



## Moscow International Symposium on Magnetism

*Dedicated to the 80<sup>th</sup> anniversary of Magnetism Department  
and the Centenary of Konstantin Belov*

August 21-25, 2011

# Book of Abstracts

*M.V. Lomonosov State University, Faculty of Physics*

### Main Topics

Spintronics and Magnetotransport  
Magnetophotonics (linear and nonlinear magneto-optics, magnetophotonic crystals)  
High Frequency Properties and Metamaterials  
Diluted Magnetic Semiconductors and Oxides  
Magnetic Nanostructures and Low Dimensional Magnetism  
Micromagnetics  
Magnetic Soft Matter (magnetic polymers, complex magnetic fluids and suspensions)  
Soft and Hard Magnetic Materials  
Magnetostructural Transition related effects (Shape-memory alloys  
and Magnetocaloric effect)  
Multiferroics  
Magnetism and Superconductivity  
Magnetism in Biology and Medicine  
Miscellaneous  
Theory

**Editors:** N. Perov  
A. Kazakov  
L. Fetisov  
A. Novikov

**Moscow 2011**

Moscow International Symposium on Magnetism (MISM),  
21-25 August 2011, Moscow  
Book of Abstracts

The text of abstracts is printed from original contributions.

Faculty of Physics M.V. Lomonosov MSU

Физический факультет МГУ имени М.В. Ломоносова

ISBN

© MISM 2011

## Contributors to MISM 2011

Moscow International Symposium on Magnetism expresses its warmest appreciation on the following organizations for their generous support



Lomonosov Moscow State University



Russian Foundation for Basic Research



Russian Academy of Science (RAS)

Scientific council of RAS on Condensed-matter Physics



Japan Society for the Promotion of Science



Institute for Theoretical and Applied Electromagnetics of Russian Academy of Sciences



The Magnetic Society of Japan



Dynasty Foundation (Moscow)



Kapitza Institute for Physical Problems

## Organizing Committee

**Chairmen:** A.Vedyaev

A.Granovsky

N.Perov

**Secretary** A.Radkovskaya

## International Advisory Committee

A. Buzdin	<i>Bordeaux</i>	D. Khomskii	<i>Koeln</i>
B. Dieny	<i>Grenoble</i>	D. Khmel'nitskii	<i>Cambridge</i>
D. Givord	<i>Grenoble</i>	C. Lacroix	<i>Grenoble</i>
B. Hernando	<i>Oviedo</i>	S. Maekawa	<i>Tokai</i>
M. Farle	<i>Duisburg</i>	D. Mapps	<i>Plymouth</i>
A. Fert	<i>Orsay</i>	S. Ovchinnikov	<i>Krasnoyarsk</i>
D. Fiorani	<i>Rome</i>	S. Parkin	<i>San Jose</i>
A. Freeman	<i>Evanstone</i>	H. Szymczak	<i>Warsaw</i>
J. Gonzalez	<i>San Sebastian</i>	V. Ustinov	<i>Ekaterinburg</i>
B. Heinrich	<i>Burnaby</i>	M. Vazquez	<i>Madrid</i>
M. Inoue	<i>Toyohashi</i>		

## National Advisory Committee

*Chairman:* V. Trukhin

*Vice-Chairman:* N. Sysoev

N. Bebenin	S. Maleev	L. Prozorova	A. Sigov
A. Lagar'kov	R. Pisarev	V. Prudnikov	A. Zvezdin

## Program Committee

*Chairman:* A. Granovsky

*Secretary:* V. Rodionova

M. Acet	<i>Duisburg</i>	N. Pugach	<i>Moscow</i>
O. Aktsipetrov	<i>Moscow</i>	A. Pyatakov	<i>Moscow</i>
B. Aronzon	<i>Moscow</i>	A. Radkovskaya	<i>Moscow</i>
B. Aktas	<i>Gebze</i>	Yu. Raikher	<i>Perm</i>
D. Berkov	<i>Jena</i>	K. Rozanov	<i>Moscow</i>
M. Chetkin	<i>Moscow</i>	E. Shalygina	<i>Moscow</i>
E. Gan'shina	<i>Moscow</i>	E. Shamonina	<i>Erlangen</i>
A. Fedyanin	<i>Moscow</i>	V. Shavrov	<i>Moscow</i>
O. Kazakova	<i>London</i>	A. Smirnov	<i>Moscow</i>
C. G. Kim	<i>Daejon</i>	L. Tagirov	<i>Kazan</i>
A. Kimel	<i>Nijmegen</i>	N. Usov	<i>Moscow</i>
N. Kreines	<i>Moscow</i>	A. Vasil'ev	<i>Moscow</i>
K. Kugel	<i>Moscow</i>	V. Veselago	<i>Moscow</i>
G. Kurlyandskaya	<i>Ekaterinburg</i>	A. Vinogradov	<i>Moscow</i>
X. Li	<i>Singapore</i>	A. Zhukov	<i>San Sebastian</i>
L. Nikitin	<i>Moscow</i>	V. Zubov	<i>Moscow</i>
L. Panina	<i>Plymouth</i>	M. Zhuravlev	<i>Moscow</i>

## Local Committee

*Chairman:* N. Perov

*Internet administrator:* N. Strelkov

N. Abrosimova	O. Kotel'nikova	G. Palvanova	A. Semisalova
T. Andreeva	S. Koptsik	E. Pankova	D. Sarafannikov
T. Andrianov	I. Kovaleva	V. Prokopieva	T. Shapaeva
I. Dementsova	A. Kudakov	M. Prudnikova	N. Strelkov
S. Granovsky	Yu. Kurbatova	N. Pugach	O. Tarakanov
L. Fetisov	A. Kuznetsov	A. Radkovskaya	M. Titova
A. Ivanov	A. Loseva	I. Rodionov	A. Vinogradov
A. Kazakov	D. Mettus	V. Rodionova	M. Vlasov
M. Khairullin	Yu. Mikhailovsky	N. Ryzhanova	A. Vompe
A. Kharlamova	L. Mironova	E. Safronova	M. Zubkov
A. Khlystov	A. Novikov	V. Samsonova	



## CONTENTS

<b>22 AUGUST .....</b>	<b>9</b>
PLENARY LECTURES .....	9
ORAL SESSIONS.....	11
“ <i>Spintronics and Magnetotransport</i> ” .....	11
“ <i>Magnetism of Nanostructures</i> ” .....	19
“ <i>Non-collinear and Spiral Structures</i> ” .....	27
“ <i>Magnetic Oxides</i> ” .....	33
“ <i>Theory</i> ” .....	41
“ <i>Magnetic Soft Matter</i> ” .....	49
“ <i>Magnetism in Biology and Medicine</i> ” .....	53
“ <i>Magnetophotonics</i> ” .....	59
“ <i>Magnetism and Superconductivity</i> ” .....	71
“ <i>Micromagnetics</i> ” .....	81
“ <i>Intermetallic Compounds</i> ” .....	85
“ <i>High Frequency Properties and Metamaterials</i> ” .....	91
POSTER SESSIONS .....	99
“ <i>Magnetism of Nanostructures</i> ” .....	99
“ <i>Magnetic Oxides</i> ” .....	167
“ <i>Magnetophotonics</i> ” .....	199
“ <i>Magnetic Soft Matter</i> ” .....	225
<b>23 AUGUST .....</b>	<b>253</b>
PLENARY LECTURES .....	253
ORAL SESSIONS.....	257
“ <i>Spintronics and Magnetotransport</i> ” .....	257
“ <i>Magnetism of Nanostructures</i> ” .....	273
“ <i>Magnetostructural Transition Related Effects</i> ” .....	289
“ <i>Theory</i> ” .....	299
“ <i>Magnetic Soft Matter</i> ” .....	313
“ <i>Magnetism in Biology and Medicine</i> ” .....	319
“ <i>Magnetophotonics</i> ” .....	329
“ <i>Magnetism and Superconductivity</i> ” .....	343
“ <i>Micromagnetics</i> ” .....	355
“ <i>High Frequency Properties and Metamaterials</i> ” .....	369
POSTER SESSIONS .....	381
“ <i>Soft and Hard Magnetic Materials</i> ” .....	381
“ <i>Theory</i> ” .....	441
“ <i>Multiferroics</i> ” .....	471
“ <i>Magnetism and Superconductivity</i> ” .....	499
<b>24 AUGUST .....</b>	<b>523</b>
PLENARY LECTURES .....	523
ORAL SESSIONS.....	527
“ <i>Diluted Magnetic Semiconductors</i> ” .....	527
“ <i>Soft and Hard Magnetic Materials</i> ” .....	537
“ <i>Magnetostructural Transition Related Effects</i> ” .....	547
“ <i>Low Dimensional Magnetism</i> ” .....	559
“ <i>Magnetic Soft Matter</i> ” .....	567
“ <i>Magnetophotonics</i> ” .....	581

“Magnetism and Superconductivity” .....	591
“Multiferroics” .....	603
“High Frequency Properties and Metamaterials” .....	613
POSTER SESSIONS .....	625
“Magnetostructural Transition Related Effects” .....	625
“Spintronics and Magnetotransport” .....	667
“Diluted Magnetic Semiconductors” .....	713
“Low Dimensional Magnetism” .....	731
“Micromagnetics” .....	745
“Magnetism in Biology and Medicine” .....	763
“High Frequency Properties and Metamaterials” .....	779
<b>25 AUGUST .....</b>	<b>809</b>
PLENARY LECTURES .....	809
ORAL SESSIONS.....	813
“Diluted Magnetic Semiconductors” .....	813
“Soft and Hard Magnetic Materials” .....	825
“Magnetic Oxides” .....	835
“Memorial Session” .....	841
“Low Dimensional Magnetism” .....	849
“Magnetic Soft Matter” .....	861
“Magnetophotonics” .....	877
“Magnetic Oxides” .....	883
“Magnetism and Superconductivity” .....	889
“Multiferroics” .....	901
“Spintronics and Magnetotransport” .....	909
<b>AUTHOR INDEX .....</b>	<b>917</b>



**22 August**

Monday

10:00-11:30

plenary lectures  
22PL-A

22PL-A-1

## ELECTRONIC PROPERTIES OF GRAPHENE

*Novoselov K.S.*

School of Physics & Astronomy, University of Manchester, Manchester, M13 9PL, UK

Among a number of unique qualities of graphene, its electronic properties attract particular attention. In my talk I'll concentrate on various ways which allow one to lift the spin/valley degeneracy in graphene, which results in flavor-polarized currents in this material. Apart of traditional spintronics, such phenomena may lead to general flavourtronics, which might be of interest for a number of applications.

22PL-A-2

## CONSERVATION LAWS OF ENERGY AND MOMENTUM IN MAGNETIC NANOSTRUCTURES

*Maekawa S.<sup>1,2</sup>*

<sup>1</sup> Advanced Science Research Center, Japan Atomic Energy Agency, Tokai 319-1195, Japan

<sup>2</sup> CREST, Japan Science and Technology Agency, Tokyo 102-0075, Japan

In magnetic nanostructures, there are two conservation laws between the conduction electrons and the magnetic moment [1]. The first is the angular momentum conservation which brings about the spin angular momentum transfer between them. The other is that of energy between them. The magnetic energy stored in the conduction electrons is released as the spin motive force. The spin-motive force is derived by extending the Faraday's law of electro-magnetism. The non-conservative force acting on the spins of conduction electrons causes the work, which brings about the spin-motive force [2]. A variety of the phenomena due to the spin motive force [3, 4] are presented.

[1] *Concepts in Spin Electronics*, ed. S. Maekawa (Oxford University Press, 2006).

[2] S. E. Barnes and S. Maekawa: *Phys. Rev. Lett.* **98**, (2007) 246601.

[3] J. Ohe, S. E. Barnes, H. W. Lee and S. Maekawa: *Appl. Phys. Lett.* **95**, (2009) 123110.

[4] P.N. Hai, S. Ohya, M. Tanaka, S.E. Barnes and S. Maekawa: *Nature* **458**, (2009) 489.

**22 August**

Monday

12:00-14:00

15:00-17:00

oral session

22TL-A

**“Spintronics and  
Magnetotransport”**

22TL-A-1

## ANOMALOUS HALL EFFECT AND SPIN CURRENT GENERATION IN 2D SYSTEMS WITH RANDOM RASHBA COUPLING

*Dugaev V.K.<sup>1</sup>, Sherman E.Ya.<sup>2</sup>, Barnaś J.<sup>3</sup>, Bruno P.<sup>4</sup>*

<sup>1</sup>Department of Physics, Rzeszów University of Technology, Rzeszów, Poland

<sup>2</sup>Department of Physical Chemistry, Universidad del Pais Vasco, Bilbao, Spain

<sup>3</sup>Department of Physics, Adam Mickiewicz University, Poznań, Poland

<sup>4</sup>European Synchrotron Radiation Facility, Grenoble, France

It is well known that Rashba spin-orbit (SO) interaction is an important element of different mechanisms of anomalous and spin Hall effects in 2D electronic systems. In many cases the Rashba coupling is zero due to the symmetry of the system. However it can be zero only in average but the system is in strongly fluctuating Rashba field. An important example is the semiconducting quantum well with the fluctuating in space Rashba coupling [1] related to the spatially fluctuating impurity density in the vicinity of quantum well.

We consider 2D electron gas in a symmetric semiconductor quantum well and the effects related to the spin-orbit coupling. Our estimations show that the magnitude of such fluctuations can be large even though it is purely relativistic effect. The main reason is that the electron wavefunction includes a superposition of atomic functions, which are localized near the atomic cores. This effect enhances enormously the magnitude of fluctuating SO field.

We consider several different effects related to this fluctuating spin-orbit interaction. First, we estimated the spin relaxation time of electrons in 2D system. It gives us an additional mechanism of spin relaxation, which can be comparable to other known mechanisms. We also calculated the combined electron dipole spin resonance and the spin pumping accompanying the absorption of light [2]. In the presented work we will mostly concentrate on a possibility of generation of the spin Hall current [3]. This effect gives us the pure spin current in the 2D electron system with zero average spin-orbit but nonvanishing fluctuations of the Rashba spin-orbit field.

Our theory can be also applied to graphene [4], where the spatially fluctuating spin-orbit field is mostly related to the ripples at the graphene surface. We calculated the corresponding spin relaxation time in graphene, and found that our estimations are in good agreement with the latest experiments. Also, we demonstrated the possibility of spin density pumping in graphene by periodic electric field in a relatively broad range of frequencies.

This work is supported by the National Science Center in Poland as a research project in years 2011-2013.

[1] M.M. Glazov, E.Ya. Sherman, V.K. Dugaev, *Physica E* **42** (2010) 2157.

[2] V.K. Dugaev, E.Ya. Sherman, V.I. Ivanov, J. Barnaś, *Phys. Rev. B* **80** (2009) 081301(R).

[3] V.K. Dugaev, M.Inglot, E.Ya. Sherman, J. Barnaś, *Phys. Rev. B* **82** (2010) 121310(R).

[4] V.K. Dugaev, E.Ya. Sherman, J. Barnaś, *Phys. Rev. B* **83** (2011) 085306.

22TL-A-2

## SPIN-TORQUE VORTEX NANO OSCILLATORS: FROM FUNDAMENTALS TO APPLICATIONS

Dussaux A.<sup>1</sup>, Locatelli N.<sup>1</sup>, Bortolotti P.<sup>1</sup>, Grollier J.<sup>1</sup>, Cros V.<sup>1</sup>, Fert A.<sup>1</sup>, Khvalkovskiy A.V.<sup>2</sup>, Krasheninnikov A.V.<sup>2</sup>, Zvezdin K.A.<sup>2,3</sup>, Zvezdin A.K.<sup>2,3</sup>, Fukushima A.<sup>4</sup>, Konoto M.<sup>4</sup>, Kubota H.<sup>4</sup>, Yakushiji K.<sup>4</sup>, Yuasa S.<sup>4</sup>, Ando K.<sup>4</sup>

<sup>1</sup> Unité Mixte de Physique CNRS/Thales and Université Paris Sud 11, 1 ave Augustin Fresnel, 91767 Palaiseau, France

<sup>2</sup> M.Prokhorov General Physics Institute of RAS, Vavilova 38, 119991, Moscow, Russia

<sup>3</sup> Istituto P.M. srl, via Grassi, 4, 10148, Torino, Italy

<sup>4</sup> National Institute of Advanced Industrial Science and Technology (AIST), Tsukuba, Japan

Spin-polarized current can excite the magnetization of a ferromagnet through the transfer of spin angular momentum to the local spin system. This pure spin-related transport phenomenon leads to alluring possibilities for the achievement of a nanometer scale, complementary metal oxide semiconductor-compatible, tunable microwave generator that operates at low bias for future wireless communication applications. Microwave emission generated by the persistent motion of magnetic vortices induced by a spin-transfer effect seems to be a unique manner to reach appropriate spectral linewidth. However, in metallic systems, in which such vortex oscillations have been observed, the resulting microwave power is much too small.

To resolve this problem two parallel route are considered: to increase the power generated by a single vortex spin-torque nano oscillators (STNO,) and to synchronize several STNO devices. In this talk we present our recent achievements in both directions. The experimental evidence of spin-transfer-induced vortex precession in MgO-based magnetic tunnel junctions, with an emitted power 5nW and the line-width of just 1 MHz is presented. This output power is already comparable with the minimal requirements imposed by applications. In contrast to other spin transfer excitations, the thorough comparison between experimental results, analytical predictions and computer simulation for this system provides a clear textbook illustration of the mechanism of spin-transfer-induced vortex precession. Computer simulations and analytical study on synchronization between two oscillated vortexes through magnetostatic interaction are presented. It is demonstrated that such synchronization could be effectively achieved through the distances larger than the single nanopillar diameter.

We acknowledge Y. Nagamine, H. Maehara and K. Tsunekawa of CANON ANELVA for preparing the MTJ films. Financial support by the CNRS and the ANR agency (VOICE PNANO-09-P231-36, ALICANTE PNANO-06-064-03) and EC FP7 grant MASTER No. NMP-FP7-212257, and RFBR (Grant No. 09-02-01423) are acknowledged.

[1] A. Dussaux, B. Georges, J. Grollier, V. Cros, A. V. Khvalkovskiy, A. Fukushima, M. Konoto, H. Kubota, K. Yakushiji, S. Yuasa, K.A. Zvezdin, K. Ando, and A. Fert. *Nature Communications*, 1:8 doi: 10.1038/ncomms1006 (2010).

22TL-A-3

## TEMPERATURE AND FIELD DEPENDENT ELECTRONIC STRUCTURE AND MAGNETIC PROPERTIES OF $\text{LaCoO}_3$

*Ovchinnikov S., Orlov Yu.*

L.V. Kirensky Institute of Physics, SB RAS, Akademgorodok, 660036, Krasnoyarsk, Russia

The old puzzle of magnetic and electric properties of  $\text{LaCoO}_3$  is solved by the band structure calculations of the strongly correlated electrons by the LDA+GTB method. The competition of the high spin (HS), intermediate spin (IS), and low spin (LS) configurations has to be included and results in the generalization of the LDA+GTB scheme. The local multielectron states of the  $\text{CoO}_6$  cluster are calculated including strong Coulomb and spin-orbital interactions and Co-O hybridization. The ground state for  $\text{Co}^{+3}$  ion is the LS one separated by a small spin gap  $e_s = 140$  K from the HS state with total moment  $J = 1$ . The intercluster hopping is treated by a perturbation theory in the Hubbard  $X$ -operators representation.

At  $T = 0$  the nonmagnetic  $\text{LaCoO}_3$  has the insulator band structure with the gap  $E_g = 1.5$  eV. At finite temperature the population of the HS increases the susceptibility and results in the in-gap states inside the insulator gap, decreasing  $E_g$  up to 0.23 eV at 100 K. Further heating provides the maximum in  $\chi(T)$  at  $T = 150$  K and decreasing the gap and metallization at  $T_{IMT} = 585$  K. Above  $T_{IMT}$  the Pauli type contribution gives the second smooth maximum in  $\chi(T)$ . The strong temperature dependence of the band structure stems from the occupation numbers of the multielectron configurations that is essential ingredient of the multielectron LDA+GTB approach.

The strong magnetic field suppress the spin gap and results in the spin crossover of the HS and LS states for  $H = 65T$ . This crossover is accompanied by the insulator-metal transition even at  $T = 0$ .

Similar changes of the electronic structure takes place for the other Mott insulators with spin crossover like magnesiowustite (Mg, Fe)O under high pressure.

This work is done with the financial support of RFBR grants 09-02-00171, 10-02-00251, Dynasty foundation, and OFN RAS program 2.3.1.

22TL-A-4

## SPIN WAVES AND SPIN CURRENTS IN MAGNETIC NANOSYSTEMS

*Demokritov S.O.<sup>1</sup>, Dzyapko O.<sup>1</sup>, Demidov V.E.<sup>1</sup>, Kurebayashi H.<sup>2</sup>, Fang D.<sup>2</sup>, Ferguson A.J.<sup>2</sup>*

<sup>1</sup> Institute for Applied Physics, University of Muenster, Muenster, Germany

<sup>2</sup> A Cavendish Laboratory, University of Cambridge, J. J. Thomson Avenue, CB3 0HE, UK

Spin currents, the flow of angular momentum without the simultaneous transfer of electrical charge, play an enabling role in the field of spintronics. Unlike the charge current, the spin current is not a conservative quantity within the conduction carrier system. This is due to the presence of the spin orbit interaction that couples the spin of the carriers to angular momentum in the lattice. This spin-lattice coupling acts also as the source of damping in magnetic materials, where

precessing magnetic moment experiences a torque towards its equilibrium orientation; the excess angular momentum in the magnetic subsystem flows into the lattice.

In this talk I will discuss our recent experiments on the YIG/Pt hybrid system [1], where we show that this flow can be reversed by the three-magnon splitting process and experimentally achieve amplification of spin current emitted by the interacting spin-waves]. This mechanism triggers angular momentum transfer from the lattice to the magnetic subsystem and enhances the spin current.

We show that the three-magnon splitting in a magnetic insulator, due to angular momentum transfer from the lattice, enhance spin-current emission at the YIG/Pt interface. This spin current enhancement is controlled by changing the frequency and the external magnetic field. These findings shed new light onto the role of nonlinear magnetic dynamics and spin waves in spintronics. In particular, the short-wavelength spin waves, usually considered to be unimportant in conventional microwave electronics, are shown to have potential for spintronic applications. From a fundamental point of view, our results clearly demonstrate the importance of the magnetic dipole interaction for the exchange of the angular momentum between magnetic and nonmagnetic subsystems, and also the importance of the angular momentum conservation law for analysis of magnetic dynamics. They also illustrate the importance of magnon-magnon interactions for developing spin-current based electronics

H. K. is grateful to the Royal Society for their financial support to this research: TG102227. Work in Muenster has been supported by the Deutsche Forschungsgemeinschaft and by the European Union through the STREP Project Master NMP3-SL-2008-212257.

[1] H. Kurebayashi, O. Dzyapko, V.E. Demidov, D. Fang, A. J. Ferguson and S.O. Demokritov, "Controlled enhancement of spin current emission by three-magnon splitting", *Nature Materials*, in consideration.

22TL-A-5

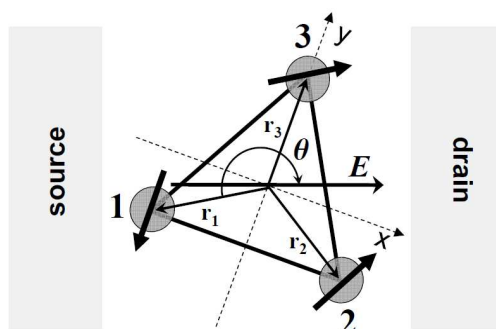
## STARK EFFECT IN SPIN SYSTEM OF COHERENTLY COUPLED QUANTUM DOTS

*Bułka B.R.<sup>1</sup>, Łuczak J.<sup>1</sup>, Kostyrko T.<sup>2</sup>*

<sup>1</sup> Institute of Molecular Physics, Polish Academy of Sciences, ul. M. Smoluchowskiego 17, 60-179 Poznań, Poland

<sup>2</sup> Faculty of Physics, A. Mickiewicz University, ul. Umultowska 85, 61-614 Poznań, Poland

We would like to present research of strongly correlated electrons in a system of coherently coupled quantum dots in the presence of an external electric field. Our interest is focused on many-electron states with different spin configurations and transition between them induced by the electric field. In particular, a system of three quantum dots (TQD) a triangular geometry is considered (see figure). Calculations are performed for the Hubbard model with a single orbital level at each quantum dot, taking into account Coulomb interactions as well as influence of the electric field. All spin configurations are



considered: quadruplet states ( $Q_{S_z}^{3/2}$ ) with the total spin  $S=3/2$ , and doublets ( $D_{S_z}^{1/2}$ ) with  $S=1/2$ . We study spin correlation functions  $\langle \vec{S}_i \cdot \vec{S}_j \rangle$  and their dependence on the electric field  $E$  and its orientation  $\theta$ . For some orientations  $\theta$  one can find a *spin dark state*, in which one of spins is decoupled from the neighborhood spins. The spin dark state can be formed either from a singlet state or from two triplet states by adding third electron to the unoccupied quantum dot. The spin dark states can be relevant for studies entanglement of three spin qubits as well as for spin dependent transport. The results are supported by studies of the Heisenberg Hamiltonian with effective exchange couplings  $J_{ij}$  between the spins, which is derived from the Hubbard model by means of a canonical transformation. The effects of the electric field on the spin system are shown to be anisotropic and include both a linear and a nonlinear part. Since electron transfer rates are anisotropic, the current characteristics are anisotropic as well, different for small and large electric fields.

Moreover, we study TQD with a triangular and a linear symmetry containing four electrons, in which one can find a transition between the singlet and the triplet state induced by the electric field. In order to understand the singlet-triplet transition, we analyse competition between a direct and super-exchange process modified by the electric field and their influence on the spin correlation functions. It is evident that one can observe the Pauli spin blockade in spin dependent transport when the system is switched from the singlet to the triplet state.

The studied model is general and can be also applied to real molecules as well as strongly correlated electrons on lattices with the triangular symmetry, to study their magnetic and optical features of interest for spintronics.

This work was supported by MNiSW from sources for science in the years 2009–2012.

22TL-A-6

## GIANT MAGNETORESISTANCE THROUGH A SINGLE MOLECULE

Bagrets A.<sup>1,2</sup>, Schmaus S.<sup>2,3</sup>, Nahas Y.<sup>2,3</sup>, Yamada T.K.<sup>3,4</sup>, Bork A.<sup>3</sup>, Bowen M.<sup>5</sup>, Beaurepaire E.<sup>5</sup>, Evers F.<sup>1,6</sup>, Wulfhchel W.<sup>2,3</sup>

<sup>1</sup> Institute of Nanotechnology, Karlsruhe Institute of Technology, 76128 Karlsruhe, Germany

<sup>2</sup> DFG-Center for Functional Nanostructures, Karlsruhe Institute of Technology, 76128 Karlsruhe, Germany

<sup>3</sup> Physikalisches Institut, Karlsruhe Institute of Technology, 76128 Karlsruhe, Germany

<sup>4</sup> Graduate School of Advanced Integration Science, Chiba University, Chiba 263-8522, Japan

<sup>5</sup> Institut de Physique et Chimie des Matériaux de Strasbourg, UMR 7504 UdS-CNRS, 67034 Strasbourg Cedex 2, France

<sup>6</sup> Institut für Theorie der Kondensierten Materie, Karlsruhe Institute of Technology, 76128 Karlsruhe, Germany

The use of single molecules to design electronic devices is an extremely challenging and fundamentally different approach to further downsizing electronic circuits. Two-terminal molecular devices such as diodes were first predicted [1] and, more recently, measured experimentally [2]. The addition of a gate then enabled the study of molecular transistors [3-5]. Furthermore, in order to increase data processing capabilities, one may not only consider the electron's charge but also its spin. This concept has been pioneered in giant magnetoresistance (GMR) junctions that consist of



thin metallic films [6,7]. Spin transport across molecules, i.e. *Molecular Spintronics* remains, however, a challenging endeavor.

As an important step in this field, we have performed [8] an experimental and theoretical study on spin transport across a molecular GMR junction consisting of a hydrogen phthalocyanine (H<sub>2</sub>-Pc) molecule deposited on the Co(111) nano-island and probed by the ferromagnetic tip of a spin-polarized scanning tunnelling microscope (sp-STM). We measure the conductance to be around 0.26G<sub>0</sub>, where G<sub>0</sub> is the quantum of conductance. Furthermore, we observe that even though H<sub>2</sub>-Pc in itself is nonmagnetic, incorporating it into a molecular junction can enhance the magnetoresistance (MR) by one order of magnitude to 60%, as compared with 5% MR of the Co tunnel junction. Our *ab initio* electron transport calculations identify strong spin-dependent hybridization of the lowest unoccupied molecular orbital (LUMO) and electrode orbitals as the cause of the large magnetoresistance.

- [1] A. Aviram, and M. A. Ratner, *Chem. Phys. Lett.* **29**, 277-283 (1974).
- [2] M. Elbing, R. Ochs, M. Koentopp, *et al.*, *Proc. Natl. Acad. Sci. USA* **102**, 8815-8820 (2005).
- [3] J. Park, A. N. Pasupathy, J. I. Goldsmith, *et al.*, *Nature* **417**, 722-725 (2002).
- [4] L. H. Yu, Z. K. Keane, J. W. Ciszek, *et al.*, *Phys. Rev. Lett.* **95**, 256803 (2005).
- [5] E. A. Osorio, T. Bjørnholm, J.-M. Lehn, *et al.*, *J. Phys.: Condens. Matter* **20**, 374121 (2008).
- [6] M. N. Baibich, J. M. Broto, A. Fert, *et al.*, *Phys. Rev. Lett.* **61**, 2472-2475 (1988).
- [7] G. Binasch, P. Gruenberg, F. Saurenbach, and W. Zinn, *Phys. Rev. B* **39**, 4828-4830 (1989).
- [8] S. Schmaus, A. Bagrets, Y. Nahas, *et al.*, *Nature Nanotechnology* **6**, 185-189 (2011).

22TL-A-7

## INTERACTION BETWEEN CONDUCTION $\pi$ -ELECTRONS AND LOCALIZED $d$ -SPINS IN MAGNETIC ORGANIC CONDUCTORS

*Swietlik R.*

Institute of Molecular Physics, Polish Academy of Sciences, ul. M. Smoluchowskiego 17,  
60-179 Poznań, Poland

Synthesis and characterization of molecular materials which combine high electrical conductivity and magnetism is an exciting area of research in contemporary materials science. The multifunctional properties can be obtained in hybrid materials that contain a conducting and magnetic sublattice, for example, in conducting charge transfer of organic donors (or acceptors) with magnetic counterions. The molecular sublattices can be independent (superposition of properties) or they can interact each other leading to new physical properties. The interaction between two sublattices can be observed when the localized magnetic moments (spins of  $d$ -electrons of transition metal ions) are coupled via the interaction with conduction  $\pi$ -electrons in organic sublattice. This indirect exchange coupling is analogous to that observed in transition and rear-earth metals (RKKY model). In organic charge transfer salts this indirect exchange interaction is expected to be rather small in comparison to the classical metals, nevertheless it was observed in many organic charge transfer salts formed by derivatives of TTF (tetrathiafulvalene) with magnetic ions with localized  $d$ -spins.

The semiconducting charge transfer salts formed by the organic donor bis(ethylenedithio)-tetrathiafulvalene (BEDT-TTF) together with M(CN)<sub>6</sub><sup>3+</sup> trianions (M = Co<sup>III</sup>, Fe<sup>III</sup>) crystallize in either triclinic [1] or monoclinic [2] lattice. Both the triclinic (or monoclinic) Co<sup>III</sup> and Fe<sup>III</sup> salts are isostructural and the BEDT-TTF molecules in conducting layers are arranged in the  $\kappa$ -type packing mode. All the crystals undergo a similar charge ordering phase transition at T<sub>CO</sub> = 150 K: at room

temperature all the BEDT-TTF molecules have the same charge +0.5 but below 150 K they have the charge 0 or +1. Moreover, there exist strong charge fluctuations above 150 K. We studied the charge fluctuations and charge ordering by IR and Raman spectroscopy. Strong changes of both electronic (IR) and vibrational features (IR, Raman) were observed. In the triclinic and monoclinic  $\text{Fe}^{\text{III}}$  salts the charge fluctuations are strong already at room temperature and grow on cooling. On the other hand, in the triclinic  $\text{Co}^{\text{III}}$  salt these fluctuations are nearly not seen above 150 K and in the monoclinic  $\text{Co}^{\text{III}}$  salt they become well pronounced below about 230 K. It is usually assumed that in BEDT-TTF salts the charge ordering is induced by the long range Coulomb interactions between charge carriers inside organic layers. However, our studies show that interactions between organic and inorganic layers should be also taken into account. We suggest that in addition to the electrostatic interactions with  $\text{M}(\text{CN})_6^{3-}$  trianions there exist also magnetic interactions between the spins of delocalized  $\pi$  electrons in BEDT-TTF layers and the spins of localized  $d$  electrons ( $\pi$ - $d$  coupling). The  $\pi$ - $d$  coupling can be responsible for the strong charge fluctuations as well as the pronounced difference between the  $\text{Co}^{\text{III}}$  and  $\text{Fe}^{\text{III}}$  salts.

[1] P. Le Maguerès, L. Ouahab et al., *Synth. Met.* **86**, 1859 (1997)

[2] A. Ota, L. Ouahab et al., *Chem. Mater.* **19**, 2455 (2007)

**22 August**

Monday

12:00-14:00

15:00-17:00

oral session

22TL-B

22RP-B

**“Magnetism of  
Nanostructures”**

22TL-B-1

## PERPENDICULAR MAGNETIC RECORDING AND ITS FUTURE EXTENSION

Honda N.<sup>1</sup>, Ariake J.<sup>2</sup>, Yamakawa K.<sup>2</sup>, Ouchi K.<sup>2</sup>

<sup>1</sup> Tohoku Institute of Technology, Sendai, Japan  
<sup>2</sup> AIT, Akita Prefectural R & D Center, Akita, Japan

Perpendicular magnetic recording (PMR) was proposed by S. Iwasaki in 1977 [1]. Under his strong leadership, the development for realization of PMR had been continued with intensive cooperation of Academic, Government, and Industry. Though the period of so called valley of death of technology, PMR has been realized as perpendicular type HDD with an areal density of 133 Gbit/in<sup>2</sup> by Toshiba in 2005. PMR is not only an improvement from conventional magnetic recording, but it should be regarded as the revolution in the technology. PMR forms a complementary relationship with in-plane magnetic recording [2], that is, magnetic recording is completed with PMR. Therefore, future magnetic recording technology should be developed based on PMR.

Recording media for PMR is based on Co-Cr alloy from the beginning. The alloy film is suitable for PMR media in that it exhibits perpendicular anisotropy due to preferred orientation along with a small grained structure. The latter is essential for high resolution and low medium noise properties. These properties have been developed remarkably using Ru based underlayer and oxide composite Co-Pt-Cr alloy, which realized smaller grains less than 10 nm surrounded by oxide. We have proposed TiO<sub>2</sub> for the oxide with better magnetic separation [3] (Fig. 1). However, from the recording resolution performance, media should have moderate inter-granular exchange coupling. The inter-granular exchange coupling increases the M-H loop slope in the film normal direction, which is also beneficial for thermal stability of recorded magnetization. The product of the loop slope of media and the field gradient of write head determine the recording resolution. Therefore, much improvement has been done for write head as well [4]. The recording layer of present perpendicular recording media has a stacked structure with well isolated and partially isolated layers (Fig. 2). The partially isolated layer offers moderate inter-granular exchange coupling.

Some extension of PMR scheme is required to achieve higher densities beyond 2 Tbit/in<sup>2</sup>. One of the promising candidates is bit-patterned media (BPM) technology. The issues and improvements of BPM technology will also be presented [5].

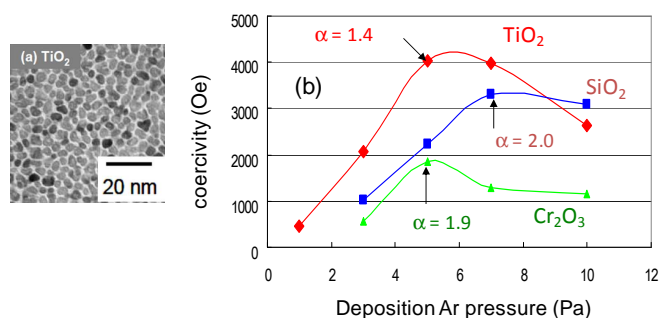


Fig. 1. (a) Plan view of TiO<sub>2</sub> oxide composite Co-Pt alloy film and (b) effect of addition of various oxides on the coercivity.

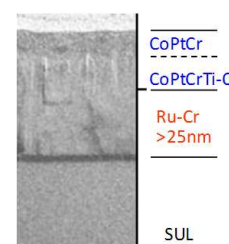


Fig. 2. TEM cross sectional view of a commercial disk medium.

The authors would like to thank Dr. S. Iwasaki for his guidance and encouragement.

[1] S. Iwasaki and Y. Nakamura, *IEEE Trans. Magn.*, **MAG-13**, 1272, 1977.

[2] S. Iwasaki, *IEEE Trans. Magn.*, **MAG-15**, 71, 1980.

- [3] J. Ariake, T. Chiba, N. Honda, *IEEE Trans. Magn.*, **41**, 3142, 2005.  
 [4] K. Ise, S. Takahashi, K. Yamakawa, N. Honda, *IEEE Trans. Magn.*, **42**, 2422, 2006.  
 [5] N. Honda, K. Yamakawa, J. Ariake, Y. Kondo, K. Ouchi, *IEEE Trans. Magn.*, **47**, 11, 2011.

22TL-B-2

## **TAILORING MAGNETIC RELAXATION CHANNELS AT THE NANOSCALE**

*Barsukov I., Lindner J., Meckenstock R., Wende H., Farle M.*

Fakultät für Physik and Center for Nanointegration, University Duisburg-Essen, Lotharstr. 1, 47057  
 Duisburg, Germany

Controlling spin relaxation is essential for spintronic and spin torque applications. Manipulating spin relaxation allows the adjustment of magnetization reversal speed at microwave frequencies. Moreover, the critical current in spin torque devices can be reduced and tuned.

In the experiment it is possible to distinguish between the intrinsic and extrinsic relaxation channels. The latter can be tailored with respect to the intensity and anisotropic behaviour. In particular, methods for inducing elementary relaxation channels of uniaxial symmetry and their impact on the magnetization dynamics are discussed in this presentation.

Fe-based thin films have been studied by means of the ferromagnetic resonance technique, by which the intrinsic and extrinsic relaxation processes can be disentangled. While the former are rather isotropic and can be adjusted via spin-orbit interaction, the latter can be modified in an advanced way. It is shown, how crystalline defects, inhomogeneities of chemical composition, and interface modifications can induce the 2-magnon scattering. Control and systematic manipulation of these parameters allow tailoring the overall spin relaxation in a desired manner.

Financial support by the DFG, SFB 491 is acknowledged.

22TL-B-3

## **ELECTRONIC CONFIGURATION AND MAGNETISM OF ATOMIC-SCALE STRUCTURES**

*Carbone C.*

Istituto di Struttura della Materia, Consiglio Nazionale delle Ricerche, Trieste, Italy

Advances in nanotechnology, like the ability of controlled atom manipulation at surfaces, have brought the properties of atomic-scale structures into the focus of research in magnetism. In a very broad class of such systems one faces the question of properly describing how the competition between electron hybridization and correlation effects ultimately determines the magnetic properties.

Selected studies making use of synchrotron radiation-based spectroscopic techniques will illustrate aspects of the magnetic and electronic interactions of single atoms and simple molecules with metal surfaces. The hierarchy of the electronic interactions will be discussed with respect to

the survival or quenching of the magnetic moment for an isolated atom as well as the charge and magnetic state for a metal center of a phthalocyanine molecule. In particular, it will be shown how atomic multiplets and local moments develops for 3d and 4f impurities on different substrates when one tunes step by step the strength of Coulomb repulsion and band formation effects. Metalphthalocyanine (CuPc, CoPc, FePc) monolayers will provide examples of charge-transfer and correlation effects on the anisotropy, spin, and orbital moments of molecular states at a metal interface.

22TL-B-4

## MAGNETIC CLUSTERS AND NANOPARTICLES: TAKING AN INTEGRATING CROSS-DISCIPLINARY APPROACH ON MULTIPLE FRONTS

*Rivas J.<sup>1</sup>, Rivas B.<sup>3</sup>, Bañobre-López M.<sup>2</sup>, López-Quintela M.A.<sup>2</sup>*

<sup>1</sup> University of Santiago de Compostela, Dpt. of Applied Physics, E-15782  
Santiago de Compostela, Spain

<sup>2</sup> University of Santiago de Compostela, Dpt. of Physical Chemistry, E-15782  
Santiago de Compostela, Spain

<sup>3</sup> University of Santiago de Compostela, Dpt. of Operative Dentistry and Endodontics, E-15782  
Santiago de Compostela, Spain

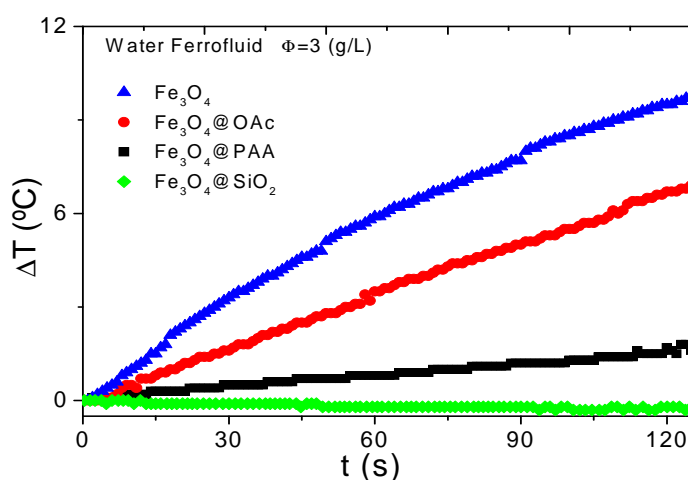
Magnetic particles play nowadays an important role in different technological areas with potential applications in fields such as electronics, energy and biomedicine. In this talk we will revise some of these applications related with the use of core-shell magnetic nanoparticles (like e.g.  $\text{Fe}_3\text{O}_4@Au$ ;  $\text{Fe}_3\text{O}_4@SiO_2$ ;  $\text{Fe}_3\text{O}_4@polymers$ ;  $\text{Fe}_3\text{O}_4@SiO_2@Au$ ;  $\text{Co}_2B@SiO_2@Au$ ; etc.) for biomolecules extractions, bio-sensing and hyperthermia treatments. As an example, figure 1 shows the large influence of the type of shell (polymers) in the temperature increase that one can achieve applying an alternating magnetic field to a dispersion of magnetite nanoparticles of 10nm.

In the last years a large interest has been devoted on the magnetic properties, which appear in small nanoparticles an clusters of diamagnetic metals, like Au, although the origin of such magnetic behavior is not understood. We will also summarize the last results in this novel area and put forward some of the explanations of such fascinating properties.

[1] V.Salgueiriño-Maceira, M.A. Correa-Duarte, M. Farle, M.A. López-Quintela, K. Sieradzki and R. Diaz. *Chem. Mater.* 18, 2701 (2006).

[2] V. Salgueirino-Maceira, M. A. Correa-Duarte, M. A. López-Quintela and J. Rivas. *Sensor Letters* 5(1), 113 (2007).

[3] M. J. Rodríguez-Vázquez, J. Rivas, M. A. López-Quintela, A. Mouriño and M. Torneiro. *Nanomaterials for Application in Medicine and Biology*. M. Giersig (ed) (Springer Verlag, 113-125, (2008).



- [4] A. B. Davila-Ibañez, M. A. Lopez-Quintela, J. Rivas and V. Salgueiriño. *J. Phys. Chem C.* 114, 7743 (2010).
- [5] E. Iglesias-Silva, J. L. Vilas-Vilela, M. A. López-Quintela, J. Rivas, M. Rodríguez, L.M. León. *J. Non-Cryst. Solids* 356 1233 (2010).
- [6] B. Santiago González, M. J. Rodríguez, C. Blanco, J. Rivas, M. A. López-Quintela, J.M. Gaspar-Martinho. *Nano Letters* 10, 4217 (2010).
- [7] Y. Piñeiro-Redondo, M. Bañobre-López, I. Pardiñas-Blanco, G. Goya, M. A. López-Quintela and J. Rivas. *Nanoscale Res. Lett.* (in press)

22TL-B-5

## **TAILORING THE PROPERTIES OF MAGNETIC NANODOTS**

*Guimarães A.P.*

Brazilian Center for Physical Research (CBPF), R. Xavier Sigaud 150, 22290-180,  
Rio de Janeiro, Brazil

Nanodots or nanodisks of magnetic materials may form magnetic vortices in their lowest energy state configuration; these are flux closure structures, with the magnetic moments generally confined to the plane, except at their cores. Vortices in nanodots have many potential applications, such as magnetic memories (VRAM's) and spin transfer nano-oscillators (STNO's). The characteristics of these vortices, including the vortex core size, can be controlled to suit these applications. This can be achieved, e.g., making use of the interface interactions in multilayers such as Co/Pt stacks [1]. We have obtained with micromagnetic simulation phase diagrams that show the change in spin configuration of the nanodots, for different anisotropies. Manipulation of the sign of the core magnetization is in principle required for the application of nanodots as memory elements, or oscillators. This can be achieved employing static, rotary, or pulsed magnetic fields; spin polarized currents have the same effect. We show here recent results obtained for dynamic properties of vortices under applied magnetic fields.

Support by CNPq and FAPERJ is acknowledged.

[1] Garcia et al. *Appl. Phys. Lett.* 97 022501 (2010).

22TL-B-6

## **MAGNETORESISTANCE BEHAVIOUR IN NANOCRYSTALLINE NiFe THIN-FILMS AND NANOWIRES**

*Atkinson D.*

Department of Physics, South Road, DH1 3LE, Durham University, Durham, UK

Anisotropic magnetoresistance (AMR) has a long history both in terms of the fundamental physics and for applications in sensor technology. More recently, AMR has become highly relevant for understanding the magnetization behaviour of magnetic structures and especially domain walls

in planar nanowires [1]. Such applications of AMR have been based on simplified assumptions [2] whilst more recent modeling has improved on these simplifications by using detailed micromagnetic structures and thickness dependent resistivity data [3]. This talk describes both the fundamental behaviour of anisotropic magnetoresistance and its application to the study of nanowires magnetization behaviour.

In order to fully develop and use AMR measurements for the rigorous interpretation of the micromagnetic configurations within nanostructures a detailed knowledge of the basic AMR dependence of the material is needed. This includes the thickness dependence of the resistivity, along with variations in grain size and texture, and importantly any magnetoresistance change as a function of thickness. The absolute size of the field dependent resistance change is more significant than simply the magnetoresistance ratio as the latter is complicated by the thickness dependent of the total resistivity.

A detailed study was made of the magnetic field dependent resistivity behaviour for Permalloy thin-films (nominal composition  $\text{Ni}_{80}\text{Fe}_{20}$ ) as a function of film thickness down to 3 nm. The films were deposited by thermal evaporation onto silicon dioxide coated silicon substrates. The magnetic behaviour of the films was measured using MOKE. The magnetic and magnetoresistance studies were complemented with detailed structural analysis using x-ray diffraction and reflectivity and TEM imaging.

Structural analysis shows that all the films are continuous, with a thin oxidation layer and have low roughness. The films are all magnetic and there is little thickness dependence to the coercivity. The grain size was about 7 nm and changes little with thickness. The resistivity of the films increases as the film thickness decreases, as expected due to surface scattering.

Most significantly, the absolute size of the magnetoresistance also changes. The field dependent resistance change falls rapidly below 10 nm to almost zero around 3 nm. The origin of this effect is not clear. However, we suggest that the fundamental mechanism giving rise to anisotropic magnetoresistance changes for film thicknesses below 10 nm and considering that a similar thickness trend was observed elsewhere in the magnetostriction of NiFe [4] we suggest that the spin-orbit coupling within NiFe films is changing below 10 nm.

Magnetoresistance measurements of individual lithographic planar nanowires with nucleation pads and single pinning structures were used to study many individual magnetic switching events as a function of magnetic field. Magnetoresistance results show the injection of individual domain walls and their interactions with pinning structures. The changes in magnetoresistance reveal considerable detail in the domain switching process. The results show significant variations in behaviour between successive switching events. Some consistencies emerge from the measurements indicating the switching process involves domain wall chirality and thermally activated switching.

[1] M. Hayashi, L. Thomas, C. Rettner, R. Moriya, X. Jiang, and S. S. P. Parkin, *Phys. Rev. Lett.* **97**, 207205 (2006)

[2] L. Thomas, and S. S. P. Parkin, in '*Handbook of Magnetism and Advanced Magnetic Materials*' vol. 2. H. Kronmüller and S. S. P. Parkin (Eds) John Wiley & Sons Ltd Chichester (2007)

[3] L. K. Bogart & D. Atkinson *Appl. Phys. Letts.* **94**, 042511 (2009)

[4] M.P. Hollingworth, M.R.J. Gibbs and E.W. Hill *J. Appl. Phys.* **93**, 8737 (2003)



22RP-B-7

## UNCOMPENSATED MOMENTS IN ANTIFERROMAGNETS AND INTRINSIC EXCHANGE BIAS

*Roshchin I.V.<sup>1,2</sup>, Badgley K.E.<sup>1</sup>, Belashchenko K.D.<sup>3</sup>, Zhernenkov M.<sup>4</sup>, Fitzsimmons M.R.<sup>4</sup>*

<sup>1</sup> Department of Physics and Astronomy, Texas A&M University, 4242 TAMU, College Station,  
Texas 77843-4242, USA

<sup>2</sup> Materials Science and Engineering Program, Texas A&M University, 3003 TAMU,  
College Station, Texas 77843-3003, USA

<sup>3</sup> Department of Physics and Astronomy, University of Nebraska-Lincoln, Lincoln,  
Nebraska 68588, USA

<sup>4</sup> Los Alamos Neutron Science Center, Los Alamos National Laboratory, Los Alamos,  
New Mexico 87545, USA

After more than 50 years since the discovery of *exchange bias*, its microscopic mechanism remains a puzzle [1]. Typically observed in a bilayer consisting of a ferromagnet (FM) and antiferromagnet (AF), exchange bias manifests itself as a horizontal shift of the ferromagnetic hysteresis loop. It is attributed to exchange coupling across the interface [1,2].

Several experimental findings demonstrate, and many models agree that uncompensated magnetization (UM) in the AF plays an important role in exchange bias [1]. Recently, the depth profile of the magnetization across the interface between a FM (Co) and an AF (FeF<sub>2</sub>) in an exchange bias bilayer has been measured [3,4]. It has been shown that the UM can form domains [5,6], affects properties of the domain structure in the FM [5,7], and may even form a parallel domain wall [8]. However, the origin of the UM remains unknown.

Here, we report studies of *AF-only*, (110)-FeF<sub>2</sub> grown on MgF<sub>2</sub> samples. Magnetometry and polarized neutron reflectivity (PNR) measurements indicate that the UM is present in this AF, and the PNR reveals the spatial distribution of the UM. This UM exhibits rather unexpected properties, including *intrinsic exchange bias*. This unusual effect enables a *new magnetic state* of matter where zero magnetic remanence cannot be achieved without heating the sample above its magnetic ordering temperature.

We argue that below  $T_N$ , the UM in FeF<sub>2</sub> is coupled to the bulk antiferromagnetic order parameter as supported by several experimental results, including high value of exchange bias field, its temperature dependence, and the absence of the training effect. We will discuss the origin of the UM based on general symmetry arguments.

Work supported by Texas A&M University, Texas A&M University – CONACyT Collaborative Research Grant Program, DOE, AFOSR, and NSF-9976899.

[1] J. Nogues and I. K. Schuller, *J. Magn. & Magn. Mater.* **192**, 203 (1999).

[2] J. Nogues *et al.*, *Phys. Rev. Lett.* **76**, 4624 (1996).

[3] S. Roy *et al.*, *Phys. Rev. Lett.* **95**, 047201 (2005).

[4] M. R. Fitzsimmons *et al.*, *Phys. Rev. B* **75**, 214412 (2007).

[5] I. V. Roshchin *et al.*, *Europhysics Letters*, **71**, 297 (2005)

[6] M. R. Fitzsimmons *et al.*, *Phys. Rev. B* **77**, 11 (2008).

[7] R. Morales *et al.*, *Appl. Phys. Lett.* **95**, 3 (2009).

[8] Z. P. Li *et al.*, *Phys. Rev. B* **76**, 8 (2007).

22RP-B-8

## HARD MAGNETIC FeCuPt NANOPARTICLES FROM THE GAS PHASE

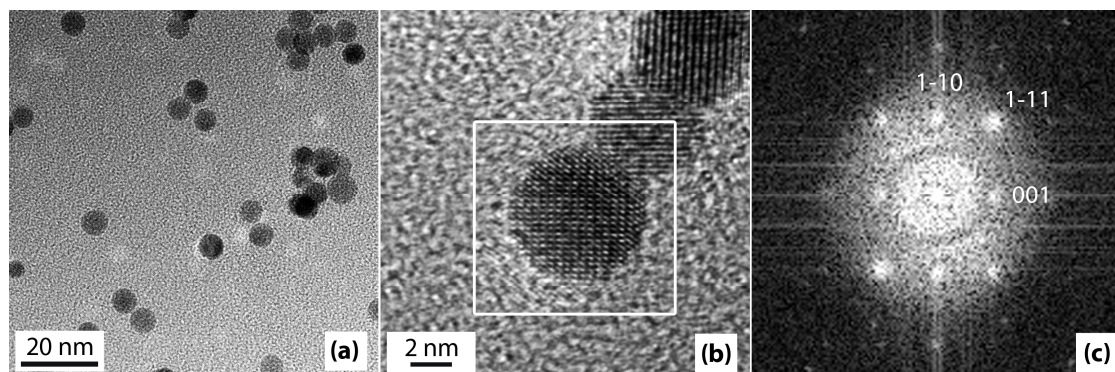
Spasova M.<sup>1</sup>, Elsukova A.<sup>1</sup>, Ünlü G.<sup>1</sup>, Acet M.<sup>1</sup>, Trunova A.<sup>1</sup>, Koplak O.<sup>2</sup>, Farle M.<sup>1</sup>

<sup>1</sup> Universität Duisburg-Essen, Fakultät für Physik and Centre of Nanointegration Duisburg-Essen (CeNiDE), Lotharstr. 1, 47048 Duisburg, Germany

<sup>2</sup> Institute of Problems of Chemical Physics, Russian Academy of Science, Ac. Semenov 1, 142432 Chernogolovka, Russia

High anisotropy magnetic nanoparticles are of immense current interest due to their potential applications such as high-performance nanocomposite permanent magnets, biosensor systems and ultrahigh density magnetic recording. A promising material for realizing such particles is FePt alloy in the chemically ordered L1<sub>0</sub> phase, since its high uniaxial magnetocrystalline anisotropy energy ( $\sim 7 \text{ MJ/m}^3$ ) allows to reduce the particle size to a few nanometers while avoiding thermal instabilities in the magnetization. However, fabrication of single crystal FePt nanoparticles in the L1<sub>0</sub> phase is a challenge. Formation of the chemically ordered phase is usually kinetically suppressed in nanoparticles, and post-preparation high-temperature annealing is required for transforming the particles into the L1<sub>0</sub> phase [1]. The latter results in nanoparticle coalescence and sintering. The gas phase preparation of nanoparticles provides the possibility of in-flight annealing of nanoparticles prior their deposition on a substrate. However, for low sputtering gas pressure where monodisperse nanoparticles can be produced, multi-twinned icosahedral morphology is predominant [2].

In this work, we show that partial replacement of Fe by Cu in FePt nanoparticles results in the formation of single crystalline L1<sub>0</sub> nanoparticles during in-flight annealing at 1273 K in the gas phase.



The figure shows (a) overview of particles in-flight annealed at 1273 K, (b) high resolution transmission electron microscopy image of FeCuPt<sub>2</sub> nanoparticle along its [110] zone axis, (c) diffractogram as obtained from the framed image in (b). {011} and {001} indicate the ordered L1<sub>0</sub> phase of the nanoparticles.

Magnetic properties of the L1<sub>0</sub> FeCuPt nanoparticles assembly were studied using SQUID magnetometry and Ferromagnetic Resonance.

Support by the Deutsche Forschungsgemeinschaft within the Sonderforschungsbereich 445 is gratefully acknowledged.

[1] Shouheng Sun, *Adv. Mater.*, **18** (2006) 393.

[2] S. Stappert, B. Rellinghaus, M. Acet, E.F. Wassermann, *J. Cryst. Growth.*, 252 (2003) 440.

**22 August**

Monday

12:00-14:00

oral session

21TL-C

21RP-C

21OR-C

**“Non-collinear and  
Spiral Structures”**

22TL-C-1

## THE HEAT CAPACITY AND THE ENTROPY LOST IN THE HELICAL MAGNET MnSi

*Stishov S.M.<sup>1</sup>, Petrova A.E.<sup>1</sup>, Shikov A.A.<sup>2</sup>, Lograsso T.M.<sup>3</sup>, Isaev E.I.<sup>4,5</sup>, Johansson B.<sup>6</sup>,  
Daemen L.L.<sup>7</sup>*

<sup>1</sup>Institute for High Pressure Physics of Russian Academy of Sciences, Troitsk,  
142190 Moscow Region, Russia

<sup>2</sup>Russian Research Center, Kurchatov Institute, Moscow 123182, Russia

<sup>3</sup>Ames Laboratory, Iowa State University, Ames, IA 50011, USA

<sup>4</sup>Department of Physics, Chemistry and Biology, SE-581 83, Linköping University, Sweden

<sup>5</sup>Department of Theoretical Physics and Quantum Technologies, National University of Science  
and Technology (MISIS), 4, Leninskii prospect, 119 Moscow, Russia

<sup>6</sup>Applied Materials Physics, Materials Science Department,

The Royal Technological University, SE-100 44 Stockholm, Sweden

<sup>7</sup>Los Alamos National Laboratory, Los Alamos, New Mexico 87545, USA

Recent studies of heat capacity, thermal expansion, resistivity and elastic properties of high quality single crystal of MnSi exposed first order features of the magnetic phase transition in MnSi. These studies revealed the existence of unexplained aspects of the phase transition, such as maxima or minima of the heat capacity, thermal expansion coefficient and temperature coefficient of resistivity on the high temperature sides of the corresponding peaks.

Here we report our study of the heat capacity of MnSi at  $B = 0$  and  $B = 4$  T in the temperature range 2.5-100 K. The frequency positions of the phonon modes in MnSi were determined in the neutron scattering experiment. The calculations of the phonon spectra and density of phonon states in MnSi were performed, which agree with available experimental data.

The analysis of the data suggest an existence of negative contributions to the heat capacity and entropy of MnSi at  $T > T_c$  in an agreement with the theoretical prediction that may mean a certain ordering in the spin subsystem. Is this “ordering” indicate tendency to the forming a skyrmion like texture remain to be seen in the future development. An evolution of the heat capacity negative term along the phase transition line at  $T \rightarrow 0$  may be of primary interest for understanding peculiar properties of the paramagnetic phase of MnSi at low temperatures and high pressures.

## SPIRAL SPIN STRUCTURE IN MONOSILICIDES OF TRANSITION METALS

*Grigoriev S.V.<sup>1</sup>, Maleyev S.V.<sup>1</sup>, Dyadkin V.A.<sup>1</sup>, Moskvina E.V.<sup>1</sup>, Menzel D.<sup>2</sup>, Eckerlebe H.<sup>3</sup>*

<sup>1</sup> Petersburg Nuclear Physics Institute, 188300 Gatchina, St-Petersburg, Russia

<sup>2</sup> Technische Universität Braunschweig, 38106 Braunschweig, Germany

<sup>3</sup> Helmholtz Zentrum Geesthacht, 21502 Geesthacht, Germany

The cubic B20-type (space group P2<sub>1</sub>3) doped compounds Mn<sub>1-x</sub>Fe<sub>x</sub>Si and the related system Fe<sub>1-x</sub>Co<sub>x</sub>Si order in a spin helix structure with a small propagation vector  $|\mathbf{k}|$ . The spin helix structure is well interpreted within the Bak-Jensen hierarchical model. The hierarchy implies that the spin helix appears as a result of the competition between the ferromagnetic spin exchange and antisymmetric Dzyaloshinskii-Moriya interaction caused by the lack of inverse symmetry in arrangement of magnetic atoms. The weak anisotropic exchange interaction fixes the direction of the spin helix propagation. We demonstrate that (i) left and right forms of the monosilicides of transition metals crystals can be grown by the Czochralski method, (ii) the magnetic chirality of all Mn<sub>1-x</sub>Fe<sub>x</sub>Si crystals follows its crystallographic counterpart, (iii) the opposite to relationship between the crystal handedness and the spin chirality has been found for seemingly similar Fe<sub>1-x</sub>Co<sub>x</sub>Si compound.

The spiral structure of cubic magnets Mn<sub>1-x</sub>Fe<sub>x</sub>Si and Fe<sub>1-x</sub>Co<sub>x</sub>Si of different  $x$  had been studied using small angle polarized neutron diffraction and SQUID measurements. On the basis of these experiments the H-T phase diagrams for each compound had been built. It is shown that the magnetic structure of all compounds can be described by the same set of the parameters: the helix wave-vector  $\mathbf{k}$ , and three characteristic fields  $H_{C1}$ ,  $H_A$ , and  $H_{C2}$ . Here  $H_{C1}$  is the field of the transformation from a multiple to a single domain structure.  $H_A$  is attributed to the rotation of the helix vector to the direction perpendicular to the field in the critical range near  $T_C$  (A-phase).  $H_{C2}$  is the field of a transition from conical to a ferromagnetic state. The interplay of these four parameters  $\mathbf{k}$ ,  $H_{C1}$ ,  $H_A$ , and  $H_{C2}$  is well interpreted in the frame of the recently developed theory for cubic magnets with Dzyaloshinskii-Moriya interaction [1]. As a result, the spin wave stiffness  $A = g\mu_B H_{C2}/k^2$ , the Dzyaloshinskii constant  $S D = Ak$ , the anisotropy constant  $F \sim H_{C1}$ , and the spin wave gap  $\Delta \approx g\mu_B H_A/\sqrt{2}$  have been obtained for different compounds Mn<sub>1-x</sub>Fe<sub>x</sub>Si and Fe<sub>1-x</sub>Co<sub>x</sub>Si.

The critical spin fluctuations in doped compounds Mn<sub>1-y</sub>Fe<sub>y</sub>Si have been studied by means of ac-susceptibility measurements and polarized neutron scattering. It is shown that these compounds undergo the transition from the paramagnetic to helimagnetic phase through continuous, yet well distinguishable crossovers: (i) from paramagnetic to partially chiral, (ii) from partially chiral to highly chiral fluctuating state. The crossover points are identified on the basis of combined analysis of the temperature dependence of ac-susceptibility and polarized SANS data. The temperature crossovers, firstly, to partially chiral and then to the highly chiral fluctuating state is associated with the enhancing influence of the Dzyaloshinskii-Moria interaction close to  $T_C$ .

Support by the Goskontrakt No 02.740.11.0874. is acknowledged.

[1] S.V. Maleyev, Phys.Rev. B, **73**, (2006) 174402.

22RP-C-3

## CHIRAL MAGNETIC NANOSTRUCTURES

*Fraerman A.A.*

Institute of Physics of Microstructures, Russian Academy of Sciences, Nizhni Novgorod, 603950  
Russia; e-mail: andr@ipm.sci-nnov.ru

Investigations of spin and spatial degrees of freedom for electrons and their interplay in conducting ferromagnets are of great interest from both theoretical and practical points of view [1]. For collinear distribution of magnetization, spatial and spin degrees of freedom for current carriers are independent. But for noncollinear distribution, the motions of electron in real and spin spaces are coupling. This can lead to the peculiarities of physical properties for noncollinear magnetic systems. In general case, distribution of magnetization in laterally-confined magnetic nanostructures is noncollinear and, what is more, – non coplanar. In the report I am going to demonstrate some examples of magnetic nanostructures with chiral distribution of magnetization and discuss connection between magnetic states and physical properties of such systems. Namely

- control of vorticity for triangle magnetic nanoparticles [1]
- antivortex state in magnetic cross-like nanostructure [2]
- spiral state in laterally confined magnetic multilayer [3]

[1] S. Yakata et al, Appl. Phys. Let. **97**, 222503, 2010

[2] V.L. Mironov et al, Phys. Rev. B **81**, 094436, 2010.

[3] A.A. Fraerman et al., J. Appl. Phys. 103, 073916, 2008.

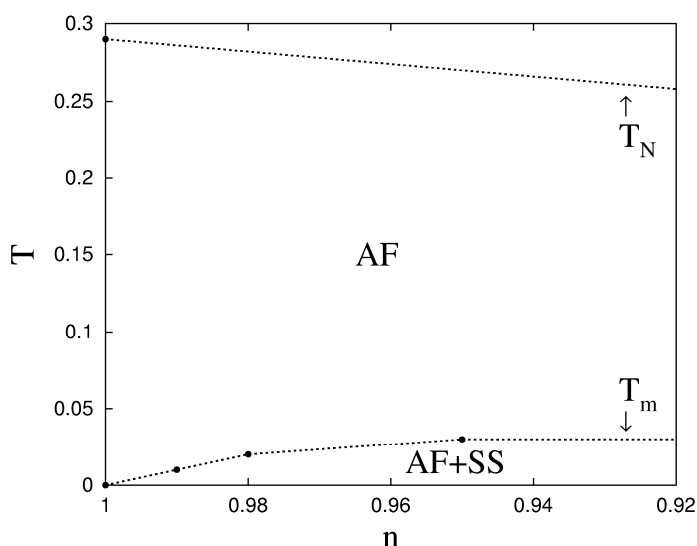
22OR-C-4

## FUNCTIONAL-INTEGRAL APPROACH TO THE INVESTIGATION OF THE SPIN-SPIRAL MAGNETIC ORDER AND PHASE SEPARATION

*Arzhnikov A.K., Groshev A.G.*

Physical-Technical Institute, Kirov Str. 132, Izhevsk 426000, Russia

Investigation of two-dimensional 2D electronic systems attracts substantial interest, which has been stimulated by the discovery of high-temperature superconducting cuprates. It is generally accepted that superconducting and magnetic properties of cuprates are closely related. At half-filling the cuprates are antiferromagnetically ordered, evolution of their magnetic properties with doping and temperature is an interesting challenge. For example, neutron scattering in  $\text{La}_{2-p}\text{Sr}_p\text{CuO}_4$  reveals the coexistence of both commensurate and incommensurate



magnetic structures in the vicinity of half-filling at low temperature, that pass to antiferromagnetic with rise of temperature. Recently the authors [1] considered the ground-state magnetic phase diagram of the two-dimensional Hubbard model with nearest and next-nearest-neighbor hopping in terms of electronic density and interaction strength. They treated commensurate ferromagnetic and antiferromagnetic as well as incommensurate spiral magnetic phases using the mean field (MF) approximation. The first-order magnetic transitions with changing chemical potential, resulting in a phase separation (PS) in terms of density, was found between ferromagnetic, antiferromagnetic, and spiral magnetic phases.

Here PS diagram is investigated depending on temperature. Our calculations are based on a two-dimensional single-band Hubbard model. We use a Hubbard-Stratonovich transformation with a two-field representation and solve this problem in a static approximation. It allows us on the one hand to obtain the solution that coincides with the MF approximation at zero temperature and on other hand to investigate the temperature behavior of PS and phase transformation taking into account the thermodynamic transverse spin fluctuations. The figure shows the change of the phase diagram with temperature in the vicinity of half-filling ( $T$  is temperature in units of the hopping integral, AF is for antiferromagnetic, SS is an incommensurate spin spiral wave). Behavior of PS (antiferromagnetic and incommensurate magnetic states) can be related to the explanation of some features observed in the one-layer compound  $\text{La}_{2-p}\text{Sr}_p\text{CuO}_4$ .

Support by RFBR N 09-02-00461 is acknowledged.

[1] P.A. Igoshev, M. A. Timirgazin, et al, Phys.Rev.B, **81** (2010) 094407





**22 August**

Monday

15:00-17:00

oral session

22TL-C

22OR-C

**“Magnetic Oxides”**

22TL-C-5

## STEPWISE MOTT TRANSITION IN COMPLEX OXIDES

*Khomskii D.I.*

II. Physikalisches Institut, Universität zu Köln, Zùlpicher Str. 77, 50937 Köln, Germany

With increasing bandwidth or decreasing correlations electron systems can go from the localized to itinerant regime (Mott transition). I will discuss this situation and show that close to such crossover several novel states, different both from the standard Mott insulators and from the normal metal, can appear. In particular, electron delocalization can occur not simultaneously in the whole sample, but first in small "clusters" (dimers, trimers), inside which electrons can already be treated as practically delocalized, the whole material still remaining insulating due to weak coupling between such "blocks". Such situation seems to occur e.g. in spinels  $\text{MgTi}_2\text{O}_4$  [1],  $\text{ZnV}_2\text{O}_4$  [2] and in  $\text{AlV}_2\text{O}_4$  [3], and also in  $\text{LiVO}_2$  [4,5]. In  $\text{TiOCl}$  under pressure, the localized-itinerant crossover is accompanied by the transition from the spin-Peierls to a conventional Peierls transition [6]. In some cases, especially in systems with orbital degeneracy, close to such crossover there may appear spontaneous charge segregation, examples being e.g. the perovskites  $\text{CaFeO}_3$  or  $\text{RNiO}_3$  [7] (R - rare earth). It seems that the possibility of occurring of novel states close to the Mott transition is a quite ubiquitous phenomenon.

This work is funded by the DFG via SFB 608.

[1] D.I. Khomskii and T. Mizokawa, *Phys. Rev. Lett.* **94** (2005) 156402.

[2] V. Pardo et al., *Phys. Rev. Lett.* **101** (2008) 256403.

[3] Y. Horibe et al., *Phys. Rev. Lett.* **96** (2006) 086406.

[4] H. Pen, J. van den Brink, D.I. Khomskii, and G. Sawatzky, *Phys. Rev. Lett.* **78** (1997) 1323.

[5] Hua Wu and D.I. Khomskii, to be published

[6] S. Blanco-Canosa et al., *Phys. Rev. Lett.* **102** (2009) 056406.

[7] I.I. Mazin et al., *Phys. Rev. Lett.* **98** (2007) 176406.

22TL-C-6

## SPIN-CHARGE-ORBITAL INSTABILITIES IN TRANSITION-METAL COMPOUNDS WITH SMALL CHARGE-TRANSFER ENERGY

*Mizokawa T.*

Department of Complexity Science and Engineering, University of Tokyo

Many insulating transition-metal compounds are known as Mott insulators, and the spin-charge-orbital orderings in the Mott insulators can be described by the Kugel-Khomskii mechanism, where the exchange interaction  $J$  is given by  $-2t^2/E_G$  ( $t$ : transfer integral,  $E_G$ : Mott gap). The Mott insulators are classified into (i) Mott-Hubbard type insulators where  $E_G$  is mainly determined by the Coulomb interaction  $U$  between the transition-metal  $d$  electrons and (ii) charge-transfer type insulators where  $E_G$  is determined by the charge-transfer energy  $\Delta$  from the ligand  $p$  state to the

transition-metal  $d$  state (Zaanen-Sawatzky-Allen scheme). A systematic photoemission study of transition-metal compounds revealed that some transition-metal oxides with high valence (such as  $\text{CaFeO}_3$ ,  $\text{PrNiO}_3$ , and  $\text{NaCuO}_2$ ) are characterized by very small (or even negative) charge-transfer energy  $\Delta$  and have strange and interesting electronic structures. In the present talk, I would like to discuss spin-charge-orbital instabilities in such transition-metal compounds with small  $\Delta$  including  $\text{BiCoO}_3$ ,  $\text{CaCu}_3\text{Co}_4\text{O}_{12}$  (perovskite and its relatives),  $\text{NiGa}_2\text{S}_4$ ,  $\text{IrTe}_2$  (triangular lattice) and  $\text{Ta}_2\text{NiSe}_5$  using photoemission experiments and model calculations. In  $\text{BiCoO}_3$  and  $\text{NiGa}_2\text{S}_4$ , the Co-O-O-Co or Ni-S-S-Ni superexchange pathways are enhanced due to small  $\Delta$  and determine the magnetic ordering or magnetic fluctuation [1,2], which should be generally seen in small- $\Delta$  systems. In contrast to the superexchange description of spin-charge-orbital instabilities, the electronic states of  $\text{NiGa}_2\text{S}_4$  and  $\text{IrTe}_2$  can be analyzed on the basis of itinerant electron models considering excitonic effect, band Jahn-Teller effect, and Peierls transition [3,4]. In  $\text{CaCu}_3\text{Co}_4\text{O}_{12}$  and  $\text{Ta}_2\text{NiSe}_5$ , the smallness of  $\Delta$  stabilizes unusual valence states of the two transition-metal sites and results in interesting ground states [5,6].

The present work has been done in collaboration with Y. Wakisaka, T. Sudayama, K. Takubo, Y. Morita, K. Ikedo, H. Wadati, G. A. Sawatzky, D. G. Hawthorn, T. Z. Regier, G. Levy, D. Fournier, A. Damascelli, M. Arita, H. Namatame, M. Taniguchi, I. Yamada, T. Saito, K. Oka, M. Azuma, Y. Shimakawa, M. Takano, N. Katayama, S. Pyon, M. Nohara, H. Takagi, Y. Nambu, S. Nakatsuji, and Y. Maeno.

- [1] T. Sudayama *et al.* submitted to Phys. Rev. B.
- [2] K. Takubo *et al.*, Phys. Rev. Lett. **99**, 037203 (2007).
- [3] K. Takubo *et al.*, Phys. Rev. Lett. **104**, 226404 (2010).
- [4] K. Ikedo *et al.*, in preparation.
- [5] T. Mizokawa *et al.*, Phys. Rev. B **80**, 125105 (2009).
- [6] Y. Wakisaka *et al.*, Phys. Rev. Lett. **103**, 026402 (2009).

22OR-C-7

## THE EFFECTS OF NON-MAGNETIC DOPING AND EXTERNAL PRESSURE UPON ORBITAL AND MAGNETIC STRUCTURES OF LANTHANUM MANGANITE

*Gonchar L.E.<sup>1,2</sup>, Firsin A.A.<sup>1</sup>, Nikiforov A.E.<sup>1</sup>, Popov S.E.<sup>1</sup>*

<sup>1</sup> Ural State University, 51 Lenin Av., Ekaterinburg, Russia

<sup>2</sup> Ural State University of Railway Transport, 66 Kolmogorov St., Ekaterinburg, Russia

The theoretical investigation of external influence on lanthanum manganite is carried out in order to describe the static and dynamic orbital states. The orthorhombic crystal; of  $\text{LaMnO}_3$  is known as a compound with the strong correlation between crystal, orbital, and magnetic structures. The non-magnetic doping of  $\text{Mn}^{3+}$  site with  $\text{Ga}^{3+}$  ion causes the collapse of the cooperative Jahn-Teller (JT) distortions [1]. The external pressure leads to collapse of orbital and magnetic orderings [1].

The crystal structure of lanthanum manganite is calculated within the framework of the shell model including Jahn-Teller energy which depends on symmetric distortions of oxygen octahedron around Mn ion [2].

The investigation of  $\text{LaGa}_x\text{Mn}_{1-x}\text{O}_3$  of  $Pmna$  space symmetry using virtual crystal model was carried out. Virtual crystal was simulated by decreasing effective linear JT constant proportional to

manganese ions amount:  $\tilde{V}_e = (1-x)V_e$ , where  $V_e$  is the linear JT constant,  $x$  is *Ga*-doping factor,  $\tilde{V}_e$  is effective linear JT constant.

The energy barrier between two stable orbital states of manganese subsystem (of  ${}^5E$  ground state) was estimated. We found that at room temperature static to dynamic Jahn-Teller effect transition becomes at *Ga*-doping factor near 0.35. Investigation of this compound at *Ga*-doping factor more 0.35 is non consistent with our model.

The pressure effect upon pure and *Ga*-doped manganite is described by adding a  $pV$ -term in the crystal energy [3].

The magnetic structure could be described for pure manganite under external pressure less than 10 GPa and for *Ga*-doped manganite with the doping rate less than 0.35. For description, we use the orbitally-dependent superexchange interaction and single-ion anisotropy [4]. The doping of non-magnetic ions leads to weakening of the magnetic interactions within the framework of *A*-type antiferromagnetic structure. The strong doping leads to ferromagnetic ordering [1] due to dynamical JT effect. The magnetic structure upon external pressure up to 10 GPa is of antiferromagnetic *A*-type. The weak ferromagnetic component decreases because of increasing superexchange and decreasing *Mn-O-Mn* angle.

The AFMR spectra are predicted in order to describe the effect of external pressure and non-magnetic doping on anisotropic magnetic interactions.

[1] J.-S. Zhou, Y. Uwatoko, K. Matsubayashi, and J.B. Goodenough, *Phys. Rev. B* **78** (2008) 220402.

[2] A.E. Nikiforov, S.É. Popov, and S. Yu. Shashkin, *Fiz. Met. Metalloved.* **87** 1(1999) 6.

[3] L.É. Gonchar', Yu.V. Leskova, A. E. Nikiforov, D. P. Kozlenko, *JETP* 111 (2010) 194

[4] L.E. Gonchar', A.E. Nikiforov, *JETP* 96 (2003) 510

22OR-C-8

## ABOUT CORRESPONDENCE BETWEEN LATTICE DISTORTIONS AND ORBITAL STRUCTURE ON THE EXAMPLE OF CE PHASE OF MANGANITES

*Sboychakov A.O.<sup>1</sup>, Kugel K.I.<sup>1</sup>, Rakhmanov A.L.<sup>1</sup>, Khomskii D.I.<sup>2</sup>*

<sup>1</sup> Institute for Theoretical and Applied Electrodynamics, Russian Academy of Sciences, Izhorskaya Str. 13, 125412 Moscow, Russia

<sup>2</sup> II. Physikalisches Institut, Universität zu Köln, Zùlpicher Str. 77, 50937 Köln, Germany

The interplay between spin, charge, orbital, and lattice degrees of freedom plays an important role in the physics of transition-metal oxides, especially those with Jahn-Teller (JT) ions, such as  $\text{Mn}^{3+}$  or  $\text{Cu}^{2+}$ . In the materials with JT ions, an orbital ordering and related lattice distortions determine a rich variety of different phenomena, and this "orbital physics" attracts now a widespread attention. Unfortunately, it is rather difficult to directly access orbital state of JT ions. Therefore, the standard way to find orbital occupation, widely used for the last 50 years, is based on structural data, with the assumption of the one-to-one correspondence between orbital occupation of an ion and corresponding JT distortion of the surrounding ligands, e.g.  $\text{O}_6$  octahedra. We demonstrate that such straightforward approach sometimes fails for the solids with orbital ordering. A well-studied layered manganite  $\text{La}_{0.5}\text{Sr}_{1.5}\text{MnO}_4$  gives a vivid example of such discrepancy. Its main structural element is a *Mn-O* plane, where manganese ions form a square lattice and each of them is surrounded by the oxygen octahedron. This compound is characterized by the charge ordering with

the checkerboard array of  $\text{Mn}^{3+}$  and  $\text{Mn}^{4+}$ , and the magnetic structure formed in the plane by zigzag ferromagnetic chains with the opposite direction of spins for neighboring chains. At the same time, the available data on the orbital structure determining the spatial distribution of valence electrons seem to be rather controversial. Analyzing the relation between the orbital structure and corresponding lattice distortions in  $\text{La}_{0.5}\text{Sr}_{1.5}\text{MnO}_4$ , we have shown that the occupation of orbitals in this compound appreciably differs from that suggested by the JT distortions [1]. To obtain correct results, it is necessary to consider self-consistently the orbital occupation, lattice distortions, and charge disproportionation.

[1] A.O. Sboychakov, K.I. Kugel, A.L. Rakhmanov, and D.I. Khomskii, *ArXiv:1007.4814; Phys. Rev. B*, in press.

22OR-C-9

### INFRARED SPECTRA OF $\text{CuO}$ AND $\text{Cu}_2\text{O}$ NANOCERAMICS

*Mostovshchikova E.V.<sup>1</sup>, Gizhevskii B.A.<sup>1</sup>, Loshkareva N.N.<sup>1</sup>, Galakhov V.R.<sup>1</sup>, Naumov S.V.<sup>1</sup>,  
Ponosov Yu.S.<sup>1</sup>, Ovechkina N.A.<sup>1</sup>, Kostromitina N.V.<sup>1</sup>, Buling A.<sup>2</sup>*

<sup>1</sup>Institute of Metal Physics, Ural Division of RAS, 620990 Ekaterinburg

<sup>2</sup>FB Physik, University of Osnabrueck, Barbarastrasse 7, D-49069 Osnabrueck, Germany

Nanomaterials based on copper oxides are interesting for both fundamental physics and practical applications.  $\text{CuO}$  is multiferroic and antiferromagnetic semiconductor with  $T_N=230$  K, a typical representative of strong correlated system.  $\text{Cu}_2\text{O}$  is the wide-gap semiconductor and a basis of the diluted magnetic semiconductors. The data about optical properties of nano- $\text{CuO}$  and  $\text{Cu}_2\text{O}$  in the IR range is very poor. Middle infrared spectra may supply data about specific defects, impurities and phonon bands of nanooxides.

We studied optical absorption (in the range 0.08-1.2 eV), Raman ( $100\text{-}1400\text{ cm}^{-1}$ ) and X-ray absorption spectra of  $\text{Cu}_2\text{O}$  and  $\text{CuO}$  nanoceramics and compared the spectra of nanooxides with those of single crystals. High-density copper oxide nanoceramics (the crystallite size 12-40 nm) were prepared from oxide powders by high pressure torsion method.

The IR spectra of nano- $\text{Cu}_2\text{O}$  and  $\text{Cu}_2\text{O}$  single crystal display two intensive bands at  $\sim 100$  and  $\sim 140$  meV (Fig.1), which are interpreted as biphonons, multiphonons or localized phonon modes [1]. The bands at 100 and 140 meV are clearly visible not only at low temperatures but at room temperature also and have weak temperature dependence. Therefore, it is unlikely that they connected with biphonons. In the spectra of nano- $\text{Cu}_2\text{O}$  we revealed the feature at 130 meV and additional band at 160 meV. These bands are absent in the spectra of the single crystal.

In the spectra of nano- $\text{CuO}$  we observed the band at the same energy 140 meV. Besides, we found a broad band with the complex structure near 190 meV, which earlier was revealed in the spectra of  $\text{CuO}$  single crystals and attributed to the transitions in  $(\text{CuO}_4)^{5-}$  clusters [2] or in terms of phonon-assisted magnetic excitations [3].

We suppose that the band at 140 meV in IR spectra of copper oxides nanoceramics is connected with presence of nonstoichiometric defects such as vacancies and cations with different valency. Concentration of such kind defects in nanostructured samples considerably more, than in equilibrium crystals.

According to the XAS data all nano-Cu<sub>2</sub>O and nano-CuO samples contain rather high concentration of Cu<sup>2+</sup> and Cu<sup>+</sup> ions respectively.

Raman spectra of nano-Cu<sub>2</sub>O demonstrate weak bands at ~100 meV and in the range of 130-150 meV. These bands are widened in comparison with similar bands in single crystals. In Raman spectra of CuO the strong band is observed at 140 meV. The band at 100 meV, observed in IR spectra, is absent.

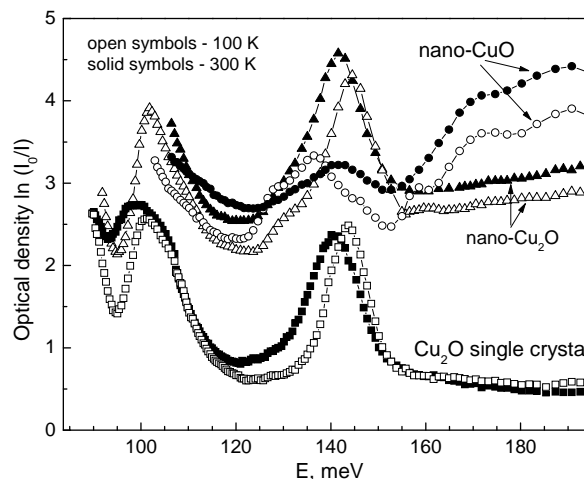


Fig.1. Optical density spectra of nano-CuO, nano-Cu<sub>2</sub>O and Cu<sub>2</sub>O single crystal

The work is supported by RFBR, grant 11-02-00252, Program of the Department of Physical Sciences of RAS “Physics of new materials and structures” and Integration project of the Ural Division – Siberian Division of RAS.

[1] M.Jorger, T.Fleck, C.Klingshirn, R.von Baltz. *Phys. Rev. B* **71** (2005) 235210.

[2] A.S.Moskvin, N.N.Loshkareva, Yu.P.Sukhorukov et al. *JETP* **78** (1994) 518.

[3] S.H. Jung, J.Kim, E.J. Choi et al. *Phys. Rev. B* **80** (2009) 140516(R).

22OR-C-10

## MAGNETOREFRACTIVE EFFECT IN MANGANITES AT VISIBLE WAVELENGTHS

Telegin A.<sup>1</sup>, Sukhorukov Yu.<sup>1</sup>, Granovsky A.<sup>2,3</sup>, Gan`shina E.<sup>2</sup>, Kaul A.<sup>2</sup>, Herranz G.<sup>4</sup>, Caicedo J.<sup>4</sup>

<sup>1</sup> Institute of Metal Physics, Ural Division of RAS, 620990, Ekaterinburg, Russia

<sup>2</sup> Moscow State University, 119992, Moscow, Russia

<sup>3</sup> Ikerbasque, Basque Foundation for Science, 48011, Bilbao, Spain

<sup>4</sup> Inst. de Ciència de Materials de Barcelona (ICMAB)-CSIC, Bellaterra, 08193 Catalonia, Spain

Associated with the drastic and rapid development of magnetophotonics, magnetic-field induced changes of optical properties of various magnetic materials have been intensively studying last years. In particularly, it was shown that magnetoreflexion and magnetotransmission of light in near-, middle- and far-infrared frequencies in magnetic multilayers, granular alloys, nanocomposites, manganites with giant, tunnel and colossal magnetoresistance (MR) are mainly due to high frequency MR, and these phenomena were named as magnetorefractive effect (MRE). MRE in manganites in the middle-infrared region can reach tens of percent near the Curie temperature [1,2]. Recently, it has been shown that a behavior of MRE in manganites is much more complicated than in artificial magnetic nanostructures and can be observed even at visible wavelengths [2-4]. There is

no consensus on the MRE mechanism at visible [3,4]. In this report we present experimental results on magnetotransmission and magnetoreflexion of optimally doped manganite films at visible wavelengths from 0.4  $\mu\text{m}$  to 1.2  $\mu\text{m}$ . The obtained data are used to clarify the origin of MRE in manganites.

The epitaxial films of different thickness and chemical composition were grown on perovskite-like crystal substrates by the method of metalloorganic chemical vapour deposition (MOCVD). The reflection spectra for unpolarized light were measured near the normal angle of light incident. The giant MRE ( $\sim 2\text{-}4\%$ ) in transmission and reflection modes for  $\text{La}_{0.7}\text{Ca}_{0.3}\text{MnO}_3$  and  $\text{La}_{0.9}\text{Ag}_{0.1}\text{MnO}_3$  films was detected at 11 kOe in the wide temperature interval from 10 K to 300 K. Although the obtained MRE magnitude at visible is less than that in the infrared region but it exceeds a level of traditional linear magneto-optical effects in this region. It was shown that there is no strict correlation between temperature dependencies of MRE and MR.

By analysis of the obtained data for structural, magnetic, magnetotransport, optical and magneto-optical data we came to the conclusion that MRE at visible is determined by the influence of magnetic field on electronic structure of manganites.

This work was supported by the RFBR (grant 10-02-00038), program of UD-SD of the RAS (grant 09-C-2-1016), program of DPS "Physics of new materials and structures" and project UD of RAS for young scientist № m-6.

- [1] Yu. Sukhorukov, A. Telegin, A. Granovsky et al., *JETP*, **138**, (2010) 3.
- [2] A. Granovskii, Yu. Sukhorukov, A. Telegin et al. *JETP*, **112**, (2011) 1.
- [3] D. Hrabovsky, J.M. Caicedo, G. Herranz et al., *Phys. Rev. B*, **79**, (2009)052401.
- [4] Yu. Sukhorukov, A. Telegin, A. Granovsky et al., to be published in *JETP* (2011).





**22 August**

Monday

12:00-14:00

15:00-17:00

oral session

22TL-D

**“Theory”**

22TL-D-1

## SPIN-PLASMONS IN TOPOLOGICAL INSULATORS

*Efimkin D.K.<sup>1</sup>, Lozovik Yu.E.<sup>1,2</sup>, Sokolik A.A.<sup>1</sup>*

<sup>1</sup> Institute of Spectroscopy RAS, 142190, Troitsk, Moscow region, Russia

<sup>2</sup> Moscow Institute of Physics and Technology, 141700, Moscow, Russia

Topological insulator is the new state of matter that was recently predicted theoretically (see the review [1] and references therein). Its two-dimensional (HgCdTe quantum wells structures) and three-dimensional realizations ( $\text{Bi}_{1-x}\text{Sb}_x$ ,  $\text{Bi}_2\text{Se}_3$  and  $\text{Bi}_2\text{Te}_3$ ) were found and studied experimentally. 3D topological insulators have insulating bulk and topologically protected helical states on the surface that are described in some cases by Dirac-like equation for massless particles.

We consider new collective excitations – spin-plasmons – in helical liquid on the surface of 3D topological insulators [2, 3] which differs essentially from ordinary surface plasmons (see, e.g., [4]). The properties of these excitations and their internal structure are studied.

Due to spin-momentum locking in helical liquid on a surface of topological insulator, the collective excitations should manifest themselves as coupled charge- and spin-density waves. The methods of experimental registration as well as possible applications of spin-plasmons are discussed.

Support by RFBR and RAN Programs is acknowledged.

[1] M.Z. Hasan, C.L. Kane, *Rev. Mod. Phys.*, 82, 3045(2010).

[2] R. Raghu, S.B. Chung, H.L. Qi and S.S. Zhang, *Phys. Rev. Lett.*, 104, 116401(2010).

[3] I. Appelbaum, H.D. Drew, M.S. Fuhrer, *Appl. Phys. Lett.*, 98, 023103 (2011).

[4] Yu.E. Lozovik, A.V. Klyuchnik, Chapter 6 in: *The Dielectric Function of Condensed Systems*, eds. L.V.Keldysh, et al., Elsevier Science Publisher B.V., 1987.

22TL-D-2

## PHASE SEPARATION INSTABILITIES, COHERENT PAIRING AND CONDENSATION IN HUBBARD NANOCLUSTERS

*Kocharian A.N.<sup>1</sup>, Fernando G.W.<sup>2</sup>, Palandage K.<sup>3</sup>*

<sup>1</sup> Department of Physics, California State University, Los Angeles, CA, USA

<sup>2</sup> Department of Physics, University of Connecticut, Storrs, CT, USA

<sup>3</sup> Department of Physics, Trinity College, Hartford, CT, USA

Phase separation instabilities and magnetic correlations with formation of various types of charge and spin pairing gaps in the ensemble of small clusters of different geometries are exactly studied in attractive and repulsive Hubbard nanoclusters with emphasis on 2x2 squares, 2x4 ladders, 8 and 10 site Betts bipartite topologies, and frustrated geometries such as tetrahedrons, square pyramid geometries, etc under variation of interaction strength, electron doping and temperature [1]. These exact calculations of charge and spin collective excitations and pseudogaps in a real space yield

intriguing insights into level crossing degeneracies and quantum critical points, phase separation instabilities and electron condensation in spatially inhomogeneous systems. Separate condensation of electron charge and spin degrees offers a new route to superconductivity in inhomogeneous HTSC systems, different from the BCS pairing scenario. The electron pairs in ensemble of clusters are complied with the Bose-Einstein statistics and in an inhomogeneous media can be fully condensed into coherent pairing state. The similarities and differences between mechanism of pairing of electron spin and charge degrees of freedom in the attractive and repulsive electrons are also discussed. The calculated exact phase diagrams at half filling and for one hole off half filling resemble a number of inhomogeneous, coherent and incoherent nanoscale phases seen using the scanning tunneling measurements in parental and doped high T<sub>c</sub> cuprates, manganites, and CMR nanomaterials [2].

[1] A.N. Kocharian, G.W. Fernando, K. Palandage, and J.W. Davenport, *Phys. Rev. B* **78** (2008) 075431.

[2] A.N. Kocharian, G.W. Fernando, and C. Yang, Spin and charge pairing instabilities in nanoclusters and nanomaterials, in *Scanning probe microscopy in nanoscience and nanotechnology*; Bhushan B. (ed.), Book chapter, 507-570 (Springer-Verlag, Berlin Heidelberg, 2010).

22TL-D-3

## **ELECTRONIC AND MAGNETIC PROPERTIES OF SEMICONDUCTING NANOCLUSTERS AND LARGE ORGANIC MOLECULES: FEATURES INTERESTING FOR SPINTRONICS**

*Uspenskii Yu.A.*<sup>1</sup>, *Kulatov E.T.*<sup>2</sup>, *Titov A.A.*<sup>2,4,5</sup>, *Tikhonov E.V.*<sup>3</sup>, *Michelini F.*<sup>4</sup>, *Raymond L.*<sup>4</sup>

<sup>1</sup> Lebedev Physical Institute of RAS, Leninskiy prosp. 53, Moscow 117924, Russia

<sup>2</sup> Prokhorov General Physics Institute of RAS, Vavilov str. 38, Moscow 119991, Russia

<sup>3</sup> Physics Department, Moscow State University, Leniskie Gory, Moscow 119991, Russia

<sup>4</sup> IM2NP UMR-6242, Aix-Marseille Université, Marseille 13397, France

<sup>5</sup> L\_Sim, SP2M, INAC, CEA, 17 av. des Martyrs, Grenoble 38054, France

Advances in nanotechnology have created smaller and smaller semiconducting systems. This progress has an evident limit in ultimate semiconducting systems as quantum dots or nanoclusters doped by a single impurity atom. Recently, the controlled creation of such systems even received the special name “solotronics” (Nature materials, 10, 91 (2011)). It is known that many properties of nanoclusters and quantum dots are different from those of corresponding bulk semiconductors. In our presentation we concentrate on changes in the electronic structure and spin properties of nanoclusters caused by their small size and single-atom doping. The key point is a reduced electron response of nanoclusters, which results in a lower dielectric function, stronger Coulomb interaction between electrons, and large many-electron effects. The same reasoning is applicable to large organic molecules containing one foreign atom. To clarify this point, we calculated: (1) the Si<sub>34</sub>DH<sub>36</sub> (D= P, As, Sb, S, Se, and Te) nanoclusters, (2) the Si<sub>35</sub>H<sub>36</sub> cluster charged by one or two electrons, (3) the metal phthalocyanine (MPc) molecules, where two central H atoms of Pc are replaced by one M-atom (M=Rh, Pd, Ag, Cd, In, and Sn). In these calculations we used three approaches: the DFT, the hybrid functionals, and the GW method. They showed that DFT calculation underestimates changes in the width of the semiconducting gap caused by the doping or charging of clusters, as compared with precise results provided by the GW method. The electron spectrum of clusters and molecules that have an odd number of electrons is spin split.

Again, DFT underestimates the value of exchange splitting by a factor of 5 to 10: such a method does not provide the adequate description of spin effects in nanoclusters and molecules. Our calculations also showed that spin effects caused by a single dopant or one added electron remain quite observable even in clusters and molecules of 3-5 nm diameter. The exchange splitting introduces important spin effects in cluster properties, in particular, spin-dependent transport through a cluster and the optical orientation of a cluster spin.

This research was supported in part by the Russian Fund for Basic Research (grants 10-02-00698a, 10-02-00118-a, 09-02-00698-a and 09-02-91078-CNRS-a), and the programs of RAS “Strongly correlated electrons in solids and structures” and “Basic investigations of nanotechnologies and nanomaterials”.

22TL-D-4

## FERROMAGNETISM, SPIRAL MAGNETIC STRUCTURES AND PHASE SEPARATION IN THE HUBBARD MODEL

*Igoshev P.A., Zarubin A.V., Katanin A.A., Irkhin V.Yu.*

Institute of Metal Physics, 620990, Ekaterinburg, S. Kovalevskoy str. 18, Russia

We analyze the magnetic phase diagram of the two-dimensional (2D) itinerant electron system on the square lattice. Relation between nearest and next-nearest neighbour transfer integrals  $t$  and  $t'$  plays an important role in this problem. Due to the van Hove singularity, for sufficiently large  $t'$  ferromagnetism can occur at moderate Hubbard repulsion  $U$ . Collinear antiferromagnetic and spiral magnetic phases are taken into account and a possible phase separation is studied.

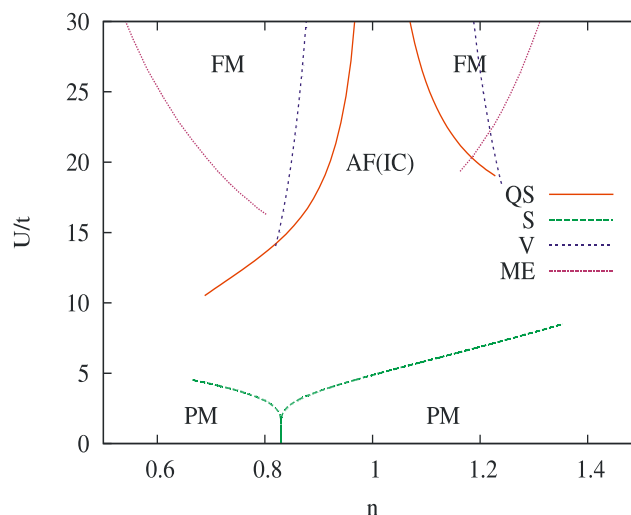


Fig. 1 Phase diagram of the 2D Hubbard model with  $t'=0.2t$ ,  $n$  being the electron concentration. *Line QS* separating ferromagnetic (FM) and antiferromagnetic (AF), including incommensurate (IC) phases is the result of the quasistatic approximation, *line S* is the boundary of FM and paramagnetic (PM) phases in the simple Stoner theory, *line V* is the Visscher's boundary of phase separation of FM–AF (Neel) phase in the limit of large  $U$ , *line ME* is the boundary of the FM and PM phases in the method of decoupling the equation of motion for the Green's functions for Hubbard's operators

The results of the mean-field approach [1] are improved with the help of quasi-static (QS) approximation [2] and renormalization group consideration [3]. A comparison is performed with the

method by Visscher (see [1]) and the result of decoupling the equation-of-motion sequence for the retarded Green's functions in the Hubbard operator representation [4]. It is shown that near half filling ( $n = 1$ ) the ferromagnetic state is characterized by of a spin-wave type instability, while away from half-filling the one-electron (spin-polaron) instability occurs. Combined magnetic phase diagram for  $t' = 0.2t$  including all the instabilities is shown in Fig. 1.

- [1] P.A. Igoshev, M.A. Timirgazin, A.A. Katanin, A.K. Arzhnikov, V.Yu. Irkhin, *Phys. Rev. B* **81**, 094407 (2010).  
 [2] P.A. Igoshev, A.A. Katanin, V.Yu. Irkhin, *Sov. Phys. JETP* **105**, 1043 (2007).  
 [3] P.A. Igoshev, A.A. Katanin, V.Yu. Irkhin, arXiv:1012.0125.  
 [4] V.Yu. Irkhin, A.V. Zarubin, *Solid State Phenomena*, **168-169**, 469 (2011).

22TL-D-5

## STRENGTH OF COULOMB CORRELATIONS IN Pnictide SUPERCONDUCTORS

*Korotin M.A.*

Institute of Metal Physics, S.Kovalevskaya, 18, Yekaterinburg 620990, Russia

Low temperature superconducting metallic compounds (NbTi, Nb<sub>3</sub>Sn, etc.) are characterized by weak electron correlations and superconductivity is described by electron-phonon interaction.

Parent compounds of high temperature cuprate superconductors (La<sub>2</sub>CuO<sub>4</sub>, YBa<sub>2</sub>Cu<sub>3</sub>O<sub>7</sub>, etc.) are Mott insulators and electron correlations are strong in them.

Superconducting iron pnictides (LaOFeAs, BaFe<sub>2</sub>As<sub>2</sub>, etc.) are metals; electron-phonon interaction of itself is not enough to provide Cooper pairs formation at observed T<sub>c</sub>'s; experimental electronic spectra of these compounds are renormalized in comparison with band structure calculation predictions. In other words, this new class of superconductors differs in properties both from low-T<sub>c</sub> and high-T<sub>c</sub> ones.

How strong are Coulomb correlations in iron pnictides? We propose a solution basing on investigation of their electronic structures within the LDA+DMFT approach (combination of Local Density Approximation and Dynamical Mean-Field Theory).

Criteria for the determination of strength of Coulomb correlations are the following:

- Correspondence between experimental and theoretical electronic spectra
- Presence of Hubbard bands and spectral weight transfer in them
- Value of iron on-site Coulomb interaction parameter
- Renormalization of electronic effective mass.

We concluded that calculated quasi-particle bands renormalization corresponding to effective mass enhancement  $m^*/m \sim 2$  observed simultaneously with the absence of Hubbard bands shows pnictide superconductors as moderately correlated systems but far from metal-insulator Mott transition.

In my talk I'll review in details the results of theoretical investigations of strength of Coulomb correlations in pnictide superconductors made in X-Ray Spectroscopy, Optics of Metals, and Theoretical Physics Labs of Institute of Metal Physics, Yekaterinburg, Russia [1-12].

- [1] S.L. Skornyakov *et al.*, *Phys. Rev. Lett.*, **106** (2011) 047007.  
 [2] A.V. Lukoyanov *et al.*, *Phys. Rev. B*, **81** (2010) 235121.  
 [3] S.L. Skornyakov *et al.*, *Phys. Rev. B*, **81** (2010) 174522.

- [4] S.L. Skornyakov *et al.*, *Phys. Rev. B*, **80** (2009) 092501.  
 [5] V.I. Anisimov *et al.*, *Physica C*, **469** (2009) 442.  
 [6] A.O. Shorikov *et al.*, *ЖЭТФ*, **135** (2009) 134.  
 [7] Ю.А. Изюмов, Э.З. Курмаев, *Высокотемпературные сверхпроводники на основе FeAs-соединений*. Москва-Ижевск, НИЦ «Регулярная и хаотическая динамика», 2009, 435 С.  
 [8] V.I. Anisimov *et al.*, *J. Phys.: Condens. Matter*, **21** (2009) 075602.  
 [9] М.А. Korotin *et al.*, *ЖЭТФ*, **134** (2008) 758.  
 [10] Ю.А. Изюмов, Э.З. Курмаев, *УФН*, **178** (2008) 25.  
 [11] E.Z. Kurmaev *et al.*, *Phys. Rev. B*, **78** (2008) 220503.  
 [12] V.I. Anisimov *et al.*, *Письма в ЖЭТФ*, **88** (2008) 844.

22TL-D-6

## SPIN-EXCITATION SPECTRUM IN CUPRATE SUPERCONDUCTORS

*Plakida N.M.*<sup>1,2</sup>, *Vladimirov A.A.*<sup>1</sup>, *Ihle D.*<sup>3</sup>

<sup>1</sup> Joint Institute for Nuclear Research, 141980 Dubna, Russia

<sup>2</sup> Max-Planck-Institute for Physics of Complex Systems, D-01187, Dresden, Germany

<sup>3</sup> Leipzig University, D-04109, Leipzig, Germany

A microscopic theory of the dynamic spin susceptibility (DSS) in superconducting cuprates within the  $t$ - $J$  model is presented. The spectrum of spin excitations is studied using an exact representation for the DSS within the Mori projection technique for the relaxation function in terms of the Hubbard operators:

$$\chi(\mathbf{q}, \omega) = -\langle\langle S_{\mathbf{q}}^+ | S_{-\mathbf{q}}^- \rangle\rangle_{\omega} = \frac{m(\mathbf{q})}{\omega_{\mathbf{q}}^2 + \omega \Sigma(\mathbf{q}, \omega) - \omega^2},$$

where the static susceptibility  $\chi(\mathbf{q}, 0) = m(\mathbf{q}) / \omega_{\mathbf{q}}^2$  and the self-energy  $\Sigma(\mathbf{q}, \omega)$  are evaluated in the mode-coupling approximation. The DSS is calculated in a wide region of hole doping  $\delta$  and temperatures  $T$  including the superconducting state. In the normal state a spin-wave-type behavior is found at low doping as in the Heisenberg model, while at higher doping a strong damping caused by hole hopping occurs, and a relaxation-type spin dynamics is observed. The local spin susceptibility and its  $\omega/T$  scaling behavior are calculated in a reasonable agreement with experimental and exact diagonalization data. At low temperatures the DSS reveals a resonance mode (RM) at the antiferromagnetic wave vector  $\mathbf{Q} = \pi(1,1)$  which is explained by a strong suppression of the damping of spin excitations caused by a spin gap at  $\mathbf{Q}$  rather than an opening of the superconducting gap [1]. This results in the observation of the RM even above superconducting temperature  $T_c$  in the underdoped region. The RM weakly depends on temperature as shown in Fig. 1 in agreement with magnetic inelastic neutron-scattering experiments.

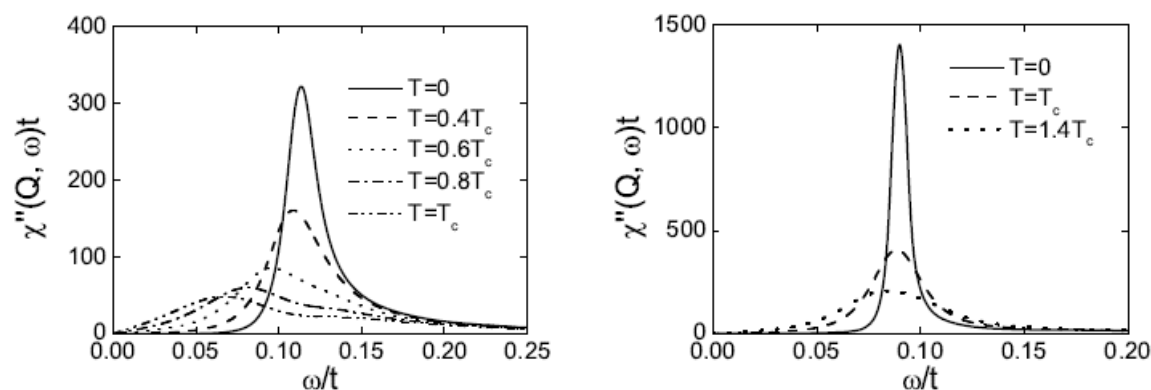


Fig.1. Temperature dependence of the spectral function  $\text{Im } \chi(\mathbf{Q}, \omega)$  in the overdoped region at hole doping  $\delta = 0.2$  (left panel) and in the underdoped region at  $\delta = 0.09$  (right panel).

[1] A.A. Vladimirov, D. Ihle, N. M. Plakida, *Phys. Rev. B*, **83** (2011) 024411.

22TL-D-7

## GENERALIZATION OF MERMIN - WAGNER THEOREM AND THE POSSIBILITY OF LONG-RANGE ORDER FOR THE ONE-DIMENSIONAL HEISENBERG MODEL

*Rudoy Yu.G.<sup>1</sup>, Kotelnikova O.A.<sup>2</sup>*

<sup>1</sup> People's Friendship University of Russia, 117198, Miklukho-Maclaya, 6, Moscow, Department of Theoretical Physics, Russia

<sup>2</sup> Lomonosov State University, Department of Magnetism, 119991, Moscow, Leninskie Gory, Russia

In the past decade the interest – both experimental and theoretical [1] was renewed concerning the low-dimensional magnetic structures, especially the problem of the magnetic phase transition possibility. One of the most known results in this field is the Mermin – Wagner (MW) theorem [2] for the isotropic Heisenberg model on the lattice with any spatial dimension  $D \geq 1$  which as a rule excludes existence of the long-range order (i.e., the spontaneous magnetization) for  $D=1$  and 2. The MW theorem is based on the fundamental exact inequalities formulated by N.N. Bogoliubov [3] and so the theoretical status of MW theorem is quite reliable.

Nevertheless, the validity of MW theorem suggests the fulfillment of some condition concerning the spatial behavior of the exchange interaction  $I(R)$ , namely the finiteness of it's second spatial moment. This assumption supposes the sufficiently rapid decay of  $I(R)$  at very long distances  $R \rightarrow \infty$ , which is evidently the case for any finite-range  $I(R)$  (including the nearest neighbors (NN) approximation); but, on the contrary, the mean-field (MF) approximation is of strictly infinite range. In this connection we recall the well known “first” Kac model [4] where  $I(R)$  is taken as the exponential of  $R$  which interpolates between these two limiting cases.

Because MF approximation is physically not quite satisfactory, Kac himself invented the “second” model [5] which is regulated by another parameter. This model is also of infinite range, but with power law (instead of exponential one) rate of decay at  $R \rightarrow \infty$ ; for this model the strict conditions of MW theorem violation are formulated.

Being inspired by the analogy of the MW condition with formally the same condition used by proof of the generalized Central Limit Theorem (CLT), or, more general, to the theory of Markov

processes we suggest to apply to the MW theorem the Montroll – Schlesinger (MS) model [6]. This model introduces an additional parameter and differs with Kac’s second model in the important aspect: it affords the magnetic sites to be arranged not strongly periodically, but in ascending geometric progression distances what relates our approach to the magnetic “networks” rather than to ordinary “lattices”.

It is important that in MS-model the so-called Levy – Khintchine, or “fractality”, index may be determined from the parameters of the model and thus one can see how to choose them in order to overcome the MW-theorem exclusions even for the 1D isotropic Heisenberg model.

- [1] H.-J. Mikeska, A.K. Kolezhuk. One-dimensional magnetism// Lecture Notes in Physics, Vol. 645, Ch. 1. 2004. [2] N.D. Mermin, H, Wagner. *Phys. Rev. Lett.* 17 (1966) 1133.
- [3] N.N. Bogoliubov. Quasiaverages in the statistical mechanics. *Preprint Dubna, Д781*, 1961.
- [4] M. Kac. *Phys. Fluids* 2 (1959) 8.
- [5] M. Kac. Mathematical mechanisms of phase transitions// *Lect. Statistical Physics*, Ed by M.Chretien, NY, 1968.
- [6] E.W. Montroll, M.F. Schlesinger. On the Wonderful World of Random Walks // *Studies in Statistical Mechanics*, Vol. XI (ed. by E.W. Montroll, J.L. Lebowitz), Amsterdam, North-Holland PC, 1984



**22 August**

Monday

12:00-14:00

oral session

22TL-E

**“Magnetic Soft Matter”**

22TL-E-1

## HEAT DISSIPATION AND MAGNETIC PROPERTIES OF MAGNETIC NANOPARTICLES FOR BIOMEDICAL APPLICATIONS

Takemura Y.

Yokohama National University, 79-5 Tokiwadai, Hodogaya, Yokohama 240-8501, Japan

In recent years, magnetic nanoparticles have attracted attention for biomedical application such as magnetic separation, MRI contrast agent, drug delivery system and hyperthermia [1]. The possibility of various magnetic nanoparticles for hyperthermia application was studied by investigating the magnetic characterization, self-heating properties under ac magnetic field, and cytotoxicity. The size and material dependences of their heat generation ability is discussed in this paper as well as the influence of surrounding environment and surface coating on their characterization.

The temperature rise of NiFe<sub>2</sub>O<sub>4</sub> nanoparticles having diameters of 242 and 7.7 nm was measured. The results of the measurement were analyzed by comparing the areas of the hysteresis loops in order to clarify the mechanism of heat dissipation in the samples. The hysteresis loops were obtained by applying both ac and dc magnetic fields. It was found that the contribution of magnetic relaxation losses to the heat dissipation was negligible in the case of NiFe<sub>2</sub>O<sub>4</sub> nanoparticle of diameter 242 nm. The contribution of the Néel relaxation [2] to the heat dissipation in the case of NiFe<sub>2</sub>O<sub>4</sub> nanoparticle of diameter 7.7 nm was observed as the difference between the areas of ac and dc hysteresis loops. From the dependences of temperature rise and hysteresis loops of the nanoparticles on the intensity and frequency of an applied magnetic field, the relaxation time for NiFe<sub>2</sub>O<sub>4</sub> nanoparticle of diameter 7.7 nm was obtained as approximately 0.5–0.7  $\mu$ s [3].

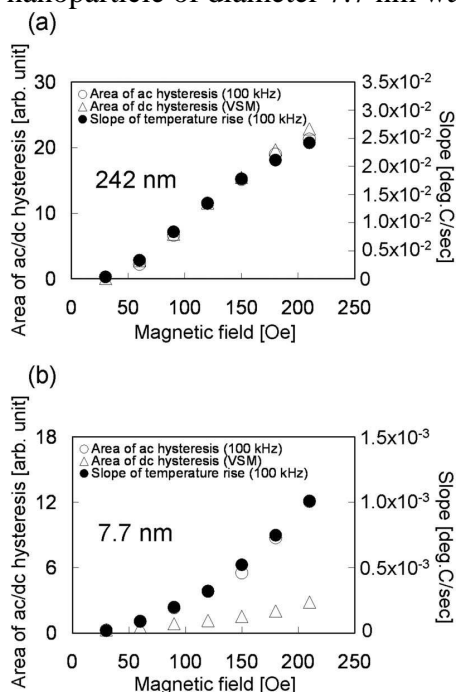


Fig.1 Field intensity dependences of the area of ac/dc hysteresis loop and slope of the temperature rise of the NiFe<sub>2</sub>O<sub>4</sub> nanoparticles with (a) diameter 242 nm and (b) diameter 7.7 nm. The frequency of the ac field was 100 kHz for the measurement of ac hysteresis and temperature rise.

- [1] Q. A. Pankhurst *et al.*, *J. Phys.*, **D 36**, R167 (2003).  
 [2] R. E. Rosensweig, *J. Magn. Magn. Mater.*, **252**, 370 (2002).  
 [3] H. Kobayashi *et al.*, *J. Appl. Phys.*, **107**, 09B322 (2010).

## OPTIMAL NANOPARTICLES FOR MAGNETIC HYPERTHERMIA : THEORETICAL AND EXPERIMENTAL RESULTS

*Mehdaoui B.<sup>1</sup>, Meffre A.<sup>1</sup>, Carrey J.<sup>1</sup>, Lacroix L.-M.<sup>1</sup>, Lachaize S.<sup>1</sup>, Goujeon M.<sup>2</sup>, Chaudret B.<sup>1</sup>,  
Respaud M.<sup>1</sup>*

<sup>1</sup> Université de Toulouse; INSA; UPS; LPCNO Toulouse, France

<sup>2</sup> Université de Toulouse; CIRIMAT, 118 Route de Narbonne, F-31062, Toulouse, France

Magnetic hyperthermia (MH) uses the heat induced in magnetic nanoparticles (NPs) by an AC magnetic field to rise the temperature of a tumour to improve the efficiency of chemotherapy or radiotherapy. NPs are characterized by their specific absorption rate (SAR). High values of SAR could permit the treatment of smaller size tumours. During the first part of this talk, recent progress obtained on the theory of MH will be shown [1]. To evaluate the heating power of NPs, it is necessary to calculate their hysteresis area, which is directly related to their SAR. It will be shown that the linear response theory and theories derived from the Stoner-Wohlfarth model are suitable to calculate the hysteresis area, but have a restricted domain of validity, which has been determined by comparison with numerical simulations of hysteresis loops. LRT is suitable for strong anisotropy NPs whereas theories derived from the Stoner-Wohlfarth model are suitable for weak anisotropy NPs. These theories are then used to determine the optimal parameters of NPs for MH. The optimal size of NPs for MH can be calculated analytically with a good accuracy. It will be shown that the central parameter for MH optimization is the anisotropy. The optimum anisotropy is simple to calculate and depends on the magnetic field used in the MH experiments and on the NP magnetization only. The theoretical optimum parameters will be compared to the one of several magnetic materials so as to draw general guidelines toward the optimization of MH. In a second part, several recent experimental results will be shown [2-6]. They have been obtained by measuring both the frequency and the magnetic field dependence of SAR on high-magnetization monodisperse Fe and FeCo NPs elaborated by organometallic chemistry [3]. Experiments have been performed on a specially-designed frequency-adjustable MH setup [2] and/or using the coil of an induction oven [5]. On the FeCo system, MH measurements have been performed on a colloidal solution of weakly-interacting NPs of 14 nm in diameter. On this system, the first experimental evidences of a behaviour typical of the Stoner-Wohlfarth regime have been obtained and quantitatively analyzed [3]. On the Fe system, MH properties have been performed on NPs, the size of which ranged from 5.5 to 30 nm [6]. Several features expected theoretically are observed for the first time experimentally in MH, in particular the fact the optimal size depends on the amplitude of the applied magnetic field. These features are a natural consequence of theories deriving from the Stoner-Wohlfarth model and are quantitatively analysed using numerical simulations. Record losses of  $11 \pm 1$  mJ/g at  $\mu_0 H_{\max} = 73$  mT have been obtained on the optimized NPs. These results open the path to a more accurate description, prediction and analysis of MH, and confirm the interest of high magnetization NPs for MH applications.

[1] J. Carrey, B. Mehdaoui, M. Respaud, *J. Appl. Phys.*, under press.

[2] L.-M. Lacroix, J. Carrey, and M. Respaud, *Rev. Sci. Instrum.* **79**, 093909 (2008)

[3] L.-M. Lacroix, R. Bel Malaki, J. Carrey, S. Lachaize, M. Respaud, G. F. Goya and B. Chaudret, *J. Appl. Phys.* **105**, 023911 (2009)

[4] L.-M. Lacroix, S. Lachaize, A. Falqui, M. Respaud, and B. Chaudret, *J. Am. Chem. Soc.* **131**, 549 (2009)

[5] B. Mehdaoui, A. Meffre, L.-M. Lacroix, J. Carrey, S. Lachaize, M. Goujeon, M. Respaud, and B. Chaudret, *J. Magn. Magn. Mat.* **322**, L49 (2010)

[6] B. Mehdaoui, A. Meffre, L.-M. Lacroix, J. Carrey, S. Lachaize, M. Goujeon, M. Respaud, and B. Chaudret, *in preparation*

## THERMAL EFFECTS IN MAGNETIC NANOPARTICLES UNDER OSCILLATING FIELDS

*Plotkin Z., Goren Y., Shenkman O., Gottlieb M.*

Chemical Engineering Dept., Ben-Gurion University, Beer-Sheva 84105, Israel

Magnetic nanoparticle (MNP) as suspensions in Newtonian liquids or when embedded in a polymeric matrix are known to generate heat when subjected to an alternating external magnetic field [1]. It has been recently demonstrated that these thermal effects may be used for treating cancer by overheating tumors and may be used to obtain magnetoactive polymers and elastomers [2]. Two separate mechanisms are responsible for the generation of heat: the Néel mechanism involving relaxation of the internal magnetic moment in the nanoparticle, and the Brown mechanism which is external to the particle and results from the viscous heating of the fluid around it as the particle turns to align with the alternating magnetic field. The Néel mechanism is prevalent when particle size is small enough, below a critical particle size which depends on the magnetic properties of the particle, such that the particle exhibits superparamagnetic properties. Yet, even for larger particles embedded in a solid matrix or polymeric elastomers particle motion is arrested and no viscous heating is possible. In the other extreme, large particles above the critical Néel domain size, suspended in a liquid will exhibit mostly Brown heating. Obviously, situations involving both mechanisms are possible in intermediate cases. The predominant approach in calculating these thermal effects is based on an “effective-medium” approach replacing the particles and the matrix (solid or fluid) by an isotropic homogeneous medium [3,4]. While quite successful in describing the behavior of the macroscopic system this approach does not allow detailed understanding of local heating effects and facilitate more judicious design of magneto-heating systems. In this work we present detailed calculations for both types of heating mechanisms.

We calculate Brownian heating by determining the flow field generated by the particle's motion. The dynamics of MNPs in suspension under an alternating magnetic field were calculated by solving analytically the Navier-Stokes equation for a simplified non-interacting particle model. We show that the “non-interaction” assumption is valid for concentrations typically employed for magnetic heating. The velocity field was subsequently used to derive the heat generation of the MNP suspension through the viscous heating term of the energy equation. It was found that through this methodology it is possible to approximate the magnitude of Brownian heating within MNP suspensions under alternating magnetic fields.

For the Néel heating we employed a multi-scale model for the heat generation and conduction into the surroundings. The model affords the determination of the unsteady-state temperature profiles in the particles and in the surrounding polymeric medium by numerically solving the equation of energy. We obtained the complete thermal history of the system as a function of all relevant parameters including particle size and distribution, particle volume fraction, thermal properties of the particle and the medium, and details of the imposed magnetic field.

Support by ISF and ERA NANOSCI+ is acknowledged.

[1] G. Glöckl, R. Hergt, M. Zeisberger, S. Dutz, S. Nagel, W. Weitschies, *J. Phys.: Condens. Matter*, **18** (2006) S2935.

[2] A.M. Schmidt *Macromol. Rapid Commun.* **27** (2006) 1168.

[3] M. Shliomis, *Sov. Phys. Uspekhi* (Engl. transl.) **17** (2) (1974) 153.

[4] R.E. Rosensweig *J. Magnetism Magn. Mater.* **252** (2002) 370.

**22 August**

Monday

15:00-17:00

oral session

22TL-E

22RP-E

22OR-E

**“Magnetism in Biology  
and Medicine”**

22TL-E-4

## TMR DETECTION OF ENDOGENOUS MAGNETIC NANOPARTICLES

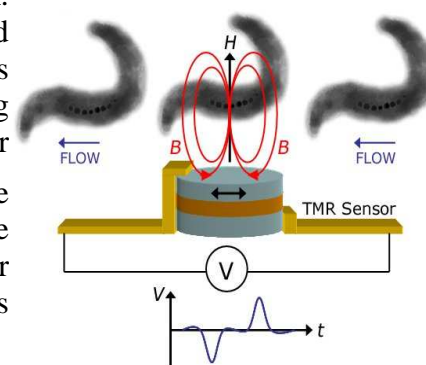
Ionescu A.<sup>1</sup>, Darton N.J.<sup>2</sup>, Vyas K.N.<sup>1</sup>, Llandro J.<sup>1</sup>

<sup>1</sup> Cavendish Laboratory, University of Cambridge, Cambridge CB3 0HE, UK

<sup>2</sup> Department of Chemical Engineering and Biotechnology, University of Cambridge, Cambridge CB2 3RA, UK

The emerging multidisciplinary field of Biomagnetism and magnetic based bio-sensors has attracted a considerable amount of interest in the last few years. This interest has been spurred on by the successful integration of magnetic nanotechnology into biomedicine and life sciences, for example in magnetic directed drug delivery by MRI [1], in hyperthermia treatment, magnetic actuation of cells [2] and in bio-assays using magnetic labels [3]. These techniques are based on magnetic nanoparticles which are normally chemically synthesised and subsequently coated for biocompatibility and ligand attachment. However one of the drawbacks of using chemically synthesised particles is their inhomogeneous size and moment distribution [4]. Particularly in magnetic nanoparticle based bio-assays these inhomogeneities lead to a poor magnetic quantification by current sensor technologies such as tunnelling magneto resistance (TMR) and giant magneto resistance effect based sensors. The question arises whether or not magnetic nanoparticles endogenously produced in magnetotactic bacteria could offer a more mono-disperse and versatile alternative for use in biomagnetic technologies.

The magnetotactic bacterium *Magnetospirillum sp.* has been cultured and the properties of its endogenous magnetic nanoparticles characterised. Electron microscopic analyses indicate that the endogenous magnetite nanoparticles in *Magnetospirillum sp.* are coated with a 3-4 nm thick transparent shell, forming a magnetosome. These magnetite nanoparticles had diameters of  $50.9 \pm 13.3$  nm in good agreement with the diameter of  $40.6 \pm 1.2$  nm extracted from magnetometry. Each *Magnetospirillum sp.* bacterium contained chains of 5 to 25 magnetosomes. Superconducting quantum interference device magnetometry results indicate that the extrinsic superparamagnetic response of the bacterial solution at room temperature can be attributed to the reversal of the magnetisation by physical rotation of the nanoparticles. The intrinsic blocking temperature of a sample of freeze dried bacteria was estimated to be  $282 \pm 13$  K. A tunnelling magneto resistance sensor (see Figure) was used to detect the stray fields of endogenous magnetic nanoparticles in static and quasi dynamic mode. Based on the tunnelling magneto resistance sensor results the magnetic moment per bacterium was estimated to be  $\sim 2.6 \times 10^{-13}$  emu. The feasibility of this detection method either as a mass coverage device or as part of an integrated microfluidic circuit for detection and sorting of magnetosome containing cells was demonstrated [5].



Support by the CamBridgeSens (EPSRC) initiative.

[1] N.J. Darton *et al.*, *Nanotechnology*, **19** (2008) 395102.

[2] Q.A. Pankhurst *et al.*, *Journal of Physics D: Applied Physics*, **22** (2009) 224001.

[3] J. Llandro *et al.*, *Medical & Biological Engineering & Computing* **48** (2010) 977.

[4] G. Micklem *et al.*, in the Introduction to "Biomagnetism and Magnetic Biosystems Based on Molecular Recognition Processes" (and publications there in), edited by J.A.C. Bland and A. Ionescu, *AIP Conf. Proc.* **1025** (2008).

[5] A. Ionescu *et al.*, *Phil. Trans. of the Roy. Soc. A.*, **398** (2010) 4371.

22TL-E-5

## MAGNETIC NANOPARTICLES FOR IMMUNOCROMATOGRAPHIC SENSORS

*Marquina C.<sup>1</sup>, de Teresa J.M.<sup>1</sup>, Serrate D.<sup>2</sup>, Marzo J.<sup>2</sup>, Arroyo F.<sup>3</sup>, Grazú V.<sup>2</sup>, Puertas S.<sup>2</sup>, Cardoso S.<sup>3</sup>, Freitas P.P.<sup>3</sup>, Ibarra M.R.<sup>2</sup>*

<sup>1</sup> Instituto de Ciencia de Materiales de Aragón (ICMA), CSIC-Universidad de Zaragoza, Facultad de Ciencias, c/Pedro Cerbuna 12, 50009-Zaragoza, Spain

<sup>2</sup> Instituto de Nanociencia de Aragón (INA), Universidad de Zaragoza, Edificio I+D, c/Mariano Esquillor s/n, 50018-Zaragoza, Spain

<sup>3</sup> Instituto de Engenharia de Sistemas e Computadores—Microsistemas e Nanotecnologias (INESC-MN) & Institute for Nanosciences and Nanotechnologies, R. Alves Redol 9, 1000-029 Lisbon, Portugal

A great effort is currently being made in the research on lateral flow tests due to their wide use nowadays in Life Sciences. Their simplicity, low cost and the large variety of analytes that can be detected by means of this technique make them suitable for a large number of applications. However, the conventional tests based on immunorecognition and the use of coloured colloidal particles have still some drawbacks that limit their use: they do not provide a quantitative determination of the analyte, and their sensitivity is limited. Our strategy to overcome these disadvantages consists in the use of superparamagnetic core-shell nanoparticles to tag the analyte, instead of the coloured colloid. The use of these magnetic labels allows us to quantify the amount of analyte present in a problem sample with a very high sensitivity, detecting their magnetic response by means of the suitable magnetic sensor.

Our method is based on measuring the magnetoresistive response of a giant magnetoresistive (GMR) sensor placed in proximity to the magnetic nanoparticles present in the lateral flow strip. Our GMR sensors are of the spin-valve type. Laser lithography techniques are used to define the active part of the sensor and the contact pads. In this talk, a brief description of our prototype and of the measurement procedure will be presented, as well as preliminary assays using our biosensor to detect the hCG pregnancy hormone in a solution. Several strategies to further increase the sensor sensitivity are currently being attempted.

The properties of the magnetic beads to be used in our test are also important to improve its performance. Therefore, different types of core-shell nanoparticles are being tested by our group, in order to make a comparative study of their magnetic response at low magnetic fields, their agglomeration, etc. Other crucial aspect to take into account in order to increase the sensitivity is the proper functionalisation of the nanoparticle shell, in order to achieve an oriented immobilisation of the antibodies to be used in the immunorecognition process. Different functionalisation and immobilisation protocols are currently being studied [1].

[1] S. Puertas, M. Moros, R. Fernandez-Pacheco, M.R. Ibarra, V. Grazu, J.M. de la Fuente, *J. Phys. D-Appl. Phys.* **43** (2010) 474012.

22TL-E-6

## CELL RESPONSES TO PULSE MAGNETIC STIMULATION

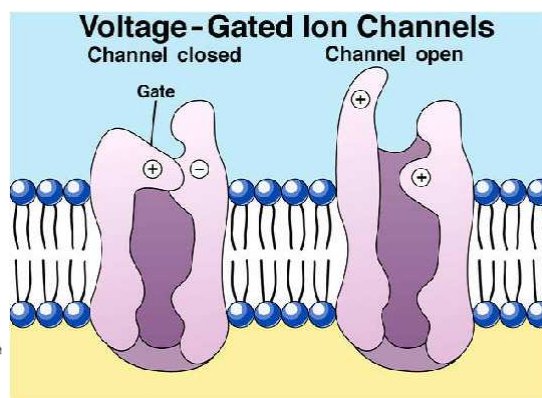
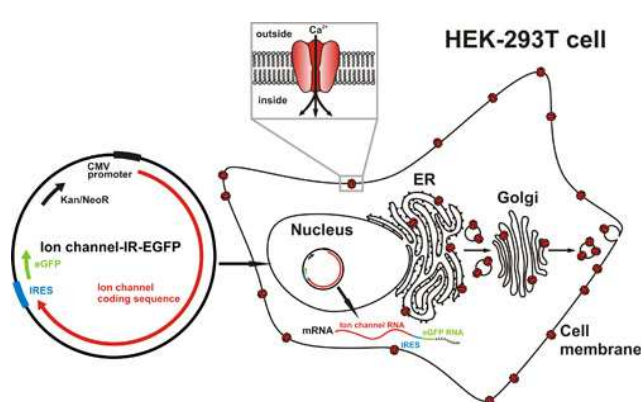
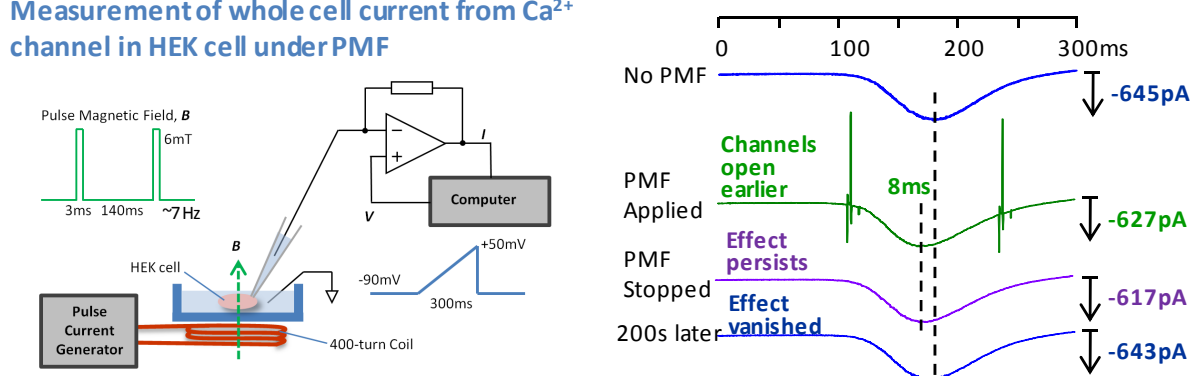
Fan J., Lee Z.H., Ng W.C., ToSoong T.H., Li X.P.\*

National University of Singapore, 9 Engineering Drive 1, Singapore 117576, Singapore

\*Correspondence to Xiaoping Li, email: mpelixp@nus.edu.sg

This study aimed to investigate the effects of pulse magnetic field (PMF) on cell electrical firing. Measurements were done on the HEK cells (Human Embryonic Kidney 293 cells), which have only Calcium ion channels (voltage gated) functioning. The whole cell current was measured by patch clamp, with the clamped voltage (imposed across the cell membrane) ramped from -90 mV to +50 mV. A PMF was generated by a 400-turn coil connected to a pulse current generator. The frequency of the pulse was 7 Hz, the width of the pulse was 3 ms, and the amplitude of the pulse (flux density) was 6 milli-Tesla. The results showed that the profile of the fired ionic current by the cell could be changed by the PMF. With the PMF applied, the cell ionic current firing reached its maximum 8 ms earlier than that without the PWF. Correspondingly, the current returned back to zero earlier. On the other hand, the maximum of the current was decreased under the influence of the PWF. When the PWF was stopped, these effects persisted for a period of time, in about 200 s, and then the current profile "recovered" to its original appearance. The change of the firing time could be due to the local electrical potential induced by the PWF, as the  $\text{Ca}^{2+}$  channels with the cell are voltage-gated. The exact mechanisms of the observed effects of PMF on the cell electrical firing are still unknown and need to be further studied.

### Measurement of whole cell current from $\text{Ca}^{2+}$ channel in HEK cell under PMF





22OR-E-7

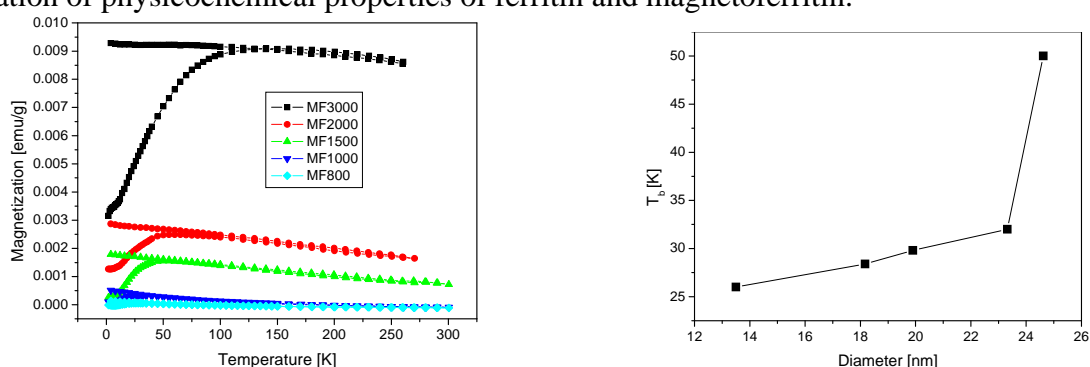
## MAGNETIC PROPERTIES OF MAGNETOFERRITIN

Timko M.<sup>1</sup>, Mitroova Z.<sup>1</sup>, Melnikova L.<sup>1</sup>, Kopcansky P.<sup>1</sup>, Kovac J.<sup>1</sup>, Pochylski M.<sup>2</sup>, Koralewski M.<sup>2</sup>

<sup>1</sup>Institute of Experimental Physics, SAS, Watsonova 47, 040 01 Kosice, Slovakia

<sup>2</sup>Faculty of Physics, Adam Mickiewicz University, Umultowska 85, 61-614 Poznań, Poland

Ferritin has previously been shown to be an excellent reaction vessel for controlled synthesis of some minerals inside its structural cage, in particular magnetite or maghemite (then it is named magnetoferritin). Magnetic nanoparticles grown in these biological moulds are usually rather homogeneous in size, free from aggregation and soluble in water. Other important advantage, especially for applications is their biocompatible character. Discovery of biological magnetite in the human brain and relation of its presence with neurodegenerative diseases have prompted investigation of physicochemical properties of ferritin and magnetoferritin.



Here we present detailed experimental study of synthesis and characterization of morphological and magnetic properties of a bioinorganic magnetic molecule – magnetoferritin with metal oxide loading values from 100 up to 3000 Fe ions per ferritin molecule. The average particle size obtained by hydrodynamic light scattering is ranging from 12 to 25 nm. Measurements of the classical magnetic properties at temperatures from 5 to 300 K and fields up to 5 T revealed a correlation between the mean particle size-and the blocking temperature. The results obtained from TEM show two important characteristics. The cores grow gradually with the iron loading and their shape is not spherical.

The superparamagnetic blocking leads to a thermal irreversibility between dc susceptibility curves measured after cooling the sample in zero field (ZFC) or under the presence of the measurement field (FC), as shown in left side figure. The linearly increasing of the blocking temperature  $T_b$  (right side figure) can be observed for small range of loading (smaller particle size). The non-linear component in this dependence was found for particle size over a smaller range (Fe loading of 2000 to 3000) due to a surface anisotropy. The anisotropy determines also the magnetic hysteresis, which shows up at sufficiently low temperatures below  $T_b$ . It was estimated that the coercive field at  $T=2$  K is largest for the sample containing the smallest nanoparticles. Since the coercive force is proportional to the average  $K$ , this result confirms the size dependence estimated from the ZFC and FC measurements.

This work was supported by Slovak Academy of Sciences, in the framework of CEX NANOFLUID, projects VEGA 0077 and 0051, APVV Sk-PI 0069-09 and Ministry of Education Agency for structural funds of EU in frame of projects Nos. 26220120033 and 26220220005.

## CARBOXYLATED MAGNETIC NANOPARTICLES AS MRI CONTRAST AGENTS. RELAXATION MEASUREMENTS AT DIFFERENT FIELD STRENGTHS

Hajdú A.<sup>1</sup>, Bányai I.<sup>2</sup>, Babos M.<sup>3</sup>, Tombácz E.<sup>4</sup>

<sup>1</sup> Laboratory of Nanochemistry, Department of Biophysics and Radiation Biology, Semmelweis University, H-1089 Budapest, Nagyvárad tér 4, Hungary

<sup>2</sup> Department of Colloid and Environmental Chemistry, University of Debrecen, 4032 Debrecen, Egyetem tér 1, Hungary

<sup>3</sup> Euromedic Diagnostics Szeged Ltd., 6720 Szeged, Semmelweis u. 1, Hungary

<sup>4</sup> Department of Physical Chemistry and Material Science, University of Szeged, Aradi vrt. tere 1., Szeged, 6720, Hungary

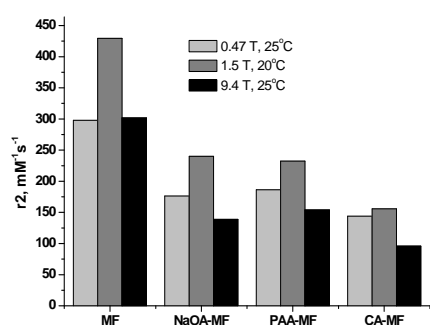


Fig 1. The  $r_2$  relaxivity parameters of the naked magnetite, and the NaOA, PAA and CA covered magnetic nanoparticles, measured at room temperature and different magnetic fields (0.47 T; 1.5 T; 9.4 T).

Biomedical applications of iron oxide nanoparticles, in particular as contrast agents in Magnetic Resonance Imaging (MRI), are nowadays in the centre of international interest [1]. The contrast between different tissues on the MRI picture is based mainly on variations in longitudinal ( $T_1$ ), and transversal ( $T_2$ ) relaxation times of water. The superparamagnetic magnetite nanoparticles have a strong  $T_2$  relaxation effect, and is planned to be used as  $T_2$  contrast agents [2]. This relaxation effect of superparamagnetic nanoparticles can be affected by numerous ways. It can be tuned with particle size, magnetic properties, but also with surface coverage and charge of the particles. Variable coatings modify the around the magnetic particles and hence

change the contrast enhancing effect in a wide range.

In the present work, magnetite nanoparticles were synthesized and stabilized in aqueous medium with carboxylic compounds (citric acid (CA), polyacrylic acid (PAA) and sodium oleate (NaOA)). Relaxation times ( $T_1$ - longitudinal,  $T_2$ -transversal) and relaxivities ( $r_1$ ,  $r_2$ ) of naked and covered magnetite nanoparticles were measured at different field strengths, i.e., 0.47, 1.5 and 9.4 T. Our goal was to show differences among the contrasting performance of the tested magnetic fluids stabilized by CA, PAA, NaOA at different field strengths using  $^1\text{H-NMR}$  and MRI devices. Considering the recent trend of MRI development, it is important to predict the behaviour of the different surface charged nanoparticles under variant magnetic fields.

The MRI and NMR measurements showed characteristic differences between the tested magnetic fluids stabilized by carboxylic compounds (Fig 1). High  $r_2/r_1$  ratios observed at each magnetic field applied show that magnetite nanoparticles could become good negative contrast agents in the future.

Support by the Hungarian Foundation NKTH-OTKA (A7-69109) and the Hungarian Science Foundation (OTKA T 49044) is acknowledged.

[1] Q.A. Pankhurst, J. Connolly, S.K. Jones, J. Dobson, *J. Phys. D: Appl. Phys.* **36** (2003) R167–R181

[2] S. Laurent, D. Forge, M. Port, A. Roch, C. Robic, L.V. Elst, R. N. Muller, *Chem. Rev.* **108** (2008) 2064–2110

**22 August**

Monday

12:00-14:00

15:00-17:00

oral session

22TL-F

22RP-F

22OR-F

**“Magnetophotonics”**

22TL-F-1

## CYCLOTRON RESONANCES AND FARADAY ROTATION IN GRAPHENE IN THE THz RANGE

*Kuzmenko A.*

Département de Physique de la Matière Condensée, Université de Genève, CH-1211 Genève 4,  
Switzerland

The key features of graphene, the single atomic layer of carbon atoms forming a honeycomb structure, are Dirac-like conical bands and the pseudospin – an extra degree of freedom due to the bi-partite crystal structure. Apart from showing beautiful physics phenomena, graphene is considered as a possible platform for novel electronic and magneto-electro-optical applications, thanks to a high tunability of its properties by external electric, magnetic and strain fields, combined with an emerging possibility of mass production.

A series of non-equidistant Landau levels (LLs), including a zero-energy level, not present in the usual semiconductors lacking pseudospin, is formed in graphene in a magnetic field. We studied the Faraday rotation induced by the cyclotron resonances corresponding to the LL transitions in the far infrared (THz) range [1]. Various samples of monolayer and multilayer graphene were grown on different faces of SiC by high-temperature annealing. The Faraday rotation, which can also be regarded as an optical Hall effect, allows measuring separately the dynamical response of electrons and holes to the external electromagnetic radiation. In highly doped monolayer graphene on the Si face of SiC, we found a quasiclassical cyclotron resonance and a Faraday rotation of several degrees, which is an extraordinary strong effect, given the atomic sample thickness. In quasineutral multilayer graphene on the C-face, we observed a series of quantum cyclotron resonances due to the low-index LL transitions, involving the zero-energy level, of both electron and hole types. Interestingly, different Fermi velocities for electrons and holes were observed.

Due to a large Faraday rotation, graphene is potentially useful in magneto-optical devices, such as polarization modulators, in the THz and microwave ranges. In this context, a unique advantage of graphene is a possibility of ambipolar doping by means of electrostatic gating, which allows the inversion of the Faraday rotation by applying electric field rather than magnetic field as in the conventional devices.

[1] I. Crassee, J. Levallois, A. L. Walter, M. Ostler, A. Bostwick, E. Rotenberg, T. Seyller, D. van der Marel and A. B. Kuzmenko, *Nature Physics* **7**, 48 (2011).

## MAGNETO-OPTICAL HARMONIC GENERATION IN SEMICONDUCTORS

Pavlov V.V.<sup>1</sup>, Pisarev R.V.<sup>1</sup>, Brunne D.<sup>2</sup>, Lafrentz M.<sup>2</sup>, Kaminski B.<sup>2</sup>, Yakovlev D.R.<sup>1,2</sup>, Bayer M.<sup>2</sup>

<sup>1</sup> Ioffe Physical-Technical Institute of RAS, 194021 St. Petersburg, Russia

<sup>2</sup> Experimentelle Physik 2, Technische Universität Dortmund, D-44221 Dortmund, Germany

Nonlinear optical phenomena may provide novel information about electronic and magnetic structures of solids comparing with linear optics. This is due to the involvement of more than a single light field into nonlinear processes. Among a vast variety of nonlinear phenomena related with frequency conversion the second-harmonic generation (SHG) and third-harmonic generation (THG) are the simplest processes. The relevant nonlinear polarization  $\mathbf{P}^{2\omega, 3\omega}$  in the electric-dipole (ED) approximation can be written as

$$\mathbf{P}^{2\omega, 3\omega} = \chi^{2\omega} : \mathbf{E}^\omega \mathbf{E}^\omega + \chi^{3\omega} : \mathbf{E}^\omega \mathbf{E}^\omega \mathbf{E}^\omega + \chi^{2\omega} : \mathbf{E}^\omega \mathbf{E}^\omega \mathbf{M}^0 + \chi^{3\omega} : \mathbf{E}^\omega \mathbf{E}^\omega \mathbf{E}^\omega \mathbf{M}^0,$$

where first two terms describe crystallographic contributions to SHG and THG, last two terms describe magnetization-induced contributions to SHG and THG.

Here we present nonlinear optical studies of diamagnetic, diluted magnetic, and magnetically ordered semiconductors in a broad spectral and temperature ranges. Several new mechanisms of SHG and THG are revealed. It is found that Landau-level orbital quantization of the band energy is a key mechanism for magnetic-field-induced second harmonic generation (MSHG) in diamagnetic semiconductors GaAs [1] and CdTe [1, 2]. The giant Zeeman spin-splitting of electronic states is essential for SHG in diluted magnetic semiconductors (Cd,Mn)Te [3]. Both mechanisms involving the optical nonlinearities of electric-dipole type take place in noncentrosymmetric semiconductors. Recently spin-induced SHG is observed at the band gap in magnetic centrosymmetric semiconductors EuTe and EuSe (see Fig. 1) [4]. This mechanism involving the optical nonlinearities of magnetic-dipole type is essential for centrosymmetric semiconductors. THG was studied in the magnetic semiconductor EuTe in external magnetic field [5]. ED THG is strongly enhanced at the photon energies close to the band gap.

The magnetic field and temperature dependencies demonstrate that the nonlinear processes arise due to novel types of optical nonlinearities caused by the external magnetic field. The observed mechanisms of optical nonlinearities open access to a wide class of centrosymmetric and noncentrosymmetric magnetic systems by harmonics generation spectroscopy.

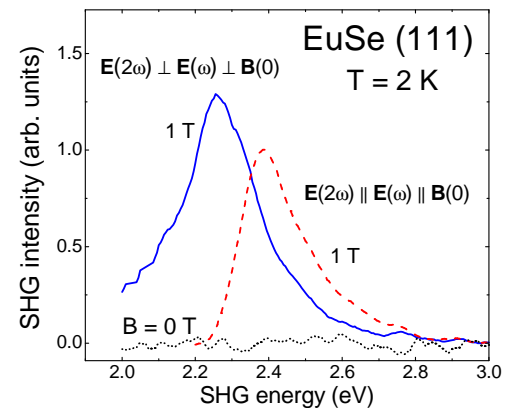


Fig. 1. SHG spectra in EuSe for zero field and for a saturation field of 1T for two different measurement geometries.

Support by RFBR, DFG, Russian Academy Program on Spintronics is acknowledged.

- [1] V.V. Pavlov, A.M. Kalashnikova, R.V. Pisarev, *et al.*, *Phys. Rev. Lett.* **94**, 157404 (2005).
- [2] I. Sanger, D. R. Yakovlev, B. Kaminski, *et al.*, *Phys. Rev. B* **74**, 165208 (2006).
- [3] I. Sanger, D.R. Yakovlev, R.V. Pisarev, *et al.*, *Phys. Rev. Lett.* **96**, 117211 (2006).
- [4] B. Kaminski, M. Lafrentz, R.V. Pisarev, *et al.*, *Phys. Rev. Lett.* **103**, 057203 (2009).
- [5] M. Lafrentz, D. Brunne, B. Kaminski, *et al.*, *Phys. Rev. B* **82**, 235206 (2010).

## PHOTOMAGNETISM IN (Ga,Mn)As FERROMAGNETIC SEMICONDUCTORS

Astakhov G.V.<sup>1,2</sup>, Ossau W.<sup>1</sup>, Brunner K.<sup>1</sup>, Molenkamp L.W.<sup>1</sup>, Korenev V.L.<sup>2</sup>, Reid A.H.M.<sup>3</sup>,  
Kimel A.V.<sup>3</sup>, Kirilyuk A.<sup>1</sup>, Rasing Th.<sup>1</sup>

<sup>1</sup> Physikalisches Institut (EP3), Universität Würzburg, Am Hubland, 97074, Germany

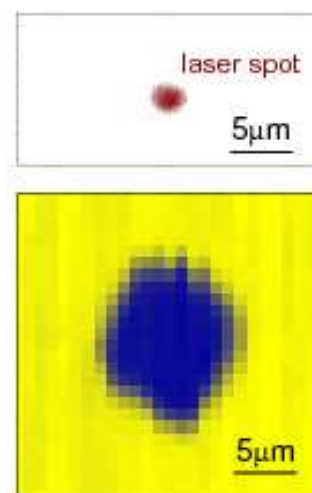
<sup>2</sup> A. F. Ioffe Physico-Technical Institute, RAS, 194021 St. Petersburg, Russia

<sup>3</sup> Institute for Molecules and Materials, Radboud University Nijmegen, 6525 AJ Nijmegen, The Netherlands

Magneto-optical (MO) recording techniques currently attract a lot of interest due to the nonvolatility, low cost, and removability of media they offer. Traditionally, the light in such devices is used to modify the strength of the magnetic interaction. Because a very large number of magnetic ions is essential to achieve ferromagnetism, the intensity of the light needed is rather high. This results in heating of the recording media, regardless of whether or not the thermomagnetic effect is the exploited physical mechanism. The resulting heat dissipation is an obviously undesirable side effect which leads to degradation of the recording media and wastes significant energy resources.

We propose a concept for MO recording which circumvents this problem by focusing our action on the depinning of domain walls (DW) instead of trying to modify the magnetic interaction. Our experiments are performed on a prototype system in the form of a low-doped (Ga,Mn)As ferromagnetic semiconductor. We find that in the vicinity of the metal-insulator transition, the coercivity is sensitive to very low intensity illumination (down to  $1 \text{ Wcm}^{-2}$ ) [1], which is several orders of magnitude lower than in alternative approaches. The coercivity can be reduced almost to zero using a single subpicosecond pulse with only 0.08 nJ of energy [2]. This compares very favorably with the 10–100 nJ of energy per bit written of current hard drives, and even with magnetic RAM (0.15 nJ) and flash (10 nJ) solid state memories. An example of the magnetic domain created using such photocoercivity effect (together with a CCD image of the focused laser beam) is shown in the figure.

The reduction of the coercivity is caused by the presence of DW pinning sites whose pinning efficiency decreases under illumination. They can be selectively addressed and switched between pinning and depinning configurations using strongly focused light pulses of appropriate power and duration [3]. This forces propagation of the DWs via controllable photoactivated jumps. We find that the time between such light-induced Barkhausen jumps (which determines how fast the magnetic domain can be rewritten) exponentially decreases with light intensity, and can be as short as 1 ns.



Support by the DFG (AS 310/2-1) and the European networks (Ultramagneton and FANTOMAS) is acknowledged.

[1] G.V. Astakhov et al., *Phys. Rev. Lett.*, **102** (2009) 187401.

[2] A.H.M. Reid et al., *Appl. Phys. Lett.*, **97** (2010) 187401.

[3] G.V. Astakhov et al., *Phys. Rev. Lett.*, **106** (2011) 037204.

## ULTRAFAST LASER-INDUCED SPIN DYNAMICS IN RARE-EARTH ORTHOFERRITES WITH TAILORED MAGNETIC PROPERTIES

de Jong J.A.<sup>1</sup>, Kalashnikova A.M.<sup>2</sup>, Kimel A.V.<sup>1</sup>, Pisarev R.V.<sup>2</sup>, Balbashov A.M.<sup>3</sup>, Kirilyuk A.<sup>1</sup>, Rasing Th.<sup>1</sup>

<sup>1</sup> Radboud University Nijmegen, IMM, 6525AJ Nijmegen, Netherlands

<sup>2</sup> Ioffe Physical-Technical Institute of RAS, 194021 St. Petersburg, Russia

<sup>3</sup> Moscow Power Engineering Institute, 111250 Moscow, Russia

Ultrafast optical manipulation of magnetic order is one of the most rapidly developing areas in modern magnetism [1]. Though most of such studies are focused on metallic or semiconducting media, it appears that magnetic dielectric materials provide a unique opportunity for investigating a broad range of various interactions between femtosecond laser pulses and ordered spin ensembles. In particular, several exciting results on novel mechanisms of ultrafast laser-induced spin-reorientation in weakly ferromagnetic orthoferrites have been reported recently [2-4]. A key property defining these unique responses of orthoferrites to ultrashort laser pulses is the presence of temperature-induced spin reorientation transitions (SRT), when a magnetization rotates from one crystallographic axis to another.

Here we report on experimental studies of the laser-induced excitation of magnetization dynamics in mixed rare-earth orthoferrites  $(\text{Sm}_{0.55}\text{Tb}_{0.45})\text{FeO}_3$ . By choosing this particular composition the magnetic properties of the orthoferrite were tailored and the SRT was shifted towards room temperature (220-270 K), while in most of the pure rare-earth orthoferrites this is observed at much lower temperatures. Figure 1 shows the laser-induced dynamics of the magnetization in  $\text{Sm}_{0.55}\text{Tb}_{0.45}\text{FeO}_3$  at temperatures below and within the SRT range. Most importantly, an ultrafast spin reorientation was observed in a wide temperature range of 190-270 K due to the thermal action of laser pulses, changing the lattice temperature.

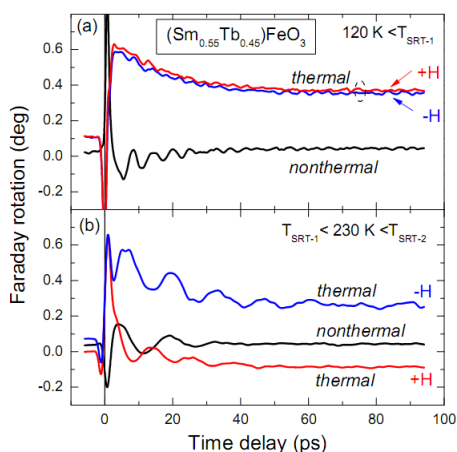


Fig. 1 Magnetization precession excited by circularly polarized 100 fs laser pulses in  $\text{Sm}_{0.55}\text{Tb}_{0.45}\text{FeO}_3$  (a) far below the SRT range at 120K and (b) within this range at 230 K. Below the SRT range excitation of the spin precession takes place only due to the inverse Faraday effect, which does require heating and thus called nonthermal [3]. At higher temperatures the spin precession is also excited but via ultrafast lattice heating [2]. The latter is called thermal and results in ultrafast reorientation of spins to the direction defined by the sign of the external magnetic field.

Moreover, the excitation of an additional resonance mode below  $T=100$  K was observed, which may indicate an extra feature present in the phase diagram of  $\text{Sm}_{0.55}\text{Tb}_{0.45}\text{FeO}_3$ . We note that in pure  $\text{SmFeO}_3$  and  $\text{TbFeO}_3$  in this temperature range no such features were reported.

Support by RFBR, EC FP7 (projects Fantomas and UltraMagnetron), NOW, and FOM is acknowledged.

- [1] A. Kirilyuk, A. V. Kimel, Th. Rasing, *Review of Modern Physics* **82** (2010) 2731.
- [2] A. V. Kimel, et al., *Nature (London)* **429** (2004) 850.
- [3] A. V. Kimel, et al., *Nature (London)* **435** (2005) 655.
- [4] A. V. Kimel, et al., *Nature Phys.* **5** (2009) 727.

## ELECTRONIC TRANSITIONS AND GENUINE CRYSTAL FIELD PARAMETERS IN COPPER METABORATE $\text{CuB}_2\text{O}_4$

*Pisarev R.V.*<sup>1</sup>, *Kalashnikova A.M.*<sup>1</sup>, *Schöps O.*<sup>2</sup>, *Bezmaternykh L.N.*<sup>3</sup>

<sup>1</sup> Ioffe Physical-Technical Institute of RAS, Petersburg, Russia

<sup>2</sup> Institute of Physics, Dortmund Technical University, Dortmund, Germany

<sup>3</sup> Institute of Physics, Syberian Branch of RAS, Krasnoyarsk, Russia

Among the wide variety of copper compounds tetragonal metaborate  $\text{CuB}_2\text{O}_4$  received a vivid attention only recently due to several interesting physical properties markedly different from those in other cuprates. From the chemical point of view this material is one of a few known examples where 12 copper  $\text{Cu}^{2+}$  ions of the same type occupy two crystallographically distinct positions ( $4b$  and  $8d$ ) in the unit cell, which leads to intricate magnetic structures and rich magnetic phase diagram with antiferromagnetic ordering below  $T_N=21\text{K}$ .

Here we present and analyse high resolution  $\alpha$ -,  $\sigma$ - and  $\pi$ -polarized absorption spectra related to  $d-d$  electronic transitions in  $\text{CuB}_2\text{O}_4$ . The spectra are characterized by exceptionally rich fine structure in the spectral range of 1.4-2.4 eV (Fig. 1). Six zero phonon (ZP) lines originating from the electronic transitions within the  $\text{Cu}^{2+}$  ions in both positions are identified.

We apply the symmetry analysis in order to explain polarization properties of the ZP lines in the  $8d$  and  $4b$  positions. Reliable assignment of all six ZP lines to specific transitions allowed us to calculate genuine cubic  $Dq$  and tetragonal  $Ds$  and  $Dt$  crystal field parameters for both positions using the crystal field theory [1]. Based on this analysis we show, in particular, that the  $(3r^2-z^2)$  state, which energy is the measure of the Jahn-Teller splitting, is the highest  $3d$ -state for the both types of  $\text{Cu}^{2+}$  ion positions. While for the ions occupying  $4b$  positions this is an obvious result, for ions in  $8d$  sites the value of the Jahn-Teller splitting is often a matter of debate. This controversy holds also for a number of other actively studied copper compounds.

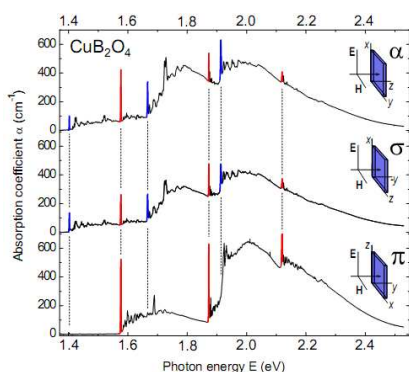


Fig. 1  $\alpha$ -,  $\sigma$ - and  $\pi$ -absorption spectra of  $\text{CuB}_2\text{O}_4$  in the range of  $d-d$  transitions measured at  $T=5\text{K}$ . Six ZP lines are identified. Three ZP lines appearing in all three spectra correspond to the  $d-d$  transitions in  $\text{Cu}^{2+}$  ion in the  $8d$  crystallographic positions, while other three - to the  $d-d$  transitions in the  $4b$  positions. Insets show the light polarization and propagation directions for the corresponding spectra.

Therefore, using the obtained crystal field parameters as the reference values we estimated  $Dq$ ,  $Ds$  and  $Dt$  for several cuprate compounds with different Cu-O bond lengths. In particular, the  $3d$  level splitting in  $\text{La}_2\text{CuO}_4$ ,  $\text{Nd}_2\text{CuO}_4$ ,  $\text{CuGeO}_3$ ,  $\text{Sr}_2\text{CuO}_2\text{Cl}_2$ , and  $\text{CuB}_7\text{O}_{13}\text{Cl}$  was analysed. Our estimates suggest that in these compounds the Jahn-Teller splitting is also larger than it was proposed previously on the grounds of experimental [2] and theoretical [3] studies.

Support by RFBR (project 09-02-00070) and FASI (grant 02.740.11.0384) is acknowledged.

[1] A. B. P. Lever, *Inorganic Electronic Spectroscopy* (Elsevier, Amsterdam, 1984).

[2] P. Kuiper, *et al.*, *Phys. Rev. Lett.* **80** (1998) 5204.

[3] D. S. Middlemiss and W. C. Mackrodt, *J. Phys.: Condens. Matter* **20** (2008) 015207.



22TL-F-6

## MAGNETOELECTRIC EFFECTS STUDIED BY X-RAY

*Staub U.*

Swiss Light Source, Paul Scherrer Insitut, CH-5232 Villigen PSI, Switzerland

The interaction of magnetic and electric fields in multiferroics is studied using x-ray diffraction in the vicinity of absorption edges. It is shown, how x-rays can be sensitive inherently to the atomic concept of the magneto-electric interaction e.g. observe “atomic” like toroidal moments, [1] and possibly even magnetic charge. [2] These quantities are of fundamental importance in multiferroic materials and possibly also for the pseudo-gap phase of high- $T_c$  superconductors, where they are called orbital flux. In the second part, it is directly shown how fast atomic spin moments can be coherently moved form one magnetic phase to another in CuO. [3] For that the antiferromagnet is excited by a femto-second laser pulse and the spin orientation probed by a femto-second x-ray pulse produced by an X-ray free-electron laser.

[1] V. Scagnoli et al., submitted.

[2] U. Staub et al., *Phys. Rev. B*, **80** (2009) 140410 (R).

[3] S. L. Johnson et al., submitted.

22RP-F-7

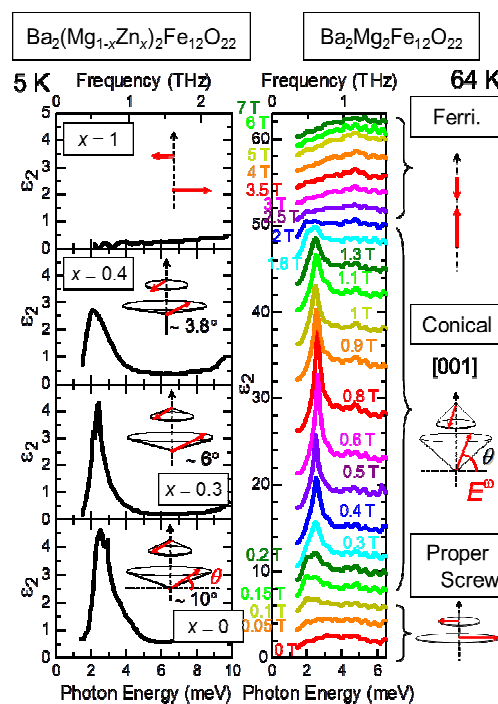
## GIGANTIC TERAHERTZ MAGNETOELECTRIC EFFECT VIA ELECTROMAGNONS IN MULTIFERROICS

*Kida N.*

Department of Advanced Materials Science, The University of Tokyo, Kashiwa 277-8561, Japan

Optical properties of solids occasionally show dramatic color changes upon various external stimulations. However, the materials showing such chromism are still rare in spite of the possible candidate for future spin electronics.

Here we show the findings of the gigantic magneto-chromism and nonreciprocal directional dichroism at terahertz frequencies. These observations are based on the successful external control of the spectral shape of the electromagnon, the magnetic resonance driven by the light electric field [1]. Among several magnetoelectrics to host electromagnons, a hexaferrite  $\text{Ba}_2\text{Mg}_2\text{Fe}_{12}\text{O}_{22}$  occupies the unique position [2]. It yields the large saturation magnetic moment in magnetic fields, which enables us to easily modify the spin structures, as compared to other magnetoelectrics with antiferromagnetic orders. Indeed, we identified the gigantic magneto-chromic change exceeding 400% even at 0.6 T (defined by the difference of the absorption



intensity with and without magnetic field) by finely controlling the spin structures in terms of the conical angle  $\theta$  from the proper screw ( $\theta=0^\circ$ ) to the ferrimagnetic ( $\theta=90^\circ$ ) through the conical spin-ordered phases ( $0^\circ<\theta<90^\circ$ ) [3].

Another unique example to host electromagnons is a multiferroic  $\text{Ba}_2\text{CoGe}_2\text{O}_7$  [4]. We observed two sharp resonances around 2 meV and 4 meV, which can be assigned to the antiferromagnetic and electromagnon resonances, respectively. Only near electromagnon resonance, we found the gigantic non-reciprocal change (defined by the difference of the absorption intensity with the reversal of magnetic field); it exceeds 200% at  $\pm 7$  T. The sign of the relative change was found to be odd with respect to the direction of the polarization and magnetization, which is a direct evidence for the emergence of the non-reciprocal directional dichroism in this compound.

This work was done in collaboration with S. Kumakura, I. Kézsmárki, S. Bordács, S. Ishiwata, Y. Onose, Y. Taguchi, and Y. Tokura.

[1] N. Kida *et al.*, *J. Opt. Soc. Am. B*, **26** (2009) A35.

[2] N. Kida *et al.*, *Phys. Rev. B*, **80** (2009) 220406(R).

[3] N. Kida *et al.*, *Phys. Rev. B*, **83** (2011) 064422.

[4] I. Kézsmárki *et al.*, *Phys. Rev. Lett.*, **106** (2011) 057403.

22RP-F-8

## SOLITARY DEFLECTION WAVES ON THE SUPERSONIC DOMAIN WALL OF YTTRIUM ORTHOFERRITE

*Chetkin M., Kurbatova Yu., Shapaeva T.*

Faculty of Physics M.V.Lomonosov Moscow State University, Leninskie Gory, Moscow 119991, Russia

The existence of antiferromagnetic (AFM) vortices in the orthoferrite domain wall (DW) was predicted theoretically by Farztdinov *et al.* [1]. But nobody observed these vortices before our works [2]. We present the experimental data on the dynamics of the solitary deflection waves (SDWs), which accompany the AFM vortices. The two- and three-fold high-speed digital photography with the help of Faraday rotation in the orthoferrites plates cut perpendicularly to the optical axis were presented. The short light pulses 200 ps duration were used in this investigation. This method is the only one applicable for the investigation of the AFM vortices dynamics. We succeeded in finding a way to generate pairs of solitary deflection waves that accompany the antiferromagnetic vortices in the orthoferrites domain wall by means of a local deceleration of a small part of supersonic DW and investigating their dynamics. From digital two- and three-fold high-speed photographs it is possible to obtain the domain wall velocity –  $v$ , the velocity of solitary deflection wave along moving domain wall –  $u$ , the total solitary deflection wave velocity –  $w$  and amplitude of this wave.

The dependences  $u(v)$ ,  $w(v)$  were obtained in the real time during one transition DW and AFM vortices. The curve  $w(v)$  demonstrates a nonlinear increase. The increase is sharper for solitary deflection waves with smaller amplitudes. Then the dependence  $w(v)$  saturates on the level 20 km/s equal to the spin wave velocity  $c$ . The  $w(v)$  saturation takes place earlier for smaller amplitudes of solitary deflection waves and smaller values of topological charges of antiferromagnetic vortices. The minimum amplitudes of the solitary deflection waves were equal to 2  $\mu\text{m}$ . The experimental

dependence  $u(v)$  first grow nonlinearly, reach a maximum magnitude and then follow the relation  $u^2+v^2=c^2$ . Positions of the maximums on the  $u(v)$  curves shift to higher velocity with an increase in the antiferromagnetic topological charges. The SDWs amplitudes are proportional to the velocity of AFM vortices along the domain wall.

So in the case of the orthoferrites we observe the new type of dynamics – antiferromagnetodynamics with very high supersonic velocities. The start of antiferromagnetodynamics in the orthoferrites was proposed in [3], where it was first time experimentally observed limiting DW velocity in the orthoferrites.

These results confirm the gyroscopic origin of the AFM vortices dynamics in the canted antiferromagnetic – yttrium orthoferrite. The theory of gyroscopic force in the domain wall of orthoferrites was elaborated by Zvezdin et al. [4]. The dynamics of solitary deflection waves, which appear on the DW crossing of the local defect, was investigated with the help numerical methods [5].

The work was supported by Russian Foundation for Basic Research (project 10-02-00594-a).

[1]. M.M. Farztdinov, M.A. Shamsutdinov, A.A. Khalifina. *Fiz.Tverd. Tela*, **21** (1979) 1522.

[2]. M.V.Chetkin, Yu.N.Kurbatova, T.B.Shapaeva. *JMMM*, **321** (2009) 800.

[3]. V.G. Bar'jakhtar, M.V. Chetkin, B.A. Ivanov, S.N. Gadetskiy, *Dynamics of Topological Magnetic Solitons*. (Springer tracts in modern physics, Berlin), vol. **129**, 1994.[4]. A.K.Zvezdin, K.A.Zvezdin. *Kratkie soobshchenia po fizike of P.N.Lebedev Physics Institute of the Russian Academy of sciences*, N 8 (2010) 22.

[5]. E.G.Ekomasov, Sh.A.Azamatov, R.R.Murtazin, A.M. Gumerov and A.D. Davletshina. *Bulletin of the Russian Academy of Sciences: Physics*, **74** (2010) 1459.

22OR-F-9

## SINGLE-SHOT IMAGING OF ULTRAFAST SPIN-REORIENTATION IN RARE-EARTH ORTHOFERRITES

*de Jong J.A.<sup>1</sup>, Razdolski I.<sup>1</sup>, Kalashnikova A.M.<sup>2</sup>, Kimel A.V.<sup>1</sup>, Pisarev R.V.<sup>2</sup>, Balbashov A.M.<sup>3</sup>, Kirilyuk A.<sup>1</sup>, Rasing Th.<sup>1</sup>*

<sup>1</sup>Radboud University Nijmegen, IMM, 6525 AJ Nijmegen, The Netherlands

<sup>2</sup>Ioffe Physical-Technical Institute, RAS, 194021 St. Petersburg, Russia

<sup>3</sup>Moscow Power Engineering Institute, 111250 Moscow, Russia

Manipulation of magnetic states of a medium by means of femtosecond laser pulses is a promising approach for achieving the fastest ever processing of magnetic information [1-3]. Here we report about single-shot time-resolved imaging and stroboscopic pump-probe experiments performed on a  $(\text{Sm}_{0.5}\text{Pr}_{0.5})\text{FeO}_3$  orthoferrite. The measurements were carried out at a temperature below the  $\Gamma_2 \rightarrow \Gamma_{24} \rightarrow \Gamma_4$  spin reorientation transition (SRT).

In the experiments, a 40-fs circularly polarized pump pulse was used to trigger the SRT. To follow the laser-induced magnetic changes, the out-of-plane component of the net magnetization was detected with a delayed probe femtosecond pulse. Fig.1 shows (a) the magneto-optical images of the sample and (b) the transient Faraday rotation measured with a subpicosecond resolution. We have found that the spin reorientation proceeds via a novel mechanism, where light has a twofold effect. Firstly, it changes the magnetic anisotropy of the medium through heating and secondly, it

determines the magnetization direction in the new phase, acting as an effective magnetic field. The direction of the field is set by the helicity of the pump polarization. It has been found that the process of the reorientation depends on the sample temperature and the pump fluence. The latter may also lead to an unusual “ring-and-core” magnetization pattern, with opposite directions of the magnetization within the pump spot.

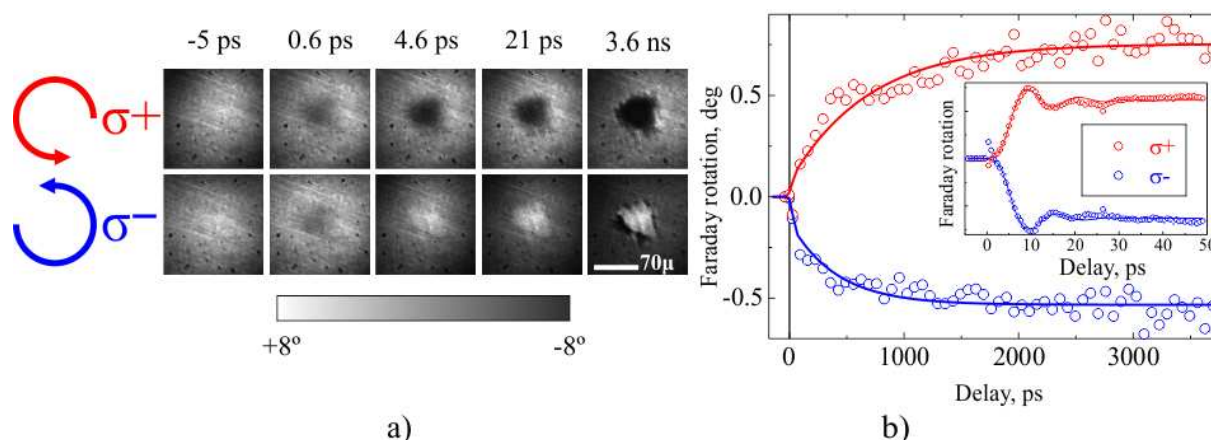


Fig.1. (a) Imaging of ultrafast reorientation and (b) stroboscopic data of the transient Faraday rotation during the laser-excited spin-reorientation transition in  $(\text{Sm}_{0.5}\text{Pr}_{0.5})\text{FeO}_3$  at  $T = 90$  K. Red and blue dots in (b), as well as the top and bottom image rows in (a) correspond to the different pump polarization helicities. The inset in Fig.1(b) shows that the ultrafast reorientation occurs within less than the first 10 ps.

[1] A. V. Kimel *et al.*, Nature **435**, 655 (2005).

[2] C. D. Stanciu *et al.*, Phys. Rev. Lett. **99**, 047601 (2007).

[3] A. V. Kimel *et al.*, Nat. Phys. **5**, 727 (2009).

22RP-F-10

## MAGNETO-SPECTROSCOPY STUDIES OF GRAPHITE NANOPLETELET FILMS

Liu H.-L.

Department of Physics, National Taiwan Normal University, Taipei, Taiwan

The very peculiar transport and electrodynamic properties of the atomically thin graphene films have been intensively studied in the past few years. While the ideal case of a single, isolated graphene sheet having macroscopic dimensions is difficult to realize, systems comprised of multiple graphene sheets can still show some of these peculiar properties. We have undertaken a THz, infrared, and magnetic-field study of moderately thick graphene films consisting of  $\sim 1.7$  nm thick nanoplatelet structures. Our THz and far-infrared results yield an electronic scattering rate of  $175 \text{ cm}^{-1}$  ( $3.3 \times 10^{13} \text{ rad/s}$ ) and plasma frequency of  $1675 \text{ cm}^{-1}$ , the latter decreasing slowly with temperature. Magneto-spectroscopy measurements at 4.2 K and in magnetic fields up to  $B = 17.5$  T show several sets of Landau level transitions (cyclotron resonance). The frequencies for some of these transitions scale as  $B^{1/2}$ , indicating a significant contribution from nearly massless Dirac Fermions (quasiparticles obeying a linear dispersion relation) [1]. This opens the possibility for observing a strong non-linear optical response in the THz spectral range, as proposed by S. A. Mikhailov [2].

Support by NSC98-2112-M-003-004-MY3 is acknowledged.

- [1] H. L. Liu *et al.*, *New Journal of Physics*, **12** (2010) 113012.
- [2] S. A. Mikhailov, *Europhysics Letters*, **79** (2007) 27002.



**22 August**

Monday

12:00-14:00

15:00-17:00

oral session

22TL-G

22RP-G

22OR-G

**“Magnetism and  
Superconductivity”**

22TL-G-1

## IRON BASED SUPERCONDUCTORS: Pnictides versus Chalcogenides

*Sadovskii M.V.<sup>1,2</sup>*

<sup>1</sup> Institute for Electrophysics, Russian Academy of Sciences, Ural Branch, Amundsen str. 106, Ekaterinburg 620016, Russia

<sup>2</sup> Institute for Metal Physics, Russian Academy of Sciences, Ural Branch, S. Kovalevskaya str.18, Ekaterinburg 620219, Russia

We present a brief review of the present day situation with studies of high-temperature superconductivity in iron pnictides and chalcogenides. Recent discovery of superconductivity with  $T_c > 30\text{K}$  in  $A_x\text{Fe}_{2-x/2}\text{Se}_2$  ( $A=\text{K,Cs,Tl},\dots$ ) represents the major new step in the development of new concepts in the physics of Fe – based high-temperature superconductors.

We compare LDA [1] and ARPES [2] data on the band structure and Fermi surfaces of novel superconductors and those of the previously studied isostructural 122 - superconductors like  $\text{BaFe}_2\text{As}_2$ . It appears that electronic structure of new superconductors is rather different from that of FeAs 122 - systems. In particular, no nesting properties of electron and hole - like Fermi surfaces is observed, casting doubts on most popular theoretical schemes of Cooper pairing for these systems. Doping of novel materials is extremely important as a number of topological transitions of Fermi surface near the  $\Gamma$  point in the Brillouin zone are observed for different doping levels.

The discovery [3,4] of Fe vacancies ordering and antiferromagnetic (AFM) ordering at pretty high temperatures ( $T_N > 500\text{K}$ ), much exceeding superconducting  $T_c$  makes these systems unique antiferromagnetic superconductors with highest  $T_N$  observed up to now. This poses very difficult problems for theoretical understanding of superconductivity. We discuss the role of both vacancies and AFM ordering in transformations of band structure and Fermi surfaces, as well as their importance for superconductivity.

Superconducting transition temperature  $T_c$  of new superconductors is discussed within the general picture of superconductivity in multiple band systems. It is demonstrated that both in FeAs – superconductors and in new FeSe – systems the value of  $T_c$  correlates with the value of the total density of states (DOS) at the Fermi level.

This work is partly supported by RFBR grant 11-02-00147 and was performed within the framework of Programs of Fundamental Research of the Russian Academy of Sciences (RAS) “Quantum physics of condensed matter” (09-II-2-1009) and of the Physics Division of RAS “Strongly correlated electrons in solid states”(09-T-2-1011).

[1] I.A. Nekrasov, M.V. Sadovskii. *JETP Lett.* **93** (2010) 166

[2] Daixiang Mou et al. *Phys. Rev. Lett.* **106** (2010) 107001

[3] Z. Shermadini et al. *Phys. Rev. Lett.* **106** (2010) 117602

[4] Wei Bao et al. ArXiv:1102.0830



## RECENT TOPICS ABOUT TOPOLOGICAL SUPERCONDUCTIVITY

*Tanaka Y.<sup>1</sup>, Yada K.<sup>1</sup>, Yokoyama T.<sup>2</sup>, Sato M.<sup>3</sup>, Nagaosa N.<sup>4</sup>*

<sup>1</sup> Department of Applied Physics, Nagoya University, Nagoya, 464-8603

<sup>2</sup> Department of Physics, Tokyo Institute of Technology, Tokyo, 152-8551, Japan

<sup>3</sup> The Institute for Solid State Physics, The University of Tokyo, Chiba, 277-8581, Japan

<sup>4</sup> The Department of Applied Physics, The University of Tokyo, 7-3-1 Hongo, Bunkyo-ku, Tokyo, 113-8656, Japan

Recently, edge state in superconductor has become a hot topic stimulated by the topological superconductivity. The edge state is a certain kind of Andreev bound state and is protected by the energy gap of the bulk Hamiltonian. In this presentation, we would like to discuss i) chiral Majorana Fermion in superconductor/topological insulator hybrid systems [1-2], ii) Helical edge modes and resulting spin current in non-centrosymmetric (NCS) superconductors [3] and iii) time reversal invariant Majorana fermion in NCS superconductors [4-5].

i) We study theoretically proximity-induced superconductivity and ferromagnetism on the surface of a topological insulator. We have clarified theoretically charge transport properties of normal metal (N) / ferromagnet insulator (FI) / superconductor (S) junction and S/FI/S junction formed on the surface of three-dimensional topological insulator (TI), where chiral Majorana mode (CMM) exists at FI/S interface. We have found that CMM generated in N/FI/S and S/FI/S junctions are very sensitively controlled by the direction of the magnetization  $\mathbf{m}$  in FI region. Especially, the current-phase relation of Josephson current in S/FI/S junctions has a phase shift neither 0 nor  $\pi$ , which can be tuned continuously by the component of  $\mathbf{m}$  perpendicular to the interface [1]. We have also studied proximity-induced superconductivity on the surface of a topological insulator (TI), focusing on unconventional pairing. The zero-energy surface state in the dxy-wave case becomes a Majorana fermion, in contrast to the situation realized in the topologically trivial high-Tc cuprates [2].

ii) We have clarified that in NCS superconductor with s+p-wave pairing, topologically nontrivial class analogous to the quantum spin Hall system is realized, when the amplitude of the p-wave pair potential is larger than that of s-wave one. The resulting helical edge modes as Andreev bound states carries spontaneous topologically protected spin current. We have found that the incident angle dependent spin polarized current flows through the interface due to the presence of the helical

iii) We have studied an Andreev bound state (ABS) and the surface density of state (SDOS) of a NCS superconductor where spin-singlet d-wave pairing mixes with spin-triplet p (or f)-wave pairing by spin-orbit coupling. For dxy + p-wave pairing, the ABS appears as a zero-energy state. The present ABS is a Majorana edge mode preserving the time-reversal symmetry. We calculate the topological invariant and discuss the relevance to a single Majorana edge mode. In the presence of the Majorana edge mode, the SDOS depends strongly on the direction of the Zeeman field [5]. We have also clarified that the present the time-reversal invariant Majorana bound state is manifested as a zero bias conductance peak when attached to normal metal.

[1] Y. Tanaka, T. Yokoyama and N. Nagaosa, Phys. Rev. Lett. 103, 107002 (2009).

[2] J. Linder, Y. Tanaka, T. Yokoyama A. Sudbo and N. Nagaosa, Phys. Rev. Lett. 103, 107002 (2009).

[3] Y. Tanaka, T. Yokoyama, A.V. Balatsky and N. Nagaosa, Phys. Rev. B 79, 060505 (2009).

[4] Y. Tanaka, Y. Mizuno, T. Yokoyama, K. Yada, and M. Sato, Phys. Rev. Lett. 105 097002 (2010).

[5] K. Yada, M. Sato, Y. Tanaka and T. Yokoyama, Phys. Rev. B, Vol. 83, 064505 (2011).

22RP-G-3

## THEORY OF JOSEPHSON TRANSPORT THROUGH FERROMAGNETIC INSULATORS AND SEMICONDUCTORS

*Kawabata S.*

Nanosystem Research Institute, National Institute of Advanced Industrial Science and Technology (AIST), Tsukuba, Ibaraki 305-8568, Japan; -kawabata@aist.go.jp

A superconducting ring with a p-junction made from superconductor (S) / ferromagnetic-metal (FM) / superconductor (S) exhibits a spontaneous current without an external magnetic field and the corresponding magnetic flux is half a flux quantum in the ground state [1]. Such a p-ring provides so-called "quiet qubit" that can be efficiently decoupled from the fluctuation of the external field [2]. However, the usage of FM gives rise to strong Ohmic dissipation. Therefore, the realization of p-junctions without FM is highly desired for qubit applications. We theoretically consider the possibility of the p-junction formation in the mesoscopic Josephson junctions with ferromagnetic insulators (FI) by taking into account the band structure of such materials explicitly [3]. In the case of the fully polarized FIs, e.g.,  $\text{La}_2\text{BaCuO}_5$  (LBCO) and  $\text{K}_2\text{CuF}_4$ , we found the formation of a p-junction and a novel atomic-scale 0-p transition induced by increasing the FI thickness  $LF$  [4, 5]. More remarkably, in the Josephson junction through the spin-filter materials such as Eu chalcogenides, the orbital hybridization between the conduction  $d$  and the localized  $f$  electron gives rise to a hybridization-induced p-junction [3]. Based on above peculiar results, we show that stable p-junction can be realized in junctions based on high- $T_c$  superconductors with LBCO barrier. Such FI-based Josephson junctions may become an element in the architecture of future quantum information devices [2].

[1] L. N. Bulaevskii, V. V. Kuzii, and A. A. Sobyenin, *JETP Lett.* **25** (1977) 291.

[2] L. B. Ioffe, V. B. Geshkenbein, M. V. Feigel'man, A. L. Fauchere, and G. Blatter, *Nature* **398** (1999) 679.

[3] S. Kawabata, and Y. Asano, *Int. J. Mod. Phys. B* **23** (2009) 4320.

[4] S. Kawabata, Y. Asano, Y. Tanaka, A. A. Golubov, and S. Kashiwaya, *Phys. Rev. Lett.* **104** (2010) 117002.

[5] S. Kawabata, and Y. Asano, *Low. Temp. Phys.* **36** (2010) 1143.

22TL-G-4

## SPIN-FERMION COUPLING IN IRON-BASED SUPERCONDUCTORS

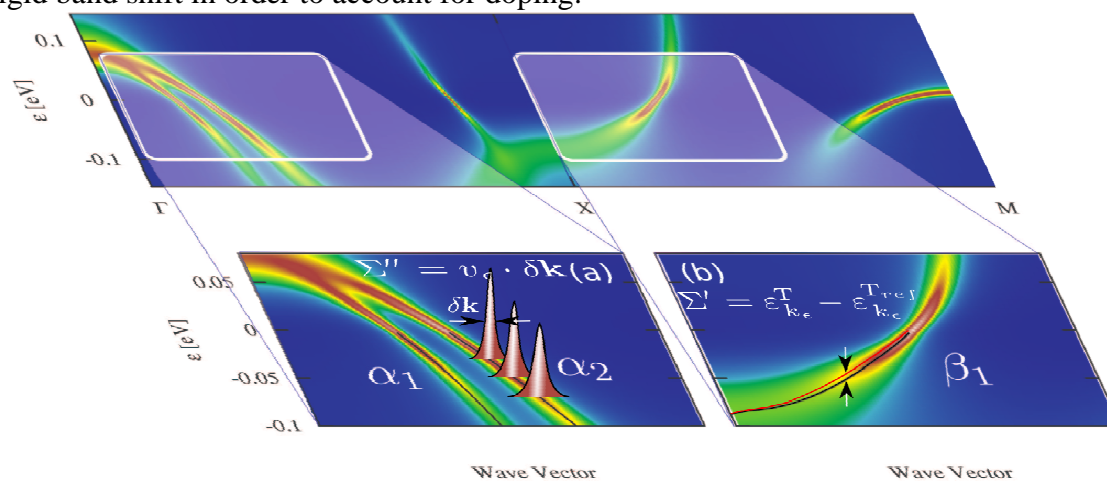
*Eschrig M., Heimes A., Grein R.*

SEPnet and Hubbard Theory Consortium, Department of Physics, Royal Holloway, University of London, Egham, Surrey TW20 0EX, United Kingdom

Magnetic inelastic neutron scattering (INS) studies of iron-based superconductors reveal a strongly temperature-dependent spectrum of the spin susceptibility in the normal conducting state [1], which develops a prominent low-energy resonance feature when entering the superconducting state [2].

Motivated by these experiments, we use a model recently introduced by us [3] of quasiparticles interacting with such a temperature dependent spin fluctuation spectrum, leading to a number of

predictions with respect to the influence of spin-fluctuations on the electronic spectrum. This includes the discussion of the quasiparticle scattering rate, the superconducting order parameter, as well as the modification of the Fermi surface. We also discuss numerically the validity of applying a rigid band shift in order to account for doping.



We apply our model to calculate observable single-particle quantities, which can be tested e.g. in angle resolved photoemission (ARPES) experiments or in scanning tunnelling spectroscopy (STS) experiments. In quantitative agreement with ARPES experiments we reproduce the quasiparticle dispersions obtained from momentum distribution curves (MDCs) as well as energy distribution curves (EDCs). We utilise an analysis of the theoretically obtained spectral functions motivated by the procedure that was applied to experimentally obtained spectra, which allows for a detailed comparison (see Figure for an example using our theoretical results). We discuss the relevance of the coupling between spin fluctuations and electronic excitations for the superconducting mechanism.

- [1] D.S. Inosov *et al.*, *Nature Physics*, **6** (2009), 178.
- [2] A.D. Christianson *et al.*, *Nature (London)*, **456** (2008), 930.
- [3] A. Heimes, R. Grein, and M. Eschrig, *Phys. Rev. Lett.*, **106** (2011) 047003.

22TL-G-5

## INTERFACE EFFECTS AND SPIN CURRENTS IN SUPERCONDUCTOR FERROMAGNET HETEROSTRUCTURES

*Belzig W.*

Department of Physics, University of Konstanz, 78457 Konstanz, Germany

Since the early work of Larkin and Ovchinnikov (1964) and Fulde and Ferrel (1965), who first pointed out the nontrivial ordered state emerging from the coexistence of superconductivity and magnetism, the search for manifestations of such novel states has been pursued. A novel twist in the last years is to use heterostructures, which allow for a greater variety in tuning the parameters governing the interplay of superconductivity and magnetism. In this way, so called  $\pi$ -Josephson junction couplings [Ryazanov *et al.* (2001)] were realized, long-range spin-triplet superconductivity was predicted [Bergeret *et al.* (2002)] and observed [Khaire *et al.* (2010)]. For the explanation of the surprising observation of a supercurrent through a half metal [Keizer *et al.* (2006)] a

microscopic treatment of the spin-scattering at an interface effects is necessary [Eschrig and Löffwänder (2008)].

The quasiclassical theory of superconductivity provides the most successful description of diffusive heterostructures comprising superconducting elements, namely, the Usadel equations for isotropic Green's functions [Usadel (1970)]. Close to interfaces, the Usadel equations have to be supplemented with boundary conditions for isotropic Green's functions. For a long time, the boundary conditions to the diffusion equation were available only for spin-degenerate contacts [Zaitsev (1984), Kupryanov and Lukichev (1988), Nazarov (1999)], which posed a serious limitation on the applicability of the Usadel description to modern structures containing ferromagnetic elements. We have closed this gap and derived spin-dependent boundary conditions for diffusive Green's functions [1,2]. We illustrate the importance of the spin-dependence of the boundary conditions by three examples:

1) We calculate the current noise of a superconductor-ferromagnet quantum point contact). This signal is qualitatively affected by the spin dependence of interfacial phase shifts acquired by electrons upon reflection on the interface potential. For a weakly transparent contact, noise steps appear at frequencies or voltages determined directly by the spin dependence of interfacial phase shifts [3,4].

2) The boundary conditions introduce a phase-shifting conductance  $G_\phi$ , which results from the spin dependence of the phase shifts acquired by electrons upon scattering on the interface. We have shown that  $G_\phi$  strongly affects the density of states and the supercurrents [6] predicted for superconducting/ferromagnetic hybrid circuits in agreement with experiments [Kontos *et al.* (2001), (2002)]

3) We investigate the Josephson current a diffusive magnetic junction with a complex magnetic structure. Using the spin-dependent quantum circuit theory, we obtain the phase diagram 0- and  $\pi$ -Josephson couplings for structures containing multiple barriers or non-collinear magnetic textures. The resulting spin-currents are interpreted as spin-torque onto the ferromagnetic structure showing a rich behavior as function of temperature and length of the junction. [5]

[1] D. Huertas-Hernando, Yu. V. Nazarov, and W. Belzig, *Phys. Rev. Lett.* **88**, 047003 (2002).

[2] A. Cottet, D. Huertas-Hernando, W. Belzig, and Yu. V. Nazarov, *Phys. Rev. B* **80**, 184511 (2009).

[3] A. Cottet and W. Belzig, *Phys. Rev. B* **77**, 064517 (2008).

[4] A. Cottet, B. Douçot, and W. Belzig, *Phys. Rev. Lett.* **101**, 257001 (2008).

[5] Z. Shomali, M. Zareyan, and W. Belzig, *Phys. Rev. B* **78**, 214518 (2008).

[6] A. Cottet and W. Belzig, *Phys. Rev. B* **72**, 180503 (2005).

22TL-G-6

**DYNAMIC PROPERTIES OF SIFS JOSEPHSON JUNCTIONS***Golubov A.A.<sup>1</sup>, Vasenko A.S.<sup>2</sup>, Kawabata S.<sup>3</sup>, Kupriyanov M.Yu.<sup>4</sup>, Bergeret F.S.<sup>5</sup>, Hekking F.W.J.<sup>6</sup>*<sup>1</sup> Faculty of Science and Technology and MESA+ Institute of Nanotechnology,  
University of Twente, 7500 AE Enschede, The Netherlands<sup>2</sup> Institut Laue-Langevin, 6 rue Jules Horowitz, BP 156, 38042 Grenoble, France<sup>3</sup> Institute of Advanced Industrial Science and Technology, Tsukuba, Ibaraki, 305-8568, Japan<sup>4</sup> Institute of Nuclear Physics Moscow State University, Leninskie gory, GSP-1, Moscow 119991,  
Russian Federation<sup>5</sup> Centro de Física de Materiales, Manuel de Lardizabal 5, E-20018 San Sebastián, Spain<sup>6</sup> Université Joseph Fourier and CNRS, 25 avenue des Martyrs, BP 166, 38042 Grenoble, France

Superconductor/insulator/ ferromagnet/ superconductor (SIFS) tunnel Josephson junctions exhibit interesting features like oscillatory behavior of the density of states (DOS) in the F-interlayer and  $0-\pi$  transitions in the Josephson current [1]. Due to combination of tunneling type of conductivity and exchange field in a ferromagnet, these junctions are suitable for applications in quantum circuits. Here we present a quantitative study of the current-voltage characteristics (CVC) of SIFS junctions. In order to obtain the CVC we calculate the DOS in the F/S bilayer for arbitrary length of the ferromagnetic layer, using quasiclassical theory. For a ferromagnetic layer thickness larger than the characteristic penetration depth of the superconducting condensate into the F layer, we find an analytical expression which agrees with the DOS obtained from a self-consistent numerical method. We discuss general properties of the DOS and its dependence on the parameters of the ferromagnetic layer. In particular we focus our analysis on the DOS oscillations at the Fermi energy. Using the numerically obtained DOS we calculate the corresponding CVC and discuss their properties. Finally, we use CVC to calculate the macroscopic quantum tunneling (MQT) escape rate for the current biased SIFS junctions.

[1] A. S. Vasenko, A. A. Golubov, M. Yu. Kupriyanov, and M. Weides, *Phys. Rev. B* **77**, 134507 (2008).

22TL-G-7

**PROXIMITY-EFFECT SUPERCONDUCTING TRIPLET SPIN VALVE***Tagirov L.R.<sup>1,2</sup>, Deminov R.G.<sup>1</sup>, Nedopekin O.V.<sup>1</sup>, Fominov Ya.V.<sup>3</sup>, Kupriyanov M.Yu.<sup>4</sup>,  
Karminskaya T.Yu.<sup>4</sup>, Golubov A.A.<sup>5</sup>*<sup>1</sup> Institute of Physics, Kazan Federal University, 420008 Kazan, Russia<sup>2</sup> Institute of Physics, Augsburg University, D-86135 Augsburg, Germany<sup>3</sup> L.D. Landau Institute for Theoretical Physics RAS, 119334 Moscow, Russia<sup>4</sup> Skobeltsyn Institute of Nuclear Physics, Moscow State University, 119992 Moscow, Russia<sup>5</sup> Faculty of Science and Technology and MESA+ Institute of Nanotechnology,  
University of Twente, 7500 AE Enschede, The Netherlands

We study the critical temperature  $T_c$  of S/F1/N/F2 core structure, where the magnetization direction of the outer F2 is kept fixed by a source of the exchange bias or induced anisotropy, or by the shape anisotropy. The nonmagnetic metal layer N in between of the F1 and F2 layers provides exchange decoupling of them. This spin-valve structure is attached to the singlet superconductor

layer S as an actuator to control the superconducting  $T_c$  of the latter. The basic idea goes up to the work by S. Oh *et al.* [1], however, we have taken into account the long-range triplet component of the superconducting pairing, which can be generated at noncollinear magnetizations of the F layers [2]. We demonstrate that  $T_c$  can be a nonmonotonic function of the angle  $\alpha$  between magnetizations of the two F layers. The minimum is achieved at an intermediate  $\alpha$ , lying between the parallel (P,  $\alpha = 0$ ) and antiparallel (AP,  $\alpha = \pi$ ) cases (see solution of the simplified problem for the S/F1/F2( $\infty$ ) structure in Ref. [3]). This implies a possibility of the “triplet” spin-valve effect: at temperatures above the minimum  $T_c$  but below the both,  $T_c^P$  and  $T_c^{AP}$ , the system is superconducting in the domain of angles around the collinear magnetizations of the F layers, but non-superconducting in the middle. At the same time, considering only the P and AP orientations, we find that both, the “normal”  $T_c^{AP} > T_c^P$ , and the “inverse”  $T_c^{AP} < T_c^P$  switching effects are possible depending on the choice of material properties and thickness of the layers [3-5]. With proper adjustment of the S-layer thickness the system can be driven into a regime of the re-entrant superconductivity as a function of the angle between magnetizations of the F1 and F2 layers [3,4]. It seems that observation of the unconventional “triplet” switching effect, or the re-entrant superconductivity in the S/F1/N/F2-type structures, could be an experimental indication of existence of the long-range odd triplet component of superconductivity in SF hybrids, predicted in Ref. [2].

This work was supported by RFBR (projects No. 11-02-00077-a, 11-02-00848-a, and 10-02-90014-Bel\_a), DFG (project No. GZ: HO 955/6-1), the Russian Ministry of Education and Science (contract No. P799), and the program “Quantum physics of condensed matter” of the RAS.

- [1] S. Oh, D. Youm, and M.R. Beasley, *Appl. Phys. Lett.* **71** (1997) 2376.  
 [2] F.S. Bergeret, A.F. Volkov, and K.B. Efetov, *Rev. Mod. Phys.* **77** (2005) 1321.  
 [3] Ya.V. Fominov, A.A. Golubov, T.Yu. Karminskaya *et al.*, *JETP Lett.* **91** (2010) 308.  
 [4] R.G. Deminov, L.R. Tagirov, O.V. Nedopekin *et al.*, *Phys. Rev. B*, submitted.  
 [5] P.V. Leksin, N.N. Garif'yanov, I.A. Garifullin *et al.*, *Phys. Rev. Lett.* **106** (2011) 067005.

22RP-G-8

## PROXIMITY EFFECT IN SFF STRUCTURES

*Karminskaya T.<sup>1</sup>, Kupriyanov M.<sup>1</sup>, Golubov A.<sup>2</sup>, Prischepa S.<sup>3</sup>*

<sup>1</sup> Institute of Nuclear Physics Moscow State University, Leninskie gory, GSP-1, Moscow 119991, Russian Federation

<sup>2</sup> Faculty of Science and Technology and MESA+ Institute of Nanotechnology, University of Twente, P.O. Box 217, 7500 AE Enschede, The Netherlands

<sup>3</sup> Belarus State University of Informatics and Radioelectronics, P. Browka 6, Minsk 220013, Belarus

Nowadays there is a considerable interest to the structures composed from superconducting (S) and ferromagnetic (F) layers. The possibility of  $\pi$ -states in SFS Josephson junctions due to oscillatory nature of superconducting order parameter induced into a ferromagnet was predicted theoretically and has been convincingly demonstrated by experiments [1]-[3]. It was also predicted that in Josephson junctions with several ferromagnetic layers it is possible to realize  $\pi$ -states even in the case when the F-layers are so thin that order parameter oscillations cannot develop there, but phase slips occur at the SF interfaces with finite transparency. This effect was predicted in [4] for

SFIFS junctions, where two SF-bilayers are decoupled by an insulating barrier 'I'. In this case phase shifts  $\delta\varphi$  occur at each of the SF interfaces and saturate at  $\delta\varphi = \pi/2$  with the increase of exchange field. As a result, total phase shift across the junction equals to  $\pi$ .

Recently, structures where two F-layers are coupled to a superconductor (FSF or SFF) attracted much attention since they may serve as superconducting spin valves, where transition temperature is controlled by angle  $\alpha$  between magnetization directions of the F-layers [5]. The SFF structures with fully transparent interfaces were studied theoretically in [6], where it was shown that critical temperature in such trilayers can be a nonmonotonic function of the angle  $\alpha$ .

In this paper we address important issue of the influence of interface transparency on singlet and triplet correlations in SFF structures and show that phase slips at both interfaces lead to a number of new peculiar phenomena. First, for parallel orientations of magnetizations in the F-layers,  $\pi$ -state in SFFIS Josephson junction can be realized as a result of two subsequent  $\pi/2$  phase shifts at the interfaces. Second, the magnitude of long-range triplet component which is generated in SFF structures with varying angle  $\alpha$  between the F-layer magnetizations, has anomalous dependence on  $\alpha$ . Namely, contrary to the previous knowledge based on analysis of symmetric FSF or SFFS structures, the triplet component in SFF structures reaches maximum not in the vicinity of  $\alpha=\pi/2$  and can be even zero for this configuration of magnetization vectors. We also show how these new effects manifest itself in the conductance of F layers and in the realization of  $0-\pi$  transition in SFFIS tunnel junctions.

Support by BFBR grant  $\Phi 10P-063$  and RFBR grant 10-02-90014-Бел-а is acknowledged.

[1] A.A. Golubov, M. Yu. Kupriyanov, and E. Il'ichev, *Rev. Mod. Phys.*, **76** (2004) 411.

[2] A.I. Buzdin, *Rev. Mod. Phys.*, **77**, (2005) 935.

[3] F.S. Bergeret, A. F. Volkov, K. B. Efetov, *Rev. Mod. Phys.*, **77** (2005) 1321.

[4] A.A. Golubov, M.Yu.Kupriyanov and Ya.V. Fominov, *JETP Letters*, **75** (2002) 190.

[5] P.V. Leksin, N.N. Garif'yanov, I.A. Garifullin,, *et al. Phys. Rev. Lett.*, **106** (2011) 067005.

[6] Ya.V. Fominov, A.A. Golubov, T.Yu. Karminskaya, *et al.*, *Pis'ma v ZhETF* **91**, (2010) 329.

22OR-G-9

## SIFS JOSEPHSON JUNCTION: FROM THE CLEAN TO THE DIRTY LIMIT

*Pugach N.G.<sup>1</sup>, Kupriyanov M.Yu.<sup>2</sup>, Goldobin E.<sup>3</sup>, Koelle D.<sup>3</sup>, Kleiner R.<sup>3</sup>*

<sup>1</sup> Faculty of Physics, M.V. Lomonosov Moscow State University, Leninskie Gory, GSP-2, Moscow 119991, Russia

<sup>2</sup> Skobeltsyn Institute of Nuclear Physics M.V. Lomonosov Moscow State University, Leninskie gory, GSP-1, Moscow 119991, Russia

<sup>3</sup> Physikalisches Institut-Experimentalphysik II, Universität Tübingen, Auf der Morgenstelle 14, D-72076 Tübingen, Germany

The interplay between dirty and clean limits for Superconductor-Ferromagnet-Superconductor (SFS) Josephson junctions is a subject of intensive theoretical studies [1,2]. SIFS junctions, containing an additional insulator (I) barrier are interesting as potential logic elements in superconducting circuits, since their critical current  $I_c$  can be tuned over a wide range, still keeping a high  $I_c R_N$  product, where  $R_N$  is the normal resistance of the junction. They are also a convenient model system for a comparative study of the  $0-\pi$  transitions for arbitrary relations between

characteristic lengths of the F-layer: the layer thickness  $d$ , the mean free path  $l$ , the magnetic length  $\xi_H = v_F/2H$ , and the nonmagnetic coherence length  $\xi_0 = v_F/2\pi T_C$ , where  $v_F$  is the Fermi velocity,  $H$  is the exchange magnetic energy, and  $T_C$  is the critical temperature of the superconducting electrodes. The spatial variations of the order parameter are described by the complex coherent length in the ferromagnet  $\xi_F^{-1} = \xi_1^{-1} + i\xi_2^{-1}$ . It is well known, that in the dirty limit ( $l \ll \xi_{1,2}$ ) described by the Usadel equations both  $\xi_1^2 = \xi_2^2 = v_F l/3H$  [3].

In this work the spatial distribution of the anomalous Green's functions and the Josephson current in the SIFS junction are calculated. The linearized Eilenberger equations are solved together with Zaitsev boundary conditions [5]. This allows comparing the dirty and the clean limits, investigating a moderate disorder, and establishing the applicability limits of the Usadel equations for such structures. We demonstrate that for an arbitrary relation between  $l$ ,  $\xi_H$ , and  $d$  the spatial distribution of the anomalous Green's function can be approximated by a single exponent with reasonable accuracy, and we find its effective decay length and oscillation period for several values of  $\xi_H$ ,  $l$  and  $d$ . The role of different types of the FS interface is analyzed. The applicability range of the Usadel equation is established.

The results of calculations have been applied to the interpretation of experimental data obtained on Nb|Al<sub>2</sub>O<sub>3</sub>|Cu|Ni|Nb Josephson junctions containing a Ni layer with moderate scattering [6].

Support by RFBR and SFB TRR-21 is acknowledged.

- [1] F. S. Bergeret, A. F. Volkov, and K. B. Efetov, *Phys. Rev. B* **64** (2001) 134506.
- [2] J. Linder, M. Zareyan, and A. Sudbo, *Phys. Rev. B* **79** (2009) 064514.
- [3] A. I. Buzdin, *Rev. Mod. Phys.* **77** (2005) 935.
- [4] A. A. Golubov, M. Yu. Kupriyanov, E. Il'ichev, *Rev. Mod. Phys.* **76** (2004) 411.
- [5] A. V. Zaitsev, *Zh. Exp. Teor. Fiz.* **86** (1984) 1742 [*Sov. Phys. JETP* **59** (1984) 1015].
- [6] A. A. Bannykh, J. Pfeiffer, V. S. Stolyarov, I. E. Batov, V. V. Ryazanov, M. Weides, *Phys. Rev. B* **79** (2009) 054501.



**22 August**

Monday

12:00-14:00

oral session

22TL-H

**“Micromagnetics”**

22TL-H-1

## MICROMAGNETIC ANALYSIS OF DOMAIN WALL DYNAMICS AND ITS APPLICATIONS

*Martinez E.*

Dpto. Física Aplicada, Universidad de Salamanca, Plaza de los Caidos s/n, Spain.

Several memory and logic devices based on the motion of magnetic domains walls (DWs) have been proposed over the last years. Traditionally, DWs were driven by magnetic field [1], but in recent years, new paradigms for DW-based devices have been made possible by the direct manipulation of DWs with spin polarized currents through the mechanism of the spin-momentum transfer [2]. Because this new architecture involves a precise understanding of the DW along ferromagnetic stripes, it is of crucial importance to determine how thermal fluctuations influence on the DW dynamics along stripes with surface roughness and on the depinning from a single notch. The study is also of fundamental interest, because the comparison between theoretical predictions and experimental observations of DW motion and DW depinning from a single notch by means of both magnetic field and/or applied current, could be used to determine intrinsic quantities such as polarization factor and the magnitude of the non-adiabatic spin torque.

This invited talk will be focused on characterizing the domain wall dynamics along both soft stripes and others with high perpendicular magnetocrystalline from a theoretical point of view, by using both a full micromagnetic description and the one-dimensional model. It will review the DW injection [3] and its subsequent motion along stripes with surface roughness driven by both static magnetic field and applied current, with emphasis on thermal effects [4]. The DW pinning and the depinning will be also analyzed under the action of static [5], oscillating [6] and pulses [7] of fields and/or currents. From these studies, some novel technological applications, such the ones which exploit the stochastic resonance phenomenon of a DW between two pinning sites [8], will be proposed and described.

- [1] D. A. Allwood et al, *Science*, **296**, 2003 (2002).
- [2] S. S. P. Parkin, *U. S. Patent*, 6834005 (2004).
- [3] J. L. Prieto et al. *Phys. Rev. B*, **83**, 104425 (2011).
- [4] E. Martinez et al. *Phys. Rev. B*, **75**, 174409 (2007).
- [5] E. Martinez et al. *Phys. Rev. Lett.* **98**, 267202 (2007);
- [6] E. Martinez et al. *J. Appl. Phys*, **106**, 043914 (2009).
- [7] E. Martinez et al. *Phys. Rev. B*, **77**, 144417 (2008).
- [8] E. Martinez et al. *Phys Rev. B*, **79**, 094430 (2009).
- [9] E. Martinez et al. *Appl. Phys. Lett.* **98**, 072507 (2011).

22TL-H-2

## FERROMAGNETIC RESONANCE MEASUREMENTS AND SIMULATIONS ON PERIODIC HOLE AND DISC ARRAYS

*Sklenar J.<sup>1</sup>, Bhatt V.<sup>2</sup>, Tsai C.C.<sup>3</sup>, Rivkin K.<sup>4</sup>, Heinonen O.<sup>5</sup>, DeLong L.D.<sup>2</sup>, Ketterson J.B.<sup>1</sup>*

<sup>1</sup> Department of Physics, Northwestern University, Evanston, IL, 60209

<sup>2</sup> Department of Physics, University of Kentucky, Lexington, KY, 40506

<sup>3</sup> Department of Engineering & Management of Advanced Technology,  
Chang Jung Christian University, Tainan 71101, Taiwan

<sup>4</sup> Seagate Technology, Bloomington, MN 55435-5489 U.S.A.

<sup>5</sup> Materials Science Division, Argonne National Laboratory, Argonne, IL, 60515

Using a broad band meander-line based technique, that allows the study of mode structure continuously as a function of applied microwave frequency, we have carried out extensive ferromagnetic resonance (FMR) measurements on arrays of e-beam patterned square-, circular- and diamond-shaped holes that form a square Bravais lattice in thin permalloy films. Such samples show multiple resonances. At higher fields, where the sample is uniformly magnetized, the behavior is non hysteretic and the overall structure of the FMR spectrum displays the symmetry of the underlying lattice. At low fields, resonances that are positioned asymmetrically with respect to positive and negative fields (and sometimes absent all together for one field direction) are observed when sweeping from positive fields through zero to negative fields; a corresponding behavior is observed when sweeping in the opposite direction. Such hysteretic effects, typically limited to studies of static characteristics, represent a relatively novel development in FMR studies, particularly with respect to their connection with symmetry-breaking (e.g. domain formation) transitions in the underlying lattice.

Simulations of the static magnetization distribution and FMR mode spectrum were carried at low and high fields using both the discrete dipole approximation (DDA) and Fourier transform methods. The DDA is adapted to incorporate the periodicity of the underlying lattice as well as the Bloch-like structure of the excitations. On the other hand the Fourier transform approach, applied to a large but finite array of holes, allows calculations at low fields where domain formation can break the translational symmetry of the hole lattice. Such calculations are generally in good agreement with the experiments with respect to field, field-angle and microwave frequency.

As a simple model of the high field FMR spectrum one can view the underlying hole lattice as a two dimensional diffraction grating that couples the essentially uniform microwave field (on the scale of the patterned array) into modes with wave vectors corresponding to the first and higher Brillouin zones associated with the lattice. Magneto-static contributions, originally described by Damon and Eshbach, result in differing dispersion for wave vector components parallel and perpendicular to the in-plane field direction resulting in the presence of multiple resonances (in addition to the uniform mode) along with a nontrivial dependence on the angle between the magnetic field and the symmetry axes of the lattice.

Supported by NSF Grant DMR-0509357, U.S. DoE Grant #DE-FG02-97ER45653 and Argonne National Laboratory operated under Contract No. DE-AC02-06CH11357.

## EDGE-SOLITON-MEDIATED VORTEX-CORE REVERSAL DYNAMICS

*Lee K.S., Yoo M.W., Choi Y.-S., Kim S.-K.*

National Creative Research Initiative Center for Spin Dynamics and Spin-Wave Devices,  
Nanospinics Laboratory, Department of Materials Science and Engineering, Seoul National  
University, Seoul 151-744, Republic of Korea; Corresponding author: sangkoog@snu.ac.kr, Phone:  
+82-2-880-5854, Fax: +82-2-885-1457

In micrometer-size (or smaller) magnetic elements, magnetic topological solitons play their crucial roles in the dynamics of ultrafast magnetization reversals [1]. One of typical examples is a well-known vortex-antivortex-pair-mediated vortex-core reversal in nanodisks; vortex-core reversals take place through the creation and annihilation of a pair of a vortex and an antivortex bulk topological solitons [2-4] while conserving the total winding number topological charge of involved solitons. However, another topological charge, the Skyrmion number decays when a pair of vortex and antivortex annihilates. Thus, the exchange energy of the Skyrmion dissipates drastically through the exchange energy explosion and subsequent spin-wave emission [2-4]. In this presentation, we are going to report a new reversal mechanism of single vortex cores in magnetic disks driven by currents flowing perpendicular to the disk plane, as found from micromagnetic simulations [5]. This mechanism is totally different from the well-known vortex-antivortex pair mediated vortex core reversal in terms of the associated topological solitons, energies, and spin-wave emissions. In this mechanism, vortex core switching occurs through serial dynamic transformations from an initial vortex to a pair of two edge solitons, again back to a newly created vortex of reversed core orientation. In contrast to the vortex-antivortex pair mediated vortex core switching, the exchange energy of the Skyrmion does not dissipate drastically through the spin-wave emission but it converts to the strong magnetostatic energy of paired edge solitons. This work provides deeper physical insights into the dynamic transformations of magnetic topological solitons in magnetic nanoscale elements.

This work was supported by Basic Science Research Program through the National Research Foundation of Korea (NRF) funded by the Ministry of Education, Science and Technology (No. 20110000441).

[1] N. D. Mermin, *Rev. Mod. Phys.* **51**, 591 (1979); O. Tchernyshyov and G. Chern, *Phys. Rev. Lett.* **95**, 197204 (2005).

[2] B. Van Waeyenberge *et al.*, *Nature* **444**, 461 (2006).

[3] Q. F. Xiao *et al.*, *Appl. Phys. Lett.* **89**, 262507 (2006); R. Hertel *et al.*, *Phys. Rev. Lett.* **98**, 117201 (2007).

[4] K.-S. Lee *et al.*, *Phys. Rev. B* **78**, 014405 (2008); K. Y. Guslienko, K.-S. Lee, and S.-K. Kim, *Phys. Rev. Lett.* **100**, 027203 (2008); K.-S. Lee *et al.*, *Phys. Rev. Lett.* **101**, 267206 (2008).

[5] K.-S. Lee *et al.*, *Phys. Rev. Lett.* **106**, 147201 (2011).

**22 August**

Monday

15:00-17:00

oral session

22TL-H

22OR-H

**“Intermetallic  
Compounds”**

22TL-H-4

## HIGH-FIELD MAGNETISM AND MAGNETOACOUSTICS IN URANIUM INTERMETALLICS ANTIFERROMAGNETS

*Andreev A.V.<sup>1</sup>, Skourski Y.<sup>2</sup>, Yasin S.<sup>2</sup>, Zherlitsyn S.<sup>2</sup>, Wosnitza J.<sup>2</sup>*

<sup>1</sup> Joint Laboratory for Magnetic Studies, Institute of Physics ASCR and Charles University, Na Slovance 2, 18221 Prague 8, The Czech Republic

<sup>2</sup> Dresden High Magnetic Field Laboratory, Helmholtz-Zentrum Dresden-Rossendorf, Dresden, 01314, Germany

We report on recent collaborated studies of the magnetic and magnetoacoustic anomalies in several uranium intermetallic antiferromagnets (AF). The uranium intermetallics are known to have huge magnetic anisotropy. For this reason, the study has been performed on the single crystals (grown by the Czochralski method in a tri-arc furnace in Prague) in pulsed magnetic fields up to 60 T (in Dresden).

The U magnetic moments of  $1.4 \mu_B$  in  $UCo_2Si_2$  ( $T_N = 82.5$  K) lie along the  $c$  axis of the tetragonal lattice. In magnetic fields applied along this axis, we observed the metamagnetic transition (MT) in 45 T (at 1.4 K). The MT is extremely sharp but exhibits a very small hysteresis. With increasing temperature, the MT becomes broader and vanishes at  $T_N$ . The magnetization gain upon the MT corresponds roughly to 1/3 of the U magnetic moment. For this reason, we suppose that the state above the MT is ferrimagnetic with the  $++-$  arrangement of the magnetic moments. Such magnetic structure exists in the ground state of the isostructural analogue  $UNi_2Si_2$ . The ultrasound measurements confirm the transition, which is accompanied by anomalies in both sound velocity and sound attenuation, and show its rather complicated temperature evolution.

In  $UCu_{0.95}Ge$  ( $T_N = 48$  K), the magnetic moments are in the basal plane of the hexagonal lattice. The MT to the forced ferromagnetic (FF) state with U magnetic moment of  $1.3 \mu_B$  occurs in the field of 38 T applied along the  $c$ -axis. The sound velocity and the sound attenuation exhibit well-pronounced anomalies at the transitions, both the spontaneous at  $T_N$  and the field-induced to the FF state. In the paramagnetic range, both acoustic characteristics show large frequency-dependent changes revealing the presence of unusual relaxation processes of a non-magnetic origin which are presumably connected with dynamics of defects in the Cu sublattice.

$U\text{IrGe}$  with  $T_N = 16$  K exhibits a large magnetic anisotropy with the hard direction along the  $a$  axis of the orthorhombic structure. Along the  $b$  and  $c$  axes, the MT towards the FF state is observed at 21 and 14 T, respectively. The sound velocity displays an anomaly of  $1 \times 10^{-4}$  at  $T_N$ . The MT along the  $b$  and  $c$  axis are accompanied by a lattice softening with a sound-velocity change of about  $1.5 \times 10^{-3}$ . Thus, the MTs affect the sound velocity much stronger than the spontaneous AF ordering.

In  $U_2Ni_2Sn$  ( $T_N = 26$  K), three metamagnetic transitions are observed at 30, 40 and 52 T in field applied along the  $c$  axis of the tetragonal lattice at 1.4 K. The magnetic moment reaches  $1.5 \mu_B/\text{f.u.}$  (formula unit) in 60 T without any trend to saturation. Magnetization curve along the  $a$  axis is a linear paramagnetic-like response up to  $0.5 \mu_B/\text{f.u.}$  in 60 T. The magnetoacoustic and neutron-diffraction studies of the  $U_2Ni_2Sn$  single crystal are in progress.

This work has been supported by grant GACR 202/09/0339 of the Czech Science Foundation and by EuroMagNET under the EU contract 228043.

## MAGNETIC PHASE TRANSITIONS IN LAYERED INTERMETALLIC COMPOUNDS

*Mushnikov N.V., Gerasimov E.G., Rosenfeld E.V., Terentyev P.B., Gaviko V.S.*

Institute of Metal Physics, Ural Branch of RAS, S. Kovalevskaya 18, 620990 Ekaterinburg, Russia

Layered magnets are either artificial or natural magnetic structures in which magnetic atoms form layers separated from each other by different layers of nonmagnetic atoms. In such structures, strong ferromagnetic interaction of magnetic atoms inside the layer can provide high temperatures of magnetic ordering. At the same time, the formation of magnetic structure as a whole is traceable to a relatively weak interlayer interaction. Such magnetic structure can in particular be sensitive to changes in magnetic field or pressure. In addition to the collinear ferromagnetic (F) or antiferromagnetic (AF) ordering in the layered magnets, there frequently emerge noncollinear and spiral magnetic structures.

We studied magnetic, thermal and magnetotransport properties of quasi-ternary layered intermetallic compounds  $R_{1-x}R'_x\text{Mn}_2\text{Si}_2$  and  $R_{1-x}R'_x\text{Mn}_6\text{Sn}_6$ . In these systems, substitution of different  $R$  atoms allows us to change gradually the interatomic distances, interlayer exchange interactions and contributions of  $R$  and Mn magnetic subsystems to the magnetic anisotropy of the compounds.

The  $\text{RMn}_2\text{Si}_2$  compounds exhibit an unusual variation of the type of interlayer Mn-Mn ordering from AF to F with increasing of the intralayer Mn-Mn distance. Temperature of the AF to F magnetic phase transition depends on the composition and is strongly influenced by magnetic field and pressure. Large linear and volume magnetostrictions and positive magnetoresistance were observed at the field-induced transition. The Mn sublattice is characterized by unusually high magnetic anisotropy in both ferromagnetic and paramagnetic states. We found a correlation between the lattice parameters and the density of states at the Fermi level. The value of  $N(E_F)$  increases with increasing the intralayer Mn-Mn distances and is almost independent of the distances between the Mn magnetic layers.

For the  $\text{RMn}_6\text{Sn}_6$  compound with a non-magnetic  $R = \text{Y}$ , the double flat spiral magnetic structure is realized below the Neel temperature 333 K. We developed a model which allows us to determine the exchange and anisotropy parameters and to predict the behavior of the spiral magnetic structure in magnetic field. Substitution of Tb for Y leads to the formation of ferrimagnetic structure in which the Tb and Mn sublattices give opposite contributions to the magnetic anisotropy of the compounds. This competition leads to the occurrence of a spin-reorientation transition. For some temperature interval around the transition, application of magnetic field in hard direction induces a first-order magnetization process. The transition field can be varied by changing the alloy composition. The obtained results show a significant role of complicated Mn-Mn and Mn- $R$  exchange interactions in formation of the magnetic structures of and magnetic phase transitions in layered intermetallic compounds.

This work was supported by the Russian Foundation for Basic Research (grant No. 09-02-00272) and by UB RAS (project 09-C-2-1016).

## UNIAXIAL $R_2\text{Co}_{17}$ FERRIMAGNETS IN HIGH MAGNETIC FIELDS

Skourski Y.<sup>1</sup>, Andreev A.V.<sup>2</sup>, Kuz'min M.<sup>3</sup>, Wosnitzer J.<sup>1</sup>

<sup>1</sup> Hochfeld-Magnetlabor Dresden, Helmholtz-zentrum Dresden-Rossendorf, Dresden, Germany

<sup>2</sup> Institute of Physics, ASCR, Na Slovance 2, 18221 Prague, Czech Republic

<sup>3</sup> Leibniz-Institut für Festkörper- und Werkstofforschung, PF 270116, 01171 Dresden, Germany

Rare-earth intermetallic compounds  $R_2\text{Co}_{17}$  and  $R_2\text{Fe}_{17}$  form an interesting group of magnetic materials and their properties have been extensively studied in the last decades. In these compounds, as generally in  $R$ - $T$  transition-metal compounds, the strongest interaction is the  $3d$ - $3d$  interaction which primarily determines  $T_C$ . The  $4f$ - $3d$  interaction, although much weaker than the  $3d$ - $3d$  interaction, is of special importance since it couples the strongly anisotropic  $R$ -sublattice moment to that one of much less anisotropic  $T$ -sublattice.  $R_2\text{Co}_{17}$  and  $R_2\text{Fe}_{17}$  compounds (crystallizing in the hexagonal  $\text{Th}_2\text{Ni}_{17}$ -type structure), where  $R$  is a heavy rare-earth element, are ferrimagnetic and high magnetic fields are needed to induce changes in the magnetic configuration.

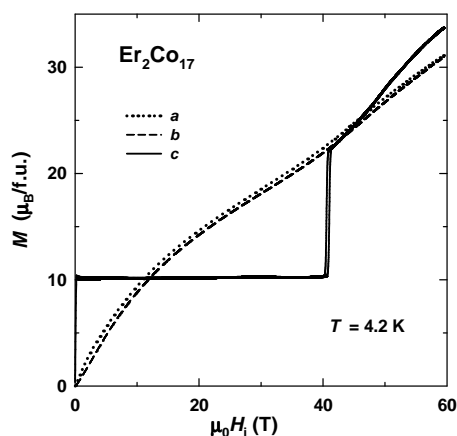


Fig. 1. Magnetization curves of an  $\text{Er}_2\text{Co}_{17}$  single crystal measured at  $T = 4.2$  K

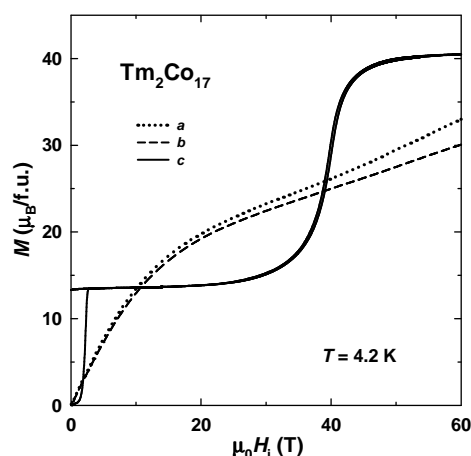


Fig. 2. Magnetization curves of a  $\text{Tm}_2\text{Co}_{17}$  single crystal measured at  $T = 4.2$  K.

For the majority of these compounds ( $\text{Er}_2\text{Fe}_{17}$  and all of them with  $R = \text{Tb}, \text{Dy}, \text{Ho}$ ), the preferred moment direction is located in the basal plane. If a sufficiently high magnetic field is applied along one of the main crystallographic directions in the basal plane, field-induced transitions will occur before the forced-ferromagnetic state is reached. The particular shape of the magnetization curves depends strongly on the magnetic anisotropy within the basal plane and is rather well understood. On the other hand, there is a small group of  $R_2\text{T}_{17}$  compounds i.e.,  $\text{Er}_2\text{Co}_{17}$ ,  $\text{Tm}_2\text{Co}_{17}$  and  $\text{Tm}_2\text{Fe}_{17}$ , in which the hexagonal  $c$  axis is the easy moment direction. In this case, the forced ferromagnetic state should be reached in high fields as well, however, the situation is more complicated than in the easy-plane compounds. We have studied high-field magnetization in two of these compounds,  $\text{Er}_2\text{Co}_{17}$  and  $\text{Tm}_2\text{Co}_{17}$  and found a markedly disparate high-field behavior. In  $\text{Er}_2\text{Co}_{17}$ , high external magnetic field applied along the  $c$  axis breaks down the ferrimagnetic ground state and drives the system towards ferromagnetic order via a non-collinear intermediate phase. This manifests itself in a jump on the magnetization curve, followed by a prolonged interval of further continuous growth (Fig. 1). In  $\text{Tm}_2\text{Co}_{17}$ , a collinear remagnetization takes place: as the applied magnetic field grows, the Tm moments disorder at first, reaching a fully disordered paramagnetic state at a critical field, then they order magnetically in the opposite sense, (Fig. 2).



22OR-H-7

## MUON-SPIN RELAXATION STUDY OF RARE EARTH AND IRON MAGNETISM IN $R\text{FeAsO}$ ( $R = \text{La, Ce, Pr, Sm, Gd AND Nd}$ )

*Pashkevich Yu.*<sup>1</sup>, *Luetkens H.*<sup>2</sup>, *Maeter H.*<sup>3</sup>, *Pascua G.*<sup>2</sup>, *Dellmann T.*<sup>3</sup>, *Khasanov R.*<sup>2</sup>, *Amato A.*<sup>2</sup>,  
*Gusev A.*<sup>1</sup>, *Lamonova K.*<sup>1</sup>, *Chervinskii D.*<sup>1</sup>, *Klingeler R.*<sup>4</sup>, *Hess C.*<sup>4</sup>, *Behr G.*<sup>4</sup>, *Büchner B.*<sup>4</sup>, *Klauss  
H.-H.*<sup>3</sup>

<sup>1</sup> A. A. Galkin Donetsk PhysTech NASU, 83114 Donetsk, Ukraine

<sup>2</sup> Lab. for Muon-Spin Spectr., Paul Scherrer Institute, CH-5232 Villigen PSI, Switzerland

<sup>3</sup> Institut für Festkörperphysik, TU Dresden, D-01069 Dresden, Germany

<sup>4</sup> Leibniz-Institut für Festkörper und Werkstofforschung (IFW), D-01171 Dresden, Germany

We report zero field muon spin relaxation ( $\mu\text{SR}$ ) measurements on layered  $R\text{FeAsO}$  with  $R = \text{La, Ce, Pr, and Sm}$  [1] as well recently studied  $R = \text{Nd and Gd}$ . We study the interaction of the  $\text{Fe}$  and rare earth electronic systems in the magnetically ordered parent compounds of  $R\text{FeAsO}_{1-x}\text{F}_x$  superconductors via a detailed comparison of the local hyperfine fields at the muon site with available Mössbauer spectroscopy and neutron scattering data. These studies provide microscopic evidence of long range commensurate magnetic  $\text{Fe}$  order with the  $\text{Fe}$  moments not varying by more than 15% within the series  $R\text{FeAsO}$  with  $R = \text{La, Ce, Pr, Sm, Nd and Gd}$ . The absolute value of low temperature iron magnetic moment, extracted from  $\mu\text{SR}$  frequencies, falls in the region 0.54-0.63  $\mu_B$  that is in nice agreement with recent neutron studies [2,3]. At low temperatures long range  $R$  magnetic order is observed. Different combined  $\text{Fe}$  and  $R$  magnetic structures are proposed for all compounds using the muon site in the crystal structure obtained by electronic potential calculations. We demonstrate that rare earth order in  $\text{Ce, Pr, Nd and Gd}$  compounds has easy - plane character. Our data point out to a strong effect of  $R$  order on the iron subsystem in the case of different symmetry of  $\text{Fe}$  and  $R$  order parameters resulting in a  $\text{Fe}$  spin reorientation in the  $R$  ordered phase in  $\text{PrFeAsO}$ . Non-collinear magnetic order of  $\text{Ce}$  and  $\text{Sm}$  is found by  $\mu\text{SR}$  in the corresponding compounds, which is explained by a weak coupling of adjacent  $R$  planes in the  $R\text{-O-R}$  layer. Our symmetry analysis proves the absence of  $\text{Fe-R}$  Heisenberg like interactions in  $R\text{FeAsO}$ . A strong  $\text{Fe-Ce}$  coupling due to non-Heisenberg anisotropic exchange is found in  $\text{CeFeAsO}$  which results in a large staggered  $\text{Ce}$  magnetization induced by the magnetically ordered  $\text{Fe}$  sublattice far above  $T_N(\text{Ce})$ . Like in the elastic neutron scattering experiment [3] in  $\text{NdFeAsO}$  we observe iron spin reorientation first order phase transition induced by  $\text{Nd}$  subsystem at the temperature above  $T_N(\text{Nd}) = 6 \text{ K}$ . Besides, below 2 K we observe strong increase of muon's spin dynamic relaxation rate pointing out on additional spin-orientation phase transition. We propose a minimal model to describe both phase transitions. Finally, we discuss the influence of the magnetic  $R\text{-Fe}$  interaction on the observed enhanced superconductivity in the  $R\text{FeAsO}_{1-x}\text{F}_x$  with a magnetic  $R$  ion.

Support by Swiss National Science Foundation (grant SNSF IZKOZ2\_134161) and Russian-Ukrainian grant No. 9-2010 are acknowledged.

[1] H. Maeter, H. Luetkens, Yu.Pashkevich, A. Kwadrin, R. Khasanov, A. Amato, A.Gusev, K.Lamonova, D. Chervinskii, R. Klingeler, C. Hess, G. Behr, B.Büchner, and H.-H. Klauss, *Phys.Rev.* **80**, 094524 (2009).

[2] N. Qureshi, et al *Phys. Rev. B* **82**, 184521 (2010)

[3] H.-F. Li, et al, *Phys. Rev. B* **82**, 064409 (2010)

[4] W. Tian et al, *Phys. Rev. B* **82**, 060514(R) (2010).

## MAGNETOELASTICITY IN $R_2\text{Fe}_{17}$ -BASED INTERMETALLICS WITH NON-MAGNETIC RARE EARTHS

Tereshina E.A.<sup>1,2</sup>, Andreev A.V.<sup>2</sup>, Watanabe K.<sup>1</sup>

<sup>1</sup> HFLSM, Institute for Materials Research, Tohoku University, 980-8577 Sendai, Japan

<sup>2</sup> Institute of Physics ASCR, 18221 Prague, Czech Republic

Since the discovery of the Invar effect in Fe-containing compounds, numerous studies of the phenomena have been performed. Apart from the classical systems such as Fe-Ni and  $\gamma$ -Fe, large magnetovolume effects have been also observed in the compounds with a high Fe content, e.g.  $R_2\text{Fe}_{17}$  ( $R$  is the rare earth metal). The peculiar magnetism of  $R_2\text{Fe}_{17}$  with anomalously low ordering temperatures across the series and with the non-collinear magnetic structures found in some of the compounds was attributed to a strong dependence of exchange interactions on the Fe-Fe interatomic distances.

$\text{Y}_2\text{Fe}_{17}$  (ferromagnetic (F)) and  $\text{Lu}_2\text{Fe}_{17}$  (ferromagnetic at low temperatures, with the transition into an antiferromagnetic (AF) phase above 130 K) show large spontaneous magnetostriction at low temperatures with the volume effect  $\sim 10^{-2}$  [1]. Noticeable field-induced magnetostriction was also observed in  $\text{Lu}_2\text{Fe}_{17}$  around the Néel temperature  $T_N \sim 274$  K [2]. In the present work, the study is performed on a series of Ru-doped compounds of  $R_2\text{Fe}_{17}$  ( $R = \text{Lu}, \text{Y}$ ), where the non-collinear AF phase is stabilized down to the lowest temperatures. The investigation is performed by the macro- (capacitor method on selected single crystals) and microscopic (X-ray diffraction in magnetic field up to 5 T) methods.

For both series of  $\text{Lu}_2\text{Fe}_{17-x}\text{Ru}_x$  ( $x = 0.5, 1$ ) and  $\text{Y}_2\text{Fe}_{17-x}\text{Ru}_x$  ( $x = 0.25, 0.5, 0.75, 1$ ), the field-induced metamagnetic AF-F transitions are manifested in the large lattice expansion along the  $c$ -axis ( $\lambda_c$ ) and in the basal plane ( $\lambda_a$ ) (see Fig. 1). However, the observed volume effects are smaller as compared to spontaneous volume magnetostriction  $\omega_s = 1.5$  % in  $\text{Lu}_2\text{Fe}_{17}$  or to the field-induced magnetostriction in another AF compound  $(\text{Lu}_{0.8}\text{Ce}_{0.2})_2\text{Fe}_{17}$  ( $\omega \sim 0.6$  % in 5 T) [3], qualitatively corresponding to the lower magnetic moment of the  $R_2\text{Fe}_{17-x}\text{Ru}_x$  compounds with the “affected” by substitution Fe sublattice. The results obtained by two independent methods agree rather well.

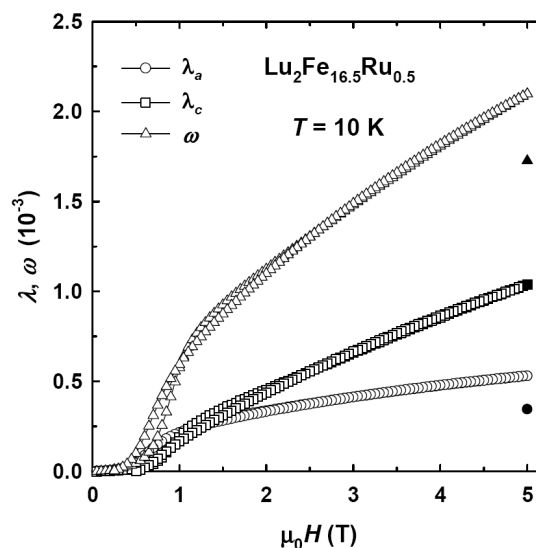


Fig.1. Comparison of the magnetostriction curves along the  $a$  and  $c$  axes of  $\text{Lu}_2\text{Fe}_{16.5}\text{Ru}_{0.5}$  single crystal measured in field applied along the  $a$  axis ( $\circ$ ) with the XRD results on a fixed random powder sample ( $\bullet$ ) at 10 K ( $\omega = 2\lambda_a + \lambda_c$  is a volume magnetostriction).

The work is supported by JSPS (No. P09227 and Grant-in-Aid No. 21-09227) and by GACR (No. 202/09/0339).

[1] A.V. Andreev, in: *Handbook of Magnetic Materials*, K.H.J. Buschow (Ed.), North-Holland, Amsterdam, 1998, Vol. 12, p. 105.

[2] S.A. Nikitin et al., *J. Magn. Magn. Mater.*, **241** (2002) 60.

[3] A.V. Andreev et al., *J. Alloys Comp.*, **477** (2009) 62.

**22 August**

Monday

12:00-14:00

15:00-17:00

oral session

22TL-O

22OR-O

**“High Frequency  
Properties and  
Metamaterials”**

22TL-O-1

## ADDITIONAL EFFECTIVE MEDIUM PARAMETERS FOR COMPOSITE MATERIALS (EXCESS SURFACE CURRENTS)

Vinogradov A.P.<sup>1</sup>, Ignatov A.I.<sup>1</sup>, Merzlikin A.M.<sup>1</sup>, Tretyakov S.A.<sup>2</sup>, Simovski C.R.<sup>2</sup>

<sup>1</sup> Institute for Theoretical and Applied Electromagnetic RAS, 13 Izhorskaya, Moscow 125412, Russia

<sup>2</sup> Department of Radio Science and Engineering, School of Science and Technology, Aalto University

The possibility of designing structure and arrangement of the elements in electromagnetic artificial materials permits one to achieve electromagnetic properties different from the properties of constituents (e.g., [1]). Most fully this possibility realizes in metamaterials, in which the interaction of the electromagnetic fields with artificial structural elements is of the resonant nature or / and the solenoidal part of the electric field plays the dominant role in this interaction. As a consequence, metamaterials exhibit advantageous and unusual electromagnetic properties (see e.g. in [2,3]). Nevertheless, it is still desirable to describe the metamaterials as homogeneous ones introducing effective constitutive parameters. Assignment of conventional effective parameters (permittivity, permeability, chirality parameter) to metamaterial samples often produces the values of the parameters whose properties differ from those of any physically possible homogeneous medium. Firstly, the retrieved parameters may depend on the sample size and surrounding environment (see e.g. [4,5]). Secondly, this approach may result in the nonzero imaginary parts of  $\epsilon$  and  $\mu$  in the absence of real dissipation (see e.g. [6]). Thirdly, the sign of these imaginary parts may contradict to the passiveness of the system [7-9] and fourthly, the frequency dispersion of material parameters may violate the causality principle [7-9]. To fix the problems, additional constitutive material parameters are often introduced. This model extension may be determined by new physical phenomena (anisotropy, artificial permeability, chirality, etc.) or by the peculiarities of the homogenization scheme [10-12]. In the latter case the additional parameters not obviously have a clear physical meaning.

Below we show that the key moment of the problems is the boundary conditions. We show that modification of the boundary conditions by introduction of additional (“excess”) surface currents can return the conventional permittivity and permeability of metamaterials their usual physical meaning, namely, the modified retrieval procedure yields values of effective impedance and refractive index through the reflection and transmission coefficients, which are independent of the system size and interface structure, whereas the susceptibilities of the excess surface currents depend on the local permittivity distribution near the interface. The accuracy of the latter procedure is the same as that of the quasi-static effective parameters.

- [1] G.W. Milton, *The Theory of Composites* (Cambridge University Press, 2002).
- [2] W. Cai, V.Shalaev, *Optical Metamaterials* (Springer, New York-Dordrecht-Heidelberg-London, 2010).
- [3] C. Caloz, T. Itoh, *Electromagnetic metamaterials: transmission line theory and microwave applications* (John Wiley & Sons Inc., Hoboken, New Jersey, 2007).
- [4] A.P. Vinogradov and A.M. Merzlikin, “On the problem of homogenizing one-dimensional systems,” *Journal of Experimental and Theoretical Physics* **94**, 482-488 (2002).
- [5] A.P. Vinogradov and A.M. Merzlikin, “Electrodynamics properties of a finely layered medium,” *Doklady Physics* **46**, 832-834 (2001).
- [6] S.M. Rytov. “Electromagnetic properties of laminated medium”. *Zh. Eksp. Teor. Fiz.* **29**, 605-616 (1955) [*Sov. Phys. - JETP.* **2**, 466-475 (1956)].

- [7] S. O'Brien, J.B. Pendry, "Photonic band-gap effects and magnetic activity in dielectric composites," *J. Phys.: Condens. Matter* **14**, 4035-4044 (2002).
- [8] D.R. Smith, S. Schultz, P. Markos, C.M. Soukoulis, "Determination of effective permittivity and permeability of metamaterials from reflection and transmission coefficients," *Phys. Rev. B* **65**, 195104 (2002).
- [9] J. Zhou, T. Koschny, M. Kafesaki, C.M. Soukoulis, "Size dependence and convergence of the retrieval parameters of metamaterials," *Photon. Nanostruct.* **6**, 96-101 (2008).
- [10] A. Ludwig, K.J. Webb, "Accuracy of effective medium parameter extraction procedures for optical metamaterials," *Phys. Rev. B* **81**, 113103 (2010).
- [11] A.K. Sarychev, D.J. Bergman, and Y. Yagil, "Theory of the optical and microwave properties of metal-dielectric films," *Phys. Rev. B* **51**, 5366-5385 (1995).
- [12] C. Fietz, G. Shvets, "Current-driven metamaterial homogenization," *Physica B* **405**, 2930-2934 (2010).

22TL-O-2

## METAMATERIALS PROGRAM IN TIME

*Klos A., Gajc M., Sadecka K., Bienkowski K., Osewski P., Stefanski A., Pawlak D.A.*  
 Institute of Electronic Materials Technology, ul. Wolczynska 133, 01-919 Warsaw, Poland

Research in electromagnetic metamaterials has steadily increased over the last 10 years, providing enhanced understanding and demonstration of novel physics at shorter and shorter wavelengths. While some evidence in this progress is being seen in radio frequency applications, optical metamaterials are still in research phase. Metamaterials program in the Institute of Electronic Materials Technology is attempting to this challenge. Our research is focused into photonic crystals and metamaterials made by self-organization [1] and especially by directional solidification of eutectics and metallodielectric structures. We use the micro-pulling down technique for growth of oxide/oxide eutectics [2-3] and metallodielectric nanocomposites [4]. This method allows obtaining various geometries of eutectic structures (Fig.1), which can exhibit different physical properties.

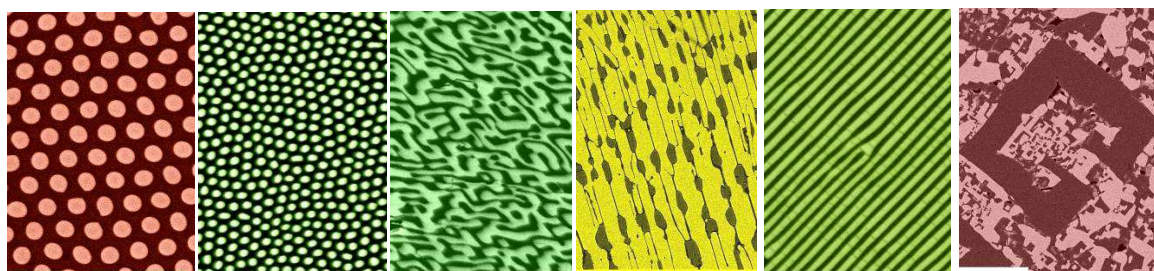


*Fig. 1. Various eutectic microstructures obtained by directional solidification in ITME.*

Directional solidification allows producing hybrid metallodielectric structures, by doping oxides with metallic nanoparticles. These composites exhibit plasmonic resonances in visible and infrared spectral range. Moreover, the metallodielectric structures are obtained by etching one phase of eutectic and filling etched areas by metal. Eutectics, including  $\text{TiO}_2$  phase, are also investigated for harvesting solar energy applications.

The authors thanks the FP7 NMP ENSEMBLE project (GA NMP4-SL-2008-213669) and the Project operated within the Foundation for Polish Science Team Programme co-financed by the EU European Regional Development for partial supporting of this work.

- [1] D.A. Pawlak, Self-organized structures for metamaterials *in* Handbook of Artificial Materials, Taylor & Francis, 2009.  
 [2] D. A. Pawlak, K. Kolodziejak, S. Turczynski, et al. Chemistry of Materials, 18, 2450 (2006).  
 [3] D. A. Pawlak, S. Turczynski, M. Gajc, et al., Adv. Funct. Mater. 20, 1116 (2010).  
 [4] A. Klos, M. Gajc, R. Diduszko, et al. ICTON 2009: 11th International Conference on Transparent Optical Networks, 1-2, 421-424 art. no. 5185322.

22OR-O-3

## TM-WAVE PROPAGATION INTO INHOMOGENEOUS MEDIUM CONSISTING OF 2D ARRAY OF NANOPARTICLE

*Ivanov A.<sup>1</sup>, Shalygin A.<sup>1</sup>, Sarychev A.<sup>2</sup>*

<sup>1</sup> Moscow State University, Faculty of Physics, 1 Leninskie Gory, 119991 Moscow, Russia

<sup>2</sup> Institute for Theoretical and Applied Electromagnetics of the RAS, 13 Izhorskaya, 125412 Moscow, Russia

The plasmonic system consisting of two-dimensional periodic array of silver cylindrical nanoparticles is investigated. The reflection of the electromagnetic wave from the inhomogeneous medium composed of metal nanoparticles, which have various diameters and inter-particle spacing, have been numerically calculated. The excitation of plasmons in nanoparticle array is studied. Electromagnetic modes, which are strongly localized around the spherical nanoparticle due to collective surface plasmon resonance, are obtained.

Since the metal permittivity is negative in the optical frequency region and it is inversely proportional to the frequency squared we can model a metal particle as an inductance L. The interaction of a metal particle with electromagnetic (EM) field can be then presented as excitation of R-L-C contour. Inductance L (with small losses described by resistance R) represents the metal particle while capacitance C represents the gap between particles. The resonance in R-L-C contour is analogous to the surface plasmon resonance in a single metal particle [1].

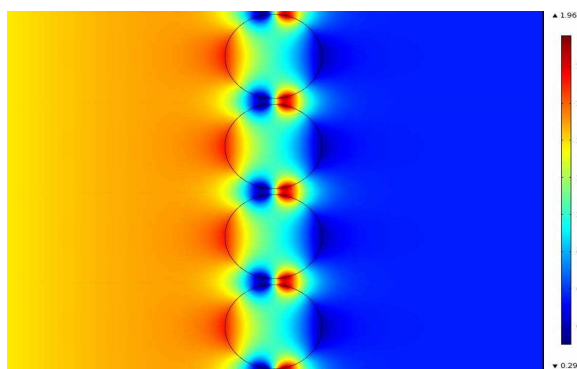


Figure 1. The exhibition of plasmon oscillations for diameter of nanoparticles  $D=10\text{nm}$ ,  $\omega = 3.53eV$

In this work we investigate the propagation of transversal electromagnetic wave in the array of closely packed silver nanocylinders. We calculate reflectance and electric field distribution as function of the frequency, diameters of the cylinders, and inter cylinder distance.

The most interesting results are obtained for the case when the distance between the cylinders is much smaller than the radius. It is shown, that the reflection of TM-wave has nonmonotonic dependence on the frequency due to excitation of the collective surface plasmon resonances in the metal nanoparticles. The plasmon modes are similar to whispering gallery modes (see fig.1). At the resonance conditions the electric field is much enhanced in the gaps between the cylinders and it could be many orders on magnitude larger than the field of the incident wave.

[1] A. Sarychev, V. Shalaev, *Electrodynamics of Metamaterials*, World Scientific, 2007.

22TL-O-4

## **MAGNETIC RESPONSE OF NANOSCALE LEFT-HANDED METAMATERIALS**

*Kafesaki M., Penciu R., Koschny Th., Shen N.H., Economou E.N., Soukoulis C.M.*

Foundation for Research and Technology Hellas (FORTH), Heraklion, Crete, Greece, and  
University of Crete, Greece; Tel: (302810) 391547, Fax: (302810) 391569,  
e-mail: kafesaki@iesl.forth.gr

Left-handed metamaterials, i.e. metamaterials with electrical permittivity and magnetic permeability both negative (resulting to negative index of refraction), are becoming recently a subject of continuously increasing attention, owing to their novel and unique properties (like backwards propagation, negative refraction, superresolution, etc) and thus the new capabilities that they can provide in the manipulation of electromagnetic waves.

These novel properties and capabilities of left-handed metamaterials have motivated strong research efforts to achieve such metamaterials operating in the infrared and optical regime, making essential thus the achievement of magnetic response and negative magnetic permeability in the optical regime. In this talk we will review the current status of the efforts to achieve optical magnetic metamaterials and left-handed metamaterials, as well as our efforts to analyze and understand the wave propagation in optical magnetic metamaterials, and to optimize such metamaterials.

22TL-O-5

## **MAGNETO-INDUCTIVE MACH-ZEHNDER INTERFEROMETER**

*Syms R.R.A.*

Optical and Semiconductor Devices Group, Electrical and Electronic Engineering (EEE)  
Department, Imperial College, London SW7 2BT, UK

Magneto-inductive waveguides are slow-wave bandpass electrical ladders operating by magnetic coupling between a set of L-C resonators arranged as a 1-D array [1]. The availability of low-loss thin-film cable [2] that can follow arbitrary curved paths without significant reflection [3] and transducers for connection to real impedance [4] is allowing the development of waveguide components analogous to those of conventional guided wave systems. Here we demonstrate

interference between magneto-inductive waves propagating at different speeds in the two arms of a Mach-Zehnder interferometer (MZI). The MZI was constructed from two 1 metre lengths of magneto-inductive cable, designed for operation at 95 MHz frequency and fitted with broadband transducers for connection to  $50 \Omega$ . The lines were excited symmetrically using a conventional 6 dB resistive power splitter, and the outputs were combined using a second 6 dB splitter (Fig. 1a). The propagation characteristics of one arm were modified, by loading with ferrites. The effect was to reduce the resonant frequency of the elements without significantly altering the coupling (Fig. 1b). Consequently, it provided a frequency-dependent phase shift, which was adjustable by varying the numbers of loading ferrites and of loaded elements. Comparison between the transmission through balanced and unbalanced interferometers (Fig. 2a) shows an additional null in the latter due to destructive interference of magneto-inductive waves propagating in the two arms. The transmission at this frequency followed the expected variation  $P_{\text{out}} = \cos^2(N\Delta ka/2)$ , where  $N$  is the number of loaded elements and  $\Delta ka$  is the phase shift per element (Fig. 2b). Similar experiments were conducted with 4-port combiners and with resonant loads.

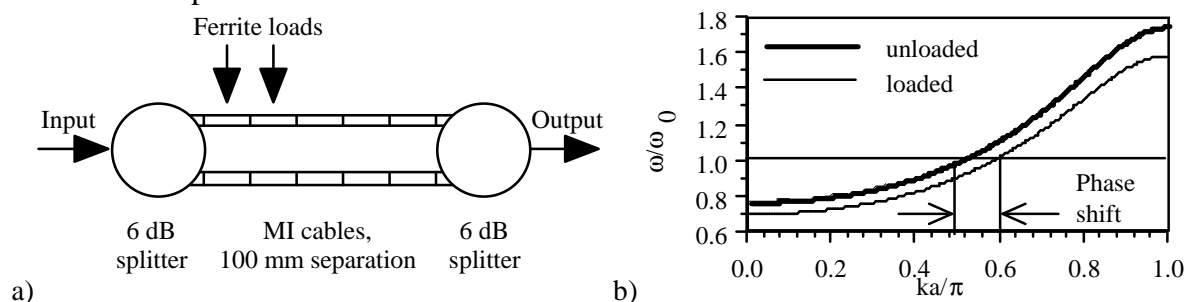


Fig. 1. a) Magneto-inductive Mach-Zehnder interferometer, and b) effect of loads in  $\omega$ - $k$  space.

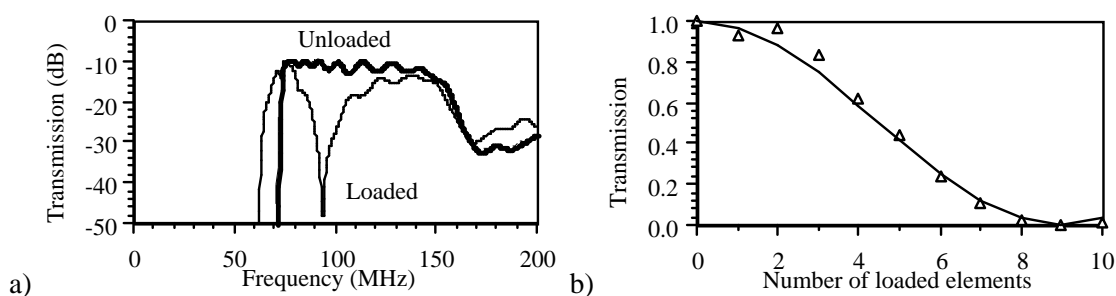


Fig. 2. a) Frequency response of loaded and unloaded interferometer, and b) interference characteristic.

- [1] E. Shamonina et al., *Elect. Lett.* 38, 371 (2002).
- [2] R.R.A. Syms et al., *J. Phys. D. Appl. Phys.* 43, 055102 (2010)
- [3] R.R.A. Syms, L. Solymar, *Metamaterials* 4, 161 (2010)
- [4] R.R.A. Syms et al., *J. Phys. D. Appl. Phys.* 43, 285003 (2010)



## METAMATERIALS WITH INTER-ELEMENT COUPLING FOR SUBWAVELENGTH IMAGING

Shamonina E.

Optical and Semiconductor Devices Group, Electrical and Electronic Engineering (EEE)  
Department, Imperial College, London SW7 2BT, UK

A mechanism for the near field imaging in metamaterials is the excitation of coupled surface plasmon polaritons at both interfaces of a metamaterial slab [1]. These surface modes interact with non-propagating evanescent part of the spatial Fourier spectrum of an object, leading to the transfer of the near field distribution from one side of the slab, where the object is located, to the opposite side. For TM polarisation, one could use a silver with  $\epsilon < 0$ , whereas for TE polarisation, analogously, one would need a metamaterial with  $\mu < 0$ , comprising, e.g., split rings.

The properties of a structure assembled from individual split rings (see e.g. Fig.1) are governed by strong interactions between individual elements [2]. A consequence of these interactions is the emergence of slow magnetoinductive waves unaccounted for in a simplified effective medium theory. These slow waves can couple to and influence the propagation of electromagnetic waves forming so-called proxiton-polaritons [3-6], similar to plasmon-polaritons in plasmas. We were able to establish the relationship between effective permeability and circuit characteristics of a split-ring metamaterial [3,4] and describes bulk modes [4] and surface modes of proxiton-polaritons at an interface air/metamaterial [5] and on a metamaterial slab [6]. Using our approach we are able to design SRR-based near field manipulating devices for TE polarisation, in full analogy to a silver slab operating as a near-perfect lens for TM polarised light. In the presentation we provide an overview of our recent results on possibilities of employing slow waves of inter-element coupling for near-field imaging. We demonstrate on a number of examples how our model can be used for the design of split-ring based near-field lenses for the desired frequency range.

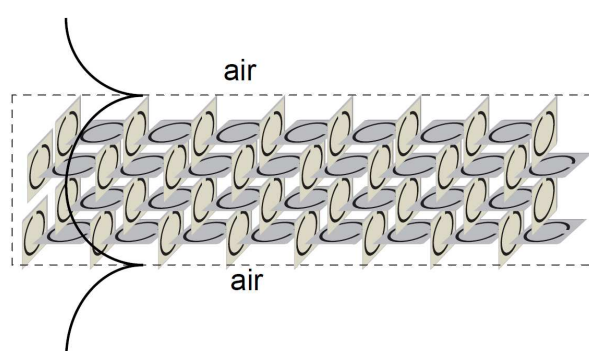


Fig.1. Imaging mechanism for a split-ring slab is inter-element coupling and excitation of surface proxiton-polariton modes.

Financial support of the the Leverhulme Trust and the DFG is gratefully acknowledged.

[1] L. Solymar and E. Shamonina, *Waves in Metamaterials* (Oxford University Press, 2009).

[2] E. Shamonina et al., *J. Appl. Phys.* **92**, 6252 (2002).

[3] R.R.A. Syms et al., *J. Appl. Phys.* **97**, 064909 (2005).

[4] A. Radkovskaya et al., *Magnetic plasmon-polaritons in split-ring metamaterials with strong coupling*, 3rd International Congress Metamaterials'2009, London, 2009.

[5] E. Shamonina and A. Radkovskaya, *Surface and bulk proxiton-polaritons in split-ring metamaterials*, 4th International Congress Metamaterials'2010, Karlsruhe, 2010.

[6] E. Shamonina, *Proxiton-polaritons on metamaterial slabs of coupled split rings*, submitted to 5th International Congress Metamaterials'2011, Barcelona, 2011.

22TL-O-7

## 'DIMER' AND 'POLYMER' DIATOMIC METAMATERIALS

*Radkovskaya A.*

Magnetism Division, Faculty of Physics, M.V. Lomonosov Moscow State University, Moscow  
119992, Russia

Properties of metamaterials assembled from individual resonators are governed by strong interactions between individual 'artificial atoms'. The coupling between individual resonators may lead to propagation of slow waves with the wavelength much shorter than that of the electromagnetic radiation. Two examples of such waves are magnetoinductive and electroinductive waves. These waves were proved to exist on arrays of 'metaatoms' in a broad frequency range from MHz to the visible, with applications including guiding and processing of signals on a subwavelength scale, detection of nuclear magnetic resonance, and subwavelength imaging [1].

Recently, we introduced 'diatomic' metamaterials with pure magnetic coupling [2]. Such structures with two metamaterial 'atoms' per unit cell are analogous to diatomic solids capable of propagating both acoustic and optical phonons. In a subsequent work [3], we proposed a diatomic chain

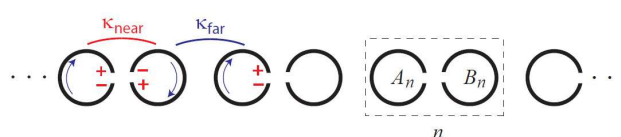


Fig. 1. Diatomic chain with alternating electric ( $\kappa_{\text{near}}$ ) and magnetic ( $\kappa_{\text{far}}$ ) coupling.

shown in Fig.1, the interesting feature of which is that the coupling alternates between electric and magnetic. The resulting dispersion characteristics are shown to be radically different from the classical acoustic and optical branches: the upper branch is a forward wave and the lower branch a backward wave. Most recently we demonstrated that it is possible to realize two types of diatomic metamaterials, a 'dimer' one and a 'polymer' one, depending on the coupling within a unit cell being larger than or equal to that between the unit cells [4]. A striking feature of the 'polymer' structure is that the gap between the two pass bands of the dispersion equation may disappear yielding a zero-phasevelocity, finite group-velocity wave. In the presentation we shall review our recent advances in studies of diatomic metamaterials, presenting experimental and theoretical data and discussing possible applications.

Financial support of the Russian Foundation of Fundamental Investigations and of the Royal Society is gratefully acknowledged.

[1] L. Solymar and E. Shamonina, *Waves in Metamaterials* (Oxford University Press, 2009).

[2] O. Sydoruk et al., *Appl. Phys. Lett.*, **87**, 072501 (2005).

[3] A. Radkovskaya et al., *Eigenmodes of diatomic metamaterials with electric and magnetic coupling*, 3rd International Congress on Advanced Electromagnetic Materials in Microwaves and Optics Metamaterials'2009, London, 2009.

[4] A. Radkovskaya et al., 'Dimer' and 'polymer' metamaterials with alternating electric and magnetic coupling, submitted to *Phys. Rev. B* (2011).

**22 August**

Monday

17:30-19:00

poster session  
22PO-I

**“Magnetism of  
Nanostructures”**

22PO-I-1

## RELAXATION MÖSSBAUER SPECTROSCOPY OF IRON OXIDES NANOPARTICLES IN SUPERFERRIMAGNETIC REGIME

Cherepanov V.M.<sup>1</sup>, Chuev M.A.<sup>1,2</sup>, Polikarpov M.A.<sup>1</sup>, Shishkov S.Yu.<sup>1</sup>

<sup>1</sup> National Research Centre “Kurchatov Institute”, 123182 Moscow, Russia

<sup>2</sup> Institute of Physics and Technology Russian Academy of Sciences, 117218 Moscow, Russia

The most important dynamical characteristic of single-domain nanoparticles is their magnetization reversal time. Typical values of the time ( $10^{-6} - 10^{-9}$  s) come into the  $^{57}\text{Fe}$  Mössbauer time window defined by the lifetime of the excited nuclear level ( $\sim 10^{-7}$  s) and Larmor precession of nuclear magnetic moments in an effective magnetic field. This is why Mössbauer spectroscopy allows one to obtain a valuable information in the field of nanoparticles diagnostic. However, up to now the Mössbauer spectra of fine magnetic particles are usually measured as a function of temperature only. Meanwhile, a substantial influence of weak magnetic fields of about kilooersted on the Mössbauer spectra shape of the nanoparticles was recently observed, which promises to give a powerful tool to estimate such important average nanoparticle parameters as anisotropy constant  $\langle K \rangle$ , saturation magnetization  $\langle M_0 \rangle$ , critical remagnetization field  $H_C$  and relaxation constant  $p_0$ . We have studied film composites based on the magnetite  $\text{Fe}_3\text{O}_4$  nanoparticles (an average size  $\langle D \rangle \approx 4$  nm) in the polyvinyl alcohol (PVA) matrix and dried ferrofluid “ARA-250” (Chemicell GmbH, Germany) with  $\langle D \rangle \approx 10$  nm by Mössbauer spectroscopy in a weak magnetic field  $H < 3.4$  kOe. The PVA Mössbauer spectrum at  $H=0$  shows a superposition of minor (poor-resolved) magnetic hyperfine structure and major collapsed spectrum typical for superparamagnetic particles. The spectra taken in magnetic fields show essential restoration of the magnetic hyperfine structure characteristic for the nanoparticles of the kind. As for the ARA-250 particles the spectrum at  $H=0$  demonstrates very unusual shape (Fig. 1, top spectrum), which demanded a special consideration. The experimental Mössbauer spectra have been analyzed within the recently developed three-level [1] and multi-level [2] relaxation models of magnetic dynamics in an ensemble of single-domain particles. These models take into account the precession and diffusion of particle’s uniform magnetization as well as the particles size distribution and interparticle interactions.

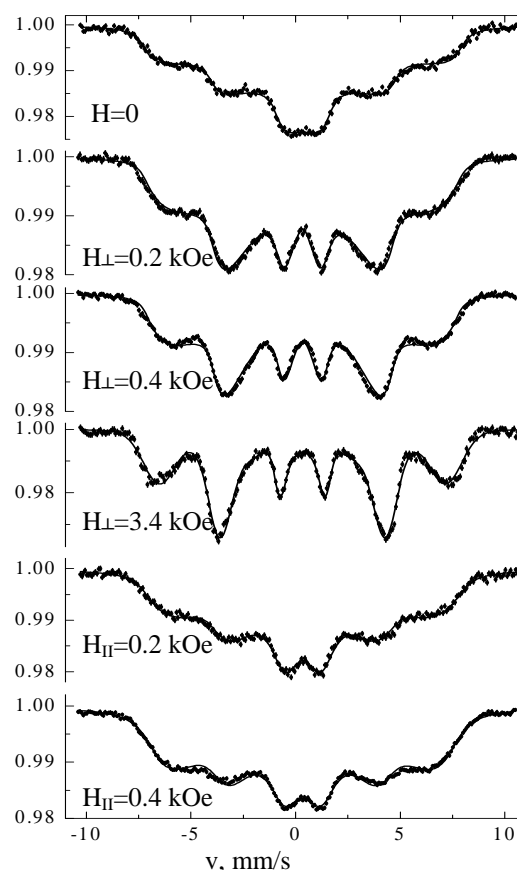


Fig 1. Room-temperature  $^{57}\text{Fe}$  Mössbauer spectra of the magnetic nanoparticles ARA-

The work was supported by RFBR.

[1] M.A.Chuev, *J.Phys.:Cond.Matt.* **20** (2008) 505201.

[2] M.A.Chuev, V.M.Cherepanov, M.A.Polikarpov, *JETP Lett.*, **92** (2010) 21.

## MICROSTRUCTURE AND MAGNETIC PROPERTIES of FeCo AND $L_{10}$ Fe/Pt THIN FILMS FOR ULTRAHIGH-DENSITY MANETIC RECORDING

*Kamzin A.S.<sup>1</sup>, Wei F.L.<sup>2</sup>, Ganeev V.R.<sup>3</sup>, Zaripova L.D.<sup>3</sup>*

<sup>1</sup>Ioffe Physical Technical Institute of RAS, St.-Petersburg, 194021, Russia

<sup>2</sup>Research Institute of Magnetic Materials, Lanzhou University, Lanzhou 730000, China

<sup>3</sup>Kazan Federal University, Kazan 420008, Russia

The ordered FePt binary alloy with tetragonal  $L_{10}$  structure possess a very high magneto-crystalline anisotropy constant, high Curie temperature and large saturation magnetization what is essential for the next generation of ultrahigh-density recording media. In order to write information in these high coercivity media, the core materials in writing heads are required to have high saturation magnetization, high permeability, and low coercivity. The bcc  $Fe_{1-x}Co_x$  alloy system have been studied extensively because they have the highest saturation magnetization up to  $\mu_0 M_s = 2.4$  T in the composition range of  $0.3 < x < 0.5$ . However, it is difficult to obtain FeCo films with excellent soft magnetic properties due to its large magnetostriction constant. In addition, the creation of the ultrahigh-density magnetic recording (UHD MR) systems of next generation requires magnetic materials as writing media with the minimum possible magnetic grain size, as well as miniaturization of the write/read magnetic heads.

This report presents the results of studies of the  $Fe_{1-x}Co_x$  films for write/read magnetic heads as well as the results of investigations of multilayer  $L_{10}$  [Fe/Pt] $_n$ . Our studies of FeCo and  $L_{10}$  FePt films have been focused on technological issues of UHD MR heads and media, respectively, as well as on the fundamental magnetic properties, such as the temperature dependence of the magnetic anisotropy constants, orientation of the easy axis and the exchange stiffness constant. The film composition was determined using inductively coupled plasma spectroscopy. The magnetic properties were studied using a SQUID and vibrating-sample magnetometers. The microstructure and the magnetic structure of the films was determined by X-ray diffraction (XRD) and Conversion Electron Mössbauer (CEM) Spectroscopy, respectively.

In result the FeCo nanostructured thin films with high magnetization ( $M_s$ ) and low coercivity  $H_c$  were obtained by utilizing suitable under-layer and optimizing the deposition conditions. It was found that the improvement of soft magnetic properties for FeCo films with an under-layer is closely related to the film texture.

In the case of FePt  $L_{10}$ -phase multilayer [Fe/Pt] $_n$  thin films have been obtained. The total thickness of multilayer [Fe/Pt] $_n$  was varied from 25 to 200 nm by changing the number  $n$  of deposited bilayers. We have studied the dependence of the microstructure, the magnetic structure, and the easy axis orientation in the [Fe/Pt] $_n$  films on the substrate temperature as well as the gas pressure during deposition, the order and thicknesses of Fe and Pt layers; and the total film thickness. The (001)-oriented  $L_{10}$  phase FePt films with high order parameter were prepared by sputtering deposition and subsequent vacuum annealing in external magnetic field (VAEMF). It is found that (001) orientation and perpendicular anisotropy can be obtained and enhanced in FePt films by VAEMF at the temperature which is near the Curie temperature of  $L_{10}$  phase FePt. These multilayers possess magnetocrystalline anisotropy ( $K_u$ ) greater compared to the existing magnetic recording media, large coercivity and saturation magnetization, high chemical stability and corrosion resistance.

The results of our studies demonstrated that prepared FeCo films and  $L_{10}$  [Fe/Pt] $_n$  multilayers meet the requirements to write/read heads and recording media, respectively, for the perpendicular recording and can be use for future UHD MR systems.

## DOMAIN WALL STRUCTURE OF WEAK FERROMAGNETS ACCORDING TO RAMAN SPECTROSCOPY

*Kuzmenko A.P.<sup>1</sup>, Abakumov P.V.<sup>1</sup>, Dobromyslov M.B.<sup>2</sup>*

<sup>1</sup> South-West State University, Russia

<sup>2</sup> Pacific State University, Russia

Domain structures in  $\text{Ni}_3\text{B}_7\text{O}_{13}\text{Br}$  (Ni – Br) and  $\text{LiNbO}_3$  have been previously studied using the spectral mapping of distribution (MSDs) [1, 2]. Full set of equipment (AIST-NT, Zelenograd) included a confocal microscope, Raman microspectrometer OmegaScope and atomic force microscope. The study of the Raman scattering spectra in  $\text{YFeO}_3$  monocrystals was made either [3] with a scanning probe microscope (with an accuracy of positioning of 0.05 nm) or with a specially designed goniometric device (with an accuracy of revolution of 5') with a two-coordinate stage. We study a single crystal transparent sample  $\text{YFeO}_3$  in the form of plate thickness of 100  $\mu\text{m}$ , cut perpendicular to the optical axis, which allows polarized light to visualize the DW and DS. Area of a sample (15×25  $\mu\text{m}$ ) was scanned using an atomic force microscope. Raman specters were measured in each point (spot ~ 0.5  $\mu\text{m}$ ). Using hyper spectral data that were presented in a graphic form we plotted the magnetization variations along the perpendicular to the DW plane (even if DW was curved, Fig.1 a, b). The DW width in  $\text{YFeO}_3$  determined in this way was equal to 2.63  $\mu\text{m}$ .

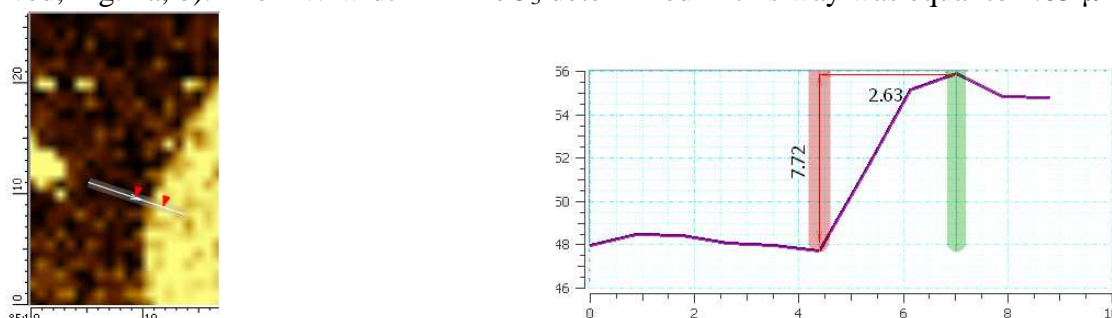


Fig. 1. Raman image of the DS and DW in  $\text{YFeO}_3$

From Fig. 1, a one can establish relations between straight ( $\Delta_0$ ) and curved ( $\Delta$ ) DW:  $\Delta = \Delta_0 \cos \alpha$  where  $\alpha$  is the angle between the normal to the straight and curved DWs. Estimation of the angle between the normal to straight DWs reaches 50°, which is consistent with the observed Raman image of DW in Fig.1, a.

[1] Iliev M.N., Hadjev V.G., Inigues J., Pascual V.G. *Acta Physica Polonica A*. **116** (1), (2009).

[2] Zelenovsky P.S., Shur V.Ya., Kuznetsov D.K., etc. *Fiz. Tver. Tela* **53** (1), (2011).

[3] Abakumov P.V., Kuz'menko A.P., Chaplygin A.N. *Proceedings of the Kursk State Technical University* **4** (33) (2010).

## FERROMAGNETIC RESONANCE IN PERMALLOY ANTIDOT ARRAYS

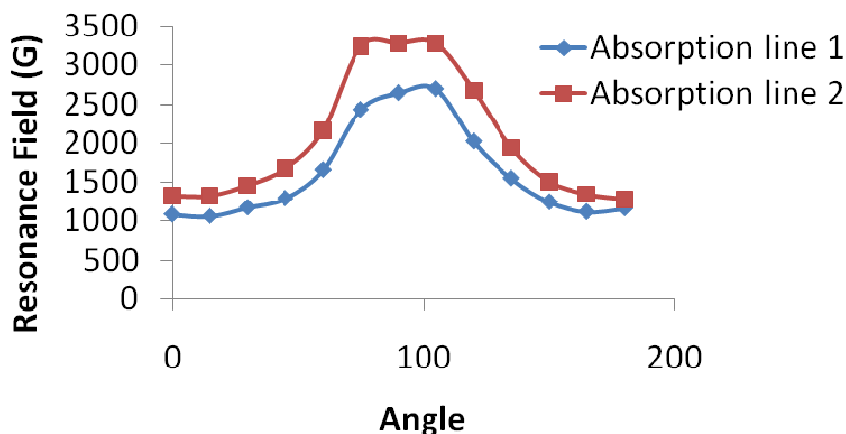
*Mateos P.<sup>1</sup>, Flores A.G.<sup>1</sup>, Raposo V.<sup>1</sup>, Iñiguez J.<sup>1</sup>, Merazzo K.J.<sup>2</sup>*

<sup>1</sup> Departamento de Física Aplicada, Universidad de Salamanca, E-37071, Salamanca, España

<sup>2</sup> Instituto de Ciencia de Materiales, CSIC, 28049 Madrid, España

Dynamic properties of magnetic nanostructures have recently been intensively studied due to their potential application in high density perpendicular recording media or magnetic sensors. At the same time, the highly oriented arrays of magnetic antidot are excellent model materials to study magnetism of low-dimensional systems. In order to understand the dynamic phenomena in these samples antidot arrays of Permalloy have been prepared by the sputtering of Ni<sub>80</sub>Fe<sub>20</sub> onto anodic alumina membrane templates. The film thickness is of 138 nm and the antidot diameters of 15 nm, for a hexagonal lattice parameter of 105 nm.

The anisotropy fields can be investigated by various techniques. One of these techniques is the ferromagnetic resonance spectroscopy (FMR) due to the fact that the resonance field depends directly on the anisotropy. Ferromagnetic resonance measurements have been carried out at a frequency of 9.54 GHz as a function of H. The sample was placed in a rectangular cavity in such a position that the angle between the applied field H and the film plane can be adjusted from 0° to 180°. The spectra show several absorption lines. The angular dependence of the resonance field for the two main absorption lines are shown in the following Figure:



As it can be seen, the

resonance field of the absorption peak increases upon changing the angle from parallel (0°) to perpendicular (90°) to the film plane. This behaviour can be explained by the relation between resonance field, frequency and anisotropy field determined by demagnetizing factors and magnetization angle respect to the sample easy axis direction after energy minimization as indicated in [1]. The results are similar to those obtained in nanowires although the easy axis is in the film plane in the case of antidot array.

[1] C.A. Ramos, E. Vasallo Brigneti, M. Vázquez, *Physica B* 354 (2004) 195–197

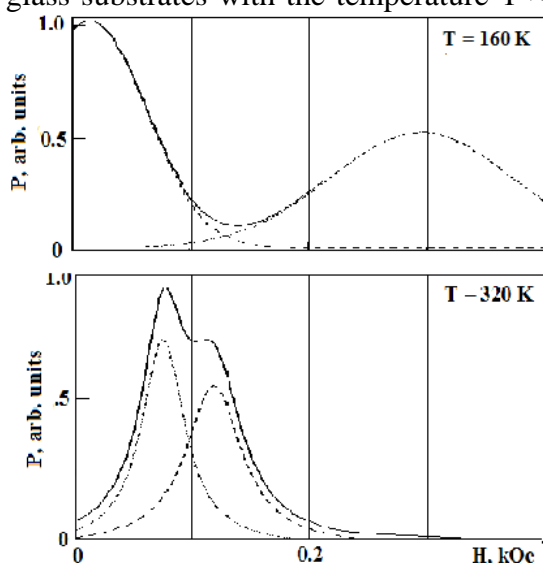
## PHYSICAL PROPERTIES OF Co/Ge/Co FILMS

Patrin G.S.<sup>1,2</sup>, Turpanov I.A.<sup>2</sup>, Kobyakov A.V.<sup>2</sup>, Patrin K.G.<sup>1</sup>, Yushkov V.I.<sup>1,2</sup>, Li L.A.<sup>1</sup>,  
Petrakovskaya E.A.<sup>1</sup>, Rautskii M.V.<sup>1</sup>

<sup>1</sup> Kirensky Institute of Physics, Russian Academy of Sciences, Siberian Branch, Krasnoyarsk,  
660036 Russia

<sup>2</sup> Siberian Federal University, pr. Svobodny 79, Krasnoyarsk, 660041 Russia

In recent years, films of the *ferromagnetic metal/semiconductor* system have attracted much attention of researches. Of great importance is the study of the spin-dependent electron transport via nonmagnetic spacers, because it significantly affects the character of the interlayer exchange coupling in these materials. We synthesized Co/Ge/Co films with different thicknesses of a nonmagnetic spacer. The films were prepared by ion-plasmas sputtering in argon atmosphere onto glass substrates with the temperature  $T \approx 373$  K. Electron microscopic investigations showed that



the films are X-ray-amorphous with the particle size  $d < 5$  nm. The patterns of the films have a shape of broadened polycrystalline rings.

We report the results of experimental studies of the interlayer interactions in the Co/Ge/Co films by SQUID magnetometry, electron and nuclear magnetic resonance, and the magnetoresistance method. As was established previously [1], the magnetic behavior of the films obtained is determined, to a great extent, by deposition rate. At high deposition rates, the temperature dependence of magnetization of the films has a thermo-induced character. In the Co/Ge/Co system, this effect is decisive in the low-temperature region; however, above a certain blocking temperature, the interlayer interactions ( $J$ ) become noticeable, which was revealed by the magnetic resonance methods. The

microwave radiation frequency was  $f_{\text{MWV}} = 9.2$  GHz. The resonance spectra measured within the temperature range from 78 to 500 K represent superposition of two lines. Temperature behavior of each line was determined by fitting the spectrum by two Lorentz lines (Fig. for the film with  $t_{\text{Co}} = 13$  nm and  $t_{\text{Ge}} = 6$  nm). It was established that the acoustic mode is more sensitive to the temperature variations, whereas the optical mode is almost temperature-independent. The experimental data were processed using the calculation of the magnetic resonance spectra for magnetic thin-film trilayers. The nonmonotonic dependence of  $J$  on thickness of the nonmagnetic spacer [2] indicates the oscillating character of the exchange coupling, which is consistent with the literature data. Comparative analysis of magnetic static and magnetoresistance data shows that a sublayer of Co-Ge solid solution is formed at the interface. The occurrence of the solid solution strongly affects the magnetic state of both Co layers and the entire Co/Ge/Co system and also influences the character of the interlayer interaction, as the features of magnetoresistance imply.

This study was supported by the Russian Foundation for Basic Research, project no. 11-02-00675-a.

[1] G. S. Patrin, C.-G. Lee, I. A. Turpanov, S. M. Zharkov et al., *JMMM*, **306** (2006) 218.

[2] A.V. Kobyakov, G. S. Patrin, I. A. Turpanov et al., *Sol. St. Phenom.*, **168-169** (2011) 273.

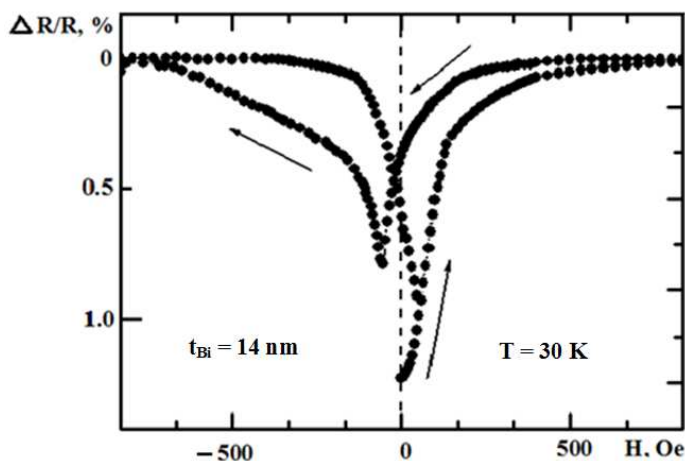


## MAGNETISM AND MAGNETORESISTIVITY IN NiFe/Bi/NiFe FILMS

Patrin K.G.<sup>1,2</sup>, Yakovchuk V.Yu.<sup>1</sup>, Patrin G.S.<sup>1,2</sup>, Yarikov S.A.<sup>2</sup>

<sup>1</sup> L.V. Kirensky Institute of Physics, Siberian Branch, Russian Academy of Sciences, Krasnoyarsk, 660036, Russia

<sup>2</sup> Siberian Federal University, prospekt Svobodny, 79, Krasnoyarsk, 660041, Russia



Multilayer magnetic films with a nonmetal spacer, in particular, those belonging to the system *ferromagnetic metal / semiconductor* [1], or with a semimetal spacer attract close attention by virtue of a great variety of effects observed in these films. When a semiconducting spacer is used, the interest of researchers is caused by the possibility of changing the current carriers concentration in a nonmagnetic layer by means of influence of external factors, which allows controlling the interlayer interaction. For this reason, currently the creation of film

structures that would keep sensitivity to external conditions and effects along with far more effective interaction between ferromagnetic layers remains the urgent problem to solve. One of the ways to accept the challenge seems to use semimetal Bi instead of semiconducting material as a nonmagnetic interlayer.

NiFe/Bi/NiFe films (Ni – 80 % at. and Fe – 20 % at.) were obtained in a single cycle by vacuum evaporation. For all films the permalloy layer thickness was  $t_{\text{NiFe}} \cong 10$  nm and bismuth spacer thickness was  $t_{\text{Bi}} = 0\text{--}15$  nm. The value  $t_{\text{NiFe}}$  was selected to be rather small, but at the same time, to keep a film continuous and magnetization of a magnetic layer independent of its thickness. Thickness of layers was determined by X-ray spectroscopy. No traces of known 3d-metal-Bi compounds were found. Magnetic measurements were made with MPMS-installation. Magnetoresistivity was measured by 4-probe technique. During the measurements magnetic field was in the film plane.

It was found [2] that the bismuth spacer formation influences essentially the system magnetization. The shape of  $\sigma(H)$  curve is changed with bismuth spacer thickness increasing. In particular, the test film with  $t_{\text{Bi}} = 0$  has the narrow hysteresis loop and magnetization curve of a ferromagnetic type. For the films with  $t_{\text{Bi}} \neq 0$  the magnetization curve width nonmonotonously depends on  $t_{\text{Bi}}$  thickness, and this is connected with inclusion of interlayer coupling. The coercive force ( $H_C$ ) is growing with increase of bismuth layer thickness having maximum at  $t_{\text{Bi}} \sim 13$  nm

Also, the magnetoresistivity of order of percent units and dependence of its value on thickness of bismuth spacer were found in these films at helium temperatures (for instance, see Fig.).

The current investigations are being undertaken at financial support of the Russian Found of Basic Researches (Grant № 11-02-00675-a)

[1] G.S. Patrin, V.O. Vas'kovskii, *Phys. Met. Metalloved.*, **101** (2006) S63.

[2] G.S. Patrin, V.Yu. Yakovchuk, D.A. Velikanov. *Phys. Lett. A*, **363** (2007) 164.

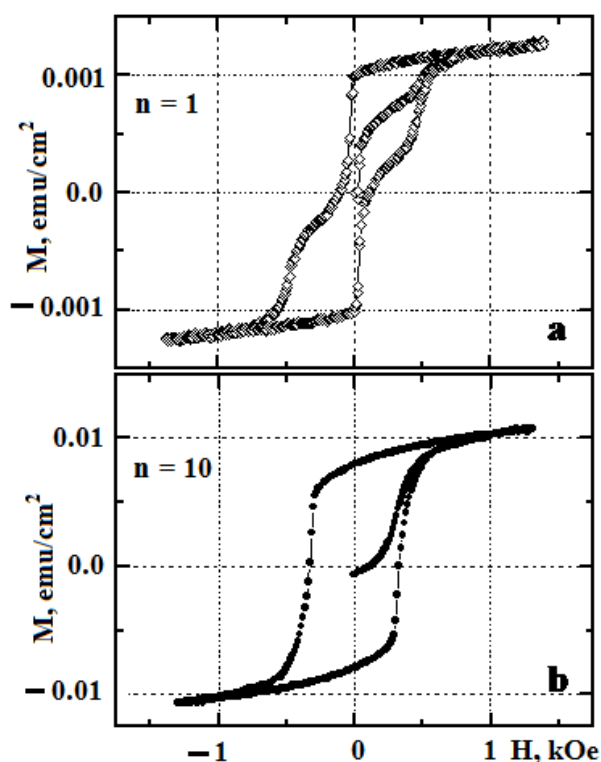
## MAGNETIC PROPERTIES OF MULTILAYER (CoNiP<sub>soft</sub>/CoP<sub>hard</sub>)<sub>n</sub> FILMS

Pal'chik M.G.<sup>1</sup>, Patrin G.S.<sup>1,2</sup>, Balaev D.A.<sup>1,2</sup>, Kiparisov S.Ya.<sup>1</sup>

<sup>1</sup> L.V. Kirensky Institute of Physics, Siberian Branch, Russian Academy of Sciences, Krasnoyarsk, 660036, Russia

<sup>2</sup> Siberian Federal University, prospekt Svobodny, 79, Krasnoyarsk, 660041, Russia

Interest to systems with spin-valve effect is caused by their practical use in spin electronics devices [1]. In it the problem of creation of spin-polarized electrons fronts on first plan. Film systems with exchange bias effect are convenient objects for decision of this task. In such systems the interlayer coupling is responsible for forming of magnetic state. Given report is devoted to study of magnetization mechanisms namely in multilayer film structures with alternate layers of soft magnetic and hard magnetic materials.



(CoNiP<sub>soft</sub>/CoP<sub>hard</sub>)<sub>n</sub> films were prepared by chemical deposition method. The content of phosphorus was 8 % at. in each layer. In hard magnetic layer the CoP was in hexagonal state and in soft magnetic layer the CoNiP was in amorphous state. In the last case the cobalt content was 57.5 % at. and nickel content was 24.5 % at. The thickness of each layer was  $t = 4$  nm. Magnetic measurements were made with vibrating-coil magnetometer in temperature range  $T = 77 \div 400$  K and in magnetic fields  $H < 10$  kOe. We investigated changes of magnetic parameters in dependence on number of layers in multilayer structure. In our experiments number of layer pairs was  $n \leq 15$ .

Earlier [2] it was established that the coercive force ( $H_C$ ) of CoP layers depends on layer thickness and  $H_C$  rises when layer thickness increases. In given case at nitrogenous temperatures the coercive forces of soft magnetic and hard magnetic layers were  $\sim 20$  Oe and  $\sim 1000$  Oe, respectively. The combination of these layers

into structure leads to substantial change of magnetic behavior of structure in whole. This is seen in Fig., where in parts **a** and in part **b** the curves of magnetization are presented for bilayer film and for film with 10 bilayers, respectively, at temperature  $T = 77.4$  K. It attracts attention that the soft magnetic layer determines the behavior of magnetization of film structure decreasing the coercive force of system. It points out that interlayer coupling has value which is comparable with exchange interaction within the layer.

The current investigations are being undertaken at financial support of the Russian Found of Basic Researches (Grant № 11-02-00675-a).

[1] I. Zutic, J. Fabian, S. Das Sarma, *Rev.Mod.Phys.*, **76** (2004) 323.

[2] A.V. Chzhan, G.S. Patrin, S.Ya. Kiparisov, et al., *Phys. Met. Metalloved.*, **109** (2010) 1.

22PO-I-8

**EPITAXIAL HETEROSTRUCTURES Co/Cu ON Si(111))***Davydenko A.V.<sup>1</sup>, Ivanov Yu.P.<sup>1</sup>, Ermakov K.E.<sup>1</sup>, Chebotkevich L.A.<sup>1,2</sup>*<sup>1</sup> Institute of physics and information technologies, Far Eastern National University, Sukhanov 8, 690950, Vladivostok, Russia<sup>2</sup> Institute for Automation and Control Processes, Far Eastern Branch of Russian Academy of Science, 5 Radio Street, 690041, Vladivostok, Russia

Since the discovery of giant magnetoresistance (GMR) [1] till nowadays there is enhanced interest of discovering systems of materials with the highest magnitude of effect. Particularly, Co/Cu multilayers have attracted much attention because of the giant magnetoresistance (MR) values [2]. Multilayer Co/Cu films grown on Si substrates are especially interesting object of investigation, because of rather simple procedure of preparation high quality epitaxial multilayers on nonconducting substrate and precise control of coverage of deposited materials. In this paper correlation of growth processes with MR properties of Co/Cu/Co deposited on Si(111) was investigated.

Epitaxial films were deposited in ultra high vacuum chamber. Vicinal substrates Si(111) with 4° misorientation towards [11-2] were used. Pressure in the system in deposition processes was less than  $5 \times 10^{-10}$  Torr. To prepare reconstructed Si(111)  $7 \times 7$  surface conventional procedure of cleaning samples was used. 11 ML Cu buffer layer was formed on Si surface to prevent formation of Co silicide. 14 ML Cu cap layer was formed to prevent samples from oxidation in the air. Structure of the films was investigated by means of reflection high energy electron diffraction (RHEED) and scanning tunneling microscopy (STM). Magnetic structure was studied by magnetic force microscopy. Hysteresis loops of magnetization were obtained by magneto-optical Kerr effect. MR properties were measured by two different four probe stations. On the first low field and precise measurements were carried out and on the second high fields up to 11 kOe were obtained. Geometry of MR measurement was current in plane, MR measurements were carried out at room temperature.

RHEED and STM investigation showed quasi layer-by-layer Co on Cu/Si(111) growth. When Cu spacer layer was deposited, 3D Cu islands 2-6 ML height were observed on the terraces. Second Co layer tended to grow 2D islands.

Magnetic and MR properties Cu(14 ML)/Co(6 ML)/Cu(d)/Co(6 ML)/Cu(11 ML)/Si(111) with coverage of Cu spacer  $d=1-7$  ML were studied. Coercive force of multilayered films was on the order of 200 Oe. Strong uniaxial magnetic anisotropy was induced by steps of Si substrate in the samples. Positive values of MR ratio  $(R(H)-R(H_{\max}))/R(H_{\max})$  for H||I and H⊥I orientations were obtained in films with Cu spacer layer (GMR effect). Probably, 3D growth of Cu spacer resulted in non uniform distribution of Cu spacer thickness between adjacent Co magnetic layers and, hence, existence of Co areas ferromagnetically and antiferromagnetically coupled. Magnitude of GMR depends on coverage of Cu spacer and orientation of magnetic field relative to easy axis of magnetization.

[1] M.N. Baibich, J.M. Broto, A. Fert, et al., *Phys. Rev. Lett.* **61**, (1988) 2472.

[2] S. S. P. Parkin, R. Bhadra, and K. P. Roche, *Phys. Rev. Lett.* **66**, (1991) 2152.

## THE MICROWAVE MAGNETIC AND STRUCTURAL PROPERTIES OF COMPOSITE AND MULTILAYER FILMS

Kotov L.N.<sup>1</sup>, Turkov V.K.<sup>1</sup>, Vlasov V.S.<sup>1</sup>, Ulyashev A.M.<sup>1</sup>, Kalinin Yu.E.<sup>2</sup>, Sitnikov A.V.<sup>2</sup>

<sup>1</sup> Syktyvkar State University, 167001 Syktyvkar, Oktyabrsky 55, Russia

<sup>2</sup> Voronezh State Technical University, 394026 Voronezh, Moskovsky Pr. 14, Russia

There are many experimental and theoretic works that devoted to research of UHF magnetic characteristics of composite and multilayer films [1-3]. This work is devoted to research of dependence of nanostructural characteristics and date of ferromagnetic resonance (FMR) of composite and multilayer films. The films of series: *A1* -  $(\text{Me1})_x(\text{Al}_2\text{O}_3)_y$ , *A2* -  $(\text{Me2})_x(\text{Al}_2\text{O}_3)_y$ , *B* -  $(\text{Me1})_x(\text{Me1-O}_a)_z(\text{Al}_2\text{O}_3)_y$ , *C* -  $\{(\text{Me1})_x(\text{Al}_2\text{O}_3)_y - (\text{Me1})_x(\text{Al}_2\text{O}_3)_y\}_{120}$ , *D1* -  $\{[(\text{Me1})_x(\text{Al}_2\text{O}_3)_y]-[\text{Si}]\}_{120}$ , *D2* -  $\{[(\text{Me2})_x(\text{Al}_2\text{O}_3)_y]-[\text{Si}]\}_{120}$ , *E* -  $\{[(\text{Me1})_x(\text{Al}_2\text{O}_3)_y]-[\text{Si:H}]\}_{120}$  were investigated, where  $\text{Me1} = \text{Co}_{45}\text{-Fe}_{45}\text{-Zr}_{10}$ ,  $\text{Me2} = \text{Co}_{45}\text{-Ta}_{45}\text{-Nb}_{10}$ ,  $0.3 < x < 0.62$ ,  $3 < y < 12$ ,  $y = 21 - 30x$ . The films were obtained in an argon atmosphere (*A1*, *A2*, *C*, *D1*, *D2* series) and with addition of oxygen (*B* series) or hydrogen (*E* series). All samples were deposited on substrates by the ion-beam sputtering method. The FMR spectra were obtained by an electron paramagnetic spectrometer at 9.45GHz with using a standard modulation method [1]. The DC magnetic field was directed along the films plane. The alternating magnetic field was perpendicular to the DC field and also was directed along to the plane of the films. The surface nanostructure and the size of metal granules of films were determined by atomic force microscopy (AFM). The dependences of FMR parameters (the width of line  $\Delta H$  and the resonance field  $H_{res}$ ) on metal concentration  $x$  of the composite and multilayer films has been carried out [2]. The dependences of the FMR parameters on  $x$  of composite films and multilayer composite-composite films are analogical. Wide maxima on the dependences  $\Delta H(x)$  of composite-semiconductor multilayer films were observed. The  $d_l(x)$  dependences of the thickness of semiconductor layer on  $x$  determined behavior of  $\Delta H(x)$  curves. In the area of maximum  $d_l(x)$  has maximal dispersion of demagnetization fields. In this case the electron exchange between composite granules through the semiconductor layers are minimal. The resonance fields for all films of different series are decreased during increasing of  $x$  according to growth of average magnetization. Based on the equations for the internal field and the FMR width of line the qualitative changes in nanostructure were determined.

This work was supported by RFBR (grant 10-02-01327).

[1] L.N. Kotov et al., *Material Science and Engineering*, **442** (2006) 352.

[2] L.N. Kotov et al., *JMMM*, **316** (2007) e20.

[3] L.N. Kotov et al., *Advanced Materials Research*, **47-50** (2008) 706.

## BIAS-CURRENT AND OPTICALLY DRIVEN TRANSPORT PROPERTIES OF THE HYBRID Fe/SiO<sub>2</sub>/p-Si STRUCTURES

Volkov N.V.<sup>1,2,3</sup>, Eremin E.V.<sup>1,2</sup>, Tarasov A.S.<sup>1,2</sup>, Varnakov S.N.<sup>1,2</sup>, Ovchinnikov S.G.<sup>1,2,3</sup>

<sup>1</sup> L.V. Kirensky Institute of Physics SB RAS, Krasnoyarsk, 660036, Russia

<sup>2</sup> Siberian State Aerospace University, Krasnoyarsk, 660014, Russia

<sup>3</sup> Siberian Federal University, Krasnoyarsk, 660041, Russia

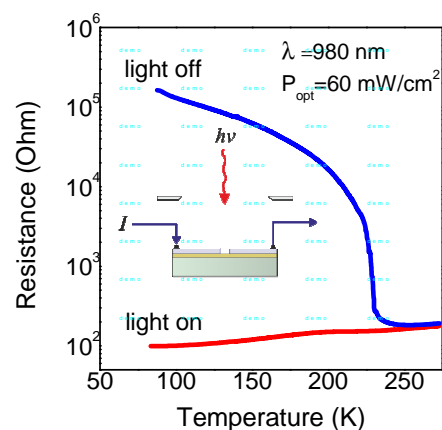
Hybrid nanostructures combining ferromagnetic metals and nonmagnetic semiconductors are very attractive for spintronic applications [1]. These structures are interesting for traditional semiconductor electronics and, simultaneously, are promising magnetic materials allowing current control by an electron spin and magnetization control by the spin-polarized current.

We studied the effect of optical radiation on the transport properties of the Fe/SiO<sub>2</sub>/p-Si hybrid structure in planar geometry. The structure was prepared by deposition of a thin (5 nm) Fe film on a p-doped Si substrate with a native SiO<sub>2</sub> layer (~ 1.2 nm). Pronounced magnetic-field- and bias-sensitive features of the transport properties of the Fe/SiO<sub>2</sub>/p-Si hybrid structure at temperature variation are found. Comparative analysis of two Fe/SiO<sub>2</sub>/p-Si samples, one with a continuous Fe film and the other with two electrodes formed from a Fe layer and separated by a micron gap, shows that these features are caused by the metal-insulator-semiconductor (MIS) transition with a Schottky barrier near the interface between SiO<sub>2</sub> and p-Si. Resistance of the MIS transition depends exponentially on temperature and bias. In the structure with a continuous ferromagnetic film, the competition between conductivities of the MIS transition and the Fe layer results in the effect of current-channel switching between the Fe layer and the semiconductor substrate.

We found one more way to control the transport properties of the Fe/SiO<sub>2</sub>/p-Si structures, specifically, optical radiation. In the structure with a gap, optical radiation gives rise to sharp (up to three orders of magnitude) decrease in resistivity of the structure below 250 K (see the figure). In the structure with a continuous ferromagnetic film, optical radiation affects current-channel switching between the Fe film and the semiconductor substrate.

The mechanism of the optical effect is photogeneration of electron-hole pairs in the semiconductor substrate near the boundary with SiO<sub>2</sub> layer. Photogenerated carriers contribute to the photocurrent across the Schottky barrier and, thus, shunt high tunnel resistance of this barrier at low temperatures.

We believe that the results obtained will be useful for various applications, in particular, fabrication of novel optically driven spintronic devices.



This study was supported by the Russian Foundation for Basic research, project no. 11-02-00367-a; Presidium of the Russian Academy of Sciences, program 21.1; the Division for Physical Sciences of the Russian Academy of Sciences, program 2.4.4.1; the Siberian Branch of the Russian Academy of Sciences, projects nos. 5 and 134; and the Federal target program, State contract NK-556P\_15.

[1] A. Fert, Thin Solid Films **2-5** (2008) 517.

## INFLUENCE OF TEMPERATURE ANNEALING ON FMR AND STRUCTURAL PROPERTIES OF SINGLE-LAYER AND MULTILAYER NANOCOMPOSITE FILMS

*Efimets Yu.Yu.<sup>1</sup>, Turkov V.K.<sup>1</sup>, Kotov L.N.<sup>1</sup>, Vlasov V.S.<sup>1</sup>, Kalinin Yu.E.<sup>2</sup>, Sitnikov A.V.<sup>2</sup>*

<sup>1</sup> Syktyvkar State University, 167001 Syktyvkar, Oktybrsky 55, Russia

<sup>2</sup> Voronezh State Technical University, 394026 Voronezh, Moskovsky Pr. 14, Russia

The work is devoted to the research of influence of annealing to ferromagnetic resonance (FMR) properties of films of A, B series with the compositions  $(\text{Co}_{45}\text{-Fe}_{45}\text{-Zr}_{10})_x(\text{Al}_2\text{O}_3)_y$ , multilayer films of the C series with compositions  $\{(\text{Co}_{45}\text{-Fe}_{45}\text{-Zr}_{10})_x(\text{Al}_2\text{O}_3)_y - (\text{Co}_{45}\text{-Fe}_{45}\text{-Zr}_{10})_x(\text{Al}_2\text{O}_3)_y\}_{120}$  and D series with compositions  $\{[(\text{Co-Fe-Zr})_x(\text{Al}_2\text{O}_3)_y] - [\text{a-Si}]\}_{120}$ . Also revealing FMR properties relationship with the structure characteristics was done. The composite and multilayer films were received in the argon atmosphere with pressure 0.04 Pa (A, C, D - series), and with the addition of oxygen with pressure  $3 \cdot 10^{-4}$  Pa (B - series) by the ion-beam sputtering method. The metal phase concentration varied in the limits  $0.26 < x < 0.63$ ,  $3 < y < 12$ ,  $y = 21-30 x$ . The FMR spectrum was obtained by the electron paramagnetic spectrometer RE-1306 on the 9.36 GHz frequency using the standard modulation index meter [1]. Annealing temperature  $T_{an}$  with the step  $\sim 50$  K changed from 300 K to 800 K. The annealing time of the samples in air atmosphere was 1 hour. The dependencies of the FMR spectra width of line  $\Delta H$  and the resonance field magnitude  $H_{res}$  on the annealing temperature  $T_{an}$  for different metal phase concentrations  $x$  were measured experimentally. For films of series A, C at increase of  $T_{an}$  growth of films absorbed power by nonuniform precession modes field lay less than the FMR was observed. The growth of absorption occurs at concentration of  $x$  below the percolation threshold threshold ( $x \leq 0.42$ ). The ratio of absorbed power for the homogeneous and inhomogeneous modes varied more than an order of magnitude with increasing annealing temperature for films of series A, C. Also during the annealing due to oxidation of the films there was increase of the  $\Delta H$  due to the growth of inhomogeneity of the films surface layers. This phenomenon was especially shown for multilayered films of series C for which thickness of composite layers much smaller than for films of series A. For films of the series C, the growth of  $\Delta H$  upon annealing after the percolation threshold was about an order of magnitude greater than for films of series A. This indicates the much greater structure changing of the films of series C compared with films of series A.  $H_{res}$  for films of series A, C at  $x$  below percolation threshold ( $x \leq 0.42$ ) during annealing slightly decreased, and after percolation ( $x > 0.42$ ) grew approximately in 2 times compared with values for films before annealing due to decreasing of average films magnetization. The nonmonotonic dependence of  $\Delta H$  on the annealing temperature  $T_{an}$  is typical for films of B series.  $\Delta H$  have the minimum for all  $x$ . At the higher  $x$  and lower  $T_{an}$ ,  $\Delta H$  starts to grow. The deepest minimum occurs at  $x \approx 0.32$ . In the temperature range of  $\Delta H$  growth for film series B decrease in the  $H_{res}$  for all  $x$  occurs, especially a strong decrease is observed for films with small  $x < 0.4$ . Gradual decrease of the  $\Delta H$  and the increase of the  $H_{res}$  are observed for films series D with the increase of the  $T_{an}$  and can be explained by decreasing average magnetization and formation of silicides and silicates. Based on the equations for the internal field and the width of line the qualitative changes in films structure were determined.

This work was supported by RFBR (grant 10-02-01327).

[1] L.N. Kotov et al., *Material Science and Engineering*, **442** (2006) 352

22PO-I-12

## CONCENTRATION AND ANGULAR DEPENDENCES OF FMR IN SINGLE-LAYER AND MULTILAYER $(\text{Co-Ta-Nb})_x\text{-(SiO}_2)_y$ FILMS

Turkov V.K.<sup>1</sup>, Kotov L.N.<sup>1</sup>, Andreev A.S.<sup>1</sup>, Vlasov V.S.<sup>1</sup>, Kalinin Yu.E.<sup>2</sup>, Sitnikov A.V.<sup>2</sup>

<sup>1</sup> Syktyvkar State University, 167001 Syktyvkar, Oktybrsky 55, Russia

<sup>2</sup> Voronezh State Technical University, 394026 Voronezh, Moskovsky Pr. 14, Russia

Research of concentration and angular dependences of resonance position and FMR width of line on magnetic field was carried out in given work for single layer and multilayer composite films of structures:  $(\text{Co-Ta-Nb})_x - (\text{SiO}_2)_y$  (series L),  $\{[(\text{Co-Ta-Nb})_x - (\text{SiO}_2)_y] - [\text{SiO}_2]\}_{56}$  (series M). Films were received by the ion-beam sputtering method in argon atmosphere at pressure  $P=4 \cdot 10^{-2}$  Pa. 45 samples for both series of films were investigated. The metal phase concentration in composite layers was increased monotonously with increasing sample number. The FMR spectrum was obtained by the electron paramagnetic spectrometer RE-1306 on the 9.36 GHz frequency using the standard modulation index meter [1].

FMR metal concentration dependences of both films series behave basically equally. The decreasing of width of resonance line was observed at the metal phase concentration area above percolation threshold with concentration increasing. It was connected with the increasing of exchange interaction between metal granules. The increasing of films metal phase concentration leads to increase in dispersion of internal demagnetization fields and FMR width of line in the metal concentration area less percolation threshold. Therefore the maximum for series L was observed on concentration dependence of width of the resonant line. Difference of films FMR spectra of series M was shown in shift of the maximum on dependence of the width of line to the area of lower concentration in comparison with films of series L and further sharper falling at increasing of metal concentration. Since 15 number of the sample the dependence of width of the line of series L and M are similar. The width of line of series L and M was decreased similar at increasing metal concentration. Thus dependences of resonant fields for series L, M of films at increasing of metal concentration were behaved similarly. The behavior of resonant fields was described by standard Kittel formula. Concentration dependences of FMR width of line correspond to theoretical model of Rubinstein [2].

Dependences of the position of resonance and width of the line on angle between the film plane and external magnetic field direction for samples of both series were received also. Angular dependences of the resonant field have the minimum at parallel and the maximum at the perpendicular orientation of the magnetic field relatively the film plane. Difference of angular dependences of the width of line consisted in maximum observed at the direction of the dc magnetic field different from perpendicular. Using Kittel formula allows calculating the effective internal magnetic fields and the g-factor of samples. The effective field was monotonously increased with increasing of metal phase concentration. That corresponds increasing of the average magnetization of films. Concentration dependences of the g-factor had the maximum in the percolation threshold area.

This work was supported by RFBR (grant 10-02-01327).

[1] L.N. Kotov et al., *Material Science and Engineering*, **442** (2006) 352

[2] M. Rubinstein et al., *Phys. Rev. B*, **50** (1994) 184

## MAGNETIC PROPERTIES OF ONE AND TWO DIMENSIONAL NANODOTS ARRAYS

Stebliy M.E.<sup>1</sup>, Ognev A.V.<sup>1,2</sup>, Samardak A.S.<sup>1</sup>, Chebotkevich L.A.<sup>1,2</sup>

<sup>1</sup>Laboratory of thin film technologies, FENU, Vladivostok, 690950, Russia

<sup>2</sup>Institute of Automation and Control Processes, FEBRAS, Vladivostok, 690041, Russia

Arrays of nanoscale objects are promising as media for data storage [1] and magnetoresistive memory cells [2]. Magnetic properties of nanostructures in the array depend not only on the parameters of its constituent elements, but also on the array's geometry, because magnetostatic interaction, which arises between nanodots has important role in the reversal process. In our work we first investigated the effect of the size of one and two dimensional nanodots arrays (1xN and NxN, N – numbers of nanodots in face of arrays) on the magnetic properties.

To prepare the samples the naturally oxidized (111) silicon substrates were coated by PMMA 950K resist, then array was fabricated by means of electron-beam lithography and lift-off techniques. The 20 nm thick Co layer was deposited by thermal evaporation in UHV and capped by 2 nm Cu to prevent oxidation. After lift-off processes the arrays of nanodots with diameter equal 600 nm were obtained. The distances between nanodots  $d = 0,2; 0,5; 1D$ , number of nanodots  $N = [2 \div 15]$ . The quality of the pattern morphology and the structure periodicity were analyzed by scanning electron microscopy (SEM) and atomic force microscopy (AFM).

Magnetic properties of arrays were investigated by magneto-optical Kerr effect (MOKE) and magnetic force microscopy (MFM). The experimental results were compared with 3D micromagnetic simulations performed by using OOMMF code [5].

It was found that the size of the array influences on the magnetic properties of nanostructures significant. It was found that with increasing N there is a change of the characteristic fields (coercivity ( $H_c$ ), the annihilation field ( $H_a$ ) and the nucleation of vortex states ( $H_n$ )). For  $N > 5$  the curves saturate. The figure shows the dependence of  $H_c$  on the size of the array for the chains and matrices nanodisks. It was found that with increasing N in the chains  $H_c$  increases and decreases in the matrices.

MSM images of the chains and arrays nanodisks with  $d = 0,3 D$  show that the magnetostatic interaction distorts the micromagnetic structure (Fig. 1b). The results are confirmed by micromagnetic modeling (Fig. 1c).

It was determined that in the close-packed two dimensional arrays biaxial anisotropy of the magnetization processes presents, and in chains – uniaxial.

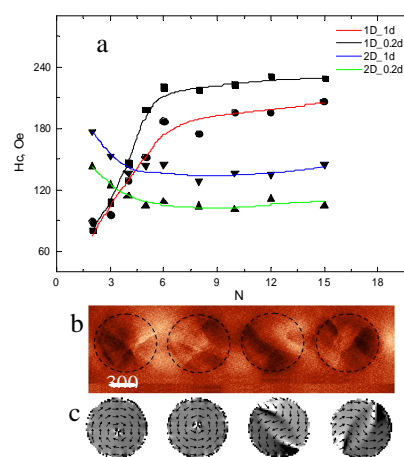


Fig. 1. The coercive force ( $H_c$ ) v.s. number of dots in face of arrays (a), MFM image of four nanodots and

Support by FCP (contracts P410, P1424), President grants and AVCP.

- [1] S. Tehrani, E. Chen, J.M. DeHerrera, J.M. Slaughter, J. Shi // J. Appl. Phys. 85, 5822, 1999.
- [2] G.M. McClelland, M.W. Hart, M. E. Best, B.D.Terris, Appl. Phys. Lett. 81, 1483, 2002.
- [3] C. Mathieu, C. Hartmann, M. Bauer, O. Büttner, S. Riedling, B. Roos, S.O. Demokritov, B. Hillebrands // Appl. Phys. Lett. 70, p. 2912, 1997.
- [4] Guslienko K. Yu. // Physics Letters A. 2001. V. 278. P. 293.
- [5] <http://math.nist.gov/oommf/>



## CHARACTERISTICS OF THE PERIODIC FINE STRUCTURE IN DOMAIN WALLS IN VACUUM-DEPOSITED FILMS

*Sagdatkireeva M.B., Rumyantseva V.V., Khasanov N.A.*  
Bashkir State University, Ufa, Validi Str., 32, 450074 Russia

The development of nanomaterials with high operational and technological properties for modern microelectronics is interesting for both scientific and practical points of view.

The dependence of the domain structure of oblique-evaporated films of quantum-well thickness and the angle of inclination of the easy-magnetization axis with respect to the normal to the quantum well plane has been studied. It is found that the self-organization of domain structures is mainly related to the quantum character of the cooperative phenomenon.

The ground state of thin ferromagnetic films composed of QWs of cubic symmetry with oblique EMA, forming an obtuse angle with the film plane, was studied based on the Hamiltonian

$$H = H_{\text{ex}} + H_{\text{elas}} + H_{\text{me}} + H_{\text{dem}},$$

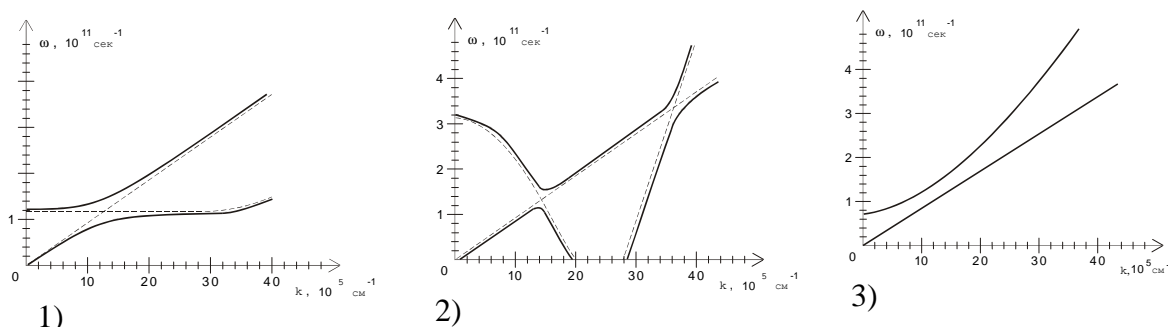


Fig.1. Magnetoelastic wave spectrum for multi-axis ferromagnetic quantum walls (QW) with 500 Å thickness with sloping anisotropy 1)  $\psi=0$  rad, 2)  $\psi=50$  rad, 3)  $\psi=67$  rad at  $K_a/K_\psi=-0.1$ ,  $\mathbf{k}$  is wave vector,  $\omega$  is the frequency of related magnetoelastic wave,  $\omega_0$  is the magnetic gap value,  $\omega_1$  is the first frequency,  $\omega_2$  is the second frequency of magnetoelastic resonance.

Self-organized stripe domain structure in evaporated QW-thick films due to the spectrum of related magnetoelastic wave (see Fig.1,  $\psi=50$  rad) is showed in the table:

The table shows that DS vary by polarity and the density of fine structure. The obtained results allow to elucidate a mechanism of effective controlling of some properties of magneto-ordered films that may be important in modern electronics.

Ph. No.	Conditions for DS existence	DW energy	DW orientation	Polarity		DS type
				DW	DS	
1	$\phi_1 < 0, \phi_2 < 0$ $\phi_2/\phi_1 =  R  \leq 1$	$E_1 = 4\phi_1 \Delta l_{2k_\lambda} [1 + R \cdot l_{2k_s}]$ $0.68 \leq k_s \leq 0.91$		-	-	$0.55 \leq k_\lambda \leq 0.91$ (negative stripes)
2	$\phi_1 < 0, \phi_2 > 0$ $ R  \leq 1$	$E_3 = 4\phi_1 \Delta l_{2k_\lambda} [1 - R \cdot l_{1k_s}]$ , $k_s \geq 0.91$		-	+	$0.55 \leq k_\lambda \leq 0.91$ (negative stripes)

Note:  $l_{1k_s} = [2E(k_s) - k_s'^2 K(k_s)]/k_s^2 K(k_s)$ ,  $l_{2k_s} = [K(k_s) - 2E(k_s)]/k_s^2 K(k_s)$ ,  $l_{1k_\lambda} = [2E(k_\lambda) - K(k_\lambda) k_\lambda'^2]/2k_\lambda$ ,  $k_\lambda'^2 = 1 - k_\lambda^2$ ;  $k_s'^2 = 1 - k_s^2$ ;  $l_{2k_\lambda} = [K(k_\lambda) - 2E(k_\lambda)]/2k_\lambda$ , where  $k_s$  and  $k_\lambda$  are the modules of elliptic integrals of I and II kinds, respectively;  $K(k_\lambda)$ ,  $K(k_s)$ ,  $E(k_s)$ ,  $E(k_\lambda)$ ;  $\lambda$  is the DS half-period; and  $s$  is the periodic fine-structure half-period.  $\phi_1, \phi_2$  are eff. constants of anisotropy.

[1] S.V. Vonsovsky, Y.S.Shur. Ferromagnetism (Gostech., Moscow, 1948).

[2] M.B. Sagdatkireeva et al., Izv. RAN, Ser. phys., 2004. P.689.

22PO-I-15

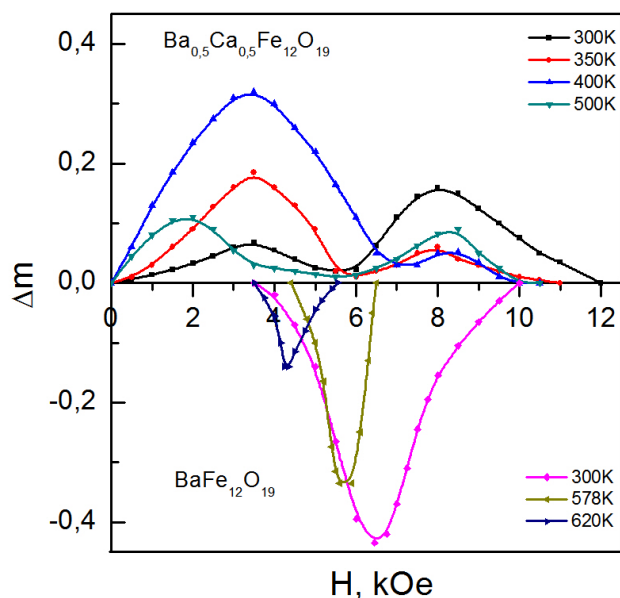
## INTERPARTICLE MAGNETIC INTERACTION IN THE CLOSE-PACKED SYSTEMS OF HIGHANISOTROPIC NANOCRYSTALS

Shurina E.V.<sup>1</sup>, Mozul K.A.<sup>1</sup>, Chernikov S.<sup>2</sup>

<sup>1</sup> Karazin Kharkov National University, Svobody Sqr. 4, Kharkov 61077

<sup>2</sup> Belgorod, Belgorod State University, Center NSMN

e-mail: [giperbola79@mail.ru](mailto:giperbola79@mail.ru)



In the formation of the magnetic properties of ensembles of small particles along with the size and surface factors that are important and moreover, an ambiguous role played the interparticle magnetic interaction. Interaction parameters depend from the intrinsic properties of the material (the magnetic moment, constant of effective magnetic anisotropy), external factors (magnetic field, temperature) and the packing density of particles in the sample.

The object of research was calcium hexagonal ferrite  $\text{Ca}_{0.5}\text{Ba}_{0.5}\text{Fe}_{12}\text{O}_{19}$  in the form of model system of lamellar nanocrystals (small Stoner-Wohlfarth particles) with the distribution by the diameter of 10-100 nm. Experimental sample

was a close-packed system of randomly oriented nanocrystals. In this paper, parameter of the resulting interparticle magnetic interaction  $\Delta m$  determined in the temperature range 300-600K and in magnetic fields from 0.5 to 12 kOe in the regime of irreversible magnetization using the Wohlfarth ratio which establishes the relationship between the remanent magnetization  $m_r(H)$  and  $m_d(H)$  followed by plotting Henkel  $m_d = f(m_r)$  and Kelly  $\Delta m = m_d - (1 - 2m_r)$ . The figure shows the dependences  $\Delta m(H)$  of experimental powder sample  $\text{Ca}_{0.5}\text{Ba}_{0.5}\text{Fe}_{12}\text{O}_{19}$  for the range temperatures in comparison with the system of nanocrystals (similar dispersion) of the base composition  $\text{BaFe}_{12}\text{O}_{19}$ . Founded two fundamental differences: if for the barium ferrite  $\Delta m < 0$  and maximum of  $\Delta m(H)$  observed at the single field value, then for the calcium ferrite  $\Delta m > 0$  and observed two peaks in the curve  $\Delta m(H)$  and with increasing temperature there is a redistribution of their intensity. For a discussion of possible reasons of the observed differences used elektron-microscopic researches and basic magnetization curves.

## SIZE AND SHAPE INFLUENCE ON MAGNETIZATION REVERSAL OF Py NANOFILM GROWN ON NIOBIUM

*Uspenskaya L.S.<sup>1</sup>, Egorov S.B.<sup>1</sup>, Chugunov A.A.<sup>2</sup>*

<sup>1</sup> Institute of Solid State Physics RASc, 142432, Chernogolovka, Russia

<sup>2</sup> Department of Fundamentals of Physical-Chemical Engineering of MSU, 119991, Moscow, Russia

Magnetic properties of artificial hybrid structures like nanolayers of hard and soft ferromagnet, ferromagnet and superconductor, are widely studied last years because of interesting physics and importance for applications. The easily switched by magnetic field soft layer plays a role of switching element, which controls the resistance of the hybrid. This layer is usually chosen by its characteristics obtained in free state. However the vicinity of second layer could vary the quality of soft magnetic layer. This is well known for the hybrids of hard-soft ferromagnet, where the coercitivity and symmetry of hysteresis loops [1], the rate of magnetization of soft ferromagnet [2] and easy axes direction [3] are known to be changed. So, it is naturally to assume that the properties of soft magnetic layer in hybrid structure of ferromagnet-superconductor can also vary.

Here we report the results of experimental study of magnetization reversal of bilayer hybrid nanofilm, consisting of permalloy layer grown on niobium layer by magnetron sputtering. The hybrid structures were shaped during growth procedure as squares, rings and stripes of micron sizes with different aspect ratios.

First of all, we have found that magnetization reversal of permalloy in hybrids and in the free permalloy layers differs not only by the value of coercitivity, by the duration of time of domain wall nucleation and by the rate of magnetization reversal, but in a qualitative sense.

Second, we have observed the dependence of kinetics of magnetization reversal upon the structures sizes and aspect ratios; smart rotational modes appear with the reduction of structure sizes below some critical size  $L$ . The surprise was not only the emergence of new modes of reversal, but the dimension of the structure under which the transition to new modes of reversal; the critical size  $L$  was much larger than the width of the domain wall in permalloy; it was of the order of several micrometers.

Next, we have seen that the coercitivity and the delay of magnetization reversal depend upon the size and shape of the structure.

And finally, we have shown the influence of the rate of magnetic field application on kinetics of magnetization reversal.

It is important to note that the experiments were performed at room temperature, that means the proximity of a superconductor could not influence the properties of the ferromagnet.

Support by RFBR grant 09-02-00856 and by RAS program "Quantum physics of condense matter" is acknowledged.

[1] I. Zutic, J. Fabian, S. Das Sarma, *Rev. Mod. Phys.*, **76** (2004) 323.

[2] L.S. Uspenskaya, *Bulletin RAS: Physics*, **74** (2010) 711; (*Izvestiya RAN, Ser. Fizicheskaya*, **74** (2010) 744.

[3] L.S. Uspenskaya, *Phys. Sol. State*, **52**, (2010) 2274; (L.S. Uspenskaya, *Fizika Tverdogo Tela*, **52**, (2010) 2131).

## THE FEATURES OF THE STRUCTURE AND MAGNETIC PROPERTIES OF Co-SiO<sub>2</sub>, Co-Al<sub>2</sub>O<sub>3</sub> COMPOSITE FILMS WITH GIANT MAGNETORESISTANCE EFFECT.

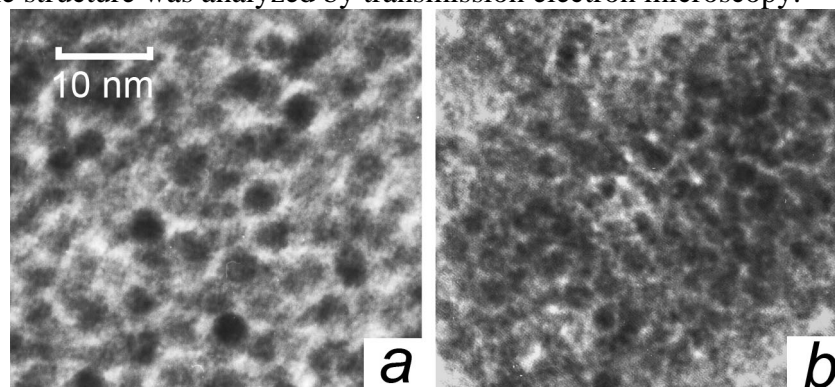
Gorkovenko A.N.<sup>1</sup>, Vas'kovskiy V.O.<sup>1</sup>, Lepalovskij V.N.<sup>1</sup>, Shchegoleva N.N.<sup>2</sup>

<sup>1</sup>Ural State University, 620000, Lenin av. 51, Ekaterinburg, Russia

<sup>2</sup>Institute of Metal Physics, 620041, S. Kovalevskoi 18, Ekaterinburg, Russia

The composite magnetic structures such as a 3d-metal-insulator interested as carriers of a some new physical phenomena – the giant Hall effect and giant magnetoresistance, but also are considered as a functional materials [1, 2].

The given work studies the influence of the structural state on the magnetic and magnetoresistive properties of film composites Co-SiO<sub>2</sub> and Co-Al<sub>2</sub>O<sub>3</sub>, which obtained by magnetron sputtering. The samples of film with thickness of 100 nm were formed onto glass substrates «Corning» by cosputtering targets of Co and SiO<sub>2</sub> (or Al<sub>2</sub>O<sub>3</sub>). The substance of metal in the films were varied from 30 to 60% for samples of type Co-Al<sub>2</sub>O<sub>3</sub> and from 40 to 60% for samples of type Co-SiO<sub>2</sub>. Magnetic properties were measured by VSM (at room temperature and magnetic fields up to 15 kOe) and SQUID-magnetometer (in the temperature range 5 ÷ 300 K in magnetic fields up to 70 kOe). The measurement of the magnetoresistance were performed at room temperature by double-probe method. The structure was analyzed by transmission electron microscopy.



The analyses of the magnetization curves and ZFC-ZC technique is shown that in certain temperature in cobalt content 50% or less for both types of films are characterized by superparamagnetic behavior. It is associated with the presence in the microstructure of thin films, which is a system of magnetic grains in the matrix of dielectric material. The estimates shown that in films with 50% of the average concentration of the metal grain size is equal about 5 nm, and it tends to increase with increasing Co content. The electron microscopy confirms the assessments and indicate a somewhat smaller grain size in the films of Co-Al<sub>2</sub>O<sub>3</sub> (Fig. 1a) as compared with films of Co-SiO<sub>2</sub> (Fig. b)

It was established that in the studied concentration of both types of films have the magnetoresistance. The maximum value of the effect observed in 50% of the Co content. In a magnetic field of 15 kOe it was about 6% and 8% for films Co-SiO<sub>2</sub> and Co-Al<sub>2</sub>O<sub>3</sub>, respectively.

[1] J.C Denardin, M Knobel, X.X Zhang, A.B Pakhomov, *JMMM*, **262** (2003) 15.

[2] W. Changzheng, Z. Peiming, Z. Libo, X. Xiaoguang, R. Yonghua, *Thin Solid Films*, **516** (2008) 3422.

22PO-I-18

## MAGNETIC BEHAVIOR AND MAGNETORESISTANCE OF NANOSIZED SUPERLATTICES Mo/Fe/Co

*Antipov S.D., Gorunov G.E., Kaminskaya T.P., Kornilov A.A., Novikov I.M., Pivkina M.N.,  
Senina V.A., Smirnitckaya G.V., Stetsenko P.N.*

M.V. Lomonosov Moscow State University, Moscow, GSP-1, Leninskie Gory, build.2,  
Faculty of Physics, Russia

In this paper we report the results on the investigation of magnetic behavior and magnetoresistance of nanosized three-components superlattice  $[\text{Mo}(12\text{\AA})\text{Fe}(x\text{\AA})\text{Co}(21\text{\AA})]_{100}$  ( $x=4\div 43$ ). Magnetic superlattices (MSL) Mo/Fe/Co have been obtained by cathode sputtering from two opposed cathodes on mica substrates (muscovite) at  $70^{\circ}\text{C}$  temperature.

Basic magnetic properties were measured along and across the planes of samples MSL at room temperature. Magnetic measurements were carried out using VSM with  $2 \cdot 10^{-7}$  emu sensitivity in fields  $\pm 8\text{kOe}$ . The surface of MSL were imaged using scanning probe microscope in semi-contact atomic force microscopy mode at room temperature. The image shows an island structure with size distributions.

The average size of islands was  $\sim 1000\text{\AA}$  across the direction of magnetic field at deposition ( $H_d$ ) and  $\sim 700\text{\AA}$  across  $H_d$ , the average value of difference of height was  $\sim (70\div 80)\text{\AA}$ .

According XRD data the samples MSL Mo/Fe/Co are in amorphous or nanocrystalline phases.

Measurements of magnetoresistance have been performed by use four-point methods in magnetic field  $(+10)\text{kOe} - 0 - (-10)\text{kOe}$  and temperature  $(10\div 220)\text{K}$  on a computerized research facility. Magnetoresistance have been recorded at the various angles between the direction of magnetic field and the plane of the sample.

It was found that there are oscillatory character spontaneous magnetization, remanent magnetization and coercivity fields on the Fe thickness with period of  $5\text{\AA}$ . It can be due to interference effects in electron waves leading to the formation of "quantum wells" in the interfaces. Some samples have drug and stepped shape of the hysteresis loops, which is connected existence of vortex type of magnetic structure and dynamics of their behavior in magnetic field. This is evidenced by studies using atomic force microscope.

We found semi conductivity temperature dependence of resistivity of investigated samples MSL.

Measurements of magnetoresistance of different temperatures were positive sign, as well as directly proportional to temperature. Asymmetry and hysteresis curves of magnetoresistance were observed. Possible reasons of this behavior of the temperature dependence of the magnetoresistance were identified.

22PO-I-19

## FERROMAGNETIC BEHAVIOR OF Pt NANOPARTICLES

*Antipov S.D.<sup>1</sup>, Gorunov G.E.<sup>1</sup>, Perov N.S.<sup>1</sup>, Pivkina M.N.<sup>1</sup>, Said-Galiyev E.E.<sup>2</sup>, Semisalova A.S.<sup>1</sup>, Stetsenko P.N.<sup>1</sup>*

<sup>1</sup> M.V. Lomonosov Moscow State University, Faculty of Physics, Moscow, GSP-1, 119991, Leninskie Gory, 1, bld.2, Russia

<sup>2</sup> A.N. Nesmeyanov Institute of Organoelement Compounds of the Russian Academy of Sciences, Moscow, GSP-1, 119991, V-334, Vavilova Str., 28, INEOS, Russia

The study of magnetic properties of 4d, 5d metal Pd and Pt nanoparticles and clusters attracts a great attention since these metals are paramagnetic in bulk state [1,2].

In this work we report the ferromagnetic behavior of the Pt nanoparticles produced by chemical methods. The metal organic chemical fluid deposition process with supercritical fluid have been used. Highly dispersed Pt clusters were fabricated on the surface of the porous spherical  $\gamma$ -Al<sub>2</sub>O<sub>3</sub> nanoparticles. The samples were produced in Institute INEOS RAS:

The particles size distributions were determined by small-angle X-rays scattering (SAXS) of Pt clusters. The bimodal particle size distribution with  $R_{1max}=20$  Å and  $R_{2max}=40$  Å was found for Pt clusters. The magnetic properties were investigated in magnetic fields up to 16 kOe at the temperature 80÷400 K by the vibrating sample magnetometer.

Pt/ $\gamma$ -Al<sub>2</sub>O<sub>3</sub> nanoparticels revealed the ferromagnetic behavior in whole temperature range 80÷400 K, the Curie temperature  $T_c$  was found to be considerably higher than 400K. The value of coercive field gradually decreased from 130 Oe to 80 Oe with temperature increase from 80 to 400 K.

Also the magnetic properties of nanoparticles Pt/SiO<sub>2</sub> fabricated by the same chemical method were investigated. The paramagnetic behavior was observed for these Pt/SiO<sub>2</sub> nanoparticles at the temperature 80÷400 K and magnetic field up to 16 kOe.

The origin of ferromagnetic behavior in Pt/ $\gamma$ -Al<sub>2</sub>O<sub>3</sub> nanoparticles prepared by chemical methods is discussed.

[1] T. Shinohara and T. Sato "Surface Ferromagnetism of Pd Fine Particles", Phys. Rev. Lett. 91, 197201 (2003).

[2] V. Kumar and Y. Kawazoe "Evolution of atomic and electronic structure of Pt clusters: Planar, layered, pyramidal, cage, cubic, and octahedral growth", Phys. Rev. B 77, 205418 (2008).

22PO-I-20

## MAGNETOTRANSPORT PROPERTIES OF GRANULAR (Cu+Co<sub>41</sub>Fe<sub>39</sub>B<sub>20</sub>)<sub>x</sub>(CuO<sub>n</sub>)<sub>100-x</sub> NANOCOMPOSITES

*Makagonov V.A., Kashirin M.A., Kudrin A.M.*

Voronezh State Technical University, Moskovsky Prospect, 14, Voronezh, Russia

The nanogranular composites consisting of a metallic grains of Cu and Co<sub>41</sub>Fe<sub>39</sub>B<sub>20</sub> in the wide-gap semiconductor CuO<sub>n</sub> matrix have been obtained in an argon atmosphere  $p_{Ar} = 3,6 \times 10^{-4}$  Torr by ion-beam sputtering. The structure of the composites have been investigated by a transmission electron microscopy.

The magnetoresistance of the investigated composites was negative and isotropic, i.e. does not depend on the relative position of the electric current and magnetic field. Field dependences of the magnetoresistance of the nanocomposites are typical for systems of ferromagnetic metal-dielectric (Fig. 1), indicating that it's a spin-dependent tunneling mechanism, as a determinative a magnetoresistance of those samples.

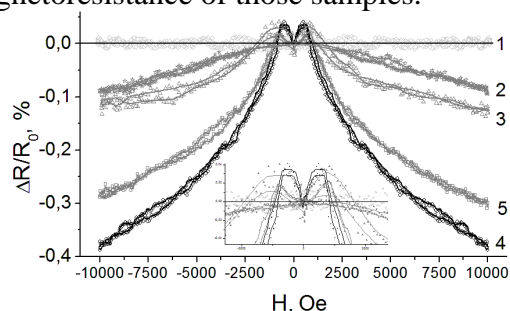


Fig. 1 Field dependences of magnetoresistance of the  $(\text{Cu}+\text{Co}_{41}\text{Fe}_{39}\text{B}_{20})_x(\text{CuO}_n)_{100-x}$  composites with different fractions (X, at.%) of amorphous conducting phase: 1 – X = 17 at.%; 2 – X = 29 at.%; 3 – X = 42,5 at.%; 4 – X = 50,2 at.%; 5 – X = 46,8 at.% (magnetic field was directed along the film plane and current direction)

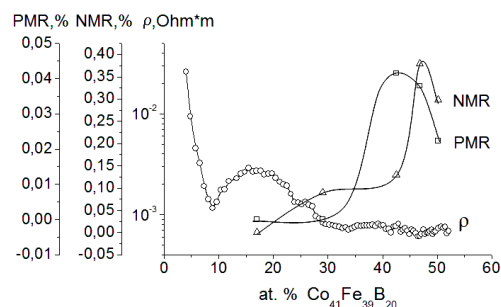


Fig. 2 Dependences of resistivity and magnetoresistance of  $(\text{Cu}+\text{Co}_{41}\text{Fe}_{39}\text{B}_{20})_x(\text{CuO}_n)_{100-x}$  composites of the fraction of the amorphous metal phase  $\text{Co}_{41}\text{Fe}_{39}\text{B}_{20}$  (X, at.%)

On the background of a negative magnetoresistance (NMR) in small fields a positive (PMR) (inset in Fig. 1) have been taken place. The influence of the composite amount to the negative and positive magnetoresistance have been showed at figure 2.

In granular ferromagnetic metal - dielectric nanocomposites maximum values NMR and PMR of concentration dependence have been observed at concentrations of the metallic phase just below the percolation threshold. NMR and PMR plots (Fig. 2) have been shown that the percolation threshold of the  $(\text{Cu}+\text{Co}_{41}\text{Fe}_{39}\text{B}_{20})_x(\text{CuO}_n)_{100-x}$  composite  $\sim 50$  at. % or higher. But at the concentration dependence of resistivity at those X no features were found. Moreover, with X greater than 30 at. % the resistivity practically does not depend on the concentration of metallic phase, which is typical for nanocomposites above the percolation threshold. This discrepancy could be explained by the presence of pure copper grains that determine the percolation threshold for electrical properties and has no effect on the magnetotransport properties.

This work was supported by RFBR (grant № 10-02-90030)

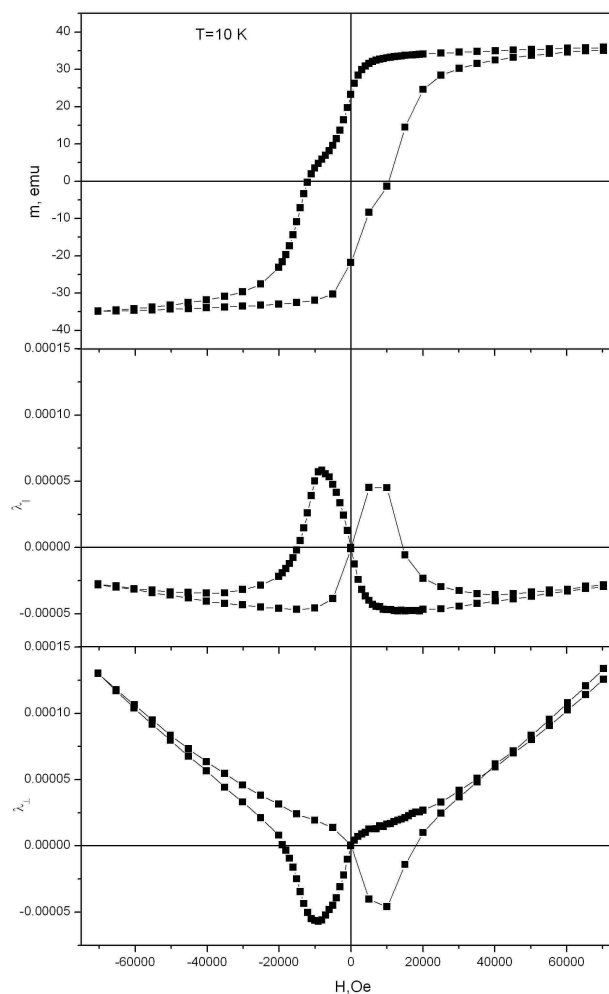
## MAGNETIC AND MAGNETOELASTIC PROPERTIES OF A BULK NANOSTRUCTURED Nd-Fe-B TYPE ALLOY MANUFACTURED BY SPARK PLASMA SINTERING METHOD

Sabiryanova E.A.<sup>1</sup>, Kudrevatykh N.V.<sup>1</sup>, Volegov A.S.<sup>1</sup>, Neznakhin D.S.<sup>1</sup>, Chuvildiev V.N.<sup>2</sup>, Lopatin Yu.G.<sup>2</sup>

<sup>1</sup> Ural State University named after A. M. Gorky, 620083, Ekaterinburg, Russia

<sup>2</sup> Lobachevsky State University of Nizhni Novgorod National Research University, 603950, Nizhni Novgorod, Russia

From the moment of their discovery, hard magnetic materials based on the Nd-Fe-B system alloys have always been and currently are in the center of attention of researchers and technologists. It concerns also the nanostructured alloys (NSA) basically manufactured by the melt spinning technique in a shape of flakes or coarse powders. This material shape does not allow to investigate their magnetoelastic properties, such as magnetostriction distortions which accompany the magnetization reversal process. Thus in this work the attempt for a bulk nanostructured Nd-Fe-B type alloy (BNSA) manufacturing has been made and its magnetic and magnetoelastic properties study were performed for the first time. The sample of BNSA Nd-Fe-B type has been obtained from the initial MQP-B brand NSA powder using a spark plasma sintering method (SPS) [1]. The final material density was about  $7.5 \text{ g/cm}^3$ . Its magnetic hysteresis properties behavior have been studied with a help of SQUID magnetometer in the fields up to  $\pm 70 \text{ kOe}$  in temperature range 10-200 K. Magnetostriction strains ( $\lambda_{\parallel}, \lambda_{\perp}$ ) were determined in the same fields and temperatures using a special small strain gauges attached on the sample surface. A typical magnetization loop ( $m(H)$ ) and longitudinal and transverse magnetostrictions ones ( $\lambda_{\parallel}(H)$ ,  $\lambda_{\perp}(H)$ ) measured at 10 K for BNSA sample are shown in figure 1. It can see that the magnetization reversal process accompanies with the essential sample length changes both along and across applied magnetic field direction which are much higher that for  $\text{Nd}_2\text{Fe}_{14}\text{B}$  single crystal along [100] or [110] axes [2]. The reasons of such  $\lambda_{\parallel}(H)$  and  $\lambda_{\perp}(H)$  behaviour for Nd-Fe-B BNSA sample in the connection with its magnetization state at different temperatures and magnetic fields will be discussed in our report.



[1] [www.tokyo-boeki.ru](http://www.tokyo-boeki.ru), Spark Plasma Sintering

[2] A.V.Andreev, A.V.Deryagin, N.V.Kudrevatykh, N.V.Musnikov, V.A. Reimer, S.V.Terent'ev, J. JETP, **90**, (1986) 1042–1050



## MAGNETIC ORDERING IN HETEROGENEOUS MULTILAYER NANOSTRUCTURES SUPERPARAMAGNETIC COMPOSITE - SEMICONDUCTOR

*Dunets O.V., Kalinin Yu.E., Sitnikov A.V., Kashirin M.A., Makagonov V.A.*  
Voronezh State Technical University, Russia

Earlier it has been observed that inserting of semiconductor layers into a superparamagnetic pre-percolation metal-dielectric composite leads to appearance of the magnetic ordering in the heterogeneous structure. This phenomenon has been investigated in a large number of different multilayered structures. All the multilayered structures were obtained by ion-beam sputtering technique and contained the same composite layers  $(\text{Co}_{40}\text{Fe}_{40}\text{B}_{20})_{33,9}(\text{SiO}_2)_{66,1}$  with a thickness of 2-5 nm separated by different semiconductor layers ( $\text{SiO}_2$ , Si,  $\text{In}_{35,5}\text{Y}_{4,2}\text{O}_{60,3}$ , SiC, C, Cu, CuO,  $\text{Bi}_2\text{Te}_3$ ,  $\text{SiO}_2$  и  $\text{Sn}_{29}\text{Si}_{4,3}\text{O}_{66,7}$ ). The thickness of the semiconductor layer was varied from 0,2 nm (non-continuous layer) to 2,5 nm (continuous layer).

The quite narrow range of semiconductor layer thicknesses (h) where significant (by several orders of magnitude) and sharp change of the electrical resistivity ( $\rho$ ) takes place have been observed in all studied multilayered system. This resistivity change is related to the formation of a continuous semiconductor layer and increase of its influence on the electron transport. The thickness value when the continuous 2D layers are being formed depends on a composition and a preparation conditions.

The dependence of the real and imaginary parts of the complex magnetic permeability on the semiconductor layer thickness has been investigated at 50 MHz. The obtained results indicate the presence of the magnetic ordering in systems with Si, C, Cu,  $\text{Bi}_2\text{Te}_3$ , and SiC layers. In the other compositions the magnetic ordering has not been observed in the studied thickness range.

The general correlation between resistivity values of the multilayer structures and presence of the magnetic ordering for all studied systems is shown of the fig.1. The experimental data allows to conclude that there is a significant contribution of charge carriers to a mechanism of the magnetic ordering in the heterogeneous systems. The possible mechanisms of the observed magnetic ordering are discussed.

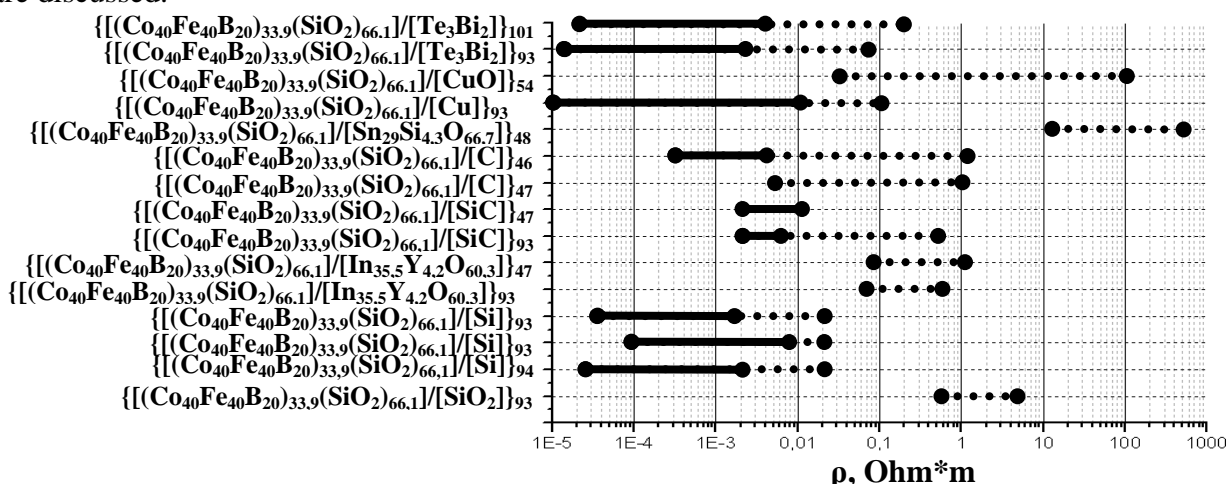


Fig. 1. Magnetic state of multilayer structure vs. electrical resistivity of the structure (dotted line - the superparamagnetic state, solid line - the magnetically ordered state).

This work was supported by RFBR (grants № 09-02-97506 p\_центр\_a)

## INFLUENCE OF THE LAYER PARAMETERS ON MAGNETIC PROPERTIES OF $\text{Fe}_{19}\text{Ni}_{81}/\text{Ti}/\text{Tb-Co}$ THIN FILMS WITH UNIDIRECTIONAL ANISOTROPY

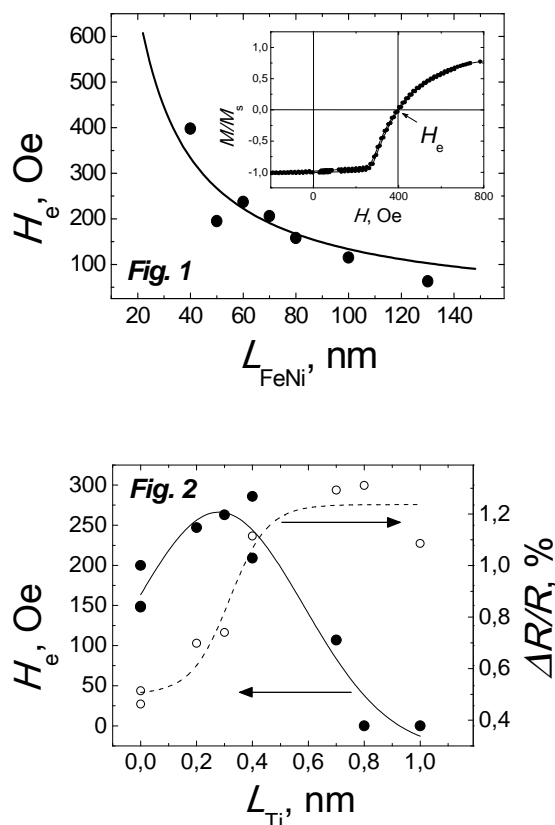
*Balymov K.G., Kulesh N.A., Sorokin A.N., Vas'kovskiy V.O.*

Ural State University named after A.M. Gorky, 620083, Ekaterinburg, Russia

Unidirectional anisotropy is an interesting feature of the of  $\text{Fe}_{19}\text{Ni}_{81}/\text{Tb-Co}$  multilayers obtained for certain conditions [1]. This work is devoted to a detailed study of the properties of  $\text{Fe}_{19}\text{Ni}_{81}/\text{Ti}/\text{Tb}_{35}\text{Co}_{65}$  multilayered structures with unidirectional anisotropy for the structures with varied thicknesses of  $\text{Fe}_{19}\text{Ni}_{81}$  layer and titanium spacer. The multilayers were prepared by rf-sputtering sequential deposition from the corresponding targets onto glass substrates in the presence of homogeneous magnetic field. The amorphous ferrimagnetic Tb-Co layers of the thickness of 120 nm had a uniaxial magnetic anisotropy. The position of the easy axis in the plane of the film was set by a technological magnetic field. Thickness of polycrystalline  $\text{Fe}_{19}\text{Ni}_{81}$  layers ( $L_{\text{FeNi}}$ ) in the series of two-layer films varied in the range  $40 \div 130$  nm,  $L_{\text{FeNi}}$  was fixed being 50 nm for the series of samples with the titanium spacer. The thickness of the nonmagnetic spacer ( $L_{\text{Ti}}$ ) varied in the range  $0.2 \div 1$  nm.

According to the data of magnetic measurements at room temperature  $\text{Fe}_{19}\text{Ni}_{81}$  layers had a unidirectional anisotropy which was manifested as a shift of the hysteresis loop along the easy axis: the value of field shift was denominated as  $H_e$  (see inset Fig. 1). It was established that the value of  $H_e$  was strongly influenced by the thickness of the  $\text{Fe}_{19}\text{Ni}_{81}$  layers as well as by state of the interlayer interface which was controlled by the thickness of Ti layer. In the first case, a monotonic decrease of the field shift was observed for  $L_{\text{FeNi}}$  increase:  $H_e$  was proportional to  $1/L_{\text{FeNi}}$  (line in Fig. 1). Changes of the value of  $H_e$  in the investigated range of the thicknesses was as high as 8 times. In the second case, the dependence of  $H_e$  on the spacer thickness had nonmonotonic character (Fig. 2) The interlayer magnetic coupling disappeared when the thickness of titanium was higher than 0.8 nm. The origin of such behavior of the field shift was discussed.

The anisotropy of the magnetoresistance  $\Delta R/R$  of  $\text{Fe}_{19}\text{Ni}_{81}/\text{Ti}/\text{Tb}_{35}\text{Co}_{65}$  films was also analyzed. The dependences of  $\Delta R/R$  on the layer parameters were obtained and interpreted (Fig. 2).



The work was supported by the RFBR (project № 11-02-00288-a).

[1] K. G. Balymov, V.O. Vas'kovskiy, A.V. Svalov, E.A. Stepanova, and N.A. Kulesh, *Phys. Met. Metallography*, **110** (2010) 6.

## MAGNETIC PROPERTIES OF GOETHITE NANOPARTICLES SYNTHESIZED WITH ADDITION OF VARIOUS SURFACE ACTIVE SUBSTANCES

*Antonov A.N.<sup>1</sup>, Novakova A.A.<sup>1</sup>, Gendler T.S.<sup>2</sup>, Kolesnikov E.A.<sup>3</sup>, Puzik I.I.<sup>3</sup>, Levina V.V.<sup>3</sup>*

<sup>1</sup> Moscow State University, Leninskie Gori, 1, 119991 Moscow, Russia

<sup>2</sup> Institute of Physics of the Earth RAS, B. Gryzinskaya, 10, 123995 Moscow, Russia

<sup>3</sup> National University of Science and Technology, Leninskiy pr.4, 119991 Moscow, Russia

To receive monosized goethite ( $\alpha$ -FeOOH) nanoparticles powders in the process of chemical precipitation from iron salt and alkali various surface active substances (SAS) with concentration 0.3% and 1% were added in water:  $C_{12}H_{25}NaO_4S$  (anion active),  $C_{12}H_{38}ClN$  (cation active) and EDTA  $C_{10}H_{14}O_8N_2Na_2$  (complexon). Investigations by means of TEM and Mossbauer spectroscopy show, that addition of 0.3% SAS increases the amount of small particles with sizes of 2-5 nm in comparison to goethite nanopowder, obtained without SAS. However application of 1% SAS differently influences on size distribution of particles: in the case of cation- active SAS only small particles with size of 2-5 nm are occurred, while in the case of anion-active SAS and complexon the growth of well-crystallized goethite particles with sizes of about 100\*20 nm takes place.

Hysteresis loops demonstrate typical for SP goethite particles linear dependence of  $J(H)$  up to applied field  $H=1T$  for all the samples, however the magnetization values  $J$  are higher for the samples obtained with using of different SAS in comparison on pure goethite nanoparticles. To examine the homogeneity of goethite nanoparticles precipitated in presence of different SAS thermomagnetic analysis (TMA) in interval 20-750°C in applied field 400mT was carried out in air using Curie balance.  $J(T)$  dependences revealed the inhomogeneous composition of goethite nanopowders precipitated with SAS: in temperature region of 200-500°C peaks of magnetization, which are unusual for heating in air of pure goethite, are occurred. Appearance of these peaks is connected with formation of ferrimagnetic intermediate phases in the course of heating. Unusual phase transitions of goethite nanoparticles can be explained by the various surface layers formed on the nanoparticles under SAS influence. The peaks have different shape and intensity depending on the type and concentration of SAS. It was found that in the case of 1% SAS all the peaks on magnetization curves are significantly weaker, than in the case of 0,3% SAS. This can be explained by weaker interactions between SAS and goethite nanoparticles surface at higher SAS concentration.

## INVESTIGATION OF PHASE TRANSITIONS OF MODEL Fe/V SUPERLATTICES

*Khizriev K.Sh.<sup>1,2</sup>, Murtazaev A.K.<sup>1,2</sup>*

<sup>1</sup> Institute of Physics Daghestan Scientific Center of Russian Academy of Sciences,  
94, Yaragskogo str., Makhachkala, Russia

<sup>2</sup> Daghestan State University, 43a, M.Gadjieva str., Makhachkala, Russia

Magnetic Fe/V superlattices with thin alternating layers of magnetic and nonmagnetic materials are convenient objects for the studying the size effects in multilayer structures. The minimum Fe-layer thickness, at which the lattice remains magnetic, is two atomic monolayers; the Curie temperature depends not only on the number of magnetic monolayers but also on the thickness of nonmagnetic vanadium layers.

The superlattices, in which the magnetizations of neighboring magnetic layers are antiparallel to each other, are of particular interest. In particular, such systems exhibit the effect of giant magnetoresistance. In Fe/V superlattices antiferromagnetic interlayer coupling occurs at vanadium and iron layer thickness of 13–14 and 2–3 monolayers, respectively. For such superlattices one can choose a range of hydrogen pressures at which the interlayer exchange interaction changes from antiferromagnetic to ferromagnetic, passing through zero.

For investigation of magnetic properties of nanoscale magnetic systems we propose model of magnetic superlattice Fe<sub>2</sub>/V<sub>13</sub>/Fe<sub>3</sub> with alternating magnetic (two and three monolayers Fe) and nonmagnetic (thirteen monolayers V) layers. The exchange interactions between the nearest neighbors in both the Fe<sub>2</sub> and Fe<sub>3</sub> layers have a ferromagnetic character and are determined by the parameter  $J_{\parallel}$  (intralayer exchange interaction). There is also interaction  $J_{\perp}$  between the atoms of the Fe<sub>2</sub> and Fe<sub>3</sub> layers via the vanadium layer (interlayer coupling). Its value and sign may change, depending on the vanadium layer thickness. Interlayer coupling for our model has the subzero sign.

The Hamiltonian of the model can be written as

$$H = -\frac{1}{2} \sum_{i,j} J_{\parallel} (S_i^x S_j^x + S_i^y S_j^y) - \frac{1}{2} \sum_{i,k} J_{\perp} (S_i^x S_k^x + S_i^y S_k^y),$$

where the first sum takes into account the exchange interaction of each magnetic atom with its nearest neighbors in the layer, and the second sum takes into consideration the interaction with the atoms from neighboring layers via the nonmagnetic layer;  $S_j^{x,y}$  are the components of the spin localized at site  $j$ .

Investigations were performed using by a single-cluster algorithm of a Monte-Carlo method for systems with periodic boundary conditions. The relation between interlayer and intralayer exchange coupling was varied in a wide limit. We have calculated spontaneous magnetization, susceptibility and specific heat as functions of the temperature and exchange parameters. The accurate method of Binder cumulants have been used for definition of the critical temperature. Temperature dependences of magnetization, susceptibility and a heat capacity for several models of a superlattice are received. In model with two and three layers of iron (Fe<sub>2</sub>/V<sub>13</sub>/Fe<sub>3</sub>) are found two maximums of a heat capacity at small values of a relation of interlayer and intralayer exchanges. Temperature dependences of thermodynamic values testify to presence in model of a superlattice Fe<sub>2</sub>/V<sub>13</sub>/Fe<sub>3</sub> of two phase transitions.

Support by FCP of the Ministry of Education and Science of the Russian Federation (goskontrakt P554) is acknowledged.

## PECULIARITY OF THE FERROMAGNETIC AND SPIN-WAVE RESONANCE IN EXCHANGE-COUPLED NiFe/X/NiFe THREE LAYER STRUCTURES (X = Ag, Cu, DyCo)

*Iskhakov R.S.<sup>1</sup>, Stolyar S.V.<sup>1,2</sup>, Yakovchuk V.Yu.<sup>1</sup>, Chizhik M.V.<sup>2</sup>*

<sup>1</sup> Kirensky Institute of Physics, Siberian Branch of RAS, Krasnoyarsk, Russia

<sup>2</sup> Siberian Federal University, Krasnoyarsk, Russia

Structures NiFe/Cu/NiFe, NiFe/Ag/NiFe and NiFe/DyCo/NiFe with the same thickness of the ferromagnetic layers (40 – 110 nm) and of various thickness of Cu and Ag interlayer (1 - 10 nm) and DyCo interlayer (45-110 nm) were investigated by FMR (9.43 GHz).

Only FMR spectra were observed for sandwiches with thickness of ferromagnetic layers 40-50 nm. The FMR spectra include two resonance modes with different intensity (“acoustic” mode and “optic” mode). The resonance field values and intensity values of FMR peak depend on interlayer thickness.

There were many resonance absorptions on the microwave spectra of investigation structures at applied field perpendicular to the film plane when thickness of ferromagnetic layers were above 50 nm. For each acoustic mode there are own optic satellite in SWR spectrum. The influence of sign of the exchange coupling strength on the field positions both for acoustic modes and their optical satellites was determined by the SWR technique. It was revealed that resonance field of the acoustic spin-wave exchanging modes considers with Kittel ratio  $H_r(n_i) \sim n_i^2$  ( $n$  - is mode number), whereas the field positions of optic satellites are described by their own dependence:  $H_r(n_i) \sim n_i^{5/2}$ .

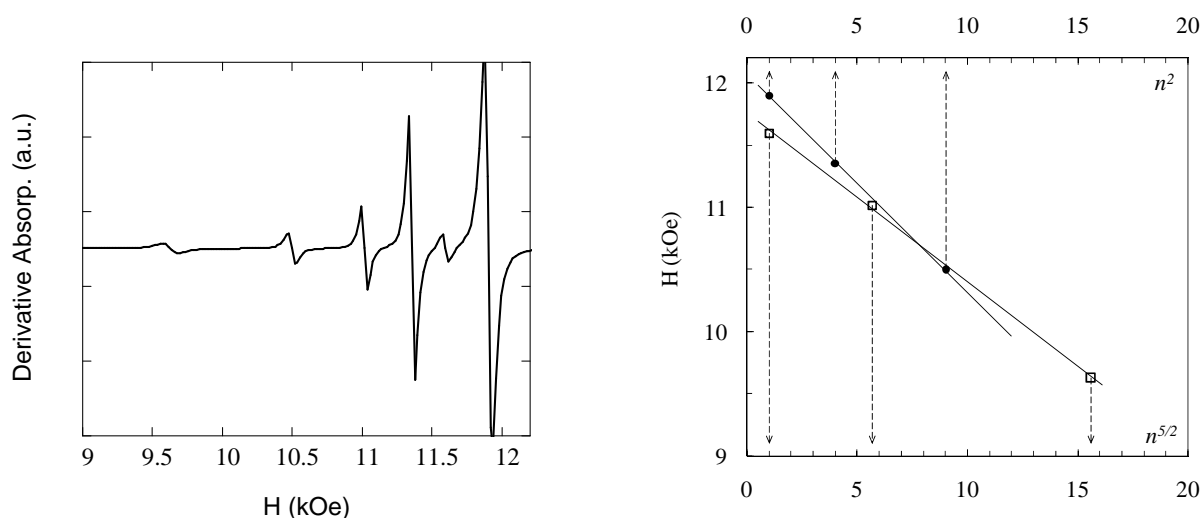


Figure shows (at the left) the SWR spectrum of NiFe(100nm)/DyCo(82nm)/NiFe(100nm) film and (on the right) dependence of resonant fields on mode number as function  $H_r(n_i) \sim n_i^2$  for acoustic mode and  $H_r(n_i) \sim n_i^{5/2}$  for optic mode.

This work was supported by the Federal Program “Development of the Scientific Potential of Higher Education” (RNP.2.1.1/3498) and by the Federal Target Program “Research and Research-Pedagogical Personnel of Innovation Russia for 2009-2013”.

## PECULIARITIES OF MAGNETIC INTERACTIONS AND STABILITY OF xFe(100-x)SiO<sub>2</sub> (x=5-95) POWDER NANOCOMPOSITES

*Kiseleva T.Yu.<sup>1</sup>, Novakova A.A.<sup>1</sup>, Gendler T.S.<sup>2</sup>, Il'inykh I.A.<sup>3</sup>, Levina V.V.<sup>3</sup>*

<sup>1</sup> Moscow M.V.Lomonosov State University, Department of Physics, Leninskie gory, 119192, Moscow, Russia

<sup>2</sup> Schmidt Institute of the Physics of the Earth, Gruzinskaya str., Moscow, Russia

<sup>3</sup> National University of Science and Technology "Moscow Institute of Steel and Alloys", Leninskiy pr. 4, 119991 Moscow, Russia

Magnetic nanoparticles exhibit magnetic properties that are strongly dependent on size effects and their specific structure features. Chemical metallization of oxides multicomponent mixture in reducing media is one of the simple methods to prepare nanocomposites consisted of metallic magnetic particles in nonmagnetic surroundings. In this work we report the study of magnetic properties and structure interdependence of Fe/SiO<sub>2</sub> nanocomposites obtained by xFeOOH-(100-x)SiO<sub>2</sub> precursors mixtures thermal metallization in hydrogen. The resulting nanocomposites series represent a powder material where Fe nanoparticles were coated or embedded into amorphous SiO<sub>2</sub> in dependence on the initial relative  $\alpha$ FeOOH and SiO<sub>2</sub> quantity and precursors homogenization type. The type of mixtures homogenization (mechanical or ultrasonic mixing) plays the principal role in the composites structure formation.

Fe<sup>57</sup> Mossbauer study of structure and magnetic state of metallic particles in obtained nanocomposites via Fe relative concentration have been performed at 78 and 300 K. Phase structure, particles sizes and morphology were studied by X-ray diffraction and TEM analyses. Hysteresis loops were measured at room temperature in applied magnetic fields up to 1 T using VFTB EM magnetometer, thermomagnetic curves M(T) were measured using Curie balance in temperature range 20 - 850 °C in applied magnetic fields 0.45 T.

Studied samples were divided into groups: with a low and high Fe content and by type of precursors homogenization (milling or ultrasound). It was found that UZ homogenization allowed to obtain a good dispersion and narrow size distribution of very small metal particles but more complicate heterogeneous phase composition ( $\alpha$ -Fe, spinel phase, amorphous SiO<sub>2</sub>, different Fe-silicate phases) than mechanically mixed nanocomposites. Mechanical treatment of precursors reveals formation of  $\alpha$ -Fe particles and amorphous SiO<sub>2</sub>.

The saturation magnetization (Js) and remanent saturation magnetization (Jrs) values of whole samples vary in almost two times for the same Fe content. Js and Jrs expect drop with SiO<sub>2</sub> increase, Hc and Hcr in opposite way increase. Hysteresis loops are quite similar in shape although they dose not achieve the saturation and show different input of para- and superparamagnetic (SP) metallic nanoparticles. Thermomagnetic curves J(T) are irreversible and demonstrate some phase transitions during heating showing the instability of all nanocomposites obtained. The temperature of main phase transition Fe→Fe<sub>3</sub>O<sub>4</sub> decreases from 370 to 317 °C with the increase of SiO<sub>2</sub> concentration what is evidently the result of very complicate microstructure.

The received nanocomposites possess perspectives of a good magnetic material for high frequency application.

Support by RFBR (Grant № 09-03-00925) is acknowledged.

## OBSERVATION OF BAND GAPS IN ONE-DIMENSIONAL MAGNONIC CRYSTAL BY SPIN-WAVE RESONANCE TECHNIQUE

*Iskhakov R.S.<sup>1</sup>, Stolyar S.V.<sup>1,2</sup>, Chekanova L.A.<sup>1</sup>, Chizhik M.V.<sup>2</sup>*

<sup>1</sup> Kirensky Institute of Physics, Siberian Branch of RAS, Krasnoyarsk, Russia

<sup>2</sup> Siberian Federal University, Krasnoyarsk, Russia

It is known that the spectrum of waves of any nature in periodic structures has band character (fig.1). Modification of exchange spin wave spectra was detected in “ferromagnetic/ferromagnetic” multilayer films with thickness  $L=N(d_1+d_2)$  ( $d_1$  and  $d_2$  are thickness of the layers) by SWR technique. It is specified by the stop-zones of magnon crystal with  $k_b=\pi/(d_1+d_2)$ , which is formed by one-dimensional modulation of the magnetic parameters. We used two type of multilayer films as initial samples -  $[\text{Co}_{98}\text{P}_2(400\text{\AA})/\text{Co}_{95}\text{P}_5(500\text{\AA})]_4$  and  $[\text{Ni}_{65}\text{Fe}_{35}(180\text{\AA})/\text{Ni}_{60}\text{Fe}_{40}(180\text{\AA})]_5$ , which

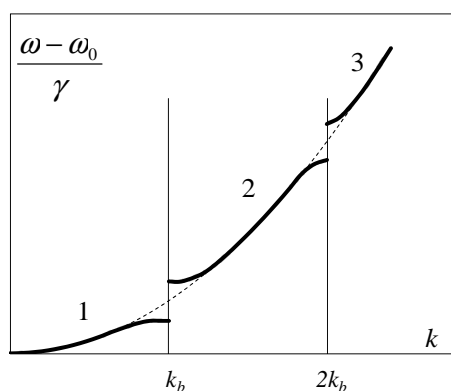


Fig.1. The forbidden zone of exchange spin wave spectra in one-dimensional magnonic crystal.

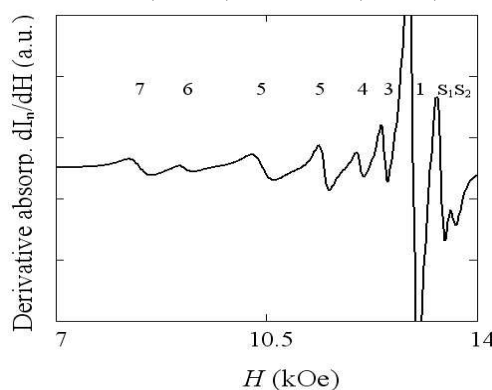


Fig.2. SWR spectra of film  $[\text{Ni}_{80}\text{Fe}_{20}(180\text{\AA})/\text{Ni}_{70}\text{Fe}_{30}(180\text{\AA})]_5$ :  
 $k_5=5\pi/N(d_1+d_2)=\pi/(d_1+d_2)=k_b$

were synthesized by chemical deposition method. Analysis of the experimental spin-wave resonance spectrum ( $k_n=n\pi/L$ ) resulted in the use of exchange doubling of the spin-wave modes ( $n=N$ ) in the “ferromagnetic/ferromagnetic” multilayer films. SWR spectra results shown in the figure 2, 3 clearly illustrate this doubling.

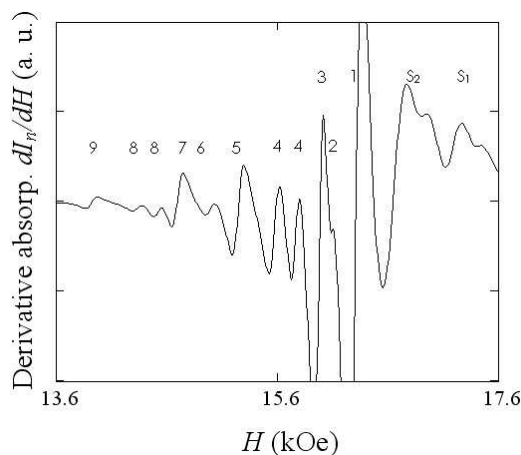


Fig.3. SWR spectra of multilayer film  $[\text{Co}_{98}\text{P}_2(400\text{\AA})/\text{Co}_{95}\text{P}_5(500\text{\AA})]_4$ :  
 $k_4=4\pi/N(d_1+d_2)=\pi/(d_1+d_2)=k_b$ ;  
 $k_8=8\pi/N(d_1+d_2)=2k_b$ .

This work was supported by the Federal Program “Development of the Scientific Potential of Higher Education” (RNP.2.1.1/3498) and by the Federal Target Program “Research and Research-Pedagogical Personnel of Innovation Russia for 2009-2013”

## MAGNETIC PROPERTIES OF CoFeB-SiO<sub>2</sub> NANOCOMPOSITE AND [(Co<sub>40</sub>Fe<sub>40</sub>B<sub>20</sub>)<sub>x</sub>(SiO<sub>2</sub>)<sub>100-x</sub>/α-Si:H]<sub>n</sub> MULTILAYER FILMS

Denisova E.<sup>1</sup>, Iskhakov R.<sup>1</sup>, Komogortsev S.<sup>1</sup>, Chekanova L.<sup>1</sup>, Balaev A.<sup>1</sup>, Kalinin Yu.<sup>2</sup>, Sitnikov A.<sup>2</sup>

<sup>1</sup> Kirensky Institute of Physics SB RAS, Krasnoyarsk, Russia

<sup>2</sup> Voronezh State Technical University, Voronezh, Russia

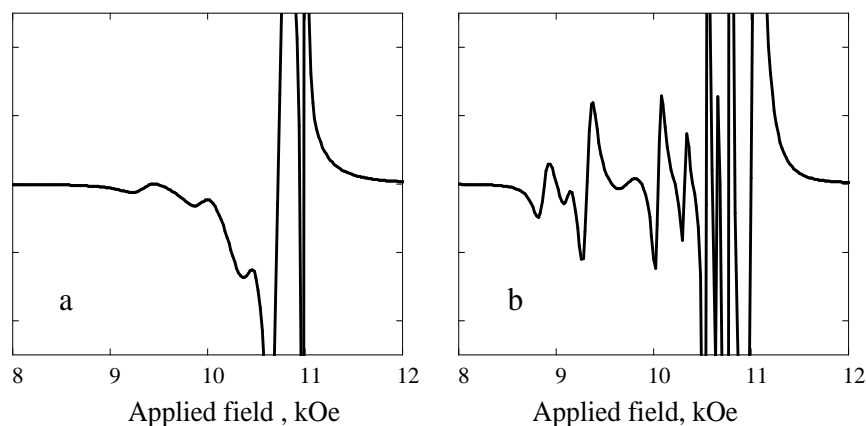


Fig.1. SWR spectrum of the Co<sub>40</sub>Fe<sub>40</sub>B<sub>20</sub>-SiO<sub>2</sub> granular films (a) and of the multilayer [(Co<sub>40</sub>Fe<sub>40</sub>B<sub>20</sub>)<sub>x</sub>(SiO<sub>2</sub>)<sub>100-x</sub>/α-Si:H]<sub>60</sub> films (b)

In this paper we investigate the magnetic and microstructure properties of nanogranular CoFeB-SiO<sub>2</sub> ultrathin layers sandwiched by α-Si:H and we focus our attention on the analysis of the results of FMR studies. The films were synthesized by the ion-beam sputtering. The magnetic properties of multilayered

[(Co<sub>40</sub>Fe<sub>40</sub>B<sub>20</sub>)<sub>x</sub>(SiO<sub>2</sub>)<sub>100-x</sub>(

t)/α-Si:H]<sub>n</sub> films with t varying in range 1.3-6 nm and (Co<sub>40</sub>Fe<sub>40</sub>B<sub>20</sub>)<sub>x</sub>(SiO<sub>2</sub>)<sub>100-x</sub> nanogranular composite films were studied using ferromagnetic resonance at X-band (9.2 GHz) and low-temperature magnetization measurements. A comparison between the magnetic properties of (Co<sub>40</sub>Fe<sub>40</sub>B<sub>20</sub>)<sub>x</sub>(SiO<sub>2</sub>)<sub>100-x</sub> granular films and [(Co<sub>40</sub>Fe<sub>40</sub>B<sub>20</sub>)<sub>x</sub>(SiO<sub>2</sub>)<sub>100-x</sub>/α-Si:H]<sub>n</sub> multilayer films was carried out. Thermal decrease of the films magnetization follows Bloch's law. Using of the standard expressions and the constant *B*, the exchange interaction constant *A* is calculated. Approach to magnetic saturation curves in the all nanocomposites follow Akulov's law  $M(H) \sim (H)^{-2}$  in the applied fields up to 3 ÷ 6 kOe. This allows us to determine the value of mean square fluctuations of local magnetic anisotropy field  $aH_a$ . Ferromagnetic resonance spectra of the (Co<sub>40</sub>Fe<sub>40</sub>B<sub>20</sub>)<sub>x</sub>(SiO<sub>2</sub>)<sub>100-x</sub> nanocomposite and layer films, [(Co<sub>40</sub>Fe<sub>40</sub>B<sub>20</sub>)<sub>x</sub>(SiO<sub>2</sub>)<sub>100-x</sub>/α-Si:H]<sub>n</sub> multilayer films are studied for various orientations of the film plane with respect to the external field. The FMR spectrum for *H* applied parallel to the film plane consists of a single absorption line. When the external field is applied perpendicular to the film plane it is possible to observe multi-peaked spectra, due to resonance absorption by standing spin-wave resonance modes. The boundary conditions for standing spin-wave in this layer are formed during sputtering process of composite films. There are four or five well-resolved peaks in the SWR spectrum of the Co<sub>40</sub>Fe<sub>40</sub>B<sub>20</sub>-SiO<sub>2</sub> granular films and up to 11 peaks in spectrum of the multilayer films (Fig.1). It is found that the  $H_r(n^2)$  dependencies are non-linear contrary to the Kittel theory. Such behavior is probably caused by the fluctuations of magnetic parameters (the magnetization and the ferromagnetic exchange interaction) in nanocomposite films.

Financial support by the RFBR (grant 11-03-00471-a) is gratefully acknowledged.



## FORMATION OF NICKEL MAGNETIC NANOWIRES IN POROUS SILICON

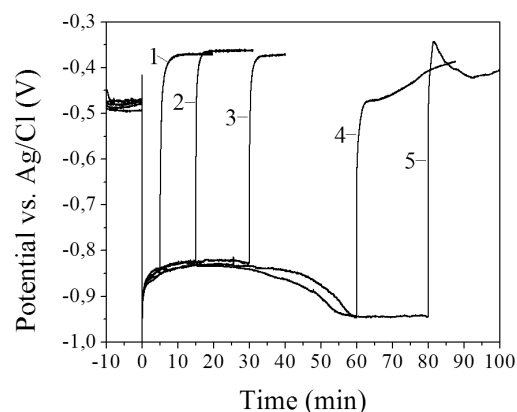
Dolgiy A.

Belarussian State University of Informatics and Radioelectronics, P. Brovka 6, Minsk, 220013,  
Belarus

Nickel-porous silicon structures are of considerable industrial interest for various applications. Anisotropy of magnetic properties of the nickel nanowires inside porous silicon conditioned by their high aspect ratio is applicable for the magnetic store production [1,2]. It is of value to study in detail the process of the nickel electrodeposition into pores of porous silicon and elaborate control methods for pore filling with magnetic metal.

The 10  $\mu\text{m}$  thick porous silicon layers with the average pore diameter of 80 nm were formed by anodizing n-type antimony doped Si wafers of 0.01 Ohm·cm resistivity in an aqueous-alcohol solution of HF acid (the ratio of HF:H<sub>2</sub>O:(CH<sub>3</sub>)<sub>2</sub>CHOH is 1:3:1 by volume parts) at a current density of 80 mA/cm<sup>2</sup>. The porosity of the layer formed was ~70%. Nickel was deposited into porous silicon in the galvanostatic regime from the aqueous solution consisted of 200 g/l NiSO<sub>4</sub>·7H<sub>2</sub>O, 25 g/l NiCl<sub>2</sub>·6H<sub>2</sub>O, 25 g/l H<sub>3</sub>BO<sub>3</sub>, and 3 g/l saccharin. An auxiliary platinum electrode was used. To study in detail the process of the nickel electrodeposition into pores of porous silicon, the electrodeposition was stopped at various process stages, namely, after 5, 15, 30, 60 and 80 min (curves 1 – 5 on the Time vs. Potential graph). The cross-sections of the samples were studied with the Hitachi-S4800 scanning electron microscope. The surface potential of the sample during the electrodeposition was recorded with the use of the reference Ag/Cl electrode.

Cross-sectional SEM studies of the samples at various deposition stages allowed the deposition mechanism to be revealed. The nickel formation inside pores is in the following way. When the electric current is passed through the porous silicon sample, the nickel grains arise inside pores at the side walls of the silicon skeleton. The diameter of every one of the grain is up to 70 nm. Referring to cross-sectional SEM images of the PS samples after the 5 and 15 min nickel electrodeposition, the nickel grains do not increase in size as the deposition time increases but new grains arise. Further increase in the deposition time increases still further a number of grains deposited and nickel grains coalesce to threads. However, single grains are distinguishable in the thread structure. It should be noted that the nickel layer formation at the sample surface was found to begin only after the pore filling. Referring to the Time vs. Potential graph and SEM images, the decrease of the surface potential corresponds to the beginning of the nickel formation at the sample surface. When a continuous nickel film is formed, further increase in the deposition time results in the increase of the film thickness, and the surface potential becomes stabilize (deposition time of 60 min and more, curves 4 and 5). Thus the moment of complete pore filling with nickel could be controlled by the surface potential of the sample.



[1] P. Granitzer, K. Rumpf, H. Krenn. *Thin Solid Films*, **515** (2006), 735.

[2] P. Granitzer, K. Rumpf, P. Pölt, A. Reichmann, H. Krenn. *Journal of Magnetism and Magnetic Materials*, **310** (2007), 838.

## MAGNETIC PROPERTIES OF AMORPHOUS AND MONOCRYSTALLINE COBALT NANOLAYERS EMBEDDED IN CARBON

Ageev N.V.<sup>1</sup>, Semisalova A.S.<sup>1</sup>, Perov N.S.<sup>1</sup>, Novikov A.I.<sup>1</sup>, Gan'shina E.A.<sup>1</sup>, Bugayev Ye.A.<sup>2</sup>, Zolotaryov A.Yu.<sup>3</sup>, Kondratenko V.V.<sup>2</sup>

<sup>1</sup> M.V. Lomonosov Moscow State University, Leninskie Gory, Moscow, 119991, Russia

<sup>2</sup> National Technical University "Kharkiv Polytechnic Institute", 61002, Ukraine

<sup>3</sup> Institute of Applied Physics, University of Hamburg, 20355, Germany

Dependence of magnetic properties of C/Co/C and C/Co/C/Co/C thin film nanocomposites has been studied upon structural state of the metal layers. Magneto-optical transverse Kerr effect (TKE) spectrometer, SQUID and vibrating sample magnetometer (VSM) were used in in-plane and out-of-plane geometry. The Co/C nanocomposites demonstrate ferromagnetic behavior which depends on Co layer thickness. Soft magnetic properties with coercitivity of  $2\pm 1$  Oe have been found for Co thickness less than 5 nm. Film composites with thicker Co layers show magnetic properties close to bulk Co with coercitivity of 50 Oe.

Transmission electron microscopy, X-ray diffraction, and *in-situ* resistivity measurements revealed the metal layer being an amorphous cobalt-carbon alloy as a result of the layer intermixing. An avalanche crystallization of the amorphous alloy took place and monocrystalline hcp-Co layers with c axis normal to the film were formed when Co thickness was more than 5 nm.

Magnetic and magneto-optical properties of the film composites contained two layers of amorphous Co alloy separated by the carbon spacer with different thickness have been studied in as-deposited state and after one hour annealing below crystallization temperature (250 °C). The one order increase of the coercitivity has been found for annealed samples in comparison with as-deposited films. Magnetic properties of the amorphous nanocomposites in as-deposited state were found to be temperature independent (down to 80 K) in contrary to annealed ones where several times increase of coercitivity has been observed. The TKE spectra of the samples with Co thickness less than 5 nm have been found to be similar to the polycrystalline Co spectrum, though the X-ray diffraction revealed the amorphous state. In addition the influence of the annealing on the magnetization value was revealed – the magneto-optical study has shown that the magnetization of annealed composites was slightly higher than for as-deposited ones, except the composite with 0,5 nm carbon layer where the decrease of magnetization was found. For this carbon thickness the strongest increase of the saturation field after the annealing was observed. Accordingly to the VSM data the magnetization was independent on the annealing for all samples. Magnetic interaction between Co layers separated by amorphous carbon of different thickness and its influence on the magnetic properties are discussed.

Support by RFBR (under project № 11-02-00906-a) is acknowledged.

## THE MAGNETIC-RESONANCE PROPERTIES STUDY OF NANOSTRUCTURES FOR SPINTRONICS BY FMR

*Kupriyanova G., Zubin A., Astashonok A., Orlova A.*

Immanuel Kant Baltic Federal University, 236041, A. Nevskogo 14, Kaliningrad, Russia  
e-mail: galkupr@yandex.ru

One of the important problems today is to create new materials and combinations for the applications of spintronics. In this work we report the study of the magnetic-resonance properties by FMR of the FM/NM/FM systems to assess their applicability in a functional magnetic tunnel junction. The present work demonstrates critical dependence of magnetic and magneto-anisotropic properties of polycrystalline structures with Fe, Fe<sub>3</sub>O<sub>4</sub> and Fe<sub>3</sub>Si on the type of spacer layer, a sequence of thin layers in the whole structure. All systems were synthesized on neutral Si/SiO<sub>2</sub> substrates by the pulsed laser deposition technique. The ferromagnetic resonance spectra of the films were taken using Radiopan electron spin resonance spectrometer operating at the X-band frequency 9.5 GHz and the modulation frequency 100 kHz. The first field derivative of the microwave power absorption was registered as a function of applied steady magnetic field at room temperature. The samples were mounted on one side of a special holder passing through the center of the TE<sub>102</sub> microwave cavity. The orientation of the film was controlled by two axial goniometers with an accuracy by 0.5°. The in plane and out-of -plane dependences of FMR spectra and linewidths have been measured for all samples. The FMR research of Fe(4nm)/Fe<sub>3</sub>O<sub>4</sub>(10nm)/MgO(3,5nm)/Fe<sub>3</sub>Si(13nm), Fe/Fe<sub>3</sub>Si/SiO<sub>2</sub>/Fe<sub>3</sub>O<sub>4</sub>Fe, Fe<sub>3</sub>Si/SiO<sub>2</sub>/Fe<sub>3</sub>O<sub>4</sub>F structures showed that the spectrum parameters depend on the sequence of layers and the formation method. The two modes with resonance fields and line widths depending on the  $\theta$  angle were observed for all samples. The angle dependence of the out-of plane resonance fields of all samples show the two fold symmetry with different constants. However, the out-plane angle dependence of the pick-to pick linewidth of the two modes shows a different behavior. The new theoretical approach for the simulation of experimental FMR results of multilayer polycrystalline structures with the exchange coupling was presented. The extracted magnetic parameters such as the effective magnetization, magnetic anisotropy and linewidths were studied.

The present work was executed within the frames of the State Contract No.02.740.11.0550

[1]. A.Goihman, G. Kupriyanova, E. Proxorenko, A. Chernenkov, Vestnik I. Kant SU, vol 4 (2010).

## SURFACE SPIN FLOP TRANSITION IN [Fe/Cr] MULTILAYERS OBSERVED BY THE NUCLEAR RESONANCE REFLECTIVITY

*Andreeva M.<sup>1</sup>, Gupta A.<sup>2</sup>, Sharma G.<sup>2</sup>, Kamali S.<sup>3</sup>, Yoda Y.<sup>4</sup>, Okada K.<sup>4</sup>*

<sup>1</sup> Faculty of Physics, M.V. Lomonosov Moscow State University, 119991, Russia

<sup>2</sup> Indore Center, UGC-DAE Consortium for Scientific Research, Indore 452017, India

<sup>3</sup> Department of Applied Science, University of California, Davis, California 95616, USA

<sup>4</sup> Japan Synchrotron Radiation Research Institute, SPring-8, Sayo, Hyogo 679-5198, Japan

The layered antiferromagnets attracts an increasing interest due to their GMR properties and peculiar behavior at the applied field (see e.g. [1, 2]).

Nuclear resonance reflectivity (NRR) is the most effective method for the investigation of the interlayer coupling [3]. NRR presents two types of data. 1. Delayed reflectivity as a function of angle is sensitive to the magnetic depth-periodicity. 2. Time spectra of reflectivity measured for the selected grazing angles show the quantum beat oscillations which originate from the interference of the waves with different frequencies of hyperfine transitions in the nucleus decay. The interference pattern is different for different magnetization direction.

We have investigated two samples [<sup>57</sup>Fe(2.0 nm/Cr(1.2nm))<sub>20</sub> and [<sup>57</sup>Fe(3.0 nm)/Cr(1.2 nm)]<sub>10</sub>. The measurements have been performed at the Beamline BL09XU of SPring-8.

Without an external magnetic field the investigated samples show the pronounced superstructure maxima (1/2 and 3/2) on the delayed reflectivity curves. That confirms the doubling of the magnetic period. At the smallest external field **50 Oe** we have not seen the change of the intensity of the 1/2 peak. However the time spectra in the L-geometry (field along the beam) and T-geometry (field perpendicular to the beam) show **some change but only at the critical angle** (Fig. 1) whereas at the higher angles the time spectra are not changed. This effect is the direct evidence of the **surface spin flop (SSF) transition**.

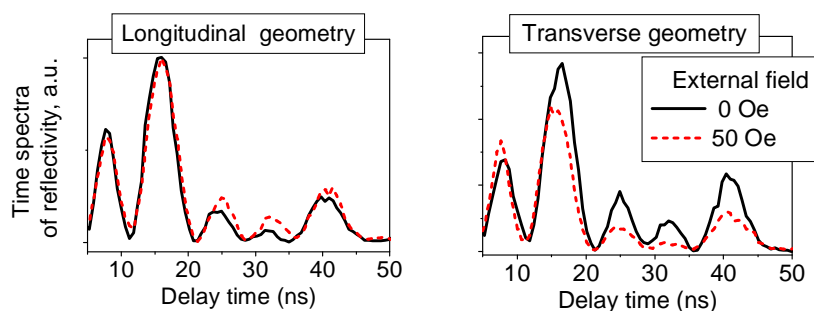


Fig. 1. The time spectra of reflectivity measured for [<sup>57</sup>Fe(3.0 nm)/Cr(1.2 nm)]<sub>10</sub> sample at the critical angle (0.218°) without and with a weak external magnetic field (50 Oe).

The delayed reflectivity curves have started to change noticeably at the external field ~ **600 Oe**. The changes in the L- and T- geometry prove that the antiferromagnetically coupled magnetizations in the <sup>57</sup>Fe layers rotate to **the perpendicular position** to the external field.

At the highest applied field **1500 Oe** the superstructure 1/2 peak disappears in the L-geometry and is essentially decreased in the T-geometry. We can conclude that we get almost a **ferromagnetic** alignment between all <sup>57</sup>Fe layers along the external field.

The work is supported by the RFBR grants No. 09-02-01293-a and No. 10-02-00768-a.

[1] V.V. Ustinov, et al. *Phys. Rev. B* **54** (1996) 15958.

[2] J. Meersschant, et al, *Phys. Rev. B* **73** (2006) 144428.

[3] M.A. Andreeva, B. Lindgren, *Phys. Rev. B* **72** (2005) 125422.

## MAGNETOOPTICAL STUDIES OF INTERLAYER COUPLING IN Fe/Si/Fe TRI-LAYERS

*Kholin D.I., Drovosekov A.B., Zasukhin S.V., Kreines N.M.*

P.L. Kapitza Institute for Physical Problems RAS, ul. Kosygina 2, 119334 Moscow, Russia

The problem of interlayer coupling in Fe/Si/Fe multilayer systems has attracted much attention for more than a decade [1-3] due to a possible use of these systems in high-tech applications. But experimental results in this field are rather contradictory mainly because of an uncontrollable diffusion of iron atoms into the silicon spacer. In this work, we study a series of Fe/Si/Fe tri-layers grown by means of the MBE technique. We varied the substrate temperature during the Si spacer formation for different samples from 300 to 77 K in order to change the concentration of Fe atoms in the spacer. The spacer thickness in each sample changed linearly from 0 to approximately 20 Å on a length of 10 mm, so that we could use the MOKE magnetometry to measure the dependence of the interlayer coupling on the spacer thickness. We had also made two samples with constant thicknesses of Si spacer, which suited for FMR and SQUID measurements [4], so we could compare the interlayer coupling parameters given by different experimental methods.

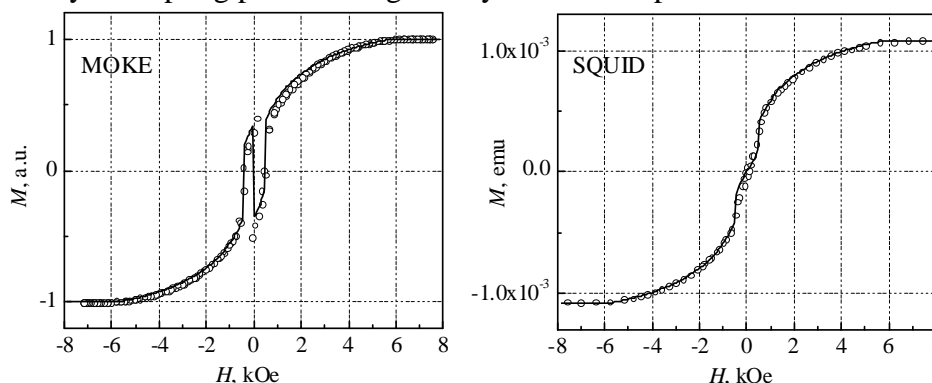


Fig. 1. Magnetization curves of a Fe(70 Å)/Si(12 Å)/Fe(70 Å) sample measured by MOKE and SQUID techniques. Dots – experimental data, solid lines – computer simulation based on the biquadratic coupling model. Magnetic field was applied in the film plane along the hard magnetisation axis of iron.

Unexpectedly, the shape of magnetisation curves measured by the MOKE and SQUID techniques differed significantly for the same samples (see Fig.1). In our talk we will show, that the results of MOKE, SQUID and FMR measurements can be all brought into conformity if we take into account a finite penetration depth of laser light and a twist of the magnetisation vector across the iron layers. This approach allowed us to obtain the dependence of the bilinear and biquadratic coupling constants on the spacer thickness for our samples.

The authors are grateful to D.E. Bürgler and R. Schreiber for the possibility to prepare the samples in Forschungszentrum Jülich. The work was partially supported by the Russian Foundation for Basic Research (grant No. 10-02-01110-a).

- [1] S. Toscano, B. Briner, H. Hopster and M. Landot, *J. Magn. Magn. Matter* **114**, L6 (1992).
- [2] D. Bürgler, M. Buchmeier, S. Cramm et al., *J. Phys.: Condens. Matter* **15**, S443 (2003).
- [3] A. Gupta, D. Kumar, and V. Phatak, *Phys. Rev. B* **81**, 155402 (2010).
- [4] A.B. Drovosekov, D.I. Kholin, N.M. Kreines, et al. *EASTMAG2010, Abstracts book*, 289 (2010).

## INFLUENCE OF THE HEAT TREATMENT ON MAGNETIC PROPERTIES OF Tb-Co FILMS AND Tb-Co/Fe<sub>19</sub>Ni<sub>81</sub> BILAYERS

*Vas'kovskiy V.O., Svalov A.V., Balymov K.G., Kulesh N.A.*

Ural State University named after A.M.Gorky, 620083, Ekaterinburg, Russia

Amorphous layers of rare earth and 3-d metal alloys are effective source of magnetic exchange bias in multilayer functional structures on the base of spin-valve [1] or anisotropic magnetoresistive [2] effects. As a specific features of these structures the large value of exchange bias field  $H_e$  and relatively high stability to external factors can be mentioned. Nevertheless, the heating is among the factors that could significantly affect the properties of amorphous layers and film structures which contain above mentioned layers. This work is devoted to the study of the effects of heating on Tb-Co amorphous and Tb-Co/Fe<sub>19</sub>Ni<sub>81</sub> layered films.

The experiment was carried out on Tb<sub>18</sub>Co<sub>82</sub>/Ti, Tb<sub>31</sub>Co<sub>69</sub>/Ti and Tb<sub>31</sub>Co<sub>69</sub>/Fe<sub>19</sub>Ni<sub>81</sub> films prepared by rf-sputtering with Ti, Tb-Co mosaic and Fe<sub>19</sub>Ni<sub>81</sub> alloy targets. The samples were deposited on the Corning glass substrates at an Ar pressure of  $10^{-3}$  Torr and in the presence of a uniform magnetic field of 150 Oe applied parallel to the plane of samples. The composition of the amorphous films was checked by the chemical analysis. The thickness of amorphous films and amorphous layers in bilayered structures was 100 nm. The thickness of the permalloy layer was 40 nm. The titanium layers of 50 nm were deposited for protection.

According to the data of the X-ray diffraction analysis the Tb-Co layers in the samples of both types were in an amorphous state. The titanium and Fe<sub>19</sub>Ni<sub>81</sub> layers were in the fine-crystalline state with a grain size of about 10 nm. Amorphous layers was also characterized by a uniaxial magnetic anisotropy, the magnitude of which depended on the composition. In bilayers the exchange bias of permalloy layer was observed. The value of  $H_e$  was 150 Oe.

Heat treatment was done in a vacuum at a pressure of  $10^{-3}$  Torr and had a cumulative character. An annealing temperature  $T_a$  was varied in the interval of 100÷250 °C. Exposure at each temperature was 1 hour. According to X-ray diffraction analysis, the annealing in the framework of these regimes does not introduce significant changes in the structural state of the samples. At the same time, the magnetic properties of the films undergo a major transformation. In the single-layered samples a reduction in the coercive force  $H_c$  and the constant of induced uniaxial anisotropy were observed. The character of these changes depends on the composition of the films. In the bilayered film along with the decrease of  $H_c$  of amorphous layer the change of the  $H_e$  field was clearly visible. The dependence of  $H_c(T_a)$  had a smooth ride, but the  $H_e(T_a)$  behavior was close to the threshold type. The sharp drop of  $H_e$  occurs at  $T_a > 200$  °C. The interpretation of the observed behaviour was proposed.

This work was supported by RFBR (grant 11-02-00288-a).

- [1] P. Ten Berge, N.J. Oliveira, T.S. Plasket, J.L. Leal, H.J. Boeve, G. Albuquerque, J. Ferreira, A.R. Morais, A.T. Sousa, L. Rodrigues, P.P. Freitas, *IEEE Trans. Magn.* **31** (1995) 2603,  
 [2] V.O. Vas'kovskiy, K.G. Balymov, A.A. Yuvchenko, A.V. Svalov, A.N. Sorokin, N.A. Kulesh, *Tech. Phys.*, **81** (2011) 83.

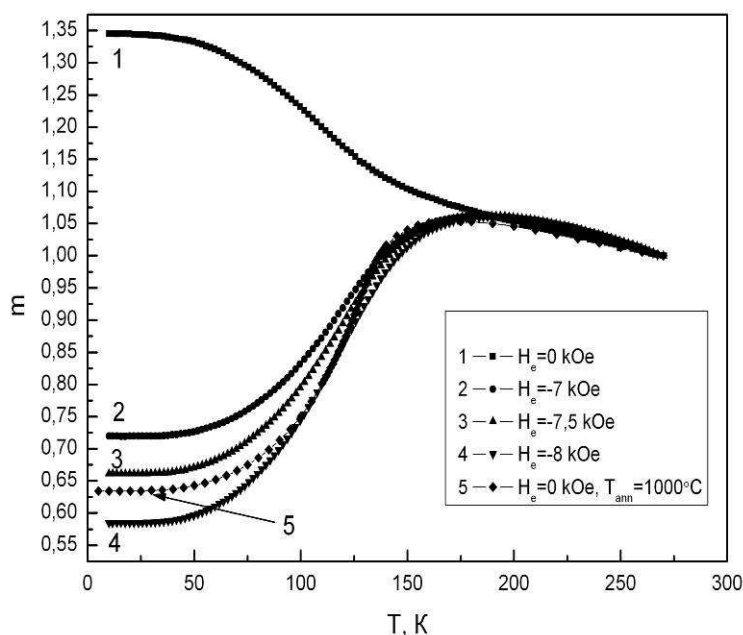
## SPIN REORIENTATION TRANSITION AND INTERGRAIN EXCHANGE INTERACTION IN NANOSTRUCTURED Nd-Fe-B-TYPE ALLOYS

Volegov A.S., Kudrevatykh N.V., Neznakhin D.S., Andreev S.V.

Ural State University, 620083 Ekaterinburg, Russia

From the moment of their discovery, nanostructured (NS) hard magnetic materials based on Nd-Fe-B system alloys have always been and currently are in the center of attention of researchers and technologists. The advantage of these materials originates from a high magneto-crystalline anisotropy, high value of saturation magnetization of the main magnetic phase ( $\text{Nd}_2\text{Fe}_{14}\text{B}$ ) and considerable exchange interaction (EI) between nanograins. In spite of a relatively long time of their study, there is no in the literature a quantitative data on EI energy.

Thus the aim of this work was to determine the EI energy value for the interface surface unit between neighbor nanograins, measuring the magnetization temperature dependences ( $m(T)$ ) for such NS alloys in “negative” magnetic fields for the spin-reorientation (SR)  $\text{Nd}_2\text{Fe}_{14}\text{B}$  phase temperature range. For such study the MQP-B and MQP-B+ brands of NS alloys were used. It was shown earlier that  $m_r(T)$  of NS alloys in SR range (curve 1 in figure) differs from that measured for large grain microstructural (MS) isotropic material (curve 5) [1]. The reason for this difference originates from exchange interaction action between nanograins in



NS alloys and its relative weakness in MS sample. So, the idea how to do that is based on the determination of the negative external magnetic field value ( $H_e$ ) which makes the  $m(T)$  of NS alloy (firstly magnetized by strong positive magnetic field) similar to that for  $m_r(T)$  MS material measured at  $H_e = 0$  in the SR temperature range. It is assumed that this NS material states are equivalent to them in the MS material at the same temperatures.

With the assumptions that the nanograins shape in NS material is cube, each grain is the single crystal of  $\text{Nd}_2\text{Fe}_{14}\text{B}$  phase and easy axes distribution is random, the EI energy density can be calculated from the formulae:

$$W = -\frac{M_s L H_e}{12}, \quad (1)$$

where:  $M_s$  – spontaneous magnetization of the  $\text{Nd}_2\text{Fe}_{14}\text{B}$  phase,  $L$  – edge length,  $H_e$  – demagnetizing (negative) field, where  $m(T)$  of NS sample is identical to that for MS one.

It was shown for the first time that its value amounts  $2.3 \text{ erg/cm}^2$  for interface between neighbor nanograins in MQP-B type NS alloys.

[1] A.S. Volegov, N.V. Kudrevatykh, I.S. Tereshina, D.S. Neznakhin, Y.A. Sabiryanova, Solid State Phenom, **168-169**, (2011), 396

## A PRESSURE INFLUENCE ON MAGNETIC PROPERTIES OF Nd-Fe-B TYPE NANOSTRUCTURAL ALLOYS

*Neznakhin D.S., Kudrevatykh N.V., Volegov A.S., Andreev S.V.*

Ural State University named after A. M. Gorky, 620083, Ekaterinburg, Russia

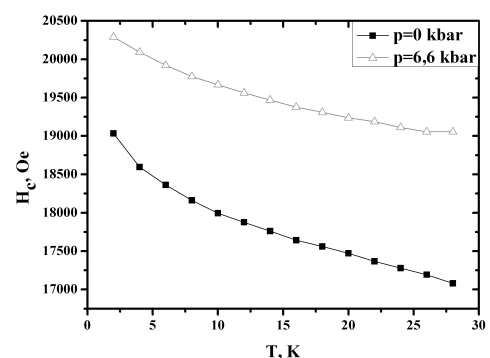
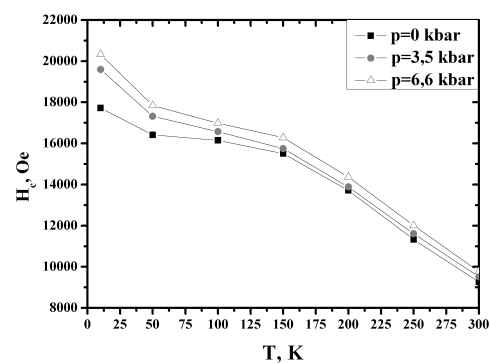
Permanent magnets produced from Nd-Fe-B type alloys have significant scientific and practical interest, which is explained by unique magnetic properties of this materials. It concerns also to the nanostructured alloys (NSA) similar composition basically manufactured by the melt spinning technique in a shape of flakes or coarse powders, which are widely used as fillers in bonded magnets. A particles of such NSA after embedding to magnet experience some internal pressures which can change their magnetic properties. Thus, the aim of this work was to study directly a pressure influence on magnetic properties of MQP-B NSA Nd-Fe-B brand. There are only few papers in literature which devoted to that subject [1, 2]. But the results of this works are contradictory. Besides, it is difficult to analyze them, because the authors didn't describe the pressure method determination (direct or non direct) [2].

We used an EasyLab Mcell 10 type pressure cell (PC) which allows to carry out magnetic measurement under hydrostatic pressures up to 10 kbar. A pressure value was determined by a tin manometer placed directly into a PC. Magnetic properties were measured with a help of SQUID magnetometer MPMS-XL-7 EC within a temperature range 2-300 K and magnetic fields up to  $\pm 70$  kOe. A relatively small amount of MQP-B powder was fixed by a soft gluer on copper plate. After its solidification the plate with a sample and manometer has been entered to the PC and fixed there. Further a PC with an oil was tightly closed, loaded at hydraulic press, attached at sample holder and mounted in SQUID magnetometer.

Magnetization and demagnetization curves were measured in two temperature ranges 50-300 K (with 50 K step) and more detailed in a range 2-30 K (with 2K step). At first range the measurements performed under three values of pressure 0, 3,5 and 6,6 kbar but in second one only for zero and 6,6 kbar. It was found that spin reorientation temperature beginning doesn't changed under pressure, but the coercivity was always higher for the loaded samples. Thus we can conclude that pressure increases coercivity of MQP-B noticeably. This is mostly visible for the low temperature range ( $\sim 10\%$  rise) and can be interpreted as the result of magnetocrystalline energy increasing in  $\text{Nd}_2\text{Fe}_{14}\text{B}$  phase lattice due to interatomic distances change.

[1] M.R. Ibarra, L. Morellona, P.A. Algarabela, C. Marquinaa, Z. Arnoldb and J. Kamarad, Pressure effects on the spin reorientation transitions in rare-earth intermetallics, *JMMM*, Volumes 104-107, Part 2, 2 February 1992, Pages 1371-1372

[2] S.V. Andreev, S.M. Zadvorkin, J.Kamarad, G.F. Korznikova, A.I.Kozlov, N.V. Kudrevatykh, E.N. Tarasov, A structure and magnetic properties of melt-spun Nd-Fe-B type alloys, The XIIIth international conference on permanent magnets, 25-29 September 2000 Suzdal, Russia, Pages 132-133





## CARBON NANOTUBE AS A SENSOR FOR SINGLE PARTICLE MAGNETIC RESONANCE DETECTION

Rod I.<sup>1</sup>, Wirtz C.<sup>1</sup>, Kazakova O.<sup>2</sup>, Cox D.<sup>2,3</sup>, Posth O.<sup>1</sup>, Lindner J.<sup>1</sup>, Meckenstock R.<sup>1</sup>, Farle M.<sup>1</sup>

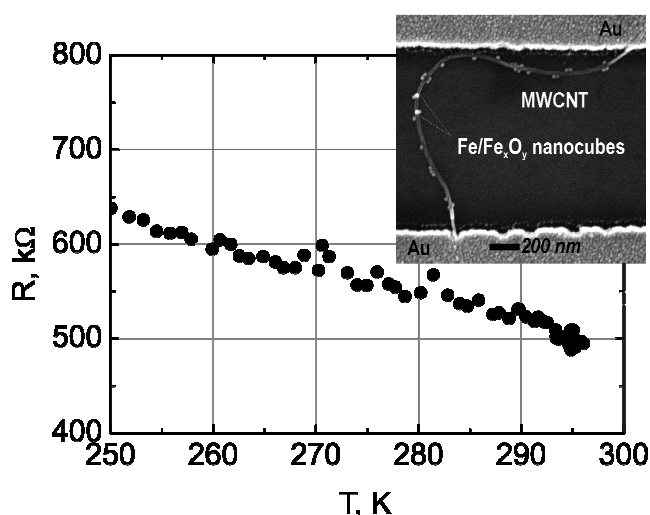
<sup>1</sup> Fakultät für Physik and Center for NanoIntegration (CeNIDE), Universität Duisburg-Essen, Lotharstr. 1, Duisburg, 47057, Germany

<sup>2</sup> National Physical Laboratory, Teddington, Middlesex, TW11 0LW, United Kingdom

<sup>3</sup> Advanced Technology Institute, University of Surrey, Guildford GU2 7XH, United Kingdom

Understanding of static and dynamic magnetic properties of individual magnetic nanoparticles and the influence of interparticle interactions is required for precise control of their properties and, therefore, reliable applications in future ultrahigh density magnetic storage media as well as magnetic nanosensors. In recent years, a variety of techniques for single magnetic nanoobject measurements have been developed (see, e.g. [1–2]).

We propose a method based on measurements of magnetic resonance in a single nanoparticle by means of bolometer detection technique [3]. This technique allows to observe an absorption of electromagnetic energy by resonant spins due to the ensuing rise in sample temperature. The temperature change can be detected by measuring the resistivity change of a bolometer attached to the sample. A carbon nanotube (CNT) is proposed for use as a very sensitive bolometer to detect magnetic resonance in individual nanoparticles. We have recently demonstrated various



experimental methods of fabricating nanoscale devices consisting of a CNT bridging metallic electrodes and decorated with magnetic iron/iron oxide nanocubes [4]. Here we report on the temperature dependence of the electrical resistance of a multi-wall (MW) CNT with attached Fe/Fe<sub>x</sub>O<sub>y</sub> nanocubes (see Figure). Rapid change of the CNT resistance with temperature (for the CNT shown in Figure,  $dR/dT = -306 \text{ } \Omega/\text{K}$  in the vicinity of room temperature) was observed experimentally. Our calculations show that temperature change of an individual magnetic nanocube with a size of 18 nm due to the resonance is equal to 0.4 K. This temperature change can be detected by

measuring the resistance change of the MWCNT whose value is of the order of milli Ohms. A temperature sensor providing the aforementioned sensitivity is expected to enable detection of magnetic resonance within individual particles attached to it.

The authors thank H. Zähres for discussion and technical support. Support by DFG, Germany (Project No. FA209-12-1) is acknowledged.

- [1] M. Jamet, W. Wernsdorfer, C. Thirion, D. Mailly et al., *Phys. Rev. Lett.*, **86** Nr. 20 (2001) 4676.
- [2] L. Hao, D. Cox, P. See, J. Gallop, O. Kazakova, *J. Phys. D: Appl. Phys.*, **43** (2010) 474004.
- [3] C.P. Pool, *Electron spin resonance*, John Wiley & Sons, 1983.
- [4] I. Rod, O. Kazakova, D. C. Cox, M. Spasova, M. Farle, *Nanotechnology*, **20** (2009) 335301.

## HEAT TREATMENT INFLUENCE ON MAGNETIC AND MAGNETOTRANSPORT PROPERTIES OF $\text{Fe}_x(\text{MgO})_{100-x}$ NANOCOMPOSITES

*Grebennikov A.A., Stognei O.V., Kashirin M.A.*

Voronezh state technical university, Moskovskiy prospect, 14, Voronezh, Russia

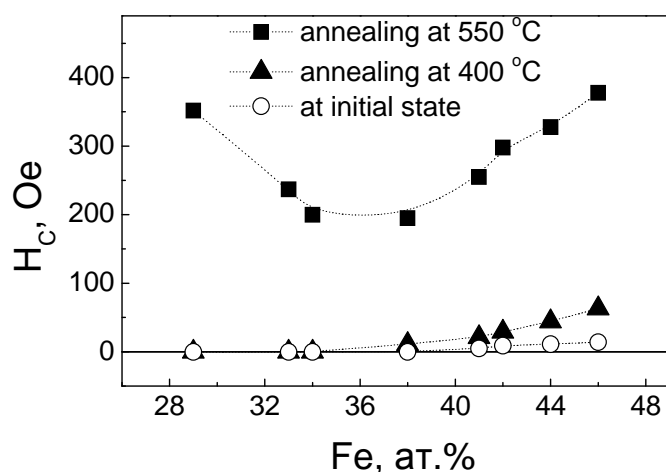


Fig. Concentration dependence of coercive force of  $\text{Fe}_x(\text{MgO})_{100-x}$  nanocomposites

The influence of thermal annealing carried out at a temperature of 400 °C and 550 °C on the magnetic and magnetotransport properties of granular composites  $\text{Fe}_x(\text{MgO})_{100-x}$  has been investigated. The film thickness was 2-3 microns. Composition of the samples was determined by electron-probe X-ray microanalysis. Magnetization processes were investigated using a vibrating sample magnetometer, magnetoresistive properties were investigated by potentiometric method with two-point technique. Nanogranularity of the samples structure was determined indirectly by studying of the magnetotransport and magnetic

properties of the samples in initial state.

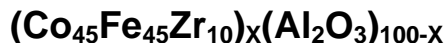
It is found that annealing at 400 °C doesn't influence on the magnetoresistance (MR) value of the  $\text{Fe}_x(\text{MgO})_{100-x}$  composites in the composition range of  $29 \leq x, \text{ at. \%} \leq 35$ . It increases from -0,6% to -2,4%. The annealing leads to decrease of the MR values in the concentration interval of 36 – 46 at. % Fe. Increase in the concentration of metal from 36 to 46 at. % didn't influence on the MR value which is equal to -2,4 % as in the initial state. The value of MR monotonously decreases from -2,4 % to -0,3 % after annealing. This result is typical for the metal-insulator composites. It is due to relaxation processes occurring in the structure of the samples during annealing. Both magnetization curves before and after annealing at 400 °C correspond to the superparamagnetic state in the composites with 29 – 35 at.% Fe. Composites with the larger metal concentration (36 – 46 at.%) exhibit a ferromagnetic properties.

A coercive force ( $H_c$ ) of these composites is higher in several times than values which were measured in the initial state. This result is due to increased of the metal granules size.

MR completely disappears after composites annealing at 550 °C. This result indirectly indicates that the nanogranular structure of composites is destructed and homogeneous material is formed as a result of annealing. Analysis of the magnetization curves of samples annealed at 550 °C shows an amazing fact: in the composites with low metal concentration the magnetic hysteresis is observed (see fig.) and  $H_c$  values of these composites are comparable with the  $H_c$  values of the samples with high metal concentration. The elemental composition of the composites allows to assume that the thermal annealing initiate formation of a magnesium ferrite.

Support of RFBR, grant N 09-02-97536-r-center-a is acknowledged.

## ELECTRICAL AND MAGNETIC PROPERTIES OF NEW MULTILAYER HETEROGENEOUS STRUCTURES BASED ON COMPOSITES



*Aleshnikov A.A., Kalinin Yu.E., Sitnikov A.V., Fedosov A.G.*

Dept. Solid State Physics, Voronezh State Technical University, Russia

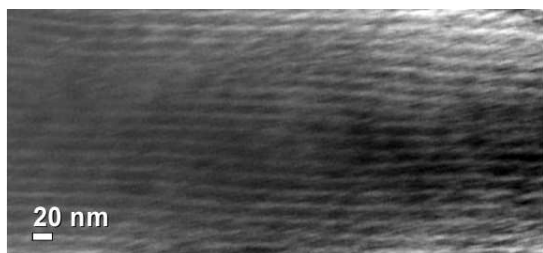


Fig. 1. Electronic microphotograph of the cross-section of multilayer heterogeneous structure  $\{[(\text{Co}_{45}\text{Fe}_{45}\text{Zr}_{10})_{55}(\text{Al}_2\text{O}_3)_{45}]/[(\text{Co}_{45}\text{Fe}_{45}\text{Zr}_{10})_{55}(\text{Al}_2\text{O}_3)_{45}+\text{O}_2]\}_{300}$

The research into magnetic properties of composites  $(\text{Co}_{45}\text{Fe}_{45}\text{Zr}_{10})_x(\text{Al}_2\text{O}_3)_{100-x}$  revealed in the films the presence of significant perpendicular component of magnetic anisotropy for compositions with high content of metal phase. It could be related to the formation of columnar structure of metal grains clusters of a composite during the film growth. The study looks at the possibility of restriction of film columnar structure growth with the help of creation of interlayers from composite produced in the active gas medium.

The films of heterogeneous systems based on ferromagnetic alloy  $\text{Co}_{45}\text{Fe}_{45}\text{Zr}_{10}$  and  $\text{Al}_2\text{O}_3$  were produced with the help of ion-beam sputtering of

composite target. Solid composites  $(\text{Co}_{45}\text{Fe}_{45}\text{Zr}_{10})_x(\text{Al}_2\text{O}_3)_{100-x}$  were synthesized. Their growth was carried out in the Ar medium, in the Ar medium with incorporation of 35 and 12 partial % of  $\text{N}_2$  and  $\text{O}_2$  respectively. Multilayer heterogeneous systems  $\{[(\text{Co}_{45}\text{Fe}_{45}\text{Zr}_{10})_x(\text{Al}_2\text{O}_3)_{100-x}]/[(\text{Co}_{45}\text{Fe}_{45}\text{Zr}_{10})_x(\text{Al}_2\text{O}_3)_{100-x}+\text{N}_2(\text{O}_2)]\}_{300}$  were also synthesized. The electronic microphotograph of cross-section of multilayer heterogeneous film (Fig. 1) showed well-formed layer structure which is repeated every 14 nm, which conforms with calculated bilayers thicknesses.

Concentration dependences of electrical resistivity ( $\rho$ ) of the investigated heterogeneous structures are typical for percolation systems with phases which differ considerably in the rate of their conductivity. Incorporation of oxygen and nitrogen leads to the increase of resistance value in composites. It is revealed that dependences of  $\rho(x)$  in the multilayer films differ insignificantly from this composite  $(\text{Co}_{45}\text{Fe}_{45}\text{Zr}_{10})_x(\text{Al}_2\text{O}_3)_{100-x}$  characteristic.

The analysis of transfer curves showed the presence of perpendicular magnetic anisotropy in composite structures with high content of metal phase. Perpendicular component of magnetization vector is not found in the films of multilayer heterostructures. Also these films are characterized by low value of coercive field, high magnetic permeability and well formed uniaxial anisotropy in the plane of the film.

Characteristics of concentration dependences of real ( $\mu'$ ) and imaginary ( $\mu''$ ) parts of complex magnetic permeability correlate with transfer curves of studied systems. Research showed that maximum values of  $\mu'(x)$  at frequency 50 MHz in multilayer structure  $[(\text{Co}_{45}\text{Fe}_{45}\text{Zr}_{10})_{57}(\text{Al}_2\text{O}_3)_{43}]/[(\text{Co}_{45}\text{Fe}_{45}\text{Zr}_{10})_{57}(\text{Al}_2\text{O}_3)_{43}+\text{O}_2]_{300}$  amount to 400, while in composite  $(\text{Co}_{45}\text{Fe}_{45}\text{Zr}_{10})_{43}(\text{Al}_2\text{O}_3)_{57}$  it is 90. Annealing heterogeneous structures at temperature 350<sup>o</sup> C during 30 minutes in magnetic field 2500 Oe applied in the plane of the film perpendicular to the axis of samples led to significant increase of  $\mu'$  and  $\mu''$  in all the studied systems.

This work was supported by RFBR (grants № 09-02-97506 p\_центр\_a)

## THE EFFECT OF *sp*-DOPANTS ON MAGNETIC PROPERTIES OF THE ORDERED $\text{Fe}_{65-x}\text{Al}_{35-y}\text{M}_{x,y}$ ( $\text{M}_{x,y}=\text{Ga,B,V}$ ; $x,y=5,10$ ) ALLOYS

Voronina E.<sup>1,5</sup>, Yelsukov Eu.<sup>1</sup>, Korolyov A.<sup>2</sup>, Klauss H.-H.<sup>3</sup>, Dellmann T.<sup>3</sup>, Granovsky S.<sup>3,4</sup>

<sup>1</sup>Physical-Technical Institute of UrB RAS, Kirov Str. 132, 426000 Izhevsk, Russia

<sup>2</sup>Institute of Metal Physics UrB RAS, S. Kovalevskoi Str. 18, 620041 Ekaterinburg, Russia

<sup>3</sup>Institut für Festkörperphysik, TU Dresden, Helmholtzstraße 10, 01062 Dresden, Germany

<sup>4</sup>Faculty of Physics, Lomonosov Moscow State University, Leninskie Gory 1, 119991 Moscow, Russia

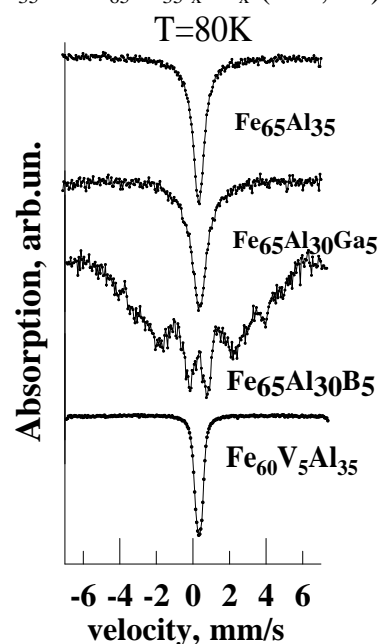
<sup>5</sup>Institute of Physics, Kazan Federal University, Kremlyovskaya Str. 18, 420008 Kazan, Russia

Magnetic moment correlations of nanometer scale interpreted as incommensurate spin density wave [1] and peculiar magnetotransport characteristics of the ordered  $\text{Fe}_{100-x}\text{Al}_x$  alloys ( $25 < x < 35$  at.%) [2] range them in a class of itinerant magnets with strong electron-electron correlations and a self-organized magnetic nanostructure. These alloys attract interest as suitable objects to study out the origin of magnetic inhomogeneities and conditions of their formation in single-phase magnets.

We present results of X-ray diffraction, complex in-field (up to 9 T) and temperature (5–300 K) magnetometric and Mössbauer studies of the ordered  $\text{Fe}_{65}\text{Al}_{35-x}\text{M}_x$  ( $\text{M}=\text{Ga, B}$ ;  $x=0,5,10$ ) and  $\text{Fe}_{65-x}\text{V}_x\text{Al}_{35}$  ( $x=5,10$ ) alloys. The materials have been produced by special heat treatment of the originally disordered nanocrystalline alloys synthesized by mechanochemistry. All the samples are a single-phase and crystallize into a  $\text{DO}_3$  or  $\text{B2}$ -type superlattice. Maximum change of *bcc* lattice parameter is about 0.2% for the alloys admixed with 10 at.% of Ga (an increase) and V (a decrease).

Analysis of the magnetometry studies shows that the systems  $\text{Fe}_{65}\text{Al}_{35}$  и  $\text{Fe}_{65}\text{Al}_{35-x}\text{Ga}_x$  ( $x=5, 10$ ) are characterized by two different magnetic states with essentially distinguishing hysteresis loops and AC susceptibility values. Low-susceptibility state is readily destroyed by external magnetic field 2.5-4 T and passes to another state (stable in a broad field and temperature range) specified by higher spontaneous magnetization and AC susceptibility. The temperature and external magnetic field values inducing the transition from one magnetic state to another are higher in the Ga-doped alloys than in reference  $\text{Fe}_{65}\text{Al}_{35}$  alloy. Significant increase of AC susceptibility value indicates a substantial realignment of local magnetic moments. The dependence of the magnetization and magnetic susceptibility on the temperature has a maximum.

The Boron addition transforms the magnetic state of the initial alloy  $\text{Fe}_{65}\text{Al}_{35}$  into a ferromagnetic exhibiting high Curie temperature, saturation magnetization and average  $^{57}\text{Fe}$  hyperfine magnetic field values (as it is seen in the Figure). Substitution of V for Fe in the ternary alloys  $\text{Fe}_{65-x}\text{V}_x\text{Al}_{35}$  results in the reduction of magnetic characteristics and collapsing of  $^{57}\text{Fe}$  hyperfine magnetic field.



Support by RFBR (Grant № 09-02-00461) is acknowledged.

[1] D.R. Noakes et al, *Phys.Rev.Let.*, **91** (2003) 217201.

[2] A.E. Yelsukova et al., *PSS*, **50** (2008) 1071.

## MAGNETIC PROPERTIES AND SPATIAL ORDERING OF FERROMAGNETIC NANOWIRES IN ARRAYS

Sukovatitsina E.V.<sup>1</sup>, Samardak A.S.<sup>1</sup>, Ognev A.V.<sup>1</sup>, Chebotkevich L.A.<sup>1</sup>, Peighambari S.M.<sup>2</sup>, Mahmoodi R.<sup>3</sup>, Hosseini M.G.<sup>3</sup>, Nasirpour F.<sup>2</sup>

<sup>1</sup> Laboratory of thin film technologies, Far Eastern Federal University, Vladivostok, Russia

<sup>2</sup> Department of Materials Engineering, Sahand University of Technology, Tabriz, Iran

<sup>3</sup> Department of Physical Chemistry, Faculty of Chemistry, Tabriz University, Tabriz, Iran

This paper is dedicated to a study of magnetic properties (coercive force and remanent magnetization) of ordered Ni nanowire arrays. The magnetic nanowires were prepared by electrodeposition of nickel from simple sulfate solutions into anodic aluminum oxide nanoporous templates (with diameter of  $d=20$  and  $40$  nm) fabricated by potentiostatic anodization. Obtained scanning electron microscope images were exploited to process spectral Fourier analysis of spatial ordering of nanowires. Magnetic properties of nanowires were investigated by the home-made vibrating sample magnetometer. We measured the angular dependence of coercivity  $H_c = f(\varphi)$  and normalized remanent magnetization  $M_r/M_s = f(\varphi)$ , where  $\varphi$  is an azimuth angle between selected direction in a sample and  $\mathbf{H}$ . Fig.1 shows dependences  $H_c = f(\varphi)$  and  $M_r/M_s = f(\varphi)$  for Ni nanowires with  $d=40$ nm. When  $\mathbf{H}$  is perpendicular to the sample plane, we found  $M_r/M_s = 0.9$  and  $H_c = 600$  Oe, while for the in-plane measurement configuration as  $\mathbf{H}$  is parallel to the sample plane,  $M_r/M_s = 0.2$  and  $H_c = 270$  Oe. It means that the array of Ni nanowires has strong perpendicular magnetic anisotropy and the in-plane component of magnetic anisotropy is considerably smaller.

For the two arrays with different spatial ordering of  $20$  nm diameter Ni nanowires we found strong difference in behavior of magnetic properties, Fig.2. As seen in Fig.2(b), the additional axes of in-plane magnetic anisotropy is caused by hexagon-like spatial ordering of nanowires in alumina matrix, Fig.2(d).

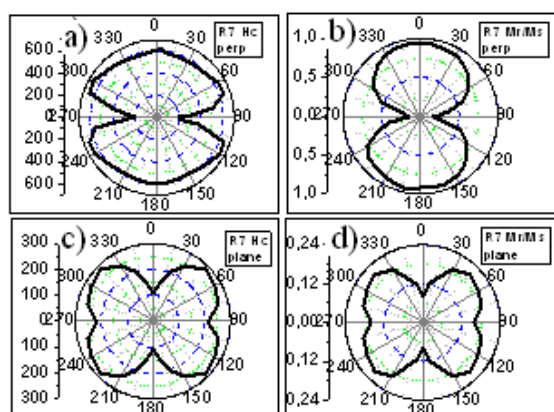


Fig.1. Angular dependences for  $40$  nm diameter Ni nanowires: (a,c) -  $H_c = f(\varphi)$ ; (b,d) -  $M_r/M_s = f(\varphi)$ ; (a,b) -  $\mathbf{H} \perp$  sample plane, (c,d) -  $\mathbf{H} \parallel$  sample plane.

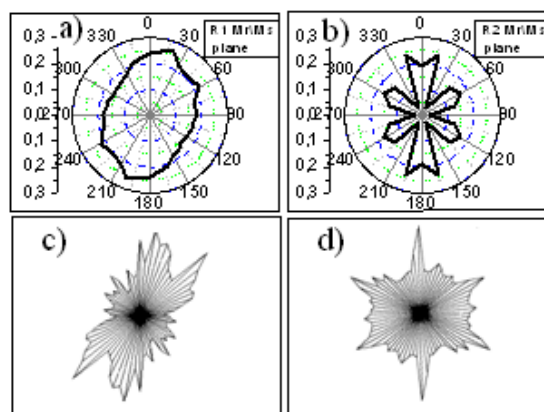


Fig.2. Angular dependence of  $M_r/M_s$  (a,b) and Fourier spectra for Ni wires ( $d=20$  nm) with different spatial ordering (samples R1 (a,c) and R2 (b,d)) when  $\mathbf{H} \parallel$  sample plane.

In conclusion, we have found that all arrays had perpendicular magnetic anisotropy induced by an oblong shape of nanowires. The reason for the multi-fold in-plane anisotropy is a nearly regular hexagonal distribution of nanowires in an alumina substrate. Manipulation by spatial ordering can help to find optimized magnetic properties of nanowires to be used in novel spintronic devices.

Support by The grant council of President of Russian Federation (MK- 942.2010.2) and Federal Program "Scientific and Research-Educational Cadres of Innovative Russia" (P1424, 02.740.11.0549) is acknowledged.

## FERROMAGNETIC Co(P) POWDERS WITH NANODIAMOND AND CORUNDUM PRECIPITATES

*Goncharova O.A.<sup>1</sup>, Chekanova L.A.<sup>2</sup>, Denisova E.A.<sup>2</sup>, Komogortsev S.V.<sup>1,2</sup>, Iskhakov R.S.<sup>1,2</sup>, Eremin E.V.<sup>2</sup>*

<sup>1</sup> Siberian State Technological University, 660049 Krasnoyarsk, Mira avenue 82, Russia

<sup>2</sup> Kirensky Institute of Physics, SB RAS, 660036 Krasnoyarsk, Akademgorodok 50/38, Russia

In recent years much attention has been given to nanocomposite materials including magnetic nanomaterials. Wide class of such materials is the composite ferromagnetic metal - nonmagnetic dielectric [1].

Powders of  $\text{Co}_{100-x}\text{P}_x$  alloy with ultradispersed corundum ( $\text{Al}_2\text{O}_3$ ) and detonation nanodiamond (DND) precipitates were synthesized by chemical deposition. In this work we report results of investigation of  $\text{Al}_2\text{O}_3/\text{Co}_{100-x}\text{P}_x$  and  $\text{DND}/\text{Co}_{100-x}\text{P}_x$  composites.

Field and temperature dependences of magnetization of composite powders were measured with PPMS in applied fields of up to 40 kOe and in the temperature range from 2 to 300 K. Ferromagnetic resonance was observed at 9.2 GHz.

Magnetization approach to saturation in the composite materials  $\text{Al}_2\text{O}_3/\text{Co}_{100-x}\text{P}_x$  and  $\text{DND}/\text{Co}_{100-x}\text{P}_x$  is characterized by following dependence of magnetization  $M$  on external field  $H$ :  $M(H) = a_{H0} - a_{H1}H^2 + a_{H2}L(H/a_{H3})$  (where  $L(x) = \text{cth}(x) - 1/x$  is the Langevin function) in fields higher than 5 kOe. It allowed us to calculate the values of root-mean-square fluctuation of local magnetic anisotropy field for ferromagnetic phase  $H_a = (a_{H1}/a_{H0})^{1/2}$ . Dependences of magnetization of the composite powders on temperature were approximated by expression  $M(T) = a_{T0} - a_{T1}T^{3/2} + a_{T2}L(a_{T3}/T)$ . The Bloch constant was calculated from approximation according to formula  $B = a_{T1}/a_{T0}$  [2]. In FMR spectra of composite powders two resonant lines in low ( $1 < H_r < 3$  kOe) and high fields ( $8 < H_r < 10$  kOe) are observed.

In the table the values of magnetic parameters of the composite powders are compared with those of  $\text{Co}_{90.5}\text{P}_{9.5}$  powder. The values of Bloch constant  $B$  for the composite powders are significantly higher than for  $\text{Co}_{90.5}\text{P}_{9.5}$  powder without precipitates.

Powder composition	Root-mean-square fluctuation of local magnetic anisotropy field $H_a$ , kOe	Bloch constant $B, \cdot 10^{-6} \text{K}^{-3/2}$	Coercive force $H_c$ , Oe	FMR linewidth in low field $\Delta H$ , kOe	FMR linewidth in high field $\Delta H$ , kOe
$\text{Co}_{90.5}\text{P}_{9.5}$	2.2	7.8	200	2	-
$(\text{DND})_{2.4}(\text{Co}_{90.5}\text{P}_{9.5})_{97.6}$	1.3	4.14	140	4	7.3
$(\text{DND})_{8.7}(\text{Co}_{90.5}\text{P}_{9.5})_{91.3}$	2.3	40.4	380	1.8	5.8
$(\text{Al}_2\text{O}_3)_7(\text{Co}_{90.5}\text{P}_{9.5})_{93}$	1.9	34.4	380	4	6.5
$(\text{Al}_2\text{O}_3)_{30}(\text{Co}_{90.5}\text{P}_{9.5})_{70}$	0.9	31.5	110	2.9	6.9

The work was supported by the target program "Development of the Scientific Potential of the Higher School", project No. 2.1.1/11470, the target federal program for 2009-2013 "Research and Educational Personnel for Innovative Russia" and Russian Foundation for Basic Research (project 11-03-00471-a).

[1] R. S. Iskhakov, S. V. Komogortsev, E. A. Denisova, Yu. E. Kalinin, A. V. Sitnikov, *JETP Lett.*, **86** (2007) 465.

[2] R. Iskhakov, E. Denisova, L. Kuzovnikova, S. Komogortsev, A. Balaev, G. Bondarenko, *J. Optoelectron. Adv. M.*, **10** (2008) 1043.

## EXCHANGE BIAS INDUCED IN POLYCRYSTALLINE Co/FeMn-STRUCTURES BY MAGNETIC FIELD COOLING

*Chechenin N.G.<sup>1</sup>, Dzhun I.O.<sup>1</sup>, Dushenko S.A.<sup>1,2</sup>, Konstantinova E.A.<sup>2</sup>*

<sup>1</sup> Skobeltsyn Institute of Nuclear Physics and

<sup>2</sup> Faculty of Physics Lomonosov Moscow State University, Lomonosov Moscow State University, Leninskie Gory, Moscow 119991, Russian Federation

Bilayer Si/Ta(30nm)/Co(7nm)/FeMn(15nm)/Ta(30nm) ferromagnetic/antiferromagnetic-based (F/AF) structures were deposited by DC magnetron sputtering in argon at the pressure of  $3 \cdot 10^{-3}$  Torr with the magnetic field of 420 Oe applied in plane of substrate during the deposition. For a comparison Si/Ta30nm/Co7nm/Ta30nm (F) structures with free ferromagnetic (F) layer were also deposited. The deposited bilayer structure was thermally annealed at  $T_{ann} = 150^{\circ}\text{C}$  for 0.5 hour and cooled down to the room temperature all in presence of a magnetic field of 1 kOe applied in the plane of the sample. Magnetic properties of the samples were studied by measuring the angular dependence of the ferromagnetic resonance (FMR) field in 115K-300K temperature range.

Though the deposition of structures in presence of magnetic field is a common way to saturate AF layer, there was no exchange bias in as-deposited bilayer structure at room temperature detected. From the temperature dependence of exchange bias the blocking temperature near 250K was obtained. The exchange bias field of 14 Oe at room temperature showed up after the thermal annealing of this structure at  $T_{ann} = 150^{\circ}\text{C}$ . Thus, the thermal treatment increased the blocking temperature from 250 K to above the room temperature. We note also that the annealing temperature is significantly lower than the Néel temperature for the bulk  $\text{Fe}_{50}\text{Mn}_{50}$  ( $T_N = 490$  K).

It is commonly accepted that in order to set the exchange bias the AF layer is to be heated above the  $T_N$ . The low setting temperature reported above indicates that in a polycrystalline structure with small non-interacting grains each AF grain can have his own critical temperature for transition into paramagnetic state, forming a distribution, corresponding to the grain size distribution  $GS(D)$ . The film thickness  $t$  is one of the most important dimensions of the grain shape affecting the transition temperature. For a unidirectional anisotropy to be set at a certain annealing temperature  $T_{ann}$  lower than the  $T_N$ , the size of the AF-grain must be smaller than a corresponding critical size,  $D < D^{(1)}$ . From the other hand the grain size must be large enough,  $D > D^{(2)}$ , to withstand the thermal fluctuations at the temperature of measuring or functioning of the AF/F structure. The range  $D^{(2)} < D < D^{(1)}$  within the GS-distribution determines the possibility and the strength of the exchange interaction from the AF-side at the AF/F interface. Further on, the strength of exchange interaction determines the exchange bias field  $H_{EB}$  to withstand the reverse magnetization of the F-film. These limitations for exchange biasing in AF/F structures are discussed in the report in connection with our experimental observations.

This work is supported by Federal Agency of Science and Innovations (contract 02.740.11.0242, contract 02.740.11.0389). The FMR study was performed at User Facilities Center of M.V. Lomonosov Moscow State University.

## MAGNETOOPTICAL KERR EFFECT ENHANCEMENT IN Co-Ti-O NANOCOMPOSITE FILMS

*Polyakov V.V.<sup>1</sup>, Polyakova K.P.<sup>1,2</sup>, Seredkin V.A.<sup>1</sup>, Patrino G.S.<sup>1,2</sup>, Tabakaev A.I.<sup>3</sup>*

<sup>1</sup>L.V.Kirensky Institute of Physics, SB RAS, 660036, Krasnoyarsk, Russia

<sup>2</sup>Siberian Federal University, 660041, Krasnoyarsk, Russia

<sup>3</sup>Siberian University named after academician M.F. Reshetnev, 660037, Krasnoyarsk, Russia

It is known, that magneto-optical properties of composite system metal-dielectric depends on properties of a dielectric component. The majority of researches are devoted to the metal with dielectric matrix or layer of SiO<sub>2</sub> and Al<sub>2</sub>O<sub>3</sub>. In this connection the magneto-optical properties of composite films in the presence TiO<sub>2</sub> with the dielectric constant exceeding corresponding value of SiO<sub>2</sub> and Al<sub>2</sub>O<sub>3</sub> are of interest.

In this report we present the results of magneto-optical investigations of Co-TiO<sub>2</sub> granular and Co/Ti<sub>2</sub> layered films. Magneto-optical spectra have been investigated in the wavelength range of visible light in a magnetic field up to 14 Oe.

We studied spectral dependence of polar Kerr effect of nanogranular films with different volume concentrations ( $X = V(\text{Co})/V(\text{Co}+\text{TiO}_2)$ ) of magnetic phase of 30 nm Co effective thickness. For films with  $x = 0.47, 0.52, 0.55$  and  $0.64$  curves shows a resonance character with a significant enhancement of the Kerr rotation angle in the wavelength range 500-700 nm. The maximum rotation angle of  $2\Theta_k = 2.5$  degree was found for films with a magnetic phase concentrations  $X = 0.55$ . This is more than five-fold in comparison with conventional Co films. The concentration dependence of the absolute value of maximum Kerr rotation has two regions of an increase in the rotation angle, one of which is in the subpercolation region and the other region is near the percolation threshold. The first maximum was observed in work [1] and was connected with the interference effects. The second region is likely explained by the percolation [1,2].

The layered structure of Co/TiO<sub>2</sub> were obtained by consistent deposition of Co layer and titanium oxide layer by ion-plasma sputtering on glass substrates. This structure consists of 10 layers. The thickness of the magnetic layer was 50 nm, the thickness of titanium oxide layer was 170 nm. Study of spectral dependence of polar Kerr effect showed that the spectrum has a pronounced resonance character with giant enhancement of angle of rotation near the resonance. It was established that the maximum Kerr rotation angle 7.3 deg was observed for 8-layer structure at a wavelength of 540 nm. It was shown that the maximum value of rotation depends on the number of layers of non-monotonic way. Also, the resonances position on the wavelength axis depends on the number of layers of intricately.

It is necessary to note that anomalies of magneto-optical spectra of the composite materials containing dielectric in the form of a layer or matrix were observed and have been predicted by theoretical calculation [3].

The mechanism of a magneto-optical rotation enhancement in nanocomposite Co-TiO<sub>2</sub> films will be discussed.

[1] A.M.Kalashnikov, V.V.Paul, Pisarev R.V., et.al., *Fiz. Tverd. Tela*, **46** (2004), 2092.

[2] Jiang Z.S., Jin G.J., Ji J.T, et.al., *J. Appl. Phys.* **78** (1995), 439.

[3] M. Abe and M. Gomi, *Jpn. J. Appl. Phys.*, **23** (1984) 1580.



## THE EMERGING OF GIANT MAGNETIC ANISOTROPY IN Au-Co NANOWIRES

Tsytar K.M., Smelova E.M., Bazhanov D.I., Saletsky A.M.  
Faculty of Physics, Moscow State University, 119899 Moscow, Russia

The progress in spintronics requires more intense and comprehensive study of the magnetic properties of low-dimensional structures [1]. Last decade special interest in theoretical and experimental investigations was devoted to the investigation of spin-dependent ballistic electron transport through magnetic nanowires and nanocontacts [2]. Especial interest was devoted to the study of mixed nanocontacts (NCs) and nanowires (NWs), the changes their elemental composition can be most effectively, controlled the magnetic and conductive properties of the system as a whole. The possibility of stable Au-Co nanoalloys formation was found in several experimental works [3]. In this paper we present a comprehensive *ab initio* study of the atomic and electronic structure of mixed Au-Co NWs. It is shown that Au-Co NWs exhibit giant magnetic anisotropy. Our self-consistent electronic-structure calculations of Au-Co wires have been performed by means of the projector augmented-wave (PAW) technique as implemented in Vienna Ab-initio Simulation Package (VASP) code [4,5] which based on the density functional theory (DFT). We investigate the properties of atomic and electronic structure of uniform and non-uniform mixed Au-Co NWs [6].

The possibility of the  $\text{Co}_2$  dimers formation was shown. It's shown that the formation of dimers leads to a non-uniform distribution of electron density and consequently leads to the rupture

between the atoms of gold at its extension. It was found that only uniformly mixed Au-Co nanowire is stable under tension to larger interatomic distances. It is first shown that the uniformly mixed Au-Co NWs have a giant magnetic anisotropy with the values of the magnetic anisotropy energy MAE~130meV per atom Co in wire comparable with the experimentally established values for the layered structures and thin films. The easy magnetization axis is perpendicular to the axis of the NW (Fig.1). As result it was found, that the mixing of noble metal atoms with ferromagnetic elements leads to the formation of stable one-dimensional nanostructures with unusual magnetic properties.

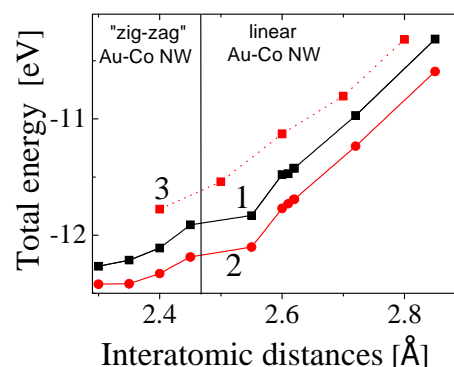


Fig.1 The total energy of Au-Co NW for both magnetic polarizations magnetic moment parallel (1) and perpendicular (2) to the wire axis and without LS interaction (3) as function of interatomic distances.

Supported by grant of RFBR No10-02-01274-a and by grant of "Dynasty Foundation".

- [1] K.M. Smelova, D.I.Bazhanov, A.M.Saletsky, et al., Phys. Rev. B. 77,033408 (2008).
- [2] J. Velev, et al. Phys. Rev. Lett. **94**, 127203 (2005).
- [3] Shigehito, JST, 80, 225(2001); H. Nabika et al., J.M.C., 12, 2408 (2002).
- [4] G. Kresse and J. Furthmuller, Phys. Rev. B, 54:11169 (1996).
- [5] M.C.Payne, et al., Rev. Mod. Phys., 64 1045 (1992), P.Bloch, Phys. Rev. B50, 17953 (1994)
- [6] E.M.Смелова и др., Письма в ЖЭТФ, 93 (3) (2011)

## TEMPERATURE DEPENDENCE OF INTERLAYER COUPLING IN Fe/Si/Fe TRILAYERS

Drovosekov A.B.<sup>1</sup>, Kholin D.I.<sup>1</sup>, Kreines N.M.<sup>1</sup>, Bürgler D.E.<sup>2</sup>, Schreiber R.<sup>2</sup>

<sup>1</sup> P.L.Kapitza Institute for Physical Problems RAS, Kosygina 2, 119334 Moscow, Russia

<sup>2</sup> Institut für Festkörperforschung, Forschungszentrum Jülich GmbH, D-52425 Jülich, Germany

Magnetic interlayer coupling between iron layers separated by a thin silicon spacer has been a subject of studies for decades [1-3]. Nevertheless, up to now, the complete understanding of the phenomenon has not been achieved. Investigations of magnetic properties of the system at varying temperature and spacer thickness can shed light upon mechanisms responsible for interlayer coupling. This report is mainly focused on temperature dependence of coupling strength in Fe/Si/Fe structures.

In this work we present results obtained for Fe(70Å)/Si( $t_{Si}$ )/Fe(70Å) trilayer samples using SQUID magnetometry and FMR technique. Two samples (S1 and S2) with  $t_{Si} \sim 10\text{Å}$  were grown by MBE technique on MgO(100) substrate with  $\sim 1000\text{Å}$  silver buffer layer. Magnetization curves were measured in 5–350K and FMR spectra in 77–300K temperature range. Magnetic field was applied in the film plane in all the experiments. The obtained data were analysed in the frame of biquadratic coupling model (BCM).

At relatively high temperatures  $\sim 300\text{K}$  the experimental data for both samples show a good agreement with the BCM. The  $M(H)$  curves can be good approximated by the BCM in the whole field range up to the saturation point. The FMR spectra demonstrate the presence of the optical branch with a typical BCM  $\omega(H)$  dependence. The absolute values of the coupling constants for two samples have the same order of magnitude,  $J_1, J_2 \sim 1 \text{erg/cm}^2$ , but the sign of the bilinear constant  $J_1$  corresponds to AFM coupling for S1 and FM for S2 sample. This difference can be explained by small deviations of the spacer thickness from  $t_{Si} = 10\text{Å}$ .

As temperature diminishes, the saturation field (and, consequently, the coupling strength) increases for both samples. The data for S1 (AFM) sample can be described by the BCM relatively good down to the lowest temperature. The resulting temperature dependences of the coupling constants are shown in the Fig.1. Both constants are increasing at cooling. On the contrary, the S2 (FM) sample demonstrates relatively strong deviation from the BCM below  $T \sim 100\text{K}$  as the saturation field is steadily growing [4].

To summarize, the investigated samples demonstrated increasing coupling strength at cooling, but the applicability of the BCM at low temperatures is under question.

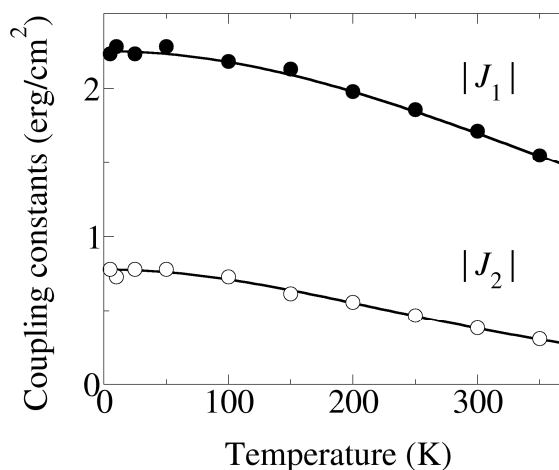


Fig.1. Temperature dependences of bilinear and biquadratic coupling constants for S1 (AFM) sample. Points are experimental data, lines are plotted for an eye.

The work is partially supported by RFBR (grant 10-02-01110).

- [1] S. Toscano, B. Briner, H. Hopster, M. Landot, *J. Magn. Magn. Matter.*, **114** (1992) L6.
- [2] G.J. Strijkers, J.T. Kohlhepp, H.J.M. Swagten, W.J.M. de Jonge, *PRL*, **84** (2000) 1812.
- [3] A. Paul, M. Buchmeier, D. Bürgler et al., *Phys. Rev. B*, **77** (2008) 184409.
- [4] A.B. Drovosekov, D.I. Kholin, N.M. Kreines et. al., *EASTMAG-2010 Abstracts* (2010) 289.

## PASSAGE OF Fe/Cr/Fe THREE LAYER FILM MAGNETIZATION CURVE BEYOND THE LIMITS OF HYSTERESIS LOOP

*Gudin S.A.<sup>1</sup>, Kurkin M.I.<sup>1</sup>, Gapontsev A.V.<sup>2</sup>*

<sup>1</sup> Institute of Metal Physics Ural Div. RAS, S. Kovalevskaya str. 18, 620219 Yekaterinburg, Russia  
<sup>2</sup> «Spetsneftegaz NPO» JSC, Beryozovsky, Zapadnay promzona 14, Russia

Nanometer thickness Fe/Cr layer films are studied intensively during last 15 years and some unusual physical properties of these structures have been discovered: the ferromagnetic, antiferromagnetic and noncollinear ordering of neighbouring magnetic layers of iron, the giant magnetoresistive effect, short and long periods of oscillations of interlayer exchange coupling. This work is encouraged by uncommon experimental results for Fe/Cr multilayers published in [1]. The conditions of the coexistence of Fe/Cr/Fe film states with parallel and antiparallel Fe layer magnetizations are obtained using the model [2-5]. Under these conditions, the transition from antiparallel (AF-) to parallel (F-) orientation in a magnetic field  $H$ , is related to the phase change of linearly polarized spin-density wave in Cr interlayer (wave node in a center of the layer is replaced with an antinode). The coexistence of these two states (AF-, F-) means that the transition of the Fe/Cr/Fe film to the ferromagnetic F- state stimulated by magnetic field  $H$  retains after  $H$  shutdown. This effect is manifested experimentally in a fact that the magnetization curve  $M(H)$  of initially antiferromagnetic Fe/Cr/Fe film would go beyond the limits of remagnetization hysteresis loop in ferromagnetic state stimulated by field  $H$  (Fig.1.).

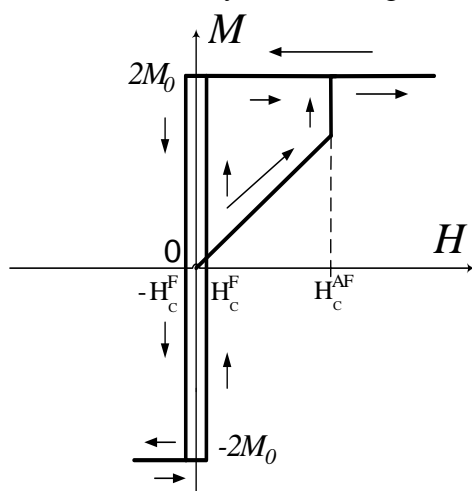


Figure 1.  
 Fe/Cr/Fe film magnetization curve and remagnetization one for the case of F- and AF- states coexistence.

This work is partially supported by RFBR, project No. 11-02-00093 and the program of Presidium of Russian Academy of Sciences.

- [1] A.B. Drovosekov, N.M. Kreines, D.I. Kholin, A.V. Korolev, M.A. Milyaev, L.N. Romashev, V.V. Ustinov JETP Lett. 88, 126 (2008).
- [2] M.I. Kurkin, S.A. Gudin, V.V Ustinov. FMM (Fizika Metallov i Metallovedenie), **96**, №5, 21 (2003)
- [3] M.I. Kurkin, S.A. Gudin, V.V Ustinov, S.A. Zlobin, FMM, **98**, №6, 8 (2004)
- [4] S.A. Gudin, A.V. Gapontsev, N.B. Bakulina, M.I. Kurkin, V.V. Ustinov PMM (Phys. Met. Metallogr.), **107**, №3, 216 (2009).
- [5] N.B. Bakulina, M.I. Kurkin, S.A. Gudin, A.V. Gapontsev. Phys. Solid. State, 52, №2, 328 (2010).

## INTERFACE STRUCTURE AND MAGNETIC PROPERTIES OF Ni-Ge FILMS

Greben'kova Yu.<sup>1</sup>, Velikanov D.<sup>1,2</sup>, Chernichenko A.<sup>1</sup>, Turpanov I.<sup>1</sup>, Mukhamedganov E.<sup>3</sup>, Li L.<sup>1</sup>, Patrin G.<sup>1,2</sup>

<sup>1</sup> L.V. Kirensky Institute of Physics, SB RAS, Krasnoyarsk, 660036, Russia

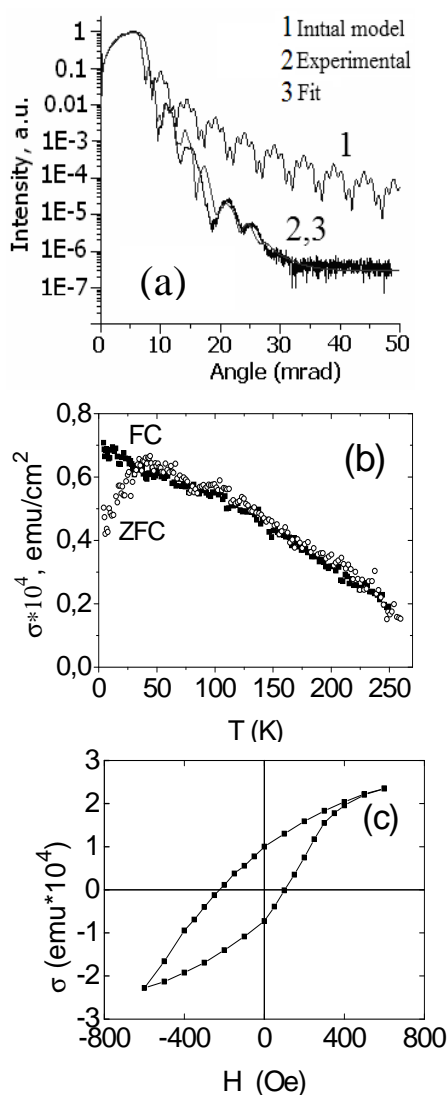
<sup>2</sup> Siberian Federal University, Krasnoyarsk, 660041, Russia

<sup>3</sup> RSC "Kurchatov Institute", Moscow, 123182, Russia

The magnetic properties of layered Ni-Ge films were investigated with the local distribution of Ni and Ge atoms and availability of the interface layer were studied also. Two-layered and five-layered films were prepared by ion-plasma sputtering at a base pressure of  $10^{-6}$  Torr in Ar atmosphere. The Ni layer thickness in the Ni-Ge structure varied from  $\sim 8$  to  $\sim 26.5$  nm and the Ge layer thickness amounted to  $\sim 47$  nm. The Ge outer layer thickness in the five-layered films amounted to  $\sim 20$  nm, the Ni layer thickness varied from  $\sim 10$  to  $\sim 20$  nm and the Ge internal layer thickness changed from  $\sim 1$  to  $\sim 10$  nm. The Ni-Ge film structure was studied by EXAFS spectroscopy and X-ray reflectometry.

Magnetization was measured with a SQUID magnetometer at 4.2-273 K in the magnetic field  $H$  up to 1 kOe. The magnetization temperature dependences were obtained in two cooling regimes - field cooled (FC) and zero field cooled (ZFC). The analysis of EXAFS - spectra shows that in the investigated samples nickel oxide was absent and the Ni layer had a crystal structure. In the Ge spectra the availability of oxide was observed, also, the absence of distant peaks said about the amorphous state of the Ge layer. Spectra of X-ray reflectivity for the Ni-Ge (15/46 nm) film are represented in Fig.a. The experimental curve 2 coincides satisfactorily with curve 3 calculated for the structure with the interface of approximately the same composition along all its depth. If it were not so, curve 2 would coincide with calculated curve 1 which is attributed to a system without an interface layer. In the last analysis the variation of the thickness/ roughness for Ni was (11,7/1,4) nm, for Ge it was (42,3/0,75) nm; the roughness of the substrate was 1,75 nm and  $Ni_xGe_y$  thickness was 93 nm. A strong difference (Fig.b) between the magnetization dependences on the temperature  $M(T)$ , in two regimes (FC and ZFC) was observed for all five-layered films. FC and ZFC curves coincided with each other only for the temperature  $T$  exceeding some temperature  $T_m \sim 40$ K. The hysteresis loops measured at 4.2 K showed that for the layered samples the loops asymmetry and its shift along the magnetic field axis took place (Fig.c).

The peculiarities observed are explained by the formation of the antiferromagnetic phase in the interface between the Ni and Ge layers, and the rough surface between the FM and AFM layers.



The support of RFBR (grant No 11-02-00675) is acknowledged.

22PO-I-50

## MAGNETO-OPTICAL PROPERTIES OF PERIODIC DOMAIN STRUCTURE IN MAGNETIC FIELD

*Eliseeva S.V., Sementsov D.I., Ostatochnikov V.A.*

Ulyanovsk State University, Lev Tolstoy 42, 432700, Ulyanovsk, Russian Federation

Single-crystal iron-garnet films with stripe domain structure is one of the most typical examples of natural product structures controlled by an external magnetic field. When the light propagates in such a structure along the axis of periodicity the selective properties of the structure should appear in the Bragg resonance region, while at propagating along the domains and domain boundaries its wave guiding properties should be manifested.

We assume that all domains have the same material parameters, their thickness  $S_j$ , where  $j=1,2$ , and period of structure  $D = S_1 + S_2$ ; periodicity of the structure is realized along  $OY$ , magnetic moments in the domains lie in the plane  $XZ$  and their directions in the readout from the axis  $OX$  are determined by the angles  $\varphi(z)$ , that depend on the applied magnetic field for each group of domains. In this case, the dielectric tensor structure is given by:

$$\hat{\epsilon}(z) = \begin{pmatrix} \epsilon_f & -if \cos\varphi(z) & 0 \\ if \cos\varphi(z) & \epsilon_f & -if \sin\varphi(z) \\ 0 & if \sin\varphi(z) & \epsilon_f \end{pmatrix}. \quad (1)$$

Magnetic gyrotropy at optical frequencies is neglected ( $\mu = 1$ ).

Taking into account the continuity of fields at the interface between the layers, we find the transformation matrix for one period of the structure, equal to the product of transformation of matrices of the two domains with different directions of magnetization  $\hat{P} = \hat{S}_1^{-1} \hat{S}_2^{-1}$ , where  $\hat{S}_j^{-1}$  is fourth-order square matrix that connects the field at the entrance to and the exit from a domain. In the absence of damping, these matrices are unimodular. The dispersion equation is fourth ordered of magnitude  $\zeta = \exp(i\kappa_{ef} D)$ , where  $\kappa_{ef}$  - is the Bloch wave number:

$$\zeta^4 + B_3 \zeta^3 + B_2 \zeta^2 + B_1 \zeta + B_0 = 0, \quad (2)$$

where the coefficients  $B_i$  are expressed through various combinations of elements of the matrix  $\hat{P}$ .

Free term of the dispersion equation  $B_0$  is equal to  $\det \hat{P} = 1$ . The report will present: a numerical analysis of the dispersion relation (2), the distribution of the wave field on domain structure, the polarization characteristics of reflected and transmitted radiation having passed through the structure, the analysis of the possibility of control over these characteristics with the magnetizing field.

This study was supported by Federal target program «Scientific and research and educational staff of the innovative Russia» on 2009-2013 years, government contract No. P2603.

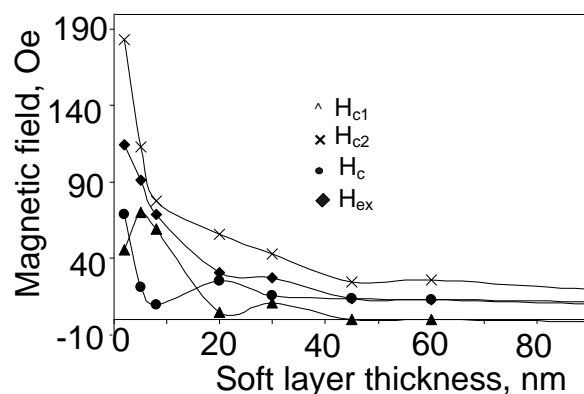
## THE COERCIVITY AND INTERLAYER EXCHANGE IN THREE-LAYER FILMS PREPARED BY CHEMICAL DEPOSITION

Chzhan A.V., Patrin G.S., Kiparisov S.Ya., Seredkin V.A.

<sup>1</sup> Kirenskii Institute of Physics, SB RAS, Krasnoyarsk 660036, Russia

<sup>2</sup> Siberian Federal University, Krasnoyarsk 660041, Russia

For obtaining of new materials and their practical applications in spintronics is necessary to monitor and control both electrical and magnetic parameters. The most interesting and informative to all other magnetic characteristics is the value of the exchange coupling between magnetic layers, which depends on many factors: the layer thickness, interface properties, etc. In this paper we report the results of studies of the exchange interaction and its influence on the coercive force in the three-layer films consisting of ferromagnetic layers based on the Co-P amorphous and polycrystalline, and a nonmagnetic layer of Ni-P obtained by chemical vapor deposition [1]. A typical hysteresis loop of soft magnetic layer has an asymmetrical form and it is characterized by exchange bias field  $H_{ex}$  respect to the zero value of the applied magnetic field  $H$  and the two critical fields  $H_{c1}$  and  $H_{c2}$ . Critical field  $H_{c1}$  corresponds to the left, and  $H_{c2}$ -right branch of the hysteresis loop. The coercivity of soft magnetic layer can be expressed in the form  $H_C = (H_{c2} - H_{c1}) / 2$ , and the bias field  $H_{ex} = (H_{c1} + H_{c2}) / 2$ . Change  $H_{ex}$  is inversely proportional to the thickness of the soft magnetic layer  $d$ . Such dependence is preserved to a thickness of  $\sim 30$ -50nm and varies from one sample to another, which, apparently, is determined by the microstructure of this layer and the interface [2]. The change of coercivity has no smooth appearance that is related to the difference in changes  $H_{c1}$  and  $H_{c2}$  the thickness of the soft magnetic layer. The value of  $H_{c1}$  first increases and then decreases, while  $H_{c2}$  decreases with increasing  $d$  (see figure). The these dependences are associated with the difference in the mechanisms of magnetization reversal in that fields. At  $H = H_{c2}$  (at the chosen experimental conditions) leads to the formation of a Bloch domain wall (BDW), while at  $H = H_{c1}$  is the annihilation of its contribution in accordance with this contribution to the coercive force of such boundaries would be asymmetrical in nature. The appearance of the DW will have to increase  $H_{c2}$ , their disappearance will have to decrease of  $H_{c1}$ .



[1] A. V. Chzhan, S. Ya. Kiparisov, V.A. Seredkin, G.S. Patrin, and M.G. Pal'chik, *Bulletin of the Russian academy of Sciences: Physics*, **73** (2009) 1161.

[2] J. Nogues, Ivan K.Shuller, *J. Magn. Magn. Mater.*, 192 (1990) 203.

## NEW MODEL FOR MAGNETISM IN ULTRATHIN FCC FE ON CU(001)

Meyerheim H.L.<sup>1</sup>, Tonnerre J.-M.<sup>2</sup>, Sandratskii L.<sup>1</sup>, Tolentino H.C.N.<sup>2</sup>, Przybylski M.<sup>1</sup>, Yildiz F.<sup>1</sup>,  
Fu X.L.<sup>1</sup>, Bontempi E.<sup>2</sup>, Ramos A.<sup>2</sup>, Grenier S.<sup>2</sup>, Kirschner J.<sup>1</sup>

<sup>1</sup> Max-Planck-Institut f. Mikrostrukturphysik, Weinberg 2, D-06120 Halle, Germany

<sup>2</sup> Institut Néel, CNRS & Université J. Fourier, F-38043 Grenoble, France

<sup>3</sup> Laboratorio di Chimica per la Tecnologia, Università di Brescia, 25123 Brescia, Italy

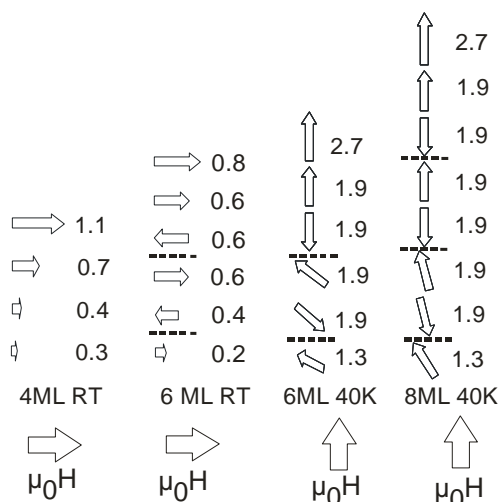


Fig.1: Spin structure for 4, 6, and 8ML fcc-Fe on Cu(001). Spin blocks are separated by dashed lines. Numbers indicate magnetic moments in Bohr Magnetons.

Using soft x-ray resonant magnetic reflectivity in combination with first-principles calculations we present a new model of the magnetic structure in fcc-Fe grown on Cu(001). Magneto Optic Kerr Effect experiments indicate an inverse spin reorientation transition, where the easy magnetization axis changes from in-plane at 4 monolayers (ML) to out of plane at 8ML thickness, while at 6 ML a hysteresis loop is found for both, in and out of plane magnetization [1].

Three samples were prepared consisting of 4, 6 and 8 ML on Cu(001) capped by 3nm Au. For each atomic layer both, the magnitude and the direction of the magnetization is fitted. Fig.1 shows the layer resolved spin structure in the samples for different magnetization directions (see arrow at the bottom) and temperatures. While at 4ML the sample is ferromagnetic, for the anti-ferromagnetic structures in the coverage range between 6 and 8 ML we find blocks with robust magnetic structure, while the relative directions between the blocks vary involving a non-collinearity within the spin structure [2]. Experimental results are supported by parameter-free calculations within the framework of the density functional theory.

We thank Urs Staub, F. Nolting and the SIM beamline staff for their support and hospitality during our (HLM, JMT, MP) stay at the SLS in Villigen.

[1] H. Jenniches, J. Shen, C.V. Mohan, S.S. Manoharan, J. Barthel, P. Ohresser, M. Klaua, and J. Kirschner, *Phys. Rev. B* **59**, (1999) 1196

[2] H.L. Meyerheim, J.-M. Tonnerre, L. Sandratskii, H.C. N. Tolentino, M. Przybylski, Y. Gabi, F. Yildiz, X. L. Fu, E. Bontempi, S. Grenier, and J. Kirschner, *Phys. Rev. Lett.* (2009) **103**, 267202

## MAGNETIC RESONANCE INVESTIGATIONS OF SINGLE CRYSTALLINE $\text{CuCr}_2\text{S}_4$ SPINEL LAYERS IN HETEROSTRUCTURE BASED ON $\text{CuCrS}_2$ SINGLE CRYSTAL

Pankrats A.<sup>1,2</sup>, Abramova G.<sup>1</sup>, Tugarinov V.<sup>1</sup>, Zharkov S.<sup>1,2</sup>, Zeer G.<sup>2</sup>, Kondyan S.<sup>2</sup>, Boehm M.<sup>3</sup>, Vorotynova O.<sup>2</sup>

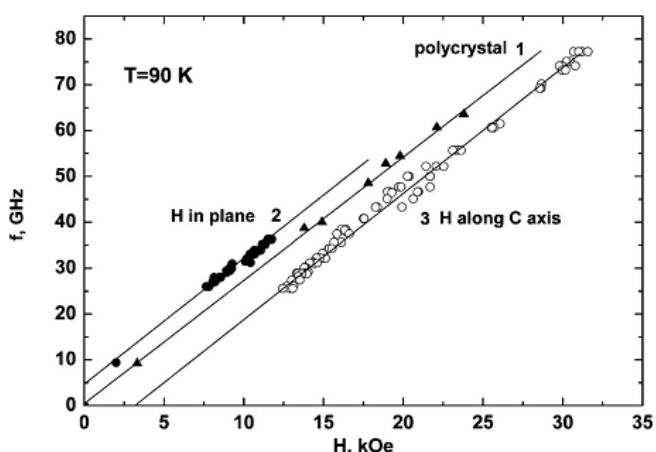
<sup>1</sup>L.V. Kirensky Institute of Physics SB RAS, Krasnoyarsk, 660036, Russia

<sup>2</sup>Siberian Federal University, Krasnoyarsk, 660041, Russia

<sup>3</sup>Institute Max von Laue-Paul Langevin, Grenoble, Cedex 9, France

A chrome-copper disulphide  $\text{CuCrS}_2$  has a layered structure with weak chemical bonds between the layers and can be considered as a dichalcogenide with  $\text{Cu}^+$  ions intercalated into the van der Waals gaps between the  $\text{CrS}_2$  layers. In this study, we present the results of the magnetic resonance study of the  $\text{CuCrS}_2$  single crystal synthesized by chemical vapor transport (CVT).

$\text{CuCrS}_2$  undergoes the paramagnet-antiferromagnet transition at  $T_N=37$  K. But in contrast to polycrystalline samples, the CVT single crystal was found to possess the strong anisotropy of the resonance properties at  $T=300$  K [1]. The magnetic anisotropy increases with the temperature decreasing, and different frequency-field dependences for parallel and perpendicular orientations of the magnetic field relative to the CVT single crystal plate were obtained at  $T=90$  K (see the figure). The observed behavior of the resonance properties of the CVT  $\text{CuCrS}_2$  single crystal can be



explained by the presence of the ferromagnetic ordered phase with easy and hard magnetization directions parallel and perpendicular to the single crystal plate, respectively. We found that the ferromagnetic properties of the CVT  $\text{CuCrS}_2$  crystal are connected with an additional  $\text{CuCr}_2\text{S}_4$  impurity phase (about 8 % by the XRD analysis) which is also single crystalline in accordance with its resonant properties. This conclusion is confirmed by the temperature dependency of the magnetic anisotropy of the impurity phase which decreases with the increasing

temperature and vanishes at approaching a temperature of about 400 K consistent with the Curie temperature of  $\text{CuCr}_2\text{S}_4$ . The presence of the single-crystal  $\text{CuCr}_2\text{S}_4$  impurity layers in the rhombohedral  $\text{CuCrS}_2$  single crystal may be attributed to the similarity of their crystal structures containing similar layers of the octahedral sites occupied by  $\text{Cr}^{3+}$ -ions. As the XRD data show, the  $\text{CuCr}_2\text{S}_4$  (111) crystal planes are parallel to the  $\text{CuCrS}_2$  (001) planes.

The studies of the microstructure and the phase composition of the sample by the scanning electron microscope JEOL JSM-7001F show that the sample can be considered as a heterostructure consisting of alternate  $\text{CuCrS}_2$  and  $\text{CuCr}_2\text{S}_4$  layers with the thickness of the spinel layers much less than 1 micron. The total amount of the spinel phase agrees with the XRD data.

The frequency-field and angular dependencies of the resonant parameters indicate that the  $\text{CuCr}_2\text{S}_4$  (111) crystal plane is an easy plane of magnetization which is characteristic for uniaxial ferromagnets. We suggest that that the lowering of the crystal symmetry in the thin layers of  $\text{CuCr}_2\text{S}_4$  occurs due to the influence of the adjacent layers of rhombohedral  $\text{CuCrS}_2$ .

[1] G. Abramova, A. Pankrats, G. Petrakovskii et al, *J. Appl. Phys.*, **107** (2010) 093914.



## FORMATION OF Cr MAGNETIC MOMENTS AND MAGNETIC ORDERING IN LAYERED COMPOUNDS $\text{Cr}_x\text{TSe}_2$ (T = Ti, V, Nb): THE ROLE OF THE PARENT COMPOUND

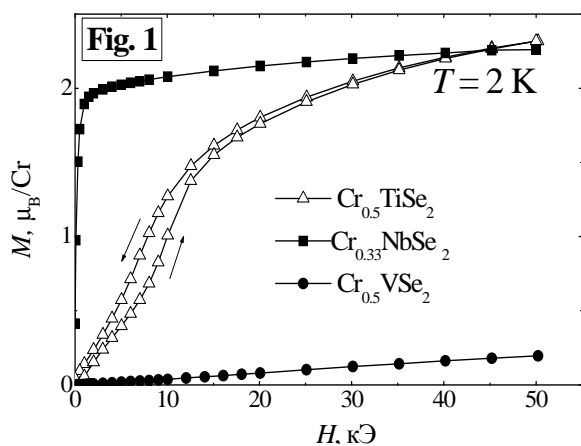
Sherokalova E.M.<sup>1</sup>, Baranov N.V.<sup>1,2</sup>, Pleschov V.G.<sup>1</sup>, Selezneva N.V.<sup>1</sup>

<sup>1</sup> Ural State University, 620083, Ekaterinburg, Russia

<sup>2</sup> Institute of Metal Physics, Russian Academy of Science, 620990, Ekaterinburg, Russia

\*e-mail: elizaveta.sherokalova@usu.ru

Layered structure of transition metal dichalcogenides  $\text{TX}_2$  (X = S, Se, Te) allows to intercalate various guest atoms with non-full filled 3d shells into space between X-Ti-X tri-layers and to obtain the quasi two-dimensional systems with alternate layers of magnetic and non-magnetic atoms [1]. The present work aims to study the crystal structure and magnetic properties of  $\text{Cr}_x\text{TSe}_2$  systems (T = Ti, V, Nb) in order to reveal how the type of the parent compound affects the formation of



magnetic moments and magnetic ordering within subsystem of intercalated Cr atoms.

The  $\text{Cr}_x\text{TSe}_2$  compounds (T = Ti, V, Nb) with Cr concentration up to  $x = 0.5$  were obtained by ampoule synthesis method [2]. The quality of all samples was checked by powder x-ray diffraction analysis by using a Bruker D8 Advance diffractometer with Cu  $K_\alpha$  radiation. The magnetic measurements were performed by using a Quantum Design SQUID magnetometer at temperatures from 2 K up to 300 K.

All compounds are observed to exhibit spin-glass or cluster-glass states at low Cr concentrations ( $x < 0.25$ ). However, further intercalation of Cr atoms leads to the appearance of a long-range antiferromagnetic order in  $\text{Cr}_x\text{TiSe}_2$  below  $T_N = 42$  K at  $x \geq 0.5$  [2], or ferromagnetic alignment of Cr moments below  $T_C = 100$  K in the case of  $\text{Cr}_{0.33}\text{NbSe}_2$  (see Figure 1). The magnetic moment per Cr atom reaches at  $H = 50$  kOe a value about of  $2.3 \mu_B$  which is lower than that expected in a local-moment model. No long-range magnetic order was detected in the  $\text{Cr}_x\text{VSe}_2$  system. The  $\text{Cr}_x\text{VSe}_2$  compounds show a spin-glass or cluster-glass behavior with freezing temperatures  $T_f < 30$  K in the whole concentration range up to  $x = 0.5$ . The values of the effective magnetic moment  $\mu_{\text{eff}}$  derived from paramagnetic susceptibility data for  $\text{Cr}_x\text{TiSe}_2$  and  $\text{Cr}_{0.33}\text{NbSe}_2$  are found to vary within  $3.1 \mu_B - 4.1 \mu_B$ , i.e. close to the spin-only value  $\mu_{\text{eff}} = 3.78 \mu_B$  for the  $\text{Cr}^{3+}$  ion. The effective moment of Cr ions in  $\text{Cr}_x\text{VSe}_2$  decreases with increasing Cr concentration from  $3.7 \mu_B$  at  $x = 0.1$  down to  $2.2 \mu_B$  at  $x = 0.5$ . The change of  $\mu_{\text{eff}}$  at the intercalation may be associated with several origins, in particular, with partial hybridization of Cr 3d states with Se 4p states and d states of T metal of the  $\text{TSe}_2$  parent compounds. The results obtained are indicative of the strong influence of the parent compound on the magnetic state of intercalated systems.

This work is supported by the Russian Foundation for Basic Research (Grant No 09-02-00441-a) and by the program of the Ministry of Education and Science (Project No 2.1.1.1682).

[1] M. Inoue, H.P. Hughes, and A.D. Yoffe, *Adv. Phys.*, **38**, (1989) 565.

[2] V.G. Pleschov, N.V. Baranov, A.N. Titov, K. Inoue, M.I. Bartashevich, T. Goto, *J. Alloys Comp.*, **320** (2001) 13–17.

## ELECTRON SPIN RESONANCE STUDY OF VANADIUM OXIDE AEROGELS

*Chernobrovkin A.L.<sup>1</sup>, Demishev S.V.<sup>1</sup>, Semeno A.V.<sup>1</sup>, Balakhonov S.V.<sup>2</sup>, Efremova M.A.<sup>2</sup>,  
Churagulov B.R.<sup>2</sup>*

<sup>1</sup> A.M.Prokhorov General Physics Institute of RAS, 38, Vavilov str., Moscow 119991, Russia

<sup>2</sup> Lomonosov Moscow State University, Lenin Hills, Moscow, 119992, Russia

Recently new vanadium oxide ( $\text{VO}_x$ ) nanoscale magnets have attracted attention due to a number of unusual magnetic properties [1]. The quantum critical behaviour of oscillating part of magnetic susceptibility has been found in  $\text{VO}_x$  nanotubes and nanorods. Moreover a strong departures from Curie-Weiss law were observed in these nanoscale magnets at temperatures  $T > 100$ , which has been explained by the presence of the antiferromagnetic (AF) dimers formed by the  $\text{V}^{4+}$  magnetic ions.

In the present work we report results of the first study of electron spin resonance (ESR) in  $\text{VO}_x$ -

aerogels, which represent the mesoporous crystalline structures from  $\text{V}_2\text{O}_5\text{-nH}_2\text{O}$  precursors by overcritical drying. Two aerogel samples marked as GS-15 and GS-17 were studied. ESR measurements at frequency 60 GHz have been carried out in the temperature range 4.2-200 K with an original cavity magneto-optical spectrometer [2]. The obtained results may be summarised as follows.

Experimental ESR spectra comprise the one broad line at all studied temperatures for the GS-15 and GS-17 samples. Calculated g-factor values were  $g = 1.96 \pm 0.01$  and were not depend on the temperature. The temperature dependence of the ESR integrated intensity for the free spins demonstrate antiferromagnetic behaviour at temperatures below  $T_C = 110$  K with  $T_{\text{AFM}} \sim 0.9$  K in GS-15 sample and  $T_{\text{AFM}} \sim 2.5$  K in GS-17 one. At the temperatures above  $T_C$  the transition to ferromagnetic behaviour with  $T_{\text{FM}} \sim 100$  K is observed in both samples.

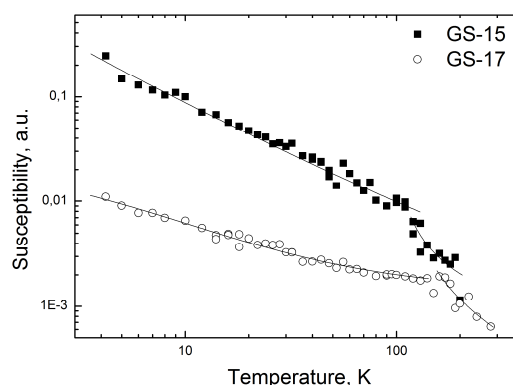
Similar FM-AFM transition at  $T \sim 110$  K was recently observed several different  $\text{VO}_x$  nanomagnets [3]. The comparison of the experimental data for various  $\text{VO}_x$  nanoparticles indicates that the most probable cause of the change in the type of magnetic interaction is a change in the concentration of  $\text{V}^{4+}$  magnetic ions.

Support from the Federal Program “Scientific and Educational Human Resources of Innovative Russia”, Programs of RAS “Strongly Correlated Electrons” and “Quantum Physics of Condensed Matter”, and the RFBR grant 09-03-00602-a are acknowledged.

[1] L. Krusin-Elbaum, D.M. Newns et al., *Nature*, **431** (2004) 672.

[2] S.V. Demishev, A.V. Semeno et al., *Phys. Sol. State*, **49** (2007) 1295

[3] S.V. Demishev, A.L. Chernobrovkin et al., *JETP Letters*, **91** (2010) 11.



## MECHANISM OF GROWTH AND MAGNETISM OF EPITAXIAL Co(111) FILMS ON ATOMIC FLAT AND VICINAL Si(111)7x7

*Ivanov Yu.P.<sup>1,2</sup>, Iljin A.I.<sup>3</sup>, Davydenko A.V.<sup>1</sup>, Zotov A.V.<sup>2</sup>*

<sup>1</sup> Far Eastern Federal University, Vladivostok, Suhkanova str. 8, Russia

<sup>2</sup> Institute of Automation and Control Processes FEBRAS, Vladivostok, Radio str. 5, Russia

<sup>3</sup> Interdisciplinary Nanoscience Center (iNANO), Aarhus, Ny Munkegade 118, Denmark

The artificial heteroepitaxial Co films adjacent to nonmagnetic metals have been intensively studied due to their importance for technical applications in magnetic or magneto-optical recording devices. Magnetic properties of ultrathin films of ferromagnetic metals on silicon substrates in conditions of epitaxial growth now are poorly investigated. It is due to the complexity of preparation of the epitaxial metal films on Si substrates consists of formation of metal silicides. The structure and morphology of ultrathin films are determined by phenomena occurring during growth. Therefore, it is of fundamental importance to characterize the growth process in order to achieve an efficient understanding of the relevant parameters and to be able to control the structure and morphology of the growing films to obtain the desired properties.

In this work, we attempt a characterization of the structure and magnetic properties taking place during the heteroepitaxy of Co on Cu(111) epitaxial buffer layer on various Si(111)7x7 substrate by means of STM, RHEED and MOKE measurements at different stages of the growth.

The experiments were performed in an Omicron UHV system. The base pressure at the deposition and STM chambers was  $3 \times 10^{-11}$  Torr. The standard preparation of Si substrates with  $<0.10$  and  $4.0$  miscut was made for reception of atomically clean surfaces Si (111)7x7. Cu and Co was evaporated from effusion cells with the rate of  $4.3$  and  $1.5$  ML/min. The Co coverage is given in monolayers, where 1 ML is defined by a one-to-one atomic ratio with the Cu(111).

In the present study we observed the regular RHEED intensity of specular beam oscillations at deposition Cu on Si(111)7x7 since the coverage of 3 ML up to 14.5 ML that testifies the layer-by-layer mode growth. The sharp RHEED pattern indicates that this is a epitaxial  $1 \times 1$  Cu(111)-R30° buffer layer.

Further we investigated the growth and magnetism of Co film deposited on the Cu buffer layers with the thickness of 11.5 ML on atomic flat and vicinal Si substrate. Our study have revealed the regular RHEED intensity of specular beam oscillations at deposition Co on epitaxial Cu buffer layer. The sharp RHEED pattern indicates that this is a epitaxial  $1 \times 1$  Co(111) film. As shown the STM studies the double-atomic and one atomic height islands is formed at the Co coverage up to 1 ML. Let's note that the Co islands decorate the Cu islands formed the double-atomic height rings with the diameter of some tens nanometers. Further the Co(111) epitaxial film grows layer-by-layer-like fashion and then passes in a multilayer growth.

MOKE measurements at RT probably demonstrate the superparamagnetic behavior up to the Co coverage of 2 ML. Since 2ML magnetic loops have revealed the ferromagnetic behavior. The magnetic behaviour of the Co films deposited on atomic flat Si(111) is different from that Co films on vicinal Si(111) at the range of the Co coverage from 2 up to 5 ML (layer-by-layer-like growth). Since 5 ML the coercitive force and the magnetic anisotropy practically do not change (multilayer growth).

The study is supported by the program the Russian Foundation for Basic Research (the grant 09-02-00022-a), the grant №2.1.1/3005, the grant № 02.740.11.0549, the grant № 02.740.11.0111.

## FORMATION AND MOTION OF DOMAIN WALLS IN COUPLED Co LAYERS WITH PERPENDICULAR ANISOTROPY

*Iunin Y.L.<sup>1</sup>, Skryabina O.V.<sup>1,2</sup>, Nikitenko V.I.<sup>1,3,4</sup>, Shull R.D.<sup>3</sup>, Chien C.L.<sup>4</sup>*

<sup>1</sup> Institute of Solid State Physics, Russian Academy of Sciences, Chernogolovka 142432, Russia

<sup>2</sup> Department of Fundamental Physical-Chemical Engineering, Moscow State University, Moscow 119991, Russia

<sup>3</sup> National Institute of Standards and Technology, Gaithersburg, Maryland 20899, USA

<sup>4</sup> The Johns Hopkins University, Baltimore, Maryland 21218, USA

Quasi-two-dimensional Co/Pt multilayers with perpendicular anisotropy have received much attention in recent years due to their relevance in fundamental science and their potential use in high-density data recording applications. These materials exhibit a number of features of magnetization reversal processes, which are not observed in bulk magnetic materials [1-3]. The reversal properties of Co/Pt multilayers are influenced by the interlayer coupling and the response of the individual Co layers to the applied magnetic field.

We studied the nucleation and motion of domain walls in ultrathin Co/Pt/Co structures with variable Pt spacer thickness in the perpendicular magnetic field. Ultrathin Co(0.6 nm)/Pt( $x$ )/Co(0.6 nm) ( $x = 0-10$  nm) structure with a wedge-shaped Pt interlayer was deposited by DC magnetron sputtering onto a Pt(10 nm) buffer layer on Si substrates and covered with a Pt(3 nm) cap. The structure has been cut into 10 samples with average Pt interlayer thicknesses  $x = 0.5, 1.5, 2.5 \dots 9.5$  nm. The domain structure evolution was investigated by magneto-optical Kerr effect microscopy which has the advantage of providing information on individual Co layers [4].

We have plotted the domain nucleation field as a function of the Pt spacer thickness. The nonmonotonic dependence of the domain nucleation field in the perpendicular field on the spacer thickness has been revealed in the thickness range 1.5–10 nm, where the perpendicular magnetization anisotropy is observed. Along with quantitative variation of coercivity, a qualitative change in the reversal mode has been revealed. Structures with the spacer thickness in the range 1.5–5.5 nm show nucleation at the same field and bounded motion of domain walls in both Co layers. An abrupt transition to the layer-by-layer reversal with independent domain wall motion in the layers is observed at thicknesses above 5.5 nm. It turned out that the order of reversal of layers in this region depends on the sweep rate of magnetic field.

The domain wall velocity as a function of the Pt spacer thickness has been measured. In the region of bounded motion of domain walls a rapid increase in the velocity is observed with the growth of the spacer thickness. In the region of the layer-by-layer reversal domain wall velocities in the layers differ by an order of magnitude and practically do not depend on the spacer thickness. When cycling the applied magnetic field, it has been revealed that the velocities of the forward and backward domain wall motion are equal in the region of bounded domain wall motion, but differ in the region of the independent domain wall motion. The nature of effects revealed is briefly discussed.

[1] Y. L. Iunin, Y. P. Kabanov, V. I. Nikitenko, et al., *Phys. Rev. Lett.* **98**, 117204 (2007).

[2] Y. L. Iunin, Y. P. Kabanov, V. I. Nikitenko, et al., *J. Magn. Magn. Mater.* **320**, 2044 (2008).

[3] P. J. Metaxas, R. L. Stamps, J. P. Jamet, J. Ferré, et al, *Phys. Rev. Lett.* **104**, 237206 (2010).

[4] M. Robinson, Y. Au, J. W. Knepper, F. Y. Yang, R. Sooryakumar, *Phys. Rev. B* **73**, 224422 (2006).

22PO-I-58

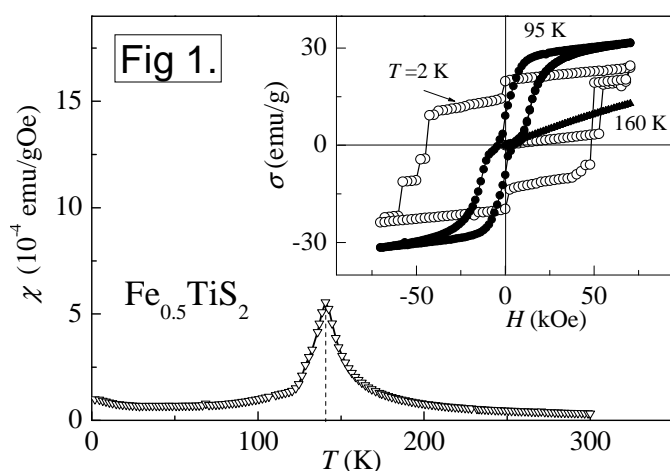
## HIGH-COERCIVE FERROMAGNETIC STATE INDUCED BY A MAGNETIC FIELD IN THE ANTIFERROMAGNETIC LAYERED COMPOUND $\text{Fe}_{0.5}\text{TiS}_2$

Baranov N.V.<sup>1,2</sup>, Sherokalova E.M.<sup>2</sup>, Volegov A.S.<sup>2</sup>, Selezneva N.V.<sup>2</sup>

<sup>1</sup> Institute of Metal Physics, Russian Academy of Science, 620990, Ekaterinburg, Russia;

<sup>2</sup> Ural State University, 620083, Ekaterinburg, Russia

Titanium dichalcogenides  $\text{TiX}_2$  ( $X = \text{S}, \text{Se}, \text{Te}$ ) being intercalated by 3d metal (M) atoms having a magnetic moment demonstrate a rich variety of magnetic behaviors ranging from spin-glass or cluster-glass states up to ferromagnetic (F) or antiferromagnetic (AF) long-range orders. The magnetic order in  $\text{M}_x\text{TiX}_2$  compounds depends both on the chemical constituents M and X, and on the concentration  $x$  of the intercalant M. Because of quasi two-dimensional crystal structure the  $\text{M}_x\text{TiX}_2$  compounds intercalated by 3d-transition metals can be considered as an analog of artificial multi-layer structures with magnetic M layers which are separated by non-magnetic tri-layers X-Ti-X.



The intercalated compounds  $\text{Fe}_{0.5}\text{TiSe}_2$  atoms is observed to exhibit a tilted antiferromagnetic structure below  $T_N = 135$  K [1], while there are contradictory data in the literature in respect to the magnetic order in  $\text{Fe}_{0.5}\text{TiS}_2$ . The magnetic state of  $\text{Fe}_{0.5}\text{TiS}_2$  was proposed to be antiferromagnetic or ferromagnetic with complicated structure as well as antiferromagnetic with inclusion of ferromagnetic clusters (see Ref. [2] and references therein).

The  $\text{Fe}_{0.5}\text{TiS}_2$  compound synthesized in the present work has a monoclinic crystal structure (space group  $I12/m1$ ) which is the

superstructure of the initial crystal structure of  $\text{TiS}_2$  ( $P\bar{3}m1$ ) owing to the ordering of Fe ions and vacancies between S-Ti-S tri-layers. The magnetic measurements were performed by using a Quantum Design SQUID magnetometer in magnetic fields up to 70 kOe. The maximum of the magnetic susceptibility observed at  $T = 140$  K (Fig.1) for the zero-field cooled sample corresponds to the Neel temperature of this compound. Application of the magnetic field below  $T_N$  induces the AF-F metamagnetic transition which is accompanied by substantial hysteresis which increases upon cooling (see inset in Fig.1). The coercive field reaches a value about of 50 kOe at low temperatures. Ising-like behavior of  $\text{Fe}_{0.5}\text{TiS}_2$  results apparently from the presence of a very high magnetocrystalline anisotropy associated with the influence of the crystal field and spin-orbital interactions [3]. The magnetic behavior of  $\text{Fe}_{0.5}\text{TiS}_2$  compound is suggested to depend substantially on the distribution of Fe ions in the layer.

This work was supported by the RFBR (Grant No 09-02-00441-a) and by the program of the presidium of RAS (Project 09-P-2-1008).

[1] N.V. Baranov, N.V. Selezneva, V.G. Pleshchev, N.V. Mushnikov and V.I. Maksimov, *Solid State Phenomena*, **168-169** (2011) 157.

[2] Y. Kuroiwa, H. Honda, Y. Noda, *Mol. Cryst. Liq. Cryst.* **341**(2000) 15.

[3] S. S. P. Parkin, R. H. Friend, *Phil. Mag. B*, **41** (1980) 65

## CRYSTAL STRUCTURE AND MAGNETISM OF $\text{Co}_{2-x}\text{Ni}_x\text{B}_2\text{O}_5$ PYROBORATE

Platunov M.S.<sup>1</sup>, Ivanova N.B.<sup>2,3</sup>, Kazak N.V.<sup>1</sup>, Bezmaternykh L.N.<sup>1</sup>, Vasil'ev A.D.<sup>1</sup>, Eremin E.V.<sup>1</sup>, Ovchinnikov S.G.<sup>1,2</sup>

<sup>1</sup> Kirensky Institute of Physics, SB of RAS, 660036, Akademgorodok, Krasnoyarsk, Russia

<sup>2</sup> Siberian Federal University, 660074, Kirensky str. 26, Krasnoyarsk, Russia

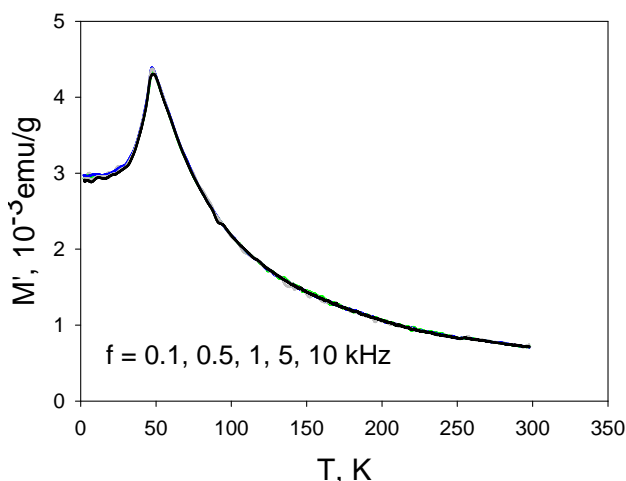
<sup>3</sup> Krasnoyarsk State Agrarian University, Mira str. 90, Krasnoyarsk, Russia

The pyroborates with general formula  $\text{MM}'\text{B}_2\text{O}_5$ , where M and M' are divalent ions Co, Mn, Fe, Mg, Ca, Sr, are interesting primarily due to their structural, magnetic and optical properties [1]. The crystal structure  $\text{MM}'\text{B}_2\text{O}_5$  can be of triclinic or monoclinic symmetry with space group  $P\bar{1}(2)$  or  $P2_1/c$ , respectively. The metal ions are placed inside distorted oxygen octahedra, which sharing edges form substructures – *ribbons*. The ribbons are extended along the crystal *b* - axis and contain two distinct crystallographic sites 1 and 2. In the heterometallic compounds ( $M \neq M'$ ) the metal ions occupy the both sites so that these materials are *intrinsically* disordered. The pyroborate group  $(\text{B}_2\text{O}_5)^{4-}$  formed by two trigonal  $(\text{BO}_3)^{3-}$  groups is the most strongly bonded. The low-dimensional substructures in the form of *ribbons* and *zigzag walls* are the common feature with the other well studied oxyborates, such as warwikites [2] and ludwigites [3].

In the present work, we synthesized the high quality single crystals of Ni – substituted  $\text{Co}_2\text{B}_2\text{O}_5$  and investigated the crystal structure and magnetic properties.

The single crystals of  $\text{Co}_{2-x}\text{Ni}_x\text{B}_2\text{O}_5$  pyroborate were prepared using a *flux method*. The crystals were dark pink in color, circa 3 mm long, they had an oblique prism shape and good optical quality. The crystal structure study has shown the monoclinic modification whereas the parent  $\text{Co}_2\text{B}_2\text{O}_5$  has the triclinic crystal structure. The obtained monoclinic lattice constants were  $a=9.23 \text{ \AA}$ ,  $b=3.16 \text{ \AA}$ ,  $c=12.36 \text{ \AA}$ ,  $\beta=104.18^\circ$ . The metal Co/Ni atoms are surrounding by deformed oxygen octahedra. We have found a strong distortion of both types of octahedra 1 and 2. The octahedron 1 is distorted much stronger than in position 2. This is indicated by the electric field gradient data and the calculation of distortion indexes.

The magnetization and magnetic susceptibility study have shown the antiferromagnetic ordering below  $T_N = 47 \text{ K}$ . The effective magnetic moment ( $\mu_{\text{eff}} = 3.49 \mu_B$ ) indicates that the magnetic ions Co(Ni) are divalent and in a high-spin state. The substitute the part of  $\text{Co}^{2+}$  ( $S = 3/2$ ) ions by  $\text{Ni}^{2+}$  ( $S = 1$ ) leads to decrease in average moment per formula unit.



This study was supported by the Russian Foundation for Basic Research (project no. 09-02-00171-a), the Federal Agency for Science and Innovation (Rosnauka) (project no. MK-5632.2010.2), the Physical Division of the Russian Academy of Science, the program “Strongly Correlated Electrons”, project 2.3.1.

[1] J.C. Fernandes et al. *Phys. Rev. B* 67, 104413 (2003).

[2] M.A. Continentino et al. *Phys. Rev. B* 64, 014406 (2001).

[3] N.V. Kazak et al. *J.M.M.M.* 323, 521 (2011).

## INFLUENCE OF METAL-DIELECTRIC NANOCOMPOSITES MORPHOLOGY ON ANOMALOUS MAGNETOTRANSPORT PROPERTIES

*Stognei O.V., Sitnikov A.V., Kashirin M.A., Belousov V.A., Bulvina Yu.S.*  
Dept. Solid State Physics, Voronezh State Technical University, Russia

A comparative investigation of magnetic, magnetoresistive and thermomagnetic properties of  $\text{Co}_x(\text{CaF})_{100-x}$  and  $\text{Co}_x(\text{Al}_2\text{O}_n)_{100-x}$  nanocomposites have been done. The samples of the composites were obtained by ion-beam sputtering of composite targets.

All studied composites exhibit tunnel magnetoresistive effect (MR). The classical negative magnetoresistivity is observed in  $\text{Co}_x(\text{CaF})_{100-x}$  nanocomposites (see fig.1 a) in a wide concentration range ( $41 < x$ , at.% Co  $< 67$ ) as in most well-known nanocomposites. In the  $\text{Co}_x(\text{Al}_2\text{O}_n)_{100-x}$  composites the anomalous **positive** magnetoresistivity was observed in addition to the usual negative MR (fig. 1 b). The positive MR value reaches 1.5 % at relatively low field (500 Oe). The

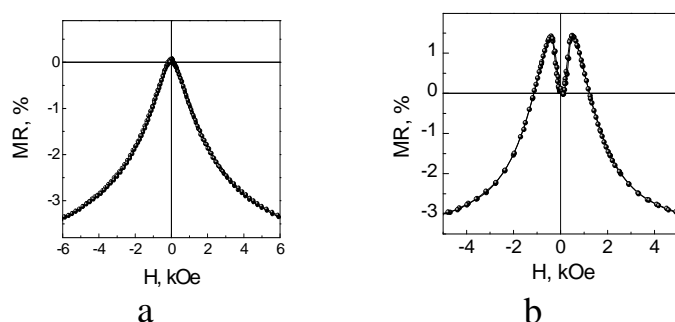


Fig. 1. Examples of magnetoresistive effect in nanocomposites with different dielectric matrix:

a -  $\text{Co}_{45}(\text{CaF})_{55}$ , b -  $\text{Co}_{58}(\text{Al}_2\text{O}_n)_{42}$

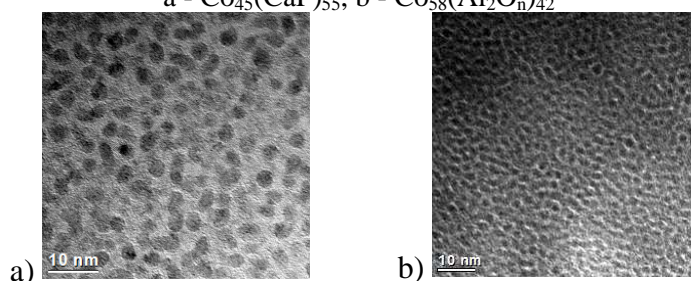


Fig. 2. HRTEM images of nanocomposites:

a -  $\text{Co}_{45}(\text{CaF})_{55}$ , b -  $\text{Co}_{58}(\text{Al}_2\text{O}_n)_{42}$

positive MR may be due to the structural peculiarities of the nanocomposite - the simultaneous presence of individual nanoparticles and clusters with large form anisotropy and dipole-dipole interaction between these structural elements.

According to HRTEM investigations a labyrinth-like structure from chains clusters is formed from 2-3 nm nanograins in  $\text{Co}_x(\text{Al}_2\text{O}_n)_{100-x}$  (fig. 2 a). In the  $\text{Co}_x(\text{CaF})_{100-x}$  composites the situation is different: the granules are larger (up to 5 nm) and they are almost completely isolated from each other in the CaF matrix. The reasons of such morphology difference are discussed.

HRTEM investigations were performed in research nanotcenter of Belgorod State University. Support by RFBR (Grant № 11-02-90437- Ukr\_f\_a) is acknowledged.

[1] O.V. Stognei et. al., *Solid State Physics*, **49** (2007) 158.

[2] A. A. Timofeev et. al., *Low Temperature Physics*, **33** (2007) 1282.

22PO-I-61

## DYNAMICS OF MAGNETIC STRUCTURE IN FRUSTRATED 2D ANTIFERROMAGNET $\text{PbBaFe}_2\text{O}_5$ AS SEEN BY ZERO-FIELD NMR

*Gervits N.E.<sup>1</sup>, Gippius A.A.<sup>1</sup>, Tkachev A.V.<sup>1</sup>, Rozova M.G.<sup>2</sup>, Tyablikov O.A.<sup>2</sup>, Pokholok K.V.<sup>2</sup>, Filimonov D.S.<sup>2</sup>*

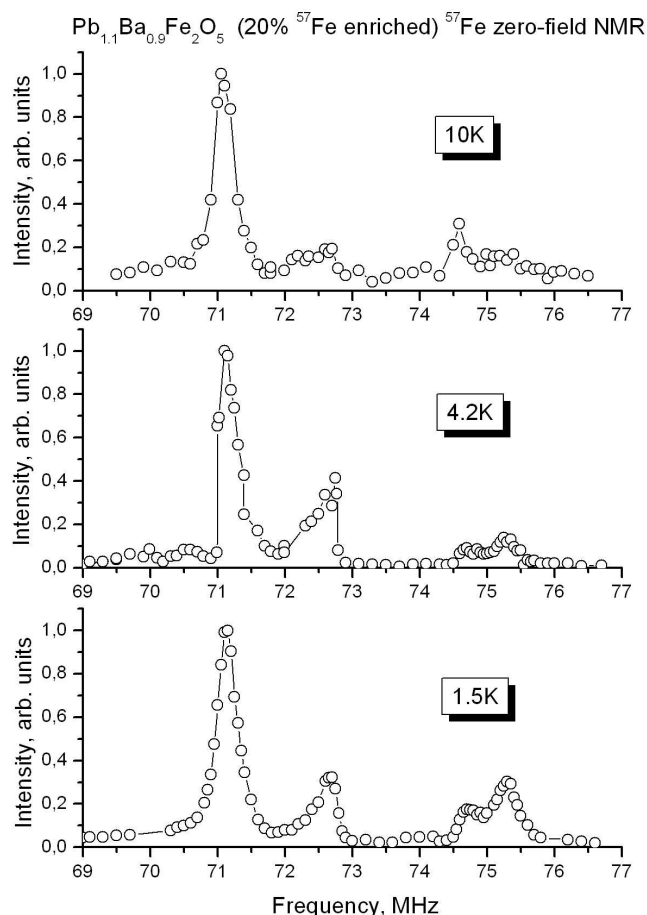
<sup>1</sup> Physics Department, M.V. Lomonosov Moscow State University, 119991, Russia

<sup>2</sup> Chemistry Department, M.V. Lomonosov Moscow State University, 119991, Russia

Introduction of the cations with a lone  $6s^2$  electron pair ( $\text{Bi}^{3+}$ ,  $\text{Pb}^{2+}$ , etc.) in the A position of the perovskite  $\text{ABO}_3$  structure leads to the structural instability toward an off-center displacement of the A cations caused by spatial character of the lone pair and the covalent type of the bonding between the A cations and oxygen atoms [1]. Such displacements lead to ferroelectricity in perovskites  $\text{BiMnO}_3$  and  $\text{BiFeO}_3$ , where the magnetic ordering also occurs due to the 3d transition metal cations at the B positions.

$\text{PbBaFe}_2\text{O}_5$  is a perovskite-like compound with a complex crystal structure: perovskite blocks are connected by crystallographic shear planes, which results in two unequivalent positions of Fe: the first six-coordinated (in the center of the octahedron  $\text{FeO}_6$ ), the second is five-coordinated (in the trigonal bipyramid  $\text{FeO}_5$ ). Moessbauer spectroscopy and neutronography show quite unusual magnetic behavior, in particular, the temperatures of the magnetic transition according to these methods are 520 and 625 K, respectively [2].

Zero-field NMR spectrum of the sample consists of four lines with different integral intensities in contradiction to the data obtained by Moessbauer spectroscopy. The ratio of integral intensities of the lines changes in wide temperature range and does not correlate with occupation numbers of two Fe sites. This fact along with the controversial data of the transition temperature evidences for dynamic character of magnetic structure in  $\text{PbBaFe}_2\text{O}_5$ . The reduction of the integral intensity of lines in the zero-field NMR spectra can be explained by presence of fast fluctuations of Fe magnetic moments.



[1] D. I. Khomskii, *J. Magn. Magn. Mater.* 306, 1 (2006).

[2] I. V. Nikolaev, *Phys. Rev. B* 78, 024426 (2008).



22PO-I-62

## “ $\gamma$ -Fe PROBLEM” AND EPITAXIAL GROWTH OF Fe ON Cu(001)

*Myagkov V.G.<sup>1,3</sup>, Bayukov O.A.<sup>1</sup>, Bykova L.E.<sup>1</sup>, Bondarenko G.N.<sup>2,3</sup>*

<sup>1</sup> Kirensky Institute of Physics, Russian Academy of Sciences, Siberian Branch, Krasnoyarsk, 660036 Russia

<sup>2</sup> Institute of Chemistry and Chemical Technology, Russian Academy of Sciences, Siberian Branch, Krasnoyarsk, 660049 Russia

<sup>3</sup> Reshetnev Siberian State Aerospace University, Krasnoyarsk, 660014 Russia

In recent years, great efforts have been focused on studying the correlation between the magnetic and structural properties of iron films grown epitaxially on Cu(001). This correlation is of fundamental importance for physics of magnetic phenomena [1, 2]. Theoretical calculations predict the dependence of the  $\gamma$ -Fe total magnetic moment on atomic volume (the so-called magnetovolume effect). Similarity of the lattice parameters of Cu (0.361 nm) and  $\gamma$ -Fe (0.359 nm) favors stabilization of the high-temperature  $\gamma$ -Fe phase as a result of its pseudomorphic growth on Cu(001). Data of most experimental studies of Fe/Cu(001) films obtained at low ( $\sim 100$  K) and room temperatures reveal the formation of various structural and magnetic types of the  $\gamma$ -Fe phase at thicknesses  $d_{\text{Fe}} < 11$  ML (monolayers). However, the results obtained are ambiguous and the presence of the magnetovolume effect in  $\gamma$ -Fe has not been experimentally proved yet. Regardless of a deposition method used and a vacuum level, at thicknesses  $d_{\text{Fe}} > 11$  ML the  $\gamma$ -Fe growth becomes unstable and the  $\alpha$ -Fe(110) phase growth epitaxially on Cu(001) in the Pitsch orientation.

In the experiments, epitaxial Cu(001) with a thickness of 100-150 nm was deposited onto identical Cu(001) surfaces. A part of Cu(001)/MgO(001) was oxidized in air, which resulted in the formation of the epitaxial  $\text{Cu}_2\text{O}$  oxide layer on the Cu(001) surface. The obtained  $\text{Cu}_2\text{O}(001)/\text{Cu}(001)$  and Cu(100) film samples were placed into a vacuum chamber again and a Fe film was deposited on the top at a temperature of 520 K. Surprisingly, the  $\alpha$ -Fe(110) layer with the Pitsch orientation grew not only on Cu(001), but also on  $\text{Cu}_2\text{O}(001)/\text{Cu}(001)$ . Measurements of the biaxial anisotropy constant yield the same value  $K_2 = (1.4 \pm 0.1) \cdot 10^5 \text{ erg/cm}^3$  ( $K_2 / M_S = 82 \text{ Oe}$ ) for both samples. Since biaxial anisotropy constant  $K_2$  is sensitive to the structure, equality of the experimental  $K_2$  values, along with similarity of the diffraction patterns for  $\alpha$ -Fe(110)/Cu(100) and  $\alpha$ -Fe(110)/ $\text{Cu}_2\text{O}(001)/\text{Cu}(001)$  films, make us draw a conclusion about identity of the epitaxial formation of the  $\alpha$ -Fe layer in both cases.

Basing on the mentioned facts, it is reasonable to suggest that the ultrathin intermediate  $\text{Cu}_2\text{O}$ -like layers are formed at the  $\alpha$ -Fe(110)/Cu(001) interface in ultrahigh-vacuum ( $< 10^{-8}$  Pa) systems. The only feature of the epitaxial growth of  $\alpha$ -Fe(110)/Cu(001) is that the thickness of the transition layer in a vacuum of  $10^{-4}$  Pa exceeds that in the ultrahigh vacuum by factors of 10-15. If our arguments are true and, indeed, the intermediate layer is formed during the epitaxial growth of  $\alpha$ -Fe(110)/Cu(001) in the ultrahigh vacuum, the current interpretation of the formation of metastable phases during the epitaxial growth on single-crystal substrates that is based on the pseudomorphic growth and stabilization of  $\gamma$ -Fe at low temperatures might be changed.

This work was supported by the Ministry of Education and Science of the Russian Federation, project no. 2.1.1/9193, the program “Development of the Research Potential of Higher Education in 2009–2011.”

[1] E. Sjöstedt and L. Nordström, *Phys. Rev. B* **54** (2002) 014447.

[2] L.T. Kong and B.X. Liu, *Appl. Phys. Lett.* **84** (2004) 3627.

22PO-I-63

## MÖSSBAUER STUDY OF CHANGES IN THE MAGNETIC STRUCTURE OF THE COMPOUNDS $\text{La}(\text{Fe}_{0.88}\text{Si}_x\text{Al}_{0.12-x})_{13}$

Serikov V.V., Kleinerman N.M., Vershinin A.V.

Institute of Metal Physics, Ural Branch of RAS, S. Kovalevskaya 18, Ekaterinburg, Russia

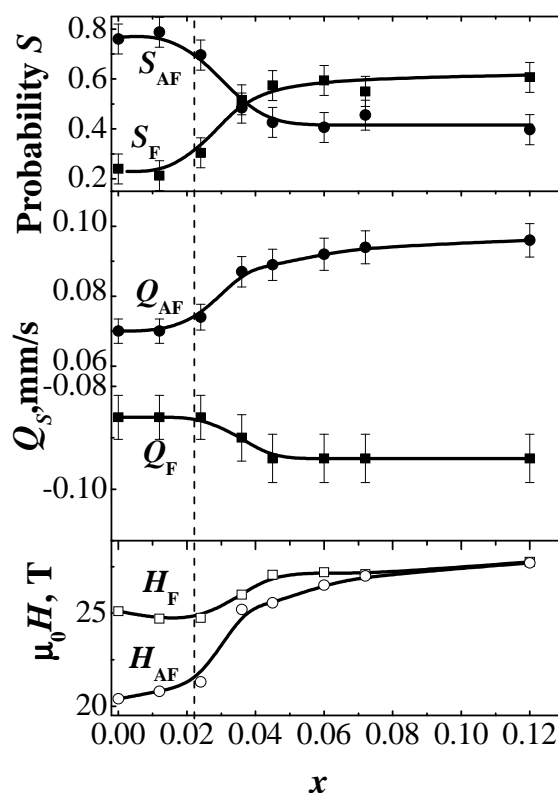
Previously [1], in the compounds  $\text{La}(\text{Fe}_{0.88}\text{Si}_x\text{Al}_{0.12-x})_{13}$  there has been discovered a concentration transition from the antiferromagnetic (AF) to ferromagnetic (F) state; however its nature is not clear so far. As a hypothesis, various options have been put forward, such as formation of F clusters or change in the electronic structure upon substitution of Al by Si.

To ascertain the nature of transition, the Mössbauer spectra were measured on these compounds at 100 K. The measurements were carried out at a spectrometer MS1101 in the constant acceleration mode; the quality of spectra was about 60%, the accuracy of maintenance of the temperature was 0.2 K. For the spectra processing the MSTOOL [2] program package was used.

From the analysis of spectra it follows that the AF state has a positive quadrupole shift while the F state has a negative one. The calculation of two core distributions of the probability density of the quadrupole splitting allowed us to establish the presence of two regions with the quadrupole splitting of different signs which we defined as clusters with different types of magnetic ordering. Figure presents the dependences of the integral probability ( $S$ ), average quadrupole splitting ( $Q$ ) and average hyperfine fields ( $H$ ). The dashed line marks the concentration corresponding to the AF-F transition.

As can be seen from Figure, both the AF and F clusters are present in all the compounds.

The transition from AF to F is related to the increase of the volume fraction of F clusters.



Support by RFBR grant № 10-02-96019 is acknowledged.

[1] S.M. Podgornykh, Ye.V. Shcherbakova, G.M. Makarova, A.A. Yermakov, *EASTMAG – 2007 “Magnetism on a nanoscale” Book of abstracts*, (2007) 166.

[2] V.S. Rusakov, *Mössbauer spectroscopy of locally inhomogeneous systems*, Alma-Ata, (2000).

## FUNDAMENTAL STUDY OF COLLIMATED SPUTTERING FOR MAGNETIC RECORDING MEDIA WITH INCLINED ANISOTROPY

Honda A., Honda N.

Tohoku Institute of Technology, Sendai, Japan

Bit-patterned magnetic recording medium (BPM) is one of promising techniques to extend recording densities of perpendicular magnetic recording beyond 1 Tbit/in<sup>2</sup>. However, when the packing density of the magnetic dots is increased, magnetostatic interaction between the dots drastically increases the switching field distribution (SFD) of the media, which limits the recording density. We have proposed a method to reduce the SFD by using inclined magnetic anisotropy for the dots [1]. Therefore, fabrication of such inclined anisotropy film is crucial for the media. Only a few studies were reported on the subject. Fundamental study of deposition of films using collimated sputtering will be presented.

Collimated sputtering was investigated to fabricate films with preferred orientation to inclined directions from the film normal. Collimators exhibited to enhance preferred orientation for stacked films of Pt/Ru/Co-Cr on a Ta seed layer as shown in Fig. 1. The orientation dispersion angle was evaluated as FWHM of the X-ray rocking curve,  $\Delta\theta_{50}$ . Upper layers showed better orientation. The inclination of the orientation direction,  $d\theta$ , was also enhanced in oblique incidence sputtering when an appropriate collimator was used (Fig. 2). It was found that the amount of inclination was much affected by the initial layer material. An inclination angle of around 8 degrees was obtained for c axis of Co-Cr alloy film using a Pt/Ru stacked under layer.

Support by the Green IT Project of NEDO is acknowledged.

[1] N. Honda, K. Yamakawa, and K. Ouchi, *IEEE Trans. Magn.*, **44**(2008), 3438-3441.

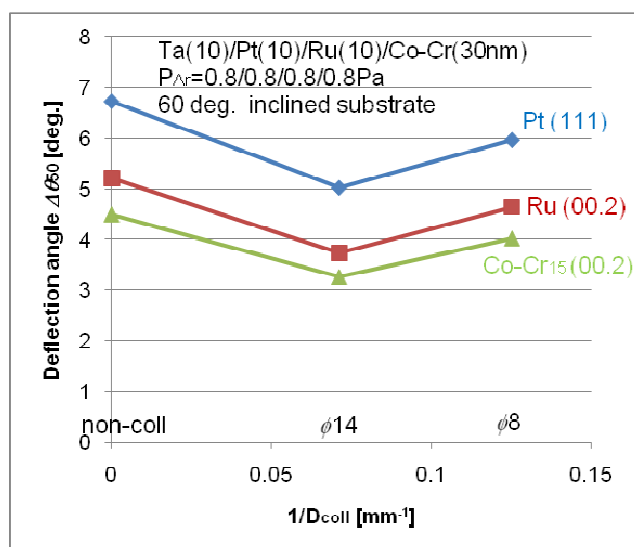


Fig. 1. Change of orientation dispersion of Pt fcc(111), Ru hcp(00.2), and Co-Cr hcp(00.2) planes with collimator.

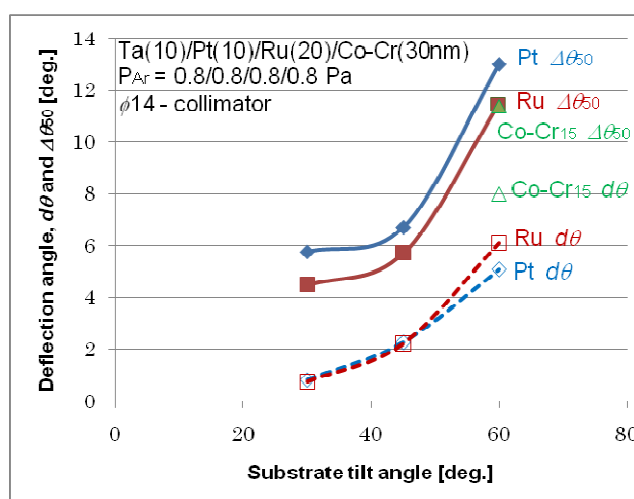


Fig. 2. Collimator angle dependence of the deflection angle,  $d\theta$ , and the orientation dispersion angle,  $\Delta\theta$ , of Pt fcc(111), Ru hcp(00.2), and Co-Cr hcp(00.2) planes for Ta/Pt/Ru films.

## MAGNETIC RELAXATION OF WEAKLY INTERACTING MAGNETIC NANOPARTICLES

*Déjardin P.-M.*

Université de Perpignan Via Domitia, 52 Avenue Paul Alduy, LAMPS, 66860 Perpignan Cedex, France

The effect of dipole-dipole interactions on the thermal fluctuations of the magnetization of an assembly of single-domain ferromagnetic particles is treated by adapting Berne's approach to the forced rotational diffusion [1] yielding a nonlinear Fokker-Planck equation governing the dynamics of the distribution function of the magnetization orientations  $W(\mathbf{u}, t)$ , namely

$$2\tau_N \partial_t W = \beta \alpha^{-1} \mathbf{u} \cdot (\partial_{\mathbf{u}} U \times \partial_{\mathbf{u}} W) + \partial_{\mathbf{u}} (\beta W \partial_{\mathbf{u}} U + \partial_{\mathbf{u}} W) \quad (1)$$

where  $\partial_{\mathbf{u}}$  is the gradient operator on the unit sphere,  $\beta = (kT)^{-1}$ ,  $k$  is Boltzmann's constant,  $T$  the absolute temperature,  $\alpha$  is a dimensionless damping constant,  $\tau_N = \beta(1+\alpha^2)M_s v / (2\alpha\gamma)$ ,  $\gamma$  is the gyromagnetic ratio,  $M_s$  is the saturation magnetization of a particle,  $v$  is the particle volume,  $U(\mathbf{u}, t) = U_s(\mathbf{u}) + V_{\text{ddi}}(\mathbf{u}, t; W)$ ,  $U_s(\mathbf{u}) = -Kv u_z^2 - M_s v H u_z$  is an effective single particle potential made of anisotropy and Zeeman energies,  $K$  is the anisotropy constant,  $H$  is the intensity of the applied field, and  $V_{\text{ddi}}(\mathbf{u}, t; W)$  is the dipole-dipole interaction potential that is a linear functional of  $W$ . Equation (1) reduces to Brown's Fokker-Planck equation for noninteracting particles [2], and allows one to treat both equilibrium and nonequilibrium properties of the assembly. We have shown that well above the mean blocking temperature, the longitudinal normalized equilibrium magnetization  $\langle u_z \rangle_0$  can be fit to

$$\langle u_z \rangle_0 = L\{M_s v H / k(T + T^*)\}, \quad (2)$$

where  $L(z) = \coth z - z^{-1}$  denotes the Langevin function and  $T^*$  is an interaction temperature. The FPE (1) can also be solved numerically to calculate the thermally activated relaxation time of the assembly. It is then shown that the relaxation time is noticeably increased while increasing the concentration, thus leading to an increase in the blocking temperature of the system, in qualitative agreement with the Dormann-Bessais-Fiorani (DBF) model [3]. Thus a model for the thermal fluctuations of interacting ferromagnetic nanoparticle systems is developed allowing one to treat the effect of dipolar interactions on static and dynamical properties of such systems. For a random space distribution of particles, the thermal instability of the magnetization may significantly be reduced with respect to that of Brown's model, but in qualitative agreement with the DBF model predicting the rise of the temperature of the peak of the zero-field cooled magnetization in samples of maghemite nanoparticles embedded in a polymer [3] with increasing the concentration of particles. At last, our treatment of dipole-dipole interactions can be extended to cases, where the orientational correlations can no longer be neglected. Thus, in this work, we have presented an adaptation of Berne's model of the forced rotational diffusion to magnetic relaxation of an assembly of single-domain ferromagnetic particles subjected to both thermal agitation and dipole-dipole interactions. This model can reproduce some features of interacting nanoparticle systems such as the rise of the temperature of the peak of the zero-field cooled magnetization as a function of the concentration found in a number of experiments [3].

[1] B. J. Berne, J. Chem. Phys., **62**, 1154 (1975).

[2] W. F. Brown Jr. Phys. Rev., **130**, 1677 (1963).

[3] J. L. Dormann, L. Bessais and D. Fiorani, J. Phys. C, **21**, 2015 (1988) ; J. L. Dormann, D. Fiorani and E. Tronc, J. Magn. Mag. Mat., **202**, 251 (1999) ; Adv. Chem. Phys., **98**, 283 (1997).

## TRANSPORT AND MAGNETOTRANSPORT PROPERTIES OF NANOCOMPOSITES $(\text{Co}_{41}\text{Fe}_{39}\text{B}_{20})_x(\text{CaF}_2)_{100-x}$ and $\text{Co}_x(\text{CaF}_2)_{100-x}$

*Kalinin Yu.E., Morozova N.A., Sitnikov A.V.*

Voronezh Technical State University, Voronezh, 394026, Russia

The results of investigation of electroresistivity as well as magnetoresistivity (MR) of granular nanocomposites  $(\text{Co}_{41}\text{Fe}_{39}\text{B}_{20})_x(\text{CaF}_2)_{100-x}$  and  $\text{Co}_x(\text{CaF}_2)_{100-x}$  are presented. The granular nanoclusters of pure metal or metal alloy (Co,  $\text{Co}_{41}\text{Fe}_{39}\text{B}_{20}$ ) randomly distributed in dielectric amorphous matrix  $\text{CaF}_2$  were obtained by ion-beam sputtering of composite targets and deposition of the material to ceramic substrates. The granular media from metal amorphous or crystal granules placed in dielectric matrix with wide and continuous spectrum of concentration were formed during simultaneous deposition of metal and dielectric phases owing to use of complicated non-symmetrical targets.

The areas of the percolation threshold for the studied composites have been determined. The temperature dependence of electrical resistance of the nanogranular  $(\text{Co}_{41}\text{Fe}_{39}\text{B}_{20})_x(\text{CaF}_2)_{100-x}$  and  $\text{Co}_x(\text{CaF}_2)_{100-x}$  composites have been investigated. It was shown that for the studied composites with low content of metallic phase at low temperatures (80 - 180 K) the dominant mechanism of charge transport is hopping conductivity via localized states of the dielectric matrix at the Fermi level with variable-range hopping. The density of localized states at the Fermi level for  $\text{Co}_{41}\text{Fe}_{39}\text{B}_{20}$  and Co metallic systems have been estimated. The electron density of states at the Fermi level for metallic phases of investigated composites correlate well with the values obtained in other systems with oxygen-containing matrices.

It was shown that the temperature range from 180 to 300 K the inelastic resonant tunneling in a finite number of conducting channels with a power dependence of the conductivity were performed. The estimation of the density of localized states at the Fermi level and the average number of localized states between the neighboring grains on the concentration of the metal component have been made. It was established that with an increase in the proportion of the metallic phase, the average number of localized states between the neighboring grains decreases. This behavior coincides with the analog dependencies for other oxygen-containing matrix composites studied previously.

It has been established that concentration dependence of MR at room temperature is similar for all studied systems: non-monotonic MR dependence on metal concentration with maximum MR values near the percolation threshold and sharp decrease of MR behind the threshold with metal rise. The concentration position of the MR maximum is determined by geometrical (morphological) peculiarities of the composites: near the percolation threshold granule magnetic moments are not still correlated but the thickness of dielectric barriers between the granules is minimum therefore the probability of polarized electron tunneling is maximum.

Support by the Russian Foundation for Basic Research (Grant N 10-02-90030) is acknowledged.

22PO-I-67

## DEPENDENCE OF MAGNETIC NANOPARTICLES PROPERTIES ON THE MORPHOLOGY AND ENVIRONMENT

*Vompe A.<sup>1</sup>, Perov N.<sup>1</sup>, Rodionova V.<sup>1</sup>, Zaichenko S.<sup>2</sup>, Chernavsky P.<sup>3</sup>, Zakharenko M.<sup>4</sup>,  
Kuznetsov A.<sup>1</sup>, Samsonova V.<sup>1</sup>, Safronova E.<sup>1</sup>*

<sup>1</sup> Faculty of Physics, MSU, Leninskie Gory, Moscow 119991 Russia

<sup>2</sup> Institute of Physical Metallurgy and Metal Physics GNC I.P. Bardin Central Institute for Ferrous Metallurgy, Russia

<sup>3</sup> Department of Chemistry, MSU, Leninskie Gory, Moscow 119991 Russia

<sup>4</sup> Taras Shevchenko National University of Kyiv, 60, Volodymyrs'ka St., 01601 Kyiv, Ukraine

The work is aimed to investigation of different properties of the magnetic nanoparticles prepared by various techniques and especially to the study of morphology and crystal structure dependency of their magnetic properties. It is inspired by rich variety of properties appeared in nonostructured materials in comparison to the bulk parent compounds. Reduced size itself results in increased surfaces energy promoting formation of metastable states like non-specific crystal structures, incomplete crystallization etc. Different techniques suitable to prepare the nanoparticles introduce even more opportunities to vary their shapes sizes and structure. Eventually surface states themselves rather different from the volume ones account for many properties of nanoparticles, especially of those which are as small as few nanometers in diameter.

Magnetic properties of the materials are rather sensitive to variation of crystal properties and morphology originated from nanostructuring. Both intrinsic and collective behaviour are affected. Modification of saturation magnetization, enhancement of the anisotropy, onset of the exchange bias, dipolar interactions and formation of chains are among the numerous phenomena known up to date.

We have prepared Fe and Fe-Cu nanoparticles in vacuum environment using evaporation technique and probed their crystal structure, morphology and magnetic properties. Experimental values of magnetization and magnetic anisotropy, acquired in the range of temperatures from 77 to 350 K, are correlated with the crystal structure parameters measured by X-ray diffraction, chemical composition analyzed by Auger-spectroscopy and morphology revealed by SEM imaging.

This researches were partially supported by RFBR grant No 11-02-90493-Укр\_ф\_a.

**22 August**

Monday

17:30-19:00

poster session  
22PO-J

**“Magnetic Oxides”**

22PO-J-1

**SPONTANEOUS GENERATION OF VOLTAGE IN SINGLE-CRYSTAL****Sm<sub>0.55</sub>Sr<sub>0.45</sub>MnO<sub>3</sub> and La<sub>0.75</sub>Ba<sub>0.25</sub>MnO<sub>3</sub>***Zashchirinskii D.M., Koroleva L.I., Morozov A.S.*

M.V. Lomonosov Moscow State University, Leninskiye Gory, 119992 Moscow, Russia

In single-crystals Sm<sub>0.55</sub>Sr<sub>0.45</sub>MnO<sub>3</sub> and La<sub>0.75</sub>Ba<sub>0.25</sub>MnO<sub>3</sub> grown by the floating zone method with the cooling in oxygen the spontaneous generation of voltage (SGV) has been observed. The voltage observed across the sample was regarded as spontaneous since a current was not supplied on sample. In single-crystal Sm<sub>0.55</sub>Sr<sub>0.45</sub>MnO<sub>3</sub> the maximum of SGV observes at  $T_m \sim 255$  K that almost does not depend from the cooling or heating rate and direction in crystal. The rate of cooling or heating changes from 1.13 to 17.5 K/min. The  $T_m$ -value far exceeds the Curie point  $T_C = 134$  K. In this time the  $T_m$ -value is closed to paramagnetic Curie point  $\theta = 270$  K. Paramagnetic susceptibility obeys the Curie-Weiss law at temperature above  $\sim 2T_C$ . Clearly in the temperature interval  $T_C < T < 2T_C$  the clusters, obtained by magnetic order, are presented. The maximum SGV-value reaches 60  $\mu$ V which is two times as big than in another compounds (FeS, TiNi, FeNi, Ce, Gd<sub>5</sub>(Si<sub>x</sub>Ge<sub>1-x</sub>)<sub>4</sub> and SmMn<sub>2</sub>Ge<sub>2</sub>). The magnetic field strongly influences on SGV-value. The maximum SGV-value decreases on  $\sim 45\%$  at  $H = 14.2$  kOe. We established that the maximum SGV-value did not change for the time 24 hours. It is obvious that SGV is nonequilibrium process with big relaxation time. We emphasize that the maximum SGV-value is bigger than in another compounds mentioned above and can to be source to supply a nanoobjects with electricity. The SGV behaviour is connected with the presence in sample the antiferromagnetic (AF) clusters of CE-type with charge-ordering since at  $T > 140$  K the clusters of this type are only. The maximum on SGV( $T$ ) curve can be caused by the simultaneous destruction of charge-ordering and AF order of CE-type since at  $T > \sim 140$  K the clusters of this type remain. Obviously, the generation of spontaneous voltage necessitates the presence in sample the regions with the opposite charges. In cluster with charge ordering Mn-ions, occupied by electrons (Mn<sup>3+</sup>), alternate with Mn-ions without electron (Mn<sup>4+</sup>). They are fixed in the cluster. So, there is voltage between cluster and paramagnetic host deprived of charge carriers. These clusters are symmetric disposed in sample from Coulombic repulsion if they are identical. In this case the electrical field from each cluster compensates the electrical field from neighboring clusters. As a whole the spontaneous voltage is absent. But the cluster sizes can distinguish and in this case the spontaneous generation of voltage can be. Obviously the distribution of cluster sizes wider in the temperature region of the phase transition from AF of CE-type phase to paramagnetic phase than in smaller temperature that explains the SGV maximum in  $T = T_m$ . We observed SGN in the La<sub>0.75</sub>Ba<sub>0.25</sub>MnO<sub>3</sub> single-crystal too. Maximum value of SGV take place in region of Curie point which is equal to 250 K. SGN.value almost does not depend from the cooling or heating rate and direction in crystal as in Sm<sub>0.55</sub>Sr<sub>0.45</sub>MnO<sub>3</sub> but it smaller on one order In this compound the ferromagnetic clusters occur in which the electrical charges are localized from  $s$ - $d$  exchange gain. They are disposed in the paramagnetic host deprived of the electrical charges. Obviously the cluster sizes can distinguish in Curie temperature region that achieves SGN.

We are acknowledged to A.M. Balbashov and Ya.M. Mukovskii for preparation of samples and their analysis.

[1] C.D. Ee, F.G. Hhh, *J. Appl. Phys.*, **33** (1999) 133.



## NEW FERRIMAGNET PEROVSKITES $\text{La}_2\text{CrA}_{0.75}\text{W}_{0.25}\text{O}_6$ AND $\text{La}_2\text{CrA}_{0.67}\text{Nb}_{0.33}\text{O}_6$ (A = Mg, Cu, Ni)

*Zakharov K., Markina M., Vasiliev A., Istomin S., Antipov E.*

Moscow State University, 119992 Moscow, Russia

We report the magnetic properties of the new family of perovskite-type compounds  $\text{La}_2\text{CrMg}_{0.75}\text{W}_{0.25}\text{O}_6$ ,  $\text{La}_2\text{CrMg}_{0.67}\text{Nb}_{0.33}\text{O}_6$ ,  $\text{La}_2\text{CrNi}_{0.75}\text{W}_{0.25}\text{O}_6$ ,  $\text{La}_2\text{CrNi}_{0.67}\text{Nb}_{0.33}\text{O}_6$ ,  $\text{La}_2\text{CrCu}_{0.75}\text{W}_{0.25}\text{O}_6$  and  $\text{La}_2\text{CrCu}_{0.67}\text{Nb}_{0.33}\text{O}_6$ .

The temperature dependences of these compounds' magnetization demonstrate ferrimagnetic behavior in good accordance with the Neel law as shown in Fig. 1, taken as an example  $\text{La}_2\text{CrMg}_{0.75}\text{W}_{0.25}\text{O}_6$ . Curves of dependences  $M(H)$  are in the form of a narrow hysteresis loop that typical for ferrimagnets, as shown in Fig. 2. The saturation in a field of 2.5 T does not occur. However, the saturation appears to be 5-6 times smaller than  $3 \mu\text{B}$  (maximum possible moment for  $\text{La}_2\text{CrMg}_{0.75}\text{W}_{0.25}\text{O}_6$ ).

The ferrimagnetism is usually associated with the presence of several different magnetic ions in the structure of the compound. However, in  $\text{La}_2\text{CrMg}_{0.75}\text{W}_{0.25}\text{O}_6$  and  $\text{La}_2\text{CrMg}_{0.67}\text{Nb}_{0.33}\text{O}_6$  there is only one type of magnetic ions ( $\text{Cr}^{3+}$ ) and it is impossible for Cr to be in nonequivalent positions in the perovskite-type structure. This behavior can be explained assuming formation of ferromagnetic (FM) domains due to the exchange through the free d-orbital of the tungsten:  $\text{Cr}^{3+} - \text{O} - \text{W}^{6+} - \text{O} - \text{Cr}^{3+}$ . Antiferromagnetic (AFM) exchange  $\text{Cr}^{3+} - \text{O} - \text{Cr}^{3+}$  on the boundaries of the domain fully compensate the contribution of the FM-domain to the total magnetization because almost all (97.6%)  $\text{Cr}^{3+}$  ions, participating in the FM exchange, also participate in the AFM exchange. When exposed to magnetic field the FM domains are oriented along the field, but boundary AFM  $\text{Cr}^{3+}$  ions will compensate this magnetic moment except for the moment, which arises due to absence the moment against the field in place of tungsten ion. Thereby, the value of the saturation moment will be the ratio of the W content to sum of W and Cr contents and is 20% of the maximum possible moment that agrees with the experimental data.

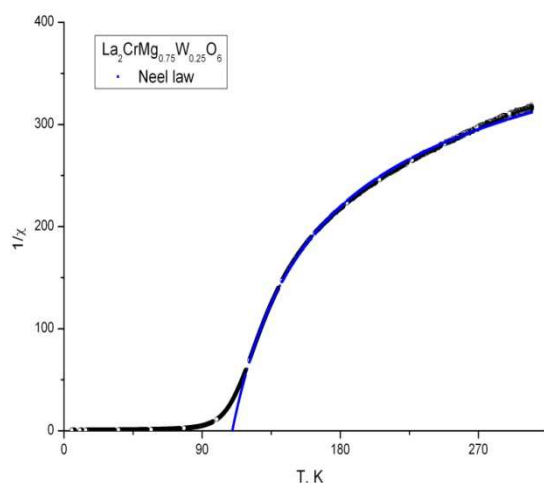


Fig. 1. Temperature dependence of reverse magnetization. Blue line is Neel law.

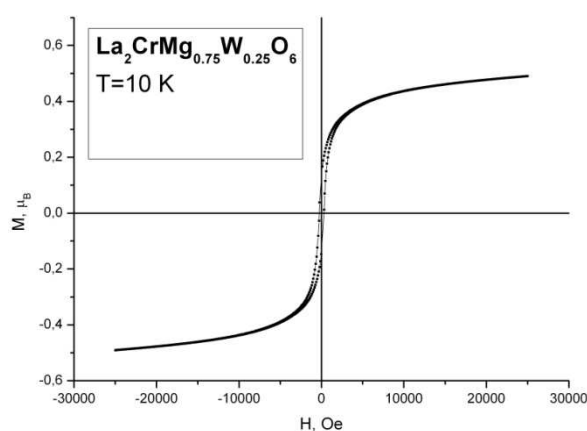


Fig. 2. Applied magnetic field dependence of magnetization at  $T=10 \text{ K}$

22PO-J-3

## TEMPATURE INFLUENCE ON KINETICS OF MAGNETIZATION REVERSAL OF LSMO THIN FILM

*Uspenskaya L.S.<sup>1</sup>, Tikhomirov O.A.<sup>1</sup>, Nurgaliev T.<sup>2</sup>*

<sup>1</sup> Institute of Solid State Physics RASc, 142432, Chernogolovka, Russia

<sup>2</sup> Institute of Electronics BASc, 72, Tzarigradsko chaussee blvd, 1784-Sofia, Bulgaria

Manganites thin films as well as hybrids of manganite and HTSC are prospective materials for spintronic applications because they exhibit the properties of resistance switching under relatively weak magnetic and electric fields. These ability of switching, the value of the effects, and the rate of the response to the fields are inevitably related with magnetic ordering and magnetic domain structure of manganites.

Here we present the results of the study of magnetic domain structure and kinetics of magnetization reversal of thin LSMO and LSMO/YBCO films in temperature range 10 K – 340 K performed by magneto-optic visualization technique, the technique which allows the real time observations of domain structure, its transformation, and direct measurements of dynamic characteristics [1]. The samples were grown by off-axes magnetron sputtering on hot (100) LAO substrates and annealed at 600 °C. The Curie temperature of LSMO film was 340 K. The main film area was free from the twins.

We discuss the correlation of magnetic domain structure with real crystal structure, we show the metastability of the structure in twin free area and the origin of two principally different types of the domains realized in the same film area, depending on magnetic prehistory; we talk about dynamic characteristics of magnetization reversal and we argue the origin of magnetic after-effects at the magnetization reversal; we show unexpected transformation of the type of magnetic domain walls at temperature ~ 170 K and corresponding cross-over of the dependence of coercitivity upon the temperature; finally, we discuss the influence of YBCO vicinity on magnetization reversal of manganite film at temperature below 90 K and explain complicated magnetic flux penetration patterns observed in LSMO/YBCO hybrids [2] via the metastability of manganite domain structure.

Support by RFBR grant 09-02-00856 and by RAS program "Quantum physics of condense matter" is acknowledged.

[1] L.S. Uspenskaya, *Bulletin RAS: Physics*, **74** (2010) 711 (*Izvestiya RAN, Ser. Fizicheskaya*, **74** (2010) 744).

[2] L.S. Uspenskaya, T. Nurgaliev, and S. Miteva, *J. Phys.: Conf. Ser.* **234** (2010) 012046

**INTERPLAY BETWEEN MAGNETIC, ORBITAL AND CHARGE ORDERINGS IN  $\text{CaCu}_x\text{Mn}_{7-x}\text{O}_{12}$  ( $0 \leq x \leq 1$ ) MANGANITES:  $^{57}\text{Fe}$  PROBE MÖSSBAUER SIAGNOSTIC**

*Presniakov I.A.<sup>1</sup>, Rusakov V.S.<sup>1</sup>, Sobolev A.V.<sup>1</sup>, Glazkova Ya.S.<sup>1</sup>, Demazeau G.<sup>2</sup>, Gubaydulina T.V.<sup>1</sup>, Gapochka A.M.<sup>1</sup>, Matsnev M.E.<sup>1</sup>, Volkova O.S.<sup>1</sup>, Vasil'ev A.N.<sup>1</sup>*

<sup>1</sup>M.V. Lomonosov Moscow State University, Moscow, Russia

<sup>2</sup>Institut de la Chemie de la Materie Condensee de Bordeaux, Bordeaux, France

Manganese perovskite-derived oxides  $\text{CaCu}_x\text{Mn}_{7-x}\text{O}_{12}$  ( $0 \leq x \leq 3$ ) containing  $\text{Mn}^{3+}$  and  $\text{Mn}^{4+}$  in six-coordinated polyhedra have attracted a wide interest due to their specific physical properties, such as structural transition and colossal magnetoresistance associated to the charge ordering (CO) and phase separation (PS) phenomena [1- 2].

Detailed  $^{57}\text{Fe}$  probe Mössbauer investigation of the double manganites  $\text{CaCu}_x\text{Mn}_{6.96-x}^{57}\text{Fe}_{0.02}\text{O}_{12}$  ( $0 \leq x \leq 1$ ) including the range of their structural and magnetic phase transitions, have been carried. On the basis of X-ray data it is proved that introduction of the  $^{57}\text{Fe}$  atoms does not perturb the manganite structure. By means of magnetic measurements the degree of influence of the probe atoms on the temperature range of structural and magnetic phase transitions of the manganites has been established. The magnetic and structural results for  $\text{CaCu}_x\text{Mn}_{7-x}\text{O}_{12}$  manganites are summarized in a  $T$ - $x$  phase diagram. In particular, it is proved that phase transition at  $T_{\text{M}2} \approx 90$  K for  $\text{CaMn}_7\text{O}_{12}$  is related with magnetic ordering of  $\text{Mn}^{3+}/\text{Mn}^{4+}$  cations, leading to formation of nonuniform magnetic microstructure. Mössbauer studies of  $^{57}\text{Fe}$  doped  $\text{CaCu}_x\text{Mn}_{7-x}\text{O}_{12}$  ( $x < 0.4$ ) confirms two phenomena: (i) the structural phase transition of the trigonal ( $R\bar{3}$ ) phase to a high-temperature cubic ( $I\bar{3}m$ ) structure in vicinity of charge ordering temperature  $T \approx T_{\text{CO}}$  with coexistence of both the phases; (ii) the existence of only non-distorted ( $\text{MnO}_6$ ) octahedra at  $T > T_{\text{CO}}$  due to the fast electronic exchange between  $\text{Mn}^{3+}$  and  $\text{Mn}^{4+}$  cations.

A model explaining nonmonotonic character of change with a chemical composition ( $x$ ) of the manganites  $\text{CaCu}_x\text{Mn}_{7-x}\text{O}_{12}$  the temperature of their magnetic ordering having a minimum at  $x = 0.4$  was proposed. This model is based on the assumption of a competition of different contributions in magnetic interactions between manganese cations: antiferromagnetic  $t_{2g}^3-p^6-t_{2g}^3$  interactions with participation of half-filled  $t_{2g}$  orbitals; and ferromagnetic "double exchange"  $e_g^1-p^6-e_g^0$  with participation of half-filled ( $\text{Mn}^{3+}$ ) and empty ( $\text{Mn}^{4+}$ )  $e_g$  orbitals of heteroaleet manganese cations.

[1] R. Von Helmut, J. Wecker, B. Holzapfel, L. Schultz, K. Samwer, Phys. Rev. Lett. 71 (1993) 2331.

[2] C.N.R. Rao, A. Arulraj, A.K. Cheetham, B. Raveau, J. Phys: Condens. Matter 12(2000) R83.

22PO-J-5

## PRODUCTION AND MAGNETIC PROPERTIES OF THE $\text{Mg}(\text{Fe}_{1-x}\text{Ga}_x)_2\text{O}_4$ BULK-SAMPLES AND FILMS ON Si

*Trukhanov A.V.<sup>1</sup>, Stognij A.I.<sup>1</sup>, Novitskij N.N.<sup>1</sup>, Trukhanov S.V.<sup>1</sup>, Ketsko V.A.<sup>2</sup>, Nipan G.D.<sup>2</sup>*

<sup>1</sup> Scientific-Practical Materials Research Centre NAS of Belarus, Belarus, Minsk,  
P. Brovki str., 19.

<sup>2</sup> Kurnakov Institute of General and Inorganic Chemistry, Russian Academy of Sciences, Russia,  
Moscow, Leninskii pr., 31.

Phase-pure  $\text{Mg}(\text{Fe}_{1-x}\text{Ga}_x)_2\text{O}_{4+\delta}$  solid solutions were prepared by the pyrohydrolytic process [1]. Structural, magnetic and electrical properties of the  $\text{Mg}(\text{Fe}_{1-x}\text{Ga}_x)_2\text{O}_{4+\delta}$  solid solutions were investigated. In our case [1], the use of citric acid as a reductant in the synthesis of  $\text{Mg}(\text{Fe}_{1-x}\text{Ga}_x)_2\text{O}_{4+\delta}$  led to the positive deviation from Vegard's law over the entire composition range. It was probably due to the transition of some  $\text{Fe}^{3+}$  cations to  $\text{Fe}^{2+}$ . The samples remained single-phase under heating to 570 K. All the prepared polycrystalline materials were soft-magnetic. The optimal compound was selected as a ceramic target for preparation thin films. This ceramic  $\text{Mg}(\text{Fe}_{0.8}\text{Ga}_{0.2})_2\text{O}_{4+\delta}$  was characterized by the highest values of conductivity ( $4 \cdot 10^{-8}$ -  $8 \cdot 10^{-8}$  S/m) and saturation magnetization ( $M \sim 28 \text{ A} \cdot \text{m}^2/\text{kg}$ ) in the range of  $\text{Mg}(\text{Fe}_{1-x}\text{Ga}_x)_2\text{O}_{4+\delta}$  solid solutions [2].

Thin films on Si substrates were obtained by oxygen ion-beam sputtering of the polycrystalline  $\text{Mg}(\text{Fe}_{0.8}\text{Ga}_{0.2})_2\text{O}_{4+\delta}$  target in high vacuum. The depth and composition of films was controlled by AES and FIB for interval thickness from 120 to 400 nm. As-prepared samples were characterized by amorphous structure and cation stoichiometry closely-like to the massive target. Afterwards the optimal conditions (temperature and time of the annealing) for crystallization of thin films were determined. The optimal thermal treatment of the past-sputtered film samples was annealing on atmosphere over a period 30...40 min ( $900^\circ\text{C}$ ). Our investigations showed that the highest values of  $\text{Mg}(\text{Fe}_{0.8}\text{Ga}_{0.2})_2\text{O}_4$  magnetization in thin films (200 nm) was approximately 16 % from the value of the magnetization massive sample. The main reason for this negative fact was active chemical interaction between the film material and Si during annealing processes.

We designed the protection layer –  $\text{TiO}_x$  (thickness 8...10 nm) on the film-substrate interface to decrease the intensity of chemical interactions there. That nanotechnology process was used to enlarge annealing temperature ( $\sim 1000^\circ\text{C}$ ). It was necessary for shaping the crystalline of better quality. It led to the increase in magnetization value  $\text{Mg}(\text{Fe}_{0.8}\text{Ga}_{0.2})_2\text{O}_4$  of thin films (200 nm). The highest value was about 44 % from magnetization value of the massive sample.

Support by BRFFR (№  $\Phi 10\text{M}-017$ )

[1] Ketsko, V.A., Beresnev, E.N., Kop'eva, M.A., et al., Specifics of the pyrohydrolytic and solid-phase syntheses of solid solutions in the  $(\text{MgGa}_2\text{O}_4)_x(\text{MgFe}_2\text{O}_4)_{1-x}$  system, *J. Inorg. Chem.*, 2010, vol. 55, no. 3. pp.427-429.

[2] A.I. Stognij, A.V. Trukhanov, V.A. Ketsko, and G. D. Nipan, Properties of  $\text{Mg}(\text{Fe}_{0.8}\text{Ga}_{0.2})_2\text{O}_{4+\delta}$  Ceramics and Films, *Inorg. Mat.*, 2011, vol. 47, no. 2, pp. 204–207.

22PO-J-6

## NUCLEATION AND DEVELOPMENT OF CLUSTERED STATE IN $\text{La}_{1-x}\text{Sr}_x\text{CoO}_3$ AND $\text{La}_{1-x}\text{Ca}_x\text{CoO}_3$ SINGLE CRYSTALS AT $x = 0.15$

*Lazuta A.V.<sup>1</sup>, Ryzhov V.A.<sup>1</sup>, Kurbakov A.I.<sup>1</sup>, Khavronin V.P.<sup>1</sup>, Molkanov P.L.<sup>1</sup>, Mukovskii Ya.M.<sup>2</sup>,  
 Pestun A.E.<sup>2</sup>, Privezentsev R.V.<sup>2</sup>*

<sup>1</sup> Petersburg Nuclear Physics Institute RAS, Gatchina, St.Petersburg, 188300, Russia

<sup>2</sup> State Technological University 'Moscow Steel and Alloys Institute' (MISIS), Moscow 119049, Russia

The origination of the ferromagnetic (F) clusters in the paramagnetic state of the doped manganites was well established. Study of this state in the doped cobaltites is the topic of the current research activity. Structure investigations (neutron diffraction), as well as the data on resistance, and magnetic properties (the *ac* linear,  $\chi''$ , and nonlinear (second  $M_2$  and third order  $M_3$ ) susceptibilities) are presented for the single crystalline  $\text{La}_{1-x}\text{Sr}_x\text{CoO}_3$  (LSCO) and

$\text{La}_{1-x}\text{Ca}_x\text{CoO}_3$  (LCCO) at  $x = 0.15$ . These insulating compounds exhibit the orthorhombic  $R3c$  space group. Although the data on  $\chi(T)$  and  $M_3(T)$  do not give direct evidences for the clustered state, they show that the clusters in LCCO can be isolated down to 80 K, whereas the F particles in LSCO can undergo a spin glass state below 80 K. According to the  $M_2(H,T)$  measurements, the F clusters nucleate in these compounds by a first order manner. On cooling, the F clusters start to form just below  $T^*$  ( $\approx 213$  K in LSCO and 255 K in LCCO). This stage is related to the cluster nucleation at the preferential sites that are likely produced by variation in the oxygen or doping stoichiometry. At the end of this stage, at  $T^{**}$  ( $\approx 130$  K in LSCO and 174 K in LCCO), the  $M_2(H)$  signal of a regular shape is observed. The well-formed isolated F clusters, which are in a single domain state, are assumed to account for it. At cooling below  $T^{**}$ , the signals begins to increase down to available  $T \approx 97$  K, indicating a growth in the cluster density in both compounds. The  $M_2(H)$  signals are very closed in these cobaltites that evidences about the practically same character of the clusters in these materials. A difference in the amplitude (5 times large in LSCO at 97 K) indicates the difference in the cluster density. It is important that a closed correspondence exists between the nucleation and growth as well as the signals of the F clusters in the doped manganites above  $T_C$  and the cobaltites. This universality is the main result of the work.

This work was supported by the Program of Presidium RAS No 21 (project 4.4.1.8) and RFBR (Grant No 09-02-01509-a).

22PO-J-7

### INFRARED SPECTROSCOPY OF $\text{SmCoO}_3$ AND $\text{EuCoO}_3$

*Kaschenko M.<sup>1,2</sup>, Kuzmova T.<sup>3</sup>, Klimin S.<sup>2</sup>, Pytalev D.<sup>2</sup>, Kamenev A.<sup>4</sup>*

<sup>1</sup> Moscow institute of physics and technology (state university), 141700 Moscow, Russia

<sup>2</sup> Institute of Spectroscopy, RAS, 142190 Troitsk, Moscow region, Russia

<sup>3</sup> Moscow State University, Chemical Department, 119899 Moscow, Russia

<sup>4</sup> Moscow State University, Materials Science Department, 119899 Moscow, Russia

The  $\text{RCoO}_3$  compounds (R - rare earth) are novel functional materials. Significant changes in conductivity can be used in various devices (sensors of temperature, pressure). They attract attention of researchers because of rich phase diagram depending on temperature, chemical composition, and pressure [1,2] (e.g., the metal-insulator transition and the high/low-spin state transition of cobalt).

In this work, we have studied the optical properties of  $\text{RCoO}_3$  (R=Eu or Sm). Transmission spectra of powder samples were registered in broad spectral (1800 – 8000  $\text{cm}^{-1}$ ) and temperature (3.5 – 300 K) ranges. The compounds have a maximum transmittance at 2000  $\text{cm}^{-1}$ . Absorption increases in the range above 3000  $\text{cm}^{-1}$  which is due to the  $d-d$  transitions in the  $\text{Co}^{3+}$  ion. Narrow lines belonging to the  $f-f$  transitions in the  $\text{R}^{3+}$  ions were observed. A scheme of the  $\text{R}^{3+}$  energy levels of was obtained and used to interpret the magnetic properties of  $\text{RCoO}_3$ .

Support from the grant of the President of the Russian Federation (№ MK-1329.2010.2) is acknowledged.

[1] M. Tachibana, et al., *Phys. Rev. B.*, **77** (2008) 094402.

[2] T. Fujita, et al., *J. Phys. Soc. Japan*, **73** (2004) 1987.

22PO-J-8

### SPIN STATES AND MAGNETIC INTERACTIONS IN ISOTOPE SUBSTITUTED $(\text{Pr},\text{Eu})_{0.7}\text{Ca}_{0.3}\text{CoO}_3$

*Kalinov A.V.<sup>1,2</sup>, Gorbenko O.Yu.<sup>3</sup>, Taldenkov A.N.<sup>4</sup>, Rohrkamp J.<sup>2</sup>, Heyer O.<sup>2</sup>, Jodlauk S.<sup>2</sup>, Babushkina N.A.<sup>4</sup>, Fisher L.M.<sup>1</sup>, Kaul A.R.<sup>3</sup>, Khomskii D.I.<sup>2</sup>, Kugel K.I.<sup>5</sup>, Lorenz T.<sup>2</sup>*

<sup>1</sup> All-Russian Electrical Engineering Institute, Krasnokazarmennaya Str. 12, Moscow, Russia

<sup>2</sup> II. Physikalisches Institut, Universität zu Köln, Zùlpicher Str. 77, 50937 Köln, Germany

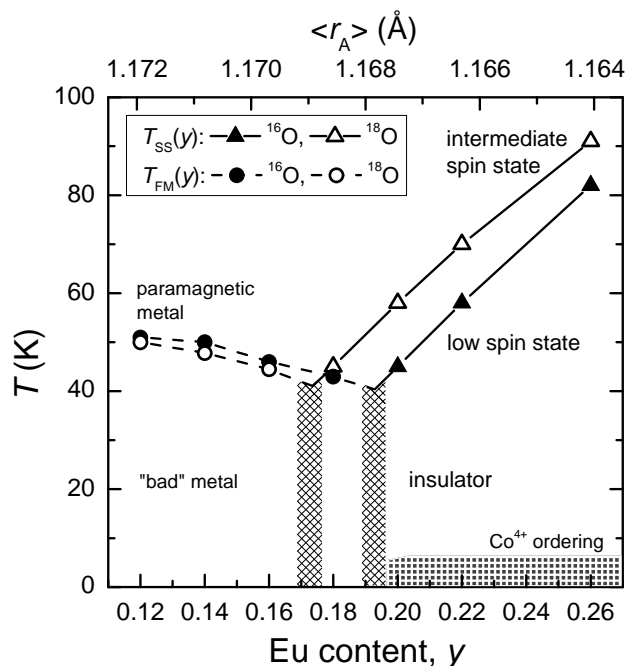
<sup>3</sup> Department of Chemistry, Moscow State University, 119991 Moscow, Russia

<sup>4</sup> Institute of Molecular Physics, Russian Research Center “Kurchatov Institute”, Moscow, Russia

<sup>5</sup> Institute for Theoretical and Applied Electrodynamics, Izhorskaya Str. 13, Moscow, Russia

Based of the measurements of the specific heat, thermal expansion, magnetization and resistivity, the magnetic/spin-state phase diagram of  $(\text{Pr}_{1-y}\text{Eu}_y)_{0.7}\text{Ca}_{0.3}\text{CoO}_3$  series was obtained. The phase diagram reveals three different states depending on the static distortions (Eu content), the oxygen-isotope mass, and the temperature. The samples with the lower Eu concentrations are ferromagnetically ordered up to moderate temperatures (about 50 K) most probably due to the low-spin  $\text{Co}^{4+}$  – intermediate-spin  $\text{Co}^{3+}$  interaction of the double-exchange type. As the Eu doping (and

the static distortion) increases, the  $\text{Co}^{3+}$  LS ( $S = 0$ ) state becomes stabilized and the magnetic ordering of the  $\text{Co}^{4+}$  ions is suppressed to temperatures well below 5 K resulting in the insulating ground state and a low-temperature anomaly in  $C_p$ . At higher temperatures, we observe a first-order spin-state transition from the LS to the IS state of  $\text{Co}^{3+}$ , which is accompanied by a decrease in the electrical resistivity, an increase in the magnetization, and a strong lattice expansion.



The isotope-effect is clearly observed for the spin-state transition  $T_{SS}$ . The temperature  $T_{FM}$  has only marginal but visible dependence on the isotope content. However for both phase boundaries [ $T_{SS}(y)$  and  $T_{FM}(y)$ ], the isotope exchange is equivalent to the change in  $y$  by approximately 0.02. This means that the static distortions due to the change in the mean ionic radius of rare-earth are somehow equivalent to changes in the lattice dynamics due to the isotope exchange, although the physical mechanisms are apparently different. An increase of Eu content leads to an increase of  $t_{2g} - e_g$  crystal field splitting, which stabilizes the LS state. On the other hand, the main effect of the oxygen isotope substitution is in the change of the effective intersite hopping, i.e., of the bandwidth.

The present work was supported by the Russian Foundation for Basic Research (Project No. 10-02-00598) and by the Deutsche Forschungsgemeinschaft via SFB 608 and the German-Russian Project No. 436 RUS 113/942/0.

22PO-J-9

## STRUCTURE AND PROPERTIES OF $\text{Ca}_{1-x}\text{Eu}_x\text{MnO}_3$ SINGLE CRYSTALS

Naumov S.<sup>1</sup>, Telegin S.<sup>1,2</sup>, Kostromitina N.<sup>1</sup>, Solin N.<sup>1</sup>, Elokhina L.<sup>1</sup>, Loshkareva N.<sup>1</sup>, Tsvetkov D.<sup>2</sup>

<sup>1</sup>Institute of Metal Physics of UD, RAS, S. Kovalevskaya st, 18, Ekaterinburg, 620990 Russia

<sup>2</sup>Ural State University, Lenin pr., 51, Ekaterinburg, 620083 Russia

Various magnetic phase transitions and transitions in the orbital/charge ordered state of calcium manganites with electronic doping  $\text{Ca}_{1-x}\text{R}_x\text{MnO}_3$  ( $R = \text{La, Pr, Nd, Sm, Eu}$ ) make these compounds by model objects for strongly correlated systems study and a subject of intensive experimental and theoretical researches, for example, [1-4].

The aim of this work is growth of single crystals  $\text{Ca}_{1-x}\text{Eu}_x\text{MnO}_{3-\delta}$  ( $x=0.1, 0.125, 0.15$ ) and study of their structure and physical properties.

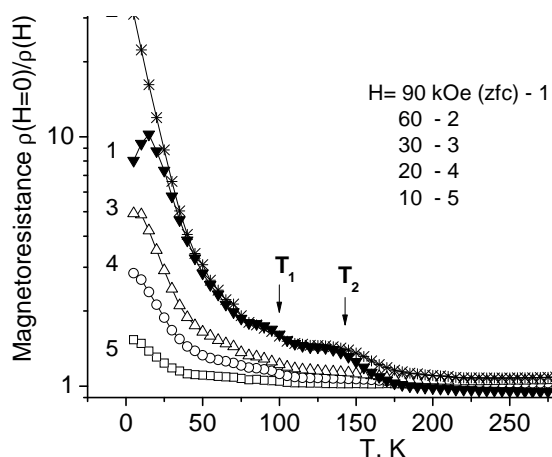
Single-crystal growth of  $\text{Ca}_{1-x}\text{Eu}_x\text{MnO}_{3-\delta}$  was performed by floating zone melting using the URN-2-3P equipment. Polycrystals and single crystals of  $\text{Ca}_{1-x}\text{Eu}_x\text{MnO}_{3-\delta}$  were investigated by x-ray diffraction, x-ray phase analysis, x-ray microanalysis. The dilatometric measurements of the polycrystalline samples were made.

The grown single crystals had the cylindrical form, with length of ~50 mm and the diameter up to 8 mm. The growth speed of single crystals amounted to 5-15 mm/h, the atmosphere of the growth was air. X-ray microanalysis showed the even distribution of elements (Ca, Eu, Mn) along the sample. Single crystal samples with approximately nominal composition and size of  $\sim 5 \times 5 \times 5$  mm<sup>3</sup> were selected from parts of the cylinder corresponding to the end of growth.

Table and Figure show the results for single crystal Ca<sub>0.85</sub>Eu<sub>0.15</sub>MnO<sub>3- $\delta$</sub> , as the example. It was determined that the direction of Ca<sub>0.85</sub>Eu<sub>0.15</sub>MnO<sub>3- $\delta$</sub>  single crystal growth coincides with the direction [100], large and small single-crystal blocks are oriented along this direction.

Table. Ca<sub>0.85</sub>Eu<sub>0.15</sub>MnO<sub>3- $\delta$</sub>  single crystal and polycrystal lattice parameters

Sample	a, Å	b, Å	c, Å	b/ $\sqrt{2}$ , Å	V/formula unit, Å <sup>3</sup>
Polycrystal	5.282	7.485	5.308	5.292	52.47
Single crystal	5.283	7.513	5.300	5.313	52.58



Magnetoresistance of Ca<sub>0.85</sub>Eu<sub>0.15</sub>MnO<sub>3- $\delta$</sub>  single crystal is represented in the Figure. Two peaks of magnetoresistance are observed near two magnetic phase transitions. T<sub>1</sub> and T<sub>2</sub> is Neel temperatures of AFM phase G-type and AFM phase C-type, respectively. Similar features were observed in single crystals of Ca<sub>1-x</sub>LaxMnO<sub>3</sub> and Ca<sub>1-x</sub>CexMnO<sub>3</sub> [3,4].

This work was supported by the Presidium of RAS project 09-P-2-1004 and a joint Project of Far Eastern Branch of RAS-Ural Branch of RAS.

- [1] I.O.Troyanchuk, N.V.Kasper, N.V.Samsonenko, et al. *J.Phys.: Condens.Matter.* **8** (1996)10627.  
 [2] S. M. Dunaevskii, *Phys.Sol.St.* **46** (2004), 193.  
 [3] N.N.Loshkareva, A.V. Korolyov, N.I. Solin et al. *JETP* 102 (2006) 248.  
 [4] N.N.Loshkareva, N.V.Mushnikov, A.V.Korolev, A.M.Balbashov, *Phys.Sol.St.* **51**, (2009) 773.

22PO-J-10

### SPIN-GLASS STATE IN SmFeTi<sub>2</sub>O<sub>7</sub>

Petrakovskii G.A.<sup>1,2</sup>, Drokina T.V.<sup>1,2</sup>, Shadrina A.L.<sup>1</sup>, Velikanov D.A.<sup>1,2</sup>, Bayukov O.A.<sup>1,2</sup>,  
 Kartashev A.V., Molokeev M.S.

<sup>1</sup> L.V. Kirensky Institute of Physics, Siberian Branch of Russian Academy of Sciences,  
 Krasnoyarsk, 660036, Russia;

<sup>2</sup> Siberian Federal University, 79 Svobodny Pr., Krasnoyarsk, 660041, Russia

Systems are contained 3d - and 4f - elements are an important class of materials on account of interesting physical properties and possible applications.

The polycrystalline sample material of Sm-containing zirconolite was synthesized from stoichiometric mixtures Sm<sub>2</sub>O<sub>3</sub>, Fe<sub>2</sub>O<sub>3</sub>, TiO<sub>2</sub> by solid-state reaction method. Thermal treatments were carried out on air in 3 stages at temperatures 1200° - 1250° C with intermediate regrindings.



The compound crystallized in orthorhombic space group Pbcn. The crystal structure of  $\text{SmFeTi}_2\text{O}_7$  contains four-, five-, six- and eight-fold oxides polyhedra [1].

The  $\text{SmFeTi}_2\text{O}_7$  results of the temperature dependence of the magnetization  $\sigma(T)$  and specific heat  $C_p(T)$  are shown in Fig. 1 and Fig. 2.

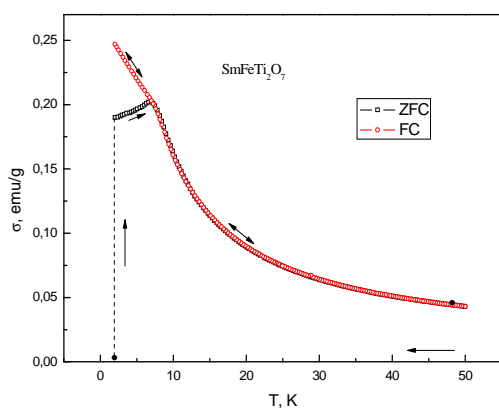


Fig.1. Temperature dependence of the magnetization for sample  $\text{SmFeTi}_2\text{O}_7$  cooled in zero field (ZFC) and cooled in magnetic field  $H=0.05$  T (FC).

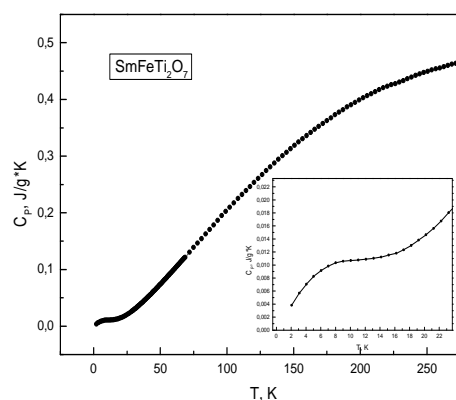


Fig.2. Temperature dependence of the specific heat in  $\text{SmFeTi}_2\text{O}_7$

The temperature dependence of the specific heat suggests the absence of long-range magnetic ordering. On the curve of  $\sigma(T)$  the hysteresis is observed for zero-field-cooled and field-cooled samples at temperatures lower than 7 K.

Thus, the analysis of the experimental results has revealed the existence of magnetic spin-glass state in  $\text{SmFeTi}_2\text{O}_7$ .

[1] E.A. Genkina, V.I. Andrianov, E.L. Belokoneva, B.V. Mill, B.A. Maximov, R.A. Tamazyan. *Kristallography*, **36** (1991) 1408

22PO-J-11

## MAGNETOACOUSTIC INVESTIGATION OF THE JAHN-TELLER EFFECT IN CHROMIUM DOPED ZnSe CRYSTAL

*Gudkov V.V.<sup>1</sup>, Bersuker I.B.<sup>2</sup>, Yasin S.<sup>3</sup>, Zherlitsyn S.<sup>3</sup>, Zhevstovskikh I.V.<sup>4</sup>, Maykin V.Yu.<sup>1</sup>, Sarychev M.N.<sup>1</sup>, Suvorov A.A.<sup>1</sup>*

<sup>1</sup> Ural Federal University, 19, Mira St., 620002 Ekaterinburg, Russia

<sup>2</sup> Institute for Theoretical Chemistry, The University of Texas at Austin, Austin, TX 78712, USA

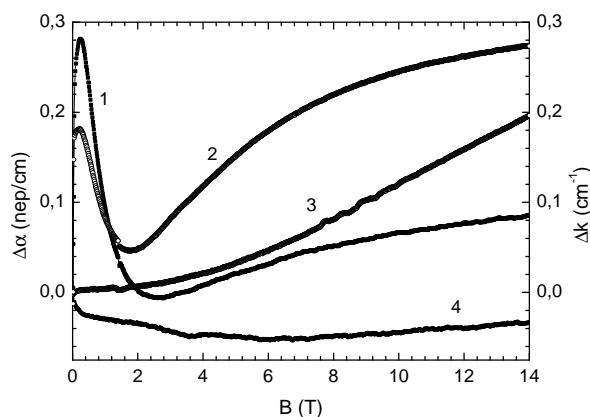
<sup>3</sup> Hochfeld-Magnetlabor Dresden, Helmholtz-Zentrum Dresden-Rossendorf, D-01314 Dresden, Germany

<sup>4</sup> Institute for Metal Physics, Ural Department of the Russian Academy of Sciences, 18, Sophia Kovalevskay St., 620041 Ekaterinburg, Russia

Our recent investigations of II-VI:3d crystals (see [1] and references therein) have shown that the Jahn-Teller effect (JTE) manifests itself as a peak in ultrasonic attenuation  $\alpha(T)$  and a minimum in

phase velocity  $v(T)$ . We have proved that ultrasonic measurements may serve as a powerful technique for evaluation of the JTE parameters.

Here we present results of ultrasonic experiments performed in external magnetic fields applied along the sound wave vector  $\mathbf{k}$ . We used the ZnSe:Cr<sup>2+</sup> crystal with concentration of the dopant  $n = 3.8 \times 10^{18} \text{ cm}^{-3}$ . It has a zinc-blende structure with tetrahedral surrounding of the Cr<sup>2+</sup>( $d^4$ ) ion in the  $^5T_2(e^2t^2)$  high spin ground state. Shear waves of the frequency  $\omega/2\pi = 23.7 \text{ MHz}$  were propagated along the [110] axis and had the polarization parallel to the  $[1\bar{1}0]$ . The temperature dependences  $\alpha(T)$  and the wave number  $k(T) = \omega/v$  measured in the fixed magnetic field  $B = 7 \text{ T}$  resemble those obtained at  $B = 0 \text{ T}$  but exhibit increase by 15% changes. The quantities  $\Delta\alpha(B) = \alpha(B) - \alpha(0)$  and  $\Delta k(B) = k(B) - k(0)$  measured at  $T = 2 \text{ K}$  and given in the figure by the curves 1 and 2, respectively, evidence for the existence of a resonant anomaly, as well as presence of monotonous contributions. At higher temperatures the anomalies disappear: see curves 3 and 4 which show  $\Delta\alpha(B)$  and  $\Delta k(B)$  at  $T = 20 \text{ K}$ . Taking in consideration the results of EPR study of this system [2] we can argue that the anomalies at  $B < 2$  correspond to the condition  $D > \hbar\omega$ , where  $D$  is a constant at  $DS_z^2$  in the spin Hamiltonian. The observed anomalies can be due to the transition in the vicinity of the crossover of the energy levels with  $M_s = 0$  and  $M_s = +1$ . Besides, tunnelling spitting [3] should be accounted for the interpretation of the results; this will be done in the nearest future.



Support by Russian Academy of Sciences Program (project No. 01.2.006 13395), Russian Foundation for Basic Research (grant No. 09-02-01389), and Welch Foundation (grant F-100) is acknowledged.

[1] V.V. Gudkov, I.B. Bersuker, I.V. Zhevstovskikh, *et al*, *J. Phys.: Condens. Matter*, **23** (2011) 115401.

[2] J.T. Vallin and G.D. Watkins, *Phys. Rev. B* **9** (1974) 2051.

[3] I.B. Bersuker, *The Jahn-Teller Effect*. (Cambridge: Cambridge University Press, 2006).

22PO-J-12

## MAGNETIC EXCHANGE INTERACTIONS AND SUPERTRANSFERRED HYPERFINE FIELDS AT <sup>119</sup>Sn PROBE ATOMS IN CaCu<sub>3</sub>Mn<sub>4</sub>O<sub>12</sub> MANGANITE

Rusakov V.S.<sup>1</sup>, Presniakov I.A.<sup>1</sup>, Sobolev A.V.<sup>1</sup>, Demazeau G.<sup>2</sup>, Gapochka A.M.<sup>1</sup>, Gubaydulina T.V.<sup>1</sup>, Matsnev M.E.<sup>1</sup>, Volkova O.S.<sup>1</sup>, Vasil'ev A.N.<sup>1</sup>

<sup>1</sup>M.V. Lomonosov Moscow State University, Moscow, Russia

<sup>2</sup>Institut de la Chimie de la Materie Condensee de Bordeaux, Bordeaux, France

The double manganite CaCu<sub>3</sub>Mn<sub>4</sub>O<sub>12</sub> is the end-member in the series of the ferromagnetic perovskites CaCu<sub>3-x</sub>Mn<sub>4+x</sub>O<sub>12</sub> ( $0 \leq x \leq 3$ ), which have attracted interest of the scientific community

due to the interesting interplay between their magnetic, electronic and structural properties. These correlations induce various physical phenomena, like colossal magnetoresistance, multiferroic properties and colossal dielectric constants which are interesting for developing basic Science as well as for potential applications.

The manganite  $\text{CaCu}_3\text{Mn}_4\text{O}_{12}$  doped with  $^{119}\text{Sn}$  atoms (~1 at. % with respect to manganese atoms) was studied by Mössbauer spectroscopy. It was demonstrated that diamagnetic tin atoms has no effect on magnetic and structural properties of the manganite. Formally tetravalent  $\text{Sn}^{4+}$  ions are substituted for isovalent manganese ions in the octahedral ( $\text{Mn}^{4+}\text{O}_6$ ) polyhedra. The covalency effects on the magnetic interactions like superexchange in  $\text{Cu}^{2+}\text{-O-Mn}^{4+}$  and  $\text{Mn}^{4+}\text{-O-Mn}^{4+}$  bonds and super-transferred hyperfine interactions of the  $^{119}\text{Sn}$  probe atoms in the manganite structure were discussed. Using a semi-quantitative nearest neighbor cluster model relating the hyperfine magnetic field on the  $^{119}\text{Sn}$  nuclei ( $H_{\text{Sn}} = 105$  kOe at  $T = 77$  K) to covalency parameters and angle characterizing the  $\text{Sn-O-M}$  ( $M = \text{Cu}, \text{Mn}$ ) bonds, it has been shown how such an analysis of supertransferred hyperfine interactions of tin probe ions can get fruitful informations about strength and sign of the super-exchange interactions between magnetic  $\text{Mn}^{4+}$  and  $\text{Cu}^{2+}$  ions.

Taking into account that the partial contributions to the hyperfine field  $H_{\text{Sn}}$  made by the  $\text{Mn}^{4+}$  and  $\text{Cu}^{2+}$  paramagnetic ions are comparable in magnitude and opposite in sign, temperature-induced changes in these contributions should be directly related to the character of the temperature dependence of the magnetization of the corresponding magnetic sublattices. A consistent description of the results of magnetic measurements and Mössbauer data in the framework of the Weiss molecular field model considering the specific local environment of tin atoms has made it possible to estimate the  $\text{Cu}^{2+}\text{-O-Mn}^{4+}$  indirect exchange coupling integrals:  $J_{\text{CuMn}} \approx -51.1 \pm 0.3$  K for  $\text{Cu}^{2+}\text{-O-Mn}^{4+}$  and  $J_{\text{MnMn}} \approx -0.6 \pm 0.2$  K for  $\text{Mn}^{4+}\text{-O-Mn}^{4+}$ . It has been shown with the use of the Goodenough-Kanamori-Anderson rules that the magnitude and sign of the intrasublattice exchange integral  $J_{\text{MnMn}}$  is consistent with both the electronic configuration of  $\text{Mn}^{4+}$  cations and the geometry of their local crystallographic environment in the title manganite.

22PO-J-13

## COMPETING INTERACTIONS AND SPIN ORBIT COUPLING IN DOPED RARE-EARTH MANGANITES

*Shah W.H.*

Department of Physics, College of Science, King Faisal University, Hofuf, 31982, Saudi Arabia  
[wiqarhussain@yahoo.com](mailto:wiqarhussain@yahoo.com)

The effect of Fe doping in  $\text{La}_{0.65}\text{Ca}_{0.35}\text{Mn}_{1-x}\text{Fe}_x\text{O}_3$  (where  $0 \leq x \leq 0.10$ ) compound on the Mn site in the ferromagnetic phase has been studied in detail. The XRD results showed that all compounds crystallized in a tetragonal phase and no appreciable change is observed in the lattice parameters with increasing Fe concentration. Resistivity measurements of the compound from ambient temperature down to 77 K exhibit a peak at temperature  $T_p$ , which decreases with increasing Fe content. Substantial rise in resistivity corresponding to the  $T_p$  and increase spin disorder are also observed with increasing doping. Two models, variable range hopping (VRH), and polaronic have been used to explain the DC transport mechanism in the insulating region above  $T_p$ . The VRH model shows better fit to the resistivity data as compared to the polaronic model. The localization length is found to decrease by increasing Fe concentration. The activation barrier,  $W$ , has been calculated and found to increase with the increase of Fe content. In the metallic region ( $T < T_p$ ) a linear decrease of  $W$  with temperature has been observed. It is observed that near to the metal-

insulator transition temperature, transport in these compounds may be described in terms of carrier hopping between states, which are localized as a result of magnetic and non-magnetic disorder. The variations in the critical temperature  $T_p$ ,  $T_c$ , confinement length, magnetic moment and magnetoresistance show a rapid change at about 4-5% *Fe*. Colossal magnetoresistance has been shifted to lower temperature, and enhanced by Fe doping. The maximum magnetoresistance is seen to increase consistently with the addition of *Fe* and increases upto 400% for 8% *Fe* concentration. However, conduction and ferromagnetism have consistently suppressed by Fe doping. The effect of *Fe* is seen to be consistent with the disruption of the *Mn-Mn* exchange possibly due to the formation of magnetic clusters. The formation of ferromagnetic and antiferromagnetic clusters and the competition between them with the introduction of  $Fe^{3+}$  ions, which do not participate in the double exchange (DE) process, have been suggested to explain the low value of magnetization at higher Fe concentration.

22PO-J-14

## THERMODYNAMIC EFFECTS OF THE SPIN ORDERING OF ELECTRONS IN HYBRIDIZED STATES ON THE IMPURITIES OF TRANSITION ELEMENTS

*Okulov V.I.<sup>1</sup>, Pamyatnykh E.A.<sup>2</sup>, Zabaznov Yu.V.<sup>2</sup>*

<sup>1</sup> Institute for Metal Physics UD RAS, Ekaterinburg, Russia

<sup>2</sup> Ural State University, Ekaterinburg, Russia

The present report shows the results of the theoretical study of the effects of manifesting the spontaneous spin polarization of electron hybridized donor d-states system in conduction band of a crystal. On the basis of the theory, developed in [1,2], we present the justification of the spin polarization phenomenon of the given type and give the description of temperature and concentration dependences of both spin splitting of electron energies and corresponding electron contributions to thermodynamic quantities (electron specific heat, elastic modulus, magnetic susceptibility), using the model of exchange Fermi-liquid interaction constants. In the framework of this model the spin splitting of the peaks of density of states, characterizing the localized component of hybridized states, is described by the constant  $\beta$ , which in the case of full polarization (one peak was filled only) proved to be equal

$$\beta = \psi n^i \quad (1)$$

Here  $\psi$  is the interaction constant and  $n^i$  is the concentration of localized component. Thereby the polarization of component  $\beta_c$ , characterizing homogeneous density (conduction electrons), takes also place and equal to:

$$\beta_c = (\psi_{ci}/\psi)\beta \quad (2)$$

Here  $\psi_{ci}$  is the interaction constant, characterizing the interaction of the components of free motion and localization of different states. Formulas (1) and (2) are valid, when the value of  $\beta$  exceeds the interval of hybridization. In the case of partial filling of spin splitting peaks the polarization is considered in [3]. Therefore we have shown that spontaneous spin polarization of electrons in hybridized states is accompanied by the polarization of conduction electrons in energy interval of hybridization. This result is of important significance as far as it gives a justified conclusion concerning the polarization of conducting electrons under the effect of direct interaction rather than indirect less effective interaction. We have considered specific low-temperature anomalies of thermodynamic properties due to hybridization of the states of polarized electrons. It

was also shown that the fact of spin polarization can be established, in particular, from the temperature dependences, the form of which is essentially dependent on the interaction parameters.

This work was supported by the Russian Foundation for Basic Research (Grant no. 09-02-01389) and by the Program of the Physical Sciences Branch of RAS (Grant no. 09-2-T2-1037) and Russian-American Program BRHE.

[1] V.I. Okulov, *Phys.Met.Metallogr.*, **100** (2005) 23.

[2] V.I. Okulov, E.A. Pamyatnykh, V.P. Silin, *Fiz.Nizk.Temp.*, **35** (2009) 891.

[3] V.I. Okulov, E.A. Pamyatnykh, Yu.V. Zabaznov, *Solid St.Phenom.*, **168-169** (2011) 489.

22PO-J-15

### OXYGEN ISOTOPE EFFECT IN ORDERED $\text{PrBaMn}_2\text{O}_6$

Taldenkov A.N., Babushkina N.A., Inyushkin A.V.<sup>1</sup>, Kalitka V.S.<sup>2</sup>, Kaul A.R.<sup>3</sup>

<sup>1</sup>NRC “Kurchatov Institute”, 123182 Moscow, Kurchatov sq.1, Russia

<sup>2</sup>Material Science Department, Moscow State University, 119991 Moscow, Russia

<sup>3</sup>Department of Chemistry, Moscow State University, 119991 Moscow, Russia

Complex transition metal oxides with the general formula  $\text{R}_{1-x}\text{A}_x\text{MnO}_3$  (R-rare earth element and Y, A – Ca, Sr or Ba) exhibit different ordering phenomena and phase transitions, e.g., antiferromagnetic (AFM) and ferromagnetic (FM) order, charge (CO) and orbital orderings, metal-insulator (MI) transitions. Among all of the manganites barium half-doped compounds  $\text{R}_{0.5}\text{Ba}_{0.5}\text{MnO}_3$  have the highest  $T_{\text{FM}}$  and a significant magnetoresistance. Recently it was discovered that an ordered structure of alternating layers of BaO-MnO-RO-MnO can be formed in these manganites. Physical properties of ordered manganite  $\text{RBaMn}_2\text{O}_6$  strongly depend on the degree of ordering. Praseodymium-based ordered manganite  $\text{RBaMn}_2\text{O}_6$  is the only composition in which the FM order parameter is suppressed by developing CO ordering (fig.1). The purpose of this study is to investigate the influence of the oxygen mass on the processes of magnetic and charge ordering in  $\text{PrBaMn}_2\text{O}_6$ .

Ordered samples of  $\text{PrBaMn}_2\text{O}_6$  were synthesized by oxygen reduction method. Raw material, disordered ceramic manganite  $\text{Pr}_{0.5}\text{Ba}_{0.5}\text{MnO}_3$ , was made by “paper synthesis”. Then oxygen-reduced ordered  $\text{PrBaMn}_2\text{O}_5$  was prepared by annealing with Fe-FeO getter. The obtained  $\text{PrBaMn}_2\text{O}_5$  was saturated with oxygen, so that an ordered manganite  $\text{PrBaMn}_2\text{O}_6$  was synthesized. Isotope substitution occurred by simultaneous prolonged annealing of the pair of  $\text{PrBaMn}_2\text{O}_6$  samples in an atmosphere of  $^{16}\text{O}$  and  $^{18}\text{O}$  (90%) at 750C, leaving the ordered structure unchanged. Temperature dependences of ac-susceptibility, magnetization and resistivity were measured in magnetic field up to 35 kOe.

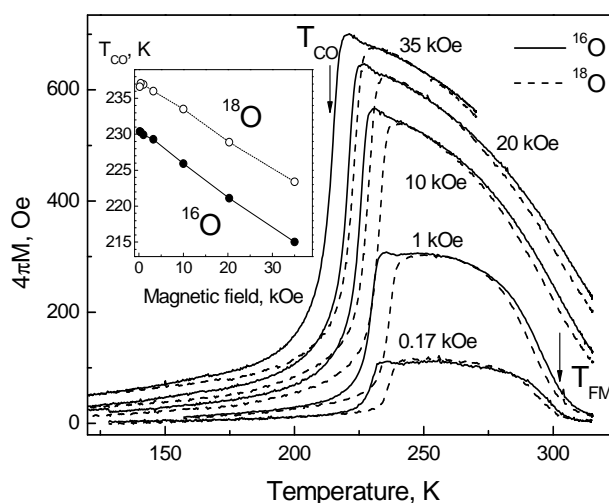


Fig.1. Temperature dependence of magnetization in permanent magnetic field. The insert shows field dependence of  $T_{\text{CO}}$ .

In agreement with the well-known results of Zhao et al. [1] obtained on disordered  $\text{La}_{0.5}\text{Ca}_{0.5}\text{Mn}^{16-18}\text{O}_3$  and  $\text{Nd}_{0.5}\text{Sr}_{0.5}\text{Mn}^{16-18}\text{O}$ , we found that heavy oxygen suppresses FM magnetic state and favors arising of CO AFM ground state. The applied magnetic field and light oxygen stabilize FM phase, thus the positive isotope shift of  $T_{\text{FM}}$  and negative isotope shift of  $T_{\text{CO}}$  occur. The shift in  $T_{\text{CO}}$  is about  $7\text{K} \div 10\text{K}$ , whereas isotope effect in  $T_{\text{FM}}$  is rather small and does not exceed  $2\text{K}$ . The MI transition coincides well with  $T_{\text{CO}}$ , and also is influenced by oxygen mass. The obtained results and possibility of site selective isotope substitution are discussed.

The work was supported by the Russian Foundation for Basic Research, project 10-02-00598-a, and by the Russian-German project DFG-GR 1484/2-1.

[1] Guo-meng Zhao et al., Phys. Rev. B, **59** (1999) 81.

22PO-J-16

## EFFECT OF ELECTRON IRRADIATION ON THE NON-STOICHIOMETRIC AND DOPED LANTHANUM MANGANITES

*Arbuzova T., Naumov S., Arbuzov V., Danilov S., Kostromitina N.*

Institute of Metal Physics of UD, RAS, S. Kovalevskaya st, 18, Ekaterinburg, 620990 Russia

The presence of  $\text{Mn}^{3+}$  and  $\text{Mn}^{4+}$  ions in lanthanum manganites leads to ferromagnetism and colossal magnetoresistance (CMR) near  $T_{\text{C}}$ . In the paramagnetic phase all the manganites have a semiconducting character of conductivity. Correlations in the ranges of limited size are considered to explain the CMR effect in the region  $T > T_{\text{C}}$ . In order to confirm the existence of magnetic polarons it is necessary to have experimental data on the magnetic properties at  $T > 2T_{\text{C}}$ , which are scarce in the literature. We measured the temperature dependences of magnetic susceptibility for the initial and electron-irradiated samples  $\text{La}_{1-x}\text{Mn}_{1-y}\text{O}_3$ ,  $\text{La}_{0.67}\text{Ca}_{0.33}\text{MnO}_3$  and  $\text{La}_{0.67}\text{Ba}_{0.33}\text{MnO}_3$ . Electron irradiation can lead to local structural changes, without varying the composition of samples. The Fig. 1 shows the temperature dependences of susceptibility  $\chi_{\text{dc}}$  in the field  $H = 90$  Oe for initial and irradiated  $\text{La}_{1-x}\text{Mn}_{1-y}\text{O}_3$  sample. The analogous dependences of susceptibility  $\chi_{\text{dc}}(T)$  for  $\text{La}_{0.67}\text{Ca}_{0.33}\text{MnO}_3$  and  $\text{La}_{0.67}\text{Ba}_{0.33}\text{MnO}_3$  are presented in Fig. 2.

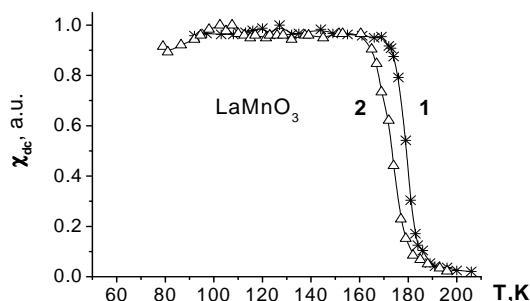


Fig.1. 1 -  $F=0$ , 2 -  $F = 9 \times 10^{18} \text{ e/cm}^2$

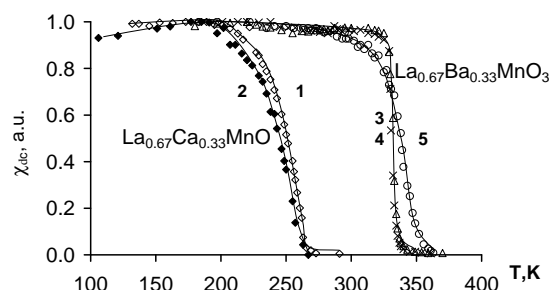


Fig.2. 1,3 -  $F=0$ ; 2,4 -  $F = 5 \times 10^{18} \text{ e/cm}^2$ ,  
5 -  $9 \times 10^{18} \text{ e/cm}^2$

Electron irradiation with fluence  $F = 5 \times 10^{18} \text{ e/cm}^2$  decreases  $T_{\text{C}}$  by  $3\text{K}$  in  $\text{La}_{1-x}\text{Mn}_{1-y}\text{O}_3$  and by  $8\text{K}$  in  $\text{La}_{0.67}\text{Ca}_{0.33}\text{MnO}_3$ . This irradiation does not influence on  $T_{\text{C}}$  of  $\text{La}_{0.67}\text{Ba}_{0.33}\text{MnO}_3$ , but at  $F = 9 \times 10^{18} \text{ e/cm}^2$  the phase transition near  $T_{\text{C}}$  is smeared, pointing to a nonuniform distribution of

defects. Curie-Weiss law starts to fulfill in the region  $T > 500\text{K}$ . When the temperature decreases the  $\mu_{\text{eff}}$  value becomes larger as compared with expected  $\mu_{\text{eff}} = 4,59 \mu_{\text{B}}$ . This indicates the presence of magnetic polarons of Varma [1]. Below 330K the continuous increase of  $\mu_{\text{eff}}$  is observed. Possible reasons for this are short-range magnetic order and correlated polarons in areas with E or CE – type structure [2]. Effective magnetic moment of the irradiated samples is larger than  $\mu_{\text{eff}}$  of the initial samples. Thus, electron irradiation leads to decrease of  $T_{\text{C}}$  and conservation of magnetic polarons till higher temperatures.

Support by program DPS RAS „Physics of new materials and structures“ and program of scientific cooperation UB of RAS and SB RAS is acknowledged.

[1] C.M. Varma. *Phys.Rev. B* **54**, (1996) 7328.

[2] T. Hotta, M. Moraghebi, A. Feiguin, et.al. – */cond-mat/* **0211049**.

22PO-J-17

## ORBITAL AND MAGNETIC STRUCTURE INVESTIGATION IN RARE-EARTH MANGANITES.

*Leskova J.V.<sup>1</sup>, Gonchar L.E.<sup>1,2</sup>, Nikiforov A.E.<sup>1</sup>*

<sup>1</sup>Ural State University, 620000, 51 Lenin Av., Ekaterinburg, Russia.

<sup>2</sup>Ural State Railway Transport University, 620034, 66 Kolmogorova St., Ekaterinburg, Russia.

The magnetic properties of perovskite are reported in a huge number of studies over a half century. The investigation of rare-earth manganites with general formula  $RMnO_3$  ( $R^{3+}=La, Pr, Nd, \dots, Tb, Dy, Ho$ ) with orthorhombic symmetry of crystal structure call a great interest. Earlier investigations of these compounds were devoted to the strong correlation between lattice, orbital, and spin degrees of freedom. This correlation becomes more complicated because of discovery of multiferroic phases of orthorhombic manganites.

The orbitally-dependent exchange interaction model was used in order to describe the superexchange interaction in all range of  $RMnO_3$  orthorhombic compounds. The model of nearest-neighbor [1] and next-nearest neighbor [2] exchange was used to describe the magnetic structures of manganites with small rare-earth ion sublattice ( $R=Dy, Tb, Ho$ ). We investigate two types –A and E – of magnetic structures. The antiferromagnetic resonance spectra of both structures have spin-flop transition region. The influence of electromagnons [3] and rare-earth sublattice magnetism [4] were

not taken into account. The E-structure AFMR spectrum has more complicated external magnetic field dependence.

The models of NMR spectra calculation of  $Mn^{3+}$  ion in  $RMnO_3$  compounds are proposed. Manganese ion spectrum consists of one broad line. It's position depends upon the type of rare-earth ion.

For different rare-earth ion in  $RMnO_3$ , the crystal lattice parameters change. Thus, the hyperfine parameter (HF) also changes. The dependence of the HF parameter is drawn at

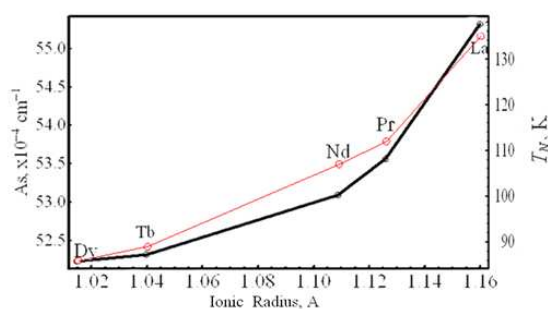


Fig 1. The dependence of hyperfine interaction parameter of  $Mn^{3+}$  upon rare-earth ion radius in  $RMnO_3$ .

Fig. 1. The magnetic interactions ( $T_N$  dependence) in several orthorhombic perovskites such as  $RCrO_3$  and  $RFeO_3$  had been investigated early [5]. For considered perovskites, the dependences of Neel temperature and HF parameters upon the type transition-metal ions share same features from the same dependences of lattice parameters. Thus, the local structures distortions determine the magnitudes of  $T_N$  and isotropic HF parameter. Perovskite crystals with different rare-earth and transition-metal ions have different types of magnetic structures. The A-type magnetic structure is considered in NMR spectra calculations in  $RMnO_3$ . The E-type magnetic structure causes no changes in zero-magnetic field case. The additional changes of spectrum could be in field dependence of HF interaction.

- [1] M. Mochizuki, N. Furukawa, *Phys. Rev. B*, **80** (2009) 134416  
 [2]. I. V. Solovyev, *Phys. Rev. B*, **83** (2011) 054404  
 [3] A.A. Mukhin et.al. *Phys. Usp.*, **52** (2009) 851  
 [4] A.A. Mukhin et al. *J. Magn. Magn. Mat.*, **226-230** (2001) 1139  
 [5] J.-S. Zhou et al. *Phys. Rev. B*, **81** (2010) 214115

22PO-J-18

## SYNTHESIS AND MAGNETIC PROPERTIES OF $Mn_2GeO_4$ SINGLE CRYSTALS

Volkov N.V.<sup>1,2</sup>, Balaev A.D.<sup>1</sup>, Sapronova N.V.<sup>1</sup>, Sablina K.A.<sup>1</sup>, Velikanov D.A., Molokeev M.S., Popkov S.I.

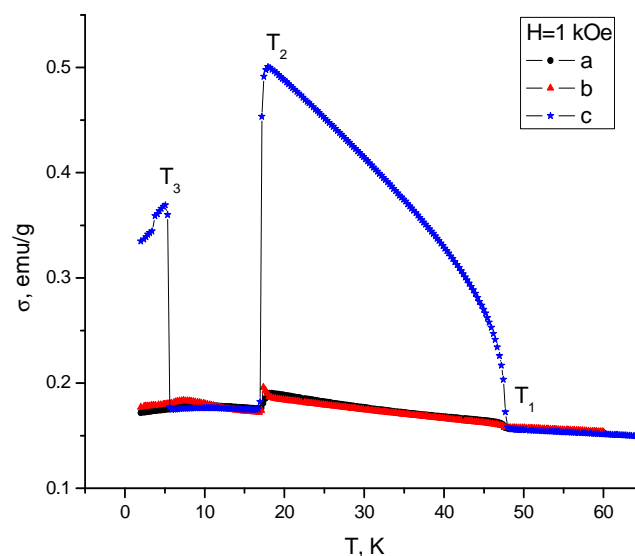
<sup>1</sup> Kirensky Institute of Physics SB RAS, Krasnoyarsk, 660036, Russia;

<sup>2</sup> Siberian Federal University, 660079 Krasnoyarsk, Russia

Within the framework of our research of manganese oxides the single crystals  $Mn_2GeO_4$  have been grown by the flux method using the original technique described in our work [1]. Also, the  $Mn_2GeO_4$  is interest of due to the fact that crystal structure is characterized by strong geometric frustration; which can lead to multiferroic properties [2]. The crystal structure, an isomorph of olivine, was determined on single crystal by X-ray diffraction method: cell parameters,  $a=10.7401$  Å,  $b=6.3116$  Å,  $c=5.0766$  Å, and the space group Pnma.

Magnetic measurements were performed on a Magnetic Property Measurement System (MPMS, Quantum Design) in the temperature range from 2 to 300 K and in magnetic fields up to 50 kOe with the exact orientation of the applied magnetic field relative to the crystallographic directions of the crystal. Figure presents temperature dependence of magnetization in the magnetic field 1 kOe. It is obvious that there are three sharp magnetic phase transition at  $T_1=47$  K,  $T_2=17.5$  K and  $T_3=5.5$  K, with phase transition at  $T_2$  depended on applied magnetic field.

Also the specific heat measurements of single crystals were carried out. The heat capacity of  $Mn_2GeO_4$  exhibits three sharp





maxima, which exactly correlate with the magnetic phase transition temperatures  $T_1$ ,  $T_2$  and  $T_3$ , respectively.

[1] Sapronova N.V., Volkov N.V., Sablina K.A., Petrakovskii G.A., Bayukov O.A., Vorotynov A. M., Velikanov D.N., Bovina A.F., Vasilyev A.D., Bondarenko G.V. *Phys. Stat. Sol. B.*, **246** (2009) 206.

[2] Khomskii D. *Physics*, **2** (2009) 20

22PO-J-19

## UNIVERSAL SCALE FOR EFFECTS OF Mn-SITE DOPING IN $\text{La}_{1/3}\text{Ca}_{2/3}\text{MnO}_3$ ON CHARGE ORDERING TEMPERATURE AND SUPERSTRUCTURE PARAMETER

*Orlova T.S.<sup>1</sup>, Laval J.Y.<sup>2</sup>, Monod Ph.<sup>2</sup>, Noudem J.<sup>3</sup>*

<sup>1</sup> Ioffe Physical-Technical Institute, 26 Polytekhnicheskaya, St. Petersburg 194021, Russia

<sup>2</sup> ESPCI, 10 Vauquelin, 75231 Paris, France

<sup>3</sup> ENSICAEN, 6 boulevard du Marechal Juin, 14050 Caen Cedex, France

The origin of charge and orbital ordered striped superstructures in the manganese perovskites ( $\text{RE}_{1-x}^{\text{3+}}\text{AE}_x^{\text{2+}}\text{MnO}_3$ , where  $\text{RE}$  is rare earth and  $\text{AE}$  is alkaline earth) is not still well understood as well as their role in magnetic and electrical behavior of these materials. Although charge ordering is considered to be primarily caused by strong Coulomb interactions among the charge carriers of near neighbors, the question on what drives the orbital ordering: Jahn-Teller distortion versus orbital-orbital superexchange is still open. Modifying the key manganese chains ( $\dots\langle\text{Mn}\rangle\text{-}\langle\text{Mn}\rangle\text{-}\langle\text{Mn}\rangle\dots$  with  $\langle\text{Mn}\rangle=\text{Mn}^{3+}$  and  $\text{Mn}^{4+}$ ), which are responsible for interplay between ion, orbital and spin ordering, through Mn-site doping could be an efficient key in understanding main factors affecting the charge-orbital ordering in the manganites.

Effects of initial doping of the Mn-sites in  $\text{La}_{1/3}\text{Ca}_{2/3}\text{Mn}_{1-y}\text{M}_y\text{O}_3$  by various cations  $\text{M} = \text{Fe}, \text{Ga}, \text{Cu}, \text{Ni}, \text{Mg}, \text{Cr}, \text{Ru}$  with different  $d$ -shell filling (without  $d$  orbital, with  $d^0$ ,  $d^{10}$  or  $d^n$ ) on striped charge-orbital ordering have been systematically studied by combining transmission electron microscopy with magnetic and transport measurements. It was found that for the dopants  $\text{M}: \text{Fe}, \text{Ni}, \text{Ga}, \text{Mg}$  (the group A) in the range  $0 \leq y \leq 0.07$  and dopants  $\text{M} = \text{Cr}, \text{Ru}$  (the group B) in the range  $0 \leq y \leq 0.05$  the temperature  $T_{\text{CO}}$  of charge ordering (CO) transition gradually decreases with dopant concentration  $y$ , but practically for each dopant  $T_{\text{CO}}(y)$  curve has own signature. However analysis of  $T_{\text{CO}}(y)$  dependences showed a unique behavior of  $T_{\text{CO}}$  change with increasing doping level through change in the effective relative concentration  $n_{\text{Mn}^{3+}} = \text{Mn}^{3+}/(\text{Mn}^{3+} + \text{Mn}^{4+})$  of  $\text{Mn}^{3+}$  ions:  $T_{\text{CO}} \sim C n_{\text{Mn}^{3+}}$  for all studied dopants. The coefficient  $C$  depends only on the valence of dopant and does not depend on its  $d$ -shell filling. This finding allows us to conclude, that none of the considered dopants is involved in charge transport in the charge ordering.

TEM studies revealed that effect of doping on the formation of extended striped superstructure critically depends on filling  $d$ -shell of doping cations. The striped superstructure was kept only in compounds doped by ions with active  $d(z^2)$  orbital ( $\text{Fe}^{3+}$  and  $\text{Ni}^{2+}$  cations). All the other dopants suppressed the superstructure formation. Analysis taking into account the electronic structure of dopants and their ability for Jahn-Teller effect showed dominant role electronic orbital-orbital (super)exchange (versus Jahn-Teller distortions interactions) in long-range superstructure formation. In the doped compounds ( $\text{Ni}$  and  $\text{Fe}$ ) the superstructure is incommensurate. It was shown

that regardless on doping element (Fe or Ni), its parameter  $q \approx (n_{Mn^{3+}} + 1/3y)a^*$  ( $a^*$  - reversal lattice parameter), i.e.  $q$ -parameter is determined by concentration of ions participated in  $d(z^2)$ -orbital ordering.

The dopants of group A decrease and ones of group B increase Weiss temperature. The transition from AFM state with insulator conductivity to FM state with conductivity of 'bad' metals (close to the Mott's criteria) was found for Ru-doped system with 7% Ru on Mn-sites. All the other doped systems remain in AFM CO state at low temperatures. Dominant role of ruthenium valence (Ru<sup>5+</sup>) in the insulator-metal phase transition is discussed.

22PO-J-20

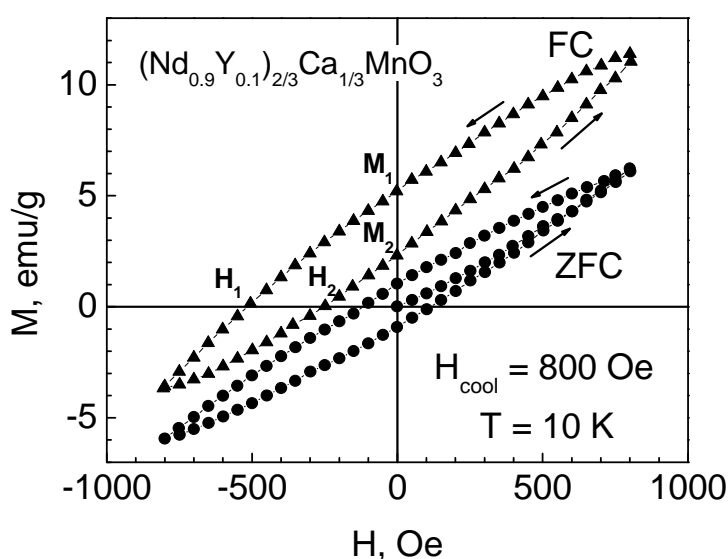
## DIRECT EVIDENCE OF THE LOW TEMPERATURE CLUSTER GLASS STATE OF $(Nd_{0.9}Y_{0.1})_{2/3}Ca_{1/3}MnO_3$ PEROVSKITE

Fertman E.<sup>1</sup>, Desnenko V.<sup>1</sup>, Beznosov A.<sup>1</sup>, Dolya S.<sup>1</sup>, Kajňaková M.<sup>2</sup>, Feher A.<sup>2</sup>

<sup>1</sup> B. Verkin Institute for Low Temp. Phys. & Engin. of NASU, Kharkov 61103, Ukraine

<sup>2</sup> Centre of Low Temp. Physics of the Faculty of Science of UPJŠ and IEP SAS, Košice, Slovakia

One of the fundamental question of the physics of manganites whether the phase segregated state (PSS) that develops in many systems can be described as a canonical spin-glass or it is a cluster-glass, representing ferromagnetic entities in nonmagnetic or antiferromagnetic matrix. To answer the question we have studied a colossal magnetoresistance (CMR) perovskite  $(Nd_{0.9}Y_{0.1})_{2/3}Ca_{1/3}MnO_3$  which possesses self-organized phase segregated state at low temperatures: two antiferromagnetic (AFM) phases and the ferromagnetic (FM) one coexist below 42 K [1]. The compound demonstrates common for the glassy magnetic systems features, such as a gap between zero field cold (ZFC) and field cold (FC) magnetization, specific frequency dependence of ac susceptibility. In this work we have shown that the compound possesses an exchange bias which is specific for cluster-glass systems.



Magnetic hysteresis loops were measured at 10 K by SQUID magnetometer technique after cooling the polycrystalline sample in zero field and after cooling in an applied field of  $H_{cool}=800$  Oe (Figure). The shifts along both magnetic field and magnetization axes have been found for FC but absent in ZFC process that manifests the exchange bias phenomenon. This effect is a result of a unidirectional exchange anisotropy interaction, which drives the FM clusters back to the original orientation when the magnetic field is removed. The magnetic field induced shift of the FC hysteresis loop was defined as

$H_{EB} = -(H_1 + H_2) / 2 \approx 387$  Oe, a coercive field was defined as  $H_C = (H_1 - H_2) / 2 \approx 132$  Oe, where  $H_1$  and  $H_2$  are the fields at which the magnetization equals zero. The vertical magnetization shift was defined as  $M_{EB} = (M_1 + M_2) / 2 \approx 3.7$  emu/g, the magnetic coercivity was defined as

$M_C = (M_1 - M_2) / 2 \approx 1.5$  emu/g, where  $M_1$  and  $M_2$  are the magnetizations at  $H=0$ . A ratio  $M_{EB} / M_s \approx 0.04$  found is large enough: its value is in a good agreement with the results for the related  $\text{Pr}_{2/3}\text{Ca}_{1/3}\text{MnO}_3$  compound [2], where nanodroplets of  $\sim 10$  Å in size were immersed within AFM host.

In summary, we have revealed intrinsic exchange coupling in the phase segregated  $(\text{Nd}_{0.9}\text{Y}_{0.1})_{2/3}\text{Ca}_{1/3}\text{MnO}_3$  at low temperatures, evident of the presence of small FM clusters immersed within the charge-ordered AFM phase.

[1] E. Fertman *et al*, *J. Magn. Magn. Mater.*, **321** (2009) 316.

[2] D. Niebieskikwiat and M. B. Salamon, *Phys. Rev. B*, **72** (2005) 174422.

22PO-J-21

## NANOPHASE SEPARATION AND MAGNETIC GLASS IN $\text{Nd}_{2/3}\text{Ca}_{1/3}\text{MnO}_3$

Kajňaková M.<sup>1</sup>, Feher A.<sup>1</sup>, Beznosov A.<sup>2</sup>, Fertman E.<sup>2</sup>, Desnenko V.<sup>2</sup>

<sup>1</sup>Centre of Low Temp. Physics of the Faculty of Science of UPJŠ and IEP SAS, Košice, Slovakia

<sup>2</sup>B. Verkin Institute for Low Temp. Phys. & Engin. of NASU, Kharkov 61103, Ukraine

Insulating perovskite  $\text{Nd}_{2/3}\text{Ca}_{1/3}\text{MnO}_3$  is a colossal magnetoresistance compound which possesses nano-phase segregated state at low temperatures: clusters of two antiferromagnetic (AF) phases and the ferromagnetic (FM) one coexist below 70 K [1]. Direct observation of magnetic domains shows that fine ferromagnetic particles are embedded in an antiferromagnetic matrix [2]. Here we have studied macroscopic low temperature magnetic properties of the compound. The data obtained, such as strongly divergent ZFC and FC static magnetizations (figure, left insert), frequency dependences of the *ac* magnetizations (figure, right insert) and the aging effect (figure), are

evident of the glassy behavior of the system. Magnetic field up to 5 T does not suppress completely the glassy state.

The rate of the frequency shift of the freezing temperature  $T_g$ , estimated as  $\partial \ln T_f / \partial \ln_{10} \omega \approx 0.02$ , is in a good agreement with analogous estimations, made for other glass systems [3].

Relaxation of the magnetization in the interval 0.5 min.  $< t < 30$  min. is described fairly well by the dependence

$M(t) = \sum_{i=0}^2 M_i \exp(-t/\tau_i)$ , where  $M_i$  are equal to 1.29, 0.004 and 0.027 emu/g for  $i = 0, 1$  and  $2$ , respectively, and corresponding relaxation times  $\tau_i$  are equal to  $\infty$ , 1.47 and 29.2 min. Weak dispersion of the dynamic magnetization (figure, right insert) points to a variety of relaxation times of the system.

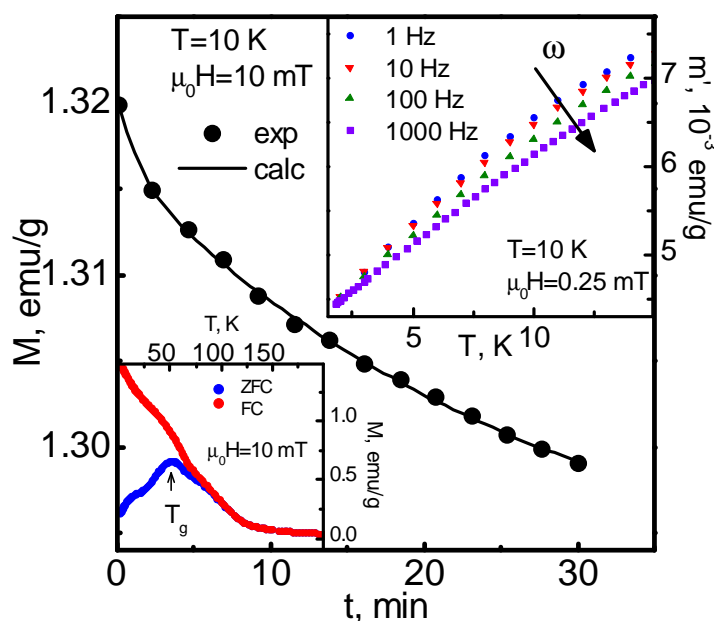


Fig. 1. Relaxation of the magnetization  $M(t)$  of the cluster glass compound  $\text{Nd}_{2/3}\text{Ca}_{1/3}\text{MnO}_3$  taken at 10 K after cooling in magnetic field 10 mT. Solid line is a fit of experimental data by a sum of two decay functions and a constant.

The data obtained permit to conclude that phase separation in the compound  $\text{Nd}_{2/3}\text{Ca}_{1/3}\text{MnO}_3$  leads to its cluster glass magnetic behavior.

The work is supported by Slovak Grant Agency VEGA-1/0159/09 and Grant of NAS of Ukraine № 01104006085.

- [1] C.D. Eee, F.G. Hhh, *J. Appl. Phys.*, **33** (1999) 133.  
 [2] Xiao-Juan Fan et al., *Phys. Rev. B* **65** (2002) 144401.  
 [3] S. Süllo et al., *Phys. Rev. Lett.* **78** (1997) 354.

22PO-J-22

## HIDDEN MARKOV MODEL AND THE PROCESSING OF OPTIC AND MAGNETO-OPTIC SPECTRA OF 3d OXIDES

Zenkov A.V.<sup>1</sup>, Zenkov E.V.<sup>1,2</sup>, Sazanova L.A.<sup>3</sup>, Inkina N.A.<sup>1</sup>, Trubina A.Yu.<sup>1</sup>

<sup>1</sup> Ural Federal University, Kuibishev St 88-43, Ekaterinburg 620100, Russia

<sup>2</sup> Institute of Metal Physics, Russian Academy of Sciences, Ekaterinburg 620219, Russia

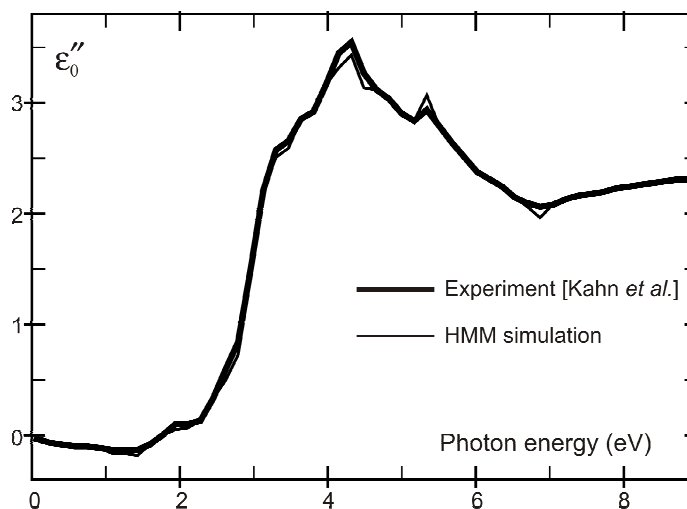
<sup>3</sup> Ural State University of Economics, Ekaterinburg 620144, Russia

The processing of experimental optic and magneto-optic spectra in the framework of some theoretical concept and the evaluation of theoretical microscopic parameters require the spectra fitting by the linear combination of Lorentz-shape dispersion lines and occasionally their derivatives with respect to resonance energy [1]. The number of parameters to be fitted (after tiny graphs in the journal publications) makes the standard least-squares method as good as inapplicable. We suggest an essentially different technique based on the hidden Markov models concept [2]. To our knowledge, no similar attempts have been made as yet.

In this concept, we associate an 'optimal' sequence of states to a sequence of observations, given the parameters of a model. A 'reasonable' optimality criterion consists of choosing the state sequence that has the maximum likelihood with respect to a given model. This sequence has been determined recursively via the Viterbi and Baum-Welch algorithms as well as the Kalman filtering [2].

As an example of our computation results, we present the figure showing the hidden Markov model simulation of an experimental spectral dependence for the yttrium iron garnet from the classical paper [3]. The agreement with the experimental data is excellent.

Using this technique allows us to obtain very reliable estimates of the microscopic parameters such as resonance energies, line widths, line strengths, etc.



The imaginary part of the diagonal component of the permittivity tensor  $\varepsilon_0 = \varepsilon'_0 + i\varepsilon''_0$  of  $\text{Y}_3\text{Fe}_5\text{O}_{12}$ : experimental data [3] (bold line) and hidden Markov model simulation result (thin line).

- [1] A.S. Moskvina, A.V. Zenkov, E.A. Gan'shina, G.S. Krinchik, M.M. Nishanova, *J. Phys. Chem. Sol.*, **54** (1993) 101.  
 [2] A.M. Fraser, Hidden Markov models and dynamical systems, SIAM, Philadelphia, 2008, 132p.  
 [3] F.J. Kahn, P.S. Pershan, J.P. Remeika, *Phys. Rev.*, **186** (1969) 891.

22PO-J-23

## MAGNETIC PROPERTIES OF SOME RARE EARTH OXYHALIDE CRYSTALS

Bunda V.<sup>1</sup>, Bunda S.<sup>1</sup>, Kovač J.<sup>2</sup>, Feher A.<sup>3</sup>

<sup>1</sup> Transcarpathian State University, Zankovetska St. 89-A, Uzhgorod 88015, Ukraine

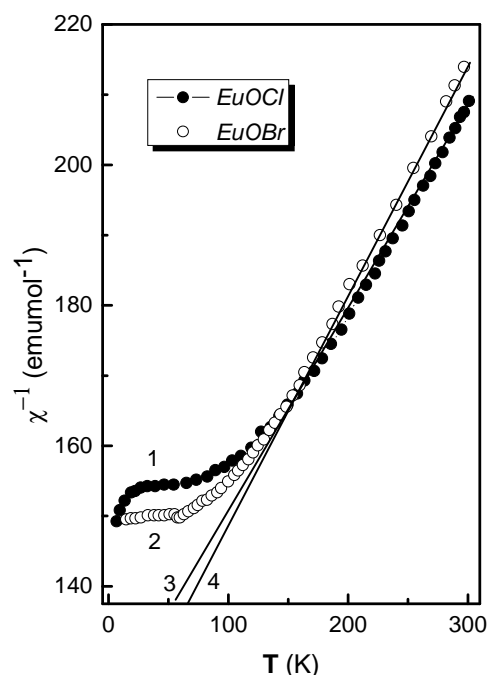
<sup>2</sup> Institute of Experimental Physics SAS, Watsonova 47, Košice, Slovakia

<sup>3</sup> P.J. Šafarik University, P. Angelinum 9, Košice 04154, Slovakia

The layered structure of rare earth oxycompounds REOHal (RE – Rare Earth; Hal= Cl, Br and I) suggests that materials of this type may exhibit 2D electronic and magnetic behavior. The quasi-2D nature of the host lattice has been confirmed e.g. by energy transfer and migration studies. The polycrystalline EuOCl and EuOBr samples were prepared by heating intimately ground mixtures of europium oxide,  $\text{Eu}_2\text{O}_3$  and ammonium halide,  $\text{NH}_4\text{Hal}$  in static  $\text{N}_2$  atmosphere. The magnetic susceptibilities for  $\text{Eu}^{3+}$  ( $\text{Eu}^{2+}$ ) ions in polycrystalline tetragonal europium oxychloride and oxybromide were measured in temperature region between 4,2 and 310 K. The susceptibilities of EuOCl and EuOBr follow the paramagnetic Curie–Weiss behavior down to low temperatures. The temperature dependence of the experimental paramagnetic susceptibility for EuOCl and EuOBr was simulated with the aid of the van Vleck formalism.

EuOCl and EuOBr samples studied thus present paramagnetic behavior down to low temperatures. However, at temperatures lower than 30–100 K, significant deviation from the linear Curie–Weiss behavior was observed for nearly every  $1/\chi_{\text{ave}}$  curve (see Fig.). This difference may be attributed either to the crystal field effect on the  $4f^N$  energy level scheme or to exchange interactions in the  $\text{Eu}^{3+}$  sublattice. The temperature dependence of the inverse magnetic susceptibility of EuOBr is complex: characteristic to a Curie–Weiss paramagnet at high temperatures, constant for the lower temperature range between 55 and 15 K and then sharply decreasing below 8 K. This behavior can be qualitatively explained by the exceptional  $^7F_J$  ( $J = 0-6$ ) ground term energy level scheme of the  $\text{Eu}^{3+}$  ion.

The  $^7F_0$  ground level is non-magnetic and gives no contribution to the susceptibility of EuOBr at low temperatures. Below 10 K, the sharp decrease in the inverse susceptibility is probably due to the presence of a slight amount of  $\text{Eu}^{2+}$  impurity. The  $\text{Eu}^{2+}$  ion with the  $4f^7$  electron configuration has high paramagnetic susceptibility. The  $\text{Eu}^{2+}$  impurity is present because of the reduction of  $\text{Eu}^{3+}$  by decomposing  $\text{NH}_4\text{Br}$  during the preparation of EuOBr.



The temperature evolution of the paramagnetic susceptibility for the EuOBr was mathematical simulated in a satisfactory manner with the van Vleck model using data for the free ion.

Support by Ukrainian Ministry of Education and Sciences and Slovakian Academy of Sciences

22PO-J-24

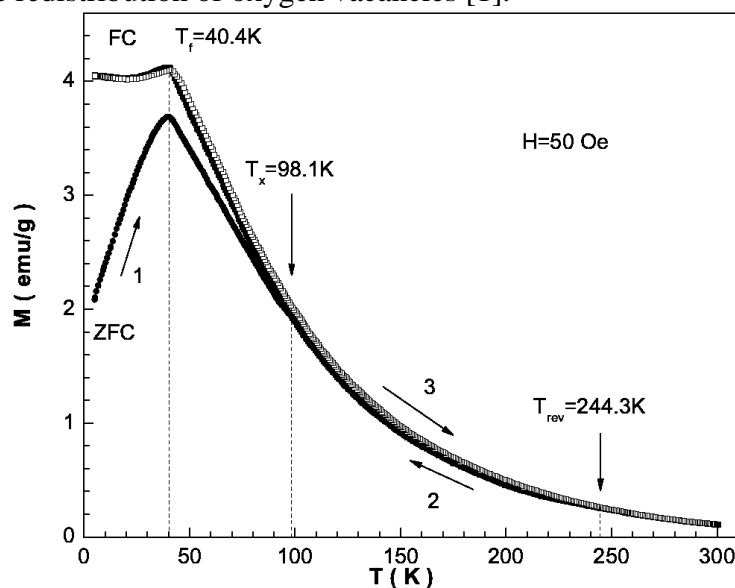
## MAGNETIC CLUSTER STATE IN THE ANION-DEFICIENT $\text{La}_{0.70}\text{Sr}_{0.30}\text{MnO}_{2.85}$ MANGANITE

*Trukhanov S.V.*

Scientific-Practical Materials Research Centre NAS of Belarus, 220072 Minsk, Belarus

(\*e-mail : [truhanov@ifttp.bas-net.by](mailto:truhanov@ifttp.bas-net.by))

The temperature and field dependences of the magnetic moment for the anion-deficient  $\text{La}_{0.70}\text{Sr}_{0.30}\text{MnO}_{2.85}$  manganite depending on the prehistory in the temperature 4-300 K range and external magnetic fields 0-140 kOe. It is established that the inhomogeneous magnetic state of the sample studied is a cluster spin glass and it is the result of the frustration of exchange  $\text{Mn}^{3+}\text{-O-Mn}^{3+}$  interactions due to the redistribution of oxygen vacancies [1].



Temperature dependence of ZFC (full circles) and FC (full squares in temperature decrease regime and open squares in temperature increase regime) specific magnetic moment in field of 50 Oe for the anion-deficient  $\text{La}_{0.70}\text{Sr}_{0.30}\text{MnO}_{2.85}$  manganite.

The increase of the external magnetic field at the beginning ( $H < 10$  kOe) leads to the fragmentation of ferromagnetic clusters, and then ( $H \geq 10$  kOe) it leads to the transition of the antiferromagnetic matrix to ferromagnetic state. The increase of the degree of polarization of local spins of manganese is observed. With increasing magnetic field up to 140 kOe the magnetic ordering temperature reaches  $\sim 160$  K [2]. The freezing temperature of the magnetic moments varies as  $T_f = 65 - 6H^{0.21}$ , while the temperature of the divergence of ZFC-and FC-curves varies as  $T_{\text{rev}} = 250 - 90H^{0.11}$ . It is established used the magnetic criterion that the phase transition into the paramagnetic state for the anion-deficient  $\text{La}_{0.70}\text{Sr}_{0.30}\text{MnO}_{2.85}$  manganite is a thermodynamic II-order phase transition. The causes and mechanism of the magnetic phase separation are discussed [3].

This work was supported by RFBR (grants № 10-02-90902 and № 11-02-90900).

- [1] S.V. Trukhanov, I.O. Troyanchuk et al., JETP Letters **83**, 33 (2006).  
 [2] S.V. Trukhanov, Technical Physics Letters, **37**, 350 (2011).  
 [3] S.V. Trukhanov, A.V. Trukhanov et al., JETP **111**, 209 (2010).

22PO-J-25

## DIVALENT AND TRIVALENT MANGANESE IN A-POSITION OF PEROVSKITE CELL OF SELF-DOPED LANTHANUM MANGANITES

*Ulyanov A.N.<sup>1</sup>, Pismenova N.E.<sup>1</sup>, Yang D.S.<sup>2</sup>, Levchenko G.G.<sup>1</sup>*

<sup>1</sup>Donetsk Physico-Technical Institute of National Academy of Sciences, 83114 Donetsk, Ukraine

<sup>2</sup>Department of Physics Education, Chungbuk National University, Cheongju 361-763, Republic of Korea

The *A*- and *B*- site substituted perovskite oxides ( $ABO_3$ ) have been studied intensively and their properties are carefully characterized in literature. The self (or vacancy)-doped  $La_{1-x}MnO_{3+\delta}$  (LMO) manganites are less carefully studied and their description contains some uncertainty. The problem is in the complexity of the self-doped manganites from the crystallochemistry point of view: how the structure accommodates the nonstoichiometry and vacancies. The magnetic and structural study of  $La_{1-x}MnO_{3+\delta}$  showed the fallout of  $Mn_3O_4$  oxide and segregation of vacancy-doped  $La_{0.9}MnO_{3+\delta}$  phase with  $x$  increase [1].

Recently, in the crystallochemistry [2] and powder neutron diffraction [3] characterizations, performed on the LMO samples with different La/Mn ratios, the *trivalent* Mn ions was suggested to substitute the La sites for La/Mn=0.91 composition. The authors of the two last papers noted that the local structure could be quite satisfactory refined in any distribution models (with and without Mn in the La sublattice) and without supporting additional evidence impossible to choose the proper one; also, at studying the  $Pr_{1-x}MnO_3$  [4] and  $La_{0.6}Sr_{0.4-x}MnTi_xO_3$  [5] compositions the *divalent* manganese in *A*-position of perovskite cell was detected.

To elucidate the noted peculiarities, we present the study of self-doped  $La_{1-x}MnO_{3+\delta}$  manganites ( $x=0.0, 0.05, 0.1$  and  $0.15$ ) with the x-ray powder diffraction analysis (XRD), magnetization measurements and x-ray absorption near edge structure (XANES) analysis. The  $x=0.0$  composition belongs to orthorhombic  $Pnma$  structure, and  $x=0.05, 0.1$  and  $0.15$  compounds exhibit the  $R\bar{3}c$  space group. No traces of any parasitic phases were detected by the XRD. Position and shape of the XANES spectra of the samples evidenced that the valence of the manganese is higher than 3+. No evidence of  $Mn^{2+}$  in the studied sample was observed. Curie temperature,  $T_C$ , of the samples equals to ~140, 160 and 180 K for the  $x=0.0, 0.05$  and  $0.1$  samples, respectively. The  $T_C$  of the  $x=0.15$  composition completely coincides with that of the  $x=0.1$  sample. All the data will be discussed (and explained) with suggesting that some amount of trivalent manganese occupy the *A*-position of perovskite cell.

- [1] P.A. Joy, S.R. Sankar, S.K. Date, *J. Phys.: Condens. Matter* **14** (2002) L663.  
 [2] R. Horyń, A. Sikora, E. Bukowska, *J. Alloys Comp.*, **353** (2003)153.  
 [3] M. Wołczyr, R. Horyń, F. Bourée, E. Bukowska, *J. Alloys Com.*, **353** (2003) 170-174.  
 [4] E. Pollert, Z. JirákJ. *Sol. State Chem.* **35** (1980) 262.  
 [5] A.N. Ulyanov, D.S. Yang, N. Chau, S.C. Yu, S.I. Yoo. *J. Appl. Phys.*, **103** (2008) 07F722.

## AB INITIO MODELING OF 3d METAL IMPURITIES INFLUENCE ON THE ELECTRONIC AND MAGNETIC PROPERTIES OF ZIRCON

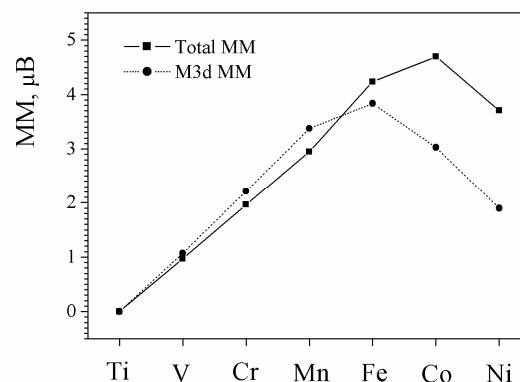
*Bannikov V.V., Shein I.R., Ivanovskii A.L.*

Institute of Solid State Chemistry, Ural Branch of RAS, Ekaterinburg,  
Pervomayskaya st., 91, Russia

In the frameworks of DFT-based band structure calculations (implemented in VASP code) we have investigated the influence of 3d-metal impurities (Ti, V, Cr, Mn, Fe, Co and Ni) on the electronic and magnetic properties of zircon. The super-cell modeling the formal stoichiometry  $Zr_{0.75}M_{0.25}SiO_4$  of doped crystal was used in the calculations.

The main results of our calculations may be summarized as follows. While the isoelectronic substitution  $Ti \rightarrow Zr$  takes place, the density of states (DOS) distribution for  $Zr_{0.75}Ti_{0.25}SiO_4$  does not suffer the significant changes as compared with pure zircon: the Ti 3d impurity states are mixed with the states of the filled valence band and empty conductivity band, therefore  $Zr_{0.75}Ti_{0.25}SiO_4$  is still non-magnetic wide band-gap semiconductor. This situation changes drastically when the V, Cr, Mn, Fe, Co and Ni impurities are introduced into zircon. The growth of the valence electrons concentration tends to partial filling of M-3d impurity states, which suffer the spontaneous spin polarization. As a result,  $Zr_{0.75}V_{0.25}SiO_4$  appears to be the magnetic semiconductor having the small band gap ( $\sim 0.5$  eV) which separates filled and empty sub-bands of V-3d $_{\uparrow}$  impurity states. At the same time,  $Zr_{0.75}Cr_{0.25}SiO_4$  is the so-called magnetic half-metal (MHM), because the sub-band of Cr-3d $_{\uparrow}$  states is partially filled, while the filled and empty Cr-3d $_{\downarrow}$  states are separated by the wide gap.  $Zr_{0.75}Mn_{0.25}SiO_4$  also has a DOS distribution of MHM type. Further,  $Zr_{0.75}Fe_{0.25}SiO_4$  is predicted to be a magnetic metal, where the maximal contribution to DOS at Fermi level ( $E_F$ ) is provided by Fe-3d $_{\uparrow}$  states, however,  $Zr_{0.75}Co_{0.25}SiO_4$  and  $Zr_{0.75}Ni_{0.25}SiO_4$  also “tend” to MHM state, where the spin-up states are of semiconducting type, while the spin-down ones contribute the non-zero DOS at  $E_F$ . In this way, the modification of  $Zr_{0.75}M_{0.25}SiO_4$  electronic properties in the M = Ti  $\rightarrow$  Ni series may be specified taking into account two factors: (I) the growth of valence electrons concentration while the atomic number Z of 3d metal increases, and (II) the shift of 3d metals impurity levels down towards  $E_F$ .

The results of calculations of atomic magnetic moments ( $MM^{at}$ ) and total magnetic moments per unit cell ( $MM^{tot}$ ) are presented in Figure. It is seen that their variation is non-monotonous, and  $Zr_{0.75}Co_{0.25}SiO_4$  exhibits the maximal values of magnetic moments. Further, it should be noted that for  $Zr_{0.75}(V,Cr,Mn)_{0.25}SiO_4$  systems the  $MM^{at} < MM^{tot}$  relation takes place, while for  $Zr_{0.75}(Fe,Co,Ni)_{0.25}SiO_4$  systems  $MM^{at} > MM^{tot}$ . This point may be explained taking into account the orientation of small magnetic moments induced by impurity on the nearest oxygen atoms. So, in  $Zr_{0.75}(V,Cr,Mn)_{0.25}SiO_4$  system they are oriented parallel to  $MM^{at}$ , while in  $Zr_{0.75}(Fe,Co,Ni)_{0.25}SiO_4$  the local anti-ferromagnetic ordering takes place. Note also, that for all doped systems under consideration the character of inter-atomic bonding does not change significantly as compared with pure zircon, being of mixed covalent-ionic type.





## THE INVESTIGATION OF PHASE TRANSITION IN THE THREE-DIMENSIONAL SITE-DILUTED POTTS MODEL

Murtazaev A.K.<sup>1,2</sup>, Babaev A.B.<sup>1,3</sup>, Aznaurova G.Y.<sup>1</sup>

<sup>1</sup> Russian Academy of Sciences Institution Kh. I. Amirkhanov Institute of Physics Daghestan Scientific Center of Russian Academy of Sciences Yaragского Str. 94, Makhachkala, Russia

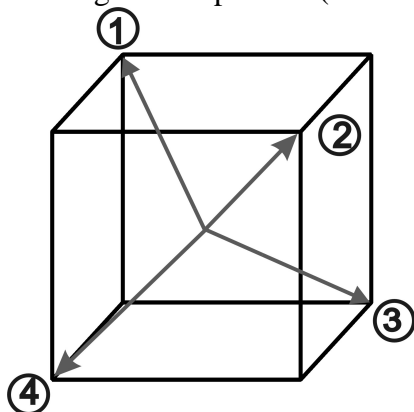
<sup>2</sup> Daghestan State University, ul. Gadzhieva 43a, Makhachkala, 367000, Russia

<sup>3</sup> Daghestan State Pedagogical University, Yaragского Str. 57, Makhachkala, 367000, Russia

An influence of impurities and different defects on the phase transitions and critical phenomena of magnetic systems is one of more actual subjects of the phase transition theory [1]. A majority of real solids contain impurities and other structure defects which influence on their thermodynamic characteristics, particularly, a behavior of the systems of the phase transitions. Therefore lately the attentions of researchers are directed at understanding how the structure defects influence on a behavior of different systems at the phase transitions. When study the critical properties of disordered spin systems are distinguished the systems with quenched and annealed impurities. In solids the impurities are usual quenched. A presence of quenched impurities is revealed as random disturbance of the local critical temperature. In a case of the spin systems, experiencing the first order phase transitions in a homogeneous state, the impurities lead to softening of this transition close to induction the second order phase transition in them [2].

In this work, the influence of quenched nonmagnetic impurities on the phase transitions in the three-dimensional 4-state Potts model was studied by the Monte-Carlo method.

Constructing three-dimensional 4-state Potts models on a simple cubic lattice one should remember that in sites of the lattice locate spins  $S_i$ , which can be in one of  $q \geq 2$  states (see Fig.1) and nonmagnetic impurities (vacancies).



The Hamiltonian of studied system can be written as:

$$H = -\frac{1}{2} J \sum_{i,j} \rho_i \rho_j \delta(S_i, S_j), \quad S_i = 1, 2, 3, 4 \quad (1)$$

where  $\delta(S_i, S_j) = \begin{cases} 1, & \text{если } S_i = S_j \\ 0, & \text{если } S_i \neq S_j \end{cases}$ ,  $S_i, S_j = \pm 1$ ,  $\rho_i = 1$ , if a site  $i$  is

occupied by the magnetic atom, and  $\rho_i = 0$ , if in a site  $i$  locates the nonmagnetic impurity,  $J$  is the exchange interaction. The investigation is carried out on the basis of Monte-Carlo method. The systems of non-linear sizes  $L_x L_x L_x$ ,  $L = 20-44$  at the spin concentrations  $p = 1.00; 0.90; 0.70; 0.65$  are researched.

By means of the fourth order Binder cumulants method the second order phase transition is shown to be observed in this model at spin concentration  $p = 0.70; 0.65$ , and for pure model ( $p = 1.00; 0.90$ ) to be occurred the first order phase transition. On the basis of the finite-size scaling theory are calculated the static critical exponents of heat capacity  $\alpha$ , susceptibility  $\gamma$ , magnetization  $\beta$  and exponent of correlation radius  $\nu$

Support by RFBR (№ 09-02-96506), PHCP (№ П554 и № 02.740.11.03.97) is acknowledged.

[1] J.M. Ziman. J.M. Ziman. *Models of disorder* (Cambridge University Press, London-New York, 1979)

[2] Y. Imry, M. Wortis, *Phys. Rev. B*, **19** (1979) 3580.

## EFFECT OF PARTIAL OXYGEN ISOTOPE SUBSTITUTION ON THE PHASE DIAGRAM OF $(\text{Pr}_{1-y}\text{Eu}_y)_{0.7}\text{Ca}_{0.3}\text{CoO}_3$ COBALTITES

*Babushkina N.A.<sup>1</sup>, Taldenkov A.N.<sup>1</sup>, Kalinov A.V.<sup>2</sup>, Kuz'mova A.V.<sup>3</sup>, Kamenev A.A.<sup>3</sup>, Kaul A.R.<sup>3</sup>*

<sup>1</sup> Institute of Molecular Physics, Research Center "Kurchatov Institute", 123182 Moscow, Russia

<sup>2</sup> All-Russian Electrical Engineering Institute, 111250 Moscow, Russia

<sup>3</sup> Department of Chemistry, Moscow State University, 119991 Moscow, Russia

The effect of  $^{16}\text{O} \rightarrow ^{18}\text{O}$  isotope substitution on the properties of  $(\text{Pr}_{1-y}\text{Eu}_y)_{0.7}\text{Ca}_{0.3}\text{CoO}_3$  cobaltites ( $0.12 < y < 0.26$ ) was studied earlier in our paper [1]. We have found that with increasing Eu content, the ground state of the compound changes from a "nearly-ferromagnetic metal" to a "weakly-magnetic insulator" at  $y < y_{cr} = 0.18$ . A pronounced spin-state transition (SST) was observed for the insulating ground state (in the samples with  $y > y_{cr}$ ), whereas in the metallic ground state (at  $y < y_{cr}$ ), the magnetic properties were quite different, without any indications of a temperature-induced SST. Using the magnetic, electrical, and thermal data, we constructed a phase diagram for this material. The characteristic feature of this phase diagram is a broad crossover range near  $y_{cr} \approx 0.18$  corresponding to a competition of the phases mentioned above. The  $^{16}\text{O} \rightarrow ^{18}\text{O}$  substitution gives rise to an increase in the SST temperature  $T_{SS}$  and to a slight decrease in the ferromagnetic transition temperature  $T_{FM}$ .

The unique sensitivity of the transition temperatures to the changes in the average oxygen mass stimulated our experiments on the partial oxygen isotope substitution, which allowed us to perform a detailed study of the phase diagram in the crossover region, where the effects of phase separation play a dominant role. We prepared a series of the cobaltite samples with the different degrees of enrichment by the heavy oxygen isotope  $^{18}\text{O}$ , namely, 90%, 67%, 43%, 17%, and 0%. This allowed us to achieve a nearly continuous tuning of the sample characteristics with the emphasis on tracing the evolution of relative content of different phases as a function of the  $^{18}\text{O}/^{16}\text{O}$  ratio. The Eu doping of the samples was chosen to be near and on the both sides of the crossover doping level  $y_{cr}$ : a composition with the high Eu content exhibiting the SST, a low-Eu composition corresponding to the nearly ferromagnetic state, and the sample at the phase crossover, where both  $T_{SS}$  and  $T_{FM}$ , were observed. For all samples, we performed the measurements of the temperature dependence of the ac magnetic susceptibility  $\chi(T)$  and electrical resistivity  $\rho(T)$ . Based on these measurements, we were able to analyze the evolution the sample properties with the change Eu and  $^{18}\text{O}$  content. An increase in the oxygen mass as well as in the Eu content gives rise to an increase in  $T_{SS}$  and to a slight decrease in  $T_{FM}$ .

The work was supported by the Russian Foundation for Basic Research, project 10-02-00598-a, and by the Russian-German project DFG-GR 1484/2-1.

[1] A.V. Kalinov, O.Yu. Gorbenko, A.N. Taldenkov, *et al.*, *Phys. Rev. B*, **81** (2010) 134427.

22PO-J-29

## EFFECT OF PRASEODYMIUM DOPING ON MAGNETIC AND KINETIC PROPERTIES OF $\text{La}_{0.6}\text{Pr}_{0.1}\text{Ca}_{0.3}\text{MnO}_3$

*Zainullina R.I.<sup>1</sup>, Bebenin N.G.<sup>1</sup>, Ustinov V.V.<sup>1</sup>, Mukovskii Ya.M.<sup>2</sup>*

<sup>1</sup> Institute of Metal Physics, UD RAS, 18 Kovalevskaya St., Ekaterinburg 620990, Russia,

<sup>2</sup> Moscow State Steel&Alloys Institute, Leninskii prospect, 4, Moscow 119049, Russia

The lanthanum manganites  $\text{La}_{1-x}\text{D}_x\text{MnO}_3$  (D=Ca, Sr, or Ba) attract attention due to colossal magnetoresistance (CMR) that is observed near Curie temperature  $T_C$ . A characteristic feature of the manganites is the strong interaction between the charge carriers, localized spins, and crystal lattice. The properties of the materials depend on the type of a divalent metal. In La-Sr and La-Ba crystals the magnetic transition always is second order while in La-Ca crystals with  $x$  around  $\frac{1}{3}$  the transition is first order, which results in strong peculiarities of magnetic, elastic, and transport properties near  $T_C$  [1, 2]. The properties of the lanthanum manganites can be changed also by substitution of Pr for La, because first the ionic radius of  $\text{Pr}^{3+}$  is less than that of  $\text{La}^{3+}$  and second in contrast to lanthanum the praseodymium ion has magnetic moment.

The aim of our work is to study temperature and magnetic-field dependences of magnetization, resistivity, thermopower in  $\text{La}_{0.6}\text{Pr}_{0.1}\text{Ca}_{0.3}\text{MnO}_3$  single crystal grown by floating zone method and to compare the data obtained with those for the crystal of  $\text{La}_{0.7}\text{Ca}_{0.3}\text{MnO}_3$

The temperature dependence of magnetization is similar to that for  $\text{La}_{0.7}\text{Ca}_{0.3}\text{MnO}_3$ . The magnetic transition in Pr doped crystal is first order as in Pr-free one but  $T_C$  is lower. Application of a magnetic field results in increase of the Curie temperature with rate  $B_M=0.8$  K/kOe. The spontaneous magnetization of  $\text{La}_{0.6}\text{Pr}_{0.1}\text{Ca}_{0.3}\text{MnO}_3$  is a little higher than that of  $\text{La}_{0.7}\text{Ca}_{0.3}\text{MnO}_3$ , which can be an evidence for the ferromagnetic coupling between Mn and Pr magnetic moments.

The low temperature resistivity obeys the relation  $\rho(T) = \rho(0) + AT^2$ , which is typical for CMR manganites in metallic state. Near  $T_C$  the well-known peak of resistivity is observed and the peak resistivity in the Pr-doped crystal is significantly greater than in Pr-free crystal. In the paramagnetic state,  $\text{La}_{0.6}\text{Pr}_{0.1}\text{Ca}_{0.3}\text{MnO}_3$  crystal is in semiconductor state with activation energy of  $E_a=88$  meV, which is close to  $E_a=78$  meV in  $\text{La}_{0.7}\text{Ca}_{0.3}\text{MnO}_3$  single crystal.

Magnetoresistance  $\frac{\Delta\rho}{\rho} = \frac{\rho(H) - \rho(0)}{\rho(0)}$  reaches maximum in the transition region and the peak value of  $\Delta\rho/\rho$  is as high as 80% in the field of 10 kOe. The temperature dependence of  $\Delta\rho/\rho$  at a given magnetic field  $H$  is well described by the relation obtained in [2]

$$\frac{\Delta\rho(T, H)}{\rho} = \frac{\rho(T - \Delta T_C(H)) - \rho(T)}{\rho(T)}$$

where  $\rho(T) = \rho(T, H = 0)$ ,  $\Delta T_C = B_M H$ .

In the magnetic transition region, the temperature dependence of thermopower of  $\text{La}_{0.6}\text{Pr}_{0.1}\text{Ca}_{0.3}\text{MnO}_3$  is sharper than that of  $\text{La}_{0.7}\text{Ca}_{0.3}\text{MnO}_3$ .

Support by RFBR grant No. 09-02-00081 and by the Program №18 of Presidium of RAS is acknowledged.

[1] R.I.Zainullina, N.G.Bebenin, V.V.Ustinov, Ya.M.Mukovskii, D.A.Shulyatev, Phys.Rev., **B76**, 0144408 (2007).

[2] N.G.Bebenin, R.I.Zainullina, N.S.Bannikova, V.V.Ustinov, Ya.M.Mukovskii, Phys.Rev., **B78**, 064415 (2008).

22PO-J-30

## LOW-FIELD MAGNETIC PROPERTIES OF $\text{La}_{0.7}\text{Sr}_{0.3}\text{Mn}_{0.9}\text{Cu}_{0.1}\text{O}_3$

Zakhvalinskii V.<sup>1</sup>, Lashkul A.<sup>2</sup>, Lähderanta E.<sup>2</sup>, Pilyuk E.<sup>1</sup>, Mashirov A.<sup>1</sup>

<sup>1</sup> Department of Physics, Belgorod State University, RUS-308015 Belgorod, Russia

<sup>2</sup> Department of Mathematics and Physics, Lappeenranta University of Technology, PO Box 20, FIN-53851 Lappeenranta, Finland

$\text{La}_{0.7}\text{Sr}_{0.3}\text{Mn}_{0.9}\text{Cu}_{0.1}\text{O}_3$  sample was obtained with the conventional solid-state reaction method [1]. Magnetization  $M$  ( $T$ ) was measured with an RF-SQUID magnetometer after cooling the sample from the room temperature down to 5 K in fields of  $B = 70$  G, 1 kG and 10 kG ( $\chi_{\text{FC}}$  or field-cooled) or in zero magnetic field ( $\chi_{\text{ZFC}}$  or zero-field cooled). Temperature dependence of the thermoremanent magnetization (TRM) was measured after cooling the sample from 300 K down to 3 K in the field of 10 G and then reducing the field to zero.

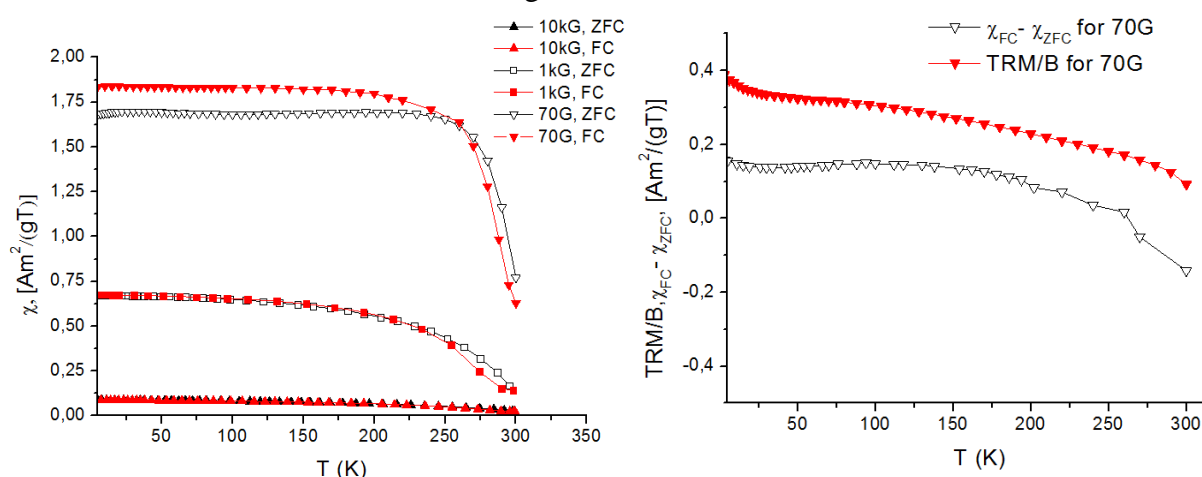


**Figure 1.** Temperature dependences of  $\chi_{\text{ZFC}}$  and  $\chi_{\text{FC}}$  in LSMCO sample at  $B = 70$  G, 1 kG, 10 kG (left panel) and temperature dependences of  $\text{TRM}/B$  and  $\chi_{\text{FC}} - \chi_{\text{ZFC}}$  (left panel).

Additional features of the magnetic irreversibility in LSMCO are displayed in the left panel of figure 1, where the plots of the  $\text{TRM}/B$  versus  $T$  are compared with the difference of  $\chi_{\text{FC}}(T) - \chi_{\text{ZFC}}(T)$ . One can see clear divergence of these plots for 70 G. The irreversible magnetic behavior in figure 1 left panel indicates a frustrated magnetic state of LSMCO. Such behavior is pertinent to spin-glass (SG) or cluster-glass (CG) phases, which set in below the onset of freezing of the magnetic moments in conditions of competing interactions between the moments [2]. In the SG phase the expression  $\text{TRM}/B(T) = \chi_{\text{FC}}(T) - \chi_{\text{ZFC}}(T)$  reflects a symmetry of the energy distribution of potential barriers in the presence or absence of the external magnetic field [3]. In the CG phase this symmetry may be broken due to the anisotropy, associated with the shape and orientation of the magnetic clusters, leading to violation of the expression above [3]. On the other hand, such behavior implies an important role of large and strongly-correlated FM clusters, attributable to percolation over a system of hole-rich FM particles.

Work at Belgorod State University was supported by Grant GC № 02.740.11.0399.

[1] Coey J M D, Viret M and von Molnar S 1999 *Adv. Phys.* **48** 167

[2] Dagotto E 2002 *Nanoscale Phase Separation and Colossal Magnetoresistance* (Berlin: Springer)

[3] Lähderanta E, Eftimova K, Laiho R, Kanani H Al and Booth J C 1994 *J. Magn. Magn. Mater.* **130** 23

## ANOMALIES OF ELASTIC PROPERTIES AT PHASE TRANSITIONS IN RARE EARTH COBALTITES $\text{RBaCo}_4\text{O}_7$ ( $\text{R} = \text{Y}, \text{Er} - \text{Lu}$ )

*Kazei Z.A., Snegirev V.V., Kozeeva L.P., Kameneva M.Yu.*

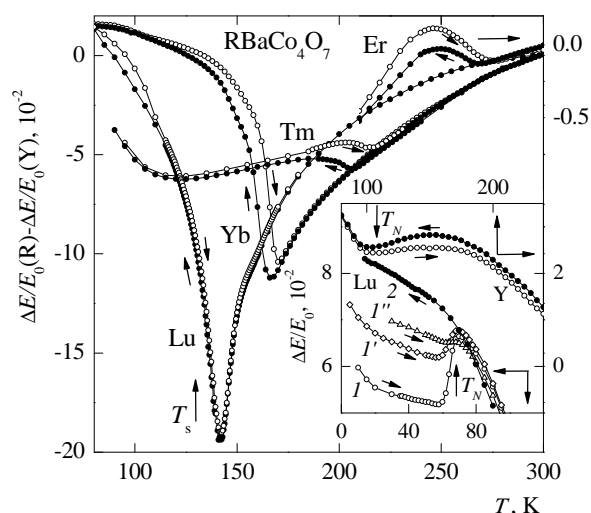
Moscow State University, 119991 Moscow, Russia

Rare earth (RE) cobaltites  $\text{RBaCo}_4\text{O}_7$  characterized by geometrical frustration of exchange interactions and coupled 3d- and 4f- subsystems have attracted considerable interest due to their remarkable magnetic and electronic properties. The hexagonal structure  $P6_3mc$  of these compounds undergoes orthorhombic distortions at temperature lowering and the temperature of structural phase transition (SPT)  $T_s$  monotonously goes down when the RE ion radius reduces. Distortion of structure at PT removes the frustration of the exchange interactions in the Kagome lattice and thus affects magnetic PT (MPT) in the Co subsystem at  $T_N < T_s$ . In the present work elastic properties for RE cobaltites  $\text{RBaCo}_4\text{O}_7$  are investigated in the range of SPT and MPT.

Young's modulus  $E$  and internal friction coefficient  $q^{-1}$  were measured by the composite resonator method at frequency  $\sim(110 - 200)$  kHz in the temperature range (4.2 - 300) K on polycrystalline samples  $\text{RBaCo}_4\text{O}_7$  ( $\text{R} = \text{Y}, \text{Er} - \text{Lu}$ ). Significant softening of Young's modulus for these cobaltites is found at temperature decrease, showing an instability of the crystal structure and accompanying with a reverse jump at SPT. The contribution to the Young's modulus due to the SPT (when taking into account the phonon contribution) exhibits a distinct regularity throughout the RE cobaltite series (Fig.). For the last Lu compound, the temperature  $T_s$  is the lowest, while the softening and jump of Young's modulus reach the maximal value  $\Delta E(T)/E_0 \approx 2 \cdot 10^{-1}$  ( $\Delta E(T) = E(T) - E_0$ ). Softening and jump decrease more than by the order of value, while the temperature  $T_s$  and hysteresis  $\Delta T_s$  enlarge from Lu- to Tm- and Er- compounds. Hexagonal structure remains stable up to lower temperatures when the RE ion size reduces. SPT is accompanied by a maximum of absorption at  $T_s$  and an additional maximum below  $T_s$ . Besides a huge absorption maximum  $q^{-1} \approx 10^{-1}$  is observed at  $T_{\text{max}} \approx 90$  K for all the RE cobaltites whose relation to SPT is not clear.

Elastic anomaly at the MPT in Lu cobaltite is less by the order of magnitude, than at SPT and its value depends on experimental conditions (insert in Fig.). For other RE cobaltites elastic anomalies at MPT are of qualitatively different character (Y cobaltite in insert).

Comparison of elastic properties at SPT is performed for RE cobaltites and RE zircons with cooperative Jahn-Teller effect. The essential softening of Young's modulus allows to assume, that the corresponding elastic constant goes to a zero at SPT in Lu- and Yb cobaltites. On the contrary, in Tm- and Er cobaltites this constant is not a "soft" mode of PT. Various models of SPT in RE cobaltites are discussed.



This work is supported by RFBR, Gr. 10-02-00532.



**22 August**

Monday

17:30-19:00

poster session  
22PO-K

**“Magnetophotonics”**

22PO-K-1

## ULTRAFAST PHOTOINDUCED MAGNETIZATION DYNAMICS IN ULTRATHIN Co/GARNET HETEROSTRUCTURES

*Pashkevich M.<sup>1,3</sup>, Atoneche F.<sup>2</sup>, Stupakiewicz A.<sup>1</sup>, Maziewski A.<sup>1</sup>, Kimel A.<sup>2</sup>, Kirilyuk A.<sup>2</sup>,  
Stognij A.<sup>3</sup>, Novitskii N.<sup>3</sup>, Rasing Th.<sup>2</sup>*

<sup>1</sup> Laboratory of Magnetism, University of Bialystok, Lipowa 41, Bialystok, Poland

<sup>2</sup> Radboud University Nijmegen, Institute for Molecules and Materials, Heyendaalseweg 135,  
Nijmegen, The Netherlands

<sup>3</sup> Scientific-Practical Materials Research Centre of the NASB, P. Brovki 19, Minsk, Belarus

Large ultrafast photoinduced magnetic anisotropy has been observed in Co substituted YIG films [1]. In such garnet films the phase of the photoinduced magnetization precession depends on the polarization of the light. After deposition of ultrathin ferromagnetic layers on a garnet film one can expect new effects of ultrafast magnetization dynamics due to the influence of the effective magnetic field of the ferromagnetic layer or a coupling between ferromagnetic layer and garnet.

The initial garnet film was grown using liquid phase epitaxy and had a thickness of 5.8  $\mu\text{m}$ . Afterwards it was thinned down to 1.8  $\mu\text{m}$  by oxygen ion beam etching in the low energy regime. Au(4nm)/Co(2nm)/garnet(1.8 and 5.8  $\mu\text{m}$ ) heterostructures were then obtained by ion-beam sputter deposition.

A strong influence of a 2 nm Co layer on the domain structure geometry, magnetization processes and coercive field has been found for 1.8  $\mu\text{m}$  garnet films. The observed magnetization reversal process in the heterostructure could be explained by both thickness-driven magnetic anisotropy of the garnet films and a strong magnetostatic coupling between Co and garnet films.

Ultrafast magnetization dynamics of garnet films and Co/garnet heterostructures were studied by time-resolved measurements using an optical pump-probe technique. The amplitude and precession frequency were measured as functions of external magnetic field and linear polarization of the pump light. These experimental results are discussed taking into account the following contributions to the total magnetic anisotropy energy in the heterostructure: cubic anisotropy, light-induced and in-plane uniaxial anisotropies.

This work was supported by the EU Seventh Framework, Programme FP7/2007-2013 under grant N214810 FANTOMAS.

[1] F.Atoneche, A.M.Kalashnikova, A.V.Kimel, A.Stupakiewicz, A.Maziewski, A.Kirilyuk, and Th.Rasing, Phys. Rev. B 81, 214440 (2010).



## MAGNETO-OPTIC EDDY CURRENT INTROSPECTIVE: MAGNETOGRAPHY VERSUS STROBOSCOPIC TECHNIQUE

Vishnevskii V.<sup>1</sup>, Berzhansky V.<sup>1</sup>, Mikhailov V.<sup>1</sup>, Pankov F.<sup>1</sup>, Levy S.<sup>2</sup>, Agalidy Yu.<sup>2</sup>

<sup>1</sup> Taurida National University, Vernadsky ave. 4, Simferopol, 95007, Ukraine

<sup>2</sup> NTUU "Kiev Polytechnic Institute", Pobedy str. 37, Kiev, 03056, Ukraine

Eddy current (EC) introspection with use of magneto-optic (MO) garnet films (GF) is a new effective tool in non-destructive control of metallic constructions mostly for the crack detection in aerospace units [1]. Known technical realizations are based on coil-type EC inductors, GF MO converters and problem-oriented software for real-time video data processing [2]. As a rule, GF are mono-crystalline, uniaxial anisotropy and low coercive. Taking into account both the films domain structure (DS) dependence on the external magnetic field distribution and the interference of EC and video framing, it is necessary to provide stroboscopic illumination. In practice MO EC image is slightly differs from the real defect geometry (Fig. 1, a, b) and this difference is conditioned by the metal type investigated, the GF's properties and EC inductor's features. Because the revelation ability of real-time MO EC introspection is limited in some cases magneto-graphic technique can be applied. Thus, besides the stroboscopic scheme the authors of this report modeled two variants of MO EC magnetographic devices: with intermediate magnetic tape and without it. For the second case MO GF was synthesized high-coercive but with artificially decreased Curie temperature  $T_C$ . Heating the garnet layer up to  $T > T_C$  during the short packet of pulses in EC inductor it was possible to observe "printed" [3] thermo-recorded MO images of inner inhomogeneities in different metallic objects such as thin welded joints in polished aluminum plates (Fig. 1, c, d). Coil-, frame- and bus-type EC inductors, bipolar and unipolar excitation currents (100 Hz-40 kHz) were approved in the experiments. GF were grown by means of liquid phase epitaxy on (111)-oriented  $Gd_3Ga_5O_{12}$  substrates. High-coercive GF's properties were: composition  $(Bi, Lu, Sm, Ca)_3(Fe, Ga, Al, Sc)_5O_{12}$ , Curie point  $T_C=55-70$  °C, coercivity ( $T=20$  °C)  $H_c=100-250$  Oe, DS period  $2w_T=4-6$   $\mu m$  (meta-stable) and  $2w_H=10-16$   $\mu m$  (stable). Low-coercive films of  $(Bi, Eu, Lu)_3(Fe, Ga, Al)_5O_{12}$  were characterized by coercivity  $H_c=0.5-0.7$  Oe and DS period  $2w=35-40$   $\mu m$ . Total Faraday rotation was  $\sim 5-6^\circ$  ( $\lambda=0.63$   $\mu m$ ). All the films were covered with TiN layers by vacuum deposition. Heating of high-coercive GF was realized by electric current pulses (3-5 A, 10 ms) propagated through the cover.



Fig. 1. Surface (a) and MO EC image (b) of 10  $\mu m$  slot in thin Al plate (stroboscopic mode); surface and MO EC image of defect-free welded joint in thick Al plate (magnetographic mode).

[1] Development of an improved magneto optic/eddy current imager. Final report DOT/FAA/AR-97/37, Office of Aviation Research, Washington DC, 20591, 1998.

[2] Y. Deng, X. Liu, Y. Fan, Z. Zeng, L. Udpa, W. Shih, *IEEE Trans. Magn.*, **42** (2006) 3228.

[3] V. Vishnevskii, A. Nesteruk, A. Nedviga, S. Dubinko, A. Prokopov, *Sens. Lett.*, **5** (2007) 29.

## LONGITUDINAL KERR EFFECT ENHANCEMENT IN 2D MAGNETOPLASMONIC CRYSTALS

*Chetvertukhin A.V.<sup>1</sup>, Baryshev A.V.<sup>2</sup>, Dolgova T.V.<sup>1</sup>, Uchida H.<sup>3</sup>, Inoue M.<sup>2</sup>, Fedyanin A.A.<sup>1</sup>*

<sup>1</sup>Lomonosov Moscow State University, Faculty of Physics, Leninskie gory 1, Moscow, Russia

<sup>2</sup>Toyohashi University of Technology, Tempaku, Toyohashi 441-8580, Japan

<sup>3</sup>Tohoku Institute of Technology, Taihaku, Sendai 982-8577, Japan

The significant enhancement of transversal Kerr effect can be achieved in presence of surface-plasmon resonance [1]. In this paper the longitudinal Kerr effect (LKE) enhancement is observed in plasmonic nickel structure.

The samples are a 2D periodical nickel columns on a bulk nickel substrate with height of approximately 50 nm and diameter of 290 nm. Columns are packed in hexagonal lattice. Period of the structure is of 500 nm (Fig. 1).

Fig. 2. shows experimental linear reflection spectra of the sample. Reflectance minimum shift in the dependence on azimuthal angle yielded by coupling of incident beam energy to resonantly excited surface plasmon-polariton (SPP).

Dependences for two angles of incidence  $40^\circ$  and  $45^\circ$  and two key azimuthal angles  $240^\circ$  and  $270^\circ$  are measured. Fig. 3. shows a LKE spectrum for azimuthal angle  $240^\circ$  (equivalent to  $300^\circ$  and  $360^\circ$  on Fig. 2.).

Significant LKE enhancement at 725 nm coincides with surface plasmon-polariton resonance at 725 nm that can be seen on Fig. 2 at azimuthal angle  $300^\circ$  and  $360^\circ$ . Experimental LKE spectra shows shift of LKE resonance together with SPP resonance while changing azimuthal angle of sample. Thus the gain of LKE effect is associated with SPP resonance.

[1] A. A. Grunin, A. G. Zhdanov, A. A. Ezhov, E. A. Ganshina, and A. A. Fedyanin, *Applied Phys. Lett.*, 97 (2010) 261908.

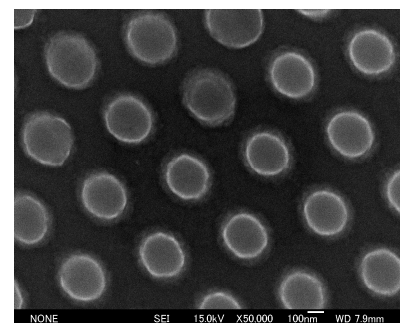


Fig 1. SEM image of experimental sample (nickel columns on bulk nickel).

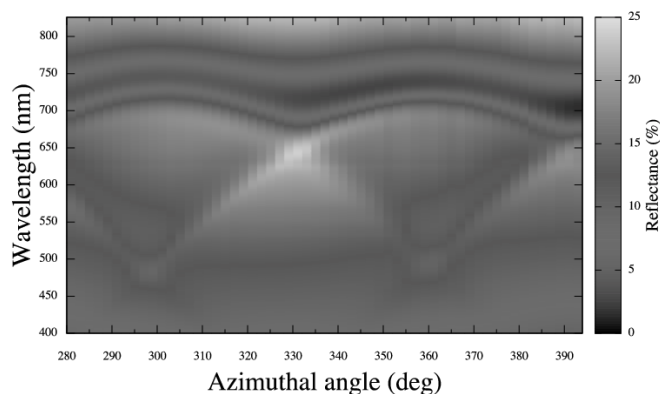


Fig. 2. Azimuthal angle linear reflectance spectra.

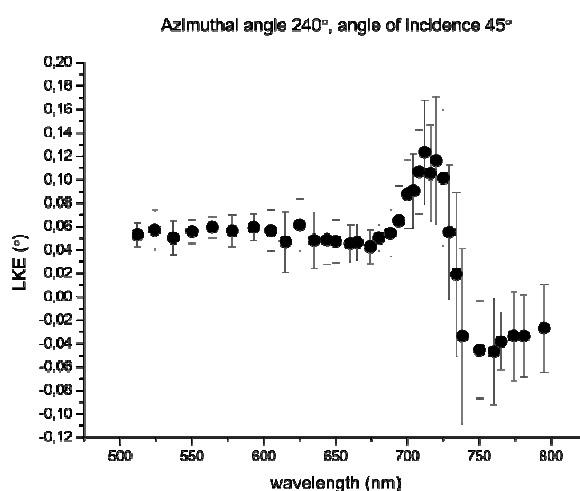


Fig. 3. LKE spectrum at azimuthal angle  $240^\circ$  and angle of incidence  $45^\circ$ .

22PO-K-4

## SPECTRA, ENERGY LEVELS, AND SYMMETRY ASSIGNMENTS FOR STARK COMPONENTS OF $\text{Eu}^{3+}(4f^{6})$ IN GADOLINIUM GALLIUM GARNET GGG ( $\text{Gd}_3\text{Ga}_5\text{O}_{12}$ )

*Gruber J.B.<sup>1</sup>, Valiev U.V.<sup>2</sup>, Burdick G.W.<sup>3</sup>, Rakhimov S.A.<sup>2</sup>, Pokhrel M.<sup>1</sup>, Sardar D.K.<sup>1</sup>*

<sup>1</sup> Department of Physics and Astronomy, The University of Texas at San Antonio, San Antonio, Texas 78249, USA

<sup>2</sup> Faculty of Physics, National University of Uzbekistan, Vuzgorodok, Tashkent 100174, Uzbekistan

<sup>3</sup> Department of Physics, Andrews University, Berrien Springs, Michigan 49104, USA

Absorption and fluorescence spectra observed between 450 nm and 750 nm at 85 K and room temperature (300 K) are reported for  $\text{Eu}^{3+}(4f^{6})$  in single-crystal Czochralski-grown garnet,  $\text{Gd}_3\text{Ga}_5\text{O}_{12}$  (GGG) [ ]. The spectra represent transitions between the  $^{2S+1}L_J$  multiplets of the  $4f^{6}$  electronic configuration of  $\text{Eu}^{3+}$  split by the crystal field of the garnet. In absorption,  $\text{Eu}^{3+}$  transitions are observed from the ground state,  $^7F_0$ , and the first excited multiplet,  $^7F_1$ , to multiplet manifolds  $^5D_0$ ,  $^5D_1$  and  $^5D_2$ . The Stark splitting of the  $^7F_J$  multiplets ( $J = 0 \div 6$ ) was determined by analyzing the fluorescence transitions from  $^5D_0$ ,  $^5D_1$ , and  $^5D_2$  to  $^7F_J$ . The  $\text{Eu}^{3+}$  ions replace  $\text{Gd}^{3+}$  ions in sites of  $D_2$  symmetry in the lattice during crystal growth. Associated with each multiplet manifold are  $(2J+1)$  non-degenerate Stark levels characterized by one of four possible irreducible representations (irreps.) assigned by an algorithm based on the selection rules for electric-dipole (ED) and magnetic-dipole (MD) transitions between Stark levels in  $D_2$  symmetry. The quasi-doublet in  $^5D_1$  was characterized by an analysis [1] of the magnetic circular dichroism (MCD) and magnetic circular polarization of luminescence (MCPL) spectra measured on the allowed (on symmetry) optical transitions observed between  $^5D_1$  and  $^7F_1$  multiplets. A parameterized Hamiltonian defined to operate within the entire  $4f^{6}$  electronic configuration of  $\text{Eu}^{3+}$  was used to model the experimental Stark levels and their irreps. The crystal-field parameters were determined through use of a Monte-Carlo method in which nine independent crystal-field parameters,  $B_q^k$ , were given random starting values and optimized using standard least-squares fitting between calculated and experimental levels. The final fitting standard deviation between 57 calculated-to-experimental Stark levels is  $5.9 \text{ cm}^{-1}$ . The choice of coordinate system, in which the nine  $B_q^k$  are real and the crystal-field  $z$ -axis is parallel to the [001] crystal axis and perpendicular to the  $xy$  - plane, is identical to the choice we used previously in analyzing the spectra of  $\text{Er}^{3+}$  and  $\text{Ho}^{3+}$  garnets [1,2].

[1] U.V. Valiev, S.A. Rakhimov, N.I. Juraeva, R.R. Rupp, L. Zhao, Z. Wang, Z. Y. Zhai, J.B. Gruber, and G.W. Burdick, *Phys. Stat Sol. (b)*, **245**, (2009), 429.

[2] G.W. Burdick, J.B. Gruber, K.L. Nash, S. Chandra, and D.K. Sardar, *Spectroscopy Lett.* **43**, (2010), 406.

## MAGNETO-OPTICAL PROPERTIES OF Co AND Ni IMPLANTED SiO<sub>2</sub>

Petrov D.A.<sup>1</sup>, Ivantsov R.D.<sup>1</sup>, Seredkin V.A.<sup>1</sup>, Edel'man I.S.<sup>1</sup>, Khaibullin R.I.<sup>2</sup>, Stepanov A.L.<sup>2</sup>

<sup>1</sup>Kirensky Institute of Physics of Russian Academy of Sciences, 660036, Krasnoyarsk, Russia

<sup>2</sup>Zavoisky Physics-Technical Institute of Russian Academy of Sciences, 420029 Kazan, Russia

The silica glasses (SiO<sub>2</sub>) were implanted with 40 keV Ni<sup>+</sup> or Co<sup>+</sup> ions to high doses in the range of 0.25–1.00×10<sup>17</sup> ions/cm<sup>2</sup>. Our early studies of these samples by coil magnetometry [1], ferromagnetic resonance [2] and high-resolution transmission electron microscope [2] showed the formation of Co and Ni spherical nanoparticles with size ~5-20 nm in the implanted near-surface region of SiO<sub>2</sub>. The ion-synthesized nanocomposites revealed in-plane magnetic anisotropy that is typical for thin granular magnetic film.

In this work we present magneto-optic (MO) studies of 3d-ion implanted samples by measurements of Faraday (FR) and Kerr rotations (KR), as well magnetic circular dichroism (MCD) in the optical spectral range in dependence on the implantation dose. MO spectra of the implanted samples are strongly modified in comparison with ones of continuous Co and Ni thin films (see figures). We observed the strong changes both in the polarity and spectral shapes. The enhanced absorption near 400 nm related to surface plasmon resonance takes place in optical spectrum of Ni-implanted samples. This feature results in MCD maximum and the reversal of FR sign.

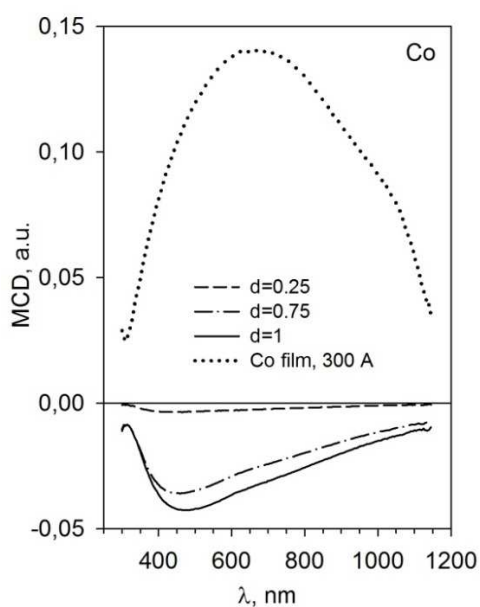


Fig. 1 MCD spectra of SiO<sub>2</sub> implanted with Co<sup>+</sup> ions to different doses (d), as well continuous film of cobalt metal

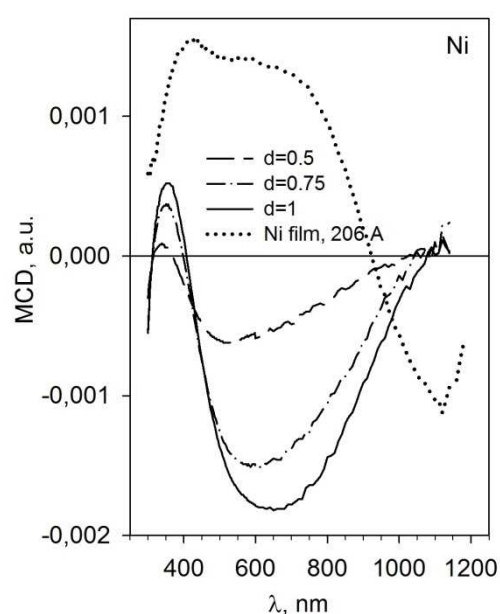


Fig. 2 MCD spectra of SiO<sub>2</sub> implanted with Ni<sup>+</sup> ions to different doses (d), as well continuous film of nickel metal

The off-diagonal components of permittivity tensor were calculated by using experimental FR, and MCD spectra of Ni and Co nanoparticles implanted in SiO<sub>2</sub> substrate and an extended Maxwell-Garnett theory including the size dependent effects.

[1] I.S. Edelman, O.V. Vorotynova, V.A. Seredkin, et al., *Phys. Solid State* **50** (2008) 2088.

[2] I.S. Edelman, E.A. Petrakovskaja, D.A. Petrov, et al., *Appl. Magn. Resonance* **40** (2011).

## THE SPIN –WAVE ACOUSTIC OF 2D MAGNETIC METAMATERIALS (EFFECTIVE MEDIUM APPROXIMATION)

*Sukhorukova O.S.<sup>1</sup>, Tarasenko S.V.<sup>1</sup>, Yurchenko V.M.<sup>1</sup>, Shavrov V.G.<sup>2</sup>*

<sup>1</sup> Donetsk Institute for Physics and Engineering named after A.A. Galkin of NASU, R.Luxemburg Str., 72, Donetsk, Ukraine, E-mail: tos1980@mail.ru

<sup>2</sup> V.A. Kotelnikov Institute of Radioengineering and Electronics of RAS, Mokhovaya Str., 11-7, Moscow, Russia, E-mail: smirnova@cplire.ru

At the present time the search of acoustic analogies of extraordinary electromagnetic properties of metamaterials (such as superlenses, cloaking, negative refraction, double negative medium etc.) is the main direction of the composite medium of modern physical acoustics. The resonance amplification by the left media of the evanescent electromagnetic waves field is a physical basis of this effect; as a consequence evanescent waves participate in the reconstruction of image. That enables to overcome a diffraction limit.

However, despite the constantly growing number of publications devoted to this theme, all theoretical and experimental works known until now were associated exclusively with non magnetic acoustic metamaterials.

The aim of this report is the theoretical studying of the possibility of resonance amplification of SH evanescent acoustic wave by means of 2D magnetic acoustic metamaterials slab. As an example of 2D magnetic acoustic material we consider the two-component acoustically continuous structure representing an elastically isotropic nonmagnetic solid matrix in which there is a set of infinite ferro- or antiferromagnetic rods of circular cross section with a metal covering.

In the frame of effective medium approximation the necessary conditions, under which for acoustically continuous structure from 2D magnetic acoustic material slab and elastically isotropic nonmagnetic layer the incident shear elastic wave (volume or evanescent) reflection coefficient is equal to zero, is determined.

The anomalies found in this work in the propagation of the shear elastic wave through a layered acoustically continuous structure containing a layer of a composite magnetic material represent an acoustic analogue of the effect of amplification of photon tunneling by a layer of the uniaxial anisotropic left medium.

[1] Joannopoulos J.D., Johnson S.G., Winn J.N. Photonic Crystals: Molding the Flow of Light. 2nd ed. Princeton:Princeton Univ. Press, 2008. 304 p.

[2] Pendry J.B. // Phys. Rev. Lett. 2000. V. 85. P. 3966–3969.

[3] Бреховских Л.М., Годин О.А. Волны в слоистых средах.М.: Наука, 1973. 416 с.

[4] Тарасенко С.В. // ЖЭТФ 2002, Т.121, №3, С.663-677.

22PO-K-7

## **SPIN DYNAMICS ON A TIME-SCALE OF THE EXCHANGE INTERACTION: AN X-RAY VIEW ON ULTRAFAST MAGNETISM**

*Radu I.<sup>1,2</sup>, Vahaplar K.<sup>1</sup>, Stamm C.<sup>2</sup>, Kachel T.<sup>2</sup>, Pontius N.<sup>2</sup>, Dürr H.A.<sup>2,5</sup>, Ostler T.A.<sup>3</sup>, Barker J.<sup>3</sup>,  
Evans R.F.L.<sup>3</sup>, Chantrell R.W.<sup>3</sup>, Tsukamoto A.<sup>4,6</sup>, Itoh A.<sup>4</sup>, Kirilyuk A.<sup>1</sup>, Rasing Th.<sup>1</sup>, Kimel A.V.<sup>1</sup>*

<sup>1</sup> Radboud University Nijmegen, Institute for Molecules and Materials, Heyendaalseweg 135, 6525  
AJ Nijmegen, The Netherlands

<sup>2</sup> Helmholtz-Zentrum Berlin für Materialien und Energie, BESSY II, Albert-Einstein-Strasse 15,  
12489 Berlin, Germany

<sup>3</sup> Department of Physics, University of York, York YO10 5DD, United Kingdom

<sup>4</sup> College of Science and Technology, Nihon University, 7-24-1 Funabashi, Chiba, Japan

<sup>5</sup> SLAC National Accelerator Laboratory, Menlo Park, CA 94025, USA

<sup>6</sup> PRESTO, Japan Science and Technology Agency, 4-1-8 Honcho Kawaguchi, Saitama, Japan

The exchange interaction, the strongest force in magnetism, is ultimately responsible for long range magnetic order. The response of the spins, however, in a magnetically ordered material to an excitation on a time-scale comparable with this exchange interaction is still a fundamental question at the frontier of modern magnetism and fast magnetic information processing. Nevertheless, the physics of these phenomena is still poorly understood which is largely due to the absence of proper experimental and theoretical techniques that can provide both the essential time resolution and the necessary spin and element specificity.

Here, by using advanced experimental (femtosecond optical excitation combined with ultrafast X-ray measurements) and computational (localized atomistic spin model) approaches, we demonstrate that in spite of the antiferromagnetic exchange interaction between Gd and Fe in the ferrimagnetic alloy GdFeCo, the ultrafast laser excitation triggers substantially different magnetization dynamics in the two sublattices (see Fig. 1). This even leads to the temporary appearance of ferromagnetic alignment of the antiferromagnetically coupled Fe and Gd magnetic moments. A coupled (antiferromagnetic) motion of Gd and Fe spins sets in only after about 10 ps, which is much longer than the characteristic time of the exchange interaction between these two sublattices (~100 fs). Our findings provide unexpected new insights into the fundamentals of ferrimagnetism, showing that two magnetic sublattices may have totally different spin dynamics even on a time scale much longer than the characteristic time of the exchange interaction between them. The discovery of this novel dynamics is important for both understanding the physics of non-equilibrium magnetic phenomena as well as for the establishment of the fundamental limits on the speed of magnetic recording and information processing technology.

Fig. 1: Ferrimagnetic alignment of the Fe and Gd magnetic moments as measured by element-specific time-resolved x-ray magnetic circular dichroism (TR-XMCD).

## EXPERIMENTAL STUDY OF THE FARADAY EFFECT IN 1D PHOTONIC CRYSTAL FOR MILLIMETER WAVEBAND

*Girich A.A.<sup>1</sup>, Polevoy S.Yu.<sup>1</sup>, Tarapov S.I.<sup>1</sup>, Merzlikin A.M.<sup>2</sup>*

<sup>1</sup> Institute of Radiophysics and Electronics of NASU, Kharkov, 61085, Ukraine

<sup>2</sup> Institute for Theoretical and Applied Electromagnetics of RAS, Moscow 125412, Russia

As it is known [1, 3], a significant enhancement of the Faraday effect can be obtained by embedding the magneto-optical media into the resonant multilayer structure. Examples of such structures are photonic crystals with defects [1] or photonic crystals, bounded by the strongly reflecting medium. As a result the Tamm surface state [2] can be formed in the transmission spectrum of such a structure.

The experimental study of amplification of the Faraday effect is presented in the given paper. The experimental structure represents the photonic crystal (air, teflon, quartz), loaded with ferrite and/or thin metal layers (Fig. 1b). The structure is placed in a circular metal waveguide. A static magnetic field is applied in parallel wave propagation. The basic mode, which is the  $TE_{11}$  mode, is excited in the structure.

An analysis of the transmission/reflection spectrum (Fig. 1a) for the unloaded photonic crystal and for the photonic crystal loaded with ferrite and metal layers (arranged sequentially), shows that the surface oscillation mode is formed in the band gap. They manifests as a “surface wave peak” in figure.

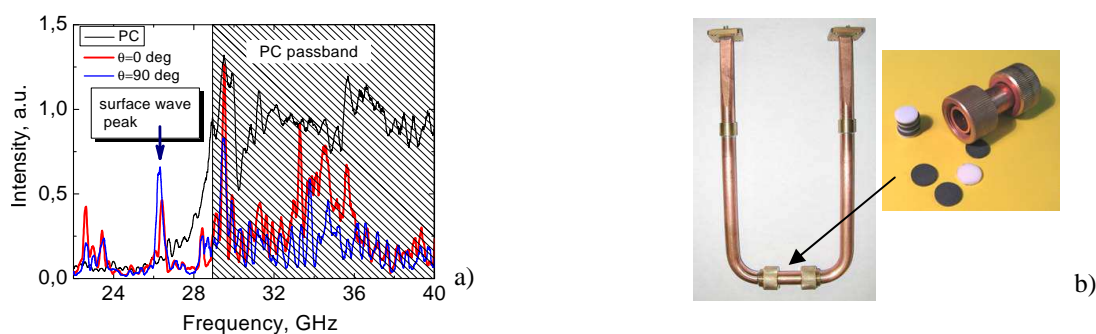


Fig. 1 – Transmission spectrum of the structure for various polarization angles (a); the measuring unit for studying the structure (b).

This mode is identified as the TM mode, which arises as a result of amplification of the Faraday effect in the ferrite layer. For the purpose of detailed study of the properties of this mode the dependencies of the mode intensity on the  $\theta$  (the angle of the analyzing waveguide), i.e. the polarization of the wave inside the measuring unit, has been analyzed. A satisfactory agreement between experiment and outcomes of numerical calculation is obtained.

This paper is partially supported by the Joint Projects RFBR-NASU (grant #7/10 on 01.06.2010).

[1] M. Inoue, R. Fujikawa, A. Baryshev, A. Khanikaev, P. B. Lim, H. Uchida, O. A. Aktsipetrov, T. V. Murzina, A. A. Fedyanin, A. B. Granovsky, “Magnetophotonic crystals,” *J. Phys. D: Appl. Phys.*, vol. 39, p. R151, 2006.

[2] A. P. Vinogradov, A. V. Dorofeenko, S. G. Erokhin, M. Inoue, A. A. Lisyansky, A. M. Merzlikin, A. B. Granovsky, “Surface State Peculiarities at One-Dimensional Photonic Crystal Interfaces,” *Phys. Rev. B*, vol. 74, N. 045128, 2006.

[3] A.V. Dorofenko, A.P. Vinogradov, A.M. Merzlikin, A.B. Granovsky, A.A. Lisyansky, "Magneto-optical Faraday effect amplified by surface waves in 1D systems", *CAOL 2008*, September 29 – October 4, Alushta, Crimea, Ukraine, pp. 192-194

22PO-K-9

## MAGNETICALLY CONTROLLED FARADAY LASER BASED ON THE TAMM STATE IN PHOTONIC CRYSTAL

*Zyablovsky A.A.<sup>1</sup>, Dorofeenko A.V.<sup>1</sup>, Vinogradov A.P.<sup>1</sup>, Pukhov A.A.<sup>1</sup>, Granovsky A.B.<sup>2</sup>*

<sup>1</sup>Institute for Theoretical and Applied Electromagnetics RAS, 13, Izhorskaya, Moscow 125412, Russia

<sup>2</sup>Faculty of Physics, Moscow State University, Leninskie Gori, Moscow 119992, Russia

Faraday laser based on the Tamm state on boundary of two photonic crystals [1,2] is proposed. Operating modes of this laser are investigated. It is shown that external magnetic field allows controlling of operating modes of laser.

In our research we use single-mode approximation of lasing. In addition, we use the slow amplitudes approach:

$$\begin{aligned}\frac{\partial E}{\partial t} + \frac{\omega}{2Q} E &= 2\pi i P \\ \frac{\partial P}{\partial t} + \frac{1}{\tau_p} P &= -i |d|^2 n E \\ \frac{\partial n}{\partial t} + \frac{1}{\tau_n} (n - n_0) &= \text{Re}[-i E^* P]\end{aligned}$$

These equations determine the amplitude of electric field, the polarization and the inverted population, respectively.

Presence of the layer wedging causes anisotropy of two linear polarizations, leading to different values of the  $Q$  factors,  $Q_x$  and  $Q_y$  [3]. Furthermore, the anisotropy can be introduced intentionally [2].

It is shown that two kinds of transition, stationary lasing/beating and stationary lasing/absence of lasing, can be observed when varying amplitude of the external magnetic field and  $Q$  factors of both the linear polarizations. The condition of switch between the operating modes is obtained.

Employing both the linear stability analysis and the numerical methods we have obtained the values of relaxation times for switching the lasing on and off.

[1] T. Goto, A. V. Baryshev, M. Inoue, A. V. Dorofeenko, A. M. Merzlikin, A. P. Vinogradov, A. A. Lisyansky, A. B. Granovsky, *Physical Review B*, **79** (2009) 125103

[2] A. D. May, P. Paddon, E. Sjerne, G. Stéphan, *Physical Review A*, **53** (1996) 2829

[3] M. I. D'yakonov, S. A. Fridrikhov, *Sov. Phys. Usp.*, **90** (1967) 837



## MAGNETO-OPTICAL PROPERTIES OF MULTILAYER NANOSTRUCTURES WITH COMPOSITE MAGNETIC LAYERS

*Gan'shina E.<sup>1</sup>, Buravtsova V.<sup>1</sup>, Novikov A.<sup>1</sup>, Kalinin Yu.<sup>2</sup>, Sitnikov A.<sup>2</sup>*

<sup>1</sup>Moscow State University, Faculty of Physics, Moscow, 119991, Russia

<sup>2</sup>Voronezh State Technical University, Voronezh, 394026, Russia

In this report we present the results of magnetic and magneto-optical (MO) studies of  $[(\text{Co}_{45}\text{Fe}_{45}\text{Zr}_{10})_Z(\text{Al}_2\text{O}_3)_{100-Z}(X)/\alpha\text{-Si}(Y)]_n$  multilayers (ML), where the granular composite based on  $\text{Co}_{45}\text{Fe}_{45}\text{Zr}_{10}$  with concentrations before the percolation threshold was used as a magnetic layer. Such structures with different thicknesses of magnetic ( $X=1,39 - 6,90$  nm) and non-magnetic ( $Y=0,18 - 1,82$  nm) layers and different  $X$  to  $Y$  ratio were investigated. This made it possible to vary the relative contributions of interfaces into MO response of the nanostructures.

It was found that the Transversal Kerr Effect (TKE) spectra  $\delta(h\nu)$  of multilayer films strongly depends on semiconductor and composite interlayer thickness. The spectra shape of the structures with  $X < 2$  nm and  $X > 4,63$  nm was similar to the spectra of metal-insulator nanocomposite [1]. For the  $X < 4,63$  nm TKE value was positive throughout the wavelength range (0.5-4.2 eV) and the TKE spectra was similar to the  $\text{Co}_{45}\text{Fe}_{45}\text{Zr}_{10}/\text{Si}$  ML spectra [2].

Measurements of the TKE field dependences  $\delta(H)$  in the near IR range has shown their abnormal behavior that was considerably differ from  $\delta(H)$  curves obtained in the visible range of spectra. The maximum of TKE was achieved at small fields ( $H < 100$  Oe), and with following increasing of magnetic field  $H$  the sign of the effect changed with further saturation at fields  $\sim 2.5$  kOe. In some cases the TKE value at maximum was 3 times greater in comparison with the saturation value. Anomalous behavior of  $\delta(H)$  disappeared with increasing of Si layers thicknesses. TKE spectra measured in small and large fields were essentially different.

The  $X$  and  $Y$  thicknesses for which the anomalous changes in the magnetic and magneto-optical properties took place are well correlated with sharp changes in the electric properties for all series. So, changes of ML transport properties in the small thickness range of silicon could be related with formation and growth of intergranular Si layer on magnetic CoFeZr granules. It means that at the granule-semiconductor interface there is a formation of new (CoFeZr)-Si or (CoFeZr)-silicides + Si composites, where a concentration of magnetic phase depends on either shapes or sizes of granules in the magnetic layer,  $X/Y$  thickness ratio and the rate of silicide formation. Increasing of Si thicknesses up to the percolation threshold range will lead to merging of neighboring granules through Si islands within the layer as well as between of adjacent layers, and hence to increasing of the magnetic phase in the (CoFeZr)- silicides + Si composite. This could be an explanation of the magnetization and TKE growth with institution of silicon. Similar conclusions can be made also from the coincidence of TKE spectra shapes and TKE magnitudes of nanocomposite-silicon and ferromagnetic-silicon ML in the range of small Si thicknesses. The maximum of magnetization values and TKE for ML structures have been observed near the percolation threshold for the (CoFeZr) - Silicides + Si composite.

Anomalous behavior in the nearest IR range most probably relates with a competition between of two contributions from different (CoFeZr)-  $\text{Al}_2\text{O}_3$  and (CoFeZr)- silicides + Si composites that have opposite sign of TKE in this spectral range.

[1] V.E. Buravtsova., V.S. Guschin., Yu.E. Kalinin.: et al.: CEJP. Vol. 2(4) 2004, p. 566.

[2] M.V. Vashuk, E.A. Gan'shina, S. Phonghirun.: et al.: Journal of Non-Crystalline Solids, 2007, V.353, 8-10, 962-964.

22PO-K-11

**SURFACE PLASMON POLARITONS AND INVERSE FARADAY EFFECT***Khokhlov N.E.<sup>1a</sup>, Belotelov V.I.<sup>1,2</sup>, Bezus E.A.<sup>3c</sup>, Kalish A.N.<sup>1d</sup>, Zvezdin A.K.<sup>2f</sup>*<sup>1</sup> M.V.Lomonosov Moscow State University, Leniskie gori 1, Moscow 119991, Russia.<sup>2</sup> A.M. Prokhorov General Physics Institute, Russian Academy of Science, Vavilov Str. 38, Moscow 119991, Russia.<sup>3</sup> Image Processing Systems Institute RAS, Molodog. st. 151, 443001 Samara, RussiaE-mail: <sup>a</sup>khokhlov@physics.msu.ru, <sup>b</sup>vladimir.belotelov@gmail.com, <sup>c</sup>evgeni.bezus@gmail.com, <sup>d</sup>kalish@physics.msu.ru, <sup>f</sup>zvezdin@gmail.com

Exciting possibility of ultrafast control of a medium magnetization at subpicosecond time scale via light was demonstrated recently [1]. It is of prime importance for modern magnetic storage systems demanding very large operation rates. At this inverse Faraday effect (IFE) takes the main role. Due to this effect, circularly polarized light induces a static magnetization in a medium:

$\mathbf{M} = \frac{\chi}{16\pi} [\mathbf{E} \times \mathbf{E}^*]$ , where  $\chi$  is the magneto-optical susceptibility,  $\mathbf{E}$  and  $\mathbf{E}^*$  are the electric field of the light wave and its complex conjugate, respectively. Thus, in order to observe pronounced value of IFE there should be a phase shift between different components of the electric field and electric field amplitudes should be sufficiently large.

In this work we investigate the IFE in the magnetoplasmonic crystals. The magnetoplasmonic crystals consist of a 1D or 2D perforated dielectric or metallic layer and a uniform paramagnetic or ferromagnetic layer. Main feature of such structures is that at some incident wavelengths surface plasmon polaritons and cavity modes can be excited. It was demonstrated that at these wavelengths the local electromagnetic field energy near the metal/dielectric interface gets increased substantially. One can assume that the plasmon-polaritons also enhance the IFE.

In accordance to numerical calculations based on the rigorous coupled-waves analysis (RCWA) the IFE in considered nanostructured materials is found to be locally increased by an order of magnitude at the spatial scale of several tens of nanometers. In addition to that the electromagnetic field intensity is got increased as well and the maxima of the intensity are usually very close to the maxima of the induced magnetic field. It leads to much more efficient influence of light on the medium around these spots as several impact mechanisms are enhanced: magnetic, thermal and energetic. Thus if the medium is magnetized it can be locally switched by means of incident circularly polarized light of moderate energy. Moreover, the loci of the enhanced dc magnetic field can be changed by shifting light wavelength or incidence angle. It is very important for possible applications related for example to the magnetization switching and magnetic data recording at record densities and rates.

The work is supported by RFBR and grant of Russia President for young scientists (MK-3123.2011.2).

[1] A.V. Kimel, A. Kirilyuk, P.A. Usachev, R.V. Pisarev, A.M. Balbashov and Th. Rasing, *Nature*, **435** (2005), 655.

22PO-K-12

## INFLUENCE OF Cu – DOPING ON THE ELECTRONIC STRUCTURE AND OPTICAL PROPERTIES OF $RNi_5$ (R = Er, Ho) COMPOUNDS

*Knyazev Yu.V.<sup>1</sup>, Lukoyanov A.V.<sup>1,2</sup>, Kuzmin Yu.I.<sup>1</sup>, Kuchin A.G.<sup>1</sup>*

<sup>1</sup>Institute of Metal Physics, Ural Division of RAS, Ekaterinburg 620990, Russia

<sup>2</sup>Ural Federal University, Ekaterinburg 62002, Russia

The  $RNi_5$ -type (R is rare-earth) compounds attract the attention not only because of diversity of their physicochemical properties, but also due to their application in hydrogen storage technology and as adiabatic cooling agents. Replacement of one rare-earth with another or substitution of Ni for some other transition metal lead to essential influence on the electric and magnetic characteristics. A number of studies indicate a direct correlation between this anomalous behavior of the physical parameters and energy structure evolution with doping content increase. The useful information about modification of energy bands upon the replacing nickel by another element can be extracted from optical study and calculation of electronic spectrum. In the present work the effect of substitution of Cu for Ni in  $(Er,Ho)Ni_{5-x}Cu_x$  ( $x = 0, 1, 2$ ) compounds on the electronic structure and optical properties has been investigated.

We report the ellipsometrical study of the optical properties of these systems in the spectral range of 0.08-5.64 eV at room temperature. It is shown that the energy dispersion of the optical conductivity  $\sigma(\omega)$  of alloys in the region of the fundamental absorption band depend considerably on the substituent concentration. The two-peak structure of  $\sigma(\omega)$  for binary  $(Er,Ho)Ni_5$  modified with an increase of Cu and display a new maximum centered at 4.5 eV for the ternary compounds. The intensity of this maximum increases with the growth in the copper content. The optical data obtained in the infrared range of spectrum were used to determine the relaxation and plasma frequencies of conduction electrons.

The electronic structure of  $(Er,Ho)Ni_{5-x}Cu_x$  ( $x = 0, 1, 2$ ) (hexagonal  $CaCu_5$  type of crystal structure) was investigated using LSDA+U method supplementing the local spin density approximation with a correction for strong electron interaction in the 4*f*-shell of rare earth element. The total and partial (for *f*- and Cu 3*d* electrons) densities of the electron states for two spin systems were calculated and used to determine interband optical conductivities of these compounds. The observed evolution of the experimental  $\sigma(\omega)$  dependencies upon replacement of Cu for Ni atoms is satisfactory described within these spin-resolved calculations of the electronic spectrum. Both the theoretical calculations and the spectroscopic data revealed the strong interband absorption peaks at range of 1 – 3 eV and the appearance of the new high-energy absorption maximum formed by Cu 3*d* → Ni 3*d* quantum transitions.

This work was supported by RFBR 10-02-00546, MK-3376. 2011. 2, scientific program of the Russian Federal Agency of Science and Innovation under Project No. 02. 740. 11. 0217.

## «MEMORY-EFFECT» IN NANOSCALE THICKNESS ION-BEAM SPUTTERED Bi:YIG FILMS

Prokopov A.R.<sup>1</sup>, Shaposhnikov A.N.<sup>1</sup>, Karavainikov A.V.<sup>1</sup>, Kotov V.A.<sup>2</sup>, Berzhansky V.N.<sup>1</sup>

<sup>1</sup>V.I Vernadsky Taurida National University, Simferopol 95007, Ukraine

<sup>2</sup>V.A. Kotelnikov IRE RAS, 11 Mohovaya St, Moscow, 125009, Russia

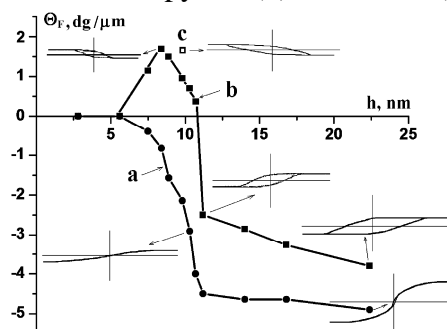
The perfection of magnetically active layers and the transition layer presence will exert the considerable influence on the magneto-optical (MO) characteristics of one-dimensional magnetophotonic crystals for short-wave visible spectrum region. Therefore, the properties of ultra-thin Bi:YIG films are of great interest. In this paper we present the results of investigation of the substrate surface crystalline state effect on the MO properties of nanoscale thickness Bi:YIG films (Faraday rotation  $\Theta_F$ , the spectra of magnetic circular dichroism MCD).

Bi:YIG films have been prepared by reactive ion-beam sputtering of  $\text{Bi}_{2.8}\text{Y}_{0.2}\text{Fe}_5\text{O}_{12}$  target on GGG (111) substrates and subsequent crystallization in air. Substrate surface crystalline state modification was performed by  $\text{Ar}^+$  treatment. It was found that the ion energy and current density significantly affect the properties of the films. This makes it possible to identify the original substrate surface crystalline state. In this sense we can say that Bi:YIG films saved the information about substrate surface crystalline structure during their preparation. This is confirmed by  $\Theta_F(h)$  dependences and Faraday hysteresis loops for the films deposited on the GGG substrates, whose surfaces have been pretreated by low-energy  $\text{Ar}^+$  glow discharge plasma (curve a, A-type films), by 1 keV and  $2.3 \text{ mA}\cdot\text{cm}^{-2}$   $\text{Ar}^+$ -beam (curve b, B-type films) and 1 keV and  $3.6 \text{ mA}\cdot\text{cm}^{-2}$   $\text{Ar}^+$ -beam (point c) (see figure).

At room temperature  $\Theta_F$  approaches zero in both film types up to thickness  $h = 5.6 \text{ nm}$ , which can be caused by size effects. A-films are characterized by in-plane magnetic anisotropy and high saturation magnetic fields as conventional Bi:YIG films. The typical for Bi:YIG films  $\Theta_F$  и MCD values occurred at  $h \approx 12 \text{ nm}$ , this corresponds to ten cell parameters approximately.

B-films have anomalous transition layer structure (opposite  $\Theta_F$  and MCD signs) in comparison with A-films. The transition layers are significantly influenced the properties of the large thickness films: at  $h \leq 70 \text{ nm}$  all B-films have perpendicular magnetic anisotropy.  $\Theta_F(h)$  and  $\text{MCD}(h)$  at  $5.6 \leq h \leq 10.3 \text{ nm}$  indicates that during crystallization process growth  $(\text{BiGdY})_3(\text{FeGa})_5\text{O}_{12}$  garnet films, whose composition varying in thickness. A corresponding  $T_C$  and  $T_{\text{comp}}$  changes in these films occurs.  $\Theta_F$  and MCD invert their signs at  $h \geq 10,7 \text{ nm}$ . Anomalous properties of B-films are due to destruction and amorphization of their substrate surfaces by ion beam treatment. As a result, during the crystallization process the film growth occurs from an amorphous layer containing both substrate and film elements oxides.

We believe that the effect of controlled ion beam pretreatment of the substrate surfaces can be used to create the MO thin film device with different types of anisotropy in the magnetically active layers.



## INFLUENCE OF ANNEALING ON NONLINEAR OPTICAL RESPONSE OF BISMUTH-SUBSTITUTED IRON GARNET FILMS

Dubrovina N.V.<sup>1</sup>, Kumar P.<sup>2</sup>, Levy M.<sup>2</sup>, Maydykovskiy A.I.<sup>1</sup>, Aktsipetrov O.A.<sup>1</sup>

<sup>1</sup>Department of Physics, Moscow State University, 119991 Moscow, Russia

<sup>2</sup>Department of Physics, Michigan Technological University, Houghton, Michigan 49931

Magneto-optical garnet films are formed of a well-known material which is currently used in various types of optoelectronic devices and are potential for the applications in nonreciprocal devices, such as optical isolators and circulators. At the same time, a task remains to figure out the technological parameters of the composition and fabrication of garnets that are responsible for the achievement of high values of magneto-optical activity and for a good crystalline quality as well. One of the possible ways to realize such films is to introduce epitaxial stress in thin garnet films. In this study, thin epitaxial garnet films of the thickness of 350÷1200 nm were epitaxially grown by RF-Magnetron sputtering method on (111) gallium gadolinium garnet (GGG) substrate and their crystallographic structure and magneto-optical response are studied using the nonlinear-optical probe of second harmonic generation (SHG). Annealing were produced during 4 hours at 700 C. We calculate the value of lattice mismatch strain and micro-strain by analysis of XRD data for annealed and unannealed films.

SHG experiments are performed using the output of the Ti-sapphire laser (at 800 nm wavelength, pulse duration of 80fs) as a fundamental radiation. For the magneto-optical characterization of the films the geometry of the transversal nonlinear magneto-optical Kerr effect (NOMOKE) is used.

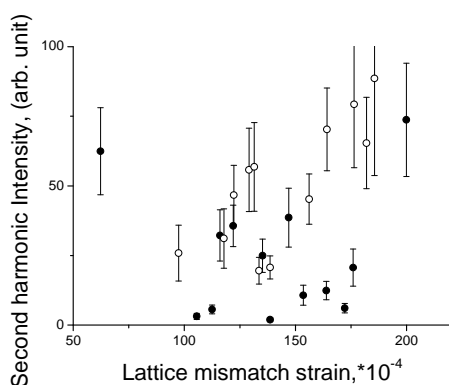


Fig. 1.

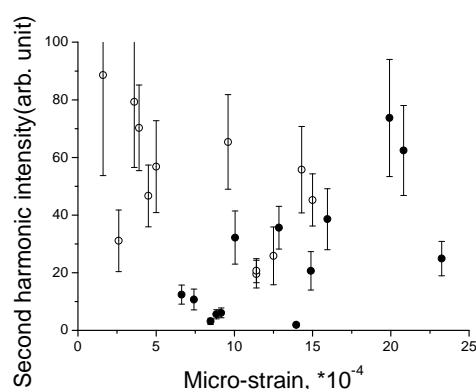


Fig. 2.

We have performed a systematic analysis on a series of BiYIG films. Figure 1 shows the SHG-dependence on lattice mismatch (LM) – the open circles corresponding to unannealed, the close circles to annealed films; it is seen that the increasing trend with LM is disturbed by annealing and second harmonic response becomes lower on average. Figure 2 shows the dependence of SHG on micro-strain (MS) before and after annealing (same notation). We observe the appearance of increase of SHG with micro-strain. Assuming quadratic growth of shg on strain we suggest that the dominant contribution into the nonlinear response before annealing is played by LM strain from interface film-substrate, whereas after annealing it is played by micro-strain defined by micro-crystallites. Magnetic contrast of NOMOKE does not depend on strain and bismuth concentration in range 0,2 - 0,3 per formula unit.

[1] M. Inoue, R. Fujikawa, A. Baryshev, et. al., *J. Phys. D: Appl. Phys.*, **39**, R151, (2006).

[2] I.E. Razdolsky, T.V. Murzina, O.A. Aktsipetrov, M. Inoue. *JETP Lett.*, **84**, p.451, (2006).

22PO-K-15

## PECULIAR OPTICAL PROPERTIES OF SELF-ASSEMBLED MAGNETIC CHAIN

*Park S.Y.<sup>1</sup>, Sandhu A.<sup>1</sup>, Lee B.W.<sup>2</sup>*

<sup>1</sup>Electronis-Inspired Interdisciplinary Research Institute, Toyohashi University of Technology, Toyohashi 441-8581, Japan.

<sup>2</sup>Department of Physics, Hankuk University of Foreign Studies, Yongin, Kyungki 449-791, Korea

Recently, self-assembled structures composed of magnetic micro-/nano-size beads are of interest in a wide range of applications such as photonic device, drug delivery, and actuator. The self-assembled structure and its motion are able to be easily controlled with not only external magnetic field but also surrounding structure. More recently, the use of self-assembled magnetic chain in solution makes it possible to develop optical modulator for optical telecommunication and optical biosensor. The motion and formation of the magnetic chain have been well-known to be described with Mason model, which is the ratio of magnetic force to hydrodynamic force. The optical response corresponding to magnetic chain has been successfully explained by diffraction of periodic linear bead array, or Mie scattering. Nevertheless, the optical properties of magnetic chain are still open to question. For instance, some of studies on optical transmittance of magnetic chain in the presence of magnetic field showed controversial result. Therefore, to elucidate the optical properties, we systematically studied the optical transmittance of magnetic chain in solution with various conditions: wavelength of light source, magnetic field strength, magnetic field direction, average length of the chain.

Magnetic bead used in this study is polystyrene bead containing superparamagnetic nanobeads. The size of the bead is from 1 to 8  $\mu\text{m}$ . The magnetization determined by vibrating sample measurement (VSM) is approximately 8 emu/g. Formation and motion of magnetic chain is controlled by two couples of Helmholtz coil, and non-polarized incoming light was guided by optical fiber, then optical transmittance was taken by spectrometer. The average length of magnetic chain was determined by high-speed optical microscope.

Optical transmittance of magnetic chain exhibits oscillation as a function of magnetic field direction. The amplitude of so-called oscillating transmittance for all bead size is found to be dependent on average length of magnetic chain. Maximum and minimum value of the amplitude are  $n\pi$ ,  $(1+n/2)\pi$ , respectively. (shown in Figure) Where  $n$  is integer. This result could be explained by the fact that light scattering in normal direction between magnetic chain and light path is greater than parallel configuration. On the other hands, at specific wavelength region, we found satellite peaks in oscillating transmittance plot, which is hardly explained by simple scattering theory. Therefore, we will discuss about that kind of peculiar optical properties of magnetic chain.

Support by EIIRIS is acknowledged.

## EVOLUTION OF OPTICAL SPECTRA OF $\text{Fe}_x\text{Ga}_{1-x}\text{BO}_3$ CRYSTALS AS A FUNCTION OF Fe CONCENTRATION

Edelman I.<sup>1</sup>, Malakhovskii A.<sup>1</sup>, Sokolov A.<sup>1</sup>, Sukhachev A.<sup>1</sup>, Zabluda V., Yagupov S.<sup>2</sup>,  
Strugatsky M.<sup>2</sup>, Postivey N.<sup>2</sup>, Seleznyova K.<sup>2</sup>

<sup>1</sup> L.V. Kirensky Institute of Physics SB RAS, 660036 Krasnoyarsk, Russia

<sup>2</sup> Taurida National University, Vernadsky ave., 4, 95007 Simferopol, Ukraine

Rhombohedral  $\text{GaBO}_3\text{:Fe}$  single crystals of high structural perfection with isomorphic substitution of  $\text{Ga}^{3+}$  ions by  $\text{Fe}^{3+}$  ions were synthesized by the solution-in-melt method. Concentration of  $\text{Fe}^{3+}$  ions varied in wide range and was determined with RFA and REM methods.

Optical absorption spectra were investigated in the spectral region of 350-1000 nm using the home made automated spectrometer (Fig. 1). A shift of the fundamental absorption edge to longer wave lengths with the Fe concentration increase was revealed. But the shift is not proportional to the Fe concentration: for the lower Fe concentrations the absorption edge shifts faster. For samples containing lower Fe concentrations absorption maxima near 380 and 450 nm are well resolved. In particular, maximum near 450 nm corresponds to that observed at 443 nm in the stoichiometric  $\text{FeBO}_3$  single crystal and can be ascribed to the  ${}^6\text{A}_{1g} \rightarrow {}^4\text{E}_g, {}^4\text{A}_{1g}$  transition between  $\text{Fe}^{3+}$  d-states. Position of this maximum does not depend on Fe concentration.

In higher concentrated sample, absorption bands associated with  ${}^6\text{A}_{1g} \rightarrow {}^4\text{T}_{1g}$  and  $\rightarrow {}^4\text{T}_{2g}$  transitions are observed. Their positions are also close to those in  $\text{FeBO}_3$  [1]. But decrease of the Fe concentration results in shift of these bands to lower wave lengths (sample 11% Fe in Fig. 1). The fine structure in the long wave length edge of the  ${}^6\text{A}_{1g} \rightarrow {}^4\text{T}_{1g}$  transition in the 67% Fe sample is similar to that observed in  $\text{FeBO}_3$  [1]. This testifies to appearance of the magnetic ordering. The spectra and their transformation depending on the Fe concentration are discussed taking into account the crystal field and spin and vibrational excitations in the crystals.

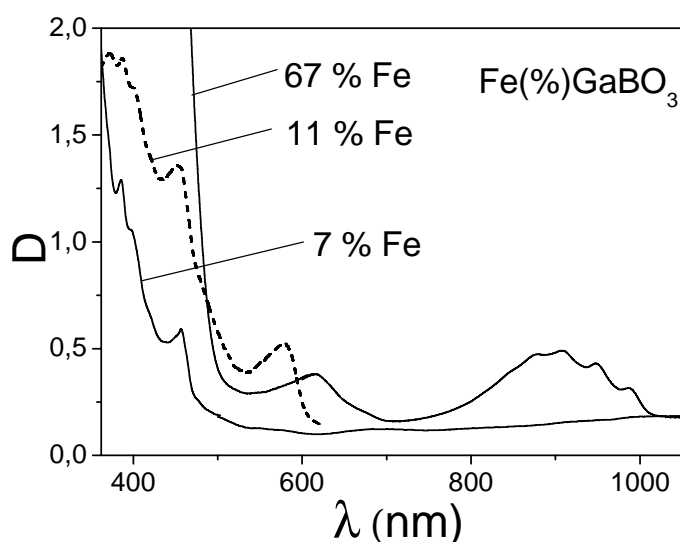


Fig.1.  $\text{Fe}_x\text{Ga}_{1-x}\text{BO}_3$  optical spectra measured at 85 K.

[1] Zabluda V.N., Malakhovskii A.V., Edelman I.S., *Phys. Stat. Sol. (b)* 751 (1984) 751.

22PO-K-17

## SINGLE CRYSTAL $\text{FeBO}_3:\text{Mg}$ AND INHOMOGENEOUS MAGNETIC PHASE

*Djuraev D.R.<sup>1</sup>, Sokolov B.Yu.<sup>2</sup>, Fayziev Sh.Sh.<sup>1</sup>*

<sup>1</sup> Bukhara State University, 11, M.Iqbol, 205018, Bukhara, Uzbekistan

<sup>2</sup> National University of Uzbekistan, VUZ gorodok, 100095, Tashkent, Uzbekistan

djuraev2002@mail.ru

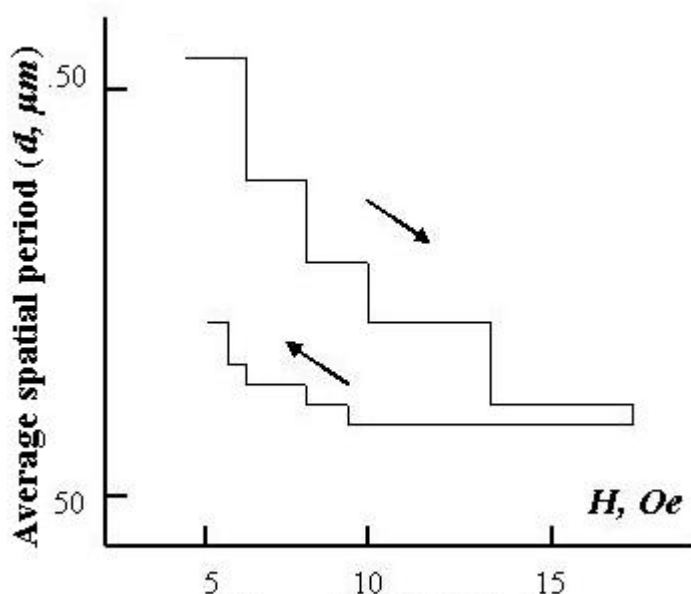


Fig.1. The magnetic field ( $H$ ) dependency of the average spatial period ( $d$ ) of the system of the bands, got under  $T = 80$  K ( $H \perp C_2$ ). The Arrows indicate the direction of the magnetization

The magnetic linear birefringence of an  $\text{FeBO}_3:\text{Mg}$  crystal is investigated as a function of the magnetic field strength and its orientation. The structure of the inhomogeneous magnetic phase of this weak ferromagnet is determined by analyzing the experimental results obtained. It is shown that, in an inhomogeneous magnetic state, the ferromagnetic moment does not deviate from the basal plane of the crystal and the angle of its deviation from the direction of the applied magnetic field is described by a one-dimensional function of the spatial coordinate along the axis of magnetization.

The transition from a homogeneous into a modulated magnetic state in weak ferromagnetic  $\text{FeBO}_3:\text{Mg}$  is studied by a magneto-optic method. At  $T < 135\text{K}$ , the application of a magnetic field in the weak plane of the crystal is shown to excite the modulation of its magnetic order parameter, which manifests itself in

a periodic deviation of the local ferromagnetism vector from the magnetization direction. The modulation period and the azimuthally angle specifying the local ferromagnetism vector direction in the modulated magnetic state of the crystal are studied as a function of temperature and magnetic field. The results obtained are discussed in terms of the of the «magnetic ripple» theory.



## MAGNONIC SPECTRUM BASED OPTICAL MAGNETOMETRY

Mansurova M.<sup>1</sup>, Kolokoltsev O.<sup>1</sup>

<sup>1</sup> Universidad Nacional Autonoma de Mexico, CCADET, Circuito Exterior S/N, C.U, DF, 04510, Mexico

In this work we present a new concept for measuring high intensity pulsed magnetic fields through the spectral analysis of magnonic excitations in thin ferrite films.

In the experiments we used a saturated yttrium-iron garnet (YIG) thin film grown on a gadolinium gallium garnet (GGG) substrate. Magnons were excited in the sample by picosecond pulsed magnetic fields applied perpendicularly to the magnetization vector. The pulsed fields were generated by a microstrip line transducer fabricated on film's surface. The magnon spectra were measured in a 0.37 - 1 GHz frequency range, with the help of the magneto-optical guided wave technique [1], [2].

Fig.1 shows the frequency of magnons vs bias DC magnetic field, at a constant value of the pulsed field. Fig.2 presents the amplitude of magnon spectral component as a function of the pulsed voltage applied to the transducer, at fixed bias field.

As seen in these figures, both experimental dependencies have a linear character.

The analysis of experimental data shows that the bias field (frequency) resolution is about 1 Oe (3 MHz), and pulsed magnetic field amplitude resolution is 10 - 30 Oe. The pulsed magnetic field sensitivity was estimated to be better than 1 Oe, for this particular configuration.

We conclude that proposed setup can be implemented into a magnetometric device, consisting of an optical fiber coupled to a YIG-GGG thin film.

Support by PAEP-2011 program is acknowledged.

[1] O.V. Kolokoltsev, Yu. A. Gaidai. *JMMM*, **204**, (1999) 101

[2] S.E Irvine, A.Y Elezzabi. *Optics Communications*, **220**, (2003) 325

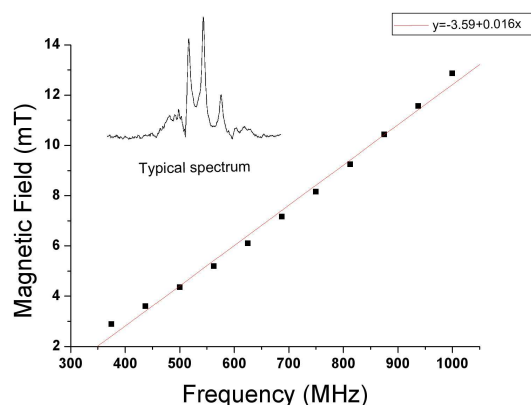


Figure 1.

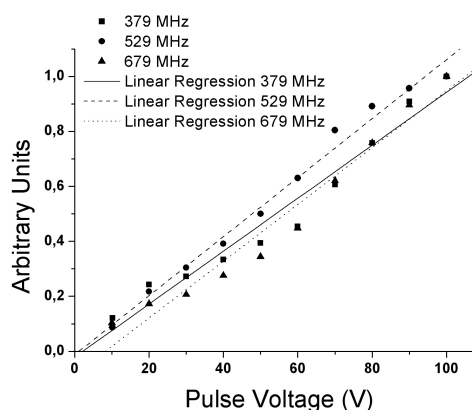


Figure 2.

## TRANSFORMATION OF ELECTRONIC STATES OF Tb<sup>3+</sup> ION IN TbFe<sup>3</sup>(BO<sup>3</sup>)<sub>4</sub> CRYSTAL UNDER THE INFLUENCE OF MAGNETIC ORDERING

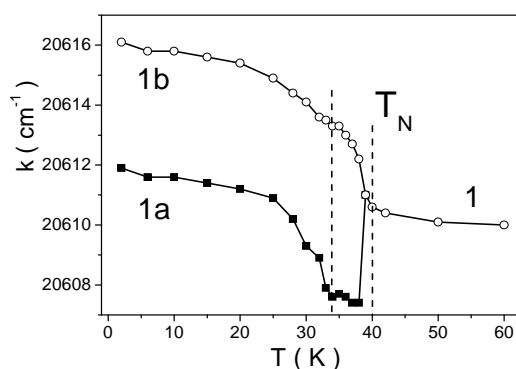
*Malakhovskii A.<sup>1</sup>, Gnatchenko S.<sup>2</sup>, Kachur I.<sup>2</sup>, Piryatinskaya V.<sup>2</sup>, Sukhachev A.<sup>1</sup>, Temerov V.<sup>1</sup>*

<sup>1</sup>L.V. Kirensky Institute of Physics, Siberian Branch of Russian Academy of Sciences, 660036 Krasnoyarsk, Russian Federation

<sup>2</sup>B. Verkin Institute for Low Temperature Physics and Engineering, National Academy of Sciences of Ukraine, 61103 Kharkov, Ukraine

Crystal and magnetic structure directly depends on the electronic structure of atoms which the crystal comprises. Electronically excited atom is, actually, an impurity atom, and, consequently, geometry of its local environment and local magnetic properties can change. Therefore, investigation of the excited state properties is of particular interest.

Optical absorption spectra of trigonal crystal TbFe<sub>3</sub>(BO<sub>3</sub>)<sub>4</sub> were studied in the region of  $^7F_6 \rightarrow ^5D_4$  transition in Tb<sup>3+</sup> ion depending on temperature (2 – 220 K) and on magnetic field (0 – 60 kOe) [1]. It was shown that the splitting of Tb<sup>3+</sup> absorption lines observed at  $T = 2$  K in zero external magnetic field result from the splitting of the excited states connected with the magnetic ordering, while the splitting observed near the Néel temperature are mainly due to the ground state splitting. Measured splitting of the absorption lines in the magnetic field permitted us to obtain the corresponding splitting of states and their Landé factors. The negative sign of the excited state splitting indicated that the orientation of the state magnetic moment is opposite to that of the ground state. In particular, this takes place for the low energy components of the exchange splitting of some of the Tb<sup>3+</sup> excited states. Determined orientations of the excited states magnetic moments permitted us to explain the ratio of the intensities of components of the lines splitting in the exchange field of the Fe-sublattice: stronger transitions occur without overturn of the magnetic moment.



Step-wise splitting of one of the absorption lines ( $\sim 20615$  cm<sup>-1</sup>) was discovered in the region of the Néel temperature (Fig.). This is shown to be due to step-wise change of equilibrium geometry of the local Tb<sup>3+</sup> ion environment only in the excited state of the Tb<sup>3+</sup> ion. Asymmetric shifts of the excited states at cooling from  $T_N$  to 2 K and the character of the temperature dependences of  $f-f$  transitions intensity indicates that the magnetic ordering is accompanied by temperature variations of the Tb<sup>3+</sup> local environment in the excited states. Crystal field splitting components have been identified according

to crystal quantum number  $\mu$  and according to irreducible representations. The identification is consistent with the experimental results. In particular, the ground state (in  $D_3$  symmetry approximation) consists of two close singlets  $\mu=0$  ( $M=\pm 6$ ) (or  $A_1$  and  $A_2$  in symbols of irreducible representations) which are split and magnetized by effective exchange field of the Fe-sublattice. The identification allowed us to explain the ratio of intensities of the crystal field splitting components.

[1] A.V. Malakhovskii<sup>1</sup>, S.L. Gnatchenko, I.S. Kachur, V.G. Piryatinskaya, A.L. Sukhachev, V.L. Temerov, *Eur. Phys. J. B* (2011), DOI: 10.1140/epjb/e2011-10806-x.

## MAGNETOREFRACTIVE EFFECT IN MANGANITE HETEROSTRUCTURES

Sukhorukov Yu.<sup>1</sup>, Telegin A.<sup>1</sup>, Bessonov V.<sup>1</sup>, Gan'shina E.<sup>2</sup>, Stepan'tsov E.<sup>3</sup>

<sup>1</sup> Institute of Metal Physics, Ural Division of RAS, 620990, Ekaterinburg, Russia

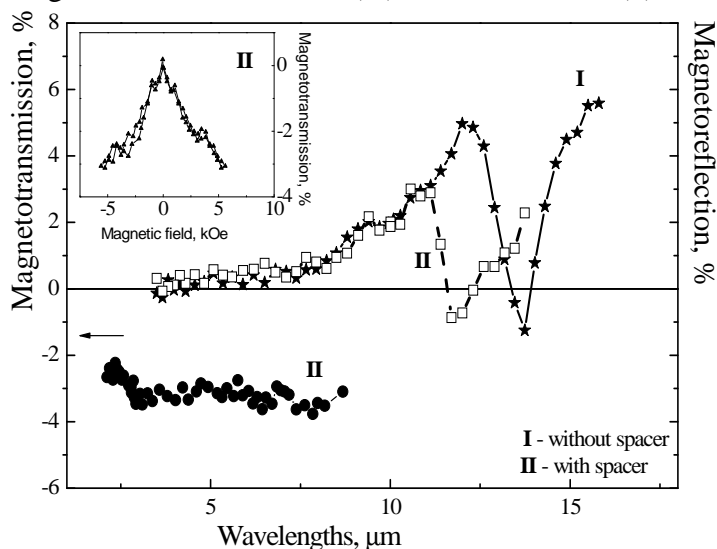
<sup>2</sup> Moscow State University, 119992, Moscow, Russia

<sup>3</sup> Institute of Crystallography of RAS, 119333, Moscow, Russia

Manganite-based structures with a colossal magnetoresistance (CMR) attract great attention because of existence of a huge high frequency (optical) responses to metal-insulator transition and CMR like as a sharp change of the infrared (IR) transmission and reflection of light near the Curie temperature ( $T_C$ ), and magnetorefractive effect (MRE) on magnetoreflexion and magnetotransmission (MT) modes [1-3]. Furthermore it was shown one can control the magnetoreflexion, magnetotransmission and magnetoresistance parameters by fabricating manganite heterostructures with layers of different compositions or geometry [4]. The goal of this work was the study of the features of MRE and influence of an artificially created interface` spacer on the magneto-optical and magnetotransport properties of manganite heterostructures.

The two type of heterostructures: **I** -  $\text{La}_{2/3}\text{Ca}_{1/3}\text{MnO}_3$  (thickness  $d = 70$  nm)/ $\text{La}_{2/3}\text{Sr}_{1/3}\text{MnO}_3$  (90 nm) and **II** -  $\text{La}_{2/3}\text{Ca}_{1/3}\text{MnO}_3/\text{SrTiO}_3$  (2 nm)/ $\text{La}_{2/3}\text{Sr}_{1/3}\text{MnO}_3$  were grown using pulsed laser deposition on single crystal substrate  $\text{SrTiO}_3$  [5].

It was obtained the magnetoreflexion (as well as resonance-like effect) and magnetotransmission effects in manganite heterostructures can reach giant values (see Fig.). It depends strongly on magnetic, and charge homogeneity of the heterostructures` layers. For the heterostructures as compared with the single-layer films: (i) there are more charge and magnetic inhomogeneities, (ii)  $T_C$  and the light intensity are decreased, (iii) magnetization is reduced, (iv) MT is lowered, (v) the temperature range of all magneto-optical effects is broadened. The dielectric non-magnetic  $\text{SrTiO}_3$  spacer influences on the temperature and spectral behaviour of magnetotransmission and magnetoreflexion and enhances the low temperature MR due to the tunnelling of spin-polarized carriers through the spacer. The obtained data is consistently explained in the framework of the developed concept of the magnetorefractive effect in the infrared spectral range for metal alloy and granular system [2,3].



Support by the RFBR 10-02-00038, program of UD-SD of the RAS № 09-C-2-1016, program of DPS "Physics of new materials and structures" and youth scientific project UD of RAS № m-6.

- [1] E. Gan'shina, N. Loshkareva, Yu. Sukhorukov et al. *J. Magn. Magn. Mater.*, **300** (2006) 62.
- [2] A. Granovskii, Yu. Sukhorukov, A. Telegin, V. Bessonov et al. *JETP*, **112** (2011) 1.
- [3] Yu. Sukhorukov, A. Telegin, A. Granovskii, E. Gan'shina, et al. *JETP*, **138** (2010) 3.
- [4] Yu. Sukhorukov, N. Loshkareva et al. *Physics of Metals and Metallography* **107**, (2009) 6.
- [5] Yu. Sukhorukov, A. Telegin, E. Gan'shina, E. Stepan'tsov et al. *Technical Physics*, **80** (2010) 8.

22PO-K-21

## SPECTRAL CROSSOVER IN PHOTONIC CRYSTALS

*Yurasov N.*

Bauman Moscow State University, Moscow, Russia, 107005

e-mail: nikyurasov@yandex.ru

The results of the theoretical investigations of the spectral crossover in photonic crystals are presented. The spectral crossover is connected with coherent waves [1]. We have found the points of spectral crossing or conditions of the coherent waves excitation. We have analyzed two cases of spectral crossover in photonic crystals. We have considered the case of the empty photonic crystal and the case of the photonic crystals embedded the ferromagnetic inclusions. Such photonic crystals are investigated experimentally [2].

We have used the periodic model of multilayer ABABA... with refractive indexes  $n_A$  and  $n_B$  [3] for the empty photonic crystal. The dispersion law is  $F(k, \omega) = \cos(ka) - f(n_A, n_B, n_A / n_B) = 0$ , where  $k$  ( $0, 0, k$ ) is the wave vector and  $n_A = 1$ ,  $n_B = n(\omega)$ , where  $\omega$  is the circle frequency of the electromagnetic wave exciting the coherent waves. The crossover condition is  $\partial F / \partial k = 0$  if another condition  $\partial F / \partial \omega \neq 0$  is satisfied. So we have equality  $ka = \pi m$ , where  $m = 1, 2, 3, \dots$  and the equation  $(-1)^m - f(1, n(\omega), 1/n(\omega)) = 0$  determines the crossover frequencies in stop-zone. In second case we have considered the Faraday's geometry. The components of the dielectric susceptibility were functions of magnetization and magnetic field, applied to photonic crystal. In this case we have used the dispersion law in form  $\sum a_n(\omega) k^n = 0$ , where  $n = 0, 1, 2, 3, \dots, 2m$ ,  $m$  is integer. Then we have the following equality  $\sum (-1)^n a_{n-1} - 1 = 0$ , where  $n = 2m, 2m-1, \dots, 1$ . So the coefficients  $a_n$  are functions of frequency, magnetic field, applied to photonic crystal the last equation determines the conditions of the crossover formation: frequencies and magnitudes of applied magnetic field. In Faraday's geometry we have spectral crossover in stop-zone also. Therefore the Bragg's peak may have the complex structure and the empty photonic crystal on the opal matrix base has one peak

[1] N.Y. Yurasov, Vestnik MGTU, Estestvennye Nauki, № 4, (2004), P. 124.

[2] V.S. Gorelik, N.Y. Yurasov, Y.P. Voinov, M.I. Samoilovich, V.V. Gryasnov, Solid State Phenomena, vol. 152-153 (2009), P.518.

[3] A. Yariv, P. Yeh, Optical wave in crystals. Wiley-Interscience Publication, New York-1984.

22PO-K-22

## THE ANALYSIS OF THE MAGNETOREFRACTIVE EFFECT IN $\text{La}_{0.67}\text{Ca}_{0.33}\text{MnO}_3$ : THIN FILMS AND SINGLE CRYSTALS

*Yurasov A.N.<sup>1</sup>, Bakhvalova T.N.<sup>1</sup>, Telegin A.V.<sup>2</sup>, Sukhorukov Yu.P.<sup>2</sup>, Granovsky A.B.<sup>3</sup>*

<sup>1</sup> Moscow State Institute of Radioengineering, Electronics and Automation (Technical University),  
119454, Moscow, Russian Federation

<sup>2</sup> Institute of Metal Physics, Ural Division of RAS, 620041, Ekaterinburg, Russian Federation

<sup>3</sup> Faculty of Physics, Moscow State University, Moscow 119991, Russia

Magnetorefractive effect (MRE) is a high frequency response on magnetoresistance (MC) and consists in variations of the coefficients of reflection and transmission of electromagnetic waves of samples with GMR, TMR or CMR under magnetization (see [1], and references therein). Recently,

it has been shown that magnetotransmission and magnetoreflexion in manganites  $\text{La}_{0.67}\text{Ca}_{0.33}\text{MnO}_3$  in the infrared spectral range (1-25  $\mu\text{m}$ ) near Curie temperature are due to MRE [2,3]. The developed theories of MRE in metallic multilayers and granular alloys with GMR and in nanocomposites with TMR are not appropriate for  $\text{La}_{0.67}\text{Ca}_{0.33}\text{MnO}_3$  [2-4]. In this report, we present results of calculations of MRE in  $\text{La}_{0.67}\text{Ca}_{0.33}\text{MnO}_3$  single crystals and thin films in the framework of the effective medium approach (EMA) supposing that  $\text{La}_{0.67}\text{Ca}_{0.33}\text{MnO}_3$  manganites consist of low and high resistivity phases with volume fractions depending on an applied magnetic field.

We considered semi-infinite single crystals and thin films 320, 180, 50 nm in thickness on the LaAlO substrate (see experimental details in [3]). The frequency-dependent conductivity for magnetized two-phases samples in the framework of EMA can be written as

$$\sigma(\omega, H) = [0.5\sigma_2 - 0.25\sigma_1 + 0.75y(\sigma_1 - \sigma_2)] \left[ 1 + \left( 1 + \frac{8\sigma_1\sigma_2}{2\sigma_2 - \sigma_1 + 3y(\sigma_1 - \sigma_2)} \right)^{1/2} \right], \quad (1)$$

where  $\sigma_2$  and  $\sigma_1$  are the conductivities of the low and high resistivity phases, correspondently,  $y$  is the volume fraction of the high conductivity phase for magnetized samples. If to denote  $x$  as the volume fraction of the high conductivity phase in the case of zero magnetic field, then

$$\sigma_2 = \frac{\sigma(\omega, H=0) [\sigma_1 [1-3x] + 2\sigma(\omega, H=0)]}{\sigma_1 + \sigma(\omega, H=0) [1-3x]}. \quad (2)$$

The values of  $\sigma_2$  were obtained from [4-6]. Then using (1,2), Frenel's formulas, the experimental data on  $\sigma(\omega, H=0)$  and  $\sigma_1$  from [4-6] we calculated MRE spectra at  $T=250\text{K}$ . It was shown that MRE spectra strongly depend on MC and optical properties. Both the magnitude and the spectral shape of the obtained MRE spectra in reflection mode are in a good agreement with the reported in [2,3] spectra of magnetoreflexion.

This work was supported by the President Grant of Russian Federation MK-2261.2011.2; by the Branch of Physical Sciences, RAS (project no. 09-T-2-1013); by the Ural and Siberian Branches, RAS (project no. 09-S-2-1016); by the Russian Foundation for Basic Research (project nos. 10-02-00038, 09-02-12455-ofi, and 09-0200309); and by the Ural Branch, RAS (youth scientific -project no. 8-m).

- [1] A.B. Granovskii, E.A. Ganshina, A.N. Yurasov et al., *J. Commun. Technol. Electron.*, **52** (2007) 1065.
- [2] Yu.P. Suhorukov, A.V. Telegin, A.B. Granovskii et al., *JETP*, **111** (2010) 355.
- [3] A.B. Granovskii, Yu.P. Suhorukov, A.V. Telegin et al., *JETP*, **112** (2011) 77.
- [4] N.G. Bebenin, *Physics Metals and Metallography*, **111** (2011) 242.
- [5] A. V. Boris, N. N. Kovaleva, A. V. Bazhenov et al., *Phys. Rev. B*, **59** (1999) R697.
- [6] Z. M. Zhang, B. I. Choi, M. I. Flik et al., *J. Opt. Soc. Am. B.*, **11** (1994) 2252

22PO-K-23

## THE NATURE OF THE FARADAY SIGNAL INDUCED DUE TO THE INVERSE FARADAY EFFECT IN PARAMAGNETIC DIELECTRICS

*Mikhaylovskiy R.V., Hendry E., Kruglyak V.V.*

School of Physics, University of Exeter, Stocker Road, EX4 4QL, Exeter, UK

The ultrafast inverse Faraday Effect has been one of the most intriguing magneto-optical phenomena over the last decade. The development of powerful ultrafast laser systems opened the prospect of experimental studies of interactions between light and magnetic materials on the femtosecond timescale. It is suggested that the inverse Faraday Effect can serve as the means for ultrafast control of the magnetic order via optical excitation [1].

We report an experimental observation of the ultrafast inverse Faraday effect in terbium gallium garnet (TGG) in an all-optical pump-probe setup at room temperature. TGG, a transparent paramagnetic dielectric material, has been chosen for the study due to its high Verdet constant at room temperature. The Faraday rotation of the probe optical pulse due to the transient magnetization induced by the circularly polarized femtosecond pump pulse was measured. The behavior of the measured signal as a function of the pump polarization and intensity revealed the magneto-optical nature of the observed effect. However, the observed amplitude of the Faraday rotation significantly exceeds that predicted by the phenomenological theory. Moreover, the study of the transverse spatial profile of the magneto-optical signal shows that it differs significantly from the simple convolution of the transverse profiles of the pump and probe pulses. Instead, we show that the contribution due to a convolution of the probe and the transient magnetic field created by the magnetic dipole induced in the sample by the pump should be taken into account. Importantly, the probe experiences rotation not only when it is overlapped with the pump spot but also when it illuminates the vicinity of the pump spot. In the latter case, the sign of the observed signal is opposite to that observed in the case of the perfect spatial pump-probe overlap. The spatial shape and amplitude of the signal depend strongly on the pump spot size, which cannot be accounted for just by the pump intensity scaling.

Therefore, our results suggest the nonlocal nature of the inverse Faraday Effect and add an additional argument to the long-lasting discussion concerning the relation between the observed magneto-optical signal and the magnetization dynamics in the sample under study.

We will also present results of the rigorous calculations of the THz magnetic fields emitted by the transient nonlinear magnetization induced in the TGG by the circularly polarized pump pulse. We will show how these fields can lead to the nonlocality of the observed signal and will discuss the different nature of the Faraday signal within the pump spot and in its vicinity.

The research leading to these results has received funding from the Engineering and Physical Research Council (EPSRC) of the UK and from the Research Council of UK (RCUK).

[1] A. Kirilyuk, A. V. Kimel, and Th. Rasing, *Rev. Mod. Phys.*, **82** (2010) 2731.

22PO-K-24

## ROBUSTNESS OF RESONANTLY ENHANCED FARADAY EFFECT

*Nechepurenko I.A.<sup>1</sup>, Dorofeenko A.V.<sup>1</sup>, Vinogradov A.P.<sup>1</sup>, Pukhov A.A.<sup>1</sup>, Granovsky A.B.<sup>2</sup>*

<sup>1</sup>Institute of Theoretical and Applied Electromagnetics RAS

<sup>2</sup>Physical Faculty, Moscow State University

At an interface of two photonic crystals the Tamm state [1,2] can exist, that is an analog of surface electron state in a crystal. The Tamm state has a frequency from the band gaps of both PC and is observed as a peak in transmission spectrum. The Tamm state, along with defect-mode of photonic crystal [3], can be used for amplification of the Faraday effect.

Being a resonance, the Tamm state is expected to be sensitive to random deviation of PC layers thickness, which always takes place in practice. Having used T-matrix technique, we have calculated the Tamm state parameters for different realizations of random system. Our analysis revealed that at realistic parameters the Tamm state is stable against 10% thickness variation. Basing on numerical and analytical techniques it was established that in the presence of the Gauss variation of thicknesses the Tamm state resonance frequency also has Gauss distribution with variances proportional to one another. The proportionality coefficient can be considered as a stability measure. The mentioned property is a consequence of linear dependence of the resonance frequency on the PC layers thickness. However, distribution of resonance width proved to have asymmetric non-Gaussian shape. This fact can be explained by nonlinear dependence of the resonance width. This is due to the fact that the resonance width depends on the quality factor which is maximal for the Tamm state.

It is known that the Faraday effect can be amplified by the Tamm state. We have considered influence of disorder on the Faraday effect.

[1] A. P. Vinogradov, A. V. Dorofeenko, S. G. Erokhin, M. Inoue, A. A. Lisyansky, A. M. Merzlikin, and A. B. Granovsky, Phys. Rev. B 74, 045128 (2006)

[2] M. Kaliteevski, I. Iorsh, S. Brand, R. A. Abram, J. M. Chamberlain, A. V. Kavokin, I. A. Shelykh, Phys. Rev. B 76, 165415 (2007)

[3] M. Inoue, T. Yamamoto, K. Isamoto, and T. Fujii, J. Appl. Phys. 79, 5988 (1996)

22PO-K-25

## NEW MAGNETO-OPTICAL SENSITIVE MEDIA FOR VISUALIZATION AND MAPPING OF INHOMOGENEOUS MAGNETIC FIELDS

*Ivanov V.E., Lepalovskij V.N.*

Ural State University, Ekaterinburg, Russia

It has been experimentally shown that at the measuring longitudinal Kerr effect in FeCo films with a plane anisotropy the complex magneto-optical imaging is observed when applying inhomogeneous magnetic field. After separation of the magneto-optical images (MOI) on the pictures corresponding polar and longitudinal Kerr effect sensitivity of the coordinate dependences of their intensity are analysed by comparison with coordinate dependences of normal ( $H_z$ ) and plane ( $H_p$ ) components of magnetic field that is shown in fig. 1a.

The MOI corresponding the polar sensitivity are analytic representation of the distribution of  $H_z$  component. The linearity of transfer characteristic, i.e. correspondence of image intensity and the field value is provided by the large form anisotropy of indicated FeCo films. This offers the new challenge of using these magnetic films for mapping of normal component of inhomogeneous magnetic fields.

The MOI corresponding longitudinal sensitivity are analytic representation of the angular dependence of  $H_p$  component (fig. 1b). The sensitivity of such image to plane component of field is high enough therefore the investigated films can be used for visualization of the hidden images possessing the low magnetic moment.

One-to-one correspondence of local intensity of MOI, value of  $H_z$  and of  $H_p$  direction in the films with the large form anisotropy is confirmed by simulation (fig. 1c). The modeling images show presence of singular points just like the experimental MOI. In these points  $H_p$  approaches to zero (fig. 1a). The quantity and topological properties of singular points characterize the form and symmetry of separate magnets as well as all magnetic system in whole.

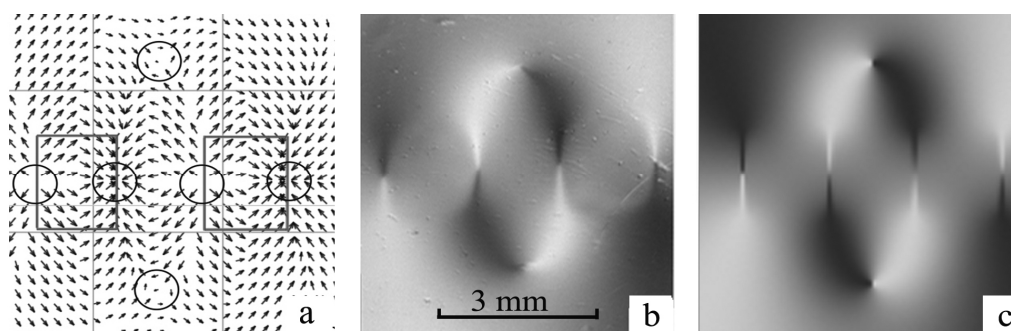


Fig. 1. Vector plot of  $H_p$ -component of inhomogeneous magnetic field (a); the experimental (b) and simulated (c) MOI corresponding the plot. One can see that specific points of MOI coincide with the singularity of vector plot of  $H_p$ .

This work was supported by the Russian Foundation for Basic Research, project no. 08-02-99081-r\_ofi.



**22 August**

Monday

17:30-19:00

poster session  
22PO-M

**“Magnetic Soft Matter”**

22PO-M-1

## STRUCTURAL STUDIES OF BIOMINERAL PARTICLES PRODUCED BY KLEBSIELLA OXYTOCA

Balasoiu M.<sup>1,2</sup>, Anghel L.<sup>3</sup>, Ishchenko L.A.<sup>4</sup>, Stolyar S.V.<sup>4,5</sup>, Meiszterics A.<sup>6</sup>, Almasy L.<sup>6,7</sup>, Rogachev A.V.<sup>1</sup>, Ivankov A.I.<sup>1</sup>, Soloviov D.V.<sup>1</sup>, Kurkin T.S.<sup>8</sup>, Jigounov A.<sup>9</sup>, Kuklin A.I.<sup>1</sup>, Raikher Yu.L.<sup>10</sup>, Iskhakov R.S.<sup>4,5</sup>, Rosta L.<sup>6</sup>, Arzumaniyan G.M.<sup>1</sup>

<sup>1</sup> Joint Institute of Nuclear Research, Dubna, 141980, Russia

<sup>2</sup> Horia Hulubei National Institute of Physics and Nuclear Engineering, P.O.Box MG-6, Bucharest, Romania

<sup>3</sup> Institute of Chemistry of ASM, Chisinau, Moldova

<sup>4</sup> Siberian Federal University, 660041, Krasnoyarsk, Russia

<sup>5</sup> Kirensky Institute of Physics, Siberian Branch of RAS, Krasnoyarsk, 660036 Russia

<sup>6</sup> Research Institute for Solid State Physics and Optics, Budapest, Hungary

<sup>7</sup> Paul Scherrer Institute, Villigen, Switzerland

<sup>8</sup> Institute of Synthetic Polymer Materials RAS, Moscow, 117393, Russia

<sup>9</sup> Institute of Macromolecular Chemistry, ASCz Prague

<sup>10</sup> Institute of Continuum Media Mechanics, Ural Branch of RAS, 614013, Perm, Russia

An important area of research in nanotechnology deals with the synthesis of nanoparticles of various chemical composition, size and controlled monodispersity. The control on the nanoparticles shape is a recent addition to the list of requirements imposed on newly emerging synthesis methods. Currently, there is a growing need in methods to produce environmentally benign nanoparticles without use of toxic chemicals in the synthesis protocol. As a result, researchers in the field of nanoparticle synthesis and assembly have turned to biological systems.

Bioproduction systems are of special interest due to their efficiency and flexibility. Microbial cells are highly organized units, regarding morphology and metabolic pathways, capable of synthesising well size-calibrated and structurized particles. Furthermore, biogenic nanoparticles often are water-soluble and biocompatible, which is essential for many applications.

Bacterium *Klebsiella oxytoca* produces several types of ferrihydrite nanoparticles in response to variation of the growth conditions (duration, exposition to light, medium content, etc.), whose properties were identified by means of Mossbauer spectroscopy and static magnetic measurements [1-3].

Studies by means of high resolution scanning electron microscopy and X-ray scattering have shown that biogenic nanoparticles removed from bacterium *Klebsiella oxytoca* are wrapped in in an organic sheath and display structural parameters resembling those of a cylinder of radius  $R = 4.87 \pm 0.02$  nm and length  $L = 2.12 \pm 0.04$  nm [4,5]. Hereby we present the results of the work aimed at further elucidation of the structural parameters and aggregation state of the aforementioned biogenic particles dispersed in water by ultrasonication.

[1] S.V. Stolyar, O.A. Bayukov, Yu. L. Gurevich et.al., *Inorganic Materials* **42** (2006) 763.

[2] Yu. L. Raikher, V.I. Stepanov, S.V. Stolyar et.al., *Physics of the Solid State* **52** (2010) 298.

[3] L.A. Ishchenko, S.V. Stolyar, V.P. Ladygina et.al., *Physics Procedia* **9** (2010) 279.

[4] M. Balasoiu, S. V. Stolyar, R.S. Iskhakov et.al, *Romanian J. Phys.*, **55** (2010) 782.

[5] M. Balasoiu, L.A. Ishchenko, S.V. Stolyar, et.al., *Optoelectronics and Advanced Materials – Rapid Communications*, **4** (2010) 2136.

## DIFFUSIVE MOTION OF NANOPARTICLES UNDER DIRECTED EXTERNAL STIMULI

*Belzik M.<sup>1</sup>, Dobbrow C.<sup>2</sup>, Schmidt A.<sup>2</sup>, Gottlieb M.<sup>1</sup>*

<sup>1</sup> Chemical Engineering Dept., Ben-Gurion University, Beer-Sheva 84105, Israel

<sup>2</sup> Department Chemie, Universität zu Köln, Köln 50939, Germany

The diffusive motion of magnetic nanoparticles suspended in a liquid is affected under the influence of external magnetic field as result of processes such as chain formation, self-assembly or micro-phase separation. The magnetic cobalt nanoparticles examined in this work are stabilized by a combination of steric and electrostatic effects. The absence of charges on the surface leads to chain-formation due to magnetic dipole-dipole interactions. By adding tri-n-octylphosphine oxide (TOPO) to the synthesis mixture, a surface charge is created, and occurring electrostatic repulsion overcomes magnetic dipole attraction and Van der Waals forces. Thus, the particle-particle interactions are dependent on the TOPO concentration as shown in Figure 1.

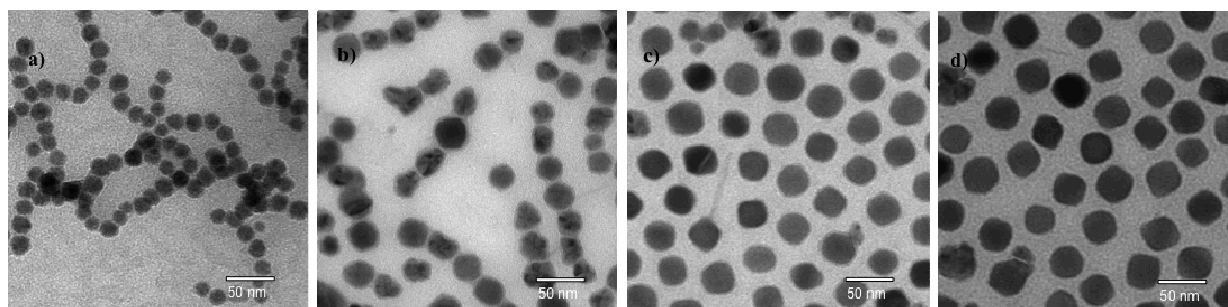


**Figure 1:** Transmission electron microscopy (TEM) images of samples with various TOPO concentration. a) no TOPO is added during the synthesis; b) 6.3 mmol/l TOPO; c) 12.7 mmol/l TOPO; d) 25.4 mmol/l TOPO.

We employed Dynamic Light Scattering (DLS) and Depolarized Dynamic Light Scattering (DDLS) to study the dynamic behavior of magnetic nanoparticle samples that differ in the amount of TOPO. Translational diffusion coefficients as function of particle concentrations were obtained by DLS measurements. Differences in the diffusion coefficient with concentration can shed light on particle-particle interactions. DDLS measurements allow determination the rotational diffusion coefficient of chain structures from which the dimension, thus the length of the chains can be deduced. Comparison of the dynamics of these systems without an external field, and while subjected to an external magnetic field of 3.7 mT has been carried out. We find that under the influence of the magnetic field the diffusion coefficient of all system examined decreases. The decrease of the diffusion coefficient is most likely due to chain formation or cluster formation under the magnetic field. We show that for particles with considerable surface charge (high TOPO concentration) the slowing down of the diffusion under an external magnetic field is a time-dependent process, which surprisingly diminishes with increasing concentration.

## VISCOELASTIC PROPERTIES OF FERROFLUIDS

*Zubarev A.Yu., Chirikov D.N.*

Urals State University, Lenina Ave 51, 620083, Yekaterinburg, Russia

Magnetic fluids (ferrofluids) present colloidal suspensions of single-domain ferromagnetic particles in a carrier liquid. The typical diameter of the particles is about 10-15 nm. In order to prevent the irreversible coagulation of the particles under the action of the colloidal dispersion forces, they are covered by special layers which screen these forces. For many modern ferrofluids the surface shells consist of surfactant molecules; the typical thickness of these layers is about 2-2.5 nm.

One of the interesting and important features of ferrofluids is their ability to change rheological properties under the action of external magnetic field. The first theories of the magnetorheological effects in ferrofluids [1,2] deal with very dilute systems, where any interactions between the particles can be ignored. The maximal magnetoviscous effect predicted by these models does not exceed several per cent. However, experiments (see, for example, [3,4,5]) carried out in recent decades with various commercial ferrofluids, demonstrate increase of their viscosity under the field by one-two orders of magnitude and the time of rheological viscoelastic relaxation which is 4-5 orders of magnitude more than that predicted by the classical models [1,2]. Analysis shows that the strong rheological effects can take place due to appearance of heterogeneous aggregates consisting of the ferrofluid particles [3-5]. Two types of the structures in ferrofluids are well-known – the linear chains and the dense bulk “drops” as well.

One can suppose that experimentally detected [5] viscoelastic phenomena in ferrofluids appear due to finite rate of evolution of ensembles of heterogeneous aggregates after alternation of macroscopical shear rate of the fluid. Characteristic time of evolution of these ensembles can determine the time of macroscopical viscoelasticity of the fluid.

We propose a simple statistical model of kinetics of evolution of the chain-like aggregates in ferrofluids and effect of this process on the macroscopical viscoelastic properties of ferrofluids. Our analysis shows that the viscoelastic phenomena can be determined by evolution of the heterogeneous aggregates in ferrofluids. In spite of the conscious oversimplification of the model, it leads to reasonable agreement with known experimental results.

We are grateful for the financial support to the Russian Fund of Fundamental Investigations (projects 10-01-96002-Ural, 10-02-96001, 10-02-00034), to the Russian Federal Education Agency, projects 2.1.1/2571 and 2.1.1/1535; to the Russian Federal Target Program, projects 02.740.11.0202, 02-740-11-5172 and NK-43P(4).

- [1] W.F. Hall, S.N. Busenberg, *J. Chem. Phys.*, **51** (1969) 137.
- [2] M.I. Shliomis, *Soviet Phys. Uspekhi (Engl. Transl)* **17** (1974) 153.
- [3] S. Odenbach, *Magnetoviscous Effects in Ferrofluids. Lectures Notes in Physics*, Springer, (2002).
- [4] L. Pop, S. Odenbach, *J. Phys.: Condens. Matter.*, **18** (2006) S2785.
- [5] J. Fleischer, *Rheologische Eigenschaften magnetischer Flüssigkeiten unterschiedlicher chemischer Zusammensetzung*. Berlin. Verlag. (2004).

22PO-M-4

## GROUND STATES OF FERROFLUID MONOLAYERS IN THE PRESENCE OF AN EXTERNAL MAGNETIC FIELD

*Kantorovich S.<sup>1,2</sup>, Danilov V.<sup>1</sup>, Prokopieva T.<sup>1</sup>, Holm C.<sup>2</sup>*

<sup>1</sup> Ural State University, Ekaterinburg, Russia

<sup>2</sup> Institute for Computational Physics Universität Stuttgart, Stuttgart, Germany

It is well known that the geometrical confinement can crucially influence the properties of the system. Thus, the microstructure of ferrofluid monolayers (thickness on the order of 40 nm) [1], differs greatly from the one in bulk magnetic fluids both for the case of the absence of an applied magnetic field and under its influence [2]. The first and important step is to analyse the ground state structures formed in a monolayer.

Computer and theoretical investigation of particle arrangements in a thin film of a magnetic liquid at low temperatures is presented. The approach developed by us combines the simplicity of simulations and accuracy of the analytical model and allows to study particle aggregates and their properties [3]. The microstructure was investigated consistently in three steps: monodisperse and bidisperse model in the absence of an external magnetic field, monodisperse model under the influence of an external field. The careful analysis of the most probable microstructures of a thin layer of a magnetic liquid has been carried out at 0K. The analysis of stability of structures under thermal fluctuations allows to draw the conclusion about the microstructure of investigated systems at low temperatures.

This research has been carried out within the financial support by RFBR Grant No.08-02-00647-a, AVCP Grant No. 2.1.1/1535, FASI No. 02.740.11.0202, and the Grant of President RF MK-6415.2010.2 and Alexander von Humboldt Foundation.

[1] Klokkenburg M. et al, *Phys. Rev. Lett*, **96** (2006) 037203.

[2] Kantorovich S. et al, *PCCP*, **10** (2008) 1883.

[3] Prokopieva T. et al, *Phys. Rev. E* **80** (2009) 031404

22PO-M-5

## MICROSTRUCTURE OF BIDISPERSE FERROFLUIDS IN MONOLAYER

*Dobroserdova A.<sup>1</sup>, Minina E.<sup>1</sup>, Cerda J.<sup>2</sup>, Pyanzina E.<sup>1</sup>, Holm C.<sup>3</sup>, Kantorovich S.<sup>1,3</sup>*

<sup>1</sup> Ural State University, Lenin av. 51, Ekaterinburg, 620000, Russia

<sup>2</sup> Institute for Cross-Disciplinary Physics and Complex System,

Campus University de les Illes Balears, 07122, Palma de Mallorca

<sup>3</sup> Institute for Computational Physics, University of Stuttgart, Pfaffenwaldring 27, 70569, Stuttgart, Germany

Ferrofluid particles can form various structures in monolayers in the absence of an external magnetic field. These clusters in constrained geometry are different from the ones in 3D. Recent quasi-2D experiments performed by cryogenic transmission electron microscopy (cryo-TEM) [1]

have demonstrated the formation of chains and rings. However, the microstructure of ferrofluids in 2D is not yet completely understood.

In the present investigation we try to describe the microstructure of bidisperse ferrofluids in quasi-2D geometry where the centres of all particles are trapped in one plane and their magnetic moments can rotate in 3D. This system is the model case of a real liquid which is polydisperse. However, the influence of the polydispersity is observed even in the bidisperse system [2].

We have performed molecular dynamics simulations for understanding the system microstructure. The simulations were realized using simulation package ESPResSO [3]. Together with the simulations we have constructed the theoretical model of the bidisperse ferrofluid. It is based on the minimization of the free energy density functional under the mass balance condition. Our theoretical analysis has allowed to determine sizes, numbers and types of the main structures in thermodynamic equilibrium. These results and data from molecular dynamics simulations have a good agreement.

We have compared the microstructure of the bidisperse ferrofluid in quasi-2D with the one in 3D [4], too. This comparison has shown the difference between them: in 2D one finds more topological configurations of chains (different combinations of small and large particle positions in the chain), rings, and, besides that, the chains in 2D are longer than in 3D. However, the longer chain can be explained only in terms of entropy, not energy. This fact has been also proven by studying pair formation probabilities.

In future we will investigate the microstructure of the bidisperse ferrofluids in constrained geometry in the presence of an external magnetic field. Besides we would study the ferrofluids with stronger interparticle interactions, and for this case the development of a new theoretical approach is needed.

This research has been carried out within the financial support by RFBR Grant No. 08-02-00647-a, AVCP Grant No. 2.1.1/1535, FASI No. 02.740.11.0202, and the Grant of President RF MK-6415.2010.2.

[1] M. Klokkenburg et al., *Phys. Rev. Lett.*, **99** (2006) 037203.

[2] A. Ivanov, S. Kantorovich, *Phys. Rev. E.*, **70** (2004) 02401-01-10.

[3] [http://espressowiki.mpip-mainz.mpg.de/wiki/index.php/Main\\_Page](http://espressowiki.mpip-mainz.mpg.de/wiki/index.php/Main_Page)

[4] C. Holm, A. Ivanov, S. Kantorovich, E. Pyanzina, E. Reznikov, *J. of Phys.: Cond. Matt.*, **18** (2006) 2737.

22PO-M-6

## **DETERMINATION OF THE MOST PROBABLE MAGNETIC MOMENT ORIENTATIONS OF A PAIR OF DIPOLAR HARD SPHERES.**

*Elfimova E., Efimova V., Ivanov A.*

Ural State University, Yekaterinburg, Russia

Classical result of the virial expansion of the pair distribution function is a power series over the ferroparticle volume concentration. For the system of dipolar hard spheres, the coefficients of the series (virial coefficients) depend on the distance between a pair of the particles and intensity of magnetodipole interaction in the absence of an external magnetic field. These coefficients are the result of averaging of the interparticle interaction potential over all possible magnetic moment

orientations and particle positions. Thus pair distribution function describes the probability density of the location of a pair of ferromagnetic particles on a certain distance.

The aim of this paper is determination of the most probable mutual orientation of the magnetic moments of a pair of dipolar hard spheres taking into consideration the influence many particle correlations. For that, the virial coefficients of the pair distribution function are not averaged over the magnetic moment orientations of a pair of ferromagnetic particles. In the obtained function, the points of local maximum are found.

In order to determine the pair distribution function it is convenient to use the diagram method for representation of the virial coefficients. The second virial coefficient corresponds to the set of double-particle diagrams; the third one is the set of three-particles diagrams and so on [1].

In the first approximation, when only double-particle diagrams are taken into account, the obtained result is rather predictable. The “head to tail” position is the most advantageous situation from the energy viewpoint.

In the second approximation it is necessary to study six three-particles diagrams. The examination of all these diagrams allows to get the most probable mutual orientation of the magnetic moments of a particle pair and to find the influence of third ferromagnetic particle on these orientations.

This research has been carried out within the financial support of Grant of President of RF MK-1673.2010.2.

[1] E.A. Elfimova, A.O. Ivanov, *J. Exp. Theor. Phys.* **111**, N.1 (2010) 146.

22PO-M-7

## THE EXPERIMENTAL SETUP FOR MEASURING THERMAL PARAMETERS OF MAGNETIC FLUIDS IN AC MAGNETIC FIELD.

*Yelkhova T.M.<sup>1,2</sup>, Plyashkevich M.L.<sup>2</sup>, Spichkin Y.I.<sup>2</sup>, Tishin A.M.<sup>1,2</sup>*

<sup>1</sup> Faculty of Physics, M.V. Lomonosov Moscow State University, 119991, Moscow, Russia

<sup>2</sup> Advanced Magnetic Technologies and Consulting LLC, 142190, Troitsk, Moscow region, Russia

The setup for measuring of heating effect of magnetic fluid in ac magnetic field has been developed. This apparatus is made for examining of magnetic fluids' thermal properties to use them in the magnetic hyperthermia procedure.

The setup consists of:

- a system of the magnetic field creation;
- a temperature measuring system.

The system of the magnetic field creation consists of generator GAG-810, an amplifier and a magnetic coil (solenoid). The signal from generator is amplified by 200 W amplifier that allows to reach the magnetic field strength of 80 Oe inside the magnetic coil with working bore of 16 mm and linear size of 43 mm. The temperature measuring system consists of differential thermocouple and voltmeter Agilent 34410A.

In the experiments a flask with the magnetic fluid is put into the solenoid working bore and the magnetic field is applied during fixed time interval. The temperature change caused by the field application is measured by the temperature measuring system. Then thermal parameters of the fluid are calculated by model equations.

## USE OF MICROSIZED FERROCOMPOSITES FOR IMMOBILIZATION OF BIOLOGICALLY ACTIVE COMPOUNDS

*Feofanov V.S., Komissarova L.Kh., Kuznetsov A.A., Brusentsov N.A.*

N.M. Emanuel Institute of Biochemical Physics of the Russian Academy of Sciences,  
Kosygin str. 4, 111977, Moscow, Russia. e-mail: komissarova-lkh@mail.ru

Magnetic nano- and microsized particles can be used for various biomedical applications: cell separation, immobilization of enzymes, detoxification of biological liquids, magnetic drug targeting and others [1-3].

We have mainly studied sorption efficiency of iron-carbon microparticles [1]. It is actual to study sorption efficiency of ferrocomposites of different chemical content and dimension in order to evaluate the possibility of using them for immobilization of biologically active compounds. It is necessary to modify the surface of these composites in order make it biocompatible. The aim of the research is to work out new modifications methods of covering the surface of microparticles ferrocomposites by biocompatible materials for the following immobilization of biologically active compounds.

We have modified the surface of composites: iron-carbon (FeC), iron-silica (FeSiO<sub>2</sub>) sized 0,5-2 mkm, magnetite (Fe<sub>3</sub>O<sub>4</sub>) sized 1-3 mkm; iron of content 90% restored iron and 10% Fe<sub>3</sub>O<sub>4</sub>, sized 0,06-0.1 mkm. Carboxilate-modified magnetic particles were obtained by albumin or gelatin coating with the following glutar-aldehyde processing, aldehyde-modified –by dextran coating with NaJO<sub>4</sub> activation. TiCl<sub>4</sub>-modified composites were obtained by TiCl<sub>4</sub> activating of gelatin-coated microparticles. We have studied immobilization of hemoglobin, hemin, barbiturates and other substances on modified particles. Adsorption of hemoglobin and other substances on modified particles was carried out in a physiological solution and in a model biological liquid (0.6% albumin in physiological solution) at 20<sup>0</sup>C (pH 7.2) at different mass ratios of composite/compound. The sorption efficiency of ferrocomposites was determined as the ratio of the quantity of the adsorbed substance to its initial amount (w/w), expressed in % and in mg/g composite (absorptive capacity) for a certain ratio of adsorbent/substance. The maximal absorptive capacity of hemoglobin was found for iron particles modified by albumin and dextran: 40.4 mg/g and 47.3 mg/g, accordingly. The maximal absorptive capacity of natrium phenobarbital (25.7 mg/g) – for iron particles modified by albumin, of barbituric acid - for composite FeSiO<sub>2</sub> (58.0 mg/g). These meanings exceed those for FeC composite. Thus, modified by albumin and dextran Fe microparticles, and FeSiO<sub>2</sub> composite can be recommended for detoxification of biological liquids from free hemoglobin and barbiturates by the method of magnetic hemosorption. The mechanism of biologically active compounds immobilization at different modifications of composites surface is discussed.

[1] L.Kh. Komissarova, A.A. Kuznetsov, V.I. Filippov et al., in: Book of reports symposium “Use of biomagnetic carriers in medicine” (2002) Moscow, p. 68-76.

[2] N.A. Brusentsov, L.Kh. Komissarova, A.A. Kuznetsov et al., Biocatalytic Technology and Nanotechnology. Nova science Publishers (2004) Moscow, p. 59-66.

[3] O.V. Salata, J. of Nanobiotechnology, **3**, No 4 (2004) p.1-6.



## MAGNETIC AND MECHANICAL PROPERTIES OF MAGNETOELASTICS

*Nikitin L.V.<sup>1</sup>, Gladkov A.A.<sup>1</sup>, Nikitin A.L.<sup>1</sup>, Stepanov G.V.<sup>2</sup>*

<sup>1</sup> Moscow State University, Physical department, Moscow, 119899, Russia

<sup>2</sup> SSC RF GNIChTEOS, 38, shosse Entuziastov, Moscow, 111123, Russia

The magnetoelastic is magnetically controllable composite material, which is able to change significantly its shape, elastic and viscous characteristics in an external magnetic field. It is a cluster of small magnetic particles in a polymer matrix. Such kind of materials is supposed to be used as elements of active suppression in mechanical oscillating systems. That's why it is of great importance to study magnetic and magnetically-dependent elastic properties of the magnetoelastic.

We have examined two series of samples:

1. With unchanging size of magnetic particles of 2000 nm and the concentration of particles ranging from 36% to 82%
2. With the unchanging concentration of magnetic particles of 62% and sizes ranging from 10 nm up to 50000 nm.

Our samples of the magnetoelastic were made on the basis of silicone rubber, with the magnetic particles infiltration in the polymerization phase of the sample.

We have examined the dependence of the magnetic characteristics of magnetoelastics on the size and concentration of magnetic particles. In addition, we studied the amplitude-frequency characteristics of the system with the damper - magnetoelastic. It is shown that the amplitude-frequency characteristics depend much on the size and concentration of magnetic particles.

In measurements we have obtained hysteresis loops for both series of samples, the values of magnetization of saturation and magnetic susceptibility. As the result of these studies we came to the conclusion: clusters of larger particles are much more strong in displaying magnetic properties, and hence the using of large particles is much more effective in magnetoelastic control. On the other hand, we should not forget that very large magnetic particles can deform the subsystem of the elastic matrix.

Also, we have obtained the amplitude-frequency characteristics of forced oscillations of the oscillating system. We have measured the amplitude-frequency response of the system with different values of external magnetic field that was applied to the magnetoelastic to show its influence on the oscillatory system. Thus it has been shown that the amplitude of the system in the resonance state decreases with increasing of external magnetic field and the resonance frequency increases. There was investigated the influence of external magnetic field on the frequency response of the system that depends on the concentration and sizes of magnetic particles in the magnetoelastic.

## MODEL OF A THIN ROD WITH VISCOELASTIC MAGNETIZABLE MATERIAL IN THE ALTERNATING MAGNETIC FIELD

Zimmermann K.<sup>1</sup>, Zeidis I.<sup>1</sup>, Naletova V.<sup>2</sup>, Kalmykov S.<sup>2,3</sup>, Turkov V.<sup>3</sup>

<sup>1</sup> Technische Universität Ilmenau, Faculty of Mechanical Engineering, Ilmenau, Germany

<sup>2</sup> Department of Mechanics and Mathematics, Lomonosov Moscow State University, Leninskie Gory, Moscow

<sup>3</sup> Institute of Mechanics, Lomonosov Moscow State University, Michurinskii Pr., 1, Moscow

Dynamics of a thin rod with magnetizable polymer in a cylindrical channel under the action of an alternating “travelling” magnetic field is considered. Magnetic field provokes periodic deformation of the rod, so the rod moves along a channel. It is proved experimentally, that the direction of its motion is opposite to a direction of a “traveling” magnetic field. An experimental installation (a channel with the system of switching electromagnetic coils) and experimental studies of the rod behavior are represented in [1]. The theoretical studies of the rod velocity based on the calculations of static deformations was performed in [2] for small frequencies of the magnetic field. The model of dynamics of a thin rod with magnetizable elastic material was used in [3] for a rod velocity calculation for an arbitrary frequency of the field.

In present paper in order to correct the model a number of new effects are taken into account. Polymer under consideration has an appreciable viscosity, so the model of thin rod with viscoelastic (using Foight model) magnetizable material is used. The equations describing the dynamics of the neutral line of thin rod under the action of external forces  $\mathbf{K}$  (magnetic, gravity and friction) are:

$$\frac{d\mathbf{P}}{dl} + \mathbf{K} = \rho S_b \frac{\partial^2 \mathbf{r}}{\partial t^2}, \quad P_n = -EJ \left( \frac{\partial^2 \theta}{\partial l^2} \right) - 3\eta J \left( \frac{d}{dt} \frac{\partial^2 \theta}{\partial l^2} \right), \quad P_t = S_b \left[ E \left( \frac{\partial l}{\partial l_0} - 1 \right) + 3\eta \frac{d}{dt} \frac{\partial l}{\partial l_0} \right].$$

Here  $\mathbf{r}$  is radius-vector of the neutral line,  $(l, \theta)$  are natural coordinates of the neutral line,  $l_0$  is Lagrange coordinate of non-deformed rod,  $S_b$  is a cross-section area of the deformed rod,  $J$  is a moment of inertia of cross-section,  $E$  is Young's modulus,  $\eta$  is viscosity coefficient.

In order to obtain edge effects for magnetic field near the coil ANSYS is used for magnetic field calculation. Friction coefficient on channel sides has a non-linear dependence on the reaction of the support. Using this model a problem of the rod motion in a vertical plane under the action of “travelling” magnetic field is solved numerically (C++ program was written).

Numerical calculations of the rod motion were performed for various parameters: length of the rod, concentration of magnetic particles in polymer,  $E$  and  $\eta$ . It was shown that viscosity and elasticity have insignificant influence on the rod velocity for small field frequencies. Magnetic properties considerably influence on the rod velocity. For high field frequencies all parameters dramatically influence on the rod velocity. It is shown the strong dependence of rod velocity on an initial rod position.

This work is supported by Russian Foundation for Basic Research (project 10-01-91333) and Deutsche Forschungsgemeinschaft (DFG Zi 540-14/1).

[1] K. Zimmermann, I. Zeidis, V.A. Naletova, V.A. Turkov, *Phys. Stat. Solid.* **1**(12) (2004) 3706

[2] K. Zimmermann, V.A. Naletova, I. Zeidis, V.A. Turkov, E. Kolev, S.A. Kalmykov, *Magneto hydrodynamics*, **44**(2) (2008) 143.

[3] V.A. Naletova, K. Zimmermann, I. Zeidis, V.A. Turkov, S.A. Kalmykov, M.V. Lukashevich, *In: ESMC2009, September 7-11, 2009, Instituto Superior Tecnico, Lisbon, Portugal*, (2009) 124.

22PO-M-11

## **MAGNETIC PROPERTIES VARIATIONS IN IRON COMPLEXES DEPENDING ON THE SYSTEM SPIN STATE**

*Khenkin L.V.<sup>1</sup>, Novakova A.A.<sup>1</sup>, Perov N.S.<sup>1</sup>, Vompe A.A.<sup>1</sup>, Sotskiy V.V.<sup>2</sup>*

<sup>1</sup> Physics Department of Lomonosov MSU, Leninskie Gory, 1, Moscow, 119991, Russia

<sup>2</sup> Chemistry Department of Ivanovo State University, Ermak str., 37, Ivanovo, 153025, Russia

In some metallo-organic complexes of transition metals, called spin-crossover materials (SCO), a central metal cation can switch the spin state (from low-spin to high-spin state) under influence of external factors, like temperature, pressure and magnetic field[1]. Simultaneously with spin state switching optic and magnetic properties of system change. This phenomenon has a wide area of applications in switching, sensing, memory and other devices. The investigations of temperature spin transition were performed by methods of a Mossbauer spectroscopy, magnetic susceptibility measurements and magnetic moment in high field measurements, which allowed to receive the information about a spin transition temperature interval and the changes of iron valent and spin states.

Complexes of bivalent and trivalent iron with ligands based on benzimidazole derivatives have been synthesized and investigated. Samples have been divided in two series by the nature of anion ( $\text{Cl}^-$  or  $\text{ClO}_4^-$ ) and within series samples ligands differed in the length of alkyl radical. The samples differed from each other by color which, as it is known, depends on a spin state. For bivalent samples temperature dependencies were obtained and spin transition temperature interval was established.

Some samples were found in a mix-valence state, that complicated spin transition observation. Combination of Mossbauer spectroscopy method and magnetic moment in high field (16 kOe) measurements in temperatures from 120 K to 350 K allowed us to establish the valence of iron ions under spin transition in our samples and spin transition temperature frameworks for these mix-valence compounds. It was found out that trivalent compounds undergo spin transition in lower temperature interval than compounds with bivalent iron ions.

[1] P. Gutlich, H. Goodwin "Spin Crossover—An Overall Perspective" // Top Curr Chem, **233** (2004), 1–47.

22PO-M-12

## **BEHAVIOR OF GAS-VAPOR INCLUSIONS IN MAGNETIC FLUIDS IN ALTERNATIVE MAGNETIC FIELDS**

*Klimenko E.M.<sup>1</sup>, Simonovsky A.Ya.<sup>1</sup>, Kholopov V.L.<sup>2</sup>*

<sup>1</sup> Stavropol State University, 1 Pushkina str., 355009 Stavropol, Russian Federation

<sup>2</sup> Institute of Mechanics, Lomonosov Moscow State University, 1 Michurinskiy ave., 119192  
Moscow, Russian Federation

Results of experimental investigation of influence of alternative magnetic fields with intensity 3 kA/m on heat flow and frequency of gas-vapor inclusions formation at the boiling of magnetic fluid are presented.

The vapor-fluids nanodisperse magnetizable system is the object of research. It was received by means of heating of magnetic fluid up to the boiling condition. Gas-vapor inclusions are the disperse phase of the system. Magnetic fluid was a dispersion medium of the system. Magnetic fluid (MF) is fulfilling role of the environment. We used magnetic fluid (MF) magnetite on kerosene type with volume concentration of solid phase of 5,75 % and density  $1040 \text{ kg/m}^3$ .

Formation frequency of gas-vapor inclusions at the boiling of magnetic fluid was measured by an inductive method. Heat flow determined by means of system of thermocouples. In the process of heating the sensor indications are recorded by a digital oscilloscope.

The Helmholtz's coils were a source of alternative magnetic field. Magnetic field direction in our experiments was perpendicular to a measuring coils axis (horizontal magnetic fields) or parallel one (vertical magnetic fields).

Observations shows that in the vertical magnetic fields (as opposed to horizontal variable magnetic fields), magnetic fluid started to boil at significantly lower temperature. The emergence of gas-vapor inclusions in the vertical magnetic fields was fixed at a temperature of the heater near  $93^{\circ}\text{C}$  (in horizontal magnetic fields at  $103^{\circ}\text{C}$ ). Frequency of gas-vapor inclusions formation in vertical magnetic fields exceed on 26% frequency in horizontal one.

Behavior of heat flow in vertical horizontal and variable magnetic fields was researched. Heat flows behavior in vertical magnetic field like to horizontal magnetic field in all intensity range. However, the flows in vertical magnetic fields at 25% above than the heat flow in horizontal magnetic fields.

The results suggest that the magnetic field is considerably influence on the behavior of gas-vapor inclusions in magnetic fluids. Therefore the efficient control of heat exchange processes in complex magnetizable systems by an alternative magnetic field is possible.

22PO-M-13

## THE RAYLEIGH-TAYLOR INSTABILITY OF A THIN FERROFLUID LAYER IN A PERPENDICULAR MAGNETIC FIELD

*Kazhan V.A.<sup>1</sup>, Korovin V.M.<sup>2</sup>*

<sup>1</sup> Moscow State University of Environmental Engineering, 127550 Moscow, Russia

<sup>2</sup> Institute of Mechanics, M.V. Lomonosov Moscow State University, 119192 Moscow, Russia

In the present work we study the influence of imposed uniform magnetic field  $H_0$  on the development of the Rayleigh-Taylor instability of a Newtonian ferrofluid layer, which wets the faced-down surface of a horizontal plate made of soft magnetic matter. The layer typical thickness is assumed to be much smaller than the capillary length  $l_c$ , and the layer lower boundary interfaces with a quiescent gas. Since the Rayleigh-Taylor instability is a gravitational instability, which develops in presence of adverse density stratification in fluid, the magnetic bulk force and magnetic normal traction effects should appear for any strength of magnetic field  $H_0$ . The Rayleigh-Taylor instability of a ferrofluid thin layer in a longitudinal magnetic field has been studied theoretically and experimentally in Ref. [1].

From experiments with nonmagnetic viscous fluid layers, it is known that the Rayleigh-Taylor instability growth leads to formation of two-dimensional patterns exhibiting different symmetries [2]. The preferred symmetries are the hexagonal and axial ones. At the latest stage of the instability development the liquid layer disintegrates into the regularly arranged stable pendant droplets, if the Bond number does not exceed the critical value of  $Bo_* = 0.04$ . The distance between two neighbor

droplets in hexagonal patterns is very close to the theoretically obtained value for the fastest growing mode wavelength.

Within the framework of ferrohydrodynamics, we have derived a nonlinear equation which describes the evolution of the local thickness of an initially flat liquid layer. The equation was obtained by asymptotic procedure of simplification applied to the full set of hydrodynamic equations and boundary conditions [3]. Considering the normal modes to be proportional to  $\exp[i(kx - \omega t)]$ , the following dispersion equation was obtained in the framework of the linearized evolution equation and boundary value problem of magnetostatics

$$\omega = \frac{i\alpha}{3\eta c} \kappa^2 (Bo + T\kappa - \kappa^2), \text{ where } i \text{ is an imaginary unit, } \kappa = kc,$$

$$Bo = \left(\frac{c}{l_c}\right)^2, \quad l_c = \sqrt{\frac{\alpha}{\rho g}}, \quad T(\mu_{r1}, \mu_{r2}, q) = \frac{q\mu_{r2}(\mu_{r1}-1)^2}{\mu_{r1}^2 \mu_{r2} + 1}, \quad q = \frac{c\mu_0}{\alpha} H_0^2, \quad \mu_0 = 4\pi \cdot 10^{-7} \frac{H}{m}$$

Here  $\rho$ ,  $\alpha$  and  $\eta$  are the ferrofluid density, surface tension and viscosity, respectively,  $g$  is the gravity acceleration,  $c$  is the layer initial thickness; and  $\mu_{r1}, \mu_{r2}$  are the relative permeabilities of the fluid and plate matter.

Dispersion equation analysis has shown that the range of unstable modes is considerably expanded for magnetic fields easily attainable for laboratory conditions. It was found that upon an increase of  $H_0, \mu_{r1}, \mu_{r2}$  the distance between neighbor pendant droplets decreases.

The work is supported by the RFBR (project 11-01-00051).

[1] V.M. Korovin, A.A. Kubasov, *JMMM*, **202** (1999) 547.

[2] M. Fermigier, L. Limat, J.E. Wesfreid, et al, *J. Fluid Mech.*, **236** (1992) 349.

[3] A. Oron, S.H. Davis, S.G. Bankoff, *Rev. Mod. Physics*, **69**, No. 3 (1997) 931.

22PO-M-14

## MAGNETIC HYDROGELS AND THEIR PROPERTIES

Nikitin L.V.<sup>1</sup>, Gladkov A.A.<sup>1</sup>, Nikitin A.L.<sup>1</sup>, Korovushkin A.E.<sup>1</sup>, Nikolaev A.L.<sup>2</sup>, Gopin A.V.<sup>2</sup>

<sup>1</sup> Moscow State University, Physical department, Moscow, 119899, Russia

<sup>2</sup> Moscow State University, Chemical department, Moscow, 119899, Russia

Hydrogels - solidlike disperse systems, characterized by the formation of the structure, which gives them the mechanical properties of solids. Unlike ordinary hydrogels magnetic hydrogels possess magnetic properties inherent in clusters of small magnetic particles. This paper investigates the conditions under which magnetic hydrogels can be created and their properties can be studied. In this work to create a magnetic hydrogels, these hydrogels have been used as source material: agar hydrogel, polyacrylamide hydrogel, a solution of Pluronic F-127, Temperature detector hydrogel. These hydrogels have been chosen as the common and well-researched. Also these hydrogels have a good repeatability of the samples.

Experiment has shown that the mass concentration of magnetic particles should not exceed a certain critical value, otherwise the polymer matrix gel will not formed. We have identified the critical mass density of magnetic particles in which the formation of magnetic hydrogels is proceeding.

Also the change of the magnetic characteristics of magnetic hydrogels samples during their drying-swelling has been studied. Was obtained hysteresis loops, magnetization of saturation and susceptibility patterns. Dependence of the elastic properties of magnetic hydrogels on the applied magnetic field was researched. It is shown that dependence of the deformation on the compressive stress is linear in agar and polyacrylamide magnetic hydrogels. Observed that with increasing magnetic field the Young's modulus in the examined samples increases.

Despite the fact that the magnetic hydrogels are completely new materials, there are already proposals for their use. It is supposed to use them as humidity sensors, new composite materials and new devices in medicine.

22PO-M-15

## STRUCTURE PROPERTIES OF POLYDISPERSE MAGNETIC FLUIDS

*Krutikova E., Anokhin D.*

Ural State University, Lenin Av, 51, Ekaterinburg, Russia

Structure properties of magnetic fluids are described by pair correlation function  $g(\vec{r}) - 1$  which means probability density for the mutual position of two randomly chosen ferroparticles, the magnetic moments of which are averaged over all orientations. The pair correlation function describes interparticle correlations which responsible for the differences between the properties of a magnetic fluid and those of an ideal paramagnetic gas. Small-angle scattering experiment allows to investigate structure properties of ferrofluids. Experimentally measured intensity of scattering make it possible to obtain the so-called structure factor, which is actually the Fourier transform of the pair correlation function of the ferroparticle system. Thus, for correct processing of experimental data, it is necessary to develop the theoretical model, which would allow to do transition from structure factor in Fourier's space to pair correlation function and back. In actuality, magnetic fluids are polydisperse, so the model is obtained in bidisperse approximation.

The ferrofluid is modeled as a system of bidisperse dipolar hard spheres. All particles were formal divided into two types – «large» and «small». They have diameters -  $d_s$ ,  $d_l$  and magnetic moments  $m_s$ ,  $m_l$ , correspondingly. For this system, the pair correlation function is a function of the typical interparticle distances:  $\vec{r}_{ss}$  («small» - «small»),  $\vec{r}_{ll}$  («large» - «large») and  $\vec{r}_{sl}$  («small» - «large»), and depends on the ferroparticle volume concentration  $\varphi = \pi n d^3 / 6$  and the dipolar coupling constant  $\lambda = m^2 / d^3 kBT$ . Here  $kBT$  is thermal energy and  $n$  is number concentration. Three different parts of pair distribution function  $g(\vec{r})$ , corresponding typical interparticle distances,  $g(\vec{r}_{ss})$ ,  $g(\vec{r}_{ll})$  and  $g(\vec{r}_{sl})$ , determine pair interactions between «small» - «small», «large» - «large» and «small»-«large» particles. Calculation method for each of these parts was described in papers [1, 2] for cases, when particles were modeled as monodisperse dipole soft/hard spheres.

We examined the diagrams which are corresponding to the second and the third virial coefficients in bidisperse case. All diagrams have been divided into three blocks, by the main characteristic distance (between particles with numbers 1 and 2), thus each pair distribution function contained on three basic diagrams – 2 - three-partial and 1 - two-partial.

As a result, we have constructed the interparticle theoretical model of polydisperse magnetic fluid within the bounds of bidisperse approximation. The pair correlation function, which describes interparticle correlations and structure properties of ferrofluid, were determined analytically. Adequacy of constructed model will examine on experimental data. This work is the subject of our further investigation.

Support by Grant of President RF No. MK-2221.2011.2 is acknowledged.

[1] E.A. Elfimova, A.O., Ivanov. *JETP.*, **111**, N1 (2010) 146.

[2] J. Cerda, E. Elfimova, V. Ballenegger, E. Krutikova, A.Ivanov, C. Holm, *Physical Review E.*, **81** (2010) 011501.

22PO-M-16

## EFFECTS IN MAGNETORHEOLOGICAL ELASTOMERS POLYMERIZED IN MAGNETIC FIELD

Bica I.<sup>1</sup>, Balasoiu M.<sup>2,3</sup>, Kuklin A.I.<sup>2</sup>

<sup>1</sup> West University of Timisoara, Department of Electricity and Magnetism, Timisoara, Romania

<sup>2</sup> Joint Institute of Nuclear Research, Dubna, Russia

<sup>3</sup> National Institute of Physics and Nuclear Engineering, Bucharest, Romania

Magnetorheological elastomers (MREs) are composite materials that include an elastic matrix into which magnetizable particles and additives are dispersed. In magnetic field, like the case of magnetorheological suspensions, the magnetizable phase forms aggregates, determining considerably changes in the physical characteristics of MREs. This property is used in various applications and studied intensively.

The materials used for manufacturing MRE are silicone rubber (SR), type RTV 3325/Bluestar Silicones (30 cm<sup>3</sup>); catalyst (C), type 60R/Rhône-Poulenc (6 cm<sup>3</sup>); iron carbonyl (IC), type Merck (18 cm<sup>3</sup>), with granulation ranging between 4.5 μm and 5.4 μm and min. 97% Fe; silicone oil (SO), type Merck, 6 cm<sup>3</sup> volume. The mixture consisting of IC and SO is brought to the temperature of 600K±5% and kept at this temperature for about 300s. IC decomposes thermally. In SO, there remains a solid phase in the form of Fe microparticles (IMs).

A homogeneous mixture consisting of SR, SO, IMs and C is formed, which is then poured in a cylindrical mould located between the poles of a Weiss electromagnet.

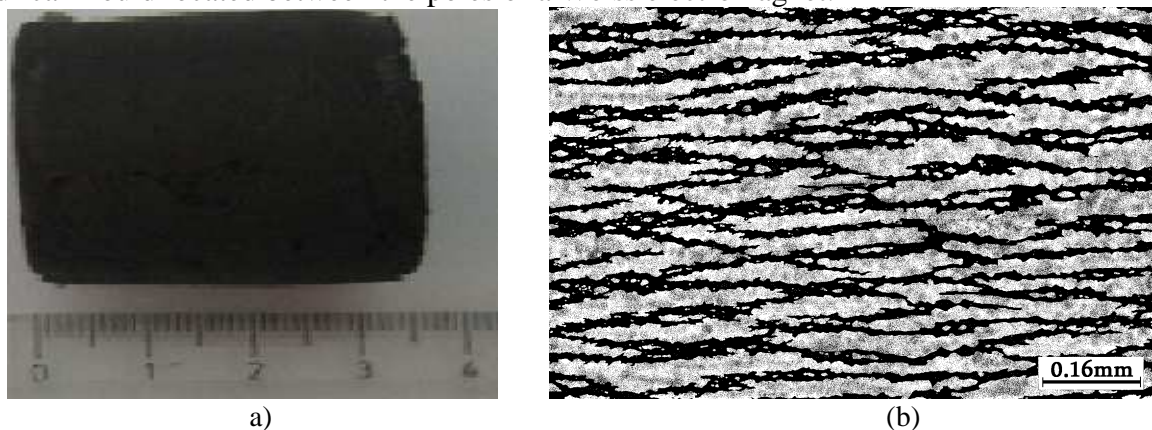


Fig.1. Magnetorheological elastomer: a) shape and size; b) microphotograph of Fe microparticles arranged in the elastic matrix, obtained by transmission in RX.

Conclusions on the study of the magnetoelasticity of the MRE sample can be resumed as follows:

- MRE in the form of a body with cylindrical symmetry, obtained by polymerization in magnetic field has its magnetizable phase in the shape of chains formed of Fe microparticles arranged on plane-parallel surfaces (Fig.1);

- In longitudinal magnetic field, MRE compresses. The relative variation of the length of the cylindrical bar, in absolute value, increases with the increase of  $\vec{H}$ , like the increase in hydrostatic pressure;

- The compression  $\varepsilon$  of the cylindrical bar is influenced by the intensity  $H$  of the longitudinal magnetic field and by the  $k$  value ( $k$  is the rigidity coefficient of a rod connecting particles). For  $k=324$  N/m, the theoretical data sufficiently approximate the experimental ones;

- Due to the magnetic interactions in the volume of the MRE sample, the Young module increases with the intensity  $H$  of the longitudinal magnetic field.

Results on small angle neutron scattering investigations of the elastomer matrix, with induced deformations due to the inclusion of micromagnetic particles, are presented.

22PO-M-17

## **SELF-ORGANIZATION OF HARD-MAGNETIC SrFe<sub>12</sub>O<sub>19</sub> PLATE-LIKE PARTICLES IN COLLOIDAL DISPERSIONS AND ON SOLID SURFACES**

*Kushnir S.E., Koshkodaev D.S., Zuev D.M., Gavrilov A.I., Kazin P.E., Tretyakov Yu.D.*

Lomonosov Moscow State University, 119991, GSP-1, Leninskie Gory 1, Russia

M-type hexaferrites are promising magnetic materials with high magnetic anisotropy, high saturation magnetization, good chemical stability and inexpensive raw materials. The hard-magnetic particles of SrFe<sub>12</sub>O<sub>19</sub> are typically plate-like. High magnetocrystalline anisotropy of strontium hexaferrite allows plate-like particles to have a magnetic moment perpendicular to the largest face of the crystallite. Such particles have properties of microscopic permanent magnets, so that under an applied magnetic field such particles in the colloid solution will orient themselves and the optical density of the solution will change. At the same time, synthesis of colloid solutions of hard-magnetic hexaferrite particles is rather problematic, because of thermodynamic instability of such solutions however, decreased concentrations of particles could extend coagulation time and make a life-time of magnetic colloids longer. The new method was developed for generation of the colloidal solutions of plate-like SrFe<sub>12</sub>O<sub>19</sub> particles based on the glass crystallization technique and on the hydrothermal method.

It's seem very attractive possibility to use thin-film materials based on single-domain hexaferrite particles in microwave technology as shields, waveguides, filter elements and generators. This is due to the fact that strontium hexaferrite has a ferromagnetic resonance frequency around 60 GHz. Hexaferrite film should be well-textured and magnetized for efficient operation of active microwave components. However, there remains the problem of obtaining simultaneously high-textured and high-coercivity hexaferrite films because the texturing leads to coalescence of grains and a sharp drop in the coercive force. To solve this problem, we used pre-synthesized particles and deposit it onto substrates. Substrates were kept in colloidal solutions in magnetic field (different value and orientation). At the same time adsorption of positively charged nanoparticles take place on a negatively charged surface of the substrate.

The aim of the present work – is to investigate self-organization processes of hard-magnetic plate-like nanoparticles in colloidal solutions and on solid surfaces under magnetic field and determine anisotropy of magnetic and magneto-optical properties of formed structures.

Obtained plate-like strontium hexaferrite nanoparticles have coercive force >800 Oe, saturation magnetization >20 e.m.u/g, mean diameter between 30 and 220 nm, aspect ratio up to 15. Coercive force of the colloidal solutions is very close to zero. In the solution particles behaved as molecules of paramagnetic gas and showed self-aligning under the applied magnetic field. Dynamic light-



scattering data of obtained magnetic fluids indicate the absence of large aggregates. The magnetic properties of the colloidal solutions show that the magnetic field of 100 Oe is enough for complete rotation of the particles in one direction (magnetic field perpendicular to the plane of the particle). Obtained magnetic fluids of SrFe<sub>12</sub>O<sub>19</sub> nanoparticles show significant linear dichroism under the applied magnetic field related to the shape anisotropy of the particles (ratio of optical densities achieved 3.8 for the wavelength 550 nm).

Mono-layers of *c*-oriented nanoparticles were obtained on glass and ITO substrates. We studied the effect of the magnetic field and exposure time on the structure of the resulting planar structures.

This work was supported by RFBR, grants 11-08-01256-a and 10-03-00694-a.

22PO-M-18

## **TRICRITICAL BEHAVIOR OF A FERRONEMATIC AT THE FREEDERICKSZ TRANSITION**

*Semenova O.R., Zakhlevnykh A.N.*

Physics Faculty, Perm State University, Bukirev St. 15, Perm 614990, Russia

Within the continuum theory we study the Freedericksz transition induced by an external magnetic field in a ferronematic. We take into account the segregation effect of magnetic particles. We consider the layer of a ferronematic, and the external uniform magnetic field is directed along the limiting plates. The axis of easy orientation of a ferronematic on the limiting surfaces is parallel to the boundaries of a layer and is directed perpendicularly to the direction of the external magnetic field. We consider ferronematic with soft homeotropic coupling between the magnetic particles and the director, and soft planar coupling between the director and the boundaries of a layer. In the latter case we take into account the surface anisotropy of fourth order, the so-called modified Rapini potential [1, 2].

We show that the ferronematic can be in one of three states with different type of ordering. One of them is the uniform state, at which the director is directed along the axis of easy orientation, and the magnetic particles are orthogonal to the director. The second one is the disturbed state when the director and magnetic particles settle down under a certain angle to the direction of an external magnetic field. The third one is the saturation state at which both the director and magnetic particles are aligned along the direction of a magnetic field. We study the transitions between these states at fixed anchoring energy on the layer boundary and on the surface of the magnetic particles. We obtain the equations determining the critical fields of this transitions (the Freedericksz field, and the saturation field).

We show that magnetic-field-induced Freedericksz transition in a ferronematic has the tricritical behavior: for strong segregation it is of the second order, and for low segregation it is of the first order. We derive the analytical expression for the tricritical segregation parameter, determining the phase-transition character change. We determine the dependence of the tricritical segregation parameter on the energy of coupling between the magnetic particles and the director and energy of coupling between the director and the boundaries of a layer for quadropolar and dipolar ferronematic mode. In case of rigid coupling on the boundaries of a layer our results confirm with the results of Ref. [3].

This work was party supported by grant 10-02-96030 from Russian Foundation for Basic Research.

- [1] G.-C. Yang, J.-R. Shj, Y. Ling, *Liquid Crystals.*, **27** (2000) 875.  
 [2] G.-C. Yang, S.-H. Zhang, *Liquid Crystals.*, **29** (2002) 641.  
 [3] D.V. Makarov, A.N. Zakhlevnykh, *Phys. Rev. E.*, **81** (2010) 051710.

22PO-M-19

## AGGREGATE SIZE DISTRIBUTION IN AQUEOUS MAGNETIC FLUID BY IN-LIQUID ATOMIC FORCE MICROSCOPY AND SMALL-ANGLE X-RAY SCATTERING

Shulenina A.V.<sup>1,2</sup>, Avdeev M.V.<sup>3,2</sup>, Besedin S.P.<sup>2,4</sup>, Volkov V.V.<sup>4</sup>, Hajdu A.<sup>5</sup>, Tombacz E.<sup>5</sup>, Aksenov V.L.<sup>2,3,1</sup>

<sup>1</sup> M.V. Lomonosov Moscow State University, Moscow, Russia

<sup>2</sup> National Research Center “Kurchatov institute”, Moscow, Russia

<sup>3</sup> Joint Institute for Nuclear Research, Dubna Moscow Region, Russia

<sup>4</sup> A.V.Shubnikov Institute of Crystallography Russian Academy of Sciences, Moscow, Russia

<sup>5</sup> University of Szeged, Szeged, Hungary

Microstructure and corresponding properties of magnetic fluids are of current interest taking into account the potential of these systems in biomedical applications (contrast medium in magnetic resonance imaging, controlled targeted drug delivery by an external magnetic field, magnetic hyperthermia, etc.). Stabilization of biocompatible magnetic fluids, which would prevent any aggregation and its subsidiary effects (e.g. clots in blood) in living organisms under various conditions, is still a challenge. In this connection, the important task is the registration and analysis of aggregation in water-based magnetic fluids.

In the given work atomic-force microscopy (AFM) in liquid conditions is used for determining the size distribution function of nanoparticle aggregates in aqueous magnetic fluid with magnetite coated by polyacrylic acid for stabilization. For anchoring the aggregates at the substrate (melted quartz) the external magnetic field is used. The obtained results are compared with the data of small-angle X-ray scattering (SAXS), as well as AFM for dried precipitates formed under evaporation of liquid medium both in absent and presence of an external magnetic field. It is shown that in-liquid AFM gives the distribution, which is closest to that obtained by SAXS. The reason for significant shifts in “dry cases” is related to the formation of additional aggregates during evaporation.

## INVESTIGATIONS OF A $\text{CoFe}_2\text{O}_4$ -FERROFLUID BASED ON MAGNETIC MEASUREMENTS

Stan C.<sup>1</sup>, Cristescu C.P.<sup>1</sup>, Balasoiu M.<sup>2,3</sup>, Perov N.<sup>4</sup>, Duginov V.N.<sup>2</sup>, Mamedov T.N.<sup>2</sup>, Fetisov L.<sup>4</sup>

<sup>1</sup> Department of Physics I, Faculty of Applied Physics, Politehnica University of Bucharest, 313 Spl. Independentei, RO-060042, Romania

<sup>2</sup> Joint Institute for Nuclear Research, 141980, Dubna, Russia;

<sup>3</sup> Horia Hulubei National Institute of Physics and Engineering, P.O. Box.MG-6, Bucharest, Romania

<sup>4</sup> Faculty of Physics, Moscow State University, Moscow, Russia

The magnetic properties of ferrofluid systems are interesting both in the development of a large spectrum of applications and from a theoretical point of view. The investigation of a system of ultrafine particles and clusters allow the study of the influence of the finite size of the system on the material properties. Nanoscale clusters make a bridge between the bulk system and the atom and their study may show how the bulk properties evolve from the atomic properties when increasing the number of atomic clusters.

In this work we present results of the experimental investigations of a  $\text{CoFe}_2\text{O}_4$  ferrofluid dispersed in water. The magnetization curves were recorded at temperatures 80 K and 300 K.

In the theoretical treatment the magnetogranulometric methods based on Langevin model and on the hypothesis of a log-normal distribution for the magnetic diameters of particles were considered.

According to the Langevin model of paramagnetism, the ferrofluid is considered as composed by non interacting spheres with a permanent dipolar magnetic moment rotating together with the particle when applying an external magnetic field. The macroscopic magnetization is obtained as a result of the combined action of an orientation induced by the external field and a destabilization produced by the Brownian motion. The magneto-granulometric analysis [1] for the ferrofluid sample performed at  $T = 300$  K, where the Langevin model is applicable, gives the parameters of the size distribution.

The experimental results obtained for  $T=80$ K cannot be treated using the Langevin model. On the assumption that the saturation magnetization is a consequence of the effect of a total orientation of all individual magnetic moments in the direction of the external field, we can compute the mean magnetic diameter at this temperature assuming the hypothesis that the density of particles does not change with temperature [2]. The reconstructed probability distributions based on the computed parameters  $D_0 = 6.30$  nm,  $S = 0.23$  for  $T = 300$  K and  $D_0 = 6.55$  nm,  $S = 0.41$  for  $T = 80$  K are shown in Fig.1. Results of the magneto-granulometric analysis are presented and discussed.

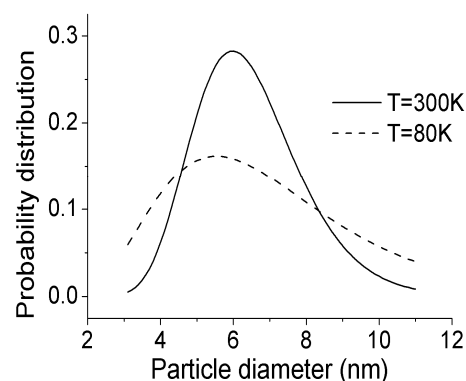


Fig.1 Probability distribution function for particle diameters.

The authors acknowledge the financial support through the grant of the Romanian Governmental Representative in the Joint Institute for Nuclear Research, Dubna no.148/15.03.2011 item 2 and the UPB-JINR cooperation scientific projects no.146/15.03.2011 item 5 and no.151/15.03.2011 item 5.

[1] M. Raşa, D. Bica, A. Philipse, L. Vékás, *Eur. Phys. J. E.*, **7** (2002) 209.

[2] C. Stan, C. P. Cristescu, M. Balasoiu, N. Perov, V. N. Duginov, T. N. Mamedov, L. Fetisov, *UPB Sci. Bull., Series A*, **73**, Issue 3 (2011).

## DYNAMICS OF A POLYMER MICRODROP SUSPENDED IN A MAGNETIC FLUID IN ELECTRIC AND MAGNETIC FIELDS

*Tkacheva E.S., Zakinyan A.R., Dikansky Yu.I.*

Department of Physics, Stavropol State University, 1 Pushkin Street, 355009 Stavropol, Russia

The study and design of new composite material systems based on magnetic fluids attracts much attention owing to wide potential applications of such systems. One of new materials based on magnetic fluid is a magnetic fluid emulsion, disperse system composed of two liquid phases one of which is a magnetic fluid. In the present work we study the behavior and dynamics of the shape of the magnetic fluid emulsion microdrops under the action of external electric and magnetic fields. The magnetic fluid emulsion studied comprises the liquid caoutchouc microdrops as a dispersed phase and the kerosene based magnetic fluid as a dispersion medium.

Droplet behavior was experimentally studied by observations with an optical microscope, which was placed between Helmholtz coils generating a uniform magnetic field in the space where the cell containing a magnetic emulsion was located. The thin cell with emulsion was assembled of two rectangular glass plates covered with a transparent conducting coating. A variable voltage applied to the plates generated the electric field between them. First we studied the droplet behavior under the action of ac electric field and then under the simultaneous action of ac electric and dc magnetic fields.

It was experimentally observed that at relatively low frequencies of electric field, the droplet is flattened taking the shape of oblate ellipsoid of revolution; at higher frequencies the droplet stretches along the force lines of the electric field becomes prolate ellipsoid. When the electric field strength rises, the droplet shape changes: a hole arises in the middle of the droplet and it takes the toroidal shape. Upon a further increasing of the electric field strength the toroidal droplet bursts into several smaller droplets. These small droplets then begin to rotate. The evolution of the droplet shape with increasing of the electric field strength at constant field frequency is shown in Fig. 1.

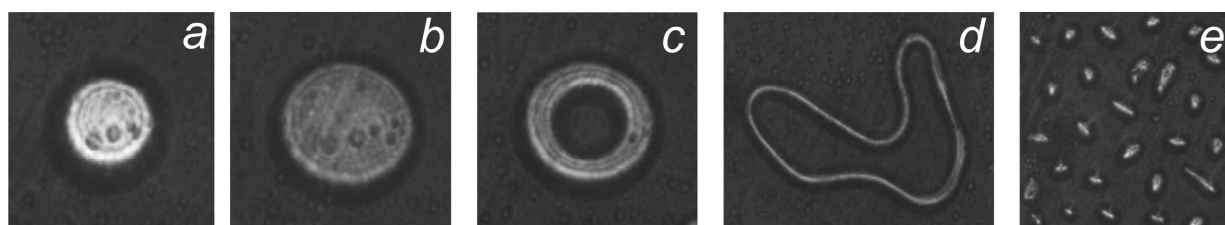


Fig. 1. Microdrop at different values of electric field strength:  $a - E = 0$ ;  $b - E = 150$  kV/m;  $c - E = 200$  kV/m;  $d - E = 315$  kV/m;  $e - E = 420$  kV/m. Initial microdrop size is  $55 \mu\text{m}$ . Electric field frequency is 8 Hz.

Additional action of constant magnetic field directed in parallel with electric field changes the droplet shape evolution. In particular, the toroidal shape does not appear when additional magnetic field acts. The frequency of rotation of small droplets formed after the breakup of initial microdrop depends on the electric field frequency and electric and magnetic fields strength. The observed peculiarities of the microdrop behavior have been analyzed and the theory of the observed phenomena has been developed.

This work was supported by the Russian Foundation for Basic Research (grant no. 10-02-90019-Bel\_a).

22PO-M-22

## HEAT CAPACITY OF A MAGNETIC FLUID: THEORY AND EXPERIMENTS

*Elfimova E.<sup>1</sup>, Korolev V.<sup>2</sup>, Korolev D.<sup>2</sup>, Titova E.<sup>1</sup>*

<sup>1</sup> Urals State University, Lenin av. 51 Ekaterinburg 620000, Russia

<sup>2</sup> Institute of solution Chemistry of RAS, Ivanovo, 153045, Russia

Specific heat capacity of a magnetic fluid was studied both experimentally and theoretically. The temperature and magnetic field dependences of specific heat capacity were investigated.

Experimentally specific heat capacity of the magnetic fluid on the base of Fe<sub>3</sub>O<sub>4</sub> has been determined by calorimetric method in the temperature range 288-353K in the magnetic field from 0 to 0.7 T. The measurement was carried out on automatic microcalorimetric installation. The microcalorimetric cell with isothermal shell was placed between two poles (60mm) of electric magnet. A volume of reaction vessel was 2 ml. Inaccuracy of measurements did not exceed 2%. The experimental results have shown that the temperature and field dependences of specific heat capacity have a complex nature [1].

For explanation of these anomalies we have developed theory. Since the magnetic fluid is a dispersion of nanoparticles, the interaction energy of ferroparticles is significant. Therefore it is necessary to take into account contribution to specific heat capacity from this interaction. For that, the magnetic fluid was modeled as a system of homogeneously magnetized monodisperse hard spheres suspended in a liquid carrier with volume  $V$ . Interactions between ferroparticles were described by the sum of the hard-sphere potential and the dipole-dipole potential. The configurational part of the Helmholtz free energy  $F$  of the magnetic fluid has been calculated for this system using virial expansion  $F$  over ferroparticle concentration. The method of virial coefficient determination is described in [2]. The computation of heat capacity is a standard procedure if the free energy is known:

$$C_{P(\text{int})} = \left( \frac{\partial}{\partial T} \left[ \left( T^2 \frac{\partial F}{\partial T} \right)_V + \left( V \frac{\partial F}{\partial V} \right)_T \right] \right)_P$$

where  $C_{P(\text{int})}$  is the contribution to specific heat capacity from ferroparticle interactions,  $T$  and  $P$  are temperature and pressure correspondently. Finally, since the magnetic fluid is heterogeneous system, the specific heat capacity was calculated on assumption of additivity of the specific heat capacity of the dispersion components:

$$C_{P(MF)} = (C_{P(fp)} + C_{P(\text{int})})\omega_{(fp)} + C_{P(lc)}\omega_{(lc)} + C_{P(sa)}\omega_{(sa)},$$

where  $C_{P(MF)}$ ,  $C_{P(fp)}$ ,  $C_{P(lc)}$  and  $C_{P(sa)}$  are specific heat capacity of magnetic fluid, solid phase, liquid carrier and surfactant accordingly;  $\omega_{(fp)}$ ,  $\omega_{(lc)}$  and  $\omega_{(sa)}$  are mass fractions of solid phase, liquid carrier and surfactant correspondently.

The theory is being tested against the experimental results.

This research has been carried out within the financial support of Grant of President of RF MK-1673.2010.2.

[1] V.V. Korolev, I.M. Arefyev, A.V. Blinov, *Journal of Thermal Analysis and Calorimetry* **92**, N.3 (2008) 697.

[2] E.A.Elfimova, A.O.Ivanov, *JETP* **111**, N.1 (2010) 146.

## THE INFLUENCE OF INTERPARTICLE CORRELATIONS ON INITIAL MAGNETIC SUSCEPTIBILITY OF A FERROFLUID

*Elfimova E., Ivanov A., Turysheva E.*

Urals State University, Lenin av. 51 Ekaterinburg 620000, Russia

Ferrofluids are stable suspensions of the one-domain nanoparticles of ferromagnetic and ferrimagnetic materials in liquid carriers. The ferrofluids synthesized by now have record-breaking high values ( $\sim 100$ ) of an initial magnetic susceptibility at room temperatures. Such ferrofluids are highly concentrated, and the intensity of interparticle dipole-dipole interaction exceeds the thermal energy. Any known theoretical model [1, 2] cannot describe so high values of the initial magnetic susceptibility (Fig.1).

In present work the statistical model, describing initial magnetic susceptibility of dense ferrofluids, has been developed. The ferrofluid is considered as a system of homogeneously magnetized monodisperse spheres. The system Hamiltonian contains the following terms: the spherical part of interparticle interactions (hard sphere potential / square-well potential) and the dipole-dipole interactions of the particle magnetic moments. The initial magnetic susceptibility is calculated using the virial expansion over ferroparticle concentration. To calculate the dipolar hard spheres virial coefficients we suggest their expansion in power series over the intensity of dipole-dipole interaction; this method is described in details in Ref. [3]. So, each virial coefficient is presented as power series over dipole-dipole interaction potential. After averaging of the virial coefficients over magnetic moment orientations and over all particle positions we obtain expression for the initial magnetic susceptibility as a function of the ferroparticle volume concentration and the dipolar coupling constant. The theory takes careful account of the many-particle correlations that play a dominant role in concentrated systems.

The theory is being tested against the experimental results and computer simulation data.

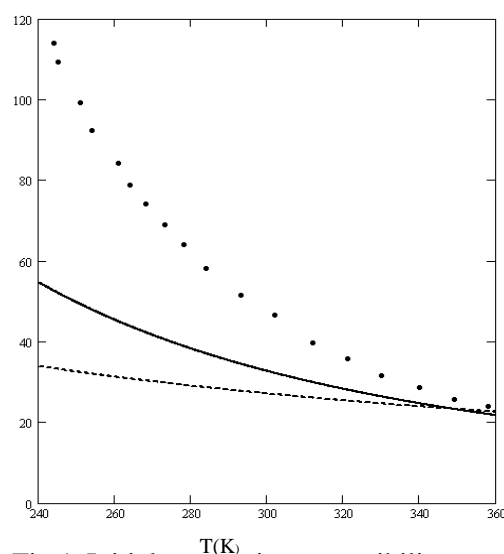


Fig.1 Initial magnetic susceptibility as a function of temperature. Points are initial magnetic susceptibility of concentrated decane-based ferrocolloid; curve 3 corresponds to Langevin model, curve 2 is the theoretical model [2].

The work was supported by the Grant No. MK-1673.2010.2 of the President of Russian Federation.

[1].M.I. Shliomis, *Usp. Fiz. Nauk*, **112** (1974) 427.

[2] A.O. Ivanov, O.B. Kuznetsova, *Phys. Rev.E.*, **64** (2001) 041405.

[3] E.A. Elfimova, A.O. Ivanov, *J. Exp. Theor. Phys.* **111**, N.1 (2010) 146.

## NON-EQUILIBRIUM MAGNETIZATION OF A DILUTE SUSPENSION OF BROWNIAN MAGNETIC PARTICLES

*Tyatyushkin A.N.*

Institute of Mechanics, Moscow State University, Michurinsky Ave., 1, Moscow 119192, Russia

Non-equilibrium magnetization is the reason due to which magnetizable substances are heated in a periodically varying magnetic field. This phenomenon can be applied for various purposes. One of the most interesting its applications is the use of the magnetic hyperthermia as a method of cancer treatment (see, e.g., [1], [2]). The goal of this work is to investigate theoretically non-equilibrium magnetization of a dilute suspension of magnetic Brownian particles and its influence on heating of the suspension in an alternating magnetic field.

Consider a suspension of spherical Brownian particles. Each particle has the moment of inertia  $J$  and the embedded magnetic moment  $\mathcal{M} = \mathcal{M}(t)$  ( $|\mathcal{M}(t)| = \mathcal{M}$  is constant). The suspension is in a uniform harmonically oscillating magnetic field with intensity vector  $\mathbf{H}(t) = \mathbf{H}_a \cos(\omega t)$ , where  $H_a$  and  $\omega$  are the amplitude and frequency of the oscillation. If  $H_a$  does not exceed some critical value at which non-linear effects can no longer be neglected, the heat production power density  $q = \chi'' \omega H_a^2 / 2$  [1], where  $\chi''$  is the imaginary part of the complex magnetic susceptibility,  $\chi' + i\chi''$ .

Let the suspension be so dilute that the interaction of a single particle with the others may be neglected. Then the equation that determines the rotation of a single particle is as follows

$$J \frac{d\mathbf{\Omega}}{dt} = \mathcal{M} \times \mathbf{H}_a \cos(\omega t) + \mathbf{K}_v + \mathbf{K}_B, \quad (1)$$

where  $\mathbf{\Omega} = \mathbf{\Omega}(t)$  is the angular velocity of the particle,  $\mathbf{K}_B$  is the moment of the stochastic force that causes the rotational Brownian motion of the particle,  $\mathbf{K}_v$  is the moment of the viscous force acting on the rotating particle. The magnetization vector of the suspension,  $\mathbf{M}$ , is calculated with the use of the equation

$$\mathbf{M}(t) \cdot \frac{\mathbf{H}}{H} = \int_0^{2\pi} \int_0^\pi \mathcal{M} n \cos\theta f(\theta_0, \varphi_0) d\theta d\varphi, \quad (2)$$

where  $n$  is the number of the particles per unit volume,  $\theta_0$  and  $\varphi_0$  are the initial angle between  $\mathbf{H}_a$  and  $\mathcal{M}$  and the corresponding azimuth angle,  $\theta = \theta(\theta_0, \varphi_0)$  is the angle between  $\mathbf{H}$  and  $\mathcal{M}$ ,  $f = f(\theta_0, \varphi_0)$  is the probability density function that describes the distribution of the initial magnetic moment vectors of the particles over directions. On the other hand,

$$\mathbf{M}(t) = \text{Re}[(\chi' + i\chi'') \exp(-i\omega t)] \mathbf{H}_a. \quad (3)$$

In order to obtain the function  $\theta = \theta(\theta_0, \varphi_0)$ , the equation (1) is solved. The obtained function is then used for the calculation of the integral in (2). The comparison of (2) and (3) yields  $\chi'$  and  $\chi''$  as functions of  $\omega$  and of the parameters of the suspension.

Knowledge of the frequency dependence of  $\chi'$  and  $\chi''$  allows controlling magnetization processes more effectively. In particular, the frequency at which  $q$  is maximal can be calculated. This can be useful in the design of apparatus in which heating in alternating magnetic fields is used, e.g., of apparatus for magnetic hyperthermia.

Support by RFBR grants 11-01-00051 and 10-01-00015 is acknowledged.

[1] R.E. Rosensweig, *J. Magn. Magn. Mat.*, **252** (2002) 370.

[2] W. Andrä et al., *J. Magn. Magn. Mat.*, **194** (1999) 197.

22PO-M-25

## HEAT EXCHANGE IN VAPOUR-LIQUID SYSTEM BASED ON MAGNETIC FLUIDS

*Yanovskiy A.A.<sup>1</sup>, Simonovsky A.Ya.<sup>1</sup>, Kholopov V.L.<sup>2</sup>*

<sup>1</sup> Department of Physics, Stavropol State University, 1 Pushkina str., 355009 Stavropol, Russian Federation

<sup>2</sup> Institute of Mechanics, Lomonosov Moscow State University, 1 Michurinskiy ave., 119192 Moscow, Russian Federation

Heat exchange in a vapour-liquid nanodispersed magnetizable system was experimentally investigated. The dispersed phase of the system is vapour bubbles and the dispersive medium is the kerosene-based magnetic fluid. The vapour-liquid system was obtained by heating the magnetic fluid to the boiling point. Interest to heat exchanging processes in vapour-liquid system is caused by possible use of a magnetic fluid as the hardening medium and as the heat transfer medium in heat exchange devices.

We used the experimental setup consists of the quartz glass cylindrical container attached to a steel plate on which the magnetic fluid boils. Heat delivery to the plate was carried out by means of the steel rod serving as a heater. The steel rod was adjoined to a central part of the plate. The plate and the rod were made of nonmagnetic steel. Two thermocouples were placed along heat-conducting rod. The experimental setup was exposed to a constant magnetic field produced by Helmholtz coils. The constant magnetic field was varied from 0 to 4.2 kA/m.

Signals from thermocouples were transmitted to the computer with analog-to-digital converter. On the basis of the temperatures indicated by thermocouples heat flow in the vapour-liquid system was calculated.

We investigated three samples of vapour-liquid system. The first sample based on magnetic fluid with density  $1.447 \text{ g/cm}^3$  and saturation of magnetization 50.9 kA/m. The second one – based on magnetic fluid twice diluted by kerosene and third – based on four times diluted initial magnetic fluid. Experiments were carried out under the action of vertical and horizontal constant magnetic field.

The experimental results have shown that the heat flow from the plate to the vapour-liquid system is incremented by 30 % in a temperature range 120-125 °C of heat exchange surface under the action of vertical magnetic field, and 50 % in a temperature range 125-130 °C under the action of horizontal magnetic field. Magnetic field influence on the second sample more feebly, the heat flow is incremented by 20 %. Magnetic field influence on the third sample was detected at temperature ~ 150 °C of heat exchange surface, the heat flow decreases by 15 %.

The obtained results indicate the possibility of guidance of heat exchange processes in the vapour-liquid magnetizable systems by means of magnetic field.

This work was supported by Russian Foundation for Basic Research (grant no. 11-01-00051-a).



## PARTICLES SIZE DISTRIBUTION IN AGGREGATED MAGNETIC FLUIDS: OPTICAL MEASUREMENTS

*Yerin C.V.*

Stavropol State University, 1 Pushkin st., 355009 Stavropol, Russian Federation

The definition of the form of particles size distribution in aggregated magnetic fluids is the important problem. Definition of a particles size distribution function in a colloid system demands the solution of an integral Fredholm's equation. The solution of such integral equations is incorrect or ill-posed problem. For the definition of particles size distribution functions of particles in magnetic fluids the wide range of regularization methods is used. One of the most simple procedures is histogram representations of an unknown distribution function or distribution function approximation simple one or two-parameter function.

Electronic microscope data of magnetic fluids as a rule can be approximated by two-parameter distribution function like to a log-normal distribution. In this work we have tried to estimate the form of particles size distribution in kerosene based magnetic fluid on the basis of optical experiments - kinetics of a magnetic birefringence in a pulsed magnetic field. The definition of the from of particles size distribution function from optical experiments essentially depends on the physical mechanism of particles orientation in a field (relation of constant and induced magnetic moments of particles and aggregates). Taking into account peculiarities of a log-normal distribution function the a relaxation of birefringence effect for aggregates of magnetic particles with an induced magnetic moment look as follows:

$$\frac{\Delta n(t)}{\Delta n_0} = \exp(-18\sigma^2) \int_0^{\infty} f(y) y^6 \exp\left(-\frac{6kT}{\pi\eta y^3 d^3} t\right) dy . \quad (1)$$

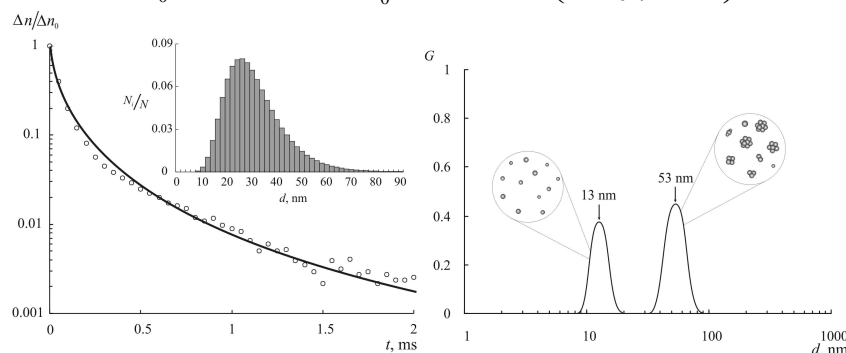


Fig. 1

Fig. 2

The experimental relaxation curve of birefringence in the magnetic colloid of a magnetite in kerosene with concentration of solid phase of 0.05 % and the histogram of particle sizes distribution which was calculated on this basis is presented on fig. 1. The dispersion of particles sizes on these data from 10 to 80 nanometers. The dispersion of particles sizes in kerosene based magnetic fluid has been measured by means of spectrometer Photocor Complex which allows to make the automated examinations by a method of dynamic light scattering and to spot a form of particles size distribution. Distribution curve gained on the Photocor Complex spectrometer (fig. 2) is the two-extreme function with the medial values of 13 and 53 nanometers corresponding to separate magnetite particles (10-20 nm) and to nanoparticles aggregate (40-80 nm).

Supported by Russian Ministry of Science and Educational in Scientific Program "Development of Scientific Potential of High School" and the Russian Foundation for Basic Research (10-02-09019Bel\_a).

## EFFECTS OF MAGNETIC FIELDS ON SURFACE TENSION AND STABILITY OF FERROFLUID INTERFACES

*Zhukov A.V.*

Institute of Mechanics, Moscow State University, Michurinskiy Pr. 1, Moscow 119192, Russia

In [1] the authors studied the dependence of surface tension at the ferrofluid-water interface on magnetic field using the phenomenological model based on surface magnetization. They used the expression for the surface thermodynamic potential  $f' = \sigma + \gamma_t \bar{H}_t^2 + \gamma_n \bar{B}_n^2$ , where both tangential and normal coefficients  $\gamma_t, \gamma_n$  have dimensions of length. This leads to new boundary conditions for magnetic field with second order derivatives and to anisotropic surface tension tensor  $\sigma_k^i = (\sigma - \gamma_n \bar{B}_n^2 + \gamma_t \bar{H}_t^2) \delta_k^i - 2\gamma_t \bar{H}_{tk} \bar{H}_t^i$ . It was found experimentally that  $\gamma_t < 0, \gamma_n > 0$ , which provides the correctness of the magnetostatic boundary value problem. The studies based on interfacial structure analysis for model one-component systems with dipolar interactions in external magnetic [2] and electric [3] fields predict, however, the opposite signs:  $\gamma_t > 0, \gamma_n < 0$ .

We investigate the structure of the flat interface between two phases in a liquid with dipolar interparticle interactions via the generalized squared gradient model (like introduced in [2]) as well as via the model with non-uniform magnetic permeability. The magnetic field is considered as a perturbation. The expressions for the coefficients  $\gamma_t, \gamma_n$  for various equations of state and the bounds for them depending on the effective interface thickness are obtained. The inequality  $\gamma_t > 0$  is shown to be valid for the small particle volume fractions.

For the case  $\gamma_t > 0, \gamma_n < 0$  the magnetostatic boundary value problem is correct for big domain size  $L$  (in the limit  $L / \max(\gamma_n, \gamma_t) \rightarrow \infty$ ) if and only if  $\mu_1^2 < q \equiv -\gamma_t / \gamma_n < \mu_2^2$ , where  $\mu_1, \mu_2$  are the relative magnetic permeabilities of phases. Small values of  $L$  have no physical sense, because the values of  $\gamma_t, \gamma_n$  are of the order of the interface thickness or even less. For  $q < 0$  the magnetostatic problem is incorrect for big domain sizes. This leads to instability of the interface.

The linear stability of the horizontal interface between two magnetizable non-conducting incompressible fluids is studied using the model [1] for surface tension. This model is also applicable to thin magnetic fluid films. The dispersion relation for gravity–capillary waves on an interface between two semi–infinite fluid domains in the external magnetic field is obtained. For big tangential fields and  $\gamma_t \neq 0$  there exists an instability due to negative surface tension eigenvalues [1]. A normal field causes the classical Rosensweig instability, with critical field values depending also on  $q$  and  $\gamma_t / \lambda_{cap}$ , where  $\lambda_{cap}$  is the capillary-gravity wavelength, which may be very small in this problem. For  $\gamma_t > 0, \gamma_n < 0$  there exists also a short-wavelength instability and the critical field value drastically decreases (if  $|q / \varepsilon_1 - 1| \ll 1$  this occurs even for relatively small  $\gamma_t / \lambda_{cap}$ ). Relations to the instability caused by capillary-wave fluctuations and generalizations of the model on curved interfaces are discussed.

Supported by the Russian Foundation for Basic Research (Grants 10-01-00015, 11-01-00051)

[1] A.N. Golubyatnikov, G.I. Subhankulov, *Magnetohydrodynamics(Engl.Transl.)*, **22** (1986) 62.

[2] V.P. Shilov, *J. Magn. Magn. Mater.*, **302** (2006) 495.

[3] V.B. Warshavsky, X.C. Zeng, *Phys. Rev. E*, **68** (2003) 051203-1.

## ABOUT CORRELATION OF MAGNETIC MOMENT OF MAGNETITE NANOPARTICLES IN FERROFLUID

*Dikansky Yu.I., Kunikin S.A., Gladkikh D.V.*

Stavropol State University, 1 Pushkin st., 355009 Stavropol, Russian Federation

Possibility of the long-range magnetic order in colloids single-domain nanoparticles was considered earlier in a considerable quantity of articles and in some of them the effects testifying in its advantage [1,2] whereas in others this possibility is sharply criticised [3]. In this work we present the investigation of well developed system magnetised aggregates which arise under certain conditions in magnetic fluids, initial samples in which can be created them, and also magnetic fluids.

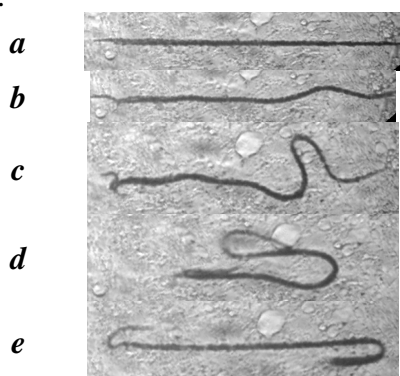


Fig. 1

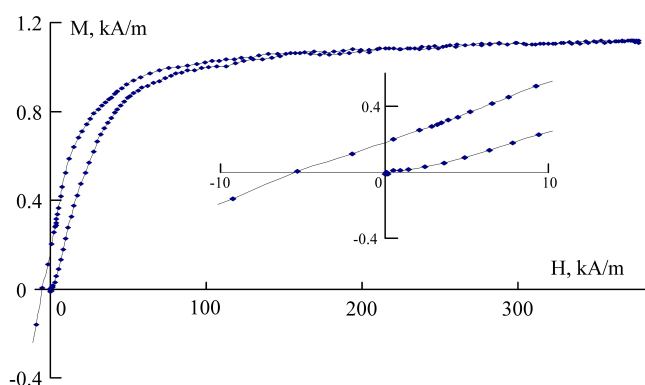


Fig. 2

We have found that in magnetic colloids with large particles (diameter more than 10 nanometers) can arise aggregates with large permanent magnetic moment. Such aggregates as a rule have considerable form anisotropy, quickly interact with an external magnetic field and without the field its oriented along magnetic field of the Earth. In some cases such aggregates have the threadlike shape and a minimum of a magnetic field energy without a magnetic field is reached at the expense of a ramification and an interlacing of aggregates. Magnetised aggregates can occur at long-term (to several tens years) storage of magnetic fluids with great value of the medial size of particles. Besides we have created such structures by simulated infringement of aggregative stability of initial homogeneous magnetic colloid at coagulant addition (surplus oleic acid). In some cases threadlike magnetised aggregative structures can possess flexibility that leads to interesting features of their motion at change a field direction. The behaviour of the threadlike magnetised aggregates is shown in fig. 1 at a change of direction of an external magnetic field (*a* – the field is directed on the right - on the left; *b, c, d, e* – a view of aggregate at regular intervals (about 1 sec) after reversing of the field direction). Complex investigation of magnetic properties of aggregate in DC and AC magnetic fields has allowed to make a conclusion that single-domain particles in this aggregates is not superparamagnetic. Their transfer in a paste-like state at increasing of concentration or introduction of polymerizing additives leads to hysteresis on magnetisation curves (fig. 2). Also such systems possess some features of magnetisation processes not to peculiar usual magnetic fluids without aggregates.

Supported by Russian Ministry of Science and Educational in Scientific Program “Development of Scientific Potential of High School” and the Russian Foundation for Basic Research (10-02-09019Bel\_a).

- [1] H. Mamiya, I. Nakatani, and T. Furubayshy *Phys. Rev. Lett.*, **84** (2000) 6106.  
 [2] D. Wei and G.N. Patey, *Phys. Rev. Lett.*, **68** (1992) 2043.  
 [3] A. F. Pshenichnikov and A. V. Lebedev *Colloid Journal*, **67** No.2 (2005) 189.

22PO-M-29

**MICRO-EXPLOSIONS IN MAGNETIC FLUIDS***Golubiatnikov A.N.*

Moscow State University, 119992 Moscow, Leninskie gory, Mech. &amp; Math. dept., Russia

As is well known, the application of sufficiently strong external magnetic field gives rise to the formation of aggregate drops in initially homogeneous magnetic liquid. The corresponding theory of structural phase transitions induced by instantaneous jumps of magnetic fields was developed earlier [1]. In the present work this theory is extended by means of addition of dissipative terms involving spatial derivatives. After the field is turned off, the diffusion of aggregate drops is accompanied by the fluid motion that in some cases results, for the model of incompressible fluid, in the concentration of kinetic energy at the centre of the spot and in the micro-explosion with the formation of a bubble [2]. In the talk the spherically- and axisymmetric problems are discussed. Hydrodynamic interaction of two aggregate drops is also investigated.

The work was supported by the RFBR (projects 11-01-00051, 11-01-00188).

- [1] A.N.Golubiatnikov, *Proc. 14 Int. Plyos Conf. Nanodisp. Magn. Fluids*, Plyos (2010) 183 (in Russian).  
[2] A.N.Golubyatnikov, A.N.Zonenko, G.G.Chernyi, *J. Appl. Math. Mech.*, **71** (2007) 661.

**23 August**

Tuesday

9:30-11:00

plenary lectures  
23PL-A

23PL-A-1

## NON-VOLATILE MRAM FOR LOW POWER ELECTRONICS

Sousa R.<sup>1</sup>, Papusoi C.<sup>1</sup>, Hérault J.<sup>1</sup>, Gapihan E.<sup>1</sup>, Bandiera S.<sup>1</sup>, Marinz de Castro M.<sup>1</sup>, Auffret S.<sup>1</sup>, Rodmacq B.<sup>1</sup>, Buda-Prejbeanu L.<sup>1</sup>, Prebeanu L.<sup>2</sup>, Ducruet C.<sup>2</sup>, Portemont C.<sup>2</sup>, Kay K.Mc.<sup>2</sup>, Vila L.<sup>3</sup>, Nozieres J.P.<sup>1</sup>, Dieny B.<sup>1</sup>

<sup>1</sup> SPINTEC, UMR8191 CEA/CNRS/UJF, INAC, CEA/Grenoble, 17 rue des Martyrs, 38054 Grenoble, France

<sup>2</sup> Crocus Technology, Grenoble, FRANCE

<sup>3</sup> Nanostructure and Magnetism, INAC/SP2M, CEA/Grenoble, 17 rue des Martyrs, 38054 Grenoble, France

In a recently published report (July 2010), the Emerging Research Devices working group of the ITRS (International Technology Roadmap for Semiconductors) identified Spin transfer torque MRAM and Redox RRAM as emerging memory technologies recommended for accelerated research and development leading to scaling and commercialization of non-volatile memories to and beyond the 16 nm generation.

The talk will first concentrate on MRAM technology and then compare the state of the art in MRAM and Redox RRAM technology

Magnetic tunnel junctions (MTJ) are very interesting elements for integrating magnetism with CMOS components because of good impedance matching with MOSFET, good down-size scalability, very large endurance (>10<sup>16</sup> cycles), intrinsic non-volatility, capability of being deposited and patterned above integrated circuits using a back-end magnetic technology. These elements are the basis of various types of MRAM under development. Besides MRAM applications, this CMOS/MTJ hybrid technology can be used to intimately combine logic and memory functions in so called logic-in-memory circuits allowing to conceive a normally-off-electronics.

In the presentation, I will review our on-going work on MRAM particularly Thermally Assisted MRAM using field or spin-transfer switching. Precessional Spin transfer MRAM allowing ultrafast switching of magnetization will also be discussed.

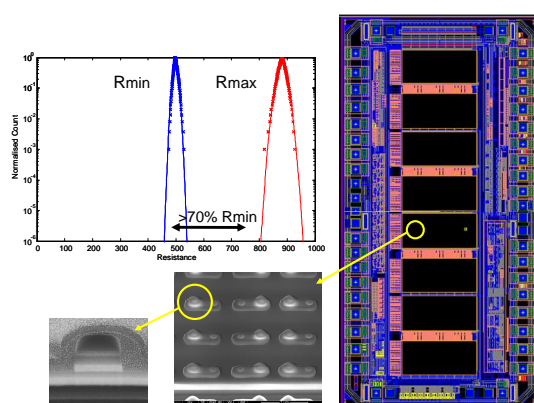


Figure 1: 1Mbit Thermally Assisted MRAM chip from Crocus Technology showing the chip layout, views of the MTJs patterned on the via emerging from the CMOS underlying wafers. Distribution of  $R_{min}$  (parallel magnetic configuration) and  $R_{max}$  (antiparallel configuration) across the 1Mbit chip.

In magnetic materials, it is well known that it is easier to switch the magnetization of a magnetic nanostructure at elevated temperature than at room temperature. This concept is used for instance in the field of hard disk drives (Heat assisted Magnetic Recording) wherein it allows combining excellent retention of the written data in standby together with the ability to write the information with moderate energy at elevated temperature.

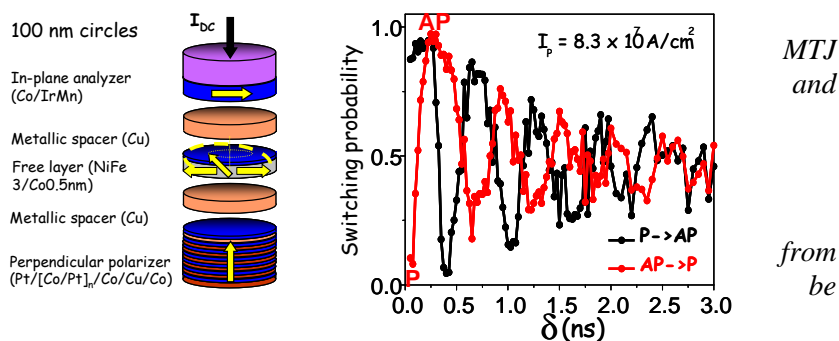
We adapted this concept to the field of MRAM written either by field or spin-transfer-torque.

In Thermally Assisted MRAM (TA-MRAM), the heating enabling the writing at about 250°C is produced by the Joule dissipation in the tunnel barrier. The concept of TA-MRAM can be implemented in various ways with in-plane magnetized or perpendicular-to-plane magnetized magnetic tunnel junctions (MTJ).

The heating takes place within a few nanoseconds with current density of the order of  $2.106\text{A}/\text{cm}^2$ . The cooling takes about 10 to 20 ns depending on the composition of the stack and especially on the thermal diffusivity to the electrodes. 1Mbit demonstrators were realized and tested by Crocus Technology and Tower Semiconductors.

We also developed precessional spin-transfer MRAM which are characterized by an ultrafast switching time of 200 ps. These precessional STT MRAM comprise a perpendicular polarizer which allows injecting electrons polarized out-of-plane in the storage layer which has in-plane magnetization. Due to the  $90^\circ$  relative orientation of injected spin-current polarization and storage layer magnetization, the spin transfer torque is at its maximum value from the very beginning of the current pulse yielding this very short switching time.

Figure 2: Illustration of spin transfer precessional switching in using a perpendicular polarizer in-plane storage layer. Oscillations of switching probability as a function of current pulse duration. The first oscillation shows that switching parallel to antiparallel state can be achieved in 200ps.



This type of memory looks particularly interesting in combination with logic applications requiring high frequency of operation.

The reliability of MTJ has been tested in accelerated conditions. Successive pulses of voltage were applied to the junctions until dielectric breakdown occurs. The results are quite encouraging for achieving a write cyclability larger than  $10^{16}$  cycles under normal operation.

In a second part of the talk, The MRAM properties (cyclability, speed, retention...) will be compared to the Redox RAM properties. This second type of memories is based on voltage induced change of resistance due to the migration of oxygen vacancies or metallic ions dispersed in insulating or semiconductor matrices.

23PL-A-2

## MAGNETOELECTRIC INTERFACES AND SPIN TRANSPORT

*Tsymbal E.Y.*

Department of Physics and Astronomy, University of Nebraska, Lincoln, NE, USA

Since the seminal discovery of giant magnetoresistance in magnetic multilayers the exploration of spin-dependent electronic transport has provided a promising avenue for applications in data storage and processing. Devices based on the electron spin typically require the application of magnetic fields or spin torques generated by large currents in the system, consuming power and producing heat, hence limiting the application of such devices. To avoid the need for large currents, there have been recent efforts toward manipulating magnetization by the application of electric fields. Such magnetoelectric effects can be induced at the surfaces and interfaces of many ferromagnetic metals affecting both the interface magnetization and the interface magnetocrystalline anisotropy. Ferroelectric materials are especially helpful in this regard because they possess a spontaneous electrical polarization which, when reversed by an electric field, can induce a large magnetoelectric response at the interface with a magnetic metal. Importantly, ferroelectric films can now be made

thin enough to allow measurable electron tunneling while still maintaining a stable and switchable polarization. Experiments and modeling show that magnetic tunnel junctions with ferroelectric barriers allow the control of spin transport by ferroelectric polarization and even lead to giant resistive-switching effects. This talk will overview recent research efforts related to magnetoelectric interfaces and the effect of ferroelectricity on charge and spin transport.



**23 August**

Tuesday

11:30-13:00

14:30-17:20

oral session

23TL-A

23RP-A

23OR-A

**“Spintronics and  
Magnetotransport”**

23TL-A-1

## PREDICTIVE MODELING OF ORGANIC MAGNETIC AND MULTIFERROIC TUNNEL JUNCTIONS

*Lopez J.M.<sup>1</sup>, Burton J.D.<sup>2</sup>, Tsymbal E.Y.<sup>2</sup>, Velev J.P.<sup>1,2</sup>*

<sup>1</sup> Department of Physics, Institute for Functional Nanomaterials, University of Puerto Rico, San Juan, PR 00931, USA

<sup>2</sup> Department of Physics and Astronomy, Nebraska Center for Materials and Nanoscience, University of Nebraska, Lincoln, NE 68588, United States

Organic materials are considered excellent candidates for certain electronics applications due to their virtually unlimited variations of functionality, mechanical flexibility, relatively low production costs, and low environmental impact. Their long spin-relaxation times make them attractive for spintronics applications as well [1]. In addition, some organics, such as the polymer poly(vinylidene difluoride) (PVDF), are ferroelectric and can form high quality ordered layers and exhibit robust ferroelectricity down to a monolayer [2]. These properties make organic semiconductors and ferroelectrics an excellent choice for barriers in magnetic tunnel junctions (MTJs), ferroelectric tunnel junctions (FTJs), and multiferroic tunnel junctions (MFTJs).

MTJs consist of magnetic electrodes separated by an insulator. The change in resistance when the orientation of the magnetization in the electrodes is switched from parallel to antiparallel is known as tunnelling magnetoresistance effect (TMR). FTJs consist of ferroelectric barrier between non-magnetic electrodes. The change of resistance due to switching the polarization orientation is known as tunneling electroresistance effect (TER). MFTJs can be thought of either as MTJs with ferroelectric barrier or FTJs with magnetic electrodes. In a recent work we have shown the existence of multiple resistance states in MFTJs associated with different magnetization and ferroelectric polarization configurations [3].

In this talk we present first-principles modeling of the properties of organic MTJs and MFTJs. Using the Landauer-Büttiker formalism implemented within a plane-wave pseudopotential method we calculate the spin-resolved conductance for parallel and antiparallel magnetization of the electrodes and/or different orientation of the polarization. First we consider crystalline Co/Alq<sub>3</sub>/Co(0001) MTJs where Alq<sub>3</sub> (tris-[8-hydroxyquinoline] aluminum) is a popular organic material due to its optoelectronics applications. TMR effect in these junction have been experimentally observed but the spin polarization of the interface transmission is a matter of debate [4]. We also study crystalline Co/PVDF/Co(0001) MFTJs with ferroelectric PVDF barriers [5]. Our calculations predict sizable TMR effect in these junctions. Moreover we predict very large TER effects in asymmetric MFTJs where a monolayer of Fe is deposited at one of the interfaces. Our results show that TER and TMR coexist in these structures. Furthermore, we investigate the role of interface oxidation in these junctions. We show that TER could arise from interface Co oxidation which is expected during PVDF deposition. The oxidation acts to make the MFTJs asymmetric. These results indicate that organic ferroelectric materials may open a new promising direction in organic spintronics.

[1] V. A. Dediu, et al., *Nat. Mater.* **8**, 707-716 (2009).

[2] A. V. Bune, et al, *Nature* **391**, 874 (1998).

[3] J. P. Velev, et al, *Nano Lett.* **9**, 427 (2009).

[4] C. Barraud, et al., *Nature Phys.* **6**, 615-642 (2010).

[5] J. M. Lopez, et al, *Nano Lett.* **11**, 599-603 (2010).

23TL-A-2

## THEORETICAL STUDIES OF THERMAL SPIN DISORDER EFFECTS IN SPIN-DEPENDENT TRANSPORT

*Belashchenko K.D.*

Department of Physics and Astronomy, University of Nebraska-Lincoln, Lincoln, Nebraska 68588, USA

First, I will present our first-principles calculations of spin-disorder resistivity (SDR) of Fe, Ni, and heavy rare-earth metals (Gd-Tm series), in which the Landauer conductance is explicitly averaged over spin disorder configurations [1]. For Fe the calculated SDR agrees very well with experiment. For Ni, comparison with experiment suggests that the average local moment in the paramagnetic state is reduced to 0.3-0.4 Bohr magnetons. The effect of magnetic short-range order on SDR is found to be weak in both Fe and Ni. Overall, the results suggest that thermal spin fluctuations in Fe and Ni have an effectively classical character. While the crystallographically averaged paramagnetic SDR for rare earth metals agrees quite well with experiments, its anisotropy systematically and significantly exceeds the available measurements. This discrepancy is critically evaluated, suggesting the need for additional experiments.

Next, I will discuss the possibility of Ohmic spin injection in semiconductors without using Schottky or tunnel barriers. Usually such a high-resistance interfacial barrier is used to overcome the conductivity mismatch problem, but this barrier limits the injected current density. A half-metal used as a spin injector overcomes this problem at zero temperature, but the situation at finite temperatures is nontrivial. I will argue that the two-current model is inapplicable to half-metals, and that barrier-free spin injection from a half-metal may be possible even at finite temperatures. I will present an intuitive model summing up multiple scatterings at the interface, as well as direct calculations of the spin injection efficiency in a simple tight-binding model with averaging over thermal spin fluctuations.

There is much interest in Gd-doped EuO as a half-metal that could be used as a spin injector. Gd doping (and, more controversially, O deficiency) sharply enhances the Curie temperature from 69 K up to as much as 170 K. I will report the results of first-principles studies of exchange interaction in Gd-doped EuO. In the virtual crystal approximation the indirect exchange through the conduction band qualitatively explains the observed doping dependence of the Curie temperature. We also considered EuO supercells with one or more substitutional Gd atom, as well as with an oxygen vacancy, and found deviations from the virtual-crystal behavior, which can be associated with local lattice relaxations.

Support by NSF (DMR-1005642, EPS-1010674, and MRSEC DMR-0820521), Defense Threat Reduction Agency, and Research Corporation is acknowledged.

[1] A. L. Wysocki, R. F. Sabirianov, M. van Schilfgaarde, and K. D. Belashchenko, *Phys. Rev. B* **80**, 224423 (2009).

## MECHANISMS OF PERPENDICULAR MAGNETIC ANISOTROPY AT Co(Fe)|MgO INTERFACES

Yang H.X.<sup>1</sup>, Lee J.H.<sup>2</sup>, Chshiev M.<sup>1</sup>, Manchon A.<sup>1,3</sup>, Shin K.H.<sup>2</sup>, Dieny B.<sup>1</sup>

<sup>1</sup> SPINTEC, UMR-8191 CEA/CNRS/UJF Grenoble 1, 38054 Grenoble, France

<sup>2</sup> Korea Institute of Science and Technology, Seoul 136-791, Korea

<sup>3</sup> KAUST, Thuwal 23955-6900, Saudi Arabia

\* Corresponding author: mair.chshiev@cea.fr

Interfacial perpendicular magnetic anisotropy (PMA) between ferromagnetic (FM) and non-magnetic layers has become of huge interest in a view of next generations of tunnel junction (MTJ) based spintronic devices. The PMA with surprisingly large values up to 1 to 2 erg/cm<sup>2</sup> have been first observed at Co(Fe)|MO<sub>x</sub> interfaces (M=Ta, Mg, Al, Ru etc) [1]. Furthermore, large PMA values have been reported for Co|MgO [2] and CoFeB|MgO MTJs [3]. The latter have been extensively studied because of Bloch state symmetry based spin filtering leading to high tunnel magnetoresistance (TMR) values [4] making them suitable for implementation in hard disk reading heads or as bit cells in magnetic random access memories (MRAM).

Here we investigate the effect of interfacial oxidation conditions on the PMA in Co(Fe)(001)|MgO(001) MTJs and elucidate mechanisms responsible for the PMA from first-principles [5]. The calculated PMA values along with moment distributions for Fe|MgO and Co|MgO structures are summarized in

TABLE I: PMA value(erg/cm<sup>2</sup>) and magnetic moment  $m(\mu_B)$  per Fe(Co) atom) for different layers of Fe(Co) in Fe(Co)|MgO MTJs with different oxidation conditions.

	Fe MgO			Co MgO
	pure	under-	over-	pure
PMA	2.93	2.27	0.98	0.38
interfacial	2.73	2.14	3.33	1.67
$m(\mu_B)$ sublayer	2.54	2.41	2.70	1.84
bulk	2.56	2.55	2.61	1.60

Table I [6] and are in agreement with recent experiments [4]. As one can see, the PMA weakens in case of overoxidized and underoxidized interfaces indicating that PMA correlates with TMR which agrees with experiment as well [7].

To elucidate the PMA origin at Fe|MgO interfaces, we performed detailed analysis of the impact of SOI on electronic band structure with out-of-plane ( $d_{z2}$ ,  $d_{xz}$ ,  $d_{yz}$ ) and in-plane ( $d_{x2-y2}$ ,  $d_{xy}$ ) Fe-3d and O- $p_z$  orbital character. When no SOI is included, the band level resulting from hybridization between Fe- $d_{z2}$  and O- $p_z$  orbitals is present. The double degenerated bands with  $\Delta_5$  symmetry related to minority Fe are also present close to the Fermi level. When spin-orbit interaction is switched on, the degeneracy is lifted and majority  $\Delta_1$  and minority  $\Delta_5$  are mixed up producing bands with both symmetry characters. As a result, band levels with  $d_{z2}$ ,  $d_{xz}$ ,  $d_{yz}$  and  $p_z$  character split around the Fermi level and this splitting is larger and the lowest band deeper for out-of-plane magnetization orientation. Thus, the lift of degeneracy of  $d_{xz}$  and  $d_{yz}$  orbitals along with their mixing with Fe- $d_{z2}$  and O- $p_z$  orbitals is at origin of perpendicular magnetic anisotropy for pure Fe|MgO interfaces. Similar analysis explains the PMA decrease in case of over and underoxidized interfaces.

Support by Chair of Excellence Program of the Nanosciences Foundation in Grenoble, France, ERC Advanced Grant Hymagine and the KRCF DRC program is acknowledged.

[1] S. Monso et al, Appl. Phys. Lett., 80 (2002) 4157; B. Rodmacq et al, J. Appl. Phys., 93 (2003) 7513

[2] L. E. Nistor et al, Phys. Rev. B, 81 (2010) 220407

[3] S. Ikeda et al, Nature Mater., 9 (2010) 271

[4] W. H. Butler et al, Phys. Rev. B, 63 (2001) 054416

- [5] G. Kresse and J. Hafner, Phys. Rev. B 47, 558 (1993); 54, 11169 (1996); Comput. Mater. Sci. 6, 15 (1996)  
 [6] H. X. Yang et al, arXiv:1011.5667  
 [7] L. E. Nistor et al, IEEE Transactions on Magnetics, 46 (2010) 1412.

23OR-A-4

## THE BEHAVIOR OF THE FERROMAGNET/WIDE-BAND POLYMER HETEROSTRUCTURE IN MAGNETIC FIELD

*Vorob'eva N.V., Lachinov A.N., Kornilov V.M.*

Institute of Physics of Molecules and Crystals URC RAS, 151, October Av., Ufa, 450075 Russia

A few years ago there has been reported a new type of magnetoresistance – huge magnetoresistance (HMR) [1]. HMR exists in the nickel electrode/ polydiphenylenephtalide (PDP) film. PDP is non-conjugated, diamagnetic polymer. The effect of HMR reveals at room temperature, it is really the reversible conductance switching controlled by the low external magnetic field. The sign of the switching is determined by the initial state of the structure.

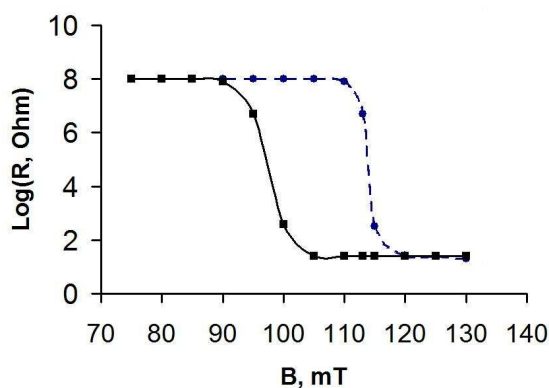
Electrical resistance dependence on the magnetic field of the experimental structure is shown in the picture [2]. Circles and squares correspond to positive and negative polarity on the ferromagnetic electrode respectively.

It is worth mentioning that the effect is really exceedingly large, the resistive change is up to million times. Also it is remarkable that PDP is wide-band dielectric material (band gap width is 4.3 eV). So it is not the ordinary material for magnetoresistive heterostructures.

The phenomena of conductivity changing in nickel/PDP system has been checked together with the strain gauge measurements. It has been proved that magnetostriction can not be the cause of the conductivity switching. Consequently the HMR is not connected with the deformation of the electrodes. Cases for the energetic character of HMR phenomena and the nature of control of the process parameters (threshold field, type and magnitude of the effect) are actuated in the report.

The ability of conductivity switching under the influence of magnetic field is closely connected with partial spin polarization of charge carriers in ferromagnetic electrode. There are some results pointing to the ability of spin transport through the polymer layer in the nickel/ PDP/ nickel spin-valve structure. It is remarkable that spin-transport polymer layer width can be up to 1200 nm.

In the same system it is possible to observe the effect which looks like the well-known tunnel anisotropic magnetoresistance. It is connected with the magnetic anisotropy of the nickel electrode. The external magnetic field permits the injected charges to overcome the potential barrier on the nickel/polymer interface. This process results in the electronic switching, that is the abrupt change of conductivity. The additional energy is acquired for such barrier overcoming. The fact that the extremum of angular dependence of magnetoresistance coincides with magnetic anisotropy direction proves the magnetic nature of this additional energy [3].



The model for the charge and spin transport in the high-conductive state is proposed in the report. It is based on the idea of two tunnel barriers at the interfaces and ballistic transport through nanosize channel in polymer layer.

Support by Physical Department of RAS project OFN-5 and Project of the Presidium of RAS 18P is acknowledged.

[1] A.N. Lachinov, N.V. Vorob'eva, A.A. Lachinov, *JETP Lett.*, **84** (2006), 604.

[2] A.N. Lachinov, et al., *Synthetic Met.* (2011), doi:10.1016/j.synthmet.2010.12.010

[3] N.V. Vorob'eva et al, *Solid State Phenomena*, **168-169** (2011), 329

23OR-A-5

## IMPROVED INTERFACIAL LOCAL STRUCTURAL ORDERING OF EPITAXIAL $\text{Fe}_3\text{Si}$ SPIN INJECTOR ON $\text{GaAs}(001)$ BY $\text{MgO}(001)$ TUNNELING BARRIER

*Makarov S.I., Krumme B., Stromberg F., Weis C., Keune W., Wende H.*

Faculty of Physics and CeNIDE, University of Duisburg-Essen, 47048 Duisburg, Germany

Although the quasi-Heusler compound  $\text{Fe}_3\text{Si}$  is a promising candidate for spintronics applications, its combination with the reactive GaAs surface is problematic since it deteriorates its beneficial attributes due to a large amount of interdiffusion at the  $\text{Fe}_3\text{Si}/\text{GaAs}$  interface [1 - 3].

Here, we report about our structural and spectroscopic analysis of the interfacial chemical ordering in epitaxial  $\text{Fe}_3\text{Si}$  thin films on  $\text{GaAs}(001)$  surface. For our conversion-electron Mössbauer investigation (CEMS) of the buried  $\text{Fe}_3\text{Si}/\text{GaAs}$  interface, we have applied the  $^{57}\text{Fe}_3\text{Si}$  tracer layer (95 % enriched in  $^{57}\text{Fe}$ ) technique. In addition, the  $\text{Fe}_3\text{Si}$  growth was analyzed with in-situ RHEED. A thin  $\text{MgO}(001)$  tunneling barrier was inserted between  $\text{GaAs}(001)$  and  $\text{Fe}_3\text{Si}(001)$  in order to prevent the atomic interdiffusion at the  $\text{Fe}_3\text{Si}(001)/\text{GaAs}(001)$  interface.

Although on both  $\text{GaAs}(001)$  and  $\text{MgO}(001)/\text{GaAs}(001)$  substrates epitaxial growth of  $\text{Fe}_3\text{Si}$  thin films was observed, our CEMS interfacial study reveals a larger disorder in  $\text{Fe}_3\text{Si}$  on  $\text{GaAs}(001)$  without insertion of the  $\text{MgO}$  tunneling barrier, as shown in Fig. 1 (upper CEMS spectrum). We confirm, however,

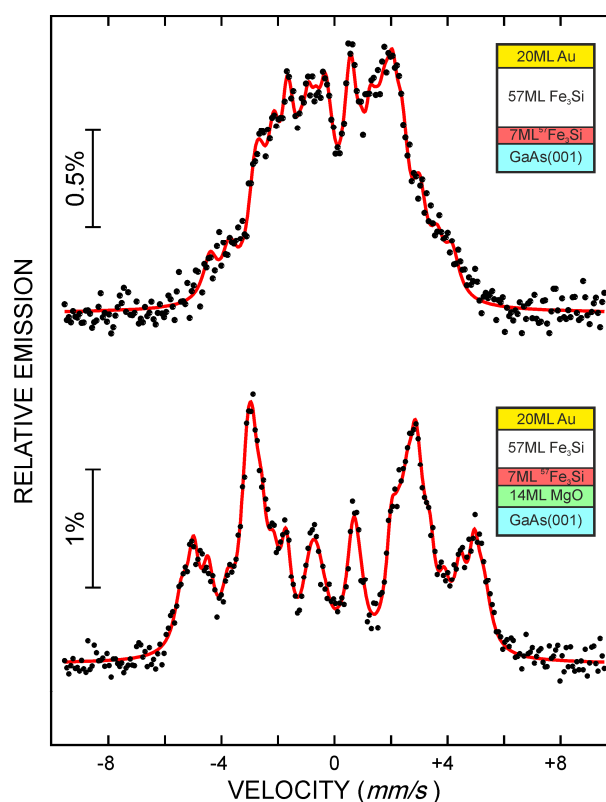


Fig. 1 CEMS spectra at room temperature (RT) from  $\text{Fe}_3\text{Si}$  thin films with  $^{57}\text{Fe}_3\text{Si}$  probe layers at the interface to  $\text{GaAs}(001)$  (upper spectrum) and at the interface to  $\text{MgO}(001)/\text{GaAs}(001)$  (lower spectrum). The black dots are experimental data; the red curve is to guide the eye.

that the insertion of an epitaxial MgO tunneling barrier prevents a chemical reaction /interdiffusion between Fe<sub>3</sub>Si and GaAs(001) and leads to a high degree of interfacial chemical ordering in Fe<sub>3</sub>Si, which is comparable to that in Fe<sub>3</sub>Si on single-crystalline (bulk) MgO(001) (see Fig. 1, lower spectrum). From a quantitative analysis of the spectra in terms of different local Fe sites we obtained the chemical order parameters of the Fe<sub>3</sub>Si films.

Support by Deutsche Forschungsgemeinschaft (SFB 491) is acknowledged.

[1] Kawaharazuka A., Ramsteiner M., Herfort J., Schönherr H.-P., Kostial H., Ploog K. H., Appl. Phys. Lett. **85**, 3492 (2004)

[2] Krumme B., Weis C., Herper H. C., Stromberg F., Antoniak C., Warland A., Schuster E., Srivastava P., Walterfang M., Fauth K., Minár J., Ebert H., Entel P., Keune W., Wende H., Phys. Rev. B **80**, 144403 (2009)

[3] Weis C., Krumme B., Herper H. C., Stromberg F., Antoniak C., Warland A., Entel P., Keune W., Wende H., J. Phys.: Conf. Ser. **200**, 072105 (2010)

23OR-A-6

## ROOM-TEMPERATURE TUNNEL MAGNETORESISTANCE IN SELF-ASSEMBLED CHEMICALLY-PREPARED NANOPARTICLES SUPERLATTICES

*Dugay J., Tan R.P., Meffre A., Blon T., Lacroix L.-M., Carrey J., Fazzini P.F., Lachaize S., Chaudret B., Respaud M.*

Université de Toulouse; INSA, UPS; LPCNO, 135, av. de Rangueil, F-31077 Toulouse, France, CNRS; LPCNO, F-31077 Toulouse, France

Chemical synthesis is a powerful way to control the size, shape and anisotropy of metallic magnetic nanoparticles (MNPs) but also to elaborate a large variety of organic tunnel barriers [1]. Using such metallic MNPs with well-controlled properties may open new opportunities in spintronics. Indeed, in the field of spin-transfer, theoretical studies predict a strong reduction of the injection current for magnetization switching and/or radio-frequency precession [2,3]. Moreover, the interaction between Coulomb blockade and magnetic field leads to a very rich physics opening the way to innovative devices [4]. To date, the single observation of tunnel magnetoresistance (TMR) in chemically-synthesized metallic NPs was obtained in 2000 by Black *et al.* on Co nanoparticles [5]. However in their experiments TMR disappeared above 20 K.

Here, we report TMR up to room temperature in millimeter-size superlattices of CoFe MNPs (TMR~25%, see Figure 1) and in networks of chemically synthesized metallic Fe nanocubes (TMR~1%) both separated by a thin organic insulating layer (long chains acids and amines). All the devices were synthesized and connected in a glove box under Ar atmosphere. The superlattices were connected using Au wires and silver paint. To elaborate Fe nanocubes devices, we trapped them between micrometric electrodes using dielectrophoresis [6]. To protect the system from

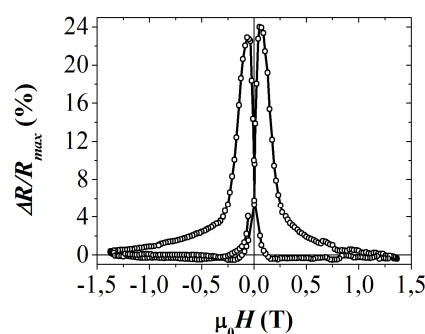


Figure 1. Magnetoresistance measurement of the CoFe superlattices for  $V = 1V$  at room temperature

oxidation this deposit was then capped by a 100 nm thick amorphous alumina layer using a RF sputtering. All the devices displayed Coulomb blockade properties at low temperature. In iron nanocubes devices, the temperature dependence of the coercitive field  $\mu_0 H_P$  ( $\pm 150$  mT) deduced from TMR curves is compared with  $\mu_0 H_C$  measured by magnetometry on NPs thin films. At low temperature,  $\mu_0 H_P$  is higher than  $\mu_0 H_C$ ; this is attributed to the fact that, in the Coulomb blockade regime, current flows preferentially through the large NPs, which display both a smaller charging energy and a larger coercive field. At  $T = 300$  K, both  $\mu_0 H_P$  and  $\mu_0 H_C$  vanish to zero, evidencing the superparamagnetic behavior of the nanocubes. The TMR decreases by only a factor 3 between low temperature and room temperature, which evidences that the organic ligands used to stabilize the nanoparticles can be efficient spin-conservative tunnel barrier without any further processing. We thus demonstrate the feasibility of an all-chemistry approach for room temperature nanoparticle-based spintronics.

- [1] Dediu, V. E., Hueso, L. E., Bergenti, I. & Taliani, C., *Nature Mater.* **8**, 707-716 (2009).  
 [2] Waintal, X. & Parcollet, O., *Phys. Rev. Lett.* **94**, 247206 (2005).  
 [3] Jalil, M. B. A. & Tan, S. G., *Phys. Rev. B* **72**, 214417 (2005).  
 [4] Seneor, P., Bernard-Mantel, A. & Petroff, F., *J. Phys.: Condens. Matter* **19**, 165222 (2007)  
 [5] Black, C. T., Murray, C. B., Sandstrom, R. L. & Sun, S., *Science* **290**, 1131-1134 (2000).  
 [6] Kumar, S., Seo, Y. K. & Kim, G. H., *Appl. Phys. Lett.* **94**, 153104 (2009).

23OR-A-7

## MAGNETOTRANSPORT BEHAVIOURS OF FEW La-BASED MANGANITES

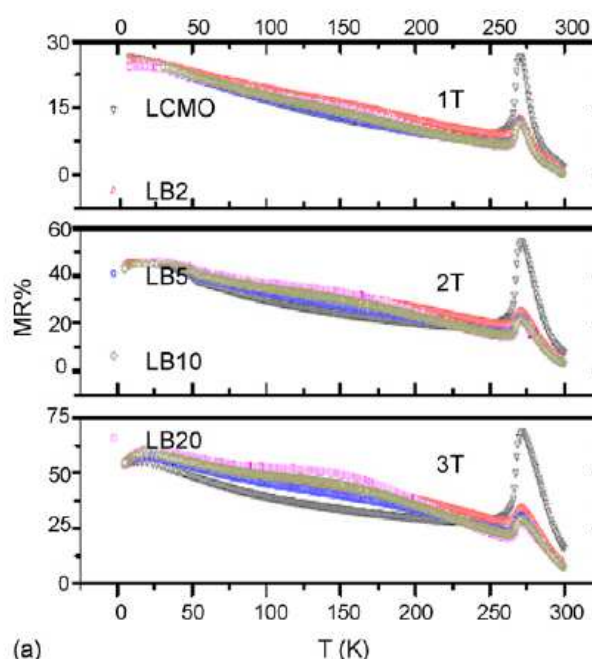
Keshri S. \*, Joshi L., Rajput S.S.

Department of Applied Physics, Birla Institute of Technology, Mesra, Ranchi – 835215, Jharkhand, India

\*E-mail ID: [s\\_keshri@bitmesra.ac.in](mailto:s_keshri@bitmesra.ac.in), [sskeshri@rediffmail.com](mailto:sskeshri@rediffmail.com)

During the last decade, the development of colossal magnetoresistive (CMR) materials [1] as well as CMR-based composites has been a source of discovery of spectacular new phenomenon, with potential applications in the fields of information technology and telecommunication. These materials show high magnetoresistance (MR) and hence useful for fabricating magnetoresistive transducers, magnetic sensors etc. The grain size of these materials as well as the nature and distribution of second phase in the composite samples play an important role in determining the properties of such materials. Therefore, understanding and controlling the structure of such material is essential to obtain desired physical properties.

The present work describes the structural, transport and magnetic properties of few CMR materials, (LCMO), (LSMO) and (LCSMO) as a



(a)

Fig.1



matrix and some of their composites using non magnetic insulators, BaTiO<sub>3</sub>(B<sub>TO</sub>), etc. as a second phase. The properties of these samples are found to depend strongly on grain size and the annealing temperature. From the conductivity measurements we observe that most of the samples show two types of transitions: intrinsic and extrinsic. The intrinsic behaviour is indicative of the alignment of Mn spin within the grain, which is governed by double exchange mechanism. The extrinsic behaviour can be attributed to the interfacial tunneling due to difference in magnetic order between core and grain boundaries.

Overall pattern of temperature dependence of resistivity have been best-fitted with the formula, where  $\rho_{PM}$  and  $\rho_{FM}$  are the resistivities of the PM and FM contents in the sample and  $f$  is the volume fraction of FM phase in the sample. Investigations on MR using magnetic field upto 3 T show enhancement of MR in the composite samples, the MR- results for LCMO-BTO composites are shown in Fig. 1. The observed linear behaviour of temperature dependent MR for a wide temperature range below T<sub>c</sub> could be useful for practical applications.

Support by University Grants Commission and Dept. of Sc. & Tech., India is acknowledged.

[1] C.N.R. Rao and B. Raveau, Review on *Colossal Magnetoresistance, Charge Ordering and Related Properties of Manganese Oxides* edited by (Singapore: World Scientific, 1998).

23OR-A-8

## INTERLAYER EXCHANGE COUPLING IN THE MULTILAYERS WITH FERROELECTRIC BARRIER

Zhuravlev M.Ye.<sup>1,2</sup>, Vedyayev A.V.<sup>3</sup>, Tsymbal E.Y.<sup>1</sup>

<sup>1</sup> Department of Physics and Astronomy, Nebraska Center for Materials and Nanoscience, University of Nebraska, Lincoln, NE 68588, USA

<sup>2</sup> Kurnakov Institute for General and Inorganic Chemistry, Russian Academy of Sciences, Moscow 119991, Russia

<sup>3</sup> Department of Physics, M.V. Lomonosov Moscow State University, Moscow 119899, Russia

Magnetizations of two ferromagnetic (FM) films separated by a thin insulating barrier layer are exchange coupled due to the tunneling spin polarization propagating across the barrier. In a three-layer system with ferroelectric barrier and different electrodes the change of the polarization of the ferroelectric barrier leads to the change of transport properties of the multilayer [1-3]. In the present work we predict a new magnetoelectric effect originating from the interlayer exchange coupling between two ferromagnetic layers separated by an ultrathin ferroelectric barrier. It is demonstrated that ferroelectric polarization switching driven by an external electric field leads to a sizable change in the interlayer exchange coupling [4]. The effect occurs in asymmetric ferromagnet/ferroelectric/ferromagnet junctions due to a change in the electrostatic potential profile across the junction affecting the interlayer coupling. The predicted phenomenon indicates the possibility of switching the magnetic configuration of a multilayer by reversing the polarization of the ferroelectric barrier layer. The multilayer systems where the effect can be enhanced are discussed.

[1] E.Y. Tsymbal, H. Kohlstedt, *Science* **313**, 181 (2006).

[2] M.Ye. Zhuravlev, R.F. Sabirianov, S.S. Jaswal, E.Y. Tsymbal, *Phys. Rev. Lett.* **94**, 246802 (2005).

- [3] M.Ye. Zhuravlev, S.S. Jaswal, E.Y. Tsymbal, R.F. Sabirianov, *Appl. Phys. Lett.* **87**, 222114 (2005).  
 [4] M.Ye. Zhuravlev, A.V. Vedyayev, E.Y. Tsymbal, *J. Phys.: Cond. Matt.* **22**, 352203 (2010).

23OR-A-9

## THERMALLY ASSISTED FIELD-WRITING IN MAGNETIC TUNNEL JUNCTIONS WITH PERPENDICULAR ANISOTROPY

Bandiera S.<sup>1</sup>, Sousa R.C.<sup>1</sup>, Marins de Castro M.<sup>1</sup>, Ducruet C.<sup>2</sup>, Portemont C.<sup>2</sup>, Vila L.<sup>3</sup>, Auffret S.<sup>1</sup>, Prejbeanu I.L.<sup>2</sup>, Dieny B.<sup>1</sup>

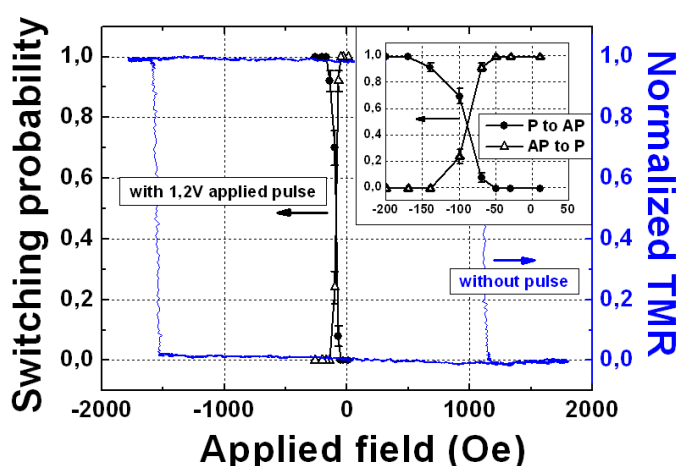
<sup>1</sup> SPINTEC, UMR(8191) CEA/CNRS/UJF-Grenoble 1/Grenoble INP, INAC, 17 Rue des Martyrs 38054 Grenoble, France

<sup>2</sup> Crocus Technology, 4 Place Robert Schumann, 38025 Grenoble, France

<sup>3</sup> SP2M/NM, CEA/Grenoble, INAC, 17 Rue des Martyrs, 38054 Grenoble, France

Magnetic tunnel junctions (MTJ) with perpendicular magnetic anisotropy (PMA) attract much interest since they allow to scale down the dimension of spintronic devices below the 45nm node, while keeping a sufficient thermal stability ( $KV/k_B T > 50$ ). In these MTJ, the magnetization can be switched either by using spin transfer torque (STT) or by field. This work shows how field writing can be used in combination with thermal assistance, as in Heat Assisted Magnetic Recording (HAMR) in order to achieve simultaneously very high coercive field in standby mode ( $H_c > 1000$  Oe) and low coercive field at the write temperature. Heating is indeed a very efficient mean to decrease the PMA of the storage layer [1] in order to reduce the field required to switch the free layer in a perpendicular-to-plane magnetized MTJ. We will show that the field required to switch a highly stable free layer can be greatly reduced thanks to current pulses.

The developed MTJ stack consists of SAF/MgO/FL, where SAF is a (Co/Pt)<sub>n</sub> based synthetic antiferromagnetic reference layer and FL is a CoFeB/(Co/Pd)<sub>n</sub> multilayer. This free layer has been optimized in such a way that it presents high PMA at room temperature but loses its anisotropy when heated to about 175°C.



The KV of such a layer is  $700k_B T$  at 300K for a 100nm diameter pillar, which gives a coercive field of 1300 Oe (blue loop). Such high anisotropy can fulfill stability requirements down to the 22nm technological node. It will be shown that if a 1.25V pulse is applied for 3ns, the coercivity is decreased to about 60 Oe (black points, see also inset), making possible magnetic field switching in MRAM cells.

Additional optimizations may further reduce the energy consumption. Ultimately, current pulses could also switch the free layer by combined thermal assistance and spin transfer torque without the need of any magnetic field.

- [1] P.J. Jensen, and K.H. Bennemann, *Phys. Rev. B*, **42** (1990) 849.

23OR-A-10

## INTEGRATION OF A PERPENDICULAR POLARIZER IN A IN-PLANE MAGNETIC TUNNEL JUNCTION

Marinz de Castro M.<sup>1</sup>, Sousa R.C.<sup>1</sup>, Bandiera S.<sup>1</sup>, Ducruet C.<sup>2</sup>, Auffret S.<sup>1</sup>, Papusoi C.<sup>1</sup>,  
Prejbeanu I.L.<sup>2</sup>, Ebels U.<sup>1</sup>, Portemont C.<sup>2</sup>, Vila L.<sup>3</sup>, Rodmacq B.<sup>1</sup>, Dieny B.<sup>1</sup>

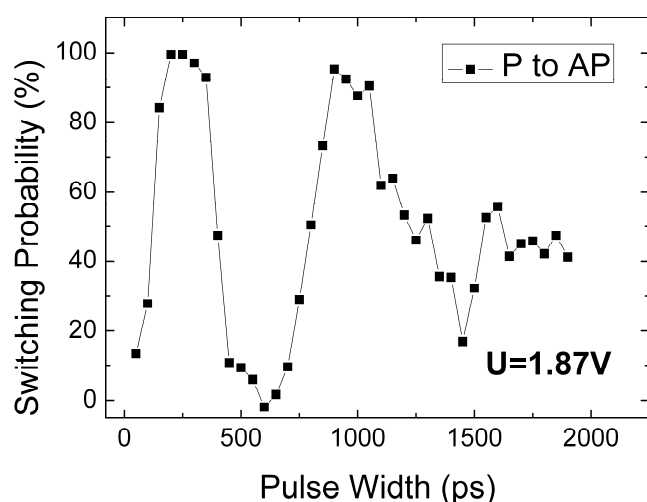
<sup>1</sup> SPINTEC, UMR CEA / CNRS / UJF-Grenoble 1 / Grenoble-INP, INAC, 17 Rue des Martyrs  
38054 Grenoble, France

<sup>2</sup> Crocus Technology, 4 Place Robert Schumann, 38025 Grenoble, France

<sup>3</sup> SP2M/NM, CEA/Grenoble, INAC, 17 Rue des Martyrs, 38054 Grenoble, France

Magnetic random access memory (MRAM) cells can be fabricated based on magnetic tunnel (MTJ) junctions with two ferromagnetic layers (reference and free layers) separated by a tunneling barrier. It has been demonstrated that the free layer magnetization can be reversed by the current spin polarized by the reference layer [1]. For applications, a fast switching of the free layer below the nano second-scale is desirable especially for CMOS/magnetic devices. This writing procedure can be improved using an additional ferromagnetic layer magnetized perpendicular-to-plane keeping the reference and free layer magnetizations in-plane [2]. The perpendicular anisotropy polarizer induces out-of-plane precessions of the free layer and consequently a faster switching can be achieved.

We show the integration of a synthetic perpendicular polarizer based on two Co/Pt multilayers separated by a Ru spacer at the bottom of an in-plane anisotropy MTJ. The figure shows the switching probability for a patterned elliptical nanopillar of 80 nm by 270 nm as a function of the pulse width plotted for 1.87 V corresponding to a current density of  $1.16 \cdot 10^7$  A/cm<sup>2</sup>. The current direction corresponds to electrons flowing from the bottom electrode to the top electrode. Square black points correspond to the parallel (P) to antiparallel transition (AP). For this transition, an ultrafast switching of less than 300 ps is achieved. Two clear oscillations of the switching probability are observed in pulse width ranging from 50 ps to 2000 ps with a period of about 750 ps.



These oscillations are due to the precessional switching of the free layer induced by the perpendicular polarizer. When the magnetization makes half a precession, or multiples thereof, the probability of switching from P to AP is maximal. If the pulse duration corresponds to a complete precession, the final resistance state is the same as the initial one. The presence of coherent pronounced oscillations of the switching probability as a function of the pulse width is in part due the synthetic antiferromagnet structure of the polarizer which considerably reduces the stray field on the free layer.

[1] J. A. Katine, F. J. Albert, R. A. Buhrman, E. B. Myers, and D. C. Ralph, *Phys. Rev. Lett.* **84**, 3149 (2000).

[2] O. Redon, B. Dieny, and B. Rodmacq, Magnetic spin polarization and magnetization rotation device with memory and writing process using such a device. US patent 6,532,164 B2 (2003).

## CURRENT INDUCED SPIN INJECTION IN Si-MOSFET

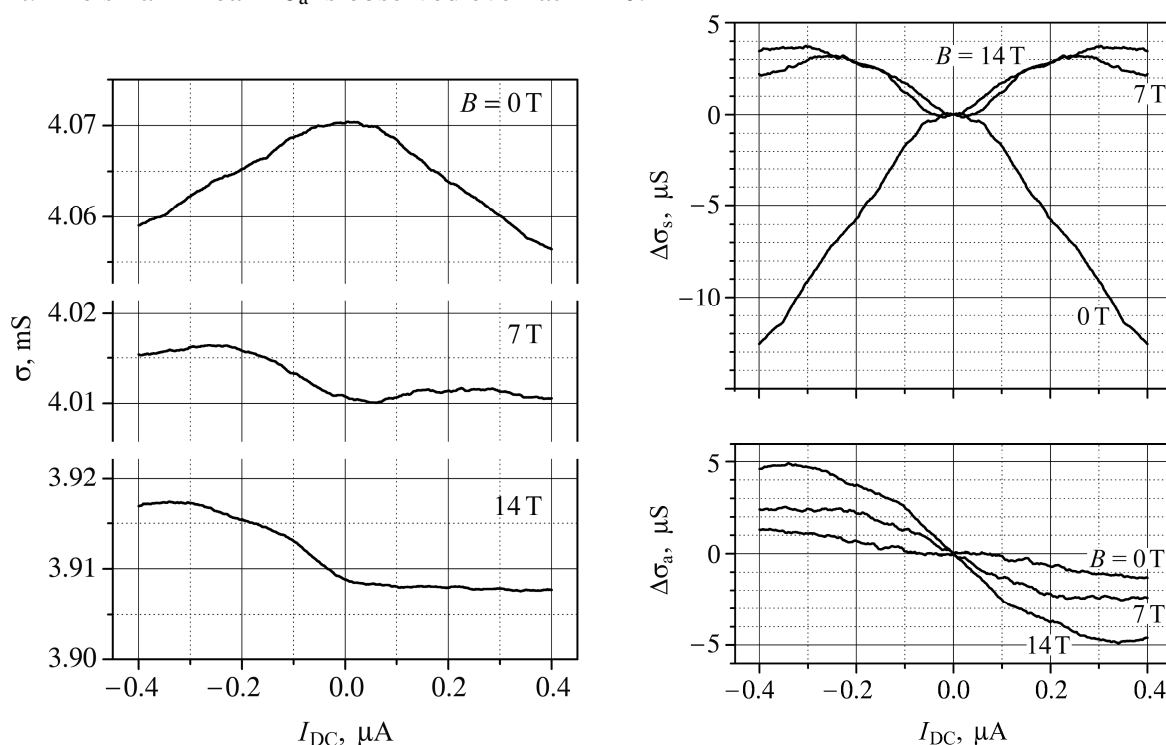
*Shlimak I.<sup>1</sup>, Butenko A.<sup>1</sup>, Golosov D.<sup>1</sup>, Friedland K.-J.<sup>2</sup>, Kravchenko S.V.<sup>3</sup>*

<sup>1</sup> Jack and Pearl Resnick Institute of Advanced Technology, Department of Physics,  
Bar-Ilan University, Ramat-Gan 52900, Israel

<sup>2</sup> Paul-Drude Institut für Festkörperelektronik, Hausvogteiplatz 5-7, 10117, Berlin, Germany

<sup>3</sup> Physics Department, Northeastern University, Boston, Massachusetts 02115, U.S.A.

Longitudinal resistivity in strong parallel magnetic fields  $B = 7$  and 14 Tesla was measured in Si-MOSFET with a narrow slot (90 nm) in the upper metallic gate that allows to apply different gate voltage  $U_G(1)$  and  $U_G(2)$  across the slot and, therefore, to control the electron density  $n_1$  and  $n_2$  in two parts of the sample independently. The experimental scheme allows us to pass through the source-drain channel the DC current ( $I_{DC}$ ) up to few  $\mu\text{A}$ , while the dynamic resistance was measured using a standard lock-in technique with the small AC current (50 nA) at a frequency of 12.7 Hz. It was observed that the sample conductivity is asymmetric with respect to the direction of DC current. Figures below show the sample conductivity  $\sigma$  and its symmetric  $\Delta\sigma_s$  and asymmetric parts  $\Delta\sigma_a$  measured in the case when  $U_G(1) = 7\text{V}$  ( $n_1 = 0.9 \cdot 10^{16} \text{ m}^{-2}$ ) and  $U_G(2) = 18\text{V}$  ( $n_2 = 2.5 \cdot 10^{16} \text{ m}^{-2}$ ) as a function of  $I_{DC}$  in fields  $B = 0, 7$  and 14 T. It is seen that  $\Delta\sigma_s(I_{DC})$  is negative at  $B = 0$ , which reflects, in our opinion, the Joule heating by  $I_{DC}$ , while at  $B = 7$  and 14 T,  $\Delta\sigma_s(I_{DC})$  is positive and weak. Asymmetric part  $\Delta\sigma_a$  first increases linearly with  $I_{DC}$  and saturates at high current. The small linear  $\Delta\sigma_a$  is observed even at  $B = 0$ .



The explanatory model of the observed phenomena is discussed in terms of spin accumulation near the slot (or depletion, depending on the direction of the electron flow) and positive magnetoresistance of Si-MOSFETs in parallel magnetic fields.

## CURRENT-INDUCED PHASE TRANSITION IN BALLISTIC AND DIFFUSIVE NANOCONTRACTS OF MAGNETICS

Bukharaev A.A.<sup>1,2</sup>, Gatiyatov R.G.<sup>1</sup>, Lisin V.N.<sup>1</sup>

<sup>1</sup> Zavoisky Physical-Technical Institute of RAS, Kazan, 420029, Russia

<sup>2</sup> Kazan Federal University, Kazan, 420008, Russia

It was recently shown in our previous study [1] on the passage of electrons through magnetic metal nanocontacts, that Joule heating of the near-contact region should be taken into account not only in diffusive nanocontacts, but also in ballistic ones. Moreover, the temperature of the near-contact region can reach its critical value at which the magnetic phase transition takes place.

The features of the transition from the ballistic electron transport regime to the diffuse one in Ni nanocontacts observed with increase in the size have been investigated. Nanocontacts with transverse dimensions in the range from 1.5 to 15 nm have been fabricated using the electrochemical technique described in [2]. The local magnetic phase transition from the ferromagnetic to the paramagnetic state in the near-contact region of Ni nanocontacts has been experimentally observed at the high current density [3]. It has been shown that the voltage  $U_C$  needed for Joule heating of the near-contact region up to the critical temperature does not depend on the contact size only in the diffuse regime. For the ballistic contact it increases with decrease in the nanocontact size. The reduction of the transport electron mean free path due to heating of nanocontacts may result in the change of the electron transport regime from ballistic to diffuse one.

A theoretical description of heating of the contact region by the current taking into account relaxation processes in the contact region of ferromagnetic electrodes has been proposed. The qualitative and quantitative agreement with the experimental results has been achieved for the case when both the energy and the energy relaxation time of electrons depend on the applied voltage when the excess energy of electrons exceeds the characteristic energies of phonons and magnons.

An important characteristic, the value of the multiplication of the transport electron mean free path by the resistivity has been found while the studying transition from the ballistic regime of electron transport to the diffuse one for the Ni nanocontacts. It allows one to estimate the electron mean free paths for the scattering of the electrons on impurities, phonons and magnons at different temperatures.

Electron transport with the high current density in Ni nanocontacts fabricated by controlled indenting of the magnetic tip of a scanning tunneling microscope into magnetic film has been studied as well. The obtained experimental dependences indicate the magnetic phase transition in the near-contact region due to its heating above the critical temperature.

This work was supported in part by the Russian Foundation for Basic Research (grant no. 09-02-00568) and the program of the Division of Physical Sciences of the Russian Academy of Sciences.

- [1] R. G. Gatiyatov, V. N. Lisin, A. A. Bukharaev, *Appl. Phys. Lett.*, **96** (2010) 093108.
- [2] R. G. Gatiyatov, S. A. Ziganshina, and A. A. Bukharaev, *JETP Letters*, **86** (2007) 412.
- [3] R. G. Gatiyatov, V. N. Lisin, and A. A. Bukharaev, *JETP Letters*, **91** (2010) 425.

23OR-A-13

## MAGNETIC PROPERTIES AND CONDUCTIVITY OF $\text{Ho}_x\text{Mn}_{1-x}\text{S}$ SOLID SOLUTIONS

*Aplesnin S.S.<sup>1</sup>, Yusifovich A.A.<sup>1</sup>, Aldashev I.A.<sup>1</sup>, Pichugin A.Yu.<sup>2</sup>, Galyas A.I.<sup>3</sup>, Yanushkevich K.I.<sup>3</sup>*

<sup>1</sup>M. F. Reshetneva Aircosmic Siberian State University, Krasnoyarsk, 660014, Russia

<sup>2</sup>Institute of Inorganic Chemistry, Siberian Branch of RAS, Novosibirsk, 630090, Russia

<sup>3</sup>State Scientific Production Association "Material Science Center of the NAS of Belarus",  
220072 Minsk, Belarus

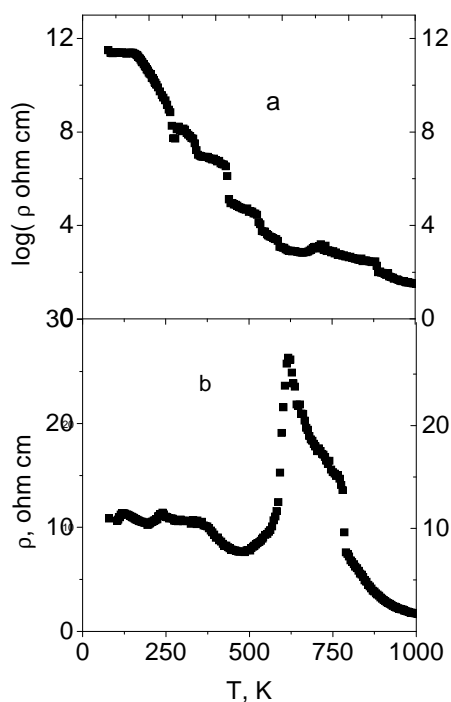
Magnetic semiconductors of manganese sulfides substituted by a trivalent of rare-earth elements reveal an unusual magnetic and electric properties. The orbital degenerate states, metal-semiconductors transition and Kondo effect in the case of d-f interaction may be expected in these solid solutions. Anomalous in the kinetic properties are possible at low and high temperatures associated with formatting of the dynamical orbital correlation.

The aim of the study is to determine the interrelation between the magnetic and electric properties for  $\text{Ho}_x\text{Mn}_{1-x}\text{S}$  compounds at the electron doping in the wide concentration region  $0 < x < 0.3$ .

According to the data of the X-ray diffraction analysis, the  $\text{Ho}_x\text{Mn}_{1-x}\text{S}$  samples possess a NaCl-type face-centered cubic lattice. All measured lattice parameters well lie down on a straight line. Magnetization of the samples in the field  $H = 0.05$  T and specific magnetization versus field were measured using a PPMS in the temperature range of  $4 \text{ K} < T < 300 \text{ K}$ . It is found the paramagnetic Curie temperature is decreased from  $\theta = 550 \text{ K}$  ( $x=0$ ) to  $\theta = 50 \text{ K}$  ( $x=0.3$ ). The magnetization dependence versus field is nonlinear and the remanent magnetic moment is found out from linear extrapolation to  $H=0$  T. This magnetic moment disappears at temperature  $T=50 \text{ K}$ .

The electrical resistivity of the synthesized samples was measured by four-probe technique at temperatures of 80-1000 K. The resistivity doesn't depend on the temperature at  $T < 160 \text{ K}$  and function of  $\ln(\rho(T))$  looks like steps at heating (Fig. 1a). For holmium concentration exceeding a percolation limit the resistivity shows a peak at  $T=611 \text{ K}$  for  $x=0.3$  compound (Fig. 1b). The sign of current carrier is changed from p-type to n with concentration rise according to results of the Seebeck coefficient. Change in sign of  $\alpha(T)$  is observed for  $\text{Ho}_x\text{Mn}_{1-x}\text{S}$  with  $x=0.1$  at the heating at  $T=450 \text{ K}$ .

Data obtained  $\rho(T)$  and  $\alpha(T)$  are explained in terms of model with the strong electron correlation and removal of electronic degeneration states in d-band for account for interorbital Coulomb interaction. Correlation between the temperature behavior of magnetic susceptibility and electrical resistance is not found.



Authors express E.V. Eremin gratitude for carrying out of magnetic measurements. This study was supported by the Russian Foundation for Basic Research project № 09-02-00554\_a; № 09-02-92001-NNS\_a.

23OR-A-14

## ANTIFERROMAGNETICALLY COUPLED SI-BASED TUNNELLING STRUCTURES

Gareev R.

University of Regensburg, Universitätstrasse 31, Germany

Thin-film ferromagnet/metal/ferromagnet structures demonstrate a rich variety of spin-dependent phenomena. Experimental observations of the antiferromagnetic coupling (AFC) and the giant magnetoresistance effect between two magnetic layers separated by a thin metallic spacer have found practical application in hard disk drives and were awarded by the Nobel Prize in Physics.

In the presented talk effects of the antiferromagnetic coupling and the tunneling magnetoresistance (TMR) in ferromagnet/semiconductor/ferromagnet epitaxial structures based on Si are described in detail. By using different techniques we demonstrate that for Fe/Si/Fe trilayers AFC is anomalously strong (reaches  $8 \text{ mJ/m}^2$ ), short-range and exponentially decaying [1]. A similar behaviour we established for Ge-containing spacers [2]. The described behavior is in a striking contrast compared to structures with metallic spacers, where AFC is weaker and oscillates with a spacer thickness [3].

The positive role of iron-silicide diffusion barriers at interfaces for suppression of pinholes and increasing of AFC is proven [4]. Our recent results on AFC across combined MgO/Si spacers as well as with Co interface “dusting” layers are presented. We demonstrate successful realization of AFC across Si with  $\text{Fe}_3\text{Si}$  magnetic electrodes taken instead of epitaxial iron as well.

Next we show that Si-based spacers form a tunneling barrier. We demonstrate that tunnelling is resonant with unusual inversion of TMR with biasing voltage, which we connect with formation of weakly spin-split magnetic impurity states inside tunneling barrier. The TMR effect for optically patterned structures does not exceed several per cent and vanishes above 50 K [5].

Finally, we present recent realization of the room-temperature magnetocurrent in AFC Fe/Si/Fe structures using ballistic electron magnetic microscopy (BEMM) techniques, which exceeds 200% and correlates well with magnetization data. We emphasize that non-destructing BEMM method enables control of spin-dependent hot-electron transport with nanometer-scaled locality and avoiding heating procedures, which can affect interface diffusion and, consequently, AFC and TMR in our patterned Fe/Si/Fe structures.

This work is supported by the German Research Society project 9209379.

[1]. R.R. Gareev, D.E. Buergler, M. Buchmeier, R. Schreiber, P. Gruenberg, *J. Magn. Magn. Mater.* **240**, (2002) 235.

[2] R.R. Gareev, D.E. Buergler, R. Schreiber, H. Braak, M. Buchmeier, P. Gruenberg, *Appl. Phys. Letts* **83** (9) (2003) 1806.

[3]. R.R. Gareev, D.E. Buergler, M. Buchmeier, D. Olligs, R. Schreiber, P. Gruenberg, *Phys. Rev. Letts*. **87** (2001) 157202.

[4]. R.R. Gareev, D.E. Buergler, M. Buchmeier, R. Schreiber, and P. Gruenberg, *Appl. Phys. Letts* **81** (2002) 1264.

[5]. R.R. Gareev, M. Weides, R.Schreiber, U. Poppe, *Appl. Phys. Letts* **88** (2006) 172105.





**23 August**

Tuesday

11:30-13:00

14:30-17:20

oral session

23TL-B

23RP-B

23OR-B

**“Magnetism of  
Nanostructures”**

23TL-B-1

**ATOMIC CLUSTERS AND MAGNETISM ON SUB-NANOMETER SCALE***Kirilyuk A.*

Radboud University Nijmegen, Institute for Molecules and Materials, Heyendaalseweg 135, 6525 AJ Nijmegen, The Netherlands

What happens to a magnetic material when we reduce its size to (sub)nanoscale dimensions? Another way of considering this is to look at the magnetic properties of a material as we construct it on an atom-by-atom basis towards the bulk. Studying free (gas-phase) atomic clusters gives us the opportunity to do exactly this, where the number of atoms in the system can be experimentally controlled. Such a bottom-up approach has the advantage that we can study the interaction of individual spins with each other in a confined, finite system. These nano-scale objects possess interesting physical properties substantially differing from the bulk [1]. It is size quantization of energy levels that could cause, sometimes, a dramatic difference of optical, electronic or chemical properties compared to the bulk. Applications in material science, health care, etc. are offered for these nano-objects [2].

The magnetic moments of Tb and Ho clusters were found to dramatically oscillate as a function of cluster size every 5 atoms. This implies that there is a repeating geometric shell structure influencing their magnetic ordering, causing 'magic numbers' in their magnetic properties. These 'magic numbers' are interestingly consistent even with clusters of different elements, not only terbium and holmium, but also gadolinium and dysprosium.

Praseodymium and rhodium clusters are interesting in that they are both non-magnetic in their bulk state, however are magnetic for all cluster sizes investigated. Furthermore, Rh clusters were not only magnetic, but also showed evidence of an extremely high magnetic anisotropy energy, high enough to overcome thermal fluctuations – above the superparamagnetic limit. These clusters therefore have possible applications in the field of high density magnetic storage, where just a few atoms may be sufficient in order to store a bit of information.

Understanding the magnetic properties of such small particles remains a challenge, making obtaining the structural information on these small particles crucial. To solve this, vibrational spectra of free clusters have been measured in the 50–1400  $\text{cm}^{-1}$  range using a free-electron laser FELIX. The structure and magnetic ordering of the clusters has then been elucidated from comparison of the measured spectra with the results of *ab initio* calculations. It is found that the actual lowest-energy geometric structure strongly depends on the spin configuration. Therefore, the magnetic order is reflected in the vibrational spectra [3].

Last but not least, theory of itinerant magnetism applied to metallic clusters show an unexpected increase of Curie temperature caused by the suppression of spin fluctuations [4].

Support by FELIX staff, the Dutch Nanotechnology initiative NanoNed and EC FP7 grants NMP3-SL-2008-214469 (UltraMagnetron) and N 214810 (FANTOMAS) is acknowledged.

[1] S. N. Khanna and A. W. Castleman, *Quantum Phenomena in Clusters and Nanostructures* (Springer, Berlin, 2003)

[2] M. Karkare, *Nanotechnology Fundamentals and Applications* (I. K. International Publishing House Pvt. Ltd., New Delhi, 2008)

[3] A. Kirilyuk, A. Fielicke, K. Demyk, G. von Helden, G. Meijer, and Th. Rasing, *Phys. Rev. B* **82**, 020405 (2010); C.N. van Dijk, D.R. Roy, A. Fielicke, Th. Rasing, A.C. Reber, S.N. Khanna, and A. Kirilyuk, *to be published*.

[4] L. Peters, M.I. Katsnelson, and A. Kirilyuk, *to be published*.

23RP-B-2

## FeCuPt ISOLATED GRAINS PREPARED BY RAPID THERMAL ANNEALING ON NANO-STRUCTURED SUBSTRATES

Itoh A., Tsukamoto A., Okame S., Mizusawa K.

College of Science and Technology, Nihon University, 7-24-1 Narashino-dai Funabashi, 274-8501 Japan

FeCuPt grains media with high magnetic anisotropy for hybrid recording prepared on two different kinds of nano-structured substrates. One of the substrates is prepared by Self-Assembled spherical Silica Particles (SASP) fabricated on Si substrates by the dip coating method and the other is close-packed array of Nano Convex Pattern (NCP) prepared by using SASP followed by inductively coupled plasma reactive ion etching (ICP-RIE). The average grain diameter ( $D_a$ ) and standard deviation of diameter (StD) of FeCuPt grains fabricated on NCP were 14.5 nm and 2.7 nm, and perpendicular magnetized FeCuPt can be obtained.

### 1. Fabrication of nano convex pattern (NCP)

We have already reported [1],[2] that the monolayer SASP made by a dipping method. The average silica particle diameter is 18 nm. Atomic force microscope (AFM) and scanning electron microscope (SEM) images of the close-packed single layer of SASP arrangement were shown in Fig. 1.

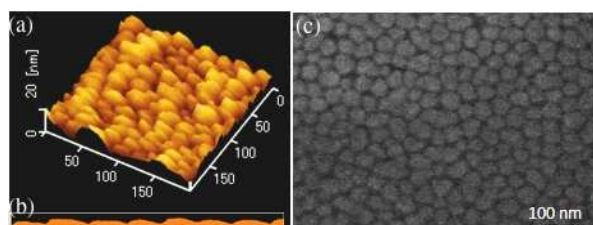


**Fig. 1** SASP (a) AFM, (b) line profile, and (c) SEM.

Then, we made the close-packed array of NC by using a single layer of SASP followed by ICP-RIE process. Fig. 2 shows the top view of SEM and AFM image of NCP (periodicity of around 24 nm).

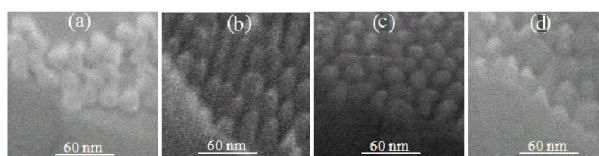


**Fig. 2** SEM images of the oblique views of the silica particles created after (a) 0 sec, (b) 8 sec, (c) 10 sec, and (d) 13 sec of ICP-RIE. The diameter of the sphere prior to ICP-RIE is 18 nm.

### 2. FeCuPt on NCP substrate.

Table 1 shows  $D_a$  and StD for FeCuPt particles fabricated by a rapid thermal annealing (RTA) method on different substrates. It is clear that the enhancement in surface ruggedness is effective to reduce grain diameter of FeCuPt.

FeCuPt isolated grains are obtained by RTA after depositing different thickness Pt/Fe/Cu (i)  $h=3.75$  nm and (ii)  $h=2.81$  nm on NCP.

Fig.3 shows X-ray diffraction profiles of  $(\text{FePt})_{86}\text{Cu}_{14}$  ( $h=3.75$  nm) grains on (a) NCP and (b) SASP.

The degree of (001) crystal orientation defined as  $I_R: I(001)/I(111)$ . (001) orientation of FeCuPt grains on NCP is three times larger than that of on SASP.

This work is partially supported by a Grant-in-Aid for scientific Research from MEXT in Japan, No. 21560368, and Storage Research Consortium, Nihon University Strategic Projects for Academic Research.

[1] A. Itoh and A. Tsukamoto, J. Magn. Soc. Jpn., 33/6-2, 507-512 (2009).

[2] K. Mizusawa, A. Tsukamoto and A. Itoh, J. Mater. Res., Vol. 26, No. 2, (2011).

**Table 1.** Summary of  $(\text{FePt})_{86}\text{Cu}_{14}$  ( $h=3.75$  nm) particles on the planar Si substrate, SASP and NCP prepared by RTA.

Substrate	Average diameter $D_a$ (nm)	Standard deviation StD of $D_a$ (nm)
Flat $\text{SiO}_2/\text{Si}$	31	8
SASP	17.2	3.2
NCP	17.8	3.6

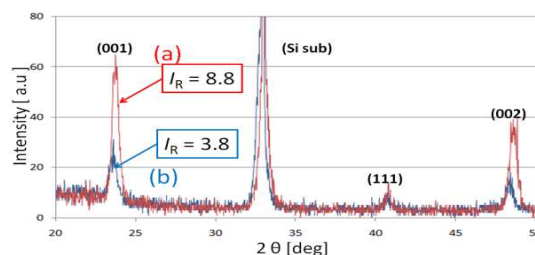


**Fig 3** XRD profiles of  $(\text{FePt})_{86}\text{Cu}_{14}$  ( $h=3.75$  nm) grains on (a) NCP and (b) SASP.

23RP-B-3

## FUNCTIONAL MAGNETIC NANOMATERIALS SYNTHESIZED BY TEMPLATE-ASSISTED ELECTROPLATING

*Prida V.M., García J., González L., Oliveira W., Hernando B.*

Depto. Física, Universidad de Oviedo, Calvo Sotelo s/n 33007-Oviedo, Spain

The synthesis of nanostructured materials with functional properties based on template-assisted techniques has drawn a huge scientific interest in the last 15 years after the discovering of the so-called two-step anodization process of aluminium by Masuda and Fukuda [1]. Highly ordered self-assembled nanoporous alumina membranes have been used since then as templates for the synthesis of a wide variety of nanomaterials, comprising nanowire and nanotube arrays of different materials, nanoparticle chains and thin films with ordered nanostructures patterned on their surface, such as antidot [2] or nanohill [3] arrays.

Among the most interesting nanomaterials synthesized so far through the template-assisted method, Pd-based ferromagnetic alloys stand out due to their interesting properties such high uniaxial magnetic anisotropy, high Kerr rotation, magnetic shape memory effect, high corrosion resistance, etc.

In this work, we highlight our recent developments in the fabrication, by means of template-assisted deposition into highly ordered nanoporous alumina membranes, of nanowire and antidot arrays of CoPd and FePd alloys, paying special attention to their basic magnetic properties and their dependence on the microstructure and morphological parameters of the ordered array.

Support by MICINN under the research projects MICINN-09-MAT2009-13108-C02-01 and MICINN-10-MAT2010-20798-C05-04 is acknowledged.

[1] H. Masuda, K. Fukuda, *Science* **268** (1995) 1466.

[2] F. Béron, K.R. Pirota, V. Vega, V.M. Prida, A. Fernández, B. Hernando, M. Knobel, *New Journal of Physics* **13** (2011) 013035.

[3] W. O. Rosa, M. Jaafar, A. Asenjo and M. Vázquez, *Nanotechnology* **7** (2009) 075301.

23TL-B-4

## INTERFACE EXCHANGE COUPLING IN FERROMAGNETIC NANOPARTICLES EMBEDDED IN ANTIFERROMAGNETIC MATRIX

*Peddis D.<sup>1</sup>, Laureti S.<sup>1</sup>, Varvaro G.<sup>1</sup>, Testa A.M.<sup>1</sup>, Agostinelli E.<sup>1</sup>, Binns C.<sup>2</sup>, Baker S.<sup>2</sup>, Trohidou K.N.<sup>3</sup>, Nordblad P.<sup>4</sup>, Hudl M.<sup>4</sup>, Mathieu R.<sup>4</sup>, Domingo N.<sup>1</sup>, Fiorani D.<sup>1</sup>*

<sup>1</sup> ISM-CNR, Institute of Structure of Matter, Area della Ricerca di Roma, Via Salaria km, 29 500, CP 10-00016 Monterotondo Scalo, Roma, Italy

<sup>2</sup> Department of Physics and Astronomy, University of Leicester, Leicester LE1 7RH, UK

<sup>3</sup> Institute of Materials Science, NCSR Demokritos, Agia Paraskevi, 15310 Athens, Greece

<sup>4</sup> Department of Engineering Sciences, Uppsala University, Box 534 SE-751 21 Uppsala, Sweden

Magnetic nanoparticles are the focus of increasing interest from both fundamental and technological point of view, for their applications in a number of different fields magnetic

memories, medicine, sensors...). In core/shell nanoparticles, the exchange coupling between the ferromagnetic (F) core and the antiferromagnetic (AF) shell has been demonstrated to increase the actual particle anisotropy, leading to an increase of the blocking temperature, thus shifting the superparamagnetic limit to lower size. In this context, films of ferromagnetic nanoparticles dispersed in an antiferromagnetic matrix provide good model systems to control the F/AF interface exchange coupling in view of exploiting as a tool for controlling the anisotropy and then the magnetic stability of magnetic nanoparticles.

In this paper, the effect of the F/AF interface exchange coupling on the magnetic properties has been investigated in three different films of nanoparticles (~2 nm) dispersed (~5 % in volume) in an antiferromagnetic matrix: Co particles in Mn matrix (Co@Mn), Fe particles in Mn matrix (Fe@Mn) and Fe particles in Cr matrix (Fe@Cr). All the films have been prepared by codepositing pre-formed mass-selected metallic clusters with an atomic vapour of Mn onto a common substrate. The structural and magnetic properties of the films were investigated by using EXAFS, XMCD, magnetometry, and theoretical modeling. For all samples, the experimental data show that the antiferromagnetic matrix provides a strong interface exchange coupling with the ferromagnetic particles, leading to a remarkable enhancement of thermal stability with respect to the same particles (same size and concentration) dispersed in a non magnetic Ag matrix. After cooling in a field  $H = 2$  T, at 5 K, exchange bias (EB) was observed in all the samples with EB field,  $H_{eb} \sim 750$  Oe, 310 Oe and 200 Oe for Co@Mn, Fe@Mn and Fe@Cr, respectively. Monte Carlo simulations reproduce very well the experimental findings.

For Co@Mn films, EXAFS measurements show the presence of a significant degree of alloying, suggesting that the well-defined particles, originally deposited, become centre of high Co concentration of CoMn alloy that evolves from pure Co at the nanoparticle centre to the pure Mn matrix within a few nm. XMCD measurements show that the Co moment is much smaller than in Co@Ag films. Electronic structure calculations confirm that the small magnitude of the core Co moment can be understood only if significant alloying occurs. Magnetization measurements show that the antiferromagnetic matrix provides through interface exchange coupling an effective long range interparticle correlation. This gives rise to a superspin glass (SSG) type freezing. This picture is confirmed by the observation of non-equilibrium dynamics at low temperatures, as shown by memory effects in zero-field-cooled magnetization curves.

23RP-B-5

## ROTATABLE ANISOTROPY AND ATHERMAL TRAINING WITHIN A GRANULAR MODEL FOR EXCHANGE BIAS

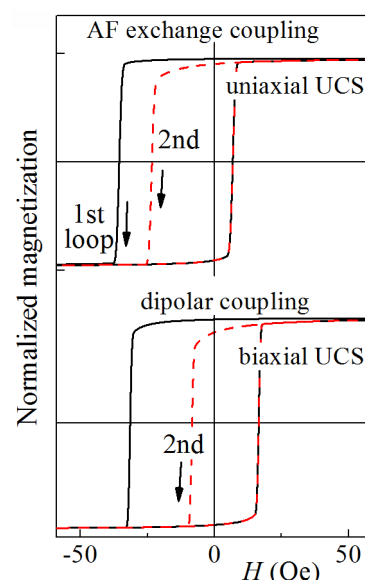
*Harres A., Geshev J.*

Instituto de Física – UFRGS, Porto Alegre, RS, Brazil

The magnetic exchange bias (EB), i.e., a shift of the magnetization curve along the magnetic field axis ( $H_{eb}$ ), comes from exchange coupling between a ferromagnet (FM) and uncompensated spins (UCS) at the interfacial region of an adjacent antiferromagnet (AF). Although discovered more than half a century ago and already used in magnetoelectronic devices, the EB continues to pose intriguing questions. One of these questions concerns the origin of the frequently observed decrease of  $H_{eb}$  upon subsequent field cycling referred to as training effect, which can be divided into thermal and athermal effects [1]. Athermal training is characterized by a shift of the descending branch of the firstly-traced hysteresis loop and persists even at very low temperatures, where the thermal training, caused by thermal activation, vanishes.

Despite the extensive efforts to model EB systems, there is still no generally-accepted theory that predicts their behaviour in real systems. In order to explain the isotropic shift in ferromagnetic resonance measurements of EB systems, an unidirectional rotatable anisotropy (RA) term of a form  $-\mathbf{M}\cdot\mathbf{H}_{\text{RA}}$  has been considered [2], where the RA field  $\mathbf{H}_{\text{RA}}$  is parallel to the external field  $\mathbf{H}$  ( $\mathbf{M}$  is the FM magnetization). It is established that the RA comes from interfacial UCS which rotate almost simultaneously with  $\mathbf{M}$ . When irreversible magnetization processes are involved, however, RA energy  $\propto -(\mathbf{M}\cdot\mathbf{H}_{\text{RA}})^2$  has been considered in order to reproduce an entire hysteresis loop [3]. Thus, the coupling with a ‘rotatable’ UCS is sensed by the FM as an additional uniaxial anisotropy with axis parallel to  $\mathbf{H}$ . Such an approach explains qualitatively both the isotropic ferromagnetic resonance field shift and the increased coercivity in bilayers with polycrystalline AF. Variations of both magnitude and easy-axis direction of the RA as  $\mathbf{H}$  is changed [4] or RA easy axis deviated from the EB direction [5,6] were also studied.

In this work we compare magnetization curves simulated within the above-cited RA models and also with loops obtained through a granular EB model for polycrystalline films. We also show that athermal training can be obtained within this model. Using realistic parameters for the magnetic anisotropy and coupling, training effects are obtained regardless the type of the anisotropy (uniaxial or biaxial) of the interface grains with UCSs, see the examples given in the figure. The experimentally-observed partial recovery of the training effects either by magnetic annealing or after application of strong magnetic fields, or even a change of the sign of  $H_{\text{eb}}$  after training are naturally attained in the framework of our model.



This work has been supported by CAPES and CNPq.

- [1] L. E. Fernandez-Outon et al., *J. Magn. Magn. Mater.* **303** (2006) 296.
- [2] R. D. McMichael et al., *Phys. Rev. B* **58** (1998) 8605.
- [3] J. Geshev, L. G. Pereira and J. E. Schmidt, *Phys. Rev. B* **66** (2002) 134432.
- [4] J. K. Kim et al., *J. Appl. Phys.* **93** (2003) 7714.
- [5] F. Radu et al., *J. Phys.: Condens. Matter* **18** (2006) L29.
- [6] J. McCord et al., *Phys. Rev. B* **78** (2008) 094419.

23OR-B-6

## MAGNETISATION REVERSAL OF PATTERNED FERROMAGNETIC THIN FILMS WITH AND WITHOUT EXCHANGE BIAS

Gornakov V.S.<sup>1</sup>, Kabanov Yu.P.<sup>1</sup>, Nikitenko V.I.<sup>1,2</sup>, Chen P.J.<sup>2</sup>, Dennis C.L.<sup>2</sup>, Shull R.D.<sup>2</sup>

<sup>1</sup> Institute of Solid State Physics, RAS, Chernogolovka, 142432, Russia

<sup>2</sup> National Institute of Standards and Technology, Gaithersburg, MD, 20899, USA

Reduced lateral size of both ferromagnet (FM) and antiferromagnet (AFM) layers in nano-structured FM/AFM systems is expected to increase the role of both edge and dipole effects on magnetic and magnetotransport properties of the devices [1]. Shape and edges in magnetic elements

with reduced dimensions play an increasingly important role in determining the magnetic structure. Conventional shapes of magnetic elements are rectangular or ellipsoid. Domain structure and micromagnetic kinetics of such type magnetic elements are intensively studied both experimentally and theoretically. However elements with mesh shape have specific boundary conditions and their micromagnetic properties are not study successfully. To determine the conditions and the origin of possible switching modes associated with the domain structure transformation in the square mesh FM layers, we have visualized successive stages of the magnetization reversal in both single layer and ferromagnetic elements exchange coupled to AFM. The polycrystalline single thin patterned films  $\text{Ni}_{81}\text{Fe}_{19}$  (30 nm) and composite systems consisting of a FM film  $\text{Ni}_{81}\text{Fe}_{19}$ (30nm) with a square mesh of an antiferromagnet  $\text{Ir}_{50}\text{Fe}_{50}$  (10 nm) were studied. In each case the square meshes have had 100-120  $\mu\text{m}$  spatial period and  $\sim 15 \mu\text{m}$  stripes width. Details of the magnetization reversal process in the patterned structures have been studied by the magneto-optical indicator film (MOIF) technique [2] depending on the external magnetic field,  $H$ . The hysteresis loops were measured with a SQUID magnetometer.

Comparison of the domain structure transformation in single layer and exchanged biased FM meshes has shown both common and distinctive properties in these elements. The MOIF imaging has revealed that in each case the micron-size square FM mesh is reversing at least in two separate steps. First, after samples saturation and a field decreasing to zero, magnetization rotation in stripes and formation of specific stable domains in the intersections of the stripes was observed. Then nucleation and extension of new domains in the FM bars took place. Analyze of an intensity of magneto-optical signals shown a significant difference between magnetization reversal of exchange biased and unbiased patterned structures as well as between patterned and non-patterned parts of exchange biased samples. Unlike unbiased FM patterned films, where magnetization reversal in stripes occurs by small domain and non-homogenous magnetization rotation, remagnetization of the FM bars in FM/AFM patterned structures from ground state is shown to happen by nucleation of domain walls, moving first along stripes parallel to applied field and then along those ones perpendicular to  $H$ . Quite different domain processes have been involved during remagnetization to ground state. The domain walls moved randomly along both parallel and perpendicular FM bars. In some cases quasivortex states were formed in the intersections of the stripes. The likely reason for the observed phenomenon is the influence of magnetic surface charges and the associated stray field at topographic step edges of ferromagnetic elements on the magnetic moments inside stripes.

[1] J.I. Martin, *et al.*, J. Magn. Magn. Mat. **256** (2003), 449-501.

[2] Yu.P. Kabanov, *et al.*, Phys. Rev. B **79** (2009), 144435.

23OR-B-7

## **NEW KIND OF A METASTABLE STATES IN A SYMMETRIC FERROMAGNETIC FILM AND SPIN-REORIENTATION PHASE TRANSITION WITH FILM THICKNESS**

*Popov A.P., Anisimov A.V.*

Moscow State Engineering-Physics Institute, 115409 Moscow, Kashirskoe shosse, 31, Russia

In the early nineties of the last century it was established that a single-domain ferromagnetic film with a competing surface and bulk anisotropy energies can be in a canted state. In this state the vector magnetization of atomic layer depends on the layer index. Also if the surface and bulk anisotropy constants satisfy some conditions then the canted state can be a ground state of a film. In

this canted state the dependence of angle between the surface plane and vector magnetization of each layer is odd with respect to the middle of a film.

In our recent article it was demonstrated that besides the ground canted state mentioned above the symmetric film (equal anisotropy constants at both sides of a film) can exhibit some other locally stable canted states that are not caused by the competition between surface and bulk anisotropy energies [1]. In the present work we had derived the analytical expressions for the criteria of appearance of solutions that correspond to these metastable states. This result allowed us to reveal the nature of these metastable states. The first kind of a metastable state is characterized by the odd dependence of orientation angles with respect to the middle of the film. It originates from the collinear state where vector moments of all layers are oriented in the film plane. The second kind of a metastable state is characterized by the odd dependence of the modified orientation angles between the normal to the surface plane and vector magnetization, with respect to the middle of the film. It originates from the collinear state where vector moments of all layers are oriented perpendicular to the surface plane.

Also in the present work we had derived the analytical expressions for the stability criterion of collinear states of a symmetric film with account of discrete location of atomic layers. Based on the results we constructed the phase diagram of magnetic states of a symmetric film. The results obtained had allowed us to describe the spin-reorientation phase transition in a sandwich Au/Co/Au from the collinear perpendicular state to again collinear in-plane state with film thickness. This phase transition goes through the intermediate ground canted state of a film. The account of non-collinear canted state is necessary for cobalt film where the domain wall width is comparable with a threshold width at which the phase transition occurs. The comparison of these theoretical results with experimental data had allowed us to restore the magnitudes of surface and bulk anisotropy constants of Co film in a Au/Co/Au sandwich. The comparison of these magnitudes of anisotropy constants with similar magnitudes for a bare cobalt film Co/Au restored in our previous work [2] allows us to state that the Neel anisotropy energy at free cobalt surface is negligible.

[1] A.P. Popov, A.V. Anisimov, O. Eriksson, N.V. Skorodumova, *Phys. Rev.*, B **81** (2010) 054440.

[2] A.P. Popov, N.V. Skorodumova, O. Eriksson, *Phys. Rev.*, B **77** (2008) 014415.

23OR-B-8

## EXPERIMENTAL ESTIMATION OF HYSTERESIS LOSSES OF SUPERPARAMAGNETIC NANOPARTICLES

*Gudoshnikov S.A.<sup>1,2</sup>, Grebenshchikov Yu.B.<sup>1</sup>, Liubimov B.Ya.<sup>1</sup>, Usov N.A.<sup>1,2</sup>*

<sup>1</sup> Pushkov Institute of Terrestrial Magnetism, Ionosphere and Radio Wave Propagation, Russian Academy of Sciences, (IZMIRAN), 142190, Troitsk, Moscow region, Russia

<sup>2</sup> Ltd. "Magnetic and Cryoelectronic Systems", 142190, Troitsk, Moscow region, Russia

The hysteresis losses of superparamagnetic nanoparticles are known to be proportional to a square of the assembly hysteresis loop. According to theoretical estimation [1] they depend considerably on the characteristic particle sizes and their magnetic parameters. In the present report the hysteresis losses of a superparamagnetic assembly of Fe<sub>3</sub>O<sub>4</sub> nanoparticles with average diameter  $D = 25$  nm are estimated experimentally in the frequency range  $f = 10 - 150$  kHz at the alternating magnetic field amplitudes  $H_0 = 100 - 300$  Oe. The low frequency hysteresis loops of the assembly (see Fig. 1) are obtained by integrating the electro-motive force signal arising in a small pick-up coil wound around a cylindrical sample of volume  $V \approx 0.01$  cm<sup>3</sup> that contains 5 - 10 mg of Fe<sub>3</sub>O<sub>4</sub> nanoparticles. For completeness, the assembly saturation magnetization,  $M_s = 370$  emu/cm<sup>3</sup>, is



obtained through a quasistatic loop measurement. It is close to the bulk magnetite value, which confirms the good quality of the assembly of  $\text{Fe}_3\text{O}_4$  nanoparticles investigated. The effective anisotropy constant is estimated to be  $K = (2-3) \times 10^5$  erg/cm<sup>3</sup>. As inset in Fig. 1 shows, the heating rate of the assembly at moderate frequencies and magnetic field amplitudes can be as high as 1° C/s. Nevertheless, the measured hysteresis losses of the sample turn out to be somewhat less than the corresponding theoretical prediction. This may be related with an agglomeration of the magnetic nanoparticles in the given assembly.

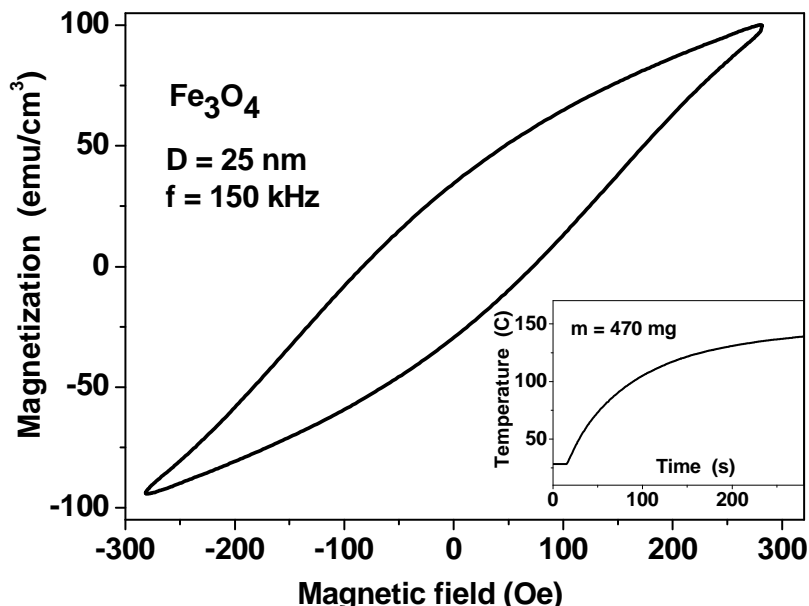


Fig. 1. Hysteresis loop of  $\text{Fe}_3\text{O}_4$  nanoparticles with diameter  $D = 25$  nm at  $f = 150$  kHz and  $H_0 = 285$  Oe. The inset shows the temperature increase in 470 mg magnetite sample subjected to the influence of alternating magnetic field with  $f = 100$  kHz and  $H_0 = 285$  Oe.

The financial supports from RFBR grant № 10-02-01394-a and grant № 4.4.1.6 of RAS Nanotechnology Program No. 21 are gratefully acknowledged.

[1] N.A. Usov, J. Appl. Phys. **107** (2010) 123909-1-12.

23OR-B-9

## MAGNETIC PROPERTIES AND MORPHOLOGY OF FERRITE NANOPARTICLE DISPERSED IN GLASS

*Edelman I.<sup>1</sup>, Ivanova O.<sup>1</sup>, Ivantsov R.<sup>1</sup>, Velikanov D.<sup>1</sup>, Zubavichus Y.<sup>2</sup>, Veligzhanin A.<sup>2</sup>, Curély J.<sup>3</sup>*

<sup>1</sup> L.V. Kirensky Institute of Physics SB RAS, 660036 Krasnoyarsk, Russia

<sup>2</sup> RRC "Kurchatov Institute", Acad. Kurchatov sq. 1, 123182 Moscow, Russia

<sup>3</sup> LOMA, Université Bordeaux-1, France

Comparative investigation of the magnetic properties and nanoparticles characteristics in oxide glasses doped simultaneously with Fe and Mn or Fe and one of the rare earth elements Dy, Tb, Gd, Ho, Er or Y and Bi were investigated. Nanoparticles arise in glasses as a result of an additional thermal treatment. The particles morphology is investigated with the high resolution electron microscopy. The glasses magnetization is investigated in the temperature interval 1.8-300 K in

magnetic field up to 5 T with a superconducting quantum interference device magnetometer (SQUID). Two cooling regimes were used – field cooled (FC) and zero field cooled (ZFC). ZFC - the sample was cooled down from the initial temperature of 300 K in the absence of an external magnetic field. FC - cooling and heating of a sample were carried out at the same magnetic field.

It is shown that as-prepared glasses demonstrate the paramagnetic behavior at temperatures higher than ~20 K. At lower temperatures the deviation from paramagnetic situation appears: in large magnetic field the temperature dependencies of magnetization obeys to Curie-Weiss law with negative Curie temperature, what is ascribed to an appearance antiferromagnetic clusters in glass.

There are common features in the temperature dependences of magnetization for all samples: (1) the difference between FC and ZFC curves (Fig. 1 left), (2) an increase in the slope of the magnetization curves at low temperatures (Fig. 1 right). Several mechanisms are considered that could be responsible for these features. The difference between FC and ZFC can be associated with the superparamagnetic state of the particles; in this case maxima in the ZFC curves determined the particles blocking temperature. The slope of magnetization curves can be due to the size effect originated from the spin disorder in the particles surface area. The different mechanisms responsible for two main peculiarities in the magnetization field and temperature dependences are proved by the difference between the blocking temperatures and temperatures when sharp slope increase appears.

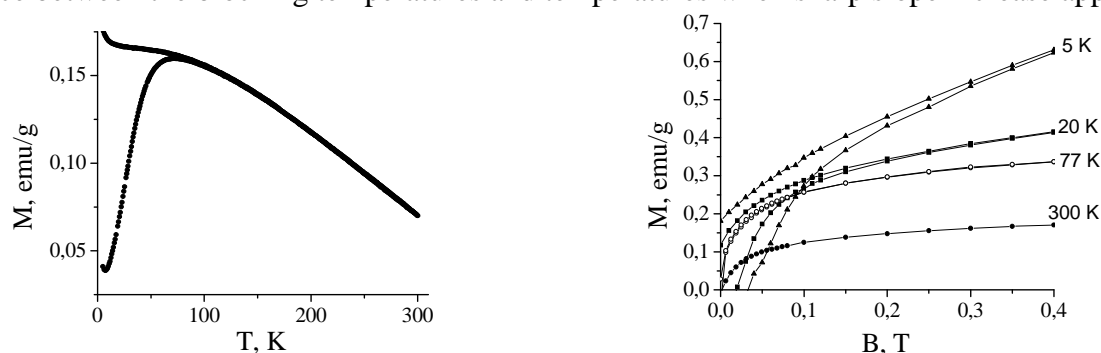


Fig.1. Left: temperature dependences of FC and ZFC magnetization curves; right: hysteresis loops measured at different temperatures for glass containing  $\text{MnFe}_2\text{O}_4$  nanoparticles of 7 nm in size.

Support by RFBR grant №11-02-00972 is acknowledged.

23OR-B-10

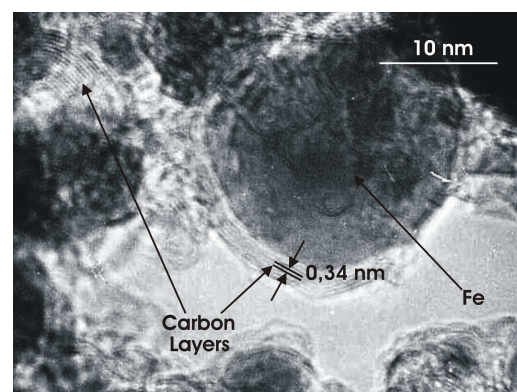
## MAGNETISM AND ELECTRONIC PROPERTIES OF "GIANT FULLERENES" ON THE BASE OF NANOCRYSTALLINE 3d-METALS ENCAPSULATED IN CARBON

*Yermakov A.Ye., Uimin M.A., Mysik A.A., Byzov I.V., Tzurin V.A., Ponosov Yu.S., Galakhov V.R., Kurmaev E.Z., Schegoleva N.N.*

Institute of Metal Physics, Ural Branch of RAS, 18, S.Kovalevskaya st., Ekaterinburg, Russia

The interest in nanosized materials have spread to other disciplines of physics, chemistry and medicine due to the possible technological application associated with them apart from the fundamental aspects. The most attractive and less studied objects are “core-shell” structure, such as, for instance, magnetic metals (Me=Fe, Co, Ni and others, so called a “Giant Fullerenes” -Me@C) in a nanocrystalline state covered by carbon as a stable platform for multimodal purposes. The detailed and systematic investigations of the above-mentioned materials are practically absent in spite of the

attractive properties for medical and technical applications. There are a lack of fundamental investigations of magnetic and electron structure for this kind of “core-shell” materials in a nanoscale range. In the present work the nanocomposites on the base of 3d-metals (Fe, Ni, Co, Fe-Co) covered by carbon and having the average size less than 10 nm including carbon coating were synthesized by gas-condensation method (on the figure Fe@C nanocomposite is shown). Structural parameters of metal-carbon nanocomposites have been studied by X-ray diffraction analysis, high resolution transmission electron microscopy, XPS, XAS, Raman and Mossbauer spectroscopy methods. It was carried out the long term photoelectron and X-ray absorption measurements of carbon-encapsulated Fe@C and Ni@C nanoparticles. We have found that carbon coating protects the metallic nanoparticles from the environmental degradation by providing a barrier against oxidation, and ensure stability of the ferromagnetic core metal inside at least more than 1 year. The observed Raman spectra of metal-carbon nanocomposites allow us to make a conclusion that the carbon coating is not perfectly complete (like fullerene structure) but those are organized from fragments of graphene planes with sizes of 10 nm lengthwise. The existence of small fractions of FCC-Fe and iron carbide in Fe@C nanocomposites were revealed by Mossbauer and XPS spectroscopy. It was shown that the specific magnetization of iron and nickel encapsulated in carbon taking into account the content of carbon coating and carbides is turned out too abnormally small as compared with the one of bulk state. At the same time a magnetization of Co@C and alloy (Fe,Co)@C nanocomposites corresponds to the magnetization of bulk state of cobalt and Fe-Co alloy considering the carbon contribution as well. The unusual magnetic properties of Fe, Ni encapsulated in carbon in the nanoscale range will be discussed in the model of non-collinear magnetic structure of metallic core.



It was carried out the long term photoelectron and X-ray absorption measurements of carbon-encapsulated Fe@C and Ni@C nanoparticles. We have found that carbon coating protects the metallic nanoparticles from the environmental degradation by providing a barrier against oxidation, and ensure stability of the ferromagnetic core metal inside at least more than 1 year. The observed Raman spectra of metal-carbon nanocomposites allow us to make a conclusion that the carbon coating is not perfectly complete (like fullerene structure) but those are organized from fragments of graphene planes with sizes of 10 nm lengthwise. The existence of small fractions of FCC-Fe and iron carbide in Fe@C nanocomposites were revealed by Mossbauer and XPS spectroscopy. It was shown that the specific magnetization of iron and nickel encapsulated in carbon taking into account the content of carbon coating and carbides is turned out too abnormally small as compared with the one of bulk state. At the same time a magnetization of Co@C and alloy (Fe,Co)@C nanocomposites corresponds to the magnetization of bulk state of cobalt and Fe-Co alloy considering the carbon contribution as well. The unusual magnetic properties of Fe, Ni encapsulated in carbon in the nanoscale range will be discussed in the model of non-collinear magnetic structure of metallic core.

Financial support by RFBR (Grant # 10-02-00323a) is acknowledged.

23OR-B-11

## STRUCTURAL CORRELATIONS OF ELECTRON TRANSPORT IN IRON FILLED CARBON NANOTUBES

*Migunov V., Spasova M., Farle M.*

Fakultät für Physik and Center for Nanointegration (CeNIDE), Universität Duisburg-Essen  
Lotharstrasse 1, 47048 Duisburg, Germany.

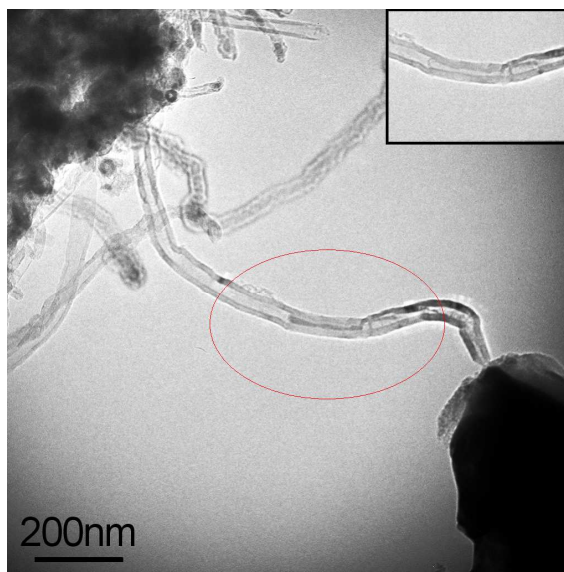
Carbon nanotubes (CNTs) are potentially the smallest building blocks for different types of future devices. A possibility to fill CNTs with magnetic materials opens horizons for promising novel applications in sensoric, magnetic storage, and magnetomechanical devices.

The Fe filled CNTs (FeCNTs) were synthesized by chemical vapor deposition in two zone quartz-tube reactor [1]. The outer diameters of the tubes are in range of 40-80 nm, the lengths varies from 1 to 10  $\mu\text{m}$ , the diameters of encapsulated iron nanowires are about 20-40 nm.

High resolution transmission electron microscopy (HR-TEM) study on atomic structure of the nanotubes shows that the metallic nanowires possess a single phase – alpha iron with bcc structure. There were no signs of oxide found.

Transport studies were carried out inside Philips CM-12 transmission electron microscope (TEM) using Nanofactory scanning probe microscopy (SPM) holder for TEM. This method allows to combine electrical measurements with simultaneous observation of morphology and atomic structure of the nanotubes in TEM. To carry out two-point resistance measurement a gold SPM tip was brought in contact with the nanotube. The I-V curves at different bias voltage ranges, magnetic fields and electron illumination conditions were recorded.

Typically the I-V curves show ohmic behavior at low current densities (up to  $10^{-7}$  A/cm<sup>2</sup>) and characteristic steps at higher current densities ( $10^{-6}$ - $10^{-4}$  A/cm<sup>2</sup>). The steps correspond to irreversible decrease of the tubes resistance. The TEM analysis show that the iron evaporates from the nanotubes because of high current density, which result in the rapid resistance drops. The figure shows a TEM micrograph of the nanotube (in the middle) attached with one end to the substrate (top left corner). The other end is contacted with the gold STM tip (right bottom corner). The iron inclusion is visible by the dark contrast in the middle of the nanotube (the area marked with red) and it disappears after the high current was passed over the tube.



The essential evaporation models will be discussed in a presentation as well as a process of FeCNTs failure. In addition the magnetic field dependent measurements will be presented.

Support by DFG in frame of SFB 445 is acknowledged.

[1] A. Leonhardt et al. *Diamond and Related Materials* **12** (2003) 790–793

23OR-B-12

## PROPERTIES OF SINGLE MOLECULE MAGNET Ni<sub>4</sub>Mo<sub>12</sub>

*Kostyuchenko V.V.*

Institute of Physics and Technology RAS, Yaroslavl Branch, Universitetskaya 21, Yaroslavl,  
150007, Russia

The core of single molecule magnet Ni<sub>4</sub>Mo<sub>12</sub> contains four ions Ni<sup>2+</sup> ( $S=1$ ) placed in the vertexes of a tetrahedron. Ligands form isolating shells that encapsulate the magnetic core. Thus the interaction between magnetic ions located in different molecules is small. The spin structure of Ni<sub>4</sub>Mo<sub>12</sub> looks rather simple. But the theoretical interpretation of magnetic properties Ni<sub>4</sub>Mo<sub>12</sub> is not a simple problem. The proper choice of spin Hamiltonian remains unclear despite intense discussions during several years [1-4].

At the present time two models can more or less describe the magnetic properties of Ni<sub>4</sub>Mo<sub>12</sub>. The first one [2] is based on assumption of essential role of non-Heisenberg exchange interactions in

$\text{Ni}_4\text{Mo}_{12}$  (biquadratic and three-spin). The second one [4] comprises two assumptions, strong violation of symmetry of exchange interactions, and strong single-ion anisotropy.

The present work is devoted to the theoretical analysis of both these models. The attention is focused on the forecasting power of these spin models. Mechanism responsible for non-Heisenberg exchange interactions is the same as mechanism resulting in interaction of spin chirality with external magnetic field. As an example, additional level splitting in magnetic field can be observed in the case of model [2]. In the case of model [4] quite different phenomena are expected. The violation of symmetry of exchange interactions inevitably leads to nonzero toroidal moment of the ground state. This effect can be observed via set of magnetoelectric phenomena.

Thus investigation of spin chirality  $\text{Ni}_4\text{Mo}_{12}$  and magnetoelectric phenomena can play a crucial role in defining the character of the magnetic interactions in  $\text{Ni}_4\text{Mo}_{12}$ . It allows us to obtain a decisive support for one of the two spin models, or reject both models.

- [1] J. Schnack, M. Bruger, M. Luban, P. Kogerler, E. Morosan, R. Fuchs, R. Modler, H. Nojiri, R. C. Rai, J. Cao, J. L. Musfeldt, X. Wei, *Phys. Rev. B*, **73** (2006) 094401  
 [2] V.V. Kostyuchenko, *Phys. Rev. B*, **76** (2007) 212404.  
 [3] J. Nehr Korn, M. Hock, M. Bruger, H. Mutka, J. Schnack, O. Waldmann, *Euro. Phys. J. B*, **73** (2010) 515  
 [4] A. Furrer, K. Kramer, T. Strassle, D. Biner, J. Hauser, H. Gudel, *Phys. Rev. B*, **81** (2010) 214437

23OR-B-13

## BIMODAL DISTRIBUTION OF BLOCKING TEMPERATURES IN EXCHANGE BIASED BILAYERS

Baltz V.<sup>1</sup>, Auffret S.<sup>1</sup>, Gaudin G.<sup>1</sup>, Vinai G.<sup>1</sup>, Moritz J.<sup>1</sup>, Rodmacq B.<sup>1</sup>, Dieny B.<sup>1</sup>, Letellier F.<sup>2</sup>, Zarefy A.<sup>2</sup>, Lardé R.<sup>2</sup>, Lechevallier L.<sup>2</sup>

<sup>1</sup> SPINTEC, 17 avenue des Martyrs 38054 Grenoble, France

<sup>2</sup> GPM, avenue de l'université 76801 Saint Etienne du Rouvray, France

The ability to pin the magnetization of a ferromagnetic layer in a fixed direction in order to define a reference direction for the spin of conduction electrons is a prerequisite to most spintronic devices [1]. Exchange bias (EB) which refers to the exchange coupling between a ferromagnet (F) and an antiferromagnet (AF) is used for that particular purpose of shifting the hysteresis loop along the magnetic field axis. Some technological applications such as magnetic random access memories, involve patterning full sheet wafers into matrix of individual submicronic cells. Industrial products qualification imposes stringent requirements on the distributions of the magnetic properties from cell to cell, including those related to EB. Randomly spread spin-glass like regions at the F/AF interface or within the bulk of the AF layer among with small grains can significantly contribute to the distributions of EB properties. By nature, the frustrations and the grains sizes are randomly spread over the wafer and thus over the memory cells after nanofabrication. As opposed to cells with few spin-glass like regions and larger grains, cells with more of such regions and smaller grains will show a weaker hysteresis loop shift at room temperature (T) and are more prone to thermal activation. Ultimately, these cells lose their spin reference direction and correlatively fail. Therefore, minimizing the amount of spin-glass like regions and enlarging the grains sizes, already at wafer level, is a requirement towards the improvement of EB properties before being able to implement it in devices.

We will discuss results on F/AF bilayers for which we evidenced bimodal distributions of blocking temperature ( $T_B$ ) [2]. The  $T_B$  distributions consist of two parts: a commonly observed high T peak associated to thermally activated reversal of the larger AF grains spin-lattice [3] and a more unconventional low T peak that is so far ascribed to both i) thermally activated reversal of the smaller AF grains spin-lattice and ii) F/AF interfacial spin-glass like regions characterized by low freezing T [4]. We will show attempts and success in understanding and controlling the low-T peak of the blocking temperature distribution: i) by tuning the growth conditions (on- vs off-axis deposition, ‘top’ vs ‘bottom’ structure, use of magnetic field during deposition...), ii) by studying the effects of annealing, and iii) by comparing various antiferromagnets exchange coupled to a Co ferromagnetic thin film: IrMn, FeMn, NiMn.

After fabricating arrays of nanopillars, we observed two-fold consequences when considering the down-size scalability of spintronic devices ascribed to grain sizes reductions due to etching and to additional formation of low freezing T regions at the edges of the nanodots [5].

Magnetic characterizations by superconducting interference magnetometry (SQUID) are complemented by atomic force microscopy (AFM) and tomographic atom probe (TAP) for structural characterizations.

[1] J. Nogués and I. K. Schuller, *J. Magn. Magn. Mater.*, **192** (1999) 203; A. E. Berkowitz and K. Takano, *ibid.*, **200** (1999) 552.

[2] V. Baltz, B. Rodmacq, A. Zarefy, L. Lechevallier, and B. Dieny, *Phys. Rev. B*, **81** (2010) 052404.

[3] E. Fulcomer and S. H. Charap, *J. Appl. Phys.*, **43** (1972) 4184.

[4] K. Takano et al *Phys. Rev. Lett.*, **79** (1997) 1130.

[5] V. Baltz, G. Gaudin, P. Somani, and B. Dieny, *Appl. Phys. Lett.*, **96** (2010) 262505.

23OR-B-14

## NANOSIZED LAYERED STRUCTURES ON A BASIS OF FERROMAGNETIC SEMICONDUCTORS AND HEUSLER ALLOYS

*Demidov E.S.<sup>1</sup>, Podolskii V.V.<sup>1</sup>, Lesnikov V.P.<sup>1</sup>, Sapozhnikov M.V.<sup>2</sup>, Karzanov V.V.<sup>1</sup>, Gribkov B.A.<sup>2</sup>,  
Gusev S.N.<sup>1</sup>, Levchuk S.A.<sup>1</sup>, Tronov A.A.<sup>1</sup>*

<sup>1</sup> Nizhni Novgorod State University, Nizhni Novgorod 603950, Russia;

<sup>2</sup> Institute for Physics of Microstructures, RAS, Nizhni Novgorod 603950, Russia;

Diluted ferromagnetics on the basis of doped by iron group 3d-impurities of compounds III-V both elementary semiconductors Ge and Si cause the big interest in connection with creation prospects on their basis of new spintronic devices. The possibility of laser synthesis of thin (50-200 nm) layers of the diluted magnetic semiconductors (DMS) on the basis of compounds III-V – GaSb, InSb, InAs, with Mn impurity, Ge and Si with Mn or Fe impurities on single crystal substrates GaAs, Si or Al<sub>2</sub>O<sub>3</sub> with ferromagnetic behavior at temperatures till 500°C was earlier demonstrated [1,2]. Recently essential progress in realization with 40-200 % GMR at a room temperature has been attained in magnetic tunnel junctions (MTJ) and spin valves on the basis of layers of similar Co<sub>2</sub>MnSi (CMS) Heusler alloys (HA) [3,4]. In the present report our experimental results of research of magnetotransport, ferromagnetic resonance (FMR) and magneto optic properties of tunnel structures with plates of alloys Co<sub>2</sub>MnSi, CoSi and dielectric interlayer MgO or Al<sub>2</sub>O<sub>3</sub>, and also single layers DMS and HA are resulted. Layers were synthesized by deposition from laser plasma and RF magnetron sputtering. The topology and distribution of magnetization of MTJ were measured by AFM and MFM probe microscopy. Magnetism of layers was controlled by

measurements of abnormal Hall effect, negative magnetoresistance (NMR), FMR and nonlinear magneto-optic Kerr effect. The characteristic features of FMR of magnetic structures with MgO dielectric interlayer (Fig.1), isotropic negative MR (Fig.2), I-V nonlinearity and hysteresis of MTJ and single DMS and HA layers at rather small density of a current  $10^4 - 10^5$  A/cm<sup>2</sup> were observed at temperatures 77-300K.

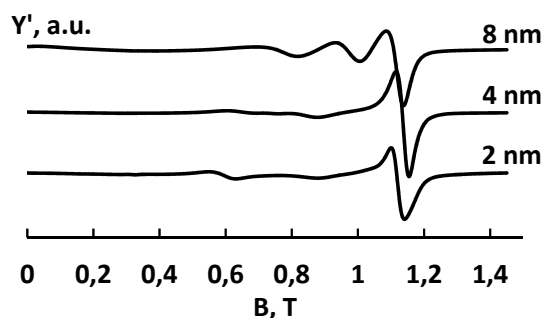


Fig.1. Acoustic and optic FMR lines of MTJ CMS/MgO(2-8nm)/CMS at room temperature.

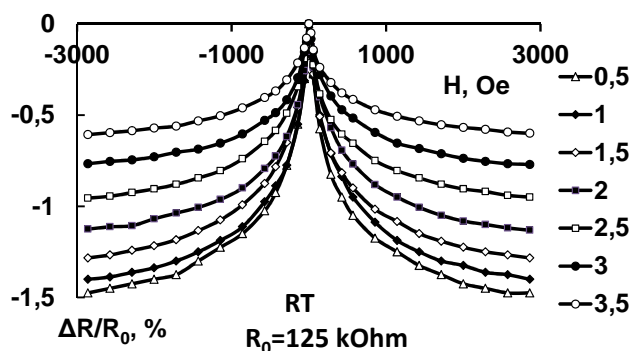


Fig.2. NMR of MTJ CMS/MgO(2nm)/CMS for 0.5-3.5 V biases at room temperature.

Supported by RFBR (08-02-01222-a, 11-02-00855-a), the Ministry of Education of Russian Federation (projects 2.1.1/2833 and 2.1.1/12029) and the State contract № 02.740.11.0672 of the Federal purpose program «Scientific and scientific-pedagogical cadre of innovative Russia» 2009-2013 is acknowledged.

- [1] E.S. Demidov, B.A. Aronzon, S.N. Gusev et al, *JMMM*, **321** (2009) 690.
- [2] E.S. Demidov, b, V.V. Podolskii, B.A. Aronzon et al, *Bull. RAS: Physics*, **74** (2010) 1389.
- [3] N. Tezuka, N. Ikeda, S. Sugimoto, K. Inomata et al, *Appl. Phys. Lett.*, **89** (2006) 252508.
- [4] T. Furubayashi, K. Kodama, T. M. Nakatani et al, *J. Appl. Phys.*, **107** (2010) 113917.

23OR-B-15

## THE INFLUENCE OF QUANTUM SIZE EFFECTS ON MAGNETIC PROPERTIES OF THIN-FILM SYSTEMS

*Shalyguina E., Rozhnovskaya A., Shalygin A.*

Faculty of Physics, Moscow State University, Leninskie Gory, 119992, Moscow, Russia

Results on the investigation of magnetic and magneto-optical properties of Fe/NML/Fe (NML: Mo, Ta) thin-film systems are presented. The examined samples were prepared by DC magnetron sputtering technique. Series of the Fe/NML/Fe trilayers with the thickness of Fe layers,  $t_{Fe}$ , equal to 2.5, 5 and 10 nm, and the nonmagnetic layer thickness,  $t_{NML}$ , varying from 0.5 to 3-4 nm, were prepared. The low-angle XRD analysis was made to check the existence of the periodic layered structures (well-defined interfaces) and to determine the layers thickness in the examined samples. The study of magnetic properties and spectral dependencies of the transverse Kerr effect was carried out employing the magneto-optical magnetometer and the magneto-optical spectrometer, respectively. Hysteresis loops were measured at two directions of the magnetic field  $H$ . In particular,  $H$  was parallel or perpendicular to the direction of the magnetic field, applied parallel to the substrate surface during the film deposition (marked as D1 and D2, respectively). The spectral dependences of TKE were measured in the  $1.4 < \hbar\omega < 4.5$  eV photon energy range, at the 65°-angle

of the light incidence from the sample normal and at  $H > H_S$  ( $H_S$  is the saturation field of the sample under study).

The hysteresis loops of the examined samples, measured at the D1 and D2 magnetic field orientations, showed the presence of an in-plane magnetic anisotropy with the easy axis of magnetization (EAM), parallel to the D1 direction. The saturation field,  $H_S$ , of the examined trilayers, was revealed to oscillate as a function of the NML layer thickness. In particular, the period of these oscillations,  $\Lambda$ , for the trilayers with Mo, Ta nonmagnetic layers and  $t_{\text{Fe}} = 2.5$  nm is equal to 0.9 and 1.2 nm, respectively. It was also discovered that the  $\Lambda$  magnitudes increase with increasing of the magnetic layer thickness. The discovered dependences of  $H_S(t_{\text{NML}})$  were explained by the presence of exchange coupling between ferromagnetic layers and its oscillatory behavior as a function of nonmagnetic spacer thickness (the switch from the ferromagnetic to the antiferromagnetic coupling). As a result, there are parallel [ferromagnetic (F) coupling] and antiparallel [antiferromagnetic (AF) coupling] orientations of the magnetization in the neighboring Fe layers. The saturation field of AF-coupled trilayers is more than  $H_S$  of the F-coupled ones. That is caused by additional energy expense for overcoming the AF exchange coupling between magnetic layers. The F-coupled trilayers were found to display nearly rectangular hysteresis loops, and the AF-coupled ones to show more complicated loops with high enough magnitudes of  $H_S$ . The experimentally found oscillation period of  $H_S$  correlated with the calculated magnitude of  $\Lambda$ , obtained in theoretical works.

It was revealed that TKE spectra of the Fe/NML/Fe systems are identical and similar to the TKE spectrum of the bulk iron but the TKE magnitudes depend on the thickness of both magnetic and nonmagnetic layers. In particular, with increasing  $t_{\text{NML}}$ , TKE values decrease. This diminution of TKE magnitudes can be explained by the decrease of the influence of the lower (with respect to the sample surface) Fe layer on the value of TKE.

The work was supported by the Russian Foundation of Basic Research, grant №10-02-00485-a.



**23 August**

Tuesday

11:30-13:00

14:30-17:20

oral session

23TL-C

23RP-C

23OR-C

**“Magnetostructural  
Transition Related  
Effects”**

23TL-C-1

## MARTENSITIC TRANSFORMATIONS IN Fe-Pd MAGNETIC SHAPE MEMORY ALLOYS: NEWS AND VIEWS FROM FIRST PRINCIPLES

*Gruner M.E.<sup>1</sup>, Weiß S.<sup>2</sup>, Fähler S.<sup>2</sup>, Schultz L.<sup>2</sup>, Entel P.<sup>1</sup>*

<sup>1</sup>Faculty of Physics and Center for Nanointegration, CeNIDE,  
University of Duisburg-Essen, 47048 Duisburg, Germany

<sup>2</sup>IFW Dresden, P.O. Box 270116, 01171 Dresden, Germany

The aim of the present contribution is to discuss the instabilities leading to the martensitic transformations in Fe-Pd magnetic shape memory (MSM) alloys with emphasis on the link to the electronic structure and magnetism. We establish an analogy to the paradigmatic Ni-Mn-Ga MSM system and demonstrate that essential prerequisites to form adaptive martensitic structures are fulfilled in the Fe-Pd system as well.

MSM alloys allow macroscopic strains of several percent to be achieved in realistic magnetic fields. Apart from the prototypical Ni-Mn-Ga full Heusler system also disordered Fe-based alloys as Fe<sub>70</sub>Pd<sub>30</sub> are considered for technological applications as actuators or sensors. In both materials, the MSM effect is related to a thermoelastic transformation from austenite to an intermediate or modulated martensitic phase. At lower temperatures a second, irreversible intermartensitic transition is reported. In Ni-Mn-Ga, the 14M modulated phase has been identified recently as a nano-twinned adaptive structure derived from the low temperature martensite.

Our computational approach relies on first principles calculations within the framework of density functional theory. Disorder is modelled either analytically, using the coherent potential approximation, or explicitly, involving large supercells with up to 500 atoms. This also allows for the optimization of the atomic positions according to their interatomic forces. In the MSM concentration range, where the energy landscape is essentially flat, such atomic relaxations prove relevant as they may shift the ground state the entire way along the Bain path from fcc to bcc [1]. The distortions arise in part from the partial pressure of the Pd 4d electrons in combination with a band-Jahn-Teller instability originating from the Fe 3d minority spin states at the Fermi level. On the other hand, we can show that magnetic excitations work in favor of the fcc austenite. These findings are corroborated by the successful epitaxial growth of strained Fe-Pd MSM films on different substrates which induce tetragonal structures covering the whole Bain path [2]. Newest experiments demonstrate furthermore the occurrence of twinned structures consisting of bct building blocks for *c/a* ratios beyond fcc, which are encountered independently in the simulations. From these we find evidence for a vanishingly small formation energy for the [110] twin boundaries which in combination with a soft acoustic phonon mode in [110] is another common feature of Fe-based and Ni-Mn-Ga MSM alloys supporting the formation of nano-twinned superstructures.

Our work is supported by the Deutsche Forschungsgemeinschaft through SPP 1239. Essential parts of the calculations were carried out using supercomputing resources kindly provided by the John von Neumann Institute for Computing (NIC) at Forschungszentrum Jülich and the Center for Computational Sciences and Simulation (CCSS) at University of Duisburg-Essen.

[1] M. E. Gruner, *Mater. Res. Soc. Symp. Proc.* **1200E** (2010) 1200-G04-04; M. E. Gruner and P. Entel, submitted to *Phys. Rev. B*

[2] J. Buschbeck *et al.*, *Phys. Rev. Lett.* **103** (2009) 216101.

23TL-C-2

## NEUTRON DIFFRACTION IN FERROMAGNETIC SHAPE MEMORY ALLOYS

*Barandiarán J.M., Gutiérrez J., Lázpita P.*

University of the Basque Country (UPV/EHU), Faculty of Science and Technology, P.O. Box 644, Bilbao, 48080, Spain

FSMA have complicated crystallographic structures with different atoms involved in their magnetic behavior, that is far from understood. In NiMnGa alloys, for instance, departures from Mn stoichiometry lead always to a reduction of the magnetic moment. In a rigid band model the electronic concentration alone will determine the final magnetic moment of the alloy. Because some isoelectronic alloys do show changes in the magnetic moment with composition, the rigid band model is questioned.

Powder and single crystal Neutron diffraction is a very appropriate tool to study preferential site occupancy and magnetic moment distribution in off-stoichiometric alloys. Such neutron studies, performed at the Institute Laue Langevin, Grenoble, France, in selected NiMnGa alloys, are reported in the present work. Direct determination of the magnetic structure from unpolarized neutron diffraction data is practically impossible, because of the faint magnetic scattered intensity. However a simple model of localized moments, based on the site occupancy, is able to explain most of the magnetic moment deviations in off-stoichiometric alloys, provided the correct exchange variations with the distance for the Mn atoms are properly taken into account [1], i.e. Mn localized 3d magnetic moments couple Antiferromagnetically (AF) at short distances and Ferromagnetically (FM) at larger ones. Special care is taken in Ni deficient alloys, where Mn excess atoms can occupy either Ni or Ga sites, giving rise to a competition between AF and FM coupling intensities.

Magnetic moment density maps have also been obtained by polarized neutron diffraction in single crystal samples. They support the above model, showing a localized moment in Mn and Ni atoms, while there is a negative spin density in the inter-atomic positions that could be assigned to a magnetic polarization of the conduction band electrons.

This work was supported by the Education and Research and the Industry Departments of the Basque Government (Grants IT-347-07 and IE05-150 respectively). We are grateful to the ILL reactor staff in charge of the instruments D20 and D10. Technical and human support from the General Research Services of the University of the Basque Country: SGIker (UPV/EHU) is also acknowledged

[1] P Lázpita, J M Barandiarán, J Gutiérrez, J Feuchtwanger, V A Chernenko and M L Richard, *New Journal of Physics* **13** (2011) 033039.

23TL-C-3

## MAGNETIC INTERACTIONS IN HEUSLER-BASED MAGNETIC SHAPE-MEMORY ALLOYS

*Acet M.<sup>1</sup>, Aksoy S.<sup>2</sup>, Titov I.<sup>1</sup>, Deen P.P.<sup>3</sup>, Mañosa L.<sup>4</sup>, Planes A.<sup>4</sup>*

<sup>1</sup> Physics Department, Duisburg-Essen University, D-47048, Duisburg, Germany

<sup>2</sup> Faculty of Engineering & Natural Sciences, Sabanci University, Tuzla, 34956 Istanbul, Turkey

<sup>3</sup> Institut Laue-Langevin, BP 156, 38042 Grenoble Cedex 9, France

<sup>4</sup> Departament d'Estructura i Constituents de la Matèria, Facultat de Física, Universitat de Barcelona, Diagonal 647, E-08028 Barcelona, Catalonia, Spain

To understand the basics underlying the magnetic shape-memory effect and to improve functional properties of magnetic shape-memory materials, we study the details of the magnetic coupling in the temperature-vicinity of the martensitic transition. Neutron polarization analysis on Ni-Mn-based martensitic Heusler systems show that at high temperatures, well within the austenite paramagnetic regime, the magnetic correlations are ferromagnetic, whereas just below the martensitic transformation, the spin structure takes up a frustrated antiferromagnetic configuration. Complementary results on ferromagnetic resonance studies show that antiferromagnetic exchange in the martensite state persists down to the lowest temperatures and coexists with long-range ferromagnetism below the martensite Curie temperature. We discuss the favorable and adverse aspects of the presence of antiferromagnetism in relation to functionalities.

23TL-C-4

## Co AND In DOPED NiMnGa: A "GIANT" MULTIFUNCTIONAL MATERIAL

*Albertini F.<sup>1</sup>, Fabbri S.<sup>1</sup>, Paoluzi A.<sup>1</sup>, Casoli F.<sup>1</sup>, Porcari G.<sup>2</sup>, Pernechele C.<sup>2</sup>, Solzi M.<sup>2</sup>, Kamarad J.<sup>3</sup>, Arnold Z.<sup>3</sup>, Serrate D.<sup>4</sup>, Algarabel P.<sup>5</sup>, Righi L.<sup>6</sup>*

<sup>1</sup> IMEM-CNR Parma, Italy

<sup>2</sup> Dipartimento di Fisica, Università di Parma & CNISM, Parma, Italy

<sup>3</sup> Institute of Physics AS CR, Prague, Czech Republic

<sup>4</sup> Facultad de Ciencias, Universidad de Zaragoza & INA, Zaragoza, Spain

<sup>5</sup> Instituto de Ciencia de Materiales de Aragon, Universidad de Zaragoza-CSIC, Zaragoza, Spain

<sup>6</sup> Dipartimento di Chimica GIAF, Università di Parma, Parma, Italy.

Ni<sub>2</sub>MnX based Heusler alloys, X being a group IIIA-VA element, belong to the family of the ferromagnetic shape memory alloys. They undergo a martensitic transition in a magnetically ordered state, and the interplay between structure and magnetism gives rise to a series of remarkable properties, such as giant magnetocaloric effect, magnetic superelasticity, and giant magnetoresistance, making them promising candidates as multifunctional materials. Among the Ni-Mn-X family, one of the most studied systems is Ni-Mn-Ga, which shows magnetic field induced strains up to 10% [1] and considerable values of the magnetocaloric effect [2]. We have recently shown that for Mn-rich NiMnGa alloys, Co substitution produces important changes in magnetism and structure, giving rise to a peculiar phase diagram showing reverse magnetostructural transformations and allowing to tune the magnetocaloric effect from direct to inverse [3]. In the present paper we show that a 2% In substitution strongly decreases the martensitic transformation

temperature moving it close to RT, produces huge effects on the main functional properties, and leads to remarkable values of the magnetocaloric effect.

Sample of composition  $\text{Ni}_{41}\text{Co}_9\text{Mn}_{32}\text{Ga}_{16}\text{In}_2$  show a Curie temperature of martensite ( $T_{\text{CM}}=244$  K) lower than Curie temperature of austenite ( $T_{\text{C}}^{\text{A}}=446$  K) and lower than martensitic transformation temperatures ( $T_{\text{AM}}=318$  K,  $T_{\text{MA}}=344$  K), giving rise to a paramagnetic gap between magnetically ordered martensite and austenite and to the occurrence of a reverse magnetostructural transformation. The same behavior has been obtained in In-free samples in a suitable Co and Mn composition range ( $\text{Ni}_{50-x}\text{Co}_x\text{Mn}_{25+y}\text{Ga}_{25-y}$ , with  $x \leq 9$ ,  $y \geq 6$ ), but showing the martensitic transformations at much higher temperatures. In doping increases the saturation magnetization jump at the transformation ( $\Delta M=65$  Am<sup>2</sup>/Kg against  $\Delta M=53$  Am<sup>2</sup>/Kg in In-free sample), too. Moreover, huge variations of volume at the transformation  $\Delta V/V$  (1.2% for In-doped and 1% for In-free sample) were obtained. These very high magnetization and volume variation allow to drive the martensitic transformation by applying a magnetic field or external pressure. The dependence of the critical temperature on field and pressure are among the highest values reported for Ni-Mn-X Heusler alloys ( $dT_{\text{M}}/dH=-5$  K/T and  $dT_{\text{M}}/dP=60.4$  K/GPa).

Direct and indirect magnetocaloric properties were measured around the martensitic transformation. The adiabatic temperature variation was evaluated in a magnetic field up to 1.9 T, exploiting a Cernox temperature sensor. A remarkable peak value ( $\Delta T_{\text{ad}}=-1.6$  K) was shown by In-doped alloy.

[1] A. Sozinov et al., *Appl. Phys. Lett.*, **80**(2002)1746.

[2] L. Pareti et al., *Eur. Phys. J.*, **32** (2003),303.

[3] S. Fabbri et al., *Appl. Phys. Lett.*, **95**(2009) 022508, *Acta Materialia*, **59**(2011) 412.

23RP-C-5

## ADIABATIC TEMPERATURE CHANGE IN FERROMAGNETIC SHAPE MEMORY ALLOYS

*Khovaylo V.V.*<sup>1</sup>, *Skokov K.P.*<sup>2</sup>, *Koshkid'ko Yu.S.*<sup>2</sup>, *Buchelnikov V.D.*<sup>3</sup>, *Kostromitin K.I.*<sup>3</sup>,  
*Sokolovskiy V.V.*<sup>3</sup>, *Zagrebin M.A.*<sup>3</sup>, *Dubenko I.*<sup>4</sup>, *Miki H.*<sup>5</sup>

<sup>1</sup> National University of Science and Technology "MISiS", Moscow 119049, Russia

<sup>2</sup> Faculty of Physics, Tver State University, Tver 170000, Russia

<sup>3</sup> Faculty of Physics, Chelyabinsk State University, Chelyabinsk 454021, Russia

<sup>4</sup> Department of Physics, Southern Illinois University, Carbondale, IL 62901, USA

<sup>5</sup> Institute of Fluid Science, Tohoku University, Sendai 980-8577, Japan

Judging by a very large isothermal magnetic entropy change  $\Delta S_{\text{m}}$ , ferromagnetic shape memory alloys (FSMAs) hold great promise for utilization in the technology of room-temperature magnetic refrigeration. However, it must be noted that in the majority of cases  $\Delta S_{\text{m}}$  has been estimated from the Maxwell relation. Considering the discrepancy of  $\Delta S_{\text{m}}$  reported for the same composition [1,2], the results of "direct" measurements [3,4] and theoretical studies [4,5], the use of the Maxwell relation alone is not suitable for a reliable evaluation of the magnetocaloric effect in the mixed-phase state of FSMAs.

Here we present results of experimental and theoretical studies of other parameter representing magnetocaloric effect – the adiabatic temperature change  $\Delta T_{\text{ad}}$  – in NiMnGa-based FSMAs. Direct measurements revealed that the adiabatic temperature change  $\Delta T_{\text{ad}}$  in FSMAs is (i) small (typically smaller than in the prototypical magnetocaloric material Gadolinium) and (ii) depends on thermal as

well as on magnetic history of a sample. It will be shown that these features of  $\Delta T_{ad}$  are easy to understand considering thermodynamics of temperature- and magnetic-field-induced martensitic transformations.

Monte Carlo simulations were performed in the framework of a model which takes account of both magnetic and elastic interactions on cubic and tetragonal lattice with periodic boundary conditions [5]. Behavior of  $\Delta T_{ad}$  in the vicinity of first-order magnetostructural transition tracked by the Monte Carlo method is in fair agreement with the experimental data.

Support from the Russian Foundation for Basic Research (grants 09-02-01274, 10-02-00721, 10-02-96020-r-ural, 10-02-92110, and 11-02-00601) and the Federal program “Scientific and pedagogical staff of innovative Russia” is acknowledged.

- [1] F. Albertini, F. Canepa, S. Cirafici, *et al.*, *J. Magn. Magn. Mater.*, **272-276** (2004) 2111.
- [2] M. Khan, S. Stadler, J. Craig, *et al.*, *IEEE Trans. Magn.*, **42** (2006) 3108.
- [3] C.P. Sasso, M. Kuepferling, L. Giudici, *et al.*, *J. Appl. Phys.*, **103** (2008) 07B306.
- [4] V.D. Buchelnikov, S.V. Taskaev, A.M. Aliev, *et al.*, *Int. J. Appl. Electromagn. Mech.*, **23** (2006) 65.
- [5] V.D. Buchelnikov, V.V. Sokolovskiy, H.C. Herper, *et al.*, *Phys. Rev. B*, **81** (2010) 094411.

23RP-C-6

## ELECTRONIC STRUCTURE OF THE HEUSLER-TYPE FERROMAGNETIC SHAPE MEMORY ALLOYS STUDIED BY PHOTOEMISSION AND AB INITIO CALCULATION

*Kimura A.*

Graduate School of Science, Hiroshima University, 1-3-1 Kagamiyama,  
Higashi-Hiroshima 739-8526, Japan

Ni-Mn based ferromagnetic shape memory alloys (FSMAs) have been widely studied owing to their various attractive properties which are related to the presence of a martensitic phase transition (MPT) that can be reversibly manipulated by an external magnetic field [1-7]. However, the origin of such an amazing phase transformation is still under discussion. Here we reveal the underlying mechanism of the MPT in the ferromagnetic state of a new class of FSMAs,  $\text{Ni}_2\text{Mn}_{1+x}\text{Sn}_{1-x}$ , by the combination of bulk-sensitive hard x-ray photoelectron spectroscopy (HAXPES) and a first-principles density-functional calculation. We have observed that the Ni 3d eg state in the cubic phase systematically shifts towards the Fermi energy with an increase in the number of Mn atoms substituted in the Sn sites. An abrupt decrease of the intensity of the Ni 3d eg states upon the MPT for  $x = 0.36\sim 0.42$  has been observed in the vicinity of the Fermi level. Our computational results reveal that the energy shift of the Ni 3d minority spin eg state in the cubic phase originates from hybridization with the antiferromagnetically coupled Mn in the Sn-site. Below the MPT temperature, the Ni 3d state splits into two levels located below and above the Fermi energy in order to achieve an energetically stable state [8].

This work was done in collaboration with M. Ye, Y. Miura, M. Shirai, Y. T. Cui, K. Shimada, H. Namatame, M. Taniguchi, S. Ueda, K. Kobayashi, R. Kainuma, T. Shishido, K. Fukushima, and T.

Kanomata. The experiments were performed at BL15XU of SPring-8 with the approval of NIMS Beamline Station (Proposal No. 2009A4800). This work was partially supported by a Grant-in-Aid for Scientific Research (Grants No. 17340112, No. 19048002, and No. 21560693) from JSPS/MEXT and by a Cooperative Research Project of RIEC, Tohoku University.

- [1] K. Ullakko et al., *Appl. Phys. Lett.*, **69** (1996) 1966.  
 [2] A. N. Vasil'ev et al., *Usp. Fiz. Nauk*, **173** (2003) 577 [*Phys. Usp.*, **46** (2003) 559].  
 [3] P. Entel et al., *J. Phys. D*, **39** (2006) 865.  
 [4] Y. Sutou et al., *Appl. Phys. Lett.*, **85** (2004) 4358.  
 [5] R. Kainuma et al., *Nature*, **439** (2006) 957.  
 [6] A. Planes, L. Manosa, and M. Acet, *J. Phys. Condens. Matter*, **21** (2009) 233201.  
 [7] A. Planes, *Physics*, **3** (2010) 36.  
 [8] M. Ye, A. Kimura, Y. Miura, M. Shirai, Y. T. Cui, K. Shimada, H. Namatame, M. Taniguchi, S. Ueda, K. Kobayashi, R. Kainuma, T. Shishido, K. Fukushima, and T. Kanomata, *Phys. Rev. Lett.*, **104** (2010) 176401.

23TL-C-7

## **METAMAGNETIC STRUCTURAL TRANSITION IN Ni-Mn-In HEUSLER ALLOY: DIRECT EVIDENCE OF AFM ORDERING IN MARTENSITE**

*Ari-Gur P.<sup>1</sup>, Buchelnikov V.<sup>2</sup>, Hernando B.<sup>3</sup>, Koledov V.<sup>4</sup>, Khovailo V.<sup>4</sup>, Ren Y.<sup>5</sup>, Rosa W.<sup>3</sup>, Garcia J.<sup>3</sup>, Gonzalez L.<sup>3</sup>, Taskaev S.<sup>2</sup>, Shavrov V.<sup>4</sup>, Enikeev R.<sup>4</sup>, Mashirov A.<sup>4</sup>*

<sup>1</sup> Western Michigan University, Kalamazoo, MI, 49008, USA

<sup>2</sup> Chelyabinsk State University, Chelyabinsk, 454001, Russia

<sup>3</sup> Depto. de Física, Universidad de Oviedo, Oviedo – Asturias, 33007, Spain

<sup>4</sup> Kotelnikov Institute of Radioengineering and Electronics of RAS, Moscow, 125009, Russia

<sup>5</sup> Argonne National Laboratory, Argonne, IL, 60439, USA

victor\_koledov@mail.ru

The phenomenon of coupled metamagnetostructural transitions (MMST) in new Heusler alloys NiMnX:Me (X = Sn, In, Sb, Me = 3d transition metal) attracts great deal of attention because of its high sensitivity to magnetic field which is crucial in applications such as magnetic refrigeration and magnetic-field-controlled shape memory effect. The nature of the magnetic ordering of the alloy is currently under discussion [1]. This report presents the survey of the works on the problem as well as original results of the experimental study of MMST in Ni<sub>50,2</sub>Mn<sub>39,8</sub>In<sub>10</sub> alloy by magnetic measurements, synchrotron (Fig. 1) and neutron diffraction (Fig. 2) techniques. The direct evidence of antiferromagnetic ordering in the martensitic state of the alloy is observed by neutron diffraction study.

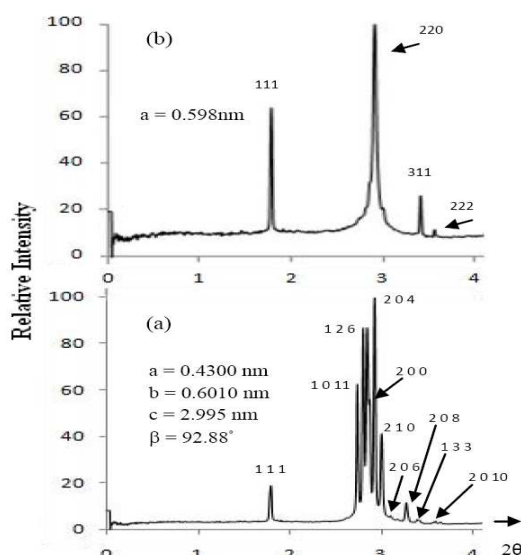


Fig. 1. MMST in  $\text{Ni}_{50.2}\text{Mn}_{39.8}\text{In}_{10}$  alloy, studied by synchrotron diffraction; (a) 290 K, martensite, (b) 314 K, austenite.

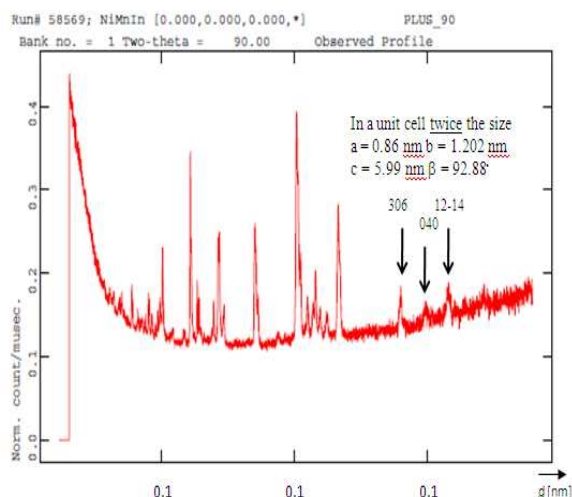


Fig. 2. Neutron diffraction studies of the martensitic state of Ni-Mn-In alloy at 290 K. The arrow identifies doubled unit cell dimension, which can not be recognized on synchrotron diffraction and may be an evidence of AFM ordering.

Based on these results, we suggest that an AFM parameter of order - L in the martensitic phase should be taken into account when calculating the entropy change at magnetic-field controlled MMST in Ni-Mn-In alloys.

The work was supported by RFBR 10-02-92662, 10-02-96020, 11-02-90502, RF President MK-1891.2010.2 and NSF 0831951 Grants. Also, beamtime awards at Argonne and Los Alamos laboratories are acknowledged.

[1] V. Buchelnikov, et al., JETP Letters 85 (2007) 560.

23RP-C-8

## EXCHANGE BIAS BEHAVIOUR AND MAGNETOCALORIC PROPERTIES IN $\text{Ni}_{50}\text{Mn}_{35.5}\text{In}_{14.5}$ ANNEALED RIBBONS AT DIFFERENT TEMPERATURES

*Sánchez T.<sup>1</sup>, Sánchez M.L.<sup>1</sup>, Santos J.D.<sup>1</sup>, Rosa W.O.<sup>1</sup>, Prida V.M.<sup>1</sup>, Escoda Ll.<sup>2</sup>, Suñol J.J.<sup>2</sup>, Koledov V.<sup>3</sup>, Hernando B.<sup>1\*</sup>*

<sup>1</sup> Dept. de Física, Universidad de Oviedo, Calvo Sotelo s/n, 33007 Oviedo, Spain

<sup>2</sup> Universidad de Girona, Campus de Montilivi, edifici PII, Lluís Santaló s/n. 17003 Girona, Spain

<sup>3</sup> Kotelnikov Institute of Radio Engineering and Electronics, RAS, Moscow 125009, Russia

\*[grande@uniovi.es](mailto:grande@uniovi.es)

Ferromagnetic shape memory  $\text{Ni}_{50}\text{Mn}_{35.5}\text{In}_{14.5}$  alloys can be directly produced as single-phase microcrystalline material by rapid solidification using melt spinning technique [1]. This alloy crystallizes in a single phase cubic B2-type austenite with a Curie point of  $T_{CA} = 284$  K that with the decreasing in temperature transforms into a martensite with  $T_{CM} = 185$  K. The direct and



reverse martensitic phase transition temperatures were  $M_s=257$  K,  $M_f = 221$  K,  $A_s = 239$  K, and  $A_f = 266$  K [2]. In this contribution the exchange bias behaviour and magnetocaloric properties of  $Ni_{50}Mn_{35.5}In_{14.5}$  melt spun ribbons after being annealed during 10 min at 1048 K, 1073 K, 1098 K and 1123 K, respectively. In each case the average elemental chemical composition was determined by EDS microanalysis. We report on the magnetocaloric properties around the structural and magnetic transitions. The comparative study of zero-field cooled and field-cooled hysteresis loops typically at 4 K revealed the existence of exchange bias anisotropy phenomena. For the annealed samples the magnetization change associated to the magnetic and structural transitions enhances for some values of the annealing temperature up to 1073 K, decreasing from this temperature value.

Support by IEEE, ARC, and ARCNN is acknowledged.

[1] X.G. Zhao et al., *Scripta Mater.* 63 (2010) 250

[2] T. Sánchez et al., *Mater. Sci. Forum* 635 (2010) 81

23RP-C-9

## MAGNETOSTRUCTURAL TRANSFORMATION AND MAGNETOCALORIC PROPERTIES OF $Ni_{49.9}Mn_{36.4}Sn_{13.7}$ HEUSLER ALLOY

Chernenko V.A.<sup>1,2</sup>, Barandiarán J.M.<sup>1</sup>, Rodríguez Fernández J.<sup>3</sup>, Rojas D.P.<sup>3</sup>, Gutiérrez J.<sup>1</sup>, Orue I.<sup>4</sup>, Lázpita P.<sup>1</sup>

<sup>1</sup> Universidad del País Vasco, Dept. Electricidad y Electronica, PO Box 644, Bilbao 48080, Spain

<sup>2</sup> Ikerbasque, Basque Foundation for Science, Bilbao 48011, Spain

<sup>3</sup> CITIMAC, Fac. Ciencias, Univ. Cantabria, Santander 39005, Spain

<sup>4</sup> SGiker, Vicerrectorado de Inv. UPV/EHU, Sarriena s/n, Leioa 48940, Spain

Ferromagnetic shape memory alloys (FSMAs), such as the prototype Ni-Mn-Ga Heusler compounds, are well-known for their ability to generate a large deformation (up to 10%) under an applied uniform magnetic field. This outstanding property stems from the magnetic field induced (de-)twinning in the martensitic phase. The other Heusler-type materials, typically Mn-rich Ni-Mn-X compounds (X=In, Sn, Sb), known as the metamagnetic shape memory alloys (MSMAs), can also exhibit a magnetic field-induced strain recovery of the preliminary mechanically detwinned martensite. In this case, the mechanism of recovery is a reverse magnetostructural transformation (MST). Usually, MST is accompanied by a large and abrupt change of the magnetization providing a physical reason for a giant magnetocaloric effect (MCE).

In this work, the MST exhibited by the polycrystalline  $Ni_{49.9}Mn_{36.4}Sn_{13.7}$  Heusler alloy was studied by DSC, thermomagnetization and X-rays diffraction measurements. This alloy shows a Curie temperature of 316 K and the forward and reverse MST at  $T_m = 239$  K and  $T_a=249$  K, respectively.

The magnetically induced entropy change has been obtained from the temperature dependencies of the specific heat,  $c_p$ , measured from 2.0 to 380K under different magnetic fields,  $\mu_0H$ , up to 8 T by using the relaxation technique implemented in a Quantum Design PPMS apparatus.

The  $c_p$  ( $T$ ) dependence exhibits a peak at MST and  $\lambda$ -anomaly at the Curie temperature,  $T_C$ . By increasing the magnetic field, the anomaly at MT shifts almost linearly with a slope equal to -1.2 K/T whereas anomaly at  $T_C$  is a nonlinear function of  $H$  with an initial slope equal to +8.1 K/T. This behavior gives rise to the ordinary MCE at  $T_C$  and an inverse MCE at MST. The peak values of the

isothermal magnetic entropy,  $\Delta S_m$ , in the vicinity of MST and  $T_C$  have been determined from the total entropy to be equal to 3 J/Kmol and -1.5 J/Kmol at 8T, respectively. The former value of  $\Delta S_m$  is within the range of giant values of MCE observed, for example, in the manganites. In addition, we found that the Debye temperature and the electronic coefficient, that are equal to  $310 \pm 2$  K and  $16.9 \pm 0.3$  mJ/K<sup>2</sup>mol, respectively, do not depend on the magnetic field within the indicated uncertainties. The latent heat at MST in zero field was estimated to be 4.5 J/g.

23OR-C-10

## FERROMAGNETIC RESONANCE IN SN-DOPED Ni<sub>50</sub>Mn<sub>34</sub>In<sub>16</sub> HEUSLER ALLOY

Aksoy S.<sup>1</sup>, Posth O.<sup>2</sup>, Acet M.<sup>2</sup>, Meckenstock R.<sup>2</sup>, Farle M.<sup>2</sup>

<sup>1</sup> Sabanci University, FENS, 34956, Istanbul, Turkey

<sup>2</sup> Duisburg-Essen University, 47048, Duisburg, Germany

Ni-Mn-based Heusler alloys undergo martensitic transformations with a strong interplay between structural and magnetic degrees of freedom, leading to several interesting properties such as magnetic shape memory, magnetic superelasticity and inverse magnetocaloric effect. Beside the magnetic field induced properties, the magnetic interactions are investigated around the martensitic transformation [1, 2]. Ferromagnetic resonance (FMR) is one of the techniques to understand magnetic behaviour in the austenite and martensite states. We report on the temperature dependence of FMR to discuss antiferromagnetic interactions in Sn-doped Ni<sub>50</sub>Mn<sub>34</sub>In<sub>16</sub> alloy and the effects of these interactions on the inverse magnetocaloric effect.

This work was supported by Deutsche Forschungsgemeinschaft (No. SPP1239).

[1] S. Aksoy et al., *Phys. Rev. B.*, **79** (2009) 212401.

[2] S. Aksoy et al., *J. Phys. Conf. Ser.*, **200** (2010) 092001.

**23 August**

Tuesday

11:30-13:00

14:30-17:20

oral session

23TL-D

23RP-D

23OR-D

**“Theory”**

23TL-D-1

## SPIN HELICES WITH DZIALOSHINSKII-MORIYA INTERACTION

Maleyev S.V.

Petersburg Nuclear Physics Institute, Gatchina, Leningrad District 188300, Russia

The Dzyaloshinskii-Moriya interaction (DMI) is responsible for the spin helical structure in different types of materials including cubic B20 metals (*MnSi* etc), *RMn<sub>2</sub>O<sub>3</sub>* multiferroics and two dimension surface layers (*Fe* on *W* etc). In all cases the DMI destroys conventional ferro or antiferromagnetic structure giving rise incommensurate helix with period  $d \sim J/D$  where  $J$  and  $D$  are exchange and DM interactions respectively. In the case of multiferroics and surface layers the DMI gives rise cycloidal order.

The DMI mixes spin waves (SW) with momenta  $\vec{q}$  and  $\vec{q} \pm \vec{k}$  and gives rise the spin-wave gap  $\Delta$  which appears as a result of the spin-wave interaction in the Hartree-Fock approximation. [1]. The magneto-elastic interaction contribute to the gap too. As a result we have  $\Delta^2 = \Delta_{Int}^2 + \Delta_{Me}^2$  where the second term is negative. Competition between these two term leads to quantum phase transition at pressure observed in *MnSi* and *FeGe*. *FeGe* [2.]

Classical energy depends on the field component along  $\vec{k}$  only. Perpendicular field components leads to the similar SW mixing along with the SW Bose condensation at  $\vec{q} = \pm nk$  where  $n=1,2,\dots$ . In the simplest case of B20 magnets due to above phenomena the spin-wave energy at  $q < k$  is given by [1,2]

$$\varepsilon_{\vec{q}} = Ak(q_{\parallel}^2 + 3q_{\perp}^4/8k^2 + \Delta^2 - 3H_{\perp}^2/8)^{1/2}$$

where  $\parallel$  and  $\perp$  denote components along and perpendicular to  $\vec{k}$  and  $A$  is the spin-wave stiffness at  $q \gg k$ . This strong SW anisotropy leads to infra-red divergences in the  $1/S$  expansion for the energy at  $H_{\perp} \rightarrow \Delta\sqrt{8/3} = H_{C2}$ . [3]. As a result convention umbrella state in the field becomes unstable at  $H = H_{C1} < H_{C2}$  and the helix vector  $\vec{k}$  rotates perpendicular to  $\vec{H}$ . This so called A-Phase exists in narrow range  $H_{C1} < H < H_{C2}$  and then the umbrella state is restored up to the transition to ferromagnetic state at  $H_C$ . Really this A-Phase is very narrow and can be observed near  $T_C$  only where it becomes broader due critical slowing down.

Rough estimations are in qualitative agreement with experimental data for *MnSi*. [3]

In general case of the helical structure there are tree critical fields:  $H_{\parallel}$  and two different perpendicular components given rise rather complex magnetic field phase diagram.

[1] S.V.Maleyev, *Phys.Rev.*,B **73** (2006) 174402..

[2] S.V.Maleyev, *J. Phys. Condensed Matter* **21** (2009) 141001.

[3] S.V.Maleyev, *ArXiv*: 1102.3524.

## NON-LINEAR SPIN FLUCTUATIONS AND PHASE TRANSITIONS IN ITINERANT ELECTRON MAGNETS: CMR MANGANITES

Solontsov A.<sup>1</sup>, Antropov V.P.<sup>2</sup>

<sup>1</sup> State Center for Condensed Matter Physics, M. Zakharova str., 6/3, 155569, Moscow, Russia

<sup>2</sup> Ames Laboratory USDOE, Ames, IA 50011 USA

Spin fluctuations (SF) in itinerant electron magnets are in the focus of condensed matter physics since the discovery of the role of paramagnons half a century ago. Since then SF were directly observed by inelastic neutron scattering in many materials, including weak itinerant magnets, heavy fermion compounds, colossal magnetoresistive (CMR) materials, etc. In weak itinerant magnets SF were shown to have a paramagnon-like nature and arise in the electron-hole continuum due to the Landau damping mechanism [1]. This quasielastic type of SF was shown to describe well the properties of weak itinerant magnets with both weak [1] and strong [2] spin anharmonicity and was recognized as a driving force of their magnetic phase transitions.

The linear Landau magnetic relaxation mechanism giving rise to the paramagnon-like SF was shown to dominate in the low-temperature region. With the rise in temperature non-linear relaxation processes due to coupling of SF may strongly affect their properties and change their nature from the linear to the non-linear one. Most important are three-mode processes of emission (absorption) of a longitudinal SF (l-SF) by magnons in isotropic ferromagnets [2] which in antiferromagnets should be accompanied by additional processes with annihilation (creation) of magnons [3]. Non-linear magnetic relaxation essentially affects the spectrum of l-SF at elevated temperatures leading to a rapid increase of the central quasielastic peak on approaching the critical temperature and to inelastic peaks near the magnon frequencies related to non-propagating longitudinal fluctuations.

Both quasielastic and inelastic l-SF were observed by inelastic neutron scattering in a series of itinerant ferro- and antiferromagnets (see [3]). Here we shall point to the CMR ferromagnetic manganites  $\text{La}_{0.7}\text{Ca}_{0.3}\text{Mn}_3$  and  $\text{Nd}_{0.7}\text{Sr}_{0.3}\text{Mn}_3$  possessing the 1<sup>st</sup> order magnetic phase transitions, where inelastic neutron scattering measurements discovered a three-peaks structure of the spectrum of magnetic excitations consisting of the central peak dominating the spectrum on approaching the phase transition which is suppressed by the magnetic field and inelastic peaks at magnon frequencies (see the review [4]).

In the present report we present a review on the non-linear dynamics of SF in itinerant electron ferro- and antiferromagnets, which in manganites should be viewed as coupled spin-lattice excitations. We analyze the scenarios of the temperature and field dependencies of the spectrum of l-SF with account of linear and non-linear relaxation mechanisms and show that they can explain the properties of quasielastic and inelastic peaks in  $\text{La}_{0.7}\text{Ca}_{0.3}\text{Mn}_3$  and  $\text{Nd}_{0.7}\text{Sr}_{0.3}\text{Mn}_3$  in terms of dynamical spin-lattice fluctuations rather than spin polarons used previously to explain their central peaks [4]. We also present evidence that non-linear quasielastic spin-lattice fluctuations may give rise to the 1<sup>st</sup> order magnetic phase transitions observed in these compounds.

Work was supported by Department of Energy-Basic Energy Sciences, under Contract No. DE-AC02-07CH11358 and by Russian Foundation for Basic Research (grant No 09-02-01475).

[1] T. Moriya, *Spin Fluctuations in Itinerant Electron Magnetism* (Springer, Berlin, 1985).

[2] A. Solontsov, *Int. J. Mod. Phys. B*, **19** (2005) 3631.

[3] A. Solontsov, A.P. Antropov, *Phys. Rev. B*, **81** (2010) 104403.

[4] Y. Zhang, F. Ye, H. Sha, P. Dai, J. A. Fernandes-Baca, E.W. Plummer, *J. Phys.: Condens. Matter*, **19** (2007) 315204.

## SPIN WAVES IN FERROMAGNETS WITH PERIODIC AND RANDOM INHOMOGENEITIES

*Ignatchenko V.A.*

L.V. Kirensky Institute of Physics SB RAS, Krasnoyarsk, 660036, Russia

A brief review of the results obtained on this problem recently at the Theoretic Division of the L.V. Kirensky Institute of Physics of the RAS is done.

1. A variant of the coherent potential approximation (the Kraichnan's approximation) is extended to the case of two wave fields of different nature with the random coupling parameter between them. Spin and elastic waves in zero-mean magnetostrictive media are considered. In this case the interactions between these two fields is due only to spatial fluctuations of the coupling parameter characterized by rms fluctuations of the magnetostriction  $\Delta\varepsilon$  and its correlation wave number  $k_c = 1/r_c$ , where  $r_c$  – correlation radius. Green's functions of the spin  $G_m(\omega)$  and elastic  $G_u(\omega)$  waves are calculated in the vicinity of the crossing point of the dispersion curves for these waves. Instead of the degeneration removal of frequencies in the wave spectrum and the appearance of two resonance peaks in the dynamic susceptibility, which are characteristic for the nonrandom coupling parameter, the sharp broadening of the self-mode peak in the crossing point has to be observed. The fine structure in the form of the narrow peak and gap appears at the center of this broad peak in the functions  $G_m''(\omega)$  and  $G_u''(\omega)$ , respectively.

2. Spin-wave spectra in the periodic superlattices with the rectangular and sinusoidal profile of the material parameter is considered. The Kronig-Penney's equation that valids for the rectangular SL with different values of the magnetization  $M_i$  or magnetic anisotropy  $K_i$  in the adjacent layers  $i = 1, 2$ , must be generalized for the case of different values of the exchange parameters  $A_i$ , because the boundary conditions in that case lead to a jump of the dynamic variable derivative that is proportional to  $A_1 - A_2$ . We obtain the upgrade form of this equation, that takes it standard form at  $A_1 = A_2$ . The general form of the relation for the sinusoidal SL with harmonic dependences of the parameters  $M(x)$  and  $K(x)$  is the equation, that contains infinite chain fractions with the same constant in the each link numerator. We extend this equation to the case of  $A = A(x)$  and show that the link numerators became different functions of both the wave number  $k$  and the number of the link  $n$ . The developed equations are used for the calculation of the 1-st and 2-nd bandgaps in the spin-wave spectrum.

3. Effects of inhomogeneities with anisotropic correlation on the spectral properties of waves in an initially sinusoidal superlattice are studied. The correlation function has different correlation radii  $k_{\parallel}$  and  $k_{\perp}$  along the superlattice axis  $z$  and in the  $xy$  plane, respectively. The gradually change of the correlation anisotropy, characterised by the parameter  $\kappa = k_{\perp}/k_{\parallel}$ , permits us to consider the transition from the isotropic 3D disorder ( $\kappa = 1$ ) to both the 1D ( $\kappa = 0$ ) and 2D ( $\kappa = \infty$ ) disorders. The changes of the Green's function and the density of states during these transitions are investigated. The transition 3D→1D is accompanied by the damping growing, the transition 3D→2D leads to appearing the asymmetry in the dynamic susceptibility.

Support by the Program No. 27.1 of the RAS Presidium, the State Contract No. 02.740.11.0220 on the FTP, and the Program RNP 2.1.1/3498 is acknowledged.

23OR-D-4

## SPIN ORDERING AT THE SURFACE OF A TOPOLOGICAL INSULATOR WITH MAGNETIC IONS

*Men'shov V.N.<sup>1,2</sup>, Tugushev V.V.<sup>1,2</sup>, Chulkov E.V.<sup>2,3</sup>*

<sup>1</sup> NRC Kurchatov Institute, Kurchatov Square 1, 123182 Moscow, Russia

<sup>2</sup> Donostia International Physics Center, P. de Manuel Lardizabal 4, 20018 San Sebastián, Spain

<sup>3</sup> Departamento de Física de Materiales, Facultad de Ciencias Químicas, UPV/EHU and Centro Mixto CSIC-UPV/EHU, San Sebastián, Basque Country, E-20080, Spain

The surface state of a topological insulator dubbed as helical is a unique metallic system, which exhibits interesting magnetic and transport properties [1]. We study in this work collective behavior of magnetic ions randomly distributed on the surface of a topological insulator. Within the framework of the proposed model of the surface states of a topological insulator, we carry out calculations of an exchange interaction between magnetic impurities, mediated by the helical electrons with Dirac spectrum. Our aim is to understand how this interaction is modified if a mean free path  $l$  due to the scattering of electrons on the impurity centers is introduced. In the presence of weak disorder, the calculations are done by a standard procedure of self-energy correction and vertex renormalization. It is found that interaction energy of two magnetic impurities separated by a distance  $\rho$  decreases exponentially  $E_{ex} \sim \rho^{-\gamma} \exp(-\rho/l)$  (in contrast to the power law  $E_{ex} \sim \rho^{-2}$  or  $E_{ex} \sim \rho^{-3}$  in the absence of disorder [2]). We obtain the effective exchange integral  $J$  as a function of chemical potential  $\mu$  or electron (hole) concentration  $n$ . As a rule, the ground state of the system under consideration is ferromagnetic (FM) with the direction of magnetization along the normal axis to the surface. In the FM phase, the average exchange field of magnetic ions induces a band gap  $\Delta$  in the surface state spectrum. Having connected the value  $\Delta$  with the average moment per magnetic ion  $\langle S \rangle$  through the self-consistent equation  $\Delta = cJ(\Delta)\langle S \rangle(\Delta)$  ( $c$  is density of magnetic ions) we describe main features of the FM ordering. We calculate the magnetic phase diagrams ( $T$  versus  $\mu$ ) and ( $T$  versus  $n$ ) of our system. Finally, experimental data on the spectroscopy of the Fe-deposited surface of the strong topological insulator  $\text{Bi}_2\text{Se}_3$  [3] are interpreted on the basis of our theoretical results.

[1] M.Z. Hasan and C.L. Kane, *Rev. Mod. Phys.*, **82** (2010) 3045.

[2] J.-J. Zhu, D.-X. Yao, S.-C. Zhang, and K. Chang, *Phys. Rev. Lett.*, **106** (2011) 097201.

[3] L.A. Wray, *et al*, *Nature Phys.*, **7** (2011) 32.

23TL-D-5

## HIGH VOLUMETRIC CAPACITANCE NEAR INSULATOR – METAL PERCOLATION TRANSITION

*Efros A.L.*

Department of Physics & Astronomy, University of Utah, Salt Lake City, Utah, 84112, USA

A new type of supercapacitor with a very high volumetric capacitance is proposed. It is based upon known phenomenon of the sharp increase of the dielectric constant of the metal-insulator mixture in the vicinity of the percolation threshold but still on the insulator side [1]. The optimization suggests that the metallic particles should be of nanoscale and that the distance between electrodes should be close to a correlation length of the percolation theory and 15-20 times larger than the average distance between particles while the area of the electrodes might be unlimited. In principle one can construct a single capacitor of any form from a large amount of such elementary plane capacitors with a volumetric capacitance of the same order or even better than capacitance of an electrolytic supercapacitor. The mean square of a random electric field in the capacitors is found to be larger than the average field corresponding to the potential difference of electrodes. This random field is responsible for a breakdown. The estimated breakdown voltage shows that the stored energy density might be significantly larger than that of electrolytic capacitors.

[1] A. L. Efros, B. I. Shklovskii, *Phys. Stat. Solidi*, **76**, 475 (1976).

23OR-D-6

## ANOMALOUSLY LARGE DAMPING OF LONG-WAVELENGTH MAGNONS CAUSED BY LONG-RANGE INTERACTION

*Syromyatnikov A.V.*

Petersburg Nuclear Physics Institute, Gatchina, Orlova Rosha 188300, Russia

We discuss the spin-wave interaction in 3D and 2D Heisenberg ferromagnets (FMs) with dipolar forces at  $T_c \leq T < \infty$  using  $1/S$  expansion. A comprehensive analysis is carried out of the first  $1/S$  corrections to the spin-wave spectrum. We observe a number of quite unusual phenomena: the spin-wave gap caused by spin-wave interaction and anomalously large damping of long-wavelength magnons in 3D FM.

We demonstrate that the spin-wave interaction leads to the gap  $\Delta$  in the spectrum  $\epsilon_k$  in both 3D [1] and 2D [2] FMs renormalizing greatly the bare gapless spectra at small momenta  $k$ . This spin-wave gap, which has been steadily ignored in the literature, resolves the problem of infrared divergent corrections to the longitudinal spin susceptibility [3] and to the spin-wave stiffness [4] in 3D FM. This gap resolves also the problem of long-wavelength magnons instability in 2D FM [5].

Expressions for the spin-wave damping  $\Gamma_k$  are derived. We observe thermal enhancement of both  $\Gamma_k$  and  $\Gamma_k/\epsilon_k$  at small momenta in both 2D and 3D FMs. In particular, a peak appears in  $\Gamma_k/\epsilon_k$  at  $k = k_c \approx \Delta/\sqrt{TD}$ , where  $D$  is the spin-wave stiffness. The height of this peak is of the order of



$T/T_c \ll 1$  in 2D FMs for  $S \ll 1$ . Thus, we conclude that magnons are well-defined quasi-particles in 2D FM at  $T \ll T_c$ . Amazingly, the spin-wave damping appears to be much larger in 3D FM: the peak height in  $\Gamma_k/\epsilon_k$  is of the order of unity at  $T \ll T_c$ . Thus, we find that long-wavelength magnons in 3D FM are heavily damped at small T. [6] Particular estimations show that  $k_c < 10^{-3} \text{ \AA}^{-1}$  in the majority of materials. Such a small value can explain the surprising fact that such an unusual phenomenon has not been observed so far. Moreover, the magnetocrystalline anisotropy normally screens this effect completely. We point out a number of real compounds with  $k_c \ll 10^{-2} \div 10^{-3} \text{ \AA}^{-1}$  and negligible anisotropy, which are suitable for experimental verification of our predictions.

- [1] A.V. Syromyatnikov, Phys. Rev. B **74**, 014435 (2006).  
 [2] A.V. Syromyatnikov, Phys. Rev. B **77**, 144433 (2008);  
 [3] B.P. Toperverg, A.G. Yashenkin, Phys. Rev. B **48**, 16505 (1993).  
 [4] T.S. Rahman, D.L. Mills, Phys. Rev. B **20**, 1173 (1979).  
 [5] A. Kashuba, Ar. Abanov, V.L. Pokrovsky, Phys. Rev. Lett. **77**, 2554 (1996); Phys. Rev. B **56**, 3181 (1997).  
 [6] A.V. Syromyatnikov, Phys. Rev. B **82**, 024432 (2010).

23OR-D-7

## **AB INITIO CALCULATION OF THE SYSTEM Cr–GaSb: A NEW HIGH-PRESSURE PHASE CONTAINING DEFECTS**

*Magnitskaya M.V.<sup>1</sup>, Kulatov E.T.<sup>2</sup>, Titov A.A.<sup>2</sup>, Uspenskii Yu.A.<sup>3</sup>, Maksimov E.G.<sup>3</sup>*

<sup>1</sup> Institute for High Pressure Physics of RAS, 142190 Troitsk, Moscow region, Russia

<sup>2</sup> General Physics Institute, Russian Academy of Sciences, 117942 Moscow, Russia

<sup>3</sup> P.N. Lebedev Physical Institute, Russian Academy of Sciences, 119991 Moscow, Russia

Recently, a new ferromagnetic compound CrGa<sub>2</sub>Sb<sub>2</sub> has been synthesized under high pressure/temperature conditions [1, 2]. This high-pressure phase crystallizes in an orthorhombic structure (space group Iba2) and remains metastable at normal pressure. CrGa<sub>2</sub>Sb<sub>2</sub> looks promising for possible spintronics applications, since it exhibits above-room-temperature ferromagnetism (the Curie temperature  $T_C \sim 350$  K) and has a very high resistivity, which implies possible semiconducting properties [2].

To study CrGa<sub>2</sub>Sb<sub>2</sub> *ab initio* (independently of experiment), we performed calculations within density functional theory (DFT) using the augmented plane-wave plus local-orbital method [3]. The generalized gradient approximation (GGA) was employed to describe the exchange-correlation potential. Spin-orbit coupling effects were included self-consistently using fully relativistic treatment for both core and valence electrons.

The structural, electronic and magnetic properties are evaluated at fully relaxed atomic positions. The equilibrium geometry properties, such as lattice parameters, interatomic distances and bond angles, are found to well agree with experiment. Our theoretical equation of state is in reasonable agreement with the experimental data on compressibility measured up to 9 GPa.

The residual resistivity of CrGa<sub>2</sub>Sb<sub>2</sub> is very high,  $\rho_{\text{exp}} \sim 250$  m $\Omega$  cm [2], which is attributable to the electron scattering by vacancies, grain boundaries and other defects inherent in the non-

equilibrium metastable phases. Notice that this compound is slightly non-stoichiometric, with the Cr deficiency of about 4% [1]. Most likely the presence of Cr vacancies is essential for the structural stability, as in the case of transition-metal carbides and nitrides. Our estimated resistivity of perfect  $\text{CrGa}_2\text{Sb}_2$  is nearly two orders of magnitude smaller than  $\rho_{\text{exp}}$ . However, this value should be increased by several times because of spin fluctuations, which are presumably large as  $T_C$  of  $\text{CrGa}_2\text{Sb}_2$  is only slightly exceeds room temperature. This estimate shows that many-electron effects can be rather important in this compound.

Calculated total magnetic moment of  $\text{CrGa}_2\text{Sb}_2$  is equal to  $\sim 2 \mu_B/\text{Cr}$  which is somewhat larger than the experimental value of  $\sim 1.6 \mu_B/\text{Cr}$ . This discrepancy may be attributed to the many-electron effects. Another possible reason is that the experimental value is reduced due to the Cr deficiency. The density of states (DOS) around the Fermi level  $E_F$  is rather low and reminds the semimetallic case. Our calculations show that this picture is also valid for the  $1 \times 2 \times 2$  supercell with 6% of Cr vacancies. Since predicting the energy gaps of semiconductors requires going beyond DFT, we applied the new MBJLDA exchange-correlation potential [4] to  $\text{CrGa}_2\text{Sb}_2$ . As a result, DOS at  $E_F$  decreased and ‘quasigap’ near  $E_F$  became wider compared to our DFT–GGA results. Our calculations confirm most of available experimental data and show that the used approach is a powerful tool in the search for new spintronics materials.

Support by Ministry of Education and Science of Russia, RAS, and RFBR (grants 09-02-91078–CNRS, 10-02-00118, 10-02-00694, 10-02-00698, and 11-02-00615) is acknowledged.

[1] W. Sakakibara, Y. Hayashi, H. Takizawa, *J. Alloys Compd.*, **496** (2010) L14.

[2] M.V. Kondrin, V.R. Gizatullin, S.V. Popova *et al.*, *arXiv:1102.5236v1* (2011).

[3] P. Blaha, K. Schwarz, G.K.H. Madsen *et al.*, *WIEN2k, An Augmented Plane Wave + Local Orbitals Program for Calculating Crystal Properties* (ed. K. Schwarz, TU, Vienna, 2001).

[4] F. Tran, P. Blaha, *Phys. Rev. Lett.*, **102** (2009) 226401.

23OR-D-8

## DESTRUCTION OF A LONG ANTIFERROMAGNETIC ORDER BY “RANDOM LOCAL FIELD” DEFECTS

*Morosov A.I.*

Moscow State Institute of Radioengineering, Electronics and Automation, (Technical University),  
pr. Vernadskogo 78, 119454 Moscow, Russia

Imry and Ma [1] showed that the negligibly small concentration of impurities, which induce a random local field conjugate to the order parameter or random anisotropy, destroys the long-range order even in the ground state in systems with the continuous symmetry of the order parameter in spaces with dimensions  $d < 4$ . In an Ising-type system with a single-component order parameter, such a destruction occurs at  $d < 2$ .

In the case of magnets, a system with defects of the random-field type appears in a diluted antiferromagnet in a uniform magnetic field. The value of the random field  $h_0$  conjugated to the antiferromagnetic order parameter  $\eta$  is directly proportional to the induction of applied magnetic field  $B_0$ :  $h_0 = \pm B_0/2$  where the sign depends on the number of sublattice in which a magnetic atom is absent. It was shown in the work [2] that the destruction of the long-range order in systems with weak easy-axis anisotropy in spaces with dimensions  $2 < d < 4$  should occur at a certain critical dimensionless concentration  $x^*$  of impurities of the random local field type:

$$x^* h_0^2 \sim K^{2-d/2} J^{d/2} \eta^2, \quad (1)$$

where  $J$  is the exchange integral, and  $K$  is the easy-axis anisotropy constant. It means that for the destruction of the long-range order the external magnetic field directed along the easy axis has to exceed the critical one. The estimation (1) corresponds to the collinear phase of an antiferromagnet. By introducing the values of magnetic inductions  $B_1$  and  $B_2$  corresponding to the spin-flop and spin-flip transition one can obtain from Eq. (1) the critical value of the induction  $B^*$ :

$$B^* \sim B_1 x^{-1/2} \left( \frac{B_2}{B_1} \right)^{\frac{d-2}{2}}. \quad (2)$$

For  $x^* \ll 1$  and the space dimension  $d \geq 2$  one has  $B^* \gg B_1$ , it means that the destruction of the long-range order in the collinear phase is impossible.

Let us consider the possibility of the destruction in the spin-flop phase of an antiferromagnet. In this phase a role of crystallographic anisotropy is played by the external field which orients the sublattice magnetizations so that the resulting magnetic moment arising due to their canting is directed along the induction vector. The effective anisotropy constant equals

$$K^* \sim B_0^2 \mu / B_2, \quad (3)$$

where  $\mu$  is the atom magnetic moment. As a result one has instead of (2)

$$B^* \propto B_2 x^{-\frac{1}{d-2}}. \quad (4)$$

For  $d \geq 2$  one has  $B^* > B_2$ .

Thus, the destruction of the long-range antiferromagnetic order by a small concentration of defects of the random-field type in the space with dimension  $d \geq 2$  is impossible.

[1] Y.Imry, S.-k. Ma, *Phys. Rev. Lett.*, **35** (1975) 1399.

[2] A.I. Morosov, A.S. Sigov, *JETP Lett.*, **90** (2009) 723.

23OR-D-9

## TAMM SURFACE STATES OF 5 NM DIAMOND BALL

*Denisov I.A.<sup>1</sup>, Belobrov P.I.<sup>2</sup>*

<sup>1</sup> Siberian Federal University, MOLPIT, 660074 Krasnoyarsk, Russia

<sup>2</sup> Kirensky Institute of Physics & Institute of Biophysics SB RAS, 660036 Krasnoyarsk, Russia

Nanodiamonds are widely used in biology, medicine and industry, but the nature of their magnetic properties are still under discussion. While diamond monocrystal is classical diamagnetic, nanodiamonds show strong paramagnetic properties. The reason of this paramagnetism, i.e. source and localization of free spins, are not known for certain yet and determine the problems of our research.

The model of electronic states of nanodiamond has been suggested for the first time in [1-3] on the basis of EPR, PEELS and Auger data and recently has been confirmed in [4, 5] by research of magnetisation and <sup>13</sup>C NMR spin-lattice relaxation and based on the representation about surface states under the shell of nanodiamond molecule. The model based on the assumption that Tamm surface states are universal and has the identical nature on a surface of diamond single crystal and

nanodiamond. The nanodiamond core form the periodic potential for the existence of bonded electronic state around and under it's surface.

The aim of our investigation was to prove the early suggested model of nanodiamond from the position of quantum mechanics. According to the  $^{13}\text{C}$  NMR 70% carbons in nanodiamond have deformed and only 30% normal  $\text{sp}^3$  hybridisation,  $\text{sp}^2$ -hybridised carbon makes up less than 1% of the material [5]. Tamm has considered diamond surface states by solving a Schroedinger equation for the Kronig-Penney potential. We are taking the 5 nm diameter diamond ball as the basis for Schroedinger equation potential to calculate surface states for that case. Tamm solution led to the understanding of electronic movement on the diamond monocrystal surface with energy of an order of diamond cohesion energy with value 0.1 eV ( $800\text{ cm}^{-1}$ ), that corresponds to de Broglie wave with 3,9 nm length. The thermodynamic stability of nanodiamond proved by fact of their fabrication (explosion method from high purity carbon black) can now be explained with stabilizing effect of de Broigle wave propagating on the angle degree of freedom inside the nanodiamond subshell wavefunction of surface Tamm state.

Also, the detailed research of magnetic properties of composite material (99.9% carbon purity) from nanodimonds powder and graphen flakes was conducted. The analysis of the magnetization data to fitting of  $M(H,T)$  by Brillouin function shows that the concentration of paramagnetic centers have amount  $5\text{-}7 \times 10^{19}$  spin/g that approximately means 7-10 free electronic spins on a particle.

The model shows the source of detected free electrons that is agrees with [5] in the nanodiamond. Qualitatively the model explains the invariance in paramagnetic properties and Auger-decay at X-ray excitation.

- [1] P.I. Belobrov, S.K. Gordeev, E.A. Petrakovskaya and O.V. Falaleev, Doklady Physics, 46 (2001) 459.
- [2] J.L. Peng, S. Bulcock, P. I. Belobrov, L.A. Bursill, Intern. J. Mod. Phys. B, 15 (2001) 4071.
- [3] P. I. Belobrov, L. A. Bursill, K. I. Maslakov and A. P. Dementjev, Appl. Surf. Sci., 210 (2003) 169.
- [4] E. M. Levin, X. W. Fang, S. L. Bud'ko, W. E. Straszheim, R. W. McCallum, and K. Schmidt-Rohr, Phys. Rev. B. 77 (2008) 054418.
- [5] XiaoWen Fang, JingDong Mao, E. M. Levin and Klaus Schmidt-Rohr, J. Am. Chem. Soc, 131 (2009) 1426.

23OR-D-10

## **ON CHIRAL MODEL OF GRAPHENE**

*Rybakov Yu.P.*

Department of Theoretical Physics, Peoples' Friendship University of Russia, 117198 Moscow, 6,  
Mikluho-Maklay str., Russia, E-mail: soliton4@mail.ru

The hybridized  $\text{sp}$ -states of valence electrons in the carbon atom can be described by  $\text{SU}(2)$  matrix considered as the order parameter. The chiral model of graphene based on this order parameter is suggested in the long-wave approximation, the ideal grapheme plane being determined by the kink-like solution. Corrugation of the graphene surface is described in the form of ripple and rings. The approximate solution corresponding to an infinite carbon nanotube is found.

23RP-D-11

## ULTRAFAST SPIN DYNAMICS IN MULTI-SUBLATTICE MAGNETS

*Mentink J.H.<sup>1</sup>, Hellsvik J.<sup>2</sup>, Afanasiev D.<sup>3</sup>, Ivanov B.A.<sup>3</sup>, Kimel A.V.<sup>1</sup>, Kirilyuk A. I.<sup>1</sup>, Eriksson O.<sup>2</sup>, Katsnelson M.I.<sup>1</sup>, Rasing Th.<sup>1</sup>*

<sup>1</sup> Radboud University Nijmegen, Institute for Molecules and Materials, Heijendaalseweg 135, 6525 AJ Nijmegen, the Netherlands

<sup>2</sup> Department of Physics and Astronomy, Division of Materials Theory, Box 516, SE-75120 Uppsala, Sweden.

<sup>3</sup> Institute of Magnetism, NASU, 03142 Kiev, Ukraine

Intense femtosecond laser pulses are able to excite and transform magnetic order of condensed matter systems on a timescale of the exchange interaction between their spins. Laser-induced demagnetization [1], change of anisotropy [2] and even complete magnetization reversal [3] has been shown to be possible. Despite of the fact that most of the studied materials consist of several non-equivalent sublattices, until now state-of-the art theories can deal only with one-sublattice ferromagnets. In this contribution we propose a general theoretical framework for the description of ultrafast spin dynamics in multi-sublattice magnets on the time scale of the exchange interaction, where we distinguish the temperature dominated and the exchange dominated regime. We show that in the temperature dominated regime non-equivalent sublattices have distinct dynamics despite their strong exchange coupling. Even more intriguing, we show that in the exchange dominated regime the sublattices can evolve against their intersublattice exchange interaction, and we derive criteria for the reversal of sublattices and total magnetization. Our results are substantiated by atomistic spin dynamics simulations and explain the recently observed laser-induced reversal of sublattices [4].

[1] E. Beaurepaire et al., Phys. Rev. Lett. **76**, 4250 (1996).

[2] A. V. Kimel et al., Nature **429**, 850 (2004);

[3] C.D. Stanciu et al., Phys. Rev. Lett, **99**, 047601 (2007).

[4] I. Radu et al. Nature, in press (2011).

23OR-D-12

## FINITE SIZE EFFECTS OF WEAK ITINERANT ELECTRON SYSTEMS ON CURIE TEMPERATURE

*Peters L., Katsnelson M.I., Kirilyuk A.*

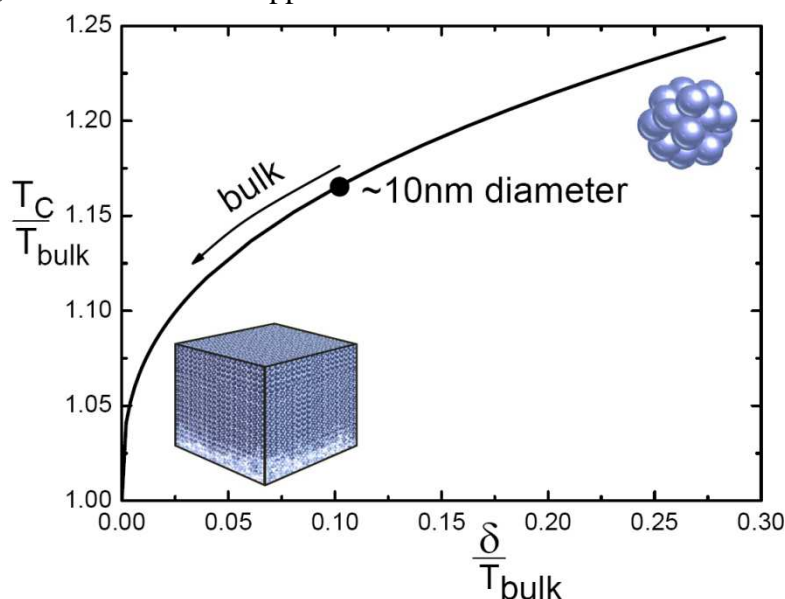
Radboud University Nijmegen, Institute for Molecules and Materials, NL-6525 AJ Nijmegen, The Netherlands

It is well established that nanoscale objects possess interesting physical properties substantially differing from the bulk. For example, small metallic particles (clusters) demonstrate unusual structural, electronic and magnetic properties. However, the precise mechanisms behind the physical and chemical properties of the clusters are still far from being understood.

Here a model for itinerant (delocalized) electron systems is presented to understand the qualitative behaviour of the Curie temperature as a function of size. Remarkably, the Curie temperature increases for decreasing cluster sizes (see figure). Here the size is defined by the volume  $V$  and  $\delta$  is

the average energy level spacing,  $\delta \sim 1/V$ ;  $T_{\text{bulk}}$  corresponds to the Curie temperature of the bulk material.

This increase of the Curie temperature actually originates from the increase in the average inter-level distance, which suppresses the spectral density of the spin fluctuations. Since the latter destroy the magnetic order, the result of such suppression is the increase of the Curie temperature.



- [1] T. Moriya, *Spin Fluctuations in Itinerant Electron Magnetism* (Springer, Berlin, 1985)  
 [2] R. Denton, B. Mühlshlegel, and D. J. Scalapino, *Phys. Rev. B* **7**, 3589 (1973)  
 [3] L. P. Gor'kov and G. M. Eliashberg, *Sov. Phys.-JETP* **48**, 1407 (1965)

23OR-D-13

## SPIN WAVE CALCULATION OF THE MAGNETIZATION AROUND AN IMPURITY IN HEISENBERG ANTIFERROMAGNETS IN A MAGNETIC FIELD

*Shinkevich S.<sup>1</sup>, Syljuåsen O.F.<sup>1</sup>, Eggert S.<sup>2</sup>*

<sup>1</sup> Department of Physics, University of Oslo, P.O. Box 1048 Blindern, N-0316 Oslo, Norway

<sup>2</sup> Department of Physics and Research Center OPTIMAS, University of Kaiserslautern, D-67663 Kaiserslautern, Germany

We consider the general case of the magnetic-field-dependent spatial magnetization pattern on the atomic scale around a general impurity embedded in a Heisenberg antiferromagnet using both an analytical and a numerical spin-wave approach [1]. This work is a followup to a Letter [2] where the magnetic response around a vacancy in an isotropic antiferromagnet was studied. The obtained results are compared to quantum Monte Carlo (QMC) simulations. The decay of the magnetization pattern away from the impurity follows a universal form that reflects the properties of the pure antiferromagnetic Heisenberg model. Only the overall magnitude of the induced magnetization depends also on the size of the impurity spin and the impurity coupling.

We have obtained results for the magnetization around a general impurity in a Heisenberg spin- $S$  antiferromagnet in a magnetic field. Away from the impurity we find that the induced magnetization is dominantly a staggered magnetization in the field direction. We have calculated

this alternating magnetization, and our results are in reasonable agreement with extensive QMC simulations that we have also carried out using the stochastic series expansion technique using directed-loop updates [3]. One important feature of the spin-wave result is that the parameters of the impurity model only affect the overall prefactor of the magnetization, while the scale and shape of the decay are universal and only reflect the properties of the host magnet and the applied field. We have analyzed how this prefactor depends on impurity properties and found that the effect on the alternating magnetization is largest for ferromagnetically coupled impurities and generally increases with magnitude of magnetic field. In order to calculate the magnetization at the impurity site we have described in detail how to diagonalize the quadratic spin-wave Hamiltonian numerically. This approach agrees well with the QMC calculations and we have outlined how the magnetization of the impurity spin depends on the coupling strength of the impurity to its neighbors.

In summary, the results can be used to predict the detailed local magnetization pattern around general magnetic and nonmagnetic impurities in isotropic antiferromagnets, e.g., from doping Zn, Co, and Ni in copper-oxide antiferromagnets. In most real materials the effects from crystal fields and other anisotropies are also important.

The QMC calculations were carried out on CPUs provided by the Notur project.

- [1] S. Shinkevich, O.F. Syljuåsen, S. Eggert, *Phys. Rev. B*, **83** (2011) 054423.
- [2] S. Eggert, O.F. Syljuåsen, F. Anfuso, and M. Andres, *Phys. Rev. Lett.*, **99** (2007) 097204.
- [3] O.F. Syljuåsen and A.W. Sandvik, *Phys. Rev. E*, **66** (2002) 046701.





**23 August**

Tuesday

11:30-13:00

oral session

23TL-E

23RP-E

23OR-E

**“Magnetic Soft Matter”**

23TL-E-1

## AN EXPERIMENTAL STUDY OF THE DYNAMIC PROPERTIES OF NANO-PARTICLE COLLOIDS WITH IDENTICAL MAGNETISATION BUT DIFFERENT PARTICLE SIZE.

*Fannin P.C.<sup>1</sup>, Marin C.N.<sup>2</sup>, Raj K.<sup>3</sup>, Couper C.<sup>1</sup>, Barvinschi P.<sup>2</sup>*

<sup>1</sup> Department of Electronic and Electrical Engineering, Trinity College, Dublin 2, Ireland

<sup>2</sup> West University of Timisoara, Faculty of Physics, V. Parvan Blv., no. 4, Timisoara, 300223, Romania

<sup>3</sup> Ferrofluidics Corporation, Nashua, NH, USA

Corresponding author. Tel 0035318961860; fax:0035316772442

E-mail address: pfannin@tcde.ie (P.CFannin)

Measurements of the frequency dependent, complex susceptibility,,  $\chi(\omega) = \chi'(\omega) - i\chi''(\omega)$  over the frequency range 0.1 to 6.0 GHz, have been used to determine the dynamic properties of three specially prepared 400 G( 0.04 T) magnetic nano-particle colloidal suspensions. The samples, namely sample 1, sample 2, and sample 3, consisted of magnetite particles of mean diameter, 6.4 nm, 7.5 nm, and 9nm respectively and were identical in terms of, carrier, surfactant, and particle material. From polarised, ferromagnetic resonant measurements, the anisotropy field, HA, of the particles was determined and sample 1 and sample 2 were found to have a much lower HA than sample 3. These determined values of HA are shown to compare favourably with those obtained by means of relevant theoretical equations reported in the literature. The Landau and Lifshitz damping parameter,  $\alpha$ , was also measured in each case and this facilitated the determination the intra-well relaxation time,  $\tau_0$ , of the particles, thereby enabling the effect of particle packing fraction on the value of  $\tau_0$  to be examined.

23OR-E-2

## MONTE-CARLO APPROACH TO THE PROBLEMS OF SUPERPARAMAGNETIC KINETICS

*Melenev P.V.<sup>1,2</sup>, Raikher Yu.L.<sup>1</sup>, Rusakov V.V.<sup>1</sup>, Perzynski R.<sup>2</sup>*

<sup>1</sup> Institute of Continuous Media Mechanics, Ural Branch of Russian Academy of Sciences  
614013, Perm, Russia

<sup>2</sup> Laboratoire PECSA, Université Pierre et Marie Curie, 75252, Paris Cedex 05, France

Monte-Carlo (MC) method is successfully used for numerical studies of various problems in magnetism, e.g. thermodynamics of Ising spin systems, aggregation patterns in ferrofluids, micromagnetic structures, etc. In the majority of cases, this approach is applied to the systems in equilibrium. On the other hand, MC method is used also for modeling of time-evolving magnetic effects [1]. However, one of the major restrictions in this area is the absence of physical time in MC-calculations, because the method, dealing as itself, exclusively with the sequences of states, does not yield estimations of the real rate of their time-change.

An successful attempt to remove this drawback was made by Nowak et al in [2]. The authors considered the free relaxation of the magnetic moment of an isolated single-domain particle with

uniaxial anisotropy. They obtained a formula expressing the time duration of the calculation step in terms of the MC angular variation of the magnetic moment. Hereby we address the MC time-quantification problem by analysing possible correspondence between two descriptions of the magnetization decay in a superparamagnetic assembly: one in terms of MC-steps and another in terms of relaxation time. The latter description is derived from the solution of Brown's kinetic equation [3]. We find that the time duration of the MC-step is proportional to the square of the MC variation amplitude. It turns out that this rule is valid much beyond the limits of the free-diffusion case, the only one, where it can be proven rigorously. Also we propose a modification of the Nowak et al relation, suitable for the particles with a finite magnetic anisotropy. Moreover, our approach may be well used to study superparamagnetic relaxation under external field.

The second problem presented hereby is the dynamic magnetic hysteresis (DMH): the magnetic response of an ensemble of superparamagnetic particles to a linearly polarized AC-field. It is shown that the results of the carried out MC-calculations agree pretty well with the data obtained by numerical integration of the kinetic Brown equation [4] for the systems with different anisotropy strength in a wide frequency range of the AC field. Comparison with the numerical experiments shows that the duration of a MC-step may be considered as practically independent on the internal stages of the DMH process. Besides that, the proportionality of this duration to the square of the MC variation amplitude, first found in the relaxation problem, holds for this essentially non-stationary case as well. We note that in the low temperature limit our MC calculations readily converge to the classical Stoner-Wohlfarth cycles. The presented evidence demonstrates efficiency of the MC-method in magnetodynamic problems. One more advantage of the MC approach, worth of mentioning, is the simplicity of including there additional factors, e.g. interparticle interactions and/or size polydispersity of the particles in the system.

The work was supported by RFBR-CNRS project 09-02-91070 (PICS 4825).

[1] D.P. Landau, K. Binder, *A Guide to Monte Carlo Simulation in Statistical Physics*. 3<sup>rd</sup> edition. *Cambridge Press*. 2009.

[2] U. Nowak, R.W. Chantrell, E.C. Kennedy, *Phys. Rev. Lett.*, **84** (2000) 163.

[3] J.L. Dormann, D. Fiorani, E. Tronc, *Adv. Chem. Phys.*, **98** (1997) 283.

[4] I.S. Poperechny, Yu.L. Raikher, V.I. Stepanov, *Phys. Rev. B*, **82** (2010) 174423.

23OR-E-3

## EFFECTIVE COERCIVE FORCE OF A UNIAXIAL SUPERPARAMAGNETIC PARTICLE

*Poperechny I.S., Raikher Yu.L., Stepanov V.I.*

Institute of Continuous Media Mechanics, Ural Branch, Russian Academy of Sciences, Perm, 614013, Russia

The essential feature of a nanoscale ferromagnetic particle is thermal diffusion (orientation fluctuations) of its magnetic moment, which intensity is controlled by the parameter  $\sigma = KV / k_B T$ , where  $K$  is the anisotropy constant and  $V$  the particle volume. Accordingly, the magnetization of a superparamagnet is determined by solving Brown's kinetic equation for the orientation distribution function. Let a magnetically uniaxial particle be subjected to an AC field  $q(t)$  (we measure it in the

anisotropy field units) of frequency  $\omega$  and amplitude  $q_0$ . In Ref. 1 the dynamic magnetic hysteresis (DMH) induced by  $q(t)$  was investigated with the angle  $\psi$  between the easy magnetization axis and the field direction being a parameter. Depending on the parameter  $\omega\tau$ , where  $\tau$  is the longest of the magnetic relaxation times, three qualitatively different regimes of DMH were found, namely, the quasi-equilibrium ( $\omega\tau < 1$ ), intermediate ( $\omega\tau \sim 1$  at  $q \sim q_0$ ) and high-frequency or polarization ( $\omega\tau > 1$ ). This classification helps one to sort out the variety of the DMH loop shapes; however, due to the dependence of  $\tau$  on the field strength,  $T$  and  $\psi$ , the above-mentioned conditions are non-trivial.

Hereby we carry on the studies of Ref.1 and analyze the effective coercive force  $q_c$  for all the DMH regimes defining it as the absolute value  $q$  of the field, at which the average (observable) projection of the particle magnetic moment on the field direction turns to zero.

In the low frequency mode the effective coercive force (ECF) increases with the particle cooling down (the temperature diminishes,  $\sigma$  grows), and evolves from virtual zero to the athermal Stoner-Wolfarth value, e.g.  $q_c = 1$  for  $\psi = 0$ . Having in possession the exact computational results, one is able to assess the validity of the conventional approximations. One of them is to use the condition  $\omega\tau(q) = 1$  as an equation determining  $q_c$ . Taking the expansion of  $\tau(q)$  from [2] and truncating it to the second order, one gets a formula that works fairly well for  $\psi < \pi/4$  but fails at larger angles. The cause is that at  $\psi > \pi/4$  the particle coercive force (at  $T = 0$ ) differs from the value of the field, at which the second minimum at the magnetic moment potential curve disappears. This peculiarity affects also well-known Kneller's formula  $q_c \propto (1 - A/\sigma)^{1/m}$ , conventionally used to estimate the ECF for assemblies of randomly oriented particles. Our comparison with the exact results confirm the type of the functional dependence but the true exponent value instead of the standard  $m = 3/2$ , see [3], turns out to be  $m = 6/5$ .

In the polarization regime the DMH curves are quasi-elliptic, the ECF increases with  $\sigma$  and rapidly attains the field amplitude value. Similar situation takes place in the intermediate regime. In both these cases, the afore-mentioned approximate formulas fail entirely as they are based on the single-relaxation time approach, which is invalid here.

Support on the part of RFBR-CNRS project 09-02-91070 (PICS 4825) is acknowledged.

- [1] I.S. Poperechny, Yu.L. Raikher, V.I. Stepanov, *Phys. Rev. B*, **82** (2010) 174423.
- [2] Yu.P. Kalmykov, *J. Appl. Phys.*, **96** (2004) 1138.
- [3] R. Skomski, *Simple Models of Magnetism*. Oxford University Press, New York, 2008.

23OR-E-4

## EXCHANGE BIAS AND VERTICAL SHIFT IN $MnFe_2O_4$ FERROFLUID NANOPARTICLES

Silva F.G.<sup>1,2</sup>, Aquino R.<sup>1</sup>, Depeyrot J.<sup>1</sup>, Tourinho F.A.<sup>1</sup>, Perzynski R.<sup>2</sup>, Stepanov V.I.<sup>3</sup>, Raikher Yu.L.<sup>3</sup>

<sup>1</sup> Complex Fluids Group, Instituto de Física, Postal box 04455, 70919-970, Brasília-DF, Brazil

<sup>2</sup> Université Pierre et Marie Curie, PECSA UMR7195, 4 Place Jussieu, 75005 Paris, France

<sup>3</sup> Lab. of Complex Fluids-Inst. of Continuous Media, Mechanics Ural Branch of RAS,  
1 Korolyov street, Perm, 614013 Russia

We present magnetization measurements carried out on magnetic colloids elaborated with 3.3 nm size nanoparticles (NPs) based on a  $MnFe_2O_4$  core protected by a maghemite shell, with a NP volume fraction  $\Phi$  ranging between 0.5 % and 11.2 %. These NPs are obtained by a chemical core/shell strategy developed for the synthesis of ferrofluids [1]. We investigate the magnetic hysteresis and the properties of the obtained  $M(H)$  loops.

Previous studies evidenced in such NPs a well-ordered ferrimagnetic core surrounded by a disordered surface layer frozen in a spin glass-like manner [2]. The temperature dependence of the core magnetization is characterized by a Bloch-like law, and the surface contribution is characterized by an exponential law with the freezing temperature  $T_f$ . Mössbauer spectroscopy has shown, that in the presence of an external field the surface spins progressively align with those of the ferrite core [3].

After cooling under a strong field we observe that the hysteresis loops shift both along  $H$  and  $M$  axes, which indicates the existence of a coupling between the spin-ordered core and the spin-glass like surface layer. The negative  $H$ -shift provides an evaluation of the exchange bias field. This field increases with the diminution of the cooling field and the NP volume content. Uncompensated pinned spins in the spin-glass like surface layer induce the positive  $M$ -shift that we observe.

The authors thank the CAPES-COFECUB program no 714/11, the RFBR-CNRS program no 09-02-91070 (PICS no4825), the Brazilian agencies CAPES, CNPq, FAPDF and the Colégio Doutoral Franco Brasileiro.

[1] J. de A. Gomes, M.H. de Sousa, F.A. Tourinho, G. da Silva, J. Depeyrot, E. Dubois, R. Perzynski *J. Phys. Chem. C*, 112 (16) (2008).

[2] R. Aquino, J. Depeyrot, M.H. Sousa, F. A. Tourinho, E. Dubois, and R. Perzynski, *Phys. Rev. B* 72 184435 (2005).

[3] E.C. Sousa, H.R. Rechenberg, J. Depeyrot, J.A. Gomes, R. Aquino, F.A. Tourinho, V. Dupuis, and R. Perzynski, *J. Appl. Phys.* 106, 093901 (2009).

23RP-E-5

## MAGNETIC NANOCOLLOIDS BASED ON NANOPARTICLES OBTAINED IN A HYDROMETALLURGY REACTOR

*Aquino R.<sup>1</sup>, Coppola P.<sup>2</sup>, Tourinho F.A.<sup>2</sup>, Moreira A.F.L.<sup>3</sup>, Depeyrot J.<sup>3</sup>*

<sup>1</sup> Universidade de Brasília, Faculdade UnB Planaltina, DF, Brazil

<sup>2</sup> Universidade de Brasília, Instituto de Química, DF, Brazil

<sup>3</sup> Universidade de Brasília, Instituto de Física, DF, Brazil

Magnetic properties of nanosized ferrites particles are a subject of great interest from both technological and theoretical research. When dispersed in a liquid carrier at room temperature, it leads to magnetic liquids, which are widely used in technological devices applications. The aim of the present work is to synthesize  $\text{MgFe}_2\text{O}_4$  and  $\text{ZnFe}_2\text{O}_4$  nanoparticles elaborated in order to perform magnetic nanocolloids. Magnesium Ferrite is one of the most important ferrite binary oxides with spinel structure, which is usually used as ferrimagnets, brown pigments, and dehydrogenation catalysts. Temperature and mechanical treatment easily leads to the disorder of Mg and Fe ions over tetrahedral and octahedral sites [1]. This disorder effect in  $\text{MgFe}_2\text{O}_4$  leads to a significant change of the Neel temperature. Also the cation distribution in spinel nanocrystals can modify significantly the saturation magnetization when compared to bulk materials. One of the most studied examples in literature is zinc ferrite, which in ideal bulk crystals presents a normal spinel structure with zinc ions located at tetrahedral sites and iron ions at octahedral sites.[2]. In this work the synthesis conditions were improved and new ferrite nanoparticles were obtained in extreme hydrothermal conditions, ie under high pressure (120 atm) and temperature up to (300 °C) using a reactor hydrometallurgy. In this case it was possible to study the influence of different synthesis parameters such as synthesis pH, temperature, pressure and reaction time. The chemical composition of the synthesized nanoparticles was verified by dicromatometry, in the case of Fe ion, and by plasma spectroscopy (ICPAES), also the atomic composition was checked by EDX. The structural characterizations of synthesized nanoparticles are performed by X-ray diffraction and Raman spectroscopy. Finally, the obtained nanocoiloid was characterized by density measurements and the volume fraction in nanoparticles is calculated using a recently published chemical core/shell model [3].

The authors thank the CAPES-COFECUB program no 714/11, the brazilian agencies CAPES, CNPq, and FAPDF.

[1] V. Sepelak, D. Baabe, F. J. Litterst, K. D. Becker, J. Appl. Phys. 88 (2000) 5884.

[2] J. A. Gomes, G.M.Azevedo, J.Depeyrot, J.Mestnik-Filho, G.J.da Silva, F.A.Tourinho, R.Perszynski. J. of Magn. Magn. Mater. 323 (2011) 1203.

[3] J. A Gomes, M. H. Sousa, F. A. Tourinho, R. Aquino, G. J. Silva, J. Depeyrot, E. Dubois, R. Perszynski, J. Phys. Chem. C 112 (2008) 6220.

**23 August**

Tuesday

14:30-17:20

oral session

23TL-E

23RP-E

23OR-E

**“Magnetism in Biology  
and Medicine”**

23TL-E-6

## TRANSMISSION LINE TYPE THIN FILM SENSOR AND ITS BIOMAGNETIC APPLICATION

*Yabukami S.<sup>1</sup>, Kojima K.<sup>1</sup>, Ozawa T.<sup>1</sup>, Kato K.<sup>1</sup>, Kobayashi N.<sup>2</sup>, Nakai T.<sup>3</sup>, Arai K.I.<sup>2</sup>*

<sup>1</sup>Tohoku-Gakuin University, 985-8537, Tagajo, Japan

<sup>2</sup>Research Institute for Electric and Magnetic Materials, 982-0807, Sendai, Japan

<sup>3</sup>Industrial Technology Institute, Miyagi Prefectural Govern., 981-3206, Sendai, Japan

A highly sensitive magnetic field sensor operating at room temperature shows promise for biomagnetic measurement. High frequency carrier type sensors [1] have potential for high-sensitivity applications similar to SQUID (Superconducting Quantum Interference Devices). In the present study we developed a transmission line type thin film sensor for biomagnetic application. The sensor element consists of coplanar pattern of Cu, ceramic substrate ( $\epsilon_r=115$ ) and amorphous CoNbZr film. The carrier current flows in the Cu conductor, not in the magnetic thin film, so the sensor is different from conventional GMI sensors with respect to this. Small magnetic field changes permeability and shifts the phase of carrier in the transmission line because of skin effect and ferromagnetic resonance. The films were deposited by RF sputtering, and anisotropy was driven by annealing. The impedance and phase difference of the sensor were measured using the S-parameter of a network analyzer (HP8752A). A small AC magnetic field was applied to the sensor element and a very small phase change was detected using a Dual Mixer Time Difference method 1). The experiments were carried out in a magnetically shielded room (Attenuation: 34 dB at 1 Hz). The resolution of magnetic field detection was about 13 pT when a small magnetic field of 1 kHz was applied. The human body lay on a bed made of SUS304. The sensor was placed several mm from the body. The sampling rate was 15 kHz. Fig. 1 shows a measured magnetocardiogram (MCG) signal and electrocardiogram (ECG). We marked the peaks of the R wave, and averaged the MCG signal 56 times, resulting in improvement of the signal-to-noise ratio. In MCG, rapid changes of the R wave and slow change of the T wave were roughly observed. MCG signals including R wave and T wave were synchronized with ECG signals (Lead I). The reasonable R wave around 100 pT was obtained.

This work was partly supported by Grants-in-Aid for Scientific Research of Japan Society for the Promotion of Science.

[1]S. Yabukami, K. Kato, Y. Ohtomo, T. Ozawa, K.I. Arai, *Journal of Magnetism and Magnetic Materials*, vol.321, pp.675-678 (2009).

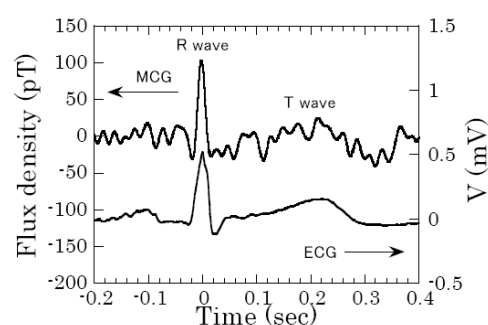


Fig. 1 Measured MCG and ECG.



23TL-E-7

## MULTIFUNCTIONAL MAGNETIC VORTEX MICRODISKS

Novosad V.<sup>1</sup>, Kim D.-H.<sup>1</sup>, Rozhkova E.A.<sup>2</sup>, Ulasov I.<sup>3</sup>, Lesniak M.S.<sup>3</sup>, Rajh T.<sup>2</sup>, Bader S.D.<sup>1,2</sup>

<sup>1</sup> Materials Science Division, Argonne National Laboratory, Argonne, IL, USA

<sup>2</sup> Center for Nanoscale Materials, National Laboratory, Argonne, IL, USA

<sup>3</sup> The Brain Tumor Ctr., The Univ. of Chicago Pritzker School of Medicine, Chicago, USA

In this work, successful interfacing of ferromagnetic nanomaterials with a spin vortex ground state and biomaterials (antibody, whole cell) will be reported. Namely, the gold-coated lithographically defined microdisks [1] with an Fe-Ni magnetic core were biofunctionalized with anti-human-IL13a2R antibody for specifically targeting human glioblastoma cells. When an alternating magnetic field is applied the vortices shift, leading to the microdisks oscillation that causes a mechanical force to be transmitted to the cell. Cytotoxicity assays, along with optical and atomic force microscopy studies, show that the spin vortex-mediated stimulus creates two dramatic effects: (a) membrane disturbance and compromising, and (b) cellular signal transduction and amplification, leading to robust DNA fragmentation and, finally, programmed cell death [2].

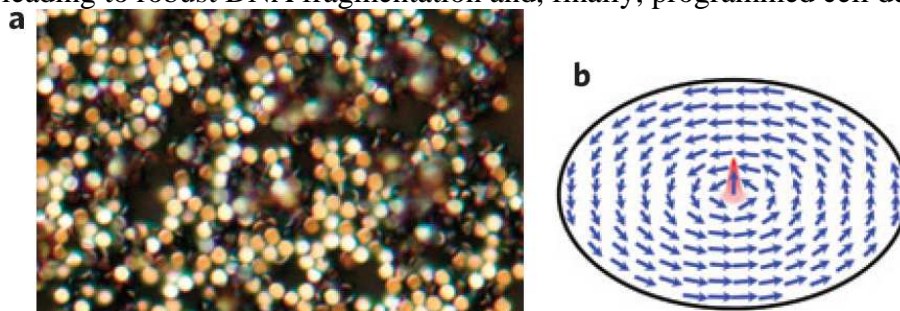


Fig. 1: Magnetic-vortex microdisks can be distantly actuated by the application of small-amplitude and low-frequency AC magnetic fields. (a) Reflection optical microscope image of the dried suspension of 60-nm-thick, ~1 micron diameter permalloy disks coated with a 5-nm-thick layer of gold on each side. The discs were prepared by means of magnetron sputtering and optical lithography. (b) Micromagnetic model of magnetic-vortex spin distribution. The magnetic vortex consists of a ~10-nm-diameter, perpendicularly magnetized vortex core, and an in-plane flux-closure spin arrangement with zero net magnetization in the remanent state.

The experiments reveals that by employing biofunctionalized magnetic vortex microdisks the magnetic fields of low frequency of a few tens of Hz and of small amplitude H of <100 Oe applied during only 10 minutes was sufficient to achieve ~90% cancer cells destruction. For comparison, magnetic fields of few hundreds Oersted, running at ~ hundreds kilohertz are typically needed to achieve another type of cytotoxicity, i.e. hyperthermia treatments using superparamagnetic particles. In other words, an external power supplied to the cell cultures in our experiments is ~100,000 s times smaller than that applied to magnetic particles that are presently used in hyperthermia applications.

Work at Argonne is supported by the US Department of Energy Office of Science, Basic Energy Sciences, under contract No DE-AC02-06CH11357.

[1] E. Rozhkova, V. Novosad, D.-H. Kim, J. Pearson, R. Divan, T. Rajh, & S.D. Bader, "Ferromagnetic Microdisks..". *Journal of Applied Physics.*, vol. **105**, 07B306 (2009).

[2] D.-H. Kim, E. A. Rozhkova, I. Ulasov, M. S. Lesniak, T. Rajh, S.D. Bader, & V. Novosad, "Biofunctionalized Magnetic Vortex Microdisks for Targeted Cancer Cell Destruction". *Nature Materials* (cover page), vol. **9**, pp. 165 - 171 (2010).

23OR-E-8

## BIODISTRIBUTION AND BIODERADATION OF NANOPARTICLES IN A BODY FROM MOESSBAUER AND MAGNETIZATION MEASUREMENTS

Chuev M.A.<sup>1,2</sup>, Cherepanov V.M.<sup>2</sup>, Mischenko I.N.<sup>2</sup>, Nikitin M.P.<sup>3</sup>, Polikarpov M.A.<sup>2</sup>,  
Panchenko V.Y.<sup>2</sup>

<sup>1</sup> Institute of Physics and Technology, Russian Academy of Sciences, 117218 Moscow, Russia

<sup>2</sup> National Research Centre “Kurchatov Institute”, 123182 Moscow, Russia

<sup>3</sup> Shemyakin-Ovchinnikov Institute of Bioorganic Chemistry, Russian Academy of Sciences, 117997 Moscow, Russia

Mössbauer spectroscopy is a powerful method for study of structural, magnetic and thermodynamic properties of magnetic nanomaterials including those delivered in a body. The main problem in interpreting the Mössbauer spectra of iron-containing magnetic nanoparticles injected into a living organism is to reliably decompose them into partial subspectra of exogenous iron atoms in nanoparticles themselves and endogenous iron atoms contained, for example, in ferritin and hemoglobin of the organism [1, 2]. The temperature evolution of the spectral shape for initial nanoparticles agrees qualitatively with the conventional behavior of the spectra of an ensemble of single-domain particles with magnetic anisotropy. Along with a noticeable increase in the linewidths of spectra of the mouse spleen after injection of nanoparticles, an effective doublet of lines in the central part of the spectra is observed. The doublet parameters are typical for Mössbauer spectra of iron in ferritin-like proteins. A conventional analysis of such spectra and their decomposition into partial components is based on a formal approach, in which continuous distributions of the magnetic hyperfine field at iron nuclei are taken into consideration, which results in only qualitative treatment of the spectra. In order to extract a quantitative information about characteristics of the samples studied one has to define a model of the magnetic dynamics in order to fit self-consistently the whole set of the experimental data, particularly, the evolution of Mössbauer spectral shape with temperature and external magnetic field as well as the magnetization curves. We have developed and performed such an analysis of the temperature- and magnetic field-dependent spectra and magnetization curves within a stochastic model for description of relaxation effects in the system of homogeneously magnetized single-domain particles [3-6], which allowed us to reliably evaluate changes in the residual nanoparticles characteristics and their chemical transformation to paramagnetic ferritin-like forms in different mouse's organs as a function of time after injection of nanoparticles. In particular, we have reliably evaluated the exogenous and endogenous iron concentrations at different stages of biotransformation of nanoparticles. Actually, the approach allows one to quantitatively characterize biodistribution, biodegradation and metabolism of magnetic nanoparticles injected into a body.

Support by RFBR is acknowledged.

[1] M.A. Chuev, V.M.Cherepanov, S.M.Deyev, et al., *AIP Conf. Proc.*, **1311** (2010) 322.

[2] M.P. Nikitin, R.R. Gabbasov, V.M. Cherepanov, et al., *AIP Conf. Proc.*, **1311** (2010) 401.

[3] M.A. Chuev, *J. Phys.: Condens. Matter*, **20** (2008) 505201.

[4] M.A.Chuev, *JETP*, **108** (2009) 249.

[5] M.A. Chuev, J. Hesse, in *Magnetic Properties of Solids* (Ed. K.B. Tamayo), Nova Science Publ., New York, 2009, pp. 1-104.

[6] M.A.Chuev, V.M.Cherepanov, M.A.Polikarpov, *JETP Lett.*, **92** (2010) 21.

## NEW CLASS OF MAGNETIC BIO CERAMICS FOR BIOMEDICAL APPLICATIONS

*Tkachenko N.V.<sup>1</sup>, Olkhovik L.P.<sup>1</sup>, Kamzin A.S.<sup>2</sup>*

<sup>1</sup> V.N.Karazin Kharkov National University, Kharkov, Ukraine

<sup>2</sup> Ioffe Physical-Technical Institute of RAS, St.-Petersburg, Russia

Different magnetic nanoparticles, including magnetite ( $\text{Fe}_3\text{O}_4$ ), maghemite ( $\text{g-Fe}_2\text{O}_3$ ), Co-ferrite ( $\text{CoFe}_2\text{O}_4$ ), Mg-ferrite ( $\text{MgFe}_2\text{O}_4$ ), etc are used for many biomedical applications such as media for biosensors, magnetic resonance imaging (MRI), immunoassay, hyperthermia, and drug-delivery systems (DDSs). The hyperthermia induced by heating effects in an AC-magnetic field of the magnetic nanoparticles, which advances cancer cell necrosis through the elevation of cell temperature to around 43 °C, was introduced recently and has attracted much attention because of its safe treatment with little physical or mental strain to the patient. However, their application as heat carriers remains subject to limited biocompatibility because the ferrite nanoparticles must be introduced into the blood vessels. Therefore, ferrite nanoparticles have been coated with biocompatible materials such as gold, polymer, silica ( $\text{SiO}_2$ ), titania ( $\text{TiO}_2$ ), and hydroxyapatite ( $\text{Ca}_{10}(\text{PO}_4)_6(\text{OH})_2$  (HAp)). Among these, HAp is the material component of bone and HAp-coated ferrite nanoparticles (HApFNP) are the most promising material. In its natural state, however, it is uncertain whether the ferrite nanoparticles are coated with HAp and HApFNP has a very low magnetic property. Therefore, it is difficult to use HApFNP in hyperthermia technique. For that reason, it is necessary to improve their magnetic properties and observe the structure of the synthesized hybrid particles.

In the present work, our attention was focused on synthesizing HAp-hexagonal ferrite (HAp-BaM) hybrid particles with higher magnetization than currently exist, to observe the structure of synthesized HAp-BaM hybrid particles, and to examine the behavior in the AC-magnetic field.

We synthesized HAp-ferrite hybrid particles using a two-step synthesis. The first step is synthesis of hexagonal ferrite particles by co-precipitation of  $\text{Fe}^{2+}$  and  $\text{Fe}^{3+}$  aqueous solutions. The hexagonal ferrite was composed mainly of maghemite ( $\text{g-Fe}_2\text{O}_3$ ) and magnetite ( $\text{Fe}_3\text{O}_4$ ). The second step is synthesis of HAp-BaM hybrid particles using ultrasonic spray pyrolysis at 1000 °C using a suspension composed of ferrite particles and  $\text{Ca}(\text{NO}_3)_2$  and  $\text{H}_3\text{PO}_4$ .

The magnetic property of the samples was examined using vibration sample magnetometer measured at room temperature with a maximum magnetic field of 10 kOe and frequency of 25 Hz. The composition of the hybrid particles was measured using an inductively coupled plasma atomic emission spectrometer. The microstructure of samples was observed using scanning electron microscopy, scanning transmission electron microscopy and Mossbauer spectroscopy. The particle size distribution of hybrid particles was measured using an electrophoretic scattering photometer.

Formation of HAp-BaM hybrid was confirmed by X-ray diffraction, composition analysis, cross sectional structure observation, magnetic property and Mossbauer effect measurements, and hyperthermia property measurements. The cross-sectional structure and of synthesized hybrid particles showed two phases (HAp and hexagonal ferrite). The hexagonal ferrite was coated with HAp. The saturation magnetization of ferrite in the HAp-BaM hybrid was 32.5 emu/g. These results show that a synthesized HAp-hexagonal ferrite hybrid particles is biocompatible and that it might be useful for magnetic transport and hyperthermia.

Thus, the synthesized hybrid ceramics HAp-BaM opens a new class of magnetic bioceramics, unifying device biocompatibility and bioactivity hydroxyapatite (HAp) and high magnetic characteristics of M type hexagonal ferrite.

23TL-E-10

## SMART MICRO-MAGNETOPHORESIS FOR ANALYSIS OF BIOMOLECULE CARRIERS

*Kim C.G. \*, Anandakumar S.*

Department of Materials Science and Engineering, Chungnam National University,  
Daejeon 305-764, South Korea

\*E-mail : [cgkim@cnu.ac.kr](mailto:cgkim@cnu.ac.kr) ; Webpage: [www.nbest.org](http://www.nbest.org)

Nanomagnetics are opening a new era not only in industrial applications especially related with information science and technology, but also in bioassays related to biomolecule translocation, biochip/sensors and multiplex bio-recognition channels. Ever since giant magnetoresistance (GMR) has been applied to a biochip sensor for recognition of biomolecule tags of magnetic particle in 1996, many researches have been carried out to enhance the resolution of the magnetic particle tags, corresponding to that of hybridized biomolecule pairs. At present, several groups in the worldwide have succeeded to enhance the sensor resolution down to a few pairs of probe-target biomolecules.

Firstly, I would like to focus on the overview and current status of magnetic bioassays. Secondly, I will introduce a novel system for translocation of magnetic bead carriers, including the magnetic characteristics of magnetic carrier, at specific sites of the sensor surface on a single chip for biosensing applications. The soft NiFe elliptical ( $9\mu\text{m}\times 4\mu\text{m}\times 0.1\mu\text{m}$ ) elements are arranged as magnetic pathways. The patterned NiFe elliptical pathways can generate different stray magnetic fields when they are subjected to the external rotating magnetic field. The in-homogeneity in stray magnetic fields can govern the magnetic bead/nanowire motion on the CNU express pathways.

Thirdly, I would like to introduce the planar Hall Resistance (PHR) effect in magnetic multilayers structures and fabrication of high sensitive PHR biosensor for biomedical diagnosis. In this context, we optimized the performance of PHR spin valve sensor for the single micro-bead of size  $2.8\mu\text{m}$  (Dynabeads® M-280) detection. The single PHE sensor exhibits a sensitivity of about  $7.2\mu\text{V}/(\text{Oe}\cdot\text{mA})$  in the magnetic field range of  $\pm 7\text{ Oe}$  approximately. And finally I will introduce novel magnetic collection pads enhancing active area of biomolecules hybridization.

23TL-E-11

## HYDROTHERMAL TREATED FERRITE NANOPARTICLES WITH HIGH DISPERSIBILITY AND THEIR BIO-MEDICAL APPLICATIONS

*Matsushita N.<sup>1</sup>, Nakagawa T.<sup>2</sup>, Fuse K.<sup>1</sup>, Makinose Y.<sup>1</sup>, Taniguchi T.<sup>3,4</sup>, Katsumata K.<sup>1</sup>, Abe M.<sup>1</sup>, Okada K.<sup>1</sup>*

<sup>1</sup> Materials and Structures Laboratory, Tokyo Institute of Technology, 4259 Nagatsuta, Midori, Yokohama 226-8503, Japan

<sup>2</sup> Dept. of Management of Industry and Technology, Osaka University, 2-1 Yamadagaoka, Suita, Osaka 565-0871, Japan

<sup>3</sup> Dept. of Applied Chemistry and Biochemistry, Kumamoto University, 2-39-1 Kurokami, Kumamoto 860-8555, Japan

<sup>4</sup> JST, CREST, 5 Sanbancho, Chiyoda-ku, Tokyo 102-0075, Japan

Recently, magnetic beads, in which magnetite nanoparticles dispersed in matrix material, attract much attention due to their potential applications in biotechnology such as magnetic resonance imaging (MRI) contrast agents, bio-screening, drug deliver and hyperthermia application. In the present study, we synthesized the ferrite particles with high dispersability and enough large magnetization by oleate-modified hydrothermal growth method, and two different types of magnetic beads ferrite GMA beads for bioscreening and ferrite alginate beads magnetic hyperthermia were investigated, respectively.

The ferrite GMA beads 300 nm in average diameter were prepared by encapsulating large numbers of ferrite nanoparticles in non specific absorption co-polymer of poly-glycidyl methacrylate and styrene. The co-precipitated ferrite particles 9 nm in diameter were grown to 13 nm by the hydrothermal process at 200 °C for 3 hours adding sodium oleate in water. The grown-up ferrite nanoparticles were highly dispersed due to the existence of oleate on the particle surface. The saturation magnetization of ferrite particles increased from 56 to 74 emu/g with the growth of ferrite particles. These ferrite nanoparticles were encapsulated in a copolymer of polystyrene and GMA by an emulsion polymerization method. The polymer coated ferrite beads having sphere shape 300 nm in average diameter exhibited a saturation magnetization of 55 emu/g, whose value was more than 6 times larger than 9.2 emu/g of the commercialized product in which ferrite nanoparticles are dispersed in SiO<sub>2</sub> matrix.

In the ferrite alginate beads, the ferrite nanoparticles are dispersed in alginate gel matrix, which is one of the most extensively used biopolymers since it is abundant, low in cost and biocompatible. The diameter of beads 50–60 μm is large enough not to outflow to the capillary blood vessel 3–10 μm in diameter. The sodium alginate aqueous solution containing ferrite nanoparticles with different average diameter sizes were dropped into a calcium chloride aqueous solution through ink-jet nozzle 60 μm in diameter. Since Alginates become rigid and dense gel quickly in the presence of calcium ions, the droplet ejected from ink jet nozzle can keep its size and shape even after alighting on the solution. Temperature rise ΔT of these beads fixed in agar was measured by applying AC magnetic field of 112 Oe and 120 kHz. The ΔT from room temperature became 8 K after 10 min for the ferrite alginate beads containing ferrite particles 13.5 nm in diameter. This result suggested that the ferrite alginate beads can be heated up the specific portion of human body to 316 K(43°C) enough high for the cancer treatment.

23RP-E-12

## MAGNETIC NANOPARTICLES IN BIOMEDICAL RESEARCH AND IN VITRO DIAGNOSTICS

*Orlov A.V.<sup>1</sup>, Nikitin M.P.<sup>1</sup>, Yuriev M.V.<sup>1</sup>, Vetoshko P.M.<sup>2</sup>, Nikitin P.I.<sup>3</sup>*

<sup>1</sup> Moscow Institute of Physics and Technology, 9 Institutskii per., Dolgoprudny,  
141700 Russia

<sup>2</sup> Institute of Radioengineering and Electronics, 11, Mokhovaya St., Moscow 103907, Russia

<sup>3</sup> General Physics Institute, RAS, 38 Vavilov St, Moscow 119991, Russia

Magnetic nanoparticles (MP) have become popular in many bioanalytical and medical applications as very attractive labels, agents for enhancement of MRI contrast and magnetic drug delivery, as heating agents in hyperthermia, etc. Therefore, quantitative detection of MP is important for these and many others applications.

In this paper, different applications of our original highly sensitive room-temperature method [1] for MP detection based on non-linear MP magnetization are discussed. In the method, MP are magnetized by ac field at two frequencies  $f_1$  and  $f_2$ . The response is recorded at combinatorial frequencies  $f = mf_1 + nf_2$ , where m and n are integers (one of them can be zero, and they may be varied to get the best signal-to-noise ratio), e.g. at  $f = f_1 \pm 2f_2$  [1-3]. The sensitivity of the method of few ng of MP in 0.5 ml volume is on the level of radioactive technique for MP based on <sup>59</sup>Fe isotope [4]. The related detectors were tested for different *in vitro* and *in vivo* applications.

In our work various formats of Magnetic ImmunoAssay (MIAtek®) have been developed that employ MP as labels for *in vitro* biochemical diagnostics. It is shown that the detection limits for different antigens in MIAtek® on 3D filters are 1-2 orders of magnitude better and the assay time is much shorter as compared with the respective values obtained with the standard ELISA [2]. Magnetic assay on immunochromatographic strips provides quantitative and rapid assays [3]. The possibility of magnetic immunoassay realization directly inside a human body is of our special scientific interest. Localization with a remote induction probe of antibody-targeted MP is promising for diagnostics of cancer, atherosclerosis or other diseases [5,6].

New class of instruments equipped with remote induction probes has been developed for mapping of MP located inside animals within 25 mm from the skin surface. The devices highly sensitive, robust and provide real-time quantitative measurements of MP concentration in blood or tissues of a living organism. The MP dynamics has been non-invasively recorded in different organs and tumors of live rats. The effects of parameters of the coils and electronic processing units on spatial resolution of MP have been established. What is important, the devices are not sensitive to linear dia- or paramagnetic materials that always surround MP in quantities, which are 9-10 orders of magnitude higher than that of the tested MP. The developed devices are promising for investigation of concentration dynamics of various MP inside animals' bodies, for selection of biodegradable MP, etc. The results demonstrate that the magnetic nanolabels in combination with developed detection devices can substitute the radioactive ones in many analytical and biomedical applications.

Support by RFFI is acknowledged.

[1] P.I. Nikitin, P.M. Vetoshko, *Patent RU 2166751* (2000), *EP 1262766 publication* (2001).

[2] P.I. Nikitin, P.M. Vetoshko, T. I. Ksenevich, *J. Magn. Magn. Mater.*, **311** (2007) 445.

[3] P.I. Nikitin, P.M. Vetoshko, T.I. Ksenevich. *Sensor Letters*, **5** (2007) 296.

[4] M.P. Nikitin, M. Torno, H. Chen, A. Rosengart, P.I. Nikitin. *J. Appl. Phys.*, **103** (2008) 07A304.

[5] M.P. Nikitin, P.M. Vetoshko, N.A. Brusentsov, P.I. Nikitin, *J. Magn. Magn. Mater.*, **321** (2009) 1658.

[6] M.P. Nikitin, M.V. Yuriev, N.A. Brusentsov, P.M. Vetoshko, P.I. Nikitin. *AIP Conference Proceedings*, **1311** (2010) 452.

23OR-E-13

## STUDY OF THE NATURE OF THE PARAMAGNETIC DOUBLET IN THE MOSSBAUER SPECTRUM USING EXTERNAL MAGNETIC FIELD.

Gabbasov R.R.<sup>1</sup>, Cherepanov V.M.<sup>1</sup>, Chuev M.A.<sup>1,3</sup>, Polikarpov M.A.<sup>3</sup>, Nikitin M.P.<sup>2</sup>, Deyev S.M.<sup>2</sup>, Panchenko V.Y.<sup>1</sup>

<sup>1</sup> National Research Center “Kurchatov Institute”, Moscow, Russia

<sup>2</sup> Shemyakin-Ovchinnikov Institute of Bioorganic Chemistry, RAS, Moscow, Russia

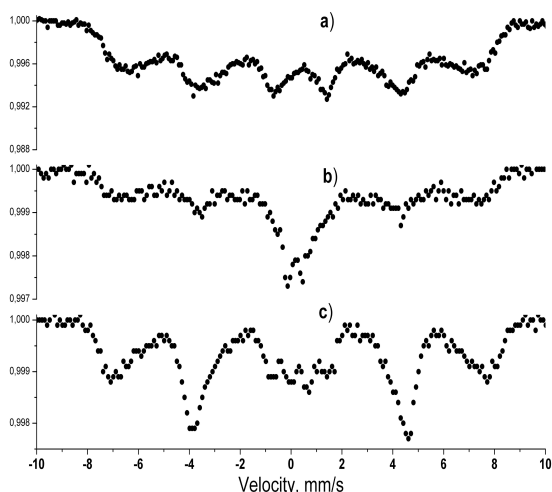
<sup>3</sup> Institute of Physics and Technology, RAS, Moscow, Russia

It was shown using Mössbauer spectroscopy of mouse's organs [1] that after the introduction of magnetic nanoparticles into the tail vein of mice, they are accumulated mainly in her liver and spleen. In this case, the shape of Mössbauer spectrum of the liver after injection of iron-containing magnetic nanoparticles (Fig. b) differs significantly from that of input nanoparticles (Fig. a). Particularly, along with the magnetic splitting component of the liver's spectrum, corresponding to that in the initial particles spectra, an additional doublet in the liver's spectrum is observed, which is typical for non-magnetic forms of iron [1]. The origin of non-magnetic doublet may be associated both with the dissolution of the particles with the subsequent formation of non-magnetic ferritin-like proteins [1] and the effect of superparamagnetism. In the latter case, reducing the size of single-domain magnetic nanoparticles decreases the relaxation time of their magnetization vectors, leading to a collapse of the hyperfine magnetic structure to the quadrupolar doublet. Applying a weak magnetic field leads to increase of relaxation time, thereby restoring the hyperfine structure due to the superparamagnetic contribution to the doublet. In the present work, to distinguish the

mechanisms of formation of the doublet, we have measured the nanoparticles and liver's Mössbauer spectra in a weak external magnetic field as described in [2]. The resulting liver's spectrum in a field is shown in Fig. c.

The evolution of both magnetic and non-magnetic spectral components within 2 months after the injection of nanoparticles was studied. Analysis of the spectra showed that both the mechanisms for forming the doublet take place.

Figure shows <sup>57</sup>Fe Mössbauer spectra of:  
 a) iron-containing magnetic nanoparticles,  
 b) mice liver 2 weeks after injection of nanoparticles,  
 c) mice liver 2 weeks after injection of nanoparticles in an external magnetic field  $H=3.4$  kOe.



The study was supported by RFBR grants 11-02-00846 and 11-02-985.

[1] M.P. Nikitin et al., *AIP Conf. Proc.*, 2010, Vol. 1311, pp. 401-407.

[2] M.A. Polikarpov et al., *J. Phys.: Confer. Ser.*, 2010, Vol. 217, No.012115 (4pp).





**23 August**

Tuesday

11:30-13:00

14:30-17:20

oral session

23TL-F

23RP-F

23OR-F

**“Magnetophotonics”**

23TL-F-1

## SPIN ORBIT INTERACTION IN COHERENT AND THERMAL ULTRAFAST MAGNETISM

*Bigot J.-Y., Vonesch H., Vomir M., Barthelemy M.*

CNRS – Université de Strasbourg, IPCMS 23 rue du Loess BP 43, 67034, Strasbourg, France

The spin dynamics induced by ultrashort laser pulses involves several mechanisms that allow manipulating the magnetization in metallic films and nanostructures. The spin orbit interaction plays a fundamental role with that respect. It is currently considered with great attention both experimentally and theoretically because it could have a strong impact for applications in Spin Nanophotonics based on light controlled spin devices. In the present lecture we will address two important aspects of the spin-photon interaction where the spin-orbit plays a fundamental role. The first one is the “conventional” spin-orbit interaction where the transfer of angular momentum between the orbital and spin moments has been recently unravelled using femtosecond Xray pulses [1]. The second aspect concerns the coherent spin-photon interaction and has its origin in the relativistic Quantum Electrodynamics of the spins interacting with the electromagnetic field of the laser [2].

The first process related to the spin-orbit interaction is present in all ferromagnetic materials having a strong magneto-crystalline anisotropy. Its simplest expression is the  $-\zeta\mathbf{L}\cdot\mathbf{S}$  scalar product in a central potential. Recently we have measured the dynamics of this coupling in CoPd films deposited on a Si<sub>3</sub>N<sub>4</sub> membrane performing a time resolved XRay Magnetic Circular Dichroism at the Bessy synchrotron beam line [1]. The experiment consisted in measuring separately the orbital  $L_z(t)$  and spin  $S_z(t)$  moments of Cobalt at the L2 and L3 edges ( $L_z$  and  $S_z$  being the projections on the direction  $z$  perpendicular to the sample plane). The results establish a delay of ~60 fs between the change of orbital and spin moments after the excitation with a 50 fs near IR laser pulse at 800 nm. Moreover both moments are reduced due to the decrease of the Magnetic Anisotropy Energy. Such dynamics occurs during the thermalisation of the charges and the spins and can therefore be understood as a “thermally” induced modification of the magneto-crystalline anisotropy.

Prior to the preceding mechanism, the spin-photon interaction contains a coherent contribution which can be observed either in a “single pulse” or a “two pulse” Magneto-optical Kerr or Faraday pump probe configuration [2]. In essence this coherent interaction is different than the inverse Faraday mechanism where circularly polarized light can transfer its momentum to the spins. Such inverse Faraday process is indeed efficient to manipulate the precession of the magnetization in Garnets [3]. The coherent spin-photon interaction that we are considering is different and has its origin in the coupling between the spins and the electric potential associated to the laser field. Like the usual spin-orbit interaction it is a relativistic term present in the quantum electrodynamics of the spin-photon interaction. We will show that it can be simply incorporated in the time dependent third order nonlinear response in the case of a simple four level system used as a toy model for understanding the spins dynamics in ferromagnetic materials.

The detailed dynamics of the above two mechanisms will be reviewed and discussed.

Support by the European Research Council: project Atomag, ERC-2009-AdG-20090325 #247452 is acknowledged.

[1] C. Boeglin, E. Beaurepaire, V. Halté, V. López-Flores, C. Stamm, N. Pontius, H. A. Dürr and J.-Y. Bigot, *Nature* **465**, (2010), 458.

[2] J.-Y. Bigot, M. Vomir, E. Beaurepaire, *Nature Physics* **5**, (2009), 515.

[3] A. V. Kimel, A. Kirilyuk, P. A. Usachev, R. V. Pisarev, A. M. Balbashov and Th. Rasing, *Nature* **435**, (2005), 655.

23TL-F-2

## THEORY OF FEMTOSECOND LASER-INDUCED DEMAGNETIZATION

*Oppeneer P.M.<sup>1</sup>, Battiato M.<sup>1</sup>, Carva K.<sup>1,2</sup>*

<sup>1</sup> Department of Physics and Astronomy, Uppsala University, P.O. Box 516,  
SE-751 20 Uppsala, Sweden

<sup>2</sup> Department of Condensed Matter Physics, Charles University, Ke Karlovu 2,  
CZ-12116 Prague, Czech Republic

More than a decade ago it was discovered that excitation of a metallic ferromagnet with an intensive femtosecond laser-pulse can cause an ultrafast demagnetization within 300 fs [1]. Meanwhile it has become clear that laser-induced demagnetization has a huge potential for applications. It represents a new, viable route to achieve magnetic recording with hitherto unprecedented speeds and is as such highly important for magnetic recording industry. However, in spite of its technological importance the mechanism underlying the femtosecond magnetization change remains highly controversial (for a recent review, see [2]). Several theories have been proposed – all based on the assumption that there must exist an ultrafast channel for the dissipation of spin angular momentum. One of the main mechanisms proposed to providing a fast spin-flip channel is currently the Elliott-Yafet electron-phonon spin-flip scattering [3].

Following a different rationale we have developed a theory for fs laser-induced magnetization dynamics, which is based on the high mobility of laser-excited spin-polarized electrons [4]. In this theory we work out the influence of fast electron dynamics of excited non-equilibrium electrons and show that it leads to spin-transport in the super-diffusive regime, causing effectively a demagnetization. Solving the derived transport equation numerically we find that super-diffusive flow of hot electrons can account for the experimentally observed demagnetization within 200 fs in Ni, without the need to invoke any spin angular momentum dissipation channel.

Further, to investigate accurately the contribution of the Elliott-Yafet electron-phonon spin-flip scattering to the femtosecond laser-induced demagnetization in Ni we compute from first-principles the Eliashberg and spin-flip Eliashberg function. From these we compute the spin-flip probability and demagnetization for various situations, *viz.* equilibrium distributions, hot electron distributions in the thermalized regime, and laser-induced non-equilibrium conditions. Hot electron distributions in the electron thermalized regime are computed to lead to larger spin-flip probabilities than equilibrium electron distributions, yet the created net demagnetization is small. A larger net demagnetization is computed for laser-induced non-equilibrium conditions. Putting our obtained results in perspective, allows us to draw conclusions regarding the relative effectiveness of the various proposed demagnetization mechanisms.

Support by FP7 EU-ITN FANTOMAS and the G. Gustafsson Foundation is acknowledged.

[1] E. Beaurepaire, J.-C. Merle, A. Daunois, J.-Y. Bigot, *Phys. Rev. Lett.* **76** (1996) 4250.

[2] A. Kirilyuk, A. Kimel, Th. Rasing, *Rev. Mod. Phys.* **82** (2010) 2731.

[3] B. Koopmans, G. Malinowski, F. Dalla Longa, D. Steiauf, M. Fähnle, T. Roth, M. Cinchetti, M. Aeschlimann, *Nature Mater.* **9** (2010) 259.

[4] M. Battiato, K. Carva, P.M. Oppeneer, *Phys. Rev. Lett.* **105** (2010) 027203.

23OR-F-3

## **THEORETICAL STUDY OF LASER-INDUCED ULTRAFAST MAGNETIZATION DYNAMICS IN ATOMIC SYSTEMS**

*Popova D., Bringer A., Blügel S.*

Peter Grunberg Institut & Institute for Advanced Simulation, Forschungszentrum Jülich and JARA,  
52425 Jülich, Germany

Ultrafast optical control of the magnetic state of a medium attracts much scientific interest. The manipulation of magnetic order by subpicosecond laser pulses is challenging for the development of novel concepts for high-speed magnetic recording, information processing and data storage. Furthermore, it uncovers magnetization dynamics in a strongly out-of-equilibrium regime. A set of experiments has revealed the direct optical control on magnetization via the inverse Faraday effect [1]. In these experiments circularly polarized high-intensity laser pulses at femtosecond time scale are used to excite the magnetic system of the sample. Although the spin-orbit interaction has been identified to be necessary to obtain an inverse Faraday effect, the fundamental mechanisms of the generation of magnetic field by light are still not understood.

In order to get insight into magnetization dynamics at femtosecond time scales we study theoretically the influence of a subpicosecond laser pulse on the magnetic states of a system. We describe the laser-induced transitions in a system of atoms in crystal field surroundings, which can lead to the change of the magnetic state of the system. We introduce the mechanism of the ultrafast inverse Faraday effect due to the stimulated Raman-like scattering process, which was suggested to be responsible for the magnetization reversal by light [2,3].

We are thankful for the support by the FANTOMAS project.

[1] A. Kimel et al., *Nature*, **435** (2005) 655.

[2] F. Hansteen et al., *Phys. Rev. B*, **73** (2006) 014421.

[3] D. Popova, A. Bringer, S. Blügel, *submitted*

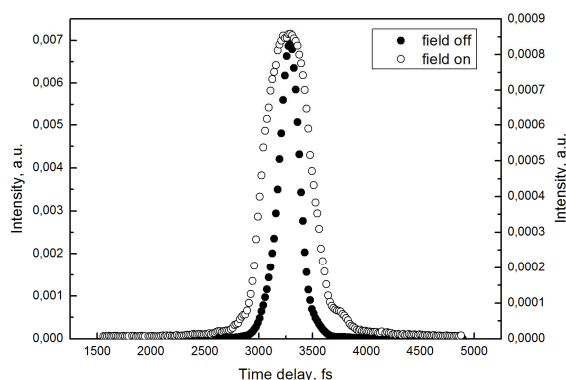
23OR-F-4

## **TIME-RESOLVED FARADAY ROTATION SPECTROSCOPY IN THIN FILMS AND MAGNETOPHOTONIC CRYSTALS**

*Dolgova T.V., Sharipova M.I., Chetvertukhin A.V., Fedyanin A.A.*

Faculty of Physics, Lomonosov Moscow State University, Moscow, Russia

One of the key features of photonic-band-gap materials is possibility to achieve very small light group velocity at the photonic band-gap edge and at the defect mode. This leads to a row of bright “slow-light” phenomena and promising applications such as enhancement of nonlinear-optical and



magneto-optical effects. In one-dimensional magneto-phonic crystals a strong increase of the Faraday rotation has been observed [1]. The effect arises from a non-reciprocity of the Faraday rotation and multiple interference inside slow-light media. A short light pulse propagating through a slow-light magnetic medium can demonstrate a nonmonotonic time dependence of Faraday rotation, if the ratio of the medium optical width to a pulse length is close to unity. In this paper the ultrafast temporal behavior of magneto-optical Faraday rotation is observed in magnetic thin films and magnetophonic

crystals by using a new polarization-sensitive femtosecond cross-correlation technique.

The samples studied are thin (few to tens microns) Bi:YIG films and magnetophonic crystals. An infrared femtosecond fiber laser with 70-MHz repetition rate, average intensity of 130 mW, wavelength of 1,55  $\mu\text{m}$ , pulse duration of 130 fs is used as a source of radiation in the cross-correlation scheme. A Glan prism splits an incoming laser pulse into two orthogonally polarized pulses. One of them goes through the sample placed in 208-Hz modulated magnetic field with 110 Oe amplitude. The difference in optical paths and thus the relative time shift of the pulses can be adjusted by the delay line. The pulses go through a 45-degree-orientated Glan prism. Both pulses are then focused at the same spot into a crystal with a  $\chi^{(2)}$  nonlinearity. If the difference in paths is small enough, so that the pulses overlap in time and space at the nonlinear crystal, the noncollinear second-harmonic generation occurs. Its intensity, which is proportional to the pulse cross-correlation function is detected by a photodiode at a magnetic field frequency as a function of the time delay. The cross-correlation function contains information about polarization rotation time dependence.

Figure shows cross-correlation function of the laser pulse measured for 30  $\mu\text{m}$ -thick magnetic film in magnetic field (open circles) and out of it (solid circles). The broadening, shape modification and asymmetry with a shoulder appearance is observed if magnetic field is applied.

The shape changes (shoulder on the right-hand side) of the polarization-sensitive cross-correlation function in the sample is the evidence of the nonmonotonic time dependence of Faraday rotation yielded by multiple interference of the pulse in the film.

[1] M. Inoue, R. Fujikawa, A. Baryshev, A. Khanikaev, P. B. Lim, H. Uchida, O. Aktsipetrov, A.A. Fedyanin, T.V. Murzina, A.B. Granovsky, *J. Phys. D: Appl. Phys.* **39**, R151–R161 (2006).

23RP-F-5

## LASER-INDUCED SPIN DYNAMICS

*Tsukamoto A., Sato T., Toriumi S., Shimizu R., Itoh A.*

College of Science and Technology, Nihon University, 7-24-1 Narashino-dai, Funabashi, Chiba 274-8501, Japan

Ultrafast laser excitation of itinerant ferromagnets as Co, Ni, or Fe leads to a demagnetization on the femtosecond time scale [1], little is known about rare-earth magnet such as Gd. In Gd, the optically excited electrons of the 5d6s band carries only 9% of the total moment while the localized 4f electrons dominate the magnetic spin moment. How and how fast the magnetic moments in

ferrimagnetic alloy system consists of Gd and FeCo sublattices are excited, with photon energies in the visible range? Here, time resolved study of magnetization response excited by 800 nm light and probed by 420 nm light shows both Gd and FeCo sublattice magnetizations are considerably reduced on the subpicosecond time scale. Delay time dependence of the change of magneto-optical Faraday rotation  $\Delta\theta_F/\theta_F$  and transmittance  $\Delta T/T$  of 20 nm thick GdFeCo were observed.  $\Delta T/T$  and  $\Delta\theta_F/\theta_F$  are responsible for the charge and the spin dynamics, respectively.

Furthermore, we demonstrate a fast precessional switching by ultra-short pulse laser via interplay of ultrafast heating and large temperature dependency of magnetic resonance. High-speed and strongly damped precessional switching was triggered by the laser irradiation with ultrafast heating of a  $\text{Gd}_{24.5}\text{Fe}_{66.1}\text{Co}_{9.4}$  across its magnetic compensation temperature  $T_M$  (~345 K) up to angular momentum compensation temperature  $T_A$ , under a static applied magnetic field.

Two kinds of compensation phenomena, around  $T_A$  and  $T_M$ , play important roles. (i) In ferrimagnetic GdFeCo having sub-lattices with different gyromagnetic ratio each other, when the temperature approaches the angular momentum compensation point  $T_A$ , both frequency of ferromagnetic resonance (FMR) mode and the Gilbert damping parameter increase significantly [2]. The magnetic system will be accelerated. (ii) By crossing the  $T_M$ , ultrafast switching from parallel to anti-parallel configuration between magnetic field and net magnetization allows excitation of magnetic systems at time scales much shorter than thermal cooling process. To initiate and investigate the magnetization reversal, we have used an all-optical pump-probe technique employing an amplified Ti:Sapphire laser system with 90 fs pulses. In particular, following the laser excitation with rather high pump fluence ( $3.3 \text{ mJ/cm}^2$ ) excitation induces a metastable opposite magnetic state[3]. After the sudden heating which causes just 30% reduction of magnetization at first breakdown, consequently magnetization was started to rotate across  $M_z = 0$  within 6 ps during first precession and finished the high damped precessional motion within few cycles into opposite direction.

This work is partially supported by PRESTO, Japan Science and Technology Agency and Nihon University Strategic Projects for Academic Research.

[1] J. Bigot, M. Vomir and E. Beaurepaire, *Nature Physics*, **5** (2009) 515.

[2] C. D. Stanciu, A. V. Kimel, F. Hansteen, A. Tsukamoto, A. Itoh, A. Kirilyuk, and Th. Rasing, *Phys. Rev. B*, **73** (2006) 220402(R).

[3] A. Tsukamoto, T. Sato, S. Toriumi, and A. Itoh, *J. Appl. Phys.*, **109** (2011) 07D302.

23TL-F-6

## SPIN DYNAMICS AT ELEVATED TEMPERATURES

Wienholdt S., Gerlach S., Schlickeiser F., Hinzke D., Nowak U.

Universität Konstanz, Universitätsstraße 10, D-78457 Konstanz, Germany

Ultrafast magnetisation dynamics has been extensively studied recently as a possibility to improve the storage density as well as the writing speed in magnetic data storage. The direct, ultrafast manipulation of the magnetisation by femtosecond laser pulses promises to become a real alternative to those techniques where magnetic field pulses are used. Recently it was demonstrated that a sub 100 femtosecond, circularly polarised laser pulse is able to reverse magnetisation on a time scale of some picoseconds, as if it acts as an equally short magnetic field pulse pointing along

the direction of light caused by the inverse Faraday effect [1,2]. In femtosecond single-shot time-resolved imaging of magnetic structures [3] it has been shown that the magnetisation reverses via a so-called ultrafast linear pathway [4] and not via precession. However, the relevant time-scales and mechanisms of these optically induced magnetisation reversal processes are not fully understood yet. So far, ultrafast all-optical magnetisation switching has been demonstrated experimentally only in ferrimagnetic materials like GdFeCo. A reason for this restriction seems to be the antiferromagnetic coupling of the two sub-lattices in these materials, which may lead to completely different dynamics as compared to a ferromagnet. It was speculated that the special properties of the ferrimagnet close to the compensation point could be relevant [3].

To understand the dynamics in these materials, we perform simulations within the framework of the Landau-Lifshitz-Bloch (LLB) equation of motion [5,6]. Simulating extended systems of up to 107 macro-spins where the exchange coupling as well as the dipolar interaction is taken into account, we find that field pulse durations as short as 250 fs can be sufficient to trigger magnetisation reversal. The magnetisation evolution after excitation with a circular polarised laser pulse of a film with an area of 10  $\mu\text{m}$  x 10  $\mu\text{m}$  can be simulated and coincides with the experimental results [3]. Furthermore, we perform atomistic spin model simulations of antiferromagnets as well as ferrimagnets, driven either by external magnetic field pulses or variation of the spin temperature and investigate the switching mechanisms in detail.

We acknowledge financial support by the EU through the collaborative research project ULTRAMAGNETRON.

[1] A. V. Kimel, A. Kirilyuk, P. A. Usachev, R. V. Pisarev, A. M. Balbashov, and Th. Rasing, *Nature* 435, 655 (2005)

[2] C. D. Stanciu, F. Hansteen, A. V. Kimel, A. Kirilyuk, A. Tsukamoto, A. Itoh, and Th. Rasing, *Phys. Rev. Lett.* 99, 047601 (2007)

[3] K. Vahaplar, A. M. Kalashnikova, A. V. Kimel, D. Hinzke, U. Nowak, R. W. Chantrell, A. Tsukamoto, A. Itoh, and Th. Rasing, *Phys. Rev. Lett.* 103, 117201 (2009)

[4] N. Kazantseva, D. Hinzke, R. W. Chantrell, and U. Nowak, *Euro. Phys. Lett.* 86, 27006 (2009)

[5] N. Kazantseva, D. Hinzke, U. Nowak, R. W. Chantrell, U. Atxitia, and O. Chubykalo-Fesenko, *Phys. Rev. B* 77, 184428 (2008)

[6] D. A. Garanin, *Phys. Rev. B* 55, 3050 (1997)

23TL-F-7

## **ELEMENT-SELECTIVE STUDIES OF MAGNETIZATION DYNAMICS: MOVING FROM NANO- TO FEMTOSECONDS**

*Schneider C.M.*

Peter Grünberg Institut, Forschungszentrum Jülich, D-52425 Jülich, Germany

The dynamic behavior of magnetic systems is of high fundamental interest and enormous technological relevance in fields of magnetic data storage and spintronics. It is determined by a complex interplay of spin-dependent interactions on different length scales. In magnetic heterosystems the situation is further complicated by the coupling between the various magnetic constituents or elements. In order to disentangle the responses of the individual magnetic components, element-selective techniques with appropriate time-resolution are needed. This can be conveniently separated by advanced x-ray pump-probe spectromicroscopy experiments, employing

circular and linear magnetic dichroism as quantitative measure of the magnetic configuration and ordering.

In order to perform element-selective magnetodynamic studies of layered heterosystems in the nano- and picosecond regime we employed soft x-ray photoemission microscopy [1]. In magnetic trilayers with interlayer exchange coupling, we observed various dynamic processes on different time scales. In the case of weak ferromagnetic coupling the interlayer exchange coupling is found to have a distinct influence on the dynamic response, which differs for domain wall motion and magnetization rotation. An additional magnetocrystalline anisotropy contribution is found to suppress magnetization rotation to a large extent.

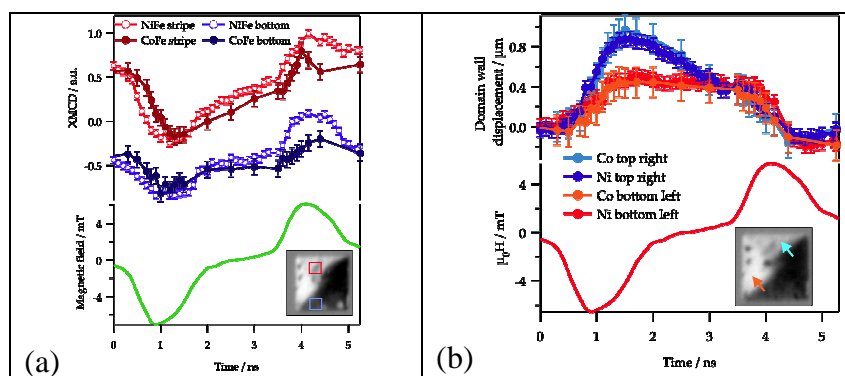


**Figure:** Magnetodynamic response of the individual NiFe and CoFe layers in a NiFe/Cr/CoFe trilayer to an ultrashort bipolar field pulse (bottom of each graph). (a) Magnetization rotation in the top and bottom layer shows a phase shift, i.e. partial “decoupling” resulting in a time-dependent twist of the layer magnetizations. (b) Domain wall motion in both layers occurs simultaneously due to local increase of the coupling via stray fields at the domain walls.

As a first step to extend this element-selective pump-probe approach into the femtosecond regime we have performed resonant magnetic reflectivity experiments at the transition metal M edges. Using a higher harmonic generation scheme with a table-top laser system we are able to study ultrafast demagnetization processes with a time resolution of better than 50 fs [2]. With this technique we can discern different demagnetization times in magnetic heterosystems.

[1] G. Schönhense, H. J. Elmers, S. A. Nepijko and C. M. Schneider, *Adv. Imag. Electron Phys.* **142** (2006) 159.

[2] C. La-O-Vorakiat, M. Siemens, M. M. Murnane, H. C. Kapteyn, S. Mathias, M. Aeschlimann, P. Grychtol, R. Adam, C. M. Schneider, J. M. Shaw, H. Nembach and T. J. Silva, *Phys. Rev. Lett.* **103** (2009) 25740.



23OR-F-8

## AN X-RAY VIEW ON ULTRAFAST MAGNETISM

Radu I.<sup>1,2</sup>, Vahaplar K.<sup>1</sup>, Stamm C.<sup>2</sup>, Kachel T.<sup>2</sup>, Pontius N.<sup>2</sup>, Dürr H.A.<sup>2,5</sup>, Ostler T.A.<sup>3</sup>, Barker J.<sup>3</sup>, Evans R.F.L.<sup>3</sup>, Chantrell R.W.<sup>3</sup>, Tsukamoto A.<sup>4,6</sup>, Itoh A.<sup>4</sup>, Kirilyuk A.<sup>1</sup>, Rasing Th.<sup>1</sup>, Kimel A.K.<sup>1</sup>

<sup>1</sup> Radboud University Nijmegen, Institute for Molecules and Materials,  
Heyendaalseweg 135, 6525 AJ Nijmegen, The Netherlands

<sup>2</sup> Helmholtz-Zentrum Berlin für Materialien und Energie, BESSY II, Albert-Einstein-Strasse 15,  
12489 Berlin, Germany

<sup>3</sup> Department of Physics, University of York, York YO10 5DD, United Kingdom

<sup>4</sup> College of Science and Technology, Nihon University, 7-24-1 Funabashi, Chiba, Japan

<sup>5</sup> SLAC National Accelerator Laboratory, Menlo Park, CA 94025, USA

<sup>6</sup> PRESTO, Japan Science and Technology Agency, 4-1-8 Honcho Kawaguchi, Saitama, Japan

Revealing the ultimate speed limit at which magnetic order can be controlled, is a fundamental challenge of modern magnetism having far reaching implications for magnetic recording industry. Exchange interaction is the strongest force in magnetism, being ultimately responsible for ferromagnetic or antiferromagnetic spin order. How do spins react after being optically excited on a timescale faster than the exchange interaction?

Here, we demonstrate that femtosecond (fs) measurements of ferrimagnetic GdFeCo alloy using X-ray magnetic circular dichroism provide revolutionary new insights into the problem of ultrafast magnetism on timescales pertinent to the exchange interaction. In particular, we show that upon fs optical excitation the ultrafast spin reversal of GdFeCo - a material with antiferromagnetic coupling of spins - occurs via a transient ferromagnetic state [1]. The latter one emerges due to different dynamics of Gd and Fe magnetic moments: Gd switches within 1.5 ps while it takes only 300 fs for Fe. Thus, by using a single fs laser pulse one can force the spin system to evolve via an energetically unfavorable way and temporary switch from an antiferromagnetic to ferromagnetic type of ordering. These observations supported by atomistic simulations, present a novel concept of manipulating magnetic order on timescales of the exchange interaction.

Funding from European Union through UltraMagnetron and FANTOMAS programs is gratefully acknowledged.

[1] I. Radu *et al.*, *Nature* **472**, (2011) 205.

## MODELLING AND COMPARISON TO EXPERIMENT OF ULTRA-FAST LASER-INDUCED MAGNETISATION DYNAMICS IN FERROMAGNETIC MATERIALS.

Chubykalo-Fesenko O., Atxitia O.<sup>1</sup>, Walowski J.<sup>2</sup>, Sultan M.<sup>3</sup>, Bovenspiensen U.<sup>2</sup>,  
Münzenberg M.<sup>2</sup>

<sup>1</sup> Instituto de Ciencia de Materiales de Madrid, CSIC, Cantoblanco, 28049, Madrid, Spain

<sup>2</sup> Physikalisches Institut, Universität Göttingen, 37077 Göttingen, Germany

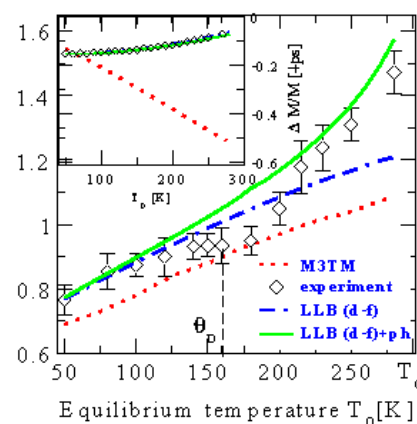
<sup>3</sup> Universität Duisburg-Essen, 47048, Duisburg, Germany

The implementation of novel magnetic recording and spintronic devices requires well-funded knowledge of the limits of spin manipulation. Recent pump-probe experiments with powerful femtosecond lasers have pushed these limits down to femtosecond timescale [1]. They also have opened a debate on the origin of the magnetization modification on this ultra-fast timescale and the role of different sub-systems.

In this work we show an excellent quantitative agreement between femtosecond optical pump-probe experiments and thermal micromagnetic modeling, using the (quantum) Landau-Lifshitz-Bloch (LLB) model in Ni and Gd, which reveals a predominant thermal demagnetization mechanism. Magnetic fluctuations are generated by a coupling via spin-flip processes to the heated electron and/or phonon systems. The coupling parameter is defined by the microscopic spin-flip rate and is two orders of magnitude larger in Ni than in Gd due to a different nature of the electrons, responsible for magnetism in these metals. In both cases the values of this parameter are consistent with the measured damping values.

In agreement with experimental results, the modeling shows that in Ni the magnetization recovers in the picosecond timescale after the optical pulse. Both the demagnetization and magnetization recovery times slow down as a function of pump fluency, consistent with the modeling based on the LLB equation [2]. The magnetization dynamics follows from the electronic temperature but is slowed down at high temperatures, according to the general behavior of the longitudinal relaxation, defined by the exchange interaction.

In Gd due to a small value of the coupling parameter, the magnetization response is tremendously slowed down with respect to the electronic temperature leading to a two-stage slow demagnetization process going up to hundreds ps timescale, consistent with experimentally found behavior [3]. We find that while in Ni a pure electron mechanism is sufficient to explain the ultra-fast demagnetisation timescales, in Gd only a combined electron (within d-f coupling model) and phonon-mediated processes can provide an agreement with the experiment. The Figure shows the comparison between the experimental and modeled demagnetisation timescales (in ps) and the inset – the absolute demagnetisation values in Gd.



[1] E. Beaurepaire et al Phys. Rev. Lett. 76 (1996) 4250.

[2] U. Atxitia et al Phys. Rev. B 81 (2010) 174401.

[3] M. Wietstruk et al, Phys. Rev. Lett. 106 (2011) 127401

23OR-F-10

## FEMTOMAGNETISM: INSIGHTS FROM HEISENBERG ENERGY-TIME UNCERTAINTY PRINCIPLE

*Kurkin M.I.<sup>1</sup>, Orlova N.B.<sup>2</sup>*

<sup>1</sup> Institute of Metal Physics UrB RAS, S. Kovalevskaya st. 18, 620041, Ekaterinburg, Russia

<sup>2</sup> Department of Applied and Theoretical Physics, Novosibirsk State Technical University,  
Karl Marx av. 20, 630092 Novosibirsk, Russia

The application of femtosecond optics for study of magnetic materials led to the discovery of a large number of mysterious phenomena not yet explained by the existing theory of spin magnetism. These phenomena are grouped in the separate section of magnetism called "femtosecond magnetism" or "femtomagnetism" [1]. It is considered that the existing theory of magnetism is not able to describe the femtomagnetic phenomena without the revision of its basic principles. The problems discussed relate only to the femtosecond magneto-optics with the pulse duration of  $\tau_p \approx (10^{-13} - 10^{-14})s$ . The effects caused by optical pumping with nanosecond duration can be perfectly described by the existing theory.

In the report we discuss three parameters of pulses that can provide such a differences: (i) the electric field amplitude  $E_p$  of the pump wave; (ii) the energy width of the pulse spectrum  $\Delta\epsilon_p$ ; (iii) the steepness of the pulse. The main focus of the report is given to a spectral width of the pulse  $\Delta\epsilon_p$ . The "energy – time" uncertainty relation allows us to estimate the ratio of the widths for femto- and nanosecond pulses  $\Delta\epsilon_p^{femto} / \Delta\epsilon_p^{nano} \approx 10^4 - 10^5$ . This allows us to get the estimation for the time of the spontaneous emission of photons  $\tau_{em}$  under the electron excitation by the optical pump with the duration  $\tau_p$ :  $\tau_{em} \approx \tau_p$ .

For femtosecond pumps, the value  $\tau_p$  can be comparable with the lifetime of the excited electron  $\tau_{rel}$  due to irreversible relaxation processes. At  $\tau_{em} \approx \tau_{rel}$ , the emission intensity becomes comparable with the intensity of the pump. Since the emission is a dynamic process, it keeps the memory of the parameters of the pump. This fact differs the emission from the irreversible relaxation; and that is important for the femtomagnetic phenomena critically depending on the discussed parameters of the pump.

The application of the "energy-time" uncertainty relation allows us to simplify the electronic Hamiltonian  $H$ , that determines the electron states between which the optical transition emerges. Here we can neglect the part that does not change significantly the electron wave function over the time  $\tau_p$ . The simplified Hamiltonian was used to analyze the transitions associated with optical excitation and emission. These processes form the nonequilibrium electron orbital angular momentum, that can fulfill the role of intermediary state between the optical pump and the electron spins responsible for femtomagnetism.

This work was partly supported by Russian Foundation for Basic Research (project 11-02-00093).

[1] A. Kirilyk, A. Kimel, Th. Rasing. Rev.Mod.Phys. **82**, 2731 (2010).

23TL-F-11

## MAGNETO-OPTIC COLLINER VOLUMETRIC HOLOGRAPHY WITH FERROMAGNETIC GARNET FILMS

*Inoue M., Lim P.B., Sakurai H., Horimai H.*

Toyohshi University of Technology, Toyohashi 441-8580, Japan

Owing to its remarkable potential in high density recording and high data transfer rate, collinear holography[1] is regarded as a promising optical memory of the next generation. Recording materials generally used for the collinear hologram memories are thick (several hundred  $\mu\text{m}$ ) photopolymer films so as to ensure large shift multiplexing of holograms. There are, however, several issues of the organic recording media; for instance, (1) they need shielding cartridge, (2) their shelf and archival lives are still uncertain, (3) they have no rewritability, and so on.

This paper presents a trial on magneto-optic collinear hologram recording with thick magnetic garnet films, which is inherently rewritable and the shielding cartridge is no need. Thermomagnetic recording is responsible for the formation of volumetric collinear holograms with a single focusing lens, while magneto-optical reading is used for retrieving the two-dimensional page data from the holograms. Polarization of the diffracted light from the hologram is subject to rotating 90 degrees from its original polarization of the incident light.

Bi-substituted iron garnet films (3.3  $\mu\text{m}$  thick) were formed by RF magnetron sputtering on SGGG substrates. They were subject to post thermal annealing at 750°C for 10 minutes for garnet crystallization. The resultant film had polycrystalline structure whose grain size was approximately 50 nm. The magnetic coupling between the magnetic grains seemed to be weak, and no clear formation of magnetic domains in the film was observed. This is favorable for forming complex magnetization arrangements corresponding to the volumetric fringe patterns. The recording pattern was found to be important parameter so as to write the holograms thermomagnetically. When the signal diameter was 260  $\mu\text{m}$ , a clear reconstructed image was obtained. Collinear shift multiplexing was also examined and we obtained reconstructed images from the overlapped magnetic holograms.

The work was supported in part by JSPS Grant-in-Aid for Scientific Research (A), No. 23246081.

[1] H. Horimai, X. Tan, N. Kitazaki, et al., "Novel features of HVD™ system," SPIE Symp. Optics & Photonics 2006, 6335-17, 124, San Diego, California, USA, (2006).

23RP-F-12

## HOLO-TABLE, A NEW STYLE OF THREE DIMENSIONAL DISPLAY

*Horimai H.<sup>1</sup>, Inoue M.<sup>2</sup>*

<sup>1</sup> HolyMine Corporation, 2032-2-301 Ooka, Numazu, Shizuoka 410-0022, Japan

<sup>2</sup> Toyohashi Univ. of Technology, 1-1 Hibarigaoka, Tenpaku, Toyohashi, Aichi 441-8580, Japan

Due to the great demand of Three-Dimensional (3D) display, development of 3D display without special glasses and smooth motion parallax is strongly desired. High density directional images displaying is one of a promising glasses-free 3D display method [1]. In this method, however, considerably large number of spatial light modulators (SLMs) corresponding to the number of spatial beam directions are needed. In contrast to the method mentioned above, Direct Light Scanning Method had been proposed by authors and demonstrated that the high-density directional 3D motion image can easily be obtained with only one SLM [2]. This paper will introduce a new style of 3D display using the direct light scanning method, named "Holo-Table". Since the holographic screen as a beam deflector sets horizontally, projected 3D image has a 360 degree full horizontal viewing angle as shown in Figure 1 schematically.

Actual Holo-Table with the newly developed RGB display optical engine is shown in Figure 2. The R/G/B LED were employed as the illuminant light source. The parallax images were projected normal to the holographic screen from the bottom side. The holographic screen rotating position was detected by a photo interrupter, and the projection images were synchronized to the rotating screen position.

Specification of the Holo-Table is summarized as: display screen size 300[mm], horizontal viewing angle ranges 360 deg., ray angle pitch 0.72 deg., number of directional images 500 per rotation, 3D resolution 1024x768 (XGA), movie frame-rate 30 fps. The switching of projected images was synchronized to the holographic screen rotation by measured disc rotating state using a photo interrupter.

Figure 3 shows an example of observed 3D images from different viewing positions which was taken by a digital camera. The displayed image can be observed by naked-eye, and sufficient motion parallax and binocular parallax (the requirement 3D image seeing) was confirmed. The displayed image was made from computer graphics, but we also have demonstrated to display actual object images taken by photographed pictures. Further investigations are now under way by employing super-high-speed SLM, such as magneto-optic SLM, to display the realistic 3D movie images.

This work is partly supported by the Organization for Hamamatsu Technopolis, Hamamatsu Optonics Cluster of MEXT (Ministry of Education, Culture, Sports, Science and Technology).

[1] Y. Takaki "A Novel 3D Display Using an Array of LCD Panels," IS&T-SPIE 5003, 1-7 (Santa Clara, U.S., 2003)

[2] Y. Aoki et al., "Direct Light Scanning 3-D Display," ACP 2009, WL113 (Shanghai, China, 2009)



Fig. 1 A new style of 3D display, "Holo-Table"

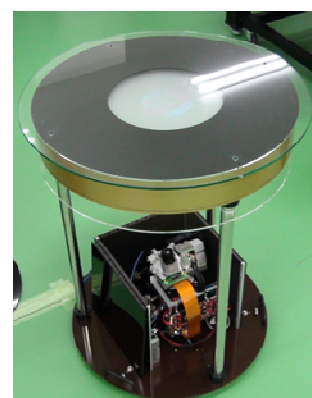


Fig. 2 Actual Holo-Table with optical engine

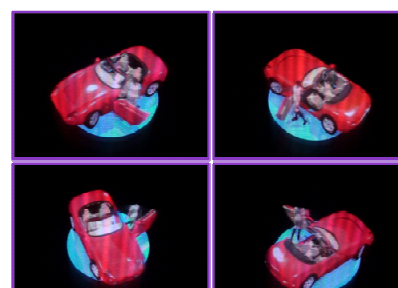


Fig. 3 The observed 3D images from different viewing angle



**23 August**

Tuesday

11:30-13:00

14:30-17:20

oral session

23TL-G

23RP-G

23OR-G

**“Magnetism and  
Superconductivity”**

23TL-G-1

## SPIN TRIPLET SUPERCURRENT IN FERROMAGNETIC JOSEPHSON JUNCTIONS

*Birge N.O., Khaire T.S., Khasawneh M.A., Klose C., Pratt Jr.W.P.*  
Michigan State University, East Lansing, MI 48824-2320, USA

The proximity and Josephson effects between a conventional superconductor (S) and a ferromagnet (F) decay and oscillate over an extremely short length scale in F due to the large exchange splitting between the spin-up and spin-down electron bands. If there were spin-triplet superconducting correlations present, however, then both the proximity and Josephson effects would persist over much longer distances. Such spin-triplet correlations have been predicted to occur in S/F systems in the presence of certain forms of magnetic inhomogeneity near the S/F interface [1]. We have observed strong evidence for spin-triplet pair correlations in S/F/S Josephson junctions containing strongly-ferromagnetic cobalt [2,3]. The experimental signature of the triplet correlations is a Josephson critical current that decays very slowly for Co thicknesses up to several tens of nm. This long-range supercurrent appears only in samples with additional ferromagnetic F' layers inserted between the central Co and outer superconducting electrodes, and is caused by non-collinear magnetizations of the F' and Co layers [4]. After application of a large in-plane magnetic field, the magnitude of the long-range supercurrent is further enhanced, contrary to expectation. I will discuss possible reasons for this additional critical current enhancement, and provide an update on our current experiments.

Support by the US DOE is acknowledged, under grant DE-FG02-06ER46341.

[1] F.S. Bergeret, A.F. Volkov, and K.B. Efetov, Phys. Rev. Lett., 86, 4096 (2001).

[2] T.S. Khaire, M.A. Khasawneh, W.P. Pratt, Jr., and N.O. Birge, Phys. Rev. Lett. 104, 137002 (2010).

[3] M.A. Khasawneh, T.S. Khaire, C. Klose, W.P. Pratt, Jr., and N.O. Birge, Supercond. Sci. Technol. 24, 024005 (2011).

[4] M. Houzet and A.I. Buzdin, Phys. Rev. B 76, 060504 (2007).



## INHOMOGENEOUS SUPERCONDUCTIVITY IN PLANAR SUPERCONDUCTOR-FERROMAGNET HYBRIDS

Koelle D.<sup>1</sup>, Werner R.<sup>1</sup>, Aladyshkin A.Yu.<sup>2</sup>, Fritzsche J.<sup>3</sup>, Guénon S.<sup>1</sup>, Kramer R.B.G.<sup>3</sup>,  
Nefedov I.M.<sup>2</sup>, Moshchalkov V.V.<sup>3</sup>, Kleiner R.<sup>1</sup>

<sup>1</sup> Physikalisches Institut and Center for Collective Quantum Phenomena in LISA<sup>+</sup>,  
Universität Tübingen, Germany

<sup>2</sup> Institute for Physics of Microstructures RAS, Nizhny Novgorod, Russia

<sup>3</sup> INPAC – Institute for Nanoscale Physics and Chemistry, K. U. Leuven, Belgium

We studied the magnetoresistance and superconducting properties of Pb thin film microbridges on top of a ferromagnetic BaFe<sub>12</sub>O<sub>19</sub> substrate, which has a well-defined stripe-like magnetic domain structure [1,2]. The nonuniform component of the magnetic field  $H$ , induced by the ferromagnet leads to a complex  $H - T$  phase diagram of the Pb bridge, with various inhomogeneous states such as reverse domain and parallel domain superconductivity, domain wall superconductivity and edge-assisted superconductivity. Here we report on integral electric transport measurements and on low-temperature scanning laser microscopy (LTSLM) imaging [3] of these nonuniform superconducting states in (i) a Pb bridge with domain walls perpendicular and (ii) a Pb bridge with a single straight domain wall along the center of the bridge. At a temperature  $T$  slightly below the transition temperature  $T_c$  of the Pb bridge and a bias current  $I$  smaller than the critical current  $I_c$ , the scanning laser spot locally destroys superconductivity by heating up the spot area above  $T_c$  or by reducing the critical current density  $j_c$  below the applied bias current density  $j$ . This results in a global change of the voltage drop  $\Delta V$ , which is detected via lock-in technique as a function of the beam spot coordinates  $(x,y)$  on the sample surface. The acquired voltage images  $\Delta V(x,y)$  confirm the formation of inhomogeneous superconducting states and external-field-controlled switching between the normal state and inhomogeneous superconductivity.

[1] J. Fritzsche, R. B. G. Kramer, V. V. Moshchalkov, *Phys. Rev. B*, **80** (2009) 094514.

[2] A. Yu. Aladyshkin, J. Fritzsche, V. V. Moshchalkov, *Appl. Phys. Lett.*, **94** (2009) 222503.

[3] J. Fritzsche, V. V. Moshchalkov, H. Eitel, D. Koelle, R. Kleiner, R. Szymczak, *Phys. Rev. Lett.*, **96** (2006) 247003.

23RP-G-3

## RECENT EXPERIMENTS WITH SIFS JOSEPHSON JUNCTIONS

Goldobin E.<sup>1</sup>, Scharinger S.<sup>1</sup>, Gürlich C.<sup>1</sup>, Mints R.G.<sup>2</sup>, Weides M.<sup>3</sup>, Kohlstedt H.<sup>4</sup>, Koelle D.<sup>1</sup>, Kleiner R.<sup>1</sup>

<sup>1</sup> Physikalisches Institut–Experimentalphysik II, University of Tübingen,  
Auf der Morgenstelle 14, 72076 Tübingen, Germany

<sup>2</sup> The Raymond and Beverly Sackler School of Physics and Astronomy, Tel Aviv University,  
Tel Aviv 69978, Israel

<sup>3</sup> Department of Physics, University of California, Santa Barbara, CA 93106, USA

<sup>4</sup> Nanoelektronik, Technische Fakultät, Christian-Albrechts-Universität zu Kiel, D-24143 Kiel,  
Germany

We have fabricated and investigated Superconductor-Insulator-Ferromagnet-Superconductor Josephson heterostructure which consists of 40 alternating 0 and  $\pi$  segments of equal lengths [1]. Such structure is proposed as a possible way to implement a so-called  $\phi$  Josephson junction, i.e., the junction having a phase drop of  $\pm\phi$  ( $0 < \phi < \pi$ ) in the ground state [2–4]. In particular we study the Josephson current density by means of low temperature scanning electron microscope (LTSEM) and the dependence of total critical current  $I_c$  on applied magnetic field  $H$ . The common theoretical approach [5], which assumes the uniform flux density  $B$ , predicts that: (a)  $I_c(H)$  has main maxima when the flux per segment is equal to half a flux quantum; (b) the other maxima of  $I_c(H)$  are much lower and almost symmetric relative to the main one; (c) the height of the main peaks is  $0.63 I_{c0}$ , where  $I_{c0} = j_c w L$  is the intrinsic critical current,  $w$  and  $L$  are the junction's width and length. In experiment, however, the secondary maxima between the two main maxima almost vanish and the main maxima of  $I_c$  are lower than expected. We demonstrate that these features are caused by a non-uniform flux density  $B$  resulting from screening currents in the electrodes in the presence of a (parasitic) off-plane field component. The results reported here also may explain inconsistent experimental data obtained earlier on YBCO-Nb and NCCO-Nb ramp zigzag 0- $\pi$  junctions [5,6].

Support by Deutsche Forschungsgemeinschaft (DFG) and German-Israeli foundation (GIF) is greatly acknowledged.

[1] M. Weides, et al., Phys. Rev. Lett. **97**, 247001 (2006).

[2] R. G. Mints, Phys. Rev. B **57**, R3221 (1998)

[3] A. Buzdin and A. E. Koshelev, Phys. Rev. B **67**, 220504(R) (2003).

[4] E. Goldobin, et al., Phys. Rev. B **76**, 224523 (2007).

[5] H.-J. H. Smilde, et al., Phys. Rev. Lett. **88**, 057004 (2002).

[6] Ariando, et al., Phys. Rev. Lett. **94**, 167001 (2005).

23OR-G-4

## INDUCED IN THE SUPECODUCTING VANADIUM MAGNETIZATION DUE TO PROXIMITY WITH THE FERROMAGNET IRON LAYER

*Khaydukov Yu.N.<sup>1,2</sup>, Nagy B.<sup>3</sup>, Zhernenkov K.N.<sup>4</sup>, Nikitenko Yu.V.<sup>5</sup>, Bottyan L.<sup>3</sup>, Aksenov V.L.<sup>2,5</sup>*

<sup>1</sup> Max-Planck Institute for Solid State Research, D-70569 Stuttgart, Germany

<sup>2</sup> Lomonosov Moscow State University, 119992 Moscow, Russia

<sup>3</sup> KFKI Research Institute for Particle and Nuclear Physics, Budapest, Hungary

<sup>4</sup> Ruhr-Universität Bochum, D 44780, Bochum, Germany

<sup>5</sup> Joint Institute for Nuclear Research, 141980 Dubna, Russia

Penetration of the superconducting order parameter inside ferromagnet metal in superconducting/ferromagnet (S/FM) heterostructures is classically called proximity effect. Theoretically was also predicted inverse proximity effect - the appearance of the induced magnetization in S layer near the S/FM interface. This effect is discussed in various theoretical works, where it is shown that the induced magnetization can have both positive and negative sign to the magnetization in the FM layer [1-3].

Here we present the first results of the Polarized Neutron Reflectometry (PNR) studies of the S/FM bilayer with composition V(40nm)/Fe(1nm). Shift of the oscillation of the experimental neutron spin asymmetries  $(R^{++}-R^{-})/(R^{++}+R^{-})$  was observed when temperature decreased below the superconducting transition temperature ( $T_c=3.8$  K) of the vanadium layer. Such a shift can only be explained by the appearance of a new magnetic sub-layer in the S layer close to the S/FM interface. Magnetization in this sub-layer is parallel to the magnetization of the FM layer and makes value of about 5% of it. This observation agrees qualitatively with the predictions of the theory [1,2].

This work was supported by grants RFBR (№ 09-02-00566) and JINR-HAS (EAI-2009/002)

[1] V.N. Krivoruchko and E.A. Koshina, Phys. Rev. B 66, 014521 (2002)

[2] F.S. Bergeret, A.F. Volkov and K.B. Efetov, Phys.Rev. B 69, 174504 (2004)

[3] F.S. Bergeret, A. Levy Yeyati and A. Martin-Rodero, Phys. Rev. B 72, 064524 (2005)

23TL-G-5

## QUANTUM FLUCTUATIONS AND CLUSTERING OF FLUCTUATION COOPER PAIRS

*Glatz A.<sup>1</sup>, Varlamov A.A.<sup>1,2</sup>, Vinokur V.M.<sup>1</sup>*

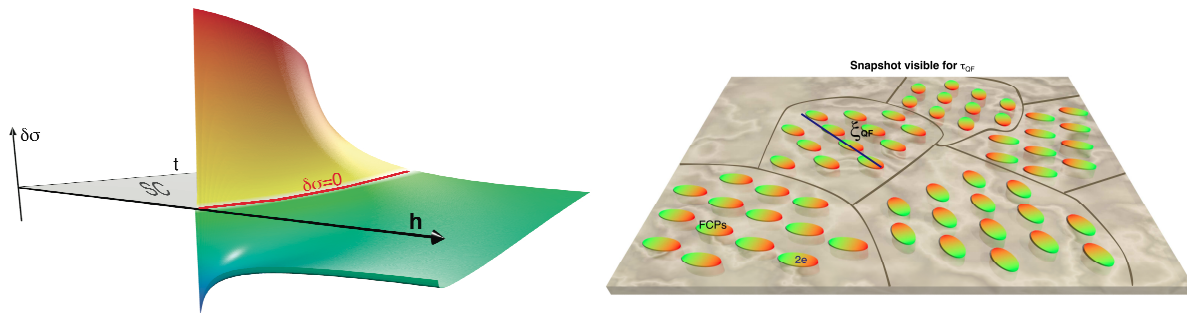
<sup>1</sup> Materials Science Division, Argonne National Laboratory, 9700 S.Cass Avenue,  
Argonne II 60439, USA

<sup>2</sup> CNR-SPIN, Viale del Politecnico 1, I-00133 Rome, Italy

The understanding of the mechanisms of superconducting fluctuations (SF), achieved during the past decades provided a unique tool obtaining information about the microscopic parameters of superconductors (SC). We derive the complete expression for fluctuation conductivity (FC) of two dimensional superconductors as a function of temperature and magnetic field valid in the whole phase diagram above the upper critical field line  $H_{c2}(T)$ . Corresponding surface  $\delta\sigma_f(T, H)$  is

shown in Fig. 1. Its striking feature consists of the fact, that the FC is positive only in the domain bound by the separatrices  $H_{c2}(T)$  and  $\delta\sigma_{fl}(T, H) = 0$  and is negative throughout all other parts of the phase diagram. Contrary to the common assumption, the FC is only positive in the domain of weak fields and temperatures above  $T_{c0}$ , the region of positive corrections depends on the magnitude of the positive anomalous MT contribution (i.e. on the value of the phase-breaking time  $\tau_\phi$ ). With increasing magnetic field, the interval of temperatures where  $\delta\sigma_{fl}(T, H) > 0$  shrinks and becomes zero close to  $H_{c2}(0)$ . In particular at low temperatures, the behavior of the FC turns out to be highly non-trivial. In this case, the surface  $\delta\sigma_{fl}(T, H)$  has a trough-shaped character and the dependence  $\delta\sigma_{fl}(T, H = const)$  is non-monotonic.

Focusing on the vicinity of the quantum phase transition near zero temperature we arrive to the conclusion that as the magnetic field approaches the critical field  $H_{c2}(0)$  from above, a peculiar dynamic state consisting of clusters of coherently rotating fluctuation Cooper-pairs forms (see Fig. 2). We estimate the characteristic size  $\xi_{QF}(H) = \xi_{BCS} / \sqrt{(H - H_{c2}) / H_{c2}}$



and lifetime  $\tau_{QF}(h) \sim \frac{\hbar \Delta_{BCS}^{-1}}{(H - H_{c2}(0)) / H_{c2}(0)}$  of such clusters and indicate in the corresponding domain of the phase diagram, where such phenomenon can be observed. The derived values  $\xi_{QF}(H)$  and  $\tau_{QF}(H)$  allow us to reproduce qualitatively the available results for the quantum fluctuation contributions to the in-plane conductivity, magnetization, and the Nernst coefficient. Finally we predict the existence of a peak in the zero temperature transverse magneto-conductivity of layered superconductors at fields above  $H_{c2}(0)$ .

23TL-G-6

## OBSERVATION OF ANDREEV BOUND STATES AT SPIN-ACTIVE INTERFACES

*Beckmann D.<sup>1</sup>, Hübler F.<sup>1,2</sup>, Wolf M.J.<sup>1</sup>, von Löhneysen H.<sup>2,3</sup>*

<sup>1</sup> KIT, Institute of Nanotechnology, Karlsruhe, Germany

<sup>2</sup> KIT, Institute of Solid State Physics, Karlsruhe, Germany

<sup>3</sup> KIT, Physikalisches Institut, Karlsruhe, Germany

Spin-active interfaces between superconductors and ferromagnets are characterized by spin-dependent transmission amplitudes as well as the relative phase shift  $\theta_s$  between spin up and down [1]. While  $\theta_s$  is an important parameter for induced triplet superconductivity at spin-active interfaces, little quantitative information is available about  $\theta_s$  so far. Recent theoretical models indicate that  $\theta_s$  may actually be quite large in structures with ultra-thin tunnel barriers [2]. One of the consequences of finite  $\theta_s$  in S/F hybrids is the presence of bound states at the interface [3]. We

report here the experimental observation of Andreev bound states in Al/Al<sub>2</sub>O<sub>3</sub>/Fe structures [4]. From the energy  $\varepsilon = \pm \Delta \cos(\theta_s/2)$  of the bound states, we can determine  $\theta_s$  with great accuracy. As predicted theoretically, we find examples of  $\theta_s \approx \pi$ , but also a significant spread from contact to contact, even within the same fabrication batch. The large spread indicates the subtle dependence of  $\theta_s$  on microscopic details of the interface.

- [1] Millis et al., Phys. Rev. B **38**, 4504 (1988).  
 [2] Grein et al., Phys. Rev. B **81**, 094508 (2010).  
 [3] Zhao et al., Phys. Rev. B **70**, 134510 (2004).  
 [4] Hübner et al., arXiv:1012.3867.

23TL-G-7

## TRIPLET SUPERCONDUCTIVITY IN A FERROMAGNETIC VORTEX

*Kalenkov M.S.<sup>1</sup>, Zaikin A.D.<sup>2</sup>, Petrashov V.T.<sup>3</sup>*

<sup>1</sup>I.E.Tamm Dept. of Theoretical Physics, P.N.Lebedev Physics Institute, 119991 Moscow, Russia

<sup>2</sup>Institute of Nanotechnology, Karlsruhe Institute of Technology, 76021 Karlsruhe, Germany

<sup>3</sup>Department of Physics, Royal Holloway, University of London, Surrey TW200EX, UK

A normal metal (N) sandwiched between two superconductors (S) goes superconducting as a result of penetration of Cooper pairs from S to N side. The range of penetration is relatively long and reaches several micrometers at low enough temperatures. This situation changes drastically provided a normal metal is replaced by a ferromagnet (F): Quantum mechanical exchange interaction on the F-side destroys spin-singlet Cooper pairs within a very short range of a few nanometers thereby suppressing conventional proximity-induced superconductivity in the ferromagnet. Despite that several experimental groups [1] reported on unexpectedly strong superconducting proximity effect in SF-structures. Later it was realized [2] that this behavior can be associated with triplet superconductivity that is compatible with the exchange interaction in a ferromagnet with non-uniform magnetization.

In this work we consider a novel situation of long range triplet pairing in ferromagnets with magnetic vortex structure. Employing quasiclassical formalism of Usadel equations we demonstrate that triplet Cooper pairs can penetrate deep into a ferromagnetic vortex and evaluate dc Josephson current in SFS-junctions containing such a vortex. We argue that the effect is well in the measurable range and can be detected in modern experiments.

[1] V. T. Petrashov et al., JETP Lett. **59**, (1994) 523; Phys. Rev. Lett. **83**, (1999) 3281; M. Giroud et al., Phys. Rev. B **58**, (1998) R11872; J. Aumentado and V. Chandrasekhar, Phys. Rev. B **64**, (2001) 054505.

[2] F.S. Bergeret, A.F. Volkov, and K.B. Efetov, Phys. Rev. Lett. **86**, (2001) 4096; A. Kadigrobov, R.I. Shekhter, and M. Jonson, Europhys. Lett. **54**, (2001) 394.

## DENSITY OF STATES MINIGAP IN A SUPERCONDUCTOR – FERROMAGNET JUNCTION

*Vasenko A.S.<sup>1,2</sup>, Golubov A.A.<sup>3</sup>, Kupriyanov M.Yu.<sup>4</sup>, Lacroix C.<sup>5</sup>*

<sup>1</sup> Institut Laue-Langevin, 6 rue Jules Horowitz, BP 156, 38042 Grenoble, France

<sup>2</sup> Department of Physics, Moscow State University, Moscow, 119992, Russia

<sup>3</sup> Faculty of Science and Technology and MESA+ Institute for Nanotechnology,  
University of Twente, 7500 AE Enschede, The Netherlands

<sup>4</sup> Nuclear Physics Institute, Moscow State University, Moscow, 119992, Russia

<sup>5</sup> Institut Néel, Université Joseph Fourier and CNRS, 25 avenue des Martyrs, BP 166,  
38042 Grenoble, France

In last years there was an intense activity in studying the so called superconducting proximity effect in the superconductor (S) – normal metal (N) and superconductor – ferromagnet (F) hybrid structures [1]. It manifests itself in superconducting correlations penetration into non-superconducting material due to the mechanism of Andreev reflection, when electron is reflected as a hole at the interface of superconductor with other material, with corresponding formation of the Cooper pair inside the superconductor.

One way to probe the superconducting proximity effect is to study the density of states (DOS) in SN and SF hybrid structures. It is well known that the DOS on the free boundary of the normal metal layer of a SN bilayer exhibits the minigap, which is a manifestation of the superconducting proximity effect. The characteristic scale of the minigap is set by the Thouless energy  $E_{Th} = D/d^2$  [2], where  $D$  is the diffusion coefficient in the normal metal and  $d$  is the thickness of the normal metal layer.

In this work we study the behaviour of the minigap in SF bilayers with respect to the parameters of the ferromagnetic metal. We can model the ferromagnet with just a single parameter – the exchange field  $h$ . It shifts the DOS for the two spin subbands in the ferromagnet in opposite directions, and therefore the critical value  $h_c$  of the exchange field at which the minigap in the spectrum closes can be roughly estimated as  $h_c \sim E_{Th}$  [3].

We have checked this prediction by self-consistent numerical calculation of the DOS in a SF bilayer and found that it is in a good agreement with our data,  $h_c \approx 0.77 E_{Th}$  [4]. However, this estimation will be different if we take into account other parameters of ferromagnetic metal. In this work we study the influence of the magnetic scattering parallel (perpendicular) to the quantization axis, and the spin-orbit scattering.

[1] A. I. Buzdin, *Rev. Mod. Phys.*, **77** (2005) 935.

[2] A.A. Golubov and M.Yu Kupriyanov, *J. Low Temp. Phys.*, **70** (1988) 83; A.A. Golubov and M. Yu. Kupriyanov, *Sov. Phys. JETP*, **69** (1989) 805.

[3] R. Fazio and C. Lucheroni, *Europhys. Lett.*, **45**, (1999) 707.

[4] A.S. Vasenko, S. Kawabata, A.A. Golubov, M.Yu. Kupriyanov, C. Lacroix, F.S. Bergeret, and F.W.J. Hekking, unpublished (arXiv: 1101.0361).

23OR-G-9

## CURRENT-PHASE RELATION IN JOSEPHSON JUNCTIONS WITH COMPLEX FERROMAGNETIC/NORMAL METAL INTERLAYER

*Klenov N.<sup>1</sup>, Bakursky S.<sup>1</sup>, Karminskaya T.<sup>2</sup>, Kupriyanov M.<sup>2</sup>*

<sup>1</sup> Physics Department Moscow State University Leninskie Gory, GSP-1, Moscow 119991, Russian Federation

<sup>2</sup> Institute of Nuclear Physics Moscow State University, Leninskie Gory, GSP-1, Moscow 119991, Russian Federation

It is well known that critical current across a Josephson junction with ferromagnetic spacer may oscillate as a function of the ferromagnetic layer thickness, thus providing an existence of Josephson structures with negative critical current, so-called  $\pi$ -junctions [1-3]. In some classical and quantum Josephson circuits it is even more interesting to create  $\varphi$ -junctions, the structures having in the ground state phase difference  $\varphi$ , ( $0 < \varphi < \pi$ ) between superconducting electrodes.

In order to have a  $\varphi$ -junction the current-phase relation (CPR)  $I_S(\varphi) = A \sin(\varphi) + B \sin(2\varphi)$  should at least contain  $\sin(2\varphi)$  contribution. Moreover the amplitude of the second harmonic must obey the conditions  $|B| > A/2$ ,  $A > 0$ ,  $B < 0$ .

In this paper we have analysed several types of SFS and SIFIS sandwiches and have found that in practically interesting range of temperatures  $T \ll 0.1T_c$  the formulated above conditions cannot be realized.

However, we have demonstrated that for the recently proposed S-NF-S variable thickness bridges [4], it is possible to choose the junction geometry providing both  $0$ - $\pi$  transition and nonsinusoidal CPR. The areas of structure parameters which ensure the  $\varphi$ -junction existence in these structures are determined and classified.

Support by RFBR grant 10-02-90014-Бел-а and 10-02-00870-а, FTP GK 14.740.11.0065 is acknowledged.

[1] A.A. Golubov, M. Yu. Kupriyanov, and E. Il'ichev, *Rev. Mod. Phys.*, **76** (2004) 411.

[2] A.I. Buzdin, *Rev. Mod. Phys.*, **77**, (2005) 935.

[3] F.S. Bergeret, A. F. Volkov, K. B. Efetov, *Rev. Mod. Phys.*, **77** (2005) 1321.

[4] T.Yu.Karminskaya, A.A.Golubov, M.Yu.Kupriyanov, A.S.Sidorenko, *Phys. Rev. B* **79**, (2009) 214509.

23RP-G-10

## SOLITARY REENTRANT SUPERCONDUCTIVITY IN ASYMMETRICAL FSF STRUCTURES

*Proshin Yu.<sup>1</sup>, Khusainov M.<sup>2</sup>*

<sup>1</sup> Kazan Federal University, Kremlevskaya, 18; Kazan 420008, Russia

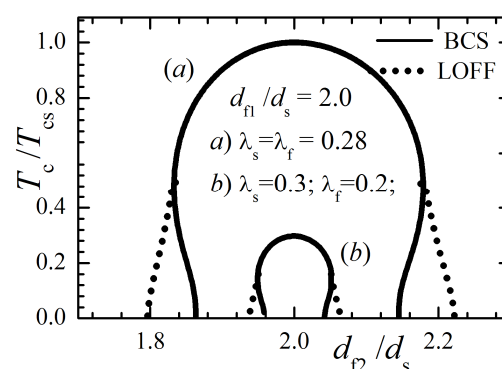
<sup>2</sup> Kazan State Power Engineering University, Krasnosel'skaya, 51; Kazan 420066, Russia

Solving the boundary value problem for the Eilenberger function, the superconducting and magnetic states of asymmetric ferromagnet-superconductor-ferromagnet ( $F_1SF_2$ ) nanostructures are

investigated. Superconductivity in the FS nanostructures is a superposition of the Bardeen-Cooper-Schrieffer (BCS) pairing with zero total momentum in the S layers and the Fulde-Ferrell-Larkin-Ovchinnikov (FFLO) pairing with nonzero three-dimensional coherent momentum in the F layers. As a rule a superconductivity occurs at  $d_f \leq d_s$ , where  $d_{f(s)}$  is the F(S) layer thickness. The typical case is the layered Gd/Nb and Fe/V structures [1]. However, the 3D superconductivity in the Gd-La superlattice not only exists at  $d_f > d_s$ , but it appears at  $T_c$  equal to the critical temperature of a bulk lanthanum sample  $T_{cs}$  [2].

It is shown that magnetic and superconducting states of pure thin  $F_1SF_2$  trilayers are controlled by the magnitude and sign of electron correlations in the  $F_1$  and  $F_2$  layers, as well as by the competition between homogeneous BCS pairing and inhomogeneous LOFF pairing. The LOFF-BCS-LOFF solitary reentrant superconductivity is predicted for  $F_1SF_2$  trilayers. A continuous control of the pair-breaking factor in the Eilenberger function and transition to the state with reentrant superconductivity is achieved by varying the thickness of the  $F_2$  layer. Sine-modulated 2D LOFF states in asymmetric  $F_1SF_2$  trilayers are possible not only for parallel, but also for antiparallel orientations of the magnetizations of the  $F_1$  and  $F_2$  layers; this fact significantly facilitates the experimental implementation of the predicted phenomena.

For the experimental observation of the predicted solitary reentrant superconductivity with the LOFF-BCS-LOFF competition, we propose the asymmetric Gd-La-Gd' trilayer system. Indeed, in the work [3], we have found that electron-electron interactions in the Gd-La superlattices with  $T_c = T_{cs} = T_{cLa} = 5K$  [2] are the same, i.e.  $\lambda_s = \lambda_f = 0.28$ , and the superconductivity exists at any ratio of the thicknesses  $d_f$  and  $d_s$ . The critical temperature dependencies with solitary reentrant peak is shown in Figure. At calculations we use "clean" limit with ideal transparent interfaces as in work [3].



The work was partially supported by the RFBR (No 09-02-01521) and by the Ministry of Education and Science of the Russian Federation.

- [1] Y.A. Izyumov, Yu.N. Proshin, M.G. Khusainov *Physics/Uspekhi*, **45** (2002) 109.
- [2] P.P. Deen, J.P. Goff, R.C.C. Ward, et al., *et al. J. Phys.: Cond. Matt.*, **17** (2005) 3305.
- [3] M.G. Khusainov, M.M. Khusainov, N.M. Ivanov, Yu.N. Proshin *JETP Lett.*, **90** (2009) 124.



23OR-G-11

## SUPERCONDUCTING PROBE OF ELECTRON CORRELATIONS AND EXCHANGE FIELD BASED ON THE PROXIMITY EFFECT IN THE F/S NANOSTRUCTURES

*Khusainov M.<sup>1</sup>, Proshin Yu.<sup>2</sup>*

<sup>1</sup> Kazan State Power Engineering University, Krasnosel'skaya, 51; Kazan 420066, Russia

<sup>2</sup> Kazan Federal University, Kremlevskaya, 18; Kazan 420008, Russia

The proximity effect in the ferromagnet/superconductor (F/S) nanostructures is microscopically investigated on base a three-dimensional boundary value problem for the Eilenberger function. The superconductivity in these systems is the superposition of the BCS pairing with zero total momentum in the S layers and the pairing through the Larkin–Ovchinnikov–Fulde–Ferrell (LOFF) mechanism with nonzero 3D momentum of pairs  $\mathbf{k}$  in the F layers [1]. It is shown that continuous matching at the F/S interface occurs only for the pair amplitudes with the same space symmetry. When two pairing types are simultaneously present, the processes of mutual transformations between LOFF and BCS pairs at the F/S interface occur as Umklapp processes through surface states. The phase diagrams of the surface states with the mixed BCS + LOFF pairing type are analyzed. Superconductivity localized at the F/S interface is predicted. The competition between the BCS and LOFF states are studied in the Cooper limit for thin F/S and F/S/F nanostructures. The dependences of the critical temperature on the exchange field  $I$ , electron correlations  $\lambda_f$ , and the thickness  $d_f$  of the F layer are derived for F/S bilayers and F/S/F trilayers. In addition, two new  $\pi$ -phase superconducting states with electron–electron repulsion in the F layers of F/S/F trilayers are predicted. A two-dimensional LOFF state in F/S/F trilayers is possible only in the presence of a weak magnetic field and the appropriate parameters of the F and S layers. The absence of the suppression of three-dimensional superconductivity in short-period Gd/La superlattices is explained and the electron–electron coupling constant in gadolinium is predicted. A method of superconducting sounding spectroscopy based on the proximity effect is proposed for determining the symmetry of the order parameter, the magnitude and sign of electron correlations, and the exchange field in various nanomagnets F.

The work was partially supported by the RFBR (No 09-02-01521) and by the Ministry of Education and Science of the Russian Federation.

[1] Y.A. Izyumov, Y.N. Proshin, M.G. Khusainov *Physics/Uspekhi*, **45**, (2002) 109.

[2] P.P. Deen, J.P. Goff, R.C.C. Ward, et al., *et al. J. Phys.: Cond. Matt.*, **17** (2005) 3305.

[3] M.G. Khusainov, M.M. Khusainov, N.M. Ivanov, Yu.N. Proshin *JETP Lett.*, **90** (2009) 124.

23RP-G-12

## JOSEPHSON SPECTROSCOPIC OBSERVATION OF FERROMAGNETIC RESONANCES

*Petkovic I.<sup>1</sup>, Aprili M.<sup>1</sup>, Barnes S.E.<sup>2</sup>, Maekawa S.<sup>3</sup>*

<sup>1</sup>Laboratoire de Physique des Solides, Bât. 510, Université Paris-Sud, 91405 Orsay Cedex, France.

<sup>2</sup>Physics Department, University of Miami, Coral Gables, 33124 FL, USA

<sup>3</sup>Advanced Science Research Center, Japan Atomic Energy Agency, Tokai, Ibaraki 319-1195, and CREST, Japan Science and Technology Agency, Tokyo 102-0075, Japan

Singlet superconductivity and ferromagnetism are antagonistic states of matter that tend to avoid one another. The challenge addressed here is that of dynamically coupling these two seemingly incompatible order parameters. The Josephson coupling in a superconducting-ferromagnetic-superconducting sandwich measures the ability of Cooper pairs to survive in the hostile ferromagnetic environment, and indeed we find the spin singlet pairs from Nb decay, at least, four times more rapidly in ferromagnetic Pd<sub>0.9</sub>Ni<sub>0.1</sub> than in the normal metal Pd.

For our magnetic junctions, the ferromagnetic resonance dynamics are coupling to those of the superconductor phase. Within the Fraunhofer interferential description of the Josephson effect, the magnetic layer acts as a time dependent phase plate. As shown in Fig.1, a magnetic resonance, of frequency  $\omega_s$  appears as a depression in the current-voltage curve when  $\hbar\omega_s = 2eV_s$  [1]. We have also investigated the possibility of measuring the dispersion of such spin-waves by varying the magnetic field applied in the plane of the junction and demonstrated the electromagnetic nature of the coupling by the observation of magnetic resonance side-bands to microwave induced Shapiro steps [2].

In the spintronics context we have thereby demonstrated the excitation of the magnetic system via singlet supercurrent and otherwise have performed a resonance experiment on about 10 millions of Ni atoms.

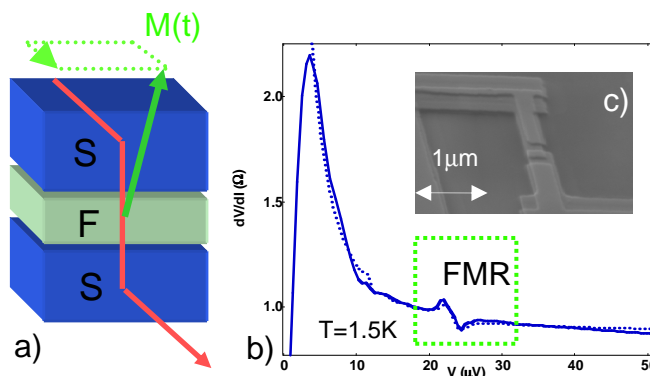


Fig.1 a) Schematic of the experiment : the AC-Josephson effect excites ferromagnetic resonance (FMR) b) Measure of the derivative of the I-V characteristics showing a resonance at the FMR frequency. c) SEM picture of the Nb/PdNi/Nb ferromagnetic Josephson junction.

Support by ANR-DYCOSMA, CREST of JST, and EPSRC (UK) is acknowledged.

[1] I. Petkovic et al., *Phys. Rev. B* **80**, (2009) 220502.

[2] S.E. Barnes et al., *Supercond. Sci. Technol.* **24** (2011) 024020.

**23 August**

Tuesday

11:30-13:00

14:30-17:20

oral session

23TL-H

23RP-H

23OR-H

**“Micromagnetics”**

23TL-H-1

**CURRENT-DRIVEN VORTEX DYNAMICS IN METALLIC NANOCONTACTS***Hrkac G.<sup>1</sup>, Schrefl T.<sup>1</sup>, Kim J.-V.<sup>2</sup>, Devolder T.<sup>2</sup>, Chappert C.<sup>2</sup>, Lagae L.<sup>3</sup>, Manfrini M.*<sup>1</sup> Department of Engineering Materials, University of Sheffield, Sheffield S1 4DU, United Kingdom<sup>2</sup> Institut d'Electronique Fondamentale, UMR CNRS 8622, Universite' Paris-Sud,  
91405 Orsay cedex, France<sup>3</sup> IMEC, Kapeldreef 75, B-3001 Leuven, Belgium

Lateral confinement in magnetic nanostructures leads to the appearance of complex magnetic states. One important example concerns the magnetic vortex, which arises in patterned structures from competing exchange and dipolar interactions. The dynamics of such vortices is largely governed by the confining potential which defines them. Recent experiments have shown resonance phenomena to be possible with such vortices, including sub-GHz excitations, below the usual ferromagnetic resonance frequency, which involve the spiralling motion of the vortex core about its equilibrium position.

Recently, it has been shown experimentally that magnetic vortices can be brought into a selfoscillatory state [1]. This is made possible with the spin-transfer effect, whereby spinangular momentum is transferred between a spin-polarized current and magnetization in a multilayer. It is well-known that spintransfer leads to an additional torque on magnetization, and it has been demonstrated that this effect can lead to steady-state vortex oscillations in nanopillars [1].

In this paper, we performed full micromagnetics simulations of metallic nano-contacts from the TUNAMOS consortium, by solving the Landau Lifshitz Gilbert Slonczewski equation simultaneously with quasi-static Maxwell equations. We take into account the spatially inhomogeneous current distribution flowing through the magnetic free layer and consequently use the Oersted field generated by this current for the magnetization dynamics.

The system we simulated was a trilayer CoFe 3.5 nm/Cu 3nm/NiFe 4nm stack. The saturation magnetization of the free layer is taken to be the same as the experimental value  $M_s = 1.1$  T, and a GMR ratio of 1% is used. We account for the inhomogeneous current distribution flowing through the free layer by computing the local current density from the local angle between the free and fixed layer magnetizations. The Oersted field is computed with the Biot-Savart law from this current distribution [2], and an asymmetric Slonczewski term for the spin transfer is used [3].

The system is discretized with a finite element method with a linear basis function and a discretization size of 4 nm, which is below the exchange length of 4.5 nm. An exchange bias field of 162 mT is applied to the reference CoFe layer to simulate pinning in the experimental stacks.

We observe that the additional spin torque drives the vortex out of the contact area and towards a stable orbit around the contact. These simulations reveal that the oscillations observed are related to the large-amplitude translational motion of a magnetic vortex. In contrast to the nanopillar geometry in which the vortex core precesses within the confining part of the Oersted field [1], the dynamics here correspond to an orbital motion outside the contact region. This behaviour can be likened to planetary orbital motion under the influence of a gravitational field; the spin-transfer torque leads to a centripetal motion of the vortex core, which is counterbalanced by the attractive potential provided by the Oersted field. Good quantitative agreement between the simulation and experimental frequencies is achieved [4]. The stability of the vortex has also been investigated using simulations. For small in-plane fields (<10 mT), a small blueshift in the frequency is observed.

This leads to an asymmetry in the field profile relative to the vortex structure and results in an elliptical motion of the vortex orbit. We have also verified in simulation that larger in-plane fields lead to a breakdown of the vortex structure. Further more we investigate the phenomena of possible

phase locking of two vortices in double/multiple point contact system and show that its field and current dependent frequency shift.

This work was supported by the European Communities programs IST STREP, under Contract No. IST-016939, the Royal Society UK and the WWTF.

[1] V. S. Pribiag et al., Nat. Phys. **3**, 498 (2007)

[2] O. Ertl *et al.*, J. Appl. Phys. **99**, 08S303 (2006).

[3] J. Xiao, A. Zangwill, and M. D. Stiles, Phys. Rev. B **70**, 172405 (2004).

[4] Q. Mistral, M. van Kampen, G. Hrkac, et al. PRL **100**, 257201 (2008)

23TL-H-2

## **INSTABILITIES OF A SPIN VALVE SYSTEM WITH PERPENDICULAR POLARIZER AND IN PLANE BIAS FIELD**

*Chang C.-R., Chang J.-H., Chen H.-H.*

Department of Physics and Center for Quantum Sciences and Engineering, National Taiwan University, Taipei 10617, Taiwan

Electronic address: crchang@phys.ntu.edu.tw, d95222013@ntu.edu.tw

For a spin-transfer-torque (STT) magnetic random access memory with a perpendicular polarizer and an in-plane (IP) bias field, a three dimensional modified asteroïd of critical strength of STT and field is derived. The modified asteroïds not only separate the multiple stable states from the single state, but also delimits the region with dynamical precessional states for STT over a critical value. Taking into account of STT, the nucleation field, coercivity, and precessional critical field for uniaxial anisotropy are rigorously determined, and the hysteresis loops for various orientation of a bias field are computed and discussed.

23TL-H-3

## **LOCALIZED AND PROPAGATING MODES FOR SPIN-TORQUE INDUCED MAGNETIC EXCITATIONS IN STRUCTURES WITH DIFFERENT DIMENSIONALITIES**

*Berkov D.V., Gorn N.L.*

Innovent Technology Development, Pruessingstr. 27B, D-07745, Jena, Germany

In this contribution we present the overview of various kinds of magnetization excitations induced by the spin transfer torque in nanodevices of various dimensionalities.

First, we briefly review simulation results for nanopillar stacks, comparing them with experimental findings. We demonstrate that already in these systems with very small lateral sizes (~ 100 nm) modes with different localization are possible. Transitions between these modes manifest themselves in discontinuities of frequency and power as functions of the current strength.

We proceed with numerical analysis of experiments in a so called point-contact geometry, where current is flowing through a nanocontact (with the diameter of several tens of nanometers) attached to a stack of extended magnetic layers. Compared to nanopillar devices, these systems demonstrate a much more complicated dynamics. Sophisticated numerical simulation analysis of experimental observations reveals that such a complexity is due to the excitation of several qualitatively different kinds of non-linear localized modes. In particular, for various experimental geometries a relatively homogeneous ‘bullet’ mode, vortex precession mode, vortex-antivortex (V-AV) pairs and even more complicated modes governed by creation and annihilation of several vortex-antivortex pairs (Fig. 1) have been found.

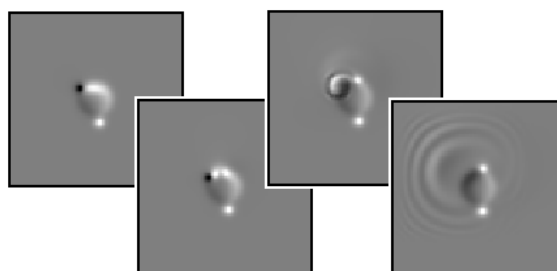


Fig. 1. Creation and annihilation of an additional V-AV pair during the oscillation of the already present V-AV pair in an extended Py layer subject to the current injection via a point contact (CPP-geometry).

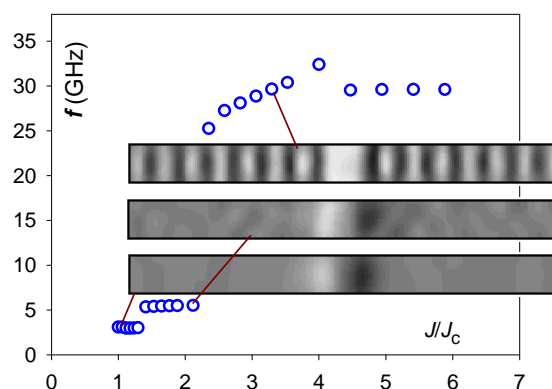


Fig. 2. Localized and propagating oscillation modes in a Py nanowire for the out-of-plane field  $H=10$  kOe. Current is injected via a FM point contact placed above the nanowire.

Finally, we present simulation results obtained for a Permalloy nanostripe with the ferromagnetic point contact placed on the top of it. We show that also in this system both localized and propagating modes are possible. For the external field directed in the nanostripe plane only localized modes have been observed, which localization is due to the stray field of the FM point contact. For sufficiently strong out-of-plane fields also a propagating mode can exist. This circumstance can be employed for the synchronization of many point contacts (placed along a nanostripe) due to a relatively weak attenuation of a propagating wave in this quasi-1d structure.

23RP-H-4

## NEW MICROMAGNETIC METHODOLOGY FOR SIMULATIONS OF NANOCOMPOSITES

*Erokhin S.<sup>1</sup>, Berkov D.<sup>1</sup>, Gorn N.<sup>1</sup>, Michels A.<sup>2</sup>*

<sup>1</sup> INNOVENT e.V., Pruessingstr. 27B, D-07745 Jena, Germany

<sup>2</sup> Laboratory for the Physics of Advanced Materials, University of Luxembourg, 162A, Avenue de la Faiencerie, BS 1.13, L-1511 Luxembourg

We developed a new micromagnetic methodology for numerical simulations of magnetic nanocomposites, which allows to calculate the magnetization distribution of a nanocrystalline material and the corresponding small-angle neutron scattering (SANS) cross-section.

The object of our interest is a nanocomposite of the Nanoperm type [1], which consists of the iron-based crystallites with typical size of 10 nm, embedded in an amorphous soft magnetic matrix. This alloy with high permeability shows the unusual angular anisotropy in the SANS cross-section. In order to prove that this phenomenon can be attributed to the magnetic structure, it is necessary to perform numerical simulations on the micromagnetic level.

The micromagnetic modelling of nanocomposites and its SANS calculations are rare [2-4], because finite difference and finite elements approaches are not really suitable for large-scale simulations of nanocomposites.

The basic components of our new method are:

(a) Generation of the mesh consisting of polyhedral finite elements, using the model of interacting spheres with short-ranged potential. This procedure assures that the shape of each polyhedron is close to spherical and that their spatial arrangement is random.

(b) Calculation of the magnetodipolar energy in the dipolar approximation. This approximation is exact only for spherical particles, but in our case, where the shape of polyhedra is close to spherical, its accuracy is sufficient.

(c) The exchange interaction is computed using the standard Heisenberg form, where the exchange constant is proportional to the volumes of neighbouring finite elements and the spacing between their centres.

SANS cross-sections, calculated from the Fourier components of simulated magnetization distributions [1], reproduce very well the experimentally measured data. This finding completely confirms that the reason for the novel effect described above is the jump in the magnetization on the phase boundary of each crystallite.

Support by DFG under the project BE 2464/10-1 is acknowledged.

[1] A. Michels, C. Vecchini, O. Moze, K. Suzuki, P.K. Pranzas, J. Kohlbrecher and J. Weissmüller, *Phys. Rev. B*, 74, 134407 (2006).

[2] J.F. Löffler, H.B. Braun, W. Wagner, G. Kostorz and A. Wiedenmann, *Phys. Rev. B*, 71, 134410 (2005).

[3] F.Y. Ogrin, S.L. Lee, M. Wismayer, T. Thomson, C.D. Dewhurst, R. Cubitt, and S.M. Weekes, *J. Appl. Phys.*, 99, 08G912 (2006).

[4] S. Saranu, A. Grob, J. Weissmüller, and U. Herr, *phys. stat. sol. (a)*, 205, 8, 1774 (2008).

23OR-H-5

## PERIODIC BOUNDARY CONDITIONS FOR SMALL ARRAYS OF MAGNETIC NANO-ELEMENTS

*Dmytriiev O.*

School of physics, University of Exeter, Exeter EX4 4QL, UK

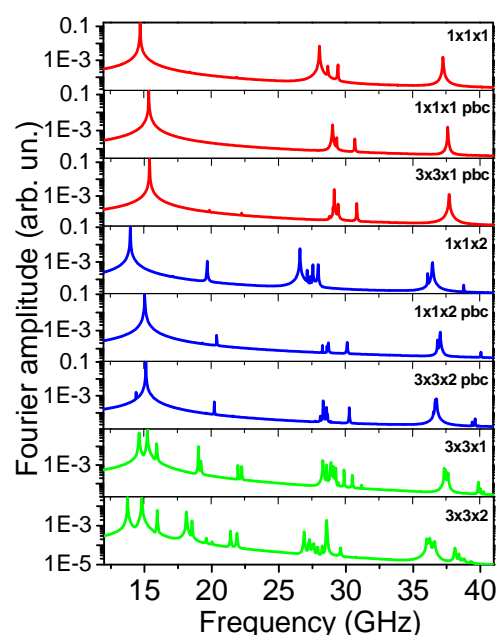
The recent advances in nanofabrication techniques have stimulated interest in studying static and dynamical properties of artificial magnetic periodic structures (magnonic crystals). Propagating and confined spin waves in such structures are a subject of one of the most recently emerged areas of modern magnetism - magnonics [1].

Due to the complex nanoscale structure of the internal field and magnetization in and the large total sizes of such objects, the determination of their magnonic spectrum is a challenging task for both analytical and micromagnetic means. One of the possibilities to circumvent the large demands on computational power in micromagnetic simulations of such objects is to use periodic boundary conditions (pbc) – extending the structure by creating virtual copies (finite and infinite number; we will consider only finite one) of some part of the array. Periodic boundary conditions have been used recently for studying standing-spin-waves resonances in the quasi-infinite arrays of antidots [2].

Although pbc allow to take correctly into account the dipole field inside of array which is a part of larger one but, generally, they give different results if we consider ‘real’ array of the same size as we obtained with using pbc. Pbc are inevitable if we want to study large (micrometer size) arrays but nobody has done systematic studies and comparison of the results obtained for the arrays with pbc and ‘real’ arrays of comparable sizes.

We report on systematic study of the spectrum of confined spin wave excitations in a single ferromagnetic disk, tri-layer (ferromagnetic disk/nonmagnetic one/ferromagnetic disk) and 3x3 their arrays with use pbc and not. We showed that the use of pbc for a single disk and a tri-layer leads only to the blue shift of the frequencies in the spectrum but not to modification of it. The use of pbc for 3x3x1 and 3x3x2 arrays leads to modification of the spectrum structure and mode profiles: they get similar to the ones in single elements and to appearance of additional mode in 3x3x2 array with pbc not typical for finite arrays.

On the figure: the spectrum of spin wave excitations in a single disk, tri-layer, 3x3 arrays of them with and without pbc in log scale along ordinate axis. Bias magnetic field  $H_{\text{bias}} = 2.5 \text{ kOe}$  is applied in the plane of the disks.



The research leading to these results has received funding from the European Community's Seventh Framework Programme (FP7/2007-2013) under Grant Agreements n°233552 (DYNAMAG)

[1] V.V. Kruglyak, S.O. Demokritov, and D. Grundler, *J. Phys. D*, **43**, 264001 (2010).

[2] S. Neusser, B. Botters, and D. Grundler, *Phys. Rev. B*, **78**, 054406 (2008).



23OR-H-6

## NUCLEATION OF MICROMAGNETIC AND DOMAIN STRUCTURES IN FERRITE-GARNET CRYSTALS

*Pamyatnykh L.A., Shmatov G.A., Pamyatnykh S.Y., Kandaurova G.S.*  
Ural State University, 620083, Yekaterinburg, Lenin Av., 51, Russia

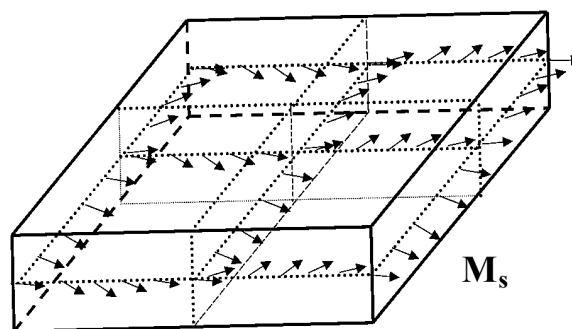
The process of nucleation of micromagnetic and domain structures with various spatial configurations in the area of orientational phase transition of the second kind on magnetic field is considered.

Experimental study of domain structure nucleation was performed in magnetic field parallel to the plane of 50  $\mu\text{m}$  thick sample-plates-(001), cut from  $(\text{EuEr})_3(\text{FeGa})_5\text{O}_{12}$  single crystal. Domain structure was revealed by means of magneto-optic Faraday effect.

It was established that at decrease of magnetic field the process of nucleation starts with formation of 2-dimensional low contrast structure. With farther decrease of magnetic field intensity this micromagnetic structure transforms into domain structure. The observed transition of micromagnetic structure into domain structure is the phase transition of the second kind. The figure shows possible distribution of magnetization vectors  $\mathbf{M}_s$  in micromagnetic structure.

The experimentally observed transition of micromagnetic structure into domain structure and backwards is described in the framework of Mitsek-Semyannikov model [1] that assumes trapezoidal distribution of magnetization vector  $\mathbf{M}_s$  in a plate's cross-section. Parameters of micromagnetic structure and equilibrium domain structure were determined via minimization of free energy of the system. Theoretical estimates are in qualitative agreement with experimental results.

Dependencies of width of stripe domains ( $D$ ) and transversal size of micromagnetic structure ( $\delta$ ) from crystal thickness ( $L$ ) were obtained numerically. It is shown that  $D(L)$  and  $\delta(L)$  are qualitatively different.



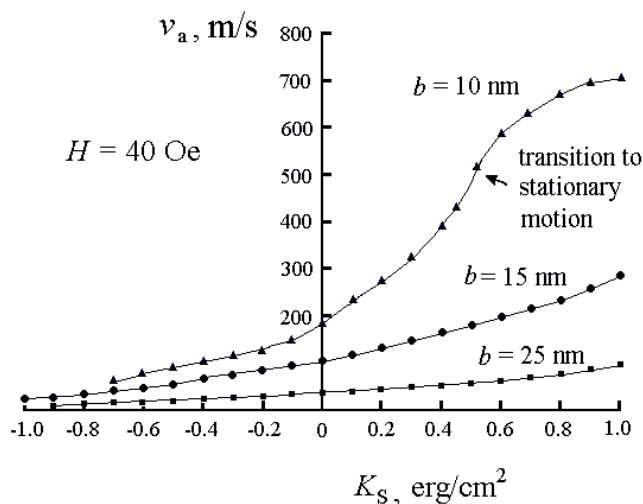
[1] A.I. Mitsek, S.S. Semyannikov, *The Physics of Metals and Metallography*, **35(6)** (1973) 1163.

## SURFACE ANISOTROPY INFLUENCE ON NÉEL-TYPE DOMAIN WALLS DYNAMICS IN MAGNETIC FILMS WITH IN-PLANE ANISOTROPY

*Dubovik M.N., Filippov B.N.*

Institute of Metal Physics, Ural Division, Russian Academy of Sciences, S. Kovalevskoy 18, Ekaterinburg, 620990 Russia

Surface anisotropy influence on Néel-type domain walls motion induced by magnetic field applied along the easy axis in magnetic films with in-plane anisotropy has been investigated on the base of Landau-Lifshitz equation numerical solution. Allowance for all main interactions (exchange, magnetically anisotropic and dipole-dipole ones) has been made in the framework of two-dimensional model of domain wall magnetization distribution. Magnetic parameters corresponding to Permalloy films of zero-magnetostriction composition have been used. The surface anisotropy constant  $K_s$  value has been varied from  $-1 \text{ erg/cm}^2$  to  $1 \text{ erg/cm}^2$ .  $K_s > 0$  corresponds to the case of easy plane-type surface anisotropy and  $K_s < 0$  corresponds to the easy axis-type one. The axis of surface anisotropy is normal to film surface. In films under consideration one-dimensional Néel-type walls are stable at film thicknesses  $b < 40 \text{ nm}$ . Till recently studying domain walls motion based on numerical methods has being dealt mainly with the thicker films in which the stable wall structure is more complex two-dimensional vortex-like Bloch-type one but recent investigation [1] showed the dynamic properties of Néel type-walls to be also nontrivial and of importance for better understanding the processes of domain walls motion in films. As in the case of thicker films and bulk crystals two regions of external field values  $H$  should be distinguished, namely, above and below certain critical field  $H_c$ . If  $H < H_c$ , wall moves with a constant velocity (stationary motion). Surface anisotropy with  $K_s > 0$  ( $K_s < 0$ ) proves to increase (decrease) the velocity of wall stationary motion. If  $H > H_c$ , the wall velocity starts to oscillate with time (nonstationary motion). Surface anisotropy with  $K_s > 0$  ( $K_s < 0$ ) proves to increase (decrease) the period of velocity oscillations and the maximal over period wall velocity. That brings about changing time-averaged velocity  $v_a$  of domain-wall nonstationary motion (see fig. 1). Also easy plane-type surface anisotropy existence leads to increasing  $H_c$  and nonstationary motion full suppression is possible that leads  $v_a$  to increase sharply.



This work has been partially supported by Russian Foundation for Basic Research, project no. 10-02-00435.

- [1] B.N. Filippov, M.N. Dubovik, L. G. Korzunin, *Phys. of Metals and Metallogr.*, in press.  
 [2] B. N. Filippov, L. G. Korzunin, F. A. Kassan-Ogly, *Phys. Rev. B.* 64 (2001) 104412.

23TL-H-8

## HYSTERESIS AND THE FIRST-ORDER REVERSAL CURVES TECHNIQUE

*Stancu A.*

Alexandru Ioan Cuza University of Iasi, Department of Physics, Faculty of Physics,  
Blvd. Carol I, 11, Iasi, 700506, Romania

Hysteretic behavior is a quite general property documented in many physical processes. Starting from previous studies made on ferromagnetic hysteresis and from the identification technique developed for the Classical Preisach Model by Mayergoyz, a decade ago it was shown that a set of First-order Reversal Curves (FORC) can provide a general experimental technique to investigate virtually any hysteretic process [1]. In this talk we show our recent results in the study of hysteresis in a number of physical systems: ferromagnetic, ferroelectric, multiferroic and in materials with spin transition. For the ferromagnetic materials the FORC method was extensively used and many studies have been published showing the qualities and the limits of this technique. Higher-order curves have also been used to evaluate separately the reversible and irreversible components of magnetization.

FORC diagram technique has been able to evidence the aging effects in ferroelectric materials which are a major technological problem of the ferroelectric memories [2].

A special attention will be given to a recent application of the Preisach model as a tool to understand the hysteretic behavior of a category of molecular magnets, the spin-transition materials. The molecules of these compounds can be found in one of the two states: low-spin (LS) or high-spin (HS). The molecules have different volumes in the two states and this phenomenon is at the origin of an inter-molecule interaction strongly dependent of the elastic properties of the crystal. The spin-transition compounds are diamagnetic in LS state and paramagnetic in HS state and show a multiple hysteretic behavior controlled by temperature, pressure and electromagnetic radiation. This intricate nonlinear phenomenon can be described with a reasonable accuracy with a special Preisach model developed by our group in recent years [3, 4]. We should mention that this technique can be used to evaluate the critical volume of spin-transition crystals under which only reversible processes are observed.

In each example, the difficulties encountered and the problems that remain unsolved for the FORC technique are presented and discussed.

Support by the Romanian CNMP PNII 12-093 HIFI, 72-186 NANOMAT and CNCSIS PNII IDEI 1994 FASTSWITCH projects are acknowledged.

- [1] A. Stancu et al., *J. Appl. Phys.*, **93** (2003) 6620.
- [2] A. Stancu et al., *Appl. Phys. Lett.*, **83** (18) (2003) 3767.
- [3] C. Enachescu et al., *Phys. Rev B*, **72** (2005) 054413.
- [4] R. Tanasa et al., *Phys. Rev. B*, **71** (2005) 014431.

23OR-H-9

## SWITCHING OF TOPOLOGICAL CHARGE OF MAGNETIC SUBMICRON PARTICLES IN VORTEX STATE

*Meshkov G.A.<sup>1</sup>, Belanovsky A.D.<sup>2</sup>, Pyatakov A.P.<sup>1,2</sup>, Zvezdin K.A.<sup>2</sup>*

<sup>1</sup> Department of Physics, M.V. Lomonosov Moscow State University, Leninskie gori, Moscow 119992, Russia

<sup>2</sup> A.M. Prokhorov General Physics Institute, 38, Vavilova St., Moscow 119991, Russia

Magnetic vortices are intensively studied structures, which are frequently found in metallic submicron magnetic particles. They arise from the competition between exchange interaction and magnetic dipole interaction. The size of particle, in which magnetic vortex can be stable, depends on magnitudes of exchange coupling and saturation magnetization.

Vortex is a good example of magnetic inhomogeneity (another example is a domain wall), which were shown to be electrically polarized [1] due to high-order contribution to free energy of a magnetic material, which takes the following form:

$$F = \gamma(\mathbf{P} \cdot [\mathbf{M}(\nabla\mathbf{M}) - (\mathbf{M}\nabla)\mathbf{M}]),$$

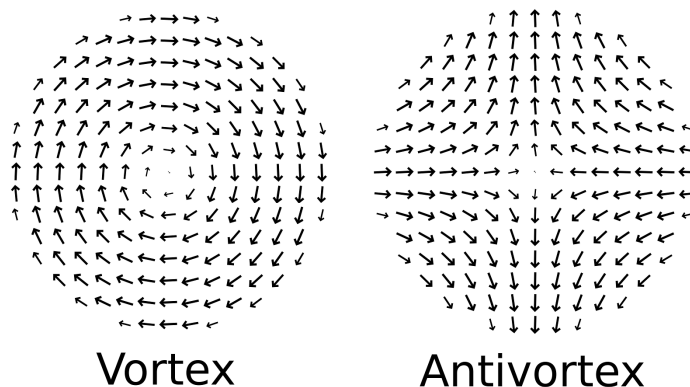
where  $\mathbf{M}$  is magnetization,  $\mathbf{P}$  is electric polarization,  $\nabla$  is differential operator and  $\gamma$  is a material-dependent coefficient. This makes possible to create and control magnetic vortices by electric field [2]. This applies even to particles with low saturation magnetization, which in the absence of electric field support only homogeneous state.

We have conducted micromagnetic simulation of nucleation, transformation and dissipation of magnetic vortices by electric field. Micromagnetic package SpinPM was used. We have shown that in a magnetic dielectric submicron particle a magnetic vortex can be created by applying electric field of a wire electrode. The electrode is running through the center of the particle perpendicular to particle plane. No currents are needed in this scheme and only static voltage is used.

When the sign of the electric field is reversed, an antivortex is created instead of vortex. Antivortex is a topological counterpart of a vortex, equally fundamental, which has negative topological charge (see figure).

In all the transformation processes vortices and antivortices arise in pairs, as topological charge conservation requires. Vortex and antivortex nucleation and dissipation processes show hysteretic behavior (the structure remains stable in electric fields, which are lower than its nucleation field).

The described effect can be used as a principle for creating memory devices. We have shown that both homogenous and vortex states can be metastable in the same particle, which provide 0 and 1. These states can be read (detected) magnetically by stray fields and written electrically as described above.



This work is supported by RFBR 10-02-13302-RT-omi.

[1] M. Mostovoy, Phys. Rev. Lett., **96** (2006), 067601

[2] A. Pyatakov, G. Meshkov, A. Logginov. Moscow University Phys. Bull., **65** (2010), 329

## THE SIMULATION OF THE NONLINEAR DYNAMICS OF MAGNETIC VORTICES IN RARE-EARTH ORTHOFERRITES

*Ekomasov E.G.<sup>1</sup>, Bogomazova O.B.<sup>1</sup>, Gumerov A.M.<sup>1</sup>, Murtazin R.R.<sup>1</sup>, Shapaeva T.B.<sup>2</sup>*

<sup>1</sup> Bashkir State University, 450074, Ufa, Zaki Validi St., 32, Russia

<sup>2</sup> Faculty of Physics M.V.Lomonosov Moscow State University, 119991, Moscow, Leninskie Gory, Russia

Theoretically, the existence possibility for two "thin" structure types of domain walls (DW) in rare-earth orthoferrites (REO) was predicted rather long ago [1]. There are also experimental results [2] which can be interpreted as observation of dynamic lines on a DW in REO moving at a supersonic speed. The question of the magnitude and type of the gyroscopic force remains central to the dynamics of the magnetic vortices in weak ferromagnetics (WFM). The theoretical description of lines dynamics, taking into account a field gyroscopic force, was carried out in [3-5]. The gyroscopic force, which is determined by the average magnetization of the sublattice constants of the Dzyaloshinski interaction and exchange interaction between sublattices, was found in [6] using a method which does not take into account the internal structure of the vortex in the DW. The equation of motion written in the collective coordinates for the resulting gyroscopic term was proposed in [7-8].

In the given work, the problem of the nonlinear dynamics of the domain walls with the thin structure of any types has been solved numerically using the Landau-Lifshitz equation in the two-sublattice model subject to an external magnetic field and dissipation. To solving the system of two second-order differential equations the finite-difference method with the explicit scheme was used. The approximation was carried out on five-point scheme "cross". The system of the differential equations is of the second order accuracy in time and space variable. The change of the structure and position of the DW over time has been determined by a written program, knowing which it is possible to calculate all the main dynamic characteristics of the DW. The stationary magnetic vortices speed has been found as a function of the DW motion speed. Comparison with the experimental data and analytical results of the perturbation theory has been carried out.

The work was supported by Russian Foundation for Basic Research (project 10-02-00594-a).

- [1] M.M. Farztdinov, M.A Shamsutdinon, A. A. Khalifina, *Fiz. Tverd. Tela*, **21** (1979) 1522.
- [2] M.V. Chetkin, Yu.N. Kurbatova, T.B. Shapaeva, *JMMM*, **258-259** (2003) 15.
- [3] A.K. Zvezdin, *Kr. Soob. po Fiz. FIAN*, **6** (1999) 28.
- [4] E.G. Ekomasov, M.A. Shabalin, *Fiz. Tverd. Tela*, **43** (2001)1211.
- [5] E.G. Ekomasov, M.A. Shabalin, O.B. Gaeva, *Functional Materials*, **11** (2004) 480.
- [6] A.K. Zvezdin, V.I. Belotelov, K.A. Zvezdin, *JETP Lett.*, **87** (2008) 381.
- [7] A.K. Zvezdin, K.A. Zvezdin, *Kr. Soob. po Fiz. FIAN*, **8** (2010) 22.
- [8] A.K. Zvezdin, K.A. Zvezdin, *Kr. Soob. po Fiz. FIAN*, **8** (2010) 33.

23OR-H-11

## NONLINEAR MAGNETIC DYNAMIC HYSTERESIS OF FINE PARTICLES

Titov S.V.<sup>1</sup>, Mrabti H.El.<sup>2</sup>, Déjardin P.-M.<sup>2</sup>, Kalmykov Yu.P.<sup>2</sup>

<sup>1</sup> Koteln'nikov's Institute of Radio Engineering and Electronics of the Russian Academy of Sciences, Vvedenskii Square 1, Fryazino, 141190, Russia

<sup>2</sup> LAMPS, Université de Perpignan, 52, Av. Paul Alduy, 66860 Perpignan, France

The dynamic hysteresis induced in magnetic nanoparticles by an external ac field is an issue of increasing interest due to its practical importance, e.g., in magnetic hyperthermia. In this work, the dynamic magnetic hysteresis in superparamagnetic nanoparticles in a strong ac magnetic field of arbitrary orientation is treated using Brown's model of coherent rotation of the magnetization  $\mathbf{M}$ . The underlying Fokker-Planck equation for the distribution function of magnetization orientations  $W(\mathbf{u}, t)$  on the unit sphere is [1]

$$2t_N \nabla_{\mathbf{u}} W = (b/a) \mathbf{u} \nabla_{\mathbf{u}} U \nabla_{\mathbf{u}} W + \nabla_{\mathbf{u}} \nabla_{\mathbf{u}} W [bW \nabla_{\mathbf{u}} U + \nabla_{\mathbf{u}} W]$$

Here  $b = v/(kT)$ ,  $k$  is Boltzmann's constant,  $T$  the absolute temperature,  $v$  is the particle's volume,  $\alpha$  is the damping constant,  $\mathbf{M} = \mathbf{u}M_s$ ,  $t_N = b(1+a^2)M_s/(2ag)$ ,  $g$  is the gyromagnetic ratio,  $M_s$  is the saturation magnetization, and  $U(\mathbf{u}, t)$  is the free energy density. As a particular example, we consider  $U = K \sin^2 \theta - [\mathbf{H}_0 + \mathbf{H}'(t)] \cdot \mathbf{M}$ , where  $\theta$  is the polar angle,  $K$  is the anisotropy constant, and  $\mathbf{H}_0$  and  $\mathbf{H}'(t)$  are the dc and ac external fields, respectively. By expanding  $W$  in terms of the spherical harmonics  $Y_{l,m}(\theta, \varphi)$ , we obtain an equation of motion for the statistical moments  $\langle Y_{l,m} \rangle(t)$ , viz.

$$\langle \dot{Y}_{l,m} \rangle(t) = \sum_{s,r} e_{l,m,l+r,m+s}(t) \langle Y_{l+r,m+s} \rangle(t),$$

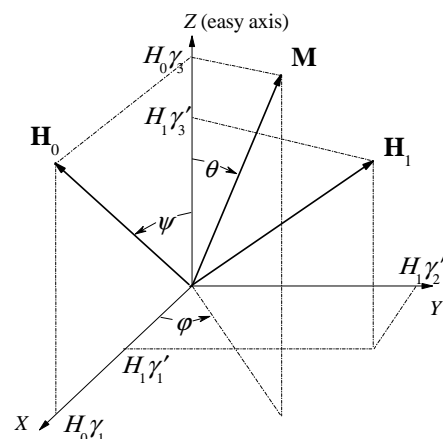
where  $e_{l,m,l+r,m+s}(t)$  are the matrix elements of the Fokker-Planck operator and the angular brackets an ensemble average over the distribution  $W$ . Expanding further the steady state moments in Fourier series leads to a system of recurring algebraic equations with three indexes that are solved using the matrix continued fractions [1]. The nonlinear ac stationary response and dependence of the area of the dynamic hysteresis loop on the temperature, frequency, damping, ac field amplitude, and orientation of the ac field are evaluated and analyzed. In the nonlinear regime, the relevant time scale for magnetization relaxation is given in terms of an effective dc field just as in Ref. 2. The results obtained extend those of Refs. 2 and 3 allowing one to handle assemblies of non-interacting superparamagnetic particles with randomly distributed easy axes. Thus they are useful for comparison with experiments on nonlinear response in strong ac fields such as the nonlinear dynamic susceptibility, nonlinear stochastic resonance, and dynamic hysteresis.

The support of the work by the Agence Nationale de la Recherche, France (Project DYSC n° ANR-08-P147-36) is gratefully acknowledged.

[1] W. T. Coffey, Yu. P. Kalmykov and J. T. Waldron, *The Langevin Equation*, 2<sup>nd</sup> Edition (World Scientific, Singapore, 2004).

[2] P. M. Déjardin and Yu. P. Kalmykov, *J. Appl. Phys.* **106** (2009) 123908; P. M. Déjardin *et al.*, *J. Appl. Phys.* **107** (2010) 073914.

[3] I. S. Poperechny, Yu. L. Raikher, and V. I. Stepanov, *Phys. Rev. B* **82** (2010) 174423; S. V. Titov *et al.*, *Phys. Rev. B* **82** (2010) 1100413(R).



23OR-H-12

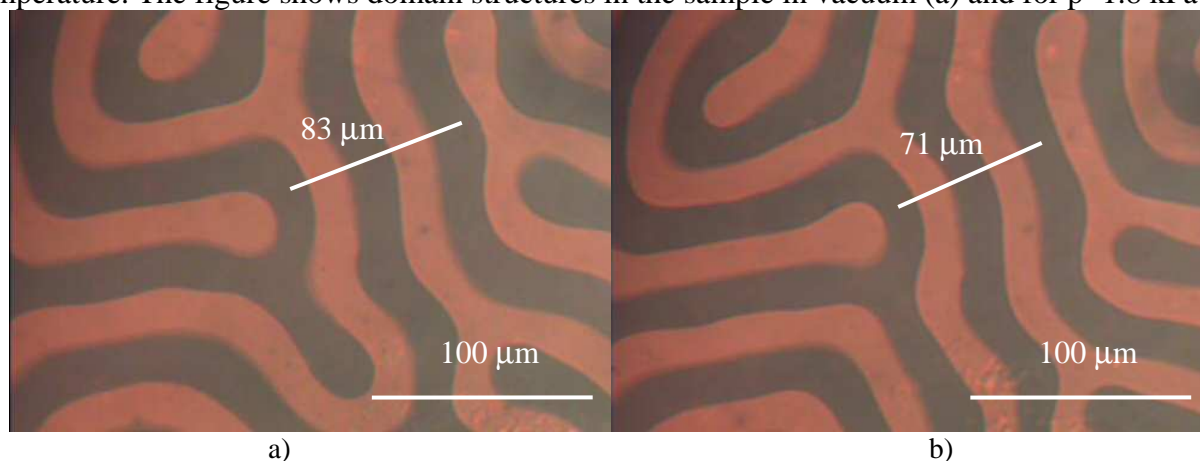
## DOMAIN STRUCTURE REVERSIBLE RECONSTRUCTION AND CHANGING DOMAINS WIDTH IN FERRITE-GARNET FILMS BY WATER MOLECULES ADSORPTION

*Zubov V.E.<sup>1</sup>, Kudakov A.D.<sup>1</sup>, Levshin N.L.<sup>1</sup>, Gusev M.Yu.<sup>2</sup>, Neustroev N.S.<sup>2</sup>*

<sup>1</sup> Faculty of Physics, M.V.Lomonosov Moscow State University, Leninskie Gory, Moscow, 119992, Russia

<sup>2</sup> Research Institute of Material Science and Technology, Zelenograd, Moscow, 124460, Russia

Influence of reversible water molecules adsorption on domain structure of vismuth-doped ferrite-garnet thin films of composition  $(\text{Bi,Lu})_3(\text{Fe,Ga})_5\text{O}_{12}$  with perpendicular magnetic anisotropy was investigated by use of magneto-optical micromagnetometer and digital camera. The thickness of films  $h=4,5 \mu\text{m}$ ,  $4\pi M_s=25 \text{Gs}$  ( $M_s$  - magnetization), domains width  $d \approx 20 \mu\text{m}$ . For the first time reversible reconstruction of domain structure and decrease of domains width was observed when introduction of water vapor into the cell with the sample took place. Maximal decrease of  $d$  was 15% for water vapor pressure  $p=1.8 \text{kPa}$ , which equal to saturated water vapor pressure for room temperature. The figure shows domain structures in the sample in vacuum (a) and for  $p=1.8 \text{kPa}$  (b).



Domains width in ferrite-garnet thin films with perpendicular magnetic anisotropy is determined by competition of  $180^\circ$  domain walls energy and energy of magnetic stray field over a film surface.

$d$  can be estimated with the help of expression  $d \sim \sqrt{\frac{\sigma h}{1,75M_s^2}}$ .  $\sigma = 4\sqrt{AK}$  - energy of domain wall

unit area,  $A$ - exchange parameter,  $K$  - constant of uniaxial perpendicular magnetic anisotropy. Domains width decreases when  $\sigma$  decreases. One can receive estimation of  $K \sim 0,8 \cdot 10^3 \text{erg/cm}^3$  by use the above-mentioned formulas and  $A=3 \cdot 10^{-7} \text{erg/cm}$ . Uniaxial magnetic anisotropy energy of unit area of film is  $K \cdot h \sim 0,4 \text{erg/cm}^2$ . Influence of water molecules adsorption on properties of magnetic is similar to a break of translation symmetry on its surface. So the water molecules adsorption can lead to appearance of the surface magnetic anisotropy, which has the same order of value as Neel surface anisotropy has ( $\sim 1 \text{erg/cm}^2$ ). Hence changing of the film domains width can be explained by reduction of effective perpendicular magnetic anisotropy constant due to water molecules adsorption.





**23 August**

Tuesday

11:30-13:00

14:30-17:20

oral session

23TL-O

23RP-O

23OR-O

**“High Frequency  
Properties and  
Metamaterials”**

23TL-O-1

## ON-CHIP NOISE SUPPRESSOR TOWARD LONG TERM EVOLUTION(LTE)-ERA RFIC RECEIVER

*Yamaguchi M., Endo Y.*

Dept. of Electrical and Communication Engineering, Tohoku University, Sendai, Japan

Ferromagnetic thin film materials with high permeability in the RF range are potential material for new passive inductive components to diversify the direction of CMOS technologies from scaling to application specific functional innovation through incorporating digital and non-digital functionality into compact systems, which is known as “More-than-Moore” approach [1]. The ongoing application trials include CMOS integrated inductors [2], [3], one-chip DC-DC converters [4] and on-chip noise suppressor for Long Term Evolution(LTE)-era RFIC receiver [5].

Among these innovative trials, this paper focuses on the on-chip noise suppressor. A coming LTE-era RFIC chip implies millions of digital gates to calibrate, control and process analogue signals on the same chip. A serious problem is that the EM noise from the digital gates migrates into the analog receiver circuit and cause desensitization. The noise currents migrate through either of conductive, capacitive or inductive paths. Since the currents yield magnetic fields, it is useful to apply soft magnetic thin film to suppress EM noise on RFIC chip, which offers; (i) small space solution (less than 5 $\mu\text{m}$ -thick), (ii) frequency-selective noise suppression based on FMR losses, (iii) suppression of both conduction noise and radiated emission, (iv) effectiveness for both noise aggressor and victim.

A conductive noise suppression of 57 dB at 6 GHz was demonstrated on thin-film coplanar line using a 2- $\mu\text{m}$ -thick CoZrNb film [6] whereas a 1.0- $\mu\text{m}$ -thick CoZrNb film was integrated onto a microprocessor chip and exhibited noise suppression of 3 to 37.8 dB at 1 to 2 GHz [7]. The loss peak frequency (maximum suppression frequency) can be defined well by the intrinsic FMR frequency and demagnetizing factor. Below the FMR frequency, traditional magnetic shielding was effectively achieved by the same magnetic film; The CoZrNb films of 0.2–2.0  $\mu\text{m}$  thick effectively suppressed magnetic near field of a LSI chip, showing that the permeability–thickness product ( $\mu\text{r} \times \text{tm}$ ) of 1450 [ $\mu\text{m}$ ] would be enough to attain 10 dB suppression [8]

This work was supported in part by the Development of Technical Examination Services Concerning Frequency Crowding by Ministry of Internal Affairs and Communications.

- [1] J. P. Kent, and J. Prasad, IEEE 2008 Custom Integrated Circuits Conference, 15-4-1, 2008.
- [2] M. Yamaguchi, M. Baba, and K-I Arai, IEEE Trans. on MTT, **49**, 2331-2335, 2001.
- [3] D-W Lee, K-P Hwang, and S. X. Wang, IEEE Trans. Magn., **44**, 4089-4095, 2008.c]
- [4] D. S. Gardner, et al, IEEE Trans. Magn., **45**, 4760-4766, 2009.
- [5] S. Muroga, Y. Endo, Y. Mitsuzuka, Y. Shimada, and M. Yamaguchi, IEEE Trans. Magn., **47**, 300-303, 2011.
- [6] K. H. Kim, S. Ohnuma, M. Yamaguchi, IEEE Trans. Magn., **40**, 3031-3033, 2004.
- [7] T. Fukushima, S. Koya, H. Ono, N. Masuda and M. Yamaguchi, J. Magn. Soc. Jpn., **30**, 531-534, 2006.
- [8] S. Muroga, Y. Endo, W. Kodate, Y. Sasaki, K. Yoshikawa, Y. Sasaki, M. Nagata and M. Yamaguchi, Submitted to IEEE T-MAG.

## HIGH FREQUENCY IRON LOSS MODEL OF Mn-Zn FERRITES AT MHz RANGE

*Tung M.J., Tong S.Y., Yang M.-D.*

Dept. of Electromagnetic Materials and Devices, Material and Chemical Research Laboratories,  
ITRI, Taiwan

Low loss Mn-Zn ferrite is mainly used for switching mode power supply (SPS) in the frequency range under 1MHz. On the other hand, only a few papers had discussed the loss mechanism of Mn-Zn ferrites in the frequency range higher than 1 MHz. This study mainly investigated the iron loss phenomenon of Mn-Zn ferrites in the frequency range between 1 MHz and 10 MHz in order to find out the loss mechanism from the point of buck impedance. The results show the effective grain-boundary capacitance play an important role at the high frequency range.

The low loss grade Mn-Zn ferrite samples were prepared by conventional ceramic process. The sintering temperature was at 1150~1250 °C with 0.1% to 3% oxygen partial pressure. Under an iron loss measuring condition with  $f \times B$  maintaining at a constant of 25 kHz\*Tesla, the low frequency loss of Mn-Zn ferrite with the grain-grain boundary structure is mainly the hysteresis loss and minimum loss of 59.3 kW/m<sup>3</sup> was obtained at 1.3 MHz. When the frequency is higher than 1.3 MHz the contribution of eddy current loss gradually increased until 3 MHz then keep constant with amount of fluctuation. The loss was influenced by the grain-grain boundary structure which corresponds to a series-parallel circuit of the resistance and capacitance to be present as the Kroop's model. According the loss analysis, the high impedance grain boundary layer will reduced due to a parallel effect of grain boundary capacitance at high frequencies, which makes the eddy current pass through grain boundary and flows through the entire bulk. Therefore the traditional theory indicating that the high impedance grain boundary restricted the eddy current didn't suitable in this frequency range, i.e., the grain boundary impedance is not advantageous to core loss at high frequencies. Thus the loss effect is not only decided by grain boundary resistance but the grain boundary capacitance. Also the dielectric loss at frequency range of 3 MHz to 10 MHz was greatly affected, whereas it did not occupy a high ratio of the total loss.

- [1] F. Fiorillo, C. Beatrice, O. Bottauscio, and A. Manzin, *Appl. Phys. Lett.* 89, (2006), 122513.
- [2] Y. Liua, S. Heb, *J. Alloys Compd.* 489 (2010) 523–529
- [3] Y. Liu, S. He, *J. Magn. Mater.* 320 (2008) 3318–3322
- [4] K.W.E. Chenga, W.S. Lee, C.Y. Tang, L.C. Chanb, *J Mater. Proc. Tech.* 139 (2003) 578–584

23RP-O-3

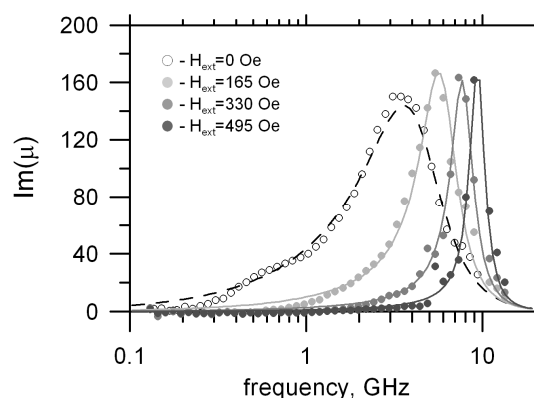
## ANALYSIS OF PROPERTIES OF FERROMAGNETIC THIN FILMS BASED ON MICROWAVE PERMEABILITY MEASUREMENTS UNDER PERMANENT MAGNETIC BIAS

*Osipov A.V., Iakubov I.T., Kashurkin O.Yu., Lagarkov A.N., Maklakov S.A., Rozanov K.N., Ryzhikov I.A., Starostenko S.N.*

Institute for Theoretical and Applied Electromagnetics RAS, Izhorskaya 13, Moscow, Russian Federation, 125412

Magnetic properties and magnetic structure of Fe-based thin films are known to depend strongly on peculiarities of manufacturing technology. A conventional approach to measuring of the microwave permeability employs shorted strip-line measurement cells [1, 2], which are typically operable up to 6 GHz. Recently, a coaxial method has been developed for films deposited on a flexible substrate [3, 4], with a long stripe of film wound into a roll-shaped coaxial sample. The coaxial technique is reported to have wider operating frequency range and better accuracy than the strip-line method. On the other hand, large uncertainty may arise in the results measured by this technique due to the magnetoelastic effect in the wound film. However, coaxial measurements under external magnetic bias may eliminate this uncertainty and provide additional data on magnetic properties of the films, e.g., estimates for magnetoelastic effect.

In the presentation, the analysis of the measured microwave permeability of thin ferromagnetic films is performed with fitting of the measured frequency dependence of permeability with the Lorentzian dispersion law, as is shown in the figure, where dots are measured data and curves are fitting curves. For a saturated film, the microwave parameters, namely, static permeability, resonance frequency, and damping factor are related to the magnetostatic parameters in accordance with well known Kittel's equations. Hence, dynamic and static properties of the films may be found. Frequency and bias field dependencies of dynamic and static magnetic parameters for single-layered thin ferromagnetic films are discussed. The difference in the microwave performance of coaxial samples made of the same film wound with ferromagnetic layer facing either inside or outside is attributed to both the anisotropy of the samples and the magnetoelastic effect. Hence, measured data obtained by coaxial measurements of these samples under magnetic bias may provide valuable data on variations of magnetic structure of the film with bias, on the effective magnetoelastic field to account for its contribution in the effective anisotropy field, on distribution of magnetic moments in the film plane, etc.



Authors are grateful to RFBR for support according to grant no. 09-08-01161.

- [1] V. Bekker, K. Seemann, H. Leiste, *J. Magn. Magn. Mater.*, **270** (2004) 327.
- [2] S. N. Starostenko, K. N. Rozanov, A. V. Osipov, *J. Appl. Phys.*, **103** (2008) 07E914.
- [3] O. Acher *et al.*, *J. Magn. Magn. Mater.*, **136** (1994) 269.
- [4] K.N. Rozanov, N.A. Simonov, A.V. Osipov, *J. Communicat. Technol. Electron.*, **47** (2002) 210.

23RP-O-4

## **AHARONI MODES IN MAGNETIC SPECTRA OF CARBONYL IRON**

*Lagarkov A.N., Semenenko V.N., Chistyayev V.A., Iakubov I.T.*

Institute for Theoretical and Applied Electromagnetics RAS, Izhorskaya str.13, Moscow, 125412,  
Russian Federation

Magnetic spectra of composite based on powder of carbonyl iron were measured at frequencies up to 30 GHz. Two previously unknown intensive high frequency resonance modes of carbonyl iron at frequencies within 15 – 25 GHz surpassing ferromagnetic resonance frequency were found. We assume that those are the Aharoni exchange resonance modes. Structure of carbonyl iron grains is analyzed. There are all the necessary conditions for exchange resonance modes excitation. The resonances are realized inside magnetically isolated nanocrystallites which constitute the carbonyl iron grains. Some estimates are made. Peculiarities of homogeneous ferromagnetic resonance of carbonyl iron are discussed also.

23TL-O-5

## **EMERGING RF AND MICROWAVE APPLICATIONS OF HEXAGONAL FERRITES**

*Geiler A.L.*

Center for Microwave Magnetic Materials and Integrated Circuits, Northeastern University, Boston,  
Massachusetts 02115

A vast body of knowledge on the structure and the properties of hexagonal ferrites has been accumulated since 1950s, driven in part by the technological significance of these materials in diverse applications, such as permanent magnets, microwave devices, and magnetic recording media. With the rapidly growing demand for bandwidth in wireless communication systems and increasing frequencies of operation of electronic devices, in recent years resurgence in scientific interest in highly anisotropic hexagonal ferrites has been observed. This interest is motivated by a number of emerging applications that pose significant materials challenges that cannot be addressed using traditional rf and microwave ferrite materials.

The principle of self-biasing non-reciprocal microwave ferrite devices by relying upon the strong magnetocrystalline anisotropy fields in hexagonal M-type ferrites was first implemented in 1959 [1]. While operation without biasing magnets was verified and extended by subsequent efforts, all the prototypes constructed thus far exhibited relatively high loss and poor isolation, which made them unsuitable for practical applications. Furthermore, due to the strong internal magnetic field in the ferrite materials utilized to develop self-biased circulators in the past, the frequency of operation was restricted above 20 GHz. In recent years, novel materials fabrication and orientation techniques have been developed that lead to exceptionally low magnetic losses [2]. Further, the aforementioned orientation techniques have been successfully applied to substituted hexagonal ferrite materials that possess low uniaxial anisotropy, thus allowing self-biased devices in the 2 to 20 GHz frequency band.

Metamaterials are artificial periodic structures which possess unique electromagnetic properties not found in naturally occurring dielectric, magnetic, and metallic materials. The band structure of an electromagnetic bandgap (EBG) metamaterial exhibits band gap and band pass regions. Within the band gap region the EBG metamaterial produces a high-impedance electromagnetic surface that

approximates a magnetic conductor [3]. Recently, it was demonstrated that by utilizing oriented hexagonal Z-type ferrite materials with controllable permittivity and permeability values antenna EBG substrates can be developed, leading to profile height reduction, as well as enhanced bandwidth and radiation efficiency[4].

For device applications there is increasing interest in enhancing the coupling between the electric and magnetic dipole moments giving rise to the ME effect. With the recent discovery of large ME effects in transition metal oxides[5], considerable effort has been devoted to magnetically frustrated systems with long-period magnetic structure. For practical applications, it will be necessary to generate and control the ME effect at room temperature (or above) and with small magnetic and/or electric fields. These advances provide promise in the simultaneous manipulation of both permittivity and permeability enhancing the dynamic response in spatial, temporal, and frequency domains. As recently as 2010, the manipulation of P with low B (<0.25 T) at room temperature in a polycrystalline Z-type hexaferrite material has been demonstrated<sup>5</sup>. The sequential switching of P using oscillating B with an amplitude between 0 and 0.25 T was demonstrated to verify the suitability of hexagonal Z-type ferrites for practical ME device applications.

These and other advances illustrate the seemingly endless capacity of hexagonal ferrites to offer unique magnetic and electronic characteristics that are highly beneficial in a wide variety of practical applications, and thus, warrant further inquiry into the structure and the properties of these materials.

- [1] H.N. Chait and T.R. Curry, *J. Appl. Phys.*, **30** (1959) 152S.
- [2] Chen, T. Sakai, T. Chen, *et al.*, *Appl. Phys. Lett.*, 88 (2006) 062516.
- [3] Sievenpiper, L. Zhang, R. F. J. Broas, *et al.*, *IEEE Trans. Microwave Theory Tech.* **47**, 2059 (1999).
- [4] Daigle, E. DuPre', A. L. Geiler, *et al.*, *IEEE Magn. Lett.*, in print.
- [5] T. Kimura, T. Goto, H. Shintani, *et al.*, *Nature (London)* **426**, 55 (2003).

23OR-O-6

## **STRUCTURE, MAGNETIC, AND MICROWAVE PROPERTIES OF GRANULAR ALLOYS $\text{Fe}_x(\text{SiO}_2)_{1-x}$ PREPARED BY MECHANOCHEMICAL SYNTHESIS**

*Lomayeva S.F.<sup>1</sup>, Rozanov K.N.<sup>2</sup>, Maratkanova A.N.<sup>1</sup>, Petrov D.A.<sup>2</sup>, Yelsukov E.P.<sup>1</sup>*

<sup>1</sup> Physical-Technical Institute UB RAS, 132 Kirov Street, 426000 Izhevsk, Russia

<sup>2</sup> Inst. for Theor. and Appl. Electromagnetics RAS, 13 Izhorskaya ul., 125412 Moscow, Russia

For high-frequency applications of nanocomposites, a special set of properties is required, such as low coercivity, high electrical and magnetic resistance, and high saturation magnetization. This combination of the properties can be obtained in granular systems, which are soft magnetic 3d-metal-based nanoparticles dispersed in a dielectric matrix of amorphous  $\text{SiO}_2$ .

Granule size, microstructure, and properties of metal-insulator interface are governed by the method and conditions of fabrication of nanocomposites. Recently, the Fe- $\text{SiO}_2$  system has been under extensive studies. Granular Fe- $\text{SiO}_2$  films may be produced by ion implantation, ion-beam sputtering, magnetron sputtering, sol-gel technology. Application of the ball milling technique to producing of Fe- $\text{SiO}_2$  nanocomposites is less studied, though the high-energy ball milling is one of the most promising techniques for obtaining nanocomposites. This method allows heterophase nanosystems with uniform distribution of phases to be obtained with easy. Structural and phase state of the nanocomposites obtained by milling, and, therefore, the magnetic and magnetotransport

properties of the nanocomposites are adjustable by a controlled variation of the milling medium and milling time, and by subsequent heat treatment.

In the presentation, structural-phase composition and magnetic properties of  $\text{Fe}_x(\text{SiO}_2)_{1-x}$  ( $x=30, 70, 90, 95$ ) nanocomposites obtained by high-energy ball milling with Ar and acetone as milling media and milling time of 1 to 64 h are studied by X-ray diffraction, FT-IR spectroscopy Mössbauer spectroscopy, electron microscopy, magnetostatic and microwave measurements.

The milling process is shown to produce isolated particles of 2 to 20 nm in size, which have a complex phase composition and may comprise Fe, FeSi alloy, oxides, silicates, carbides depending on milling medium and milling time. The effect of milling conditions on the saturation magnetization and coercivity has also been studied. The saturation magnetization and the coercivity are functions of fraction of phases containing oxygen and carbon in the particle.

The microwave permittivity and permeability of composites comprising 20% of the milled powders are measured in the frequency range of 0.1 to 5 GHz. The size of ferromagnetic particles is found to affect greatly the permeability of the composites at frequencies below 1 GHz. A typical measured frequency dependence of permeability is shown in the figure.

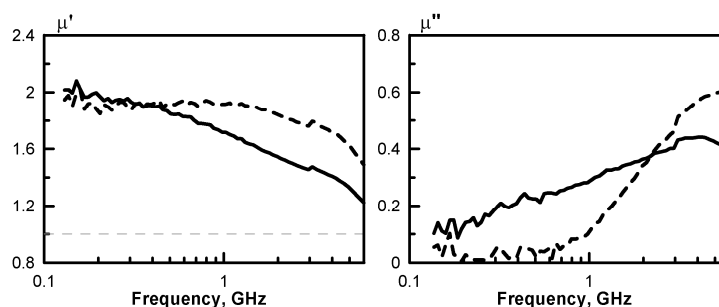


**Figure.** The measured frequency dependences of real (left) and imaginary permeability (right) of composites comprising 22 % vol. of milled  $\text{Fe}_x(\text{SiO}_2)_{1-x}$  powders ( $x=0.95$ ) with particle size of 5 to 40  $\mu\text{m}$  (solid lines) and 1 to 4  $\mu\text{m}$  (dashed lines)

The study was partially supported by the Russian Foundation for Basic Research, grant no. 09-08-00158.

23OR-O-7

## MICROSTRUCTURE, STATIC AND DYNAMIC MAGNETIC PROPERTIES OF THIN Co FILMS

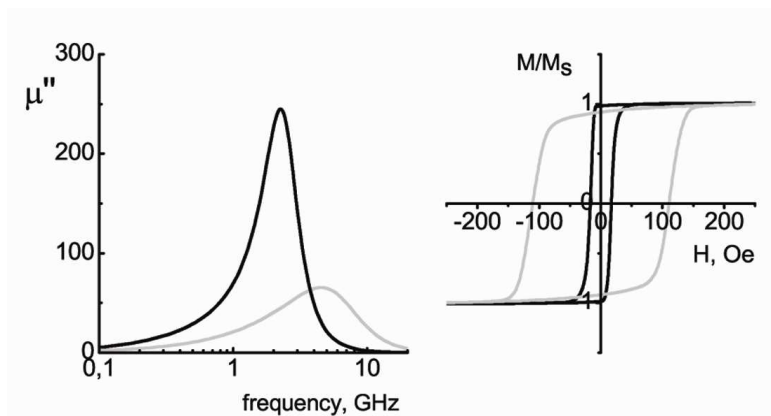
*Maklakov S.S.<sup>1</sup>, Maklakov S.A.<sup>1</sup>, Ryzhikov I.A.<sup>1</sup>, Rozanov K.N.<sup>1</sup>, Osipov A.V.<sup>1</sup>, Kashurkin O.Yu.<sup>1</sup>, Amelichev V.A.<sup>2</sup>*

<sup>1</sup> Institute for Theoretical and Applied Electromagnetics RAS, 125412 Moscow, ul. Izhorskaya, d. 13/19, Russia

<sup>2</sup> Moscow State University, Chemistry Department, 119991 Moscow, Russia

Thin magnetic films are widely used for magnetic applications. Such applications are microwave antennas and recording devices. To develop materials with given microwave permeability it is necessary to know a relationship between magnetic properties and microstructure of magnetic matter.

The results of a comparative study of magnetic properties and microstructure of thin Co films are given. Materials investigated were obtained using DC magnetron sputtering in an Ar flow. The films structure was studied using TEM and GIXD techniques. Magnetic hysteresis loops and magnetic permeability frequency dispersions in a range from 0.1 to 10 GHz were measured.



Fabrication parameters variation leads to different types of Co films obtaining with resonant frequencies from 2 to 6 GHz. Nanocrystalline structure of these films is discovered. Increasing of crystalline size from 5 to 100 nm leads to increasing of resonant frequency from 2 to 5 GHz and increase of coercivity from 15 to 110 Oe.

The relationship obtained allows one to develop new pathways for magnetic materials production.

23OR-O-8

### HIGH FREQUENCY PROPERTIES OF NI SPINEL FERRITES

Nosov A.<sup>1</sup>, Rinkevich A.<sup>1</sup>, Ronkin M.<sup>1</sup>, Gribov I.<sup>1</sup>, Moskvina N.<sup>1</sup>, Karpova T.<sup>2</sup>, Vladimirova E.<sup>2</sup>, Vasiliev V.<sup>2</sup>

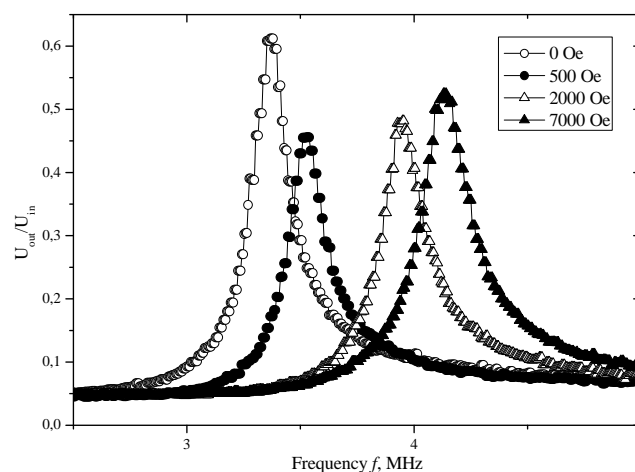
<sup>1</sup> Institute of Metal Physics, Ural Division of RAS, S.Kovalevskoi str.18, 620990, Ekaterinburg, Russia

<sup>2</sup> Institute of Solid State Chemistry, Ural Division of RAS, Pervomaiskaya str.91, 620990, Ekaterinburg, Russia

The spinel ferrites of general formula  $MFe_2O_4$ , where  $M=Mn, Co, Ni, Zn$ , attract considerable interest as soft magnetic materials for applications in magnetic field sensing, ferrofluids, magnetic drug delivery, magnetic information storage, high frequency devices *etc.* Understanding peculiarities of their radiofrequency behavior under application of *dc* magnetic field  $H$  is of considerable interest both to fundamental physics and potential applications. The purpose of this study is to investigate the high frequency magnetic properties of Ni-based spinel ferrites under the influence of *dc* biasing.

The  $NiFe_2O_4$  and  $Ni_{0.8}Zn_{0.2}Fe_2O_4$  spinel ferrites were prepared by decomposition of citrate complexes of corresponding metals. The pellet shaped samples with typical dimensions of 10 mm in diameter and thickness of 1 mm were prepared by isostatic compacting the powders and final heat treatment in air. X-ray diffraction patterns confirmed the phase purity of the compositions investigated. Magnetic properties were characterized by measurements of *dc* hysteresis loops and magnetostriction.

High frequency magnetic properties were measured in a circuit consisting of two coils (inner and outer) wired on a sample. Each coil





had about 40 turns. Their axes were mutually orthogonal. The  $ac$  signal from generator of the frequency range from 20 kHz to 30 MHz could be applied to either of the coils and the signal, excited in the second one, have been recorded. Experimentally the ratio of the excited signal to the  $ac$  signal from generator was monitored as a function of frequency, excitation voltage, and  $dc$  magnetic field applied in a sample pane.

Typical frequency response of the system under application of  $H$  is shown in the figure. Data for the  $\text{NiFe}_2\text{O}_4$  spinel ferrite are presented. In the absence of  $dc$  magnetic field the resonant oscillatory circuit is formed by the coils with ferromagnetic sample inside. The resonant frequencies were in the range of units of megahertz depending on the sample composition. Shift of resonant frequency with  $dc$  magnetic field is caused by variation of the magnetic permeability of the sample material  $dc$  upon magnetization. The dynamic longitudinal and transverse components of magnetic permeability tensor have been estimated from the experimental data.

Support by the Program of the Presidium of RAS No.22, Project of joint research of Ural and Siberian Branches of RAS No.09-S-2-1016, Program of the Department of physical sciences of RAS "Spin phenomena in solid-state structures and spintronics" is acknowledged.

23TL-O-9

## EVALUATION OF ABSORPTIVE PROPERTIES AND PERMEABILITY OF THIN SHEET MAGNETO-DIELECTRIC MATERIALS

*Koledintseva M.Y., Razmadze A.G., Gafarov A.Y., Drowniak J.L.*

EMC Lab, Missouri University of Science and Technology, 4000 Enterprise Dr.,  
HyPoint Industrial Park, Rolla, MO, 65401, U.S.A.

Thin absorbing layers containing magnetic alloy or ferrite inclusions can be effectively used for attenuating common-mode currents on extended structures, such as power cords, cables, edge-coupled microstrip lines, shielding enclosures, or susceptible circuits from electromagnetic immunity (EMI) point of view. To design or choose an appropriate absorbing material, it is important to evaluate per-unit-length attenuation of the common-mode currents over the given frequency range by an absorbing layer of particular thickness. An analytical model to evaluate attenuation on the coaxial line with the central conductor coated with a magneto-dielectric layer is proposed and validated by the experiments and numerical modeling.

The analytical model is based on finding a complex propagation constant and the corresponding surface impedance associated with the  $\text{TM}_z$  mode propagating along a coaxial line with a central conductor coated with a thin magneto-dielectric layer. Frequency characteristics of permittivity and permeability are supposed to be known. Indeed, they are measured using a traditional Nicholson-Ross technique [1] on a washer punched out of a thin sheet material under test, and the washer completely filling the cross-section of the coaxial airline. The proposed model is based on the vector potential matching on the boundaries of the conductor-lossy material-air, and the rigorous solution of the transcendental equation for wave numbers for the modes propagating in the air region at the boundary with the lossy magneto-dielectric medium [2], [3]. The attenuation of quasi-TEM-mode propagating in the air-filled coaxial line with the coated central conductor is analyzed using the concepts of surface displacement [4] and degraded conductivity due to the thin coating. The effective RLGC parameters of the structure, different from those in a lossless coaxial line, are then extracted. The S-parameters for a section of the coaxial line with the coated central conductor then can be calculated using the transition from the RLGC parameters to the ABCD matrix

parameters. A few examples of commercially available thin sheet noise-suppressing magneto-dielectric materials have been tested, and both measured and modeled frequency dependences of attenuation are presented. This approach allows for comparing absorptive properties of different thin sheet magneto-dielectric materials, as well as when using the same material, but of different thickness or length on the conductor. This is important for developing a metrics of attenuation due to the presence of the noise-suppression material on a conducting surface. The analytical results for the transmission coefficient ( $S_{21}$ ) are also compared with numerical simulations using the finite-element method in CST Microwave Studio, and the results agree well over the frequency range of interest, 900 MHz-12 GHz.

Another useful outcome of this model is that it lays the basis for the technique to extract permeability of thin sheet magneto-dielectric materials by wrapping them around a central conductor of the coaxial airline. The results of extracting permeability are compared with those extracted using a washer sample.

The authors acknowledge the partial support of this work by the NSF grant no. 0855878 through the Industry-University Research Center (I/UCRC) program.

- [1] A.M. Nicholson, G.F. Ross, *IEEE Trans. Instrum. Meas.*, **19** (1970), 377-382.
- [2] R.E. Collin, *Field Theory of Guided Waves*, 2<sup>nd</sup> ed., IEEE, Wiley (1991), ch. 11.
- [3] G. Goubau, *J. Appl. Phys.*, **21**, 1950, 1119-1128.
- [4] A.E. Sanderson, in *Advances in Microwaves*, **7** (1971), Academic Press, 2-57.

23OR-O-10

## **A CALIBRATION TECHNIQUE FOR PERMEABILITY MEASUREMENTS IN A SHORTED STRIPLINE**

*Starostenko S.N., Rozanov K.N.*

Institute for Theoretical and Applied Electromagnetics RAS, Russian Federation, Moscow, Izhorskaya, 19

Microwave measurements of thin film are usually performed in small all-in-one shorted stripline cells [1]; the highest operating frequency of a cell is associated with its resonance frequency. But the smaller is the cell length, the higher partial volume of this cell is occupied by non-uniform field in the vicinity of coaxial to stripe coupling (CSC). Besides, the smaller is the coupling, the poorer is its matching, the lower is its transparency, the lower is the field strength and the smaller is the zone of uniform field inside the cell. This very zone limits the measured sample size. The sample cross-section and the coupling matching define the lowest permeability measured with a particular network analyser. Numerical procedures [2, 3] that account for field non-uniformity are too complicated for practice, therefore the measurement of low permeability samples is still a challenging problem.

The difficulty arises from unknown S-parameters of a built-in CSC, since the standard calibration procedure employing zero, infinite and matched loads is inapplicable to an all-in-one single-port cell with an internal CSC inhomogeneity. It is possible to neglect their contribution to the measured reflectivity response only at frequencies below the resonance of the measurement cell. Therefore this neglect limits the highest operating frequency [1-3]. Several calibration procedures are known to be appropriate for single-port all-in-one cells. The conventional one is similar to a sliding-short method, and is based on measurement of reflectivity response as a function of sample position

relative to a short at each frequency. A drawback is that the wider is the frequency band, the higher should be the sample-slide length and the more measurements are needed. The technique is cumbersome and is limited by cell design. An alternative procedure is based upon a partial calibration with a reference sample of known constitutive parameters. The prototype procedure [4] takes into account sample sizes and shape, but neglects one of S-parameter of CSC.

The proposed technique is based on measurement of two complimentary reference samples. The first one is a permeable composite similar to one in the paper [4]. The second sample may be a dielectric with high permittivity or a stripe of impermeable metal. The dimensions of both reference samples are selected to obtain approximately opposite reflectivity phases within the operating frequency band. The calibration procedure includes the reflectivity measurement of an empty cell and of the cell loaded with each of reference samples.

The measurements are performed in 30cm-long stripline cell, where the CSC is well matched and the low-susceptible samples may be large enough for reliable permeability measurement. Another advantage of a long cell is that the calibration errors are visualised, as the cell resonance is well below the highest operating frequency.

The proposed technique has been tested by measurements of samples with known permeability spectra; the measurement accuracy is almost tenfold higher than in [4]. The technique may be applied for calibration of different types of all-in-one transmission lines.

Partial support by RFBR Grant No 09-08-0 1161 is acknowledged.

- [1] V. Bekker, K. Seemann, H. Leiste, *J. Magn. Magn. Mater.*, **270**, 327, 2004.
- [2] Y.Q. Wu, Z.X. Tang, Y.H. Xu, B.G. Zhang, X. He, *IEEE Trans Magn.*, **46**, 886, 2010.
- [3] Y. Liu, L.F. Chen, C.Y. Tan, H.J. Liu, C.K. Ong, *Rev. Sci. Instr.* **76**, 063911, 2005
- [4] S.N. Starostenko, K.N.Rozanov, A.V.Osipov, *J. Appl. Phys.* **103**, 07E914, 2008

23OR-O-11

## **TAMM AND SHOCKLEY STATES IN MAGNONIC SUPERLATTICES**

*Kłos J.W.*

Faculty of Physics, Adam Mickiewicz University, Umultowska 85, 61-614 Poznań, Poland

The idea of surface states was introduced in the 1930s in pioneer works by Tamm [1] and Shockley [2] regarding electronic states. The mechanism of induction of surface states in finite (or semi-infinite) periodic potentials was discussed in the following decades. One of the clearest classifications, proposed by J. Zak [3], segregates surface states into two categories: Shockley states, induced by only breaking the translational symmetry of the crystal by cutting the crystal potential at a symmetry point, and Tamm states, which necessitate a potential perturbation near the surface.

The concept of Tamm and Shockley states can be applied to surface states in other media, too. We investigate the occurrence of Tamm and Shockley states in magnonic superlattices. In these systems the dynamic component of magnetization, describing the propagation of spin waves, has the form of a Bloch function. As in the case of electronic states, the exponential decay of surface states inside the magnonic superlattice will result from complex wave-vector values in frequency ranges corresponding to bandgaps in the magnonic spectrum.

We investigate 1D magnonic crystals consisting of periodically alternating layers of two ferromagnetic materials. We use two calculation methods: (1) the transfer matrix technique for

analytical calculations, and (2) the plane wave method (PWM) for numerical computation. In each method the surface is introduced differently. The analytical approach is applied to semi-infinite structures. In the PWM we consider a superstructure with a series of periods separated by wide spacers in each supercell.

The spin-wave spectra are calculated by a continuous model based on the Landau-Lifshitz equation in the linear approximation. We take into account both the exchange and dipolar interactions by adding extra terms to the effective field. Damping is neglected.

Shockley states are calculated for the in-plane external magnetic field configuration, in which the static demagnetizing field is negligible. To investigate the induction of Tamm states, we modify the surface cell of the magnonic superlattice by controlling the width of the layers in the surface cell and its material parameters.

We also examine the occurrence of surface states in the out-of-plane configuration of the external field, with strong static demagnetizing field at the interfaces between adjacent layers. In this case the surface cell is perturbed by the static demagnetizing field in a different way than inner cells.

The research was supported by European Community's Seventh Framework Programme (FP7/2007-2013), Grant Agreement no. 228673 (MAGNONICS).

- [1] I. Tamm, Phys. Z. Sowjetunion, **1** (1932) 733.
- [2] W. Shockley, Phys. Rev., **56** (1939) 317.
- [3] J. Zak, Phys. Rev., B **32** (1985) 2218.

**23 August**

Tuesday

17:30-19:00

poster session  
23PO-I

**“Soft and Hard  
Magnetic Materials”**

23PO-I-1

## THE ORIGIN OF VARIABLE THERMOELECTRIC EFFECT IN MAGNETIC VISCOSITY ALLOY $\text{Fe}_{86}\text{Mn}_{13}\text{C}$

*Abylkalykova R.B.<sup>1</sup>, Kveglis L.I.<sup>2</sup>, Semchenko V.V.<sup>2</sup>, Volochaev M.N.<sup>3</sup>*

<sup>1</sup> East Kazakhstan Technical University of D.Serikbaeva, 070004, Ust Kamenogorsk, Kazakhstan

<sup>2</sup> Siberian Federal University, 660041, Krasnoyarsk, Russia

<sup>3</sup> Siberian Aerocosmic University, Krasnoyarsk, Russia

[kveglis@iph.krasn.ru](mailto:kveglis@iph.krasn.ru)

In given work the thermal electromotive force was detected at various points in the shock-deformed samples of alloy  $\text{Fe}_{86}\text{Mn}_{13}\text{C}$ . The electromotive force was established that as a result of long mechanical loading on an austenitic alloy  $\text{Fe}_{86}\text{Mn}_{13}\text{C}$ . In its structure, besides known phases of deformation martensite, Frank-Kasper structures can be formed. The variable temperature dependence of thermal electromotive force in samples of alloy  $\text{Fe}_{86}\text{Mn}_{13}\text{C}$  has been detected. It has been noticed that at heating of the sample, its property are identical to properties of the thermocouple. If the sample has not been subject to shock strain value the contact potential difference effect was absent. It is determined that in Fe-Mn and Fe-Mn-C alloys there is the complicated magnetic order similar to an order in spin glass, which is installed thanks to coexistence of interacting antiferromagnetic and ferromagnetic phases. Structural studies of alloy  $\text{Fe}_{86}\text{Mn}_{13}\text{C}$  may indicate such states and give the answer to the cause of magnetic viscosity. Electronic structure calculations for nanocrystalline  $\text{Fe}_{87}\text{Mn}_{13}$ , by the scattered waves method, were showed the presence of energy gaps in the spectra of the electron density of states of nanocrystalline having a structure of the Frank-Kasper. They are most easily formed from the nonequilibrium state in metallic alloys. Sign thermo electromotive force may vary depending on the temperature. The reason for its appearance is connected with the contact potential difference at the interface of two phases: the antiferromagnetic austenite and ferromagnetic martensite deformation. The nature of the appearance of variable thermoelectric effect can be explained from the standpoint of coexistence in the samples of the inhomogeneous crystal and magnetic structures. The effect of magnetic viscosity in samples of alloy  $\text{Fe}_{86}\text{Mn}_{13}\text{C}$  and its change under the influence of long-term impact of mechanical loading was detected.

23PO-I-2

## <sup>11</sup>B NMR STUDY OF AMORPHOUS $\text{Fe}_{85-x}\text{Cr}_x\text{B}_{15}$ (x=0-20) ALLOYS

*Pokatilov V.S.*

Moscow State Institute of Radio-Engineering, Electronics and Automation, pr. Vernadskogo 78, Moscow, 117454 Russia

Local atomic and magnetic structures of Fe-B amorphous alloys have been studied in sufficient detail. The short-range order of these alloys have been determined (for example, [1, - 3]). Amorphous alloys based on Fe and B that have been used in engineering contains s-, p- and d-atoms. The influence of these atoms on the local atomic and magnetic structures of these alloys has not been practically investigated. In this work, it was studied the effect of substitution of chromium

atoms for iron atoms on the short-range order in the  $\text{Fe}_{80-x}\text{Cr}_x\text{B}_{15}$  ( $x = 0 - 20$ ) amorphous alloys by  $^{11}\text{B}$  NMR method.

The  $\text{Fe}_{80-x}\text{Cr}_x\text{B}_{15}$  ( $x = 0 - 20$ ) amorphous alloys were produced by ultra fast quenching of a melt-spinning process. The local atomic and magnetic structures of Fe-B-Cr amorphous alloys were studied on a nuclear magnetic resonance spectrometer at  $^{11}\text{B}$  nuclei in the frequency range 1-50 MHz at a temperature of 4.2K.

It has been revealed that the substitution of chromium atoms for iron atoms gives rise to an additional contribution to the  $^{11}\text{B}$  NMR spectra in the low frequency range. In the  $\text{Fe}_{80-x}\text{Cr}_x\text{B}_{15}$  ( $x = 0 - 20$ ) amorphous alloys, the chromium atoms substitute for iron atoms in the nearest coordination shells of boron atom. These alloys consist of nanoclusters in which boron atoms have short-range order of the tetragonal  $(\text{Fe,Cr})_3\text{B}$  and  $\alpha - \text{Fe}(\text{Cr})$  phase type. It has been found that the substitution of chromium atoms disturbs the local magnetic moments of iron atoms.

[1] V. Pokatilov, N. Djakonova, *Hyperfine Interact.* **59** (1990) 525.

[2] V.S. Pokatilov, *Phys. Solid State* **49** (12) (2007) 2217

[3] V.S. Pokatilov, *Phys. Solid State* **51**(12) (2007) 2217.

23PO-I-3

## THE INFLUENCE OF NANOSTRUCTURE PARAMETERS ON A MAGNETIZATION REVERSAL PROCESSES OF R-Zr-Co-Cu-Fe ALLOYS

*Suponev N.P., Semenova E.M., Lyakhova M.B., Kurtanov N.I., Velichko E.S.*

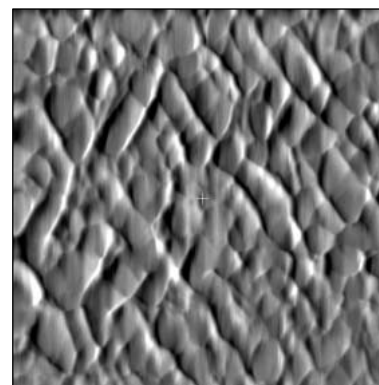
Tver State University, 170002, Sadoviy lane 35, Tver, Russia

Investigations of magnetization reversal processes and structure of large group of R-Zr-Co-Cu-Fe (R=Sm, Gd) alloys were carried out. Magnetic measurements were executed by a vibrating sample magnetometer. The microstructure and magnetic domain structure was studied by methods of optical and scanning probe microscopy. For realization of a high coercivity state alloys were exposed homogenizing at 1170–1190°C during 3–6 hours and isothermal ageing at 800°C during 2–24 hours. The further cooling was carried out by two ways: hardening up to room temperature or slow cooling up to 400°C. Such variation of heat treatment has allowed realizing a wide spectrum of coercivity values of the investigated alloys.

The method of atomic force microscopy had been established the presence of a cellular microstructure [1] at R-Zr-Co-Cu-Fe alloys already after ageing at 800°C during 5 hours (see fig.). The subsequent increase of processing duration was accompanied by only small increase of the cells sizes. Cells of a microstructure had the average sizes from 50 nm to 100 nm depending on a mode of thermal processing and a chemical compound of R-Zr-Co-Cu-Fe alloys.

However the coercivity values of R-Zr-Co-Cu-Fe alloys is determined mainly by duration of ageing at 800°C, and also way of cooling, at slow cooling the majority of alloys from 800°C there is an about twice increase of  $H_C$  values.

The received results testify that the coercivity values of R-Zr-Co-Cu-Fe alloys is mainly defined not by the cells size, and a



Typical cellular  
microstructure of alloys

chemistry difference of inside areas and a boundary phase of cells of a microstructure.

Redistribution of elements between phases of cellular structure occurs both during isothermal ageing at 800°C and at slow cooling up to room temperature. Result of both processes is formation of high gradients of magnetic constants in a microstructure of alloys, is especial on borders of cells. Due to boundary phases of cells become the effective centers of domain wall pinning.

The peculiarities of magnetic reversal processes of alloys found out in work are discussed in the model of the mixed mechanism of a magnetic hysteresis [2]: irreversible rotation of a magnetization vector in the central areas of cells and a domain wall pinning on boundary phase of cells.

Support by RFBR №09-02-01274 and the Federal program Scientific and pedagogical staff of innovative Russia.

[1] A.E. Ray, *J. Appl. Phys.*, **55** (1984) 2094.

[2] N.P. Suponev, R.M. Grechishkin, M.B. Lyakhova, Yu.E. Pushkar, *J. Magn. Magn. Mat.*, **157–158** (1996) 367.

23PO-I-4

## **EFFECT OF HEAT TREATMENT ON THE MICROSTRUCTURE AND MAGNETIC PROPERTIES OF Fe<sub>2</sub>NiAl-BASED ALLOYS**

*Menushenkov V.P., Sviridova T.A., Shelehov E.V., Savchenko A.G.*

National Research Technological University “MISiS”, 119049 Leninsky prospekt 4, Moscow, Russia

The crystal structure and magnetic properties of hard magnetic Fe<sub>2</sub>NiAl-based alloy with composition Fe<sub>46.4</sub>Ni<sub>24.5</sub>Al<sub>26.7</sub>Si<sub>12.4</sub> were investigated by transmission electron microscopy, X-ray diffraction and magnetostatic methods after different heat treatments. This alloy belongs to a group of alloys with insolubility gap at state diagram. The high coercivity is related with special microstructure which forms during cooling below the solubility curve when  $\alpha$ -solid solution decomposes into a mixture consisting of two isomorphic cubic phases'  $\alpha \rightarrow \alpha_1 + \alpha_2$ . Maximum of coercive force achieved after cooling with critical rate  $V_{cr} = 4-6^\circ\text{C/s}$  from 1200°C to room temperature (RT).

Water-quenching from 1200°C ( $V = 55^\circ\text{C/s}$ ) fixes a non-homogeneous  $\alpha$ -solid solution with the low coercive force ( $H_c < 4$  Oe). X-ray diffraction analysis showed the superposition of two phases:  $\alpha_1$ -phase with a bcc-structure (A2), which can be partly ordered in Cu<sub>2</sub>MnAl-type structure (L<sub>21</sub>) and  $\alpha_2$ -phase, which is partly ordered with the formation of the CsCl-type structure (B2). Both phases have almost equal lattice parameters, i.e.,  $a = 0.2877$  nm.

The cooling from 1200°C with a critical rate  $V_{cr} = 4.5^\circ\text{C/s}$  transforms the alloy into the high-coercivity state ( $H_c = 650$  Oe). During cooling in a high temperature range from 950 to  $\sim 800^\circ\text{C}$ , ferromagnetic  $\alpha_1$ -platelets are formed within the weakly ferromagnetic NiAl-rich matrix ( $\alpha_2$ -phase). The magnetic anisotropy and coercivity originate from a difference in the demagnetizing factors of  $\alpha_1$ -platelets and a difference in the saturation magnetization of  $\alpha_1$ -particles and  $\alpha_2$ -matrix. But the value of coercivity is low because of the high magnetic interaction between  $\alpha_1$ -particles. During cooling below 800°C, continuous changes in the composition take place via the redistribution of Fe and Ni-Al atoms between  $\alpha_1$  and  $\alpha_2$  phases. Improvement of magnetic insulation of  $\alpha_1$ -particles due



to the process of second decomposition related with NiAl precipitation around  $\alpha_1$ - particles increases coercive force.

It is known that  $H_c$  of Fe<sub>2</sub>NiAl-based alloys are not sensitive to thermomagnetic treatment because of the temperature of solid solution decomposition (~950°C) is higher than Quire temperature of ferromagnetic  $\alpha_1$ -phase. But the thermomagnetic treatment may be effective when the cooling rate from 1200°C to RT is higher than the critical rate and the solid solution decomposition is uncompleted. Appreciable improvements of magnetic characteristics (the remanence and magnetic energy) of Fe<sub>46.4</sub>Ni<sub>24.5</sub>Al<sub>26.7</sub>Si<sub>2.4</sub> alloy were reached using the cooling of the samples at cooling rates that are higher than the  $V_{cr}$  corresponding to the formation of optimal microstructure of magnets. The subsequent tempering treatment at 710°C in magnetic field  $H = 3$  kOe increases the remanence  $B_r$  and the energy product  $(BH)_{max}$  by up to 15-25%. In this case, the thermomagnetic treatment leads to the growth of  $\alpha_1$ -platelets within grains, which are mainly parallel to the direction of the magnetic field applied during aging and, thus, the remanence of magnets increases.

This work was supported by Ministry of Education and Science of the Russian Federation (2.1.2/13549 grant).

23PO-I-5

## THERMAL DEPENDENCE OF MAGNETIC PROPERTIES OF SINTERED MAGNETS ND-FE-B ALLOYED BY REM ALLOYS WITH TRANSITION METALS

*Melnikov S.A.<sup>1</sup>, Piskorskiy V.P.<sup>2</sup>, Belyaev I.V.<sup>3</sup>, Valeev R.A.<sup>2</sup>, Verklov M.M.<sup>1</sup>, Ivanov S.I.<sup>4</sup>,  
Ospennikova O.G.<sup>2</sup>, Parshin A.P.<sup>1</sup>*

<sup>1</sup> JSC «VNIHT», Kashirskoe road, 33, Moscow, 115409, Russia

<sup>2</sup> FSUE «VIAM», Radio st., 17, Moscow, 105005, Russia

<sup>3</sup> JSC «SPU «Magnetron», Kuibysheva st., 26, Vladimir, 600026, Russia

<sup>4</sup> JSC «VNINM», Rogova st., 5a., Moscow, 123060, Russia

The present paper studies the effect of additives in the form of REM (dysprosium) alloys with transition metals of the following compositions: Dy<sub>32.1</sub>Al<sub>55.2</sub>Co<sub>12.7</sub>, Dy<sub>37.7</sub>Al<sub>32.5</sub>Co<sub>29.8</sub>, DyCu<sub>5</sub>, DyCo<sub>2</sub> and, also, in the form niobium alloy Nb<sub>3</sub>Co<sub>7</sub> on magnetic properties of sintered magnets based on main alloy Nd<sub>15.25</sub>Fe<sub>73.5</sub>Co<sub>1.6</sub>Ti<sub>1.4</sub>Cu<sub>0.5</sub>Al<sub>0.25</sub>B<sub>7.5</sub>.

It is proved that dysprosium additives introduced to sintered magnets led to increase of coercive force  $iH_c$  from 994.4 to 1369.0 kA/m or growth from 25 to 70 % of values  $iH_c$  of unalloyed sintered magnets. Drop of residual induction in this case makes 1.7 to 4.7 % for cobalt-free additives, and for introduction of DyCo<sub>2</sub> residual induction is increased by 6.6 %. Alloying of sintered magnets by addition Nb<sub>3</sub>Co<sub>7</sub> results in insignificant growth of  $iH_c$  by 3.2 % and high increase of residual induction by 9.6 %.

It is established that trend of curves of temperature dependence for relative values of coercive force and residual induction practically coincide for all studied compositions of sintered magnets.

Introduction of alloying additives (also including cobalt) does not considerably effect the thermal stability of hysteresis performances of sintered permanent magnets Nd-Fe-B. Thermal coefficients of residual induction  $\alpha$  and coercive force  $\beta$  vary within  $\alpha = -(0,13...0,074)$  % °C<sup>-1</sup> and  $\beta = -(0,8...0,6)$  % °C<sup>-1</sup>. Increase of operating temperature for sintered magnets is possible due to coercive force  $iH_c$  growth as a result of alloying.

## ATOMIC FORCE MICROSCOPY MEASUREMENTS OF MAGNETOSTRICTION OF SOFT-MAGNETIC FILMS

Harin E.V.<sup>1</sup>, Sheftel E.N.<sup>1</sup>, Krikunov A.I.<sup>2</sup>

<sup>1</sup> Baikov Institute of Metallurgy and Materials Science RAS, 119991, Moscow, Leninskii prospekt 49, Russia

<sup>2</sup> Institute of Radio Engineering and Electronics RAS, 141120, Moscow Region, Fryazino, Vvedenskii Square 1, Russia

The soft magnetic properties magnitude of a ferromagnet (the magnetic permeability, coercive force) under magnetization is determined by contributions of magnitocrystalline and magnetoelastic energies. The magnitocrystalline anisotropy of nanocrystalline ferromagnet with a grain size, which is lower substantially than the exchange ferromagnetic interaction length, is enough small and, thus, does not affect the level of soft-magnetic properties. In this case, the role of magnetoelastic anisotropy which to a great extent is determined by magnetostrictive processes increases. To prepare nanocrystalline ferromagnet films, planar technologies are used; in terms of the technologies, films are formed on substrates. The experimental determination of the magnetostriction of the films located on a substrate is a complicated experimental task. This is related to the fact that the presence of a substrate determines the consideration of the “film-substrate” system as a bimaterial bending under the action of elastic stresses induced in the thin-film layer.

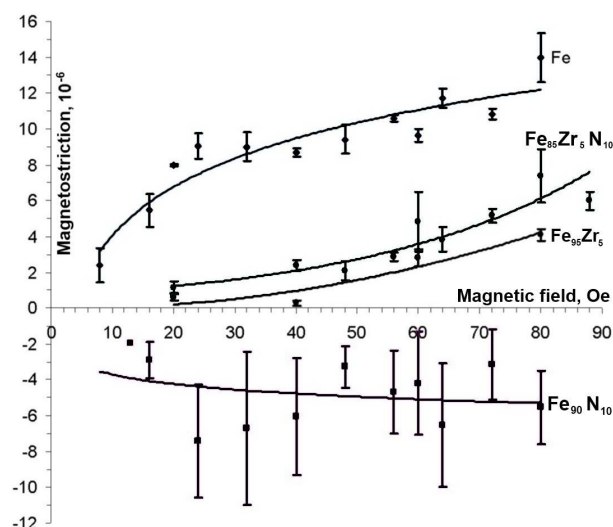
In the present study, we report results of measurements of the magnetostriction of films located on substrates using an atomic force microscope and a technique developed by us. The measurements were performed for Ni, Fe, Fe<sub>90</sub>N<sub>10</sub>, Fe<sub>95</sub>Zr<sub>5</sub>, and Fe<sub>85</sub>Zr<sub>5</sub>N<sub>10</sub> films deposited on quartz substrates by magnetron sputtering. The films chemical composition determined by EDX, the phase-structural state was studied by XRD. The magnetostriction of films as a function of the magnetic field applied along the film plane was measured by a cantilever method based on the determination of substrate bending induced by the applied magnetic field. The bending was measured along the long side of sample and perpendicular to the side. The deformation along the applied field was calculated by expression:

$$\lambda = \frac{D}{3} \frac{h_s^2}{h_f l^2} \frac{E_s / (1 + \nu_s)}{E_f / (1 + \nu_f)},$$

where  $D$  is the substrate bending;  $h_f$  and  $h_s$  are the film and substrate thicknesses, respectively;  $E_f$  and  $E_s$  are the Young modules of the film and substrate, respectively;  $l$  is the film length, for which the bending was measured;  $\nu_f$  and  $\nu_s$  are the Poisson coefficients of the film and substrate, respectively. The in-film magnetostriction, which can be compared with the linear magnetostriction of volume materials, is:

$$\lambda = \frac{2}{3} (\lambda_{\parallel} - \lambda_{\perp}).$$

The effect of chemical composition and phase and structural states of the films under study on the magnetostriction is discussed.



This study was supported by the President Foundation supporting leading scientific schools, project 02.120.11.7075-NSh.

23PO-I-7

## MOSSBAUER STUDY OF MAGNETIC TRANSFORMATIONS IN ALLOYS $\text{Pr}(\text{Fe}_{1-x}\text{Al}_x)_2$

*Solodov E.*

Lomonosov Moscow State University, GSP-1, Leninskie Gory, Moscow, 119991, Russian Federation

In frames of this experimental work were synthesized high pressure phases in the quasibinary system  $\text{Pr}(\text{Fe}_{1-x}\text{Al}_x)_2$ . Chosen experimental methods were X-ray diffraction of polycrystals, magnetic measurements and low temperature Mössbauer spectroscopy (90 ÷ 370K). We studied phase structure, atomic-crystal structure, phase transformations and hyperfine interactions into system of alloys for  $0 \leq x \leq 1$  at step  $x=0.1$ .

By the X-ray investigations were studied the phase constitution and crystal structure of synthesized alloys as well as were determined their crystal parameters.

Mössbauer spectra were obtained at the temperature in range of 90 ÷ 370K. Experimental Mössbauer spectra were fitted as a superposition of sextets (responsible for the magnetically ordered state) and doublets (which characterize the paramagnetic state). Region  $x = 0.2-0.3$  is a two-phase region of coexistence of structures C15 and C14. Therefore, the spectra are complex and can be represented by a superposition of at least three sextets and three doublets. This number corresponds to the the three main probability of finding aluminum atoms in the nearest neighborhood of iron atoms in the cubic lattice of C15.

The concentration area  $x = 0.4$  is a single-phase region of the hexagonal C14-type structure. A large amount of aluminum in the alloy led to the fact that the spectra are mainly a superposition of paramagnetic doublets. The sample with  $x = 0.4$ , unfortunately, contains an admixture of  $\alpha\text{-Fe}$ , which gives a characteristic sextet with a field  $H = 330\text{kOe}$ .

In our samples, we measured the magnetic moment on temperature during cooling in a magnetic field of 100 Oe.

The dependence of the area sextets on the temperature, which determines the boundaries of the phase transitions of the types “order-disorder” was carried out. It is in good agreement with data from direct magnetic measurements.

23PO-I-8

## MAGNETIC PROPERTIES OF $\text{Ba}_6\text{Mn}_{24}\text{O}_{48}$

Cherny A.S.<sup>1</sup>, Rykova A.I.<sup>1</sup>, Khatsko E.N.<sup>1</sup>, Yeremenko A.V.<sup>1</sup>, Shevchenko A.D.<sup>2</sup>, Uvarov V.N.<sup>2</sup>,  
Pomerantseva E.A.<sup>3,4</sup>, Goodilin E.A.<sup>3,4</sup>, Tretyakov Yu.D.<sup>3,4</sup>

<sup>1</sup> B.I.Verkin Institute for Low Temperature Phys. & Engineering of NAS of Ukraine,  
47 Lenin Ave., Kharkov 61103, Ukraine

<sup>2</sup> G.V. Kurdyumov Institute for Metal Physics of the NAS of Ukraine,  
36, Academician Vernadsky Dlvd., UA-252680 Kiev-142, Ukraine

<sup>3</sup> Department of Materials Science, Lomonosov Moscow State University, Lenin Hills, 119992,  
Moscow, Russia

<sup>4</sup> Department of Chemistry, Lomonosov Moscow State University, Lenin Hills, 119992, Moscow,  
Russia

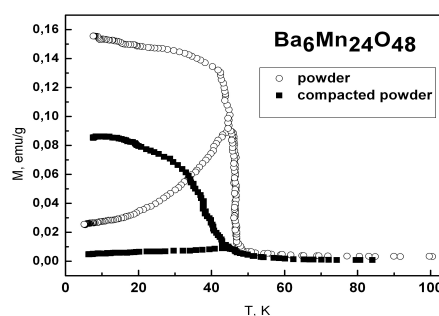
It have been investigated static and dynamic magnetization  $M$  for manganite  $\text{Ba}_6\text{Mn}_{24}\text{O}_{48}$  in the temperature range 4,2-300 K and in external magnetic fields up to 6000 Oe. It have been studied samples  $\text{Ba}_6\text{Mn}_{24}\text{O}_{48}$ : sample number 1 - was obtained by compressing the powder under the pressure of 7.5 GPa, the sample number 2 - powder. The  $M(T)$  are characterized by the presence of the anomaly around 40 K, which is due to a transition study of the magnetic system in two states (the powder pressed under the pressure of 7.5 GPa and powder) in a magnetically ordered state.

Temperature dependence of the static magnetization of both samples measured during heating after cooling in zero magnetic field (ZFC) and in magnetic fields (FC), differ greatly in appearance, indicating that the phase separation and spin-glass state. The interval of the magnetic field varies from 24 to 6000 Oe. The temperature  $T^*$  the beginning of the divergence between  $M_{\text{ZFC}}(T)$  and  $M_{\text{FC}}(T)$  for both samples are weakly dependent on the external magnetic field, which is consistent with the results of the possibility of glass behavior of systems without relaxation. It should be noted

the presence of significant differences in the behavior of the temperature dependence of the static  $M_{\text{ZFC, FC}}(T)$  for sample number 1 and number 2 (see Fig.). The figure shows that the 4.2 K magnetization ratio for samples number 1 and number 2 ( $M_{\text{FC1}}/M_{\text{FC2}} \approx 1,8$ ). This difference may be due to different kind and magnitude of the interaction between the particles of powder and pressed powder. Conducted a study of the temperature dependence of the dynamic magnetization of pressed powder  $\text{Ba}_6\text{Mn}_{24}\text{O}_{48}$  in the frequency range 10 - 10000 Hz allowed us to determine the frequency dependence of the freezing temperature  $T_f$ . Accordingly, using the data, determined the rate of frequency shift of the

freezing temperature  $\delta T_f = \frac{\partial \ln T_f}{\partial \log_{10} \omega} \approx 0.013$ , which in magnitude is consistent with similar

estimates for the spin - glass systems.



Temperature dependence of magnetization  $\text{Ba}_6\text{Mn}_{24}\text{O}_{48}$  in the ZFC and FC in a magnetic field 200 Oe

23PO-I-9

## LOCAL STRUCTURE OF HIGH-COERCIVITY Fe-Ni-Al ALLOYS

Menushenkov A.P.<sup>1</sup>, Menushenkov V.P.<sup>2</sup>, Chernikov R.V.<sup>1,3</sup>, Sviridova T.A.<sup>2</sup>, Grishina O.V.<sup>1</sup>,  
Sidorov V.V.<sup>1</sup>

<sup>1</sup> National Research Nuclear University "MEPhI", 115409 Kashirskoe sh. 31, Moscow, Russia

<sup>2</sup> National University of Science and Technology "MISIS", 119049 Leninskiy pr. 4, Moscow, Russia

<sup>3</sup> HASYLAB at DESY, 22603 Notkestrasse 85, Hamburg, Germany

Hard magnetic Fe-Ni-Al alloys belong to a group of alloys with insolubility field at state diagram. On cooling below the solubility curve solid solution decomposes to a mixture of two isomorphic cubic phases  $\beta \rightarrow \beta + \beta_2$ . Maxima of coercitive force  $H_c$  achieved at intermediate decomposition stage is related with nonequilibrium microstructure which is formed at aging of homogeneous solid solution (heat treatment I), or at solid solution cooling with critical rate (heat treatment II).  $H_c$  value reached by heat treatment II is 1.5 times as large as  $H_c$  value reached by heat treatment I. Data on structural transformations in Fe-Ni-Al alloys are contradictory and need to be specified [1]. This work summarizes our studies of crystal structure and local environment of iron and nickel in Fe-Ni-Al alloy after different heat treatment by means of X-ray absorption spectroscopy (EXAFS).

The samples with nominal composition of  $\text{Fe}_{46.4}\text{Ni}_{24.5}\text{Al}_{26.7}\text{Si}_{2.4}$  were prepared by induction melting in Ar atmosphere followed by casting in a copper mould. Three schemes of heat treatment were used. Phase identification was carried out at powder samples by X-ray diffraction using  $\text{Co-K}\alpha$  radiation. EXAFS measurements above iron and nickel K-edge absorption were performed at E4 beamline of HASYLAB synchrotron centre (DESY, Hamburg, Germany).

Quenching from 1200°C in water (N1) fixes solid solution with low coercitive force ( $H_c < 4$  Oe). X-ray structure analysis showed the superposition of two phases:  $\beta_2$ -phase which is partly ordered in CsCl-manner structure (B2) and  $\beta$ -phase with bcc-structure (A2). The cooling with critical rate (N2) transforms the alloy to the high-coercivity state ( $H_c = 650$  Oe). The diffraction pattern shows peaks broadening and increase of intensity of additional superstructural reflections belonging to  $L2_1$  phase. Aging of sample N2 at 780°C for 10 min (N3) reduces coercitive force to  $H_c = 320$  Oe and leads to decrease of the intensity of superstructural reflections of  $L2_1$  phase.

According to EXAFS spectra analysis, parameters of coordination shells around iron atoms are practically identical in all samples N1-N3. However analysis of the EXAFS-function measured above K-Ni edge showed the strong difference of the nickel local environment in sample N2 from the environment in sample N1 and N2.

Quenching from 1200°C (N1) fixes initial stage of solid solution decomposition into two phases:  $\beta_2$ -phase (B2 structure) and  $\beta$ -phase (bcc-structure A2). The cooling with critical rate (N2) transforms the alloy to high-coercivity state with  $\beta$ -phase partly ordered in  $\text{Cu}_2\text{MnAl}$ -like structure ( $L2_1$ ). Annealing at 780°C (N3) transfers the alloy to initial phase state: parameters of coordination spheres around Fe and Ni are restored to values corresponding to sample N1 ( $A2+B2$  structures) due to disordering of  $L2_1$ -phase and its transformation into A2 phase.

Support by Federal Program "Scientific and scientific-pedagogical staff of innovative Russia" and Russian Foundation for Basic Researches (grant 11-02-01174-a) is acknowledged.

[1] V.P. Menushenkov, T.A. Sviridova, E.V. Shelekhov, *Proceedings of the 19-th Int. Metallurgical and Materials Conference "Metal-2010"* (Roznov pod Radhostem, Czech Republic, 18-20 May 2010) 807.

## XAFS STUDIES OF MAGNETIC COMPOUNDS, BASED ON THE RARE-EARTH IONS

Menushenkov A.P.<sup>1</sup>, Yaroslavtsev A.A.<sup>1,2</sup>, Grishina O.V.<sup>1</sup>, Chernikov R.V.<sup>1,3</sup>, Kovnir K.A.<sup>4</sup>, Shatruk M.M.<sup>4</sup>

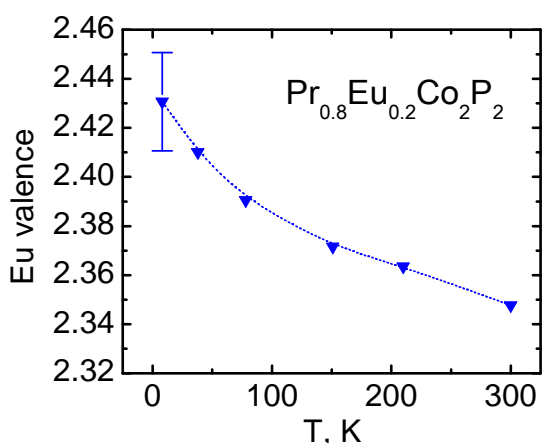
<sup>1</sup> National Research Nuclear University "MEPhI", Kashirskoe sh. 31, 115409, Moscow, Russia

<sup>2</sup> NRC "Kurchatov Institute", Akademika Kurchatova pl., 123182, Moscow, Russia

<sup>3</sup> HASYLAB at DESY, Notkestrasse 85, D-22603 Hamburg, Germany

<sup>4</sup> Florida State University, Tallahassee, FL 32306, USA

The peculiarities of local crystalline and electronic structure such as interatomic distances, local disordering factors and rare-earth valences were investigated by means of XAFS spectroscopy in  $\text{RCo}_2\text{P}_2$  ( $\text{R} = \text{La}, \text{Ce}, \text{Pr}, \text{Eu}$ ) itinerant magnets. Magnetic ordering in such materials is dictated by peculiarities of electronic band structure at the Fermi level and could be modified e.g. by applying external pressure to the sample [1]. The similar modification of an itinerant magnet can be induced by chemical pressure with non-isoelectronic substitution in the rare-earth sublattice. In  $\text{LaCo}_2\text{P}_2$  ( $T_C = 132$  K [2]) the Ce-substituted phases studied herein behave quite differently from the Pr- and Nd-substituted ones. This might be due to Ce intermediate valence state. Another studied compound  $\text{Pr}_{0.8}\text{Eu}_{0.2}\text{Co}_2\text{P}_2$  is unexpectedly ferromagnetic ( $T_C = 290$  K), while the pure  $\text{PrCo}_2\text{P}_2$  and  $\text{EuCo}_2\text{P}_2$  are antiferromagnets.



The X-ray absorption spectra were collected at C beamline of HASYLAB (DESY, Hamburg, Germany) in transmission mode above the  $L_3$ -rare-earth and  $K$ -Co absorption edges. The evaluation of different valence components contribution into the  $L_3$ -XANES spectra was performed using the conventional fitting of complicated absorption peaks with combinations of analytical functions. The analysis showed that the average valence of Eu in  $\text{Pr}_{0.8}\text{Eu}_{0.2}\text{Co}_2\text{P}_2$  increases from +2.35 at 300 K to +2.43 at 8 K (see Fig.). The Ce valence in  $\text{La}_{1-x}\text{Ce}_x\text{Co}_2\text{P}_2$  samples increases from +3.02 at 300 K to 3.08 at 8 K and also increases with the Ce concentration. The change can be explained by

a gradual lattice contraction upon cooling and corresponding rise of the chemical pressure, which favors the smaller in volume  $\text{Eu}^{3+}$  and  $\text{Ce}^{4+}$  states. The EXAFS spectroscopy study performed with the standard technique of  $\chi(k)$  function extraction and Fourier-analysis showed the splitting  $\sim 0.14$  Å of rare-earth coordination shells around Co in all samples consistent with the smaller ionic radii of cerium and europium. The Ce/Eu-Co interatomic distances decrease upon cooling. In such compounds the R-Co interatomic distance characterizes the chemical pressure and interaction between the rare-earth  $4f$  states and Co  $3d$  states. Thus, the rare-earth valence states and R-Co distances behavior upon cooling indicates a fast fluctuation of an electron between localized  $4f$  and delocalized  $3d$  levels which impacts the electronic band structure and drastically alters the magnetic properties.

This work was partially supported by RFBR (grant No. 11-02-01174-a), FTP "Scientific and scientific-pedagogical staff of innovative Russia" (State Contract No. 16.740.11.0139).

[1] M. Chefki, M.M. Abd-Elmeguid, H. Micklitz, et al., *Phys. Rev. Lett.*, **80** (1998) 802.

[2] K. Kovnir, C.M. Thompson, H.D. Zhou, et al., *Chem. Mater.*, **22** (2010) 1704.

23PO-I-11

## EFFECT OF HEAT TREATMENT ON THE MICROSTRUCTURE AND MAGNETIC PROPERTIES OF AS-CAST $\text{SmCo}_5$ BASED ALLOYS

*Menushenkov V.P.<sup>1</sup>, Sviridova T.A.<sup>1</sup>, Shelekhov E.V.<sup>1</sup>, Belova L.M.<sup>2</sup>, Menushenkov A.P.<sup>3</sup>, Chernikov R.V.<sup>3</sup>, Sidorov V.V.<sup>3</sup>, Grishina O.V.<sup>3</sup>*

<sup>1</sup> National University of Science and Technology «MISIS», 119049 Leninsky prospekt 4, Moscow, Russia

<sup>2</sup> Dept. Materials Science and Engineering, Royal Institute of Technology, Stockholm, 100 44 Sweden

<sup>3</sup> National Research Nuclear University «Moscow Engineering Physics Institute» Kashirskoe shosse, 31, 115409 Moscow, Russia

A post sintering heat treatment (HT) is an important stage of  $\text{SmCo}_5$  based magnets processing. The conventional HT included slow cooling from 1120 to 850°C increases  $H_{ci}$  of sintered magnets from 0,1 to more than 3,5 T. The phase-transformation-induced coercivity mechanism in  $\text{SmCo}_{5-x}$  sintered magnets was proposed on the basis of X-ray diffraction data [1]. In this work, we have investigated the microstructure, crystalline and local structure of  $\text{SmCo}_5$  phase in as-cast hypo- and hyperstoichiometric  $\text{Sm}_y\text{Co}_{100-y}$  alloys after various heat treatment using X-ray diffraction, X-ray absorption spectroscopy and metallographic methods. It was established that complicated microstructure of hyperstoichiometric alloys forms in nonequilibrium conditions during crystallization of the ingots and the subsequent cooling to room temperature. XRD study of the lattice parameters of  $\text{SmCo}_5$  phase in as-cast  $\text{SmCo}_5$  based alloys after different heat treatments shows evidence of the Sm enrichment of the  $\text{SmCo}_5$  phase. The behavior of the lattice parameters of  $\text{SmCo}_5$  phase in Sm-rich alloys when subjected to aging between 1220°C and 700°C can be related to the phase transformation of  $\text{SmCo}_5$  into  $\text{SmCo}_{5-x}$  phases. EXAFS analysis shows that stacking faults in  $\text{SmCo}_5$  phase appear in hyperstoichiometric alloys confirming the hypothesis of the phase-transformation-induced coercivity mechanism.

This work was supported by Ministry of Education and Science of the Russian Federation (State Contract П11024 from May 27, 2010).

[1] V.P. Menushenkov. *J. Appl. Phys.*, **99** (2006), 08B523-1 - 08B523-3.

23PO-I-12

## MAGNETIC HYSTERESIS AND MAGNETOIMPEDANCE PROPERTIES OF ELASTICALLY DEFORMED SOFT MAGNETIC $\text{Co}$ -BASED WIRES DC CURRENT ANNEALED

*Semirov A.V., Derevyanko M.S., Kudryavtcev V.O., Bukreev D.A., Moiseev A.A.*  
East Siberian State Academy of Education, Irkutsk, Russia

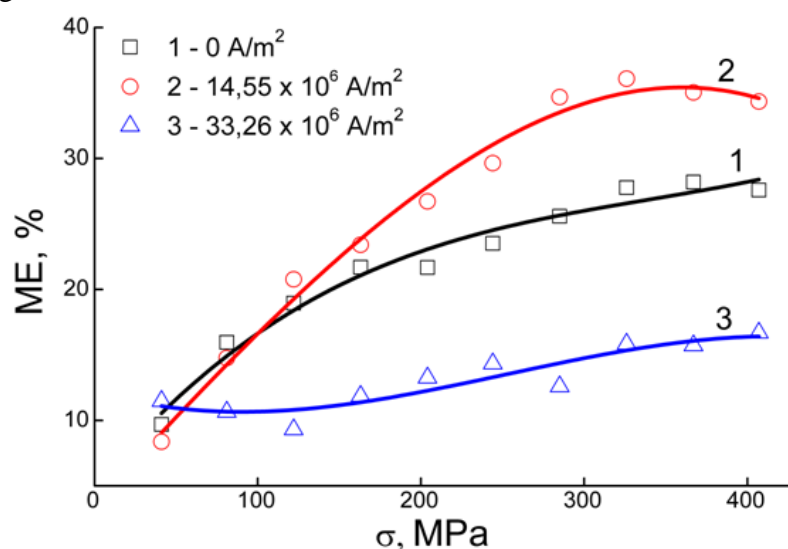
An influence of the dc current annealing on the magnetic hysteresis and magnetoimpedance properties of the amorphous  $\text{Co}_{66}\text{Fe}_4\text{Nb}_{2.5}\text{Si}_{12.5}\text{B}_{15}$  wires elastically deformed was investigated. The diameter of the wires was 175-180  $\mu\text{m}$  and length was 26-30 mm. The annealing was done by direct

electrical current at the air during 5 minutes. The value of the annealing current density ( $j$ ) was varied from 0 to  $37.4 \times 10^6 \text{ A/m}^2$ .

The magnetic hysteresis properties were determined from hysteresis loops derived by the induction method. The value of the external magnetic field  $H$  applied along the sample length was  $\pm 15 \text{ Oe}$ . The frequency  $f$  of the remagnetizing field was 2 kHz. The external mechanical tensile stresses  $\sigma$  were varied from 0 to 400 MPa. The magnetization changing under the mechanical stress influence, called the magnetoelastic effect (ME-effect), was calculated by the relative residual induction as  $((\Delta B_r/B_s)/(B_r/B_s))_\sigma = ((B_r/B_s)_\sigma - (B_r/B_s)_{\sigma=0})/(B_r/B_s)_{\sigma=0} \times 100\%$ .

The magnetoimpedance measurements were done using the impedance analyzer Agilent 4294A in the frequency range (0,001 ÷ 60) at the effective value of the current 1 mA. The field dependences of the impedance were analyzed for the wires annealed at the different dc current densities. Also the impedance dependences on the mechanical stresses values  $\sigma$  were analyzed.

The values of the ME-effect for three wires heat treated at the different dc values are shown at the figure.



It can be seen that ME-effect dependences on mechanical stresses have the monotonously increasing behavior for the wires heat treated at the dc current density values below  $15 \times 10^6 \text{ A/m}^2$ . Also we can observe from the figure that the ME-effect values of the wires 1 (without annealing) and 2 (annealing at the dc current density  $14.55 \times 10^6 \text{ A/m}^2$ ) are near equal right up to the  $\sigma$  value about 160 MPa.

The ME-effect increasing occurs greater with the further  $\sigma$

growing for the sample 2 than for the sample 1. The ME-effect of the sample 3 (annealing at the dc current density  $33.26 \times 10^6 \text{ A/m}^2$ ) poorly changes in the whole range of the tensile stresses.

The maximum value of the ME-effect equals about 16.5 % for the wires 3 in the tested  $\sigma$  range. Whereas it equals 28 % for the wires 1 and 35 % for the wires 2.

The comparative analysis of the dc current annealing influence on the magnetoimpedance was carried out for the amorphous  $\text{Co}_{66}\text{Fe}_4\text{Nb}_{2.5}\text{Si}_{12.5}\text{B}_{15}$  wires elastically deformed.



23PO-I-13

## HYDROGEN ABSORPTION AND MAGNETIC PROPERTIES OF $\text{Ho}_2\text{Fe}_{14}\text{BH}_x$ HYDRIDES

*Damianova R.<sup>1</sup>, Nikitin S.A.<sup>2</sup>, Bezdushnyi R.V.<sup>3</sup>, Tereshina I.S.<sup>4</sup>, Tereshina E.A.<sup>2</sup>, Burkhanov G.S.<sup>4</sup>,  
Chistyakov O.D.<sup>4</sup>, Iliev L.<sup>5</sup>*

<sup>1</sup> University of Forestry, 10, Kliment Ohridski bld., Sofia 1756, Bulgaria

<sup>2</sup> Department of Physics, Lomonosov Moscow State University, GSP-1, Leninskie Gory, Moscow, 119991, Russian Federation

<sup>3</sup> LHEP JINR, 141980 Dubna, Moscow region, Russia

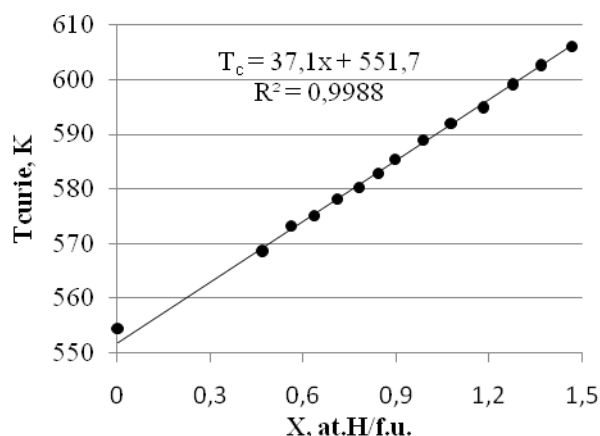
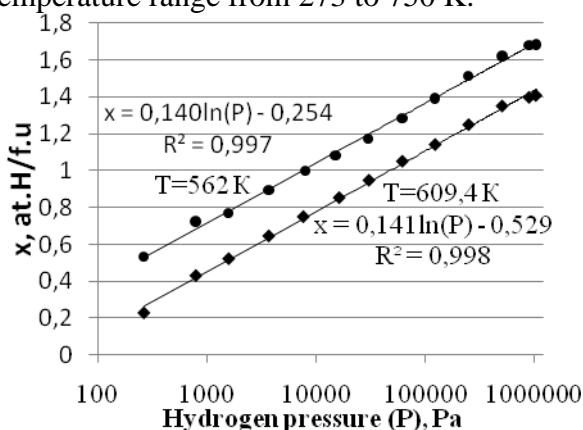
<sup>4</sup> Baikov Institute of Metallurgy and Material Science RAS, Leninskii pr. 49, Moscow, 119991, Russia

<sup>5</sup> Department of Condensed Matter, Faculty of Physics, Sofia University, Sofia 1126, Bulgaria

Magnetism and the hydrogen absorption properties for intermetallic compound  $\text{Ho}_2\text{Fe}_{14}\text{BH}_x$  were investigated. Measurements of the temperature dependencies of magnetization have been performed with the permanent control of the hydrogen content. The dependencies of Curie ( $T_C$ ) temperatures on hydrogen pressure and concentration variation were determined together with the dependencies of the hydrogen concentration on pressure at constant temperatures (near  $T_C$ ) and on the temperature at constant pressures.

The  $\text{Ho}_2\text{Fe}_{14}\text{B}$  compound was prepared by arc melting in a high-purity helium atmosphere using a water-cooled copper bottom and a non-consumable tungsten electrode. The phase composition was checked by the X-ray diffraction analysis. The quantity of impurity phase ( $\alpha\text{-Fe}$ ) estimated by both the X-ray and thermomagnetic analyses was found to be  $\sim 3\%$ .

Magnetization measurements at 78-700 K were performed using an apparatus constructed on a principle of vibrating-sample magnetometer and under the gas pressure up to 16 atm. During measurements of the temperature dependence of magnetization ( $\sigma(T)$ ), the sample was placed in a chamber with a constant hydrogen pressure. In order to determine the hydrogen concentration  $x$  in the sample at any temperature ( $x(T)$ ), a volumetric-type experimental set-up has been used to study the hydrogen absorption-desorption properties at hydrogen pressures up to 16 atm in the temperature range from 273 to 750 K.



The dependences of hydrogen concentration on the pressure display logarithmic behavior in the vicinity of  $T_C$ ; no plateau on the curves was observed up to the maximum pressures. The Curie temperatures increase with the hydrogen concentration rise and depend linearly on the hydrogen content  $x$ . At hydrogen concentration 1.47 atoms per formula unit (at.H/f.u.), the increase of  $T_C$  reaches  $51.5^\circ$ .

The work has been supported by the Science Research Foundation of Sofia University - Grant №102/08.04.2010.

## EFFECT OF MAGNETOSTRICTION OF $RFe_2$ COMPOUNDS ON THE STRUCTURE OF THEIR HYDRIDES

*Gaviko V.S., Stashkova L.A., Mushnikov N.V., Terent'ev P.B., Gerasimov E.G.*

Institute of Metal Physics, Urals Branch of RAS, S. Kovalevskaya 18, 620990 Ekaterinburg, Russia

Crystal structure of the rare earth intermetallics  $Er_{1-x}Tb_xFe_2$  and  $Sm_{1-x}Tb_x(Fe,Co)_2$  and their hydrides was investigated using X-ray diffraction. The compounds possess a cubic structure of the  $MgCu_2$ -type (Laves phases C15) in paramagnetic state. In the magnetically ordered state the compounds undergo magnetoelastic rhombohedral distortions of the lattice. The sign of rhombohedral magnetoelastic distortions is controlled by the sign of the Stevens factor  $\alpha$  for a rare earth atom, which characterizes the shape anisotropy of the 4f-shell and is negative for Tb ions and positive for Sm and Er ions. The difference in the signs accounts for the compensation of the magnetostriction in the quasi-binary  $Er_{1-x}Tb_xFe_2$  and  $Sm_{1-x}Tb_x(Fe,Co)_2$  Laves phases while varying concentration  $x$ . The aim of the present work is to reveal possible correlations between initial spontaneous magnetostriction distortions of the rare earth intermetallic lattice and the lattice deformations which occur due to the hydrogen ordering in hydrides with low and high hydrogen contents.

It was found that in hydrides with a low hydrogen concentration the “seed” magnetoelastic distortions of the lattice result in an ordering of hydrogen atoms so that the thus born lattice stresses enhance the initial deformation. In the hydrides  $TbFe_2H_y$  with  $y \sim 0.1$  the sign of the rhombohedral lattice distortion is positive, whereas in  $Sm(Fe,Co)_2H_y$ , negative. The amount of these deformations is by the order of magnitude higher than that of the “seed” magnetoelastic distortions. Samples with low hydrogen contents were produced in different ways:  $TbFe_2H_y$  – by polishing of the  $TbFe_2$  plates in an electrolyte based on the orthophosphoric acid;  $Sm(Fe,Co)_2H_y$  – by holding of the powders in air, since these compounds are able to spontaneously absorb some hydrogen from atmosphere (see [1]).

Hydrides with a high content of hydrogen ( $y > 3$ ) were synthesised using a Siverts-type reactor. They contain a rhombohedral phase, but, unlike the compounds with low hydrogen content, the sign of rhombohedral deformations is found to be negative independently of the sign and amount of the initial magnetoelastic distortion of the lattice. The rhombohedral structure of the hydrides at high hydrogen contents results from hydrogen ordering over the interstitials of the lattice. It is known from neutron diffraction studies that the  $A_2B_2$  position ( $A$  is the R atom and  $B$  is the 3d-atom) with a center at the 96g site is favorable for filling with hydrogen [2]. However, at  $y > 3$  part of hydrogen atoms occupy the tetrahedral interstices of the  $AB_3$  type with a center at the position 32e. It is this fact that, in our opinion, conditions the rhombohedral distortions of lattice of the hydrides with high hydrogen contents.

Support by UB RAS (project 09-P-2-1021) is acknowledged.

[1] V.S. Gaviko, A.V. Korolyov, N.V. Mushnikov, *J. Less Comm. Met.* **167** (1990) 119.

[2] L. Pontonnier, D. Fruchart, G.L. Soubeyroux, G. Triantafillidis, Y. Berthier. *J. Less-Common Met.* **172-174** (1991) 191.

23PO-I-15

## STRUCTURE AND MAGNETIC PROPERTIES OF ALLOYS IN SYSTEM (SmTb)Fe<sub>2</sub>

*Umkhaeva Z.<sup>1</sup>, Ilyushin. A.<sup>2</sup>*

<sup>1</sup> Chechen University, Grozny, Russia

<sup>2</sup> Moscow State University, Moscow, Russia

The compounds RB<sub>2</sub>, where R is rare earth metal and B is transitional metal have received a considerable attention of scientists. These compounds are particularly interesting from the point of view of magnetism, because they exhibit the wide variety of magnetic behaviours, including structural and magnetic phase transitions and spin reorientation phenomena.

Some compounds with light rare earth metals could be synthesized only under high pressures with using of special equipments.

Synthesis and investigation of pseudobinary (Sm<sub>1-x</sub>Tb<sub>x</sub>)Fe<sub>2</sub> powder system were carried out. Synthesis of the alloys was realized in the chamber of a Toroid type [1] by quenching from the melt at temperatures of up to 2000 K and a pressure of 8 GPa. The alloys were synthesized from the powders of at least 99.9% purity. The alloys of the system (Sm<sub>1-x</sub>Tb<sub>x</sub>)Fe<sub>2</sub> were synthesized within the range of constitution (*x*) 0; 0,1; 0,2; 0,25; 0,3; 0,4; 0,5; 0,75; 1,0.

The phase composition and atomic crystal structure of the alloys were examined by X-ray diffraction of polycrystals. It was ascertained that in the compounds of these systems the formation of a cubic phase takes place on the whole concentration range and this cubic phase is isotypic to the Laves phase of the C15 structure type.

The precise studies of X-ray data received at the room temperature showed that structures of all alloys have small rhombohedral distortions ( $\sim 10^{-3}$ ). Accordingly the Messbauer measurements the direction of the easy magnetisation is  $\langle 111 \rangle$ .

Using the low temperature X-raying in the range of 5-300 K with special equipment we have studied structures of all samples. As a result we have gotten the thermal expansion curves for all samples. Dependencies lattice parameter  $a(T)$  and volume of unit cell  $V(T)$  showed some anomalies for alloys with composition  $0 \leq x \leq 0,4$ . Diffractonal maxima in X-ray spectra of these alloys have had many transformations. It means that type of distortions of unit cells are changed. It was found that in the range of composition  $0 \leq x \leq 0,4$  and in the range of temperature  $\sim 200$  K direction of easy magnetisation is changing. By using of the method of interpretation developed in [2] was found the field on spin reorientation diagram with direction of easy magnetisation along  $\langle 110 \rangle$ .

From the Messbauer experimental data were obtained values of hyperfine magnetic fields for all alloys.

From magnetic measurements and X-ray temperature measurements were obtained values of Curie points as well as temperatures of spin reorientations.

[1] Khvostatsev L.G., Vereschagin L.F., Novikov A.P. *High Temp-High Press.* **9**, (1977) 637.

[2] Ilyushin A.S. Introduction to the structural physics of rare earth intermetallics. M. MSU (1991)

## AUTOMATIC REGISTRATION OF DYNAMIC HYSTERESIS LOOPS IN WIDE RANGE OF MAGNETIC FIELD FREQUENCIES

*Gorin A., Logunov M.*

National Research Mordovia State University, 430005 Saransk, Russia

The dynamic hysteresis loop is one of the basic characteristics of magnetic reversal processes of magnetic material. In connection with multifactorial dependence of magnetic reversal mechanisms for research of properties of magnetic material registration of set of dynamic hysteresis loops is required at various values of frequency  $f$  and amplitude  $H_a$  of magnetic field, temperatures, etc. In such conditions rather actual there is a problem of automation of registration process of dynamic hysteresis loops.

The experimental setup which is carrying out automatic registration of dynamic hysteresis loops of magnetic material in a wide range of magnetic field frequency  $f$  is developed for the decision of this problem. Registration of hysteresis loops is carried out with use oscilloscope method [1-3]. The program of setup control is designed with use of programming environment LabVIEW.

The program allows to set ranges of change of magnetic field amplitude  $H_a$  and frequency  $f$ , and also steps of their change. The step of change of each parameter can be variable that is convenient for mapping of the received dependences in various formats, for example, in logarithmic and linear scales. Integration of induced secondary voltage is software-based and it allows to carry out registration of hysteresis loops in a wide range of frequencies without change of setup elements.

Features of the setup are stabilization of magnetic field amplitude at change of its frequency and a high sensitivity due to decrease in noise and drift of the apparatuses. During registration of dynamic hysteresis loops at frequency scanning the set of field amplitude  $H_a$  is supported. For this purpose on each magnetic reversal frequency the transfer ratio of the measuring apparatus is calculated and the voltage amplitude on an output of the signal generator which is necessary for assignment of the fixed field amplitude  $H_a$  is set.

For small samples the increase of the signal/noise ratio  $K_{sn}$  is actual. Averaging registered signal of induced secondary voltage is made under several oscillograms for  $K_{sn}$  ratio increase by means of the most developed program. Automatic updating of drift of the registered hysteresis loops is made at change of measurement conditions.

Parameters of the experimental setup are defined by parameters of used physical equipment. The architecture of the designed computer program allows to carry out fast addition of support of the new generating and registering equipment. For some equipment libraries of the virtual devices are designed, allowing to carry out control of them from the programming environment LabVIEW.

[1] A. Goldman, *Modern Ferrite Technology*, Springer (2006) 438.

[2] P. Kis, M. Kuczmann, J. Füzi, A. Iványi, *Physica B*, **343** (2004) 357.

[3] Z. Polik, T. Ludvig, M. Kuczmann, *J. Electrical Engineering*, **58** (2007) 236.

## FABRICATION AND CHARACTERIZATION OF NiFe FILMS ON PATTERNED Si SUBSTRATES

Sakharov V.<sup>1</sup>, Khivintsev Y.<sup>1,2</sup>, Nikitov S.<sup>2,3</sup>, Filimonov Y.<sup>1,2</sup>

<sup>1</sup> Saratov Branch of Kotel'nikov Institute of Radio-engineering and Electronics of RAS, 38 Zelenaya St., Saratov, Russia

<sup>2</sup> Saratov State University, 83 Astrakhanskaya St., Saratov, Russia

<sup>3</sup> Kotel'nikov Institute of Radio-engineering and Electronics of RAS, 11-7 Mokhovaya St., Moscow, Russia

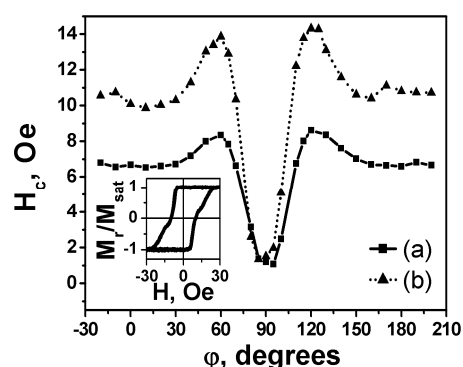


Fig. 1.  $H_C(\varphi)$  for Py stripes with (a)  $P=10\ \mu\text{m}$  and (b)  $P=15\ \mu\text{m}$ . The inset shows the hysteresis loop for  $P=10\ \mu\text{m}$ ,  $\varphi=0^\circ$ .

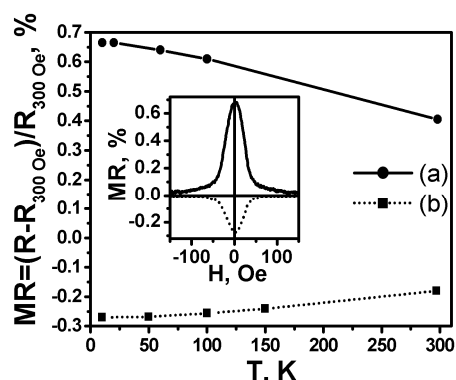


Fig. 2. MR vs. temperature for field applied perpendicular to the stripes and current aligned along (a) and perpendicular (b) to the stripes. The inset shows a typical MR curve at 10 K

Patterned magnetic media are the subject of the strong interest because of possible application in data storage devices and magnetic field sensors. In this work we studied magnetic properties of structures obtained by deposition of continuous permalloy (Py) films on silicon substrates patterned in a form of 1D and 2D periodical structure with micron sized lateral dimensions.

The structures were fabricated using photolithography, ion etching and magnetron sputtering. The patterned substrates had the same etched grooves width of about  $3.5\ \mu\text{m}$  but different periods ( $P$ ).

Magnetic measurements involved vibrating sample magnetometry, magnetic-force microscopy (MFM), the method of ferromagnetic resonance (FMR) and the four-probe method for magnetoresistance (MR) measurements.

Domain structure observed using MFM was sensitive to the pattern type and Py deposition parameters.

Angular dependence of coercivity ( $H_C$ ) (see Fig. 1) showed different mechanisms of magnetization reversal in our samples for various angles ( $\varphi$ ) between field direction and etched grooves.

MR depended on the fabrication conditions, etching depth and pattern type. The maximum value of MR (up to 2.2 %) was found for the samples with striped pattern. MR effect gradually increased in absolute value as the temperature decreased (see Fig. 2).

FMR measurements showed appearance of additional resonances in the patterned films.

This work was supported by RFBR (grants # 09-07-00186 and 11-07-00233), Federal Grant-in-Aid Program «Human Capital for Science and Education in Innovative Russia» (governmental contract # П485, 02.740.11.0014 and 14.740.11.0077), Federal Agency of Education of the Russian Federation (project # 2.1.1/2695) and the Grant from Government of Russian Federation for Support of Scientific Research in the Russian Universities Under the Guidance of Leading Scientists (project No. 11.G34.31.0030).

23PO-I-18

## OPTIMIZATION OF FORCE VERSUS ASPECT RATIO IN PERMANENT MAGNETS

*Iñiguez J., Raposo V., Flores A.G.*

Departamento de Física Aplicada, Universidad de Salamanca, E-37071, España, Spain

As is well known, magnetic springs are usually designed to provide either a constant assisting or resisting force [1,2]. The generation of a force that is independent of the stroke makes magnetic springs preferable for balancing weight forces in vertical drive applications. The mode of operation is based on the attractive or repulsive forces of permanent magnets. The special design of the flow-guiding components and the magnets translates the strongly non-linear relationship between force and displacement in magnet-iron arrangements into a constant force curve. Clearly, a previous stage in the design of magnetic springs is the maximization of forces between the magnets forming the magnetic spring system.

Magnetic actuators based on rare earth permanent magnets can be optimized using the adequate amount of material by a correct choice of the aspect ratio and volume. A systematic numerical and experimental study of the force that exhibit two cylindrical magnets is performed as a function of the aspect ratio, size and distance. The magnetization will be fixed along the axis of the cylinders and forces will be calculated by finite element simulations [3].

The main results are summarized as follows. For a particular value of the distance between magnets and constant volume of the magnetic material, there is an optimum aspect ratio that maximizes the repulsive or attractive force between them. This can be qualitatively explained taking into account the interactions of the magnetic surface charges at the end of the magnets. For very long cylinders the amount of charge is very small and so the resulting force is weak. In contrast, for very flat magnets (slab-like magnets) positive and negative magnetic charges are very close and, although the total magnetic charge is strongly increased, the magnetic field and also the force are significantly reduced. In fact, for an infinite magnetic slab, the magnetic induction outside it is null. Finally for an adequate aspect ratio the amount of magnetic charge and its separation is optimum and the force will be maximized.

Changing the distance that separates the magnets requires a different aspect ratio for maximize the forces, as we can understand again by the balance of the separation of the magnetic charges at both bases and the distance between magnets.

Finally, for a fixed aspect ratio the force obviously increases with magnet volume, but it is possible to obtain a compromise by calculating the force vs volume relation, that again presents an optimum value. Finally a set of experimental results corroborating the numerical calculations is presented.

In conclusion, it is possible to obtain the maximum force using a constant volume of magnets and the optimum force versus volume relation for actuators, magnetic levitation, magnetic springs or any other application based on magnetic forces. The qualitative behaviour can be easily extended to other magnet shapes but the general design guidelines for optimizing the forces are established based on the results for cylinders.

Support by Junta de Castilla y León and the Ministerio de Educación y Ciencia of Spain is acknowledge.

[1] [http://www.linmot.com/fileadmin/doc/MagSpring/Overview\\_MagSpring\\_e\\_recent.pdf](http://www.linmot.com/fileadmin/doc/MagSpring/Overview_MagSpring_e_recent.pdf)

[2] [http://www.magspring.com/Datasheets/MagSpringOverview\\_V2.0e\\_040924.pdf](http://www.magspring.com/Datasheets/MagSpringOverview_V2.0e_040924.pdf)

[3] FEMM is a freeware Windows-based program for analyzing 2D planar and axisymmetric problems in magnetism via the finite-element method

## APPROACH TO MAGNETIC SATURATION AND RANDOM MAGNETIC ANISOTROPY IN NANOCRYSTALLINE ALLOY $\text{Fe}_{73.5}\text{CuNb}_3\text{Si}_{13.5}\text{B}_9$

Komogortsev S.V.<sup>1,2</sup>, Iskhakov R.S.<sup>1,2</sup>, Kuznetsov P.A.<sup>3</sup>, Balaev A.D.<sup>1</sup>, Bondarenko G.N.<sup>1</sup>

<sup>1</sup> Kirensky Institute of Physics, SB RAS, Akademgorodok 50, bild. 38, Krasnoyarsk, Russia

<sup>2</sup> Siberian State Technological University, 82 Mira Prospect, Krasnoyarsk, Russia

<sup>3</sup> Central Research Institute of Structural Materials, "Prometey", 191015, St-Petersburg, Russia

Nanocrystalline Fe–Cu–Nb–Si–B soft magnetic alloys, commercially known as Finemet, continue to fascinate researchers both from fundamental and applied points of view. These magnetic nanocomposites consist of ferromagnetic nanocrystalline grains with the intragrain easy axis of magnetization varying randomly in orientation from grain to grain embedded in an amorphous ferromagnetic matrix. Within the framework of the random anisotropy model ultrasoft magnetic properties in such systems are thought to arise from the averaging out of the local random magnetic anisotropy by the exchange interaction, operating between the nanocrystalline grains and mediated by the amorphous matrix spins in the intergranular region, in a way similar to that in ferromagnets in the amorphous state. According to this approach, the spin system of a ferromagnet is described in terms of the following microscopic parameters: exchange  $A$ , magnetization  $M_s$ , local anisotropy with the energy  $K$  and localized at the scales  $2R_c$  and dimensionality of grain packing  $d$  in the nanocomposite. There are numerous experimental and theoretical papers where were shown that investigation of approach to magnetic saturation curve in ferromagnetic with random magnetic anisotropy allow one to obtain numerical values of  $R_c$ ,  $K$ ,  $A$ ,  $M_s$ ,  $d$  [1]. In the present work we report about investigation of approach to magnetic saturation curve in  $\text{Fe}_{73.5}\text{CuNb}_3\text{Si}_{13.5}\text{B}_9$  amorphous ribbon and obtained as result of different annealing conditions, as well as the annealing-temperature dependence of the crystallite size, coercive field.

The ribbons of amorphous alloys  $\text{Fe}_{73.5}\text{CuNb}_3\text{Si}_{13.5}\text{B}_9$ , 20  $\mu\text{m}$  thick, are synthesized by quenching from liquid state. The samples of ribbons were annealed for different times (from 10 min to 8 hours) and at different temperatures (from 430°C to 700°C). The range of annealing conditions were chose to investigate the alloy  $\text{Fe}_{73.5}\text{CuNb}_3\text{Si}_{13.5}\text{B}_9$  according our measurements program at the different stages of nanocrystallization well established for present moment.

The X-ray diffractograms reveal the phase composition (bcc solid solution Fe(Si)+amorphous alloy) and behavior the grain size with annealing time and temperature. There are two stages of crystallizations At annealing temperature above 500°C the stable enough nanocrystalline alloy was formed with the grain size about 10 nm that steeply increases to annealing under 600°C (fig.1). At annealing temperature above 600°C there is rapid crystallization to the alloy with the grain size about 60 nm. According magnetic measurements annealing results in increase of saturation magnetization  $M_s$  and exchange constant  $A$  determined from convenient Bloh's  $T^{3/2}$  law treatment. Approach magnetization to saturation curves were processed using technique described in [1]. There are the typical for nanocrystalline alloys crossover from  $M \sim H^{-(4-d)/2}$  to  $M \sim H^{-2}$  on log-log  $\Delta M(H)$  plot with increasing applied field for the as-sputtered and annealed samples. In the terms of the method developed in [3], the  $R_c$ ,  $K$ ,  $A$ ,  $M_s$  and  $d$  values were determined. It is surprise result that the value of  $d$  is less than 3 and not integer. This fact is discussed in the report.

Support by Federal Program "Development of the Scientific Potential of Higher Education" (project no. RNP 2.1.1/11470), Federal Target Program "Research and Research-Pedagogical Personnel of Innovation Russia for 2009-2013", Russian Foundation for Basic Research (project 11-03-00471-a) are acknowledged.

[1] R.S. Iskhakov, S.V. Komogortsev, *Bull. Russ. Ac. Sci.: Physics*, **71** (2007)1620.

23PO-I-20

## RESEARCH OF CRYSTALLIZATION KINETICS NEODYMIUM-IRON-BORON ALLOY WITH ZIRCONIUM ADDITIONS

*Glebov V.A.<sup>1</sup>, Glebov A.V.<sup>1</sup>, Bakulina A.S.<sup>1</sup>, Yagodkin Yu.D.<sup>2</sup>, Shchetinin I.V.<sup>2</sup>*

<sup>1</sup> All-Russian Research Institute of Inorganic Materials, Moscow Russia

<sup>2</sup> National University of Science and Technology, Moscow, Russia, 119049, ingvar@misis.ru

Research the possibility of using the Kolmogorov-Avrami equation to describe kinetics of crystallization of alloys based on the  $\text{Nd}_2\text{Fe}_{14}\text{B}$  compound. For determine the transformed volume using the results of magnetic measurements. Established that kinetics of crystallization of rapidly quenched alloys of neodymium-iron-boron with zirconium additions, based on measurements of magnetic characteristics (coercive force and saturation magnetization) made it possible the following conclusions. From the analysis of magnetization that doping with zirconium leads to a drastic change in the kinetic parameters in the equation of Kolmogorov-Avrami. Simultaneously doping with zirconium alloys Nd-Fe-B promotes the formation of crystallization more dispersed microstructure of the alloy. However analysis of the coercive force showed that the crystallization of the alloy doped with zirconium, is divided into two stages. At the first stage values of the kinetic parameters coincide with the values determined from analysis of magnetization. The second stage is characterized by a decrease in the parameter of the nucleation rate and growth of new phase.

23PO-I-21

## STRUCTURE AND MAGNETIC PROPERTIES OF NANOCRYSTALLINE Fe-Cr-Co ALLOYS FOR PERMANENT MAGNETS

*Ushakova O., Malinina R.*

Moscow Institute of Steel&Alloys, Moscow, Russia

Magnetic properties of alloys containing Fe and 28-30%Cr, 12-15 % Co with addition of 2-5 % Mo after cold rolling with reduction of 70 % at each stage were carried out.

At present time magnetic properties of Fe-Cr-Co-Mo alloys about 1.5-2 times less than theoretically predicted. That is why the process of high coercive condition forming in investigated alloys represents the practical interest.

Disintegration of the alloyed ferrite on two isomorphous phases  $\alpha_1$  and  $\alpha_2$  occurs at TMT and step aging. High coercive condition is reached by optimization of phases compositions, their shape, oblongness and mutual orientation of  $\alpha_1$  and  $\alpha_2$  particles.

It is known that anisotropy of elastic energy can bring essential contribution to texture forming during recrystallization of metals and alloys with cubic lattice under special conditions: existence of free from defects subgrains, a high level of anisotropy of elasticity (the factor of anisotropy > 2) and significant strains (in comparison with the limit of elasticity). The stage of preliminary low temperature annealing at 600-650°C was added to traditional scheme of heat treatment to realize advantages of anisotropy of elastic energy in texture forming.

Stoner-Volfart model gives the overestimated value of coercive force compared with really reached one. Good correlation of reversal induction (theoretical and experimental) confirms that quantities and compositions of  $\alpha_1$  and  $\alpha_2$  phases are practically optimal.



It was shown that  $H_c$  of Fe-Cr-Co-Mo alloys with cubic texture of recrystallization increases up to 30 %:  $H_c \approx 80$  kA/m.

It was supposed that additional reserves of magnetic properties are in creation of more perfect crystallographic and magnetic texture.

23PO-I-22

## STEP-LIKE HYSTERESIS LOOPS OF Co-BASED AMORPHOUS MICROWIRES SETS

*Akmaldinov K., Rodionova V., Perov N.*

Magnetism Department, Faculty of Physics, M.V. Lomonosov Moscow State University, Leninskie Gory 1-2, 119991 Moscow, Russia

Nowadays there are the numerous applications for using amorphous ferromagnetic microwires due to their small size and unique properties like extra-soft magnetic behaviour or rectangular hysteresis loop. In the present work we consider the possibility of creation of the decoding system based on the set of Co-based non-bistable microwires contrary to the common decoding system based on magnetically bistable Fe-based microwires [1], and the remagnetisation processes in the various sets of Co-based amorphous microwires are investigated.

The magnetization reversal in the single and in the sets of Co-based amorphous microwires with different length was investigated using Vibrating Sample Magnetometer. Co-based microwire with diameter of 30  $\mu\text{m}$  was produced by quenching and drawing technique [2]. The number of the wires composed the sets was varied from 1 to 5. The distance between the wires in the sets was made equal to 0, 1 or 2 diameters of microwire. The lengths of the sets changed from 0.5 up to 2 cm.

The hysteresis loops for the single Co-based microwire with different length of 1-2 cm and the hysteresis loops for the set of 5 Co-based microwires with length of 1.5 cm, located close to each other are shown in the figure. The hysteresis loop for single microwire has a shape usual for the wire with circular anisotropy whereas the hysteresis loop for 5 microwires set has step-like behaviour.

It was found that the microwire length increase leads to changing the hysteresis loops near the saturation fields (see Figure) but keeps the coercivity. When the length was 1 cm and more, the remagnetization of the sets occurs one-by-one in consecutive order – the hysteresis loops have the step-like (see Figure) shape, the height of each step corresponds to one wire magnetic moment change. The width of the step depends on the inter-wires distance and their length.

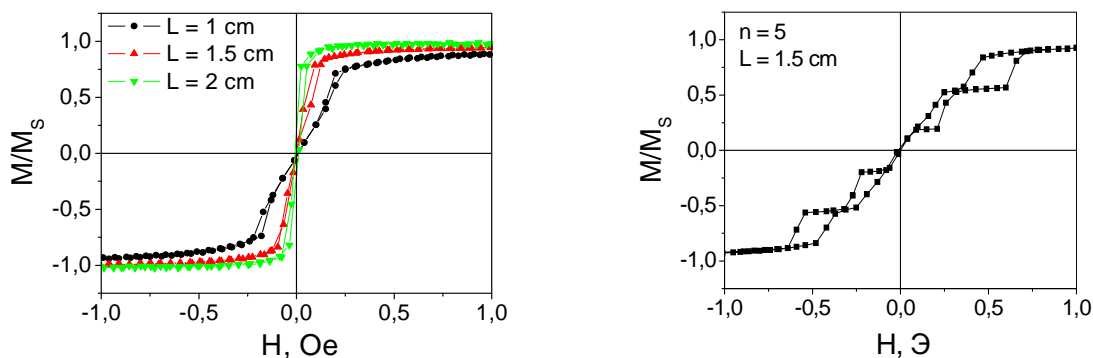


**Figure:** The hysteresis loops for the single Co-based microwire with different length of 1-2 cm and the hysteresis loops for the set of 5 Co-based microwires with length of 1.5 cm, located close to each other.

Support from RFBR (under project № 11-02-00906-a), MES (under project № 16.513.11.3073) and U.M.N.I.K. program is acknowledged.

[1] Zhukov A., *J. Magn. Magn. Mater.* 242-245 (2002) 216-223.

[2] Abe Y., *Trans. Iron and Steel Institute of Japan* 27 (12) (1987) 929-935.

23PO-I-23

## **MAGNETIC PROPERTIES OF NANOCRYSTALLINE Co-BASED ALLOYS PRODUCED BY DYNAMIC COMPACTION AND PLASMA SPRAY DEPOSITION**

*Kuzovnikova L.<sup>1</sup>, Denisova E.<sup>1</sup>, Kuzovnikov A.<sup>2</sup>, Iskhakov R.<sup>1</sup>, Lepeshev A.<sup>3</sup>*

<sup>1</sup> Kirensky Institute of Physics SB RAS, Krasnoyarsk, 660036, Russia

<sup>2</sup> JSC «Pulse technologies», Krasnoyarsk, 660036, Russia

<sup>3</sup> Siberian Federal University, Krasnoyarsk, 660041, Russia

Obtaining of bulk nanostructured materials having special physical properties of nanoparticles will allow to expand of their application field. The important aspect in the nanostructured materials compaction is how to achieve high density without loss a nanoscale microstructure. Some of amorphous alloy powders may be used as a precursor to production of nanocrystalline materials by controlled crystallization during compaction process.

In the present work the powders of the cobalt-based alloys (Co(P) – amorphous and crystalline) have been synthesized by reduction of metal ions in aqueous solution by use  $\text{NaH}_2\text{PO}_2$ . Magnetic properties of these powders were detailed investigated early [1]. The bulk samples were prepared by dynamic compaction and a plasma spray deposition techniques. The investigations of structure and magnetic properties of bulk samples were carried out by X-ray diffraction, electron microscopy and correlation magnetometry. The regimes of dynamic compaction were selected so that the basic magnetic characteristics (such as the saturation magnetization -  $M_0$ , the exchange stiffness constant -  $D$ , the local magnetic anisotropy field -  $H_a$ , the FMR linewidth -  $\Delta H$ , the coercivity) remain unchanged. Plasma spray deposition is a process by which the high temperature of plasma is employed to melt powders of metallic materials and spray them onto a substrate, forming a dense covering.

Approach to magnetic saturation curves in the all nanocomposites follow Akulov's law  $M(H) \sim (H)^{-2}$  in the applied fields up to  $3 \div 11$  kOe. This allows us to determine the value of mean square fluctuations of local magnetic anisotropy field  $aH_a$ . The value of  $aH_a$  is occurred to decrease during formation of bulk samples (for initial amorphous powder  $aH_a = 1.4$  kOe, for compact 1.3 kOe, for covering 1.1 kOe). It is found that approach to magnetic saturation curves follow law  $M(H) \sim (H)^{-0.5}$  in the applied fields less than 2.5 kOe. Such behavior  $M(H)$  indicates that the bulk material produced by both technique is nanostructural [2].

The results of magnetic measurements lead to a conclusion that the dynamic compaction and a plasma spray deposition techniques allow to obtain bulk nanostructured materials with remaining physical properties nanoparticles the same.

Support by RFBR № 11-03-00471-a is acknowledged.

[1] R.S. Iskhakov, E.A. Denisova, L.A. Chekanova, *IEEE Trans. Magn.*, **33** (1997) 3730.

[2] R.S. Iskhakov, S.V. Komogortsev, *Bull. Russ. Ac. Sci.: Physics*, **71** (2007) 1620.

## THE TEMPERATURE HYSTERESIS OF THE MAGNETIC PROPERTIES OF PRETREATED AMORPHOUS Fe-BASED RIBBONS

*Semenov A.L., Gavriljuk A.A., Pelmeneva A.V., Morozova N.V., Mokhovikov A.Yu., Zubritsky S.M.*  
Irkutsk State University, 20 Gagarina bvd, Irkutsk, Russia

This research is devoted to investigating of the influence of the thermo-cycling on dynamic magnetic properties of amorphous  $\text{Fe}_{64}\text{Co}_{21}\text{B}_{15}$  ribbons, which quenched promptly from melt. The furnace annealing of samples was carried out on air, so that pretreatment temperature range varied from  $150^{\circ}\text{C}$  up to  $360^{\circ}\text{C}$  ( $T_{\text{pre}}$ ) and processing time was 1 hour. After that, dynamic hysteresis loops were observed, thus the magnitude of the magnetic field was 1 kA/m with the frequency of 1 kHz, and the interval of thermo-cycling ( $T_{\text{cycl}}$ ) was from  $20^{\circ}\text{C}$  up to  $300^{\circ}\text{C}$ . For each sample, there were several cycles of “heating-cooling” with the temperature step of  $12^{\circ}\text{C}$ .

Discovered that non-hysteresis behavior (relative to temperature) of magnetic parameters was observed for samples, which were pretreated annealed at  $T_{\text{pre}} > 340^{\circ}\text{C}$ , in all cycles “heating-cooling”. While magnetic parameters were changing enough strongly (relative changes of  $B_r$  and  $H_c$  achieved to 20%) at the heating process.

As shown, the pretreatment of samples leads to the insignificant temperature hysteresis of magnetic parameters (less than 10%) at temperature range from  $320^{\circ}\text{C}$  up to  $340^{\circ}\text{C}$  in the first cycle of “heating-cooling”. At further thermo-cycling, magnetic parameters were provided to be rather thermo-stable (relative changes of  $B_r$  and  $H_c < 5\%$ ).

Experimental results will be used for modeling of magnetic parameters behavior versus temperature for amorphous  $\text{Fe}_{64}\text{Co}_{21}\text{B}_{15}$  alloys in the frame of Weiss' molecular field theory.

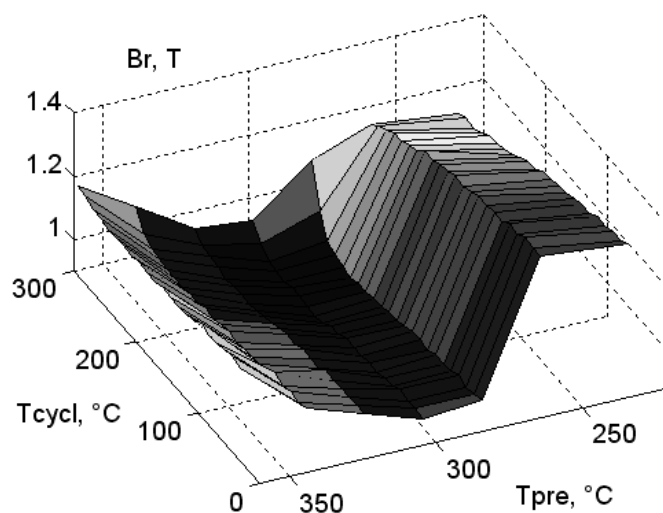


Fig.1 Dependence  $B_r(T_{\text{pre}}, T_{\text{cycl}})$  of the remanence versus heating temperature (at the first thermo-cycling) and temperature annealing.

This research was supported by the Russian Foundation for Basic Research (project № 11-08-00362-a) and by the Federal Agency for Science and Innovations (analytical departmental targeted program Development of the Scientific Potential of Higher Education Institutions, project № RNP.2.2.1.1/3297).

## MAGNETIC PROPERTIES OF PRE-TREATED AMORPHOUS Fe-BASED WIRES

*Gavrilyuk A.A., Semenov A.L., Mokhovikov A.Yu., Korzun A.Yu., Morozova N.V., Morozov I.L.*  
Irkutsk State University, 20 Gagarina bvd, Irkutsk, Russia

In this study we have investigated the effect of ac current annealing and length on dynamic magnetic properties of amorphous  $\text{Fe}_{75}\text{Si}_{10}\text{B}_{15}$  wires, which had produced by the melt spinning technique.

Samples of 140  $\mu\text{m}$  diameter and length from 0.02 m to 0.1 m were pretreated on air by dc current, which had been applied along the wire length. Density of dc current was varied from 0 up to 65  $\text{MA}/\text{m}^2$ , and processing time was 2 minutes. After that, dynamic hysteresis loops were observed, thus the magnitude of the magnetic field was 1 kA/m with the varying frequency from 0.1 kHz to 10 kHz.

It was found out that magnetic parameters behavior in amorphous phase indicate on the transition of wire core from multi-domain state to single domain at increasing of wire length (at  $l > 5\text{cm}$ ).

Furthermore, it has been shown that abrupt increasing of coercivity, decreasing of remanence (fig.1) and maximum differential magnetic permeability could be evidenced about the intensive crystallization process at the density of dc current higher than 52  $\text{MA}/\text{m}^2$ . Changing of the frequency of the reversal magnetic field doesn't exert influence on qualitative dependence of magnetic parameters versus density of dc current annealing and sample length.

In this research, it has been analyzed the effect of annealing and wire length on the stability of domains inside the inner core

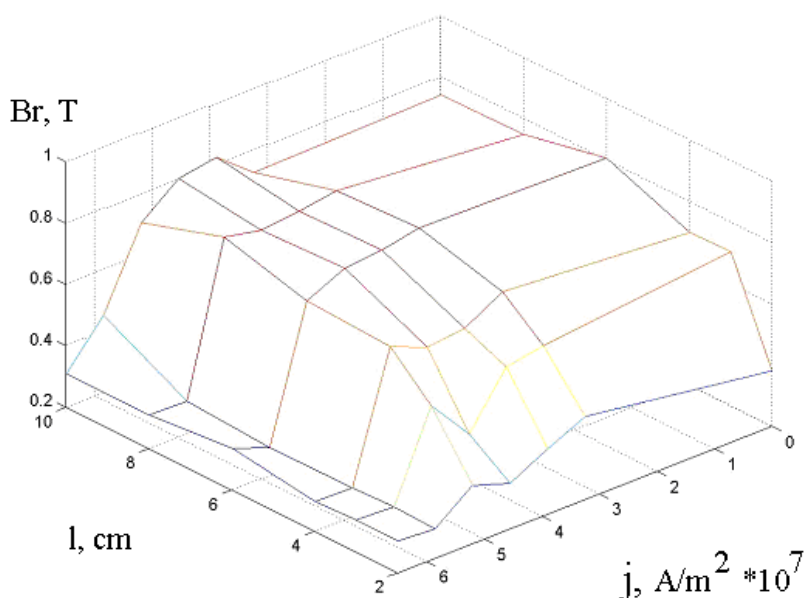


Fig.1 Dependence of remanence versus wire length and density of dc current for frequency of reversal magnetic field of 5 kHz.

This research was supported by the Russian Foundation for Basic Research (project № 11-08-00362-a) and by the Federal Agency for Science and Innovations (analytical departmental targeted program Development of the Scientific Potential of Higher Education Institutions, project № RNP.2.2.1.1/3297).

23PO-I-26

## MAGNETIC PROPERTIES AND ORDER-DISORDER TRANSITION IN CoPt NANOPARTICLES

Komogortsev S.V.<sup>1,2</sup>, Chizhik N.A.<sup>3</sup>, Filatov E.Yu.<sup>4</sup>, Korenev S.V.<sup>4</sup>, Shubin Yu.V.<sup>4</sup>, Velikanov D.A.<sup>1</sup>, Yurkin G.Yu.<sup>1</sup>

<sup>1</sup> Kirensky Institute of Physics, SB RAS, Akademgorodok 50, bild. 38, Krasnoyarsk, Russia

<sup>2</sup> Siberian State Technological University, 82 Mira pr., Krasnoyarsk, Russia

<sup>3</sup> Siberian Federal University, Svobodny pr. 79, Krasnoyarsk, Russia

<sup>4</sup> Nikolaev Institute of Inorganic Chemistry SB RAS, Lavrentyev Ave. 3, Novosibirsk, Russia

CoPt nanoparticles have attracted much attention for their prospective use in magnetic applications, including ultrahigh-density magnetic storage media.

Co–Pt alloys of near-equiatomic composition exhibit a typical disorder–order transformation from the disordered A1 phase to the ordered L1 phase when the temperature is lowered below 1098 K. The A1 phase, with a disordered fcc structure, is a soft magnetic phase. The L1<sub>0</sub> phase is an ordered fct structure with Pt at the [1/2 1/2 1/2] sites and Co at the [0 0 0] sites. It is magnetically hard phase with a very high uniaxial magnetocrystalline anisotropy field ( $H_a = 13$  T at room temperature) [1], the easy magnetization direction being along the  $c$  axis. Its Curie temperature is around 773 K, being slightly lower than that of the fcc phase. Here we report about magnetic and structural investigations of equiatomic CoPt nanoparticles synthesized by decomposition of precursor compound  $[\text{Pt}(\text{NH}_3)_4][\text{Co}(\text{C}_2\text{O}_4)_2(\text{H}_2\text{O})_2] \cdot 2\text{H}_2\text{O}$  [2]. The X-ray diffraction pattern reveals that as-prepared nanoparticles are in disordered cubic phase with size of the crystallites about 3–4 nm. Further annealing at 673 and 773 K during from 2 to 16 hours in helium atmosphere results in appearance of superstructure reflections on XRD patterns corresponding to structural transformation A1 - L1 phase. The value of ordering degree is obtained by XRD patterns modeling algorithm [2]. The ordering degree in the CoPt nanoparticles increases with annealing time up to 80%. According SEM and XRD annealing results also in sintering of nanoparticles and crystalline growth up to 35 nm.

Field and temperature dependence of magnetization were measured by MPMS-Quantum Design. The range of magnetic fields changed from -50 to 50 kOe and temperature varies from room to helium temperature. The major hysteresis loops including reversible and irreversible part of magnetization curve are obtained. The value of coercivity in the CoPt nanoparticles increasing with annealing and reaches the value 3.3 kOe at room temperature and 4.9 kOe at 5 K for nanoparticles annealed at 673 K during 16 hours. The value of ordering in these nanoparticles is evaluated as 35 %. The value of magnetic anisotropy energy (MAE) of CoPt nanoparticles was obtained from approach magnetization to saturation curves processing according to Akulov's law. The value of MAE increases with annealing and ordering degree of CoPt particles.

The temperature dependence of magnetization characterized by negative curvature and the value of gradient about 5% in the temperature range 5 – 275 K i.e. reveals ferromagnetic behavior of investigated nanoparticles. It is occur that  $M(T)$  doesn't follow expressions from spin wave theory (Bloch's law). The possible ways of describing the temperature dependences of magnetization for CoPt nanoparticles are discussed in this report.

The work has been partially supported by RFBR Grant 11-03-00168-a, Government of the Novosibirsk region grant for young scientists and engineers, Federal Program “Development of the Scientific Potential of Higher Education” (project no. RNP. 2.1.1/11470), Federal Target Program “Research and Research-Pedagogical Personnel of Innovation Russia for 2009–2013”.

[1] F. Bolzoni, F. Leccabue, et al. *IEEE Trans. Magn.Mag.*, **20** (1984) 1625.

[2] A. Zadesenets, E. Filatov, P. Plyusnin, et. al. *Polyhedron*, **30** (2011) 1305–1312.

## EFFECT OF MILLING IN VARIOUS MEDIA AND ANNEALING ON THE STRUCTURE AND MAGNETIC PROPERTIES OF STRONTIUM HEXAFERRITE POWDER

*Ketov S.V., Lopatina E.A., Bulatov T.A., Yagodkin Yu.D., Menushenkov V.P.*

National Research Technological University "MISiS", 119049 Leninsky prospekt 4, Moscow,  
Russia

Owing to relatively high magnetic properties, chemical stability and low cost, the SrFe<sub>12</sub>O<sub>19</sub> strontium hexaferrite is widely used for the production of permanent magnets. The magnetic properties of the strontium ferrite powder can be increased when producing it in the nanocrystalline state, in particular, by the mechanical activation followed by annealing [1,2]. After such a treatment, the coercive force of the powder increases up to  $\mu_0 H_{ci} > 0,4$  T. The final state of strontium hexaferrite powder depends on mechanical activation conditions, in particular, on the milling medium. The present work is aimed at the study of the effect of kinetics of milling in various media and subsequent annealing on the structure and magnetic properties of strontium hexaferrite powders.

The milling was performed in various media using a SAND-1 planetary ball mill and a rotation speed of ~ 230 rpm. The phase composition, average crystallite sizes ( $\langle D \rangle$ ), and lattice microstrains ( $\langle \epsilon \rangle$ ) were determined by X-ray diffraction analysis. The particle-size distributions for the powders were studied using a Fritsch Analysette-22 Nanotech laser analyzer. Moreover, the morphology and sizes of powder particles and crystallites present in these particles were studied by scanning electron microscopy (SEM) using a JEOL JSM-6700F electron microscope. The magnetic properties were measured at room temperature in applied magnetic fields of up to 2 T using a LDJ VSM-9600 vibrating-sample magnetometer.

The milling of strontium ferrite powder leads to an abrupt decrease in the powder particle size and an increase in lattice microstrains of the SrFe<sub>12</sub>O<sub>19</sub> phase. During milling, two peaks in the particle-size distribution also appear. No changes in the phase composition were observed during milling in toluene and oleic-acid-containing toluene, whereas during mailing in water, the Fe<sub>2</sub>O<sub>3</sub> phase (type H1.1) forms. The saturation magnetization and remanence decrease after the milling; this is likely to be due to an increase in the content of lattice defects. At the same time, the coercive force is unchanged with increasing milling time.

High resolutions scanning electron microscopy analysis has revealed that, after annealing, SrFe<sub>12</sub>O<sub>19</sub> powder particles consist of nanocrystals whose sizes decrease with increasing time of milling. The annealing allowed us to increase the magnetic properties of the powder. Moreover, their values depend on the medium and time of milling. The annealed powders are characterized by the following magnetic properties:  $\mu_0 H_{ci} = 0,42 \div 0,49$  T,  $B_r = 0,23 \div 0,24$  T,  $(BH)_{max} = 13-15$  kA/m<sup>3</sup>.

[1] Ketov S.V., Yagodkin Yu.D., Lebed A.L., Chernopyatova Yu.V., Khlopkov K. Structure and magnetic properties of nanocrystalline SrFe<sub>12</sub>O<sub>19</sub> alloy produced by high-energy ball milling and annealing // *J. Magn. Magn. Mater.*–**300** (2006), Issue 1, p. e479-e481

[2] Ketov S.V., Yagodkin Yu.D., Menushenkov V.P., Structure and magnetic properties of strontium ferrite anisotropic powder with nanocrystalline structure//*J. Alloys and Compd.*, **510** (2011) 1065-1068

## MAGNETIC PROPERTIES, STABILITY, STRUCTURE OF (Fe, Co)-BASED NANOCRYSTALLINE SOFT MAGNETIC ALLOYS WITH ADDITION OF Gf, Mo, Zr

*Dmitrieva N.V., Lukshina V.A., Volkova E.G., Potapov A.P., Gaviko V.S., Filippov B.N.*  
Institute of Metal Physics UD RAS, 620990, Ekaterinburg, Kovalevskaya st. 18, Russia,

Aiming of the development of materials with high thermal stability, the following alloys  $(\text{Fe}_{0.6}\text{Co}_{0.4})_{86}\text{Hf}_7\text{B}_6\text{Cu}_1$ ,  $(\text{Fe}_{0.7}\text{Co}_{0.3})_{88}\text{Hf}_7\text{B}_4\text{Cu}_1$  and  $(\text{Fe}_{0.7}\text{Co}_{0.3})_{88}\text{Hf}_4\text{Mo}_2\text{Zr}_1\text{B}_4\text{Cu}_1$  were produced by quenching from the melt onto a rotating drum and investigated. To obtain nanocrystallised state after quenching, alloys were subjected to thermal- (TA) or thermo-stress- (TSA) annealing in air at temperatures 520-620°C. TSA included heating, holding and cooling of the samples in the presence of tensile stresses. The influence of conditions of TA and TSA on the magnetic properties of alloys, their thermal stability and structure was studied.

Optimal TA conditions for realization of minimal coercive force ( $H_c$ ) in the alloys were determined. The magnetic state of the ribbon sample with a length of 100 mm was controlled by the hysteresis loops measured in an open magnetic circuit by the ballistic method using a microvebermeter F-190. The coercive force,  $H_c$ , the maximum induction,  $B_m$ , residual magnetization,  $B_r$ , and the ratio  $B_r/B_m$  were determined from the hysteresis loops measured in magnetic fields up to 4000 A/m applied along the axis of the ribbon. Structural state of the alloy  $(\text{Fe}_{0.6}\text{Co}_{0.4})_{86}\text{Hf}_7\text{B}_6\text{Cu}_1$  was studied by X-ray diffraction. Observation was carried out on the contact surface of the ribbons using DRON-6 (monochromatic radiation  $K_\alpha$  Cr). Structural state of the alloys  $(\text{Fe}_{0.7}\text{Co}_{0.3})_{88}\text{Hf}_7\text{B}_4\text{Cu}_1$  and  $(\text{Fe}_{0.7}\text{Co}_{0.3})_{88}\text{Hf}_4\text{Mo}_2\text{Zr}_1\text{B}_4\text{Cu}_1$  was investigated by transmission electron microscopy (TEM) using a microscope JEM 200CX.

It is shown that in all three alloys, nanocrystallization in course of the TSA in above mentioned temperature range leads to an induction of the longitudinal magnetic anisotropy with an easy magnetization direction aligned with the axis of the ribbon.

The samples of the alloys after TA and TSA have different functional characteristics. The lowest  $H_c = 20$  A/m in the alloys  $(\text{Fe}_{0.6}\text{Co}_{0.4})_{86}\text{Hf}_7\text{B}_6\text{Cu}_1$  and  $(\text{Fe}_{0.7}\text{Co}_{0.3})_{88}\text{Hf}_7\text{B}_4\text{Cu}_1$  is obtained after TA at 600-620°C during 20 min. The lowest  $H_c$  of the alloy  $(\text{Fe}_{0.7}\text{Co}_{0.3})_{88}\text{Hf}_4\text{Mo}_2\text{Zr}_1\text{B}_4\text{Cu}_1$  is achieved after TA at 520-570°C during 20 min and makes up 100 A/m. It is shown that the large values of  $H_c$  for the samples of the  $(\text{Fe}_{0.7}\text{Co}_{0.3})_{88}\text{Hf}_4\text{Mo}_2\text{Zr}_1\text{B}_4\text{Cu}_1$  alloy are likely connected with the appearance in the course of TA and TSA of coarse grains of the  $\alpha$ -Fe solid solution.

It is established that the alloy  $(\text{Fe}_{0.7}\text{Co}_{0.3})_{88}\text{Hf}_4\text{Mo}_2\text{Zr}_1\text{B}_4\text{Cu}_1$  annealed in the course of TSA at 620°C (20 min) has its best thermal stability of magnetic properties: the values of  $B_r/B_m$ ,  $H_c$  and  $B_m$  did not change during subsequent annealing without external influences at 550°C for 26 hours. This alloy after TA at 620°C (20 min) possesses, also, a good thermal stability of  $B_m$  whose value did not change, as well, during the next after TA annealing at 550°C for 26 hours. Nevertheless, the ratio  $B_r/B_m$  increases from 0.4 to 0.5, and  $H_c$  reduced by 37%.

It is established that the alloys  $(\text{Fe}_{0.6}\text{Co}_{0.4})_{86}\text{Hf}_7\text{B}_6\text{Cu}_1$  and  $(\text{Fe}_{0.7}\text{Co}_{0.3})_{88}\text{Hf}_7\text{B}_4\text{Cu}_1$  are not thermally stable at 550°C judging by the behavior and  $H_c$  and  $B_m$ .

Support by the Presidium of Russian Academy of Sciences (project no. 09-T-2-1015) is acknowledged.

## MAGNETIC PROPERTIES AND MICROSTRUCTURE OF THIN POLYCRYSTALLINE NICKEL FILMS WITH (200) TEXTURE

*Dzhumaliev A.S., Nikulin Y.V., Filimonov Y.A.*

Saratov Branch of Kotel'nikov IRE RAS, Saratov, Zelenaya 38, Russia

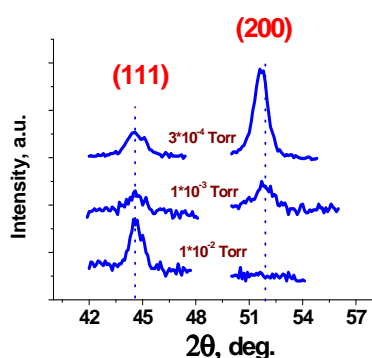


Fig.1 XRD pattern of Ni film  $d \approx 170$  nm grown at different Ar pressure. Cu-K $_{\alpha}$   $\lambda = 0.1541$  nm

a) Before annealing      b) Annealing,  $T \approx 350^{\circ}\text{C}$

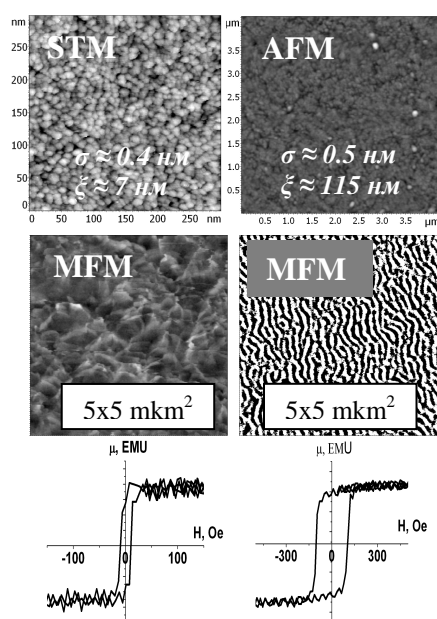


Fig.2 STM, MFM images and VSM magnetic loops of Ni (200) film,  $d \approx 44$  nm before and after annealing.

Magnetic properties of thin film are determined by its microstructure [1]. In turn, microstructure formation is strongly depends on working gas pressure, deposition rate, substrate temperature and postgrowth annealing. To our knowledge all studies of polycrystalline Ni films are concerned films with (111) texture. In this report we describe results of investigation of polycrystalline Ni films with (200) texture. Films with thicknesses  $15 \div 650$  nm were produced by DC sputtering at rates 17 and 36 nm/min on SiO $_2$ /Si substrates. Deposition starts at room temperature and 8 minutes later substrate temperature rises to  $80^{\circ}\text{C}$  and  $200^{\circ}\text{C}$  for films grown at rates 17 and 36 nm/min respectively. Postgrowth annealing was carried out in vacuum at  $150^{\circ}\text{C} \div 400^{\circ}\text{C}$  during 30 minutes.

Films grown at Ar pressure  $1 \cdot 10^{-3}$  Torr show (200) texture, but films grown at  $1 \cdot 10^{-2}$  Torr show (111) texture (Fig.1). Grain size  $\xi$  of Ni (200) films increases from 7 to 16 nm as thickness increases to 650nm. Surface roughness  $\sigma_{\text{rms}}$  changes in the range  $0.3 \div 0.8$  nm. Annealing at  $T > 200^{\circ}\text{C}$  causes grain sizes to increase on  $15 \div 30$  times,  $\sigma_{\text{rms}}$  to increase in  $2 \div 5$  times and interplanar distance to decrease on  $0.37 \div 0.57\%$ .

The thickness dependence of ferromagnetic resonance (FMR) linewidth have nonmonotonic character with minima  $\Delta H \approx 150$  Oe at  $d \approx 50 \div 90$  nm. After annealing at  $T > 200^{\circ}\text{C}$   $\Delta H$  values increase in 1.5...3 times.  $4\pi M$  values for annealed films are  $20 \div 30\%$  higher with respect to unannealed films. At thicknesses  $d_{\text{crit}} \approx 120$  nm ( $v \approx 36$  nm/min) and  $d_{\text{crit}} \approx 180$  nm ( $v \approx 17$  nm/min)  $H_c$  increases in 3.5 and 2 times respectively.  $H_c$  increasing is accompanied by decreasing  $M_r/M_s$  from  $0.85 \div 0.97$  to  $0.5 \div 0.6$ . At  $d_{\text{crit}}$  domain structure changes to stripes with period increasing from 290 to 460 nm with thickness. Domain period of films grown at 36 nm/min is  $15 \div 25\%$  higher with respect to films grown at 17 nm/min. Films with  $d \approx 40 \div 320$  nm after annealing at  $T \approx 350^{\circ}\text{C}$  have stripe domain structure (Fig.2) with period linearly increasing with thickness. Domain period also rises on 25% as annealing temperature increases from  $150^{\circ}\text{C}$  to  $400^{\circ}\text{C}$ .

This work was supported by RFBR (grants № 09-07-00186 and 11-07-00233), Federal Grant-in-Aid Program "Human capital For Science and education in Innovative Russia".

[1] J. B. Yi, Y. Z. Zhou, Z. J. JMMM, **284** ( 2004) 303.



## THE RESIDUAL STRAINS IN NANOCRYSTALS AND INDUCED MAGNETIC ANISOTROPY AS A RESULT OF THE TENSILE STRESS ANNEALING IN FINEMETS WITH THE DIFFERENT SILICON CONTENT

*Ershov N.V.<sup>1</sup>, Chernenkov Yu.P.<sup>2</sup>, Fedorov V.I.<sup>2</sup>, Lukshina V.A.<sup>1</sup>, Potapov A.P.<sup>1</sup>*

<sup>1</sup> Institute of Metal Physics, Ural Division of RAS, Yekaterinburg, Russia

<sup>2</sup> St.-Petersburg Institute of Nuclear Physics, RAS, Gatchina, Russia

As a result of heat treatment under tensile load in nanocrystalline FeSi-based alloys (FINEMET), the state with anisotropy of the magnetic properties is formed. The character of the anisotropy depends on the silicon content [1].

Atomic structure of the  $\text{Fe}_{87-X}\text{Si}_X\text{B}_9\text{Nb}_3\text{Cu}_1$  ( $X = 0, 6, 8, 9.5, 11, 13.5$ ) alloys was studied by X-ray diffraction analysis in transmission geometry. Diffraction patterns of the ribbon samples in the initial state formed by rapid quenching of the melt on a rotating copper disk, after crystallizing annealing (120 minutes,  $T = 520^\circ\text{C}$ ) and after tensile stress annealing (TSA – 120 minutes,  $T = 520^\circ\text{C}$ , mechanical stress in 400-440 MPa) were measured twice: with the scattering vector parallel and perpendicular to the axis of the ribbon.

It was shown that in the initial state, all the alloys are in the nanocrystalline (average grain size of about 2 nm), and their structure is independent of the direction and silicon content. After crystallizing annealing, the intensity distribution remains isotropic, but with increasing crystallite size up to 10-12 nm, a complete set of reflections corresponding bcc lattice of the  $\alpha$ -FeSi alloy is allowed. With silicon concentration increasing, the interplanar distances vary in full compliance with their change in bulk samples. When  $X > 9.5$  the superstructure peaks of  $\text{D0}_3$  phase -  $(\frac{1}{2} \frac{1}{2} \frac{1}{2})$  and (100), whose intensity increases with the silicon concentration, appear in the diffraction patterns. Other peaks of this phase, either coincide with the Bragg reflections from the bcc lattice, or are very weak.

After the TSA in all the samples, the extensions of the nanocrystal lattice in the direction of load application and their compression in the transverse direction are observed. Regardless of the silicon concentration the nanocrystal lattice distortions are nonisotropic. The distortion magnitude is greater the greater the angle between the direction ( $hkl$ ) and the nearest axis  $\langle 111 \rangle$ . In the [111] direction the distortions are minimum or absent, in the [100] they are maximum. Thus, after the TSA treatment, the residual strains are of tetragonal character.

With the silicon content increasing, the phase composition of the nanocrystals is complicated. At high silicon concentrations in the specimens there is a significant fraction of the ordered phase  $\text{Fe}_3\text{Si}$  (at  $X = 11$ , more than half of, and at  $X = 13.5$ , more than 80 % of the Fe-Si solution volume) in whose lattice after TSA the similar anisotropic distortions take place. It can be concluded that if  $X \leq 8$ , then the longitudinal anisotropy is induced due to the residual tetragonal strain of the bcc lattice of nanocrystals with the disordered  $\alpha$ -FeSi phase, which is characterized by a positive magnetoelastic coupling constant (longitudinal Villari effect). The transverse magnetic anisotropy in nanocrystals at  $X > 9.5$  is caused by the residual strains of the  $\text{Fe}_3\text{Si}$  phase, which has a negative magnetoelastic coupling (transversal Villari effect).

Support by RFBR (project no. 10-02-00435) and Presidium of RAS (project no. 09-II-2-1035) is acknowledged.

[1] V.V. Serikov, N.M. Kleinerman, E.G. Volkova, V.A. Lukshina, A.P. Potapov, A.V. Svalov, *Phys. Met. Metallogr.* **102** (2006) 268.

23PO-I-31

## THE EFFECT OF PLASTIC DEFORMATION ON SOME PROPERTIES OF Fe-22%Cr-15%Co HARD MAGNETIC ALLOY

*Korzniikova G.F.<sup>1</sup>, Milyaev I.M.<sup>2</sup>*

<sup>1</sup> Institute of Problems of Metal Superplasticity, Russian Academy of Sciences,  
Khalturin str. 39, Ufa, 450001, Russia

<sup>2</sup> Baikov Institute of Metallurgy and Materials Sciences, Russian Academy of Sciences,  
Leninskii pr. 49, Moscow, 119991, Russia

Almost all materials for permanent magnets are brittle and have low strength characteristics. Alloys of the Fe–Cr–Co system belong to a group of deformed hard magnetic materials of the precipitation hardening class. Magnets made from these alloys have a good combination of fairly high magnetic properties, corrosion resistance, and workability. As a rule, they are processed at a homologous temperature  $T = (0.60 - 0.75) T_m$  corresponding to the hot deformation temperature. The magnetic properties of Fe–Cr–Co alloys achieved after thermomagnetic treatment are higher than those of Fe–Al–Ni–Co (ALNICO) alloys, which are their closest analogue in magnetic properties.

In this work, we investigate the Fe–22% Cr–15% Co alloy belonging to this group of alloys. There are several methods of improving the mechanical properties of brittle materials. It is known that grain refinement and the formation of composite structures increase the strength characteristics of brittle materials. Deformation in Bridgman anvils increases the mechanical properties of permanent magnets but somewhat decreases their magnetic characteristics. However, the specimen sizes are small, which significantly narrows the area of their practical application.

The complex of magnetic and mechanical characteristics can be improved by the formation of gradient structures in magnets. Such gradient structures were prepared in planar specimens of Fe–Cr–Co alloys when they were deformed by upsetting with torsion and in cylindrical specimens deformed by tension with torsion [1]. However, to produce long workpieces with a uniaxial anisotropy in industry, more productive deformation schemes, such as drawing and rolling in profiled rolls are used.

The aim of this work was to investigate the processes of structure formation during warm plastic deformation and their influence on the magnetic properties of Fe–22% Cr–15% Co alloy upon its rolling in profiled rolls.

(1) We revealed a nonmonotonic dependence of the magnetic characteristics of anisotropic specimens of an Fe–22% Cr–15% Co alloy on the degree of plastic deformation. It was shown that an increase in the strain to 11.6% increases the remanence and the maximum energy product; a further increase in the strain to 28.5% leads to a decrease in the magnetic properties.

(2) In anisotropic samples of the Fe–22% Cr–15% Co alloy, warm uniaxial deformation decreases the maximum energy product and retains the coercive force unchanged.

(3) Warm plastic deformation leads to the formation of a composite structure consisting of hard magnetic fragments with a modulated structure bounded by deformation bands, in which a soft magnetic solid solution forms during the dissolution of the initial  $\alpha_1$  and  $\alpha_2$  phases.

[1] G. Korzniikova, A. Korzniikov, *Materials Science & Engineering A* **503** (2009) 99.

## SYNTHESIS OF FERRITE NANO-PARTICLE AGGREGATE AND THEIR CHARACTERISTICS

Kazuhiro N.<sup>1</sup>, Ryoma M.<sup>1</sup>, Nobuhiro M.<sup>2</sup>, Mitsuteru I.<sup>2</sup>

<sup>1</sup> Suzuka National College of Technology, Shiroko-cho, Suzuka-city, Mie 510-0294, Japan

<sup>2</sup> Tokyo Institute of Technology, Midori-ku, Yokohama-city, Kanagawa 226-8503, Japan

<sup>3</sup> Toyohashi University of Technology, Tempaku-cho, Toyohashi-city, Aichi 441-8580, Japan

We have been reported room temperature synthesis of ferrite nano-particles [1]. This abstract introduces the room temperature synthesis in open air without draft chamber. A pH adjusting solution of NaOH (concentration of 1 mol/l and variable volume of 12 – 30 ml) was added to a reaction solution of  $\text{FeCl}_2\cdot 4\text{H}_2\text{O}$  +  $\text{FeCl}_3\cdot 6\text{H}_2\text{O}$  (each concentration of 0.08 mol/l and constant volume of 30 ml) in an open vessel. Dissolved oxygen oxidizes some  $\text{Fe}^{2+}$  to  $\text{Fe}^{3+}$ . We obtained the ferrite nano-particles at shorter reaction time of a few seconds. Then we took an aging time for them. We investigated the aging time after synthesis. The aging time varied from 0 to 1 month as shown in Fig.1. Finally we obtained ferrite nano-particle aggregate by filtering and drying over 1 week in open air. Their particles were spinel structure as revealed by X-ray diffractometry. They had a typical broad peak of nano-particles.

When volume of NaOH solution is low, magnetization value decreases because of low pH value as shown in Fig.1. Their magnetization values increase with increasing aging time and they were saturated over 1 day.

Figure 2 shows that magnetization values increase gradually with increasing aging time when volume of NaOH is constant of 18 ml. The aging time is important to increase magnetization value.

Their nano-particle aggregate is black color. The color changes to reddish-brown by milling. These properties will be presented at this conference.

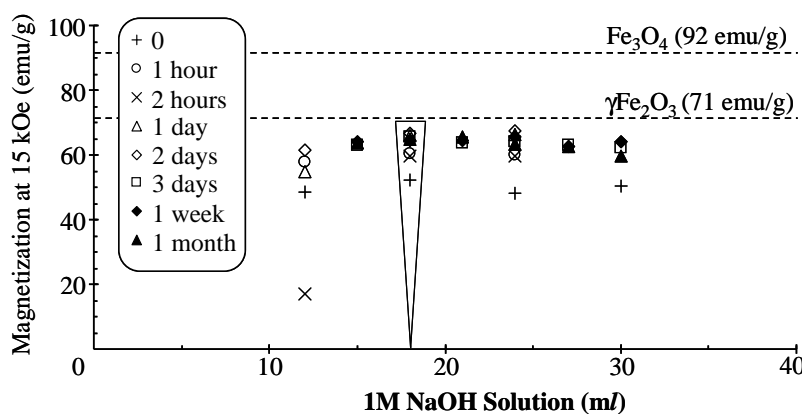


Fig.1. Magnetization at 15 kOe as function of volume of NaOH solution

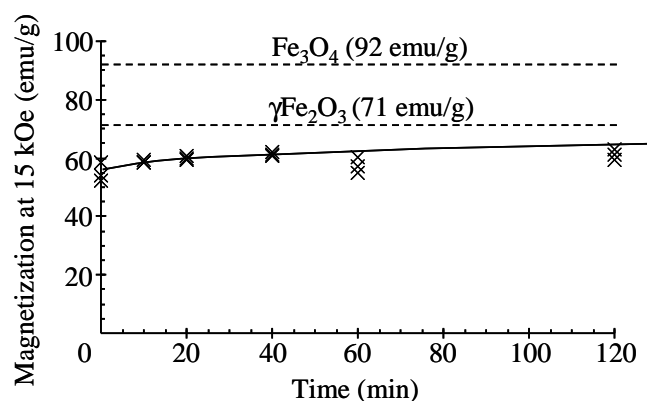


Fig.2. Magnetization at 15 kOe as function of aging time after synthesis

[1] K. Nishimura, M. Abe, M. Inoue, *IEEE Trans. Magn.*, **38** (2002) 3222.

## EFFECT OF INITIAL COMPOSITION ON THE PHASE COMPOSITION AND MAGNETIC AND MECHANICAL PROPERTIES OF HIGH-STRENGTH Fe-Cr-Co-BASED MAGNETIC MATERIALS

*Kleinerman N.M., Serikov V.V., Vershinin A.V., Belozarov E.V., Mushnikov N.V.*

Institute of Metal Physics, Ural Branch, RAS, ul. S.Kovalevskoi 18, Ekaterinburg, Russia

Along with conventional applications of Fe-Cr-Co based alloys, a new one, as materials for high-speed engines, has recently been found. This was favored by a series of studies in which the authors managed to realize a good combination of magnetic and mechanical properties in the Fe-22wt%Cr-15wt%Co alloys via alloying with Ga and W and different heat treatments [1]. Structure investigations using different methods allowed a conclusion to be made that in the materials under consideration a specific structure is formed in terms of phase composition and morphology. An essential contribution was made by the Mossbauer method which helped to pick out different regions constituting the structure and estimate their compositions and volume fractions. Further studies were aimed at searching a way of gaining the required properties on the alloys with lowered concentrations of Cr and Co, and compositions with improved mechanical properties were obtained, though with a somewhat lowered coercivity [2]. The processes taking place in the structure of these alloys need special research. The work presented was performed using the Mossbauer technique. Spectra of alloys with different concentrations of Co, Cr, and W, that of Ga being constant (0.5%), were taken at room temperature and processed using the program package MSTOOLS [3]. Multi-core distributions enabled us to pick out, first, structure components already known as a W-enriched paramagnetic phase, low-field regions with variable Cr composition, and Fe-Co-based regions with a high field and to compare them for different alloys (see Fig.1). At the next step, based on the data of direct fitting of the spectra and sequential subtracting the subspectra, the multi-core distribution were constructed just for the high-field part of the spectra (see Fig.2). It turned out possible to separate a region which, according to the spectral parameters, can be ascribed to a structure component that just contains Ga. The results for different alloys are compared and analyzed.

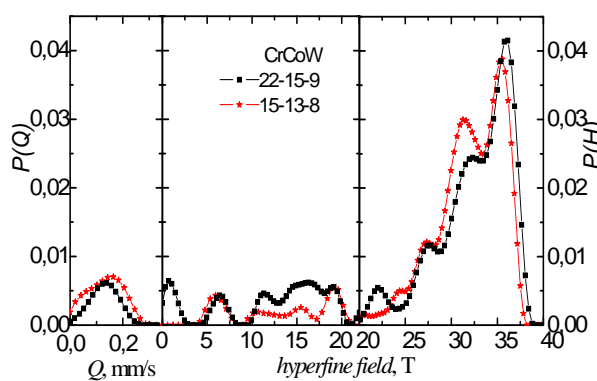


Fig. 1

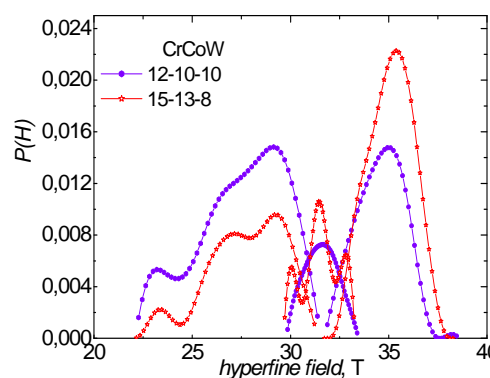


Fig. 2

This work was supported by the Ural Division of RAS (grant № 09-P-2-1035).

[1] E.V. Belozarov, M.A. Uimin, A.E. Ermakov, V.V. Serikov, N.M. Kleinerman and G.V. Ivanova, *Phys. Met. Met.*, **106**, N5, 2009, pp.472-480.

[2] E.V. Belozarov, G.V. Ivanova, N.N. Shchegoleva, N.V. Mushnikov, M.A. Uimin, *Phys. Met. Met.*, in press

[3] V.S. Rusakov, *Mossbauer spectroscopy of locally inhomogeneous systems*. Alma-Ata (2000).

## MAGNETIC PHASE TRANSITIONS IN $\text{La}_{1-x}\text{R}_x\text{Mn}_2\text{Si}_2$ ( $\text{R} = \text{Gd}, \text{Tb}, \text{Dy}$ ) COMPOUNDS

*Gerasimov E.G., Mushnikov N.V., Gaviko V.S.*

Institute of Metal Physics, Ural Division of Russian Academy of Sciences,  
Sofia Kovalevskaya 18, 620990 Ekaterinburg, Russia

The ternary intermetallic  $\text{RMn}_2\text{X}_2$  compounds ( $R$  is a rare earth,  $X$  is Si or Ge) crystallize in the body-centered tetragonal  $\text{ThCr}_2\text{Si}_2$ -type structure (space group  $I4/mmm$ ) consisting of alternating atomic layers of  $-R-X-Mn-X-R-$  aligned perpendicular to the  $c$ -axis. The compounds exhibit an unusual correlation between the intralayer Mn-Mn distance ( $d_{\text{Mn-Mn}}$ ) and interlayer magnetic arrangement of the Mn magnetic moments. A critical distance for intralayer Mn atoms exists in the compounds and is considered to be equal to  $d_c \approx 0.285\text{-}0.287$  nm at room temperature. As a rule, at  $d_{\text{Mn-Mn}} > d_c$ , the Mn layers are ordered ferromagnetically along the  $c$ -axis, whereas at  $d_{\text{Mn-Mn}} < d_c$ , they are ordered antiferromagnetically. In the  $\text{RMn}_2\text{X}_2$  compounds with magnetic rare earths, competition of the Mn-Mn,  $R$ -Mn and  $R$ - $R$  exchange interactions and anisotropies of the rare earth and manganese sublattices can strongly effect on magnetic structures at low temperatures.

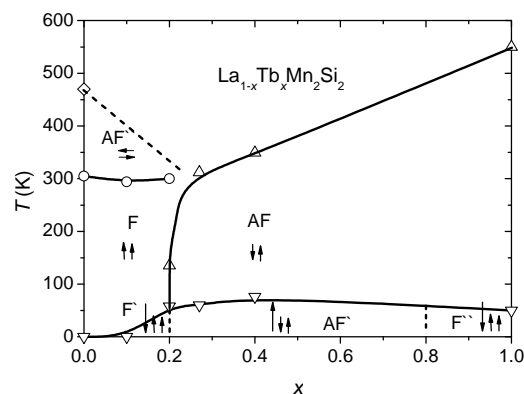
The aim of the present work was to study magnetic structure and magnetic properties of the  $\text{La}_{1-x}\text{R}_x\text{Mn}_2\text{Si}_2$  ( $R$  is Gd, Tb, Dy;  $0 \leq x \leq 1$ ) compounds in which there is possibility to gradually change the intralayer Mn-Mn distances from  $d_{\text{Mn-Mn}} > d_c$  ( $x=0$ ) to  $d_{\text{Mn-Mn}} < d_c$  ( $x=1$ ) and the  $R$ -Mn,  $R$ - $R$  exchange interactions by increasing  $R$  content.

Magnetic properties of the  $\text{La}_{1-x}\text{R}_x\text{Mn}_2\text{Si}_2$  ( $R$  is Gd, Tb, Dy;  $0 \leq x \leq 1$ ) compounds were investigated using magnetic measurements on quasi-single crystals. The  $x$ - $T$  concentration magnetic phase diagrams are constructed.

All obtained  $x$ - $T$  magnetic phase diagrams are similar to that presented on figure for the  $\text{La}_{1-x}\text{Tb}_x\text{Mn}_2\text{Si}_2$  compounds where short arrows describe Mn-Mn arrangement and long arrows show direction of the  $R$  magnetic sublattice. Six various magnetic structures are realized in the compounds at different concentration  $x$ . With increasing  $R$  content up to  $x=0.27$ , the intralayer Mn-Mn distance becomes close to the critical  $d_c$ , which leads to the  $F^-$ - $AF^+$ ,  $F$ - $AF^+$  transitions.

The  $AF^-$ - $F^-$  transition can be connected with the enhancement of negative  $R$ -Mn exchange interactions upon increasing  $R$  content. Thus, the changes in the type of the interlayer Mn-Mn ordering at  $T = 4.2$  K in  $\text{La}_{1-x}\text{R}_x\text{Mn}_2\text{Si}_2$  are caused by both the existence of the critical intralayer Mn-Mn distance and the competition of the interlayer Mn-Mn and negative  $R$ -Mn exchange interactions.

It was shown that all compounds have strong magnetic anisotropy with the  $c$ -axis easy direction. The magnetic anisotropy strongly increases with increasing Tb, Dy content as a result of growth of contribution of the rare-earth magnetic anisotropy to the magnetic anisotropy of the compounds. For the compounds with  $x = 0.2$ , the irreversible magnetization processes are observed which can be connected with the existence of compensation point at which the  $R$  and Mn magnetic sublattices compensate each other. The nature of spontaneous and field-induced  $F$ - $AF^+$ ,  $F^-$ - $AF^+$  phase transitions are also studied.



This work was supported by the Russian Foundation for Basic Research (grant No. 09-02-00272) and by Ural and Siberian Divisions of the Russian Academy of Science.

## MAGNETOCRYSTALLINE ANISOTROPY OF $R_2(\text{Fe}_{1-x}\text{V}_x)_{17}$ COMPOUNDS WITH $R = \text{Y}$ AND $\text{Sm}$

*Terentyev P.B., Mushnikov N.V., Ivanova G.V.*

Institute of Metal Physics, Ural Division, Russian Academy of Sciences, S. Kovalevskoi 18, Ekaterinburg, 620219 Russia

Intermetallic compounds  $R_2\text{Fe}_{17}$ , which have a crystal structure with a uniaxial symmetry and exhibit high values of the magnetic moment owing to the high iron content, are attractive materials to be used as permanent magnets. Unfortunately, all these compounds, except for those containing Ce and Lu, exhibit an easy-plane magnetic anisotropy at room temperature and rather low Curie temperatures [1]. However, the magnetic properties of these compounds can be changed markedly using additions of different substitutional or interstitial impurities. For example, the substitution of Ga, Al, and Si for Fe increases the Curie temperature and changes the easy-axis orientation from planar (within the basal plane) to axial (along the  $c$  axis) [2].

In this work, we studied the effect of the substitution of V for Fe on the magnetic anisotropy of the  $R_2\text{Fe}_{17}$  compounds with  $R$  - Y and Sm. In these compounds, Y atoms are nonmagnetic, whereas Sm atoms have a magnetic moment. The Y-containing compounds were used to study the magnetic anisotropy of the Fe sublattice and to estimate its contribution to the magnetic anisotropy of the  $\text{Sm}_2(\text{Fe}, \text{V})_{17}$  compounds.

It was shown that the Curie temperature  $T_C$  of the  $\text{Y}_2(\text{Fe}_{1-x}\text{V}_x)_{17}$  and  $\text{Sm}_2(\text{Fe}_{1-x}\text{V}_x)_{17}$  compounds increases and the saturation magnetization decreases with increasing  $x$  up to  $x = 0.05$ . The V content  $x = 0.05$  corresponds to the maximum solubility of V in the Fe sublattice. All compounds exhibit easy-plane anisotropy. At 77 K, the anisotropy constant  $K_1$  of the Y-containing compounds decreases monotonically with increasing  $x$  (Fig. 1); the  $K_1(x)$  dependence of the Sm-containing compound shows a maximum at  $x = 0.02$ . The anisotropy constants  $K_1$  of the Sm and Fe sublattices are negative and their contributions to the magnetocrystalline anisotropy of the  $\text{Sm}_2(\text{Fe}_{1-x}\text{V}_x)_{17}$  compounds are virtually the same (Fig. 1). The nonmonotonic behavior of the  $K_1(x)$  dependence is likely to be related to changes in the crystalline fields at Sm atoms. The substitution of V for Fe leads to an increase in the higher-order contributions (higher than the second order) to the anisotropy.

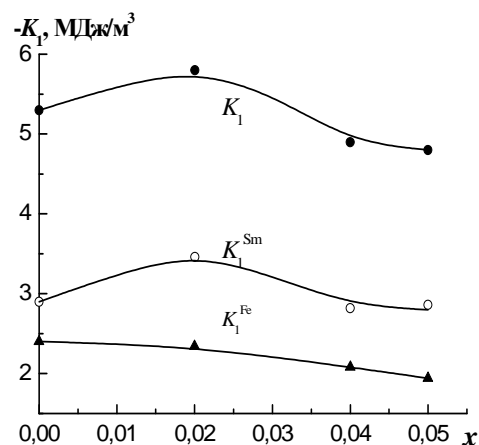


Fig. 1 Concentration dependences of  $K_1$  for  $\text{Sm}_2(\text{Fe}_{1-x}\text{V}_x)_{17}$ ,  $K_1^{\text{Fe}}$  for  $\text{Y}_2(\text{Fe}_{1-x}\text{V}_x)_{17}$  and  $K_1^{\text{Sm}} = K_1 - K_1^{\text{Fe}}$  at 77 K.

This work was supported by Russian Foundation for Basic Research (grant № 09-02-00272).

[1] X Kou X.C., de Boer F.R., Grossinger R., Wiensinger G., Suzuki H., Kitazawa H., Takamasu T., Kido G. *J. Magn. Magn. Mater.* **177-181**, (1998) 1002.

[2] W. Zarek, *J. Magn. Magn. Mater.*, **158** (1996) 91.

## MAGNETOIMPEDANCE AND COIL-LESS FLUXGATE EFFECT IN ELECTRODEPOSITED NiFe/Cu WIRE

Yagmur V., Atalay F.E., Bayri N., Atalay S.

Inonu University, Science and Arts Faculty, Physics Department, 44069 Malatya, Turkey

All electrochemical experiments were performed in a three-electrode glass cell with a volume of 85 ml, using a homemade computer controlled electrochemical workstation. The working electrode (Cu wire) was located vertically at the center of a high-density platinum gauze electrode and then one end of working electrode was fixed and the other end was twisted for different angles between  $0^\circ$  and  $360^\circ$  to apply torsion during the electrodeposition process. The total length of the magnetic film deposited onto  $50\ \mu\text{m}$  Cu wire is 3 cm and the thickness of the magnetic layer is about  $10\ \mu\text{m}$ . EDX microanalysis also showed that the magnetic layer has a composition of  $\text{Ni}_{80}\text{Fe}_{20}$ . In the coil-less fluxgate measurements, the second harmonic of the output signal from the ends of the wire,  $U_{\text{wire}}$ , was measured using a lock-in amplifier as a function of magnetic field, details are given in [1].

All samples showed single peak in MI curves (Figure 1). The maximum MI change was observed in the sample produced under the effect of zero torsion and MI effect magnitude decreases with increasing torsion applied during the electrodeposition process. This can be related to the increase in the induced anisotropy with increasing torsion. The magnitude  $\%(\Delta Z/Z)$  are 282%, 260%, 235% and 119% for samples produced under 0, 22.4, 44.8, 89.7 rad/m torsion values, respectively at driving frequency of 160 kHz. Figure 2 shows coil-less fluxgate (CF) curve for sample produced under 89.7 rad/m torsion at 50 kHz driving current frequency. The second harmonics of output voltage detected from the ends of wire shows a linear variation at low magnetic field region. Since the coil-less fluxgate requires helical magnetization component, the sensitivity of coil-less output increases with increasing torsion and maximum sensitivity was observed in the sample produced at 89.7 torsion.

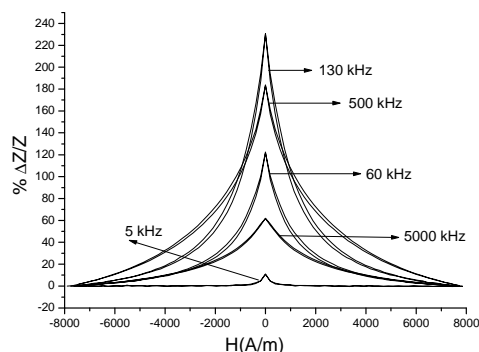


Fig. 1. MI curves of sample produced under 44.8 rad/m torsion.

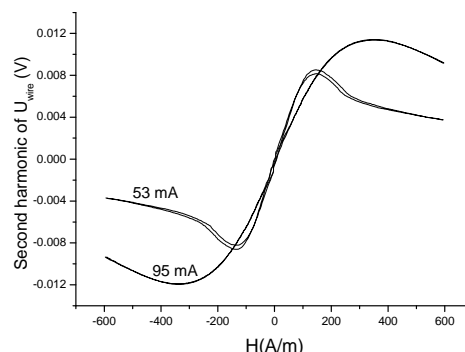


Fig. 2. CF curves sample produced under 89.7 rad/m torsion.

This project was supported by TUBITAK with project number 109T361.

[1] S. Atalay, N. Bayri, T. Izgi, F.E. Atalay, V.S. Kolat, *Sensors and Actuators A*, **158** (2010) 37–42.

23PO-I-37

## COIL-LESS FLUXGATE EFFECT IN AMOPHOUS $\text{Co}_{71}\text{Fe}_1\text{Mo}_1\text{Mn}_4\text{Si}_{14}\text{B}_9$ RIBBONS

*Fidan A., Atalay S., Bayri N., Yagmur V.*

Inonu University, Science and Arts Faculty, Physics Department, 44069 Malatya, Turkey

In this study, coil-less fluxgate effect of nearly zero magnetostrictive ( $<0.2 \cdot 10^{-6}$ )  $\text{Co}_{71}\text{Fe}_1\text{Mo}_1\text{Mn}_4\text{Si}_{14}\text{B}_9$  amorphous ribbon was investigated. Coil-less fluxgate is a new type of magnetic field sensor without a coil [1-2]. It is based on helical anisotropy and deep circumferential magnetic saturation in the ferromagnetic fluxgate core. A detailed measurement system was given in [2].

The ribbon has 30  $\mu\text{m}$  thicknesses and was cut to 1 mm wide, 6 cm long. The samples were annealed at 480 mA current under the effect of 3, 12.5 and 25 rad/m torsion.

Figure 1 shows coil-less fluxgate curve for as-received and the current annealed ribbons under the effect of 25 rad/m torsion for 30 kHz driving current frequency. The second harmonics of output voltage detected from the ends of wire shows a linear variation at low magnetic field region. The sensitivity of annealed sample is about 570 V/T, which is comparable with the previously reported fluxgate sensitivity values. The presented sensor has no coil so it is much easy to reduce the size of sensor and easy to fabricate it.

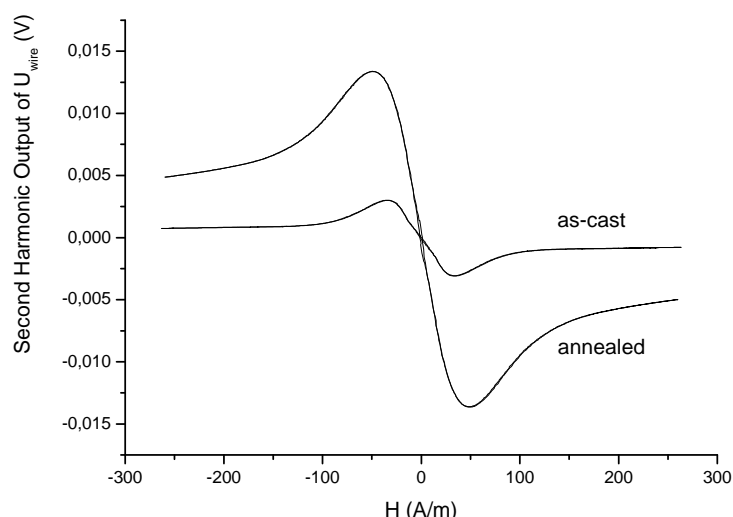


Figure 1. The second harmonic voltage output of as-cast and annealed sample under the effect of 25 rad/m torsion.

This project was supported by TUBITAK with project number 109T361.

[1] M. Butta, P. Ripka, S. Atalay, F.E. Atalay, X.P. Xli, *J. Magn. Magn. Mater.* **320** (2008) e974–e978.

[2] S. Atalay, N. Bayri, T. Izgi, F.E. Atalay, V.S. Kolat, *Sensors and Actuators A*, **158** (2010) 37–42.



## SHORT-RANGE ORDER FORMATION AND MAGNETISM IN Fe-Si AND Fe-Al ALLOYS

Kuznetsov A.R.<sup>1,2</sup>, Gornostyrev Yu.N.<sup>1,2</sup>, Gorbatov O.<sup>1,2</sup>, Ruban A.V.<sup>3</sup>, Ershov N.V.<sup>1</sup>, Chernenkov Yu.P.<sup>4</sup>, Fedorov V.I.<sup>4</sup>, Lukshina V.A.<sup>1</sup>, Kleinerman N.M.<sup>1</sup>, Serikov V.V.<sup>1</sup>

<sup>1</sup>Institute of Metal Physics UD RAS, 620990, Ekaterinburg, Russia

<sup>2</sup>Institute of Quantum Materials Science, 620107, Ekaterinburg, Russia

<sup>3</sup>Royal Institute of Technology (KTH), SE-100 44, Stockholm, Sweden

<sup>4</sup>B.P.Konstantinov Petersburg Nuclear Physics Institute RAS, 188300, Gatchina, Russia

Fe-Si and Fe-Al alloys constitute the basis of soft magnetic materials and have been intensively studied for decades. There are few doubts that appearance of so-called induced magnetic anisotropy is closely connected with the certain type of short-range order (SRO) in these alloys, however the mechanism of SRO formation is still under debate. Both these alloys exhibit the change of the type of ordering from D0<sub>3</sub> to B2 when temperature increases above Curie point,  $T_C$ , and the SRO observation also follows this trend. In particular, the neutron scattering experiments reveal the D0<sub>3</sub> type SRO in Fe-Si for  $T < 600^\circ\text{C}$  and Si concentration above 6 at.% [1]. The B2 type SRO has been observed in the X-ray diffuse scattering studies in Fe-Si alloys quenched from  $T = 850^\circ\text{C}$  with the Si concentration of 5-8 at.% and the D0<sub>3</sub> type SRO appeared after annealing at  $450^\circ\text{C}$ . The high-temperature states ( $T > T_C$ ) of Fe-Al alloy show a tendency towards the B2 structure and the D0<sub>3</sub> type SRO formation takes place for low temperatures. In particular, the B2 type SRO observed [2] in Fe-21.9 at.% Al as for  $T > T_C$  ( $T = 800^\circ\text{C}$ ) as well for  $T < T_C$  ( $T = 600^\circ\text{C}$ ) while D0<sub>3</sub> type SRO has been found in Fe-19.4 at.% Al for  $T < 400^\circ\text{C}$ .

Short-range order formation in dilute Fe-Si and Fe-Al alloys has been investigated by statistical Monte Carlo simulations with effective interactions deduced from first principles calculations for different magnetic structures of bcc Fe [3]. We have found that the effective interactions depend on the global magnetic state. These results reveal the key role of magnetism in the formation of the atomic SRO in these alloys. In particular, the B2 type chemical SRO forms preferably in the paramagnetic state ( $T > T_C$ ) and the D0<sub>3</sub> type SRO corresponds to the equilibrium state of alloys in the ferromagnetic state ( $T < T_C$ ). Our results provide a support for the concept that the induced magnetic anisotropy in Fe-Si and Fe-Al is due to the presence of solute-solute pairs at the second coordination shell and their ordering in a magnetic field or an under external load. These pairs can not appear during annealing at  $T < T_C$  however they can be inherited by cooling from the paramagnetic state.

Support by RFBR (project No. 10-02-00435) and Presidium of RAS (project No. 09-II-2-1035) is acknowledged.

- [1] K. Hilfrich, W. Kölker, W. Petry, O. Schärpf, E. Nembach, *Acta Metal. Mater.*, **42** (1994) 743.
- [2] B. Schönfeld, R. Bucher, M.J. Portmann, and M. Zolliker, *Z. Metallkd.*, **97** (2006) 240.
- [3] O.I. Gorbatov, A.R. Kuznetsov, Yu.N. Gornostyrev, A.V. Ruban, N.V. Ershov, V.A. Lukshina, Yu.P. Chernenkov, V.I. Fedorov, *JETP*, **139** (2011).

## MAGNETIC PROPERTIES OF A $\text{DyFe}_5\text{Al}_7$ SINGLE CRYSTAL

Gorbunov D.I.<sup>1,2</sup>, Andreev A.V.<sup>1</sup>

<sup>1</sup> Institute of Physics ASCR, Na Slovance 2, 182 21 Prague 8, The Czech Republic

<sup>2</sup> Institute of Metal Physics, Kovalevskaya 18, 620990 Ekaterinburg, Russia

The  $\text{RFe}_5\text{Al}_7$  (R – Y, Sm-Lu) compounds crystallizing in the tetragonal  $\text{ThMn}_{12}$ -type structure are very interesting objects for research due to their unusual magnetic properties: “negative magnetization”, strong thermal and magnetic hysteresis, time-dependent effects [1,2]. Although single crystals of these compounds are desirable due to their high magnetic anisotropy, they have never been grown and investigated. In the present work magnetic studies of a  $\text{DyFe}_5\text{Al}_7$  single crystal are performed.

Magnetic moments of the  $\text{DyFe}_5\text{Al}_7$  compound lie in the basal plane. The  $c$ -axis is the hard magnetization direction. At low temperatures, large anisotropy within the basal plane is observed as well between the [100] and [110] axes.

Temperature dependence of magnetization taken from magnetization isotherms along the [100] and [110] axes displays a typical ferrimagnetic behavior (Fig. 1) with the compensation point  $T_{\text{comp}} = 93$  K and Curie temperature  $T_C = 231$  K.

Magnetization isotherms measured along the [100] and [110] axes intersect due to strong bending of magnetic moments (with a higher susceptibility along the latter axis) after the domain-wall movement is completed. The magnetization along the [110] axis becomes higher. Along the easy [100] axis a field-induced transition is observed at  $75 \leq T \leq 100$  K in magnetic fields up to 14 T. Above the transition magnetization curves along both axes coincide. The transition field has a steep temperature dependence. High-field measurements are needed to obtain more data on the field-induced transition in  $\text{DyFe}_5\text{Al}_7$  at  $T < 75$  K.

The  $\text{DyFe}_5\text{Al}_7$  single crystal displays strong hysteresis with coercive field attaining  $\sim 3$  and 2.5 T at 2 K along the [100] and [110] axes, respectively. The coercive field decreases exponentially up to 20 K and much more slowly at higher temperatures. At  $T = T_{\text{comp}}$  it goes through a weak maximum.

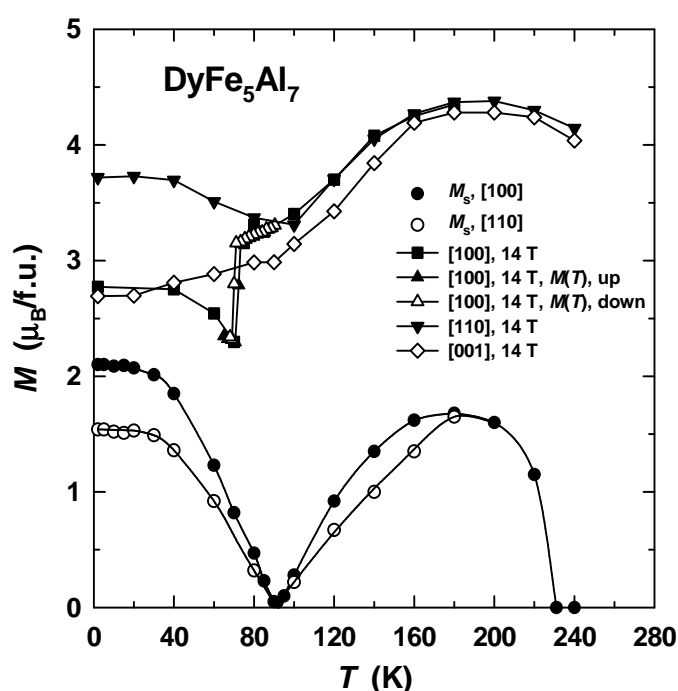


Fig. 1. Temperature dependence of spontaneous magnetization (bottom) and magnetization measured in 14 T (top) taken from magnetization isotherms along the principal axes. For the [100] axis, the  $M(T)$  data in 14 T are shown as well.

The work is a part of research project AVOZ10100520 and was supported by grant 202/09/0339 of the Czech Science Foundation.

[1] I. Felner, I. Nowik, M. Seh, *J. Magn. Magn. Mater.* **38** (1983) 172.

[2] I. Felner, I. Nowik, K. Baberschke, G.J. Nieuwenhuys, *Solid State Commun.* **44** (1982) 691.

## THE EFFECT OF THE MAGNETOCHEMICAL TREATMENT ON MAGNETIC PROPERTIES OF FeN THIN-FILM SYSTEMS

*Shalyguina E.<sup>1</sup>, Tarakanov O.<sup>1</sup>, Rozhnovskaya A.<sup>1</sup>, Kharlamova A.<sup>1</sup>, Ryjikov I.<sup>2</sup>*

<sup>1</sup> Faculty of Physics, Moscow State University, Leninskie Gory, 119992, Moscow, Russia

<sup>2</sup> Institute for Theoretical and Applied Electromagnetics, 13/19 Izhorskaya st., 127412 Moscow, Russia

The results on magneto-optical investigation of the magnetochemical treatment effect on morphology and magnetic properties of FeN thin-film systems are presented. The thin-film systems were obtained by the magnetron sputtering of iron in argon atmosphere under a pressure of  $10^{-4}$  Torr. The multilayer thin-film systems consisted of alternating silicon oxide and FeN layers. The thickness of FeN single-layer sample was equal to  $0.25\ \mu\text{m}$ , and the thickness of FeN layers in three-layer systems was  $0.07\ \mu\text{m}$ . The samples were chemically treated by phosphoric acid both in a magnetic field applied parallel or perpendicular to the sample surface and without magnetic field. The study of the surface morphology and the near-surface local magnetic properties of the thin-film systems was carried out employing a high-resolution microscope connected to computer by a digital camera and with the help of scanning Kerr microscopy.

The investigation of chemical treatment on the surface morphology of the samples was performed with the help of the familiar method, based on using a low-coercitive ferrite-garnet (FG) film as an indicator of stray fields. The initial FG film had the labyrinth domain structure (typical for this kind of materials) which was observed by means of the Faraday effect. Then the domain structure of the FG film was observed by making optical contact with the surface of the investigated samples. It was found that in the case of initial and chemically treated in a zero magnetic field samples the domain structure of the FG film remains labyrinth. However, after chemical etching in the presence of the magnetic field parallel or perpendicular to the sample surface, the FG film displays stripe or cylindrical domains, respectively. The obtained data can be explained by the enhancement of longitudinal and vertical defects on the surface of the FeN thin-film samples, which cause the appearance of the near-surface relief, predetermining the distribution of stray fields. These fields modify the domain structure, observed in the FG film.

The influence of the described above changes in the surface morphology of the samples on their magnetic properties was investigated. The near-surface local magnetization curves for the studied samples were measured employing scanning Kerr microscopy by registering the magneto-optical signals from a surface area of  $50\text{-}\mu\text{m}$  diameter. The initial samples were found to be characterized by a rather high homogeneity of the local magnetic properties. In particular, the difference in the local values of the saturation field,  $H_S$ , was no more than 9%. However, after chemical treatment in the presence of a magnetic field, the difference of  $H_S$  rises to 30-36 %, and the absolute values of  $H_S$  increase 1.5-2 times as compared to the initial samples. This result was explained by the appearance of the above heterogeneities on the sample surfaces, which cause enhancement of the stray fields influence on the measurable magnetic characteristics.

The work was supported by the Russian Foundation of Basic Research, grant №10-02-00485-a.

## FERROMODULATION EFFECT USAGE FOR THE MAGNETIC FILM ANISOTROPY INVESTIGATION

*Ubizskii S.B.<sup>1</sup>, Pavlyk L.P.<sup>1</sup>, Syvorotka I.I.<sup>2</sup>*

<sup>1</sup> Lviv Polytechnic National University, 2, Profesorska St., Lviv, 79013, Ukraine

<sup>2</sup> Scientific Research Company „Carat”, 202, Stryjska St., Lviv, 79031, Ukraine

Magnetic anisotropy is one of the key properties of the magnetic substances determining their domain structure and their behaviour in magnetic field. At the same time it belongs to parameters that are not easy to measure experimentally if a sample has small magnetic moment and weak anisotropy. It means it is difficult to do for many subjects being interesting and prospective now for investigation especially if the problem of magnetic anisotropy parameters' determination is put for non-destructive technique.

This contribution reports about an experimental proof of the phenomenological model [1] describing a ferromodulation response of the magnetic film being subjected to magnetization reversal under magnetic field changing its direction as pendulum oscillation [2] in the film plane and is a part of the investigation aimed on development a method of the magnetic anisotropy characterization. The pendulum-like magnetization reversal is driven by two orthogonal magnetic fields lying in the film plane – the permanent bias field being enough to saturate a film and relative small excitation field. The ferromodulation effect consists in the appearance of the additional modulation of an inductive EMF response being registered by the pick-up coil in the direction of the excitation field or the bias field as even or odd harmonics respectively [3]. It was shown before [4] that ferromodulation response is proportional to the magnetic moment of the film and sensitive to magnetic anisotropy being in dependence on angular position of easy magnetisation axes in the film plane.

The experiments were carried out by means of recording of the ferromodulation response dependencies upon an angular position of the disk sample in the film plane. The thin polycrystalline permalloy film with an induced uniaxial anisotropy in the film plane and (111)-oriented epitaxial iron garnet film of  $Y_3(FeSc)_5O_{12}$  composition which possessed the intrinsic cubic crystalline magnetic anisotropy as well as a small ( $5^\circ$ ) misorientation of [111] axis from the film plane were used for experiments. The angular dependencies reflect the symmetry of the in-plane magnetic anisotropy and are well described by the phenomenological model. The two-fold symmetry was observed in the case of uniaxial anisotropy and respectively six-fold symmetry in the case of epitaxial iron garnet film of (111) orientation. The last was somewhat disturbed presumably by misorientation of the film plane. The registered signal behaviour dependence upon magnetization reversal conditions allows identifying easy and hard axes in the film plane and can be considered as a mean of magnetic orientation. When the bias field is decreasing bifurcation appear near the hard axes directions due to nucleation of domains.

Performed investigation allows concluding that the developed method is sensitive enough and can be applied to different problem solving in the field of the magnetic anisotropy study and its quantitative parameters estimation.

This work is fulfilled in frames of the project DB/Neos. Authors thank to Dr. A.F. Kravets for a permalloy sample used in this investigation.

[1] S.B. Ubizskii, L.P. Pavlyk, International Conference „Functional Materials” (ICFM'2009), Ukraine, Crimea, Partenit, 2009, Abstracts, p. 449.

[2] S.B. Ubizskii, L.P. Pavlyk, *Sensors & Actuators A* **141** (2008) 440.

- [3] S.B. Ubizskii, L.P. Pavlyk, E.M. Klimovich, European Magnetic Sensors and Actuators Conference (EMSA'2008), Caen, France, 2008, Abstracts, p. 134.
- [4] S.B. Ubizskii, L.P. Pavlyk, Joint European Magnetic Symposia (JEMS'2008), Dublin, Ireland, 2008, Abstracts, p. MS 003.

23PO-I-42

## STRUCTURE AND MAGNETIC PROPERTIES OF HARD MAGNETIC NANOCRYSTALLINE ALLOYS BASED ON OXIDES

*Menushenkov V.P., Savchenko A.G., Yagodkin Yu.D.*

National University of Science and Technology «MISIS», 119049 Leninsky prospekt 4, Moscow, Russia

Recently, hard magnetic nanocrystalline materials are the objects of numerous investigations. The alloys based on oxides, particularly based on strontium hexaferrite  $\text{SrFe}_{12}\text{O}_{19}$  and alloys of Fe-Co-O system, are a special group among these materials. The goal of the present work was to analyze the structure and magnetic properties of these alloys.

Due to good combination of high magnetic properties, chemical stability and low cost, strontium hexaferrites in a microcrystalline state are widely used as permanent magnet materials.

However, the coercive force ( $H_{ci}$ ) of such magnets usually does not exceed 240-280 kA/m. The nanocrystalline hexaferrites are produced by various techniques, in particular, by the chemical coprecipitation method, by the glass crystallization, by the high-energy milling [1]. In the last case the milling results in formation of an amorphous phase and in decrease of the magnetic properties. The subsequent annealing of the milled powders leads to considerable increase of the properties caused by formation of  $\text{SrFe}_{12}\text{O}_{19}$  phase with the nanocrystalline structure. The average size of such phase crystallites, determined from broadening of X-ray diffraction lines and by scanning electron microscopy, was  $\langle D \rangle = 150\text{-}200$  nm. However, such powder could not be textured by pressing in an applied magnetic field due to random orientation of hexaferrite nanocrystallites in powder particles.

The milling at smaller intensity of the process enable to produce the powder in which the amorphous phase is missed, but  $\text{SrFe}_{12}\text{O}_{19}$  crystallites have the high lattice microstrains. The subsequent intermediate low-temperature annealing in a magnetic field and finishing high-temperature annealing without the field allow to obtain anisotropic powders, which can be textured in a magnetic field, with  $\langle D \rangle \sim 102$  nm and sufficiently great coercive force of 320-360 kA/m [2]. Considerably greater values of the coercive force are specific to  $\text{SrFe}_{12}\text{O}_{19}$  powders produced by the oxide glass crystallization.

Alloys based on magnetite  $\text{Fe}_3\text{O}_4$  are of interest, too. It was shown that nanomaterials, comprising  $\text{Fe}_3\text{O}_4$  and Fe phases with crystallites sizes of 10-30 nm, can be produced by mechanochemical technique and subsequent annealing from  $\text{Fe}_2\text{O}_3+\text{Fe}$ ,  $\text{Fe}_2\text{O}_3+\text{Fe}+\text{Co}$  and  $\text{FeO}+\text{Co}$  powder mixtures. Unlike the starting materials, these nanomaterials have the hard magnetic properties. Cobalt is dissolved in  $\text{Fe}_3\text{O}_4$  and Fe phases. The phase abundance and properties of these nanomaterials depend, first of all, on composition of the starting mixtures. It was shown that the coercive force of the powders, containing about 80 vol.%  $(\text{Fe},\text{Co})_3\text{O}_4$  phase, reaches 65 kA/m [3].

[1] Yu.D.Yagodkin, Yu.V.Lyubina, *Metal Science and Heat Treatment*, 2 (2009) 3

[2] S.V.Ketov, V.P.Menushenkov, Yu.D.Yagodkin, *Journal of Alloys and Compounds*, 509 (2011) 1065

[3] E.S.Shandrovskaiy, Yu.D.Yagodkin, *Metal Science and Heat Treatment*, 5 (2011) 22

## MAGNETOSTRICTION AND THERMAL EXPANSION OF PHASES FORMING DURING HEAT TREATMENT OF FERROMAGNETS

Gubernatorov V.V.<sup>1</sup>, Dragoshanskii Yu.N.<sup>1</sup>, Sycheva T.S.<sup>1</sup>, Olkov S.A.<sup>2</sup>, Pyatygin A.I.<sup>2</sup>

<sup>1</sup>Institute of Metal Physics, Ural Division of RAS, 620990 Ekaterinburg, Russia

<sup>2</sup>OOO VIZ-Stal, 620028 Ekaterinburg, Russia

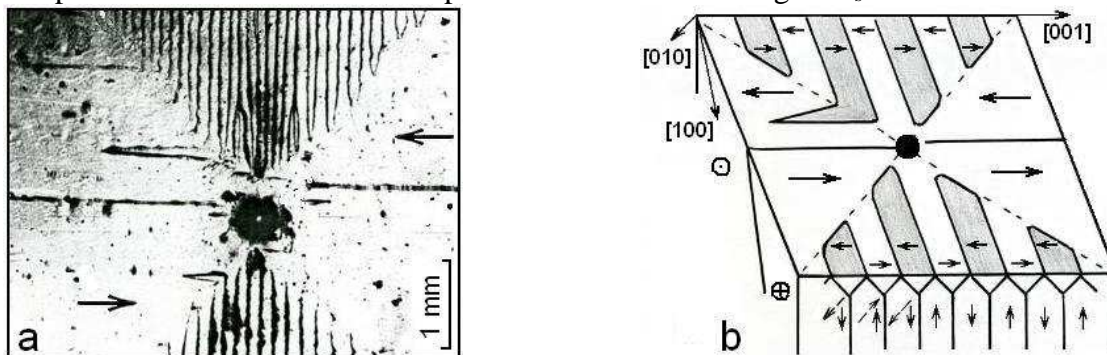
It is known that the saturation magnetostriction ( $\lambda_s$ ) significantly depends on the presence of internal residual stresses in ferromagnetic materials, which lead to formation of the  $90^\circ$  magnetic domains. Change in magnetization orientations of the  $90^\circ$  domains occurs in longitudinal magnetic field and makes the contribution to  $\lambda_s$ .

This study is concerned with one of possible sources of stress arising in ferromagnets, particularly during their cooling after the final high temperature annealing, which is carried out to obtain certain crystallographic texture, crystallite (grain) size and internal grain structure (substructure).

During cooling from high temperatures the first- and second- order phase transitions may occur in ferromagnets (in agreement with the state diagram), phase hardening accompanies it. Phase hardening causes dynamic strain aging with the formation of new phases [1]. These phases differ from the adjacent matrix by the structure, chemical composition and, consequently by the mechanical and physical properties, including the thermal expansion coefficient (TEC). During subsequent cooling the stresses will arise due to the TEC difference of the matrix and newly formed phases. The stresses will cause  $90^\circ$  domains formation.

The evidence has been shown by model experiment. The figure (a - the specimen, b – the scheme; arrows indicate magnetization directions) demonstrates how stripe domain structure A develops into  $90^\circ$  domain structure B with the transverse magnetization in (110)[001] crystal of Fe-3%Si alloy, which is caused by stresses after local indenter deformation. Similar picture was found [2] when the stresses were caused by local laser irradiation of the Fe-Si crystals.

The analysis of literature data of Fe-Si, Fe-Al, Fe-Ga, and Fe-Co alloys shows that  $\lambda_s$  change is well consistent with the phase formation in ferromagnets during the cooling from the high temperatures: the larger volume fraction of phases and the more significant TEC difference between matrix and phases means the more developed structure B and the higher  $\lambda_s$ .



The work has been partially supported by RFBR (grant No. 11-02-00931) and the integration project IMP – IEP UD RAS № 09-И-2-2002.

[1] V.V. Gubernatorov, T.S. Sycheva, *JMMM*, **254-255** (2003) 404.

[2] T. Nozawa, Y. Matsuo, H. Kobayashi et al., *J. Appl. Phys.*, **63** (1988) 2966.

## MAGNETIZATION CORRELATIONS AND RANDOM MAGNETIC ANISOTROPY IN NANOCRYSTALLINE FILMS $\text{Fe}_{78}\text{Zr}_{10}\text{N}_{12}$

*Iskhakov R.S.<sup>1,3</sup>, Komogortsev S.V.<sup>1,3</sup>, Sheftel E.N.<sup>2</sup>, Harin E.V.<sup>2</sup>, Krikunov A.I.<sup>4</sup>, Eremin E.V.<sup>1</sup>*

<sup>1</sup> Institute of Physics SB RAS, Krasnoyarsk 660036, Russia

<sup>2</sup> Institute of Metallurgy and Materials Science RAS, Moscow 119991, Russia

<sup>3</sup> Siberian University of Technology, Krasnoyarsk, 660049, Russia

<sup>4</sup> Institute of Radio Engineering and Electronics RAS, Fryazino, 141120, Russia

The nanocrystalline films of quasi-eutectic alloys Fe-ZrN represent the new type of magnetically soft ferromagnetic materials, characterized by high magnetization and thermal stability [1]. Extraordinary magnetic softness in nanocrystalline ferromagnetic is described in the terms of random magnetic anisotropy model. It is assumed that easy axes of individual grains are randomly oriented. Local magnetization in this case is randomly inhomogeneous and can be described by magnetization correlation function. The important parameter of magnetization correlation function is the magnetic correlation length  $R_L$  – the scale of area where the local magnetization is uniform. It is established that the extremely magnetic softness in such materials is realized under the condition  $2R_L \gg D$  where  $D$  is the grain size.

In this report we compare the parameters of the magnetization correlation function of the nanocrystalline film  $\text{Fe}_{78}\text{Zr}_{10}\text{N}_{12}$  obtained by two experimental techniques: correlation magnetometry (the technique of analysis of magnetization approach to saturation curves) [2] and by magnetic force microscopy. The main parameters of the random magnetic anisotropy in the  $\text{Fe}_{78}\text{Zr}_{10}\text{N}_{12}$  films: magnetic anisotropy energy and the correlation radius of the local magnetic anisotropy are determined by correlation magnetometry as well.

The experimental samples are films  $\text{Fe}_{78}\text{Zr}_{10}\text{N}_{12}$  with the thickness of 0.8  $\mu\text{m}$  synthesized by reactive magnetron sputtering at the direct current and annealed at 400  $^{\circ}\text{C}$  during 1 hour. According to X-ray investigations annealed the films are characterized by mixed amorphous-nanocrystalline structure [3]. Evaluation of the magnetization correlation length ( $R_L$ ), performed by the correlation magnetometry yields the value  $\sim 0.13 \mu\text{m}$ . The images of the film surface obtained by magnetic force microscopy reveal the contrast, visualizing the film magnetization heterogeneity. Calculation of magnetization correlation functions using these images shows that: 1) the character of magnetization correlation function in nanocrystalline film  $\text{Fe}_{78}\text{Zr}_{10}\text{N}_{12}$  is nonmonotonic, and 2) the value of the magnetization correlation length  $R_L$  is about 0.12  $\mu\text{m}$ .

Support by Federal Program “Development of the Scientific Potential of Higher Education” (project no. RNP.2.1.1/2584), Federal Target Program “Research and Research-Pedagogical Personnel of Innovation Russia for 2009-2013” and RF President grant No. 02.120.11.7075-NSh are acknowledged.

[1] E.N. Sheftel', O.A. Bannykh, *Russian Metallurgy*, 5 (2006) 394.

[2] R.S. Iskhakov, S.V. Komogortsev, *Bull. Russ. Ac. Sci.: Physics*, **71** (2007)1620.

[3] E.N. Sheftel', A.V. Shalimova, G.S. Usmanova et. al., *Phys. Met. Metal.*, **96** (2003) 414.

23PO-I-45

**ELECTRONIC AND SPIN STRUCTURE OF METAL PHTHALOCYANINES***Tikhonov E.V.<sup>1</sup>, Uspenski Yu.A.<sup>2</sup>, Kulatov E.T.<sup>3</sup>, Belogorokhov I.A.<sup>4</sup>, Khokhlov D.R.<sup>1</sup>*<sup>1</sup> Physics Department, Moscow State University, GSP-1, Leninskie Gory, Moscow, 119991, Russia<sup>2</sup> Lebedev Physical Institute of RAS, 119991 Moscow, Leninskij prospekt, 53, Russia<sup>3</sup> Prokhorov General Physics Institute of RAS, 119991, Moscow, Vavilov Str., 38, Russia<sup>4</sup> Federal State Research and Design Institute of Rare Metal Industry, 119017, Moscow, B. Tolmachevsky lane, Building 5-1, Russia

Metal phthalocyanines (MPc) form a large class of complex semiconducting compounds widely used in modern technology and, particularly, in electronics. The molecule of MPc may be imagined as a molecule of phthalocyanine  $C_{32}N_8H_{18}$ , where two central hydrogen atoms are replaced for one metal atom. The substitution of different metal atoms significantly affects the electronic structure, geometry, electrical, optical and magnetic properties of MPc molecules. Changes in the HOMO-LUMO energy gap, optical and magnetic properties of MPc are most practically important. In this presentation we consider a series of 3d- and 4d-metal phthalocyanines (M=Ni, Cu, Zn, Rh, Pd, Ag, Cd, In, and Sn) using first-principles calculations with the GGA and hybrid functionals. It is found that metal phthalocyanines with odd number of electrons are spin-polarized and the exchange splitting of their electron spectrum is of 1 eV near the Fermi energy. Using CuPc, as an example, we considered optical and magneto-optical spectra of metal phthalocyanines. Comparing calculated results with experimental ones, we found that the hybrid functionals provide much better description of electron and optical spectra than the GGA method.

This research was supported in part by the Russian Fund for Basic Research (grants 10-02-00698a, 10-02-00118-a, 09-02-00698-a and 09-02-91078-CNRS-a) and the programs of RAS “Strongly correlated electrons in solids and structures” and “Basic investigations of nanotechnologies and nanomaterials”.

23PO-I-46

**MAGNETIC PROPERTIES OF INTERMETALLIC COMPOUND  $Ti_3Al$  WITH DEUTERIUM***Patselov A., Milyaev M., Eshchenko R.*

Institute of Metal Physics, Ekaterinburg, Russia

Hydrogen is known to change magnetic and electronic properties of alloys and intermetallics in a wide range [1]. Intermetallics based on titanium are used as a special structural materials in modern technology. Therefore, study of their interaction with hydrogen (deuterium) is a challenging problem. This paper presents the results of magnetization measurements of the intermetallic  $Ti_3Al$  samples doped with different concentrations of deuterium.

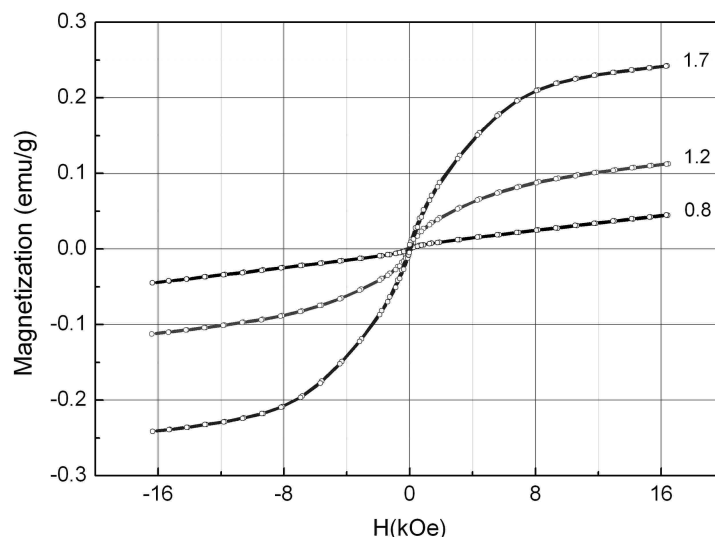
Saturation with deuterium was carried out at 700 °C. Exposure to this temperature for 1.5 hours ensured complete absorption of the samples for given volume of gas. Samples with a concentration of deuterium,  $D/Me = x = 0.8; 1.2; 1.7$  were chosen for the study. Magnetization measurements



were performed at room temperature using a vibrating sample magnetometer on polycrystalline samples with composition close to stoichiometric.

Magnetization of deuterides with  $x = 0.8$  has similar values to magnetization of samples without deuterium. At deuterium concentration  $x > 0.8$  magnetization is growing and at  $x = 1.7$  magnetization is increasing by more than 5 times (figure). Increase in magnetization after deuterium introduction is assumed to be due to the changes in the density of electronic states and phase transition initiated by deuterium.

More detailed study of structural changes in magnetization of  $Ti_3Al$  deuterides was carried out by shear under pressure technique. All the samples had the same treatment parameters: quasi-hydrostatic pressure 12 GPa, and the same true logarithmic strain. The structure of deformed deuterides varies depending on the concentration of deuterium that was shown in [2] on X-ray based and electron microscopic data. After the above-mentioned deformation treatment magnetization was measured again and the increase in



magnetization of the samples with concentration  $x = 0.8$  was experimentally observed. At the same time the decrease in magnetization of  $Ti_3Al$  deuterides with  $x = 1.7$  was observed. Based on these findings the relationship of structural transformations and magnetization of deuterides is discussed.

This study was supported under the Russian Academy of Sciences (RAS) plan (subject "Impulse", reg. no. 01.2.006 13394) with partial financial support from the RAS Program (project no. 09-P-2-1019).

[1] Hydrogen in metals / edited by G. Alefeld and J. Volkl, Berlin; New York: Springer-Verlag, (1978), 426.

[2] R. N. Eshchenko, A. M. Patselov, and V. P. Pilyugin *Bulletin of the Russian Academy of Sciences: Physics*, **73** (2009), No. 9, 1262.

23PO-I-47

## LOCAL AND ATOMIC STRUCTURE OF AMORPHOUS ALLOYS

### $Fe_{75}Cr_{10}B_{15}$

*Dmitrieva T., Pokatilov V.*

Moscow State Institute of Radioengineering, Electronics and Automation (Technical University),  
119454 Moscow, pr. Vernadskogo, 78, Russia

Amorphous magnetic metal alloys on the basis of iron-boron draw wide attention of researchers as they are a base of magnetic soft and hard materials which have found wide application. Despite intensive studies of these alloys throughout more than 30 years, the local atomic and magnetic

structure of these alloys remains practically unknown. It should be noted, that local structure was studied enough only for amorphous alloys Fe-B where it had been shown, that these alloys consisted of microranges (nanoclusters) with several types of the short-range (SR) order. Numbers and types of SR orders depend on the content of boron and iron [e.g., 1]. Amorphous alloys based on Fe and B that have been used in engineering, as a rule, additionally contain s, p, and d atoms. The influence of these atoms on the local atomic and magnetic structures of the alloys under consideration has not been adequately investigated. Amorphous alloys Fe-B-Cr, generally, were studied after high-heat treatments above crystallization temperature. The SR atomic and magnetic order of these alloys in amorphous state was not studied.

In the presented work the SR order of Fe atoms in amorphous alloy Fe<sub>75</sub>Cr<sub>10</sub>B<sub>15</sub> was explored by a Mössbauer effect method. Mössbauer spectra were studied in the temperature field 12-500K. Distributions P(H) of hyperfine fields (HFF), isomer P( $\delta$ ) and quadrupole P( $\epsilon$ ) shifts and model interpretation of experimental spectra were made by means of programs DISTRI and SPECTR [2]. Curie and Debye temperatures of this alloy was measured as well. At temperatures 140-160K abnormal behavior HFF and width of distribution P(H) was found. Distribution P( $\epsilon$ ) at T > T<sub>C</sub> contains, at least, two most probable states of Fe atoms differing quadrupole and isomer shifts. It points out the complex local atomic and magnetic structures. Distribution P(H) at 12K consists also, at least, of two most probable states of Fe atoms with various local HFF. Effects of short-term annealing and a quenching of amorphous alloys at temperatures both low and above crystallization temperature on Mössbauer spectra and also X-ray analysis of these samples show that amorphous alloys Fe<sub>75</sub>Cr<sub>10</sub>B<sub>15</sub> contain microranges (nanoclusters) with SR order of tetragonal boride (Fe, Cr)<sub>3</sub>B and  $\alpha$ -Fe(Cr) types.

[1]. V.S.Pokatilov. FTT **51** (2009), № 1, p.1354.

[2]. V.S.Rusakov. *Mössbauer spectroscopy of locally inhomogeneous systems*. (Almaty, Kazakhstan 2000, (in Russian)).

23PO-I-48

## MAGNETIC ANISOTROPY AND MAGNETOSTRICTION OF AMORPHOUS TbCo FILMS

*Kulesh N.A., Balymov K.G., Stepanova E.A., Vas'kovsky V.O.*  
Ural State University named after A.M. Gorky, Yekaterinburg, Russia

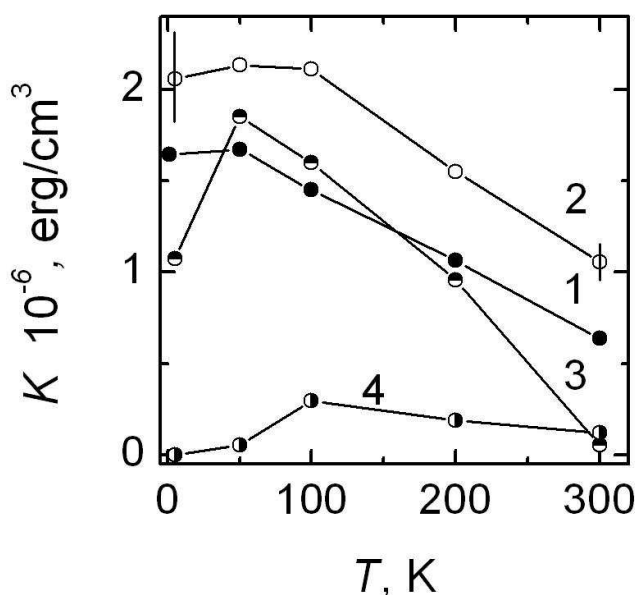
Magnetic properties of Tb<sub>x</sub>Co<sub>100-x</sub> amorphous thin films for x = 8÷43 at.% were investigated. Samples were prepared by rf-sputtering of the mosaic target in the Ar media with 1 mTorr pressure. During the deposition, the homogeneous in-plane magnetic field of 150 Oe was applied. Corning cover glass was used as a substrate; in all cases the Tb-Co layer was covered by additional 50 nm Ti top layer to avoid an oxidation. Thickness of Tb-Co layers were 100 nm, compound was controlled by chemical analysis. For investigation of the magnetic properties at room temperature VSM with a 17 kOe field range was used. For low-temperature measurements the SQUID-magnetometer MPMS-7EC-XL with a 70 kOe operating field range was used.

According to our investigation, all samples have a sophisticate magnetic anisotropy. Also, it was found that there is a strong in-plane unidirectional anisotropy parallel to the direction of the external field which was applied during the deposition. It is supposed that it has a magnetoelastic nature.

Figure demonstrates a numerical characterization of this anisotropy for several samples of different compounds (1 - Tb<sub>8</sub>Co<sub>92</sub>; 2 - Tb<sub>18</sub>Co<sub>82</sub>; 3 - Tb<sub>22</sub>Co<sub>78</sub>; 4 - Tb<sub>31</sub>Co<sub>69</sub>). The anisotropy constant K was determined as a difference of an area under demagnetization curve measured along

easy axis (EA) and an area under curve measured along hard axis. It was found that terbium-rich samples have relatively weak anisotropy. This can be explained by high dispersion of the easy axis, which could be cause of strong local fluctuations of the EA due to sperrimagnetic order of atomic magnetic moments of terbium [1].

We performed an estimation of the magnetostriction constant in amorphous Tb-Co films of various compositions. For that we used a method of the magnetic anisotropy induction by application of the elastic stress. The induced anisotropy was registered using the magnetoresistive effect of permalloy layer, which was deposited on the amorphous layer.



Supported by RFBR (grant 11-02-00288-a).

[1] A.S. Andreenko, S.A. Nikitin., APS, **167** (1997) 605.

23PO-I-49

## DESTROYING OF NONEQUILIBRIUM FERROMAGNETIC STATE IN PrB<sub>6</sub>

Samarin N.A.<sup>1</sup>, Anisimov M.A.<sup>1</sup>, Bogach A.V.<sup>1</sup>, Glushkov V.V.<sup>1</sup>, Demishev S.V.<sup>1</sup>, Filipov V.B.<sup>2</sup>,  
Shitsevalova N.Yu.<sup>2</sup>, Kuznetsov A.V.<sup>3</sup>, Sluchanko N.E.<sup>2</sup>

<sup>1</sup> Low Temperatures and Cryogenic Engineering Department, A.M. Prokhorov General Physics  
Institute of Russian Academy of Science, 38 Vavilov str., Moscow 119991, Russia

<sup>2</sup> I.N.Frantsevich Institute for Problems of Material Science of NASU, 3 Krzhizhanovskii str., Kiev  
03680, Ukraine

<sup>3</sup> Moscow Engineering Physics Institute, 31 Kashirskoe sh., Moscow 115409, Russia  
E-mail: anisimov.m.a@gmail.com, nes@lt.gpi.ru

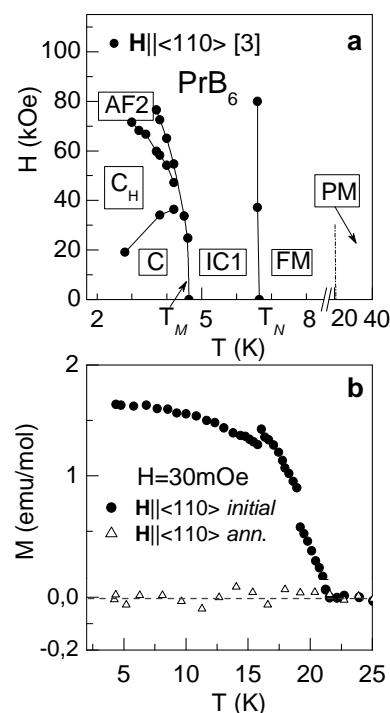
Rare earth hexaborides RB<sub>6</sub> are bcc compounds that demonstrate a variety of magnetic properties and ground states. The investigations of praseodymium hexaboride (PrB<sub>6</sub>) show the strong anisotropy of transport and magnetic properties in this antiferromagnet (AF) [1-3]. In the absence of magnetic field two successive phase transitions in AF incommensurate (IC1) and commensurate (C) states are observed at  $T_N \sim 6.7\text{K}$  and  $T_M \sim 4.6\text{K}$ , respectively [2]. The increase of magnetic field at temperatures in the range  $T < T_M$  is accompanied by the several transitions from AF C to collinear (C<sub>H</sub>) and then to the new antiferromagnetic (AF2) phase for direction  $\mathbf{H} \parallel \langle 110 \rangle$  [3] (Fig.a). Moreover the recent studies of magnetization [4] for PrB<sub>6</sub> allow to detect a new ferromagnetic (FM) transition at  $T_C \sim 20\text{K}$  (Fig.a).

To shed more light on the ground state formation the comprehensive study of transverse magnetoresistance (MR) and magnetization has been carried out on the high quality single crystals of PrB<sub>6</sub> in the wide range of temperatures 2-40K and magnetic fields up to 80 kOe. In order to estimate the contribution of boron vacancies to FM ordering the experiments were made on the ordinary (initial state) and annealed ( $T_{an} \sim 1700^\circ\text{C}$ ,  $t \sim 10$  hours) single crystals of PrB<sub>6</sub>. The high

quality of the samples was controlled by X-ray diffraction and electron microscopy. The MR ( $\mathbf{I} \parallel \langle 110 \rangle$ ) and magnetization measurements were fulfilled in magnetic field  $\mathbf{H} \parallel \langle 111 \rangle$ ,  $\mathbf{H} \parallel \langle 110 \rangle$ .

The data obtained allow to establish the appearance of spontaneous magnetization with a relatively small magnetic moment  $M \sim 1.6$  emu/mol for initial crystal of  $\text{PrB}_6$  below 21 K (see the symbols  $\bullet$  on Fig.b). After annealing the curve  $M(T)$  shows the absence of spontaneous magnetization (the symbols  $\Delta$  on Fig.b). However for initial and annealed state of crystals the results of MR investigation reveal the similar behavior and the same AF magnetic phase transitions (AF IC1 and AF C). The analysis of the data obtained allows to conclude in the favour of boron vacancies contribution (see [5]) to FM ordering of  $\text{PrB}_6$  at  $T_C \approx 21$  K.

- [1] M.Sera, M-S.Kim et al., J. Phys. Soc. Jpn., **73**, (2004) 3422.  
 [2] M.A.Anisimov, A.V.Bogach, V.V.Glushkov et al., JETP, **109** (2009) 815.  
 [3] N.E.Sluchanko et al., JETP Lett., **90**, (2009) 152.  
 [4] P.A.Alekseev, K.Flachbart, S.Gabani et al., Phys.Sol.St., **52** (2010) 914.  
 [5] M.M.Korsukova, V.N.Gurin et al., J.Less-Comm. Met., **117** (1986) 73.



23PO-I-50

## HIGH PRESSURE SYNTHESIS AND MAGNETIC PROPERTIES OF CUBIC B20 MnGe and CoGe

*Tsvyashchenko A.V.<sup>1,2</sup>, Sidorov V.A.<sup>1,3</sup>, Fomicheva L.N.<sup>1</sup>, Krasnorussky V.N.<sup>1</sup>, Sadykov R.A.<sup>1,4</sup>, Thompson J.D.<sup>3</sup>, Gofryk K.<sup>3</sup>, Ronning F.<sup>3</sup>, Ivanov V.Yu.<sup>5</sup>*

<sup>1</sup> Vereshchagin Institute for High Pressure Physics, RAS, 142190 Troitsk, Russia

<sup>2</sup> Skobeltsyn Institute of Nuclear Physics, MSU, Vorob'evy Gory 1/2, 119991 Moscow, Russia

<sup>3</sup> Los Alamos National Laboratory, Los Alamos, NM 87545, USA

<sup>4</sup> Institute for Nuclear Research, RAS, 142190 Troitsk, Russia

<sup>5</sup> Prokhorov General Physics Institute, RAS, Vavilov Str., 38, 119991, Moscow, Russia

Samples of MnGe and CoGe having cubic B20 structure were prepared by melting the constituent elements at the high pressure of 8 GPa. Magnetic measurements showed that CoGe is a Pauli paramagnet, but MnGe exhibits antiferromagnetic-type ordering below  $T_N = 175$  K. The magnetic susceptibility of MnGe follows a Curie-Weiss law above 300 K with an effective magnetic moment  $\mu_{\text{eff}} = 3.68 \mu_B/\text{f.u.}$  and  $\theta_p = +231$  K. The large positive value of  $\theta_p$  indicates a strong ferromagnetic exchange. The value of the effective moment is close to the free  $\text{Mn}^{4+}$  ion ( ${}^4F_{3/2}$ ) value  $3.87 \mu_B/\text{f.u.}$  At temperatures below  $\sim 50$  K the magnetic susceptibility of MnGe shows zero field cooled and field cooled hysteresis, possibly from formation of ferromagnetic-like domains (Fig.1). From measurements of magnetization of MnGe in fields up to 60 kOe and in the temperature range 2-350 K, we constructed its T-H magnetic phase diagram (Fig.2) which is similar to that proposed for MnSi-type compounds with a helical magnetic order. Specific heat measurements reveal that the total magnetic entropy of MnGe relative to nonmagnetic CoGe is equal to  $3.55 \text{ J/mole-K}$  ( $0.62R \ln 2$ ) and 93% of this value is released below  $T_N = 175$  K. The remaining magnetic entropy was found in

the range 175-250 K. The electrical resistivity of polycrystalline samples also was measured. Both MnGe and CoGe have resistivities  $\sim 350 \mu\Omega \text{ cm}$  at room temperature which decrease smoothly on decreasing temperature.

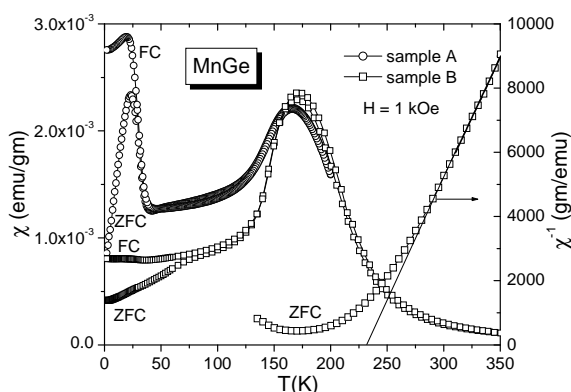


Fig. 1.

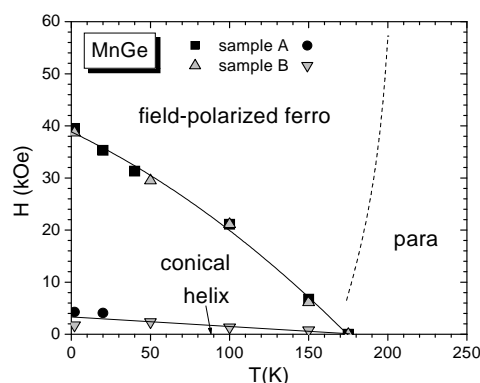


Fig. 2.

This work was supported by the Russian Foundation for Basic Research (Grant 11-02-00029). Work at Los Alamos National Laboratory was performed under the auspices of the US DOE/ Office of Basic Energy Sciences, Division of the Material Sciences and Engineering.

23PO-I-51

## NEW MIXED-VALENCE TELLURATE SYSTEM $\text{Li}_{1-x}\text{Mn}_{2+x}\text{TeO}_6$ : MAGNETIZATION AND EPR STUDIES.

Zvereva E.A.<sup>1</sup>, Savelieva O.A.<sup>1</sup>, Samohvalov E.A.<sup>1</sup>, Volkova O.S.<sup>1</sup>, Vasiliev A.N.<sup>1</sup>, Nalbandyan V.B.<sup>2</sup>,  
Evstigneeva M.A.<sup>2</sup>, Wolter A.<sup>3</sup>, Büchner B.<sup>3</sup>

<sup>1</sup> Faculty of Physics, Moscow State University, 119991 Moscow, Russia

<sup>2</sup> Chemistry Faculty, Rostov State University, Rostov-on-Don 344090, Russia

<sup>3</sup> Leibniz Institute for Solid State and Materials Research IFW Dresden, D-01171 Germany

We report on static and dynamic magnetic properties of new mixed-valence tellurate system  $\text{Li}_{1-x}\text{Mn}_{2+x}\text{TeO}_6$ . The samples have been prepared by conventional solid-state reactions. They represent a new triclinic structure type [1] derived from orthorhombic  $\text{Li}_2\text{TiTeO}_6$ . Temperature dependencies of magnetic susceptibility and magnetic field dependencies of magnetization have been measured by SQUID magnetometer in the range  $T=2-300 \text{ K}$ ,  $B \leq 5 \text{ T}$ , electron paramagnetic resonance (EPR) studies have been carried out using X-band spectrometer ( $f \approx 9.4 \text{ GHz}$ ,  $B \leq 0.7 \text{ T}$ ,  $T=6-470 \text{ K}$ ).

It was found that all samples of various compositions demonstrate the common features in the magnetic properties. Temperature dependence of the magnetic susceptibility has a complicated character and reveals the presence of two distinct anomalies at low temperatures: the first one at  $T_1=12 \text{ K}$  and the second at  $T_2=20 \text{ K}$ . Upon an increase of manganese content amplitude of the first anomaly monotonously increases, while the magnitude of the second one remains practically unchanged (Fig. 1). At temperatures higher  $T_2$  the magnetic susceptibility follows the Curie-Weiss law  $\chi = \chi_0 + C/(T - \Theta)$ . Curie-Weiss temperatures weakly depends on compound composition and is on average ( $\Theta \approx 90-95 \text{ K}$ ), indicating antiferromagnetic interaction between Mn ions. Effective magnetic moments estimated from the Curie constant values  $C$  was found to be  $7.6-8.0 \mu_B$  that is in

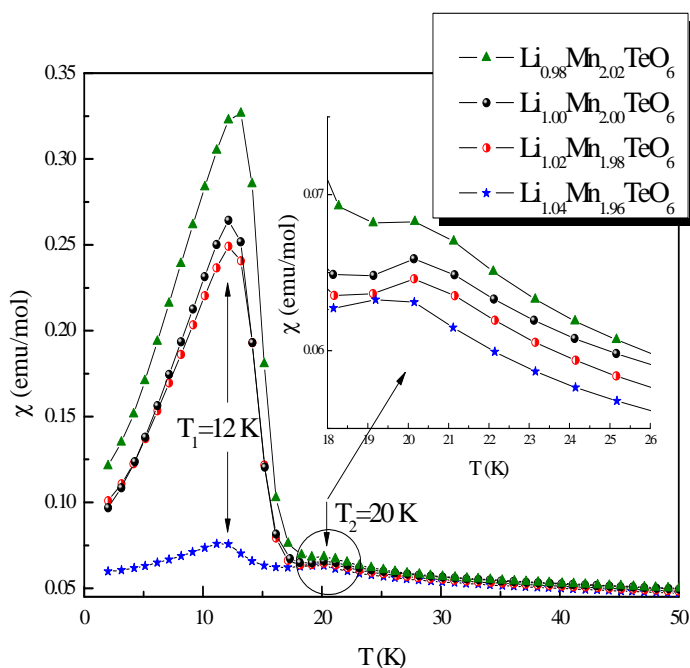


Fig. 1. Temperature dependence of magnetic susceptibility for  $\text{Li}_{1-x}\text{Mn}_{2+x}\text{TeO}_6$  samples at various composition.

a satisfactory agreement with theoretical estimations for given concentration of manganese in mixed valence state: half of Mn ions per formula unit is in high-spin  $\text{Mn}^{2+}$  ( $S=5/2$ ) state and another half - in high-spin  $\text{Mn}^{3+}$  ( $S=2$ ) state.

EPR spectra of samples studied show inhomogeneously broaden absorption line probably originated from  $\text{Mn}^{3+}$  ions in weakly distorted octahedral coordination. Thorough analysis of the line shape indicates that absorption line is a superposition of two spectral components (broad 1 and narrow 2 ones) with rather different effective g-factors: at  $T=300$  K -  $g_1=1.52\pm 0.01$  and  $g_2=2.15\pm 0.01$ . This is likely to correspond to the presence of four crystallographically non-equivalent Mn sites in the structure [1]. With decreasing temperature down to helium temperature the EPR linewidth essentially increases by analogy with behavior of other antiferromagnetic and spin-glass systems.

The work was supported by the Russian Foundation for Basic Research (grant 11-03-01101).

[1] V.B. Nalbandyan, A.A. Pospelov et al. Submitted to *Solid State Sciences*.

23PO-I-52

## MAGNETIC STRUCTURE OF $\text{La}_{0.54}\text{Ho}_{0.11}\text{Sr}_{0.35}\text{MnO}_3$ MANGANITES Cu DOPED

Craus M.-L.<sup>1,2</sup>, Anitas E.<sup>2,3</sup>, Cornei N.<sup>4</sup>, Islamov A.<sup>2</sup>, Oprea A.<sup>2</sup>, Garamus V.<sup>5</sup>

<sup>1</sup> Institute of Research and Development for Technical Physics, Mangeron 47, Iasi, Romania;

<sup>2</sup> Joint Institute for Nuclear Research, Joliot-Curie 6, 141980 Dubna, Russia;

<sup>3</sup> Horia Hulubei National Institute of Physics and Nuclear Engineering, Atomistilor 407, Bucharest - Magurele, Romania;

<sup>4</sup> Faculty of Chemistry, "Al.I.Cuza" University, Carol I 11, Iasi, Romania;

<sup>5</sup> GKSS Research Centre, Max-Planck-Str., Geesthacht, Germany.

The colossal magnetoresistance, observed in perovskite manganites, involves the double exchange mechanism and electron-phonon interactions. In contrast with the classical ferromagnets in the manganites, there is a strong coupling between the charges, spin and lattice degree of freedom. The  $\text{La}_{0.54}\text{Ho}_{0.11}\text{Sr}_{0.35}\text{Mn}_{1-x}\text{Cu}_x\text{O}_3$  manganites were obtained by sol-gel method using oxides and acetates and investigated by X-ray diffraction using a HUBER diffractometer with GUINIER CAMERA

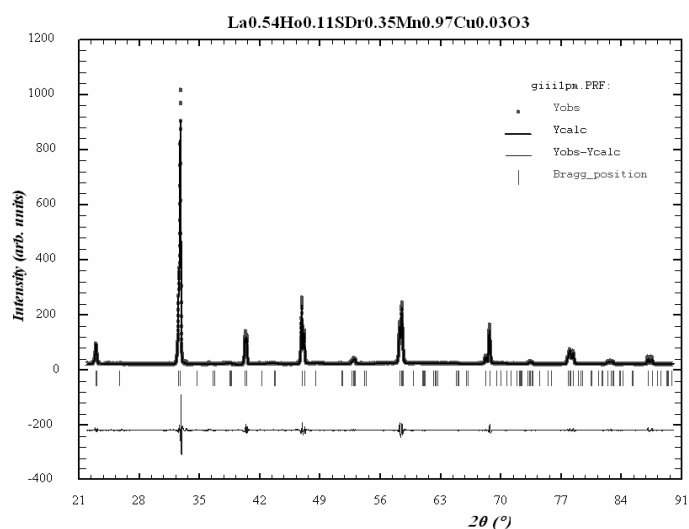


Figure 1. The observed ( $Y_{obs}$ ) and calculated ( $Y_{calc}$ ) diffractograms, the difference between them ( $Y_{obs}-Y_{calc}$ ) and the Bragg positions for  $\text{La}_{0.54}\text{Ho}_{0.11}\text{Sr}_{0.35}\text{Mn}_{0.97}\text{Cu}_{0.03}\text{O}_3$  manganite (FullProf method)

momentum transfer in the range  $0.005 < q < 0.015 \text{ \AA}^{-1}$  is characterized by a Porod law behavior ( $I(q) \sim q^{-4}$ ) while in the second region, when  $0.015 < q < 0.2 \text{ \AA}^{-1}$ , the scattering intensity shows a power law behavior with the module of the exponent varying between 2 and 3 and is characteristic to scattering from mass fractal aggregates. After subtraction of nuclear scattering from total scattering we obtained magnetic scattering. An indirect Fourier transform (IFT) procedure has been applied for determination of the pair distance distribution function (PDDF). The results show the formation of magnetic clusters, with radius which depend on the Cu concentration.

670 and a  $\text{CuK}\alpha_1$  radiation. Space group, lattice constants, average size of the crystalline blocks and positions of cations/anions in the unit cell were obtained with FullProf code.

The distribution and average sizes of magnetic clusters have been determined at room temperature, without magnetic field, by SANS measurements. The aim of present work is to investigate the correlation between crystalline/magnetic structure and transport mechanism characteristics

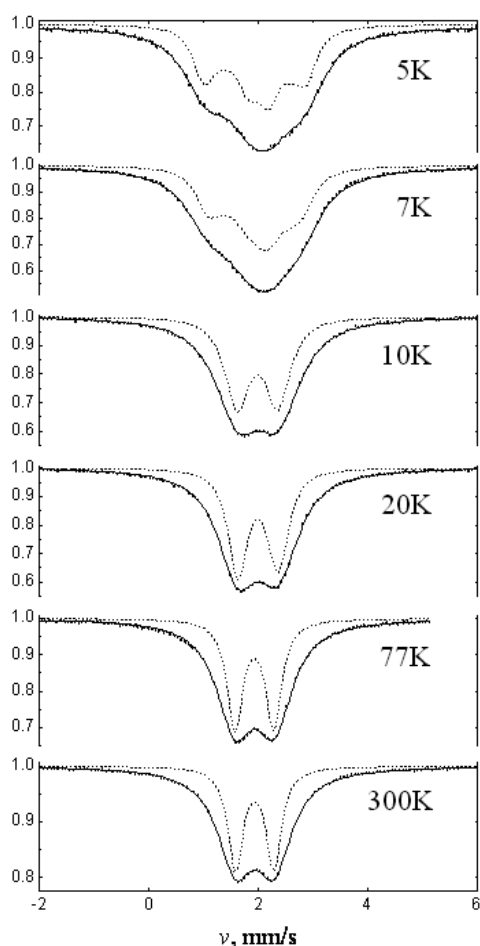
in  $\text{La}_{0.54}\text{Ho}_{0.11}\text{Sr}_{0.35}\text{Mn}_{1-x}\text{Cu}_x\text{O}_3$  manganites with variation of Cu concentration. The SANS data versus variation of Cu concentration shows clearly two different regions. The first region, corresponding to the module of the

## MÖSSBAUER SPECTROSCOPY OF ANTIFERROMAGNETIC FLUCTUATIONS IN HEAVY FERMION COMPOUND CePdSn

Polikarpov M.A.<sup>1</sup>, Cherepanov V.M.<sup>1</sup>, Chuev M.A.<sup>1,2</sup>

<sup>1</sup> National Research Centre “Kurchatov Institute”, 123182, Moscow, Russia

<sup>2</sup> Institute of Physics and Technology, Russian Academy of Sciences, 117218 Moscow, Russia



CePdSn is a heavy-fermion compound which shows an antiferromagnetic ordering at low temperatures ( $T_N \approx 7$  K) and single-ion Kondo effect at higher temperatures. An analysis of the neutron diffraction data evidenced for the presence of incommensurate magnetic structure with modulation vector that differs from the half of reciprocal lattice vector [1]. At the same time experimental data on the muon spin precession in local magnetic field showed the presence of several well-resolved Fourier components in the time spectra of muon spin depolarization, which do not require the introduction of any distribution of the local magnetic field related to the incommensurate magnetic structure. The main purpose of this study was to elucidate the reasons for this discrepancy by studying the spin fluctuations in CePdSn for  $T > T_N$  by Mössbauer spectroscopy. The temperature evolution of the experimental spectra is found to be well consistent with the calculations within a two-level relaxation model [2]. This allows us to treat previously proposed «spin-slip» model [1] of the magnetic structure CePdSn as a simple partition of the sample on the nanometer-scale antiferromagnetic domains. A direct consequence of an adequate description of the spectra in this model was the ability to monitor the temperature dependence of the frequency fluctuations magnetizations of domains and the distribution density of itinerant conduction electrons near the tin atoms in the process of RKKY interaction.

<sup>119</sup>Sn Mössbauer spectra (points) of CePdSn as a function of temperature and theoretical spectra (solid lines) calculated within a two-level relaxation model. Dotted lines show the absorption spectra of the sample without its convolution with the Lorentzian source line.

The authors thank T. Takabatake for the samples CePdSn and Russian Foundation for Basic Research for financial support.

[1] G.M. Kalvius A. Kratzer, K.H. Münch, F.E. Wagner, S. Zwirner, H. Kobayashi, T. Takabatake, G. Nakamoto,

H. Fujii, S.R. Kretzman, R. Kiefl. *Physica B.*, **186-188** (1993) 412.

[2] M.A. Polikarpov, V.M. Cherepanov, M.A. Chuev, S.S. Yakimov. *J. Magn. Magn. Mater.*, **135** (1994) 361.



## INFLUENCE OF HYDROGENATION ON MAGNETIC AND STRUCTURAL PROPERTIES OF $\text{ErFe}_2$ .

Sherstobitova E.A., Gubkin A.F., Pirogov A.N., Mushnikov N.V.

Institute for Metal Physics, RAS, 620990 Yekaterinburg, S. Kovalevskoy st. 18, Russia

The crystalline  $\text{ErFe}_2\text{H}_x$  hydrides possess a cubic structure of the C15 type for  $x \leq 3.2$ , the rhombohedral structure for  $3.2 < x < 3.7$  and again the C15-type structure for  $x \approx 4$  at the room temperature [1,2]. According to the x-ray powder diffraction study [2], in  $\text{ErFe}_2\text{H}_x$  compounds with  $x \approx 3.2$  the rhombohedral-to-cubic phase transition was observed upon heating in the temperature range 260-320 K. The transition was assumed to be controlled by redistribution of hydrogen over the interstitials. However the contribution of hydrogen atoms to the x-ray diffraction scattering is

negligible and, hence, there is no experimental proof for the proposed model. According to magnetic measurements [3], temperature dependence of the magnetization of  $\text{ErFe}_2\text{H}_{3.1}$  sample shows a pronounced hysteresis around the transition temperature which implies the rhombohedral-to-cubic phase transition in the  $\text{ErFe}_2\text{H}_{3.1}$  compound is of the first-order type. In order to clarify the influence of hydrogen on the crystal structure and magnetic properties of  $\text{ErFe}_2\text{H}_{3.1}$  compounds we carried out neutron diffraction experiments in a wide temperature range 12 K – 450 K for the  $\text{ErFe}_2\text{H}_{3.1}$  compound close to the rhombohedral-to-cubic phase transition. Bearing in mind the large incoherent scattering cross section of hydrogen, the neutron diffraction study of deuteride  $\text{ErFe}_2\text{D}_{3.1}$  has been done in order to determine the localization of deuterium atoms.

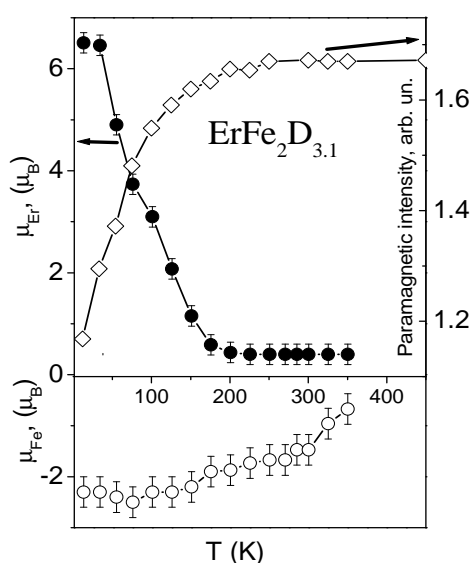


Fig.1 Sublattice magnetization and paramagnetic scattering intensity as a function of temperature for  $\text{ErFe}_2\text{D}_{3.1}$ .

It has been found that at 450 K the cubic crystal structure of  $\text{ErFe}_2\text{H}_{3.1}$  and  $\text{ErFe}_2\text{D}_{3.1}$  compounds is ascribed to the  $F23$  space group, which is a subgroup of the  $Fd3m$  space group commonly applied to the  $\text{ReFe}_2\text{H}_3$ -type hydrides. The deuterium and hydrogen ions partially

occupy two types of the 48h sites, which are centers of  $\text{A}_2\text{B}_2$  interstitials (where  $\text{A} = \text{Er}$ ,  $\text{B} = \text{Fe}$  atoms). At 320 K the structure transition from cubic to monoclinic structure is observed. The Curie temperature  $T_c$  of the hydride and deuteride is considerably lower than that of the parent  $\text{ErFe}_2$  (370 K for  $\text{ErFe}_2\text{H}_{3.1}$  versus 575 K for  $\text{ErFe}_2$ ). We found that  $\text{ErFe}_2\text{H}_{3.1}$  and  $\text{ErFe}_2\text{D}_{3.1}$  are ferrimagnets below the Curie temperature with the magnetic moment of Fe directed opposite to that of Er. Temperature dependences of the sublattice magnetic moments of  $\text{ErFe}_2\text{D}_{3.1}$  compound and intensity of paramagnetic scattering are shown in Fig.1. At 12 K the value of Er magnetic moment is significantly reduced in the  $\text{ErFe}_2\text{D}_{3.1}$  compound ( $6.5 \mu_B$  versus  $9 \mu_B$  in  $\text{ErFe}_2$ ) and drops steadily with increasing temperature. These results indicate that the exchange interactions involving the Er atoms are markedly weakened in the hydrides.

This work is partially supported by UB RAS (project 09-P-2-1021)

[1] Fruchart D., Berthier Y., de Saxce T., Vulliet P.J. *Less-Common Met.* **130**, (1987), 89.

[2] Andreev A.V., Deryagin A.V., Yezov A.A., Mushnikov N.V. *Phys. Metal. Metallogr.* **58(6)**, (1984), 124.

[3] Shreder L.A., Gaviko V.S., Mushnikov N.V., Terent'ev P.B., Solid State Phenom. **152-153**, (2009), 33.

23PO-I-55

## MAGNETIC PROPERTIES OF HIGH-PRESSURE PHASE $\text{Fe}_{1-x}\text{Co}_x\text{Ge}$ (B20)

*Tsvyashchenko A.V.*<sup>1,2</sup>, *Sidorov V.A.*<sup>1</sup>, *Fomicheva L.N.*<sup>1</sup>, *Thompson J.D.*<sup>3</sup>, *Tobash P.H.*<sup>3</sup>,  
*Pokatilov V.S.*<sup>4</sup>

<sup>1</sup> Vereshchagin Institute for High Pressure Physics, RAS, 142190 Troitsk, Russia

<sup>2</sup> Skobeltsyn Institute of Nuclear Physics, Moscow State University,  
Vorob'evy Gory 1/2, 119991 Moscow, Russia

<sup>3</sup> Los Alamos National Laboratory, Los Alamos, NM 87545, USA

<sup>4</sup> Moscow State Institute of Radioengineering, Electronics, and Automation  
(Technical University), pr. Vernadskogo 78, Moscow, 119454 Russia

The samples of  $\text{Fe}_{1-x}\text{Co}_x\text{Ge}$  (B20) for magnetic and electrical resistivity studies were prepared at a constant pressure of 8.0 GPa by the melting of the constituent materials.

From the measurements of the temperature and field dependences of magnetization for the  $\text{Fe}_{(1-x)}\text{Co}_{(x)}\text{Ge}$  compounds, a ferromagnetic behavior up to  $x = 0.8$  and a Pauli paramagnetic behavior for  $x = 0.90, 0.95, 1$  were revealed. Thus, a concentration point of a quantum transition at the cobalt concentration  $x = 0.9$  was found. As seen from the concentration dependences of the Curie temperature  $T_c(x)$  (see Fig.1) and saturation magnetization  $M_s(x)$  (see Fig.2), some modification of the magnetic structure in the region  $x = 0.5$  may take place. The magnetic structure modification is confirmed by Mossbauer measurements.

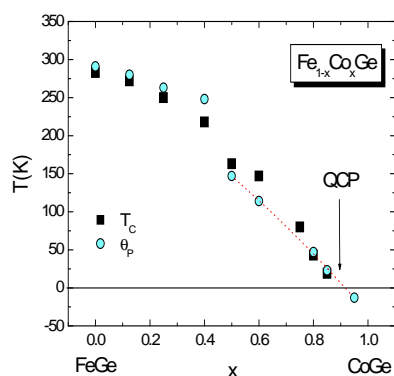


Fig. 1.

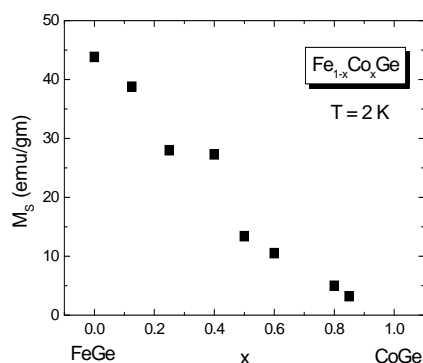


Fig.2.

This work was supported by the Russian Foundation for Basic Research (Grant 11-02-00029).

23PO-I-56

## MAGNETIC PROPERTIES OF HIGH-PRESSURE PHASE $\text{Mn}_{1-x}\text{Co}_x\text{Ge}$ (B20)

*Tsvyashchenko A.V.<sup>1,2</sup>, Sidorov V.A.<sup>1</sup>, Fomicheva L.N.<sup>1</sup>, Krasnorusski V.N.<sup>1</sup>, Sadykov R.A.<sup>1,3</sup>*

<sup>1</sup> Vereshchagin Institute for High Pressure Physics, RAS, 142190 Troitsk, Russia

<sup>2</sup> Skobeltsyn Institute of Nuclear Physics, Moscow State University, Vorob'evy Gory 1/2, 119991 Moscow, Russia

<sup>3</sup> Institute for Nuclear Research, Russian Academy of Sciences, 142190 Troitsk, Russia

The samples of  $\text{Mn}_{1-x}\text{Co}_x\text{Ge}$  (B20) for magnetic and electrical resistivity studies were prepared at a constant pressure of 8.0 GPa by the melting of constituent materials. Fig.1 presents the concentration dependences of the lattice parameter for the series of compounds  $\text{Mn}_{1-x}\text{Co}_x\text{Ge}$  (B20) and  $\text{Fe}_{1-x}\text{Co}_x\text{Ge}$  (B20).

From the measurements of temperature dependences for the  $\text{Mn}_{(1-x)}\text{Co}_x\text{Ge}$  compounds, an antiferromagnetic behavior up to  $x = 0.3$  and a complex ferromagnetic behavior for  $x$  greater than 0.3 but less than 0.9 were revealed. Fig.2 shows a preliminary sketch of the phase diagram.

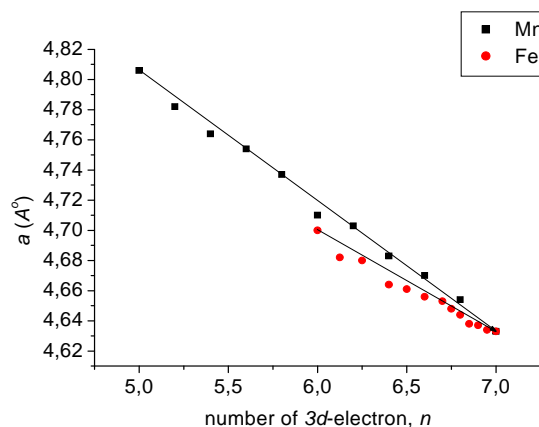


Fig.1.

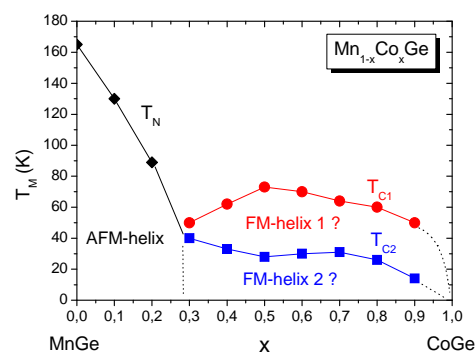


Fig.2.

This work was supported by the Russian Foundation for Basic Research (Grant 11-02-00029).

23PO-I-57

## THE EFFECT OF HYDROGEN ON THE INTERSUBLATTICE INTERACTION IN *R*-Fe INTERMETALLICS

*Tereshina I.*<sup>1,2</sup>, *Doerr M.*<sup>3</sup>, *Skourski Y.*<sup>4</sup>, *Tereshina E.*<sup>5,6</sup>, *Watanabe K.*<sup>5</sup>, *Chistyakov O.*<sup>1</sup>, *Telegina I.*<sup>7</sup>, *Drulis H.*<sup>8</sup>

<sup>1</sup> Baikov Institute of Metallurgy and Materials Science RAS, 119991 Moscow, Russia

<sup>2</sup> International Laboratory of High Magnetic Fields and Low Temperatures, 53-421 Wroclaw, Poland

<sup>3</sup> Technische Universität Dresden, Institut für Festkörperphysik, D-01062 Dresden, Germany

<sup>4</sup> Hochfeld-Magnetlabor Dresden (HLD), Helmholtz-Zentrum Dresden-Rossendorf, 01314 Dresden, Germany

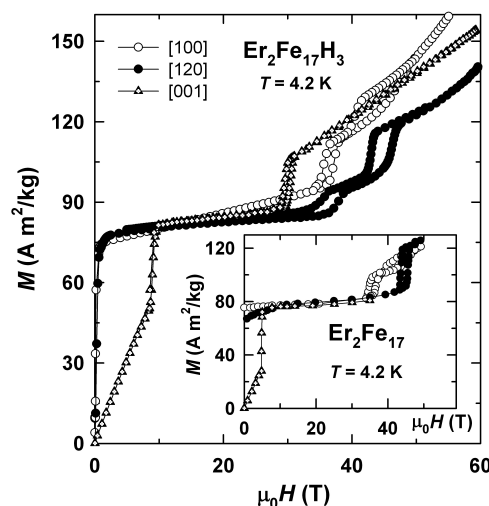
<sup>5</sup> HFLSM, Institute for Materials Research, Tohoku University, 980-8577 Sendai, Japan

<sup>6</sup> Institute of Physics ASCR, 18221 Prague, Czech Republic

<sup>7</sup> Lomonosov Moscow State University, Faculty of Physics, 119991 Moscow, Russia

<sup>8</sup> Institute of Low Temperature and Structure Research PAS, 50-950 Wroclaw, Poland

In *3d-4f* intermetallics, the coupling between the rare earth (*R*) and Fe moments is either parallel for the first half or antiparallel for the second half of the rare earth series. At sufficiently high magnetic fields, the antiparallel coupling can be destroyed, and the field-induced first-order magnetic transitions along the easy magnetization axis provide information on the strength of the intersublattice coupling. For the *R*-Fe intermetallics with a high Fe content, the importance of this fundamental problem is revealed in the number of works dedicated to the study of  $R_2Fe_{17}$  and  $R_2Fe_{14}B$  compounds (see e.g. [1,2]). The present work is aimed at investigation of the high-field magnetization process in the hydrogen-charged  $R_2Fe_{17}H_3$  ( $R = Ho, Er$ ) and  $R_2Fe_{14}BH_{2.5}$  ( $R = Er$ ) single crystals in order to clarify the effect of the interstitial hydrogen on the strength of the intersublattice molecular field (i.e. the field created by the Fe sublattice and acting on the *R* sublattice).



The magnetization data for  $R_2Fe_{17}$ ,  $R_2Fe_{14}B$ , and their hydrides  $R_2Fe_{17}H_3$  and  $R_2Fe_{14}BH_{2.5}$  were measured at 4.2 K in fields up to 14 T applied along the principal axes using a superconducting magnet and a capacitance magnetometer. At 4.2 K, the high-field magnetization study up to 60 T was performed using a pulsed-field magnet with the 20 ms pulse duration. The intersublattice molecular fields were estimated by analyzing the first magnetization jump (i.e. its height and the critical field of the transition) in the curves measured in field applied along the easy magnetization direction [1]. Hydrogenation is found to result in a small decrease (~5-6 %) of the inter-sublattice molecular fields in all the compounds studied.

The work is supported by RFBR, pr. No. 10-03-00848 and by EuroMagNET II under the EU contract 228043. E.A.T. gratefully acknowledges the financial support of JSPS (grant No. P09227 and No. 21-09227).

[1] J.J.M. Franse and R.J. Radwanski, in: K.H.J. Buschow (ed.), *Handbook of Magnetic Materials*, North-Holland, Amsterdam, **7** (1993) 307.

[2] J. F. Herbst, *Rev.Mod.Phys.* **63** (1991) 819.

[3] M.D. Kuzmin, Y. Skourski, K.P. Skokov, K.-H. Müller, *Phys.Rev.B.* **75** (2007) 184439.

## LOCAL ELECTRONIC AND CRYSTALLINE STRUCTURE PECULIARITIES OF MAGNETIC INTERMETALLIC COMPOUND

### $\text{Ce}_2\text{Fe}_{17-x}\text{Mn}_x$ : XAFS DATA ANALYSIS

Yaroslavtsev A.A.<sup>1,2</sup>, Menushenkov A.P.<sup>1</sup>, Grishina O.V.<sup>1</sup>, Chernikov R.V.<sup>1,3</sup>, Kuchin A.G.<sup>4</sup>

<sup>1</sup> National Research Nuclear University "MEPhI", Kashirskoe sh. 31, 115409, Moscow, Russia

<sup>2</sup> NRC "Kurchatov Institute", Akademika Kurchatova pl., 123182, Moscow, Russia

<sup>3</sup> HASYLAB at DESY, Notkestrasse 85, D-22603 Hamburg, Germany

<sup>4</sup> Institute of Metal Physics UB RAS, S. Kovalevskoy 18, 620041, Ekaterinburg, Russia

For the first time the X-ray absorption spectroscopy (EXAFS) above the  $K$ -Ce absorption edge (40443 eV) was applied to investigate the Ce local environment restructuring vs. Mn substitution and temperature in  $\text{Ce}_2\text{Fe}_{17-x}\text{Mn}_x$  intermetallics with the complicated magnetic phase diagram: the basic state is ferromagnetic, but in the range  $x = 0.5-1$  it is helical antiferromagnetic [1]. Under the same conditions the valence state of Ce was studied by XANES spectroscopy above the  $L_3$ -Ce absorption edge (5723 eV). The correlation between local electronic and crystal structure changes and the magnetic properties was found. The XAFS spectra were collected at C beamline of HASYLAB (DESY, Hamburg, Germany) in transmission mode.

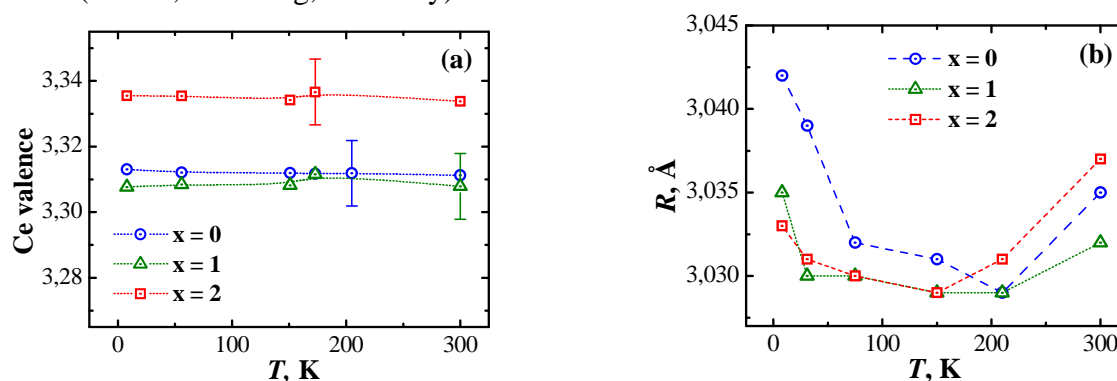


Fig. The temperature dependences of a) Ce valence; b) the radius of first Ce coordination shell with 7 Fe/Mn atoms in  $\text{Ce}_2\text{Fe}_{17-x}\text{Mn}_x$  ( $x = 0, 1, 2$ ) samples

The Ce valence doesn't depend on temperature but depends on Mn concentration (see. Fig.(a)), besides, in ferromagnets  $x = 0, 2$  it appears slightly bigger than in antiferromagnet  $x = 1$ . The 3<sup>rd</sup> coordination shell radius or the Ce-Ce interatomic distance monotonously decreases with the temperature increase and correlates with the temperature dependence of lattice parameter  $c$  [2]. Whereas, temperature dependences of the 1<sup>st</sup> (see Fig.(b)) and the 2<sup>nd</sup> coordination shell radii behave nonmonotonously and qualitatively correlate with the cell volume. Unlike the Ce-Ce distance the 1<sup>st</sup> and the 2<sup>nd</sup> shells are sensitive to the magnetic transformations because they contain only  $3d$  metal atoms, 7 and 12 respectively. The approaching of  $3d$  atoms close to each other induces the rise of negative and the decrease of positive  $3d-3d$  exchange interactions defining the magnetic properties.

This work was partially supported by RFBR (grant No. 11-02-01174-a), FTP "Scientific and scientific-pedagogical staff of innovative Russia" (State Contract No. 16.740.11.0139) and UD RAS (No. 09-P-2-1008).

[1] A.G. Kuchin, A.N. Pirogov, V.I. Khrabrov, et al., *J. Alloys Compds.*, **313** (2000) 7.

[2] O. Prokhnenko, Z. Arnold, A. Kuchin, et al., *J. Appl. Phys.*, **100** (2006) 013903 (9).

23PO-I-59

## NANOHETEROMICROSTRUCTURE AND SOFT MAGNETIC PROPERTIES OF FeSiBCuP NANOCRYSTALLINE ALLOYS WITH ADDITIONS

Lupu N.<sup>1,2</sup>, Makino A.<sup>2</sup>, Kubota T.<sup>2</sup>, Zhang Y.<sup>2</sup>, Zhang Z.Q.<sup>2</sup>, Inoue A.<sup>3</sup>

<sup>1</sup> National Institute of Research and Development for Technical Physics, 700050 Iasi, Romania

<sup>2</sup> Institute for Materials Research, Tohoku University, 980-8577 Sendai, Japan

<sup>3</sup> WPI Research Center, Tohoku University, 980-8577 Sendai, Japan

Nowadays, the energy saving is one of the most important requirements for the most of the power applications. In this regard, the minimization of power losses is one of the key issues for soft magnetic materials used in transformers, inductors and motors, independent of their structural features (i.e. crystalline Fe-Si steels, amorphous or nanocrystalline materials). Up to now, the most reduced power losses for relatively high magnetic induction values are obtained for amorphous and nanocrystalline Fe-based alloy systems [1]. Despite of their lower  $B_s$  compared with Si steels, Fe-based amorphous and nanocrystalline materials present reduced effective magnetocrystalline anisotropy. Normally, an increase of  $B_s$  is achieved when Fe is partially substituted with Co and the amount of early transition metal (Nb, mainly) is reduced [2]. Very recently, it was proved that a Nb-free nanocrystalline Fe-based material show high  $B_s$  up to 1.9 T and excellent magnetic softness [3]. Thus, it would be interesting to know which might be the effect of small additions of Co and/or Ni on the soft magnetic behaviour of Nb-free nanocrystalline Fe-based alloys. This paper presents some of our recent studies in this regard.

The replacement of Fe with small amounts of Co or Ni (1-2 at.%) enhances the nanoheteromicrostructure of  $Fe_{83.3-84.3}Si_4B_8P_{3-4}Cu_{0.7}$  nanocrystalline melt-spun ribbons and refines the  $\alpha$ -(Fe,Co) nanograins. By controlling the nanocrystallization process the soft magnetic (Fe,Co)-based grains can be reduced to 5-15 nm in diameter and their distribution into the residual amorphous matrix is very homogeneous. The nanocrystallized alloys show extremely high saturation magnetic induction of 1.8-2 T depending on the Co or Ni substitution, exhibit low coercive fields below 10 A/m and core losses of 1-3 W/kg at 50 Hz, comparable with the ones of Fe-3.5wt.%Si [3]. Additionally, the relative magnetic permeability reaches values of  $1.8-2 \times 10^4$ , the targets values being obtained after annealing at temperatures between 425 and 475°C, depending on the composition of the substituted alloys. These materials have a great potential for engineering applications, mainly contributing to the energy saving and its transportation.

[1] M. Ohta and Y. Yoshizawa, *J. Phys. D: Appl. Phys.*, **44** (2011) 064004.

[2] K.J. Miller, A. Leary, S.J. Kernion, A. Wise, D.E. Laughlin, M.E. McHenry, V. Keylin, J. Huth, *J. Appl. Phys.*, **107** (2010) 09A316.

[3] A. Makino, H. Men, T. Kubota, K. Yubuta, A. Inoue, *J. Appl. Phys.*, **105** (2009) 07A308.

23PO-I-60

## THE STUDY OF AMORPHOUS MICROWIRES WITH MAGNETO-OPTICAL METHOD

*Nikitin L.V., Zotova O.V.*

Moscow State University, Physical department, Moscow, 119899, Russia.

Magneto-optical spectroscopy has been used successfully for the analysis of amorphous fine crystalline and other inhomogeneous states of the samples. Most efforts are aimed at studies of the magnetization processes in microwire and the distribution of local anisotropy axes.

In this paper we attempt to study amorphous microwires on the basis of alloys of iron and cobalt. The data obtained on amorphous ribbons and films have been used for the analysis of the results.

A method for the study of the dispersion curves of equatorial MOKE at the microwire in a wide range of photon energies of the incident light ( $\hbar\omega = 1 - 5 \text{ eV}$ ) have been developed. On the microwires of various compositions with different geometric parameters the dispersion, angular and field dependence of equatorial MOKE have been investigated. Found that x-ray amorphous microwires based on alloy, according  $\text{Co}_{81.73}\text{B}_{9.26}\text{Si}_{5.91}\text{Mn}_{9.9}$  to the diameter of metal wires may be in the fine-crystalline, amorphous or inhomogeneous state.

In the study of x-ray amorphous microwires on the basis of iron alloys was observed the influence of structure on the conditions of amorphization of microwires metal core. In the angular dependence of the equatorial MOKE, the phenomenon of magneto optical interference was found.

Using a geometric model of the light was analyzed the influence of various geometrical parameters of the microwire and optical properties of glass on the nature of the interference. Comparison of these experimental results with theoretical calculations revealed changes in the optical properties of microwires glass cover. In the microwires based on a high iron content alloy in the metal-glass border a transition layer whose optical properties differ from those of metal wires and glass coating was detected. It is shown that such a transition layer changes the nature of magneto-optical interference during the transition into the ultraviolet spectrum.

23PO-I-61

## PHYSICAL AND MAGNETIC PROPERTIES OF $\text{Sm}_{0.2}\text{Gd}_{0.8}\text{Ni}_4\text{B}$ COMPOUND

*Özçelik B.<sup>1</sup>, Kantarci N.<sup>1</sup>, Nane O.<sup>1,2</sup>, Yakinci M.E.<sup>3</sup>*

<sup>1</sup> Department of Physics, Faculty of Sciences and Letters, Cukurova University 01330, Adana, Turkey

<sup>2</sup> The Faculty of Engineering, Hakkari University, Turkey

<sup>3</sup> Department of Physics, Faculty of Sciences and Letters, İnönü University 44069, Malatya, Turkey

Physical properties of the  $\text{Sm}_{0.2}\text{Gd}_{0.8}\text{Ni}_4\text{B}$  compound have been investigated by means of the X-ray powder diffraction, DC and AC susceptibility techniques. The compound studied crystallizes in  $\text{CeCo}_4\text{B}$  type structure with  $P6/mmm$  space group. The unit-cell parameters  $a$  and  $c$  are determined as 5.01 and 6.95 Å, respectively, and the unit-cell volume  $V$  is calculated as 151.08 Å<sup>3</sup>. All these parameters are in good agreement with previously reported values in the literature [1]. DC and AC magnetic measurements present the visible magnetic phase transition from paramagnetic to ferromagnetic, around definite transition temperature. The magnetic phase transition temperature of

the compound is obtained from DC magnetization, AC susceptibility and the well known Kouvel-Fisher method [2] as 36.6, 35.74 and 35.2 K, respectively. The saturation magnetization ( $M_s$ ) and the coercive fields ( $H_c$ ) of the compound are found to be  $3.7\mu_B/\text{f.u}$  and 277 Oe, respectively, by using the hysteresis loops at 9.5 K. We have also investigated the non-linear AC susceptibility of the compound, around its ferromagnetic transition temperature, as a function of temperature, frequency and amplitude of the AC driving field. In order to explain the measured experimental results, we have used the theory developed for ferromagnetic, based upon the mean field model [3]. The measurements exhibit both frequency and amplitude dependencies. Observed dependencies are compared with the existing theories of linear and nonlinear susceptibilities with reference to short- and long-range interactions. In Kouvel-Fisher method [2], one plots  $1/\chi_I^*(d\chi^{-1}/dT)$  against  $T$ , obtaining a straight line. The slope of this line gives the critical exponent  $\gamma$ , and it intersects the  $T$  axis at  $T_c$ . In order to obtain  $d\chi^{-1}/dT$  and the best straight line, we used a two-point numerical differentiation program and linear regression method, respectively. The critical exponent  $\gamma$  of the sample is calculated to be  $2.78 \pm 0.05$ .

This work was supported by the Research Fund of Cukurova University, Adana, Turkey, under grant contracts no. FEF2008YL30.

- [1] N.M Hong, T. Holubar, G. Hilscher, IEEE Trans. Magn. 30, No:6 (1994) 4966.
- [2] Kouvel J S and Fisher M E 1964 Phys. Rev. 136 A1626
- [3] Ozcelik B, Kiymac, K, J. Phys.: Condens. Matter 6 (1994) 8309–21.



**23 August**

Tuesday

17:30-19:00

poster session  
23PO-J

**“Theory”**

23PO-J-1

## THEORY OF NANODIAMOND TAMM STATES

*Belobrov P.I., Denisov I.A.*

Siberian Federal University, MOLPIT, Institute of Biophysics SB RAS, Krasnoyarsk, Russia

In the first time I.E. Tamm has introduced three collective phenomena. In 1925 he shown urgent role of orbital moment in quantum theory of paramagnetism [1]. In 1930 he introduced the concept of vibrational quanta in solid [2] later called phonons by Ya.I. Frenkel. In 1932 "Tamm levels" - certain electron states were due to the existence of the surface calculated by him [3]. Nature of free spin at the thermodynamically stable diamond ball  $\sim 5$  nm (nanodiamond) is explained his idea that "any system with virtual separated charges should have magnetic moment". There is proof here of self-consisted model of nanodiamond free spin coexists with electronic-vibrational Tamm surface state.

For the evidence we used Fermi 3D-brane surface and some special boundary conditions for satisfy the Bloch's theorem by self-consisting of the Abrikosov's quasi particle and antiparticle pairs. These "antiparticles" are completely analogous to the antiparticles of elementary particle theory, e.g., positrons. The widely used name "hole" is a misleading one, since that term is commonly used to describe a different object, i.e., a vacant state in an unfilled band [4].

The ground state at  $T \neq 0$ , as well as any excited state, are constructed from the  $T = 0$  equilibrium state by transferring particles from inside to outside the Fermi sphere. In each transfer a particle appears outside the Fermi sphere while an empty state or an "antiparticle" is created inside. These particles and antiparticles are the quasi particles describing excited states of nanodiamond. Their energies must be measured from the Fermi level  $\mu(0)$  that lies in the middle of band gap. Particle-like quasi particles with momenta between  $p_m \sim 1/3.6 \text{ \AA}^{-1}$  and  $p_0 \sim 1/50 \text{ \AA}^{-1}$  have an energy  $\xi_p(p)$ .  $v = p_m/m$  being the velocity on the Fermi sphere (exterior of 3D-brane). Antiparticles, on the other hand, have momenta below  $p_0$ , and their energies  $\xi_a(p)$  are measured in the opposite direction [4]. Interior of Fermi 3D-brane in reciprocal space has graphane-like structure [5] in real structure of nanodiamond surface.

Following Abrikosov's approach [4] we together with a few suppose took into account two limit cases. (1) The tight-binding approximation. This model is never applicable in practice to valence electrons, but electrons into the distorted core/shells of nanodiamond can be treated this way. (2) The nearly-free electron approximation. This model does not provide a correct description of valence electrons either, but can be sometimes justified for free collective Tamm's electron in nanodiamond.

The preliminary comparison of our model with existed experimental data allows to call the quasiparticles as tammon and antitammon.

Support by RFBR (# 09-08-98002-p\_sibir\_a), MES RF (# 2.2.2.2/5309), and U.S. CRDF (# RUX0-002-KR-06/BP4M02) is acknowledged.

[1] Ig. Tamm. Zur Quantentheorie des Paramagnetismus. *Z. Phys.* **32** (1), 582-595 (1925).

[2] Ig. Tamm. Über die Quantentheorie der molekularen Lichtstreuung in festen Körpern. *Z. Phys.* **60** (5-6), 345-363 (1930).

[3] Ig. Tamm. Über eine mögliche Art der Elektronenbindung an Kristalloberflächen *Z. Phys.* **76** (11-12), 849 -850 (1932).

[4] A.A. Abrikosov. Introduction to the theory of normal metals. Acad. Press, 1972. 293 p.

[5] D.C. Elias *et al.*, Graphene's Properties by Reversible Hydrogenation: Evidence for Graphane. *Science*, **323**, 610-613 (2009).

23PO-J-2

## ANALOGY BETWEEN BENDING OF COMPOUND ELASTIC ROD AND MAGNETIZATION OF MULTILAYER MAGNETIC SYSTEM

*Zakharov Yu.<sup>1</sup>, Vlasov A.<sup>2</sup>, Avakumov R.<sup>1</sup>*

<sup>1</sup> Siberian state technological university, 660049 Krasnoyarsk, Mira av. 82, Russia

<sup>2</sup> Siberian state aerospace university, 660014 Krasnoyarsk, Krasnoyarsky rabochy av. 31, Russia

In present paper we draw an analogy between two physical problems. The first one is problem of bending of two-parts elastic rod with inelastic connection between parts. Second problem is problem of magnetization of multilayer thin magnetic film. The film consists of two soft magnetic layers separated by nonmagnetic spacer. This magnetic system applied to stiff magnetic substrate. The parallel between two problems takes place because both of physical processes may be described by differential equation of nonlinear pendulum [1, 2].

The analogy between bilayer system with the ferromagnetic-on-antiferromagnetic-substrate type and elastic rod was drawn in paper [3]. In present paper we research behavior of compound elastic and magnetic systems with different connections between parts. Also, we investigate how non-magnetic spacer influence on threshold fields in multilayer magnetic system. We found out that two thresholds appeared in such system by appointed ratio of physical characteristics of nonmagnetic interlayer and soft magnetic layers. It takes place because of rivalry between exchange interaction between soft magnetic layer and stiff magnetic substrate and interaction between soft magnetic layers via nonmagnetic interlayer.

A computer model we construct has shown that following process takes place. At first, upper layer lose stability and its magnetization tend to orientate along applied field when it reaches first threshold value. Than lower layer lose stability because transverse component of magnetization does appear in upper layer. When magnetization of upper layer reaches saturation magnetization of lower layer orientates against applied field. Than applied field span follows when no magnetization process takes place. Finally, lower layer loses stability and reaches saturation when applied field reaches second threshold value.

The same situation takes place in elastic system consisting of two rods with inelastic connection. Bending deformation directs antiparallel to external force. This fact gives ability to educe new results for magnetic systems.

[1] A. Aharoni, E.H. Frei and S. Shtrikman, *J. Appl. Phys.*, **30** (1959) 1956-1961.

[2] Yu.V. Zakharov, K.G. Okhotkin, *J. Appl. Mech. Tech. Phys.*, **43** (2002) 739-744.

[3] Yu.V. Zakharov, *PhysicsDoklady*, **40** (1995) 464-468.

23PO-J-3

## SPIN-WAVES IN STONER FERROMAGNETIC PHASE OF A TWO-DIMENSIONAL ELECTRON SYSTEM

*Esmailian A.H.<sup>1</sup>, Kanjouri F.<sup>2</sup>, Mohammadi N.<sup>1</sup>, Mahloojian M.R.<sup>1</sup>, Abbasi N.<sup>1</sup>*

<sup>1</sup>Department of Physics, Qom Branch, Islamic Azad University, Qom, Iran

<sup>2</sup>Physics Department, Tarbiat Moallem University, Tehran, Iran

We have studied the collective excitations (spin-wave energies) in the ferromagnetic ground state of a two – dimensional (2D) electron system using the random phase approximation (RPA). To do so, we have calculated the magnetic transverse susceptibility in 2D electron system by Hartree – Fock (HF) approximation of Hubbard model at T=0 which is generally referred to as the Stoner model[1]. We have also obtained the intensity of the Stoner excitations with the wave –vector transfer  $q$  and the energy  $\hbar\omega$  for 2D electron system. The spin-waves dispersion of three – dimensional (3D) electron system due to its quadratic behavior starts from zero at  $q \rightarrow 0$ [2-4] while our numerical results show that the spin-waves dispersion of 2D electron system starts from the value  $\Delta$ , known as exchange splitting energy, even at  $q=0$ .

[1] E. C. Stoner, *Proc. R. Soc. London A.*, **165** (1938) 372.

[2] R. M. White, *Quantum Theory of Magnetism*, Springer Ser. Solid-State Sci., vol. 32 (Springer, Berlin, Heidelberg 2006).

[3] J. F. Cooke, J. A. Blackman, and T. Margan, *Phys. Rev. Lett.*, **54** (1985) 718.

[4] T. Izuyama, E. J. Kim, and R. Kubo, *J. Phys. Soc. Japan.*, **18** (1963) 1025.

23PO-J-4

## ELECTRON TRANSPORT THROUGH MAGNETIC MOLECULE: CORRELATION EFFECTS

*Kudasov Yu.B.<sup>1,2</sup>, Maslov D.A.<sup>1,2</sup>*

<sup>1</sup> Russian Federal Nuclear Center - VNIIEF, pr. Mira 37, 607188, Russia

<sup>2</sup> Sarov Physics and Technology Institute, National Research Nuclear University “MEPhI”, Dukhov str. 6, Sarov, 607188, Russia

Enormous experimental and theoretical efforts were applied to the investigation and controlling of quantum electron transport at the molecular scale during last decades. Single molecules, self-assembled monolayers, chains of metal atoms and other systems have been investigated. One of the most interesting phenomenon observed is the negative differential resistance (NDR) effect. In particular, nitro-substituted molecule consisting of three benzene rings demonstrates NDR effect up to room temperature [1]. That makes it possible to develop molecular electronic devices based on bistable cell [2].

If the molecule is attached to metal contacts with a wide flat electronic bands, like gold nanoparticles, mechanism of the NDR is different from semiconductor resonance-tunneling diodes. That is why, few novel theoretical models were proposed to elucidate the nature of the NDR: coupling of electrons to vibrons, recharging of the molecule and others.

Since a molecular wire is weakly bound to leads as compared to an interatomic bond in solids the relative strength of intramolecule Coulomb interactions drastically increases. That is why, the

strong correlations play an important role in the electron transport through the molecular wires and drastically change the transport properties [3].

We present a new technique for theoretical investigation of the steady nonequilibrium transport through a magnetic molecule and discuss the correlation mechanism of the NDR in molecular systems that was proposed earlier phenomenologically [4]. It is demonstrated by an example of a magnetic molecule attached to two leads

$$H = \sum_{\sigma=\uparrow,\downarrow} \varepsilon_{\sigma} n_{\sigma} + U n_{\uparrow} n_{\downarrow} + \sum_{\alpha k \sigma} \varepsilon_{\alpha k} n_{\alpha k \sigma} + \sum_{\alpha k \sigma} (V_{\alpha k \sigma} c_{\alpha k \sigma}^{\dagger} d_{\sigma} + \text{H.c.}),$$

where  $\alpha = R, L$  denotes the left and right leads,  $\mathbf{k}$  is the wave vector.

A closed system of equations of motion for Green functions is obtained. It contains equations for spectral functions to define a nonequilibrium distribution on the molecule. It is shown that a population of the molecular levels approximately obeys to pseudoequilibrium distribution [5]. Current through the molecule is computed in the framework of Landauer formalism.

According to suggested model the NDR can be observed when one of the levels is localized and the other is strongly coupled to the leads. Asymmetric coupling of the localized level reinforces the effect. The total spin of the molecule depends on the applied voltage.

Support by Russian Foundation for Basic Research (#10-02-00530-a) and Russian Federal Education Agency (AVCP#2.1.1/7216) is acknowledged.

- [1] J. Chen, W. Wang et al., *Phys. Rev. Lett.*, **77** (2000) 1224.
- [2] M.A. Reed, J. Chen et al., *Appl. Phys. Lett.*, **78** (2001) 3735.
- [3] P. Delaney, J.C. Greer, *Phys. Rev. Lett.*, **93** (2004) 036805.
- [4] Yu.B. Kudasov, *Bull. Rus. Acad. Sci.: Phys.*, **72** (2008) 172.
- [5] A.-P. Jauho, N.S. Wingreen, Y. Meir, *Phys. Rev. B*, **50** (1994) 5528

23PO-J-5

## INDUCING MAGNETISM IN GRAPHENE NANOMESH

*Yang H.<sup>1</sup>, Chshiev M.<sup>1</sup>, Waintal X.<sup>2</sup>, Roche S.<sup>3,4</sup>*

<sup>1</sup> SPINTEC, UMR-8191, CEA/CNRS/UJF-Grenoble 1, 38054 Grenoble, France

<sup>2</sup> SPSMS-INAC-CEA, 17 rue des Martyrs, 38054 Grenoble, France

<sup>3</sup> CIN2 (ICN-CSIC) and Universitat Autònoma de Barcelona, 08193 Barcelona, Spain

<sup>4</sup> ICREA, Instituci Catalana de Recerca i Estudis Avancats, 08010 Barcelona, Spain

Corresponding author: mair.chshiev@cea.fr

Recent reports on possibility of inducing localized spin polarization and magnetic moments at one-dimensional zigzag edges in graphene nanoribbons [1] open the way to novel concepts of building nanoscale spintronic devices [2]. On another hand, recent reports on possibility of experimental fabrication of graphene nanomesh (GNM) gave rise to possibility of introducing of large scale patterned defects into graphene [3].

Using first-principles calculations, we explore the electronic and magnetic properties of graphene nanomesh, a regular network of large vacancies in graphene, produced either by lithography or nanoimprint. When removing an equal number of A and B sites of the graphene bipartite lattice, the zigzag (armchair)-like edge type nanomesh exhibits antiferromagnetic (paramagnetic) ground state. In contrast, in situation of sublattice symmetry breaking, stable ferrimagnetic states are obtained [4]. For hydrogen-passivated nanomesh [insets in Fig. 1], the ground state is found strongly depending

on the vacancy shape and size. As shown in Fig. 1, the obtained net magnetic moments increase with the number difference between A and B sublattices ( $\Delta_{AB}$ ) in good agreement with Lieb's theorem [5]. However, such induced moments are found to be larger for zigzag-rich edge nanomesh, a result beyond the Lieb's theorem predictions. Our findings indicate that using highly asymmetric vacancies stabilize ferrimagnetic ground states with very high exchange splitting values ( $\sim 0.5$  eV) making GNM a promising candidate material for room temperature carbon based spintronics [4].

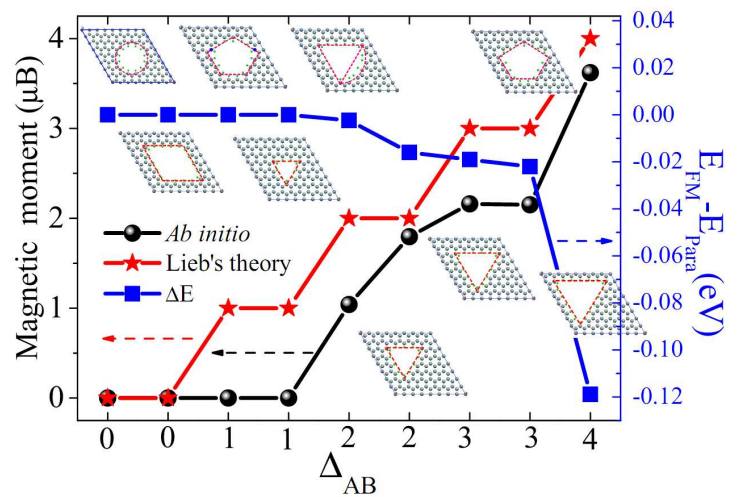


**Figure 1:** *Ab initio* calculated and Lieb's theorem predicted Magnetic moment and energy difference between ferrimagnetic and paramagnetic states as a function of number difference of A and B sites for various GNMs.

This work is supported by Chair of Excellence Program of the Nanosciences Foundation in Grenoble, France, by the ANR NANOSIM-GRAPHENE and EU CONCEPT-GRAPHENE.

- [1] Y.-W. Son et al, Nature, **444** (2006) 347; O. Yazyev et al, Phys. Rev. Lett., **100** (2008) 047209.
- [2] A. Fert et al, *Mat. Sci. Eng. B*, **84** (2001) 1; S. A. Wolf et al, Science, **294** (2001) 1488.
- [3] J. Bai et al, Nature Nanotechnology, **5** (2010) 190.
- [4] H. X. Yang et al, arXiv:1103.4188
- [5] E. H. Lieb, *Phys. Rev. Lett.* **62**, 1201 (1989).

23P-J-6

## THE PHASE TRANSITIONS OF THE DILUTED SPIN -1 ISING MODEL WITH RANDOM INTERACTIONS ON A BODY CENTERED CUBIC CRYSTAL

*Ghazale J.J., Saber F.S.*

Physics Department, University of Guilan, Rasht, Iran

The Ising model has been used successfully to investigate a numbers of physical phenomena in different fields of physics, such as phase transitions associated with order–disorder in several systems.

The Ising model is one of the most activity studied systems in statistical mechanics and takes into account the crystal field, the transverse and the longitudinal field. In this work the magnetization, quadrupolar moments, phase diagrams of the diluted transverse Spin-1 Ising Model with random interaction are investigated on the simple cubic lattice in the effective field theory within the framework of a single site cluster theory including using a probability distribution method that adopted the nearest neighbors exchange coupling with probability distribution law based on the use of generalized Van Der Warden identities. The critical temperature at which the longitude magnetization vanishes is studied as a function of concentration (p) and transverse field.

If  $P$  is larger than critical value  $P_c$  then the transverse field may cause a phase transition from order to the disorder phase. Also, the effects of transverse and longitude magnetic fields on the thermal and magnetic properties of the spin system are investigated. A number of interesting phenomena such as reentrant phenomena, two critical lines have been found.

It is especially found when  $P$  increases upper than 0.4 the reentrant phenomena disappeared and two ferromagnetic areas appeared by two critical lines.

- [1] J.W. Tucker, M. Saber, L. Peliti. *J.Physica A.*, **206** (1994) 497.  
 [2] T. Bouziane, M. Saber, *J.Magn. Magn. Mater.*, **321** (2008) 17.  
 [3] Y.Q. Liang, G.Z. Wei, *J.Magn. Magn. Mater.*, **320** (2008) 1680.

23PO-J-7

## NON-EQUILIBRIUM CRITICAL RELAXATION OF HEISENBERG FERROMAGNETS WITH LONG-RANGE CORRELATED DEFECTS

*Medvedeva M., Prudnikov P.*  
 Omsk State University, Mira 55A, Russia

In this paper one present a numerical study of the influence of structural long-range (LR) correlated defects on the non-equilibrium critical behavior of complex systems described by the Heisenberg model, with Hamiltonian  $H = -J \sum_{i,j} p_i p_j \vec{S}_i \vec{S}_j$ . A special type of such a disorder has been considered at first by Weinrib and Halperin [1]. They showed that the disorder with power law correlation  $g(x) \sim x^{-a}$  for large separations  $x$  is relevant  $a < d$ . As a result, the existence of LR correlations in the disorder gives significant effect and wider class of disordered systems can be characterized by a new universality class of critical behavior. The power law decay for the impurity-impurity pair correlation function  $g(x)$  allows a direct geometrical interpretation. So, for integer  $a$  it corresponds to the lines (at  $a = d-1$ ) or the planes (at  $a = d-2$ ) of impurities of random orientation. In this paper the case  $a = 2$  corresponding to linear defects were considered. We used the following method for creating impurity configurations: the lines parallel to the coordinate axes were deleted randomly from a filled three-dimensional lattice spins in order to acquire a given concentration of impurities. Therefore, the models with LR-correlated quenched defects have both theoretical interest due to the possibility of predicting new types of critical behavior in disordered systems and experimental interest due to the possibility of realizing LR-correlated defects in the  $^4\text{He}$  in aerogels [2], polymers, and disordered solids containing fractal-like defects or dislocations near the sample surface [3].

We have used a short-time dynamics (STD) approach to obtain the values of dynamic and static critical exponents. The completely ordered state has been chosen as the initial configuration. In this case, the initial state corresponds to  $T = 0$  (when all the spins are oriented in one direction). Scaling analysis for STD shows that, for an ordered initial state quenched to  $T_C$ , the order parameter behaves as  $M(t) \sim t^{-\beta/z\nu}$  and  $\partial_\tau \ln M \sim t^{1/z\nu}$ . In addition, a cumulant  $F_2$  can be defined, which behaves as  $F_2(t) \sim t^{d/z}$  and these power law relations enable us to determine all the critical exponents. We have used cubic lattice of linear size  $L=128$  at the critical temperature  $T_C = 1.197(2)$  to carried out simulation. The total spin concentration in the system was chosen to be  $p = 0.80$ .

The influence of a leading correction to the scaling on asymptotic values of exponents were considered to obtain accurate values of the critical exponents. We have found dynamic and static critical exponents  $z = 2.245(59)$ ,  $\nu = 0.757(26)$ ,  $\beta = 0.388(15)$  and exponent of scaling correction

$\omega = 0.786(46)$ . The obtained value of the dynamic critical exponent is in good agreement with results of the theoretical work of  $z = 2.2644$  [4].

This work was supported in part by Ministry of Education and Science of Russia through project 02.740.11.0541, by the RFBR through Grants 10-02-00507 and 10-02-00787 and by Grant MK-3815.2010.2 of Russian Federation President. Our simulations were carried out on the SKIF-MSU in the Moscow State University.

- [1] A. Weinrib, B.I. Halperin, *Phys. Rev. B.*, **27** (1983) 413.  
 [2] C. Vasquez R., R. Paredes V., A. Hasmy, R. Jullien, *Phys. Rev. Lett.*, **90** (2003) 170602.  
 [3] M. Altarelli, M. D. Nunez-Regueiro, M. Papoular, *Phys. Rev. Lett.*, **74** (1995) 3840.  
 [4] V.V. Prudnikov, P.V. Prudnikov, A.A. Fedorenko, *Phys. Rev. B.*, **62** (2000) 8777.

23PO-J-8

## NON-EQUILIBRIUM CRITICAL DYNAMICS OF FERROMAGNETS WITH LONG RANGE CORRELATED DEFECTS

*Kulikov D.<sup>1</sup>, Prudnikov P.<sup>1</sup>*

<sup>1</sup> Omsk State University, Mira prospekt 55-A, Omsk, 644077, Russia

The renormalization group analysis in [1] shows that if the initial state of a ferromagnetic system is characterized by a sufficiently high degree of the chaotization of spin variables with the relative magnetization far from the saturation state ( $m_0 \ll 1$ ), the process of the relaxation of the system from a given initial non-equilibrium state at the critical point at macroscopically small times is accompanied not by a decrease, but an increase in magnetization with time according to a power law with the exponent characterized by a independent dynamical critical exponent  $\theta'$ :

$$m(t) \sim t^{\theta'}$$

To describe the critical behaviour of structurally disordered Ising systems in the equilibrium state, we use the Ginzburg–Landau–Wilson Hamiltonian. In this work, to describe the effect of complex extended defects on the critical behaviour of system we investigate the Weinrib–Halperin model with the long range isotropic correlation between defects:

$$g(x-y) \sim |x-y|^{-a},$$

where  $a$  is the correlation parameter of structural defects.

**Table.** Results of the calculations of the dynamical critical exponent  $\theta'$  using the Padé–Borel (PB) and Padé–Borel–Leroy (PBL) summation method, as well as the self similar approximation (SSA) for various values of the correlation parameter  $a$  in comparison with the results of the computer simulation (CS)

$a$	PBL	PB	SSA	Total	CS
3.00	0.1482	0.1174	0.1207	0.129(10)	0.127(16) [2]
2.80	0.1513	0.1160	0.1201	0.129(11)	
2.60	0.1550	0.1164	0.1212	0.131(12)	
2.40	0.1588	0.1174	0.1229	0.133(13)	
2.20	0.1624	0.1189	0.1248	0.135(14)	
2.00	0.1654	0.1206	0.1269	0.138(14)	0.149(11) [3]

We obtained series for  $\theta'$  in two loop approximation directly for  $d = 3$ . Using summation methods, we calculated the critical exponent  $\theta'$  of the non-equilibrium evolution of the system as a function of the parameter  $a$  (see Table). The comparison of the  $\theta'$  exponent values presented in Table with the



computer simulation of the Ising model for the uncorrelated structural defects ( $a = 3.0$ ) and for uniformly distributed linear defects ( $a = 2.0$ ) indicates good agreement within the statistical error already in the two loop approximation.

This work was supported in part by Ministry of Education and Science of Russia through project 02.740.11.0541, by the RFBR through Grants 10-02-00507 and 10-02-00787 and by Grant MK-3815.2010.2 of Russian Federation President.

[1] H.K. Janssen, B. Schaub, B. Schmittmann, *Z. Phys. B.*, **73** (1989) 539.

[2] V.V. Prudnikov, P.V. Prudnikov, I.A. Kalashnikov, et al. *JETP*, **110** (2010) 253.

[3] V.V. Prudnikov, P.V. Prudnikov, B. Zheng et al., *Prog. Theor. Phys.*, **117** (2007) 973.

23PO-J-9

## FIELD-THEORY DESCRIPTION OF THE NONEQUILIBRIUM CRITICAL DYNAMICS OF SPIN SYSTEMS

*Kalashnikov I., Prudnikov P.*

Omsk State University, pr. Mira, 55a, Omsk, 644047 Russia

Field-theoretic renormalization group approach is applied to investigate the short-time nonequilibrium critical behavior of pure and diluted spin systems with nonmagnetic impurities in 3-loop approximation.

Short-time critical relaxation of systems with initial small macroscopic magnetization  $m_0 = m(0) \ll 1$  leads to universal short-time scaling behavior for order parameter  $m(t)$  and order parameter correlations. The scaling behavior of these quantities is characterized by initial slip exponents  $\theta$  and  $\theta'$ . Exponent  $\theta$  describes the two-time power dependence for order parameter correlation functions and  $\theta'$  is responsible for short-time growth of order parameter. At the first time, the calculation of these dynamic critical exponents of the short-time evolution is carried out at fixed dimension  $d=3$  for pure and diluted spin systems without the use of  $\epsilon$ -expansion.

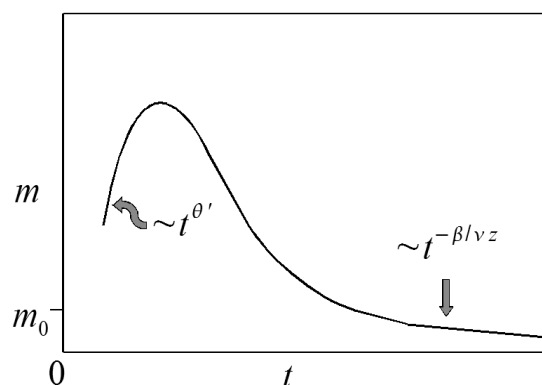
To describe the critical behavior of spin systems in the equilibrium state, the Landau-Ginzburg model Hamiltonian is used:

$$H_{GL}[s] = \int d^d x \left\{ \sum_{\alpha=1}^n \frac{1}{2!} \left[ (\nabla s_{\alpha}(\mathbf{x}))^2 + \tau s_{\alpha}^2(\mathbf{x}) + V(\mathbf{x}) s_{\alpha}^2(\mathbf{x}) \right] + \frac{g}{4!} \left( \sum_{\alpha=1}^n s_{\alpha}^2(\mathbf{x}) \right)^2 \right\},$$

where  $s(\mathbf{x})$  is the order parameter field,  $\tau$  is reduced temperature,  $g$  is coupling constant,  $V(\mathbf{x})$  is a random potential of nonmagnetic impurities with distribution characterized by moments

$$\langle\langle V(\mathbf{x}) \rangle\rangle = 0; \quad \langle\langle V(\mathbf{x})V(\mathbf{y}) \rangle\rangle = v\delta(\mathbf{x}-\mathbf{y}).$$

Pure system is a special case of this model with  $v = 0$ . Initial influence  $s(\mathbf{x}, 0) = s_0(\mathbf{x})$  on critical evolution can be prepared using distribution  $P[s_0] \sim \exp(-H_0[s_0])$ , where



Order parameter short-time growth for non-equilibrium critical relaxation

$$H_0[s_0] = \int d^d x \left( \frac{\tau_0}{2} [s_0(\mathbf{x}) - m_0(\mathbf{x})]^2 \right).$$

We investigate dissipative relaxation dynamics of non-conserved order parameter which is known as Model A in classification of Halperin-Hohenberg.

Renormalization group (RG) approach was realized to calculate exponents  $\theta$  and  $\theta'$  in 3-loop approximation. We performed RG and diagrams calculations at fixed dimension  $d = 3$ . The obtained series expansions for RG functions and exponents were resummed with the use of special methods for the summation of asymptotic series. The values of exponents were compared with results  $\varepsilon$ -expansion application and with results of Monte Carlo simulations of spin systems in the short-time regime.

This work was supported in part by the RFBR through Grants 10-02-00507 and 10-02-00787 and by Grant MK-3815.2010.2 of Russian Federation President.

23PO-J-10

## INVESTIGATION OF THE AGEING PHENOMENA IN TWO-DIMENSIONAL XY-MODEL

*Alekseyev S., Prudnikov V., Prudnikov P.*  
Omsk State University, pr. Mira 55a, Russia

The slow dynamics of the two-dimensional XY model has been widely studied both numerically and theoretically. In nonequilibrium dynamics temporal correlations do not show time translational invariance. In the so-called ageing regime the correlation function  $C(t, t_w)$  of any observable is a two-time function depending on both a waiting time  $t_w$  and  $t$ , the total time. In this paper we numerically investigated ageing phenomena in two-dimensional XY-model at the low temperatures through measurement of autocorrelation function  $A(t, t_w)$  by means Monte-Carlo methods starting from the ordered state for waiting times  $t_w=100, 500, 1000$  MCs/s.

Two-time dependence of autocorrelation function for  $T \leq T_{KT}$  can be defined in the following scaling form [1]:

$$A(t, t_w) = \frac{1}{(t - t_w)^{\eta(T)/2}} \left[ \frac{(1 + \lambda)^2}{4\lambda} \right]^{\eta(T)/4}$$

for times  $t - t_w \gg a^2$ , where  $a$  is a ultraviolet cutoff,  $\lambda \equiv t/t_w$ ,  $\eta(T)$  - critical exponent. For times  $t - t_w \ll t_w$  autocorrelation function as following:

$$A(t, t_w) \sim \frac{1}{(t - t_w)^{\eta(T)/2}}.$$

This is the quasi-equilibrium regime. The dynamic functions decay at long time separations  $t - t_w \gg t_w$  as power laws:

$$A(t, t_w) \sim \frac{1}{t^{\eta(T)/4}}.$$

The crossover between the two regimes takes place at time  $t - t_w \sim t_w$ . Spin-spin correlation function can be written in the following form:

$$C(x - x') \sim (x - x')^{-\eta(T)}.$$

We have obtained critical exponent  $\eta(T)$  from the following form:

$$\langle m^2(T, L) \rangle \sim L^{-\eta(T)}$$

**Table.** Exponents for spatial correlation function and autocorrelation function, obtained for different temperatures  $T$ , waiting times  $t_w$  and asymptotic time intervals

T/J	$\eta(T)$	$t_w=100$		$t_w=500$		$t_w=1000$	
		[0;60]	[1000;10000]	[0;60]	[1000;10000]	[0;100]	[10000;20000]
0,1	0,0161(6)	0,0093(2)	0,0045(1)	0,0097(1)	0,0044(1)	0,0096(2)	0,0048(1)
0,2	0,0334(5)	0,0185(4)	0,0091(1)	0,0197(3)	0,0093(1)	0,0190(3)	0,0093(1)
0,4	0,0716(6)	0,0379(8)	0,0193(1)	0,0400(6)	0,0203(1)	0,0389(5)	0,0206(1)
0,6	0,1161(10)	0,0603(10)	0,0313(1)	0,0635(9)	0,0322(1)	0,0620(6)	0,0356(1)
0,8	0,1805(10)	0,0903(12)	0,0477(8)	0,0948(12)	0,0483(1)	0,0931(8)	0,0534(1)
0,89	0,2315(42)	0,1112(15)	0,0623(9)	0,1176(40)	0,0649(2)	0,1164(9)	0,0597(2)

This work was supported by Ministry of Education and Science of Russia through project 02.740.11.0541 and by the RFBR through Grant 10-02-00507. Simulations were carried out on the SKIF-MSU in the Moscow State University.

[1] L. Berthier, P.C.W. Holdsworth, M.J. Sellitto *Phys. A.* **34** (2001) 1805.

23PO-J-11

## DESCRIPTION OF SUBSTITUTIONAL ADSORPTION OF MAGNETIC IONS ON METALLIC SURFACES WITH FORMATION OF MONOLAYER FERROMAGNETIC FILMS USING THE SPIN-DENSITY FUNCTIONAL METHOD

*Klimov S., Mamonova M., Prudnikov V.*

Omsk State University, pr. Mira, 55a, Omsk, 644047 Russia

At present time, a large number of experimental works have been devoted to the study of magnetic ordering in Fe, Co, and Ni ultrathin films [1, 2]. It has been established that the long-range ferromagnetic order arises in films at some effective film thickness. However, the nature and regularities of this phenomenon remain not quite clear.

In paper [3] it was developed in terms of the spin-density functional theory the description of influence of the temperature and ferromagnetic ordering on the adsorption of Fe, Co, and Ni transition metal ions on a nonmagnetic substrate with the formation of a submonolayer films. For case of nonactivated adsorption the conditions for the formation of magnetic monoatomic films stable with respect to island adsorption with a change in the coverage parameter  $\Theta$  are revealed. It was demonstrated that the inclusion of the ferromagnetic ordering substantially affects the adsorption energy and leads to its considerable increase.

In this work the further development of the proposed in [3] technique is realized to describe more complex processes of activated adsorption. The activated adsorption is accompanied by mixing adsorbed atoms with substrate atoms. These substitutional adsorption processes can be energetically more favorable than the nonactivated adsorption processes for room temperatures. We carry out the theoretical description and calculation of energy and structural characteristics of activated adsorption of Fe, Co, and Ni transition metal ions on a copper nonmagnetic substrate at different orientations of its surface face with taking into consideration the inhomogeneous distribution of magnetization in surficial region.

Results of calculation show that the temperature and ferromagnetic ordering lead to material effect on surface reconstruction and characteristics of adsorption at depending on the coverage parameter  $\Theta$ . So, for adsorption Co and Fe it is revealed that substitutional processes are energetically more favorable for case with small values of coverage parameter  $\Theta$  when "sandwich"-structures or close to these are generated. However, with growth  $\Theta$  and approaching to  $\Theta = 1$  the interaction of magnetic ions and appearance of spontaneous magnetization lead to formation of monolayer film Co or Fe on a surface without involvement of substrate atoms.

The substitutional processes for adsorption Ni strongly depend on orientations of copper surface faces than for adsorption Co and Fe: on close-packed surface face Cu(111) processes of reconstruction don't depend on temperature and are entirely defined by coverage parameter  $\Theta$ ; on face Cu(100) effects of surface reconstruction are similar to adsorption Fe and Co; on the "loose" face Cu(110) substitutional processes of atoms Ni are very poor.

This work was supported in part by Ministry of Education and Science of Russia through projects No. 02.740.11.0541 and No. 2.1.1/13956.

[1] C.A.F. Vaz, J.A.C. Bland, G. Lauhoff *Reports Progr. Phys.* **71** (2008) 056501.

[2] G. Bihlmayer, P. Ferriani, S. Baud, et al. Ultra-Thin Magnetic Films and Magnetic Nanostructures on Surfaces. *NIC Symposium*. **32** (2006) 151.

[3] M.V. Mamonova, N.S. Morozov, V.V. Prudnikov *Phys. Solid State*. **51** (2009) 2169.

23PO-J-12

## NONEQUILIBRIUM SHORT-TIME CRITICAL DYNAMICS OF FERROMAGNETS

*Prudnikov P.*

Omsk State University, Mira 55A, Russia

The determining features of the nonequilibrium critical behavior of systems in second-order phase transitions and first-order phase transitions close to the second-order ones are the critical slowing of an increase in the relaxation time and anomalously large correlation times of various states of a system. These features lead to the dynamic scaling behavior even when the system is in states far from the equilibrium state. The renormalization group analysis in [1] shows that if the initial state of a ferromagnetic system is characterized by a sufficiently high degree of the chaotization of spin variables with the relative magnetization far from the saturation state ( $m_0 \ll 1$ ), the process of the relaxation of the system from a given initial nonequilibrium state at the critical point at macroscopically small times is accompanied not by a decrease, but an increase in magnetization with time according to a power law with the exponent characterized by a new independent dynamical critical exponent  $\theta'$ :

$$m(t) \sim t^{\theta'}$$

In this case, with an increase in time, the short-time dynamics of an increase in the order parameter changes to the convenient long-time dynamics of a decrease in the order parameter with the time, according to a power law  $m(t) \sim t^{-\beta/z\nu}$  with the exponents  $\beta/z\nu$  involving the static critical exponents  $\beta$  and  $\nu$  and the dynamical critical exponent  $z$ .

The simultaneous effect of nonequilibrium initial states and defects of the structure on the evolution of anisotropic disordered systems at the critical point has been analyzed. The field theory

description and Monte Carlo investigation of the nonequilibrium critical behavior of three-dimensional disordered systems with uncorrelated [2] and long-range correlated defects [3] has been given and the dynamical critical exponent of the short-time evolution has been calculated.

The values of the exponents, obtained by renormalization-group description with the use asymptotic summation methods are in good agreement with results of numerical investigations. Comparison with the results which have been obtained in various works were given.

The Monte Carlo investigations of the short-time critical behavior of weakly disordered systems starting from the initial states with  $m_0 \ll 1$  has revealed three stages of the dynamic evolution: early time stage, which are typical for the pure system, stage characterized by crossover behavior and stage of the dynamic evolution, which corresponds to behavior of disordered system. For strong disordered systems early stage, which corresponds to behavior of pure system are not observed.

This work was supported in part by Ministry of Education and Science of Russia through project 02.740.11.0541, by the RFBR through Grants 10-02-00507 and 10-02-00787 and by Grant MK-3815.2010.2 of Russian Federation President. Our simulations were carried out on the SKIF-MSU in the Moscow State University.

[1] H.K. Janssen, B. Schaub, B. Schmittmann, *Z. Phys.* **73** (1989) 539.

[2] P.V. Prudnikov, A.N. Vakulov, E.A. Pospelov, et al. *Phys. Rev. E* **81** (2010) 011130.

[3] P.V. Prudnikov, D.N. Kulikov, *JETP Letters*, **93** (2011) 103.

23PO-J-13

## AUTORESONANT CONTROL OF MAGNETIC ENVELOPE SOLITONS

*Batalov S.V., Shagalov A.G.*

Institute of Metal Physics, Ural Division, Russian Academy of Sciences, ul. S. Kovalevskoi 18, Ekaterinburg, 620990 Russia

Many recent papers on magnetic phenomena concerned with some kind of nonlinear objects such as spiral patterns, magnetic vortexes, domain walls etc. The ability to control such nonlinear structures plays a major role in developing new applications and devices. In this work a new approach to control an amplitude of a weakly nonlinear spin wave is suggested.

We consider the problem of controlling nonlinear waves of magnetization with the aid of an external ac magnetic field in magnets with an easy axis anisotropy. The dynamics of the magnetic system is described by the nonlinear Schroedinger equation (NSE) obtained from the Landau–Lifshitz equation within the limit of small deviations of the magnetization from the ground state. The nonlinearity of these equations causes the existence of solutions in the form of solitary waves – solitons. External magnetic field enters NSE as a perturbation term and can cause a slow evolution of such soliton parameters as amplitude and velocity. The existence of such waves of magnetization in real magnets was demonstrated in a number of theoretical and experimental works.

By the control of the magnetization wave we understand a controlled change in its amplitude, which allows one, in particular, to considerably increase the wave amplitude or even change the amplitude according to some complex scenario. To realize the control, we use the effect of the nonlinear phase locking (autoresonance) of the soliton by an external perturbation, whose parameters slowly vary in time. The effect of phase locking is based on the fact that upon the satisfaction of some threshold conditions the difference between the phase of pumping and the phase of the soliton remains limited for a long time [1]. The phase locking allows to control the

amplitude of the soliton by slow variation of the pumping frequency. It is important to note that the phase locking is supported due to the nonlinearity of the system rather than due to the special selection of the time dependence of the external field. This property of the autoresonance makes it very attractive for practical applications.

We found configurations of the external magnetic field appropriate for the autoresonant control [2]. In the case of easy axis magnets and standing magnetic solitary wave, the field rotating around easy axis (with small enough perpendicular components) could be appropriate for the control of the wave amplitude. In general, the external field should initially be in resonance with a nonlinear wave and its parameters should satisfy some threshold conditions. Then slow variation of the pumping frequency results in variation of the soliton parameters.

[1] S. V. Batalov, E. M. Maslov, A. G. Shagalov. *Zh. Eksp. Teor. Fiz.*, **135** (5), 1021 (2009).

[2] S. V. Batalov, A. G. Shagalov. *Fiz. Metallov i Metallovedenie*, **109** (1), 3 (2010).

23PO-J-14

## DYNAMIC INTERACTION OF MAGNONS IN ORTHORHOMBIC ANTIFERROMAGNETS IN EXTERNAL MAGNETIC FIELD

*Kharrasov M.Kh., Kyzyrgulov I.R., Sharafullin I.F.*

Bashkir State University, 450074, Ufa, Russia

The search for new magnetically materials stimulates the investigation of physical systems, which are subject to various exposures. In this regard, great attention is paid to study the effect of external magnetic and electric fields in crystals and superconducting materials [1, 2].

In this study, ferromagnetic crystal is investigated as «the easy plane» with orthorhombic symmetry. The Hamiltonian system considers influence of the external magnetic and electric fields, linear magnetoelectric effect, and also additional magnetic anisotropy directed by a polarization vector. Having carried out in a Hamiltonian a transition to birth and annihilation operators of magnons and segnetons, we will pass to the Hamiltonian, which takes into account nonlinear processes of interaction between magnons.

$$H_M = E_0 + \sum_{k_i} \varepsilon_{k\alpha}^M c_{k3\alpha}^+ c_{k3\alpha} + \sum_{k_i} J^{\alpha\beta} \Delta(k_1 + k_5 - k_2 - k_6) c_{k1\alpha}^+ c_{k5\alpha}^+ c_{k2\alpha} c_{k6\alpha} + \\ + \sum_{k_i} \{ \Phi_1 \Delta(k_1 + k_8 - k_2) c_{k1\alpha}^+ c_{k8\alpha}^+ c_{k2\alpha} + \Phi_2 \Delta(k_1 - k_2 - k_7) c_{k1\alpha}^+ c_{k2\alpha} c_{k7\alpha} \}$$

The spin-wave spectrum in the linear approximation is calculated. The spin-wave velocity is calculated by the dispersion law at small values of wave vectors. Influence of external electric and a magnetic field for various directions concerning crystallographic axes on parameter of magnetoelectric interaction is considered. The dependence of the temperature contribution to the free energy is defined due to magnon interaction with each other. It was defined using the Green's temperature function [3]:

$$\beta \Delta F = \left(-\frac{1}{2}\right) \sum_{\bar{k}', \bar{k}''} J_{\alpha\beta} n_{\bar{k}'} n_{\bar{k}''} + \frac{1}{2} \sum_{\bar{k}, \bar{k}', \bar{k}''} \frac{J_{\alpha\beta}^2}{\beta} n_{\bar{k}'} n_{\bar{k}''} n_{\bar{k}} (1 + n_{\bar{k}}) - \\ - \frac{1}{8} \sum_{\bar{k}, \bar{k}', \bar{k}''} \frac{J_{\alpha\beta}^2}{\beta^3} \frac{n_{\bar{k}'} n_{\bar{k}''} (1 + n_{\bar{k}} + n_{\bar{k}'+\bar{k}''-\bar{k}}) - n_{\bar{k}} n_{\bar{k}'+\bar{k}''-\bar{k}} (1 + n_{\bar{k}'} + n_{\bar{k}''})}{\varepsilon_{\bar{k}'} + \varepsilon_{\bar{k}''} - \varepsilon_{\bar{k}} - \varepsilon_{\bar{k}'+\bar{k}''-\bar{k}}}$$

The attenuation of magnons is determined due to the processes of scattering and fusion. In a high-temperature limit the contribution to the attenuation of the processes of merging and splitting is proportional to temperature. In a low-temperature area the contribution to the damping, due to merge of magnons, decreases exponentially with the temperature. It is shown that the damping due to the interaction of spin waves larger than the magnon and segneton damping.

- [1] D.-X. Yao, E. W. Carlson, *Phys.Rev.B*, **78** (2008) 052507.  
 [2] A.M. Savchenko, M.B. Sadovnikova, J.G. Karchev *J. Bulletin of Moscow University. Series 3. Physics. Astronomy*. **6** (2008), 51.  
 [3] B.I. Sadovnikov, A.M. Savchenko, *J. Appl. Phys.*, **271**, (1999) 411.

23PO-J-15

## TUNNELING OF ACOUSTIC WAVES THROUGH THE GAP BETWEEN TWO FERROMAGNETIC CRYSTALS WITH THE RELATIVE LONGITUDINAL MOVING

*Moiseyev A., Vilkov E.*

Ul'yanovsk Branch of Institute of Radio Engineering and Electronics of Russian Academy of Sciences, Goncharova 48, 432011, Ul'yanovsk, Russia

The purpose of research is studying features of distribution magnetoelastic waves in system of two ferromagnetic crystals with the relative longitudinal moving, divided a vacuum gap. The tunneling of a plane monochromatic acoustic wave via a gap between two ferromagnetic crystals exhibiting relative longitudinal displacement has been studied. It is shown that, at a gap width comparable with the wavelength, the acoustic wave can exhibit complete transmission at the Damon–Eshbach mode frequency. This is confirmed by the numerical calculation of the dependence of the magnitude of the reflection coefficient on the incidence angle, which is shown in Fig. 1. If the gap width is much smaller than the wavelength, the complete transmission takes place at two resonance frequencies ( $\omega = \omega_0$ ,  $\omega = \omega_0 + \omega_m$ ), however, only in the range of glancing angles of incidence (Fig. 2). Because of the similarity of the dependences  $R(\theta)$  for these frequencies, Fig.2 shows only the curves corresponding to the frequency  $\omega = \omega_0$ .

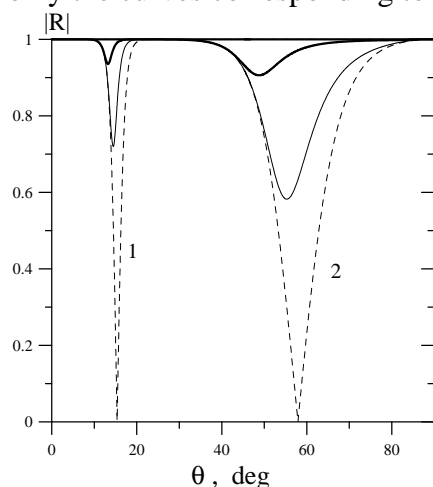


**Fig. 1.** Dependence  $R(\theta)$  for the frequency  $\omega = \omega_0 + \omega_m / 2$ . 1 -  $k_h \approx 16$ , 2 -  $k_h \approx 4$ . Dashed curves -  $V = 0$ , thin lines -  $V = 3.5 \text{ m/s}$ , thick curves -  $V = 17.5 \text{ m/s}$ .

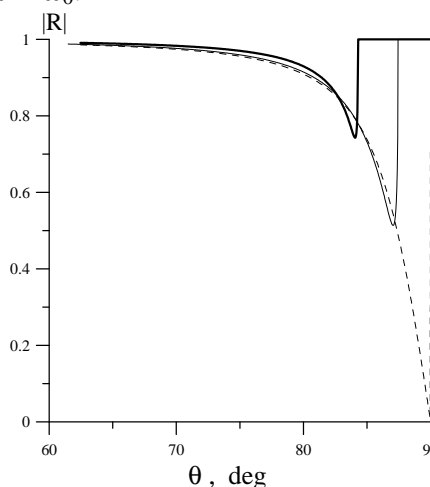


**Fig. 2.** Dependence  $R(\theta)$  for the frequency,  $\omega = \omega_0$  ( $k_h \approx 0.004$ ). Dashed -  $V = 0$ , thin lines -  $V = 3.5 \text{ m/s}$ , thickened curves -  $V = 17.5 \text{ m/s}$ .

Allowance for the longitudinal displacement of one crystal leads in all cases to violation of the resonance conditions, which results in a significant decrease in the transmission coefficient. The greater the velocity of crystal displacement, the stronger the decrease in the acoustic wave transmission through the gap between ferromagnetic crystals [1].

[1]. E.A.Vilkov, A.V.Moiseyev, V.G.Shavrov, "Magnetoelastic wave tunneling via a gap between ferroelectric crystals with relative longitudinal displacement", *Pi'sma v Zhurnal Tekhnicheskoi Fiziki*, 2009, Vol. 35, No. 9, pp. 876–878.

23PO-J-16

## INCOMMENSURATE MAGNETIC ORDER IN THE TWO-DIMENSIONAL HUBBARD MODEL

*Timirgazin M.A.<sup>1</sup>, Arzhnikov A.K.<sup>1</sup>, Vedyayev A.V.<sup>2</sup>*

<sup>1</sup> Physical-Technical Institute, Ural Branch of Russian Academy of Sciences, Kirov str. 132, Izhevsk 426001, Russia

<sup>2</sup> Faculty of Physics, M.V. Lomonosov Moscow State University, Leninskie Gory, 119992, Moscow, Russia

In the last decade more materials were revealed in which various incommensurate magnetic orderings were realized. In particular, many high-temperature superconducting compounds have such magnetic structure under certain conditions. Superconducting properties in these materials are strongly connected with magnetic ones. Despite the obvious meaning of the problem there is no sufficient theoretical description of the conditions of such magnetic order formation in  $3d$  transition metals.

We have carried out a comparative theoretical investigation of various incommensurate magnetic states in the framework of mean-field approximation in the 2D Hubbard model. First of all, the spiral magnetic states were considered. We have taken into account both pure states and the mixed ones in which the phase separation is realized. The magnetic phase diagrams in terms of the Hubbard model parameters have been constructed for several values of the next-nearest neighbor hopping parameter. The spiral states occupy a wide region in these diagrams, with the mixed states being realized in the vicinity of half-filling. It was found that paramagnetic phase does not take part in the phase separation. For large  $U$  the phase separation of ferromagnetic and antiferromagnetic states takes place and its boundary agrees well to the analytical result.

The spiral incommensurate magnetic order is hardly distinguishable from collinear incommensurate magnetic order (spin-density wave) in experiment. The collinear state is rarely considered in the framework of the Hubbard model because of mathematical complexities which arise when diagonalizing the model Hamiltonian. We have solved this problem and have compared the energy of the collinear states with the spiral ones. The phase diagram have been constructed which takes into account both incommensurate types of magnetic order and the possibility of phase separation. The collinear spin-density wave have been found to be the ground state for the small and moderate  $U$ .

The data obtained qualitatively agree to the experimental data for some quasi-2D structures such as  $\text{La}_{2-x}\text{Sr}_x\text{CuO}_4$  superconductor, in which incommensurate magnetic order is observed for some values of doping.

Both the phase separation of spiral states and the collinear spin-density wave accompany by strong charge separation. The additional Coulomb energy originating from the electronic



inhomogeneities is not taken into consideration within the Hubbard model. Possible influence of the account of this energy on the conclusions drawn above is discussed.

23PO-J-17

## THE INFLUENCE OF SPIN WAVES ON THE ULTRAFAST DEMAGNETIZATION OF Gd STUDIED WITH ATOMISTIC SPIN DYNAMIC SIMULATIONS

*Rossen S.<sup>1,2</sup>, Mentink J.H.<sup>1</sup>, Iusan D.<sup>3</sup>, Eriksson O.<sup>3</sup>, Rasing Th.<sup>1</sup>*

<sup>1</sup> Radboud University Nijmegen, Institute for Molecules and Materials,  
Heijendaalseweg 135, 6525 AJ Nijmegen, the Netherlands

<sup>2</sup> Forschungszentrum Jülich, Peter Grunberg Institute-1, 52428 Jülich, Germany

<sup>3</sup> Department of Physics and Astronomy, Division of Materials Theory, Box 516,  
SE-75120 Uppsala, Sweden.

In pump-probe experiments it is observed that a femtosecond laser pulse can demagnetize a ferromagnetic metal within 1ps for the transition metals and within 40 ps for the rare earth Gd [1]. These observations, first obtained in 1996 for Ni [2], are rather intriguing as they are much faster than expected from thermodynamics (~1ns). Nevertheless, the microscopic understanding of this ultrafast demagnetization is limited. In particular, the role of spin waves on the microscopic level has hardly been explored. In this work we address this problem using atomistic spin dynamics simulations [3] of Gd, with exchange parameters calculated from first principles. With the use of these parameters we were able to reproduce static properties of Gd which are in good agreement with experiments, provided that interactions with neighbouring spins up to at least 3 lattice units are taken into account.

Following [4], the effect of the laser pulse was modelled in the simulations by a time dependent temperature of the heat bath coupled to the magnetic system. The spin wave spectrum as a function of time is calculated by performing an inverse Holstein-Primakoff [5] transformation at different instants of time during demagnetization. Furthermore the influence of spin waves with different wave vectors is explicitly studied for this Gd system by performing simulations with these specific spin waves in the initial state. Interestingly, spin waves with low energies were found to demagnetize faster than high energy spin waves. The results could be well understood in terms of the characteristic time scales of the spin waves.

[1] M. Wietstruk *et al.*, 2011 *Phys. Rev. Lett.* **106**, 127401

[2] E. Beaurepaire *et al.*, 1996 *Phys. Rev. Lett.* **76**, 4250

[3] B. Skubic *et al.*, 2008 *J. Phys. Condens. Matter* **20**, 315203

[4] N. Kazantseva *et al.*, 2008 *Europhys. Lett.* **81**, 27004

[5] T.Holstein and H.Primakoff, 1940 *Phys. Rev. Lett.* **58**, 1098

## EXTENDED DYNAMIC SPIN-FLUCTUATION THEORY WITH APPLICATION TO IRON

Reser B.I.<sup>1</sup>, Melnikov N.B.<sup>2</sup>, Grebennikov V.I.<sup>1</sup>

<sup>1</sup>Institute of Metal Physics RAS, 18, Kovalevskaya St., 620990 Ekaterinburg, Russia

<sup>2</sup>Moscow State University, Leninskie Gory, 119991 Moscow, Russia

The Gaussian approximation (GA) of the dynamic spin-fluctuation theory (DSFT) [1] is insufficient to properly account for the interaction of the spin fluctuations as it yields a jump phase transition to the paramagnetic state. We eliminate the jump and obtain a continuous second-order phase transition by taking into account higher-order terms of the free energy of electrons in the fluctuating exchange field [2, 3], thus renormalizing the mean field and spin susceptibility. This renormalized Gaussian approximation (RGA) is enhanced further by taking into account uniform fluctuations (UF) along with the local ones. The extended theory is applied to the calculation of magnetic properties of iron. As can be seen from Fig. 1, a sharp increase of the fluctuations and sharp decrease in magnetization at high temperatures, which occurred in the GA of the DSFT, disappear in the RGA+UF. In the latter, the calculated curve for the magnetization gives a good fit to the experimental one. The local magnetic moment  $m_L(T)$  calculated in the RGA+UF by formula (39) in [3] does not strongly depend on temperature.

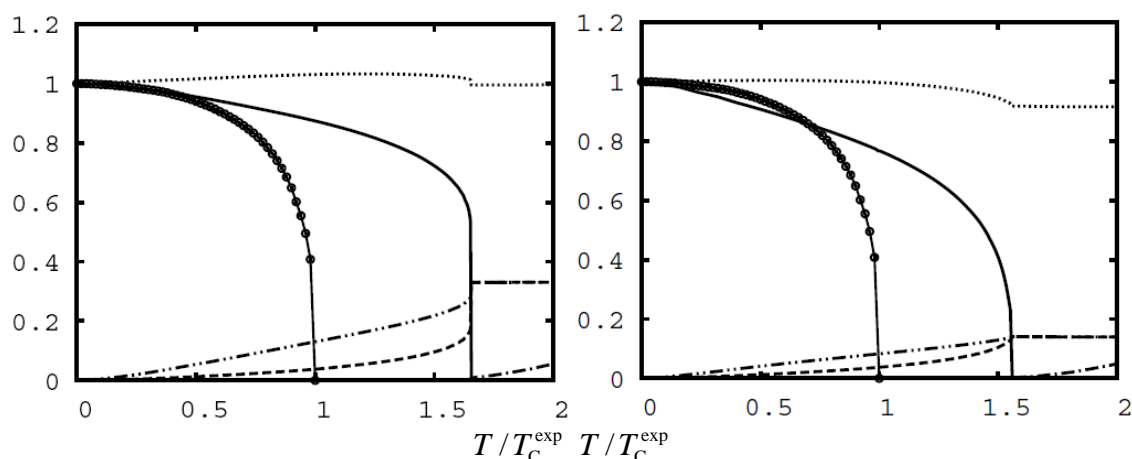


Fig. 1. The magnetization  $m(T)/m(0)$  (— calculation,  $\circ\circ\circ\circ$  experiment [4]), the mean square of fluctuations  $\langle \Delta V_x^2 \rangle(T)$  (- · -) and  $\langle \Delta V_z^2 \rangle(T)$  (- - -) in units of  $\langle V_z \rangle^2(0)$ , the reciprocal paramagnetic susceptibility  $\chi^{-1}(T)$  (- · -) in units of  $T_C^{\text{exp}} / \mu_B^2$ , and the local moment  $m_L(T)/m_L(0)$  (····) of iron calculated in the GA of the DSFT (left) and in the RGA+UF of the DSFT (right).

Support by RFBR (grant nos. 11-01-00795 and 11-02-00093) and by the Ministry of Education and Science of the Russian Federation (grant no. 2.1.1/2000) is acknowledged.

[1] B.I. Reser, V.I. Grebennikov, *Phys. Met. Metallogr.*, **85** (1998) 20.

[2] N.B. Melnikov, B.I. Reser, V.I. Grebennikov, *J. Phys. A: Math. Theor.*, **43** (2010) 195004.

[3] N.B. Melnikov, B.I. Reser, V.I. Grebennikov, *J. Phys.: Condens. Matter*, (submitted).

[4] J. Crangle, G.M. Goodman, *Proc. Roy. Soc. A*, **321** (1971) 477.

## STUDY OF SPIN AND ELASTIC WAVES WITH THE RANDOM COUPLING PARAMETER BY THE CPA METHOD

*Ignatchenko V.A., Polukhin D.S.*

L.V. Kirensky Institute of Physics SB RAS, Krasnoyarsk, 660036, Russia

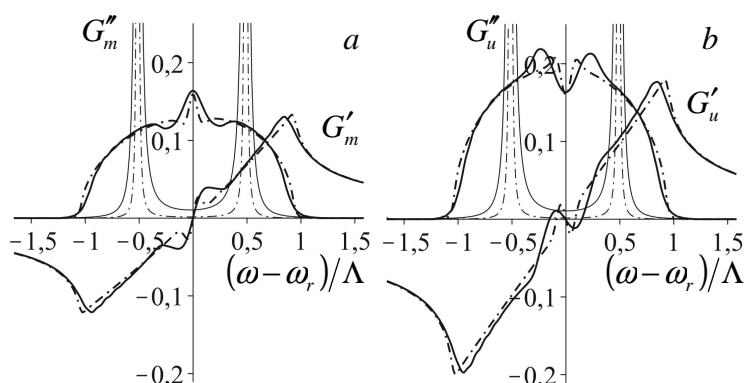


Fig. 1. Green's functions of the spin  $G_m(\omega)$  and elastic  $G_u(\omega)$  waves, at  $k_c/\sqrt{\eta k_r} = 1.6 \cdot 10^{-2}$  (solid curves) and  $2.5 \cdot 10^{-3}$  (dot-dashed curves).

A variant of the coherent potential approximation (the Kraichnan's approximation) is extended to the case of two wave fields of different nature with the random coupling parameter between them. Spin and elastic waves in zero-mean magnetostrictive media are considered. In this case the interactions between these two fields is due only to spatial fluctuations of the coupling parameter characterized by rms fluctuations of the magnetostriction  $\Delta\varepsilon$  and its correlation wave number  $k_c = 1/r_c$ ,

where  $r_c$  - correlation radius. Green's functions of the spin  $G_m(\omega)$  and elastic  $G_u(\omega)$  waves are shown in Fig. 1 in the vicinity of the crossing point of the dispersion curves for these waves ( $k = k_r$ ,  $\omega = \omega_r$ ). The imaginary parts of the Green's functions (thin solid and dot-dashed curves) in the first approximation (Bourret approximation) have the form of two peaks in the points  $\omega = \omega_r \pm \Lambda/2$ , where  $\Lambda = \eta(2\omega_u\omega_m)^{1/2}$ ,  $\eta = (\Delta\varepsilon)M/(\mu\alpha)^{1/2}$ ,  $\omega_u = vk_r$ ,  $\omega_m = gM$ ,  $\alpha$  is the exchange parameter,  $g$  is the gyromagnetic ration,  $M$  is the magnetization,  $v = \sqrt{\mu/p}$  is the speed of elastic wave,  $p$  is the matter density, and  $\mu$  is the elastic force constant. This picture is similar to the picture of the usual magnetoelastic resonance, which occurs due to the nonrandom coupling parameter in the homogeneous magnetoelastic medium [1]. However, the next approximations completely destroy this picture: the number of peaks in the both function  $G_m''(\omega)$  and  $G_u''(\omega)$  grow and the magnitude of these peaks decrease. As a result, for  $G_m''(\omega)$ , as well for  $G_u''(\omega)$  the broad single mode resonance line is formed with the linewidth  $\sim 2\Lambda$  (bold solid and dot-dashed curves in Fig. 1.). So, instead of the degeneration removal of frequencies in the wave spectrum and the appearance of two resonance peaks in the dynamic susceptibility, the sharp broadening of the self-mode peak in the crossing point has to be observed. The fine structure in the form of the narrow peak and gap appears at the center of this broad peak in the functions  $G_m''(\omega)$  and  $G_u''(\omega)$ , respectively. The widths of the fine structure peak and gap grow with the  $k_c$  increase.

Support by the Program No. 27.1 of the RAS Presidium, the State Contract No. 02.740.11.0220 on the FTP, and the Program RNP 2.1.1/3498 is acknowledged.

[1] A.I. Akhiezer, V.G. Bar'yakhtar, S.V. Peletminskii, *Zh. Eksp. Teor. Fiz.*, **35** (1958) 228.

## DYNAMICS OF THE MAGNETIC NONHOMOGENITIES OF THE MAGNETIC WITH 1D NONHOMOGENITIES MODULATION OF THE MAGNETIC ANISOTROPY PARAMETERS

*Ekomasov E.G., Gumerov A.M., Bogomazova O.B., Murtazin R.R., Rakhmatullin I.I.*

Bashkir State University, 450074, Ufa, Zaki Validi St., 32, Russia

The presence of structural and chemical nonhomogeneities, which may give rise to the local changes in the material magnetic parameters [1] is typical for real crystals in magnetics. Such changes in the parameters can be also caused by local effects (mechanical, thermal or solar). As it is usually difficult to make a precise (microscopic) calculation, one is to model the functions, which describe the parameters of a non-homogeneous material. The case is especially interesting, when the size of a magnetic non-homogeneity and the size, describing a non-homogeneity of parameters of a stuff, are of the same order. It results in considerable complication of Landau-Lifshitz equation for the magnetization. Although the task of excitation and distribution of the magnetization waves, under certain conditions, is reduced to the studies of the modified sine-Gordon equation with floating factor [2-4]. The investigation of the big perturbations influence on the solution of the modified sine-Gordon equation in general case can be investigated only with the help of numerical methods [4-6]. In dynamic, when a temporally or spatial non-homogeneous perturbation acts in the area of such non-homogeneities (or defects), under certain conditions, a strongly non-linear waves of magnetic character can be aroused. Such waves are weakly investigated.

This research considers our studies of the domain walls (DW) dynamics in ferromagnetics with an optional size one dimensional modulation of the magnetic anisotropy constant in terms of stimulation and radiation of the nonlinear waves. For the nonhomogeneity of the constant of the magnetic anisotropy (NCMA) case the reflection of the DW from the NCMA region was observed. It was connected with the DW resonant interaction with the magnetic nonhomogeneity of the breather type, stimulated in the NCMA region. On the bases of the collective variables method [7] an analytical model that adequately describes the obtained numerical results of interaction of the DW with the localized magnetic nonhomogeneity was created. Also the possibility of the DW quasitunneling involving several NCMA regions (i.e. when the particle crosses the barrier with the speed below ultimate) and the origin of the magnetic nonhomogeneities of the multi-soliton type in the form of kink and breather bound state cophased and antiphased with the oscillating breathers was shown.

[1] S.V. Vonsovskii, Magnetism, Nauka, Moscow (1971).

[2] D.I. Paul, J.Phys.C: *Solid State Phys*, **12** (1979) 585.

[3] M.A. Shamsutdinov, I.U. Lomakina, V.N. Nazarov, A.T. Harisov, D.M. Shamsutdinov, Ferro- and antiferromagnitodynamic. Nonlinear oscillations, waves and solitons, Nauka, Moscow (2009).

[4] E.G. Ekomasov, Sh.A. Azamatov, R.R. Murtazin, *FMM*, **105** (2008) 341.

[5] E.G. Ekomasov, Sh.A. Azamatov, R.R. Murtazin, *FMM*, **108** (2009) 566.

[6] A.M. Gumerov, E.G. Ekomasov, R.R. Murtazin. Simulation of the domain wall dynamics in weak ferromagnets // Chronicles of the Consolidated Fund of Electronic Resource <Science and education>, №5 (2010). URL: <http://ofernio.ru/portal/newspa-per/ofernio/2010/5.doc>.

[7] O.M. Braun, Y.S. Kivshar. The Frenkel-kontorova Model: Concepts, Methods, And Applications, Springer-Verlag, (2004).

## LOCAL MOMENTS IN THE DYNAMIC SPIN-FLUCTUATION THEORY OF METALLIC MAGNETISM

Melnikov N.B.<sup>1</sup>, Reser B.I.<sup>2</sup>, Grebennikov V.I.<sup>2</sup>

<sup>1</sup> Moscow State University, Leninskie Gory, 119991 Moscow, Russia

<sup>2</sup> Institute of Metal Physics RAS, 18, Kovalevskaya St., 620990 Ekaterinburg, Russia

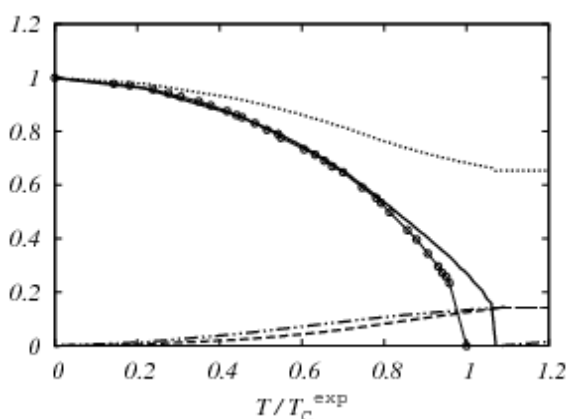


Fig. 1. The magnetization  $m(T)/m(0)$  (— calculation,  $\circ\circ\circ\circ$  experiment [4]), the mean square of fluctuations  $\langle \Delta V_x^2 \rangle(T)$  (- · -) and  $\langle \Delta V_z^2 \rangle(T)$  (- - -) in units of  $\langle V_z \rangle^2(0)$ , the reciprocal paramagnetic susceptibility  $\chi^{-1}(T)$  (- · · -) in units of  $T_C^{\text{exp}} / \mu_B^2$ , and the local magnetic moment  $m_L(T)/m_L(0)$  (····) of  $\text{Fe}_{0.65}\text{Ni}_{0.35}$  Invar calculated in the RGA+UF of the DSFT.

magnetic volume change,  $\omega_m(T) = (D_0/B)M_0^2[(m_L(T)/m_L(0))^2 - 1]$ , where  $D_0$  is the magneto-volume coupling constant for  $q = 0$ ,  $B$  is the bulk modulus and  $M_0$  is the uniform magnetization at  $T = 0$  K, for  $\text{Fe}_{0.65}\text{Ni}_{0.35}$ , we obtain  $\omega_m(T_C) = -0.017$  in good agreement with the experimentally estimated value  $-0.019$  [5].

The dynamic spin-fluctuation theory (DSFT) [1], based on the Gaussian approximation (GA) of the free energy of electrons in the fluctuating exchange field, has been extended by taking into account higher-order terms of the free energy [2, 3]. We call this approximation of the DSFT the renormalized Gaussian approximation (RGA). The effect of nonlocal spin correlations has been enhanced by taking into account uniform fluctuations (UF) along with the local ones [3]. Finally, simple computational formulae for local magnetic moment  $m_L(T)$  have been derived.

The extended DSFT is applied to the calculation of  $m_L(T)$  of the  $\text{Fe}_{0.65}\text{Ni}_{0.35}$  Invar. As can be seen from Fig. 1, the  $m_L(T)$  calculated in the RGA+UF of the DSFT strongly depends on temperature: with temperature increasing from zero to  $T_C$ , the local moment decreases by 35%. This change is considerable and quite sufficient for an explanation of the Invar effect. Using our calculated value  $m_L(T_C)/m_L(0) = 0.65$  and experimentally estimated value  $D_0/B \approx 10^{-6}$  (emu/g)<sup>-2</sup> in formula for the

Support by RFBR (grant nos. 11-01-00795 and 11-02-00093) and by the Ministry of Education and Science of the Russian Federation (grant no. 2.1.1/2000) is acknowledged.

[1] B.I. Reser, V.I. Grebennikov, *Phys. Met. Metallogr.*, **85** (1998) 20.

[2] N.B. Melnikov, B.I. Reser, V.I. Grebennikov, *J. Phys. A: Math. Theor.*, **43** (2010) 195004.

[3] N.B. Melnikov, B.I. Reser, V.I. Grebennikov, *J. Phys.: Condens. Matter*, (submitted).

[4] J. Crangle, G.C. Hallam, *Proc. Roy. Soc., A* **272** (1963) 119.

[5] M. Shiga, *Inst. Phys. Conf. Ser.*, **55** (1981) 241.

## NONLINEAR DYNAMICS OF THE DOMAIN WALLS IN MAGNETICS WITH AN OPTIONAL ONE-DIMENSIONAL MODULATION OF THE MAGNETIC PARAMETERS

*Ekomasov E.G., Murtazin R.R., Nazarov V.N., Almuchametova A.R.*

Bashkir State University, 450074, Ufa, Russia

It is known that in real magnetics the appearance of magnetic parameters local changes happens due to structural and chemical nonhomogeneities and local influence (mechanical, thermal or solar). As it is usually difficult to make a precise (microscopic) calculation, one is to model the functions, which describe the parameters of a nonhomogeneous material [1]. The defects have a strong effect on the magnetics static and dynamic characteristics, coercive force and stickiness in particular. Such defects can lead to the appearance of the spatially localized oscillation modes and different types of magnetic nonhomogeneities. Direct experimental investigation of the defects often turns out to be difficult, and that is why the indirect methods are used. One of the theoretical ways of study of the defects influence on the magnetic nonhomogeneities is the accounting of the material parameters spatial dependence in the network of the thermodynamics theory. It results in considerable complication of Landau-Lifshitz equation for the magnetization. Although the task of excitation and distribution of the magnetization waves, under certain conditions, is reduced to the studies of the modified sine-Gordon equation with floating factor [2]. The research of the big perturbations influence on the solution of the modified sine-Gordon equation in general case can be investigated only with the help of numerical methods [3]. In dynamic, when a temporally or spatial nonhomogeneous perturbation acts in the area of such nonhomogeneities (or defects), under certain conditions, a strongly non-linear waves of magnetic character can be aroused. Such waves are poorly investigated.

This research considers our studies of the DW dynamics in ferromagnetics with an optional size one-dimensional modulation of the magnetic parameters in terms of stimulation and radiation of the nonlinear waves. We examined several types of magnetic parameters variations: Gaussian decrease, square well, etc. For the calculation a program was written. For the nonhomogeneity of the constant of the magnetic anisotropy case and exchange constant  $A$  the dependence of the DW minimal speed required to cross the defect region was studied analytically and numerically. The oscillations of the DW localized in the nonhomogeneity region under the influence of the changing magnetic field were considered and the dependence of the resonance frequency (i.e. the translational mode of the DW oscillation) on nonhomogeneity region parameters was obtained. It was found out that after the DW leaves the defect, this region preserves localized oscillations of the environment magnetization, which under certain conditions lead to the origin of the magnetic nonhomogeneities of breather and soliton type. The regions of the defect parameters similarly to [3], defining the existence of the magnetic nonhomogeneities of breather and soliton type were specified. The dependence of the internal modes of breather and soliton oscillations on defect parameters was obtained. We propose a formula describing the dependence of the established soliton amplitude on the parameters of the defect.

[1] S.V. Vonsovskii, Magnetism, Nauka, Moscow (1971).

[2] D.I. Paul, J.Phys.C: Solid State Phys. v.12 (1979) 585.

[3] E.G. Ekomasov, Sh.A. Azamatov, R.R. Murtazin, FMM **105** (2008) 341.

## SPIN WAVES IN MULTILAYERS WITH DIFFERENT MAGNITUDES OF THE MAGNETIZATION, EXCHANGE AND ANISOTROPY

*Ignatchenko V.A., Tsikalov D.S.*

L.V. Kirensky Institute of Physics SB RAS, Krasnoyarsk, 660036, Russia

Spin-wave spectra in the one-dimensional magnon crystals – periodic superlattices (SL) – with the rectangular and sinusoidal profile of the material parameter is considered. The general form of the dispersion relation for the rectangular SL with different values of the magnetization  $M_i$  or magnetic anisotropy  $K_i$  in the adjacent layers  $i = 1, 2$  is the standard Kronig-Penney's equation [1], as in the case of the dielectric constant  $\varepsilon_i$  difference in photonic crystals. But for the case of different values of the exchange parameters  $A_i$  this equation must be generalized, because the boundary conditions in that case lead to a jump of the dynamic variable derivative that is proportional to  $A_1 - A_2$ . As a result, the dispersion law was obtained in the form [2]

$$\cos d_1 \sqrt{v_1} \cos d_2 \sqrt{v_2} - \frac{1}{2\sqrt{v_1 v_2}} \left[ v_1 \frac{A_1}{A_2} + v_2 \frac{A_2}{A_1} \right] \sin d_1 \sqrt{v_1} \sin d_2 \sqrt{v_2} = \cos kL, \quad (1)$$

where  $v_i = (M_i / 2A_i)(\omega / g - H - 2K_i / M_i + 4\pi M_i)$ . At  $A_1 = A_2$  Eq. (1) takes the standard form. The general form of the relation for the sinusoidal SL with harmonic dependences of the parameters  $M(x)$ ,  $K(x)$  or  $\varepsilon(x)$  on the  $x$  coordinate is the equation, that contains infinite chain fractions [3] with the same constant in the each link numerator. We extend this equation to the case of  $A = A(x)$

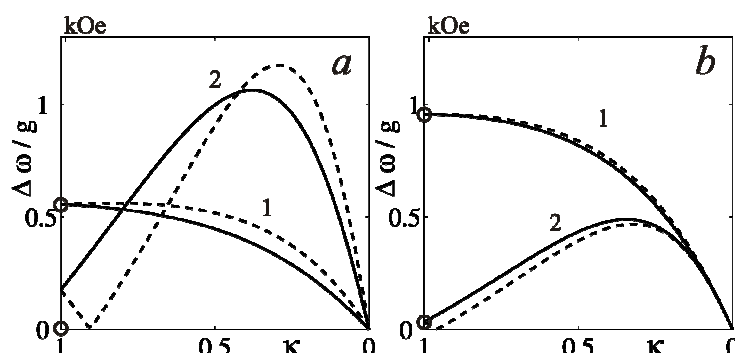


Fig. 1. Dependence of the 1-st (curves 1) and 2-nd (curves 2) bandgap on the  $\kappa = d_1/d_2$  for the cases of difference of  $A_i$  (a),  $(A_1 - A_2)/\bar{A} = \pm 0.1$ , and  $K_i$  (b),  $(K_1 - K_2)/\bar{K} = \pm 0.3$ , where  $\bar{A}$  and  $\bar{K}$  are the mean values. Solid curves correspond to the sign “+” and dashed to the “-”. Bandgaps for the sinusoidal SL are shown by circles at  $\kappa = 1$ .

and show that link numerators became different functions of both the wave number  $k$  and number of the link  $n$ . The obtained equations are used for the calculation of the dependences of the 1-st and 2-nd bandgaps in the spectrum on the ratio of the layer thicknesses  $\kappa = d_1/d_2$  (Fig.1). It is seen, that 1-st bandgap has the maximum at  $\kappa = 1$  and then decreases with the  $\kappa$  decrease. The 2-nd bandgap has the maximum between  $\kappa = 1$  and  $\kappa = 0$ . It is seen, that its width can be considerable increased by the corresponding choice of the ratio  $\kappa$  between  $d_1$  and  $d_2$ .

Support by the Program No. 27.1 of the RAS Presidium, the State Contract No. 02.740.11.0220 on the FTP, and the Program RNP 2.1.1/3498 is acknowledged.

[1] R.D. Kronig and W.G. Penney, Proceedings of the Royal Society London, **130** (1931) 499.

[2] V.V. Kruglyak and A.N. Kuchko, Physica B, **339** (2003) 130.

[3] T. Tamir, K.F. Casey, and Z. Kaprielian, IEEE Trans., **13** (1965) 297.

23PO-J-24

## **GENERAL TRAVELLING-WAVE SOLUTION OF THE AKHIEZER–BOROVIK PROBLEM**

*Ostrovskaya N.V.*

Moscow State Institute of Electronic Technology (Technical university), Solnechnaya Alleya, 5,  
Zelenograd, Moscow, 124498, Russia

The Landau–Lifshits equation for uniaxial ferromagnetic has been considered with use of only classical methods of differential equations eschewing as the inverse scattering so and finite-gap methods. Its general travelling-wave solution was obtained in the form of Jacobi elliptic integral of the first kind. The solution contains four independent constants of integration, two of which are just shearing ones, and the additional (fifth) external parameter is the wave velocity. The bifurcation manifold for the solution in three-dimensional bifurcation space consists of three surfaces and several isolate lines out of them. There is only one isolate line that corresponds to the solution with zero asymptotic (the Akhiezer–Borovik soliton [1]). Another one corresponds to parameters of dark solitons family [3]. The rest refer to localized solutions with nonzero asymptotic. For the parameter combinations out of these surfaces there are the regions of real periodic cnoidal solutions, such as ones that were obtained in [2], and the regions without any real solutions, but with complex ones only including instantons.

[1] A.I. Akhiezer, A.E. Borovik, *JETP*, **51** (1966) 508.

[2] A.M. Kamchatnov, *JETP*, **102** (1992) 1006.

[3] N.V. Ostrovskaya, *Journal of Physics: Conference series*, **200** (2010) 042020.

23PO-J-25

## **MAGNETIC EXCITATIONS IN LOKALLY NON-EQUILIBRIUM MEDIA**

*Kabychenkov A.*

Institute of Radio Engineering and Electronics of Russian Academy of Sciences, Russia,  
Moscow region, Fryazino, Vvedenskogo 1. e-mail: akab@mail.cplire.ru

In frame work of locally non-equilibrium thermodynamics the equation of motion for magnetization is derived. This equation takes the form of standard equation of motion in case of locally equilibrium high-symmetry medium, ignoring the surface moments. The equations of magnetization and electromagnetic field are interrelated through vortices of the magnetization and magnetic vector potential. In magnetic non-ordered media (paramagnetic, diamagnetic, magnetic glasses, neutron liquid) the linear coupled waves of vector potential and magnetization are considered. The dispersion and attenuation of the waves are determined [1]. It is shown, that there is the discrete number of frequencies for which waves propagate without attenuation or waves dump at constant phase and the real and imaginary parts of the wave numbers are equal (skin-effect). In high wave number region the dispersions of electromagnetic-spin and spin-electromagnetic modes are linear function and attenuations are constant.

In locally non-equilibrium magneto-non-ordered media the fluctuation spectrum and attenuation are determined, too. Imaginary part of frequency satisfies a fifteenth-degree equation. Each decision of the equation produces two branch of spectrum. The electromagnetic-spin modes have the energy gap at zero wave number. The magnitude of the gap is characterized by the typical relaxation times.



The dominant homogeneous mode has continuous oscillation and other modes have damped oscillation. Some of the modes have the local minimum similar to the roton spectrum. Spin-electromagnetic modes have not the gap. Oscillations of nearly zero frequency are caused by translation invariance, the absence of restoring force. However, in this case it is essential to take account of nonlinear effects. As a result frequency will be depended on amplitude, when the frequency is approached to zero, the amplitude is approached to zero, too [2]. In diamagnetic in high wave number region there are two unstable modes. The range of instability is confined by spatial dispersion. The amplitudes of these modes are limited by nonlinear effects.

In bounded volume the spectrum and attenuation of localized modes are considered, too. If the volume is parallelepiped that attenuation and dispersion are determined by the above equations in which continual wave number substitute for discrete wave number.

The equations of motion for electric polarization and electric current have the similar to equation for magnetization form. When considering the vector potential as a field momentum, an analogy between the equations of motion of medium with internal rotation and the equations of electrodynamics arises [3]. In particular thermo-magnetic effect will be similar thermo-spin effect. The vector potential and magnetization can be considered as the polarization vectors of spin charges in the spaces of displacements and rotations [4].

[1] A. Kabychenkov. Bulletin of Russian Academy of Sciences, Physics, 2010, V.74, N10, p.1376

[2] A. Kabychenkov. IV International symposium on surface waves in solid and layered structures. Proceedings, 1998, pp.83-87

[3] A. Kabychenkov. Technical Physics, 2009, V.54, N8, p.1116

[4] A. Kabychenkov. Moscow International Symposium on Magnetism, 2005, Books of Abstracts, pp.549-550

23PO-J-26

## THEORETICAL INVESTIGATION OF THE MAGNETIC ORDER IN FeAs

*Dobysheva L.V., Arzhnikov A.K.*

Phys.-Techn. Institute UrBr Russian Ac. Sci., 426001, Izhevsk, Kirova str., 132, RUSSIA

The FeAs attracts large interest due to extraordinary properties of its close relatives such as LaFeAsO, BaFe<sub>2</sub>As<sub>2</sub>, and NaFeAs, which are attributed to the presence of FeAs planes with the same local structure as in the iron monoarsenide. Using an ab-initio method of the electron structure calculation (FP LAPW that is realized in WIEN2k package), we have studied the magnetic structure of FeAs, both GGA and LDA potentials being used in calculations. After finding the optimum lattice parameters, we have considered a few magnetic configurations with a collinear structure. There are a ferromagnetic FM and three kinds of antiferromagnetic AFM structures found. The AFM structures have lower total energies than the FM one. For all four structures, the calculations with spin-orbit term included have been conducted and the magnetic anisotropy has been studied.

The existence of different types of collinear ordering gives rise to a presumption that a noncommensurate spin wave is the most stable state with a lowest energy in this system. Using a package version for the noncollinear magnetism, the dependence of the total energy on the wave vector  $q$  has been obtained.

With a model Hamiltonian, it has been shown that magnetic anisotropy results in a spin spiral wave with a corresponding difference in the spin amplitudes, so that the spin spiral becomes elliptical.

Support by RFBR (grant N 09-02-00461) is acknowledged.

## QUANTUM THEORY OF MAGNETISM AND THE PROBLEM OF MAGNETIC ORDERING IN CARBON-BASED SYSTEMS

*Kuzemsky A.L.*

Joint Institute for Nuclear Research, 141980 Dubna, Moscow Reg., Russia  
(e-mail:kuzemsky@theor.jinr.ru; <http://theor.jinr.ru/~kuzemsky>)

The development of experimental techniques over the recent years opened the possibility for synthesis and investigations of a wide class of new substances with unusual combination of properties. Transition and rare-earth metals and especially compounds containing transition and rare-earth elements possess a fairly diverse range of magnetic properties. The construction of a consistent microscopic theory explaining the magnetic properties of these substances encounters serious difficulties when trying to describe the collectivization-localization duality in the behaviour of magneto-active electrons. This problem appears to be extremely important, since its solution gives us a key to understanding magnetic, electronic, and other properties of this diverse group of substances. Quantum theory of magnetism deals with variety of the schematic models of magnetic behaviour of real magnetic materials. In paper [1] we presented a comparative analysis of these models; in particular, we compared their applicability for description of complex magnetic materials. The concepts of broken symmetry, quantum protectorate, and quasiaverages were analysed in the context of quantum theory of magnetism, especially for the low-dimensional systems, in paper [2]. As a rule, magnetic materials can be metals, semiconductors or insulators which contain the ions of the transition metals or rare-earth metals with unfilled shells. However during the last decade the search for macroscopic magnetic ordering in exotic materials has attracted big attention. In particular, the carbon-based materials were pushed into the first row of researches. Carbon materials are unique in many ways. They are characterized by the various allotropic forms that carbon materials can assume. In spite of the fact that graphite is diamagnetic, in 2001 an “observation of strong magnetic signals in rhombohedral pristine C60, indicating a Curie temperature near 400-500K” was reported. Recently a “room-temperature ferromagnetism of graphene” [3] was claimed. Some evidence that proton irradiation on highly oriented pyrolytic graphite samples may triggers ferro- or ferrimagnetism was reported. The possibility of a magnetism in grapheme nanoislands was speculated and a defective graphene phase predicted to be a room temperature ferromagnetic semiconductor was conjectured. Thus the natural question arises: can carbone-based materials be magnetic and what is the mechanism of the appearing of the magnetic state from the point of view of the quantum theory of magnetism? In the present work, these questions were analysed and reconsidered to elucidate the possible relevant mechanism (if any) which may be responsible for observed peculiarities of the “magnetic” behaviour in these systems, having in mind the quantum theory of magnetism criteria. On the basis of this analysis the conclusion was made that the thorough and detailed experimental studies of this problem only may lead us to a better understanding of the very complicated problem of magnetism of carbon-based materials.

- [1] A.L. Kuzemsky, Statistical Mechanics and the Physics of Many-Particle Model Systems. *Physics of Particles and Nuclei*, 40 (2009) 949-997.
- [2] A.L. Kuzemsky, Bogoliubov's Vision: Quasiaverages and Broken Symmetry to Quantum Protectorate and Emergence. *Int.J. Mod. Phys.*, B24 (2010) 835-935.
- [3] Yan Wang et al., Room-Temperature Ferromagnetism of Graphene. *Nano Letters*, 9 (2009) 220-224.

## ELECTRONIC STRUCTURE OF NONCOLLINEAR MAGNETIC MANGANITE PHASES IN THE TIGHT- BINDING APPROXIMATIONS

*Dunaevsky S.M.*

Petersburg Nuclear Physics Institute, Orlova Grave, Gatchina, 188300 Russia

A remarkable property of the doped manganites  $R_xA_{1-x}MnO_3$  ( $R = La, Pr, Nd, Sm$ ;  $A = Ca, Sr, Ba$ ) with a perovskite structure is that their magnetic structures exhibit a rich variety. Depending on the chemical composition and doping level, these compounds can either be in the ferromagnetic state or have different types of antiferromagnetic (AF) order. Apart from simple antiferromagnetic structures of the  $G$ ,  $A$ , and  $C$  types, there can arise more complex structures consisting of ferromagnetic chains AF ordered with respect to each other. The best known examples of such structures are provided by structures of the  $CE$  and  $E$  types. All the aforementioned magnetic phases are collinear. However, the experiment has demonstrated that undoped manganites contain not only collinear but also noncollinear (spiral) magnetic structures.

In this paper, it has been shown how the tight-binding method should be modified to calculate the  $E(\mathbf{k})$  spectrum of  $e_g$  electrons and the total energy of spiral (commensurate and incommensurate) magnetic structures of manganites. In these compounds, the magnetic structure is formed by the manganese  $t_{2g}$  electrons, which are considered to be localized. The effective Hamiltonian used to describe the properties of manganites in this study include the standard double – exchange Hamiltonian for the degenerated  $e_g$  level, the Heisenberg Hamiltonian and the Hamiltonian of the electron–phonon interaction.

The transformation of the spinor components  $U(\theta_i, \varphi_i)$  appears as a result of the rotation of the local system of the coordinates at each manganese atom, which accompanies any translation by the direct lattice vector. In this case, the translation invariance of the lattice is retained, which makes it possible to use the Bloch theorem for constructing the wave function and calculating the spectrum of noncollinear magnetic structures [1]. In the tight - binding method, the matrix element of the Hamiltonian of a noncollinear magnetic structure between the nearest spinors  $\alpha(\beta)$  at atoms with indices  $i$  and  $j$  has the form

$$H_{ij\sigma\sigma'}^{\alpha\beta}(k) = \sum_{ij} t_{ij}^{\alpha\beta} (U_j^\dagger U_i)_{\sigma\sigma'} e^{ik(\mathbf{R}_j - \mathbf{R}_i)} \quad (\sigma, \sigma' = \uparrow, \downarrow) \quad (1)$$

Thus, the main result of transformation  $U(\theta_i, \varphi_i)$  is the appearance of the off diagonal (in spin indices) matrix elements of the Hamiltonian between the nearest neighbors.

Expression (1) allows us at once to obtain explicit expressions for the matrix of the Hamiltonian  $H(\mathbf{k}, \mathbf{q})$  of the noncollinear manganite structures with the wave vector  $\mathbf{q}$  when the quantities  $\varphi_i(\mathbf{q})$  and  $\theta_i(\mathbf{q})$  are specified. We have  $\theta_i = \theta_j$  and  $\varphi_j - \varphi_i = \mathbf{q}(\mathbf{R}_j - \mathbf{R}_i)$  for the spiral and  $\theta_j - \theta_i = \mathbf{q}(\mathbf{R}_j - \mathbf{R}_i)$  and  $\varphi_j = \varphi_i$  for the flat cycloid. Thus one can analytically describe the matrix of the Hamiltonian  $H(\mathbf{k}, \mathbf{q})$ , where  $\mathbf{q}$  is the wave vector of the specified spiral structure and  $\mathbf{k}$  is the wave vector of the crystal lattice under consideration. In fact, this study is the generalization of the approach proposed in [2], where the spectrum and the ground state of the magnetic structures formed by four local spins in the unit cell of manganite were calculated using the tight-binding method with the complete Hamiltonian and spinor transformation  $U(\theta_i, \varphi_i)$ .

[1] L. N. Sandratskii, *Adv. Phys.*, **47** (1998) 91.

[2] S. M. Dunaevsky and V. V. Deriglazov, *Phys. Rev. B*, **71**, (2005) 094 414.

23PO-J-29

**MAGNETICS WITH LARGE SINGLE-ION ANISOTROPY***Sizanov A., Syromyatnikov A.*

Petersburg Nuclear Physics Institute, 188300 Saint-Petersburg, Russia

We propose a new representation for spin operators. It's useful for investigation of spin systems with ground state close to  $S_z=0$  on all sites. Using this representation we consider spin systems with integer spin, exchange interaction and large single-ion easy-plane anisotropy. For these systems the spectrum of low-lying excitation is calculated up to the 2<sup>nd</sup> order of  $J/D$  for  $S > 1$  and up to the 3<sup>rd</sup> order for  $S = 1$ . It's shown that there is a good agreement of our result with previous results obtained by Monte-Carlo calculations. Also this approach is used for considering  $\text{NiCl}_2\text{-4SC(NH}_2)_2$  compound known as DTN. We obtain for the first time consistent description of DTN properties at large and small magnetic field simultaneously.

23PO-J-30

**TRANSITIONS IN THREE-DIMENSIONAL MAGNETS WITH EXTRA BROKEN SYMMETRIES***Sorokin A.O., Syromyatnikov A.V.*

Petersburg Nuclear Physics Institute, 188300, Saint Petersburg, Russia

In a phase transition, symmetry plays crucial role determining the universal properties of the systems at critical point. The order parameter space is the symmetry broken upon transition. In particular, for XY and Heisenberg ferromagnets the order parameter space is manifold  $\text{SO}(2)$  and  $\text{SO}(3)/\text{SO}(2)$  correspondingly, i.e. one- and two-dimensional sphere, describing a set of probable direction of spontaneous magnetization. In three dimensions for the systems the second order transition occurs with origin of collinear order.

For helimagnets and triangular antiferromagnets the order is planar. For XY spins in these systems  $\text{Z}_2 \otimes \text{SO}(2)$  symmetry is broken, and additional order parameter is chirality. For Heisenberg spins broken symmetry is  $\text{SO}(3)$ , and order is described by two orthogonal vectors. In three dimensions the transition is weak first order with pseudo-universal behavior.

We introduced and considered by Monte Carlo simulations two models of three-dimensional classical magnets with more complicated order parameter space. The first model is the stacked three-exchange model on a simple cubic lattice with one interlayer ferromagnetic exchange between nearest neighbor spins and three intralayer exchanges between spins of first three order of range. The second model is antiferromagnet on a stacked-triangular lattice with two competing interlayer exchanges.

Ground state of these systems is planar, but because of two helical structures are present, the broken symmetry in case of Heisenberg spins is  $\text{Z}_2 \otimes \text{SO}(3)$  similar to magnets with non-planar order. In this case we found first order transition but with probable pseudo-universal behavior. We obtained critical exponents which are in agreement with exponents of other systems of this class [1,2].

In case of XY spins the broken symmetry is  $\text{Z}_2 \otimes \text{Z}_2 \otimes \text{SO}(2)$  with two chiral order parameters. We found distinct first order transition.

- [1] H. Kunz, G. Zumbach, *J. Phys. A* **26** (1993) 3121.  
 [2] H.T. Diep, A. Ghazali, P. Lallemand, *J. Phys. C* **18** (1985) 5881.

23PO-J-31

## MONTE CARLO SIMULATION OF MAGNETIC PROPERTIES OF RARE-EARTH AMORPHOUS ALLOYS

*Bondarev A.V., Ozherelyev V.V., Bataronov I.L., Barmin Yu.V.*

Voronezh State Technical University, 14 Moskovskii prospekt, 394026 Voronezh, Russia

In the amorphous alloys of the  $\text{Re}_{100-x}\text{T}^{\text{4f}}_x$  ( $\text{T}^{\text{4f}} = \text{Gd, Tb, Dy, Ho, Er}$ ), ( $x=20-91$  at. %) systems in a wide compositional region, the sharp maximum on temperature dependence of magnetic susceptibility  $\chi(T)$  and irreversibility of magnetization  $M(T)$  are observed. This magnetic phase transition is typical for spin glasses. The observed magnetic phase transition is typical for spin glasses. At the intermediate concentrations ( $x=33-65$  at. %), the  $\text{Re}_{100-x}\text{Gd}_x$  amorphous alloys turn into the reentrant spin-glass state. These phase transitions take place if the concentration of the rare-earth atoms exceeds the critical value  $x_c=8-20$  at. %. The existence of the critical concentration can be explained within the frame of percolation theory. The spin-glass-like transition takes place only if the percolation cluster of the rare-earth atoms is formed [1].

Then we constructed the molecular dynamics models of atomic structure of the Re-Tb amorphous alloys and of pure amorphous Tb. Using the Monte Carlo method in the frame of the Heisenberg model we carried out simulation of magnetic properties of Re-Tb amorphous alloys and of pure amorphous Tb. The model Hamiltonian was chosen in the following form [2]:

$$H = -\frac{1}{2} \sum_{i,j} J_{ij} (\vec{S}_i \cdot \vec{S}_j) - D \sum_i (\vec{n}_i \cdot \vec{S}_i)^2 - \mu h \sum_i S_i^z$$

where  $J_{ij}$  is exchange integral between the nearest neighbours  $i$  and  $j$ ;  $D$  is local uniaxial anisotropy (varied from 0 to  $20J$ );  $\vec{S}_i$  is Heisenberg spin;  $\vec{n}_i$  is unit vector determining the direction of the local anisotropy axes;  $h$  is external magnetic field.

The temperature dependencies of spontaneous magnetization, Edwards–Anderson order parameter and magnetic susceptibility were calculated. At  $D/J > 8$  and  $x \geq 13$  at. % Tb the transition to the spin-glass state was observed. With increasing concentration of Tb atoms, the transition temperature linearly increases, this dependence agrees with the experimental results.

We calculated the magnetization curves, hysteresis loops, remanent magnetization, coercive field, spin-spin correlation functions at different temperatures and different  $D/J$  values. These materials show very high coercivity at low temperatures. They do not reach magnetic saturation even under very high magnetic fields up to 1000 kOe. The temperature dependencies of magnetization in the presence of magnetic field after field cooling and after zero field cooling (FC and ZFC curves) were also calculated.

- [1] Yu.V. Barmin, I.L. Bataronov, A.V. Bondarev, *NATO Sci. Ser. II*, **184** (2005) 209.  
 [2] R. Harris, M. Plischke, M.J. Zuckermann, *Phys. Rev. Lett.*, **31** (1973) 160.

## SPIN AND ORBITAL SUSCEPTIBILITY OF 2D RASHBA ELECTRONS IN A STRONG MAGNETIC FIELD

*Novokshonov S.G.*

Institute of Metal Physics, Ural Division of RAS, Ekaterinburg, 620990, S. Kovalevskaya str., 18, Russia

The analytical expression for magnetic moment,  $M$ , of 2D Rashba electron gas in a strong orthogonal magnetic field,  $B$ , is received. We take, as the starting point, the thermodynamical Maxwell relation  $(\partial M / \partial \zeta)_B = (\partial n / \partial B)_\zeta$ , where  $\zeta$  is the chemical potential and  $n$  is the concentration of electrons. The following expression

$$\left( \frac{\partial M}{\partial \zeta} \right)_B = \frac{1}{\pi B} \text{Im} \left\{ \int_{-\infty}^{\zeta} \text{Tr} G^A(E) dE - \text{Tr} \left[ \zeta - \frac{1}{2} \vec{n} \cdot (\vec{\sigma} \times \vec{\pi}) \right] G^A(\zeta) \right\}$$

can be received from the Maxwell relation by means of a sequence of some identically transformations. Here symbol  $Tr$  denotes the trace over both orbital and spin degrees of freedom,  $G^A(E)$  is the averaged advanced one-particle Green function of 2D Rashba electron in an orthogonal magnetic field,  $\alpha$  is the Rashba spin-orbit coupling,  $\vec{\pi}$  is the operator of kinematic electron momentum,  $\vec{\sigma}$  is the vector formed by Pauli spin matrices, and  $\vec{n}$  is the unit normal vector to the considered 2D system. The analysis of the magnetic fields and Fermi energy  $E_F$  dependencies of  $M$  was made using the exact relation between  $G^A(E)$  and Green function of electron with ideal value of  $g$ -factor ( $g_0 = 2$ ) and without spin-orbit interaction [1].

If  $E_F$  lies above bottom of the upper subband, then the smooth part of total magnetic moment of 2D Rashba electron gas combined from usual paramagnetic Pauli and diamagnetic Landau contributions. The main period of de Haas-van Alphen (dHvA) oscillations is defined by energy  $E_F + m\alpha^2$  and is equal to  $\Delta(1/B) = |e| / \pi c n$ . The location of the  $k$ -th node of the oscillations beatings is determined by condition

$$B_k = \frac{2mc}{|e|} \frac{2k_F \alpha}{\sqrt{4k^2 - (g-2)^2}}, \quad k = 1, 2, 3, \dots$$

where  $g$  is the effective  $g$ -factor.

This behavior is drastically changed, if  $E_F$  moves down below bottom of the upper subband. First of all, it is accompanied by disappearance of the dHvA oscillations beatings. Secondly, the Fermi level turns the monotone decreasing function on the magnetic field and, consequently, the simple relation between period of dHvA oscillations and electron concentration is violated. Furthermore, it leads to the failure of well known relation between para- and diamagnetic terms of total magnetic moment and to appearance of the smooth magnetic field dependence (parallel with the oscillations) of these quantities.

The work was done within RAS Program (Low-Dimensional Nanostructures).

[1] S.G. Novokshonov, A.G. Groshev, Phys. Rev. **B74** (2006) 245333.

**23 August**

Tuesday

17:30-19:00

poster session  
23PO-K

**“Multiferroics”**

23PO-K-1

## EVOLUTION OF SPIN-MODULATED MAGNETIC STRUCTURE IN MULTIFERROIC COMPOUND $\text{Bi}_{(1-x)}\text{Sr}_x\text{FeO}_3$

*Tkachev A.V.<sup>1</sup>, Gippius A.A.<sup>1</sup>, Gervits N.E.<sup>1</sup>, Pokatilov V.S.<sup>2</sup>, Kononova A.O.<sup>2</sup>*

<sup>1</sup> Physics Department, M.V. Lomonosov Moscow State University, 119991, Russia

<sup>2</sup> Moscow Institute of Radioengineering, Electronics and Automation, 119454, Russia

$\text{BiFeO}_3$  is a perovskite-like compound with magnetic and electrical long-range order with antiferromagnetic transition temperature about 670 K. It has space modulated magnetic structure of cycloidal type with the period  $\lambda = 620 \pm 20 \text{ \AA}$  incommensurate with the lattice parameter. This structure results in space modulation of local field on  $^{57}\text{Fe}$  nuclei as well as space periodic spin-spin relaxation time. It leads to specific NMR line shape presented on the top panel of the figure.

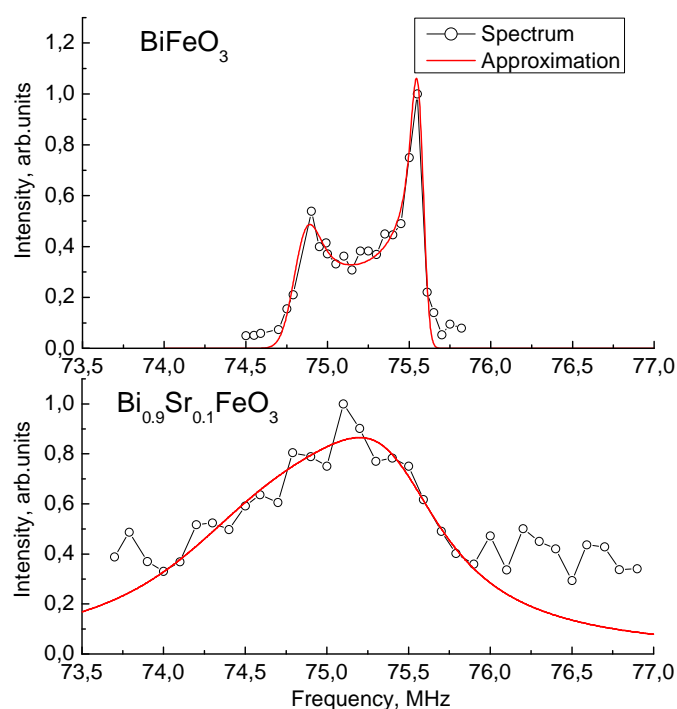
The space modulated magnetic structure can be described by the spatial distribution of  $\theta$ , the angle between magnetization and threefold c-axis. It is determined by the elliptic function

$$\cos \theta = \text{sn} \left( \pm \frac{4K(m)}{\lambda} x, m \right),$$

where  $m$  is anharmonic parameter,  $\text{sn}(x, m)$  is the elliptic Jacobi function and  $K(m)$  is the complete elliptic integral of the first order [1]. Applying this equation with given frequency and line width anisotropy [2] one can approximate the  $^{57}\text{Fe}$  NMR spectrum (red line in the figure).

Substitution for bismuth atoms destroys the space modulated structure. Several samples with substitution of strontium for bismuth  $\text{Bi}_{1-x}\text{Sr}_x\text{FeO}_3$  were studied. A significant broadening of spectrum was observed already at  $x = 10\%$  as shown on the bottom panel of the figure. The frequency range slightly shifts to the lower values and the line width increases more than by a factor of ten. Thus the specific line shape is almost indistinguishable and the spectrum looks like a single slightly asymmetric peak. This phenomenon evidences for destruction of the spatial modulated structure at  $x \sim 0.1$ .

It is worth to mention that substitution of lanthanum for bismuth causes similar changes at  $x \sim 0.2$  [2]. Therefore we conclude that heterovalent substitution for bismuth destroys space modulated magnetic structure at lower amount of substituent than homovalent substitution.



[1] A.V.Zalessky, et al., Europhys. Lett. 50, 547 (2000)

[2] A.V.Zalessky, et al., Solid State Physics 45(1), 134 (2003)



23PO-K-2

## SPATIALLY MODULATED STRUCTURES IN ANTIFERROMAGNETIC MULTIFERROIC WITH BIAXIAL ANISOTROPY

*Kulagin N.E.<sup>1</sup>, Popkov A.F.<sup>2</sup>, Zvezdin A.K.<sup>3</sup>, Soloviov S.V.<sup>2</sup>*

<sup>1</sup> State University of Management, Ryazanskii pr. 99, Moscow, 109542 Russia

<sup>2</sup> Moscow Institute of Electronic Technology, pr. 4806, str. 5, Zelenograd, Moscow, 124489 Russia

<sup>3</sup> Prokhorov General Physics Institute, Russian Academy of Sciences, ul. Vavilova 38, Moscow, 119991 Russia

In connection with the opening feasibility of controllable electric switching of the crystal magnetic state and electric property control using magnetic fields, multiferroics are promising for applications in spintronics and magnetoelectronics. Therefore, it is urgent to study the mechanism of appearance and disappearance of magnetically ordered structures induced by spontaneous polarization of the crystal and phase transitions between them [1, 2].

In this study possible types of spatially modulated periodic antiferromagnetic structures in a rhombohedral multiferroic with BiFeO<sub>3</sub> crystal symmetry were studied depending on the ratio of anisotropy and magnetoelectric interaction parameters. Detailed consideration of inhomogeneous magnetoelectric interactions in BiFeO<sub>3</sub> uniaxial multiferroics with space group R3c detected the presence of spatially modulated antiferromagnetic structures principally differing in the structure, energy and periodicity.

Analysis of inhomogeneous multiferroic states which represent antiferromagnet with flexomagnetoelectric interaction, take into consideration the small destruction of sublattices, when the total magnetization is small and the spatial change in the antiferromagnetic moment magnitude can be neglected. The free energy density of the system in this approximation includes the exchange energy, the flexomagnetoelectric energy and energy of the magnetic anisotropy.

In this study detailed analysis of spatially modulated antiferromagnetic structures for multiferroic with biaxial anisotropy were studied. We suppose that biaxial anisotropy may be caused by magnetocrystalline uniaxial anisotropy and the anisotropy induced by an external magnetic field. Investigation of spin-wave spectrum of the multiferroic in the homogeneous state shows that for some values of normalized anisotropy parameter this state is unstable with respect to the spin-wave excitation in the direction perpendicular to the antiferromagnetic vector. Helical and cone spatially modulated antiferromagnetic structures having lower energies are preferable for these regions. We show that helical solutions lose their stability and branch out for certain values of varied anisotropy parameters. At the existence boundaries of cone and helical structures their period becomes infinite. Phase diagram of possible antiferromagnetic structures was composed on the plane of anisotropy parameters.

We discuss also possible existence of antiferromagnetic vortex structures in the considered materials.

[1] A.M. Kadomtseva, Yu.F. Popov, A.P. Pyatakov, G.P. Vorob'ev, A.K. Zvezdin, and D. Viehland. *Phase Transitions* **79** 1019 (2006).

[2] N.E. Kulagin, A.F. Popkov, A.K. Zvezdin, *Fiz. Tverd. Tela* **53** 912 (2011) [*Phys. Solid State* **53** 970 (2011)].

23PO-K-3

**<sup>63,65</sup>Cu NMR STUDY OF THE MULTIFERROIC CuCrO<sub>2</sub>**

Ogloblichev V.<sup>1</sup>, Smolnikov A.<sup>1</sup>, Sadykov A.<sup>1</sup>, Yakubovsky A.<sup>2,3</sup>, Kumagai K.<sup>2</sup>, Piskunov Yu.<sup>1</sup>,  
Gerashenko A.<sup>1</sup>, Verkhovskii S.<sup>1</sup>, Barilo S.<sup>4</sup>

<sup>1</sup> Institute of Metal Physics, UB RAS, 620990 Yekaterinburg, Russia

<sup>2</sup> Russian Research Centre, "Kurchatov Institute", 123182 Moscow, Russia

<sup>3</sup> Department of Physics, Faculty of Science, Hokkaido University, 060-0810 Sapporo, Japan

<sup>4</sup> Institute of Solid State and Semiconductor Physics, 220072 Minsk, Belarus

We present the results of <sup>63,65</sup>Cu NMR research into paramagnetic and ordered states of a single crystal of the antiferromagnet CuCrO<sub>2</sub> having a triangular lattice consisting of Cr atoms. <sup>63,65</sup>Cu NMR spectra were taken in a wide range of temperatures (4-300) K and of magnetic fields  $H = (0-94)$  kOe directed in the plane  $ab$  and along the  $c$  axis of the crystal. The components of electric field gradient (EFG) tensor and of magnetic shift tensor ( $K_{ab,c}$ ) were obtained. The temperature dependences of  $K_{ab}(H||ab)$ ,  $K_c(H||c)$  are well described by the Curie-Weiss law for paramagnetic state and they resemble the magnetic susceptibility ( $\chi_{ab,c}$ ) behavior. The hyperfine field at copper sites  $H_{loc,ab,c} = 33$  kOe/ $\mu_B$  has been determined using the  $K_{ab,c}$  vs  $\chi_{ab,c}$  diagrams. The direction of the principle axis of EFG is aligned with the  $c$ -axis. The quadrupole frequency  ${}^{63}\nu_Q = 27.0(4)$  MHz and the parameter of asymmetry  $\eta$  is equal to 0. Below  $T = 24.2(3)$  K, the NMR line sharply broadens and with further decreasing  $T$ , the NMR spectrum becomes consisting of two peaks characteristic of incommensurate phases. The distance between the edge peaks in orientation  $H||c$  is five as large as that in  $H||ab$ .

Support by UB RAS (grant for young scientists No.3-m), RFBR (No 11-02-00354, No 09-02-00310), BRFFR (No F09K-017, No F10P-152), from the President of Russia through the grant for young scientists (MK-1232.2011.2) is acknowledged.

23PO-K-4

**SCATTERING OF LIGHT IN THE REGION OF FIELD INDUCED SPIN-ORIENTATION PHASE TRANSITION IN TbFe<sub>3</sub>(BO<sub>3</sub>)<sub>4</sub> SINGLE CRYSTAL**

Gnatchenko S.L.<sup>1</sup>, Kachur I.S.<sup>1</sup>, Piryatinskaya V.G.<sup>1</sup>, Bedarev V.A.<sup>1</sup>, Pashchenko M.I.<sup>1</sup>,  
Malakhovskii A.V.<sup>2</sup>, Bezmaternykh L.N.<sup>2</sup>, Sukhachev A.L.<sup>2</sup>, Temerov V.L.<sup>2</sup>

<sup>1</sup> B. Verkin Institute for Low Temperature Physics and Engineering,  
National Academy of Sciences of Ukraine, 61103 Kharkov, Ukraine

<sup>2</sup> L.V. Kirensky Institute of Physics, Siberian Branch of Russian Academy of Sciences, 660036  
Krasnoyarsk, Russian Federation

Spectroscopic and magneto-optical investigations of magnetic field induced spin-orientation phase transition in the single crystal TbFe<sub>3</sub>(BO<sub>3</sub>)<sub>4</sub> were performed. Behavior of the absorption spectra in the region of the phase transition testifies to the existence of a magnetic intermediate state with the periodic alternation of domains of low-field and high-field magnetic phases. In the same interval of magnetic fields the considerable reduction of light transmission of the crystal is observed (Fig. 1), which is a consequence of strong light scattering arising in the region of the phase transition.

Visual polarization investigations of the domain structure of the magnetic intermediate state were performed. It was shown that the high-field magnetic phase arises as cylindrical domains which are transformed into a labyrinth domain structure with the increasing field (Fig. 2). The strong scattering of light by the crystal is the result of the magnetic two-phase domain structure.

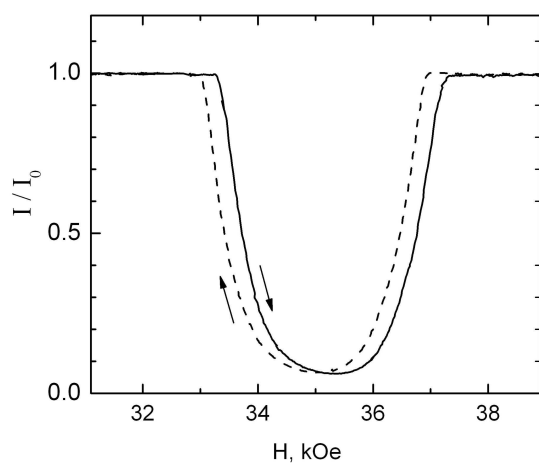


Fig. 1. Field dependence of light transmission of  $\text{TbFe}_3(\text{BO}_3)_4$  in the region of the phase transition.  $\mathbf{H} \parallel \mathbf{C}_3$ ,  $\mathbf{k} \parallel \mathbf{C}_3$ ,  $T = 2$  K.

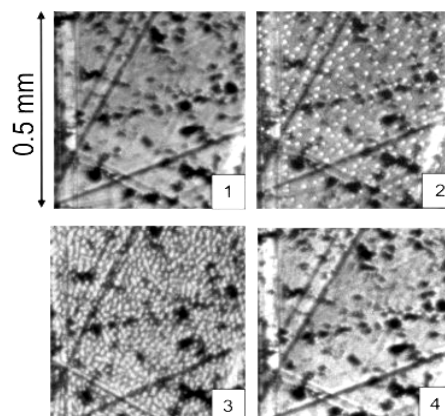


Fig. 2. Domain structure of intermediate magnetic state:  $H = 37.6$  kOe (1);  $38.8$  kOe (2);  $40.1$  kOe (3);  $42.6$  kOe (4).  $T = 8.3$  K.

The measurements of Faraday rotation and magnetic linear birefringence at  $\mathbf{H} \parallel \mathbf{k} \parallel \mathbf{C}_3$  were performed. In the high-field magnetic phase, the large magnetic circular birefringence appears, which is an order of magnitude larger than the value of the linear birefringence. This allows to infer that the main mechanism of the light scattering on the domains is related to the large value of the Faraday rotation in the high-field magnetic phase domains.

23PO-K-5

## HYBRID ELECTROMAGNETIC–SPIN-WAVE SPECTRUM OF MULTIFERROIC STRUCTURE WITH HIGH MAGNETIC ANISOTROPY

*Grigorieva N.Yu., Kalinikos B.A.*

Saint-Petersburg Electrotechnical University, St. Petersburg, 197376 Russian Federation

In the last years multiferroic layered structures based on hexaferrite and ferroelectric films draw much attention in connection with their dual tunability (electrical and magnetic) in terahertz frequency range [1-3]. Recent advances in growth technology of thin ferroelectric films, which are sputter deposited on the surface of the gold coated hexaferrite film, having low loss at microwaves, make these structures attractive for a variety of tunable microwave components and devices for millimeter-wave and terahertz applications [2]. Thus, the investigation of propagation characteristics of spin waves in such structures is now of great importance. Besides, it is well-known that fabrication of such complex layered structures in one technological cycle causes an uncontrollable spin pinning on the magnetic film interfaces. Therefore, an accounting of the asymmetrical spin-pinning conditions on two surfaces of the hexaferrite film is needed.

Here we present the analytical theory for hybrid dipole-exchange electromagnetic-spin waves propagating in multiferroic layered structure. The theory was elaborated in the frames of spin-wave

modes approach and takes into account a high magnetic volume anisotropy of the hexaferrite film, as well as an arbitrary type of spin-pinning conditions on both surfaces of the ferrite film.

The considered multiferroic layered structure (Fig. 1) is magnetized by a static magnetic field, oriented perpendicular to its plane. The direction of the bias magnetic field is chosen so as to make maximum use of the uniaxial anisotropy field characteristic for a hexaferrite film, which is perpendicularly oriented. The relation of propagation characteristics of the hybrid dipole-exchange electromagnetic-spin waves with surface spin-pinning conditions in the considered multiferroic layered structure is established. Hybrid dipole-exchange electromagnetic-spin wave spectrum is calculated for several values of spin-pinning parameters on the surfaces of the hexaferrite film. The dependence of the size of the dipole gaps in spin-wave spectrum vs. spin-pinning parameters is calculated.

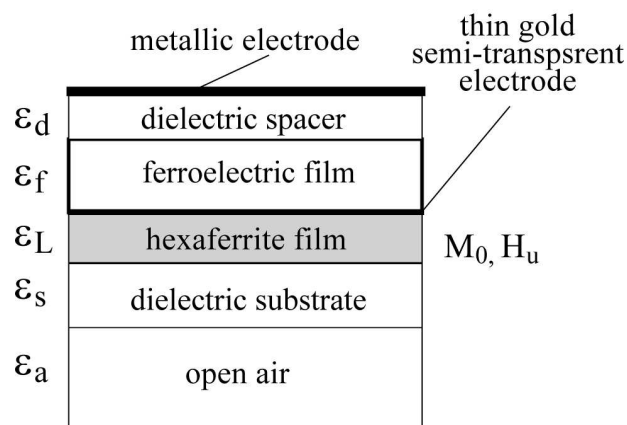


Fig.1

This work was supported in part by the Russian Foundation for Basic Research, by the RF Ministry of Education and Science under contracts 02.740.11.0231 and 02.740.11.0465, and the grant of the President of RF NSh-3783.2010.2.

- [1] Ce-Wen Nan, Bichurin, M.I., Shuxiang Dong, Viehland, D., and Srinivasan, G., *J. Appl. Phys.*, **103** (2008) 031101
- [2] Das, J., Kalinikos, B.A., Barman, A.R., and Patton, C.E., *Appl. Phys. Lett.*, **91** (2007) 172516
- [3] Grigoryeva, N.Yu., Sultanov, R.A., Kalinikos, B.A., *Electronics Letters*, **47**(1) (2011) 35
- [4] Kalinikos, B. A., Slavin, A. N., *J. Phys. C: Solid State Phys.*, **19** (1986) 7013

23PO-K-6

## COUPLED OSCILLATIONS OF ELECTRONIC AND NUCLEAR SPINS AND SPONTANEOUS POLARIZATION IN MULTIFERROIC $\text{BiFeO}_3$ : NMR PECULIARITIES

*Tankev A.P., Smagin V.V., Borich M.A.*  
Institute of Metal Physics, Yekaterinburg 620041, Russia

Epitaxial  $\text{BiFeO}_3$  films attract significant physical interest because of their multiferroic properties. They possess more than one ferroic order parameter simultaneously (ferroelectric, ferromagnetic and ferroelastic). The magnetization and the electric polarization reach large values in  $\text{BiFeO}_3$  films even at the room temperature. The materials are the interesting objects for modern microelectronics, magnetic memory and sensor technique (see [1,2] for example).

The work presents the results of theoretical investigation of coupled oscillations of electronic spins, nuclear spins and spontaneous polarization in single-phase epitaxial  $\text{BiFeO}_3$  films. The normal frequencies and dynamic susceptibility tensor are calculated. The peculiarities of the susceptibility tensor components in the vicinity of nuclear magnetic resonance (NMR) frequency

are investigated. The possibilities of the experimental detection of radically new types of NMR in these films are discussed. The first one consists in the excitation of NMR by radio-frequency magnetic field followed by detection of the dynamic component of spontaneous polarization at the frequency close to NMR frequency. The second one represents the excitation of oscillations of spontaneous polarization at the frequency close to NMR frequency by the driving electric field followed by detection of the dynamic component of magnetization (the principal possibilities of observation of these phenomena were discussed in [3,4]). These unusual types of NMR differ one from another in their basic characteristics, such as the enhancement factors, the dynamic frequency shifts and integral intensities of NMR signal. The comparative analysis of the proposed mechanisms of excitation and detection of NMR signal in multiferroic films BiFeO<sub>3</sub> is carried out.

The work was partially supported by the President of Russia sciences support program, grant No MK-1232.2011.2.

- [1] A.G. Zhdanov, A.K. Zvezdin et. al. *Phys. Tverdogo Tela*, **48** (2006) 83.  
 [2] I.E. Dzaloshinskii *Lett. Journal Exploring the Frontiers Physics*, **83** (2008) 67001.  
 [3] M.I. Kurkin, V.V. Leskovetc et. al. *Phys. Tverdogo Tela*, **45** (2003) 653.  
 [4] V.V. Leskovetc, E.A. Turov *Phys. Tverdogo Tela*, **42** (2000) 879.

23PO-K-7

## MAGNETIC PROPERTIES OF Nd<sub>0.6</sub>Dy<sub>0.4</sub>Fe<sub>3</sub>(BO<sub>3</sub>)<sub>4</sub>

Demidov A.A.<sup>1</sup>, Gudim I.A.<sup>2</sup>, Eremin E.V.<sup>2</sup>

<sup>1</sup> Bryansk State Technical University, 241035 Bryansk, Russia

<sup>2</sup> Kirensky Institute of Physics, Russian Academy of Sciences, 660036 Krasnoyarsk, Russia

The Nd<sub>0.6</sub>Dy<sub>0.4</sub>Fe<sub>3</sub>(BO<sub>3</sub>)<sub>4</sub> compound belongs to the family of rare-earth ferrobates, which exhibits a variety of phase transitions and some multiferroic features. In NdFe<sub>3</sub>(BO<sub>3</sub>)<sub>4</sub> at  $T < T_N \approx 31$  K magnetic moments of Nd and Fe lie in the basal plane *ab*. In DyFe<sub>3</sub>(BO<sub>3</sub>)<sub>4</sub> the magnetic moments of Dy and Fe are directed along the trigonal axis *c* at  $T < T_N \approx 39$  K and it shows the spin-flop transition for  $\mathbf{B} \parallel \mathbf{c}$ . Thus, as a result of competition of different contributions to the magnetic anisotropy of Nd<sub>1-x</sub>Dy<sub>x</sub>Fe<sub>3</sub>(BO<sub>3</sub>)<sub>4</sub> the rearrangement of the magnetic structure between the easy-axis and easy-plane states appears to be possible [1, 2]. With the increase of the parameter *x* the contribution from the Dy subsystem will more stabilize the easy-axis state of Nd<sub>1-x</sub>Dy<sub>x</sub>Fe<sub>3</sub>(BO<sub>3</sub>)<sub>4</sub> and the temperature of spontaneous spin-reorientation transition shifts toward higher temperatures. In this work the experimental and theoretical investigation of the field and temperature dependences of magnetization and the temperature dependences of the initial magnetic susceptibility of Nd<sub>0.6</sub>Dy<sub>0.4</sub>Fe<sub>3</sub>(BO<sub>3</sub>)<sub>4</sub> has been performed.

The single crystals have been grown using procedure particularly described in [2]. In the calculations we used a theoretical approach which has been successfully applied for description of the magnetic properties of the RFe<sub>3</sub>(BO<sub>3</sub>)<sub>4</sub> (see e.g. [3]). This approach is based on a crystal field model for the R ion and on the molecular field approximation. Comparison of calculation results with experimental data allowed to determine a set of parameters for Nd<sub>0.6</sub>Dy<sub>0.4</sub>Fe<sub>3</sub>(BO<sub>3</sub>)<sub>4</sub>: the intrachain Fe-Fe exchange field  $B_{dd1} \approx 56$  T, the f-d exchange fields  $B_{fd}^{Nd} \approx 11.5$  T and  $B_{fd}^{Dy} \approx 2.3$  T, the Fe-Fe exchange field, which includes the interchain interaction  $B_{dd2} \approx 28$  T.

Analysis of the experimental data and performed calculations showed that in  $\text{Nd}_{0.6}\text{Dy}_{0.4}\text{Fe}_3(\text{BO}_3)_4$  at low temperatures and  $B = 0$ , the magnetic moments of the  $\text{Nd}_{0.6}$ ,  $\text{Dy}_{0.4}$  and Fe-subsystems are oriented along the trigonal axis  $c$  (collinear phase). It can be seen from Fig. 1 that the experimental (symbols) and calculated (lines) magnetization curves  $M_c(B)$  at  $T = 2$  K in a magnetic field  $B_{\text{SF}} \approx 1.9$  T are characterized by a magnetization jump due to the spin-flop transition in the Fe subsystem from the initial collinear phase to the flop phase. Good agreement of experimental and calculations magnetization curves  $M_{c,\perp c}(B)$  at  $T = 2-40$  K and the temperature dependences of magnetic susceptibility  $\chi_{c,\perp c}(T)$  in the ordered and paramagnetic regions was achieved.

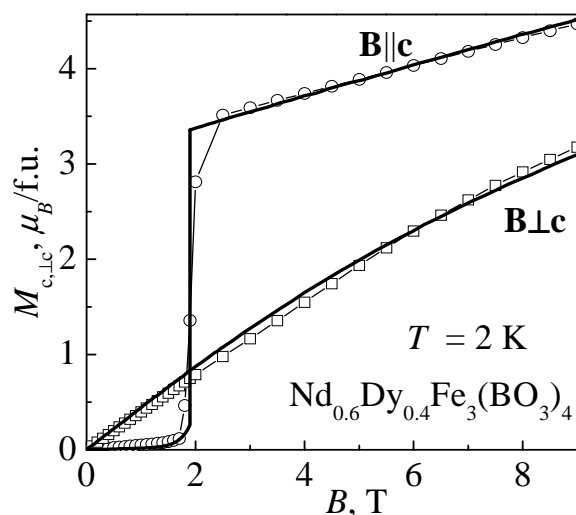


Fig. 1. Magnetization curves for  $\mathbf{B}_{\parallel, \perp c}$ .

Support by Grant of the President of the Russian Federation MK-497.2010.2 is acknowledged.

- [1] Yu.F. Popov, A.M. Kadomtseva, G.P. Vorob'ev et al., *JETP Lett.*, **89** (2009) 345.  
 [2] I.A. Gudim, E.V. Eremin, V.L. Temerov, *J. of Cryst. Growth*, **312** (2010) 2427.  
 [3] E.A. Popova, D.V. Volkov, A.N. Vasiliev et al., *Phys. Rev. B*, **75** (2007) 224413.

23PO-K-8

## STRUCTURAL TRANSITION AND MAGNETOELECTRIC COUPLING IN MULTIFERROIC $\text{BiFeO}_3$ AND $(\text{Bi}_{0.95}\text{Nd}_{0.05})\text{FeO}_3$ CERAMICS

Ding Y.<sup>1,2</sup>, Wu K.T.<sup>1,3</sup>, Tu C.S.<sup>1,3</sup>, Wang T.H.<sup>1</sup>, Ku C.S.<sup>4</sup>, Lee H.Y.<sup>4</sup>, Yao Y.D.<sup>1</sup>

<sup>1</sup> Graduate Institute of Applied Science and Engineering, Fu Jen Catholic University, Taipei 242, Taiwan

<sup>2</sup> Teaching Center of Natural Sciences, Minghsin University of Science and Technology, Hsinchu 304, Taiwan

<sup>3</sup> Department of Physics, Fu Jen Catholic University, Taipei 242, Taiwan

<sup>4</sup> National Synchrotron Radiation Research Center, Hsinchu Science Park, Hsinchu 30076, Taiwan

*In-situ* high-resolution synchrotron x-ray diffraction, magnetization, dielectric permittivity, grain size, and current density were carried out as a function of temperature in  $\text{BiFeO}_3$  (BFO) and  $(\text{Bi}_{0.95}\text{Nd}_{0.05})\text{FeO}_3$  ceramics synthesized by the solid-state-reaction method. The temperature-dependent synchrotron x-ray diffraction reveals a rhombohedral – orthorhombic – cubic transition sequence near 820 and 850 °C in BFO upon heating. As shown in Fig. 1,  $(\text{Bi}_{0.95}\text{Nd}_{0.05})\text{FeO}_3$  ceramic exhibits a transition sequence of rhombohedral – orthorhombic – cubic near 710 and 750 °C, respectively. Upon heating, the dielectric permittivity exhibits a pronounced frequency-dependent dielectric maxima in the region of and 300-500 °C in both  $\text{BiFeO}_3$  and  $(\text{Bi}_{0.95}\text{Nd}_{0.05})\text{FeO}_3$  ceramics. It suggests a coupling between ferroelectric and magnetic parameters near the antiferromagnetic (AFM) – paramagnetic (PM) transition, which may trigger a magnetoelectric response to cause the

dielectric maximum response under application of measuring electric field. The rhombohedral distortion angle  $\alpha_R$  shows a local minimum near 400 °C in both BFO and  $(\text{Bi}_{0.95}\text{Nd}_{0.05})\text{FeO}_3$  ceramics, implying a maximum distortion of the perovskite structure as temperature approaches the AFM–PM transition near 400 °C. In addition, as shown in Figure 2, BFO exhibits an antiferromagnetic behavior, whose magnetization curve is linear with the field at room temperature. Similar antiferromagnetic behavior occurs in  $(\text{Bi}_{0.95}\text{Nd}_{0.05})\text{FeO}_3$  ceramics sintered at 890-960 °C.  $(\text{Bi}_{0.95}\text{Nd}_{0.05})\text{FeO}_3$  ceramics sintered at 960 exhibit a weak ferromagnetic phenomenon with remanent magnetizations of  $\sim 0.006$  emu/g at room temperature. The magnetic susceptibilities of BFO and  $(\text{Bi}_{0.95}\text{Nd}_{0.05})\text{FeO}_3$  ceramics are about  $1.9 \times 10^{-5}$  and  $8.4 \times 10^{-6}$  (emu/g·Oe), respectively. A frequency-dependent and broad dielectric maximum was observed in both BFO and  $(\text{Bi}_{0.95}\text{Nd}_{0.05})\text{FeO}_3$  upon heating. This dielectric response is likely triggered by the antiferromagnetic (AFM) – paramagnetic (PM) transition near the Néel temperature. Grain size of  $(\text{Bi}_{0.95}\text{Nd}_{0.05})\text{FeO}_3$  ceramics exhibits a significant growth as sintering temperature increases. The current density was also carried out as a function of temperature, which exhibits a slope change as temperature approaches the Néel temperature. This further confirms a magnetoelectric coupling in the AFM–PM transition region. This work was supported by the Sapintia Education Foundation.

23PO-K-9

## ELLIPSOMETRIC STUDY OF ANISOTROPY PERMITTIVITY OF HEXAGONAL MANGANITES $\text{RMnO}_3$ ( $R = \text{Ho}, \text{Tm}, \text{Yb}$ )

*Makhnev A.A.<sup>1</sup>, Nomerovannaya L.V.<sup>1</sup>, Balbashov A.M.<sup>2</sup>*

<sup>1</sup>Institute of Metal Physics UD RAS, 620041, Ekaterinburg, Russia

<sup>2</sup>Moscow Power Engineering Institute, 105835, Moscow, Russia

Hexagonal manganites  $\text{RMnO}_3$  ( $R = \text{Ho-Lu}, \text{Y}$ ) are compounds in which a ferroelectric and an antiferromagnetic order may coexist (multiferroic). Hexa- $\text{RMnO}_3$  exhibit changes in physical properties depending on the rare-earth ( $R$ ) element. The anisotropy of permittivity was not studied in  $\text{RMnO}_3$  except for  $\text{YMnO}_3$  and  $\text{HoMnO}_3$ . To understand the physics involved in  $\text{RMnO}_3$ , it is necessary to know their electronic structure. Such information can be extracted from optical data.

We report the ellipsometric study of anisotropy real  $\varepsilon_1(E)$ , and imaginary,  $\varepsilon_2(E)$ , parts of the complex permittivity of hexa- $\text{RMnO}_3$  ( $R = \text{Ho}, \text{Tm}, \text{Yb}$ ) single crystals in the 0.8 - 4.8 eV spectral range at the temperature  $T = 300$  K. The samples were grown by the floating-zone method with radiation heating. The measurements of optical constants were carried out for polarizations  $\mathbf{E} \perp c$  and  $\mathbf{E} \parallel c$  for the samples with cleanest surface (as grown) and with polished.

At  $T = 300$  K the strong anisotropy of  $\text{RMnO}_3$  optical function manifests itself in both the character of the spectral dependence and their different numerical values. The spectral dependences of the  $\varepsilon_1(E)$  and  $\varepsilon_2(E)$  for  $\text{HoMnO}_3$ ,  $\text{TmMnO}_3$  and  $\text{YbMnO}_3$  single crystals were qualitatively similar. The spectra  $\varepsilon_2(\omega)$  of three the materials show interband optical transitions located at the near frequencies. The spectrum of the  $\varepsilon_2(E)$  for polarization  $\mathbf{E} \perp c$  exhibits a very intense asymmetric narrow band at near 1.5 eV, an extended plateau centered at near 2.4 eV and an asymmetric broad band at  $\sim 4.6$  eV. For polarization  $\mathbf{E} \parallel c$  the  $\varepsilon_2(E)$  function has the bands at  $\sim 3.4$  and  $\sim 4.7$  eV, and the narrow band is shifted to  $\sim 1.7$  eV and its intensity decreases. This similar in the optical spectra of the hexa- $\text{RMnO}_3$  is the starting point of our analysis of their electronic structure. This most likely is due to close degree of anisotropy of the lattice parameters  $c/a$  and the fact that the electron transitions involving rare-earth ions do not give a significant contribution to the energy range 1.0-5.0 eV. The optical transitions in hexa- $\text{RMnO}_3$  should be regarded as an interband charge transfer

excitation from the O(2p) states strongly hybridized with Mn(3d) to Mn(3d) states. The spectra are analyzed on the basis of a band model of the anisotropy interband transitions [1]. The experimental character of anisotropy of the complex permittivity is not suitable for explaining the electronic structure of hexa- $RMnO_3$  compounds. The agreement is not so good. Our experiment have confirmed that the energy of the intense electronic transition near 1.5 eV is changed as the radius of the  $R$  ion change like as in number of hexa- $RMnO_3$  ( $R=Gd-Ho, Y$ )-family film samples [2]. The position the peak for body single crystals is 1.57, 1.52, 1.50 eV for  $HoMnO_3$ ,  $TmMnO_3$  and  $YbMnO_3$ , respectively. The broad absorption band appears in the  $\epsilon_2(E)$  spectra of study compounds in the near-infrared region. It is possible, that the origin of the near-infrared  $\epsilon_2(E)$  absorption is associated with 4f-4f transitions of  $R^{3+}$  ions, which were founding in the transmission spectra at the energies below the fundamental absorption edge [3].

[1] M. Qian, J. Dong, D.Y. Xing, *Phys. Rev.*, **B 63** (2001) 155101.

[2] W.S. Choi, D.G. Kim, S.S.A. Seo, S.Y. Moon, D. Lee, J.H. Lee, H.S. Lee, D.Y. Cho, Y.S. Lee, P. Murugavel, J. Yu, and T.W. Noh, *Phys. Rev.*, **B 77** (2008) 045137.

[3] N.N. Loshkareva, E.V. Mostovshchikova, A.S. Moskvina, S.V. Naumov, N.V. Kostromitina, and A.M. Balbashov, *Solid State Phenomena*, **168-169** (2011) 549.

23PO-K-10

## PERMITTIVITY AND MULTIFERROIC STUDIES OF $SiO_2/Co/SiO_2$ FILMS

*Ding Y.<sup>1,2</sup>, Yao Y.D.<sup>1</sup>, Wu K.T.<sup>3</sup>, Hsu J.C.<sup>3</sup>, Hung D.S.<sup>4</sup>, Wei D.H.<sup>5</sup>*

<sup>1</sup> Graduate Institute of Applied Science and Engineering, Fu Jen University, Taipei, 242, Taiwan

<sup>2</sup> Center of General Edu., Ming Hsin Univ. of Sci. and Techn., Hsinchu 304, Taiwan

<sup>3</sup> Department of Physics, Fu Jen University, Taipei 242, Taiwan

<sup>4</sup> Dept. of Inform. and Tele. Engn., Ming Chuan Univ., Taipei 111, Taiwan

<sup>5</sup> Dept. of Mech. Engn., Taipei Univ. of Techn., Taipei 106, Taiwan

Co inserted layer with different thickness on the dielectric permittivity of  $SiO_2(60\text{ nm})/Co(x\text{ nm})/SiO_2(60\text{ nm})$  thin films fabricated on glass B270 substrates by the reactive sputtering technique was studied. The variation of dielectric constant for films is dependent on the thickness of the Co inserted layer observed from 40 Hz to 30 MHz. The dielectric constant is around 7.4 for B270 glass substrate and  $SiO_2/B270$  film. However, for the  $SiO_2/Co/SiO_2$  films, it is raised up to 55 for even with a 2 nm thick Co inserted layer. This large enhancement behavior of the dielectric constant could be explained due to the growth mechanism of the Cobalt inter-layer from island clusters to continuous Co layer for samples with  $x$  between 1 and 2 nm. For the magnetic induced ferroelectric variation, the variation of the dielectric constant increased with thickness of Co for samples with  $x$  larger than 2 nm. However this increase behavior is roughly saturated for applied magnetic field roughly above 60 Oe. A direct observation of a 0.04 ~ 0.20 % dielectric tunability is achieved.



23PO-K-11

**GROWTH AND PROPERTIES OF MULTIFERROIC THIN FILMS  $\text{YMnO}_3$** *Andreev N.V.<sup>1</sup>, Chichkov V.I.<sup>1</sup>, Sviridova T.A.<sup>1</sup>, Tabachkova N.Yu.<sup>1</sup>, Volodin A.P.<sup>2</sup>, Mukovskii Ya.M.<sup>1</sup>*<sup>1</sup> National Science and Technology University "MISiS", Leninskii prosp., 4, Moscow, Russia<sup>2</sup> Katholieke Univ Leuven, Lab Solid State Phys & Magnetism, Celestijnenlaan 200 D, BE-3001 Leuven, Belgium

Single crystal thin films  $\text{YMnO}_3$  were grown by RF magnetron sputtering on (001)  $\text{Al}_2\text{O}_3$  and (111)  $\text{SrTiO}_3$  substrates with (111) platinum functional sublayer. X ray analysis and electron microscopy have shown epitaxial growth of platinum to a single crystalline substrate and manganite to platinum. The surface topography of the films was observed by atomic force microscopy and a piezo-force microscope has been used to demonstrate the ferroelectric nature of the films. The magnetic phase transition in samples takes place at  $T_N \sim 40$  K. In the ZFC case when heating in the field one can see distinct antiferromagnetic response, and in the FC case one can see the magnetization due to induced ferromagnetism.

23PO-K-12

**ELASTIC MODEL FOR THE STUDY OF MOLECULAR MAGNETS***Enachescu C., Stoleriu L., Stancu A.*

Faculty of Physics, Alexandru Ioan Cuza University, 700506, Iasi, Romania

The spin transition compounds are molecular magnets, switchable between two states in thermodynamic competition: the diamagnetic low spin state (LS) and the paramagnetic high spin state (HS). When the elastic interactions in these systems are stronger than a threshold value, the abrupt transition is accompanied by complex hysteresis processes like thermal or pressure hysteresis, which makes them suitable for a wide range of applications.

We model here the hysteretic and relaxation behavior in spin transition compounds, considering the molecules situated in a bi-dimensional hexagonal lattice and interacting by the way of elastic connecting springs [1-3], that stand for both long range and short range interactions. Even if the present model uses less parameters, it is able to simulate all the main experimental curves, and predict the clustering and nucleation phenomena. At high temperature, the molecules are in the HS state; by lowering the temperature they pass to LS state, if able to exceed the elastic force from the closest springs. The switch of individual molecules is checked randomly by a Monte Carlo procedure. When a molecule changes its state, the new equilibrium positions of all molecules are calculated. The transition of a molecule from a state to another corresponds to a change of its volume (HS molecules have a bigger volume) and modifies the global interactions in the system and finally the position of each molecule.

In Fig. 1a we present how the interactions are influencing the width and shape of the hysteresis: smooth transition showing no hysteresis in absence of interactions and steeper hysteresis for increasing interactions, similar to experimental curves presented elsewhere. The effect of the system size is presented in fig. 1b and show a behavior in good agreement with very recent experimental data on spin crossover nanoparticles (width increasing for larger system sizes). For moderate values of the spring constant, some clusters form, but on average the HS and LS molecules are distributed randomly in the sample during the relaxation process (Fig. 2a). If the spring constant is high enough

then the clusters are bigger and develop faster throughout the sample leading to fluctuations, and nucleation and growth phenomenon (Fig 2b). An infinite avalanche process is then leading to non-random distributions of HS and LS complexes [4].

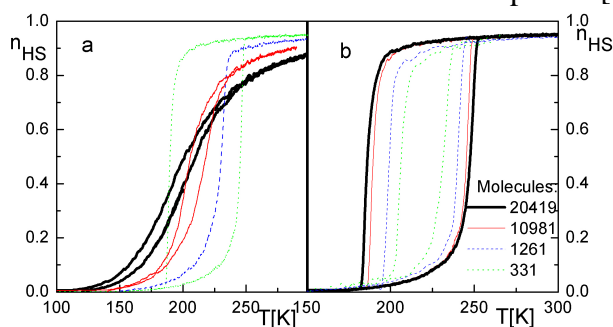


Fig.1 Thermal hysteresis for different interactions (a) and system sizes.(b)

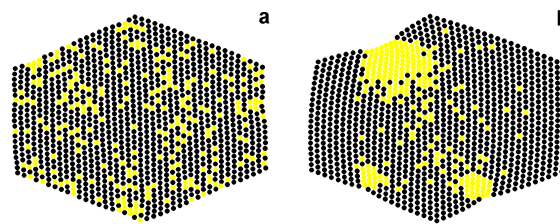


Fig. 2 Snapshots of spin configurations when around 10% of molecules are in the LS state showing the difference between the behavior observed for weak (a) and strong (b) interactions

Support by Romanian CNCSIS (TE 182/2010) is acknowledged.

- [1] C. Enachescu, L. Stoleriu, A. Stancu, A. Hauser, *Phys. Rev. Lett.*, **102**, 257204, 2009  
 [2] C. Enachescu, M. Nishino, S. Miyashita, L. Stoleriu, A. Stancu, A. Hauser, *EPL*, **91**(2), 27003, 2010  
 [3] C. Enachescu, L. Stoleriu, A. Stancu, A. Hauser, *Phys. Rev. B*, **82**(10), 104114, 2010  
 [4] M. Nishino, C. Enachescu, S. Miyashita, F. Varret, *Phys. Rev. B*, **82**(2), 020409, 2010

23PO-K-13

## EVIDENCE OF p-d AND d-d CHARGE TRANSFER AND INSULATOR-TO-METAL PHASE TRANSITIONS IN NONLINEAR OPTICAL RESPONSE OF $(La_{0.6}Pr_{0.4})_{0.7}Ca_{0.3}MnO_3$

Ivanov M.<sup>1</sup>, Mishina E.<sup>1</sup>, Firsova N.<sup>1</sup>, Moshnyaga V.<sup>2</sup>, Fiebig M.<sup>3</sup>

<sup>1</sup> Moscow State Institute of Radioengineering, Electronics and Automation, prosp. Vernadskogo 78, 119454 Moscow, Russia

<sup>2</sup> Universitaet Goettingen, Friedrich-Hund- Platz 1, 37077, Goettingen, Germany

<sup>3</sup> Universitaet Bonn, Nussallee 14-16, 53115, Bonn, Germany

We report the evidence of p-d and d-d charge transfer transition and insulator-to-metal phase transitions in optical second harmonic generation (SHG) in  $(La_{0.6}Pr_{0.4})_{0.7}Ca_{0.3}MnO_3$  (LPCMO) thin film. LPCMO perovskite is an  $O'$ - orthorhombic manganate with  $P6_3/mmm$  space group with four- and three-electron energy levels of the  $Mn^{3+}(d^4)$  and  $Mn^{4+}(d^3)$  states, respectively, in octahedral crystal field.

SHG spectra for specific light polarization combinations show two bands at 3.4 and 2.8 eV. Considering the influence of applied magnetic field and Jahn-Teller effect on the SHG spectra, as well as taking into account the data on electronic structure of the orthorhombic manganites we conclude that the observed energy bands correspond the doubled energy of the well known charge transfer transitions  $Mn(^5\Gamma_1 \square > ^5\Gamma_6)$  and  $Mn(^5\Gamma_1 \square > ^5\Gamma_5)$  at 1.725 eV and 1.4 eV, respectively [1].

Colossal magnetoresistance manganites, particularly LPCMO, are characterized by electronic phase separation with coexisting paramagnetic insulating and ferromagnetic metallic phases [2]. In

LPCMO an insulator-to-metal transition temperature,  $T_{IM}$ , is very close to Curie temperature,  $T_C$ , i.e.  $T_{IM}=T_C=190\text{K}$ . To distinguish insulator-to-metal transition the temperature measurements of SHG intensity at resonant laser pump energy of 1.725 eV were carried out. The SHG intensity decreases significantly near  $T_{IM}$  as the temperature increases. A minimum of the SHG signal at  $T_{IM}=190\text{K}$  is shifted by about 15 K when magnetic field of 6 kOe is applied; this is consistent with the field-induced shift of insulator-to-metal transition, observed by other techniques [3].

The work is partly supported by DAAD.

[1] A. S. Moskvina et al., Phys. Rev. B **82**, 035106 (2010).

[2] G. Singh-Bhalla, A. Biswas, A.F. Hebard. Phys. Rev. B **80**, 144410 (2009).

[3] T.Z. Ward et al., Nature Phys. **5**, 885 (2009).

23PO-K-14

### <sup>57</sup>Fe MOSSBAUER STUDY OF MULTIFERROIC $\text{Bi}_{0.65}\text{Sr}_{0.35}\text{FeO}_3$

*Konovalova A., Pokatilov V.*

Moscow State Institute of Radioengineering, Electronics, and Automation (Technical University),  
Vernadsky pr. 78, Moscow, 119454 Russia

Perovskites based on  $\text{BiFeO}_3$  are interesting objects for studying the magnetoelectric effect [1].  $\text{BiFeO}_3$  exhibits long-range antiferromagnetic ( $T_N=640\text{ K}$ ) and ferroelectric ( $T_C=1083\text{ K}$ ) ordering [1]. The compound has a rhombohedral distorted perovskite structure and a spatial spin-modulated structure (SSMS) of the cycloidal type with  $T_N\approx 640\text{ K}$  and the modulation period  $\lambda\approx 620\text{ \AA}$ , which is incommensurate with the crystal lattice parameters [2]. The values of electric  $P_0$  and magnetic  $M_0$  polarizations in  $\text{BiFeO}_3$  are small because the SSMS averages  $P_0$  and  $M_0$  [3]. As noted in [3], the destruction of the SSMS in the  $\text{BiFeO}_3$  compound must lead to increasing both  $P_0$  and  $M_0$ . It was found the ions  $\text{Sr}^{2+}$  substitution for ions  $\text{Bi}^{3+}$  leads to suppression of the SSMS in the rhombohedral structure with Sr content  $x=0.1\text{ mol.}\%$  [4]. The aim of the present work is to study in detail the local valence and magnetic states of the  $\text{Bi}_{0.65}\text{Sr}_{0.35}\text{FeO}_3$  sample by <sup>57</sup>Fe Mossbauer spectroscopy.

The  $\text{Bi}_{0.65}\text{Sr}_{0.35}\text{FeO}_3$  sample was prepared in air by a conventional solid-state synthesis. X-ray diffraction measurements showed that the samples were single-phase and had a cubic structure and  $a=0.3943\text{ nm}$ . The sample was studied by <sup>57</sup>Fe Mossbauer spectroscopy at 87, 295 and 670 K (above the Neel temperature). Mossbauer spectra were processed for the Lorentzian line shape by the least squares method using DISTRI (restoration of distributions of hyperfine interactions parameters) and SPECTR (model analysis) programs [5]. The temperature of the magnetic phase transition of the  $\text{Bi}_{0.65}\text{Sr}_{0.35}\text{FeO}_3$  sample was determined using the technique for temperature scanning of the count rate of  $\gamma$  quanta  $N(T)$  and  $T_N=667\pm 5\text{ K}$ .

A detailed analysis of these spectra at 87, 295 and 670 K using the DISTRI program suggests that it is necessary for their good description to introduce: a superposition of at least two overlapping doublets, differing in isomer shift and quadrupole splitting which corresponds to two non-equivalent crystallographic states above  $T_N$ ; a superposition of four sextets which corresponds to four non-equivalent magnetic states below  $T_N$ . However, three sextets with the equal isomer shifts ( $\delta_1 \approx \delta_2 \approx \delta_3 = 0.35\text{ mm/s}$ ) correspond to the ions  $\text{Fe}^{3+}$  in the octahedral oxygen environment; in the fourth sextet, the ions  $\text{Fe}^{3+}$  are in the squared pyramidal environment ( $\delta_4 = 0.25\text{ mm/s}$ ). These four

magnetic states are due to different values of local magnetic moments ions  $\text{Fe}^{3+}$  caused by the appearance of ions  $\text{Sr}^{2+}$  in the near environment of ions  $\text{Fe}^{3+}$ .

This work was supported by the Russian Foundation for Basic Research, project No 09-02-00072a.

- [1] Venevtsev Yu. N., Gagulin V. V., Lyubimov V.N., *Ferroelectromagnets* (Nauka, Moscow, 1982) [in Russian].  
 [2] I. Sosnowska, R. Przenioslo, P. Fischer and V.A. Murashov. *J. Magn. Magn. Mater.* **160**, p. 383 (1996).  
 [3]. Zvezdin A. K., Pyatakov A. P., *Usp. Fiz. Nauk* **174** (4), p. 465 (2004) [in Russian].  
 [4] Pokatilov V.S., Pokatilov V. V., Sigov A. S., Konovalova A. O., *Bull. of the Russian Academy of Sciences: Physics*, **174** (8), p.1115 (2010).  
 [5] Rusakov V.S. *Mossbauer spectroscopy of locally inhomogeneous systems*. (Almaty, Kazakhstan 2000, [in Russian])

23PO-K-15

## SPECIFIC HEAT OF QUASI-ONE-DIMENSIONAL ANTIFERROMAGNET $\beta\text{-TeVO}_4$

*Bludov O.M.<sup>1</sup>, Savina Yu.O.<sup>1</sup>, Pashchenko V.A.<sup>1</sup>, Gnatchenko S.L.<sup>1</sup>, Szewczyk A.<sup>2</sup>,  
Lemmens P.<sup>3</sup>, Berger H.<sup>4</sup>*

<sup>1</sup> B.I. Verkin Institute for Low Temperature Physics and Engineering, NASU, 47 Lenin Ave., 61103 Kharkov, Ukraine

<sup>2</sup> Institute of Physics, PAS, al. Lotników 32/46, PL-02-668 Warsaw, Poland

<sup>3</sup> Institute for Condensed Matter Physics, TU Braunschweig, D-38106 Braunschweig, Germany

<sup>4</sup> Institute of Physics of Complex Matter, EPFL, 1015 Lausanne, Switzerland

Temperature dependence of specific heat  $C_p(T)$  of single crystal  $\beta\text{-TeVO}_4$  was measured in the temperature range 2.5-300 K at zero magnetic field. The crystal structure consists of zigzag chains formed by slightly distorted square pyramids  $\text{VO}_5$  sharing corners. The magnetic susceptibility data of the compound shows behavior, which is characteristic for an infinite uniform spin- $1/2$  chain with the intrachain antiferromagnetic (AF) exchange coupling  $J/k_B=21.4$  K [1]. Fig. 1 shows the temperature dependence of specific heat of the crystal up to 32K. Two features were observed on temperature dependence  $C_p(T)$ :

1) two  $\lambda$ -anomalies at temperatures 4.6K and 3.2K which can be interpreted as phase transitions to a long-range-ordered AF state and the further modification of the ordered phase of the studied quasi-one-dimensional spin system;

2) a broad maximum at temperature near 10K. This kind of specific heat behavior is typical for one-dimensional AF spin systems. In low temperature range the specific heat can be described as the sum  $C_p(T) = C_{mag}^{1D}(T) + C_{lat}(T)$ , where  $C_{mag}^{1D}(T)$  is the specific heat of the infinite AF spin- $1/2$  chain [2],  $C_{lat}(T)$  is the lattice contribution. The lattice contribution can be expressed as  $C_{lat}(T) = 264 * R * (T/\theta_D)^3$  in low temperature limit. In the temperature range 5-20K the best fit was obtained for the following parameters: the AF exchange constant  $J/k_B=19.7$ K and the Debye temperature  $\theta_D=167$ K.

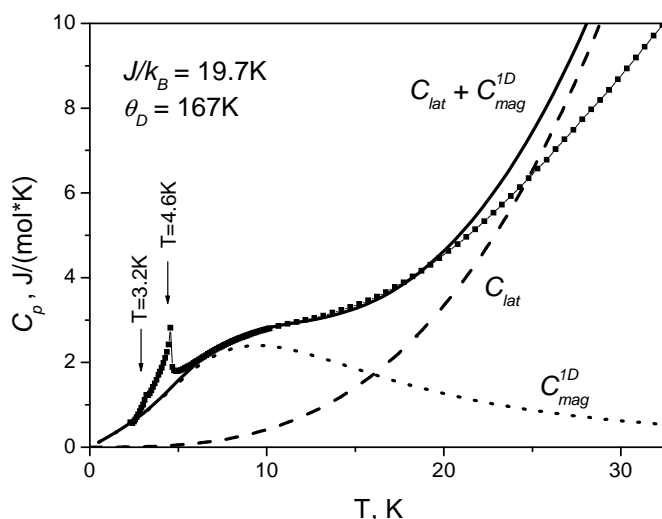


Fig. 1 Temperature dependence of specific heat  $C_p(T)$  of single crystal  $\beta$ -TeVO<sub>4</sub>. Solid square – the experimental data, solid line – the sum of magnetic and lattice contributions, dotted line – the magnetic contribution of AF spin-1/2 chain  $C_{mag}^{1D}(T)$ , dashed line – the lattice contribution  $C_{lat}(T)$ .

- [1] Yu.O. Savina, O.M. Bludov, V.A. Pashchenko, S.L. Gnatchenko, P. Lemmens, and H. Berger, “Magnetic properties of the antiferromagnetic spin-1/2 chain system  $\beta$ -TeVO<sub>4</sub>” [in press].  
 [2] D.C. Johnston, R.K. Kremer, M. Troyer, X. Wang, A. Klumper, S.L. Bud’ko, A.F. Panchula, P.C. Canfield, Physical Review B **61**, 9558, 2000.

23PO-K-16

## HIGH-TEMPERATURE ( $T \gg T_C$ ) FERROMAGNETIC CLUSTERS IN $\text{Pr}_{1-x}\text{Ca}_x\text{MnO}_3$ ( $x=0.15 - 0.30$ ): THE MAGNETIC, RESISTIVE AND DIELECTRIC DATA

Tarasenko T.N.<sup>1</sup>, Makovetskii G.I.<sup>2</sup>, Radyush Yu.V.<sup>2</sup>, Yanushkevich K.I.<sup>2</sup>

<sup>1</sup> Donetsk Institute for Physics and Engineering named after O.O. Galkin, NAS of Ukraine, R.Luxemburg Str., 72, 83114, Donetsk, Ukraine

<sup>2</sup> Scientific-Practical Materials Research Center, NAS of Belarus, P.Brovka Str., 19, 220072, Minsk, Belarus

Interesting property of mixed-valence manganites is the existence of phase separation state [1]. Above the temperatures of ferromagnetic (FM)  $T_C$ , antiferromagnetic (AFM)  $T_N$  and charge ( $T_{CO}$ ) ordering some region (temperature window), where the clusters of these states coexist, is present [1]. It is possible that this window have properties of pseudo-gap as in high temperature superconductors. It is known [1-4] that the  $\text{Pr}_{1-x}\text{Ca}_x\text{MnO}_3$  system has a complex ( $x, T$ ) phase diagram [2] and undergoes some concentration magnetic phase transitions.

The investigations of magnetic, transport and dielectric properties of polycrystalline  $\text{Pr}_{1-x}\text{Ca}_x\text{MnO}_3$  ( $x=0.15, 0.25$  and  $0.30$ ) have been performed in a wide temperature range. Ceramic samples of  $\text{Pr}_{1-x}\text{Ca}_x\text{MnO}_3$  were prepared through conventional solid state reaction. In accordance with the X-ray diffraction study the samples are single-phase and have an orthorhombic structure (Pbnm - symmetry). All samples under study reveal an unusual high values of specific magnetization  $\sigma(T)$  at  $T \gg T_C$ . We can assert the importance of magnetic clustering below temperatures  $\approx 6T_C$  in  $\text{Pr}_{1-x}\text{Ca}_x\text{MnO}_3$  ( $0.15 \leq x \leq 0.30$ ). The temperature dependences of the inverse magnetic susceptibility  $1/\chi(T)$  have a typical ferromagnetic form, in which long-range ordering is destroyed, but short-range ordering is still retained. Obtained experimental data on the magnetic properties of  $\text{Pr}_{1-x}\text{Ca}_x\text{MnO}_3$  manganites can be explained on the basis of model of spatial phase

separation. In [3] it was shown that charge ordering rare-earth manganites (including  $Pr_{0.7}Ca_{0.3}MnO_3$ ) appear properties of multiferroics.

All samples under study show semiconductor properties in the temperature range  $77 \leq T \leq 850$  K. Compositions with  $x=0.15$  and  $x=0.3$  expressly have transition to intrinsic conductivity at high temperatures. Therefore one can estimate the energy gap width of semiconductor component of conductivity using dependence of  $\ln\sigma=f(10^3/T)$ . The  $Pr_{0.85}Ca_{0.15}MnO_3$  sample has the energy gap width  $\Delta E=0,432$  eV and  $Pr_{0.7}Ca_{0.3}MnO_3$  -  $\Delta E=0,484$  eV. The observed strong dispersion of both components of dielectric permeability ( $\epsilon'$  and  $\epsilon''$ ) testifies to powerful polarization of samples. The large values of  $\epsilon'$  and  $\epsilon''$  in  $Pr_{1-x}Ca_xMnO_3$  are related to a high dc conductivity (through conductivity), what the large values of dielectric dissipation testify to ( $tg\delta > 1$  at room temperatures even for 1MHz). There is some correlation between temperature dependences of specific resistance and specific magnetization in temperature region 600-700 K.

Thus a new scale  $T^* \approx 600-700$  K for cluster formation in multiferroic  $Pr_{1-x}Ca_xMnO_3$  is determined. The temperature window  $T_C \leq T \leq T^*$ , where FM and AFM clusters coexist, is discussed.

Support by the Joint project of FRSF of Ukraine (№F41.1/020) and Belarusian RFFR (№ F11K-054).

[1] E.Dagotto et al., *Phys.Rep.*, **344**, (2001) 1.

[2] C. Martin et al., *Phys.Rev.***B60**, (1999) 3233.

[3] C.R.Serrao et al., *J.Phys.:Cond.Matter.***19**,496217 (2007).

[4] V.S. Kolat et al., *JMMM*, **322**, (2010) 427.

23PO-K-17

## ELECTRIC FIELD CONTROL OF MICROMAGNETIC STRUCTURE BY MEANS OF SCANNING PROBE MICROSCOPY

*Bodunova A.S.<sup>1</sup>, Pyatakov A.P.<sup>1</sup>, Temiryazeva M.P.<sup>2</sup>, Lisovskii F.V.<sup>2</sup>, Logginov A.S.<sup>1</sup>*

<sup>1</sup> Physics Department, M.V. Lomonosov Moscow State University, Moscow, Russia

<sup>2</sup> The Institute of Radioengineering and Electronics of RAS, Fryazino, Russia

Recently much attention is paid to studies of magnetoelectric and multiferroic materials. The influence of electric field on magnetic properties of the sample can appear as micromagnetic structure transformation rather than macroscopic changes of magnetic properties. In this context the scanning probe technique (SPM) is needed to induce and measure magnetic domain-wall motion/transformation at the local level [1-3].

In this paper the SPM technique is used to verify the hypothesis about the electric polarization associated with magnetic domain walls due to the local reducing of crystal symmetry in the magnetic inhomogeneities [4]. As the samples there were chosen iron garnets films as their micromagnetic structure can be readily visualized by magneto-optical observation in this type of materials. Furthermore the electric field controlled displacement of magnetic domain walls was demonstrated in these films [5].

In view of the global miniaturization the substantial improvement of the electric field control can be the transition to the nanoscale using the tip of SPM probe (see the Figure). These are magneto-optical images of iron garnet film containing stripe domain structure. The dark area is the SPM probe used as the source of static electric field. In the selected area we can see the attraction of the

domain head under the positive electric potential. For better view the difference image of the structure in the initial state and the transformed one is also shown.



Figure. Displacement of the domain walls a) Original position b) Displacement under the influence of an electric field c) difference image.

Also SPM technique can be used for local probing the electric polarization of magnetic domain walls in Kelvin mode of SPM measurements and the correlation of electric and magnetic properties could be the proof for electric polarization of the magnetic domain walls.

Support of RFBR grant №10-02-13302-RT-omi is gratefully acknowledged.

- [1] Tien-Kan Chung, Gregory P. Carman, Kotekar P. Mohanchandra, *APL*, **92** (2008) 112509.
- [2] V. R. Palkar and K. Prashanthi, *APL*, **93** (2008) 132906.
- [3] D.V. Karpinsky, R.C. Pullar, Y.K. Fetisov, K.E. Kamentsev, A.L. Kholkin, *J. Appl. Phys.*, **108** (2010) 042012.
- [4] V.G.Bar'yakhtar, V.A.L'vov, D.A.Yablonskii, *JETP Lett.* **37** (1983) 673.
- [5] A.S. Logginov, G.A. Meshkov, A.V. Nikolaev, E.P. Nikolaeva, A.P. Pyatakov, A.K. Zvezdin, *APL*, **93** (2008) 182510

23PO-K-18

### MULTIFERROIC AS A LEFT-HANDED MEDIUM

*Kulagin D.V.<sup>1</sup>, Levchenko G.G.<sup>1</sup>, Savchenko A.S.<sup>1</sup>, Tarasenko A.S.<sup>1</sup>, Tarasenko S.V.<sup>1</sup>, Shavrov V.G.<sup>2</sup>*

<sup>1</sup> Donetsk Institute for Physics & Engineering of the National Academy of Sciences of Ukraine,  
P.O. 83114, 72, R. Luxemburg str., Donetsk, Ukraine

<sup>2</sup> Kotel'nikov Institute of Radio Engineering and Electronics of the Russian Academy of Sciences,  
P.O. 125009, 11, Mokhovaya str., Moscow, Russia

As is well known, the left-handed medium simultaneously exhibits at least two effects [1]: the negative refraction effect (the opposite signs of the projections of the group velocities of the incident and refracted waves on the interface of the media) and the negative phase velocity effect (the opposite signs of the projections of the phase velocities of the incident and refracted waves on the normal to the interface). To date, the possibility of the left-handed effect in the single-phase magnetoelectric materials were analyzed in a number of works [2–6]. However, all those studies were based on some restrictions. First, only the isotropic magnetoelectric interaction was usually considered. Second, even though the magnetoelectric interaction was considered anisotropic, the frequency dependence of the magnetoelectric coefficients was neglected. As a result, the possibility that the negative phase velocity effect can exist simultaneously with the negative refraction effect was not discussed for multiferroic.

In this report, using an example of a multiferroic with the uniform antisymmetric magnetoelectric interaction of  $[\mathbf{ML}]\mathbf{P}$  type, we show that the properties of the left-handed medium appear. We study the case, when the ground state of the multiferroic under consideration is characterized by the following equilibrium orientation of the ferromagnetism  $\mathbf{M}_0$ , antiferromagnetism  $\mathbf{L}_0$ , and electric polarization  $\mathbf{P}_0$  vectors:  $\mathbf{M}_0\parallel\mathbf{X}$ ,  $\mathbf{L}_0\parallel\mathbf{Y}$ ,  $\mathbf{P}_0\parallel\mathbf{Z}$ . The wave vector  $\mathbf{k}$  of the propagating electromagnetic wave is in the YZ plane. The outward normal  $\mathbf{n}$  to the interface between magnetoelectric multiferroic and a nonmagnetic dielectric coincides with the positive direction of the Z axis. In particular with respect to chiral and magnetoelectric properties of magnetic medium it is study :

- 1) the effect of negative phase velocity;
- 2) the limiting volume wave of TM- or TE- type (the vector of group velocity is strictly parallel to interface between the multiferroic and a nonmagnetic dielectric and a vector of phase velocity is not collinear to interface);
- 3) the effect negative refraction is possible.
- 4) the necessary conditions for left –handed medium existence

It is shown that the above mentioned phenomena depends on the magneto-optical configuration.

[1] V. G. Veselago, *Usp. Fiz. Nauk* **92**, (1967) 517 [*Sov.Phys. Usp.* **10**, (1967) 509]

[2] Jian Qi Shen, *Phys. Rev. B* **73**, (2006) 045113.

[3] Cheng-Wei Qiu and Said Zouhdi, *Phys. Rev. B* **75**, (2007) 196101.

[4] Jian Qi Shen, *Phys. Rev. B* **75**, (2007) 196102.

[5] Cheng-Wei Qiu, Hai-Ying Yao, Le-Wei Li, et al., *Phys. Rev. B* **75**, (2007) 155120.

[6] Cheng-Wei Qiu, Hai-Ying Yao, Le-Wei Li, et al., *Phys. Rev. B* **75**, (2007) 245214.

23PO-K-19

## SPECTRUM OF THE COUPLED WAVES IN MAGNETICS HAVING THE FERROMAGNETIC SPIRAL

*Bychkov I.V.<sup>1</sup>, Buchelnikov V.D.<sup>1</sup>, Kuzmin D.A.<sup>1</sup>, Shadrin V.V.<sup>2</sup>*

<sup>1</sup> Chelyabinsk State University, 454001, Chelyabinsk, Street Br. Kashirinyh, 129, Russia

<sup>2</sup> Magnitogorsk State University, 455038, Magnitogorsk, Lenin avenue 114, Russia

Recently the major attention is given to studies of photon crystals (periodic layered structures). Since photon crystals are hard to obtain, it is useful to simulate them by crystals having spiral, both magnetic and dipole, structures (for example MnSi, CsCuCl<sub>3</sub>, TbMnO<sub>3</sub>).

The spiral magnetic structures contribute a number of features in a spectrum and dynamics of spin excitation in magnetic materials. Coupled electromagnetic both spin and electromagnetic, spin and elastic waves in spiral magnetic structure of type «simple spiral» are investigated earlier. However the spectrum and dynamic properties magnets in a phase «ferromagnetic spiral» are not enough studied. The spectrum of the coupled spin and electromagnetic waves in spiral magnetic structure of type «ferromagnetic spiral» is investigated in the present work. Two types of spirals – with exchange and relativistic interactions are considered. The basic condition of a crystal is described by a vector of magnetization with components  $M_x = M_0 \sin \theta \cos qz$ ,  $M_y = M_0 \sin \theta \sin qz$ ,  $M_z = M_0 \cos \theta$ , where  $M_0$  - magnetization of saturation,  $q$  - wave number of a spiral,  $\theta$  - an angle between a direction of magnetization and a spiral axis  $z$ .  $\theta$  is defined by value of an external magnetic field.



Tensor of magnetic susceptibility of a crystal with ferromagnetic spiral structure is received. It has been shown that all tensor components, a spectrum and consequently also all dynamic properties of considered structure depends from  $\theta(H)$ .

Researches of spectra of the connected fluctuations in the modulated magnetic structures are spent in approach  $L \gg a$ , where  $L = 2\pi/q$  - the spiral period,  $a$  - the lattice constant.

The electromagnetic-spin interaction on the related fluctuations in crystals with spiral magnetic structure is researched. It has shown that it essentially differs from the related fluctuations in crystals with ferromagnetic and antiferromagnetic material sequencing. Also it was shown, that the related fluctuations in structure with an exchange spiral essentially differ from fluctuations in structure with a relativistic spiral. Excitation spin and electromagnetic waves depends from  $\theta(H)$ . Longitudinal spin fluctuations are absent in case of small fields. The spectrum is zoned in helical crystals with a ferromagnetic spiral. The value of the forbidden zones, arising at interaction of spin and electromagnetic branches, does not depend from  $q$ , and is defined by anisotropy, parameter of electromagnetic-spin interaction and  $\theta(H)$ . Speed of a quasi-electromagnetic wave in comparison with speed of a noninteracting electromagnetic wave decreases for two-three order in long-wave area. The contribution to activation of quasi-spin waves from an electromagnetic subsystem is same, as well as in magnets without spiral structure. The carried out researches have shown that the spectrum and dynamic properties of structures with a ferromagnetic spiral can be operated effectively by external magnetic field.

23P-K-20

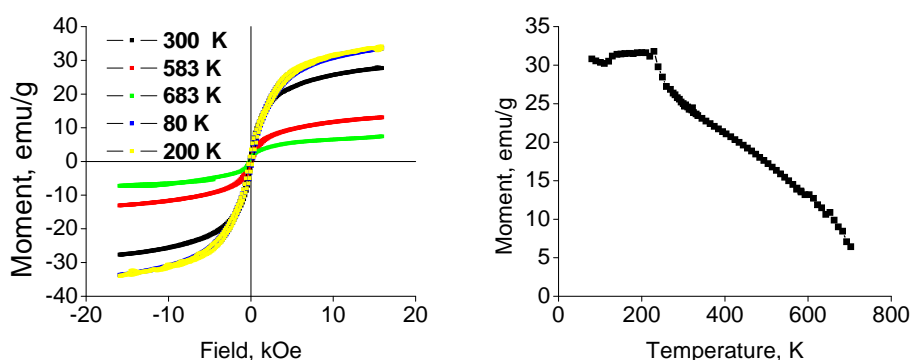
## ZONE CRYSTALLIZATION, ELECTRICAL AND MAGNETIC PROPERTIES OF Sr-Co-HEXAFERRITES

*Fetisov L.Y.<sup>1,2</sup>, Perov N.S.<sup>1</sup>, Bush A.A.<sup>2</sup>, Kamentsev K.E.<sup>2</sup>, Shkuratov V.Y.<sup>2</sup>*

<sup>1</sup> Faculty of Physics M.V. Lomonosov Moscow State University, Leninskie Gory, Moscow, 119991 Russia

<sup>2</sup> Institute of Informatics MIREA, pr. Vernadskogo 78, Moscow, 117454 Russia

The low-field ( $< 300$  Oe) magnetoelectric effect (ME) was discovered in ceramic samples of Sr-Co Z-type hexaferrites of content  $\text{Sr}_3\text{Co}_2\text{Fe}_{24}\text{O}_{41}$  at room temperatures [1]. It's value is 50 times larger than ME effect in  $\text{Cr}_2\text{O}_3$ . Therefore more detailed studies of the ME effect in such type of hexaferrites are required, especially in monocrystalline samples. In our research we investigated the technology for manufacturing of hexaferrite single crystals using the floating-zone method and



Hysteresis loops (a) and magnetization temperature dependence (b) of the samples

magnetic and electrical properties of the samples.

At the first stage cylindrical samples 8 mm in diameter and 90 mm length were synthesized by the ceramic technology method from the original components  $\text{SrCO}_3$ ,  $\text{Co}_3\text{O}_4$ , and  $\text{FeO}$  in air atmosphere at  $1100^\circ\text{C}$ . Then the samples were crystallized using the zone melting facility URN-2-3P with optical heating under linear velocity of crystallization of 5.5 mm/h. The X-ray analysis of the samples was carried out using the diffractometer Dron-3 ( $\text{CuK}\alpha$  -radiation) and showed that they are almost single-phase and composed of Sr-Co hexaferrite of W-type. The samples had hexagonal unit cell with parameters  $a = 5.562(5) \text{ \AA}$  and  $c = 32.65(5) \text{ \AA}$ .

Magnetic and dielectric properties of the samples were measured. The figures show that magnetization of the hexaferrite decreases with increasing temperature and vanishes at  $T_c \sim 720 \text{ K}$ . Temperature dependences of dielectric permittivity  $\epsilon(T)$ , losses parameter  $\text{tg}\delta(T)$ , and specific resistivity  $\rho(T)$  had a monotonous behavior in the temperature range 100-250 K and frequency range 0.1 – 200 kHz. No any abnormal changes typical to phase transition have been observed.

The work was supported by the Russian Foundation for Basic Research and Ministry of Education and Science of Russia.

[1] Y. Kitagawa et. al. Nature Materials. 2010. V.9. P.797.

23PO-K-21

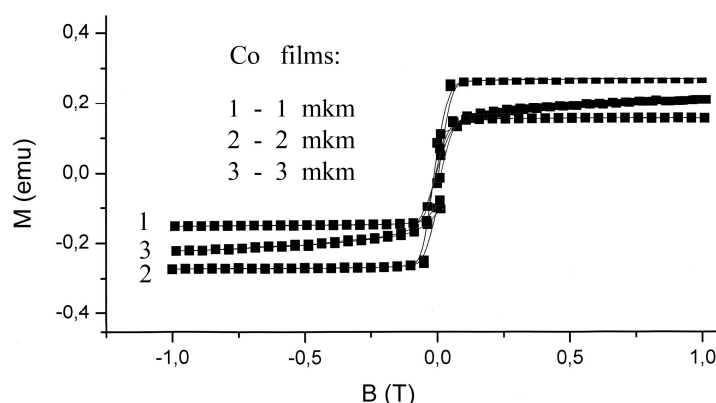
## MAGNETO-ELECTRIC EFFECT AND MINIMAL LAYER THICKNESS IN PZT ( $h < 20 \mu\text{m}$ )/Co ( $d < 6 \mu\text{m}$ ) MULTILAYERED HETEROSTRUCTURES

Stognij A.I.<sup>1</sup>, Novitskii N.N.<sup>1</sup>, Poddubnaya N.N.<sup>1</sup>, Sharko S.A.<sup>1</sup>, Szymczak H.<sup>2</sup>, D'yakonov V.P.<sup>2</sup>

<sup>1</sup> Scientific-Practical Materials Research Centre NAS of Belarus, 19 P.Brovki Street, Minsk, 220072, Belarus, [stognij@iftf.bas-net.by](mailto:stognij@iftf.bas-net.by)

<sup>2</sup> Institute of Physics, Polish Academy of Science, 02-668 Warsaw, Poland

Interface formation of ferromagnetic – ferroelectric in controllable conditions is the principle problem for mass production of sensors on the base of magnetoelectric effect in heterogeneous layered structures [1]. Particularly an open question concerning the origin of magnetoelectric interaction between the polycrystalline ferroelectric ceramics and ferromagnetic film as in case of Co-PZT interface still remains [2]. One should take into account that in the



general case the ceramic tablet of ferroelectric is not a vacuum microelectronic material. The problems of PZT surface preparation for ferromagnetic films of cobalt or permalloy reproducibly growth are discussed in the present report. First ion-beam sputter deposition of cobalt film thicker than three micrometers, its tearing off from ceramics, and second deposition with thickness of 2-3  $\mu\text{m}$  are shown to be sufficient for formation of continuous thermostable interface without bulging and peeling of the film during the multiple polarization – depolarization cycles at  $300^\circ\text{C}$ . The

selection of thickness range of permalloy and cobalt deposited onto real Co-PZT interface prepared by proposed way was made on the base of magnetic loops shown in **fig**.

Impossibility of support of approximate equality of volume part of ferroelectric and ferromagnetic phases in such multilayered structures [1] at low thicknesses of ferromagnetic film is associated with the lack of film adhesion to the polycrystalline ferroelectric surface consist of monocrystal grains of the order of one micrometer. The accumulation of mechanical pressures takes place in films of more than three micrometers formed onto flat areas of ferroelectric grains.

The ways of achievement of magnetoelectric effect up to 100 mV/(cm·Oe) in magnetic field to 100 Oe in PZT ( $h < 20 \mu\text{m}$ )/Co ( $d < 6 \mu\text{m}$ ) six-layered structures of 6...8 mm in diameter with yield not less than 0.6 are discussed in the present report. Such heterostructures are one of the suitable design for application in sensors.

Support by F10 GCST-002 (Poland – Belarus)

[1] C.-W. Nan, M.I. Bichurin, S. Dong, D. Viehland, G. Srinivasan, Multiferroic magnetoelectric composites: Historical perspective, status, and future directions, *J. Appl. Phys.*, **103** (2008) 031101.

[2] N.N. Poddubnaya, V.M. Laletin, A.I. Stognij, N.N. Novitskii, Dependence of magnetoelectric effect in layered lead zirconate-titanate / nickel heterostructures on the interface type *Functional Materials* **17**, (2010) No.2.

23PO-K-22

### MAGNETIC RESONANCE OF MONOCRYSTAL $\text{GdMnO}_3$

*Yatsyk I.V.*<sup>1</sup>, *Eremina R.M.*<sup>1</sup>, *Gavrilova T.P.*<sup>1</sup>, *Mukovskii Ya.M.*<sup>2</sup>, *Krug von Nidda H.-A.*<sup>3</sup>

<sup>1</sup> E. K. Zavoisky Physical-Technical Institute, 420029 Kazan, Russia

<sup>2</sup> Moscow Institute of Steel and Alloys, Leninskii pr. 4, Moscow, 119049 Russia

<sup>3</sup> Experimentalphysik V, Elektronische Korrelationen und Magnetismus, Universität Augsburg, 86135 Augsburg, Germany

Recently there has been an increasingly growing interest in the substances, where the magnetic and electric degrees of freedom are linked (multiferroics). This is due not only to new physical

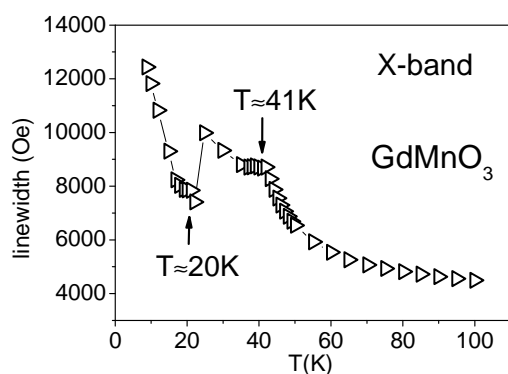


Fig. 1. Temperature dependence of ESR linewidth in a single crystal  $\text{GdMnO}_3$  in X - band (triangles). Arrows indicate the phase transition temperature, external magnetic field is parallel to the  $a$  axis

properties of these substances, but also the ability to control their condition with the help of external magnetic or electric fields, which opens up good prospects for the creation of new functional materials and devices based on them. The literature discusses several models to explain the coexistence of magnetic and ferroelectric orderings. One of them is a change of symmetry. Distortion in the substance of spatial inversion leads to the formation of modulated spin structures, but it is possible the opposite effect: spatial modulation of spin can lead to the disappearance of the center of symmetry from among the elements of crystal symmetry and the appearance of electric polarization. Such a mechanism is believed to be determines the

appearance of electric polarization in orthorhombic manganites [1] and explains the control the electric polarization by a magnetic field [2].

We investigated of EPR spectra temperature and angular dependence in the single crystal GdMnO<sub>3</sub> in the X- and Q-bands. One exchange narrow line was observed in all temperature regimes. The linewidth of the magnetic resonance line decreases with increasing temperature. An exception is the region near 20 K - temperature of the transition from the canted antiferromagnetic state in the sinusoidal (spiral) antiferromagnet, where a sharp increase in the ESR linewidth at 2500 Oe (Fig.1).

[1] A. M. Kadomtseva, Yu. F. Popov, G. P. Vorob'ev, V. Yu. Ivanov, A. A. Mukhin and A. M. Balbashov, JETP Letters, Volume **82**, Number 9, 590-593 (2005)

[2] Kimura T., Goto T., Shintani H., Ishizaka K., Arima T., Tokura Y. Nature **426**, 55-58 (2003)

23PO-K-23

## UNUSUAL SPONTANEOUS AND MAGNETIC FIELD INDUCED PHASE TRANSITIONS IN MULTIFERROIC $\text{Mn}_{0.85}\text{Co}_{0.15}\text{WO}_4$

Ivanov V.Yu.<sup>1</sup>, Mukhin A.A.<sup>1</sup>, Balbashov A.M.<sup>2</sup>, Iskhakova L.D.<sup>3</sup>, Vorob'ev G.P.<sup>4</sup>, Popov Yu.F.<sup>4</sup>, Kadomtseva A.M.<sup>4</sup>

<sup>1</sup> Prokhorov General Physics Institute of the Russian Acad. Sci., 119991, Moscow, Russia

<sup>2</sup> Moscow Power Engineering Institute, 105835, Moscow, Russia

<sup>3</sup> Fiber Optics Research Center of the Russian Acad. Sci., 119333, Moscow, Russia

<sup>4</sup> M.V. Lomonosov Moscow State University, 119992 Moscow, Russia

In the last years new kinds of multiferroics possessing electric polarization induced by non-centro-symmetrical helix (cycloid) spin structures were discovered. MnWO<sub>4</sub> is one of the prototypes of such multiferroic family which was recently extended by Co-substituted Mn<sub>1-x</sub>Co<sub>x</sub>WO<sub>4</sub> compositions exhibiting new spin structures and magnetoelectric properties [1-4]. In this work we have studied magnetic and magnetoelectric properties of Mn<sub>0.85</sub>Co<sub>0.15</sub>WO<sub>4</sub> single crystals having monoclinic *P2/c* crystal structure and revealed that this multiferroic system possesses even richer magnetoelectric spin structures, both spontaneous and magnetic-field-induced ones, than was suggested so far [1, 2].

In addition to three transitions from a paramagnetic state to collinear paraelectric AF4 phase at  $T_N \sim 17$  K, then - to collinear paraelectric AF1 phase (containing a minor ferroelectric cycloid AF2 phase) at 10 K and then - to ferroelectric cycloid phase AF5 at  $\sim 7$  K observed in Ref. [2], we have revealed below  $\sim 3.5$  K the new transition to some modification of the AF5 phase - AF5\*, which keeps up to  $\sim 7$  K during heating. We have found that Mn<sup>2+</sup> (Co<sup>2+</sup>) spin easy direction (*x*-axis) in the collinear AF1 and AF4 phases is in the *ac*-plane at the angle  $\sim 35^\circ$  from *a*-axis.

New field induced states exhibiting unusual ferroelectric features were observed at low temperatures by cooling either in a zero magnetic field (ZFC) or field cooling (FC). In particular, a new ferroelectric phase having polarization  $\sim 50$   $\mu\text{C}/\text{m}^2$  along *a*-axis was observed at low temperatures by cooling in *H*//*b* ( $H \geq 20$  kOe), while after ZFC regime this state was not reached even in the fields up to 200 kOe. Magnetic field *H*//*a*-axis extends the stability range of the AF2 ferroelectric (*P*//*b*) phase to the low temperatures. Two step phase transitions were found in the  $P_b(H_a)$  dependencies in the pulsed fields. Unusual change of sign of the  $P_b(T)$  polarization was observed during cooling in the *H*//*c*-axis being accompanied simultaneously by induced  $P_a$  component. *H-T* phase diagrams were obtained for *H*//*a*-, *b*- and *c*-axes. Besides, the phase transition from the paraelectric AF1 state to ferroelectric AF2 one was observed in *H*//*x*-easy axis

which was accompanied by magnetic susceptibility jump and appearance of  $P_b$  polarization similar to that found in pure  $\text{MnWO}_4$ .

In a frame of magnetoelectric coupling based on the inverse Dzyaloshinskii-Moria interaction [5] as well as symmetry properties of studied monoclinic system possible magnetic cycloid structures and its reorientation in magnetic field were analyzed.

This work was supported by RFBR (09-02-01355) and (10-02-00846).

[1] Y.-S. Song et al., Phys. Rev. B **79** (2009) 224415.

[2] R.P. Chaudhury, et al., Phys. Rev. B **82** (2010) 184422.

[3] Y.-S. Song et al., Phys. Rev. B **82** (2010) 214418.

[4] V.Yu. Ivanov, et al. Proc. of Int. Meeting ODPO-13, Rostov-on-Don-Loo (2010) v.1, p.163.

[5] H. Katsura et al., Phys. Rev. Lett. **95** (2005) 057205.

23PO-K-24

## BENDING MODES AND MAGNETOELECTRIC EFFECTS IN ASYMMETRIC FERROMAGNETIC-FERROELECTRIC STRUCTURE

*Petrov V.M.<sup>1</sup>, Bichurin M.I.<sup>1</sup>, Srinivasan G.<sup>2</sup>*

<sup>1</sup> Novgorod State University, B. S. Peterburgskaya St. 41, Veliky Novgorod 173003, Russia

<sup>2</sup> Oakland University, Rochester, MI 48309, USA

Magnetoelectric (ME) couplings in bilayers of magnetostrictive and piezoelectric phases are mediated by mechanical deformation. A model is discussed here for the resonance enhancement of such magnetoelectric (ME) interactions at frequencies corresponding to bending oscillations. The thickness dependence of stress, strain and magnetic and electric fields within a sample are taken into account so that the bending deformations could be considered in an applied magnetic or electric field. The frequency dependence for longitudinal and transverse ME voltage coefficients have obtained by solving electrostatic, magnetostatic and elastodynamic equations.

We consider boundary conditions corresponding to bilayers that are free to vibrate at both ends, or simply supported at both ends, or fixed at one end. The explicit expressions for ME voltage coefficients are derived for each of these end conditions. It is shown that the bending resonance and consequent enhancement in ME coupling occurs at the lowest frequency for a bilayer that is fixed at one end and free at the other end.

The model is applied to a specific case of permendur-lead

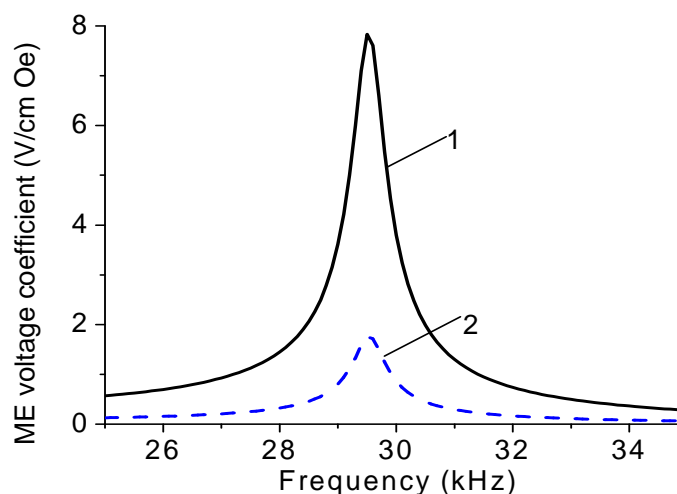


Fig. 1. Frequency dependence of transverse (1) and longitudinal (2) ME voltage coefficients for a bilayer of permendur and PZT free at both ends

zirconate titanate bilayer of length 9.2 mm and total thickness 0.7 mm. For a bilayer that is free at both ends the ME voltage coefficient stays constant with frequency except for a resonance enhancement at bending mode expected at about 29.5 kHz which is an order of magnitude smaller than the longitudinal acoustic mode frequency. Due to the absence of demagnetization effects, the transverse coefficient at resonance is a factor of five higher than the longitudinal case as in Fig. 1. One notices a significant decrease in the resonance frequency to 13 GHz for a bilayer with simply supported ends and a 10% increase in the peak ME coefficient to 10 V/cm Oe. Further decreasing in the resonance frequency can be achieved by using a bilayer that is clamped at one end and free at the other. In this case, the frequency is a factor of four smaller than for a bilayer that is free to vibrate at both ends.

Theoretical ME voltage coefficients versus frequency profiles are in excellent agreement with data. The resonance ME effect is therefore a novel tool for enhancing the field conversion efficiency in the composites.

23PO-K-25

## EFFECTS OF R AND Fe RESONANCE MODE INTERACTION IN RFe<sub>3</sub>(BO<sub>3</sub>)<sub>4</sub> MULTIFERROICS

*Kuzmenko A.M.<sup>1</sup>, Mukhin A.A.<sup>1</sup>, Ivanov V.Yu.<sup>1</sup>, Bezmaternikh L.N.<sup>2</sup>*

<sup>1</sup> A.M. Prokhorov General Physics Institute of the RAS, 119991 Moscow, Russia

<sup>2</sup> Institute of Physics SB RAS, 660036 Krasnoyarsk, Russia

Rare-earth iron borates RFe<sub>3</sub>(BO<sub>3</sub>)<sub>4</sub> have proved to be a new class of multiferroics possessing non-centrosymmetrical trigonal crystal structure (R32) and showing a significant dependence of magnetic and magnetoelectric properties on the paramagnetic rare-earth (R) subsystem exchange-coupled with antiferromagnetically ordered Fe ions ( $T_N = 30-40$  K). We have studied the submillimeter magnetic resonance properties of easy plane Nd, Sm, Gd iron borates to get additional data on R-Fe interaction and its effect on magnetic excitations in Fe- and R-subsystems. Transmission spectra of single crystalline *a*-cut plates were measured by submillimeter quasioptical backward-wave-oscillator technique at the frequency range 3-20 cm<sup>-1</sup> at the temperatures 3-300 K. One or two resonance modes were observed for both ac electro-magnetic field polarizations (*h*//*b*, *e*//*c* and *h*//*c*, *e*//*b*) in contrast to our results in the easy plane Y and Eu iron borates revealing only single high frequency antiferromagnetic resonance (AFMR) mode for (*h*//*b*) [1]. The modes were identified as magnetic excitations in the exchange coupled Fe- and R-subsystems. Their origin is associated with the Fe AFMR modes ions and electron transitions inside a ground state (doublet) of R ions split by R-Fe exchange field (R-modes). A qualitatively different behavior of the resonance modes was found in the Nd, Sm, Gd iron borates. A strong dynamical coupling of the magnetic Fe and R ions oscillations accompanied by their anti-crossing and a redistribution of corresponding mode strengths were established both experimentally and theoretically.

As a result of such anti-crossing we observed in NdFe<sub>3</sub>(BO<sub>3</sub>)<sub>4</sub> the increase of the Nd-mode frequencies (up to 13 cm<sup>-1</sup>) as compare with the static exchange Nd<sup>3+</sup> doublet splitting (8.8 cm<sup>-1</sup>) while the underlying Fe AFMR mode (*h*//*b*) was soften. The mode anti-crossing was reduced with dilution of Nd ions in Nd<sub>0.4</sub>Y<sub>0.6</sub>Fe<sub>3</sub>(BO<sub>3</sub>)<sub>4</sub>. Similar increasing of Sm-mode frequency as compare with the Sm<sup>3+</sup> doublet splitting was also observed for *h*//*c* polarization in SmFe<sub>3</sub>(BO<sub>3</sub>)<sub>4</sub>. However, for the *h*//*b* polarization we found at low temperatures not only increase of the Sm mode frequency but also the Fe mode raising in contrast to NdFe<sub>3</sub>(BO<sub>3</sub>)<sub>4</sub>. This is explained by a significant anisotropy of exchange Sm-doublet splitting in the easy plane and easy axis states ( $\Delta_{\perp} = 13.2$  cm<sup>-1</sup>  $\gg$   $\Delta_{\parallel}$ ), while for the Nd<sup>3+</sup>  $\Delta_{\perp} \sim \Delta_{\parallel}$ . Unexpectedly nothing Gd<sup>3+</sup>-modes was found in

pure  $\text{GdFe}_3(\text{BO}_3)_4$ . It was shown that their missing is attributed to a peculiar compensation of contributions of Fe and Gd ions to permeability for the high frequency (exchange) mode due to almost equality of their gyromagnetic ratios. However, in mixed  $\text{Gd}_{0.5}\text{Nd}_{0.5}\text{Fe}_3(\text{BO}_3)_4$  system the missing Gd-modes were well observed along with Nd ones. Their frequencies ( $\sim 17 \text{ cm}^{-1}$ ) turned out more then two times higher of Gd levels exchange splitting.

An explanation and quantitative description of the observed effects have been performed and corresponding parameters of magnetic interactions and ground state of R-ions have been extracted. A role and contribution of magnetoelectric (electro dipolar active) excitations, i.e. electromagnons in the phenomena studied have been also analyzed.

This work was supported by RFBR (10-02-00846 and 09-02-01355).

[1] A.M. Kuzmenko, A.A. Mukhin, V.Yu. Ivanov, A.M. Kadomtseva, L.N. Bezmaternykh, JETP, **112**, No. 5 (2011).

23PO-K-26

## NEUTRON DIFFRACTION, MAGNETIC AND MAGNETOELECTRIC STUDY OF PHASE TRANSITIONS IN $\text{Mn}_{0.9}\text{Co}_{0.1}\text{WO}_4$ MULTIFERROICS

*Urcelay-Olabarria I.<sup>1</sup>, Ressouche E.<sup>1</sup>, Skumryev V.<sup>2</sup>, García-Muñoz J.L.<sup>3</sup>, Balbashov A.M.<sup>4</sup>, Mukhin A.A.<sup>5</sup>, Ivanov V.Yu.<sup>5</sup>, Vorob'ev G.P.<sup>6</sup>, Popov Yu.F.<sup>6</sup>, Kadomtseva A.M.<sup>6</sup>*

<sup>1</sup> Institute Laue-Langevin, 15638042 Grenoble Cedex 9, France

<sup>2</sup> Institut Català de Recerca i Estudis Avançats (ICREA) and Departament de Física, Universitat Autònoma de Barcelona, 08193Bellaterra, Spain

<sup>3</sup> Instituto de Ciencia de Materiales de Barcelona, CSIC, E-08193 Bellaterra (Barcelona), Spain.

<sup>4</sup> Moscow Power Engineering Institute, 105835, Moscow, Russia

<sup>5</sup> Prokhorov General Physics Institute of the Russian Acad. Sci., 119991, Moscow, Russia

<sup>6</sup> M.V. Lomonosov Moscow State University, 119992 Moscow, Russia

It was found recently that substitution of  $\text{Mn}^{2+}$  ions by  $\text{Co}^{2+}$  ones in  $\text{Mn}_{1-x}\text{Co}_x\text{WO}_4$  multiferroics results in significant changes of its magnetic structure and related ferroelectric properties [1-2]. We have studied the spontaneous and magnetic field induced phase transitions of  $\text{Mn}_{0.9}\text{Co}_{0.1}\text{WO}_4$  multiferroic by means of magnetic, magnetoelectric and neutron diffraction measurements. The single crystals of  $\text{Mn}_{0.9}\text{Co}_{0.1}\text{WO}_4$  possessing a monoclinic crystal structure  $\text{P2}/c$  were grown by a floating zone method. The single crystal neutron diffraction experiments in magnetic field up to 5 T were carried out at the ILL (Grenoble, France). Magnetic measurements were performed by SQUID-magnetometer. Electric polarization was studied by pyroelectric measurements in a static field up to 5 T as well as in pulsed fields up to 20 T.

Our measurements show two magnetic phase transitions, at  $T_N = 13 \text{ K}$  and  $T_2 \approx 10.5 \text{ K}$ . Refinement of the magnetic structure using neutron diffraction data at 12 K reveals that the spins are collinear on the  $ac$  plane, sinusoidally modulated with the propagation vector  $\mathbf{k} = (-0.222(1) \ 0.5 \ 0.472(1))$  and the amplitude of  $2.535(8) \mu_B$  (similar to the so called AF3 magnetic phase of the pure  $\text{MnWO}_4$ ). The magnetic moments make an angle of  $35.8(5)^\circ$  with the  $a$  axis. Below 10 K the spins rotate in the  $ac$  plane, keeping the propagation vector, and transform to the elliptical helix (cycloid), with the spin plane perpendicular to the  $b$  axis. The refinement of the data at 2 K shows that the cycloid becomes more circular and the modulus of the moments increases. The magnetic structure is the so called AF2\* magnetic phase [1]. The phase transition to this magnetic structure is

accompanied by an appearance of the electric polarization both along a-axis ( $\sim 100 \mu\text{C}/\text{m}^2$ ) and c-axis ( $\sim 30 \mu\text{C}/\text{m}^2$ ) allowed in this phase by the symmetry of the spin-current mechanism in this system [3].

Applying a magnetic field along c-axis, at  $H_{cr} \sim 30$  kOe the rotation plane of the elliptical structure AF2\* flops on  $90^\circ$  and spins become perpendicular to the external magnetic field in a new magnetic structure AF2\*\*. This transition is accompanied by a jump of magnetic susceptibility and disappearance of both components  $P_a$  and  $P_c$  of the electric polarization in agreement with a magnetoelectric coupling based on the inversed Dzyaloshinskii-Moriya interaction [3]. Similar phase transition attending also cycloid plane flopping was observed by magnetoelectric measurements for  $H||a$ -axis in pulsed fields at  $H_{cr} \sim 85$  kOe. No effects for the electric polarization (and thus magnetic structure) were found for  $H||b$ -axis in fields up to 200 kOe. The obtained data exhibit a significant reduction of magnetic anisotropy in ac-plane due to Co substitution resulting in stabilizing the cycloidal ac-plane spin structure.

This work was supported by RFBR (09-02-01355) and (10-02-00846) and MAT2009-09308.

- [1] Y.-S. Song et al., Phys. Rev. B **79** (2009) 224415; Phys. Rev. B **82** (2010) 214418.  
 [2] V.Yu. Ivanov, et al. Proc. of Int. Meeting ODPO-13, Rostov-on-Don-Loo (2010) v.1, p.163.  
 [3] H. Katsura et al., Phys. Rev. Lett. **95** (2005) 057205.

23PO-K-27

## MAGNETOELASTIC EFFECTS IN THE NEODYMIUM FERROBORATE

Zvyagina G.<sup>1</sup>, Zhekov K.<sup>1</sup>, Zvyagin A.<sup>1,2</sup>, Bilych I.<sup>1</sup>, Gudim I.<sup>3</sup>, Temerov V.<sup>3</sup>, Volkov N.<sup>3</sup>

<sup>1</sup> B.I. Verkin Institute for Low Temperature Physics and Engineering of the National Academy of Sciences of Ukraine, Kharkov, 61103, Ukraine

<sup>2</sup> Max-Planck-Institut für Physik komplexer Systeme, 01187 Dresden, Germany

<sup>3</sup> L.V. Kirensky Institute for Physics, Siberian Branch of the Russian Academy of Sciences, 660036, Krasnoyarsk, Russia

Rare-earth ferrobates with the common formula  $\text{RFe}_3(\text{BO}_3)_4$  ( $\text{R}=\text{Y}, \text{La-Nd}; \text{Sm-Er}$ ) are studied intensively during last years, because they possess a set of interesting optical, magnetic, and magneto-electric properties. Belonging of these crystals to the class of multiferroics makes them very perspective subjects for the creation of new multifunctional devices [1].

Magnetic properties of the rare-earth ferrobates are determined by the presence there of two types of magnetic ions, which belong to 3d and 4f elements. The specifics of their magnetic properties is defined, first, by the behavior of the magnetic iron subsystem, and second, by the characteristic features of the electron structure of the rare-earth ion, which is formed by the crystalline electric field, and, naturally, by the f-d interaction.

In all compounds of this family the antiferromagnetic ordering of the iron subsystem takes place at the temperatures 30 K-40 K. The ions  $\text{R}^{3+}$  bring an essential contribution to the orientation of the  $\text{Fe}^{3+}$  magnetic ions in the ordered state, and the magnetic anisotropy. The presence of the essential coupling between the magnetic, electric, and elastic subsystems of ferrobates yields to the onset of multiferroelectric effects, which reveal themselves most sharply in the vicinities of the spontaneous and magnetic field-induced phase transformations [1, 2]. This is why, the investigation of the elastic properties of such compounds in the vicinities of phase transitions is very interesting.



We have performed low-temperature ultrasonic investigations of the  $\text{NdFe}_3(\text{BO}_3)_4$  single crystal in the external magnetic field. The temperature range was 1.7–300 K and magnetic field range was up to 5,5T.

The transition to the antiferromagnetically ordered state is manifested at  $T_N \approx 30.6$  K in the temperature behavior of the sound velocity and absorption of the neodymium ferroborate.

The features in the temperature behavior of elastic characteristics of and its behavior in the external magnetic field, applied in the basic (*ab*)-plane of the crystal, permit us to suppose that the transition to the incommensurate spiral phase [3] is realized in the system. This phase transition behaves as the first order one.

The phase H-T diagrams for  $\text{NdFe}_3(\text{BO}_3)_4$  for the cases  $\mathbf{H} \parallel \mathbf{a}$  and  $\mathbf{H} \parallel \mathbf{b}$  have been constructed.

We have constructed the phenomenological Landau-like theory, which qualitatively describes the behavior of the sound velocity as the function of the temperature and the field. The spiral phase is caused by the nonzero spontaneous electric polarization. The weak inplane anisotropy modifies the spiral structure, giving rise to the onset of odd harmonics for the spatial distribution of the vector of antiferromagnetism.

Acoustic “inhomogeneity” of the sample, which causes the multi-phase behavior of the acoustic signal, and which is revealed in the behavior of the transverse  $C_{44}$  mode in the range of temperatures 10 – 30 K can be the evidence of the process of the creation of domains in a crystal.

[1] A.N. Vasiliev and E.A. Popova, *Low Temp. Phys.* **32**, 735(2006).

[2] A.M. Kadomtseva et al., *Low Temp. Phys.* **36**, 511 (2010)]

[3] M. Janoschek et al., *Phys. Rev. B* **81**, 094429, (2010).



**23 August**

Tuesday

17:30-19:00

poster session

23PO-M

**“Magnetism and  
Superconductivity”**

23PO-M-1

## **Z<sub>2</sub>—VORTEX UNBINDING TRANSITION FOR TWO-DIMENSIONAL FRUSTRATED ANTIFERROMAGNETS**

*Ignatenko A.N.*

Institute of Metal Physics, 620990, Ekaterinburg, Russia

Two-dimensional frustrated Heisenberg antiferromagnet with non-collinearly ordered ground state at finite temperature is known to have transition related to the decay of vortex pairs [1]. In contrast to the famous Berezinsky-Kosterlitz-Thouless (BKT) phase transition, which appears in systems with abelian XY-like symmetry, in the present case even without vortices magnetic fluctuations are so strong that they not only destroy magnetic order, which is in accordance with Mermin-Wagner theorem, but also produce finite correlation length at any finite temperature and the phenomenon of quasi-long range order does not occur.

In this contribution the influence of magnetic classical and quantum fluctuations on the vortex subsystem is studied. If one simply neglects fluctuations by considering vortices inserted at some points into ideally ordered background, one obtains an ensemble of point particles equivalent to classical Coulomb plasma in two dimensions. In this picture long-range logarithmic potential at low temperatures is able to bind *all* vortices into pairs (dipoles); the latter begin to dissolve only at Kosterlitz-Thouless temperature. Therefore neglect of fluctuations leads to usual BKT phase transition.

It is shown that magnetic fluctuations exponentially screen the interaction between vortices at distances  $r \gg \xi$  ( $\xi$  is correlation length). Correspondingly the energy of one vortex which is equal to half the energy of infinitely large pair is finite. Hence even at arbitrary small temperatures not all vortices are bound into pairs, and there exist finite, but exponentially small, density of free  $Z_2$  – vortices. Therefore there is no principal difference between low and high temperature regimes: at high temperatures density of vortices is simply much larger than at low temperatures. *Thereby the process of dissociation of  $Z_2$  – vortex dipoles is a crossover and not phase transition.*

In the renormalized classical region ( $T$  is low in comparison with ground state spin stiffness) this crossover is sufficiently narrow due to exponentially large correlation length  $\xi \sim \exp(1/T)$ . At distances  $1/T \ll r \ll \xi$  the repulsive double logarithmic interaction  $-T \log(r)^2$ , which is induced by fluctuations in addition to bare attractive logarithmic potential  $\log(r)$ , leads to substantial reduction of the crossover temperature. Under the enhancement of frustration, when the system is approached to quantum phase transition into spin liquid ground state, the crossover is smeared by quantum fluctuations.

Backward influence of  $Z_2$  – vortices on the spin fluctuations (spin correlation functions), in particular the possibility of vortex mechanism of spinon's confinement, is also discussed.

[1] H. Kawamura and S. Miyashita, J. Phys. Soc. Japan **53** (1984) 9; **53** (1984) 4138.

23PO-M-2

## MAGNETIC ANISOTROPY OF MANGANITE $\text{La}_{0.7}\text{Sr}_{0.3}\text{MnO}_3$ FILMS INVESTIGATED BY MICROWAVE RESONANCE METHODS

*Demidov V.V., Borisenko I.V., Ovsyannikov G.A., Petrzhik A.M.*

Kotel'nikov Institute of Radio Engineering and Electronics of RAS, Mokhovaya 11-7, Moscow, 125009, Russia.

The generalized analysis of experimental data for ascertainment of the dependence for in-plane magnetic anisotropy of  $\text{La}_{0.7}\text{Sr}_{0.3}\text{MnO}_3$  (LSMO) films with mechanical stresses induced by mismatch between crystallographic parameters of film and substrate is made. The films were deposited on  $\text{NdGaO}_3$  (NGO) substrate, in which the crystallographic plane (110)NGO was tilted around [110] NGO direction on the angles  $\gamma = 0 \div 25.7$  degrees related the surface of the substrate. This method allows the controllable changing of mismatch leaving other characteristics of film invariable. Parameters of magnetic anisotropy were determined by two independent methods: the examination of FMR spectra measured at 10 GHz and the recording of absorption spectra by Q-meter at 300 MHz. The latter method is very simple and useful for determination of a hard axis direction for uniaxial magnetic anisotropy. The increasing of uniaxial magnetic anisotropy with the increasing of the angle due to film strain was found. The model that explains changing of anisotropy magnetic energy with angle increasing was suggested. This model describes all experimental data for in-plane magnetic anisotropy of LSMO films well enough [1].

Support by Program for Basic Research of the Russian Academy of Sciences, Russian Foundation for Basic Research Project 11-02-01234, Scientific School Grant 5423.2010.2, Ministry of Education and Science of the Russian Federation, contract 02.740.11.0795

[1] V.V. Demidov, I.V. Borisenko, A.A. Klimov, G.A. Ovsyannikov, A.M. Petrzhik, S.A. Nikitov. Magnetic anisotropy in strain epitaxial manganite. *JEPT*, **139** (2011) N4.

23PO-M-3

## POSSIBLE SCENARIO FOR SUPERCONDUCTIVITY AND MAGNETIC PENETRATION DEPTH IN UNDERDOPED CUPRATES

*Eremin M.V., Sunyaev D.A.*

Kazan Federal University, Kremlevskaya 18, Russian Federation

We have analysed a possible energy band schema and superconductivity for underdoped cuprates, focusing on the temperature dependencies of magnetic penetration depth  $\lambda_{ab}$  in Cu-O plane. In Fig. 1 we demonstrate that the temperature dependence of superfluid density  $1/\lambda_{ab}^2$  is very sensitive to the ratio  $2\Delta/k_B T_c$ . It is about 5 for overdoped compounds, but strongly increases as we approach the underdoped side of phase diagram.

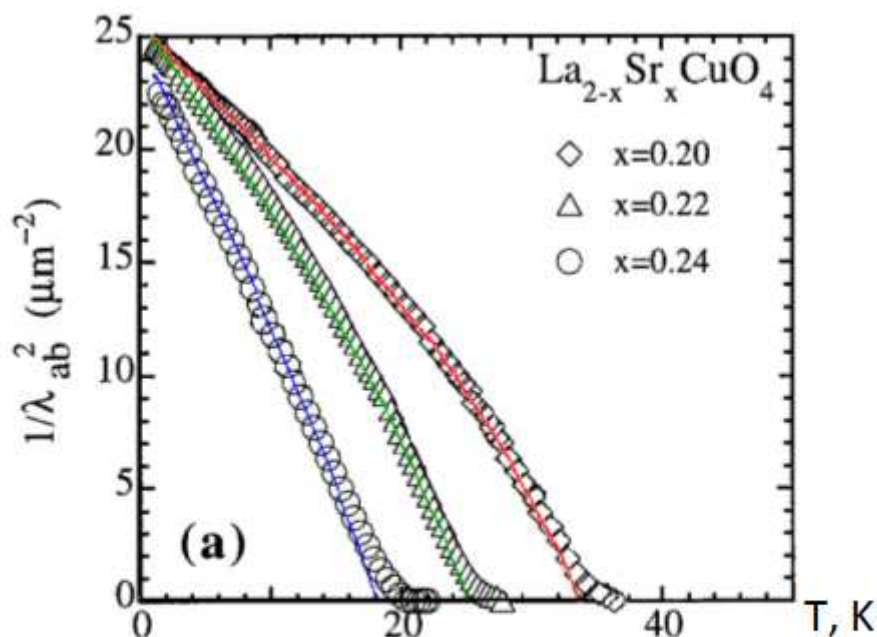


Fig.1. Temperature dependencies of superfluid densities  $\text{La}_{2-x}\text{Sr}_x\text{CuO}_4$ . Symbols (diamonds, triangles and circles) – experimental data from Ref. [1], solid lines – our calculations. The  $2\Delta_0/k_B T_c$  ratios are:  $(6.1 \pm 0.1)$ ,  $(5.9 \pm 0.1)$  and  $(5.3 \pm 0.1)$ , for  $x=0.20$ ,  $x=0.22$  and  $x=0.24$ , correspondently.

We argue that this behaviour of ratio  $2\Delta/k_B T_c$  as a function of hole concentration can be explained in two band scenario, like suggested in paper [2]. In underdoped regime there are two bands near the Fermi level with different energy dispersions. Both are coupled via “hybridization” or pseudogap parameter. The superconducting pairing in one band dominates with respect to other one. Using this two-component model we have calculated the ratio  $2\Delta/k_B T_c$  as well as the superfluid density. Our results are very similar to those observed in experiment.

Support by RFBR Grant 09-02-00777-a, and Swiss National Science Foundation, Grant IZ73Z0 128242 is acknowledged.

[1] Panagopoulos, B. D. Rainford, J. R. Cooper, W. Lo, J.L. Tallon, J. W. Loram, J. Betouras, Y. S. Wang and C. W. Chu, *Phys. Rev. B*, **60** (1999) 14617.

[2] Kai-Yu Yang, T. M. Rice, Fu-Chun Zhang, *Phys. Rev. B*, **73** (2006) 174501.

23PO-M-4

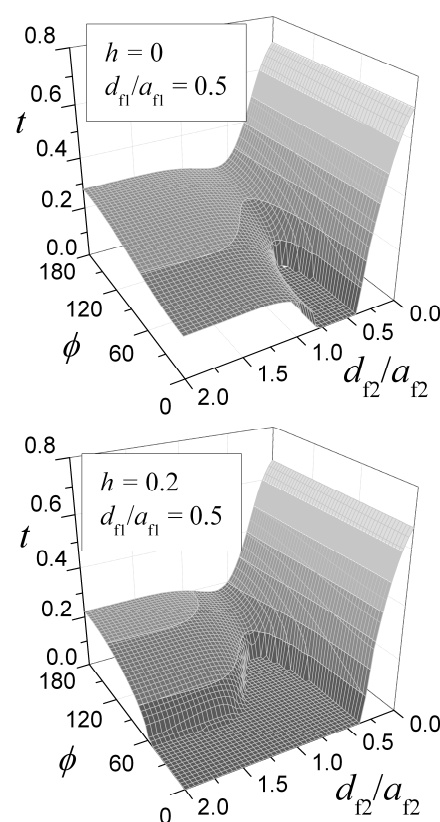
## PROXIMITY EFFECT FOR ASYMMETRICAL TREE LAYERED FS STRUCTURES IN EXTERNAL MAGNETIC FIELD

Avdeev M., Khusainov M., Proshin Yu., Tsarevskii S.

Kazan Federal University, Kremlevskaya, 18, Kazan 420008, Russian Federation

We consider asymmetrical trilayers  $F_1F_2S$  and  $F_1SF_2$  structures in an external parallel magnetic field. The different mutual orientations of the F layers magnetizations are examined. At this condition the triplet component of the superconducting condensate is arisen [1,2]. Assuming that all F and S layers are dirty, we solve the boundary value problem for the Usadel function [3]. Using these solutions and self-consistency equation, we calculate the critical temperature for the  $F_1F_2S$  and  $F_1SF_2$  systems as function of the F layers thicknesses  $d_{f1,2}$  in external magnetic field  $H$  [3].

For example, in Figure we show the dependence of the reduced critical temperature  $t = T_c/T_{cs}$  on the reduced thickness  $F_2$  layer  $d_{f2}/a_{f2}$  and angle between the direction of magnetization  $\phi$  for the  $F_1SF_2$  system in the external magnetic field  $h = H/H_c$  ( $T_{cs}$  is critical temperature of S metal,  $H_c$  is critical parallel field of the thin film,  $a_f = v_F/2I$  is spin stiffness length,  $v_F$  is Fermi velocity and  $I$  is exchange field in the F metal). The parameters of system are chosen as follows: the S layer thickness is  $d_s/\xi_{s0} = 0.8$ ; free path lengths are  $l_s/\xi_{s0} = 0.2$ ,  $l_{f1,2}/a_{f1,2} = 0.4$  for the S and F layers, respectively; the  $F_1S$  and  $SF_2$  interface transparencies are  $\sigma_{s1,2} = 3$ , the Sharvin conductance is  $n_{sf1,2} = 1.2$  and the ratio  $I_{1,2}/\pi T_{cs}$  equals 6.8. The external magnetic field suppresses a superconductivity of the contact and may significantly alter the critical temperature dependence. It is very important for possible spin-valve applications of the FS trilayer because they are controlled by external magnetic field. We also consider the influence of asymmetry of FS structures on the phase diagram  $T_c(d_{f1}, d_{f2})$ .



The work was partially supported by the RFBR (the project 09-02-01521) and by the Ministry of Education and Science of Russian Federation.

- [1] Ya.V. Fominov, A.A. Golubov, T.Yu. Karminskaya, M.Yu. Kupriyanov, R.G. Deminov, L.R. Tagirov, *Pi'sma v ZhETF.*, **91** (2010) 329  
 [2] Ya.V. Fominov, A.A. Golubov, M.Yu. Kupriyanov, *JETP Letters.*, **77** (2003) 510  
 [3] M.V. Avdeev, M.G. Khusainov, Yu.N. Proshin, S.L. Tsarevskii, *Supercond. Sci. Technol.*, **23** (2010) 105005

## VIBRATIONAL AND MAGNETIC CONTRIBUTIONS IN THE HEAT CAPACITY OF $Tm_{1-x}Yb_xB_{12}$

Sluchanko N.E.<sup>1</sup>, Azarevich A.N.<sup>1</sup>, Bogach A.V.<sup>1</sup>, Glushkov V.V.<sup>1</sup>, Demishev S.V.<sup>1</sup>, Filipov V.B.<sup>2</sup>, Shitsevalova N.Yu.<sup>2</sup>, Gabani S.<sup>3</sup>, Flachbart K.<sup>3</sup>, Gavrilkin S.Yu.<sup>4</sup>, Mitzin K.V.<sup>4</sup>

<sup>1</sup> A.M. Prokhorov General Physics Institute of RAS, 38, Vavilov str., Moscow, 119991, Russia

<sup>2</sup> Institute for Problems of Materials Science, 3, Krzhizhanovsky str., Kiev, 03680, Ukraine

<sup>3</sup> Center of Low Temperature Physics, IEP SAS, 04001 Košice, Slovakia

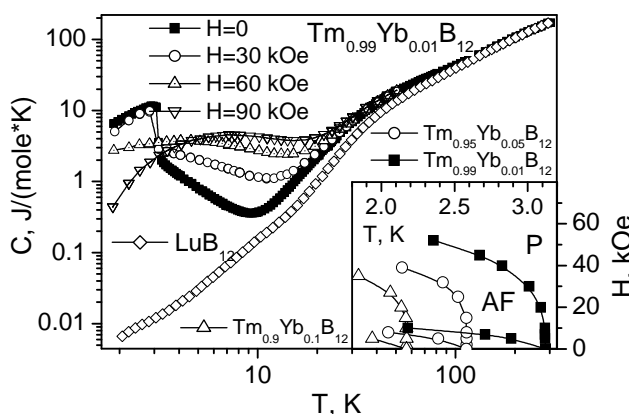
<sup>4</sup> P.N.Lebedev Physical Institute of RAS, 53 Leninskii prospect, 119991 Moscow, Russia

Quantum criticality and the associated magnetic quantum phases of heavy fermion metals from one side and the metal-insulator transition (MIT) in strongly interacting electron systems from another are of extensive current interest [1-2]. The picture of a magnetic metal transformation into paramagnetic (P) insulator has been subjected to experimental testing in recent years. In particular it was found in [3] that in the family of compounds  $Tm_{1-x}Yb_xB_{12}$  the substitution of Tm by Yb causes a transition from antiferromagnetic metal (AF)  $TmB_{12}$  ( $T_N \approx 3.2K$ ) to Kondo-insulator  $YbB_{12}$ . Very recently the transition to unconventional cage-glass state was detected in the heat capacity and Raman measurements of the nonmagnetic dodecaboride  $LuB_{12}$  [4].

To shed more light on the transformation of thermal properties in the strongly correlated system with MIT and vibrational instability we have studied the heat capacity  $C(H,T)$  of  $Tm_{1-x}Yb_xB_{12}$  substitutional solid solutions ( $0 < x < 0.85$ ). The experiments have been carried out on the high quality single crystals in wide range of temperatures (1.8-300K) in magnetic fields up to 90 kOe on the Quantum Design PPMS-9 installation.

The typical example of the  $C(H,T)$  data obtained in this study is shown in Figure for Tm-rich solid solution  $Tm_{0.99}Yb_{0.01}B_{12}$ . It is discerned from Fig. that antiferromagnetic transition at  $T_N \approx 3.1K$  depresses in magnetic field allowing to determine both the field induced AF-P transitions and H-T phase diagram (see insert in Fig.). For comparison in Fig. the specific heat of reference compound  $LuB_{12}$  is also presented.

It was established evidently that a quasi-local mode (Einstein oscillator,  $\theta_E = 140-150K$ ) forms the main vibrational contribution to the heat capacity in  $Tm_{1-x}Yb_xB_{12}$  compounds and the Einstein temperature is happened to be noticeably smaller when compared with  $\theta_E = 160K$  in  $LuB_{12}$ . It was shown that the single-site crystal field effect is not appropriate to describe the features of magnetic contribution  $C_m$  in  $C(T,H)$ . Moreover,  $C_m$  in  $Tm_{1-x}Yb_xB_{12}$  may be attributed to the response from nanoclusters of magnetic moments consisting from the Tm and Yb rare earth ions.



Support by the RAS Program “Strongly Correlated Electrons in Semiconductors, Metals, Superconductors and Magnetic materials” and RFBR is acknowledged.

[1] Q.Si, S.Rabello, K.Ingersent, J.L.Smith, *Nature* **413**, 804 (2001).

[2] A.Akbari, P.Thalmeier, P.Fulde, *Phys.Rev.Lett.* **102**, 106402 (2009).

[3] N.E.Sluchanko et al., *JETP Lett.* **89**, 256 (2009).

[4] N.E. Sluchanko et al., *JETP* in print (2011).



## BULK AND LOCAL MAGNETIZATION OF SUBSTITUTIONAL SOLID SOLUTIONS $Tm_{1-x}Yb_xB_{12}$

Bogach A.V.<sup>1</sup>, Sluchanko N.E.<sup>1</sup>, Glushkov V.V.<sup>1</sup>, Demishev S.V.<sup>1</sup>, Azarevich A.N.<sup>1</sup>, Filipov V.B.<sup>2</sup>, Shitsevalova N.Yu.<sup>2</sup>, Gabani S.<sup>3</sup>, Flachbart K.<sup>3</sup>, Vanacken J.<sup>4</sup>, Moshchalkov V.V.<sup>4</sup>

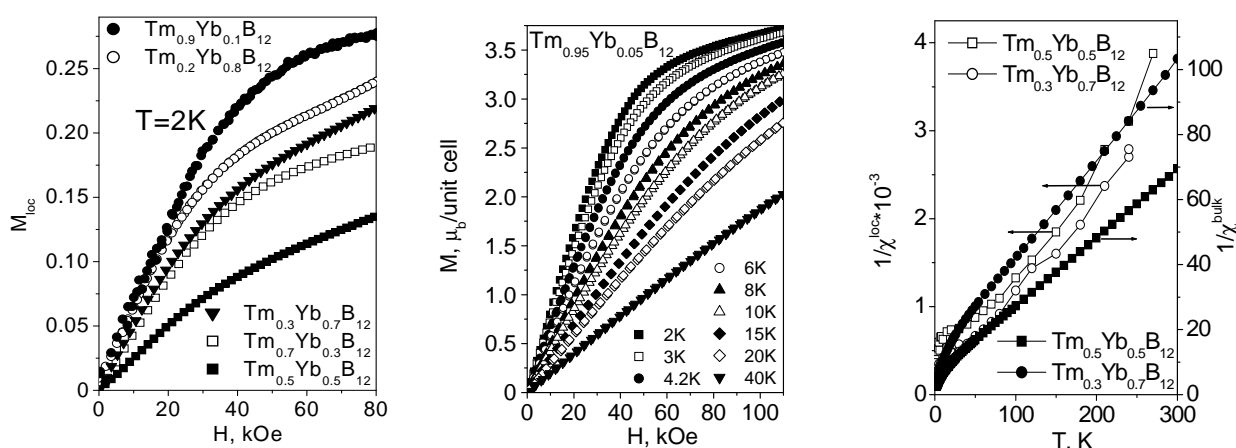
<sup>1</sup> A.M. Prokhorov General Physics Institute of RAS, 38, Vavilov str., Moscow, 119991, Russia

<sup>2</sup> Institute for Problems of Materials Science, 3, Krzhyzhanovsky str., Kiev, 03680, Ukraine

<sup>3</sup> Center of Low Temperature Physics, IEP SAS, 04001 Košice, Slovakia

<sup>4</sup> Institute for Nanoscale Physics and Chemistry of KUL, Celestijnenlaan 200D, B-3001 Leuven, Belgium

$RB_{12}$  cage-cluster compounds have attracted considerable interest in recent years due to the unique combination of their physical properties, such as high melting point, hardness, thermal and chemical stability, and a variety of magnetic properties. Among them, the rare earth dodecaborides  $Tm_{1-x}Yb_xB_{12}$  demonstrate two simultaneous transitions - the metal-insulator and antiferromagnetic - paramagnetic ones and a monotonous decrease of the Neel temperature ( $T_N$ ) is observed along the  $RB_{12}$  series from  $TbB_{12}$  ( $T_N \approx 19.2K$ ) to  $Tm_{0.7}Yb_{0.3}B_{12}$  ( $T_N \approx 0.8K$ ) with a filling of the  $4f$  shell of rare earth ions.



To shed more light on the charge scattering mechanisms in paramagnetic and AF phases of these compounds the transverse magnetoresistance (MR) and magnetization  $M(H,T)$  measurements have been carried out in this study on single crystalline samples of  $Tm_{1-x}Yb_xB_{12}$  ( $0 < x < 0.85$ ) in wide temperature range (1.8-40K) in magnetic fields up to 110 kOe. The examples of the MR and  $M(H,T)$  data obtained for the samples with different Yb content are shown in Figures a and b respectively. It was established evidently that the only regime of negative quadratic magnetoresistance is observed for all the substitutional solid solutions  $Tm_{1-x}Yb_xB_{12}$  under investigation. Moreover, it was found that both the root square of MR  $M_{loc}(H) = \sqrt{-\Delta\rho/\rho}$  (Fig. a) and magnetization  $M(H)$  (Fig.b) demonstrate Brillouin type dependences with the tendency to saturation in strong magnetic fields. It was shown that the above mentioned negative contribution (-)MR can be interpreted quantitatively in the framework of Yosida model [1]. On the basement of the approach [1] the local (Fig.a) and bulk (Fig.b) magnetization dependences may be compared and additionally the Currie-Weiss type analysis is approximately carried out.

Support by the RAS Program “Strongly Correlated Electrons in Semiconductors, Metals, Superconductors and Magnetic materials” and RFBR (project 10-02-00998a) is acknowledged.

[1] K. Yosida, Phys. Rev., **107** (1957) 396.

23PO-M-7

## DOPING EFFECT ON THE ANOMALOUS BEHAVIOR OF THE HALL EFFECT IN ELECTRON-DOPED SUPERCONDUCTOR $\text{Nd}_{2-x}\text{Ce}_x\text{CuO}_{4+\delta}$

Charikova T.B.<sup>1</sup>, Shelushinina N.G.<sup>1</sup>, Harus G.I.<sup>1</sup>, Neverov V.N.<sup>1</sup>, Petukhov D.S.<sup>1</sup>, Ivanov A.A.<sup>2</sup>

<sup>1</sup> Institute of Metal Physics RAS, S.Kovalevskaya str.,18, Ekaterinburg, 620990, Russia,

<sup>2</sup> Moscow Engineering Physics Institute, Kashirskoye highway, 31, Moscow, 115409, Russia

The in-plane longitudinal  $\rho_{xx}$  and Hall  $\rho_{xy}$  components of the resistivity are measured as the functions of perpendicular to the ab-plane magnetic field  $B$  up to 9T in single crystal films of electron-doped superconductor  $\text{Nd}_{2-x}\text{Ce}_x\text{CuO}_{4+\delta}$  at helium temperatures  $T=(0.4 - 4.2)\text{K}$ .

The evolution of the Hall coefficient value in the normal state above the upper critical field  $B_{c2}$  is traced with a variation of Ce doping. It is found that low temperature normal state Hall coefficient  $R_H^n$  is negative for underdoped ( $x=0.14$ ) and optimally doped ( $x=0.15$ ) films, positive for highly overdoped ( $x=0.18$ ) films and has  $R_H^n \cong 0$  for slightly overdoped ( $x=0.17$ ) films in accordance with previous results for normal state  $R_H^n$  at  $T > T_c$ .

Such a behavior of  $R_H^n(x)$  may be naturally explained by a coexistence of electrons (of concentration  $n$ ) with holes (of concentration  $p$ ) even in nominally electron-doped cuprate system [1]. In agreement with the ARPES results [2] the two types of carriers may originate from electronlike and holelike parts of the Fermi surface in cuprates.

Proceeding from a relation  $n \sim x$  for ideal electron doping we have carried out a division of electron and hole contributions and have come to a conclusion about rather rapid increase of  $p(x)$ .

As in the most cuprates we have found an anomalous change of a sign of the Hall effect in the mixed state  $R_H^f$  just below  $B_{c2}$ : from negative to positive for  $x=0.14$ ;  $0.15$  and from positive to negative for  $x=0.18$ . This Hall anomaly has been previously interpreted using a lot of different assumptions, most of which were closely connected with the peculiarities of magnetic flux dynamics in the mixed state of superconductors.

We have adopted a semiphenomenological description of a mixed state Hall effect by flux-flow model of Bardeen and Stephen modified by coexistence of electrons and holes with rather different superconducting gaps (and thus with different  $B_{c2}$ ) [2]. It turns out possible to describe qualitatively both the behavior of  $R_H^f$  as a function of magnetic field and the temperature evolution of this picture due to  $B_{c2}(T)$  dependencies.

This work was done within RAS Program (project N 09-P-2-1005 Ural Division RAS) with partial support of RFBR (grant N 09-02-96518).

[1] N.Luo, cond-mat/00030074.

[2] J.E.Hirsch, F.Marsiglio, Phys.Rev.B, **43** (1991) 424.

[3] N.P.Armitage et al., phys.Rev.Lett., **88** (2002) 257001.

## SUPERCONDUCTING TRIPLET SPIN VALVE F2F1S – GENERAL MODEL WITH ARBITRARY LAYER THICKNESSES AND BOUNDARY TRANSPARENCIES

*Deminov R.G.<sup>1</sup>, Tagirov L.R.<sup>1,2</sup>, Nedopekin O.V.<sup>1</sup>, Fominov Ya.V.<sup>3</sup>, Karminskaya T.Yu.<sup>4</sup>, Kupriyanov M.Yu.<sup>4</sup>, Golubov A.A.<sup>5</sup>*

<sup>1</sup> Institute of Physics, Kazan Federal University, 420008 Kazan, Russia

<sup>2</sup> Institute of Physics, Augsburg University, D-86135 Augsburg, Germany

<sup>3</sup> L.D. Landau Institute for Theoretical Physics RAS, 119334 Moscow, Russia

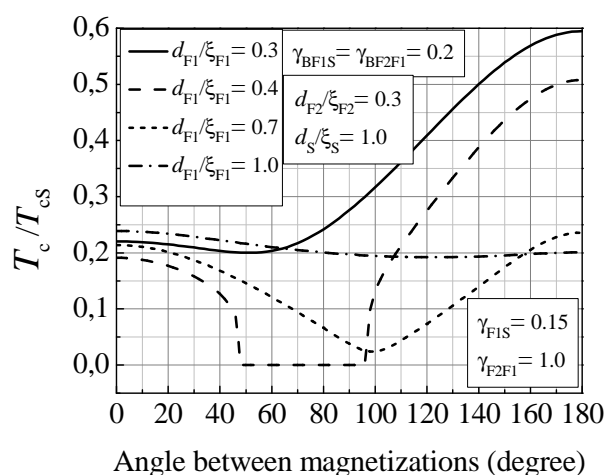
<sup>4</sup> Skobeltsyn Institute of Nuclear Physics, Moscow State University, 119992 Moscow, Russia

<sup>5</sup> Faculty of Science and Technology and MESA+ Institute of Nanotechnology, University of Twente, P.O. Box 217, 7500 AE Enschede, The Netherlands

We study the critical temperature  $T_c$  of F2F1S trilayers (S is a singlet superconductor, Fi is a ferromagnetic metal), where the long-range triplet superconducting component is generated at noncollinear magnetizations of the F layers [1].

The F2NF1 heterostructure (N is a non-magnetic normal metal) with arbitrary thickness of the layers is a conventional spin-valve which plays a role of control element in the F2NF1S tetralayers. Earlier we demonstrated that  $T_c$  in such structures can be a non-monotonic function of the angle  $\alpha$  between magnetizations of the two F layers [2,3]. The absolute minimum is achieved at an intermediate  $\alpha$ , lying between the parallel (P,  $\alpha = 0$ ) and antiparallel (AP,  $\alpha = \pi$ ) configurations, we called this feature the “triplet” spin-valve effect. The role of the N layer in the F2NF1S structure reduces to separating magnetically the two ferromagnetic layers allowing them to rotate independently. If thinner than the coherence length, it has very small impact on superconductivity in the structure [3]. Therefore we can study the simplified F2F1S structure.

Figure shows dependence of the transition temperature  $T_c$  on the angle  $\alpha$  between magnetizations, the outer ferromagnetic layer F2 having fixed thickness (see the legend). Here  $T_{cS}$  is the superconducting transition temperature for an isolated S layer. Transparencies of the interfaces were taken typical for the SF-proximity systems (see the Figure legends). At small thicknesses  $d_{F1}$  of the middle ferromagnetic layer F1 ( $d_{F1}/\xi_{F1} = 0.3$ ) the switching effect is standard, while at larger  $d_{F1}$  ( $d_{F1}/\xi_{F1} = 1.0$ ) the effect is inverse. Curve for  $d_{F1}/\xi_{F1} = 0.7$  demonstrates the triplet spin-valve effect. Moreover, the reentrant  $T_c(\alpha)$  dependence ( $d_{F1}/\xi_{F1} = 0.4$ ) is possible. In this situation the triplet spin-valve effect takes place even at  $T = 0$ . Figure shows a possibility of the spin-valve effect enhancement at approximately equal thicknesses of the F layers.



This work was supported by RFBR (prs. Nos. 11-02-00077-a, 11-02-00848-a, and 10-02-90014-Bel\_a), DFG (pr. No. GZ: HO 955/6-1), the Russian Ministry of Education and Science (contract No. P799), and the program “Quantum physics of condensed matter” of the RAS.

[1] F.S. Bergeret, A.F. Volkov, and K.B. Efetov, *Rev. Mod. Phys.*, **77** (2005) 1321.

[2] Ya.V. Fominov, A.A. Golubov, T.Yu. Karminskaya *et al.*, *JETP Lett.*, **91** (2010) 308.

[3] R.G. Deminov, L.R. Tagirov, O.V. Nedopekin *et al.*, *Phys. Rev. B*, submitted.

## INVESTIGATION OF MULTICRITICAL PHENOMENA IN COMPLEX MODELS OF MAGNETICS BY MONTE-CARLO METHODS

Murtazaev A.<sup>1</sup>, Ibaev J.<sup>2</sup>

<sup>1</sup> Institute of Physics DSC RAS, Makhachkala, Yaragskogo 94, Russia

<sup>2</sup> Dagestan State University, Makhachkala, Gadjieva 43a, Russia

Besides a problem of the critical phenomena (the second-order phase transitions) many researchers direct the attention to the study of more complex types of behavior in situations conditionally called as multicritical phenomena. The cross points of two or more lines of the singularities in a plane of the thermodynamic states of the system are belong to them [1].

Experimental situation near the critical points is more complex than in objects with common critical points. This complexity is connected with a presence of crossover phenomena and a correct accounting of distorting factors. At the same time a strict theoretical investigation of similar systems leads to variety of complex nonlinear differential equations.

Therefore the application of computational physics methods is one of the most reliable techniques for exploration of similar phenomena.

In this work we present a research of Ising magnetic with positive values of the exchange integrals for nearest neighbors and negative values for next neighbors along Z axes (so called ANNNI-model (Fig.1)) by the Monte-Carlo (MC) methods based on the standard Metropolis algorithm.

The studied model is characterized by an occurrence of multicritical Lifshitz-like point in the phase diagram, where three phases coexist simultaneously: ferromagnetic, paramagnetic, and incommensurate phases [2].

Modeling was carried out on cubic systems with periodic boundary conditions and sizes of  $L \times L \times L$   $L=12 \div 64$ . The spin number was  $N_{eff}=1728 \div 262144$ . Markovian chains of  $\tau=1000\tau_0$  in length ( $\tau_0=10^4$  MC steps/spin is a length of non-equilibrium part) were generated by means of computers. The thermodynamic parameters for the system were averaged along this chain. Furthermore, the averaging was performed by ten different initial configurations. According to experimental results was plotted the phase diagram of the model and the critical exponents were calculated along the bounds of second-order "ferromagnetic-paramagnetic" phase transitions in the neighborhood of Lifshitz point.

A change in values of critical exponents when increasing the absolute value of interaction parameter of the neighbors following the next ones indicates the occurrence of the crossover from Ising critical behavior to the multicritical.

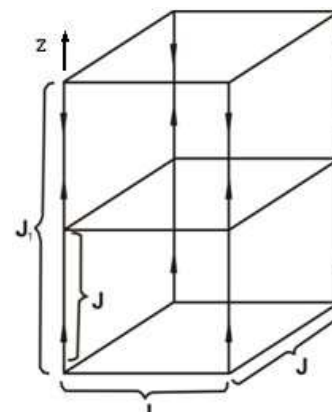


Fig. 1. ANNNI-model

Support by RFBR (№ 09-02-96506), PHCP (№ П554 и № 02.740.11.03.97) is acknowledged.

[1] P.A. Fleury *Science.*, 211, (1981). 125

[2] Yu.A. Izumov, V.M. Siromiatnikov Phase transition and symmetry crystal M.: Science (1984) 241.

23PO-M-10

## SUPERCONDUCTING FILM FLUX TRANSFORMER FOR A SENSOR OF A WEAK MAGNETIC FIELD

*Ichkitidze L.P.<sup>1</sup>, Mironyuk A.N.<sup>2</sup>*

<sup>1</sup> Moscow State Institute of Electronic Technology, dep. BMS, MIET, pas. 4806, bld. 5, Zelenograd, Moscow, 124498, Russia

<sup>2</sup> Institute of nanotechnology of microelectronics of the Russian Academy of Sciences, Leninsky Prospekt, 32A, Moscow, 119991, Russia

The magnetic sensitivity of sensors of a weak magnetic field (SWMF) can be considerably improved by the use of the superconducting film flux transformers (SFFT).

The object of study is the geometry of SWMF with a magnetosensitive element (ME) based on the giant magnetoresistance effect when ME and the narrow SFFT operative strip over it are separated by a dielectric layer. Performed is the nanostructuring of the SFFT operative strip in the form of parallel branches with nanometer widths.

Carried out is the search for the SFFT gain factor growth  $F_m$  maximum value by varying the widths of the slits and branches, their number and topological location, and also the SFFT material characteristics. During the search for the optimal splitting of the SFFT operative strip into parallel branches, corresponding to the maximum value of  $F_m$  for a given configuration, calculated is the magnetic field on ME created by the superconducting currents in the branches, taking into account the non-uniform currents distribution and total branches inductance. Considered is only the magnetic field component with the most significant impact on ME.

Calculation of  $F_m$  is performed for different variants of the SFFT operative strip nanostructure with the following parameters used in the work [1]: the critical current density of  $10^6$  A/cm<sup>2</sup>, the London penetration depth of 50 nm, the SFFT operative strip width of 7000 nm, the SFFT operative strip thickness of 150 nm. For example, at the minimum width of the slits of 80 nm  $F_m \approx 100$  is achievable and the threshold magnetic sensitivity of SWMF can be reduced by the same factor.

Thus the topological nanostructuring of the operative strip of the superconducting film flux transformer increases its efficiency by approximately two orders of magnitude relative to the non-nanostructured operative strip. Respectively, the resolution of the sensor of a weak magnetic field improves and the threshold magnetic sensitivity reaches a value of  $\leq 100$  fT.

[1] Pannetier M., Fermon C., Le Goff G., Simola J., Kerr E., Science, **304** (2004) 1648-1650.

23PO-M-11

## FERMI-SURFACE TOPOLOGY OF $\text{Ce}_{1-x}\text{Yb}_x\text{CoIn}_5$

*Ignatchik O.<sup>1</sup>, Polyakov A.<sup>1</sup>, Wosnitza J.<sup>1</sup>, Bianchi A.D.<sup>2</sup>, Prevost B.<sup>2</sup>, Blackburn S.<sup>2</sup>, Côté M.<sup>2</sup>, Capan C.<sup>3</sup>, Hurt D.<sup>3</sup>, Fisk Z.<sup>3</sup>*

<sup>1</sup> Dresden High Magnetic Field Laboratory (HLD),

Helmholtz-Zentrum Dresden Rossendorf, D-01328 Dresden, Germany

<sup>2</sup> Department of Physics, University of Montreal, Montreal H3C 3J7, Canada

<sup>3</sup> Department of Physics and Astronomy, University of California, Irvine CA 92697-4575, USA

$\text{CeCoIn}_5$  is a well known heavy-fermion Pauli-limited superconductor with  $T_c = 2.3$  K. A quantum critical point (QCP) is appearing when superconductivity is suppressed by a magnetic field. The nature of the ground state has been the subject of many speculations, but it seems likely to be of antiferromagnetic only. The QCP is located not exactly at the upper critical field  $H_{c2}$ , but at a slightly lower field and antiferromagnetic fluctuations are present also in the superconducting state. More recently, it was discovered that the field-induced antiferromagnetic order couples to the superconductivity close to  $H_{c2}$  [1]. In many studies of a broad range of strongly correlated electron systems hosting a QCP doping has been used as a tuning parameter to move from a superconducting to an antiferromagnetic ground state.

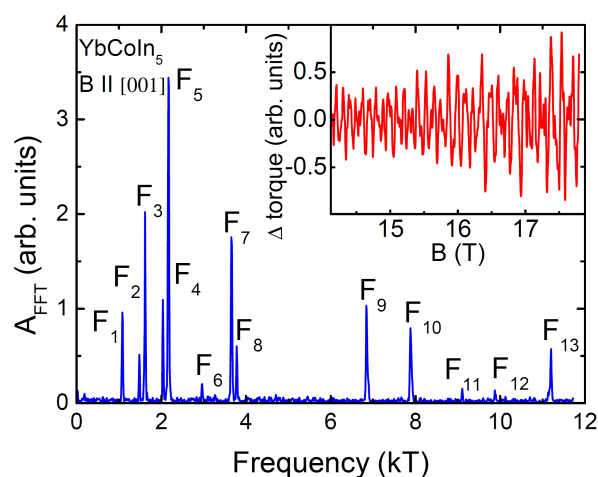


Fig. 1. Fourier spectrum of dHvA signal measured for  $\text{YbCoIn}_5$  sample. Magnetic quantum oscillations after background subtractions in the insert.

We present a detailed study of the evolution of the Fermi surface of  $\text{Ce}_{1-x}\text{Yb}_x\text{CoIn}_5$  as a function of Yb. Yb acts as a non-magnetic divalent substitute for trivalent Ce, equivalent to hole doping on the rare-earth site. The effect of Yb doping on  $\text{CeCoIn}_5$  was investigated via de Haas-van Alphen (dHvA) measurements (Fig. 1). The high-quality single crystals of  $\text{Ce}_{1-x}\text{Yb}_x\text{CoIn}_5$  cover the range from heavy-fermion superconductors to non-superconducting Pauli paramagnets [2]. The dHvA data have been obtained with Yb concentrations of:  $x = 0.1, 0.55, 0.85, 0.95$ , and 1 by use a capacitive torque magnetometer in a dilution refrigerator with base temperature of 20 mK equipped with a superconducting 20 T magnet. Superconductivity has been observed for Yb concentrations of up to  $x = 0.8$ . According to our dHvA measurements, only low effective masses could be detected for the samples with Yb concentrations larger than  $x = 0.55$ . The Fermi-surface topology of the  $\text{Ce}_{1-x}\text{Yb}_x\text{CoIn}_5$  family resembles partly that of  $\text{CeCoIn}_5$  and consists as well of highly corrugated quasi-2D cylindrical and small ellipsoidal sheets.

[1] M. Kenzelman et al., *Science* **321**, 1652, (2008)

[2] C. Capan et al., *Europhys. Lett.* **92**, 47004 (2010).

23PO-M-12

## ELECTRON TRANSPORT IN HYBRID SUPERCONDUCTING HETEROSTRUCTURES WITH MAGNETICALLY ACTIVE LAYERS

*Petrzhik A.M.<sup>1</sup>, Kislinskii Y.V.<sup>1</sup>, Constantinian K.Y.<sup>1</sup>, Ovsyannikov G.A.<sup>1,2</sup>, Shadrin A.V.<sup>1,2</sup>,  
Zaitsev A.V.<sup>1</sup>*

<sup>1</sup> Kotel'nikov Institute of Radio Engineering and Electronics RAS, Mokhovaya 11-7, Moscow, Russia

<sup>2</sup> Department of Microtechnology and Nanoscience, Chalmers University of Technology, S41296, Gothenburg, Sweden.

We report on electron transport in oxide heterostructures with superconducting/magnetic (S/M) thin film interfaces. The investigated hybrid mesa-heterostructures consist of a cuprate superconductor, a nonsuperconducting cuprate (antiferromagnetic) or manganite (ferromagnetic) interlayer with thickness  $d_M = 5 \div 50$  nm and a conventional superconductor (Nb). The superconducting critical current ( $I_C$ ) with a critical current density  $j_C = 5 \cdot 10^2 \text{ A/cm}^2$  (for  $d_M = 12$  nm) and a characteristic voltage  $I_C R_N = 100 \div 200 \mu\text{V}$  ( $R_N$  is normal resistance) are observed at liquid helium temperature for  $\text{Ca}_x\text{Sr}_{1-x}\text{CuO}_2$  antiferromagnetic cuprate interlayers with thickness  $d_M = 12 \div 50$  nm. Thus, a long-range proximity effect for  $\text{Nb}/\text{Au}/\text{Ca}_{1-x}\text{Sr}_x\text{CuO}_2/\text{YBa}_2\text{Cu}_3\text{O}_{7-\delta}$  heterostructures was observed with experimentally determined decay length  $8 \div 9$  nm [1].

The superconducting current-phase relation of heterostructures deviates from the regular sine-type and demonstrating a second harmonic component. These hybrid heterostructures with S/M interfaces show unusually high sensitivity to external magnetic field [2].

When substituting the cuprate interlayer by a manganite ( $\text{LaMnO}_3$ ,  $\text{La}_{0.7}\text{Ca}_{0.3}\text{MnO}_3$  or  $\text{La}_{0.7}\text{Sr}_{0.3}\text{MnO}_3$ ) film with  $d_M = 5 \div 20$  nm, no critical current was observed although the manganite interlayer was made several times thinner (down to  $d_M = 5$  nm).

Using semi-classical analytical approach for conductivity of heterostructures with manganite interlayer it was demonstrated that at temperatures lower than the critical temperature of Nb,  $T_{C(\text{Nb})}$ , in the case of low transparency of superconductor/manganite interface, the conductance is specified by the proximity effect and strongly depends on interface transparency. At low temperatures  $T \ll T_{C(\text{Nb})}$  conductance peak appears within the voltage range, which is determined by exchange field of manganite interlayer [3]. At intermediate temperatures  $T_{C(\text{Nb})} < T < T_{C(\text{YBCO})}$  we experimentally observed conductance singularities close to  $V=0$ , caused by superconductivity of the YBCO electrode.

Support by the Russian Academy of Sciences, Russian Foundation of Basic Research (11-02-01234-a), Scientific school grant 5423.2010.2, Ministry of Education and Science of Russian Federation, contract 02.740.11.0795 is acknowledged.

[1] G.A. Ovsyannikov, K.Y. Constantinian, Yu.V. Kislinski et al., *Superconductor Sci. and Technol.*, **24** (2011) 055012.

[2] Y.V. Kislinskii, K.Y. Constantinian, G.A. Ovsyannikov, et al., *JETP*, **106** (2008) 800.

[3] A.M. Petrzhik, G.A. Ovsyannikov, et al. *JETP*, **112**, No 5 (2011) to be published.

23PO-M-13

## MAGNETIC HYPERFINE FIELDS FOR $^{119}\text{Sn}$ IMPURITY ATOMS IN THE LAVES PHASES $\text{GdAl}_2$ AND $\text{TFe}_2$ (T= Y, Sc, Hf) CRYSTALLIZED AT HIGH PRESSURE

*Krylov V.I.<sup>1</sup>, Tsvyashchenko A.V.<sup>1,2</sup>, Fomicheva L.N.<sup>2</sup>*

<sup>1</sup> Skobeltsyn Institute of Nuclear Physics, Moscow State University, Vorob'evy Gory 1/2, 119991 Moscow, Russia

<sup>2</sup> Vereshchagin Institute for High Pressure Physics, Russian Academy of Sciences, 142190 Troitsk, Russia

The hyperfine interactions for diamagnetic atoms are very sensitive to the electronic structure of the intermetallic compounds. The evidence of metastability an electronic structure of the compounds  $\text{RE}_2\text{T}_2$  (RE is rare earth metals and, T is Fe, Co) crystallized under high pressure has been found by hyperfine magnetic field (HF) studies on  $^{119}\text{Sn}$  nuclei in Refs. [1, 2].

The structural and magnetic properties of the compounds  $\text{GdAl}_2$  and  $\text{TFe}_2$  (T= Y, Sc, Hf) crystallized under high pressure have been investigated by X-rays technique and Mössbauer spectroscopy for  $^{119}\text{Sn}$  impurity atoms. The components of each alloy doped by a small amount of  $^{119}\text{Sn}$  or  $^{119\text{m}}\text{Sn}$  were melted under pressure of 8 GPa [3]. The Laves structures: cubic C15 ( $\text{MgCu}_2$ ) and hexagonal C14 ( $\text{MgZn}_2$ ) have been detected for  $\text{GdAl}_2$ ,  $\text{YFe}_2$  and  $\text{ScFe}_2$ ,  $\text{HfFe}_2$ , respectively. The lattice parameters of all compounds are found to be the similar of that observed for the samples melted under "normal" conditions.

It has been shown that the  $^{119}\text{Sn}$  impurity atoms occupy both crystallographically nonequivalent positions in the structure C15 ( $\text{GdAl}_2$  and  $\text{YFe}_2$  compounds) and, all three ones in the structure C14 ( $\text{ScFe}_2$  and  $\text{HfFe}_2$  compounds). The HFs for  $^{119}\text{Sn}$  atoms equal to  $|B_1|= 39.17(6)$  T (the sign of the  $B_1$  was not measured) and  $B_2=-28.94(3)$  T at 5 K are found to be present in Gd- and Al-sites, respectively. The large difference in values of the HFs for  $^{119}\text{Sn}$  atoms in T- and in Fe-sites ( $B_1$  and  $B_2$ , respectively) of  $\text{TFe}_2$  compounds has been detected at 5K. The HFs are positive and, equal to  $B_1=43.2(2)$ ,  $34.4(1)$  and  $43.8(2)$  T for  $^{119}\text{Sn}$  atoms in Y-, Sc- and Hf-sites, respectively. The HFs  $B_2$  are anisotropic for  $^{119}\text{Sn}$  atoms in Fe-sites of  $\text{YFe}_2$ :  $B_2(1)=-2.19(6)$  T and  $B_2(2)=-3.6(3)$  T. The HFs  $B_2$  at 5 K are also different for  $^{119}\text{Sn}$  atoms in 2a- and 6h-sites:  $B_2(2a)=-2.75(3)$  T,  $B_2(6h)=-5.62(1)$  T for  $\text{ScFe}_2$  and,  $B_2(2a)=-9.0(1)$  T,  $B_2(6h)=-6.67(1)$  T for  $\text{HfFe}_2$ .

[1] V.I. Krylov, A.V. Tsvyashchenko, *Hyperfine Interactions*, **59** (1990) 391

[2] A.V. Tsvyashchenko, V.I. Krylov, *Hyperfine Interactions*, **59** (1990) 399

[3] A.V. Tsvyashchenko, *J. Less-Common Met.*, **99** (1984) L9.



23PO-M-14

## COEXISTENCE OF FERROMAGNETISM AND SUPERCONDUCTIVITY IN COMPLEX IRON-VANADIUM LAYERED NANOSTRUCTURES.

*Tsaregorodsev R.O.<sup>1</sup>, Khaydukov Yu.N.<sup>1,2</sup>, Nikitenko Yu.V.<sup>3</sup>, Perov N.S.<sup>1</sup>, Mukhamedzhanov E.Kh.<sup>4</sup>, Jernenkov K.N.<sup>5</sup>, Aksenov V.L.<sup>3,4</sup>*

<sup>1</sup> Lomonosov Moscow State University, 119992 Moscow, Russia

<sup>2</sup> Max Planck Institute for Solid State Research, D-70569 Stuttgart, Germany

<sup>3</sup> Joint Institute for Nuclear Research, 141980 Dubna, Russia

<sup>4</sup> RRC Kurchatov Institute, 123182, Moscow, Russia

<sup>5</sup> Ruhr-Universität Bochum, D 44780, Bochum, Germany

Study of influence of superconductivity (S) on ferromagnetism (FM) in layered nanostructures is an actual problem both for fundamental science and for practical applications. Theoretically predicted, that due to proximity effects between S and FM layers various scenarios of influence of superconductivity on ferromagnetism are possible: formation of domain structure (so-called cryptoferromagnetic state [1]), effect of magnetization "leakage" from FM to S layer [2, 3], change of direct and indirect exchange coupling of FM layers [4], etc. In FM/S/FM structures with non-collinear magnetization the existence of triplet superconductor pairs is predicted. Such pairs are not subject to destroying influence of an exchange field [5] and therefore more "alive" in FM layer. Practical importance of studying of such systems for needs of spintronics is connected with non trivial magnetic response of such systems on occurrence of superconductivity.

In the present work results of research of influence of superconductivity on magnetism in periodic systems of type  $[S/F]_n$ . Part of experimental data of polarized neutron reflectometry (PNR) with initial interpretation has been presented earlier in articles [6,7]. In this work we present results of complex analysis of structural, magnetic and superconducting properties of the systems based on data of synchrotron, neutron and VSM experiments.

Work was supported by RFBR grant (project № 09-02-00566).

[1] P.W.Anderson, H. Suhl, Phys. Rev., V.116 p. 898 (1959)

[2] V.N. Krivoruchko and E.A. Koshina, Phys. Rev. B 66, 014521 (2002)

[3] F. S. Bergeret, A. F. Volkov and K. B. Efetov, Phys. Rev. B 69, 174504 (2004)

[4] Sa de Melo C.A.R. Phys.Rev. B 62 12303 (2000)

[5] Volkov A. F., Bergeret F. S., and Efetov K. B. PRL. V 90. P 117006 (2003)

[6] V.L. Aksenov, K.N. Jernenkov, Yu.N. Khaidukov et al, Physica B V. 356, 9-13 (2004)

[7] V. L. Aksenov, Yu. V. Nikitenko, A. V. Petrenko et al, Crys. Rep. V.52(3),p. 381, 2007

## SUPERCONDUCTING PHASE TRANSITION IN SUPERCONDUCTOR/FERROMAGNET MULTILAYERS

*Kushnir V.N.<sup>1</sup>, Prischepa S.L.<sup>1</sup>, Cirillo C.<sup>2</sup>, Attanasio C.<sup>2</sup>, Kupriyanov M.Yu.<sup>3</sup>, Aarts J.<sup>4</sup>*

<sup>1</sup> Belarus State University of Informatics and RadioElectronics, P. Browka 6, Minsk 220013,  
Belarus

<sup>2</sup> CNR-SPIN Salerno and Dipartimento di Fisica "E.R. Caianiello" Università degli studi di Salerno,  
Fisciano (Sa) I-84084, Italy

<sup>3</sup> Institute of Nuclear Physics, Moscow State University, Moscow 119992, Russia

<sup>4</sup> Kamerlingh Onnes Laboratory, Leiden University, P.O. Box 9504, 2300 RA Leiden,  
The Netherlands

The nucleation of superconductivity in finite multilayers consisting of alternate ferromagnet (F) and superconducting (S) layers has been investigated both experimentally and theoretically. We found that the transition width  $\Delta T_c$  increases with increasing number  $N_{bl}$  of S/F bilayers in the multilayer in a well-defined manner, even though structural analysis indicates that interface roughness and thickness variations of the individual layers are small. Also, step-like features start to appear in the transition. The theoretical analysis made in terms of eigenvalues-eigenfunctions problem for the microscopic equations of the superconducting critical state derived in the diffusive limit (linearized Usadel equations).

For the preparation, we used weakly ferromagnetic  $\text{Pd}_{81}\text{Ni}_{19}$  and superconducting Nb. The samples consist of  $\text{Si}/N_{bl} \times (\text{Pd}_{81}\text{Ni}_{19}/\text{Nb})/\text{Pd}_{81}\text{Ni}_{19}$  and were grown on Si(100) substrates by diode sputtering in an ultrahigh vacuum system as described in [1]. The structural properties were characterized by X-ray reflectometry (XRR) [2]. The series has formed by samples with  $N_{bl}$  running the values from 1 to 14 and the layer thicknesses  $d_S = 18.7$  nm and  $d_F = 2.2$  nm.

For the theoretical investigation of the critical states of prepared structures, the boundary problem for the set of Usadel equations is solved by the matrix method [3]. As a result, for each structure of the series, the set of  $N_{bl}$  critical eigenstates with eigen critical temperatures  $T^{(k)}$  ( $k = 0, 1, \dots, N_{bl}-1$ ), which enumerated in accordance with numbers of the eigenfunctions nodes, is derived. The parameters of the model are estimated by the simultaneous fitting of the experimental dependence of the critical temperature  $T_c$  of  $\text{Pd}_{81}\text{Ni}_{19}/\text{Nb}$  bilayers (which belongs to the considered layered system) versus thickness of Nb layer [4], and the asymptotic of experimental  $T_c(N_{bl})$  dependence.

The result of the comparison of the experimental and theoretical data is the following. The set of eigenvalues  $T^{(k)}$  covers, and, for large  $N_{bl}$ , almost precisely matches to the transition width  $\Delta T_c$ . We elaborated a model of a multistep phase transition by passing of the eigenstates with different  $T^{(k)}$ . This model includes the mechanisms of interaction of the bias transport current with induced spontaneous vortex current [3,5].

Support by BFFR, grant F10R-063 (K.V.N., P.S.L.) and by RFFR, grant 10-02-90014-Bel-a (K.M.Yu.) is acknowledged.

[1] C. Cirillo et al., *Phys. Rev B*, **75** (2007) 104510.

[2] A. Vecchione et al., *Surface Science*, submitted.

[3] V.N. Kushnir, M.Yu. Kupriyanov, *Pis'ma v ZhETP*, submitted.

[4] C. Cirillo et al., *Phys. Rev B*, **80** (2009) 094510.

[5] S.L. Prischepa et al., *Pis'ma v ZhETP*, **88** (2008) 431 [*JETP Lett.* 88 (2008) 375].

23PO-M-16

**NMR INVESTIGATION OF SPIN GAP CHARACTERISTICS IN Na<sub>3</sub>Cu<sub>2</sub>SbO<sub>6</sub>***Lue C.S.<sup>1</sup>, Kuo Y.K.<sup>2</sup>, Young B.-L.<sup>3</sup>*<sup>1</sup> Department of Physics, National Cheng Kung University, Tainan 70101, Taiwan<sup>2</sup> Department of Physics, National Dong Hwa University, Hualien 97401, Taiwan<sup>3</sup> Department of Electrophysics, National Chiao Tung University, Hsinchu 30010, Taiwan

We report the results of a <sup>23</sup>Na nuclear magnetic resonance (NMR) study on the quasi-one-dimensional compound Na<sub>3</sub>Cu<sub>2</sub>SbO<sub>6</sub> at temperatures between 4 and 300 K. The temperature-dependent NMR shift exhibits a character of low-dimensional magnetism with a broad maximum at  $T_{max} \sim 95$  K, consistent with the magnetic susceptibility result. The transferred hyperfine coupling constant is obtained to be 2.7 kOe. Below  $T_{max}$ , the NMR shift and spin-lattice relaxation rate clearly indicate thermally activated behavior, confirming the spin gap formation in Na<sub>3</sub>Cu<sub>2</sub>SbO<sub>6</sub>. The NMR shift data can be fitted well to the alternating chain model, yielding a spin gap of about 65 K. Such the result suggests that the alternating chain picture could be a proper scenario for the understanding of spin gap nature in Na<sub>3</sub>Cu<sub>2</sub>SbO<sub>6</sub>.

23PO-M-17

**LOW-TEMPERATURE HEAT CAPACITY OF SINGLE CRYSTAL MANGANITES La<sub>1-x</sub>Ba<sub>x</sub>MnO<sub>3</sub> IN MAGNETIC FIELD***Abramov N.<sup>1</sup>, Chichkov V.<sup>1</sup>, Lofland S.E.<sup>2</sup>, Mukovskii Y.M.<sup>1</sup>*<sup>1</sup> National University of Science and Technology "MISIS", Leninskii prosp. 4, Moscow 119049, Russia<sup>2</sup> Rowan University, 201 Mullica Hill Rd., Glassboro, New Jersey 18028-17001, USA

We have measured the specific heat  $c_p$  of single crystal colossal magnetoresistance manganites of the type La<sub>1-x</sub>Ba<sub>x</sub>MnO<sub>3</sub> ( $x = 0.15, 0.17, 0.32$ ) at low temperatures in magnetic field. The data fit were fit as a function of temperature  $T$  and magnetic field  $H$  by  $c_p = \gamma T + \beta T^3 + c_{mag}(T,H) + c_{Schottky}(T,H)$  where  $c_{mag}(T,H)$  takes into account the magnon contribution while magnetic  $c_{Schottky}(T,H)$  arises because of the hyperfine field of the <sup>55</sup>Mn nuclear moment. For metal-like La<sub>0.68</sub>Ba<sub>0.32</sub>MnO<sub>3</sub>, the Sommerfeld constant electronic  $\gamma = 3.0$  mJ/mol K and the spin-wave stiffness coefficient  $D = 160$  meV Å<sup>2</sup> while for the insulating compounds  $\gamma = 0$  and  $D \sim 90$  meV Å<sup>2</sup>. Other parameters such as the Debye temperature  $\Theta_D$  and the hyperfine field  $H_{hyp}$  are similar for all compositions, with  $\Theta_D \approx 435$  K and  $H_{hyp} \approx 36.5$  T. The observed decrease of the specific heat under magnetic field is completely consistent with a suppression of magnons in a magnetic field, suggesting no unusual or exotic magnetic behavior.

The work was supported in part by NSF Grant DMR 0908779 and and Joint RFBR-NSF Grant 09-02-92661. NA was supported by the Programme of Creation and Development of the NUST "MISIS".

## PHASE TRANSITION IN FRUSTRATED HEISENBERG ANTIFERROMAGNET ON A TRIANGULAR LATTICE WITH NEXT- NEAREST NEIGHBOR INTERACTIONS

*Murtazaev A.K.<sup>1,2</sup>, Ramazanov M.K.<sup>1,3</sup>, Badiev M.K.<sup>1</sup>*

<sup>1</sup> Institute of Physics, Dagestan Scientific Center, RAS, 367003 Yaragskogo, 94, Makhachkala, Dagestan, Russian Federation

<sup>2</sup> Dagestan State University, 367003 Makhachkala, Dagestan, Russian Federation

<sup>3</sup> Dagestan State Pedagogical University, 367003 Makhachkala, Dagestan, Russian Federation

The study of phase transitions and critical phenomena in frustrated spin systems is one of the fundamental problems in statistical physics [1]. Recent advances in understanding phase transitions and critical phenomena in frustrated systems have largely been achieved by applying of Monte Carlo methods, because most attempts to calculate the critical exponents and characterize the mechanisms of the critical behavior of such systems by conventional theoretical and experimental methods are confronted by serious difficulties [2,3].

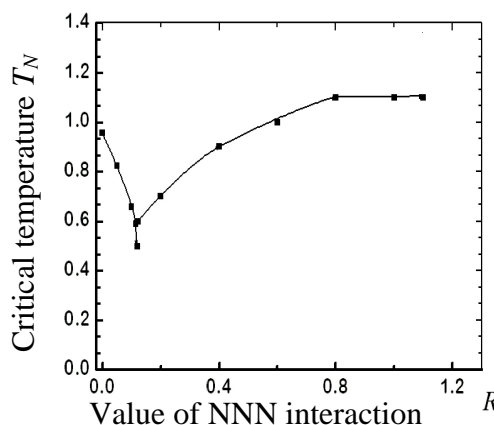
In the given work, we attempt whenever possible, with maximum accuracy, with observance of a uniform technique, and with a reliable and tested scheme, based on a replica exchange algorithm of the Monte Carlo method, to determine the value of the critical parameters of the three-dimensional frustrated Heisenberg antiferromagnetic model on a triangular lattice with allowance for next-nearest neighbor interactions. The Hamiltonian of the Heisenberg antiferromagnetic model can be represented in a following form [4]:

$$H = -J \sum_{\langle ij \rangle} (\vec{S}_i \cdot \vec{S}_j) - J' \sum_{\langle ij \rangle} (\vec{S}_i \vec{S}_j) \quad (1)$$

where  $\vec{S}_i$  is a three-component unit vector  $\vec{S}_i = (S_i^x, S_i^y, S_i^z)$ ,  $J < 0$  and  $J' < 0$  are antiferromagnetic exchange interaction constants.  $J'/J = R = 0.0 \div 0.1$  is the value of next-nearest neighbor interaction.

Figure shows a phase diagram characterizing the dependence of critical temperature  $T_N$  from value of next-nearest neighbor (NNN) interaction  $R$ . On this diagram we see area of coexistence of three phases. As approaching a point where three phases co-exist, the temperature of phase transition is displaced aside lower temperatures.

The static magnetic and chiral exponents specific heat  $\alpha$ , susceptibility  $\gamma$  and  $\gamma_c$ , magnetization  $\beta$  and  $\beta_c$ , correlation length  $\nu$  and  $\nu_c$  were calculated by using the finite-size scaling theory [2,3].



This study was supported by the Russian Foundation for Basic Research project no. 10-02-00130 and project no. 09-02-96506.

[1] Vik.S. Dotsenko, *Usp. Fiz. Nauk*, **165** (1995) 481.

[2] A.K. Murtazaev, M.K. Ramazanov, *Phys. Rev. B*, **76** (2007) 174421.

[3] A.K. Murtazaev, M.K. Ramazanov, M.K. Badiev, *JETP*, **105** (2007) 1011.

[4] H. Kawamura, *J. Phys. Soc. Jpn.*, **56** (1987) 474.

23PO-M-19

## MAGNETO-OPTICAL STUDY OF HTSC TAPES ON MAGNETIC AND NONMAGNETIC SUBSTRATES

*Rudnev I.A., Sedin Yu.Yu., Osipov M.A., Pokrovskiy S.V., Podlivaev A.I.*

National Research Nuclear University MEPhI, Moscow, Russia

Magneto-optical imaging (MOI) is an excellent tool to visualize magnetic flux patterns in superconductors with high spatial as well as temporal resolution. Furthermore, quantitative MOI allows the determination of main properties of the critical state, such as Meissner and critical current density distributions, electric fields, flux velocity fields and the local activation barrier for thermally activated flux creep. Magneto-optical imaging offers also a unique and useful method for quality control of real 2G HTSC tapes. In this report, flux profiles visualized by MOI technique will be presented at different experimental conditions. Some types of 2G HTSC tapes on both magnetic and nonmagnetic substrates are used in this study. Three cases are investigated: application of external magnetic fields; application of external dc currents; and application of external ac currents. The behaviors and peculiarities of complicated flux penetration into the samples at different conditions will be discussed in detail.

23PO-M-20

## TOPOLOGICAL HYSTERESIS AND QUANTUM TUNNELING OF NORMAL-SUPERCONDUCTOR INTERFACES IN TYPE-I Pb SUPERCONDUCTORS

*Vélez S.<sup>1</sup>, García-Santiago A.<sup>1</sup>, Zarzuela R.<sup>1</sup>, Hernandez J.M.<sup>1</sup>, Tejada J.<sup>1</sup>, Chudnovsky E.M.<sup>2</sup>*

Grup de Magnetisme, Departament de Física Fonamental, Facultat de Física, Universitat de Barcelona,

<sup>1</sup> c. Martí i Franquès 1, planta 4, edifici nou, 08028 Barcelona, Spain and Institut de Nanociència i Nanotecnologia IN2UB, Universitat de Barcelona, c. Martí i Franquès 1, edifici nou, 08028 Barcelona, Spain

<sup>2</sup> Physics Department, Lehman College, The City University of New York, 250 Bedford Park Boulevard West, Bronx, New York 10468-1589, USA

Evidence of how temperature takes part in the magnetic irreversibility in the intermediate state in a cylinder and various disks of pure type-I superconducting lead (Pb) is presented [1]. Isothermal measurements of first magnetization curves and magnetic hysteresis cycles are analyzed in a reduced representation that reveals the univocal definition of an equilibrium state for flux penetration in all the samples and concurrently exposes the thermal dependence of flux expulsion in the disks and its lack in the cylinder. The results are discussed in terms of the contributions of the shape-dependent geometrical barrier (which is the origin of the so-called topological hysteresis [2,3]) and the energy barriers associated to stress defects that act as pinning centers on normal-superconductor interfaces (NSI). The effect of the defects is to enhance the capability of the system to trap magnetic flux along the descending branch of the hysteresis cycle driving the system in a set of metastable states that would originate the occurrence of time-dependent phenomena. A first exploration of the thermal dependence of the relaxation rate reveals that the dynamics of the intermediate state of a type-I superconductor with defects is ruled by nonthermal processes for low

enough temperatures [4]. It is attributed to quantum tunneling of NSI mediated by the formation/flattening of bumps at the defects of the sample. The value of the tunneling barriers is estimated in average, and the temperature of crossover from the thermal to the quantum regime is obtained from the Caldeira-Leggett theory. Comparison between theory and experiment points to tunneling of interface segments of a size comparable to the coherence length, by steps of the order of 1 nm. The effect of an applied magnetic field on both the crossover temperature and the quantum relaxation rate is also explored [5]. A decreasing magnetic field dependence of the strength of these energy barriers, which control both the value of the crossover temperature and the onset of metastability of the system, is invoked to explain all the results obtained.

- [1] S. Vélez, A. García-Santiago, J. M. Hernandez, and J. Tejada (submitted to Phys. Rev. B).  
 [2] S. Vélez, C. Panadès-Guinart, G. Abril, A. García-Santiago, J. M. Hernandez, and J. Tejada, Phys. Rev. B **78**, 134501 (2008).  
 [3] R. Prozorov, Phys. Rev. Lett. **98**, 257001 (2007).  
 [4] E. M. Chudnovsky, S. Vélez, A. García-Santiago, J. M. Hernandez, and J. Tejada, Phys. Rev. B **83**, 064507 (2011).  
 [5] S. Vélez, R. Zarzuela, A. García-Santiago, and J. Tejada, (submitted to Phys. Rev. B).

23PO-M-21

## STUDIES ON TEMPERATURE DEPENDENT ELECTRICAL AND MAGNETOCALORIC PROPERTIES OF $\text{La}_{0.9}\text{Sr}_{0.1}\text{MnO}_3$

*Shinde K.P.<sup>1,2</sup>, Pawar S.S.<sup>1,2</sup>, Thorat N.D.<sup>2</sup>, Pawar S.H.<sup>1,2</sup>*

<sup>1</sup> Department of Physics, Shivaji University, Kolhapur-416 004 (MS), India

<sup>2</sup> Centre For Interdisciplinary Research, D. Y. Patil University, Kolhapur – 416 006 (MS), India

Magnetic refrigeration is an emerging technology that is expected to be more energy efficient and environmentally green compared to the conventional gas compression refrigeration technique. The working principle of the magnetic refrigerator is based on the magnetocaloric effect (MCE), which refers to an adiabatic temperature change ( $\Delta T_{ad}$ ) or an isothermal magnetic entropy change ( $\Delta S_M$ ) upon application or removal of a magnetic field. Although the magnetic refrigeration using adiabatic demagnetization of paramagnetic salts had been in use for many years to obtain temperatures below 1 K, ferromagnetic materials with tunable Curie temperatures (TC) are being explored to achieve room temperature cooling applications.

In the present investigation, nanocrystalline sample of  $\text{La}_{0.9}\text{Sr}_{0.1}\text{MnO}_3$  (LSMO) has been successfully synthesized by the Solution combustion method. The X-ray diffraction studies show rhombohedral crystal structure without any impurities. The surface morphology studied by Scanning Electron Microscope and TEM analysis shows the particle size increases with annealing temperature. The low temperature resistivity measurement shows that LSMO shows semiconducting behavior. The magnetic properties were studied by VSM and SQUID. The maximum saturation magnetization and lower coercivity found for the sample heat treated at 1200 °C are 52.5 emu/gm and 10.7Oe respectively. The maximum change in entropy found to be 0.135 J/kg.K with 1.5T applied field at Curie temperature for sample heat treated at 600°C.

## THE JOSEPHSON CURRENT IN THE SFS SANDWICH TAKING INTO ACCOUNT PROXIMITY EFFECT AND UMKLAPP PROCESSES

*Tumanov V., Proshin Yu.*

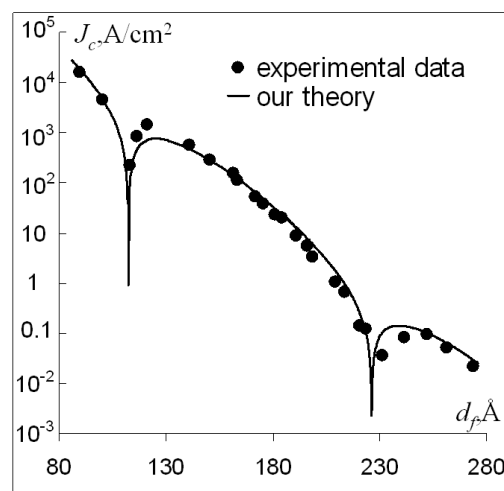
Institute of Physics, Kazan University, Kazan, Russian Federation.

We analyze the symmetrical superconductor-ferromagnetic-superconductor (SFS) Josephson system in the dirty limit. The transformation the BCS pairs to the Fulde-Ferrell-Larkin-Ovchinnikov pairs (and vice versa) at passing through SF (FS) borders may be accompanied by Umklapp processes. Thus the value of the Cooper pair's quasimomentum in the SF border plane may be varied on  $q_f$  [1]. The system is considered close the critical temperature  $T_c$ . The solution of the Usadel equations with the boundary conditions [1] allows us to determine the critical temperature [1] and the Josephson current [2] as a function of the F layer thickness  $d_f$ . To estimate the proximity effect influence on the Josephson current density  $J_s$  we use the expansion of superconductor energy in the powers of an order parameter and we get the expression:

$$J_s(\varphi) = (2e/\hbar)N(0) \left( -10.24T_c d_s \frac{\partial}{\partial \varphi} T_c(\varphi) + \frac{\Phi_0 J_{c0} \sin \varphi}{2\pi c N(0)} \right), \quad (1)$$

where  $\Phi_0$  is the magnetic flux quantum,  $N(0)$  is the electron density of state,  $d_s$  is the S layer thickness,  $\varphi$  is the phase difference of the order parameter between the S layers,  $J_{c0}$  is the critical Josephson current density without dependence of the critical temperature  $T_c$  from the phase difference  $\varphi$ . First term in (1) gives the main contribution near  $T_c$  and it may be evaluated as  $\partial T_c / \partial \varphi \approx (1/2)(T_c(\pi) - T_c(0)) \sin \varphi$  ( $T_c(0)$  and  $T_c(\pi)$  is the critical temperature when  $\varphi$  is 0 and  $\pi$ ).

The experimental dependence of current density  $J_c$  of the F layer thickness  $d_f$  for the Nb/Cu<sub>0.47</sub>Ni<sub>0.53</sub>/Nb system [3] and our theoretical curve are presented in Figure. We took for the parameters  $\xi_{s0} = 430 \text{ \AA}$  (the BCS coherence length),  $\xi_s = 80 \text{ \AA}$  (coherence length),  $d_s = 110 \text{ nm}$  from the work [3]. The transparency of the SF boundaries  $\sigma_s = 0.27$  have found from the analysis of  $T_c$  ( $d_s = 11 \text{ nm}$ ) behavior [3]. Such low value of transparency allows us to analyze  $J_c(d_f)$  using the linearized Usadel equation [2]. We do not take into account the  $s$ - $d$  scattering processes, as in [4]. Good agreement is obtained by taking into account the Umklapp processes (fitting parameters are the spin-stiffness length  $a_f = 0.029\xi_{s0}$ ,  $a_f q_f = 1.32$ , the mean free path in the F layer  $l_f/a_f = 1.65$ ).



The work was partially supported by RFBR (the project 09-02-01521) and by Ministry of Education and Science of Russian Federation.

[1] Yu.A. Izyumov, *et al.*, *Physics/Uspekhi*, **45** (2002) 109.

[2] A.I. Buzdin, *Rev.Mod.Phys.*, **77** (2005) 950.

[3] V.V. Ryazanov, *et al.*, *Low Temp. Phys.*, **136** (2004) 385.

[4] A.V. Vedyayev, N.V. Ryzhanova, N.G. Pugach, *JMMM*, **305** (2006) 53.

23PO-M-23

## GIANT MAGNETOSTRICTION OF HTSC SINGLE CRYSTAL $\text{Bi}_2\text{Sr}_{(2-x)}\text{La}_x\text{CuO}_6$ ( $x=0.8$ ) IN NONCONDUCTING STATE

Krynetskii I.<sup>1</sup>, Moskvina A.<sup>2</sup>, Shabanova N.<sup>3</sup>, Krapf A.<sup>4</sup>, Martovitsky V.<sup>3</sup>, Gavrilkin S.<sup>3</sup>, Kovalenko V.<sup>3</sup>

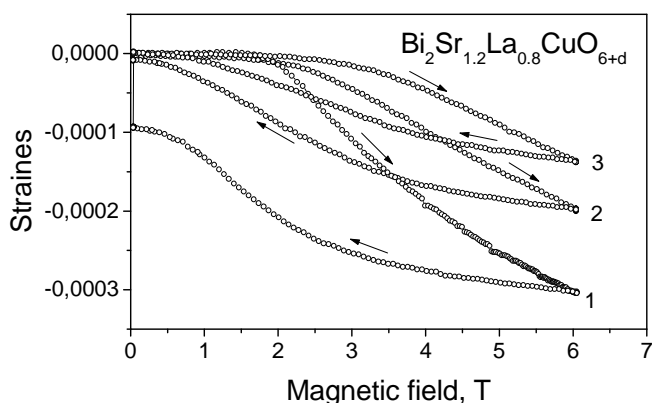
<sup>1</sup> Lomonosov Moscow State University, 119899 Moscow, Russia

<sup>2</sup> Ural State University, 620083 Ekaterinburg, Russia

<sup>3</sup> Lebedev Physical Institute of the Russian Academy of Science, 119991 Moscow, Russia

<sup>4</sup> Humboldt University Berlin, Institute of Physics, 12489 Berlin, Germany

The magnetostriction measurements of heavily underdoped single layer cuprate  $\text{Bi}_2\text{Sr}_{2-x}\text{La}_x\text{CuO}_6$  ( $x=0.8$ ) for concentration of charge carriers corresponding to the metal-insulator transition were performed at magnetic fields up to 6 T in temperature range 6.3 – 70 K. The single crystals of  $\text{Bi}_2\text{Sr}_{2-x}\text{La}_x\text{CuO}_6$  ( $x=0.8$ ) were grown by the method of free crystallization in flux cavities at cooling from 1020<sup>o</sup> C down to 920<sup>o</sup> C at the rate of 1-2<sup>o</sup> C/h followed by cooling to room temperature at the rate of 100<sup>o</sup> C/h. The magnetostriction measurements were performed with a homemade strain gauge dilatometer with the relative resolution of  $5 \times 10^{-7}$ . The crystal strains were measured along some direction in (ab)-plane, external magnetic field was applied parallel the strain direction and perpendicular to (ab)-plane. Figure shows the longitudinal magnetostriction curve of  $\text{Bi}_2\text{Sr}_{1.2}\text{La}_{0.8}\text{CuO}_{6+d}$  single crystal at T=6.3 (1), 10 (2) and 20 K (3).



The surprisingly large  $\lambda$  value for nonsuperconducting La-Bi2201 sample exceeds all the magnetostriction data ever reported for single crystal samples of high- $T_c$  cuprates well in depth of superconducting state [1]. The magnetostriction curves had a hysteretic behavior with strong temperature dependence. Transversal magnetostriction for La-Bi2201 single crystal revealed a behavior which was dramatically differed from that for longitudinal magnetostriction. It had opposite (positive) sign with the both maximal magnitude at 6 T and remnant strains on the

order of  $10^{-6}$ . The giant magnetostriction of nonconducting La-Bi2201 single crystal was explained in the frame of model of residual, or fluctuating superconductivity La-Bi2201 cuprate.

The RFBR Grants No. 10-02-01339-a and 10-02-96032-a are acknowledged for financial support.

[1] Ikita H., Hirota N., Nakayama Y., Kishio K., and Kitazawa K., Phys. Rev. Lett. **70**, 2166 (1993).



## NON-ZHANG-RICE BEHAVIOR OF THE $\text{CuO}_4$ HOLE COPPER CENTERS IN $\text{La}_2\text{Li}_{0.5}\text{Cu}_{0.5}\text{O}_4\text{:Fe}$ AS SEEN BY NMR

Gippius A.A.<sup>1</sup>, Gervits N.E.<sup>1</sup>, Tkachev A.V.<sup>1</sup>, Presniakov I.A.<sup>2</sup>, Sobolev A.V.<sup>2</sup>, Rusakov V.S.<sup>1</sup>,  
Moskvin A.S.<sup>3</sup>

<sup>1</sup> Department of Physics, Moscow State University, 119991 Moscow, Russia

<sup>2</sup> Department of Chemistry, Moscow State University, 119991 Moscow, Russia

<sup>3</sup> Ural State University, 620083 Ekaterinburg, Russia

The nature of the doped-hole state in the cuprates with nominally  $\text{Cu}^{2+}$  ions such as  $\text{La}_2\text{CuO}_4$  is a matter of great importance in understanding both the normal state behavior of the cuprates and the mechanism leading to the high-temperature superconductivity. Single ( $d_{x^2-y^2}$ )-hole state of  $\text{Cu}^{2+}$  ion is typical for copper with the square planar coordination of oxygen ions. An unique opportunity to study the doped hole state ( $\text{CuO}_4^{5-}$  center to be a cluster analogue of  $\text{Cu}^{3+}$  ion) in isolated  $\text{CuO}_4$  clusters without the confounding contributions of the nearest neighbor antiferromagnetically correlated  $\text{CuO}_4$  clusters is provided in  $\text{La}_2\text{Cu}_{1-x}\text{Li}_x\text{O}_4$  at  $x = 0.5$ .

Our  $^7\text{Li}$  NMR measurements in  $\text{La}_2\text{Li}_{0.5}\text{Cu}_{0.5}\text{O}_4\text{:Fe}$  samples reveal a dramatic change in the  $^7\text{Li}$  NMR lineshape and unusual temperature effects despite a very low concentration of Fe atoms. It seems, the Fe substitution stimulates a strong change of Cu-O electronic structure within a rather large volume around Fe center. An unexpectedly large inhomogeneous broadening with a marked asymmetry of the lineshape was observed below  $T=180\text{K}$  in comparison with the  $^7\text{Li}$  line in  $\text{La}_2\text{Li}_{0.5}\text{Cu}_{0.5}\text{O}_4$  [1]. An anomalous temperature dependence of the  $^7\text{Li}$  spin-lattice relaxation rate  $1/T_1$  which can be approximated by a sum of the almost T-independent low temperature contribution ( $T < 150\text{K}$ ), and high temperature activated process:  $1/T_1 \sim \exp(-E_a/kT)$  with  $E_a \approx 65$  meV. Such a behavior reflects the magnetic/quadrupole fluctuations within the Cu-O subsystem [2]. The distinct asymmetry of the  $^7\text{Li}$  NMR signal at  $T < 160$  K is consistent with contributions from nearby oxygen ion orbital magnetic moments to dipolar field on  $^7\text{Li}$  nuclei.  $^7\text{Li}$  NMR together with  $^{57}\text{Fe}$  Moessbauer data performed for the  $\text{La}_2\text{Li}_{0.5}\text{Cu}_{0.5}\text{O}_4\text{:}^{57}\text{Fe}$  powder sample unambiguously point to a non Zhang-Rice nature of the ground state of the hole  $\text{CuO}_4^{5-}$  centers.

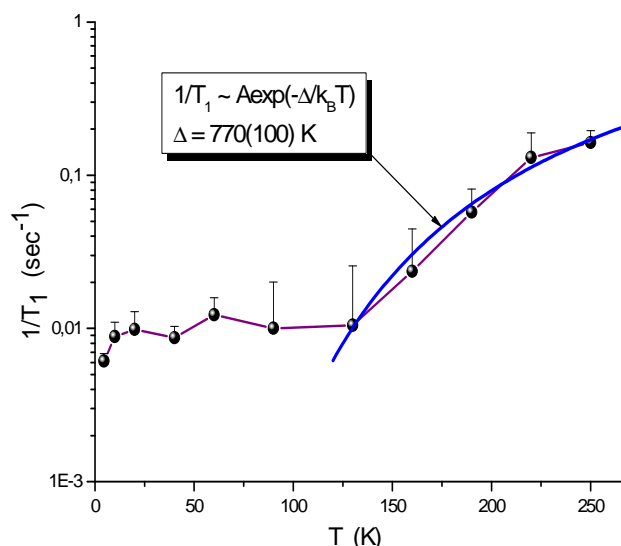


Fig.1.  $^7\text{Li}$  spin-lattice relaxation rate in  $\text{La}_2\text{Li}_{0.5}\text{Cu}_{0.5}\text{O}_4\text{:Fe}$  measured at  $H = 4.88$  T and  $F = 80.12$  MHz.

[1] A.I. Rykov, H. Yasuoka, and Y. Ueda, *Physica C* **247** (1995) 327.

[2] Y. Yoshinari, et al., *Phys. Rev. Lett.* **77** (1996) 2069.



Wednesday

**24 August**

9:30-11:00

plenary lectures  
24PL-A

24PL-A-1

## ULTRAFAST OPTICAL MANIPULATION OF MAGNETIZATION: CHALLENGES AND OPPORTUNITIES

*Rasing T.*

Radboud University Nijmegen, The Netherlands, Institute for Molecules and Materials

The interaction of sub-picosecond laser pulses with magnetically ordered materials has developed into an extremely exciting research topic in modern magnetism and spintronics[1]. From the discovery of sub-picosecond demagnetization over a decade ago[2] to the recent demonstration of magnetization reversal by a single 40 femtosecond laser pulse[3], the manipulation of spins by ultra short laser pulses has become a fundamentally challenging topic with a potentially high impact for future spintronics, data storage and manipulation and quantum computation.

Single-shot pump-probe magneto-optical imaging results show that circularly polarized subpicosecond laser pulses steer the magnetization reversal in a Transition Metal-Rare Earth alloy along a novel and ultrafast route, which does not involve precession but occurs via a strongly nonequilibrium state[4]. However, the nature of this phase and the dynamics of the individual TM and RE moments remained elusive so far. Recent experiments indicate a possible difference in the dynamics of the TM and RE moments at time scales that are currently limited by the pulse widths of the optical excitations employed (~100 fs). To investigate such highly nonequilibrium phases requires both excitation and probing at ultra short time scales and selectivity for the individual moments[5].

In addition, when the time-scale of the perturbation approaches the characteristic time of the exchange interaction (~10-100 fs), the magnetic dynamics may enter a novel coupling regime where the exchange interaction may even become time dependent. Using ultrashort excitations, we might be able to manipulate the exchange interaction itself. Such studies require the excitation and probing of the spin and angular momentum contributions to the magnetic order at timescales of 10 fs and below, a challenge that might be met by the future fs X-ray FEL's.

- [1] A.Kirilyuk et al, Rev. Mod. Phys. 82, 2731-2784 (2010)
- [2] E. Beaurepaire et al, Phys.Rev.Lett.76, 4250 (1996)
- [3] C.D.Stanciu et al, Phys.Rev.Lett.99, 047601 (2007)
- [4] K.Vahaplar et al, Phys.Rev.Lett.103, 117201 (2009)
- [5] I. Radu et al, Nature 472, 205-208 (2011)

## RECENT ADVANCES IN BIOMAGNETICS

Ueno S.<sup>1,2,3</sup>

<sup>1</sup> Professor Emeritus, Graduate School of Medicine, the University of Tokyo, Tokyo, Japan

<sup>2</sup> Department of Applied Quantum Physics, Kyushu University, 6-10-1 Hakozaki, Higashi-ku, Fukuoka, 812-8581 Japan

<sup>3</sup> Faculty of Medical Technology, Teikyo University, Fukuoka, 4-3-124 Shinkattachi-machi, Omuta, Fukuoka, 836-8505 Japan

Biomagnetics is an interdisciplinary field where magnetics, biology and medicine overlap. Biomagnetics has a long history since 1600 when William Gilbert published his book “De Magnete”. Recent advances in biomagnetics have enabled us not only to detect extremely weak magnetic fields from the human brain but also to control cell orientation and cell growth by extremely high magnetic fields. Pulsed magnetic fields are used for transcranial magnetic stimulation (TMS) of the human brain, and both high frequency magnetic fields and magnetic nanoparticles have promising therapeutic applications for the treatments of cancers and brain diseases such as Alzheimer’s and Parkinson’s. On the imaging front, magnetic resonance imaging (MRI) is now a powerful tool for basic and clinical medicine. New methods of MRI based on the new principles of imaging of impedance of the human body, called impedance MRI, and the imaging of neuronal current activities in the human brain, called current MRI, are also being developed.

The plenary lecture focuses on the recent advances in biomagnetics and bioimaging based on achievements obtained mostly in our laboratory in recent years. The lecture describes (1) a method of localized magnetic stimulation of the human brain by TMS with a figure-eight coil, (2) magnetoencephalography (MEG) or measurements of extremely weak magnetic fields related to neuronal electrical activities in the brain by superconducting quantum interference device (SQUID) systems, (3) electrical property mapping and imaging with MRI such as impedance MRI and current MRI, (4) cancer therapy and control of iron-ion release from, and uptake into, ferritin, an iron storage protein, by using both high frequency and pulsed magnetic fields and magnetic nanoparticles, and (5) magnetic control of cell orientation and cell growth by static high magnetic fields.

These new biomagnetic approaches will open new horizons in brain research, brain treatments, and regenerative medicine.

Some references [1-9] related to five subjects are given below.

Support by the Grant-in-Aid for Specially Promoted Research (No. 12002002) from the Ministry of Education, Culture, Sports, Science and Technology, Japan, and by the Grant-in-Aid for Scientific Research (S) (No. 17100006) from the Japan Society for the Promotion of Science (JSPS) is acknowledged.

[1] S. Ueno, T. Tashiro, K. Harada, *J. Appl. Phys.*, **64** (1988) 5862.

[2] S. Ueno, T. Matsuda, M. Fujiki, *IEEE Trans. Magn.*, **26** (1990) 1539.

[3] S. Ueno, N. Iriguchi, *J. Appl. Phys.*, **83** (1998) 6450.

[4] S. Ueno, *IEEE Eng. Med. Biol.*, **18** (1999) 108.

[5] M. Ogiue-Ikeda, S. Kawato, S. Ueno, *Brain Research*, **1037** (2005) 7.

[6] M. Sekino, Y. Inoue, S. Ueno, *IEEE Trans. Magn.*, **41** (2005) 4203.

[7] S. Ueno, M. Sekino, *J. M.M.M.*, **304** (2006) 122.

[8] O. Cespedes, S. Ueno, *Bioelectromagnetics*, **30** (2009) 336.

[9] S. Sekino, H. Ohashi, S. Yamaguchi-Sekino, S. Ueno, *IEEE Trans. Magn.*, **45** (2009) 4841.



Wednesday

**24 August**

11:30-13:00

14:30-17:20

oral session

24TL-A

24RP-A

24OR-A

**“Diluted Magnetic  
Semiconductors”**

24TL-A-1

## DILUTE FERROMAGNETIC SEMICONDUCTORS AT THE HOLE LOCALIZATION EDGE

*Dietl T.*

Laboratory for Cryogenic and Spintronic Research, Institute of Physics,  
Polish Academy of Sciences  
Institute of Theoretical Physics, University of Warsaw (dietl@ifpan.edu.pl)

The question of whether disorder, and the resulting Anderson–Mott localization, enhances or reduces magnetic correlations is central to the physics of magnetic alloys. Particularly intriguing is the case of (Ga,Mn)As and related magnetic semiconductors, for which diverging theoretical scenarios have been proposed. I will present recent works on (Ga,Mn)As at the localisation edge [1] including studies of magnetotransport properties of InAs:Mn quantum wells [2] and magnetisation as a function of the gate voltage in metal-insulator-(Ga,Mn)As structures [3] as well as I will refer to investigations of local density of states by scanning tunnelling microscopy [4]. I will argue [1,3] that the disappearance of ferromagnetism associated with carrier localization proceeds by means of the emergence of a superparamagnetic-like spin arrangement. This implies that carrier localization leads to a phase separation into ferromagnetic and non-magnetic regions, which are attributed to critical fluctuations in the local density of states, specific to the Anderson–Mott quantum transition [4].

[1] T. Dietl, Interplay between carrier localization and magnetism in diluted magnetic and ferromagnetic semiconductors, *J. Phys. Soc. Jpn.* 77, 031005 (2008).

[2] U. Wurstbauer, C. Śliwa, D. Weiss, T. Dietl, and W. Wegscheider, “Hysteretic magnetoresistance and thermal bistability in a magnetic two-dimensional hole system”, *Nature Phys.*, in press.

[3] M. Sawicki, D. Chiba, A. Korbecka, Yu Nishitani, J. A. Majewski, F. Matsukura, T. Dietl, and H. Ohno: “Experimental probing of the interplay between ferromagnetism and localization in (Ga, Mn)As”, *Nature Phys.* 6, 22 (2010).

[4] A. Richardella, P. Roushan, S. Mack, B. Zhou, D. A. Huse, D. D. Awschalom, and A. Yazdani “Visualizing critical correlations near the metal-insulator transition in  $\text{Ga}_{1-x}\text{Mn}_x\text{As}$ ”. *Science* 327, 665 (2010).



## ELECTRIC FIELD CONTROL OF FERROMAGNETISM IN III-V FERROMAGNETIC SEMICONDUCTOR STRUCTURES

*Chiba D.<sup>1,2,3</sup>, Kobayashi K.<sup>1</sup>, Ono T.<sup>1</sup>, Matsukura F.<sup>3,4</sup>, Ohno H.<sup>3,4</sup>*

<sup>1</sup> Institute for Chemical Research, Kyoto University, Gokasho, Uji, Kyoto 611-0011, Japan

<sup>2</sup> PRESTO, Japan Science and Technology Agency (JST), 4-1-8 Honcho Kawaguchi,  
Saitama 322-0012, Japan

<sup>3</sup> Laboratory for Nanoelectronics and Spintronics, Research Institute of Electrical Communication,  
Tohoku University, 2-1-1 Katahira, Aoba-ku, Sendai 980-8577, Japan

<sup>4</sup> Center for Spintronics Integrated Systems, Tohoku University, 2-1-1 Katahira, Aoba-ku,  
Sendai 980-8577, Japan

Electric-field control of ferromagnetism adds a new dimension to the future spin based information processing methods [1-7]. Ferromagnetic properties in III-V ferromagnetic semiconductors are electrically tunable by control of their carrier concentration. We have shown in the past that Curie temperature and coercivity can be manipulated by applying electric-fields [1-3]. Recently, we have reported the possibility of magnetization switching through the direct control of magnetic anisotropy solely by applying electric field [5,8]. This method is believed to open up a new route to novel electrical magnetization switching and to make it fully compatible with semiconductor integrated circuits. We show that it is experimentally possible by using a gating technology in a ferromagnetic semiconductor (Ga,Mn)As field effect structure.

Another topic is the formation of ferromagnetic nano-dots by electric field [9]. To realize this, we utilize electric field to modulate the in-plane distribution of carriers in a (Ga,Mn)As film with a meshed gate structure having a large number of nano-scaled windows. We believe this approach becomes a powerful tool for controlling and studying collective phenomena at nanoscale because it may enable us to electrically tune the size of the ferromagnetic dot as well as the interaction among them.

This work was supported in part by ERATO and PRESTO from JST, Grant-in-Aids from MEXT/JSPS, Information Technology Program from MEXT, the FIRST Program from JSPS, and the GCOE program at Tohoku University.

[1] H. Ohno *et al.*, *Nature* **408**, 944 (2000).

[2] D. Chiba *et al.*, *Science* **301**, 943 (2003).

[3] D. Chiba *et al.*, *Appl. Phys. Lett.* **89**, 162505 (2006).

[4] M. Weisheit *et al.*, *Science* **315**, 349 (2007).

[5] D. Chiba *et al.*, *Nature* **455**, 515 (2008).

[6] T. Maruyama *et al.*, *Nature Nanotechnology* **1**, 406 (2009).

[7] M. Endo *et al.*, *Appl. Phys Lett.* **96**, 212503 (2010).

[8] D. Chiba *et al.*, *Appl. Phys. Lett.* **96**, 192506 (2010).

[9] D. Chiba *et al.*, *Nano Lett.*, **10**, 4505 (2010).

24OR-A-3

## PERCOLATIVE METAL-INSULATOR TRANSITION IN MAGNETIC SEMICONDUCTORS

*Meilikhov E.Z., Farzetdinova R.M.*

Kurchatov Institute, 123182 Moscow, Russia

The role of large-scale fluctuations of the electric potential in traditional (non-magnetic) doped semiconductors is well known. Such a fluctuating potential appears usually in highly-compensated semiconductors where concentrations of charged impurities (donors and acceptors) are high and the concentration of screening mobile charge carriers is low, that results in a large screening length, defining the spatial scale of electric potential fluctuations. In that case, the average amplitude of the fluctuation potential is also high that leads to the localization of charge carriers and results in the activation character of the system conductivity: it is controlled by the thermal activation of charge carriers from the Fermi level to the percolation level and falls down exponentially with lowering temperature. In the absence of the impurity compensation, the charge carrier concentration is so high that any perturbations of the electro-static nature are effectively screened, and the spatial scale of the potential coincides with the extent of impurity density fluctuations. The depth of such a short-scale potential relief is relatively shallow and does not lead to the charge carrier localization - the conductivity keeps to be metal one.

In diluted (but nevertheless, highly-doped) magnetic semiconductors (of  $\text{Ga}_{1-x}\text{Mn}_x\text{As}$  type), in addition to above mentioned fluctuations of the electric potential, the new perturbation source appears - specifically, fluctuations of the “magnetic potential” concerned with fluctuations of the local magnetization in such a semiconductor. That potential is, in fact, the potential of the exchange interaction of mobile charge carriers with magnetic impurities (for instance, via the RKKY mechanism) which fluctuates in accordance with fluctuations of the concentration and the local magnetization of those impurities.

Within the “wells” of the magnetic potential, mobile charge carriers with a certain spin direction are accumulated while the carriers of the opposite spin direction are pushed out. The spatial scale of magnetic fluctuations is now determined not by the electrostatic screening but by the characteristic length of the magnetic interaction of impurities and the correlation length of their arrangement in the semiconductor bulk. However, in diluted magnetic semiconductors, there is usually  $l \sim l_s$  and, thus, spatial scales of the magnetic (exchange) and Coulomb potentials agree closely.

That means the constructive superposition of both reliefs, and so the average total amplitude of the potential relief becomes to be higher. The medium arises where the concentration and the spin polarization of charge carriers are strongly non-uniform, and the degree of that non-uniformity is substantially defined by the local magnetization of the system. Increasing magnetization with lowering temperature promotes strengthening the spatial localization of charge carriers and in a number of cases could stimulate the metal-insulator transition. Percolative metal conductivity, characteristic for non-uniform systems, changes into the conductivity of the activation type. That occurs when under some external factors (such as temperature, magnetic field, etc.) the Fermi level falls below the percolation level. One of possible mechanisms is as follows. The fluctuating potential leads to appearing the density of states tail into which both the percolation and Fermi levels are pulled. Rates of those levels' movement are different, and if they change the relative position the metal-insulator transition occurs.

It is just the model that is investigated in the present work.

24OR-A-4

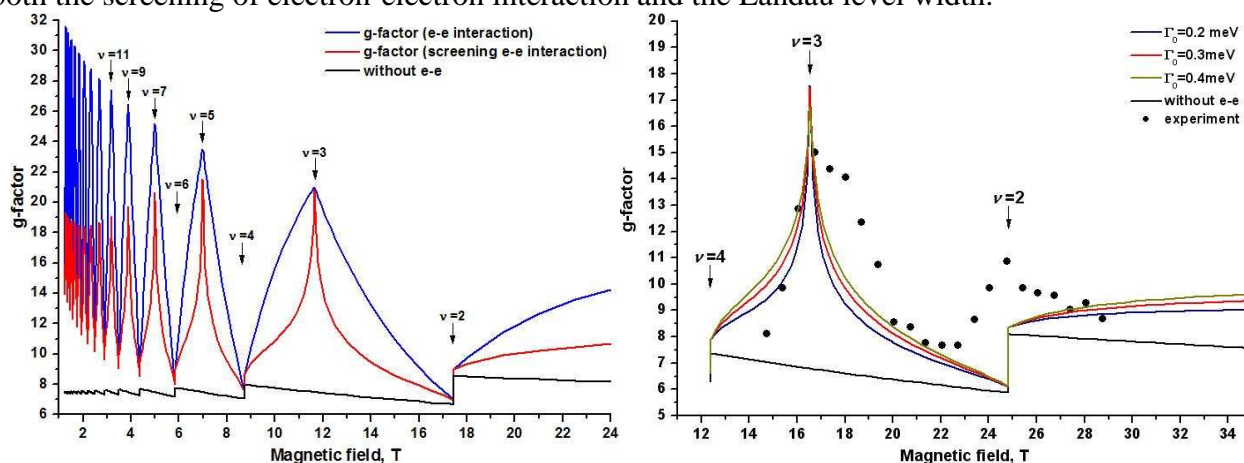
## THE $g$ -FACTOR ENHANCEMENT IN NARROW-GAP QUANTUM WELL HETEROSTRUCTURES

*Krishtopenko S.S.<sup>1</sup>, Gavrilenko V.I.<sup>1</sup>, Goiran M.<sup>2</sup>*

<sup>1</sup> Institute for Physics of Microstructures RAS, GSP-105, 603950, Nizhny Novgorod, Russia

<sup>2</sup> Laboratoire National des Champs Magnetiques Intenses (LNCMI-T), CNRS UPR 3228 Université de Toulouse, 143 Avenue de Rangueil, F-31400 Toulouse, France

We report on the study of the exchange enhancement of the  $g$ -factor in 2D electron gas in  $n$ -type narrow-gap semiconductor heterostructures that features a strong nonparabolicity of the energy-momentum law. To give a general description of the energy states, we used 8-band  $\mathbf{k}\cdot\mathbf{p}$  Hamiltonian for the envelope wave functions as a single-particle operator of the kinetic energy. This approach allows one to directly take into consideration the influence of nonparabolicity, lattice-mismatch deformation and spin-orbit coupling on the electron energy spectrum. The electron-electron interaction was taken into account in the “screened” Hartree-Fock approximation. The Coulomb Green function was obtained by solving the problem on electron motion in a flat-layered medium with spatial dispersion. Calculations of the dielectric function describing the screening effect were performed within the Thomas-Fermi long-wave approximation. We demonstrate that the exchange  $g$ -factor enhancement not only shows maxima at odd values of Landau level filling factors but, due to the band nonparabolicity, persists at even filling factor values as well (left panel). The magnitude of the exchange enhancement, the amplitude and shape of the  $g$ -factor oscillations are governed by both the screening of electron-electron interaction and the Landau level width.



The “enhanced”  $g$ -factor values calculated for the 2D electron gas in InAs/AlSb quantum well heterostructures are compared with our earlier experimental data [1] and with those obtained by Mendez et al. [2] in magnetic fields up to 30 T (right panel). As easy to see from the right panel, the  $g$ -factor peak, observed at the filling factor of 3, is reasonably described by the theoretical curve and is indeed related to the exchange enhancement of the 2D electron  $g$ -factor. The second peak, corresponding to even filling factor corresponds to the “jump” of the  $g$ -factor value at the Fermi level due to the nonparabolicity of energy-momentum law. Our results demonstrate that the significant effect of the nonparabolicity on many-body phenomena such as the exchange enhancement of the spin-splitting in a 2D electron gas in the presence of magnetic field.

[1] V.Ya. Aleshkin, V.I. Gavrilenko, A.V. Ikonnikov, S.S. Krishtopenko, Yu.G. Sadofyev, K.E. Spirin, *Semiconductors* 42 (2008) 828.

[2] E.E. Mendez, J. Nocera, W.I. Wang, *Phys. Rev. B* 47, (1993) 13937.

24TL-A-5

## FANO-ANDERSON EFFECT IN DILUTE SEMIMAGNETIC SEMICONDUCTORS

*Averkiev N.S., Rozhansky I.V.*

Ioffe Institute, S.-Petersburg, 194021, Russia

Heterostructures with paramagnetic impurity spatially separated from free carriers of a charge by a tunneling transparent barrier are new perspective objects for research of magnetic interactions in a solid state. Spatial division keeps high mobility of free carriers, but thus, influence of impurity on spin polarization of free carriers remains unexpectedly considerable.

The aim of the report is to give a brief talk on crystal GaAs: Mn magnetic properties and in frame of the model to account for peculiarities of magnetophotoluminescence of quantum structures based on GaInAs:Mn.

The main feature of deep center MnGa in GaAs is strong exchange interaction between a hole localized near the defect and 3d<sup>5</sup> electrons. As result the ground state of the hole characterizes the total momentum equals to 1 and the spin of 3d electrons is antiparallel to the hole total momentum.

Nanostructures under consideration[1] based on GaAs/InGaAs, containing a quantum well and manganese delta-layer, separated from the quantum well on 3-6 nanometers. A new theory allowing to consider simultaneously exchange interaction of holes with ions of manganese and tunneling in frame of configuration interaction and Bardin's tunnel Hamiltonian is offered. Theoretical calculation of a photoluminescence spectra due to recombination between a hole and a photoexcite electron in the quantum well in a magnetic field and their comparison with experimental data is carried out. The proposed theory explains observable degree of circular polarization of a luminescence, temperature dependence and unusually weak dependence from tunnel distance between the delta-layer and the quantum well[1]. In a zero magnetic field the manganese level changes continuous energy spectrum in the quantum well being with it in a resonance. It leads to increase of a photoluminescence near to the resonance. Splitting of levels of the hole on MnGa in a magnetic field results to that for holes with a moment projection  $j = + 3/2$  and  $j = -3.2$  resonances are located in different parts of a spectrum that leads to observable polarization of a luminescence. The splitting value between states with  $j = + 3/2$  and  $j = -3.2$  is defined by exchange interaction in a ferromagnetic state and decreases above Curie temperature approximating to Zeeman splitting.

The work is supported partly by RFFI and the Russian Ministry of Science and Education (contract 14.740.11.0892)

[1] S.V.Zaitsev et.al. JETP Let.,v.90,N.10, p.658(2010)

## TRANSPORT IN DILUTE MAGNETIC SEMICONDUCTOR HETEROSTRUCTURES

*Tripathi V.<sup>1</sup>, Dhochak K.<sup>1</sup>, Aronzon B.A.<sup>2,3</sup>, Rylkov V.V.<sup>2,3</sup>, Davydov A.B.<sup>2</sup>, Raquet B.<sup>4</sup>, Goiran M.<sup>4</sup>,  
Kugel K.I.<sup>3</sup>*

<sup>1</sup> Department of Theoretical Physics, Tata Institute of Fundamental Research,  
Homi Bhabha Road, Navy Nagar, Mumbai 400005, India

<sup>2</sup> Russian Research Center “Kurchatov Institute”, Kurchatov Square 1, Moscow, 123182 Russia

<sup>3</sup> Institute for Theoretical and Applied Electrodynamics, Russian Academy of Sciences,  
Izhorskaya Str. 13, Moscow, 125412 Russia

<sup>4</sup> CNRS INSA UJF UPS, UPR 3228, Laboratoire National des Champs Magnétiques Intenses,  
University de Toulouse, 143 avenue de Rangueil, F-31400 Toulouse, France

We study experimentally and theoretically the resistivity and its noise in semiconductor heterostructures  $\delta$ B-doped with Mn. The two-dimensional nature of transport as well as ferromagnetism make their properties different from their three-dimensional counterparts. We observe anomalies in the temperature dependence of resistivity and noise in both metallic and insulating samples and interpret them as evidence for significant ferromagnetic correlations. The insulating samples are particularly interesting as they provide valuable clues to the nature of ferromagnetism in these structures [1].

Following the approach reported in [2], we show how the interplay of disorder and nonlinear screening leads at low carrier densities to the formation of hole puddles in the transport layer. We find that in this droplet phase, ferromagnetic correlations result in anomalies in the resistivity at temperatures below the Curie temperature, and even in the absence of long-range ferromagnetic order. This is to be contrasted with bulk Mn-doped semiconductors where resistivity anomalies are expected above and near to the Curie temperature, and are associated with a ferromagnetic phase transition.

The ferromagnetic correlations also affect the resistivity noise directly through their effect on the fluctuations of relative orientations of the magnetization at the droplets and indirectly through their effect on the hole number fluctuations. We propose simple models for the resistivity noise in the droplet phase in the presence of these ferromagnetic correlations. Finally, we discuss possible models for ferromagnetism that are consistent with the observed behaviour of resistivity and its noise in these heterostructures.

The work was supported by the Russian Foundation for Basic Research (projects 09-02-92675-IND and 11-02-00363) and by the Indo-Russian Collaboration Program (grant. INT/RFBR/P-49). We also acknowledge the partial support of EuroMagNET under EU Contract No. RII3-CT-2004-506239. V.T. and K.D. acknowledge the support of TIFR.

[1] V. Tripathi, K. Dhochak, B.A. Aronzon, V.V. Rylkov, A.B. Davydov, B. Raquet, M. Goiran, K.I. Kugel, ArXiv:1012.5456.

[2] V. Tripathi, M.P. Kennett, *Phys. Rev. B*, **74** (2006) 195334.

24TL-A-7

## SPIN-POLARIZED HALF-METALLIC STATE OF A FERROMAGNETIC DELTA LAYER EMBEDDED IN A SEMICONDUCTING MATRIX

*Caprara S.<sup>1</sup>, Tugushev V.V.<sup>2</sup>, Chulkov E.V.<sup>3</sup>*

<sup>1</sup> Dipartimento di Fisica - Università "La Sapienza", I-00185, Rome, Italy

<sup>2</sup> RRC Kurchatov Institute, 123182, Moscow, Russia

<sup>3</sup> Donostia International Physics Center, 20018, San Sebastian, Basque Country, Spain

We propose a model to describe the occurrence of a spin-polarized half-metallic state around a delta layer of magnetic transition metal atoms embedded into a non-magnetic semiconducting matrix. We show that the intrinsic physical properties of a single delta layer are responsible for ferromagnetic order in this system. The relevant physical ingredients our model are the hybridization of the d electron states of the metal and of the (s,p) electron states of the semiconductor, the charge redistribution around the delta layer, and the electron-electron correlation on the d orbitals of the transition metal atoms, which is the driving force of ferromagnetism. We discuss the mean-field phase diagram of the model at zero and finite temperature, both for fixed chemical potential and for fixed density of particles on the delta layer. We finally comment on the relevance of our results to interpret the outcomes of numerical ab initio calculations and of experiments on the so-called digital magnetic heterostructures, both in the absence and in the presence of a quantum-well carrier channel.

24RP-A-8

## HYBRID HETEROSTRUCTURE WITH NANOLAYER OF DILUTED Ga-In(Mn)As-Sb SEMICONDUCTOR AND 2D-SEMIMETAL CHANNEL AT THE TYPE II BROKEN-GAP HETEROINTERFACE FOR SPIN-DEPENDENT ELECTRON TRANSPORT

*Moiseev K.D.<sup>1</sup>, Berezovets V.A.<sup>1,4</sup>, Mikhailova M.P.<sup>1</sup>, Parfeniev R.V.<sup>1</sup>, Lesnikov V.P.<sup>2</sup>, Podolski V.V.<sup>2</sup>, Kudriavtsev Yu.<sup>3</sup>, Nizhankovskii V.<sup>4</sup>, Kaczorowski D.<sup>5</sup>*

<sup>1</sup>A.F. Ioffe Physical-Technical Institute RAS, St Petersburg, 194021, Russia

<sup>2</sup>Lobachevsky State University, Nizhniy Novgorod, 603021, Russia

<sup>3</sup>CINESTAV-IPN, Av. Instituto Politécnico Nacional 2508 07360 Mexico D.F., Mexico

<sup>4</sup>Intern. Laboratory of High Magnetic Fields and Low Temperatures, Wrocław, 50-204, Poland

<sup>5</sup>Institute of Low Temperature and Structure Research PAN, Wrocław, 50-950, Poland

Production of diluted magnetic semiconductors using a method of laser ablation of Mn atoms onto the epitaxial layer of the quaternary GaInAsSb solid solution grown by liquid phase epitaxy has been proposed and developed [1]. The obtained heterostructures were investigated by high-resolution x-Ray diffraction method in symmetrical Bragg's and glancing incidence geometry for structural analysis, SIMS and AFM methods were used for study of a layered profile. It was shown that deposition of 2-3 ML atomic Mn on binary InAs surface leads to occurrence of binary Mn<sub>x</sub>As<sub>y</sub> inclusions at the heterointerface. Under substituting InAs by the quaternary GaInAsSb solid solution lattice-matched with InAs substrate formation of the quinary GaInMnAsSb nanolayer (of about 200 nm) was revealed. Pseudomorphic GaInAsSb/InAs single heterostructure with planar and abrupt heteroboundary provides formation of 2D-semimetal channel with high carrier mobility

( $6.0 \times 10^4 \text{ cm}^2 \text{V}^{-1} \text{s}^{-1}$ ) and electron concentration of  $n_e = 9.2 \times 10^{11} \text{ cm}^{-2}$  due to electrons and holes subsystems are localized in self-consistent quantum wells on both sides of the type II broken-gap heterointerface [2]. Planar and vertical quantum magnetotransport in the 2D-semimetal channel in the type II broken-gap p-InAs/p-GaInAsSb heterostructure with Mn nanolayer has been studied in high magnetic fields under the quantum Hall regime up to 35 T at low temperatures  $T = 1.5 \text{ K}$ . An asymmetric potential profile of the quantum wells at the type II heteroboundary leads to Rashba spin-splitting of 2D-electron states near Fermi level in an absence of a magnetic field [3]. Taking into account s-d exchange interaction of Mn ions in the p-doped InAs substrate and 2D-electrons at the heterointerface results in an enhancing of Landau levels spin-splitting. Spin-related structures for the lowest Landau level of 2D-electrons in the channel were observed as steps in I-V characteristics and spikes in the tunneling conductance ( $dI/dU$ ) measured at quantum Hall regime ( $B > 12 \text{ T}$ ). For filling number of  $\nu = 2$  the value of  $dI/dU$  in co-linear case was higher in an order than for one in non-co-linear case and their ratio increases with magnetic field increasing [4].

Work was supported in part by RBRF grant #09-02-00063, by programs of the Presidium of RAS and Leading Scientific Schools. Yu. K. acknowledges to CONACYT (grant #79812).

- [1] K.D. Moiseev et al, *Semicond.* 45, 788 (2011).
- [2] M.P. Mikhailova et al, *Semicond. Sci. Technol.* 19, R109 (2004).
- [3] E.I. Rashba, *Sov. Phys. Solid States* 2, 1109 (1960).
- [4] R.V. Parfeniev et al, *J. Magn. Magn. Mat.* 321, 712 (2009).

24TL-A-9

## **ELECTRICAL CONTROL OF MAGNETIZATION IN FERROMAGNETIC MATERIALS**

*Rokhinson L.<sup>1</sup>, Chernyshov A.<sup>1</sup>, Overby M.<sup>1</sup>, Lyanda-Geller Y.<sup>1</sup>, Liu X.<sup>2</sup>, Furdyna J.<sup>2</sup>*

<sup>1</sup> Department of Physics, Purdue University, West Lafayette, Indiana 47907, USA

<sup>2</sup> Department of Physics, University of Notre Dame, Notre Dame, Indiana 46556, USA

The current state of information technology accentuates dichotomy between processing and storage of information, with logical operations performed by charge-based devices and non-volatile memory based on magnetic materials. The major obstacle for a wider use of magnetic materials for information processing is the lack of efficient control of magnetization. Reorientation of magnetic domains is conventionally performed by non-local external magnetic fields or by externally polarized currents. Efficiency of the latter approach is greatly enhanced in materials where ferromagnetism is carrier-mediated. In such materials externally induced spin-dependent anisotropy of carriers' spectrum effects the magnetization direction. I will discuss two types of magnetization control in a model magnetic semiconductor (Ga,Mn)As: via externally applied strain [1] and via spin-orbit magnetic field [2]. In both cases we demonstrate reversible domain rotation and hysteretic switching of magnetization between two orthogonal easy axes. In addition, I will show that some particular properties of ferromagnetic materials, such as anisotropic traverse magnetoresistance, allows direct all-electrical measurements of SO effective magnetic field, both magnitude and direction.

- [1] M. Overby, A. Chernyshov, L. P. Rokhinson, X. Liu, and J. K. Furdyna, "GaMnAs-based hybrid multiferroic memory device", *Applied Physics Letters* 92, 192501 (2008)

[2] A. Chernyshov, M. Overby, X. Liu, J.K. Furdyna, Y. Lyanda-Geller and L.P. Rokhinson, "Evidence for reversible control of magnetization in a ferromagnetic material by means of spin-orbit magnetic field", *Nature Physics* 5, 656 - 659 (2009)



Wednesday

**24 August**

11:30-13:00

14:30-17:20

oral session

24TL-B

24RP-B

**“Soft and Hard  
Magnetic Materials”**

24TL-B-1

## TAILOR-MADE NANO MATERIALS WITH MODULATED SPIN STRUCTURE FOR HIGHLY QUALIFIED SPIN RELATED DEVICES

*Takahashi M.*<sup>1,2,3</sup>

<sup>1</sup> Department of Electronic Engineering, Graduate School of Engineering,  
Tohoku University, Japan

<sup>2</sup> New Industry Creation Hatchery Center (NICHe), Tohoku University, Japan

<sup>3</sup> Center for Nanobioengineering and Spintronics, Chungnam National University, Korea  
migaku@ecei.tohoku.ac.jp

Highly qualified spin related devices such as ultra-high density hard disk drive (HDD) and magnetic random access memory (MRAM), inductor and antenna for high frequency use are inevitable requirements for the recent IT technology. Tailor-made spin nano materials by precisely controlled fabrication technology with nano-scale in each devices and understanding their nanomagnetism are essential from the view point of material, process, and physics. Artificial control of the exchange coupling among ferromagnetic layers through the RKKY interaction (indirect) and the direct exchange coupling represented as the exchange bias at the ferromagnetic (FM)/antiferromagnetic (AFM) interface are paid hot attention to induce the newly modulated spin structures in conventional simple ferromagnetic material.

Exchange coupled stacked media between ferromagnetic hard/ soft, or positive-/ negative- Ku layers (modulation of ferromagnetic spin structure in hard magnetic materials) and the giant exchange anisotropy at FM/ AFM interface (uncompensated spin structure with ferromagnetic order of AFM at the hetero-interface) have been attracted much attention from the view point of real applications [1-3].

Conventional metallic ferromagnetic material for high frequency response in GHz range has a frequency limit determined by Snoek's law. To overcome this physical limit, we newly proposed magnetic-dielectric material consisting of magnetic nanoparticle assembly, which shows superparamagnetic response, with polymer hybridization (frustrated spin structure in super spin glass). This new concept hybrid nano-material will be a promising candidate for possible application to the high-frequency devices [4].

To realize ideal tailor-made nano structured materials, control of ultra-thin thickness, surface morphology, grain size, and interface are the required key issues. Ultra clean (UC) dry-process proposed by us [5] has provided fruitful results on film growth of seed, underlayer, and magnetic layers for the currently used hard disk (HD) [6, 7], MRAM and spin-valve (SV) head [8-10]. While, chemical synthesis of the magnetic nanoparticles can precisely control the size with nanometer scale, narrow size distribution, shape and monodispersion state of the nanoparticles [11, 12].

Within the frame work of the present paper, correlation between tailor-made nano material and unique magnetic properties developed for each categorized research items mentioned above will be widely discussed in connection with spin related devices.

[1] M. Takahashi and S. Saito *J. Magn. Magn. Mat.* 320, 2868 (2008).

[2] M. Takahashi, M. Tsunoda and S. Saito, *J. Magn. Magn. Mat.* 321, 539 (2009).

[3] M. Takahashi, M. Tsunoda and S. Saito, *ECS Trans.* 16, 19 (2009).

[4] D. Hasegawa, H. Yang, T. Ogawa and M. Takahashi, *J. Magn. Magn. Mat.* 321, 746 (2009).

[5] e. g. M. Takahashi, A. Kikuchi and S. Kawakita, *IEEE Trans. Magn.* 33, 2938 (1997).

[6] M. Takahashi, H. Shoji, D. Djayaprawira and S. Yoshimura, *IEEE Trans. Magn.* 36, 2315 (2000).

[7] N. Itagaki, S. Saito and M. Takahashi, *J. Appl. Phys.* 105, 07B734 (2009).

- [8] M. Tsunoda, D. Takahashi and M. Takahashi, J. Appl. Phys. 93, 6513 (2003).  
 [9] K. Imakita, M. Tsunoda and M. Takahashi, J. Magn. Soc. Jpn. 28, 368 (2004).  
 [10] Y. Ashizawa, H. Ohyama, K. Sunaga, Y. Watanabe, M. Tsunoda and M. Takahashi, J. Magn. Soc. Jpn. 31, 411 (2007).  
 [11] H. Yang, F. Ito, D. Hasegawa, T. Ogawa and M. Takahashi, J. Appl. Phys. 101, 09J112 (2007).  
 [12] H. Yang, T. Ogawa, D. Hasegawa, and M. Takahashi, J. Appl. Phys. 103, 07D526 (2008).

24TL-B-2

## **MAGNETIC NANOWIRES. PREPARATION, PROPERTIES, APPLICATIONS**

*Chiriac H.*

National Institute of Research and Development for Technical Physics, 700050 Iasi, Romania

The metallic nanowires are generally prepared by different chemical or physico-chemical methods. Among them, the electrodeposition into the nanopores of different templates is widely used for preparing magnetic simple or multilayered nanowires. Our recent studies shown that the diameter of the electrodeposited nanowires could vary from 30 to 400 nm and their length is limited by the thickness of the template (usually 40 or 50  $\mu\text{m}$ ). Additionally, the large density of the nanowires per  $\text{cm}^2$  ( $10^7$ - $10^8$ ) is influencing strongly the magnetic and magnetotransport properties [1]. Thus, it is desirable to prepare single nanowires with controllable diameters and lengths, and with both ends free for making electrical contacts.

Very recently, our group reported the preparation of glass-coated magnetic nanowires with diameters down to 100 nm by a rapid quenching technique [2]. Due to the constraints of the method of preparation the compositions of such glass-coated nanowires are restricted to the ones with glass-forming ability. However, rapidly solidified magnetic nanowires have low production costs and their properties can be accurately tailored through a variety of parameters: the diameter of the metallic nucleus, the glass coating thickness, their ratio, and the composition, which decides the sign and magnitude of the magnetostriction constant. These tailoring parameters are adjustable through the preparation process. Post-production processing, such as various types of annealing (furnace, Joule heating, field-annealing, stress-annealing) as well as the post-production partial or full removal of the glass coating can be also used to tailor the magnetic properties. Another obvious advantage of the rapidly solidified amorphous nanowires is that they can be prepared at sample lengths which basically exceed all the current requirements of applications based on nanowire samples.

By combining the glass-coating and electrodeposition techniques, we succeeded preparing single metallic nanowires with diameters of 100-200 nm and different compositions, and not only from the ones suitable for the glass-coating rapid quenching technique. By using the new method, we succeeded preparing single glass-coated [NiFe(50 nm)/Cu(20 nm)] x n multilayered nanowires by switching between the deposition potentials of the two constituents (-1.4 V and -0.3 V for NiFe and Cu deposition, respectively). The magnetic characteristics as well as the magnetoresistance of the newly prepared glass-coated single NiFe/Cu multilayered nanowire are comparable with the ones reported for NiFe/Cu multilayered nanowires, which we prepared by electrodeposition in alumina templates with thicknesses of only 40  $\mu\text{m}$  [1]. The new prepared nanowires have lengths in the mm range, and can be easily used for logic devices or biomedical applications.

Financial support from the NUCLEU Programme (PN 09-43 01 02) is acknowledged.

- [1] H. Chiriac, O.G. Dragos, M. Grigoras, G. Ababei, N. Lupu, *IEEE Trans. Magn.*, **45** (2009) 4077.  
 [2] H. Chiriac, S. Corodeanu, M. Lostun, G. Stoian, G. Ababei, T.-A. Óvári, *J. Appl. Phys.*, **109** (2011) 063902.

24TL-B-3

## ADVANCES IN AMORPHOUS AND NANOCRYSTALLINE MATERIALS

*Hasegawa R.*

Metglas, Inc., 440 Allied Drive, Conway, SC 29526, USA

The demand for advanced soft magnetic materials is increasing in light of needs for energy efficient magnetic devices, used especially in electrical power generation and transmission. This trend began in the mid-1970s when the first petroleum embargo took place and has been intensified by a decreasing supply of fossil fuel in the world where the demand for electrical power is increasing rapidly. This in turn accelerates global warming, which must be mitigated as soon as possible. Some solutions are being provided by renewable energy production through wind and solar power, which require energy-efficient magnetic devices. In responding to the energy shortage in the mid-1970s, the development of amorphous magnetic materials was prompted. The early material development is described in Ref. [1], following which a concerted effort of its application in energy efficient electrical transformers was made [2]. Thus application of amorphous magnetic materials had a good start but was slowed down as the energy crisis eased. The new crisis of global warming added to the old problem of coping with ever-increasing global energy needs have been forcing us to address the need for new soft magnetic materials which provide energy-efficient magnetic devices. A recent related effort is described in Ref. [3]. In this work, a new amorphous alloy was introduced which showed a saturation magnetic induction  $B_s$  of 1.64 T which is compared with  $B_s=1.57$  T for a currently available Fe-based amorphous alloy and decreased magnetic losses. Such combination is rare but can be explained in terms of induced magnetic anisotropy being changed by the alloy's chemistry and its heat treatment. It has been found that the region of magnetization rotation in the new alloy is considerably narrowed, resulting in reduced audible noise from the magnetic devices utilizing the material. Efforts to increase  $B_s$  also have been made for nanocrystalline alloys. For example, a  $Fe_{85}Si_2B_8P_4Cu_1$  nanocrystalline alloy with a  $B_s$  of 1.8 T is reported to exhibit a magnetic core loss of about 0.2 W/kg at 50 Hz and at 1.5 T induction [4]. Another example is provided by a nanocrystalline alloy having a composition of  $Fe_{80.5}Cu_{1.5}Si_4B_{14}$  with  $B_s$  exceeding 1.8 T [5]. The iron loss at 50 Hz and at 1.6 T induction in a toroidal core of this material is 0.46 W/kg which is 2/3 that of a grain oriented silicon steel. At 20 kHz/ 0.2 T excitation, the iron loss is about 60% of that in an Fe-based amorphous alloy which is widely used in power electronics. This article is a review of these new developments and their impacts on energy efficient magnetic devices.

- [1] R. Hasegawa, *J. Magn. Magn. Materials*, **100**, 1-12 (1991)  
 [2] H. Ng, R. Hasegawa, A.C. Lee and L. A. Lowdermilk, *Proc. IEEE*, **79**, 1608-1623 (1991)  
 [3] R. Hasegawa and D. Azuma, *J. Magn. Magn. Materials*, **320**, 2451-2456 (2008)  
 [4] A. Makino, T. Kubota, P. Sharma, A. Urata, H. Matsumoto, S. Yoshida and A. Inoue, presented at the Annual Conf. on Magnetism and Magnetic Materials, November 2010.  
 [5] M. Ohta and Y. Yoshizawa, *J. Phys. D*, **43**, 064004 (2010)

24TL-B-4

## OBSTACLES TO THE USE OF FERROMAGNETIC AMORPHOUS MATERIALS FOR VOLUME APPLICATIONS

*Kiessling A., Reiningger T.*

Festo AG & Co. KG, Rüter Strasse 82, 73734 Esslingen, Germany

Despite the fact that amorphous and nanocrystalline ferromagnetic alloys show excellent soft-magnetic properties which can be tailored over a wide range, their application within modern electronics still is an unsolved challenge.

We describe the difficulties and obstacles relating to coherence encountered during the development of sensor products for factory automation when using amorphous or nanocrystalline ribbons and wires as the sensor element.

Our main motivation in carrying out these investigations was to improve on performance of the well-known types of sensors, especially silicon-based Hall sensors, AMR sensors and GMR-sensors – familiar from the series production of mobile phones and electronic storage devices like hard discs and others - in terms of cost-effectiveness and functionality.

The following systems have been investigated:

1. Ring core fluxgate sensors based on wound or laser-cut stacked amorphous ribbons.
2. Inductive displacement sensors with a core of nanocrystalline ribbons stacked and glued together to form a square-shaped or rectangular stack of  $1.5 \times 1.5 \times 200 \text{ mm}^3$ .
3. Magneto-impedance sensors based on FeNiBo and FeNiCo amorphous wires 3 to 10mm long soldered on a PCB surface.

We have learned that simple processes like cutting, gluing, bending, heating, soldering, packaging and installing in a housing destroy the excellent magnetic properties of these excellent ferromagnetic materials and are the main reasons why these are not used in present-day products.

We are convinced that close collaboration between development and manufacturing engineers on the one hand and materials scientists on the other will be necessary in order to turn these materials into a commercial success.

A short survey is given of the problems arising when using these materials and also the possible ways of improving the situation.

## MAGNETIC AND TRANSPORT PROPERTIES OF GRANULAR AND HEUSLER-TYPE GLASS-COATED MICROWIRES

Zhukov A.<sup>1,2</sup>, Garcia C.<sup>3</sup>, Ilyn M.<sup>2</sup>, Varga R.<sup>4</sup>, del Val J.J.<sup>2</sup>, Granovsky A.<sup>1,5</sup>, Zhukova V.<sup>2</sup>

<sup>1</sup> Ikerbasque, Basque Foundation for Science, 48011 Bilbao, Spain

<sup>2</sup> Dpto. Fisica de Materiales, Fac. Quimicas, UPV/EHU, 20018 San Sebastian, Spain

<sup>3</sup> Bogazici Univ, Dept Phys, TR-34342 Istanbul, Turkey

<sup>4</sup> Inst. Phys., Fac.Sci., UPJS, Park Angelinum 9, Kosice, Slovakia

<sup>5</sup> Moscow State University, Moscow, 119991, Russian Federation

Recently, special attention has been paid to the studies of thin microwires produced by Taylor-Ulitovsky technique allowing the fabrication of long (from few meters to few km) composite glass-coated metallic amorphous or nanocrystalline microwires (metallic nucleus diameters ranging from 1 and 30  $\mu\text{m}$  and the thickness of glass coating between 0.5 and 20  $\mu\text{m}$ ) owing to high enough quenching rate [1, 2]. These microwires are quite suitable for many technological applications owing to quite peculiar magnetic properties such as the magnetic bistability (MB) and the giant magnetoimpedance (GMI) effects [1-3]. On the other hand, recently has been reported on preparation and properties of microwires with granular structure (Co, Fe, Ni-Cu alloys) [4], with magnetocaloric effect [5] and from Heusler alloys [3, 6].

In this paper, we present a brief review of structural, magnetic, magnetotransport properties of various types of glass-coated microwires obtained by Taylor-Ulitovsky method focusing on last results on granular  $\text{Co}_x\text{-Cu}_{1-x}$  ( $5 < x < 40$  at%) and Heusler-type  $\text{Ni}_2\text{MnGa}$  microwires. In the case of Heusler-type microwires their main advantage is related with composite character of microwires, allowing production of relatively long pieces of microwire coated by glass, which is the case of brittle Ni-Mn-Ga alloy. Annealed  $\text{Ni}_2\text{MnGa}$  microwires showed ferromagnetic behaviour with Curie temperature about 330 K and polycrystalline structure with space group  $I4/mmm$  and lattice parameters  $a = 3.75 \text{ \AA}$  and  $c = 6.78 \text{ \AA}$ . We observed noticeable magnetocaloric effect that makes these type of microwires promising for multifunctional applications. The structure and properties of Co-Cu microwires strongly depend on Co volume fraction and the ratio of the total microwire diameter to the diameter of metallic core. In the case of low Co content XRD indicates that Co atoms are distributed within the Cu crystals. Then Co volume fraction increases up to 10% accordingly to XRD the structure of the metallic core becomes granular with two phases: the main one, fcc Cu (lattice parameter 3.61  $\text{ \AA}$ ) and fcc  $\alpha$ -Co (lattice parameter 3.54  $\text{ \AA}$ ). Depending on composition and geometry these microwires exhibit Kondo-type magnetoresistance, small positive magnetoresistance, or considerable giant magnetoresistance

Supporting by projects “SoMaMicSens” (MANUNET-2010-Basque-3, ERA-NET), “EM-safety” project (FP7), MAT2010-18914 (Spanish Ministry of Science and Innovation), Saiotek (S-PE09UN38) and by Slovak VEGA grant No.1/3076/09 and No. 2/0167/10.

- [1] A. Zhukov, J. Gonzalez, J.M. Blanco et al., *J. Mater. Res.*, 15 (2000) 2107.
- [2] V. Zhukova, M. Ipatov and A Zhukov, *Sensors* 9 (2009) 9216.
- [3] M. Vazquez, H. Chiriac, A. Zhukov et al., *Phys. Stat. Sol. (a)*, 208 (2011) 493.
- [4] A. Zhukov, J. Gonzalez, V. Zhukova, et al., *J. Magn Magn. Mater.*, 294 (2005) 165.
- [5] M. I. Ilyn, V. Zhukova, J. D. Santos et al., *Phys. Stat. Sol. (a)*, 205 (2008) 1378.
- [6] C. García, V. M. Prida, V. Vega et al., *Phys. Stat. Sol. (a)*, 206 (2009) 644.
- [7] D. C. Dunand and P. Müllner: *Adv. Mater.*, 23, (2011) p216

24RP-B-6

## MULTI-LAYERED Nd-Fe-B/ $\alpha$ -Fe THICK FILM MAGNETS

Fukunaga H.<sup>1</sup>, Nakayama H.<sup>1</sup>, Kamikawatoko T.<sup>1</sup>, Yanai T.<sup>1</sup>, Nakano M.<sup>1</sup>, Yamashita F.<sup>1</sup>

<sup>1</sup> Faculty of Engineering, Nagasaki University, Nagasaki 852-8521, Japan

<sup>2</sup> Minebea Co., Ltd., 1743-1 Asana, Fukuroi, Shizuoka 437-1193, Japan

Multi-layered Nd-Fe-B-based nanocomposite thick magnets are one of promising candidates for magnets used in a small motor [1], because the isotropic nature and large remanence  $M_r$  of a nanocomposite magnet enables us to magnetize it multi-polarly and to obtain large output torque of a motor [1]. Previously, we proposed a method of preparing multi-layered nanocomposite film magnets with the thickness of several tens of microns by the pulsed laser deposition (PLD) method [2,3]. In this contribution, we report magnetic properties of Nd-Fe-B/ $\delta$ -Fe nanocomposite film magnets and clarify the relationship between their microstructure and magnetic properties.

The multi-layered films with the thickness of 8.1–28.4  $\mu\text{m}$  were deposited from a rotating  $\text{Nd}_{2.6}\text{Fe}_{14}\text{B}/\alpha\text{-Fe}$  composite target (6.5 rpm) by the PLD method using a YAG laser ( $\lambda=355\text{ nm}$ ). The output power of the laser PL was varied between 3 and 7 W. As the deposited films were amorphous, they were crystallized with an infrared furnace for hardening.

A reduction in the laser power caused increases in  $M_r$  and  $(BH)_{\text{max}}$  as well as decreases in the Nd content and  $H_c$  (Fig.1). The highest  $(BH)_{\text{max}}$  and  $M_r$  values were obtained for a film with  $\text{N}/(\text{Nd}+\text{Fe}) = 0.098$  deposited

with  $LP = 3\text{ W}$ , and were  $90\text{ kJ/m}^3$  and  $1.0\text{ T}$ , respectively (Fig.2). Magnetic properties for some RE-TM isotropic thick film magnets are shown in Table 1. The film obtained in this study has the largest  $M_r$  and  $(BH)_{\text{max}}$  values in the films shown in the table.

The average thickness of a set of Nd-Fe-B and  $\alpha\text{-Fe}$  layers calculated from the film thickness was  $19.1\text{ nm}$ . This thickness is reasonable for obtaining a nanocomposite magnet. The squareness of a hysteresis loop and the spring-back ratio of a demagnetization curve of our film suggested that the large remanence can be attributed to the strong intergrain exchange interaction in our film.

Table 1 Magnetic properties of isotropic RE-TM thick film-magnets.

Alloy	Thickness ( $\mu\text{m}$ )	$H_c$ (kA/m)	$M_r$ (T)	$(BH)_{\text{max}}$ ( $\text{kJ/m}^3$ )	Ref.
Nd-Fe-B	14.9	430	1.0	90	This Work
Nd-Fe-B	500	1380	0.59	61	Rieger et al.
Nd-Fe-B	300	760	0.45		B. Pawlowski et al.
Nd-Fe-B	10-50	860	0.5		S. Schwarzer et al.
Sm-Co	30	1200	0.75	90	T. Budder et al.
Sm-Fe-N	~45	1440	0.55		J. Aketo et al.

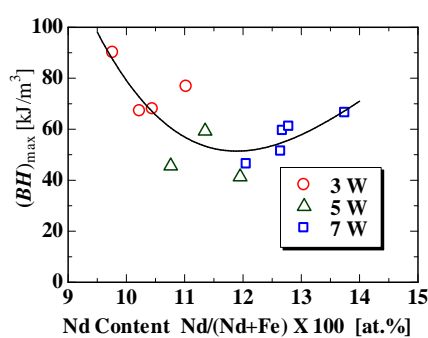


Fig.1 Maximum energy product  $(BH)_{\text{max}}$ .

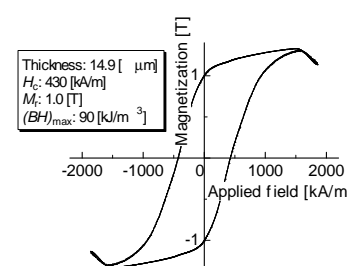


Fig.2 Hysteresis loop of multi-layered film magnet deposited with  $LP = 3\text{ W}$ .

[1] F. Yamashita et al., IEEE Trans. Magn. 46 (2010) 2012.

[2] H. Fukunaga et al., J. Alloys Compound 408-412, (2006) 1355.

[3] H. Fukunaga et al., J. Phys. Conf. Series 266 (2011) 12027.

24RP-B-7

## Nd-Fe-B THICK FILM MAGNETS PREPARED BY VACUUM ARC DEPOSITION

*Nakano M.<sup>1</sup>, Sahara M.<sup>1</sup>, Yanai Y.<sup>1</sup>, Yamashita F.<sup>2</sup>, Fukunaga H.<sup>1</sup>*

<sup>1</sup> Faculty of Engineering, Nagasaki Univ., 1-14 Bunkyo-machi, Nagasaki, Japan

<sup>2</sup> Rotary Component Tech., Div., Minebea Co., Ltd., 1743-1 Asana, Fukuroi, Shizuoka Japan

A lot of studies on anisotropic Nd-Fe-B thick film magnets have been carried out in order to advance micro-electro-mechanical-systems (MEMS) [1-7]. Although (BH)max of an isotropic Nd-Fe-B film is inferior to that of an anisotropic one [8,9], the flexibility of magnetization is attractive in the practical applications such as miniaturized motors. For example, Töpfer et al. reported a multipolarly-magnetized isotropic Nd-Fe-B film prepared by a screen printing method [10]. Yamashita et al. also indicated that a multipolarly-magnetized isotropic thick film was effective to enhance the torque of a milli-size motor compared with that of a motor comprising an anisotropic one [11]. We have already reported on the isotropic Nd-Fe-B thick film magnets prepared by using a PLD (Pulsed Laser Deposition) method and applied them to several micro machines [12]. The characteristic of the method was the high deposition rate up to 90  $\mu\text{m}/\text{h}$  on a 5 mm $\times$ 5 mm substrate by taking advantage of small particles (droplets) emitted from an Nd-Fe-B target.

In this report, we introduce a preparation of thick film magnets by using a Vacuum Arc Deposition [13]. The method also utilizes small particle, however they are liquid droplets which are different from solid ones synthesized by PLD method. Isotropic Nd-Fe-B thick film magnets were prepared by the method with the deposition rate of approximately 10  $\mu\text{m}/\text{h}$  followed by pulse-annealing. It is also reported that an optimum amount of Nb additive is effective to enhance coercivity without the deterioration of remanence and (BH)max values of the isotropic thick films.

- [1] F. Dumas-Bouchat *et al.*, *Appl. Phys. Lett.* **96** (2010) 102511.
- [2] A. Walther *et al.*, *J. Magn. Magn. Mater.* **321** (2009) 590.
- [3] N. M. Dempsey *et al.*, *Appl. Phys. Lett.* **90** (2007) 092509.
- [4] M. Uehara, *J. Magn. Magn. Mater.* **284** (2004) 281.
- [5] L. K. B. Serrona *et al.*, *Appl. Phys. Lett.* **82** (2003) 1751.
- [6] B. A. Kapitanov *et al.*, *J. Magn. Magn. Mater.* **127** (1993) 289.
- [7] S. Yamashita *et al.*, *J. Appl. Phys.* **70** (1991) 6627.
- [8] T. Spelitos *et al.*, *J. Magn. Magn. Mater.* **272-276** (2004) e877.
- [9] A. Melsheimer *et al.*, *Physica B.* **299** (2001) 251.
- [10] J. Töpfer *et al.*, *Proceedings of the 18th Int. Workshop on High Performance Magnets and Their Applications*, (2004) 828.
- [11] F. Yamashita *et al.*, *IEEE Trans. Magn.* **46** (2010) 2012.
- [12] M. Nakano *et al.*, *IEEE Trans. Magn.* **43** (2007) 2672.
- [13] M. Nakano *et al.*, *J. Appl. Phys.* **107** (2010) 09A744-1.



24RP-B-8

## MAGNETO-OPTICAL STUDY OF DOMAIN WALL DYNAMICS AND GIANT BARKHAUSEN JUMP IN MAGNETIC MICROWIRES

Chizhik A.<sup>1</sup>, Zhukov A.<sup>1</sup>, Blanco J.M.<sup>2</sup>, Gonzalez J.<sup>1</sup>

<sup>1</sup> Dpto. Fisica de Materiales, Fac. de Quimica, Universidad del Pais Vasco, San Sebastian, Spain

<sup>2</sup> Dpto. Fisica Aplicada I, EUPDS, UPV/EHU, 20018 San Sebastian, Spain

The investigation of the surface domain walls (DW) motion in magnetic microwires is related to the elucidation of the basic mechanisms of giant magnetoimpedance effect. The aim of this work is to carry out for the first time the investigation of the main peculiarities of the circular magnetic DW motion in magnetic Co-rich microwires.

The measurements were performed on the amorphous glass-coated microwire of the composition  $\text{Co}_{67}\text{Fe}_{3.85}\text{Ni}_{1.45}\text{B}_{11.5}\text{Si}_{14.5}\text{Mo}_{1.7}$  (the diameter of metallic nucleus of  $21.4\ \mu\text{m}$  and total diameter of  $26.2\ \mu\text{m}$ ). Surface domain wall motion has been investigated using magneto-optical Kerr effect (MOKE) modified Sixtus-Tonks method [1] in the presence of circular and axial magnetic field.

The circular DW motion was induced by the pulsed circular magnetic field. The single domain wall motion along the wire was registered as two successive jumps of the MOKE signal. This motion is associated with the circular magnetic bistability related to the giant Barkhausen jump of circular magnetization (Fig. 1). During the experiments our attention was focused of the influence of the dc axial magnetic field on the surface circular DW motion.



Fig. 1. Foto (a) and schematic picture (b) of single circular domain in microwire.

It was found the strong influence of the dc axial magnetic field on the surface circular domain wall motion – depending on the value of the dc axial magnetic field, it could accelerate or decelerate DW motion. In the performed experiments the velocity of the circular DW reached the value of 2000 m/sec. Also it was discovered the axial field induced transformation of the magnetic profile of the moving DW. In particular, dc axial field causes the formation of the extended part inside the circular DW with magnetization directed along the dc axial field.

[1] A. Chizhik A, R. Varga, A. Zhukov, J. Gonzalez, J.M. Blanco, *J. Appl. Phys.*, **103** (2008) 07E707.

24TL-B-9

## HIGH FREQUENCY STUDY OF THE GIANT MAGNETOIMPEDANCE (GMI) EFFECT AND ITS HYSTERETIC BEHAVIOR BY MEANS OF FORC METHOD

*Pirota K.R., Arzuza L.C.C., Béron F., Valenzuela L.*

Instituto de Física Gleb Wataghin, Universidade Estadual de Campinas, Rua Sergio Buarque de Holanda, 777, Cidade Universitária "Zeferino Vaz", Campinas 13083-859, SP, Brazil

Soft amorphous ribbons with a well-defined transversal domain structure generally present (quasi) anhysteretic magnetization curve under an axial applied field. Another effect, called giant magnetoimpedance (GMI), is related to the magnetization process of the magnetic system. It consists of the variation of the electric impedance of soft magnetic materials in the presence of static magnetic field. Its highest sensitivity allows to experimentally obtain a well defined hysteretic area on the GMI curve of these amorphous ribbons. First-order reversal curve (FORC) method represents a powerful experimental technique to probe the irreversible processes occurring in a system, which yield to hysteretic behavior [1]. Mainly applied to magnetization vs field curves, a proper FORC analysis gives the statistical distribution of the parameters from elementary (local) hysteretic process, in opposition to global ones in the case of major hysteresis curves.

In this work, the FORC formalism was applied to hysteretic giant magnetoimpedance (GMI) curves of FeCoSiB amorphous ribbons with transversal anisotropy FORC in a higher and broader frequency range (10 MHz to 1 GHz), using a vector network analyzer (VNA). The first striking observation is that the FORCs are not confined to the hysteretic area, even exceeding the major curve amplitude at some point. They can be separated into three groups depending of the reversal field value, based on their behavior. An interlinked hysteron/anti-hysteron model is proposed to interpret it, which allows analyzing the influence of frequency and magnetostriction upon the hysteretic GMI effect. Our results shows that the hysteresis present in the real part of impedance decreases when increasing the current frequency, while the imaginary part does not present any hysteresis for the whole frequency range studied. The results are interpreted considering transitions in the domain wall structure induced by the external applied field [2]. The method appears a suitable tool to investigate the mechanisms responsible for the hysteretic behaviour in amorphous ribbons, when magnetization curve exhibits too weak hysteresis in order to be able to apply adequately the FORC method.

[1] I. D. Mayergoyz, Phys. Rev. Lett. **56**, 1518 (1986)

[2] F. Béron, L. A. Valenzuela, M. Knobel, K.R. Pirota, submitted to Phys. Rev. B

Wednesday

**24 August**

11:30-13:00

14:30-17:20

oral session

24TL-C

24RP-C

24OR-C

**“Magnetostructural  
Transition Related  
Effects”**

24TL-C-1

## THE EFFECT OF MAGNETIC ANISOTROPY ON THE GIANT MAGNETOCALORIC EFFECT

*Szymczak R.<sup>1</sup>, Kolano-Burian A.<sup>2</sup>, Dyakonov V.P.<sup>1</sup>, Szymczak H.<sup>1\*</sup>*

<sup>1</sup> Institute of Physics, Polish Academy of Sciences, Warszawa, Poland

<sup>2</sup> Institute of Non-Ferrous Metals, Gliwice, Poland

\* corresponding author; e-mail : szymh@ifpan.edu.pl

The search for improve working parameters of materials exhibiting excellent magnetocaloric properties near room temperature is one of the most important directions in physics and applications of magnetic materials. Intensive effort is concentrated at present in the study of the giant magnetocaloric effects discovered in  $Gd_5Si_2Ge_2$  and in  $LaFe_{13}$  and  $MnAs$  families of compounds. Our main goal in this work is to investigate the effect of magnetic anisotropy on the magnetocaloric behavior of these well-known magnetic refrigerant materials. This effect is seen in two different ways: (1) the magnetic field direction in relation to the magnetization is kept constant and the modulus of the field is varied. This effect is usually observed near order-disorder phase transition. It will be shown that that the magnetocaloric effect measured with the magnetic field applied along the easy magnetization axis is larger than that along the hard direction; (2) the magnetic field direction in relation to the magnetization is not fixed because of the occurrence of the spin reorientation phase transition. In this case the magnetic anisotropy strongly affects magnitude and sign of the magnetocaloric effect.

A mean field theory will be used in order to explain the presented experimental results.

This work was financially supported by European Fund for Regional Development (Contract No. UDA-POIG.01.03.01-00-058/08/00).

24TL-C-2

## SPIN CROSSOVERS IN MOTT-HUBBARD INSULATORS AT HIGH PRESSURE

*Lyubutin I.S.<sup>1</sup>, Ovchinnikov S.G.<sup>2</sup>*

<sup>1</sup> Shubnikov Institute of Crystallography, RAS, 119333, Moscow, Russia.

<sup>2</sup> Institute of Physics, Siberian Division of RAS, 660036, Krasnoyarsk, Russia.

The commonly accepted mechanisms of the insulator-metal transition (IMT) in strongly correlated d-electron systems are the band-width controlled IMT (driven by the broadening of the d-bands), and filling-controlled IMT, induced by the doping of charge carriers into the parent insulator compound. However recently, a new mechanism of IMT in Mott-Hubbard insulators have been discovered experimentally and explained theoretically [1,2]. This mechanism can be initiated by the lattice compression at high pressure and it is driven by a spin transition in 3d5 ions from the high-spin (HS) state to the low-spin (LS) state. The evidence of the spin-crossover transition in a set

of 3d metal oxides follows from the Mössbauer and NFS measurements and it is supported by XES experiments [2]. The collapse of the magnetic moment and radical drop of the local spin of 3d<sup>5</sup> ions are substantial evidences for the spin-crossover transition in these systems. We found that the HS-LS spin-crossover suppresses the effective Hubbard parameter  $U_{\text{eff}}$  down to the value enabling the insulator-metal transition according to the Mott mechanism  $U_{\text{eff}}/W \approx 1$  ( $W$  is a half of the d-bandwidth). This type of a Mott-Hubbard IMT was first observed experimentally in the multiferroic BiFeO<sub>3</sub> [1], and similar mechanism must be effective for other 3d<sup>5</sup> transition-metal compounds such as FeBO<sub>3</sub>, GdFe<sub>3</sub>(BO<sub>3</sub>)<sub>4</sub>, RFeO<sub>3</sub> (R= La, Nd, Pr, Lu), Y<sub>3</sub>Fe<sub>5</sub>O<sub>12</sub>,  $\alpha$ -Fe<sub>2</sub>O<sub>3</sub>, Fe<sub>3</sub>O<sub>4</sub>, MnO where the spin crossover was found along with insulator-metal or insulator-semiconductor transitions [2]. We call the new IMT mechanism as the "Hubbard energy control" mechanism, to distinguish from the well known "bandwidth control" and "band-filling" mechanisms of the IMT. The influence of the spin-crossovers on magnetic and electronic properties of the 3d<sup>n</sup> metal compounds will be reviewed, and the classification of possible scenarios of metallization will be presented.

This work is supported by the Russian Foundation for Basic Research grant, #11-02-00636a and by the Program of Russian Academy of Sciences under the Project "Strongly correlated electronic systems".

[1] I.S. Lyubutin, S.G. Ovchinnikov, A.G. Gavriliuk, V.V. Struzhkin. Spin-crossover induced Mott transition and the other scenarios of metallization in 3d<sup>n</sup> metal compounds, Phys. Rev. B 79 (2009) 085125.

[2] I.S. Lyubutin and A.G. Gavriliuk, "Research on phase transformations in 3d-metal oxides at high and ultrahigh pressure: state of the art", Physics – Uspekhi 52 (2009) 989-1017. effect.

24RP-C-3

## MAGNETOELASTIC AND ELASTOCALORIC EFFECTS IN THE RARE-EARTH METALS AND COMPOUNDS

*Nikitin S.A.*

Department of Physics, Lomonosov Moscow State University, GSP-1, Leninskie Gory, Moscow, 119991, Russia

The phenomenon of giant magnetostriction in the rare-earth metals and compounds has opened the way to the development of new magnetostrictive materials with high characteristics for generation of sound and ultrasound waves, optoelectronics, hydraulics arrangements.

This article discusses experimental data and their theoretical explanation for the volume magnetostriction, spontaneous magnetostriction, a change of magnetization under pressure, elastocaloric effects.

Particular attention has been given to the behaviour of these effects in the region of magnetic phase transitions. The volume paraprocess magnetostriction  $\Delta V/V$  was investigated near Curie temperature  $T_c$  as a function of magnetization for rare-earth metals and compounds.  $\omega$  was calculated by thermodynamic theory from a change of magnetization under pressure. From these data we obtained a dependence of exchange integrals on the lattice cell volume.

The magnetization dependence of paraprocess magnetostriction for the rare-earth alloys may be ascribed to Landau theory for magnetic phase transition. A giant magnetoelastic caloric effect was found in a region of magnetic phase transition in rare-earth compounds and alloys. This effect is of particular value for a creation of new refrigerators.

It was established that in  $R\text{Co}_2$  compounds a giant volume magnetostriction is caused by 3d-sublattice, in which the magnetic moment critically increases with magnetic field at  $T > T_c$ .

The investigation revealed that the giant volume magnetostriction occurs over the whole region of magnetic phase transition in  $R_2\text{Fe}_{17}$  compound. The temperature dependence of the magnetostriction constants and their values may be explained within the standard Theory of Magnetostriction [1], where exchange and magnetocrystalline interactions are strongly strain dependent. The magnetization dependence of a volume magnetostriction is attributable to contributions from the second and fourth powers of magnetization in the Gibbs potential, as determined by the thermodynamic theory for the ferromagnetic–paramagnetic transitions. Giant values of the volume magnetostriction have its origin in the strong strain dependence of exchange interaction and 3d-electron bandwidth, that results from the effective 3d-electron coulomb repulsion and also by the particular local density of magnetic moment [1]. A special attention should be paid to the fact that  $\text{Y}_2\text{Fe}_{17}$  exhibits a large magnetostriction in moderate magnetic fields at room temperatures, providing an opportunity of this effect applications in hydraulic devices.

The work was supported by RFBR grant #10-02-00721

[1] A. del Moral, Handbook of Magnetostriction and Magnetostrictive Materials, vol.1 of chapter. 4-6, 10, Del Moral Publisher S.L.Spain, 2008.

24TL-C-4

## MAGNETOCALORIC EFFECT AND MULTIFUNCTIONAL PROPERTIES OF Mn-BASED HEUSLER ALLOYS

*Dubenko I.<sup>1</sup>, Pathak A.K.<sup>1</sup>, Kazakov A.<sup>2</sup>, Prudnikov V.N.<sup>2</sup>, Stadler S.<sup>3</sup>, Granovsky A.B.<sup>2,4,5</sup>, Ali N.<sup>1</sup>*

<sup>1</sup> Southern Illinois University at Carbondale, Carbondale IL, 62901, USA

<sup>2</sup> Moscow State University, Moscow, 119991, Russian Federation

<sup>3</sup> Louisiana State University, Baton Rouge, LA 70803, USA

<sup>4</sup> Basque Country University, 20080, San Sebastian, Spain

<sup>5</sup> Ikerbasque, Basque Foundation for Science, 48011, Bilbao, Spain

The magnetic states of austenitic (AP) and martensitic (MP) phases of some magnetic off-stoichiometric Heusler alloys are characterized by different magnetic moments and in some cases by different types of magnetic ordering. As a result off-stoichiometric Heusler alloys exhibit giant inverse magnetocaloric effect, field induced magneto-structural transitions, exchange bias, giant magnetoresistance, non-reciprocal effects in magnetization, and so on (see Ref. [1] and references therein).

In this report we summarize our results on the studies of magnetocaloric properties, phase transitions and phenomena related to magnetic heterogeneity in the vicinity of martensitic transition in Ni-Mn-In and Ni-Mn-Ga off-stoichiometric Heusler alloys. The crystal structure, phase transitions, magnetocaloric effect (MCE) and magnetotransport properties were studied for the following alloys:  $\text{Ni}_{50}\text{Mn}_{50-x}\text{In}_x$  ( $x = 13.5, 15, 15.05, 15.2, 15.5, 16$ );  $\text{Ni}_{50-x}\text{Co}_x\text{Mn}_{35}\text{In}_{15}$  ( $x = 1, 2, 3, 5$ ),  $\text{Ni}_{50}\text{Mn}_{35-x}\text{Co}_x\text{In}_{15}$  ( $x = 1, 2, 3$ ),  $\text{Ni}_{50}\text{Mn}_{35}\text{In}_{14}\text{Z}$  ( $Z = \text{Al}, \text{Ge}$ ),  $\text{Ni}_{50}\text{Mn}_{35}\text{In}_{15-x}\text{Si}_x$  ( $x = 1, 2, 3, 4, 5$ );  $\text{Ni}_{50-x}\text{Co}_x\text{Mn}_{25+y}\text{Ga}_{25-y}$  ( $x = 0, 4, 6, 7, 8$ ;  $y = 6, 7, 8$ );  $\text{Ni}_{50-x}\text{Co}_x\text{Mn}_{32-y}\text{Fe}_y\text{Ga}_{18}$  ( $x = 0, 8$ ,  $y = 1, 1.5, 2$ ). It was found that the magnetic entropy changes,  $\Delta S$ , associated with inverse MCE in the vicinity of the temperature of magneto-structural transition,  $T_M$ , persists in a range (125-20) J/(kgK) for a magnetic field change  $\Delta H = 5$  T. The transition temperatures vary from 240 K to 370K with

composition. The martensitic transformation in  $\text{Ni}_{50}\text{Mn}_{50-x}\text{In}_x$  ( $x=13.5$ ) results in transition between two paramagnetic states. Associated with the paramagnetic-paramagnetic transition  $\Delta S = 24 \text{ J}/(\text{kgK})$  was detected for  $\Delta H = 5 \text{ T}$  at  $T = 350 \text{ K}$ . It was shown that variation in composition of  $\text{Ni}_2\text{MnGa}$  can drastically change the magnetic state of MP below and in the vicinity of  $T_M$ . The presence of the MP with magnetic moment much smaller than that in AP above  $T_M$  leads to the large inverse MCE in  $\text{Ni}_{42}\text{Co}_8\text{Mn}_{32-y}\text{Fe}_y\text{Ga}_{18}$  system. The adiabatic temperature changes ( $\Delta T_{\text{ad}}$ ) in the vicinity of the  $T_C$  and  $T_M$  of  $\text{Ni}_{50}\text{Mn}_{35}\text{In}_{15}$  and  $\text{Ni}_{50}\text{Mn}_{35}\text{In}_{14}\text{Z}$  ( $Z=\text{Al}$  and  $\text{Ge}$ ) were studied using an adiabatic magnetocalorimeter. The largest changes  $\Delta T_{\text{ad}} = -2\text{K}$  and  $2\text{K}$  near  $T_M$  and  $T_C$  were obtained for  $\Delta H = 1.8 \text{ T}$ , respectively. It was observed that  $|\Delta T_{\text{ad}}| \approx 1\text{K}$  for relatively small field changes ( $\Delta H = 1 \text{ T}$ ) for both types of transitions.

We also discuss recent results on resistivity, magnetoresistance, ordinary and anomalous Hall effect in some  $\text{NiMn-In-Z}$  alloys and promising applications of these multifunctional materials.

This research was supported by the Russian Foundation for Basic Researches, by the Basque Foundation for Science, by the Office of Basic Energy Sciences, Material Sciences Division of the U. S. Department of Energy.

[1] I. Dubenko, M. Khan, A. Pathak et al., *J. Magn. Magn. Mat.*, **321** (2009) 754.

24TL-C-5

## THEORETICAL MODEL FOR STUDY THE MAGNETIC, STRUCTURAL AND MAGNETOCALORIC PROPERTIES OF HEUSLER ALLOYS

*Buchelnikov V.D.<sup>1</sup>, Sokolovskiy V.V.<sup>1</sup>, Taskaev S.V.<sup>1</sup>, Entel P.<sup>2</sup>*

<sup>1</sup> Chelyabinsk State University, Br. Kashirinykh Str., 129, 454001, Chelyabinsk, Russia

<sup>2</sup> Faculty of Physics and CeNIDE, University of Duisburg-Essen, 47048, Duisburg, Germany

Ferromagnetic Heusler Ni-Mn-X ( $X = \text{Ga}, \text{In}, \text{Sn}, \text{Sb}$ ) alloys have attracted much attention in view of their unique properties such as the shape memory effect, giant magnetocaloric effect, large magnetoresistance and other interesting magnetic properties like a coupled magnetostructural phase transition [1-3].

In this work we constructed a theoretical model for detailed description of the magnetic, structural and magnetocaloric properties of Heusler Ni-Mn-X ( $X = \text{Ga}, \text{In}, \text{Sn}, \text{Sb}$ ) alloys using the *ab initio* investigations of magnetic exchange parameters combined with Monte Carlo simulations.

In the proposed model, we consider the three-dimensional cubic lattice with real unit cell of Heusler alloys and with periodic boundary conditions. For description of magnetic part of whole system, we use the Heisenberg model for study a second-order magnetic phase transition and the Potts model which allows us to simulate a first-order magnetic phase transition [1, 4, 5]. Values of magnetic exchange integrals have been taken from first-principles *ab initio* calculations by employing Lichtenstein's formula [6] and the Munich SPR-KKR package [7] in combination with the single-site coherent potential approximation (KKR-CPA) in the 1<sup>st</sup>, 2<sup>nd</sup> and 3<sup>rd</sup> coordination spheres for the cubic  $L2_1$  and tetragonal  $L1_0$  structures of the Heusler alloys. The structural part describes by the degenerated three states Blume-Emery-Griffiths model [4, 5, 8] for modeling of a martensitic transformation.

The calculated temperature dependencies of the magnetic and lattice contribution to the total specific heat as well as the evaluation of the isothermal magnetic entropy  $\Delta S_{\text{mag}}(T, H_{\text{ext}})$  and

adiabatic temperature  $\Delta T(T, H_{ext})$  changes around the magnetic, magnetostructural and metamagnetostructural transitions in an external magnetic field agree fairly well with the experimental data. In particular, results for  $\Delta S_{mag}(T, H_{ext})$  and  $\Delta T(T, H_{ext})$  may be used to speculate about designing new magnetic Heusler alloys with better magnetocaloric properties, i.e. larger  $\Delta T(T, H_{ext})$  values.

Support by RFBR grants 10-02-96020-r-ural, 11-02-00601, 10-02-92110 and RF President grant MK-1891.2010.2 is acknowledged.

- [1] P. Entel et al. *Mater. Sci. Forum* **583** (2008) 21.
- [2] Y. Sutou et al. *Appl. Phys. Lett.* **85** (2004) 4358.
- [3] T. Krenke et al. *Phys. Rev. B* **73** (2006) 174413.
- [4] V.D. Buchelnikov et al. *Phys. Rev. B* **81** (2010) 094411.
- [5] V.D. Buchelnikov et al. *Phys. Rev. B* **78** (2008) 184427.
- [6] A.I. Liechtenstein et al. *J. Magn. Magn. Mater.* **67** (1987) 65.
- [7] H. Ebert, *Electronic Structure and Physical Properties of Solids*, ed. H. Dreyssé (Berlin: Springer, Lecture Notes in Physics, 1999) Vol. 535, p. 191.
- [8] M. Blume, V.J. Emery and R.B. Griffiths, *Phys. Rev. A* **4** (1971) 1071

24TL-C-6

## UNDERSTANDING MAGNETISM OF MARTENSITIC STATE OF Ni-Mn BASED SMA: XAS AND XMCD STUDIES

*Priolkar K.R.<sup>1</sup>, Lobo D.N.<sup>1</sup>, Emura S.<sup>2</sup>*

<sup>1</sup> Department of Physics, Goa University, Taleigao Plateau, Goa 403206 India

<sup>2</sup> Institute of Scientific and Industrial Research, Osaka University, 8-1 Mihogaoka, Ibaraki,  
Osaka 567-0047, Japan

Shape memory alloys of the type  $\text{Ni}_2\text{Mn}_{1+x}\text{Z}_{1-x}$  ( $Z = \text{In, Sn, Sb}$ ) have attracted a lot of attention due to their significantly different magnetic properties in comparison to those of prototype  $\text{Ni}_2\text{MnGa}$ . These Ni-Mn-Z alloys have significantly smaller magnetization in the martensitic state than that in austenitic state [1]. In addition, these alloys exhibit other interesting properties like inverse magnetocaloric effect [2], giant magnetoresistance [3], giant magnetothermal conductivity [4] and an exchange bias effect [5].

According to recent neutron diffraction results the magnetic correlations in the martensitic phase are antiferromagnetic (AF) in nature [6]. The origin of these correlations is still far from being understood. Theoretical efforts based on monte-carlo simulations indicate the AF correlations are due to RKKY interactions between Mn atoms occupying its own sub-lattice and those occupying the Z sub-lattice [7]. However, another first principles calculation predicts superexchange interactions as the cause of antiferromagnetic interactions [8]. This scenario is supported by photoelectron spectroscopy which provides evidence for hybridization between Ni 3d states and 3d states of excess Mn atoms in the martensitic phase [9].

In this paper, with the help of temperature dependent XAS and XMCD studies, we propose strong Ni-Mn hybridization in the martensitic phase as the cause of antiferromagnetic interactions in the martensitic phase.



- [1] Y. Sutou et al., Appl. Phys. Lett. 85 (2004) 4358.
- [2] T. Krenke et al., Nature Mater. 4 (2005) 450.
- [3] S.Y. Yu et al., Appl. Phys. Lett. 89 (2006) 162503.
- [4] B. Zhang et al., Appl. Phys. Lett. 91 (2007) 012510.
- [5] M. Khan et al., Appl. Phys. Lett. 91 (2007) 072510.
- [6] S. Aksoy et al., Phys. Rev. B 79 (2009) 212401.
- [7] V. Buchelnikov et al., Phys. Rev. B 78 (2008) 184427.
- [8] E. Şaşıoğlu et al., Phys Rev B 77 (2008) 064417.
- [9] M. Ye et al., Phys. Rev. Lett. 104 (2010) 176401.

24OR-C-7

## FIRST-PRINCIPLES DESCRIPTION OF THERMALLY INDUCED MAGNETIC EXCITATIONS IN SIMULATIONS OF STRUCTURAL PHASE TRANSITIONS

*Abrikosov I.A.<sup>1</sup>, Ekholm M.<sup>1</sup>, Ruban A.V.<sup>2</sup>, Alling B.<sup>1</sup>, Marten T.<sup>1</sup>, Steneteg P.<sup>1</sup>*

<sup>1</sup> Department of Physics, Chemistry and Biology, IFM, Linköping University,  
SE-581 83 Linköping, Sweden

<sup>2</sup> Applied Material Physics, Department of Materials Science and Engineering,  
Royal Institute of Technology, SE-10044 Stockholm, Sweden

In magnetic alloys, the effect of finite temperature magnetic excitations on phase stability is poorly investigated. At zero temperature most (though not all) magnetic materials exhibit relatively simple ferromagnetic or antiferromagnetic ordered arrangements of local magnetic moments, which are most often assumed in simulations, while paramagnetic phases are often (and erroneously) considered as non-magnetic. In reality, temperature induced magnetic excitations modify this picture, and are essential for the predictive description of materials properties below, as well as above the Curie temperature, because many systems undergo phase transitions in this temperature range. We demonstrate the importance of accounting for the finite temperature magnetic excitations in theoretical simulations of structural properties and phase transitions for two systems, Fe-Ni permalloy and CrN.

Considering random Ni-rich Fe-Ni alloys, which undergo chemical order-disorder transition approximately 100 K below their Curie temperature, we demonstrate from ab initio calculations that deviations of the global magnetic state from ideal ferromagnetic order due to temperature induced magnetization reduction have a crucial effect on the structural transition temperature. We propose a scheme where the magnetic state is described by partially disordered local magnetic moments and combine it with Heisenberg Monte Carlo simulations of the magnetization. Although our theoretical approach is based on a number of assumptions concerning the finite temperature magnetic excitations, the type of magnetic and atomic configurational Hamiltonians, and the coupling of the chemical and magnetic degrees of freedom, we are able to reproduce quite accurately not only the experimental ordering transition temperature, but also its behavior as a function of the alloy composition [1].

Using first-principles calculations we study the effect of magnetic disorder above the magnetic transition temperature on the structural and thermodynamic properties of CrN, a material which undergoes a structural transition from orthorhombic antiferromagnetic to cubic paramagnetic phase around room temperature. The need of a treatment of electron correlations effects beyond the local density approximation is proven. When magnetic disorder and strong electron correlations are taken

into account simultaneously, pressure- and temperature-induced structural and magnetic transitions in CrN can be understood [2].

In summary, our work points out the general importance of temperature induced magnetic effects for alloy stability in the magnetically ordered, as well as disordered states. It adds a new aspect to the development of accurate *ab initio* theory of magnetostuctural transitions.

[1] M. Ekholm, H. Zapolsky, A. V. Ruban, I. Vernyhora, D. Ledue, and I. A. Abrikosov, Phys. Rev. Lett. **105**, (2010) 167208.

[2] B. Alling, T. Marten, and I. A. Abrikosov, Nature Materials **9**, (2010) 283; Phys. Rev. B **82**, (2010) 184430.

24OR-C-8

## MAGNETOCALORIC PROPERTIES OF MAGNETIC IN WEAK MAGNETIC FIELDS

*Aliev A.M.<sup>1</sup>, Koledov V.V.<sup>2</sup>, Hernando B.<sup>3</sup>, Kalitka V.S.<sup>4</sup>*

<sup>1</sup> Amirkhanov Institute of Physics, Daghestan Scientific Center of RAS,  
Makhachkala 367003, Russia

<sup>2</sup> Kotelnikov Institute of Radio Engineering and Electronics, RAS, Moscow 125009, Russia

<sup>3</sup> Depto. de Física, Facultad de Ciencias, Universidad de Oviedo, Calvo Sotelo s/n,  
33007 Oviedo, Spain

<sup>4</sup> Moscow State University, Moscow 119899, Russia

Study of the magnetocaloric effect in weak magnetic fields is of interest due to that the fine peculiarity of interaction of magnetic and phonon subsystems can appear. In high magnetic fields the features are suppressed in partly. Especially clear the effects can be observe in magnetic materials in which the magnetic transitions occur simultaneously or close to the structural, and charge (orbital) transitions.

Various magnetic materials, such as a gadolinium, Heusler alloys, and A-site ordered manganites are studied in the paper. Possibility of carrying out of reliable measurements of MCE in weak magnetic fields became practicable due to creation of a technique of direct measurements of MCE by modulation of a magnetic field [1].

Behavior of MCE in classical magnetocaloric material gadolinium in weak and strong fields essentially doesn't differ. Even in weak fields the MCE resulted from spin - reorientation is observed. Near Curie point the field dependences of MCE in weak and strong fields are different. While in strong fields MCE saturates, in weak fields the strengthening of MCE dependence on magnetic field is observed.

In Heusler alloys, in addition to paramagnetic-ferromagnetic transition, structural transition accompanied by sharp reduction of magnetization takes place, too. Vanish of magnetization with decrease of temperature leads to the inverse MCE. In the studied compositions of rapidly quenched ribbons  $Mn_{50}Ni_{40}In_{10}$  and  $Ni_{50}Mn_{37}Sn_{13}$  Heusler alloys both direct and inverse magnetocaloric effects associated with magnetic (paramagnet - ferromagnet - antiferromagnet) and structural (austenite - martensite) phase transitions are found. Additional inverse magnetocaloric effects of small value are observed around the ferromagnetic transitions. At the same time, in bulk samples of Heusler alloys, this effect does not occur.

In A-site ordered manganites  $PrBaMn_2O_6$  and  $NdBaMn_2O_6$  direct and inverse magnetocaloric effects also are observed. In  $NdBaMn_2O_6$  direct and inverse effects are observed in very narrow

temperatures region. In weak magnetic fields direct and inverse effects take place both at heating and cooling. In higher magnetic fields both effects are observed only at cooling mode while at heating the inverse effect corresponding to the ground antiferromagnetic state of this composition is revealed only.

This work was supported by RFBR (11-02-01124, 09-08-96533), and Physics Branch of RAS is acknowledged.

[1] A.M. Aliev, A.B. Batdalov, V.S. Kalitka. JETP Letters **90**, 663–666 (2009).

24OR-C-9

## STRUCTURAL, MAGNETIC AND ELECTRONIC PROPERTIES OF A NEW SILICIDE Mn-Pt-Si

*Gamza M.<sup>1,2</sup>, Ackerbauer S.<sup>1</sup>, Leithe-Jasper A.<sup>1</sup>, Schnelle W.<sup>1</sup>, Rosner H.<sup>1</sup>, Grin Yu.<sup>1</sup>*

<sup>1</sup> Max Planck Institute for Chemical Physics of Solids, Dresden, Germany

<sup>2</sup> Institute of Materials Science, University of Silesia, Katowice, Poland

Recent results concerning giant exchange-derived magnetoelastic coupling and tricriticality in the metamagnet MnCoSi (TiNiSi-type structure) [1] as well as intriguing magnetic properties of the isostructural compounds MnTX (T = transition metal element; X = Si, Ge) [2] stimulated the search for consecutive members of this family. Here, we report on the crystal structure, electronic structure and magnetic properties of the new compound MnPtSi. First principles electronic structure calculations indicate an interesting spin state of Mn with a magnetic moment of 3.2  $\mu_B$ . This finding is in agreement with the saturation magnetisation of 3  $\mu_B$  in the ordered state. Further, the effective moment derived from high-temperature magnetic susceptibility supports the  $S \approx 3/2$  spin state of Mn. Thermodynamic measurements revealed two successive magnetic phase transitions at  $T_C \approx 340$  K and  $T_N \approx 326$  K. The FM to AFM transition is accompanied by a large magneto-volume effect ( $\Delta V/V \sim 1.4\%$ ) and a change in Mn-Mn distances of up to 1%.

[1] Barcza A. et al.; Phys. Rev. Lett. (2010) 104 247202

[2] Eriksson T. et al.; Phys. Rev. B (2005) 71 174420 and references there in

24OR-C-10

## NEUTRON DIFFRACTION STUDY OF Ni-Mn-Ga MSM ALLOY

Ari-Gur P.<sup>1</sup>, Garlea V.O.<sup>2</sup>, Coke A.<sup>2</sup>, Ge Y.<sup>3</sup>, Aaltio I.<sup>3</sup>, Söderberg O.<sup>3</sup>, Hannula S.-P.<sup>3</sup>, Kimmel G.<sup>4</sup>

<sup>1</sup> Mechanical & Aeronautical Engineering, Western Michigan University, Kalamazoo, MI, USA

<sup>2</sup> Neutron Scattering Sciences Division, Oak Ridge National Lab, Oak Ridge, TN 37831, USA

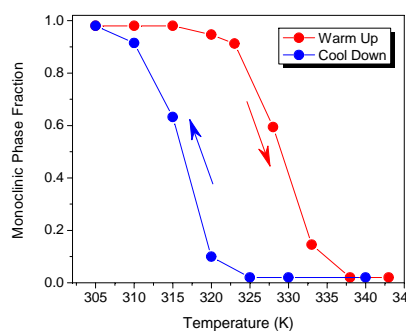
<sup>3</sup> Department of Materials Science and Engineering, Aalto University, Espoo, Finland

<sup>4</sup> Faculty of Engineering Sciences, Ben-Gurion University of the Negev, Beer-Sheva, Israel

Alloys demonstrating magnetic field induced strains (MFIS) attracted much attention in the last decade; non-Stoichiometric Ni-Mn-Ga alloys, specifically, are considered promising for numerous industrial applications [1]. Their performance, though, is sensitive to variations in their composition, crystal structure and quality [1]. Substantial amount of work was published on the crystal structure of Ni-Mn-Ga alloys (see e.g. [2]), however more information is still needed about the chemical order in the crystal of the different Ni-Mn-Ga alloys [3]. The order (or lack of it) is very important, as it affects the distance between Mn atoms and, as a result, the magnetic properties too.

In the current work, single crystals of non-stoichiometric Ni-Mn-Ga were grown and milled to produce a powder with particles in the range of 56-105  $\mu\text{m}$ . The powder was heat treated at 825°C for 2 hours, to eliminate the effects of milling. Crystal and magnetic structures, phase transformations and chemical order were investigated using neutron powder diffraction. Measurements revealed that, above 340 K, the alloy crystallizes in a L2<sub>1</sub> Heusler structure with a lattice constant of  $a = 0.584$  nm, in agreement with X-ray results [2]. Rietveld refinements of site occupancies for all three elements indicate the following composition Ni<sub>2</sub>Mn<sub>1</sub>Ga<sub>0.76</sub>. The fact that neither Mn nor Ni occupy the vacant sites of Ga means that the interatomic distance of the Mn atoms remains unchanged compared to the stoichiometric phase. The refined ferromagnetic moment on the Mn site was obtained to be 2.8  $\mu\text{B}$ .

At lower temperature, a phase transition to a 10M modulated monoclinic phase (P12/m 1) takes place. The lattice constants of this phase are:  $a = 0.423$  nm,  $b = 0.558$  nm,  $c = 2.101$  nm,  $\beta = 90.328^\circ$ . The figure to the right, describes the phase transformations upon cooling and warming, expressed as the monoclinic phase fraction. The magnetic structure remains collinear ferromagnetic, with no significant change in the magnitude of Mn moment



Change of monoclinic (P12/m 1) phase fraction for the warming and cooling cycles of the sample

The authors wish to acknowledge the US National Science Foundation award #0831951, FRACAA award # 08-050, beam time at Oak Ridge and the support of the Academy of Finland.

[1] K. Rolf, A. Mecklenburg, J.-M. Guldbakke, R.C. Wimpory, A. Raatz, J. Hesselback, R. Schneider, *J. Mag. and Mag. Mat.*, 321 (2009) 1063.

[2] Y. Ge, O. Söderberg, N. Lanska, A. Sozinov, K. Ullakko, V.K. Lindros, *J. Phys. IV* 112 (2003) 921.

[3] I. Glavatskyy, N. Glavatska, A. Dobrinsky, J.-U. Hoffmann, O. Söderberg and S.-P. Hannula, *Sripta Materialia* 56 (2007) 565.

24OR-C-11

## GIANT AND REVERSIBLE STRAIN-MEDIATED MAGNETOCALORIC EFFECT IN $\text{La}_{0.7}\text{Ca}_{0.3}\text{MnO}_3$ FILMS

Moya X.<sup>1</sup>, Hueso L.E.<sup>2,3</sup>, Maccherozzi F.<sup>4</sup>, Tovstolytkin A.I.<sup>5</sup>, Podyalovskii D.I.<sup>5</sup>, Ducati C.<sup>1</sup>, Phillips L.<sup>1</sup>, Ghidini M.<sup>1</sup>, Hovorka O.<sup>2</sup>, Berger A.<sup>2</sup>, Vickers M.E.<sup>1</sup>, Dhesi S.S.<sup>4</sup>, Mathur N.D.<sup>1</sup>

<sup>1</sup>Department of Materials Science, University of Cambridge, Cambridge, CB2 3QZ, United Kingdom.

<sup>2</sup>CIC nanoGUNE Consolider, Tolosa Hiribidea 76, E-20018 Donostia - San Sebastian

<sup>3</sup>IKERBASQUE, Basque Foundation for Science, E-48011 Bilbao, Spain.

<sup>4</sup>Diamond Light Source Ltd., Harwell Science and Innovation Campus, Chilton, Didcot, Oxfordshire, OX11 0DE, United Kingdom.

<sup>5</sup>Institute of Magnetism, 36b Vernadsky Blvd., Kyiv 03142, Ukraine.

Concomitant magnetic and structural phase transitions are important in many applications, i.e. magnetostriction, magnetoresistance and magnetocalorics [1]. However, structural phase transitions arise in only a few classes of magnetic materials. Here, we report the existence of extrinsic magnetostructural transitions in ferromagnetic  $\text{La}_{1-x}\text{A}_x\text{MnO}_3$  ( $A = \text{Sr}, \text{Ca}$ ) manganite films due to strain from ferroelastic-ferroelectric  $\text{BaTiO}_3$  substrates. Macroscopic techniques (magnetometry and calorimetry) will be presented in order to demonstrate magnetically driven entropy changes in our films. The results are comparable with the best magnetocaloric materials [2] and we will discuss the use of these extrinsic transitions for magnetocaloric applications. Photoemission electron microscopy with x-ray magnetic circular dichroism contrast and ferromagnetic resonance will also be presented for microscopic insight into the underlying physical mechanisms that permit these extrinsic magnetocaloric effects.

[1] *Magnetism and Structure in Functional Materials*, edited by A. Planes, Ll. Mañosa and A. Saxena, Materials Science Series, Vol. 79 (Springer-Verlag, Berlin, 2005).

[2] K.A. Gschneider, Jr. and V.K. Pecharsky, *Annu. Rev. Mater. Sci.* **30**, 387–429 (2000).



Wednesday

**24 August**

11:30-13:00

14:30-17:20

oral session

24TL-D

24OR-D

**“Low Dimensional  
Magnetism”**

24TL-D-1

## MAGNETIC MONOPOLES IN SPIN ICE

*Holdsworth P.*

Ecole Normale Supérieure de Lyon

Models for the frustrated magnetic material “spin ice” show the remarkable property of fractionalization of magnetic moments into effective free magnetic charge: magnetic monopoles [1,2]. The development of experimental signatures of the presence of monopoles in spin ice materials, Holmium and Dysprosium Titanate is hence one of the most engaging and exciting challenges of condensed matter physics.

In this talk I will present a theory of diffusive monopole dynamics, motivated by magnetic relaxation measurements on both materials [3]. I will show that the relaxation rate of the underlying network of constraints, which are classical analogues of Dirac strings, is in quantitative agreement with that for magnetic relaxation in  $\text{Dy}_2\text{Ti}_2\text{O}_7$ [4]. This agreement provides an explanation for the non-standard nature of spin freezing in spin ice compounds and gives strong evidence for the presence of monopoles. I will also review recent experiments giving direct measurement of the magnetic charge through the Wien effect [5,6].

- [1] Castelnovo, C., Moessner, R. & Sondhi S. « Magnetic monopoles in spin ice ». *Nature* 451, 42.
- [2] Ryzhkin, I. A. Magnetic relaxation in rare-earth oxide pyrochlores. *J. Exp. Theor. Phys.* 101, 481-486 (2005).
- [3] L. Jaubert and P. C. W. Holdsworth, « Signature of magnetic monopole and Dirac string dynamics in spin ice », *Nature Physics* 5, 258.
- [4] Snyder, J. et al. « Low temperature spin freezing in  $\text{Dy}_2\text{Ti}_2\text{O}_7$  spin ice ». *Phys. Rev. B* 69, 064414 (2004).
- [5] S. T. Bramwell, S. R. Giblin, S. Calder, R. Aldus, D. Prabhakaran, T. Fennell, « Measurement of the charge and current of magnetic monopoles in spin ice » *Nature*, 461, 956, (2009).
- [6] - S. R. Giblin, S. T. Bramwell, P. C. W. Holdsworth, D. Prabhakaran and I. Terry, « Creation and Measurement of Long-Lived Magnetic Monopole Currents in Spin Ice, *Nature Physics* 7, 252-258 (2011).



24TL-D-2

## **Li<sub>2</sub>CuO<sub>2</sub>: FUNDAMENTAL NOVEL INSIGHTS INTO FRUSTRATED QUASI-1D QUANTUM ANTIFERROMAGNETIC**

*Klingeler R.<sup>1</sup>, Nishimoto S.<sup>2</sup>, Drechsler S.-L.<sup>2</sup>, Kuzian R.<sup>2,5</sup>, Malek J.<sup>2,3</sup>, Richter J.<sup>7</sup>, Lorenz W.E.A.<sup>2</sup>, Wizen N.<sup>1,2</sup>, Loewenhaupt M.<sup>4</sup>, van den Brink J.<sup>2</sup>, Skourski Y.<sup>6</sup>, Büchner B.<sup>2</sup>*

<sup>1</sup>Kirchhoff Institute for Physics, University of Heidelberg, Germany

<sup>2</sup>Leibniz-Institut für Festkörper- und Werkstoffforschung (IFW) Dresden, Germany

<sup>3</sup>Institute for Problems of Materials Science, Kiev, Ukraine

<sup>4</sup>Institut für Festkörperphysik, Technische Universität Dresden

<sup>5</sup>Institute of Physics, ASCR - Prague, Czech Republic

<sup>6</sup>Hochfeld-Magnetlabor Dresden, Helmholtz-Zentrum Dresden-Rossendorf, Dresden, Germany

<sup>7</sup>University of Magdeburg, Inst. of Theoretical Physics, Germany

Li<sub>2</sub>CuO<sub>2</sub> is the first and most frequently studied compound of the growing class of edgeshared spin-chain cuprates. Being a model edge-shared quasi-one-dimensional (quasi-1D) frustrated quantum spin magnet, we have explored in detail its magnetic and thermodynamic properties. Our results provide new insight which can be extended to the class of quasi-1D frustrated quantum spin magnets in general. In particular, our inelastic neutron diffraction studies detect long-sought quasi-1D magnetic excitations with a large dispersion along the CuO<sub>2</sub>-chains. The total dispersion is governed by a surprisingly large ferromagnetic (FM) nearest neighbor exchange integral  $J_1 = -228$  K. An anomalous quartic dispersion near the zone center and a pronounced minimum near (0,0.11,0.5) r.l.u. point to the vicinity of a 3D FM-spiral critical point. Interchain coupling turns out to be the essential parameter governing the magnetic phase diagram. Remarkably, for a wide range of frustrated spin-chains the saturation field is completely independent of intra-chain interactions. We show that in the isotropic approximation the inter-chain coupling can be read off directly from the saturation field determined by pulsed field studies which hence represents a novel sensitive and attractive method to determine even weak inter-chain interactions of the order of few K. Detailed studies of the thermal expansion, specific heat and magnetostriction allow to determine the resulting complex phase diagram and reflect signatures of critical fluctuations and the close vicinity to a critical point.

Support by DFG via KL1824/2 is gratefully acknowledged.

[1] W. Lorenz et al., EPL 88, 37002 (2009)

[2] S.-L. Drechsler et al., JPCS 200 12028 (2010)

[3] S. Nishimoto et al., arXiv:1004.3300

24TL-D-3

## INTERPLAY BETWEEN PARAMAGNETISM AND PARAELECTRICITY IN THE FRUSTRATED SPIN CHAIN MAGNET $\text{Li}_2\text{ZrCuO}_4$

*Kataev V.<sup>1</sup>, Vavilova E.<sup>1,2</sup>, Moskvin A.S.<sup>1,3</sup>, Arango Y.<sup>1</sup>, Sotnikov A.<sup>1,4</sup>, Drechsler S.-L.<sup>1</sup>, Klingeler R.<sup>5</sup>, Volkova O.<sup>6</sup>, Vasiliev A.<sup>6</sup>, Büchner B.<sup>1</sup>*

<sup>1</sup> Leibniz Institute for Solid State and Materials Research IFW Dresden, D-01171 Dresden, Germany

<sup>2</sup> Zavoisky Physical Technical Institute of the Russian Academy of Sciences, 420029, Kazan, Russia

<sup>3</sup> Ural State University, 620083, Ekaterinburg, Russia

<sup>4</sup> A. F. Ioffe Physico-Technical Institute of RAS, 194223, St.-Petersburg, Russia

<sup>5</sup> Kirchhoff Institute for Physics, University of Heidelberg, D-69120 Heidelberg, Germany

<sup>6</sup> Moscow State University, 119992 Moscow, Russia

$\text{Li}_2\text{ZrCuO}_4$  is a recently discovered quantum spin-1/2 chain compound in a close vicinity to the quantum critical point to ferromagnetism that exhibits very unusual magnetic properties. In this talk a detailed experimental study of this material by means of nuclear magnetic resonance and electron spin resonance spectroscopies complemented by measurements of dielectric constants will be reviewed. We have observed a new peculiar effect of the interaction between two sublattices that uniquely coexist in this material: the above mentioned sublattice of frustrated spin-1/2 chains and a sublattice of Ising-like reorienting electric dipoles due to tunneling  $\text{Li}^+$  ions. The electrical sublattice orders glass-like at  $T_g \sim 70$  K yielding non-equivalent spin sites in the chains. We suggest that such a remarkable interplay between two subsystems may strongly influence the properties of the spiral spin state in  $\text{Li}_2\text{ZrCuO}_4$  and might be responsible for the missing multiferroic behavior present in other helicoidal magnets.

24TL-D-4

## UNCONVENTIONAL TEMPERATURE ENHANCED MAGNETISM IN IRON TELLURIDE

*Zaliznyak I.A.<sup>1</sup>, Xu Z.<sup>1</sup>, Tranquada J.M.<sup>1</sup>, Gu G.<sup>1</sup>, Tsvelik A.M.<sup>1</sup>, Stone M.B.<sup>2</sup>*

<sup>1</sup> CMP&MS Department, Brookhaven National Laboratory, Upton, New York 11973, USA

<sup>2</sup> Oak Ridge National Laboratory, 1, Bethel Valley Road, Oak Ridge, Tennessee 37831, USA

Discoveries of copper and iron-based high-temperature superconductors (HTSC) have challenged our views of superconductivity and magnetism. Contrary to the pre-existing view that magnetism, which typically involves localized electrons, and superconductivity, which requires freely-propagating itinerant electrons, are mutually exclusive, antiferromagnetic phases were found in all HTSC parent materials. Moreover, highly energetic magnetic fluctuations, discovered in HTSC by inelastic neutron scattering (INS), are now widely believed to be vital for the superconductivity. In two competing scenarios, they either originate from local atomic spins, or are a property of cooperative spin-density-wave (SDW) behavior of conduction electrons. Both assume clear partition into localized electrons, giving rise to local spins, and itinerant ones, occupying well-defined, rigid conduction bands. Here we report an INS study of spin dynamics in iron telluride, a parent material of one of the iron-based HTSC families, which shows that this very assumption

fails, and that conduction and localized electrons are fundamentally entangled. In the temperature range relevant for the superconductivity we observe a remarkable redistribution of magnetism between the two groups of electrons. The effective spin per Fe at  $T \approx 10$  K, in the antiferromagnetic phase, corresponds to  $S \approx 1$ , consistent with the recent analyses that emphasize importance of Hund's intra-atomic exchange. However, it grows to  $S \approx 3/2$  in the disordered phase, a result that profoundly challenges the picture of rigid local and itinerant bands.

24TL-D-5

## MAGNETIC RESONANCE IN THE SPIN-LIQUID AND ORDERED PHASES OF $S=1/2$ ANTIFERROMAGNET $\text{Cs}_2\text{CuCl}_4$

*Smirnov A.I.<sup>1</sup>, Povarov K.Yu.<sup>1</sup>, Starykh O.A.<sup>2</sup>, Petrov S.V.<sup>1</sup>, Shapiro A.Ya.<sup>3</sup>*

<sup>1</sup> P. L. Kapitza Institute for Physical Problems, RAS, 119334 Moscow, Russia

<sup>2</sup> University of Utah, Salt Lake City, Utah 84112, USA

<sup>3</sup> A.V.Shubnikov Institute of Crystallography, RAS, 119333 Moscow, Russia

The spin system of  $\text{Cs}_2\text{CuCl}_4$  is formed by localized  $S=1/2$  spins coupled antiferromagnetically within 2D layers with distorted triangular lattice. This magnet remains in a quantum spin-liquid state at temperatures far below Curie-Weiss temperature 4 K and exhibits a transition with a spiral ordering only at  $T_N=0.6$  K. [1] We studied spin excitations in  $\text{Cs}_2\text{CuCl}_4$  by means of electron spin resonance (ESR) at temperatures down to 0.05 K in the range 9-140 GHz. An unexpected energy gap of 14 GHz and a splitting of ESR were found for the spin-liquid phase. We describe quantitatively both the shift and splitting of ESR for different orientations of the magnetic field, as well the pronounced influence of the polarization of microwaves, considering the spinon excitations in presence of a uniform Dzyaloshinskii-Moriya (DM) interaction. This DM interaction provides an effective magnetic field, the sign of which is opposite for the right- and left-moving spinons. This causes the shift and splitting of ESR. At cooling below  $T_N$  the above spinon-ESR survives deep in the ordered phase at frequencies above 50 GHz, while magnetic resonance spectrum is strongly modified at frequencies below 40 GHz. Thus, in the ordered phase we observe a crossover from the low-energy spectrum of a spiral AFM to the spinon-type spectrum of a quasi-1D spin liquid at higher energies. This novel phenomena are consequences of fractionalized spinon excitations of spin chains, which are effectively decoupled in  $\text{Cs}_2\text{CuCl}_4$  due to the frustration. The experiments demonstrate a novel probe of spinon excitations.

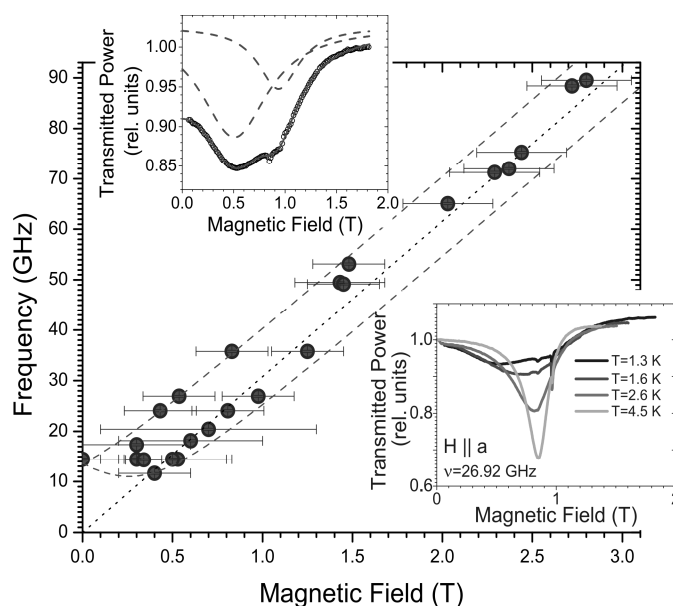


Fig. 1. Frequency-field dependence at  $T=1.3$  K and  $\mathbf{H}||\mathbf{a}$ . Dotted line is a paramagnetic resonance at  $T=10$  K, dashed lines present theory [2]. Upper insert: splitted line as a sum of two Lorentzians. Lower insert: temperature evolution of ESR line with cooling.

Other modes of spin excitations of the ordered phase at low fields may be well described by a macroscopic approach for a spiral magnet. Excitations observed in high field phases still remain unclassified.

[1] O. A. Starykh, H. Katsura, L. Balents, Phys. Rev. B 82, 014421 (2010).

[2] K.Yu. Povarov, A.I.Smirnov, O.A.Starykh, S.V.Petrov, and A.Ya.Shapiro, preprint arXiv:1101.5275v1[[str-el](#)]

24TL-D-6

## ORTHOGONAL SPIN ARRANGEMENT AS POSSIBLE GROUND STATE OF A THREE – DIMENSIONAL SHASTRY – SUTHERLAND NETWORK IN THE “PAPER-CHAIN” COMPOUND $\text{Ba}_3\text{Cu}_3\text{In}_4\text{O}_{12}$

*Volkova O.S.<sup>1</sup>, Maslova I.S.<sup>1</sup>, Klingeler R.<sup>2,3</sup>, Abdel-Hafiez M.<sup>3</sup>, Wolter A.U.B.<sup>3</sup>, Büchner B.<sup>3</sup>, Vasiliev A.N.<sup>1</sup>*

<sup>1</sup> Low Temperature Physics and Superconductivity Department, Moscow State University, Moscow 119991, Russia

<sup>2</sup> Kirchhoff Institute for Physics, University of Heidelberg, D-69120 Heidelberg, Germany

<sup>3</sup> Leibniz Institute for Solid State and Materials Research, IFW Dresden, D-01069 Dresden, Germany

The barium-copper indate  $\text{Ba}_3\text{Cu}_3\text{In}_4\text{O}_{12}$  stands for unique topology of the magnetic subsystem. It consists of rotated by  $90^\circ$  relative to each other “paper-chain” columns made of vertex-sharing  $\text{Cu}^{\text{I}}\text{O}_4$  and  $\text{Cu}^{\text{II}}\text{O}_4$  planar units. At high temperatures, the magnetic susceptibility in  $\text{Ba}_3\text{Cu}_3\text{In}_4\text{O}_{12}$  follows the Curie-Weiss law with positive Weiss temperature  $\Theta \sim 52$  K indicating the predominance of ferromagnetic coupling. With lowering temperature, it gives way to antiferromagnetic coupling which results in the formation of the magnetically ordered state at  $T_N = 12.7$  K. At low temperatures, the  $\text{Ba}_3\text{Cu}_3\text{In}_4\text{O}_{12}$  experiences non-trivial succession of field-induced transformations consisting of two distinct spin-flop-like transitions and two distinct spin-flip-like transitions reaching full saturation  $\sim 3 \mu_B/\text{f.u.}$  in modest magnetic fields  $\sim 5.2$  T. These observations can be explained self-consistently presuming three-dimensional orthogonal arrangement of the  $\text{Cu}^{2+}$  ( $S = 1/2$ ) magnetic moments forming three virtually independent antiferromagnetic sub-subsystems. In accordance with the “paper-chain” structural motif, the nearest-neighbor exchange interaction in  $\text{Ba}_3\text{Cu}_3\text{In}_4\text{O}_{12}$  is ferromagnetic due to  $\sim 90^\circ$   $\text{Cu}^{\text{I}} - \text{O} - \text{Cu}^{\text{II}}$  bond. This exchange is frustrated by antiferromagnetic next-nearest-neighbor intrachain exchange interaction via  $\text{Cu}^{\text{II}} - \text{O} - \text{O} - \text{Cu}^{\text{II}}$  pathways. The intrachain next-nearest-neighbor interaction is intrinsically frustrated itself due to the tetrahedral arrangement of  $\text{Cu}^{\text{II}}$  ions within the columns. Moreover, the interchain interaction in  $\text{Ba}_3\text{Cu}_3\text{In}_4\text{O}_{12}$  is heavily frustrated because the overall pattern of the copper ions is that of a three-dimensional generalized Shastry-Sutherland network. The formation of the orthogonal spin structure lifts all these multiple frustrations. In this arrangement, favored by magnetocrystalline anisotropy, pseudodipolar and Dzyaloshinskii-Moriya interactions, the quantum fluctuations provide the coupling between three mutually orthogonal magnetic subsystems resulting in an impressive “order by disorder” effect.

24OR-D-7

## MAGNETIC STRUCTURE OF QUASI-ONE-DIMENSIONAL FRUSTRATED ANTIFERROMAGNET $\text{LiCu}_2\text{O}_2$

*Buettgen N.<sup>1</sup>, Bush A.A.<sup>2</sup>, Gippius A.A.<sup>3</sup>, Kraetchmer W.<sup>1</sup>, Prozorova L.A.<sup>4</sup>, Svistov L.E.<sup>4</sup>*

<sup>1</sup> Center for Electronic Correlations and Magnetism EKM, Experimentalphysik V, Universitat Augsburg, D86135 Augsburg, Germany

<sup>2</sup> Moscow Institute of Radiotechnics, Electronics, and Automation, 119454 Moscow, Russia

<sup>3</sup> Moscow State University, Moscow, 119991 Russia

<sup>4</sup> P.L.Kapitza Institute for Physical Problems RAS, 119334 Moscow, Russia

We present results of NMR and ESR study of the frustrated  $S=1/2$  chain cuprate  $\text{LiCu}_2\text{O}_2$ . A kind of frustration in quasi-one-dimensional chain magnets is provided by competing interactions, when the intra-chain nearest neighbor exchange is ferromagnetic and the next-nearest neighbor exchange is antiferromagnetic. The measurements were made on the single crystal samples without twinning.

ESR spectra obtained, can be described in the frame of the planar spiral spin structure with strong uniaxial anisotropy of the “easy axes aligned along “a” direction of the crystal. This type of the anisotropy is unexpected for the  $\text{LiCu}_2\text{O}_2$  because the axis of the local symmetry for  $\text{Cu}^{2+}$  ions is aligned along c-direction. We present the data of NMR spectra obtained on nuclei of nonmagnetic ions of  $\text{Li}^+$  measured in a broad field and temperature range. The NMR spectra obtained can be well described in the frame of spiral magnetic structure with uniaxial anisotropy aligned along “a” direction. The NMR data shows that the magnetic ordering in  $\text{LiCu}_2\text{O}_2$  occurs in two stages. First, the component of spiral structure along “a”-direction is ordered and then the second component.

It was shown, that NMR spectra are sensitive to the direction of chirality vector of spiral structure. It was obtained experimentally the NMR spectra from both magnetic domains with opposite directions of chirality vector.

24OR-D-8

## LOW-ENERGY DYNAMICS OF SPIN-GAP MAGNETS STUDIED BY ELECTRON SPIN RESONANCE

*Glazkov V.N.<sup>1</sup>, Smirnov A.I.<sup>1</sup>, Zheludev A.<sup>2</sup>, Sichelschmidt J.<sup>3</sup>, Sales B.C.<sup>4</sup>, Yankova T.<sup>5</sup>*

<sup>1</sup> Kapitza Institute for Physical Problems RAS, 119334 Moscow, Russia

<sup>2</sup> Department of Solid State Physics, ETH Zurich, Switzerland

<sup>3</sup> Max Planck Institute for Chemical Physics of Solids, Dresden, Germany

<sup>4</sup> Oak Ridge National Laboratory, Oak Ridge, USA

<sup>5</sup> Department of Chemistry, M.V.Lomonosov Moscow State University, Moscow, Russia

Spin gap magnets are one of the current focus topics of magnetism. Due to the special geometry of exchange bonds (usually a dimer-based network) or quantum effects related to the reduced geometry of the spin subsystem these magnets remains in the disordered spin-liquid state down to lowest temperature. Stability of this unordered ground state is ensured by the energy gap separating singlet ground state from the triplet excitations. At certain critical field  $H_c$  a quantum phase transition into the field-induced antiferromagnetically ordered state occurs. This phase transition is widely discussed in connection with the popular model of Bose-Einstein condensation (BEC) [1]. Electron spin resonance technique allows to probe low energy dynamics of a magnet at the energies

as small as 0.05 meV (corresponding to microwave frequency of 10 GHz), which is hardly accessible by other methods.

We present here results of the study of one-dimensional magnet NTENP [2], and two-dimensional magnet PHCC

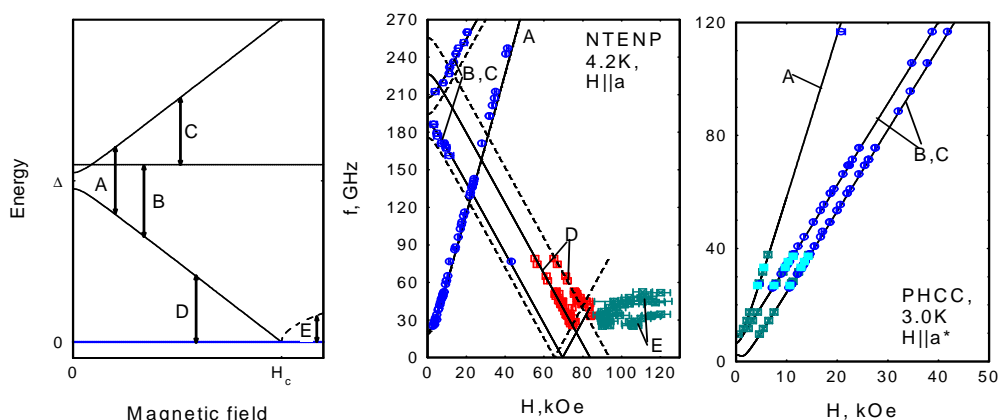


Fig. 1 Left panel: Scheme of the spin-gap magnet energy levels field dependence and possible resonance transitions. Middle and right panels: Frequency-field diagrams for NTENP and PHCC. Symbols – experiment, lines – model calculations.

(Figure 1). We observe experimentally different sorts of resonance modes, which can be identified by characteristic frequency-field and temperature dependences: thermally activated transitions between triplet sublevels (A,B,C), direct overgap transitions (D) and antiferromagnetic resonance above  $H_c$  (E). Observation of these transitions, analysis of their frequency-field and temperature dependences provides precise details on the zero-field splitting of the triplet sublevels, gap dependence close to the critical field and gap reopening in high-field phase.

Authors acknowledge support from Russian Foundation for Basic Research and Russian Presidential Grant for Support of Scientific Schools.

[1] T.Giamarchi, C. Rugg and O.Tchernyshyov, Nature Physics **4** (2008) 198

[2] V.N.Glazkov, A.I.Smirnov, A.Zheludev, B.C.Sales, Phys.Rev.B **82** (2010) 184406

**24 August**

Wednesday

11:30-13:00

14:30-17:20

oral session

24TL-E

24RP-E

24OR-E

**“Magnetic Soft Matter”**

24TL-E-1

## NONLINEAR ABSORPTION OF SURFACTED FERROFLUID INVESTIGATED WITH THE Z-SCAN TECHNIQUE

*Espinosa D.<sup>1</sup>, Soga D.<sup>1</sup>, Alves S.<sup>2</sup>, Figueiredo Neto A.M.<sup>1</sup>*

<sup>1</sup> Instituto de Física, Universidade de São Paulo, cp: 66318, 05314-970, São Paulo, SP, Brazil

<sup>2</sup> Instituto de Ciências Ambientais, Químicas e Farmacêuticas, Universidade Federal de São Paulo, Diadema, SP, Brazil

Ferrofluids are potential candidates to present remarkable nonlinear optical properties due to the nanometric dimension of the magnetic particles (typical diameter  $D$ ). Parameters like  $\chi(3)$ , the third-order optical susceptibility, was shown to depend inversely  $D$  [1]. One of the parameters used to calculate  $\chi(3)$  of a material is the nonlinear absorption coefficient  $\beta$ . The absorption coefficient of a material is written as:  $\alpha(I) = \alpha_0 + \beta I$  (eq. 1), where  $\alpha_0$  and  $I$  are the linear absorption coefficient and the irradiance. The Z-Scan (ZS) technique [2, 3] was employed to measure  $\beta$  in different timescale regimes, from the thermal (ms) to the electronic one (fs). In this technique, a lens focuses a pulsed laser beam, and the ferrofluid thin sample is scanned along the beam direction, passing through the focus point. All the transmitted light is recovered with another lens and detected by a photodetector as a function of the sample position  $z$ . In the case of the thermal regime a chopped CW laser was used. In the electronic regime experiments, the laser is itself pulsed. The wavelength employed in all the experiments was  $\lambda = 532$  nm. The ferrofluid used is made by magnetite nanograins, typical diameter of about 10 nm, coated with oleic acid and dispersed in mineral oil. The concentration of magnetic material in the samples and  $\alpha_0$  were 0.36 vol% and  $40.1 \text{ cm}^{-1}$ , except in the case of the ms experiments where these values were 0.036 vol% and  $4.01 \text{ cm}^{-1}$ . Table 1 shows the values of the pulse width  $\tau$  (FWHM), frequency of the pulses  $f$ , pulse energy  $E_p$  and nonlinear absorption coefficient  $\beta$ .

Table1: Experimental parameters (see text for definitions) and nonlinear absorption  $\beta$ .

$\tau$	$f$	$\beta(\text{cm} / \text{GW})$	$E_p(\text{nJ})$
15 ms	30 Hz	$5.2 \times 10^9$	21600
100 ps	20 Hz	$5.2 \times 10^1$	3300
280 fs	10 kHz	$2.2 \times 10^3$	0.091
280 fs	3 kHz	$5.0 \times 10^2$	0.091
120 fs	1 kHz	8.4	18

The values of  $\beta$  were obtained with the theoretical fitting of the experimental data according to ref. [3]. In the femtosecond timescale with  $f = 1$  kHz, the nonlinear absorption effect (NLA) is expected to be caused by the two photons absorption (TPA) process. However, for higher frequencies and in the picosecond timescale, the increasing values of  $\beta$  indicate that TPA is not the

only physical process responsible for the NLA. Free-carrier absorption (FCA) process may also occur and  $\beta$  doesn't have anymore the physical meaning of the TPA coefficient. In this case, eq. 1 may be replaced by  $\alpha(I) = \alpha_0 + \beta I + \sigma N(I)$  (eq. 2), where  $\sigma$  is the FCA cross section and  $N$  is the density of excited carriers [4]. In the millisecond time-scale, the nonlinear effect is expected to be only due to FCA, and eq. 2 may be replaced by  $\alpha(I) = \alpha_0 + \sigma N(I)$  (eq. 3).

Support by FAPESP, CNPq, CAPES and INCT on Complex Fluids is acknowledged.

[1] D. Soga, S. Alves, A. Campos, F.A. Tourinho, J. Depeyrot, and A.M. Figueiredo Neto, *J. Opt. Soc. Am. B*, **24** (2007) 49.

[2] M. Sheik-bahae, A. A. Said and E. W. Van Stryland, *Opt. Lett.*, **14** (1989) 955.

[3] M. Sheik-bahae *et al*, *IEEE J. Quantum Electron.*, **26** (1990) 760.

[4] E. W. Van Stryland *et al*, *Prog. Crystal Growth and Charact.*, **27** (1993) 279.



## GLASSY DYNAMICS OF MAGNETIC NANOPARTICLES IN A SUPERCOOLED LIQUID

*Dubois E.<sup>1</sup>, Chushkin Y.<sup>2</sup>, Robert A.<sup>3</sup>, Perzynski R.<sup>1</sup>*

<sup>1</sup> Université Pierre et Marie Curie, PECSA UMR7195, 4 Place Jussieu, 75005 Paris, France

<sup>2</sup> European Synchrotron Radiation Facility - 6 rue J. Horowitz BP 220, 38043

Grenoble Cedex 9 France

<sup>3</sup> SLAC National Accelerator Laboratory, Linac Coherent Light Source, 2575 Sand Hill Rd, Menlo Park CA 94025 - USA

Magnetic Fluids present a glassy transition at large concentration and strong interparticle repulsion. This has been observed at room temperature with electrostatically stabilized  $\gamma\text{-Fe}_2\text{O}_3$  nanoparticles dispersed in water at pH=7 and moderate ionic strength ( $\sim 3 \cdot 10^{-2}$  M) where the freezing of both the translational and rotational degrees of freedom of the nanoparticles have been probed [1, 2]. X-ray Photon Correlation Spectroscopy (XPCS) measurements performed at ID10C beamline of ESRF – Grenoble have shown dynamic heterogeneities, which become anisotropic under-field [3,4]. Here we are concerned with the two following questions : - What happens when the solvent itself undergoes a glassy transition? - How this glass transition interferes with that of the colloidal dispersion at large volume fraction of nanoparticles?

We thus present XPCS experiments performed as a function of T with Magnetic Fluids based on  $\gamma\text{-Fe}_2\text{O}_3$  nanoparticles (10 nm in diameter) stabilized with a commercial surfactant in Dibutylphtalate, a solvent undergoing a glassy transition at 182 K. In the experiment the volume fraction  $\Phi$  of nanoparticles varies between 1% and 15%, and the interparticle interaction is repulsive on average at room temperature.

At low volume fraction ( $\Phi = 1\%$ ), the interparticle interaction is negligible and we probe the freezing dynamics of the solvent passing from the hydrodynamic limit at high temperatures to a heterogeneous dynamics at lower temperatures. The inverse characteristic time  $\Gamma$  of the correlation functions scales as  $Q^\alpha$  with  $\alpha \sim 2$  at 202.5 K, signature of nanoparticle diffusion, and with  $\alpha \sim 1$  at 196 K where experimental observations support the existence of cooperative processes, probed here at the spatial scale of the dynamical heterogeneities.

At  $\Phi = 3\%$ , the interparticle interactions begin to enter in play shifting to a higher temperature than 196K the low temperature limit of the hydrodynamic regime.

Under an applied field H, the situation is more complicated and largely depends on  $\Phi$  and T. For example at  $\Phi = 1\%$ , H= 1200 Oe and T= 202.5 K, the relaxations are isotropic. Under field at lower temperatures the experiment is limited by a phase separation in two coexisting phases of different concentrations. Indeed decreasing temperature transforms the interparticle interaction from repulsive (on average) at high T to attractive (on average) at low T. This phase separation depends on  $\Phi$ , T and on the applied field H.

[1] A. Robert, E. Wandersman, E. Dubois, V. Dupuis, R. Perzynski, EuroPhysics Lett., 75 (2006) 764.

[2] E. Wandersman, V. Dupuis, E. Dubois, R. Perzynski, Phys. Rev. E 80 (2009) 041504.

[3] E. Wandersman, A. Duri, A. Robert, E. Dubois, V. Dupuis, R. Perzynski, J. of Physics: Condensed Matter 20 (2008) 155104.

[4] E. Wandersman, Y. Chushkin, E. Dubois, V. Dupuis, G. Demouchy, A. Robert, R. Perzynski Braz. J. Physics 39 (2009) 210

24OR-E-3

## LOCAL STRUCTURE OF SPINEL-TYPE NANOCRYSTALS OF FERROFLUIDS: NON EQUILIBRIUM CATION DISTRIBUTIONS

Depeyrot J.<sup>1</sup>, Gomes J.A.<sup>1</sup>, Martins F.H.<sup>1</sup>, Paula F.L.O.<sup>1</sup>, Tourinho F.A.<sup>2</sup>, Aquino R.<sup>3</sup>, Mestnik Filho J.<sup>4</sup>, Perzynski R.<sup>5</sup>

<sup>1</sup> Complex Fluids Group, Instituto de Física, Universidade de Brasília, Brazil.

<sup>2</sup> Complex Fluids Group, Instituto de Química, Universidade de Brasília, Brazil.

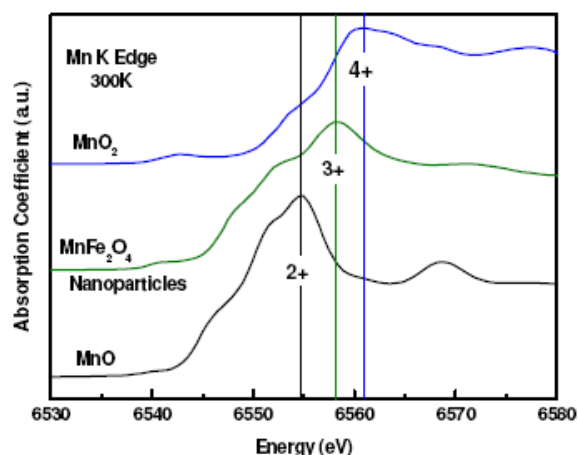
<sup>3</sup> Complex Fluids Group, Faculdade UnB Planaltina, Universidade de Brasília, Brazil.

<sup>4</sup> Instituto de Pesquisas Energéticas e Nucleares, São Paulo, Brazil.

<sup>5</sup> Laboratoire PECSA, Université Pierre et Marie Curie, Paris, France.

Magnetic nanocolloids constitute a very attractive and promising class of nanomaterials as they may be confined, displaced, deformed and controlled by an external magnetic field. These unique and striking features make them suited for a quite large number of applications, from engineering to biomedical. We are currently working on the synthesis of magnetic nanoparticles based on composites of metal oxides (ferrites) and on their dispersion in acidic and neutral media or in more complex systems like clays or liquid crystals. A core-shell strategy has been developed to protect the stoichiometric ferrite nanocore by a maghemite shell [1]. In this work, we explore the local structure of magnetic nanocrystals based on Zn-, Cu- and Mn-ferrite core. Measurements of neutron

diffraction realized at Laboratoire Léon Brillouin (LLB-Saclay/France), of X-ray absorption spectroscopy (XAS) and X-ray Diffraction performed at the Brazilian Synchrotron Light Laboratory (LNLS) are undertaken to investigate the cations distribution, their valence state and coordination. The combined analysis suggest in all samples, a non equilibrium cation distribution among interstitial sites of the spinel-type nanocrystals structure. As an example, this cation inversion is responsible for the observed enhancement of the magnetic response of Zn-ferrite nanoparticles [2]. In Mn-ferrite nanoparticles, Rietveld refinement of neutron diffraction patterns shows that more than 50 % of Mn ions are located at octahedral sites. Moreover, the oxidation state of the manganese ions is 3+, a result different from bulk ferrite. Then, the presence of a shoulder before the main absorption peak may be attributed to Mn<sup>3+</sup> ions in octahedral environment and the expected Jahn-Teller distortions.



XANES spectra and valence state of Mn ions.

diffraction patterns shows that more than 50 % of Mn ions are located at octahedral sites. Moreover, the oxidation state of the manganese ions is 3+, a result different from bulk ferrite. Then, the presence of a shoulder before the main absorption peak may be attributed to Mn<sup>3+</sup> ions in octahedral environment and the expected Jahn-Teller distortions.

We acknowledge the Brazilian agencies CNPq, CAPES and FAP/DF.

[1] J. A. Gomes, M. H. Sousa, F. A. Tourinho, R. Aquino, G. J. da Silva, J. Depeyrot, E. Dubois, R. Perzynski, *J. Phys. Chem C* 112, 6220 (2008).

[2] J. A. Gomes, G. M. Azevedo, J. Depeyrot, J. Mestnik-Filho, G. J. da Silva, F. A. Tourinho, R. Perzynski, *J. Magn. Mater.* 323, 1203 (2011).

24RP-E-4

## STRUCTURE OF AGGREGATES IN WATER-BASED FERROFLUIDS

*Avdeev M.V.<sup>1,2</sup>, Aksenov V.L.<sup>1,2</sup>, Vekas L.<sup>3</sup>*

<sup>1</sup> Frank Laboratory of Neutron Physics, Joint Institute for Nuclear Research,  
Joliot-Curie str. 6, 141980 Dubna Moscow Reg., Russia

<sup>2</sup> National Research Centre "Kurchatov Institute", Akademika Kurchatova pl. 1, 123182 Moscow,  
Russia

<sup>3</sup> Laboratory of Magnetic Fluids, Center for Fundamental and Advanced Technical Research,  
Romanian Academy/Timisoara Branch, Mihai Viteazul str. 24, 300223 Timisoara, Romania

Colloidal stability of water-based ferrofluids for technical and biomedical applications is of great practical importance. The appearance of aggregates stimulated by magnetic interaction reduces the efficiency of these systems in most cases. Thus, the knowledge of aggregation regimes in ferrofluids is a key point for their development.

The present work summarizes the structural data for aggregates observed in various types of water-based ferrofluids by scattering methods (light, X-ray/synchrotron radiation, neutrons). Different aggregate classes depending on the stabilization mechanism (steric/electrostatic stabilization) of magnetic particles (magnetite) are distinguished. It is shown that aggregates in water-based ferrofluids form both at the preparation stage and then in final solutions showing often multilevel structural organization. In the general case this organization is strongly affected by the thermodynamic parameters (temperature, concentration, external magnetic field). The problems in the complementary use of different methods for characterizing the inner atomic and magnetic structures of aggregates in ferrofluids are discussed.

24TL-E-5

## DOXORRUBICIN LOADED MAGNETIC POLYMERSOMES: A MULTIFUNCTIONAL NANOCARRIER FOR THERANOSTIC

*Sanson C.<sup>1</sup>, Thévenot J.<sup>1</sup>, De Oliveira H.<sup>1</sup>, Ibarboure E.<sup>1</sup>, Brûlet A.<sup>2</sup>, Miraux S.<sup>3</sup>, Thiaudière E.<sup>3</sup>,  
Tan S.<sup>4</sup>, Brisson A.<sup>4</sup>, Lecommandoux S.<sup>1</sup>, Sandre O.<sup>1</sup>*

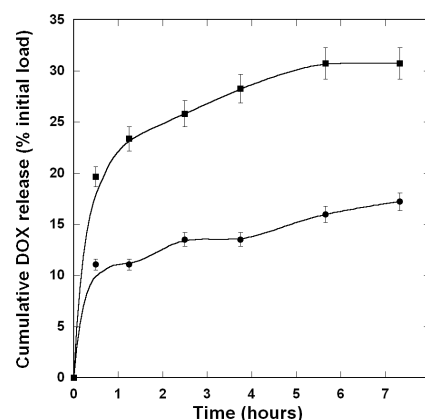
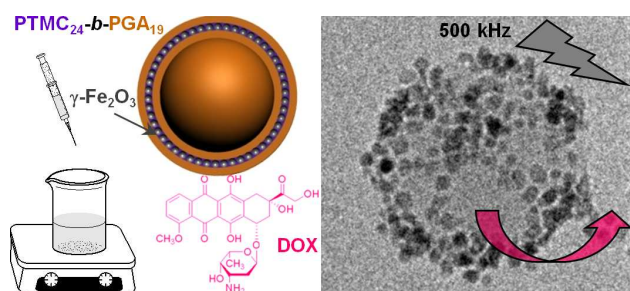
<sup>1</sup> Université de Bordeaux, LCPO, ENSCBP 16 avenue Pey Berland, 33607 Pessac Cedex, France

<sup>2</sup> CEA Saclay, LLB, 91191 Gif sur Yvette, France

<sup>3</sup> Université de Bordeaux, RMSB, 146 rue Léo Saignat, 33676 Bordeaux, France

<sup>4</sup> Université de Bordeaux, CBMN, IECB, 33402 Talence Cedex, France

Hydrophobically modified maghemite nanoparticles can be embedded within the rubbery membrane of poly(butadiène)-b-poly(L-glutamic acid) polymersomes leading to soft magnetic vesicles that can be deformed by a static magnetic field.[1-3] We adapted the method for a semi-crystalline copolymer such as poly(trimethylene carbonate)-b-poly(L-glutamic acid) with a fusion temperature in the range 35-40°C.[4] The nanoprecipitation process forms highly magnetic vesicles (ratio of  $\gamma$ -Fe<sub>2</sub>O<sub>3</sub> to copolymer up to 70 wt %) together with a good control over the vesicles' size in the range 100-400 nm depending on conditions. Nanoprecipitation enables also the simultaneous loading of  $\gamma$ -Fe<sub>2</sub>O<sub>3</sub> nanoparticles (up to 50 wt %) and of an anticancer drug, doxorubicin (up to 12 wt %). Like in our previous systems,[1-3] the deformation of the vesicles' membrane under an applied magnetic field has been evidenced by small angle neutron scattering. These dual-loaded



vesicles display enhanced contrast properties in Magnetic Resonance Imaging and can be guided in a magnetic field gradient. The feasibility of controlled drug release by radio-frequency magnetic hyperthermia was evidenced in the case of encapsulated doxorubicin, showing a proof of concept of “magneto-chemotherapy”. These magnetic polymersomes can thus be used as efficient multifunctional nano-carriers for combined therapy and imaging.

Cryo-TEM image and sketch of the preparation of dually-loaded vesicles by addition of an aqueous buffer into a mixture of PTMC-*b*-PGA copolymer, hydrophobically coated magnetic iron oxide nanoparticles and doxorubicin drug. The excitation by a radiofrequency magnetic field (500 kHz, 2.6 mTesla) accelerates the DOX release by a factor around two.

Financial support was provided by the European Commission through the Seventh Framework Program (FP7) for Research & Development (CP-IP 213631-2 NANOTHER).

- [1] S. Lecommandoux, O. Sandre, F. Chécot, J. Rodriguez-Hernandez, R. Perzynski, *Adv. Mat.*, 17 (2005) 712.  
 [2] S. Lecommandoux, O. Sandre, F. Chécot, J. Rodriguez-Hernandez, R. Perzynski, *J. Magn. Magn. Mater.*, 300 (2006) 71  
 [3] S. Lecommandoux, O. Sandre, F. Chécot, R. Perzynski, *Prog. Sol. St. Chem.*, 34 (2006) 171.  
 [4] C. Sanson, O. Diou, J. Thévenot, E. Ibarboure, A. Soum, A. Brûlet, S. Miraux, E. Thiaudière, S. Tan, A. Brisson, V. Dupuis, O. Sandre, and S. Lecommandoux, *ACS Nano* 5 (2011), 1122.

24TL-E-6

## MAGNETIC HYPERTHERMIA WITH HIGH-COERCIVITY NANOPARTICLES

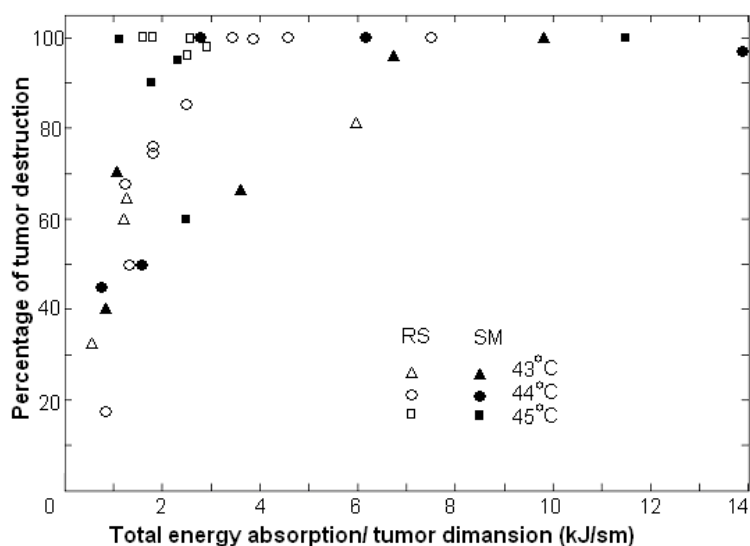
*Kashevsky B.<sup>1</sup>, Istomin Yu.<sup>2</sup>, Kashevsky S.<sup>1</sup>, Ulaschik S.<sup>3</sup>, Prokhorov I.<sup>1</sup>*

<sup>1</sup> V.A. Luikov Heat and Mass Transfer Institute, Belarus Academy of Sciences, P. Brovka str. 15, Minsk, 220072, Belarus

<sup>2</sup> N.N. Alexandrov National Cancer Center of Belarus, Lesnoy-2, Minsk, 223040, Belarus

<sup>3</sup> Institute of Physiology, Belarus Academy of Sciences, Akademicheskaiy str. 28, Minsk, 220072, Belarus

The key problem which predetermines the technical implementation of local magnetic hyperthermia is posed by the choice of magnetic particles. Presently, attention is given mainly to ultrasmall (~10 nm) superparamagnetic particles and relatively weak alternating magnetic fields of high (sub-megahertz) frequencies. As an alternative we consider bigger particles with magnetic



recognized restrictions on the field parameters and the particle characteristics, we analyze conditions of practical low-frequency magnetic hyperthermia, describe producing and relevant properties of suitable high-coercive nanoparticles, present computerized equipment for low-frequency hyperthermia on small animals, and illustrate this method with the results of controlled treatment of model tumors on rats. The developed experimental setup generates the field with amplitude of up to 900 Oe and the frequency of 3.70 kHz. Its feedback system provides strict control of the temperature elevation at the site of a thermocouple (TC) which we place into healthy tissue, right under a heated tumor. Another TC is placed at the tumor center. During treatment, the system automatically stores the two temperatures and the energy absorption rate. 36 tumors of two types have been treated with different temperatures and heating durations (43°C, 30 min, 44°C, 20 min and 45°C, 15 min). The tumors were of different shape, with volumes between 1.2 and 3.6 ml. The amount of particles syringed into each tumor was predetermined from the developed model of heating, with the average content equal to 120 mg per 1ml of tumor. The effect of tumor destruction was estimated in 24 hours after the session using a vital staining. The figure presents the percentage of tumors destruction vs a treatment parameter representing the ratio of the total absorbed energy to the characteristic tumor radius.

The presented results indicate prospects of using high-coercivity nanoparticles for local magnetic hyperthermia.

24RP-E-7

## POWER LOSSES IN A SUSPENSION OF MAGNETIC DIPOLES UNDER A ROTATING FIELD

*Raikher Yu.L., Stepanov V.I.*

Institute of Continuous Media Mechanics, Ural Branch, Russian Academy of Sciences, Perm, 614013, Russia

Energy absorption due to viscous friction in a dilute suspension of single-domain ferromagnetic particles subjected to a rotating field is considered. The problem is treated in the framework of kinetic approach. The behavior of specific loss power (SLP) as a function of the field amplitude  $H$  and frequency  $\omega$  is studied. The cases of a rotating field and linearly polarized AC field are compared, and the essential differences are revealed. The results obtained enable one to assess the

allowable or optimal field parameters for a given magnetic suspension intended for rotational magneto-inductive heating on the basis of the following simple rules [1]:

- (i) under fixed frequency of rotation the absorbed power grows quadratically with the field amplitude and attains a virtually maximal value at  $H_* \propto 6\omega\eta V_h / M_s V_m$ ; any further increase of  $H$  is inefficient;
- (ii) under fixed amplitude of the field the absorbed power grows quadratically with the field frequency and attains a virtually maximal value at  $\omega_* \propto M_s H V_m / 6\eta V_h$ ; any further increase of  $\omega$  is inefficient.

Here  $V_h$  is the hydrodynamic particle volume,  $V_m$  the volume of magnetic-domain kernel  $M_s$  the magnetization of the particle material.  $\eta$  the viscosity of the carrier liquid.

To transform these estimates in dimensional form, we assume  $V_h \sim 10V_m$ ,  $M_s \approx 400$  (ferrite) and  $\eta \propto 10^{-2}$  Ps (water). Then for the rotation frequency of the field  $\omega/2\pi = 10$  kHz one has  $H_* \sim 90$  Oe. Under the above-adopted number values, the parameter  $\omega H / 2\pi$  is about  $10^6$  Oe/s, which falls well within the Brezovich's restriction rule that establishes the physiological tolerance of hyperthermia.

Comparison of the two types of the field viz. rotating and linearly polarized (AC), leads to the following conclusions. In the linear magnetization regime, the rotating field technique has an advantage in doubling of the SLP [2] because, unlike that of the AC field, the strength of the rotating field is always maximum. This advantage is lost in the nonlinear (high-field) regime due to fundamental difference between the asymptotic field dependencies of SLP since the latter saturates with the field amplitude in the rotation case but grows linearly in the AC one.

In general, the obtained parametric dependencies establish a universal conclusion with respect to heat generation induced by a suspension of non-interacting rigid dipoles: in any field configuration, SLP at given frequency is the higher the greater is the ratio  $V/T$ ; at a constant temperature this means the use of larger particles. In other words, for this class of suspensions the upper limit for the particle size (and thus, SLP) is imposed, if any, not from physical but from some other (e.g. physiological) considerations.

Partial financial support from RFBR projects 10-02-96022 and 09-02-91070 is gratefully acknowledged.

[1] Yu.L. Raikher, V.I. Stepanov, *Phys. Rev. E* **83** (2011) 021401.

[2] V.A. Sharapova, M.A. Uymin, A.A. Mysik, A.E. Yermakov, *Phys. Met. Metallogr.* **110** (2010) 5.

24OR-E-8

## MAGNETOCALORIC EFFECT AND HEAT CAPACITY OF MAGNETIC FLUIDS

*Korolev V., Korolev D., Ramazanova A., Yshkova V.*  
Institute of solution Chemistry of RAS, Ivanovo, 153045, Russia

Magnetocaloric effect (MCE) investigation is of great interest because it can provide the information on magnetic phase transitions in magnetic materials as the largest MCE values are observed in the region of phase transitions. Experimental study of MCE jointly with heat capacity

of magnetic material lets obtain more additional information on the nature of magnetic ordered state as well as on interaction of magnetic and thermal characteristics.

In the work presented the magnetocaloric properties (MCE and heat capacity) of magnetic fluids based on alkaren 11 and D24 and polyethylsiloxanes (PES) were studied by microcalorimetric method over temperature range of 278-343 K.

It has been found experimentally that for nano-sized stabilized magnetite in magnetic fluids the MCE value by one order higher as compared with the value in aqueous suspensions where magnetite is micro-sized. It was established for the first time that nano-sized magnetite in magnetic fluids on the base of PES within temperature interval of 336-340 K has magnetic phase transition "order-order" type whereas non-stabilized superfine magnetite passes into antiferromagnetic hematite under oxidation [1]. In magnetic liquids based on alkaren 11 and D24, in contrast to the ones on the base of polyethylsiloxanes, for temperature dependences of MCE and heat capacity there is no anomalous behavior. In concentrated magnetic fluids with high magnetization abrupt increasing of MCE in low magnetic fields is observed.

The specific heat capacity in zero field is a third higher for nanomagnetite in magnetic fluids as compared with micro-magnetite. Magnets specific heat capacity depends strongly on magnetic field magnitude. For all magnetic particles studied in the work the extreme dependence of specific heat capacity on magnetic field value with a maximum at  $0.3\div 0.4$  T was revealed. The decreasing of the heat capacity at  $B > 0.4$  T could be explained by decreasing of heat capacity magnetic constituent as the result of magnetic ordering of the system. For temperature dependences of specific heat capacity in the region of phase transitions there are maxima and minima. Moreover it was observed that the heat capacity weak depended on magnetic field at temperatures near the phase transitions ones [2].

This research has been carried out within the financial support of Grant of RFBR № 08-03-00532a.

[1] Korolev V.V., Arefyev I.M., Ramazanov A.G. The magnetocaloric effect of superfine magnets // *Journal of Thermal Analysis and Calorimetry*. – 2008. – V. 92. – N 3. – P. 691-695.

[2] Korolev V.V., Arefyev I.M., Blinov A.V. Heat capacity of superfine oxides of iron under applied magnetic fields // *Journal of Thermal Analysis and Calorimetry*. – 2008. – V. 92. – N 3. – P. 697-700.

24RP-E-9

## **MAGNETIC FLUIDS WITH ORGANIC CARRIERS: INFLUENCE OF COMPOSITION ON COLLOIDAL STABILITY, MAGNETIC AND FLOW BEHAVIOR**

*Susan-Resiga D.<sup>1</sup>, Socoliuc V.<sup>1</sup>, Marinica O.<sup>2</sup>, Avdeev M.V.<sup>3</sup>, Vékás L.<sup>1</sup>*

<sup>1</sup> Romanian Academy-Timisoara Branch, CFATR, Lab. MF, Timisoara, Romania

<sup>2</sup> Politehnica University Timisoara, NCESCF, Timisoara, Romania

<sup>3</sup> Joint Institute for Nuclear Research, FLNP, Dubna, Russia

The macroscopic behavior of magnetic fluids and their compatibility with various media and exploitation conditions of devices with magnetic fluids are determined by composition and structural characteristics. Many of the applications, e.g., rotating seals, bearings, dampers or sensors, require magnetic fluids with high magnetization and at the same time, with long-term colloidal stability. These requirements are difficult to fulfill simultaneously and implies severe

conditions on the MNP synthesis/stabilization/ dispersion procedures applied during the preparation of magnetic nanofluids.

In this paper the particle surface coating and volume fraction, as well as the size distribution and magnetic moment density of dispersed particles will be considered in correlation with colloidal stability, magnetic and flow properties of magnetizable fluids. Based on previous small angle neutron scattering results concerning the efficiency of various chain length (C12-C18) carboxylic acids in sterical stabilization of magnetite nanoparticles in a non-polar organic carrier [1], we present a study on the colloidal stability of a series of mineral oil based magnetic nanofluids with particle solid (physical) volume fraction ranging from 1 % to 21 % by means of rheological, magnetization, TEM, dynamic and static light scattering experiments. The dependence of the dynamic viscosity on solid volume fraction it was found to fit well with the Krieger-Dougherty formula. From the fit the thickness of the effective surfactant (oleic acid) layer was estimated at 1.4 nm, in very good agreement with the value found from previous SANS investigations. A major change of flow behavior and magnetic properties is achieved by dispersing micron sized Fe particles in a high concentration magnetite nanofluid, with saturation magnetization in the range of 80-100 kA/m [2]. The resulting extremely bidisperse magnetizable fluid samples show strongly non-Newtonian flow properties and up to 103 times increase of effective viscosity. The magnetization curves  $M=M(H)$  of the nano-micro structured magnetizable fluid samples show a Fröhlich-Kennelly type dependence and their saturation magnetization attains 900 kA/m. A comparison is presented with similar properties of conventional MR fluids.

Support by the European project FP7 No. 229335 MAGPRO<sup>2</sup>LIFE and the Romanian project 83EU/2010 is acknowledged. Thanks are due to ROSEAL Co. (Odorhei, Romania) for magnetic fluid samples.

[1] M.V. Avdeev, D. Bica, L. Vékás, V. L. Aksenov, A.V. Feoktystov, O. Marinica, L. Rosta, V.M. Garamus, R. Willumeit, J. Colloid&Interface Sci., 334 (2009)37-41

[2] Daniela Susan-Resiga, Doina Bica, L.Vekas, J. Magn. Magn. Mater., 322 (2010)3166-3172

24RP-E-10

## COULOMETRY AND VOLTAMMETRY OF ULTRASMALL COLLOIDS: INTRODUCTION TO A NEW FIELD

*Tourinho F.A.<sup>1</sup>, Marinho E.P.<sup>1</sup>, Filomeno C.L.<sup>1</sup>, Depeyrot J.<sup>2</sup>*

<sup>1</sup> Complex Fluids Group - Instituto de Química - Universidade de Brasília - DF - Brazil

<sup>2</sup> Complex Fluids Group - Instituto de Física - Universidade de Brasília - DF - Brazil

The characterization of aqueous colloidal dispersions based on spinel ferrite nanoparticles by ordinary spectroscopy methods UV-VIS-IR is usually difficult because of the high optical absorption coefficient of these materials. On the other hand, a set of electrochemical techniques can be used, such as potentiometry and conductometry, which have recently proved to be a powerful tool to measure the surface charge density and for the study of the pH-dependent phase diagram [1]. In this work we investigated a new electrochemical field based on the electrolysis of ultrasmall colloids at the interface electrode/dispersion under conditions of complete polarization. A square wave voltammetry (SWV) of a collection of non-interacting magnetic nanoparticles based on maghemite and cobalt ferrite revealed voltammetric diffusion-controlled currents that differ from those obtained with true solutions (free ions). The Nernst potential corresponding to the peak



intensity is attributed to the reduction of iron ions of the nanostructure from Fe(III) to Fe(II). This peak is shifted about 1 V in the direction of cathodic potential when compared to the free ions case indicating that the reduction process is easier for the later. Then, we realize a controlled-cathode-potential electrolysis (potentiostatic coulometry) of the same samples. In this case, the integrated current leads to the concentration of iron ions involved in the reduction process by using the Faradays law. For maghemite nanoparticles, the results indicate that only two thirds of the iron atoms, present in the octahedral sites of the nanocrystal structure, were reduced. Then, oxygen vacancies have to be considered to achieve the electroneutrality. For cobalt ferrite based nanoparticles, the results show that all iron atoms of the cobalt ferrite core are reduced. These results well matches the core-shell characteristics of the synthesized nanoparticles [2].

The authors thank the Brazilian agencies CNPq, CAPES and FAPDF.

[1] A. F. C. Campos, E. P. Marinho, M. A. Ferreira, F. A. Tourinho, F. L. O. Paula; J. Depeyrot, Braz. J. Phys. 39, 230 (2009).

[2] J. A. Gomes, M. H. Sousa, F. A. Tourinho, R. Aquino, G. J. Silva, J. Depeyrot, E. Dubois, R. Perzynski, J. Phys. Chem. C 112, 6220 (2008)

24RP-E-11

## FREE ENERGY OF MAGNETIC FLUIDS UNDER EXTERNAL MAGNETIC FIELD. BIDISPERSE MODEL

*Elfimova E., Kuznetsov A., Mendeleev V.*

Urals State University, Lenin av. 51 Ekaterinburg 620000, Russia

The simplest theoretical model of a magnetic fluid is a system of monodisperse dipolar hard spheres. The magnetostatic, thermodynamic and structure properties of magnetic fluids were predicted on the basis of this model (for example [1, 2]). In spite of good agreement between theory and computer simulation data the quantitative differences between theory and physical experiments exist. First of all it is connected with polydispersity of the real magnetic fluids. In the present work the polydispersity of the magnetic fluids is considered within the framework of bidisperse approximation. The Helmholtz free energy of the magnetic fluids under external magnetic field is studied theoretically.

The magnetic fluid is modeled as a system of homogeneously magnetized bidisperse hard spheres. Interactions between ferroparticles are presented by the sum of the hard sphere repulsion potential and the dipole-dipole potential. Under applied uniform magnetic field the particle magnetic moments are additionally interacted with an external field. The Helmholtz free energy is obtained on the basis of virial expansion over the ferroparticle concentration. It is convenient to use diagram representation for each virial coefficient (Fig. 1). The  $p$ -particle diagram corresponds to  $p^{\text{th}}$  virial coefficient; the diagram vertices are the ferroparticles, the bonds between  $i$  and  $j$  vertices conform to the Mayer functions:

$$f(ij) = \exp(-\beta U_s(ij) - \beta U_d(ij)),$$

where  $\beta = 1/kT$ ,  $kT$  is the thermal energy,  $U_s(ij)$  is hard sphere potential,  $U_d(ij)$  is dipole-dipole pair potential. In the bidisperse

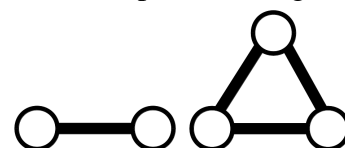


Fig.1 Diagrams correspond to the second and third virial coefficients in expansion of free energy over ferroparticle concentration.

system, when all particles are divided into small and large ones, each  $p$ -particle diagram is replaced by the sum of  $p$ -particle diagrams of following classes with proper combinatorial factors: the diagram with only large particles, the diagram with only small particles and the diagrams with large and small particles. For each diagram we suggest Mayer function expansion in power series over the intensity of dipole-dipole interaction. So, to calculate the  $p^{\text{th}}$  dipolar hard spheres virial coefficient the corresponding  $p$ -particle diagrams must be averaged (integrated) over the orientations of all magnetic moments and position of all particles. This method is described in details in Ref. [3] for monodisperse ferroparticle system. In the present work, the second and third virial coefficients have been calculated; dipole-dipole interparticle interactions have been taken into account by expanding to the second order with respect to the dipole-dipole potential.

The obtained Helmholtz free energy has been conveniently expressed as explicit function of the small and large ferroparticle volume concentrations, the dipolar coupling constant and the dimensionless magnetic field (Langevin parameter).

This research has been carried out within the financial support of Grant No. MK-1673.2010.2 of the President of Russian Federation.

[1] A.O. Ivanov, O.B. Kuznetsova, *Phys. Rev.E.*, 64 (2001) 041405.

[2] J.J.Cerda and others *J.M.M.M.*, 323 (2011) 1246.

[3] E.A. Elfimova, A.O. Ivanov, *J. Exp. Theor. Phys.* **111**, N.1 (2010) 146.

24OR-E-12

## SPIN TRANSITION OF MOLECULAR COMPOUNDS UNDER PRESSURE

*Levchenko G.*

Donetsk Physical & Technical Institute NAS of Ukraine named after A.A. Galkin;  
e-mail: g-levch@ukr.net, Ukraine

The study of the molecular magnets is very interesting and the most fundamental problem in modern science [1]. This area of research includes three directions of investigations: high spin – low spin transition (ST) of magnetic ions in coordinated compounds; long range ordering in molecular materials; and molecules with large magnetic moment. This talk is devoted to elucidation of the ST phenomenon and is based on our study of the pressure influence on the temperature induced ST in mononuclear molecular compounds and in one, two and three- dimensional polymeric compounds. For beginning, here is discussed the state of these kind of investigations before our starting. It is shown that there were some well recognized statements; like that the transition pressure always increases with pressure increase according to expression:

$$T_{1/2} = (T_0)_{1/2} + (P\Delta V_{HL}) / \Delta S(1)$$

where  $T_{1/2}$  is a transition temperature under pressure,  $(T_0)_{1/2}$  is a transition temperature at atmospheric pressure,  $P$  – external pressure,  $\Delta V_{HL}$  -change of the volume at transition and  $\Delta S$  -change of the entropy under transition. Second statement was that the temperature hysteresis under pressure always decreases with pressure increase and here is a critical pressure higher of which the transition becomes gradual. The main wrong conclusion of these investigations was that if it is necessary to receive compound with a big hysteresis at room temperature, having the compound with transition at low temperature, it cannot be achieved using high pressure for increasing of the transition temperature

Using a high pressure cell adapted for SQUID magnetometer, we have studied the pressure influence on ST for many compounds with nanodimensions in one two or three directions. The result is that the ST temperature can be increased or decreased by pressure, according to equation:

$$T_{1/2} = (T_0)_{1/2} + (P\Delta V_{HL} + \Delta_{elast} - \Gamma) / \Delta S(2)$$

where  $\Delta_{elast}$  is an elastic energy and  $\Gamma$  is an interaction energy.

The hysteresis width also can be increased or decreased by pressure and we never did observed transformation of the ST with histeresis at atmospheric pressure into gradual under pressure. The equation (2) is in the contradiction of (1), because in accordance to (1) the interaction parameter does not influence on transition temperature under pressure, however according (2) the  $\Gamma$  influences on transition temperature and with increase of  $\Gamma$  under pressure the transition temperature can decrease, what one can observe in experiments.

The second part of the talk is devoted to the study of pressure induced spin transition at room temperature. This study allows to comperе two types of transition induced by temperature and induced by pressure and also interaction parameters received from two types of ST. As a result we have concluded that temperature induced and pressure induced spin transitions are determined with the same interaction parameters, but not always with the same change of elastic energy. We also observed the difference of ST pressure at room temperature in two types of experiments for some compounds. This difference is also discussed.

[1] Левченко Г. Г., Христов А.А. Молекулярный магнетизм: фазовые переходы высокий спин – низкий спин / Донецк, изд-во «Ноулидж», (2010), 264 с.

24OR-E-13

## EXTENSION OF THE OPERATING TEMPERATURE RANGE OF MAGNETIC FLUIDS

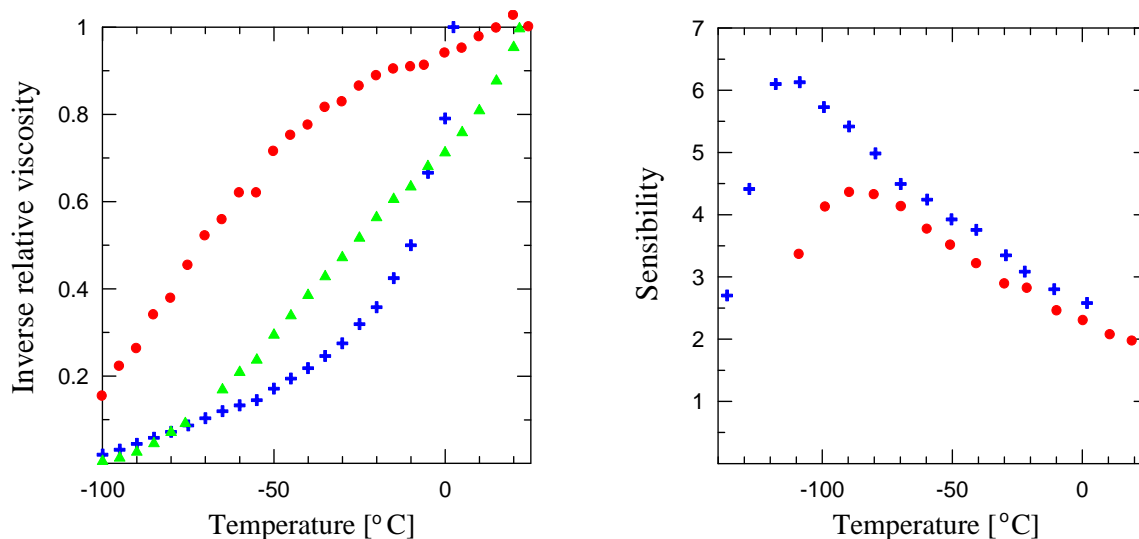
*Lebedev A.V.<sup>1</sup>, Lysenko S.N.<sup>2</sup>*

<sup>1</sup> Institute of Continuous Media Mechanics, UB RAS, Korolev Str. 1, Perm, 614013, Russia

<sup>2</sup> Institute of Technical Chemistry, UB RAS, Korolev Str. 3, Perm, 614013, Russia

Magnetic fluids [1] (colloidal solutions of fine dispersed magnetics) due to a combination of magnetic properties and fluidity inherent in classical fluids have much promise for fundamental investigation and practical application [2]. The lower boundary of the working temperature range is defined by the type of surfactants covering the particles. For a typical magnetite-based fluid stabilized with oleic acid this lower limit is -60°C.

In Ref. [3], the authors describe a new multifunctional stabilizer – polypropylene glycol (PPG). One of the advantages of PPG is that it extends the range of working temperatures. It has been found that the temperature range limit depends on the type of the base fluid. The best results have been obtained with the magnetic fluid based on propyl alcohol. The fluid preserves fluidity up to -115°C. This observation is illustrated by the figure, which compares the inverse relative viscosity data for magnetic fluids based on propanol (•), diethyl ether (+), and tholuol (Δ).



The analysis made has shown that PPG-stabilized fluids can be used for studying the inter-particle interactions in magnetic fluids at low temperatures. The most suitable base medium for such fluids is diethyl ether, in which mechanical blocking of the particles occurs at lowest temperatures.

The investigations have been supported by the RFBR, grant № 10-02-96022-r\_ural\_a.

- [1] M. I. Shliomis, Usp. Fiz. Nauk 112 (1974) 427 [Sov. Phys. Usp. 17 (1974) 153].
- [2] S. Odenbach, Lecture Notes in Physics, Vol. m71 (Springer, Berlin, 2002).
- [3] A. V. Lebedev and S. N. Lysenko Appl. Phys. Lett. 95 (2009) 013508.
- [4] A. V. Lebedev and S. N. Lysenko, JMMM, 323 (2011) 1198-1202.

**24 August**

Wednesday

11:30-13:00

14:30-17:20

oral session

24TL-F

24RP-F

24OR-F

**“Magnetophotonics”**

24TL-F-1

## **VECTOR CHIRAL SPIN LIQUID PHASE IN FINITE QUASI-ONE-DIMENSIONAL Fe-DOUBLE CHAINS ON Ir(100)**

*Blugel S.*

Peter Grunberg Institut and Institute for Advanced Simulation, Forschungszentrum Julich and JARA, D-52425 Julich, Germany

Combining spin-polarized scanning tunneling microscopy experiments with density functional theory calculations and Monte Carlo simulations, we present evidence for a complex magnetic order in individual bi-atomic Fe chains of finite length supported by an Ir surface. Using spin-polarized scanning tunneling microscopy we find in these chains an atomic-scale 120 degree spin-spiral structure. Quantitative theory reveals the Dzyaloshinskii-Moriya interaction as the driving force behind the formation of this non-collinear magnetic order in competition with a very weak Heisenberg exchange inter-action. Simulations show that the magnetization is lost at finite temperature, but the vector chirality survives as a new order parameter and the finite quasi-one dimensional Fe-double chains on Ir(100) is in the vector chiral spin liquid phase at finite temperature. Thermally activated magnetization reversal in magnetic chains on surfaces is studied by classical atomistic spin-dynamics simulations.

24TL-F-2

## **MAGNETO-OPTICS OF MAGNETIC NANOSTRUCTURES**

*Maziewski A.<sup>1</sup>, Kisielewski J.<sup>1,2</sup>, Kisielewski M.<sup>1</sup>, Stupakiewicz A.<sup>1</sup>, Tekielak M.<sup>1</sup>*

<sup>1</sup> Faculty of Physics, University of Bialystok, Lipowa 41, Bialystok, Poland

<sup>2</sup> Radboud University Nijmegen, Heyendaalseweg 135, Nijmegen, The Netherlands

This work is focused on results of recent studies of Co nanostructures. Magnetic properties of sandwiched ultrathin Co layers can be effectively tuned by: (i) structure of either an overlayer [1] or/and underlayer [2,3]; (ii) local irradiation by either ions [4,5] or light [6]. Magnetic ordering could be also modified when changing bilayer number N in (Co/Au)<sub>N</sub> multilayers [7]. Magnetic nanostructures with spatially changeable properties are usually specially designed. Magneto-optical Kerr effects (MOKE) based magnetometry is very powerful for such nanostructures local studies of magnetic ordering and vectorial-3D magnetization processes. Examples of such investigations will be presented. Application of femtosecond laser pulses for local magnetic anisotropy will be also discussed.

This work was supported by : (i) the EU Seventh Framework, Programme FP7/2007-2013 under grant N214810 FANTOMAS and (ii) Polish SPINLAB project in the frame of the EU programme Innovative Economy, Priority 2.2.

[1] M. Kisielewski et al., Phys.Rev.Lett. 89, 8, 87203 (2002).

[2] A. Stupakiewicz et al., Phys. Rev. Lett., 101, 217202 (2008).

[3] A. Wawro et al., PHYSICAL REVIEW B 83, 092405 (2011).

- [4] J. Jaworowicz et al., *Appl. Phys.Lett.*, 95, 022502 (2009).  
 [5] M. Urbaniak et al., *Phys.Rev.Lett.*, 105, 067202 (2010).  
 [6] J. Kisielewski et al., *Solid State Phenomena*, 140, 69 (2008).  
 [7] M. Tekielak et al., *IEEE TRANSACTIONS ON MAGNETICS*, 44, 11, 2950 (2008).

24OR-F-3

## NONLINEAR OPTICS OF MAGNETIC NANOSTRUCTURES

*Kolmychek I.A.<sup>1</sup>, Mitrukovskiy S.I.<sup>1</sup>, Krutyanskiy V.L.<sup>1</sup>, Nikulin A.A.<sup>1</sup>, Gan'shina E.A.<sup>1</sup>,  
 Murzina T.V.<sup>1</sup>, Zayats A.<sup>2</sup>*

<sup>1</sup> Department of Physics, Moscow State University, 119992 Moscow, Russia

<sup>2</sup> Department of Physics, King's College London, Strand, London WC2R 2LS, UK

Magnetic nanostructured materials attract much attention due to their unique properties that can be absent for the case of bulky crystals. In particular, magnetic anisotropy induced by a pronounced shape of nanostructures as well as plasmon assisted optical and magneto-optical properties are of special attention as they can find new applications in storage and optoelectronic devices. On the other hand, novel structures can reveal new effects that are interesting from the point of view of fundamental science. Among various experimental methods a distinguished place belongs to optical second harmonic generation (SHG) due to its intrinsically high sensitivity to structural, electronic, magnetic etc. properties of surfaces and nanostructures. One of the advantages of the SHG method is the possibility to study the optical response both at the fundamental and SHG wavelengths, which enlarges the spectral range available for the investigation and provides as well nondestructive character of the diagnostics. Moreover, due to the surface

In this work the SHG studies of plasmonic magnetic nanostructures are presented. The main aim of this research was to reveal the modification of the nonlinear-optical response of nanostructures in the spectral vicinity of the LSP excitation.

The studied samples are magnetic (1) core/shell ( $\text{Fe}_2\text{O}_3/\text{Au}$ ) nanoparticles of about 30 nm in diameter in a polymer matrix [1], (2) Au/Co/Au nanodisks of 60 nm and 110 nm in diameter, the total height of 32 nm [2], and (3) nickel nanorods with the aspect ratio of 7 [3]. These structures reveal the excitation of localized surface plasmons in the visible spectral range. Nonlinear-optical studies were performed when using the output of a femtosecond Ti-sapphire (wavelength range 710-850 nm) or nanosecond OPO laser system (wavelength range 450-700 nm) lasers as the fundamental radiation; the reflected SHG signal was detected by a PMT. For the magnetic measurements, the samples were placed in a transversal DC magnetic field of 3 kOe.

The main results obtained on the SHG properties of these structures are the following.

(1) SHG response from a spatially inhomogeneous array of core/shell nanoparticles in the presence of DC magnetic field reveals a coherent contribution that vanishes without the magnetic field; it originates from the appearance of plasmon-assisted magnetization induced magneto-dipole SHG component.

(2) The ratio of magnetic to nonmagnetic parts of the SHG polarization in Au/Co/Au nanodisks differs strongly from that of a continuous trilayer structure. The key role here belongs to the anisotropy of the local field factors at the fundamental and SHG wavelengths.

(3) A strong SHG magnetic anisotropy and spectral dependence of the SHG intensity and of the SHG magnetic contrast is observed in the reflection from Ni nanorods. These effects are attributed to the excitation of the two plasmonic modes excited at the SHG and fundamental frequencies in elongated magnetic nanostructures.

- [1] P. Gangopadhyay, S. Gallet, E. Franz et. al, *IEEE Trans. Magnetics*, **41**(10) (2005) 4194.  
 [2] J.B. Gonzalez Diaz, A. Garcia Martin, J.M. Garcia Martin et. al., *Small*, **4** (2008) 202.  
 [3] A. A. Stashkevich, Y. Roussigné, P. Djemia, et.al., *Phys. Rev. B* **80** (2009) 144406.

24RP-F-4

## **MAGNETIZATION REVERSAL BY LASER INDUCED HEAT PULSE IN NANOSTRUCTURED FERRIMAGNETIC THIN FILMS**

*Le Guyader L.<sup>1</sup>, El Moussaoui S.<sup>1</sup>, Nolting F.<sup>1</sup>, Mengotti E.<sup>2</sup>, Heyderman L.<sup>2</sup>, Tsukamoto A.<sup>3</sup>, Itoh A.<sup>3</sup>, Kirilyuk A.<sup>4</sup>, Rasing Th.<sup>4</sup>, Kimel A.V.<sup>4</sup>*

<sup>1</sup> Swiss Light Source, Paul Scherrer Institut, 5232 Villigen, Switzerland

<sup>2</sup> Laboratory for Micro- and Nanotechnology, Paul Scherrer Institut, 5232 Villigen, Switzerland

<sup>3</sup> CST, Nihon University, Chiba, Japan

<sup>4</sup> Spectroscopy of Solids and Interfaces, Institute of Molecules and Materials (IMM) Radboud University Nijmegen, Heyendaalseweg 135, 6525 AJ Nijmegen, The Netherlands

The exchange interaction is the strongest force in magnetism that typically corresponds to magnetic fields of up to several 100 T. Recent experiments have nevertheless shown that the magnetic order can be manipulated by an ultrafast laser pulse which heats the spin system on the time scale of the exchange interaction[1]. Whether such an excitation can be employed for the ultimately fast magnetization reversal triggered with just an ultrafast heat pulse is the question we tried to address here experimentally.

We report on our investigation of laser induced magnetization switching in structured GdFeCo ferrimagnetic thin films. To exclude any effect on the switching observed of the stray field or domain wall motion from the region outside the laser pulse, we have structured these thin films into arrays of squares and circles of various sizes ranging from 1 micron down to 100 nm using electron beam lithography. Employing X-ray magnetic circular dichroism (XMCD) in a photoemission electron microscope (PEEM) we have been able to image the magnetization configuration of these sub-wavelength nanostructures. Furthermore, by performing in-situ focusing of a single high energy femtosecond linearly polarized laser pulse and subsequently imaging the resulting magnetic states, we have succeeded to demonstrate that the magnetization of these structures permanently reverses each time the laser pulse excites the magnetic sublattices on the time scale of the exchange interaction between the Gd and Fe. We have also investigated the fluence threshold dependence of this switching as a function of the size of the structures. Time resolved studies of the laser induced magnetization reversal in the GdFeCo nanostructures are presently in progress.

- [1] I. Radu, K. Vahaplar, C. Stamm, T. Kachel, N. Pontius, H.A. Dürr, T.A. Ostler, J. Barker, R.F.L. Evans, R. W. Chantrell, A. Tsukamoto, A. Itoh, A. Kirilyuk, Th. Rasing and A. V. Kimel, "Transient ferromagnetic-like state mediating ultrafast reversal of antiferromagnetically coupled spins", *Nature* (2011)



24OR-F-5

## MAGNETO-OPTIC FRAUNHOFER DIFFRACTION ON 2D MAGNETIC DOMAIN PATTERNS

Logunov M.<sup>1</sup>, Nikitov S.<sup>2</sup>, Gerasimov M.<sup>1</sup>, Kashkin D.<sup>1</sup>, Loginov N.<sup>1</sup>, Spirin A.<sup>1</sup>

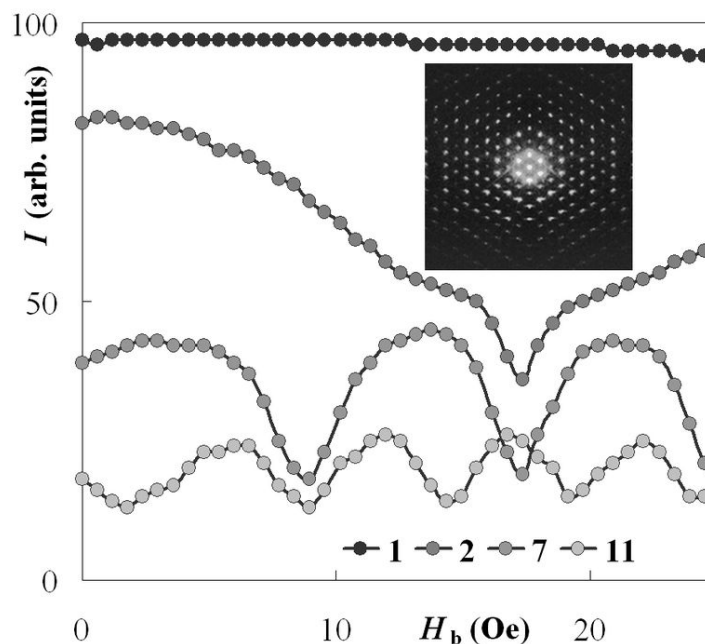
<sup>1</sup>National Research Mordovia State University, 430005 Saransk, Russia

<sup>2</sup>Kotel'nikov Institute of Radio Engineering and Electronics of RAS, 125009 Moscow, Russia

Magneto-optic materials and magneto-photonics crystals are of interest for physics and technics as a basis for effective devices of light beaming control [1]. An opportunity of formation of strictly ordered 2D domain patterns in soft magnetic films draws attention [2-4]. Such patterns consist from topologically modified magnetic bubble domains. Reorganization of patterns in the same film is possible. The patterns are statically steady after reorganization.

In the present work magneto-optic Fraunhofer diffraction on 2D domain patterns is studied. In this case the 2D domain pattern represents a phase diffraction grating. Properties of such two-dimensional grating can be controlled by means of a magnetic field. He-Ne laser was used for diffraction experiments on domain patterns. The diffraction pattern from 2D domain pattern with *Cmm6* symmetry is shown on fig. Numerous diffraction maxima testify to spatial uniformity of domain pattern. Magneto-optic Fraunhofer diffraction on domain patterns with *Cmm6*, *Pab2*, and *P6* symmetry has been studied.

Phase diffraction optical elements do not absorb optical radiation, and redistribute it on diffraction orders. The picture of redistribution at the same symmetry and the period of domain pattern depends on factor of filling of the pattern (a parity of the area of domains). It is well visible on dependences of relative intensity  $I$  of  $N$ -order diffraction maxima from magnetic bias field  $H_b$  (fig.). Thus, 2D domain patterns can be a basis of controlled 2D phase diffraction gratings.



[1] S.G. Erokhin, A.P. Vinogradov, A.B. Granovsky, M. Inoue, *Phys. of the Solid State*, **49** (2007) 497.

[2] F.V. Lisovskii, E.G. Mansvetova, *JETP Lett.*, **55** (1992) 32; **58** (1993) 784.

[3] M.V. Logunov, M.V. Gerasimov, *JETP Lett.*, **74** (2001) 491.

[4] E. Ascitutto, C. Roland, C. Sagui, *Phys. Rev. E*, **72** (2005) 021504.

24RP-F-6

## SPIN-PHOTONICS DEVICES FOR HIGH-SPEED OPTICAL NETWORKS

Zayets V., Saito H., Yuasa S., Ando K.

Spintronics Research Center, National Institute of Advanced Industrial Science and Technology (AIST), Umezono 1-1-1, Tsukuba, Ibaraki 305-8568, Japan

Magneto-optical (MO) materials are important for variety of photonics applications, because of their unique properties of such as non-reciprocity and an ability to memorize data. Because time-inversion symmetry is broken in MO materials, the optical properties of MO material are different for two opposite direction along magnetization and important optical components such as an optical isolator and circulator can be only made utilizing MO materials.

At present, there is a significant commercial demand for optical isolator and circulator, which could be integrated into photonic integrated circuit. We proposed to use (Cd,Mn)Te as a magneto-optical material for such isolator. The (Cd,Mn)Te exhibits a huge Faraday effect and can be grown on a semiconductor substrate. For (Cd,Mn)Te waveguide with (Cd,Zn)Te grown on GaAs substrate we achieved a high Faraday rotation of 2000 deg/cm, a high isolation ratio of 27 dB, a low optical loss of 0.5 dB/cm, and a high magneto-optical figure-of-merit of 2000 deg/dB/kG in a wide 25-nm wavelength range [1]-[3]. These values are comparable or better to that of commercial discrete isolators.

We predicted theoretically [4] and prove experimentally [5] the effect of non-reciprocal loss in hybrid semiconductor/ferromagnetic metal waveguides. This effect can be use for new design of waveguide optical isolator. Because the structure of this isolator is similar to that of laser diode, such design is beneficial for integration. The bistable laser diode with non-reciprocal amplifier was proposed to be used for high-speed optical logic [6].

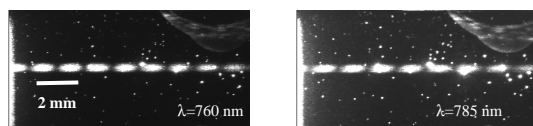


**Fig. 1:** TE component of mode propagating in (Cd,Mn)Te waveguide. Intensity oscillations is due to polarization rotation. Value of Faraday rotation is high with low wavelength dispersion [3]

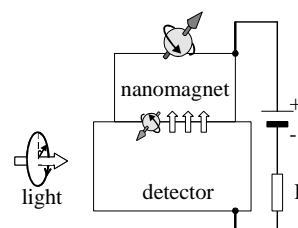


**Fig. 2:** Design of spin-photon memory cell [7]

We proposed the non-volatile high-speed optical memory, which utilize the magnetization reversal of nanomagnet by spin-polarized photo-excited electrons. It was demonstrated experimentally that one selected pulse from train of two optical data pulses with interval of 450 fs can solely excite the spin-polarized electrons without a disturbance from the unselected optical data pulse [7]. That proves feasibility for recording data into the memory with speed of 2.2 TBit/sec. The reading function for the memory was demonstrated [8].

- [1] W. Zaets and K.Ando, *Appl. Phys.Lett.* **77** (2000) 1593.
- [2] V. Zayets, M. C. Debnath, and K.Ando, *Appl. Phys.Lett.* **84** (2004) 565.
- [3] M. C. Debnath, V. Zayets, and K.Ando, *Appl. Phys.Lett.* **91** (2007) 043502.
- [4] W. Zaets and K.Ando, *IEEE Photon. Techn. Lett.* **11** (1999) 1012.
- [5] V. Zayets and K.Ando, *Appl. Phys.Lett.* **86** (2005) 261105.
- [6] W. Zaets and K.Ando, *IEEE Photon. Techn. Lett.* **13** (2001) 185.
- [7] V. Zayets and K.Ando, *Appl. Phys.Lett.* **94** ( 2009) 121104.
- [8] V. Zayets, H. Saito, S. Yuasa, and K.Ando *Optics Letters* **35** (2010) 931.

## MAGNETOPHOTONIC CRYSTALS WITH NOBLE METAL SURFACES

Baryshev A.V.<sup>1,2</sup>, Kawasaki K.<sup>1</sup>, Goto T.<sup>1</sup>, Inoue M.<sup>1</sup>

<sup>1</sup> Toyohashi University of Technology, Toyohashi 441-8580, Japan

<sup>2</sup> Ioffe Physico-Technical Institute, Saint-Petersburg 194021, Russia

Artificial materials with periodicity on the nanoscale and sub-micron scale—photonic crystals (PhCs)—have attracted a great attention, since they are considered as miniature building elements and effective components for various demands of today's needs from medicine to communication and computer technologies. Modern fabrication approaches allow structuring and combining different materials with the idea of creation of artificial matter with principally new performances, and also tuning characteristics of known conventional matter.

In this work we demonstrate that tailoring of surfaces of magnetophotonic crystals (MPhCs) [1] provides a new approach to engineer their responses that can be useful for optical sensor applications. One-dimensional MPhCs with multilayer structures terminated by noble metal (gold) layers were fabricated onto quartz substrates using sputtering. Experimental samples had multilayer or microcavity structures, where the thickness of Au film did not exceed 50 nm. The samples provided a large enhancement of the Faraday rotation associated with light coupling to magneto-optical constituents (ferrimagnetic garnets). Parameters of these multilayers were chosen such that they supported an optical resonance (so-called optical Tamm state, OTS; and the Fabry-Perot resonance, FPR) originating from periodicity of their lattices and the surface plasmons resonance (SPR) on gold films' interfaces. In experiments the OTS (FPR) and SPR modes were excited simultaneously by light from a selected spectral range. Later was observed in reflection spectra as a spectral overlap of the resonances. Responses from the samples were studied in the regime of plasmon excitation (Kretschmann geometry). Tuning/detuning the overlapping of these two intrinsic resonances by a variation of analytes' refractive index and by the binding of avidin to biotin resulted in the sharp change of measured optical and magneto-optical responses. Index resolution of the order of  $10^{-7}$  was achieved when probing changes in the reflected intensity. Magneto-optical responses are in favor of that a better sensitivity is attainable. These data were compared with that obtained for identical gold films at the same experimental conditions. For the fabricated samples, the comparison showed that the sensitivity of the PC/Au system was one order of magnitude higher by than that measured using thin gold films.

[1] T. Goto, A. V. Dorofeenko, A. M. Merzlikin, A. V. Baryshev, A. P. Vinogradov, M. Inoue, A. A. Lisyansky, and A. B. Granovsky, *Phys. Rev. B*, **79**, (2009) 125103.

[2] M. Inoue, R. Fujikawa, A. Baryshev, A. Khanikaev, P. B. Lim, H. Uchida, O. Aktsipetrov, A. Fedyanin, T. Murzina, and A. Granovsky, *J. Phys. D: Appl. Phys.*, **39**, (2006) R151.

## APPLICATION OF MAGNETO-OPTIC GARNET TO WAVEGUIDE OPTICAL ISOLATORS FOR PHOTONIC INTEGRATED CIRCUITS

Mizumoto T., Shoji Y., Takei R.

Tokyo Institute of Technology, 2-12-1 Ookayama, Meguro-ku, Tokyo 152-8552, Japan

Optical nonreciprocal devices such as an optical isolator and an optical circulator are indispensable to prevent lightwave from propagating in unwanted directions. The function of an optical isolator is used to protect optical active devices from unwanted reflection. A magneto-optic effect is to be implemented for obtaining the optical nonreciprocal function. A magneto-optic garnet is the best candidate in an optical fiber communication wavelength range because of its low absorption and large magneto-optic effect.

Currently available optical isolators are basically composed of bulk optics. They are not suitable for integrating with other photonic devices. A waveguide optical isolator is to be developed for the application to photonic integrated circuits in which non-magneto-optic materials like III-V compound semiconductors, silicon and silica are used as a waveguide platform.

The waveguide optical isolator that is based on nonreciprocal loss mechanism has been demonstrated with an isolation of 14.7 dB/mm at a 1550-nm wavelength region [1]. Also, the integration with a DFB laser has been demonstrated in [2]. It uses the difference in propagation loss between forward and backward propagation generated by the large magneto-optic effect of ferromagnetic material. The propagation loss that the forward wave experiences is compensated by the gain of built-in semiconductor optical amplifier.

We developed a surface activated direct bonding technique to integrate a magneto-optic garnet on commonly used waveguide platforms of III-V and silicon [3]. Using this technique, we fabricated an interferometric isolator that was composed of a GaInAsP guiding layer [4]. Employing the nonreciprocal phase shift generated by the first-order magneto-optic effect, the interferometer is designed so that the constructive and destructive interference occurs in the forward and backward direction, respectively. A similar approach was successfully taken to realize an optical isolator in a silicon waveguide fabricated on an SOI wafer. An isolation of 21 dB has been demonstrated at a wavelength of 1559 nm in the silicon interferometric waveguide isolator, where a Ce:YIG cladding layer was directly bonded on a silicon rib waveguide [5]. The surface activation process of oxygen plasma is used for bonding Ce:YIG onto silicon at 250 °C.

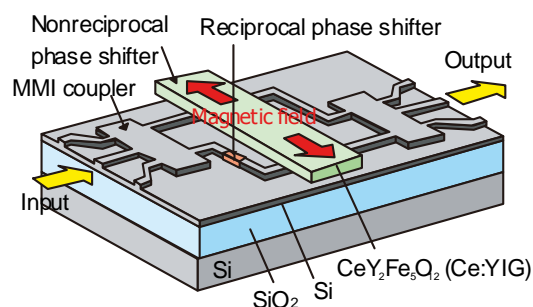


Fig. 1 Interferometric waveguide optical isolator on an SOI platform.

- [1] H. Shimizu and Y. Nakano, *J. Lightwave Technology*, **24** (2006) 38.
- [2] H. Shimizu and Y. Nakano, *Photon. Technol. Lett.*, **19** (2007) 1973.
- [3] R. Takei, K. Yoshida, and T. Mizumoto, *Jpn. J. Appl. Phys.*, **49** (2010) 086204.
- [4] H. Yokoi, T. Mizumoto, N. Shinjo, N. Futakuchi, and Y. Nakano, *Applied Optics*, **39** (2000) 6158.
- [5] Y. Shoji, T. Mizumoto, H. Yokoi, I-Wei Hsieh, and Richard M. Osgood, Jr., *Applied Physics Letters*, **92** (2008) 071117.

24RP-F-9

## FREQUENCY INVERSION AND TIME REVERSAL VIA A DYNAMIC MAGNONIC CRYSTAL

Chumak A.V.<sup>1</sup>, Tiberkevich V.S.<sup>2</sup>, Karenowska A.D.<sup>3</sup>, Serga A.A.<sup>1</sup>, Gregg J.F.<sup>3</sup>, Slavin A.N.<sup>2</sup>, Hillebrands B.<sup>1</sup>

<sup>1</sup> Fachbereich Physik and Forschungszentrum OPTIMAS, Technische Universität Kaiserslautern, Kaiserslautern 67663, Germany

<sup>2</sup> Department of Physics, Oakland University, Rochester, Michigan 48309, USA

<sup>3</sup> Department of Physics, Clarendon Laboratory, University of Oxford, Oxford OX1 3PU, UK

Artificial media with spatially periodic variations in their magnetic properties – so-called magnonic crystals (MCs) – are the magnetic analog of photonic and sonic crystals. Spin-wave excitation spectra of such structures exhibit a range of interesting features including band gaps over which spin wave propagation is prohibited. Especially interesting in the context of both fundamental research and microwave signal processing is a recently developed dynamic magnonic crystal (DMC) – an artificial crystal with a lattice whose properties can be modified while a wave packet propagates inside it [1]. It is based on a ferrite spinwave waveguide placed in a periodically varying current-controlled magnetic field (see Fig. 1a). We have demonstrated that the rejection band depth and width in such a crystal can be tuned using the applied current. Furthermore, the crystal can be switched from full transmission to full rejection with a transition time ten times smaller than the spin-wave relaxation time [1].

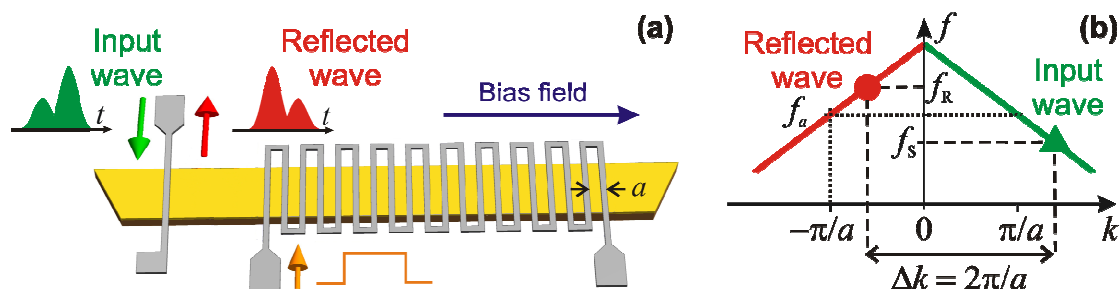


Fig. 1. All-linear time reversal by a dynamic magnonic crystal. (a) The experimental DMC system which comprises a planar current-carrying meander structure positioned close to the spin-wave waveguide. (b) The schematic illustration of the frequency inversion process.

We have shown that a DMC may provide a linear means to perform spectral transformations, including frequency inversion and time reversal [2], which, until now, have only been possible through nonlinear mechanisms (Fig. 1b). The crystal is switched from a homogeneous state to one in which its properties vary with spatial period  $a$ , while a propagating wave packet is inside. As a result, a linear coupling between wave components with wave vectors  $k \approx \pi/a$  and  $k' = k - 2\pi/a \approx -\pi/a$  is produced, which leads to spectral inversion, and thus to the formation of a time-reversed wave packet. The reversal mechanism is entirely general and so is applicable to artificial crystal systems of any physical nature.

[1] A.V. Chumak, T. Neumann, A.A. Serga, B. Hillebrands and M.P. Kostylev, *J. Phys. D: Appl. Phys.* **42**, 205005 (2009).

[2] A. V. Chumak, V. S. Tiberkevich, A. D. Karenowska, A. A. Serga, J. F. Gregg, A. N. Slavin, and B. Hillebrands, *Nat. Commun.* **1**:141 doi: 10.1038/ncomms1142 (2010).

24RP-F-10

## MAGNONIC META-MATERIALS

*Mikhaylovskiy R.V., Dvornik M., Dmytriiev O., Kruglyak V.V.*

School of Physics, University of Exeter, Stocker Road, EX4 4QL, Exeter, UK

Born as a result of the remarkable technological, experimental, and theoretical advances, magnonics is a field of study of spin waves in magnetic nanostructures, with magnonic crystals having played a decisive role in defining its identity so far [1]. On the other hand, a lot of interest has been generated by the prospectus for creation of effectively continuous magnonic meta-materials [2,3].

In this talk, we will review our most recent results along this research direction. In particular, we will focus opportunities resulting from the use of magnonic resonances in magnetic nano-structures and the ways how they could be modelled and studied experimentally.

The research leading to these results has received funding from the European Community's Seventh Framework Programme (FP7/2007-2013) under Grant Agreements n°233552 (DYNAMAG) and n°228673 (MAGNONICS) and from the Engineering and Physical Research Council (EPSRC) of the UK.

[1] V. V. Kruglyak, S. O. Demokritov, and D. Grundler, *J. Phys. D – Appl. Phys.* **43** (2010) 264001.

[2] V. V. Kruglyak, P. S. Keatley, A. Neudert, R. J. Hicken, J. R. Childress, and J. A. Katine, *Phys. Rev. Lett.* **104** (2010) 027201.

[3] R. V. Mikhaylovskiy, E. Hendry, and V. V. Kruglyak, *Phys. Rev. B* **82** (2010) 195446.

24TL-F-11

## THE X-RAY VIEW OF ULTRAFAST MAGNETISM

*Durr H.A.*

SLAC National Accelerator Laboratory, Menlo Park CA 94025, USA

Polarized soft x-rays have been used over the past 20 years to obtain fascinating new insights into nanoscale magnetism. The separation of spin and orbital magnetic moments, for instance, enabled detailed insights into the interplay of exchange and spin-orbit interactions at the atomic level. The now available polarized soft x-ray pulses with only 100 fs duration allow us to observe the magnetic interactions at work in real time. The ultimate goal of such studies is to understand how spins may be manipulated by ultrashort magnetic field, spin polarized current or light pulses. In this talk I will focus on fs laser induced spin-orbit dynamics in 3d transition metals and 4f rare earth systems. Using fs x-ray pulses from the BESSY II femtoslicing facility I will show how fs excitation of the electronic system modifies the spin-orbit interaction enabling ultrafast angular momentum transfer between spin, orbital and lattice degrees of freedom. I will also show first results demonstrating how the intense coherent fs x-ray pulses from the LCLS X-ray free electron laser allows us to access the nm length scale

Wednesday

**24 August**

11:30-13:00

14:30-17:20

oral session

24TL-G

24RP-G

24OR-G

**“Magnetism and  
Superconductivity”**

24TL-G-1

## QUANTUM SUPERPOSITION OF MAGNETIC FLUX STATES IN A SUPERCONDUCTING LOOP

*Il'ichev E.*

IPHT, 07745, A. Einstein str. 9, Jena, Germany

Nowadays there is clear and convincing proof that artificially fabricated macroscopic solid state systems can behave according to the laws of quantum mechanics. Recent experiments have demonstrated that superconducting Josephson circuits can be in superposition of macroscopically distinct quantum states. This has important implications, for instance, for the quantum measurement theory, for the description of the interaction between light and matter as well as for implementation of new generation of quantum limited detectors and quantum information processing devices.

In the talk both – theoretical description and practical realization of superconducting qubits will be discussed.

24RP-G-2

## IMPLEMENTATION OF SFS $\pi$ -SHIFTERS IN SUPERCONDUCTING QUANTUM CIRCUITS

*Feofanov A.K.*

Institut Néel, CNRS & Université Joseph Fourier, 38042, Grenoble, France

High operation speed and low energy consumption may allow the superconducting digital single flux quantum circuits to outperform traditional complementary metal-oxide-semiconductor logic. The remaining major obstacle to a high density of elements on a chip is a relatively large cell size necessary to hold a magnetic flux quantum  $\Phi_0$ . Inserting a  $\pi$ -type Josephson junction [1, 2] in the cell is equivalent to applying flux  $\Phi_0/2$  and thus makes it possible to solve this problem [3]. Moreover, using  $\pi$ -junctions in superconducting qubits may help to protect them from noise [4, 5]. Here we demonstrate the operation of two superconducting circuits — one of them is classical and one quantum — which both utilise such  $\pi$ -phase shifters realised using superconductor-ferromagnet-superconductor sandwich technology [6]. The classical circuit is based on single-flux-quantum cells, which are shown to be scalable and compatible with conventional niobium-based superconducting electronics. The quantum circuit is a-biased phase qubit, for which we observe coherent Rabi oscillations. We find no degradation of the measured coherence time compared to that of a reference qubit without  $\pi$ -junction.

[1] Bulaevskii, L. N., Kuzii, V. V. & Sobyenin, A. A. Superconducting system with weak coupling to the current in the ground state. JETP Lett. 25, 290-294 (1977).

[2] Buzdin, A. I., Bulaevskij, L. N. & Panyukov, S. V. Critical-current oscillations as a function of the exchange field and thickness of the ferromagnetic metal (F) in an S-F-S Josephson junction. JETP Lett. 35, 178-180 (1982).

[3] Ustinov, A. V. & Kaplunenko, V. K. Rapid single-qubit quantum logic using  $\pi$ -shifters. J. Appl. Phys. 94, 5405-5407 (2003).



[4] Ioffe, L. B., Geshkenbein, V. B., Feigelman, M. V., Fauchère, A. L. & Blatter, G. Environmentally decoupled sds-wave Josephson junctions for quantum computing. *Nature* 398, 679-681 (1999).

[5] Blatter, G., Geshkenbein, V. B. & Ioannidis, L. B. Design aspects of superconducting-phase quantum bits. *Phys. Rev. B* 63, 174511 (2001).

[6] Ryazanov, V. V. et al. Coupling of two superconductors through a ferromagnet: evidence for a  $\pi$ -junction. *Phys. Rev. Lett.* 86, 2427-2430 (2001).

24RP-G-3

## REENTRANCE SUPERCONDUCTIVITY IN SF STRUCTURES AND ITS APPLICATION FOR THE SPIN-SWITCH DESIGN

*Sidorenko A.S.<sup>1,2</sup>, Tagirov L.R.<sup>3,4</sup>*

<sup>1</sup> Institute of Electronic Engineering and Industrial Technologies ASM, MD-2028 Kishinev, Moldova

<sup>2</sup> Institute of Nanotechnology, Karlsruhe Institute of Technology, D-76021 Karlsruhe, Germany

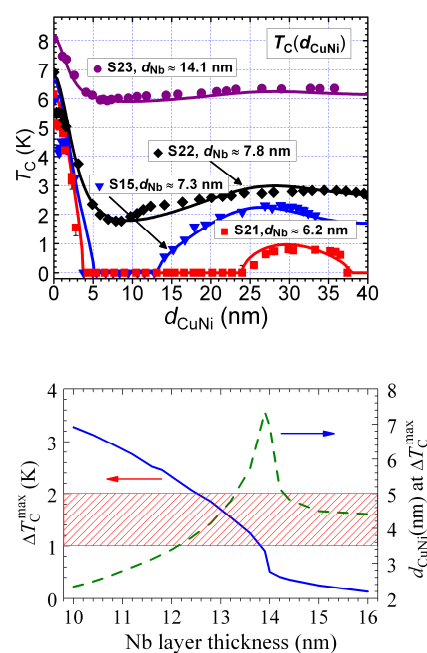
<sup>3</sup> Kazan Federal University, 420008 Kazan, Russian Federation

<sup>4</sup> Institut für Physik, Universität Augsburg, D-86159 Augsburg, Germany

Superconductivity (S) and ferromagnetism (F) are antagonistic long-range orders which cannot coexist in a homogeneous material. Heterostructures comprising nanometer scale layers of superconducting and ferromagnetic layers offer new physical picture of the interaction of superconductivity and magnetism, in which the superconducting pairing function penetrates in the ferromagnetic layers in an oscillating manner. If the oscillation scale, and the pairing function decay length are comparable with the ferromagnetic layer(s) thickness, various interference effects can be expected. In this review presentation we focus on the mesoscopic oscillations of the

superconducting transition temperature  $T_c$  which arise as a result of modulation of coupling between the superconducting and ferromagnetic layers when varying the ferromagnetic layer thickness (see the top figure). By fitting the experimental data with the quasiclassical theory the physical parameters of the Nb/CuNi alloy had been found [1]. One superconducting layer and two ferromagnetic layers already offer functionality determined by mutual alignment of magnetic moments of the ferromagnetic layers. This functionality can be utilized to build a superconducting spin valve of the F/S/F design. Using physical parameters established for the Nb/CuNi couple from the experiments on S/F bilayers [1] we estimated superconducting spin-valve effect which can be obtained with the materials mentioned above. The results of  $\Delta T_c = T_c^{AP} - T_c^P$  calculations

(where  $T_c^P$  and  $T_c^{AP}$  are the superconducting transition temperatures of the F/S/F trilayer for the parallel and antiparallel alignment of magnetizations, respectively) are presented in the bottom figure. The optimal range of the layers thickness, which falls in the intersection of the two curves with the shaded area in the bottom figure, provides the spin-valve effect magnitude more than 1 K.



Support by Deutsche Forschungsgemeinschaft (DFG) under the grant No GZ: HO 955/6-1 and by the A.v.Humboldt Foundation, the AvH-Project 2C0704 "Nonuniform superconductivity in layered SF-nanostructures Superconductor/Ferromagnet" is gratefully acknowledged.

[1] V.I. Zdravkov, J. Kehrle, G. Obermeier, et al. Phys. Rev. B **82**, 054517 (2010).

24OR-G-4

## SUPERCONDUCTING CRITICAL TEMPERATURE AND MAGNETIC INHOMOGENEITIES IN SUPERCONDUCTOR/FERROMAGNET/SUPERCONDUCTOR TRILAYERS

*Prischepa S.L.<sup>1</sup>, Kushnir V.N.<sup>1</sup>, Cirillo C.<sup>2</sup>, Attanasio C.<sup>2</sup>, Kupriyanov M.Yu.<sup>3</sup>*

<sup>1</sup> Belarus State University of Informatics and RadioElectronics, P. Brovka 6,  
Minsk 220013, Belarus

<sup>2</sup> CNR-SPIN Salerno and Dipartimento di Fisica "E.R. Caianiello",  
Università degli Studi di Salerno, Fisciano (Sa) I-84084, Italy

<sup>3</sup> Institute of Nuclear Physics, Moscow State University, Moscow 119992, Russia

The effect of the exchange energy variations in weakly ferromagnetic alloys on the superconductive resistive transition of Superconductor/Ferromagnet/Superconductor (S/F/S) trilayers is studied. Critical temperature,  $T_c$ , and resistive transitions versus the F-layer thickness,  $d_F$ , have been analyzed in Nb/Cu<sub>0.41</sub>Ni<sub>0.59</sub>/Nb and Nb/Pd<sub>0.81</sub>Ni<sub>0.19</sub>/Nb trilayers. We show that the  $T_c(d_F)$  dependence and the width of the resistive transition curves  $R(T)$  are sensitive to magnetic inhomogeneities in the F-layer for values of  $d_F^*$  corresponding to thickness where the  $\pi$ -superconducting state is established.

In particular we observe that, for the Nb/Cu<sub>0.41</sub>Ni<sub>0.59</sub>/Nb trilayers, a broadening of the  $R(T)$  transitions is observed in the  $\pi$ -phase thickness region, for  $d_F \square d_F^*$ , where the width  $\Delta T_c = 0.6$  K, while for thickness  $d_F \ll d_F^*$  and  $d_F \gg d_F^*$  the resistive transitions are sharp and  $\Delta T_c \approx 0.1$  K. It was proposed that such broadening at  $d_F \square d_F^*$  can be due to in-plane inhomogeneity of both S and F materials which generates a network of Josephson 0- and  $\pi$ - contacts with a subsequent spontaneous nucleation of vortices [1]. On the other hand for the Nb/Pd<sub>0.81</sub>Ni<sub>0.19</sub>/Nb trilayers the  $R(T)$  transitions are sharp and  $\Delta T_c$  do not exceed 0.1 K for all the values of  $d_F$ .

Since the specular X-ray reflectivity measurements performed on these samples revealed similar values of the interfacial roughness for both the studied systems [2,3], we exclude the possible geometrical inhomogeneity of the samples as a reason for  $R(T)$  broadening. At the same time the Ni clustering is much more pronounced in Cu<sub>0.41</sub>Ni<sub>0.59</sub> films with respect to Pd<sub>0.81</sub>Ni<sub>0.19</sub> one.

For this reason the experimental data have been analyzed applying the approach developed by Tagirov to describe superconducting/strong ferromagnetic systems [4,5]. In the present case the aim was to take into account the possible presence of Ni segregation in the alloys. The model successfully reproduces with reasonable values of parameters the data for the Nb/Cu<sub>0.41</sub>Ni<sub>0.59</sub>/Nb system, as well as for the Nb/Pd<sub>0.81</sub>Ni<sub>0.19</sub>/Nb one. The results of the fitting procedure confirm the absence of strong Ni clustering in Pd<sub>0.81</sub>Ni<sub>0.19</sub> films, while the quantitative estimate of the exchange energy in the Ni clusters present in Cu<sub>0.41</sub>Ni<sub>0.59</sub> films is in good agreement with the literature.

Support by BFFR, grant F10R-063 (P.S.L., K.V.N.) and by RFFR, grant 10-02-90014-Bel-a (K.M.Yu.) is acknowledged.

- [1] S.L. Prischepa et al., *Pis'ma v ZhETP*, **88** (2008) 431 [*JETP Lett.* 88 (2008) 375].  
 [2] S.L. Prischepa et al., *Solid State Phenomena*, **152-153** (2009) 478.  
 [3] A. Vecchione et al., *Surface Science*, submitted.  
 [4] L.R. Tagirov, *Physica C*, **307** (1998) 145.  
 [5] B.P. Vodopyanov, L.R. Tagirov, H.Z. Durusoy, A.V. Berezhnov, *Physica C*, **366** (2001) 31.

24RP-G-5

## SUPERCONDUCTING THERMO-ELECTRIC BOLOMETER WITH HIGH IMBALANCE OF TUNNELING THROUGH THE SIN TUNNEL JUNCTION

Kuzmin L.<sup>1,2,3</sup>, Pugach N.<sup>2</sup>

<sup>1</sup> Chalmers University of Technology, 412 96 Gothenburg, Sweden

<sup>2</sup> M.V. Lomonosov Moscow State University, Faculty of Physics and SINP, Moscow, Russia

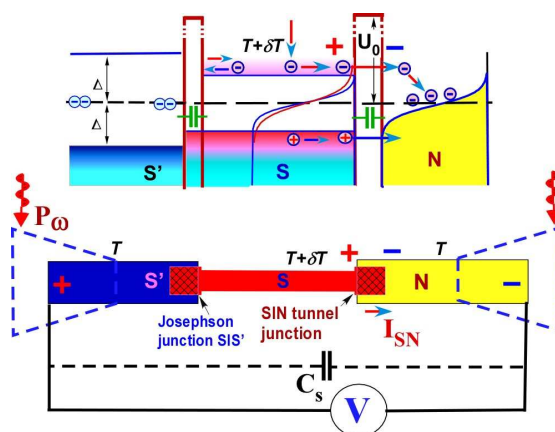
<sup>3</sup> LCN Alexeev NSTU, N. Novgorod, Russia

The novel concept of the Zero-Biased Thermo-Electric Bolometer (TEB) has been recently proposed [1]. The bolometer is based on a charge-to-voltage conversion in a Superconductor-Insulator-Normal (SIN) Tunnel Junction. The absorption of photons in the superconducting absorber leads to excitation of quasiparticles, tunneling through the SIN junction in zero-biased mode with some imbalance of quasielectrons and quasiholes and generation of voltage. The thermoelectric voltage is determined by accumulation of tunneling charge in an external capacitance. Conversion efficiency is very high and voltage response comparable with a superconducting gap is easily achieved. All properties of the TEB are determined by charge imbalance in absorption and tunneling. The imbalance was quite low for previously realized systems with SIN tunnel junction (0.01 for Smith-Tinkham realization [2]).

Fig 1. Sketch of the proposed Thermo-Electric Bolometer (TEB) based on a Charge-to-Voltage Conversion of quasiparticles excited in superconducting nanoabsorber by an RF signal. The converter is working in a novel mode as an integrator of charge that has tunneled through the SIN junction. The self-biased SIN tunnel junction is used for the generation of a voltage which appears due to the different probability of tunneling for quasielectrons and quasiholes to the normal metal.

We propose a radically new method of advanced TEB with high imbalance of quasielectrons and quasiholes tunneling through the SIN junction. The concept is fully based on large difference in tunneling probability of quasielectrons and quasiholes through the low potential barrier SIN junctions. For that goal, the TEB with AlOx barrier of height  $U_0=1.7$  meV should be replaced Cr-based or Ti-based systems with a low potential barrier. Estimation of tunneling probability and imbalance for Pb/Cr<sub>2</sub>O<sub>3</sub>/Pb junction with  $U_0=20$  meV, superconducting gap  $2\Delta=2.7$  meV, thickness of the barrier  $d=5$  nm [3] using quantum-mechanical transparency gives Imbalance = 0.7 (!) that is very high figure for TEB [1].

Having a bias-free thermo-electric bolometer working at low temperatures is very attractive for applications. However, the thermo-electric Seebeck coefficient is dramatically decreased at low temperatures for ordinary metals and semiconductors. In contrast, the proposed TEB with



imbalance of tunneling show quite high thermo-electric coefficient. Possible intrinsic imbalance of quasielectrons and quasiholes in superconductor could be added to this effect.

Support by SNSB, RFBR, SI, and by the Act 220 of Russian Government is acknowledged.

- [1]. L. Kuzmin, *Physica C: Superconductivity*, 470, 1933-1935 (2010).
- [2]. A.D. Smith, M. Tinkham, and W.J. Skocpol, *PRB*, **22**, 4346 (1980).
- [3]. C. Y. Fu and T. Van Duzer, *IEEE Trans on Magn*, 17, 290 (1981).

24TL-G-6

## PHASE DIAGRAM OF Fe BASED SUPERCONDUCTORS

*Büchner B.*

Institut für Festkörperforschung, IFW Dresden  
Institut für Festkörperphysik, TU Dresden

Focusing on  $\text{REO}_{1-x}\text{F}_x\text{AsFe}$  ( $\text{RE} = \text{La}, \text{Sm}, \text{Ce}$ ) we have studied the phase diagram as well as magnetic and electronic properties of iron pnictide superconducting using a broad spectrum of experimental techniques, such as NMR  $\mu\text{SR}$ , ARPES, magnetometry, x-ray diffraction, and transport measurements. Details of the phase diagram, the magnetic ordering properties of the superconducting state and the normal state electronic properties in the superconducting regions of the phase diagram are derived from these experimental studies. In the paramagnetic normal state, NMR on three different nuclei in  $\text{LaO}_{1-x}\text{F}_x\text{AsFe}$  shows that the local electronic susceptibility rises with increasing temperature. In addition, the relaxation rate as determined from NMR studies points to the presence of antiferromagnetic fluctuations, which are most pronounced in the underdoped systems close to the magnetically ordered phase. Moreover, measurements of the electrical field gradient by NQR yield clear-cut evidence for nanoscale order of charges and/or orbitals which are reminiscent to the famous stripe order found in cuprates and other strongly correlated systems.

In addition I will report evidence for unconventional triplet superconductivity that we find in some high quality single crystals of  $\text{LiFeAs}$ , which is a stoichiometric pnictide superconductor with  $T_c \sim 18$  K. This evidence is obtained from NMR data and from quasiparticle interference as extracted from STM measurements.

- [1] H.-J. Grafe et al., *Phys. Rev. Lett.* 101, 047003 (2008), *New J. Phys.* 11, 35002 (2009)
- [2] H.-H. Klauss et al., *Phys. Rev. Lett.* 101, 077005 (2008)
- [3] H. Luetkens et al., *Phys. Rev. Lett.* 101, 097009 (2008)
- [4] R. Klingeler et al., *Phys. Rev. B*, 81, 024506 (2010)
- [5] H. Luetkens et al., *Nature Materials* 8 305, (2009)
- [6] C. Hess et al., *Europhys. Lett.* 87, 17005(2009)
- [7] V. Zabolotnyy et al., *Nature* 457, 569 (2009)
- [8] G. Lang et al., *Phys. Rev. Lett.* 104, 097001 (2010)
- [9] S.V. Borisenko et al., *Phys. Rev. Lett.* 105, 067002 (2010)
- [10] I. Morozov et al., *Cryst. Growth Des.* 10(10), 4428 (2010)
- [11] S.-H. Baek et al., preprint
- [12] T. Hänke et al., preprint

24TL-G-7

## PHYSICAL PROPERTIES OF AROMATIC HYDROCARBON ADDED MgB<sub>2</sub> BULKS, WIRES AND TAPES

*Gencer A.<sup>1</sup>, Babaoğlu M.G.<sup>1</sup>, Yanmaz E.<sup>2</sup>, Ertekin E.<sup>1</sup>, Ağıl H.<sup>3</sup>, Safran S.<sup>1</sup>, Çiçek Ö.<sup>1</sup>, Belenli I.<sup>2</sup>*

<sup>1</sup> Ankara University, Faculty of Sciences, Department of Physics, 06100-Tandoğan, Ankara, Turkey

<sup>2</sup> Karadeniz Technical University, Science Faculty, Physics Department, Trabzon, Turkey.

<sup>3</sup> Hakkari University Rectorate, Hakkari, Turkey.

Corresponding e-mail: gencer@science.ankara.edu.tr

In this paper, we report on the structural and superconducting properties of aromatic hydrocarbon addition in MgB<sub>2</sub>. Benzene, ethyl-toluene and toluene chosen as aromatic hydrocarbon for in-situ processed MgB<sub>2</sub> samples. Structural characterization of samples was performed by the X-ray powder diffraction (XRD) and Scanning Electron Microscopy (SEM) measurements. Magnetic properties were determined by zero field cooled M-T, *M-H* hysteresis and AC susceptibility measurements. Ball-milling was used to reduce average particle size down to nano-scales with more homogeneous mixture for regularly distributed pinning sites. Pressed bulk tablets were heat treated in argon gas under high pressures to prevent Mg escape. To determine optimum preparation conditions, ball-milling timing, sintering temperature and heat treatment cycles were changed. Hydrocarbon addition in MgB<sub>2</sub> enhances critical current density by a factor 2 via pinning mechanism while critical temperature is lowered as expected. Experimental results are also compared with direct C addition in MgB<sub>2</sub>. We note that MgB<sub>2</sub> reacts with added hydrocarbons while we observe abnormality in the flux pinning mechanism at temperatures around 5 K as an indication of flux avalanches being field and temperature dependent. Amplitude dependent ac susceptibility data gives an estimate of critical current density in the vicinity of critical temperature which depends on the content of carbon in the main matrix of MgB<sub>2</sub>. Further analysis of experimental data has been performed with Bean critical state model for potential applications. It appears that there exists a limiting case for a potential increase of the critical current density especially in the vicinity of 4.2 K. We note that the main challenge is the improvement of the material homogeneity and precursor purity and grain size, new performance levels due to homogeneously distributed flux pinning sites and finally densification of MgB<sub>2</sub>. Aromatic hydrocarbon adding results in an increase in critical current density by about a factor of 2, however the material becomes rather un-stable to sustain higher critical currents at lower temperatures. Ball-milled nano-powders with new and innovative preparation methods are key issues of the work to be presented. The resulting powders were used to make wires and tapes based on home-made powder-In-Tube (PIT) and Continuous Tube Folding and Filling (CTTF) techniques. Properties of such wires are being investigated.

This work has been supported in part by The Scientific and Technological Research Council of Turkey (TÜBİTAK) under contract no: 109T106 and Ankara University Research Fund.

## X-RAY SPECTRA AND ELECTRONIC STRUCTURE OF FeAs-SUPERCONDUCTORS

*Kurmaev E.Z.<sup>1</sup>, McLeod J.A.<sup>2</sup>, Moewes A.<sup>2</sup>, Skorikov N.A.<sup>1</sup>, Anisimov V.I.<sup>1</sup>, Finkelstein L.D.<sup>1</sup>*

<sup>1</sup> Institute of Metal Physics, Russian Academy of Sciences-Ural Division,  
620041 Yekaterinburg, Russia (kurmaev@ifmlrs.uran.ru)

<sup>2</sup> Department of Physics and Engineering Physics, University of Saskatchewan, 116 Science Place,  
Saskatoon, Saskatchewan S7N 5E2, Canada

The results of resonant inelastic X-ray scattering (RIXS) measurements and density functional theory (DFT) calculations of REO<sub>1-x</sub>F<sub>x</sub>FeAs (RE=La, Sm) [1], LiFeAs, NaFeAs [2], CaFe<sub>2</sub>As<sub>2</sub> [3] and KFe<sub>2</sub>As<sub>2</sub> are presented. The experimental RIXS spectra are found to be consistent with DFT calculations. Both theory and experiment show that the Fe *3d*-states dominate on the Fermi level and the low Hubbard *d*-band typical for correlated systems is not found. RIXS measurements at Fe *L*<sub>2,3</sub>-edges show that I(*L*<sub>2</sub>)/I(*L*<sub>3</sub>) intensity ratio is small, close to that of Fe-metal and quite different with respect to correlated FeO which is indicative of itinerant character of Fe *3d*-electrons. The comparison of experimental RIXS spectra with LDA+DMFT (Local Density Approximation combined with Dynamical Mean-Field Theory) calculations [4] shows a good agreement between theory and experiment (with the average Coulomb repulsion  $U = 3\div 4$  eV and Hund's exchange  $J = 0.8$  eV) only when Fe *3d*-As *4p* hybridization is taken into account. This Fe *3d*-As *4p* hybridization weakens electron correlations and therefore one can conclude that FeAs-superconductors belong to weakly or moderately weakly correlated systems.

This work is partly supported by the Russian Science Foundation for Basic Research (Projects 11-02-00022, the Natural Sciences and Engineering Research Council of Canada (NSERC), and the Canada Research Chair program.

- [1] E.Z. Kurmaev, R.G. Wilks, A. Moewes, N.A. Skorikov, Yu.A. Izyumov, L.D. Finkelstein, R.H. Li, and X.H. Chen, *Phys. Rev. B* **78**, 220503(R) (2008).
- [2] E.Z. Kurmaev, J. McLeod, N.A. Skorikov, L.D. Finkelstein, A. Moewes, M.A. Korotin, Yu.A. Izyumov and S. Clarke, *J. Phys.: Condens. Matter* **21**, 345701 (2009).
- [3] E.Z. Kurmaev, J.A. McLeod, A. Buling, N.A. Skorikov, A. Moewes, M. Neumann, M.A. Korotin, Yu.A. Izyumov, N. Ni and P.C. Canfield, *Phys. Rev. B* **80**, 054508 (2009).
- [4] V. I. Anisimov, E.Z. Kurmaev, A. Moewes, Yu.A. Izyumov, *Physica C* **469**, 442 (2008).

24TL-G-9

## VORTEX STRUCTURES IN Fe-BASED SUPERCONDUCTING SINGLE CRYSTALS

Vinnikov L.Ya.

Institute of Solid State Physics RAS, Chernogolovka Moskow region, Academician Osipyan Str.2,  
Russia

Unabated interest in Fe-based high- temperature superconductors of the pnictide family discovered in 2008 [1] has stimulated studies of superconductivity in simpler iron compounds in particular iron-chalcogenides [2]. As well as cuprates superconducting pnictides and chalcogenides are layered compounds but theirs theirs theirs theirs vortex structures in single crystals is dramatically different [3-5]. Single crystals of the pnictide family are characterized by unusually high critical currents and the regular vortex structure is absent in a wide range of magnetic fields from several mT to 9 T for example in Ba(FeCo)<sub>2</sub>As<sub>2</sub> [3].

Review of observation vortex structures in Fe-based superconductors has been performed.

The vortex structure of the single crystals electron-doped SmFeAs(OF)-1111 type- and hole-doped BaKFe<sub>2</sub>As<sub>2</sub>-122 type- superconductors with different doping degrees were investigated by the decoration method [4]. A familiar study for the iron-chalcogenides Fe(TeSe) [5] -11 type-as well as novel superconductor K<sub>0.8</sub>F<sub>2</sub>Se<sub>2</sub> and BaFe<sub>2</sub>(AsP)<sub>2</sub> -122 type-were carried out. The main results of the observation of magnetic flux structures in all investigated Fe-containing single crystals is absence of the regular vortex lattice.

The disordered vortex structure is discussed in view of the vortex pinning in single crystals.

Support by RFBR grant 10-02-01297 is acknowledged.

[1] Y. Kamihara, T. Watanabe, M. Hirano and H. Hosono, *J. Am. Chem. Soc.*, **130** (2008) 3296

[2] F. S. Hsu, J. Y. Lup, K.W.Yeh, et al., *Proc. Nat. Acad. Sci. USA*, **105**, (2008) 14262

[3] M.R. Eskildsen, L.Ya. Vinnikov, T.D. Blasius et al., *Phys. Rev. B*, **79**, (2009)100501(R);  
*Physica C*, **469**, (2009) 529

[4] L.Ya.Vinnikov, T.M.Artemova, I.S.Veshchunov, et al., *JETP Lett.*, **90**, (2009) 299

[5] ] L.Ya.Vinnikov, A.V. Radaev, I.S.Veshchunov, et al., *JETP Lett.*, **93** (2011) 287

24RP-G-10

## PHYSICS OF CORRELATED ELECTRONS AT COMPLEX OXIDE INTERFACES

Chakhalian J.

Physics Department, University of Arkansas, Fayetteville

Complex oxides are a class of materials containing a variety of competing strong interactions that create a subtle balance to define the lowest energy state, which leads to a wide variety of interesting properties (e.g. superconductivity, exotic magnetism,...). By utilizing the bulk properties of these materials as a starting point, interfaces between different classes of complex oxides offer a unique opportunity to break the symmetry present in the bulk and alter the local environment. Utilizing the

recent advances in oxide growth, we can now combine materials with distinctly different and even competing orders to create new materials in the form of heterostructures. The broken symmetry, strain, and altered atomic environments at the interfaces then provide an exciting avenue to manipulate this subtle balance and perhaps even create new quantum phases. The understanding of these phases, however, requires detailed microscopic studies of the heterostructure properties. Here we will demonstrate how synchrotron based X-ray probes offer the ability to probe bulk vs. interface properties to gain unique insight into the emerging many-body physics of cuprate, manganite and nickelate based ultra-thin heterostructures.

24RP-G-11

## DUAL FEATURES OF MAGNETIC SUSCEPTIBILITY IN SUPERCONDUCTING CUPRATES

*Eremin M.V.<sup>1</sup>, Shigapov I.M.<sup>1</sup>, Eremin I.M.<sup>2</sup>*

<sup>1</sup> Kazan Federal University, 420008, 18 Kremlyovskaya St., Kazan, Russian Federation

<sup>2</sup> Institute für Theoretische Physik III, Ruhr-Universität Bochum, D-44801 Bochum, Germany

The hour-glass-shape dispersion observed in neutron scattering below  $T_c$  naturally calls for the explanation of the spin response in terms of dual character of the excitations. While the upward dispersion resembles the collective spin wave branch like in quasi-two dimensional antiferromagnet with short range spin fluctuation, the downward dispersion in the superconducting state can be nicely attributed to the feedback effects of the d-wave order parameter on the itinerant component. There is much evidence about dual character of the spin excitations also from NMR experiments at Cu and O nuclei in copper-oxygen planes. However, usually an interaction between both would introduce the repulsion between both branches and it is not 'a-priori' clear how the total spin response would look in this case. Starting from the singlet-correlated band model [1], we discuss the spin response in the superconducting cuprates taking into account both local and itinerant spin components which are coupled to each other self-consistently. The value of superconducting energy gap extracted from the temperature dependencies of the nuclear relaxation rate [2] and superfluid density [3] for  $\text{YBa}_2\text{Cu}_3\text{O}_{6+y}$ . The energy dispersion information is available from ARPES data. Our analytical and numerical results show that the obtained analytical expression for the spin susceptibility reproduces well the characteristic features of the experimental data in  $\text{YBa}_2\text{Cu}_3\text{O}_{6+y}$  compounds near optimal doping level including the dispersion of the spin excitations in the normal and superconducting state as well its frequency and temperature dependence. While the structure of the spin excitations in the normal state can be attributed to the mostly overdamped localized magnetic modes, the strong feedback of the d-wave superconductivity on the itinerant electrons reveals the formation of the spin exciton with the characteristic downward dispersion of the spin excitations in the superconducting state. In addition, the high energy spin excitations still originate from the localized excitations. Remarkable that both modes merge at the  $\omega_{\text{res}}$  which is a result of the single pole structure at  $Q = (\pi, \pi)$ . At  $\omega \rightarrow 0$  the contribution to total susceptibility related to quasi-two dimensional short range spin fluctuation is dominated. BCS like equation yields a d-wave pairing with  $2\Delta / k_B T_c = 4.2$ .

Support by RFBR Grant 09-02-00777-a, and Swiss National Science Foundation, Grant IZ73Z0 128242 is acknowledged.



- [1] M.V. Eremin, A.A. Aleev, and I.M. Eremin, Zh. Eksp. Teor. Fiz. **133**(4), 862 (2008) [JETP **106**(4), 752 (2008)]  
 [2] T. Mayer, M. Eremin, I. Eremin and P.F. Meier, J. Phys.: Condens. Matter **19**, 116209 (2007)  
 [3] M.V. Eremin, I.A. Larionov, and I.E. Lyubin, J. Phys. Condens. Matter **22**, 185704-185709 (2010)

24OR-G-12

## ON THE SUPERCONDUCTIVITY OF HIGH-SPIN TRANSITION-METALL COMPOUNDS

Zaitsev R.O.

Moscow Institute of Physics and Technology, Dolgoprudny, Moscow region, 141700, Russia

The possibility of existence of Cooper instability in transition-metal compounds has established on the basis of idea about the strong interaction in a single unit cell. The phase diagram of the existence of the superconducting ordering depending on the degree of underfilling of the 3d shells has been obtained. The nonephonon BCS constant has been calculated.

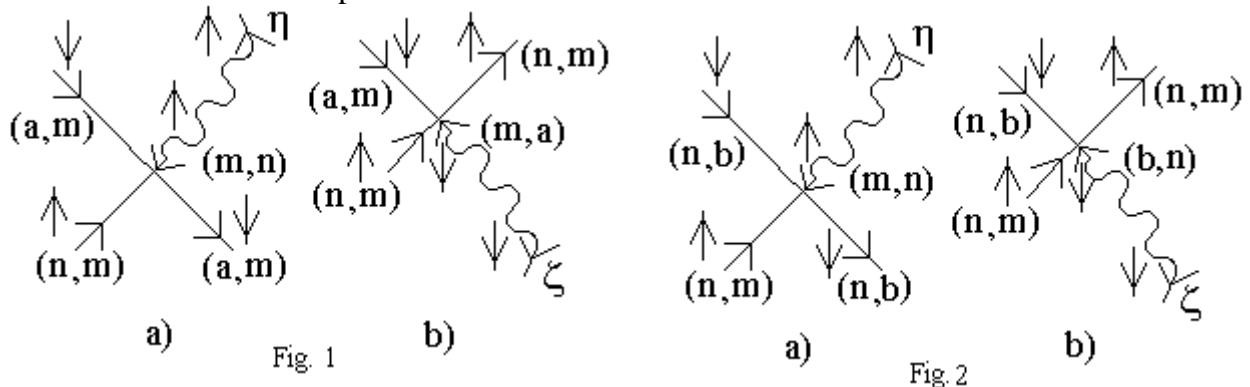


Fig. 1

Fig. 2

The two single-particle scattering amplitudes are determined as the coefficients of the products of two  $X_\lambda X_\nu$ -operators obtained in the calculation on the commutators  $\{X_\alpha [X_\beta \hat{H}]\}$  [1], there  $\hat{H}$  is Hamiltonian operator expressed in terms of the  $X$ -operator. As a result, the four vertex parts determining for the kinematic interaction for four diagrams given in Figs. 1a, 1b and 2a, 2b are obtained.

As shown by Gor'kov [2], to obtain the conditions for the appearance of superconductivity, it is sufficient to consider the homogeneous system of ladder equations. Since the zeroth vertex part in the case of kinematic interaction depends only on the output momenta, corresponding equations have the form:

$$\Gamma_{i=k} = -\lambda_{i=k} \sum_{p,n,m} e_i^v(\vec{p}) e_k^v(-\vec{p}) \frac{\mu}{\xi_p^v} \tanh\left(\frac{\xi_p^v}{2T_c}\right) e_n^v(\vec{p}) e_m^v(-\vec{p}) \Gamma_{nm},$$

where  $\lambda_{i=k} = \frac{-1}{1+[h_d]}$ , for each integer interval  $[h_d] \leq h_d \leq 1+[h_d]$ , ( $0 < h_d < 5$ ).

$$\Gamma_{i \neq k} = -\lambda_{i \neq k} \sum_{p,n,m} [e_i^v(\vec{p}) e_k^v(-\vec{p}) + e_k^v(\vec{p}) e_i^v(-\vec{p})] \frac{\mu}{\xi_p^v} \tanh\left(\frac{\xi_p^v}{2T_c}\right) e_n^v(\vec{p}) e_m^v(-\vec{p}) \Gamma_{nm},$$

where  $\lambda_{i \neq k} = -1, \frac{-11}{24}, \frac{-1}{6}, \frac{1}{16}, \frac{4}{15}$ , for the corresponding intervals:  $0 < h_d < 1$ ,

$1 < h_d < 2$ ,  $2 < h_d < 3$ ,  $3 < h_d < 4$ ,  $4 < h_d < 5$ ;  $e_k^v(\vec{p})$  – the ortonormalize eigen vectors,  
 $\xi_p^v$  – the excitation energy,  $\mu$  – the chemical potential.

[1] R.O. Zaitsev, *JETP Letters*, **92** (2010) 146; [2] L.P. Gor'kov, *JETP*, **34** (1958) 735.

**24 August**

Wednesday

11:30-13:00

14:30-17:20

oral session

24TL-H

24RP-H

**“Multiferroics”**

24TL-H-1

**MULTIFERROICITY IN RARE-EARTH ORTHOFERRITE SYSTEMS**Tokunaga Y.<sup>1,2</sup>, Furukawa N.<sup>2,3</sup>, Sakai H.<sup>1</sup>, Iguchi S.<sup>4</sup>, Taguchi Y.<sup>1</sup>, Arima T.<sup>5,6</sup>, Tokura Y.<sup>1,2,7</sup><sup>1</sup> Cross-Correlated Materials Research Group (CMRG) and Correlated Electron Research Group (CERG), RIKEN Advanced Science Institute (ASI), Wako, Saitama 351-0198, Japan<sup>2</sup> Multiferroics Project, ERATO, Japan Science and Technology Agency (JST), Wako, Saitama 351-0198, Japan<sup>3</sup> Department of Physics and Mathematics, Aoyama Gakuin University, Sagamihara, Kanagawa 229-8558, Japan<sup>4</sup> Institute for Materials Research, Tohoku University, Sendai 980-8577, Japan<sup>5</sup> Department of Advanced Materials Science, University of Tokyo, Kashiwa, 277-8561, Japan<sup>6</sup> RIKEN SPring-8 Center, Hyogo 679-5148, Japan<sup>7</sup> Department of Applied Physics, University of Tokyo, Bunkyo-ku, Tokyo 113-8656, Japan

Since 1970s, some of rare-earth orthoferrite and orthochromite systems have been theoretically studied from the viewpoint of magnetic symmetry and predicted to be promising candidates as magnetoelectric and/or multiferroic materials, in which not only the magnetic ordering of  $3d$  spins of transition metals but also that of  $4f$  moments of rare-earth ion contribute to their magnetoelectric coupling [1, 2]. In this talk, we present the experimental demonstration of the multiferroicity in rare earth orthoferrite systems. We found that perovskite ferrite systems  $\text{GdFeO}_3$  and  $\text{DyFeO}_3$  have "ferromagnetic-ferroelectric", i.e., genuine multiferroic states below the ordering temperatures of rare-earth moments. Here, weak ferromagnetic moment is caused by Dzyaloshinskii-Moriya interaction working on Fe spins and electric polarization originates from the striction due to symmetric exchange interaction between Fe and Gd(Dy) spins [3, 4]. Both materials showed large electric polarization ( $>0.1 \mu\text{C}/\text{cm}^2$ ) and strong magnetoelectric coupling. In addition, we succeeded in mutual control of magnetization and polarization with electric- and magnetic-fields in  $\text{GdFeO}_3$ , and attributed the controllability to novel, composite domain wall structure. We will also discuss the recent progress in the exploration of the stronger clamping between electric polarization and magnetization in these systems.

This work was in part supported by JSPS FIRST program.

[1] T. Yamaguchi and K. Tsushima, *Phys. Rev. B* **8**, 5187. (1973).

[2] A. K. Zvezdin and A. A. Mukhin, *JETP Lett.* **88**, 505 (2008)

[3] Y. Tokunaga et al., *Phys. Rev. Lett.* **101**, 097205 (2008).

[4] Y. Tokunaga et al., *Nature Mater.* **8**, 558 (2009).

24TL-H-2

## TOPOLOGICAL DEFECTS AND DYNAMIC MAGNETOELECTRIC COUPLING IN MULTIFERROIC MATERIALS

*Mostovoy M.<sup>1</sup>, Artyukhin S.<sup>1</sup>, Jensen N.<sup>2</sup>, Argyriou D.<sup>3</sup>, Nomura K.<sup>4</sup>, Nagaosa N.<sup>4,5</sup>*

<sup>1</sup> Zernike Institute for Advanced Materials, University of Groningen, Nijenborgh 4, 9747 AG, Groningen, The Netherlands

<sup>2</sup> Risø National Laboratory for Sustainable Energy, Frederiksborgvej 399, DK-4000 Roskilde, Denmark

<sup>3</sup> European Spallation Source ESS AB, P.O Box 176, SE-221 00 Lund, Sweden

<sup>4</sup> Correlated Electron Research Group (CERG), RIKEN-ASI, Wako 351-0198, Japan

<sup>5</sup> Department of Applied Physics, The University of Tokyo, Hongo, Bunkyo-ku, Tokyo 113-8656, Japan

The control of domains in ferroic devices lies at the heart of their potential for technological applications. Multiferroic materials offer another level of complexity as domains can be both ferroelectric and magnetic nature. The composite multiferroic domain walls give rise to complex magnetoelectric switching phenomena in  $\text{GdFeO}_3$  where the electric polarization is induced by the coupled magnetic orders of rare earth and transition metal spins [1]. I will discuss the origin of an unusual incommensurate state in  $\text{TbFeO}_3$  orthoferrite recently discovered using neutron diffraction under an applied magnetic field [2]. This state has a very long incommensurate period ranging of  $\sim 340 \text{ \AA}$  and exhibits an anomalously large number of higher-order harmonics, which makes possible to identify it with the periodic array of sharp domain walls of Tb spins separated by many lattice constants. The Tb domain walls interact by exchanging spin waves propagating through the Fe magnetic sublattice. The resulting Yukawa-like force has a very long range that determines the period of the incommensurate state.

I will also discuss a new magnetoelectric interaction in multi-orbital Mott insulators. Unlike the well-known ‘inverse Dzyaloshinskii-Moriya’ mechanism and the Heisenberg exchange striction, this interaction is dynamical in nature: it couples electric field to the time derivative of the local magnetization. This coupling works for all crystal lattices and does not involve the relativistic spin-orbit coupling. It gives rise to unusual effects, such as the displacement of spin textures in ferromagnetic insulators induced by an applied electric field, which may find applications in dissipationless spintronics. The effect of the dynamic magnetoelectric coupling is dramatically enhanced for topological magnetic objects. I will discuss the resonant absorption of circularly polarized light by Skyrmions and magnetic vortices [3].

Support by FOM is gratefully acknowledged.

[1] Y. Tokunaga *et al.*, *Nature Mater.*, **8** (2009) 558.

[2] S. Artyukhin *et al.*, preprint arXiv:1103.4275.

[3] M. Mostovoy, K. Nomura, N. Nagaosa, *Phys. Rev. Lett.*, **106** (2011) 047204.

## GIANT MAGNETODIELECTRIC EFFECT IN $RFe_3(BO_3)_4$ MULTIFERROICS

Mukhin A.A.<sup>1</sup>, Vorob'ev G.P.<sup>2</sup>, Ivanov V.Yu.<sup>1</sup>, Kadomtseva A.M.<sup>2</sup>, Popov Yu.F.<sup>2</sup>,  
Kuzmenko A.M.<sup>1</sup>, Bezmaternykh L.N.<sup>3</sup>, Gudim I.A.<sup>3</sup>

<sup>1</sup> Prokhorov General Physics Institute of the Russian Acad. Sci., 119991, Moscow, Russia

<sup>2</sup> M.V. Lomonosov Moscow State University, 119992 Moscow, Russia

<sup>3</sup> Kirensky Institute of Physics, Siberian Branch of the Russian Acad. Sci., Krasnoyarsk, Russia

We have observed the giant magnetodielectric effect in rare-earth iron borates  $RFe_3(BO_3)_4$  – new family of multiferroics ( $T_N = 30-40$  K) possessing non-centrosymmetrical trigonal crystal structure (R32) and exhibiting a strong dependence of their properties on exchange interactions between antiferromagnetic Fe and paramagnetic rare-earth (R) ions. More than threefold increase in the dielectric constant  $\epsilon_a$  ( $\epsilon_b$ ) at  $T < T_N$  and its suppression from  $\epsilon \sim 48$  to the primary level  $\sim 15$  in the magnetic field of  $\sim 5$  kOe applied in the basal  $ab$  plane was found in the easy plane  $SmFe_3(BO_3)_4$  [1]. The frequency dependence of  $\epsilon$  was almost absent between 10 -200 kHz. A qualitatively different behavior was observed for  $\epsilon_a(H_{a,b})$  and  $\epsilon_b(H_{a,b})$ . A close relation of this effect to anomalies in the field dependence of the electric polarization and magnetization in  $SmFe_3(BO_3)_4$  has been established. Similar magnetodielectric effects were also observed in  $NdFe_3(BO_3)_4$ ,  $Nd_{0.5}Gd_{0.5}Fe_3(BO_3)_4$ ,  $Nd_{0.4}Y_{0.6}Fe_3(BO_3)_4$  accompanied, however, by more reduced changes of  $\epsilon_a$  ( $\epsilon_b$ ).

The theoretical explanation of the observed phenomena has been proposed. It has been shown that the observed magnetodielectric effect is due to the contribution to the dielectric constant from the electric susceptibility related (via magnetoelectric coupling) to the rotation of  $Fe^{3+}$  spins in the easy  $ab$  plane at  $T < T_N$ , which is suppressed by the magnetic field. The observed difference in the  $\epsilon_a(H_{a,b})$  and  $\epsilon_b(H_{a,b})$  behavior is determined by the different magnetoelectric coupling for  $P_x \sim L_x^2 - L_y^2$  and  $P_y \sim -2L_x L_y$  [2], where  $L_{x,y}$  are the components of antiferromagnetic moment in the basal plane. The high value of the observed magnetodielectric effect  $\Delta\epsilon \sim (2P_t^0)^2/K$  in  $SmFe_3(BO_3)_4$  is explained by the relatively high electric polarization  $P_t^0 \sim 400 \mu C/m^2$  in the basal plane. In the easy plane state, this polarization easily rotates in the electric field due to the low magnetic anisotropy energy  $K$  in the basal plane. A realistic model taking into account the induced magnetoelastic anisotropy in the basal plane was elaborated. It allowed consistently describe the main features of the observed behavior of the dielectric constants, electric polarization and magnetization in the magnetic field for  $SmFe_3(BO_3)_4$ .

A relatively small value of the magnetodielectric effects observed in other rare-earth iron borates is explained by a small electric polarization  $P_t^0$ , since  $\epsilon \sim (P_t^0)^2$ . Another reason of the reduced magnetodielectric effect occurs for  $NdFe_3(BO_3)_4$ , where  $P_t^0$  is closed to  $SmFe_3(BO_3)_4$  one. The increase of the rotation contribution to the dielectric constant is suppressed in  $NdFe_3(BO_3)_4$  below  $\sim 20$  K due to the transition to the spiral spin state. As a result the magnetic fields, which destroyed the spiral phase at  $\sim 9$  kOe, simultaneously reduce the magnetodielectric effect. The analysis of the temperature dependences of the observed phenomena has allowed us to conclude on the prevailing contribution of the R-subsystem to the considered magnetoelectric effects in the rare-earth iron borates. The fundamental spin excitations both in Fe- and R-subsystems (electromagnons) responsible for the found effects have been also analyzed.

This work was supported by RFBR (09-02-01355) and (10-02-00846).

[1] A.A. Mukhin, G.P. Vorob'ev, V.Yu.Ivanov, A.M. Kadomtseva, et al. JETP Lett.93, 275 (2011)

[2] A.K. Zvezdin, G.P. Vorob'ev, A.M. Kadomtseva, et al.,JETP Lett. 83, 509 (2006).

24TL-H-4

## RECENT ACHIEVEMENTS IN THE FIELD OF SPIN INDUCED FERROELECTRIC OXIDES AND SULFIDES

Maignan A.<sup>1</sup>, Martin C.<sup>1</sup>, Singh K.<sup>1</sup>, Simon Ch.<sup>1</sup>, Damay F.<sup>2</sup>

<sup>1</sup> Laboratoire CRISMAT, UMR 6508 CNRS ENSICAEN, 6, bd du Maréchal Juin, France,

<sup>2</sup> Laboratoire Léon Brillouin CEA-Saclay 91191 Gif-sur-Yvette Cedex,

There exists a large variety of metal-transition oxides that exhibit multiferroic properties. Among them, the delafossites form a class of spin induced ferroelectrics which electric polarization cannot be explained by the spin current model. To test the robustness of alternative models [1] implying metal-oxygen hybridization, the structural, electrical and magnetic properties of AgCrS<sub>2</sub> sulfides have been investigated [2, 3]. They show the existence of spin induced ferroelectricity in a monoclinic polar structure which undergoes a collinear 4L antiferromagnetic structure. The strong magnetostriction below T<sub>N</sub> is believed to induce local atomic displacements responsible for the polarization contrasting with the mechanisms involved in the corresponding AgCrO<sub>2</sub> delafossite.

For the delafossite oxides, a second mechanism has also been recently discovered: in CuFe<sub>0.5</sub>V<sub>0.5</sub>O<sub>2</sub> [4] and CuCr<sub>0.5</sub>V<sub>0.5</sub>O<sub>2</sub>, two spin glasses, the local disorder induced by the cation mixing at the M site in CuMO<sub>2</sub>, is found to induce a relaxor behaviour. These materials are belonging to the so-called “dipolar glasses”.

[1] T.H Arima, *J. Phys. Soc. Jpn* **76**, 073702 (2007)

[2] K. Singh, A. Maignan, C. Martin and Ch. Simon, *Chem. Mater* **21**, 5007 (2009)

[3] F. Damay, C. Martin, V. Hardy, G. André, S. Petit and A. Maignan, *Cond-Mater* Xiv:1009.2616

[4] K. Singh, A. Maignan, Ch Simon, V. Hardy, E. Pachoud and C. Martin, *J. Phys. Cond. Matter*: **23**, 126005 (2011).

24TL-H-5

## HARD X-RAY DICHROISMS STUDIES OF MULTIFERROIC GaFeO<sub>3</sub> CRYSTALS

Rogalev A.<sup>1</sup>, Wilhelm F.<sup>1</sup>, Bosak A.<sup>1</sup>, Goulon J.<sup>1</sup>, Smekhova A.<sup>1,2</sup>, Gan'shina E.A.<sup>2</sup>,  
Bezmaternykh L.N.<sup>3</sup>, Kazak N.V.<sup>3</sup>, Ovchinnikov S.G.<sup>3</sup>

<sup>1</sup> ESRF, 6, rue Jules Horowitz, 38000 Grenoble, France

<sup>2</sup> M.V.Lomonosov Moscow State University, Moscow, Russia

<sup>3</sup> L.V. Kirensky Institute of Physics, Krasnoyarsk, 660036, Russia.

Ferroelectric and ferrimagnetic ordering coexist in gallium ferrate - GaFeO<sub>3</sub>. The multiferroic properties of this compound have been extensively studied since early sixties by many different experimental techniques. In order to study these properties on a microscopic level we have measured various X-ray reciprocal and non-reciprocal dichroisms at the Fe K-edge. The results of these experiments carried out at the ESRF beamline ID12 on a high quality untwined single crystal of GaFeO<sub>3</sub> are presented here. X-ray magnetochiral dichroism and X-ray non-reciprocal magnetic linear dichroism, which are a direct measure of the Fe orbital anapole and higher order magnetoelectric multipole, are disentangled experimentally for the first time. These two dichroic signals are compared to usual X-ray magnetic circular dichroism which is a measure of orbital

magnetic moment carried by Fe atoms. Moreover, X-ray natural circular dichroism has been also measured on this biaxial non-enantiomorphous crystal. All these dichroisms are analyzed with the help of a set of the sum rules. This analysis allowed us to deduce the expectation values of different effective operators related to multiferroic properties of GaFeO<sub>3</sub>.

24RP-H-6

## MAGNETIC AND MAGNETOELECTRIC PROPERTIES OF PYROXENE MATERIALS ACrX<sub>2</sub>O<sub>6</sub>: FROM LOW DIMENSIONALITY TO MAGNETIC FRUSTRATION

*Nénert G.<sup>1</sup>, Isobe M.<sup>2</sup>, Kim I.<sup>3</sup>, Ritter C.<sup>1</sup>, Vasiliev A.N.<sup>4</sup>, Kim K.H.<sup>3</sup>, Ueda Y.<sup>2</sup>*

<sup>1</sup> Institut Laue-Langevin, Boîte Postale 156, 38042 Grenoble, Cedex 9, France; nenert@ill.eu

<sup>2</sup> Institute for Solid State Physics, University of Tokyo, 5-1-5 Kashiwa, Chiba 277-8581, Japan

<sup>3</sup> CeNSCMR, Department of Physics and Astronomy, Seoul National University, Seoul 151-747, South Korea

<sup>4</sup> Low Temperature Physics Department, Moscow State University, Moscow 119991, Russia

In recent years, the coupling between magnetic and dielectric properties in transition-metal oxides gave rise to a significant research effort [1-3]. This effort is governed by the emergence of new fundamental physics and potential technological applications [2-4]. Multiferroic materials exhibit simultaneously (ferro)magnetic, pyroelectric, and ferroelastic properties. Contrary to multiferroic materials, magnetoelectric materials show an induced electrical polarization by a magnetic field. A proper understanding of the interplay between the various physical properties of these two types of materials relies heavily on the knowledge of the detailed crystal and magnetic structures.

One new class of compounds which have been investigated in this context is the class of pyroxene materials. They have the general formula AMX<sub>2</sub>O<sub>6</sub> where A is an alkali (+I) or alkali-earth ion (+II), M is a transition metal ion (+II or +III) while X = Si, Ge. These materials have been extensively investigated due to their importance in mineralogy [5] and their low dimensional magnetic properties [6]. The recent work by Jodlauk *et al.* shed some new light on these materials motivated by the idea that this family could be a good representative of a magnetically frustrated lattice [7]. The existence and possible interplay of low dimensionality and magnetic frustration resulting in multiferroic and/or magnetoelectric properties in the pyroxenes will probably open new avenues to tune and investigate the richness of the physics in this family.

We aim here to present our findings on the magnetic and magnetoelectric properties of the Cr<sup>3+</sup> containing pyroxenes. We will present our results which show that Cr<sup>3+</sup> pyroxene materials exhibit simple magnetic structure compatible with a linear magnetoelectric effect but so far no multiferroic properties. In addition, while pyroxene materials have been considered so far as good representatives of low dimensional magnetism, their magnetic ground state is likely to be mostly driven by magnetic frustration [8].

[1] M. Fiebig, J. Phys. D **38**, R123 (2005).

[2] W. Eerenstein, N. D. Mathur, and J. F. Scott, Nature (London) **442**, 759 (2006).

[3] S.-W. Cheong and M. Mostovoy, Nat. Mater. **6**, 13 (2007).

[4] A. Pimenov, A. A. Mukhin, V. Yu. Ivanov, V. D. Travkin, A. M. Balbashov, and A. Loidl, Nat. Phys. **2**, 97 (2006); A. B. Sushkov, R. V. Aguilar, S. Park, S. W. Cheong, and H. D. Drew, Phys. Rev. Lett. **98**, 027202 (2007).



- [5] T. Arlt, R. J. Angel, R. Miletich, T. Armbruster, T. Peters; *American Mineralogist* **83**, 1176 (1998)
- [6] J. van Wezel, *et al.*; *Europhys. Lett.* **75**, 957 (2006) ; P. Millet, *et al.*; *Phys. Rev. Lett.* **83** 04176 (1999).
- [7] S. Jodlauk, *et al.*, *J. Phys.: Condens. Matter* **19**, 432201 (2007). 064416-7.
- [8] G. Nénert, *et al.*, *Phys. Rev. B* **79**, 064416 (2009) ; G. Nénert, *et al.* *Phys. Rev. B* **80**, 024402 (2009) ; G. Nénert, *et al.*, *Phys. Rev. B* **81**, 184408 (2010); G. Nénert, *et al.*, *Phys. Rev. B* **82** 024429 (2010).

24RP-H-7

## DIRECT AND INVERSE MAGNETOELECTRIC EFFECT IN THE ELECTROMECHANICAL RESONANCE RANGE

*Bichurin M.I., Petrov V.M., Averkin S.V.*

Novgorod State University, B.S.-Peterburgskaya Str.41, Veliky Novgorod 173003, Russia

Magnetolectric (ME) coupling in the composites is mediated by the mechanical stress and one would expect orders of magnitude stronger coupling when the frequency of the ac field is tuned to acoustic mode frequencies in the sample than at non-resonance frequencies. Two methods of theoretical modeling can be used for calculating the frequency dependence of ME coefficients by solving the medium motion equation. First approach rests on considering the structure as an effective homogeneous medium and implies the preliminary finding the effective low-frequency material parameters. The second approach is based on using the initial material parameters of components. This report is focused on modeling of the ME effect in ferrite-piezoelectric layered structures in EMR region. We have chosen cobalt ferrite (CFO) - barium titanate as the model system for numerical estimations. The ME voltage coefficients  $\alpha_E$  have been estimated for transverse field orientations corresponding to minimum demagnetizing fields and maximum  $\alpha_E$ . As a model, we considered a ferrite-piezoelectric layered structure in the form of a thin plate with the length  $L$ . We solved the equation of medium motion taking into account the magnetostatic and elastostatic equations, constitutive equations, Hooke's law, and boundary conditions. The resonance enhancement of ME voltage coefficient for the bilayer is obtained at antiresonance frequency. ME voltage coefficient,  $\alpha_{E,13}$  increases with increasing barium titanate volume, attains a peak value for  $\nu = 0.5$  and then drops with increasing  $\nu$  as in Fig.1.

To obtain the inverse ME effect, a pick up coil wound around the sample is used to measure the ME voltage due to the change in the magnetic induction in magnetostrictive phase. The measured static magnetic field dependence of ME voltage has been attributed to the variation in the piezomagnetic coefficient for magnetic layer. The frequency dependence of the ME voltage shows a resonance character due to longitudinal acoustic modes in piezoelectric layer. Here we take into account only stress components along  $x$  axis, because close to EMR we can assume  $T_1 \gg T_2$  and  $T_3$ . Expressing the stress components via the deformation components and substituting these expressions into the equation of the medium

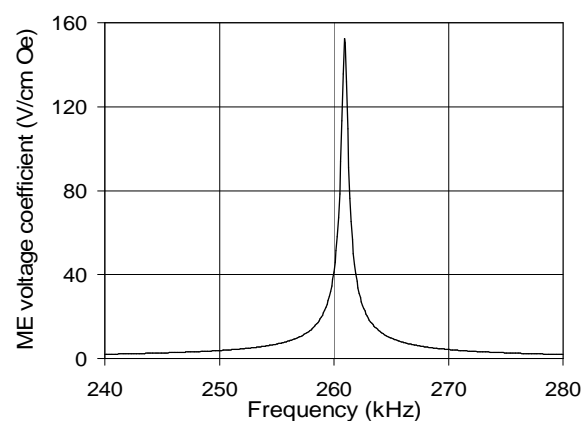


Fig.1. Frequency dependence of  $\alpha_{E,13}$  for the bilayer with  $\nu=0.5$

motion, we obtain a differential equation for the  $x$  projection of the displacement vector of the medium ( $u_x$ ). Taking into account the fact that the trilayer surfaces at  $x=0$  and  $x=L$  are free from external stresses, we find the solution to this equation.

In real structures, there are losses that occur first of all in the contacts. These losses can be taken into account by substituting  $\omega$  for  $\omega' - i\omega''$  with  $\omega''/\omega' = 1/Q$  where  $Q$  is the measured quality factor of EMR. We obtained a very good agreement between theory and data. The investigations carried out have enabled us to establish a relation between efficiencies of the direct and the inverse ME interactions and their frequency dependences.

24RP-H-8

## STUDY OF MULTIFERROIC MANGANITES $RMn_2O_5$ ( $R=Tb, Sm$ ) BY RARE EARTH SPECTROSCOPY

*Chukalina E.P.<sup>1</sup>, Popova M.N.<sup>1</sup>, Pisarev R.V.<sup>2</sup>, Kohn K.<sup>3</sup>*

<sup>1</sup> Institute of Spectroscopy RAS, Troitsk 142190, Moscow region, Russia

<sup>2</sup> Ioffe Physical-Technical Institute of RAS, 194021, St.-Petersburg, Russia

<sup>3</sup> Department of Physics, Waseda University, Tokyo 1698555, Japan

Manganites with the general formula  $RMn_2O_5$  ( $R$ =rare earth, Y, or Bi) demonstrate a strong coupling between lattice, orbital, and magnetic degrees of freedom, which results in a rich variety of phase transitions and of interesting structural, dielectric, magnetic, and magnetoelectric properties depending on a particular  $R^{3+}$  ion. A giant magnetoelectric effect has been observed in  $RMn_2O_5$  with  $R=Eu, Gd, Tb, Dy, Ho, Y,$  and  $Bi$  which is a promising finding in view of possible applications. In particular, magnetically recorded ferroelectric memory on the base of  $TbMn_2O_5$  was reported [1]. Despite intense experimental studies, the detailed nature of the magnetoelectric coupling and observed phase transitions still remains unclear. Atomic displacements giving rise to ferroelectricity were searched for by neutron, X-ray, and Raman experiments. However, no reliable experimental results exist up to now because the displacements are expected to be very small. Another possible mechanism of the ferroelectricity could be the charge transfer transitions between the manganese and oxygen, resulting in a spin polarization of the oxygen sites [2].

To get additional information on subtle changes of the lattice, electronic, and magnetic structures in  $RMn_2O_5$ , we have performed the optical absorption study of the  $f$ - $f$  transitions in  $TbMn_2O_5$  and  $SmMn_2O_5$ . The  $R^{3+}$  ions in the orthorhombic structure of  $RMn_2O_5$  with the space group  $Pbam$  are surrounded by eight oxygen ions and occupy a single fourfold  $C_s$  symmetry position. Relatively narrow lines of the  $f$ - $f$  transitions provide a sensitive probe of the local crystal structure and the local internal magnetic field in a crystal. While  $TbMn_2O_5$  is one of the best studied members of the  $RMn_2O_5$  family, only sparse data on  $SmMn_2O_5$  are available [3].

Single crystals of terbium and samarium manganites were grown by the flux method. For optical measurements, thin platelets cut perpendicular to the  $a$ ,  $b$ , and  $c$  crystallographic axes for  $TbMn_2O_5$  and non-oriented for  $SmMn_2O_5$  single crystals were prepared. Absorption spectra were measured in the temperature range from 1.5 to 300 K in the spectral region 1500-10000  $cm^{-1}$  using a Fourier-transform spectrometer Bruker IFS 125HR.

Temperature dependences of the line positions and intensities in the spectra of  $TbMn_2O_5$  exhibit pronounced peculiarities at the phase transitions found from earlier neutron scattering experiments, specific heat, magnetic, and dielectric measurements. In particular, a splitting of some lines was clearly observed at the ferroelectric transition. Since  $Tb^{3+}$  is a non-Kramers ion, this splitting unambiguously evidences the appearance of new structural positions due to low-symmetry lattice distortions. Unlike the  $Tb^{3+}$  ion,  $Sm^{3+}$  is a Kramers ion, and the observed line splitting in the spectra

of  $\text{SmMn}_2\text{O}_5$  below  $\sim 35$  K points to the magnetic ordering. The data analysis reveals also the existence of several structurally inequivalent positions. This conclusion is in agreement with the  $Pb21m$  space group for manganites at low-temperature with two distinct positions for the rare-earth ion in the unit cell as recently suggested by some authors.

This work was supported in part by the Russian Foundation for Basic Research (Grant №10-02-01071) and by the Russian Academy of Sciences under the Programs for Basic Research.

- [1] N. Hur, S. Park, P.A. Sharma, J.S. Ahn, S. Guha, and S.-W. Cheong, *Nature* **429** (2004) 392.
- [2] Th. Lottermoser, D. Meier, R. V. Pisarev, and M. Fiebig, *Phys. Rev. B*, **80** (2009) 100101(R).
- [3] T. Fujita and K. Kohn, *Ferroelectrics*, **219** (1998) 155.



Wednesday

**24 August**

11:30-13:00

14:30-17:20

oral session

24TL-O

24RP-O

24OR-O

**“High Frequency  
Properties and  
Metamaterials”**

24TL-O-1

## BRILLOUIN SCATTERING OF LIGHT BY SPIN WAVES IN FERROMAGNETIC NANORODS

*Stashkevich A.A.<sup>1</sup>, Roussigné Y.<sup>1</sup>, Djemia P.<sup>1</sup>, Yushkevich Y.<sup>1</sup>, Chérif S.M.<sup>1</sup>, Evans P.R.<sup>2</sup>,  
Murphy A.P.<sup>2</sup>, Hendren W.R.<sup>2</sup>, Atkinson R.<sup>2</sup>, Pollard R.J.<sup>2</sup>, Zayats A.V.<sup>2</sup>*

<sup>1</sup>LSPM CNRS (UPR 3407), Université Paris 13, 93430 Villetaneuse, France

<sup>2</sup>Centre for Nanostructured Media, Queen's University of Belfast, Belfast BT7 1NN, UK

**Summary.** In this talk we discuss the experimental and theoretical aspects of magneto-optical interactions of light with dipole-exchange spin waves (SW) localized on arrays of ferromagnetic metal nanorods (Ni and Co).

**Main text.** Arrays of self-assembled metallic nanorods grown in dielectric matrices are characterised by very rich physics of electromagnetic wave phenomena. Such structures can manifest pronounced plasmonic (in noble metals) behaviour in the visible spectral range [1]. On the other hand, in the case of ferromagnetic materials employed for fabrication of the nanorods (Ni, Co, Permalloy) [2], the nanorod assemblies can be regarded as periodic artificial media featuring magnonic effects, i.e. supporting collective Bloch modes formed from dipole-exchange oscillations localised on individual nanorods [3] or as magnons, the latter term being traditionally applied to the SW of thermal nature. There is consequently a growing research effort in the field of electromagnetic properties of such structures both in optical and microwave frequency bands.

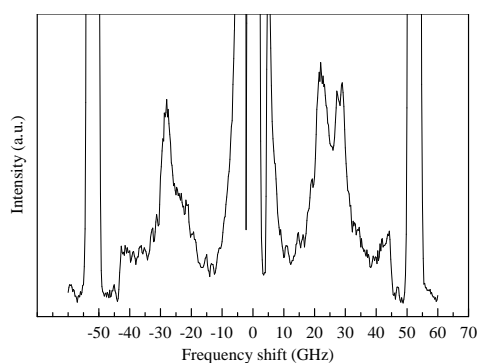


Fig. 1. Typical BLS spectrum.

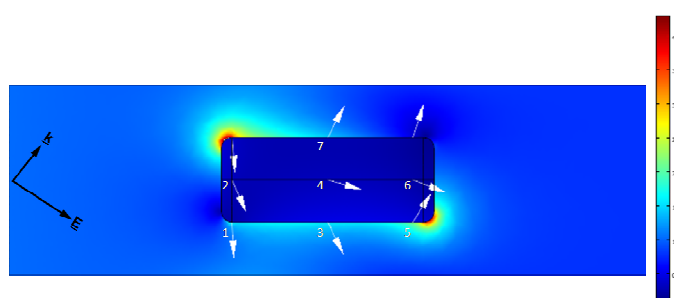


Fig.2. Near-field MO diffraction (finite element simulations).

In the context of this paper, we focus on optical mechanisms underlying magneto-optical (MO) Brillouin light scattering (BLS) mechanisms by magnons with the frequencies in the 3-30 GHz range. Special attention will be paid to the mechanisms of the MO near-field interactions in metal nanoparticles of cylindrical shape. Major experimental effort was realized on Ni and Co nanorods of nanometric size, grown in a  $\text{Al}_2\text{O}_3$  matrix by electrodeposition. Below, among others, are illustrated two features that will be discussed in the context of this talk: a) fine structure and Stokes/anti-Stokes asymmetry of BLS spectral lines (Fig.1), b) Near field pattern of the diffraction of light (Fig.2), leading to the magnetic cylinder being “flown over” by the optical wave, which leads to light penetrating inside from all sides

[1] R. J. Pollard et al, Phys. Rev. Lett. 102, 127405, 2009.

[2] P. Evans et al, Nanotechnology 17, 5746-5753, 2006.

[3] A.A. Stashkevich et al, Phys. Rev. B 80, 144406, 2009.

24OR-O-2

## SPIN-WAVE EXCITATIONS IN FERRITE MAGNONIC CRYSTALS

*Filimonov Yu.<sup>1</sup>, Nikitov S.<sup>2,3</sup>, Pavlov E.<sup>2</sup>, Vysotsky S.<sup>1</sup>*

<sup>1</sup> Kotel'nikov SBIRE RAS, Zelenaya str., 38, Saratov, Russia

<sup>2</sup> Kotel'nikov IRE RAS, Mokhovaya str., 11-7, Moscow, Russia

<sup>3</sup> Saratov State University, Astrakhanskaya str., 83, Saratov, Russia

Spin-wave excitation in 1D and 2D periodic magnetic structures (magnonic crystals (MC)) based on yttrium iron garnet (YIG) films with micron size features and period  $\Lambda$  were investigated by VNA techniques. Both propagating magnetostatic waves (MSW) and localized excitations were studied.

For MSW propagating in MC the clearest feature is Bragg diffraction at surface periodic structure results in arising of forbidden gaps in their spectra. We have investigated collinear Bragg diffraction of surface (MSSW), forward and backward volume MSW in 1D and 2D MC and noncollinear Bragg diffraction of MSSW propagating in 1D MC (depending of angle between the directions of MSSW wave vector and periodic structure's axis). Besides in case of 1D MC spin-wave spectra quantization induced by surface microstructure was observed.

Bragg resonances' formation was investigated depending both on MSW power and condition of propagating. Particularly an influence of MSSW parametric instability processes on forbidden gap's parameters was studied. It was shown that both spatial nonuniformity of dispersion and nonlinear losses induced by parametric instability might destroy the synchronism between incident and reflected MSSW and leads to suppression of Bragg resonances in magnonic crystal. Both transmitted MSSW power and reflected from input transducer microwave power dependencies on incident MSSW power clear demonstrate disappear of Bragg resonances.

Influence of metallization of MC's surface on formation of forbidden gaps was experimentally investigated in case of MSSW propagation in 1D MC. It is well-known that 1) in ferrite-dielectric-metal structure the shape of MSW dispersion curve depends on thickness  $t$  of dielectric layer, 2) MSSW propagating in opposite directions are keep close to different surfaces of ferrite film. In fact it was experimentally proved that decreasing of  $t$  down to  $t < \Lambda/\pi$  leads to disappear of Bragg resonances.

Eigen spin-wave excitations of 2D MC with rhombic and square lattices were experimentally studied depending on both the value of bias tangential magnetic field  $H_0$  and on angle between direction of  $H_0$  and MC's axis. Resonant spin-wave spectra include region I ("angle-independent") and region II where angular dependence of resonances position correlate to symmetry of MC. Using micromagnetic modelling of internal magnetic field's distribution in MCs it was shown that I and II regions can be associated with spin wave excitations of central part of unit cell of MCs and "waveguide-like" parts of unit cell parallel to their axis, respectively.

Support by RFBR (grants # 09-07-00186 and 11-07-00233), Federal Grant-in-Aid Program "Human Capital for Science and Education in Innovative Russia" (governmental contract # П485, 02.740.11.0014 and 14.740.11.0077), Federal Agency of Education of the Russian Federation (project # 2.1.1/2695) and the Grant from Government of Russian Federation for Support of Scientific Research in the Russian Universities Under the Guidance of Leading Scientists (project No. 11.G34.31.0030) is acknowledged.

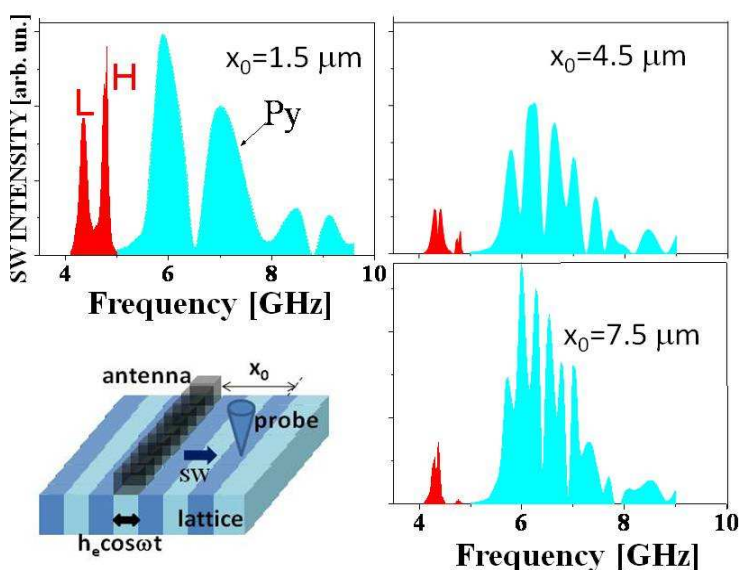
24OR-O-3

## SPIN WAVE PROPAGATION IN LATERAL PERIODIC MAGNETIC STRUCTURES

*Polushkin N.I.*

Instituto Superior Tecnico and ICEMS, Av. Rovisco Pais 1, 1049-001, Lisbon, Portugal

A common feature of periodic systems is the occurrence of stop bands for wave propagation across them. It is pervasive that these bands appear to be very narrow gaps due to Bragg resonances at the Brillouin zone boundaries. Out of the gaps the transparency of a periodic heterogeneous medium, as a rule, is close to that of a uniform one. We find [1] that this general picture is violated in lateral periodic magnetic structures. We show theoretically that an alternating magnetic field applied locally to the structure excites the spin oscillations that propagate across it within narrow ( $\Delta\omega/\omega < 5\%$ ) frequency bands. Only these bands are allowed for the spin-wave (SW) transmission. Our model system is a periodic array of closely packed (without any separation) alternating stripes with two different saturation magnetizations,  $M_1$  and  $M_2$ . Importantly, some realistic systems, notably laser-patterned heterostructures [2], can be employed as prototypes for such a model. By numerical computation of the amplitude-frequency characteristics, we show that, due to the absence of Bragg scattering, the lowest frequency bands, L and H, are comparatively transparent for dipolar spin waves, so that their transparency is substantially higher than that of adjacent higher-frequency bands. In the figure presented here we compare the SW intensity at different distances  $x_0$  from the excitation source in a uniform permalloy (Py) layer with that in a 2.0- $\mu\text{m}$ -period lattice where  $4\pi M_1 = 10.0$  kG, which corresponds to the magnetization of Py, and  $4\pi M_2 = 5.0$  kG. We identify a mechanism that contributes to the narrowing of the transmission bands in our system. This mechanism is associated with the effects of spin pinning at the lateral interfaces. The pinning condition prevents the SW modes from their further transmission across the system, with formation of a potential well in which destructive SW interference occurs. We believe that the features reported here can be of potential interest for developing band-pass magnetic filters that are incorporated into the design of signal processing microwave devices.



Work was supported by the Russian Foundation for Basic Research (grant #07-02-01305) and by the Foundation for Science and Technology in Portugal via the program "Ciencia 2008".

[1] N. I. Polushkin, Phys. Rev. B, **82** (2010) 172405.

[2] N. I. Polushkin et al., Phys. Rev. Lett., **97** (2006) 256401; Phys. Rev. B, **77** (2008) 180401.



## SUPERCRITICAL DYNAMICS OF THREE- BOSON COUPLED EXCITATIONS IN MAGNETS

*Preobrazhensky V.<sup>1,2</sup>, Yevstafyev O.<sup>2,3</sup>, Pernod P.<sup>2</sup>, Bou Matar O.<sup>2</sup>*

Joint International Laboratory LEMAC:

<sup>1</sup> Wave Research Center, A.M. Prokhorov General Physics Institute RAS, 38 Vavilov str., Moscow 119991, Russia

<sup>2</sup> Institute of Electronics, Micro-electronics and Nanotechnology (IEMN-UMR CNRS 8520), PRES University North of France, ECLille, 59651 Villeneuve d'Ascq, France

<sup>3</sup> V. I. Vernadsky Taurida National University, 4, Vernadsky Ave. Simferopol 95007, Ukraine

Magneto-ordered media can be considered as model objects for studies of multi-boson coupled excitations in general physics. Spin subsystem of magnets is strongly nonlinear by nature that favors observation and investigation in details of multi-boson processes on examples of magnons or hybridized magneto-elastic waves (quasi-phonons). Three quasi-phonon coupled excitations were recently predicted and observed experimentally in “easy plane” antiferromagnets (AFEP) under transversal electromagnetic pumping [1,2]. The features of such processes are the explosive instability and spatial localization of excitations with the threshold value of pumping dependent on initial number of bosons. The main restriction for observation of supercritical explosion of excitations at finite time of pumping was found to be nonlinear frequency shift (NFS) of the coupled quasi-phonons. In the present talk the review of the last experimental and theoretical results on supercritical explosive dynamics of quasi-phonons in AFEP  $\alpha$ -Fe<sub>2</sub>O<sub>3</sub> and FeBO<sub>3</sub> is presented. Compensation of NFS effect by the proper choice of the pumping phase modulation allowing observation of supercritical explosion is demonstrated (fig.1)[2]. The anharmonic and strongly nonlinear theories of explosive dynamics of quasi-phonon triads are developed and compared with the experimental results. The theories are generalized on excitation of magnon triads in magnetic films.

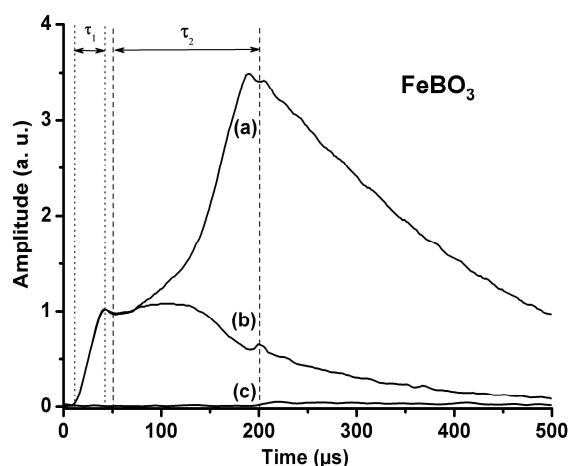


Fig.1 Time dependencies of amplitude of three quasi-phonon supercritical excitations observed in FeBO<sub>3</sub> crystal at 77K: (a) with pumping phase modulation, (b) without modulation, (c) without initial excitation;  $\tau_1$  and  $\tau_2$  are the durations of the initially exciting and pumping pulses respectively.

The work was supported by RFBR (grant 09-02-00602-a), Program of RAS “Acoustic diagnostics of natural media”, French Ministry of Foreign Affairs (Embassy) in Ukraine.

[1] V.Preobrazhensky, O.Bou Matar, P.Pernod. *Phys.Rev.E*. 78 (2008) 046603.

[2] V.Preobrazhensky, O.Yevstafyev, P.Pernod, V.Berzhansky. *JMMM* 322 (2010) 585-588; *JMMM* 323 (2011) 1568-1573.

## EFFECT OF DC BIAS CURRENT ON MAGNETOIMPEDANCE IN AMORPHOUS MICROWIRES

Ipatov M.<sup>1</sup>, Zhukova V.<sup>1</sup>, Gonzalez J.<sup>1</sup>, Zhukov A.<sup>1,2</sup>

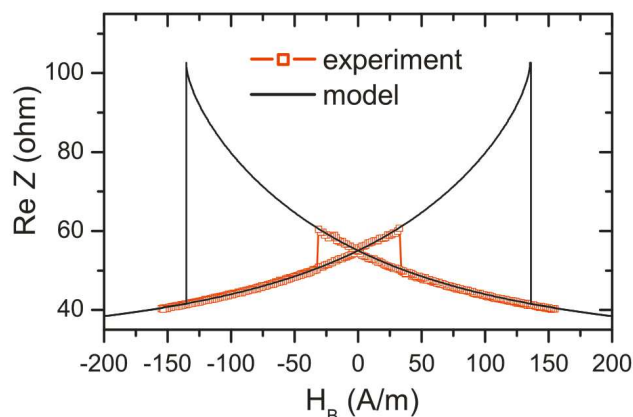
<sup>1</sup> Dpto. Fisica de Materiales, Fac. Quimicas, UPV/EHU, 20018 San Sebastian, Spain

<sup>2</sup> IKERBASQUE, Basque Foundation for Science, 48011 Bilbao, Spain

The magnetoimpedance (MI) effect has received much attention during the last two decade due to its potential for small-size magnetic field sensor applications. This effect is intrinsically related to high magnetic softness and special magnetic anisotropy. In particular, these conditions are fulfilled in magnetically soft amorphous microwires with low and negative magnetostriction constant  $\lambda_s \approx -10^{-7}$  where MI effect more than 500% was observed [1].

The MI effect is usually considered as the dependence of conductor impedance  $Z$  on an applied external magnetic field  $H_E$ . If a static bias current  $I_B$  is applied to the conductor, circumferential bias field  $H_B$  is created inside the conductor. Then, the MI is defined not only by external magnetic field  $H_E$  but also by this internal circumferential static bias field  $H_B$ . Recently we have theoretically and experimentally demonstrated that in a conductor with helical magnetic anisotropy, the high frequency impedance depends on the dc bias current  $I_B$  (or the corresponding bias field  $H_B$ ) and this dependence is hysteretic [2, 3]. We have experimentally observed a change of impedance more than 35% upon changing the bias current (see figure).

Here we present our recent result on investigation of the impedance dependence of magnetically soft microwire on the internal circumferential magnetic field  $H_B$  created by the dc bias current  $I_B$  and discuss the possible applications for this effect.



[1] A. Zhukov and V. Zhukova, *Magnetic Properties and Applications of Ferromagnetic Microwires with Amorphous and Nanocrystalline Structure*, Nova Science, New York, 2009.

[2] M. Ipatov, V. Zhukova, A. Zhukov, and J. Gonzalez, *Appl. Phys. Lett.*, **97** (2010), 252507.

[3] M. Ipatov, V. Zhukova, A. Zhukov, J. Gonzalez, and A. Zvezdin, *Phys. Rev. B*, **81** (2010), 134421.

24OR-O-6

## MAGNETIC PROPERTIES AND MAGNETOIMPEDANCE OF ELECTROPLATED WIRES

*Kurlyandskaya G.V.<sup>1,2</sup>, Jantaratana P.<sup>3</sup>, Bebenin N.G.<sup>4</sup>, Vas'kovskiy V.O.<sup>2</sup>*

<sup>1</sup> University of the Basque Country UPV-EHU, Dept. Electricity and Electronics,  
Campus of Leioa, 48940, Leioa, Spain

<sup>2</sup> Ural State University, Dept. Magnetism and Magnetic Nanomaterials, Lenin Ave. 51, 620083,  
Ekaterinburg, Russia

<sup>3</sup> Kasetsart University, Dept of Physics, Bangkok 10900, Thailand

<sup>4</sup> Institute of metal Physics, UD RAS, Kovalevskaya 18, 620041, Ekaterinburg, Russia

The technology of preparation of composite wires with a thin magnetic electroplated coating was developed long ago being requested by applications of such materials in magnetic memory devices [1]. In 1996 Beach et al [2] have rediscovered these materials for technological applications (low magnetic field sensors) and basic studies of non-linear processes. Later on many attempts were made in order to take into account the domain structure contribution in order to describe giant magnetoimpedance (GMI) behaviour.

Non-linearity of the magnetization processes was proved for different compositions of the electroplated [3] and composite [4] wires by Fourier analysis of the induced voltage (the high harmonics generation) and nonlinear dependence of the induced voltage on the driving current amplitude. It has been established that the high harmonics can show larger variation under application of an external magnetic field than the fundamental one. In order to explain the extraordinary high sensitivity of the harmonics up to an order of the tens of thousands %/Oe various theoretical models were proposed [2-4]. It was shown that for FeCoNi electroplated wires the strong nonlinear effects are consequence of the high value of the transverse susceptibility at the points of re-orientational phase transitions in the magnetic layer and that the high-order magnetic anisotropy may play a key role [3].

In this work, some recent results of the experimental and theoretical studies of physical processes in the electroplated wires with high GMI effect under conditions of strong nonlinearity are discussed. Special attention is paid to model calculations, which demonstrate that taking into consideration magnetic anisotropy of high order, namely, the second order anisotropy is essential. We also discuss some new applications of the GMI electroplated wires as sensitive elements of a small magnetic field detector for biosensing and non-destructive testing.

Support by SAIOTEK MAGNOSEN and ACTIMAT Grants is acknowledged.

[1] B.D. Cullity, Introduction to Magnetic Materials, Addison-Wesley, Reading, MA, USA, 1972.

[2] R.S. Beach, N. Smith, C.L. Platt, F. Jeffers, A.E. Berkowitz, *Appl. Phys. Lett.* **68** (1996) 2753.

[3] G.V. Kurlyandskaya, H. Yakabchuk, E. Kisker, N.G. Bebenin, H. García-Miquel, M. Vazquez, V.O. Vas'kovskiy, *J. Appl. Phys.* **90** (2001) 6280.

[4] A.S. Antonov, N.A. Buznikov, A.F. Prokoshin, A.L. Rakhmanov, I.T. Iakubov, A.M. Yakunin, *Technical Physics Letters*, **27** (2001), 313.

24TL-O-7

## PRECISE PROBING SPIN WAVE DYNAMICS IN CIRCULAR MAGNETIC DOTS

*Aliev F.G.<sup>1\*</sup>, Awad A.A.<sup>1</sup>, Guslienko K.Y.<sup>2</sup>, Dieleman D.<sup>1</sup>, Lara A., Metlushko V.<sup>3</sup>*

<sup>1</sup> Dpto. Física de la Materia Condensada, CIII, Universidad Autónoma de Madrid, 28049 Madrid, Spain

<sup>2</sup> Dpto. Física de Materiales, Universidad del País Vasco, 20018 Donostia-San Sebastian, Spain

<sup>3</sup> Dept. of Electrical and Computer Engineering, University of Illinois at Chicago, Chicago, Illinois, USA

(\*) farkhad.aliev@uam.es

Vortices are encountered many natural systems ranging from galaxies to superconductors and superfluids. Spin wave dynamics in Permalloy dots with magnetic vortex and situated in the applied external in-plane magnetic field could be considered as a simple toy model to investigate dynamics of single vortex state in the confined stratified media.

First we discuss dependence of spin wave modes excited by in-plane magnetic field on dots aspect ratio [1]. The frequency splitting of two lowest azimuthal modes was observed and described by dynamic splitting model accounting the spin waves and vortex gyrotropic mode interaction [2]. Secondly, we describe precise measurements of spin dynamics in the vortex state of the circular magnetic dots by exciting spins in different in-plane directions with respect to applied in-plane bias magnetic field [3]. Spin wave dynamics was measured using FMR-VNA technique [4,5]. We unambiguously demonstrate experimentally and by micromagnetic simulations the existence of two distinct dynamic vortex (stable and metastable) regimes. Dynamic response in the metastable state strongly depends on relative orientation of the external rf pumping and bias magnetic fields. Parallel rf pumping is shown to be unique tool to observe spin excitation modes localized near the strongly shifted vortex core for the bias field between the vortex nucleation and annihilation fields. Meanwhile, the perpendicular rf pumping which excites the spin waves throughout the entire dot, reveals crossover between two dynamic vortex regimes near the nucleation field. Finally, we shall present preliminary results on spin wave dynamics of dipolar (20nm separation) or exchange (0.9nm separation) vertically coupled Py dots.

Our findings open new possibilities for development of magnetic devices with precise control over the magnetization switching process. They also underscore importance of understanding of dynamic response in different nanostructured materials with vortices in confined and stratified conditions.

[1] A. Awad, et al., *Appl. Phys. Lett.*, **96**, 012503 (2010).

[2] K.Guslienko, et al., *Phys. Rev. Lett.*, **101**, 247203 (2008).

[3] F.G. Aliev, et al., *Phys. Rev.* **B79**, 174433 (2009).

[4] J. F. Sierra, et al., *Appl. Phys. Lett.*, **93**, 172510 (2008).

[5] J. F. Sierra, et al., *Appl. Phys. Lett.*, **94**, 012506 (2009).

24OR-O-8

## LOW TEMPERATURE FMR IN THE SYSTEM OF NON-INTERACTING MAGNETIC NANODISKS

*Nedukh S.<sup>1</sup>, Tarapov S.<sup>1</sup>, Belozorov D.<sup>2</sup>, Kakazei G.<sup>3</sup>, Kharchenko A.<sup>1</sup>*

<sup>1</sup> Institute of Radiophysics and Electronics NAS of Ukraine, 12 Ac. Proskura St., Kharkov, 61085, Ukraine

<sup>2</sup> National Scientific Center - "Kharkov Institute of Physics and Technology", 1, Akademicheskaya St., Kharkov, 61108, Ukraine

<sup>3</sup> IFIMUP-IN/Department of Physics, University of Porto, Rua do Campo Alegre, 687, Porto, 4169-007, Portugal

The main direction of developing the contemporary microelectronics is the miniaturization and reducing of energy consumption. The spintronic is one such a promising directions. However, now the development of spintronic is impossible without the magnetic materials usage. Thus the investigation of the magnetic properties of micro-and nanoscale magnetic is an important and actual task.

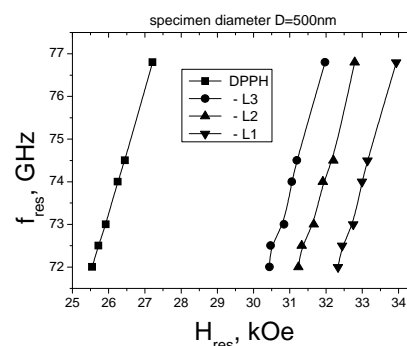
This paper elucidates the experimental study of magnetodynamic properties of systems of magnetic micron-size nanodisks in the microwave range at low temperatures.

Several systems of permalloy nanodisks deposited onto a glass substrate have been studied. In the each system, the distance between the disks is equal to twice the diameter. Disks diameters ( $D$ ) were: 4000nm, 2000nm, 1500nm, 1000nm, 500 nm, 250nm. The thickness of every specimen equals to 40 nm. This ratio between the disk diameter and the distance between the disks allowed us to explore both the ensemble of weakly interacting disks (for  $D=250$  nm, 500 nm) as well as the array of almost non-interacting microdisks ( $D=4000\text{nm}-1500\text{nm}$ ).

The magnetoresonance investigations were performed in 70-80 GHz frequency band and at a temperature of 4.2 K. The static external magnetic field was applied perpendicularly to the disks array.

As a result the magnetoresonance absorption spectra, containing not only the fundamental mode but the modes corresponding to spin waves has been obtained. The resonance frequency-field dependence for the specimen with  $D = 500$  nm is shown in the figure.

A comparative analysis of the results obtained with the X-band results executed at  $T = 300\text{K}$  [1] is performed.



Research were partially supported by STCU Project #5210

[1] G.N. Kakazei, T. Mewes, P.E. Wigen et al. J. Nanoscience and Nanotechnology, **8** (2008) 281

24RP-O-9

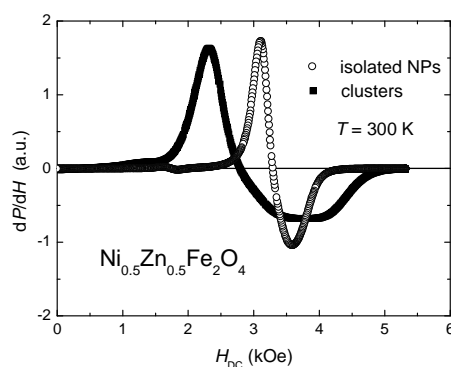
## MICROWAVE ABSORPTION IN NANOSTRUCTURED FERRITES

Valenzuela R.<sup>1</sup>, Herbst F.<sup>2</sup>, Ammar S.<sup>2</sup>

<sup>1</sup> Departamento de Materiales Metálicos y Cerámicos, Instituto de Investigaciones en Materiales, Universidad Nacional Autónoma de México, 04510, México

<sup>2</sup> ITODYS, UMR-CNRS 7086, Université de Paris-Diderot, 75205 Paris, France

Ferrite nanoparticles (NPs) of composition  $\text{Zn}_{0.5}\text{Ni}_{0.5}\text{Fe}_2\text{O}_4$  were synthesized by forced hydrolysis in polyol from the corresponding zinc, nickel and iron acetates. By varying the preparation conditions, different aggregation states were obtained, ranging from isolated nanoparticles with average diameter of 5-8 nm, to clusters of some 50 nm, formed as well by nanoparticles with average diameter in the 5-8 nm range. X-ray diffraction (XRD) characterization showed a single spinel phase well crystallized in all cases. High-resolution transmission electron microscopy (HRTEM) confirmed that depending on preparation conditions, this method allows the preparation of isolated nanoparticles, as well as clusters made of a few hundreds of NPs. Additionally, HRTEM showed that there is an epitaxial arrangement of nanoparticles within clusters; i.e., there is a good agreement of crystal planes between neighboring nanoparticles.



The ferromagnetic resonance (FMR) of samples was investigated in the X-band (9.45 GHz) at 77 K and at room temperature. The resonance field for isolated samples exhibited a lower value than that for clusters; this difference in resonance field can be attributed to the epitaxial character of clusters, which increases the internal field in the clusters. The opposite was observed for resonance linewidths; clusters exhibited very broad linewidths as compared with isolated NPs. Such broadening of resonance lines can be interpreted in terms of a random distribution of the anisotropy axes. Isolated NPs, in contrast, are essentially superparamagnetic, as revealed by magnetization measurements. These results are discussed.

Partial support by a ANR (France)-CONACyT (Mexico) grant is acknowledged

24OR-O-10

## ANTIFERROMAGNETIC RESONANCE AND MAGNETIC INVESTIGATIONS OF RARE-EARTH FERROBORATES

*Tugarinov V.<sup>1</sup>, Pankrats A.<sup>1,2</sup>, Petrakovskii G.<sup>1,2</sup>, Kondyan S.<sup>2</sup>, Velikanov D.<sup>1</sup>, Temerov V.<sup>1</sup>*

<sup>1</sup>L.V. Kirensky Institute of Physics SB RAS, 660036, Krasnoyarsk, Russia

<sup>2</sup>Siberian Federal University, 660041, Krasnoyarsk, Russia

The borate compounds with general formula  $RA_3(BO_3)_4$  ( $R^{3+}$  - rare-earth ion or  $Y^{3+}$  and  $A=Al, Ga, Sc, Cr, Fe$ ) have attracted considerable attention as materials for nonlinear optics and laser technics. They crystallize in the trigonal crystal system and have the structure of the *huntite* mineral with high-temperature space group  $R\bar{3}2$ , which transforms to  $P3_121$  with temperature decreasing for the crystals with small ionic radius of the  $R^{3+}$ . Many  $RFe_3(BO_3)_4$  crystals are multiferroics. The  $RA_3(BO_3)_4$  crystals have interesting magnetic properties due to an interaction between subsystems of  $Fe^{3+}$  and  $R^{3+}$  magnetic ions. In the present work we present data on antiferromagnetic resonance (AFMR), magnetic properties, heat capacity and magnetic phase diagrams of  $GdFe_3(BO_3)_4$ ,  $GdFe_{2.1}Ga_{0.9}(BO_3)_4$ ,  $EuFe_3(BO_3)_4$  and  $Pr_{1-x}Y_xFe_3(BO_3)_4$  system with  $x=0\div 1$ .

The AFMR investigations of pure  $GdFe_3(BO_3)_4$  showed [1] that the competition of  $Fe^{3+}$  and  $Gd^{3+}$  contributions to total magnetic anisotropy of the crystal results in spontaneous reorientation at  $T=10$  K between states with “easy plane” (EP) and “easy axis” (EA) anisotropy. EP magnetic ordering occurs at the Neel temperature  $T_N=38$  K. Magnetic phase diagram was constructed from AFMR and magnetic measurements.

Diamagnetic substitution of  $Fe^{3+}$  leads to decreasing of the Néel temperature in  $GdFe_{2.1}Ga_{0.9}(BO_3)_4$  to  $T_N=16.3$  K. From magnetic and AFMR data the magnetic phase diagram was constructed. It follows from the data that the spontaneous reorientation does not occur in Ga-substituted ferroborate and the crystal remains easy-axis in a whole ordering area.

The investigations of magnetic and resonance properties of  $Pr_{1-x}Y_xFe_3(BO_3)_4$  system showed the following: the crystal with  $x=1$  ( $YFe_3(BO_3)_4$ ) is an easy-plane antiferromagnet [2], the AFMR investigations of the crystal with  $x = 0$  ( $PrFe_3(BO_3)_4$ ) crystal confirm that it is an easy-axis antiferromagnet in all temperature range below  $T_N=32$  K [3]. The energy gap  $\nu_c=130$  GHz allow to estimate the Pr contribution to total magnetic anisotropy as exceeding almost two times the Fe one in magnitude.

A dilution of the  $Pr^{3+}$  subsystem by diamagnetic yttrium reduces the anisotropy of the subsystem and can lead to a spontaneous transition from EA to EP state at some yttrium content. The single crystals  $Pr_{1-x}Y_xFe_3(BO_3)_4$  with yttrium content  $x=0.25, 0.5$  and  $x=0.75$  were grown. Magnetic and resonance investigations show that the crystal with  $x = 0.25$  is EA antiferromagnet with the energy gap close to 75 GHz at  $T=4.2$  K but the crystals with  $x=0.5$  and  $0.75$  are EP one.

The crystal  $EuFe_3(BO_3)_4$  is EP antiferromagnet throughout the temperature range below the Neel temperature. AFMR data show that the energy gap is about 120 GHz at  $T=4.2$  K, which is close to the value of the gap in the yttrium ferroborate. Thus, the contribution of rare-earth subsystem to the magnetic anisotropy is negligible in Eu ferroborate.

Thus, the value of the total magnetic anisotropy depends strongly on the type of the rare-earth ion, which determines the magnetic structure of the crystal.

Work is supported by RFBR grant 10-02-00765.

[1] A.I. Pankrats, G.A. Petrakovskii, L.N. Bezmaternyh, O.A. Bayukov, JETP, 126, 887 (2004).

[2] A.I. Pankrats, G.A. Petrakovskii, L.N. Bezmaternyh, V.L. Temerov, FTT 50, 77 (2008).

[3] A. M. Kadomtseva, Yu. F. Popov, G. P. Vorob'ev etc., JETP Lett., 87, 45 (2008).

24OR-O-11

## MAGNETIC RESONANCE IN STRONGLY CORRELATED METALS

Demishev S.V.<sup>1</sup>, Semeno A.V.<sup>1</sup>, Bogach A.V.<sup>1</sup>, Glushkov V.V.<sup>1</sup>, Lapa P.N.<sup>1</sup>, Samarina N.A.<sup>1</sup>,  
Ishchenko T.V.<sup>1</sup>, Filipov V.B.<sup>2</sup>, Shitsevalova N.Yu.<sup>2</sup>, Sluchanko N.E.<sup>1</sup>

<sup>1</sup> A.M. Prokhorov General Physics Institute of RAS, Vavilov street, 38, 119991 Moscow, Russia

<sup>2</sup> Institute for Problems of Materials Science of NASU, 3, Krzhizhanovsky Str., Kiev 03680, Ukraine

Studying of the magnetic resonance in strongly correlated metals (SCM) has recently attracted much attention [1-3]. These systems are characterized by strong spin fluctuations, which should broaden the resonance line to practically undetectable values [1]. Therefore any observation of the magnetic resonance in this class of materials is very unusual. For experimental study of the ESR in SCM we proposed new experimental procedure of absolute calibration of the resonant magnetoabsorption line [4,5] which allows finding full set of the resonant parameters, namely the dynamic magnetization  $M_0$ ,  $g$ -factor and the line width,

whereas in the standard approach only two latter quantities can be found. The developed approach implies special geometry of the cavity experiment [4,5] excluding effects of inhomogeneity of the magnetic field in the sample due to demagnetization factor. This technique has been verified in the case of  $\text{EuB}_6$  [4], where good coincidence between measured and simulated ESR line shapes in the range 9-100 GHz is obtained. The suggested experimental method was applied to the case of the ESR in  $\text{CeB}_6$ , where magnetic resonance is specific to the phase II (so-called antiferro-quadrupole phase) was studied. It is found that approaching to the phase II-paramagnetic phase (phase I) transition temperature  $T_{\text{I-II}}$  results in strong broadening of the resonance (the line width increases 3 times in the range  $1.8 \leq T \leq 3.8$  K) whereas  $g$ -factor  $g=1.59$  remains temperature independent. The ESR data suggests that the magnetization of  $\text{CeB}_6$  in the phase II consists of several contributions, one of which,  $M_0$ , is responsible for the observed magnetic resonance. This term in magnetization is missing in the paramagnetic phase and corresponds to *ferromagnetically* interacting localized magnetic moments (LMMs) in agreement with the theoretical predictions [2-3], although total magnetization  $M$  shows *antiferromagnetic* correlations (fig. 1). Determination of  $M_0$  allows finding saturation magnetization and corresponding quantum number  $J$  for the oscillating LMMs (fig. 1). We obtained  $J=1/2$  for  $\text{CeB}_6$ , which suggests that the ground state of  $\text{Ce}^{3+}$  ion is  $\Gamma_7$  rather than  $\Gamma_8$ . Thus the antiferro-quadrupole model of orbital ordering contradicts to the experimental data on the magnetic resonance in  $\text{CeB}_6$ , and development of the theory of static and dynamic magnetic properties of this heavy fermion metal appears on the agenda.

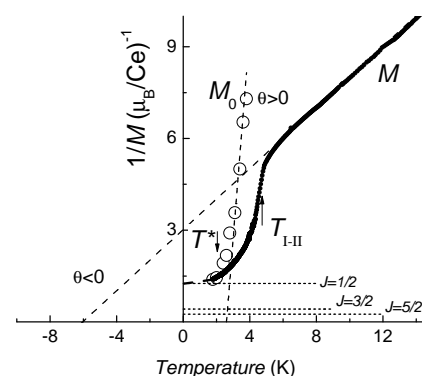


Fig. 1. Magnetisation structure of the phase II of  $\text{CeB}_6$  (60 GHz cavity experiment).

The ESR data suggests that the magnetization of  $\text{CeB}_6$  in the phase II consists of several contributions, one of which,  $M_0$ , is responsible for the observed magnetic resonance. This term in magnetization is missing in the paramagnetic phase and corresponds to *ferromagnetically* interacting localized magnetic moments (LMMs) in agreement with the theoretical predictions [2-3], although total magnetization  $M$  shows *antiferromagnetic* correlations (fig. 1). Determination of  $M_0$  allows finding saturation magnetization and corresponding quantum number  $J$  for the oscillating LMMs (fig. 1). We obtained  $J=1/2$  for  $\text{CeB}_6$ , which suggests that the ground state of  $\text{Ce}^{3+}$  ion is  $\Gamma_7$  rather than  $\Gamma_8$ . Thus the antiferro-quadrupole model of orbital ordering contradicts to the experimental data on the magnetic resonance in  $\text{CeB}_6$ , and development of the theory of static and dynamic magnetic properties of this heavy fermion metal appears on the agenda.

The work was supported by the Programme of the Russian Academy of Sciences “Strongly correlated electrons” and by the Federal Programme “Scientific and Educational Human Resources of Innovative Russia”.

- [1] J. Sichelschmidt, et al., *Phys. Rev. Lett.*, **91** (2003) 156401.
- [2] E. Abrahams and P. Wölfle, *Phys. Rev. B*, **78** (2008) 104423.
- [3] P. Schlottmann, *Phys. Rev. B*, **79** (2009) 045104.
- [4] A.V. Semeno, et al., *Phys. Rev. B*, **79** (2009) 014423.
- [5] S.V. Demishev, et al., *Phys. Rev. B*, **80** (2009) 245106.



Wednesday

**24 August**

17:30-19:00

poster session

24PO-I1

**“Magnetostructural  
Transition Related  
Effects”**

24PO-I1-1

## MAGNETOCALORIC EFFECT IN Ni-Mn-In BASED HEUSLER ALLOYS: DIRECT MEASUREMENTS OF ADIABATIC CHANGES OF TEMPERATURE NEAR PHASE TRANSITIONS

*Prudnikov V.N.<sup>1</sup>, Saletsky A.M.<sup>1</sup>, Kazakov A.P.<sup>1</sup>, Dubenko I.S.<sup>2</sup>, Granovsky A.B.<sup>1,3,4</sup>,  
Konovalov P.N.<sup>1</sup>, Ivanova O.S.<sup>1</sup>, Prudnikova M.V.<sup>1</sup>, Pathak A.K.<sup>2</sup>, Ali N.<sup>2</sup>, Zhukov A.P.<sup>3,4</sup>*

<sup>1</sup> Moscow State University, Moscow, 119991, Russian Federation

<sup>2</sup> Southern Illinois University Carbondale, IL, 62901, USA

<sup>3</sup> Basque Country University, 20080 San Sebastian, Spain

<sup>4</sup> Ikerbasque, Basque Foundation for Science, 48011, Bilbao, Spain

The magnetic materials that exhibit large magnetocaloric effects (MCE), i.e. ability to absorb or produce heat as the result of the application of external magnetic fields (H), are of significant interest because of their potential impact for application in new ecological refrigeration devices. Besides, MCE can be considered as a probe of phase transformations. The MCE originates from the change in magnetization induced by the magnetic field, and characterized by a change in magnetic entropy  $\Delta S_M$  and, therefore, in the temperature  $\Delta T_{ad}$  of the sample. Magnetic systems that undergo field-induced phase transitions, characterized by large, sharp changes in magnetization near or above room temperature, are of considerable interest as promising MCE materials. One such system is the off-stoichiometric  $Ni_{50}Mn_{50-x}In_x$  Heusler alloys in the vicinity of  $x=15$ . These alloys exhibit a temperature-induced first-order structural phase transition (at  $T_M$ ) from a high-temperature austenitic phase with cubic  $L2_1$  or  $B_2$  crystal structure, to a low-temperature martensitic phase, characterized by a crystal cell of lower symmetry. Large negative (normal) and positive magnetic entropy changes  $\Delta S_M$ , attributed to the first- (at  $T_M$ ) and second-order transitions (at  $T_C$ ), correspondingly, were observed in these materials near room temperature ([1,2] and references therein). However, most studies were concentrated on the  $\Delta S_M$  evaluation from isothermal magnetizations measurements but not on the direct measurements of adiabatic changes in temperature  $\Delta T_{ad}$ .

We studied the adiabatic temperature changes  $\Delta T_{ad}$  in the vicinity of the Curie ( $T_C$ ) and martensitic ( $T_M$ ) transition temperatures of  $Ni_{50}Mn_{35}In_{15}$  and  $Ni_{50}Mn_{35}In_{14}Z_1$  ( $Z=Al$  and  $Ge$ ) Heusler alloys using the updated adiabatic magnetocalorimeter MagEq MMS in (250-350) K temperature interval for applied magnetic field changes up to  $\Delta H=1.8$  T. We improved software of this set up to handle experimental data automatically. The largest measured changes were  $\Delta T_{ad} = -2K$  and  $2K$  near the martensitic (first order) and ferromagnetic (second order) transitions for  $\Delta H=1.8$  T, respectively. It was observed that  $\Delta T_{ad} = 1$  K for relatively small changes in  $\Delta H=1$  T for both types of transitions. It was shown that the characteristic temperatures of phase transitions and the temperature ranges of large  $\Delta T_{ad}$  can be tuned in quaternary alloys  $Ni_{50}Mn_{35}In_{14}Z_1$  by varying  $Z$ . Therefore these materials should be further explored as potential working materials in magnetic refrigeration applications.

This research was supported by the Russian Foundation for Basic Researches, by the Basque Foundation for Science, by the Office of Basic Energy Sciences, Material Sciences Division of the U. S. Department of Energy.

[1] I. Dubenko, M. Khan, A. K. Pathak et al., *J.Magn.Magn.Mat.*, **321** (2009) 754.

[2] S. Aksoy, T. Krenke, M. Acet et al., *Appl. Phys. Lett.*, **91** (2007) 241916.

24PO-I1-2

## MAGNETOCALORIC EFFECT IN MANGANITES

Koroleva L.I.<sup>1</sup>, Zashchirinskii D.M.<sup>1</sup>, Morozov A.S.<sup>1</sup>, Szymczak R.<sup>2</sup>

<sup>1</sup> M.V. Lomonosov Moscow State University, Vorobyevy gory, Moscow 119992, Russia

<sup>2</sup> Institute of Physics of PAS, ul.Lotnicov 32/46, Warsaw 02668, Poland

Magnetocaloric effect (MCE) was studied in  $\text{La}_{1-x}\text{Sr}_x\text{MnO}_3$ ,  $\text{Sm}_{0.55}\text{Sr}_{0.45}\text{MnO}_3$  and  $\text{PrBaMn}_2\text{O}_6$  manganites. It has been found that the maximum value of MCE, measured by direct method, is far less than is obtainable by computation from the change of the magnetic entropy in Curie temperature. This phenomenon is explained by presence in above listed manganites of the magnetic two-phase ferromagnetic – antiferromagnetic state. So in  $\text{La}_{1-x}\text{Sr}_x\text{MnO}_3$  the negative contribution from the lesser antiferromagnetic portion of sample lowers the summary MCE and modifies of  $\text{MCE}(T)$  curve form displacing its maximum to the better temperature than Curie point on 20-30 K. At the same time the cooling in the oxygen atmosphere of the  $\text{Sm}_{0.55}\text{Sr}_{0.45}\text{MnO}_3$  single-crystal sample, which restores the Mn-V-Mn broken connections and in doing so increases in it the summary volume of clusters with the CE-type antiferromagnetic order, results to that the maximum on  $\text{MCE}(T)$  curve is disposed at the Neel temperature of clusters with the CE-type antiferromagnetic order (243 K) and not into Curie point of ferromagnetic clusters (134 K). Magnetic field, applied to sample at MCE measurement, transfers these antiferromagnetic clusters in ferromagnetic state and in Neel temperature both are destroyed. At the same time the maximum on  $\text{MCE}(T)$  curve of  $\text{Sm}_{0.55}\text{Sr}_{0.45}\text{MnO}_3$  is disposed near Curie point in the cooling in the air single-crystal sample and ceramic sample. The  $\text{PrBaMn}_2\text{O}_6$  manganite has the layer crystalline structure with A-site ordering. (Here A = Pr, Ba) [1]. In compound with the 95% mentioned ordering the two phase transactions take place: paramagnetic – antiferromagnetic at  $T_C = 295$  K and ferromagnetic – antiferromagnetic at  $T_N = 231$  K. Phase with spontaneous magnetization obtains the understated magnetic moment. in comparison to that would be at ferromagnetic ordering of moments  $\text{Mn}^{3+}$ ,  $\text{Mn}^{4+}$  and  $\text{Pr}^{3+}$  ions. The curve  $\text{MCE}(T)$  measured in magnetic field 14,2 kOe has two extremes: the wide maximum around 291 K (near  $T_C$ ) and the sharp minimum at 234 K (near  $T_N$ ). But the MCE-values in both extremes are small: 0,13 K in maximum and 0,2 K in minimum. This is connected with the presence of antiferromagnetic interactions in the ferromagnetic phase and ferromagnetic interactions in antiferromagnetic phase.

So the understated values of MCE of manganites received by straight method evidence about the presence in its of magnetic two phase ferromagnetic – antiferromagnetic state. The presence in manganites of the colossal magnetoresistance and the giant volume magnitostriktion [2] point out that this magnetic two-phase state provokes by strong *s-d* exchange and consists from the insulating antiferromagnetic phase and the ferromagnetic phase in which the charge carriers are concentrated.

Authors is acknowledged to A.M. Balbashov and A.R. Kaul for the preparation of samples and their analysis.

[1] T. Nakajima, H. Kageyama and Y. Ueda, *J. Phys. Chem. Solids*, **63** (2002) 913.

[2] L.I. Koroleva. *Magnetic Semiconductors*. Publ.Phys.Dept MSU (2003) (In russian).

## THEORETICAL STUDY OF TWINS' BOUNDARY MOTION IN HEUSLER Ni-Mn-Ga ALLOYS BY MONTE CARLO METHOD

*Kostromitin K.I.<sup>1</sup>, Buchelnikov V.D.<sup>1</sup>, Sokolovskiy V.V.<sup>1</sup>, Entel P.<sup>2</sup>*

<sup>1</sup> Faculty of Physics, Chelyabinsk State University, Br. Kashirinykh Str., 129, 454001, Russia

<sup>2</sup> Faculty of Physics and CeNIDE, University of Duisburg-Essen, 47048, Duisburg, Germany

In this work we present a theoretical model for description of twins' boundary moving of Heusler Ni-Mn-Ga alloys in an external magnetic field by Monte Carlo technique. In the proposed model, we consider a two-dimensional lattice with open boundary conditions and with interaction between nearest neighbors in magnetic and structural subsystems. We do not consider Ni and Ga atoms because of their magnetic moment are much more less then magnetic momentum of Mn atoms. For description of magnetic and structural parts we have chosen the classical Ising model with magnetostructural interaction. We consider only two variants of low-temperature martensite. The total Hamiltonian can be written as

$$H = -J_{mag} \sum_{\langle i,j \rangle} S_i S_j - J_{el} \sum_{\langle i,j \rangle} \sigma_i \sigma_j - U \sum_{\langle i,j \rangle} \sigma_i S_i S_j - g \mu_B H_{ext} \sum_i S_i$$

Here,  $J_{mag}$  and  $J_{el}$  are exchange constants in magnetic and structural subsystems;  $S_i$  is a spin variable;  $\sigma_i$  is a microdeformation variable, values  $\sigma_i = \pm 1$  correspond to two martensitic variants;  $U$  is a magnetoelastic constant;  $H_{ext}$  is the external magnetic field;  $g$  is the Lande factor;  $\mu_B$  is the Bohr magneton. Sums are performed over all nearest-neighbor pairs. In our model the coordination number is equal four. In the Hamiltonian the first and second terms describe interactions in the magnetic and structural subsystem, the third term characterizes the magnetoelastic interaction, and, finally, the last term shows an influence of an external field.

The Monte Carlo simulations have been carried out using the standard Metropolis algorithm. The number of sites in the lattice was equal to  $N=500$ . As the time unit we used one Monte Carlo step, which is consisting in  $N$  attempts of the change  $S_i$  and  $\sigma_i$  variables. For given the temperature, the number of Monte Carlo steps on each site varies from  $10^3$ . The martensitic phase consists of five twin variants with spin  $S_i = \pm 1$  and strain  $\sigma_i = \pm 1$ .

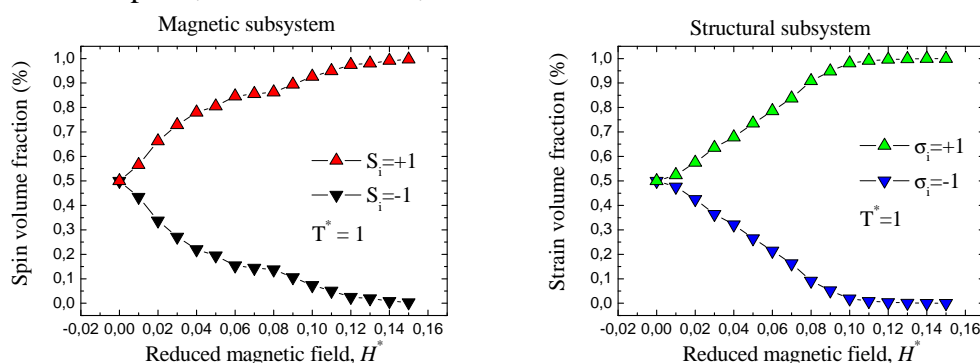


Fig. 1. The magnetic field dependencies of the spin and strain volume fractions at different temperatures.

It is shown that an applying of the magnetic field leads to moving of twins' boundary (Fig.1). An unfavourable martensitic variant passed in another variant, which has the same direction as an external field. The theoretical results have the same trend as experimental observations [1].

Support by RFBR grants 10-02-96020-r-ural, 11-02-00601, 10-02-92110 is acknowledged.

[1] A.A. Likhachev, K. Ullakko, Physics Letters A 275, 142–151 (2000).

## MAGNETOCALORIC EFFECT IN (Tb, Dy, Gd)Co<sub>2</sub> MULTICOMPONENT COMPOUNDS WITH HIGH-PURITY RARE-EARTH METALS

*Tereshina I.<sup>1</sup>, Politova G.<sup>1</sup>, Burkhanov G.<sup>1</sup>, Chistyakov O.<sup>1</sup>, Chzhan V.<sup>1</sup>, Cwik J.<sup>2</sup>, Zaleski A.<sup>3</sup>, Palewski T.<sup>2</sup>, Drulis H.<sup>3</sup>*

<sup>1</sup> Baikov Institute of Metallurgy and Material Science RAS, Moscow, Russia

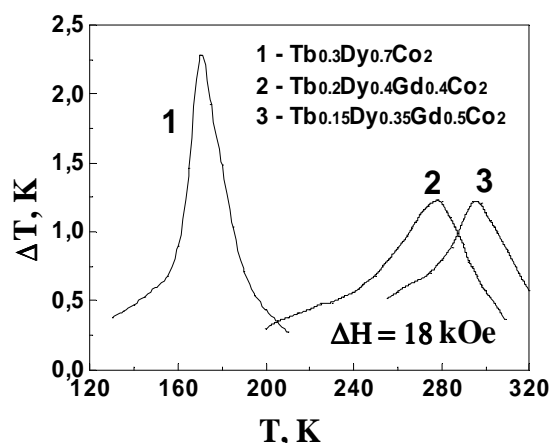
<sup>2</sup> International Laboratory of High Magnetic Fields and Low Temperatures, Wroclaw, Poland

<sup>3</sup> Institute of Low Temperatures and Structural Researches, Wroclaw, Poland

Up to date, the search for new materials for magnetic refrigeration exhibiting large magnetocaloric effect (MCE) at temperatures ranging from the lowest up to those well above the room temperature, is one of the important tasks of applied physics [1-3]. In the present work, the investigation was carried out among the multicomponent compounds of the RCo<sub>2</sub> type. A series of Tb<sub>x</sub>Dy<sub>y</sub>Gd<sub>z</sub>Co<sub>2</sub> ( $x + y + z = 1$ ) single-phase alloys was prepared by arc-melting using the high purity rare-earth metals with a simultaneous control of metallic and aerogenic impurities. The study was aimed at the following goals. (i) Reliable data collected with the use of high-purity samples. (ii) Determination of the alloys with the optimal characteristics by varying the composition within the rare-earth sublattice. (iii) Comprehensive investigation of magnetic and thermal properties (MCE, specific-heat and magnetization experiments) of the compounds under study. The measurements of the magnetocaloric effect were performed by a direct method. The specific-heat and magnetization experiments were carried out by a standard relaxation method on PPMS installation (Quantum Design, USA).

Figure shows the temperature dependence of MCE for selected Tb<sub>x</sub>Dy<sub>y</sub>Gd<sub>z</sub>Co<sub>2</sub> compounds. In Tb<sub>0.3</sub>Dy<sub>0.7</sub>Co<sub>2</sub>, MCE is observed at  $T = 170$  K, where the first-order transition from paramagnetic into a magnetically-ordered state takes place (the type of the magnetic phase transitions was examined in terms of Landau theory), and it consists of 2.3 K adiabatic temperature change under the magnetic field variation from 0 up to 18 kOe.

Partial substitution of Tb and Dy ions for Gd leads to 1) a considerable increase of the Curie temperature; 2) changes the magnetic phase transition type from the first to the second one; 3) results in a two-fold decrease of the MCE value. As it is also seen from the picture, the MCE value is less sensitive to the Gd content change in the concentration range  $0.4 \leq z \leq 0.5$  than the Curie temperature of the compounds. Therefore, the investigated Gd-containing alloys, which possess large magnetization and a considerable MCE in the vicinity of the room temperature, deserve attention as potential cooling agents for magnetic refrigeration.



The work is supported by RFBR, project No. 10-03-00848.

[1] A.S. Andreenko, K.P. Belov, S.A. Nikitin, A.M. Tishin., *Sov. Phys. VSP* **32** (1989) 649

[2] K.A. Gschneidner, V.K. Pecharsky, A.V. Tsokol., *Rep.Progr.Phys.* **68** (2005) 1479

[3] A.M. Tishin, Y.I. Spichkin., *The magnetocaloric effect and its applications* Institute of Physics Publishing, Bristol, Philadelphia (2003) 475 p.

## A NOVEL FAMILY OF GLASS-COVERED MICROWIRES: Ni-Mn-In HEUSLER ALLOYS

Mikhailovsky Yu.O.<sup>1</sup>, Kazakov A.P.<sup>1</sup>, Prudnikov V.N.<sup>1</sup>, Granovsky A.B.<sup>1,2,3</sup>, Zhukov A.<sup>2,3</sup>, Perov N.S.<sup>1</sup>, Rodionova V.V.<sup>1</sup>, Hasanov S.<sup>4</sup>, Larin V.S.<sup>5</sup>

<sup>1</sup> Moscow State University, Moscow, 119991, Russian Federation

<sup>2</sup> Basque Country University, 20080 San Sebastian, Spain

<sup>3</sup> Ikerbasque, Basque Foundation for Science, 48011, Bilbao, Spain

<sup>4</sup> Institute of Solid State Physics, 142432, Moscow Region, Russian Federation

<sup>5</sup> Microfir Tehnologii Industriale, 2021, Kishinev, R. Moldova

Magnetic amorphous and nanocrystalline glass-covered microwires prepared by Taylor-Ulitovsky technique have been studied intensively for a long time because of their unique soft magnetic properties and numerous applications [1]. It was realized that this technique allows fabricating microwires with magnetic, magnetotransport, mechanical and structural properties, which are extremely sensitive to the initial composition of metallic ingot, technological parameters, thickness of the metallic core and glass cover and the type of glass. This technique was used successfully to produce also granular microwires and microwires from Ni<sub>2</sub>MnGa Heusler alloys. Recently found Ni<sub>50</sub>Mn<sub>50-x</sub>Z<sub>x</sub> (Z=In, Sb, Sn) compounds that also belong to the class of Heusler alloys have attracted a great interest (see [2], and references therein), especially for x having martensitic transition temperatures near room temperature. We present the results of the first attempt to fabricate microwires from this novel family of Heusler alloys and demonstrate for the case of near-stoichiometric composition Ni<sub>2</sub>MnIn that their magnetic and transport properties are quite different from those for the bulk samples.

Magnetic properties of annealed at 770 K in air microwires were measured by VSM (Lake Shore 7400 System) in the temperature interval 77-400K in the range H=0.005-15 kOe. We performed ZFC and FC measurements as it was done previously for bulk samples Ni-Mn-In-Co in [3]. The crystal structure was determined by x-ray diffraction technique. The resistivity and longitudinal magnetoresistance was studied in the same temperature range.

The stoichiometric composition Ni<sub>2</sub>MnIn is known to order ferromagnetically at T<sub>C</sub>= 315 K, does not undergo a martensitic transition, while the Mn-rich off-stoichiometric composition Ni<sub>50</sub>Mn<sub>50-x</sub>In<sub>x</sub> exemplifies a martensitic transition with the transition temperature highly sensitive to the Mn:In ratio. In the case of fabricated from Ni<sub>2</sub>MnIn microwires T<sub>C</sub> ≈ 275 K, there is no evidence of martensitic transformation, ZFC and FC curves coincide only at H > 10 kOe, but differ from each other at T < T\* < T<sub>C</sub>, where T\* is about 225-250 K depending on magnetic field. We observed quasi-diamagnetic behavior at ZFC measurements in small magnetic fields similarly to that was reported in [3]. All parameters of hysteresis curves for microwires differ from that were reported in literature for bulk samples of the same composition.

The obtained results are encouraging on the way to get microwires with martensitic transformation close to room temperature and tunable magnetic properties.

This research was supported by the Russian Foundation for Basic Researches and by the Basque Foundation for Science.

[1] A. Zhukov and V. Zhukova, Magnetic properties and applications of ferromagnetic microwires with amorphous and nanocrystalline structure, Nova Science Publ., NY, 2009, 162 p.

[2] I. Dubenko, M. Khan, A. K. Pathak et al., *J. Magn. Magn. Mat.*, **321** (2009) 754.

[3] V.N. Prudnikov, A.P. Kazakov, I.S. Titov et al., *Phys. Solid State*, **53** (2011) 490.

24PO-I1-6

## ANOMALOUS AND ORDINARY HALL EFFECTS IN Ni-Mn-In-Z HEUSLER ALLOYS

Kazakov A.P.<sup>1</sup>, Prudnikov V.N.<sup>1</sup>, Granovsky A.B.<sup>1,2,3</sup>, Prudnikova M.V.<sup>1</sup>, Dubenko I.S.<sup>4</sup>,  
Pathak A.K.<sup>4</sup>, Ali N.<sup>4</sup>, Zhukov A.P.<sup>2,3</sup>

<sup>1</sup> Moscow State University, Moscow, 119991, Russian Federation

<sup>2</sup> Basque Country University, 20080 San Sebastian, Spain

<sup>3</sup> Ikerbasque, Basque Foundation for Science, 48011, Bilbao, Spain

<sup>4</sup> Southern Illinois University Carbondale, IL, 62901, USA

The strong interest to Heusler alloys is mainly due to the two unique properties: half-metallic behaviour and martensitic phase transition. The first feature leads to the 100% spin polarization of the electronic states at the Fermi level and makes these systems extremely attractive for spintronics. The second feature leads to magnetic shape memory effect, magnetic superelasticity, large magnetocaloric effect, exchange bias, metamagnetism, giant magnetoresistance, giant Hall effect, kinetic arrest [1,2]. Therefore Heusler alloys offer an excellent opportunity to investigate a rich collection of novel, interconnected physical properties that related to the various aspects of magnetic and structural phase transformations. Besides, Heusler alloys can be considered as multifunctional smart materials promising for spintronics, magnetic refrigeration, and magnetic sensors. In this report, we present experimental results on structural, magnetic and magnetotransport properties of Ni-Mn-In-Z (Z=Co, Cu, Si) alloys focusing on the specific behavior of magnetoresistance and Hall effect.

The Ni<sub>50</sub>Mn<sub>35</sub>In<sub>15</sub>, Ni<sub>50-x</sub>Co<sub>x</sub>Mn<sub>35</sub>In<sub>15</sub> (x=1, 2), Ni<sub>50</sub>Mn<sub>35</sub>In<sub>15-x</sub>Si<sub>x</sub> (x=1, 3, 4), Ni<sub>48</sub>Cu<sub>2</sub>Mn<sub>35</sub>In<sub>15</sub> samples were fabricated using the conventional arc-melting method. The magnetization M(T,H) was measured using VSM (Lake Shore 7400 System) and SQUID (Quantum Design) magnetometers in the temperature interval 4-400K and magnetic field up to 50 kOe. Magnetotransport measurements were carried out by the standard four-probe method using a fully automated system in a temperature interval 77-400K at magnetic fields in the range 0.005-15 kOe.

Using the data on magnetization, magnetoresistance and Hall resistivity obtained for the same samples and at the same conditions we determined the ordinary Hall effect (OHE) and anomalous Hall effect (AHE) coefficients in low temperature martensitic and high temperature austenitic phases as well as in the close vicinity of martensitic transformation. In spite of resistivity, total Hall resistivity and OHE resistivity are quite different at  $T < T_A$  and at  $T > T_A$ , where  $T_A$  is the characteristic temperature of martensitic transformation, the AHE coefficients in both phases are positive and are of the same order of magnitude. The temperature dependence of AHE coefficients and their magnitude are not consistent with theories of AHE in disordered alloys based on the side jump mechanism and the Berry phase contribution. In the near vicinity of the martensitic transformation, the field dependences of the Hall resistance are complex and nonmonotonic, indicating a change in the relative concentrations of the austenite and martensite phases in strong fields.

This research was supported by the Russian Foundation for Basic Researches, by the Basque Foundation for Science, by the Office of Basic Energy Sciences, Material Sciences Division of the U.S. Department of Energy.

[1] Ferromagnetic Shape Memory Alloys II, Ed. V.A. Chernenko, J.M. Barandiaran, Trans. Tech. Publ. Ltd, Switzerland, 210 p., 2009.

[2] I. Dubenko, A. Pathak, S. Stadler et al., *Phys.Rev.B*, **80**, (2009) 092408.

## TEMPERATURE DEPENDENCES OF THE ACOUSTIC HARMONICS AMPLITUDES IN FERROMAGNETIC SHAPE MEMORY ALLOY Ni-Mn-Ga

*Beznosikov D.S.<sup>1</sup>, Vlasov V.S.<sup>1</sup>, Kotov L.N.<sup>1</sup>, Koledov V.V.<sup>2</sup>, Shavrov V.G.<sup>2</sup>, Ulyashev A.M.<sup>1</sup>*

<sup>1</sup> Syktyvkar State University, 167001 Syktyvkar, Oktybrsky 55, Russia

<sup>2</sup> Institute of Radioengineering and Electronics of RAS, 125009 Moscow, Mokhovaya 11-7, Russia

The properties of ferromagnetic shape memory alloys Ni-Mn-Ga as the giant magnetoinduced strains, the reversible shape memory effect, large magnetocaloric effect in the room temperature range allow us to say about great perspectives of industrial application of these alloys [1]. These unusual properties are due to the thermo-elastic martensitic transformation from the high temperature cubic (or austenite) phase to the low temperature tetragonal (or martensitic) phase [1]. The temperature dependence of the ultrasonic attenuation of waves and the harmonic generation in the area of a structural transformation provides insight into the nature of the transition [2].

The temperature dependence of the ultrasonic attenuation was measured in a Ni<sub>2</sub>MnGa single crystal in the temperature range from 290 K to 380 K. Data of the electric response amplitudes of piezoelectric transducers recording elastic displacement of the longitudinal waves passing through the crystal. The first harmonic waves were recorded at 5 MHz frequency and the second harmonic at 10 MHz generated in the sample. In the temperature range 310 - 328 K where the transition occurred from the austenitic phase to martensitic phase the response amplitude of the first harmonic in the transition region the broad minimum due to the presence of the metastable phase was observed. Besides in the central area of the minimum for the first harmonic the narrow peak was observed. The narrow peak may be coupled with the easy magnetization axes changing in the crystal. Longitudinal wave begins to propagate along the direction close to the easy axis which corresponds to decreasing of the magnetoelastic interaction and decreasing the acoustic waves attenuation consequently. Also in the minimum area on the temperature range 313 - 325 K the maximum second-harmonic generation was observed demonstrating the increase of nonlinear wave interaction with the crystal lattice. Nonlinearity in the transition area may be increased by due to the presence of the reorientation of the magnetization vector and due to restructuring of the domain structure [1]. In the area of the Curie point of the studied sample (near 80 °C) also slight increasing of second-harmonic amplitude is observed which may be caused by decreasing of the anisotropy constants or magnetic softening. Far from the phase transition temperature dependences of the first and second harmonics amplitudes are gradual character. This suggests that at zero DC magnetic field the acoustic waves attenuation in single-crystal alloy Ni<sub>2</sub>MnGa is mainly determined by the waves interaction with changing domain structure and the scattering of waves on micro- and nano-crystalline inhomogeneities in the crystal.

Support by RFBR (grant 10-02-01327).

[1] V.D. Buchelnikov, et al, *JMMM*, **313** (2007) 312.

[2] J. Worgull, E. Petti, and J. Trivisonno, *Phys.Rev. B*, **54** (1996) 54.



24PO-I1-8

## MAGNETOCALORIC EFFECT IN HEUSLER ALLOY Ni-Mn-In

Musabirov I.<sup>1</sup>, Mulyukov Kh.<sup>1</sup>, Hernando B.<sup>2</sup>, Garcia J.<sup>2</sup>, Gonzalez L.<sup>2</sup>, Mashirov A.<sup>3</sup>, Koledov V.<sup>3</sup>, Khovailo V.<sup>3</sup>, Schavrov V.<sup>3</sup>

<sup>1</sup> Institute for Metals Superplasticity Problems of RAS, Ufa, 450001, Russia

<sup>2</sup> Dep. de Física, Universidad de Oviedo, Oviedo, Asturias, 33007, Spain

<sup>3</sup> Kotelnikov Institute of Radioengineering and Electronics of RAS, Moscow, 125009, Russia  
[a.v.mashiorv@mail.ru](mailto:a.v.mashiorv@mail.ru)

In the last years the investigations of the strong magnetocaloric effect (MCE) in Heusler alloys Ni-Mn-In system were carried out in much of works. However only very recently the reasonable doubts was expressed that signs of the contribution of structural and magnetic subsystems to the peak-to-valley entropy change are coincident during the magnetostructural transition (MST) [1]. Thus the MCE during MST is hardly to deserve to be called “giant”. In the same time the physical question of the reliable subsystems contributions determination is opened, because the majority of experiments in this field are either indirect or inaccurate.

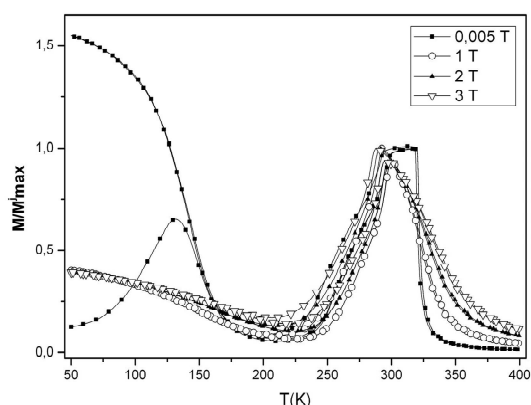


Fig. 1. Dependence  $M$  (T) in fields 0.005, 1, 2 and 3 T.

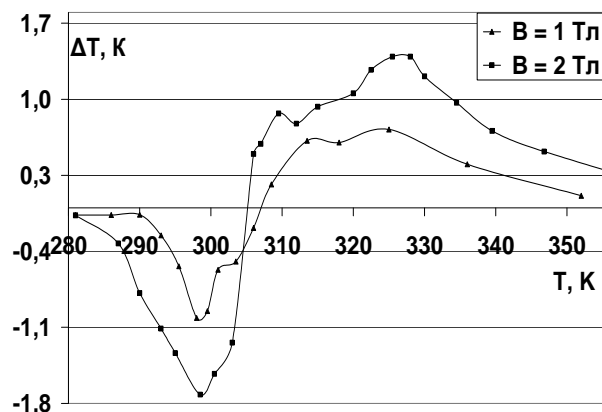


Fig. 2. Adiabatic temperature change  $\Delta T$  the sample in fields 1 и 2 T

In this work the polycrystalline alloys Ni-Mn-In systems were produced by arc melting technique. The MCE was experimentally tested by the measurements of temperature dependence of magnetization and the adiabatic change of temperature  $\Delta T$  in the magnetic fields 1 and 2 T induction. The typical dependences for Ni<sub>50.2</sub>Mn<sub>39.8</sub>In<sub>10</sub> are shown in fig. 1 and 2. It is seen, that the  $\Delta T$  peaks around the Curie temperature (325 K) and MST (300 K) are approximately modulo equal and opposite on sign. We can conclude that that the magnetic subsystem impact to MCE is opposite by sign to structural one. This means, that when the structural subsystem is transformed under turning on of the magnetic field from the martensitic the to austenitic state the energy is absorbed which is given by the magnetic subsystem, transformed from (weakly magnetic) martensite to ferromagnetic austenite. The adequate quantitative model reconstruction of the thermodynamic processes is possible only after the improvement of modern experimental methods and the resolution of problem of the thermal capacity measurement in magnetic field around MST.

The work was supported by RFBR 10-02-92662, 10-02-96020, 11-02-90502.

[1] S. Kustov, I. Golovin, M.L. Corro, E. Cesari, J. Appl. Phys. 107, 053525 (2010)

24PO-I1-9

**MAGNETOCALORIC EFFECT IN  $R\text{Co}_2$  COMPOUNDS***Ovchenkova I.A., Tskhadadze G.A., Zhukova D.A., Ivanova T.I., Nikitin S.A.*M.V.Lomonosov Moscow State University, Physics Dept., Moscow, 119899 Vorobiev Gory,  
Russia

In this work we present the results of investigations of magnetization and magnetocaloric effect (MCE), measured by the direct method on compounds based on  $R\text{Co}_2$  ( $R = \text{Tb}, \text{Ho}$ ) with substitutions in rare earth and 3d- sublattice by nonmagnetic elements (Y, Al, Ga).

The  $R\text{Co}_2$  compounds are the ferrimagnetic compounds with two magnetic subsystems – rare earth and Co. For  $\text{Ho}(\text{Co}_{1-x}\text{Al}_x)_2$  with  $x \leq 0.06$  the Stoner's-Wohlfarth's condition of the itinerant magnetism is realized [1,2], so in these compounds the first type phase transitions from magnetically ordered to disordered state are observed. In the range of these transitions we determined the abrupt change of the linear dimensions of the sample and the giant MCE ( $\sim 3 \div 3.5$  K at  $H = 13.5$  kOe). In compounds with the Curie temperature ( $T_C$ ) larger than 150 K ( $\text{Ho}(\text{Co}_{1-x}\text{Al}_x)_2$   $x > 0.06$ ,  $\text{Ho}(\text{Co}_{1-x}\text{Ga}_{0.05})_2$ ,  $(\text{Tb}_{1-x}\text{Y}_x)\text{Co}_2$ ,  $\text{Tb}(\text{Co}_{1-x}\text{Al}_x)_2$ ) the phase transition from magnetically ordered to disordered state becomes the second type phase transition. So the observed value of MCE in the region of this transition is essentially lower than for compounds with the phase transition of the first type ( $\Delta T \sim 0.8 \div 1.3$  K at  $H = 13.5$  kOe).

Due to the peculiarities of the density of states near Fermi level of these compounds [2,3] the small impurities of nonmagnetic Al or Ga into Co subsystem reinforce the magnetism of these compounds and increase their Curie temperature. This effect is observed as in series of samples based on  $\text{TbCo}_2$ , as on  $\text{HoCo}_2$ . The concentration dependence of MCE is different. First, the MCE is increasing with  $x$  simultaneously with the Curie temperature, but after some concentration of Al the reverse effect occurs:  $T_C$  increases while MCE begins to decrease. This tendency is observed both in series with the phase transitions of the first type and the second type.

The analysis of the magnetization curves showed that  $C_3$  doesn't change with temperature for these compounds. Hence, the dependence of MCE from  $M^2$  must be linear in the area of  $T_C$ , which is in good accordance with the experimental.

The work has been supported by RFBR grant # 10-02-00-721.

[1] E.C.Stoner. Proc.Roy.Soc.Ser.A. 154 (1936) 656.

[2] R.Z.Levitin, A.S.Markosian. Uspekhi Fizicheskikh Nauk (Russian), 155 (1988) 647.

[3] V.V.Aleksandrova, K.P.Belov, R.Z.Levitin, A.S.Markosian, V.V.Snegiriev. JETP Letters (Russian), 40 (1984) 77.

[4] J.Inoue, M.Shimizu. J.Phys.F, Met.Phys., 18 (1988) 2487.

24O-I1-10

## MAGNETIC PROPERTIES OF GLASS-COVERED Ni-Mn-Ga HEUSLER ALLOY MICROWIRES

Rodionova V.<sup>1,4</sup>, Ilyn M.<sup>2</sup>, Zhukova V.<sup>2</sup>, Zhukov A.<sup>2,3</sup>, Gonzalez J.<sup>2</sup>, Fetisov L.<sup>1</sup>, Perov N.<sup>1</sup>, Goikhman A.<sup>4</sup>, Shusharina N.<sup>4</sup>, Hasanov S.<sup>5</sup>, Granovsky A.<sup>1,2,3</sup>

<sup>1</sup> Moscow State University, Moscow, 119991, Russia

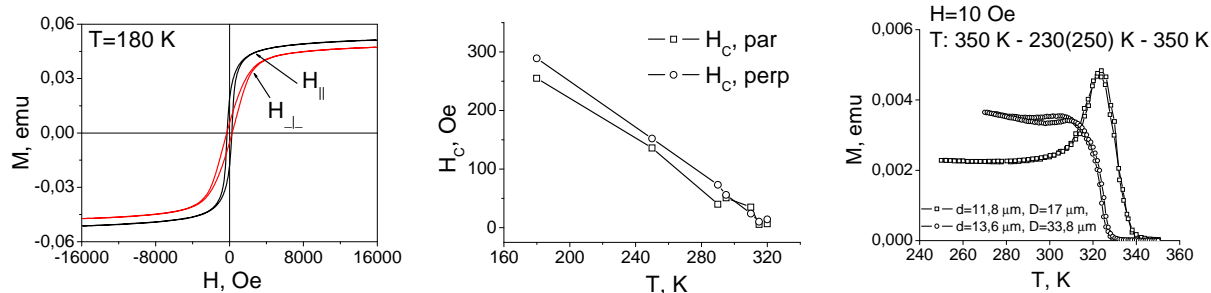
<sup>2</sup> Basque Country University, 20080 San Sebastian, Spain

<sup>3</sup> Ikerbasque, Basque Foundation for Science, 48011, Bilbao, Spain

<sup>4</sup> Immanuel Kant Baltic Federal University, 236041 Kaliningrad, Russia

<sup>5</sup> Insitute of of Solid State Physics, 142432, Chernogolovka, Moscow Region, Russia

We present experimental results on magnetic properties of the glass-covered Ni-Mn-Ga Heusler microwires fabricated by Taylor-Ulitovsky technique. The ingot of near-stoichiometric Ni<sub>49.5</sub>Mn<sub>25.4</sub>Ga<sub>25.1</sub> composition was used to make a microwire with the total diameter D of 17, 33.8 and 79.2  $\mu\text{m}$  and the diameter of metallic core d of 11.8, 13.6 and 49.6  $\mu\text{m}$ , correspondingly. The chemical composition of metallic core of microwires was close to the composition of the ingot as was checked by AES. XRD and magnetic measurements did not reveal martensitic transition in as cast samples but demonstrated the appearance of martensitic phase below 290 K in the samples annealed 30 min at 780 K in air. Intrinsic for the Taylor-Ulitovsky technique rapid solidification and large stress, originated from the difference in thermal expansion coefficients of the glass and metal, affect the crystal structure of the metallic core and therefore the magnetic properties of the fabricated Heusler microwires are different from their bulk and thin film counterparts.



Magnetic properties of annealed microwires were measured by SQUID magnetometer from 5 to 400 K in the fields up to 50 kOe and by VSM (Lake Shore 7400 System) in the temperature interval 77-400 K in the range 0.005-15 kOe. Magnetic field was applied along the microwire axis and perpendicular to the microwire axis. To enhance the sensitivity the measurements were performed for the array of microwires. The typical hysteresis behavior for microwires at low temperatures is shown in Fig.(a). The temperature dependence of coercivity (Fig.(b)) clearly demonstrates that below 290 K microwires are not isotropic.  $M(T)$  curves (Fig.(c)) depend on the microwires thickness that is due to the influence of stresses on the magnetic properties. We discuss the difference of magnetic parameters of Ni-Mn-Ga microwires (saturation magnetization, saturation field, coercivity, Curie temperature) with those for bulk crystals and possible applications of these novel microwires for actuators, magnetic and stress sensors.

This research was supported by the Russian Foundation for Basic Researches, by the Ministry of Education and Science of Russia, and by the Basque Foundation for Science.

24O-I1-11

## MAGNETOCALORIC EFFECT AND MAGNETIC PROPERTIES OF HIGH-PRESSURIZED RhFe COMPOUND

Samanta T.<sup>1</sup>, Dubenko I.<sup>1</sup>, Krylov V.I.<sup>2</sup>, Tsvyashchenko A.V.<sup>2,3</sup>, Fomicheva L.N.<sup>3</sup>, Sadykov R.A.<sup>3,4</sup>, Ali N.<sup>1</sup>

<sup>1</sup> Southern Illinois University, Carbondale IL, 62901, USA

<sup>2</sup> Skobeltsyn Institute of Nuclear Physics, Moscow State University, Vorob'evy Gory 1/2, 119991 Moscow, Russia

<sup>3</sup> Vereshchagin Institute for High Pressure Physics, RAS, 142190 Troitsk, Russia

<sup>4</sup> Institute for Nuclear Research, Russian Academy of Sciences, 142190 Troitsk, Russia

FeRh compound is the one of oldest candidate in giant magnetocaloric material family, which exhibits giant magnetocaloric effect (MCE) around room temperature due to first order magnetic transition (FOMT) from ferromagnetic (FM) to antiferromagnetic state with decreasing in temperature [1]. It has been established that pressure modifies the FM-AFM transition temperature [2]. Keeping above mentioned characteristics of FeRh in mind, we have carried out the study of MCE of metastable FeRh compound synthesized under pressure 8 GPa.

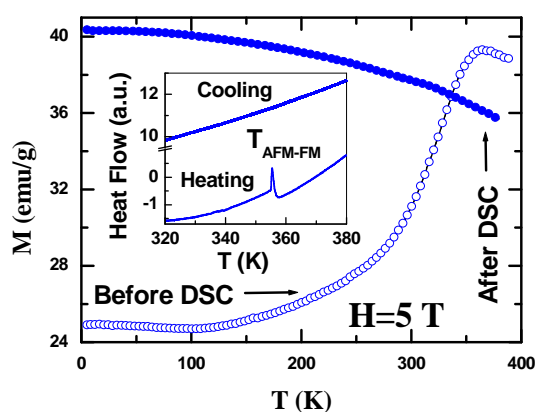


**Fig. 1** ZFC M(T) curve for 5 T. Inset: DSC heat flow curve

A sharp change in magnetization (M) of RhFe has been observed in zero-field-cooled (ZFC) M(T) curve around 338 K measured at H=5 T, which is associated with FOMT from FM to AFM state (see Fig. 1). Magnetic entropy changes ( $\Delta S$ ) have been calculated using M(H) isotherms in the temperature interval 90-380 K for magnetic field change ( $\Delta H$ ) up to 5 T. The observed inverse MCE has been related to strong AFM nature of the system below FOMT. The  $\Delta S(T)$  curve exhibits maximum value in vicinity of FOMT. The observed maximum  $\Delta S$  and, refrigerant capacity values of 0.8 J/kg K and, 44 J/kg, respectively has been detected for  $\Delta H=5$  T at 338K.

The heat flow curve of differential scanning calorimetric (DSC) measurement during heating from 173 to 573 K exhibits anomaly around FM-AFM transition temperature typical for FOPT. However, no such anomaly has been observed during cooling cycle which is the signature of metastable behaviour of the system (see Inset of Fig. 1). Using the same piece of sample as for DSC measurement, we have carried out magnetization measurement and observed the large difference in ZFC M(T) curves of the sample annealed during DSC and original sample (see Fig.1) at H=5 T. Therefore, the transition detected by DSC is irreversible as confirmed by magnetization measurements. Mössbauer spectra for <sup>57</sup>Fe atoms have been measured at the temperatures 4.2 – 300 K.

Support by the grants of the Russian Foundation for Basic Research (project nos. 11-02-00029) and Material Sciences Division of the U. S. Department of Energy are acknowledged.

[1] S. A. Nikitin et. Al., *Phys. Letters A*, **148** (1990) 363

[2] R. C. Wayne, *Phys. Rev.*, **170** (1968) 523

24O-I1-12

## MARTENSITIC TRANSFORMATION AND MAGNETIC ENTROPY CHANGE IN $\text{Ni}_{44}\text{Mn}_{45}\text{Sn}_{11-x}\text{Al}$

Wang R.L.<sup>1</sup>, Xu L.S.<sup>1</sup>, Marchenkov V.V.<sup>2</sup>, Medvedeva I.V.<sup>2</sup>, Yang C.P.<sup>1\*</sup>

<sup>1</sup> Faculty of Physics & Electronic Technology, Hubei University, Wuhan, 430062,  
People's Republic of China

<sup>2</sup> Institute of Metal Physics, 620041, Ekaterinburg, Russia

Email address: cpyang@hubu.edu.cn, Tell: +86-27-88665447; fax: +86-27-88663390.

The off-stoichiometric  $\text{Ni}_{50}\text{Mn}_{25+x}\text{Z}_{25-x}$  (X=In, Sb, or Sn) Heusler alloys that undergo martensitic transition (MT) at  $T_M$  below the ferromagnetic ordering temperature have attracted attention because of their giant magnetocaloric effect (MCE), and therefore have potential applications in environmentally friendly magnetic refrigerators. Much effort has been made to increase the magnetic entropy change by enlarging the magnetization changes ( $\Delta M_{sf}$ ) across the martensitic transition through adjusting the ratio of Ni and Mn and/or doping other transition elements. Actually, according to Maxwell relation, the value of  $\Delta S_M$  is determined by the value of  $dM/dT$  other than  $\Delta M_{sf}$  itself. So, reducing the martensitic transition temperature range (MTTR) between  $A_s$  and  $A_f$  may be another efficient method to improve the value of  $\Delta S_M$ . In this letter, we substituted Al for Sn in  $\text{Mn}_{44}\text{Ni}_{45}\text{Sn}_{11}$  alloys and studied the influence of Al substitution on the Martensitic transition and magnetic entropy change. The experimental results show that the MT temperatures increase with the increase of Al content due to the cell contraction, while the MTTR decreases rapidly. This can be attributed to the increase of  $\Delta M_{sf}/\text{MTTR}$ .

24PO-I1-13

## AB-INITIO INVESTIGATION OF THE ELECTRONIC STRUCTURE AND ELASTIC PROPERTIES OF IDEAL AND OFF-STOICHIOMETRIC HEUSLER ALLOYS

Kulkova S.<sup>1,2</sup>, Hu Q.M.<sup>3</sup>, Li C.M.<sup>3</sup>, Yang R.<sup>3</sup>

<sup>1</sup> Institute of Strength Physics and Materials Science SB RAS, pr. Akademichesky 2/4, Tomsk  
634021, Russia

<sup>2</sup> Tomsk State University, pr. Lenina 36, Tomsk 634050, Russia

<sup>3</sup> Shenyang National laboratory for Materials Science, Institute of Metal Research,  
Chinese Academy of Sciences, 72 Wenhua Road, Shenyang 110016, China

The coupling between the magnetic and structural properties of Heusler results in its unique thermo-magneto-mechanical properties. Alloys showing perspective magneto-elastic properties are basically off-stoichiometric ones. The study of the electronic properties and magnetic states of the off-stoichiometric Heusler alloys are crucial for understanding their properties. First-principles methods based on the density-functional theory are ideal tools for these purposes. We report the first principle study of the electronic structure, magnetic and elastic properties of some ideal Heusler alloys with composition  $\text{X}_2\text{MnZ}$ , where X=Ni, Co, Fe, Z = Al, Ga, In, Sn, Sb, as well as off-stoichiometric  $\text{Ni}_2\text{MnGa}$ -based alloys performed by the pseudopotential approach implemented in the VASP code and exact muffin-tin orbitals (EMTO) method with coherent-potential

approximation. The formation energies of several kinds of defects (atomic swaps, antisites, vacancies) were estimated for  $\text{Ni}_2\text{MnZ}$  series. The peculiarities of the Fermi surface cross-sections and nesting for both paramagnetic and magnetic phases as well as the behavior of the generalized susceptibility are analyzed. We considered nine types of off-stoichiometric  $\text{Ni}_2\text{MnGa}$  alloys with 12 different composition in order to study the influence of site occupancy and off-stoichiometric composition on the magnetic and elastic properties. The free energy and electronic energy for alloys with different composition were estimated. It was shown that for most of the off-stoichiometric alloys, the normal site occupation is favorable, i.e., the excess atoms of the rich component occupy the sublattices of the deficient components. In the case of the Ga-rich alloys, the excess Ga atoms always prefer to take the Mn sublattice no matter if Mn is deficient or not. The influence of site occupancy on the local magnetic properties on each sublattice was analyzed. It was found that a Mn atom changes its magnetic moment when occupying different sublattices. The magnetic moments of Mn on own, Ni and Ga sites are roughly  $3.5 \mu_B$ ,  $-2.5 \mu_B$  and  $\pm 3.2 \mu_B$ , respectively. So, Mn atom can be ferromagnetically or antiferromagnetically coupling with Mn atom on its own sublattice, depending on composition of alloy. In general, it was found that the bulk modulus increases with increasing  $e/a$  ratio. The shear moduli  $C'$  and  $C_{44}$  change oppositely:  $C'$  decreases but  $C_{44}$  increases with increasing  $e/a$ . Since the Mn-rich Ga-deficient alloys deviate significantly from this general trend we have investigated the influence of magnetic coupling between Mn atoms on Ga sublattice ( $\text{Mn}_{\text{Ga}}$ ) and Mn atoms on Mn sublattice ( $\text{Mn}_{\text{Mn}}$ ) on the elastic moduli. It was found that for large concentration  $x$  the state with antiparallel  $\text{Mn}_{\text{Ga}}\text{-Mn}_{\text{Mn}}$  magnetic coupling is slightly more stable than that with parallel coupling, whereas with increasing of  $x$  they trend to be degenerated. It was shown that for the antiparallel  $\text{Mn}_{\text{Ga}}\text{-Mn}_{\text{Mn}}$  magnetic coupling, the shear modulus  $C'$  versus the martensitic transformation temperature  $T_M$  is in line with the general  $C'\text{-}T_M$  relationship for  $\text{Ni}_2\text{MnGa}$ -based alloys, in contrast to the case for the parallel  $\text{Mn}_{\text{Ga}}\text{-Mn}_{\text{Mn}}$  magnetic coupling.

Support by RFBR (grant № 08-02-92201\_NSCF) and NSCF (grant № 50871114) is acknowledged.

24PO-I1-14

## MAGNETIC PROPERTIES OF A-SITE CATION DOPED, DOUBLE LAYERED $\text{LaMn}_2\text{O}_7$ COMPOUNDS

*Samancıoğlu Y.<sup>1</sup>, Coşkun A.<sup>1</sup>, Irmak A.E.<sup>1</sup>, Taşarkuyu E.<sup>1</sup>, Aktürk S.<sup>1</sup>, Ünlü G.<sup>1</sup>, Acet M.<sup>2</sup>*

<sup>1</sup>Department of Physics, Faculty of Science, Mugla University, 48000 Kotecli Mugla, Turkey

<sup>2</sup>Experimental Physics, Duisburg-Essen University, 47048 Duisburg, Germany

The  $\text{La}_{1.4-x}\text{Ba}_x\text{Ca}_{1.6}\text{Mn}_2\text{O}_7$  ( $x=0.0, 0.2$  and  $0.4$ ) compounds were prepared by the sol-gel method and sintered in air at  $1400^\circ\text{C}$  for 24 h. The magnetic properties of the compounds were investigated to explore the effects of A-site cation Ba-doping on the magnetic properties. From the measurements, the Curie temperatures and the isothermal magnetic entropy changes were determined. The Curie temperature of the sample with  $x=0$  doping is determined as 265 K, and it decreases with increasing Ba concentration up to a value of 258 K for  $x=0.20$ . It then increases again to 265 K for  $x=0.40$ . The magnetic entropy-change in a field-change of 1T is determined to be  $3.1 \text{ J/kg}^{-1}\text{K}^{-1}$  for  $x=0$ ,  $0.75 \text{ J/kg}^{-1}\text{K}^{-1}$  for  $x=0.20$  and it increases up to  $2.0 \text{ J/kg}^{-1}\text{K}^{-1}$  for  $x=0.40$ . The results indicate that the Curie temperature and the magnetic entropy-change show similar trends with respect to the doping concentration.

24PO-I1-15

## THE EFFECT OF POTASSIUM DOPING ON $\text{La}_{1.4}\text{Ca}_{1.6}\text{Mn}_2\text{O}_7$ TWO-LAYERED PEROVSKITE MANGANITES

Ünlü G.<sup>1</sup>, Acet M.<sup>3</sup>, Samancıoğlu Y.<sup>1</sup>, Coşkun A.<sup>1</sup>, Aktürk S.<sup>1</sup>, Sarıkürkcü C.<sup>2</sup>, Taşarkuyu E.<sup>1</sup>, Irmak A.E.<sup>1</sup>, Aksoy S.<sup>3</sup>, Yücel A.<sup>1</sup>, Demirci Ç.E.<sup>1</sup>

<sup>1</sup>Department of Physics, Faculty of Sciences and Letters, Muğla University, 48000, Muğla, Turkey

<sup>2</sup>Department of Chemistry, Faculty of Sciences and Letters, Muğla University, 48000, Muğla, Turkey

<sup>3</sup>Experimentalphysik, Universität Duisburg-Essen, 47057 Duisburg, Germany

<sup>4</sup>Faculty of Engineering and Natural Sciences, Sabancı University 34956, Tuzla, İstanbul, Turkey

We investigate the effect of potassium doping on the structural, magnetic and magnetocaloric properties of  $\text{La}_{1.4}\text{Ca}_{1.6}\text{Mn}_2\text{O}_7$  polycrystalline two-layered perovskite manganites. The samples have been prepared by the sol-gel route. They were sintered at 1673 K, and X-ray diffraction analysis indicated that all samples are single phase and crystallize in the tetragonal  $\text{Sr}_3\text{Ti}_2\text{O}_7$ -type crystal structure with the  $I4/mmm$  space group. An isothermal magnetic entropy change of 5.8 J/kg K in 2 T and an adiabatic change of temperature of 2.4 K in 5 T is obtained at 240 K in  $\text{La}_{1.0}\text{K}_{0.4}\text{Ca}_{1.6}\text{Mn}_2\text{O}_7$ .

[1]Y. Maritotmo, A. Asamitsu, H. Kuwahara, Y. Tokura, Nature (London) **380**, 141 (1996).

[2]H. Asano, J. Hayakawa and M. Matsui, American Inst. of Phys. **96**, 3 (1996).

[3]C.N.R. Rao, P. Ganguly, K. K. Singh, and R.A. Moham Ram, J. Solid State Chem. **72**, 14 (1988).

[4]T.I. Arbutzova, S.V. Naumov, and V. L. Arbutzov, Phys. of the Solid State **45**, 1513 (2003).

24PO-I1-16

## MONTE CARLO STUDY OF THE MAGNETIC AND MAGNETOCALORIC PROPERTIES OF $\text{La}_{0.67}\text{Ca}_{0.33}\text{MnO}_3$

Pavlukhina O., Buchelnikov V., Sokolovskiy V., Zagrebin M.  
Chelyabinsk State University, 454001 Chelyabinsk, Russia

The magnetocaloric effect is a magneto-thermodynamic phenomenon in which a reversible change in temperature of a suitable material is caused by exposing the material to a changing magnetic field. It has great importance in the technology of magnetic refrigeration. The magnetic materials with large values of magnetocaloric effect can be applied as work substances in magnetic cooling devices such as industrial and household refrigerators, air conditioners, heat pumps etc.

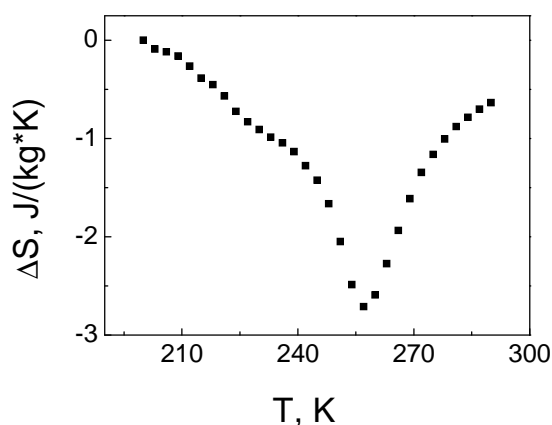
Experimental studies have shown that the manganites are also attractive for the application in magnetic refrigeration [1].

Manganite  $\text{La}_{0.67}\text{Ca}_{0.33}\text{MnO}_3$  crystallizes in a perovskite structure in which trivalent  $\text{Mn}^{3+}$  and tetravalent  $\text{Mn}^{4+}$  ions are distributed in to the lattice forming a simple cubic array. In our simulation model, magnetic  $\text{Mn}^{3+}$  and  $\text{Mn}^{4+}$  ions are described by classical Heisenberg spins, while oxygen, lanthanum and calcium ions are considered as non-magnetic. Three types of bonds are considered:

$\text{Mn}^{3+}(\text{eg})\text{-O-Mn}^{4+}(\text{d3})$ ,  $\text{Mn}^{3+}(\text{eg}')\text{-O-Mn}^{4+}(\text{d3})$  and  $\text{Mn}^{3+}(\text{eg}')\text{-O-Mn}^{3+}(\text{eg})$  with exchange parameters  $J_{\text{ab1}}$ ,  $J_{\text{ab2}}$  and  $J_{\text{ab3}}$ , respectively. Restrepo-Parra et al. [2] reported values of exchange parameters  $J_{\text{ab1}}=7.77$  meV,  $J_{\text{ab2}}=1.35$  meV and  $J_{\text{ab3}}=4.65$  meV.

In our work, using the Heisenberg's Hamiltonian we present Monte Carlo calculations of exchange magnetic constants and the temperature and field dependence of magnetization, and entropy changes, and determined the Curie temperature ( $T_C$ ). Curie temperature obtained during the theoretical simulations ( $T_C=258$  K) agrees well with experimental data ( $T_C=259$  K) [3] and with theoretical result for this compound ( $T_C=260$  K) [2].

The Figure shows the calculated temperature dependence of the entropy change at changing of magnetic field from 0 to 2 T for  $\text{La}_{0.67}\text{Ca}_{0.33}\text{MnO}_3$ . The maximum of the entropy change in a magnetic field 2 T is found to be 2.75 J/(kgK).



Support by RFBR grants 10-02-96020-r-ural, 11-02-00601, and 10-02-92110 is acknowledged.

[1] Yu B. et al., *Int. J. Refrig.*, **26** (2003) 622.

[2] Restrepo P. et al, *J. Magn. Magn. Mater.*, **323** (2011) 1477.

[3] Phan M. et al., *J. Magn. Magn. Mater.*, **308** (2007) 325.

24PO-II-17

## FRUSTRATED MAGNETIC STATES IN RARE-EARTH INTERMETALLIC COMPOUNDS $\text{R}_5\text{Pd}_2$

Gubkin A.F.<sup>1</sup>, Terent'ev P.E.<sup>1</sup>, Sherstobitova E.A.<sup>1</sup>, Korolev A.V.<sup>1</sup>, Teplykh A.E.<sup>1</sup>, Baranov N.V.<sup>1,2</sup>

<sup>1</sup> Institute for Metal Physics, RAS, 620990 Yekaterinburg, S. Kovalevskoy st. 18, Russia

<sup>2</sup> Ural State University, 620000 Yekaterinburg, Lenin ave. 51, Russia

The  $\text{R}_5\text{Pd}_2$  (R=Tb, Dy, Ho, Er) compounds have the largest content of the rare-earth metal within the R-Pd series and crystallize in the cubic crystal structure of the  $\text{Dy}_5\text{Pd}_2$  type (space group  $Fd\bar{3}m$ ) [1]. The triangular-like arrangement of rare-earth atoms in 4f site and a random distribution of rare-earth atoms over half-filled 32e crystallographic positions imply the existence of a complex magnetic state. The  $\text{R}_5\text{Pd}_2$  compounds are observed to exhibit a rich variety of field-induced phase transitions in [2-3]. The giant magnetocaloric effect associated with the field-induced metamagnetic phase transition has been found in  $\text{Ho}_5\text{Pd}_2$  [4]. The presence of a complex magnetic behavior in  $\text{R}_5\text{Pd}_2$  was suggested to result from the RKKY-type exchange interaction and frustrations effects [3].

In this work the study of the magnetic state of  $\text{Ho}_5\text{Pd}_2$  and  $\text{Tb}_5\text{Pd}_2$  rare-earth intermetallic compounds was carried out using neutron diffraction technique, DC and AC magnetic measurements in a wide temperature range. According to the neutron diffraction data the  $\text{Tb}_5\text{Pd}_2$  and  $\text{Ho}_5\text{Pd}_2$  compounds do not exhibit a long-range magnetic order down to low temperatures. However, the appearance of a set of broad diffuse maxima of magnetic origin was detected in the low angle region of the neutron diffraction patterns for both compounds with decreasing temperature (Fig. 1a). These maxima can be attributed to the appearance in  $\text{Tb}_5\text{Pd}_2$  and  $\text{Ho}_5\text{Pd}_2$  of



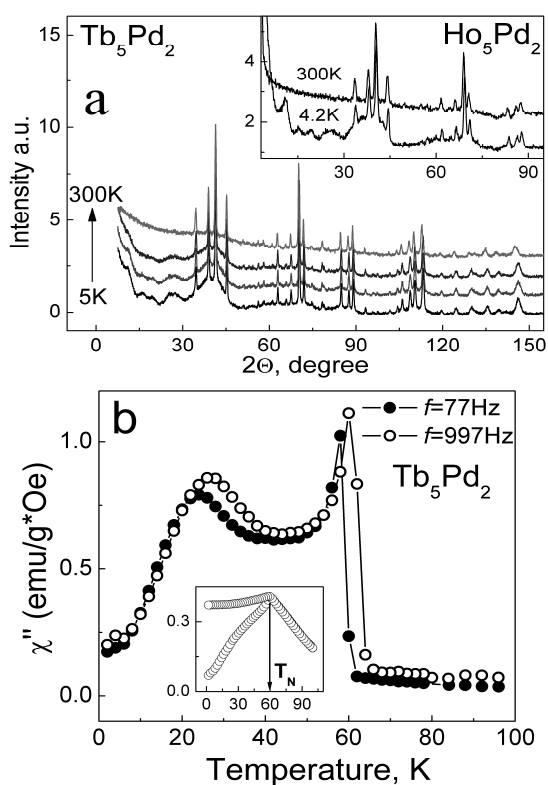


Fig. 1.a) neutron diffraction patterns for  $\text{Tb}_5\text{Pd}_2$  and  $\text{Ho}_5\text{Pd}_2$  powder samples and b) temperature dependence of  $\chi''$  for  $\text{Tb}_5\text{Pd}_2$ . ZFC-FC curves are shown in the inset.

short-range antiferromagnetic correlations within clusters below critical temperatures  $T_{cr} \approx 60$  K and  $T_{cr} \approx 30$  K, respectively. The AC-susceptibility measurements on a polycrystalline  $\text{Tb}_5\text{Pd}_2$

sample have revealed an unusual temperature dependence of the out-of-phase component  $\chi''$  (Fig. 1b) and frequency dependence of the susceptibility. The results obtained in the present work show that the magnetic state of  $\text{Ho}_5\text{Pd}_2$  and  $\text{Tb}_5\text{Pd}_2$  compounds is of the cluster-glass type, which originates apparently in the presence of structural disorder within R-sublattice and oscillating RKKY-type exchange interactions.

This work was supported by the program of RAS (Projects № 10-2-III-516, 09-II-2-1035).

- [1] M. L. Fornasini, A. Palenzon, *J. Less-Common Metals*, **38**, (1974) 77-82.  
 [2] J. K. Yakinthos et al., *J. Less-Common Metals*, **51** (1977) 113-116.  
 [3] M. Klimczak, E. Talik, A. Winiarski, R. Troc, *J. Alloys and Compounds*, **423** (2006) 62–65.  
 [4] T. Samanta, I. Das, S. Banerjee, *Applied Physics Letters*, **91** (2007) 082511.

24PO-II-18

## THE MAGNETOCALORIC EFFECT IN MULTIPHASE NANOCOMPOSITES Y-Fe

Karpenkov D.Yu., Karpenkov A.Yu., Skokov K.P., Semenova E.M., Smirnov R.F., Airiyan E.L.,  
Arefev A.I., Pastushenkov Yu.G.

Department of Physics, Tver State University, Sadoiy lane, 35, Tver, 170002, Russia

Creation of nanocomposite based on binary compound and determination of dependence between the values of magnetocaloric effect (MCE) and the dimensional factor of such specimens became the purpose of this work.

It was established that if we subject the initial alloy containing some phases with different characteristics, for instance Nd-Fe-B[1], to rapidly quenching and reduce the grain size down to several nanometers, exchange interaction will appear between grains. The consequences of formation of nanostructure are increasing the magnetization and insignificant reduction of coercivity.

The majority of materials with high values of MCE which are used as working bodies of magnetic refrigerators are not homogeneous. Some phases possess high values of MCE, but unfortunately they have high Curie temperature too ( $T_c$ ), maximum of MCE is observed near this temperature. At the same time there are phases with low temperatures of phase transitions in an alloy. The idea of the research is creation of nanocomposite, which will unite characteristics of both phases with the

purpose of increasing of values of MCE. The binary alloys of system Y-Fe with a ratio 25:75 and 35:65 were taken as objects of research, as the difference between the Curie temperatures of two phases is big enough to distinguish the contribution of each phase in total value of MCE.

Fig.1(a) shows the results of measuring of magnetocaloric effect of  $Y_{25}Fe_{75}$  alloy in field 18,3 kOe. As shown in diagrams, MCE of micro- and nanocrystalline samples  $Y_{25}Fe_{75}$  alloy are  $0,68^{\circ}C$  and  $0,86^{\circ}C$  accordingly. As shown in diagrams (Fig. 1(b)) for alloy  $Y_{35}Fe_{65}$  two characteristic peaks on the curve for the initial sample are observed. However there is a merge of these peaks for the rapidly quenched sample that leads to increasing of MCE from  $0,62^{\circ}C$  to  $0,72^{\circ}C$ .

The results of the investigation show, that reduction of the grain size down to 50-80 nanometers on nanocrystalline samples of  $Y_{25}Fe_{75}$  and  $Y_{35}Fe_{65}$  alloys leads to increasing of value of MCE from comparison with values on microcrystalline samples by 20-25 %.

This work was supported by grant RFBR № 10-02-00721-a, №09-02-01274 and the Federal program Scientific and pedagogical staff of innovative Russia.

[1] O. Gutfleisch, A. Bollero, A. Handstein, D. Hinz, A. Kirchner, A. Yan, K. -H. Müller, L. Schultz. Nanocrystalline high performance permanent magnets\\ *Journal of Magnetism and Magnetic Materials, Volumes 242-245, Part 2, April 2002, Pages 1277-1283*

24PO-I1-19

## MAGNETOCALORIC PROPERTIES OF A-SITRE ORDERED MANGANITES

Aliev A.M.<sup>1</sup>, Batdalov A.B.<sup>2</sup>, Gamzatov A.G.<sup>3</sup>, Kamilov K.I.<sup>1</sup>, Kalitka V.S.<sup>2</sup>

<sup>1</sup> Amirkhanov Institute of Physics, Daghestan Scientific Center of RAS, Makhachkala 367003, Russia

<sup>2</sup> Moscow State University, Moscow 119899, Russia

A-site ordered manganites  $RBaMn_2O_6$  (R-rare earth) have attracted the attention of researchers because of their unique physical properties. The most significant structural feature of these materials is that  $MnO_2$  plane located between two RO and BaO layers, which have significantly different sizes, resulting in highly distorted  $MnO_6$  octahedra. This implies that the structural and physical properties of  $RBaMn_2O_6$  can not be explained using only the tolerance factor, as for the cation-disordered  $R_{0,5}Ba_{0,5}MnO_3$  manganites. In addition, this strain may have an additional effect on the interaction of the charge, orbital, spin and lattice degrees of freedom. Depending on the rare-earth element, the observed phase transition temperatures are significantly different. In addition, the properties of these materials strongly depend on the sample preparation conditions.

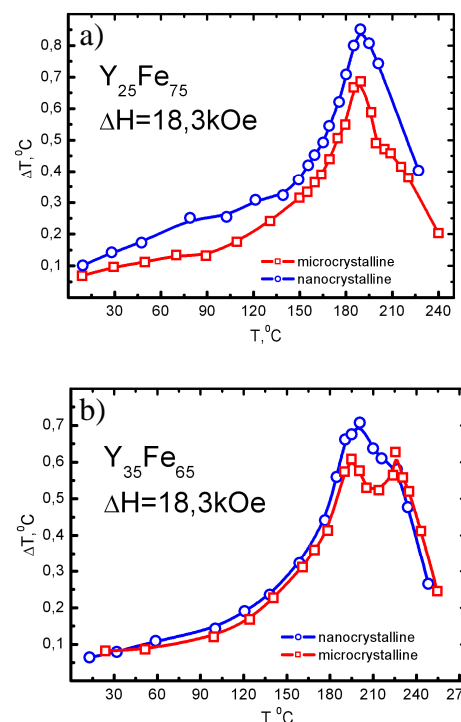
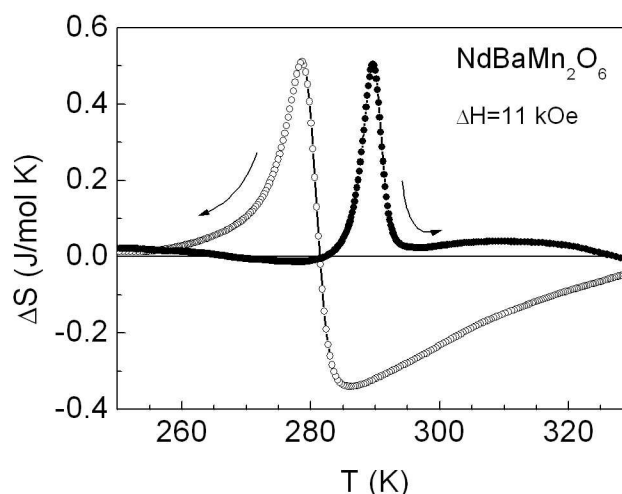


Fig.1 Magnetocaloric effect in field 18,3 kOe of micro and nanocrystalline samples  $Y_{25}Fe_{75}$  (a) and  $Y_{35}Fe_{65}$  (b) alloys

The magnetocaloric effect (MCE) of A-site ordered  $\text{PrBaMn}_2\text{O}_6$  and  $\text{NdBaMn}_2\text{O}_6$  manganites has been studied by direct methods and by the specific heat measurements. Direct measurements of the MCE in low magnetic fields were performed using recently proposed modulation technique and by classic direct method in high fields.

Direct and inverse MCE are observed at Curie and Neel points correspondingly. In  $\text{PrBaMn}_2\text{O}_6$  the value of inverse MCE in the heating run is less than in the cooling regime. This effect can be attributed to competition between ferromagnetic and antiferromagnetic interactions. Indirectly estimated and direct MCE values differ around first order AF transition.

The MCE in the  $\text{NdBaMn}_2\text{O}_6$  compound has anomalous behavior. In low magnetic fields abrupt transitions between direct and inverse magnetocaloric effect are observed. In a relatively strong magnetic field  $H = 11$  kOe the direct and inverse effects take place only at cooling, while at heating mode only an inverse MCE is observed. The value of the MCE ( $-\Delta S = 0.7$  J / kg K and  $\Delta S = 1.02$  J / kg K for  $\Delta H = 11$  kOe) does not reach high values, but the proximity of the effects observed at room temperatures, believes the use of both effects in the magnetic cooling technology.



This work was supported by RFBR (11-02-01124, 09-08-96533), and Physics Branch of RAS.

24PO-I1-20

## NUMERICAL SIMULATION OF MAGNETIC COOLING CYCLES

*Skokov K.<sup>1</sup>, Karpenkov A.<sup>1,2</sup>, Pastushenkov Yu.<sup>2</sup>, Gutfleisch O.<sup>1</sup>*

<sup>1</sup> IFW Dresden, Institute for Metallic Materials, PO Box 270116, D-01171 Dresden, Germany

<sup>2</sup> Faculty of Physics, Tver State University, 170002, Sadovy lane, 35, Tver, Russia

Any refrigerator must simultaneously meet two basic criteria, temperature span and cooling power. The concept of magnetic refrigeration (MR) is based on the magnetocaloric effect (MCE). The performance of a MR depends upon a variety of design decisions which will impact efficiency. In this work the design temperature span and cooling power are used in combination with field strength and material volume to define a performance metric specific to an MR.

In general, a magnetic refrigerator should include the following main parts: magnetic working body (refrigerant), magnetization system, hot and cold heat exchangers. Because gadolinium is a well-studied material that produces a relatively large magnetocaloric effect near room temperature ( $T_C=293$  K) [1] we selected it as the refrigerant.

We have simulated an ideal Brayton refrigeration cycle and Brayton cycle with regenerator. The general operational principle of refrigerator is as follows: thermal contact of working body (WB) with regenerator; the adiabatically magnetization of the WB, which causes a rise in the temperature of WB by the value of the MCE; then the magnetized material is set in thermal contact with the hot heat exchanger (HHE) and is cooled back to the temperature of HHE; thermal contact of WB with

regenerator; the adiabatically demagnetization, which causes a decrease in the temperature of WB by the value of the MCE; the last step is thermal contact with the cold heat exchanger (CHE).

First, we simulated open no-load system, with parameters: mass of WB=1 kg, mass of CHE=10 kg, mass of HHE=10<sup>3</sup> kg and mass of regenerator=10 kg, applied magnetic field  $\mu_0 H=1.5$  T. Temperature dependences of MCE and heat capacities of Gd under action of different magnetic fields were measured experimentally. Calculation shows that temperature span was 4.11 K with start temperature 294 K for ideal cycle and 7.81 K for cycle with regenerator (Fig.1). Further, we calculated the double Brighton cycle, when two WB are used. Temperature span was 4.11 K for ideal cycle and 7.81 K for cycle with regenerator, but number of cycles was reduced by half (Fig.1).

Calculations of up-load cycles shows that maximum cooling power without losses on heat exchange for single Brayton cycles was 1200 W and for double cycles was 2400 W (Fig.2).

Support by RFBR № 10-02-00721-a, №09-02-01274 and the Federal program Scientific and pedagogical staff of innovative Russia.

[1] A.M. Tishin, Y.I. Spichkin, *The Magnetocaloric Effect and Its Applications*, Institute of Physics Publishing, Bristol, Philadelphia (2003) 475.

24PO-I1-21

## GIANT MAGNETOCALORIC EFFECT IN THE REGION OF MAGNETIC PHASE TRANSITION IN Mn(As,Sb) INTERMETALLIC COMPOUNDS

Pankratov N.Yu.<sup>1</sup>, Mitsiuk V.I.<sup>2</sup>, Krokhotin A.I.<sup>1</sup>, Smarzhenskaya A.I.<sup>1</sup>, Govor G.A.<sup>2</sup>, Nikitin S.A.<sup>1</sup>, Ryzhkovskii V.M.<sup>2</sup>

<sup>1</sup> Physics Faculty, M.V. Lomonosov Moscow State University, Moscow, Russia

<sup>2</sup> SSPA "Scientific-Practical Materials Research Center of NAS of Belarus", Minsk, Belarus

The magnetocaloric effect (MCE) is important because of its potential application in the domestic and industrial refrigeration markets [1-3]. The MCE is characterized by the adiabatic temperature variation and the isothermal entropy change. The MnAs is a ferromagnetic which demonstrates phase transition at room temperature region with a change of both magnetic and structural properties. The MCE in MnAs and doped Mn(As,Sb) compounds have been studied by indirect investigation [4]. The objective of this work was to investigate the MCE in the crystals of doped Mn(As<sub>1-x</sub>Sb<sub>x</sub>) compounds with low concentration of Sb, by using a direct study of adiabatic temperature change  $\Delta T$  at magnetic fields up to 12 kOe.

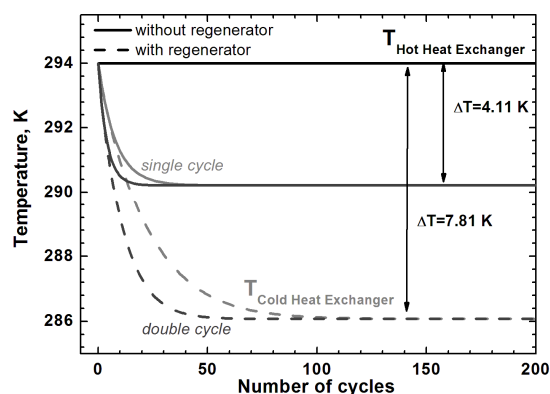


Fig.1

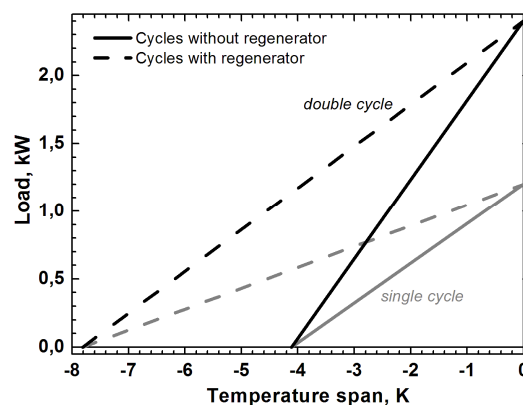


Fig.2

The crystalline alloys were obtained by the Stockbarger-Bridgman method and were characterized by X-ray diffraction at room temperature. The magnetization was measured by Vibrating Sample Magnetometer (Cryogenic Limited) in fields up to 140 kOe and by the SQUID magnetometer in fields up to 50 kOe. The MCE was obtained by direct method by measuring a temperature change at adiabatic field variation from 0 to 12 kOe.

Our results show that for MnAs the maximum value of MCE is  $\Delta T = 0.28$  K on heating (at 308 K) and  $\Delta T = 0.88$  K on cooling (at  $T = 306$  K). In doped Mn(As,Sb) compounds the temperature dependence behavior of MCE is similar to MnAs. All investigated compounds demonstrate a strong temperature and field hysteresis of magnetic properties in magnetic field less than 40 kOe. A low concentration of doped atoms (no more that 2 atom%/f.u.) leads to small increase of the phase transition temperature. In the MnAs<sub>0.98</sub>Sb<sub>0.02</sub> the maximum value of MCE is 0.85 K (at  $T = 311$  K) and 0.88 K (at  $T = 310$  K) on heating and cooling, respectively. It should be noted, that the magnitude of  $\Delta T$  on heating and cooling in MnAs<sub>0.98</sub>Sb<sub>0.02</sub> is about to equal.

Isothermal entropy changes ( $\Delta S$ ) were calculated from magnetization isotherms. The curves were obtained with temperature step 5 K. The result shows, that the maximum change of magnetic entropy of MnAs is about 40 J/kg·K at 140 kOe. We have found that the magnitude of cooling capacity for MnAs  $q = 442$  J/kg. The value of the magnetocaloric effect is calculated by  $\Delta T = T/C_p \cdot \Delta S$  equation, using the obtained  $\Delta S$  value ( $C_p$  is the specific heat [6]). In the field 140 kOe the maximum value of  $\Delta T$  is 13 K.

We have shown that the partly replacement of As by Sb leads to slightly decrease of temperature hysteresis of MCE and magnetization. At the same time a small concentration of Sb ( $x < 5$ ) preserves the phase transition at room temperature region.

The work is supported by the RFBR-BRFBR under the joint grant No.10-02-90016.

- [1] A.S. Andreenko, K.P. Belov, S.A. Nikitin, A.M. Tishin, Magnetocaloric Effects in Rare-earth magnetic materials, *Sov. Phys. Usp.* 32 (1989) 649-664.  
 [2] A.M. Tishin, Y.I. Spichkin, *The Magnetocaloric Effect and its Applications*, Institute of Physics, Bristol and Philadelphia, 2003.  
 [3] K.A. Gschneidner Jr., V.K. Pecharsky, A.O. Tsokol, *Rep. Prog. Phys.* 68 (2005) 1479-1539.  
 [4] H. Wada, Y. Tanabe, *Appl. Phys. Lett.* 79 (2001) 3302-3304.  
 [6] F. Gronvold, et al., *Acta Chemica Scandinavica.* 24 (1970) 285-298.

24PO-I1-22

## STRUCTURAL AND MAGNETIC PROPERTIES OF OFF-STOICHIOMETRIC HEUSLER ALLOYS Ni<sub>2</sub>MnIn

*Granovsky S.A.<sup>1,2</sup>, Gaidukova I.Yu.<sup>1</sup>, Doerr M.<sup>2</sup>, Ritter C.<sup>3</sup>, Skourski Y.<sup>4</sup>, Loewenhaupt M.<sup>2</sup>*

<sup>1</sup> M.V.Lonomossov Moscow State University, 119991 Leninskie Gory Moscow, Russia

<sup>2</sup> Institut für Festkörperphysik TU Dresden, 01062 Dresden, Germany

<sup>3</sup> Institut Laue-Langevin, F-38042 Grenoble Cedex 9, France

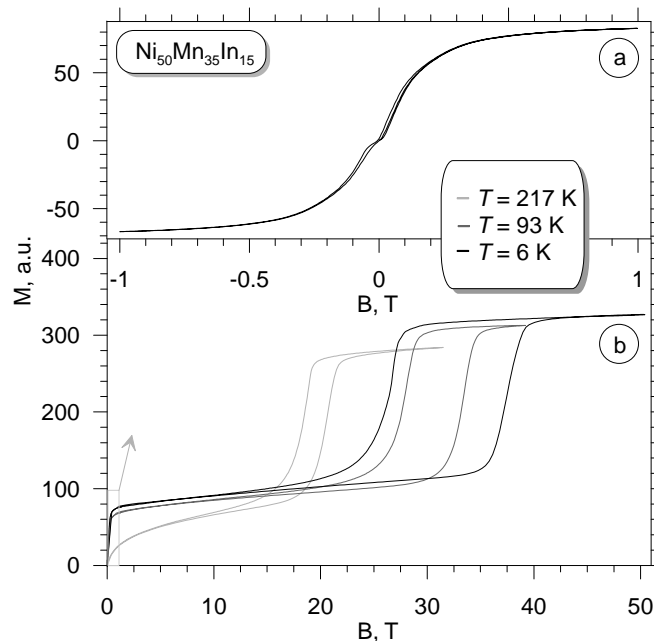
<sup>4</sup> Dresden High Magnetic Field Laboratory, Helmholtz-Zentrum Dresden-Rossendorf, 01314 Dresden, Germany

Investigation of shape-memory alloys attracts considerable attention for fundamental condensed matter physics. As the martensitic transition is based on the tiny energy balance, it can be driven by relatively small variation of temperature, chemical pressure and, in number of cases, by magnetic

field. The field-induced martensitic transitions observed in Heusler alloys  $\text{Ni}_{50}\text{Mn}_{50-x}\text{Z}_x$  ( $Z = \text{Ga}, \text{Sn}, \text{Sb}, \text{In}$ ) in the room temperature range make them suitable for practical applications.

The high temperature austenitic modification of  $\text{Ni}_{50}\text{Mn}_{50-x}\text{In}_x$  alloys is ferromagnetic for  $x > 14.5$  and the ordering temperature  $T_c \approx 315\text{K}$  is practically not depending on (Mn:In) ratio. The martensitic transition takes place for  $x \leq 15.8$  and the concentration dependency of “martensitic start” temperature  $M_s$  is not well understood as yet. It is considered that the main parameter, responsible for  $M_s$  is the free electron density  $e/a$ , however, there is no evidence, that this dependence is valid, at least, in  $\text{Ni}_2\text{MnIn}$  series. Thus, the sample with  $x = 15.8$  shows the transition at 205 K while the alloys with concentration  $x \geq 15.9$  exhibit no structural change.

Magnetism of off-stoichiometric Heusler alloys is not well understood. Furthermore, there is a controversy in experimental results, published by different authors, first of all, concerning structural characteristics. Compounds with the higher Mn-excess and higher  $A_s$  were not sufficiently studied, experiments with high magnetic fields are missing too. These circumstances motivated us for comprehensive study of structural, magnetic and transport properties of  $\text{Ni}_{50}\text{Mn}_{50-x}\text{In}_x$  system in the wide concentrations range, paying the special attention to the microscopic investigations and experiments in high magnetic fields.



The magnetization loop measured on  $\text{Ni}_{50}\text{Mn}_{35}\text{In}_{15}$  at  $T = 6\text{ K}$  (a) and several magnetization isotherms, obtained at high pulsed magnetic fields (b).

This work was supported by RFBR (09-02-01475-a).

24PO-I1-23

## MAGNETOCALORIC EFFECT IN Ni-Fe-Mn-Ga AND Ni-Co-Mn-Ga HEUSLER ALLOYS

*Fayzullin R.R.<sup>1</sup>, Drobosyuk M.O.<sup>1</sup>, Buchelnikov V.D.<sup>1</sup>, Taskaev S.V.<sup>1</sup>, Khovaylo V.V.<sup>2</sup>*

<sup>1</sup> Chelyabinsk State University, Br. Kashirinykh Str., 129, 454001, Chelyabinsk, Russia

<sup>2</sup> National University of Science and Technology “MISiS”, Lenin Av. 4, 119049 Moscow, Russia

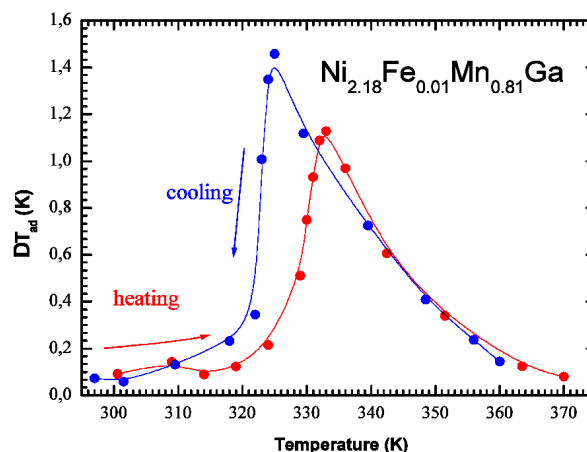
The magnetocaloric effect (MCE) is the ability of magnetic materials to heat up or cool down when placed in or removed from an external magnetic field. It has great importance in the technology of magnetic refrigeration. The magnetic materials with large values of MCE can be applied in the magnetic refrigeration technique [1]. Recent experimental studies have shown that Ni-Mn-Ga Heusler alloys are also attractive for the application in magnetic refrigeration [2].

In this work we study experimentally MCE in  $\text{Ni}_{2.19-x}\text{Fe}_x\text{Mn}_{0.81}\text{Ga}$  ( $x=0.01, 0.02, 0.03, 0.04$ ) and  $\text{Ni}_{2.16-x}\text{Co}_x\text{Mn}_{0.84}\text{Ga}$  ( $x=0.03, 0.06, 0.09$ ) Heusler alloys. Polycrystalline ingots with nominal compositions were prepared by an arc-melting method. Since the weight loss during the arc-melting

was small (0.2%) it was assumed that the real compositions correspond to the nominal ones. The ingots were annealed at 1100 K for 9 days quenched in ice water. Samples for MCE measurements were cut from the middle part of the ingots.

The MCE measurements were performed by the setup produced by AMT&C [3]. In this setup, the adiabatic temperature change  $\Delta T_{ad}$  was measured by a direct method with help of a thermocouple. Magnetic field up to 2 T was created by Halbach permanent magnet. The magnetic field strength was measured by Hall probe. Signals from the thermocouple and Hall probe were recorded simultaneously what allowed us to measure  $\Delta T_{ad}$  as a function of magnetic field H. The phase transition temperatures were determined from temperature dependencies of low field magnetization measured by original setup using Hall effect.

The temperature dependencies of  $\Delta T_{ad}$  for  $\text{Ni}_{2.19-x}\text{Fe}_x\text{Mn}_{0.81}\text{Ga}$  ( $x=0.01, 0.02, 0.03, 0.04$ ) and  $\text{Ni}_{2.16-x}\text{Co}_x\text{Mn}_{0.84}\text{Ga}$  ( $x=0.03, 0.06, 0.09$ ) Heusler alloys for the magnetic field change  $\Delta H = 2$  T were measured. It is shown that maximal MCE takes place near the structural and magnetic phase transition and its value changes from 0.5 to 2 K. The example of MCE measurements for  $\text{Ni}_{2.18}\text{Fe}_{0.01}\text{Mn}_{0.81}\text{Ga}$  alloy is presented on the Figure. So, we can conclude that investigated alloys are perspective for magnetic refrigeration.



Support by RFBR grants 10-02-96020-r-ural, 11-02-00601, 10-02-92110 and RF President grant MK-1891.2010.2 is acknowledged.

[1] K. Gschneidner, Jr. and V.K. Pecharsky, *Int. J. Refrig.*, **31** (2008) 945.

[2] A. Planes, L. Manosa, and M. Acet, *J. Phys.: Condens. Matter.* **21** (2009) 233201.

[3] Y.I. Spichkin Y.I., et al, *Proc. 3rd IIF-IIR Intern. Conf. Magnetic Refrigeration at Room Temperature*, IIF/IIR (2009) 173.

24PO-I1-24

## MAGNETOCALORIC EFFECT IN Ni-Mn-Ga HEUSLER ALLOYS

*Drobosyuk M.<sup>1</sup>, Buchelnikov V.<sup>1</sup>, Taskaev S.<sup>1</sup>, Khovaylo V.<sup>2</sup>*

<sup>1</sup> Chelyabinsk State University, Br. Kashirinykh str. 129, 454001 Chelyabinsk, Russia

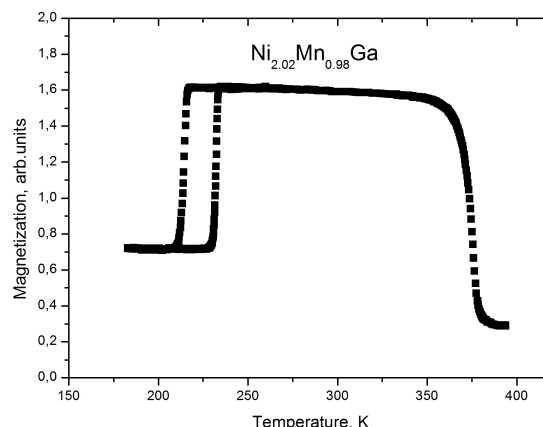
<sup>2</sup> National University of Science and Technology 'MISIS', Lenina Av. 4, 119049 Moscow, Russia

The magnetocaloric effect (MCE) is the ability of magnetic materials to heat up or cool down then they are placed in or removed from an external magnetic field. The magnetic materials with large values of MCE can be applied as work substances in magnetic cooling devices.

In this work the magnetic and magnetocaloric properties of the ferromagnetic shape memory alloys  $\text{Ni}_{2+x}\text{Mn}_{1-x}\text{Ga}$  ( $x=0.02; 0.03; 0.04; 0.07; 0.08; 0.09; 0.18; 0.27; 0.33; 0.36; 0.39$ ) were experimentally studied. MCE and magnetization of alloys were measured by direct methods.

Polycrystalline ingots with  $\text{Ni}_{2+x}\text{Mn}_{1-x}\text{Ga}$  nominal compositions were prepared by a conventional arc-melting method. The ingots were annealed at 1100 K for 9 days in evacuated quartz ampoules and quenched in water. Samples were cut from the middle part of the ingots [1].

The magnetocaloric measurements were performed by the help of the setup produced by Advanced Magnetic Technologies and Consulting Ltd (AMT&C) [2]. In this setup adiabatic temperature change ( $\Delta T_{ad}$ ) was measured by a direct method. The thermocouple junction was fixed directly on the sample, which was rigidly fastened to the sample placed on a fluoroplastic pad on a sample holder made from nonmagnetic metal. The sample holder was located in a chamber also made from non magnetic stainless steel and the chamber was sealed so the sample did not touch its sides. The magnetic fields (up to 2 T in the setup) are created by a Halbach permanent magnet magnetic field source. Magnetic field was measured by a Hall probe. The thermocouple and the Hall probe signal were recorded simultaneously, which allowed measuring  $\Delta T_{ad}$  versus magnetic field strength ( $H$ ). The temperature was changed by an electric heater.



Phase transition temperatures were determined from temperature dependencies of low field magnetization measured by original setup using Hall effect (example of temperature dependence of magnetization is presented on the Figure).

All alloys exhibit the positive MCE typical near the second-order phase transitions and can have the negative MCE close the structural transitions at low values of magnetic field. Our MCE measurements of Ni<sub>2+x</sub>Mn<sub>1-x</sub>Ga have shown that the maximal MCE is observed near the Curie point [3]. The maximal values of MCE are 0.2 – 1.5 K near the room temperature.

Support by RFBR grants 10-02-96020-r-ural, 11-02-00601, 10-02-92110 and RF President grant MK-1891.2010.2 is acknowledged.

[1] V. V. Khovaylo, V. D. Buchelnikov et al., *Phys. Rev. B*, **72** (2005) 222408.

[2] Y.I. Spichkin Y.I., et al, *Proc. 3rd IIF-IIR Intern. Conf. Magnetic Refrigeration at Room Temperature*, IIF/IIR (2009) 173.

[3] V. D. Buchelnikov, M.O. Drobosyuk et al., *Solid State Phenomena*, **168-169** (2011) 165.

24PO-I1-25

## MAGNETOOPTICAL SPECTROSCOPY OF HEUSLER ALLOYS: BULK SAMPLES, THIN FILMS AND MICROWIRES

Novikov A.I.<sup>1</sup>, Gan'shina E.A.<sup>1</sup>, Granovsky A.B.<sup>1,2,3</sup>, Zhukov A.<sup>2,3</sup>, Chernenko V.A.<sup>3,4</sup>

<sup>1</sup> Moscow State University, Moscow, 119991, Russian Federation

<sup>2</sup> Chemistry Faculty, Basque Country University, 20080, San Sebastian, Spain

<sup>3</sup> Ikerbasque, Basque Foundation for Science, 48011, Bilbao, Spain

<sup>4</sup> University of Basque Country Faculty, Dpt. Electricity & Electronics, P.O. Box 644, Bilbao 48080, Spain

We report the magneto-optical spectra of the Heusler bulk alloys Ni-Mn-In, thin films Ni-Mn-Ga, microwires Ni-Mn-In and Ni-Mn-Ga in the martensitic and austenitic states. Bulk samples of compositions Ni<sub>50</sub>Mn<sub>35</sub>In<sub>15</sub>, Ni<sub>50</sub>Mn<sub>34</sub>In<sub>16</sub>, Ni<sub>50-x</sub>Co<sub>x</sub>Mn<sub>35</sub>In<sub>15</sub> (x=1, 2), Ni<sub>50</sub>Mn<sub>35</sub>In<sub>15-x</sub>Si<sub>x</sub>



( $x = 1, 3, 4$ ),  $\text{Ni}_{48}\text{Cu}_2\text{Mn}_{35}\text{In}_{15}$  were fabricated by the conventional arc-melting of high purity metal components in an argon atmosphere, followed by annealing at 850C for 24 hours in vacuum.  $\text{Ni}_2\text{MnGa}/\text{MgO}(100)$  thin films were prepared by magnetron sputtering and their magnetic, micromagnetic, and texture properties were described in [1]. The Taylor-Ulitovsky technique [2] was used to fabricate  $\text{Ni}_2\text{MnGa}$  and  $\text{Ni}_2\text{MnIn}$  glass-covered microwires. In the latter case we used the stack of microwires. The transverse Kerr effect (TKE) was studied at an angle of light incidence of  $68^\circ$  with respect to the sample plane in the energy range  $1.5 \text{ eV} < E < 3.5 \text{ eV}$  at temperatures of 50–350 K in a magnetic field of up to 3.5 kOe. The temperature dependences of the Kerr effect were measured during heating at a rate of 1–3 K/min.

The obtained TKE spectra for austenitic state of  $\text{Ni}_2\text{GaMn}$  thin films are consistent with the data reported for bulk samples in [3]. Surprisingly, the TKE spectra profile does not change too much at martensitic transformation, only magnitudes of characteristic maxima decrease. Therefore the TKE in  $\text{Ni}_2\text{MnGa}$  Heusler alloys is mostly due to the single ion optical transitions in Mn, which are not sensitive to the change of electronic structure and nearest to Mn surrounding.

For most of studied bulk samples the TKE signal is weak (about  $10^{-5}$ ) and in many cases could not be detected at all in spite of strong spin-orbit interaction in Heusler alloys and quite large anomalous Hall effect studied for the same samples. It means that magnetic properties of Heusler alloys at interfaces differ from those in the bulk and strongly depend on the quality of optically or electrochemically polished surfaces, prehistory and stress.

This research was supported by the Russian Foundation for Basic Researches and by the Basque Foundation for Science.

[1] V.A. Chernenko, R.L. Anton, J. M. Barandiaran et al., *IEEE Trans. Magn.*, **44** (2008) 3040.

[2] A. Zhukov and V. Zhukova, Magnetic properties and applications of ferromagnetic microwires with amorphous and nanocrystalline structure, Nova Science Publ., NY, 2009, 162 p.

[3] S.J. Lee, Y.P. Lee, Y.H. Yan, Y.V. Kudryavtsev, *J. Appl. Phys.*, **93** (2002) 6975.

24PO-I1-26

## INVESTIGATION OF THE GIANT ROTATING MCE IN $\text{NdCo}_5$ SINGLE CRYSTALS IN THE SPIN-REORIENTATION REGION

*Koshkid'ko Yu.S.<sup>1</sup>, Skokov K.P.<sup>1,3</sup>, Pastushenkov Yu.G.<sup>1</sup>, Nikitin S.A.<sup>3</sup>, Ivanova T.I.<sup>3</sup>, Palewski T.<sup>4</sup>*

<sup>1</sup> Tver State University, 170100 Zheliabova 33, Tver, Russia

<sup>2</sup> Moscow State University, 119992 Leninskie Gory 1, Moscow, Russia

<sup>3</sup> Leibniz Institute for Solid State and Materials Research Dresden (IFW Dresden)

<sup>4</sup> International Laboratory of High Magnetic Fields and Low Temperatures, 53-421 Wroclaw, Poland

In the majority of works, concerning magnetocaloric effect (MCE), the subject of investigation is the MCE, caused by the change of magnetic part of entropy in the paraprocess region. However besides the contribution of paraprocess in MCE it is possible to allocate the next one, connected with the process of magnetization vector rotation, founded by Akulov and Kirensky [1]. The value of MCE due to the process of magnetization vector rotation [1] was considerably lower than the MCE of the paraprocess. Higher values of the MCE of this kind were found in the work [2] in the region of spin-reorientation transitions (SRT). The conclusion is that the maximum values of the MCE, connected with the process of magnetization vector rotation, are observed in the magnetic

materials with high values of magnetic anisotropy constants. From this point of view,  $\text{RCO}_5$  intermetallic compounds (R=Pr, Nd, Tb, Dy, Ho), which have SRTs and high values of anisotropy constants, are of profound interest in MCE investigation [3].

As the result of the investigations [4,5] the giant rotating MCE in  $\text{NdCo}_5$  single crystals in the spin-reorientation region [4] was found. That is why it is a matter of great interest to provide a more detailed investigation of this phenomenon. In order to investigate the giant rotating MCE two models were proposed. The first model was based on the calculation of the rotating MCE from the MCA constants and turn angles of the magnetization vector [6]. The second model allowed to carry out calculations of the rotating MCE from the rotating moment curves, calculated at the same value of the magnetic field at which the calculation of the MCE was carried out.

The investigations showed that the model, based on the method of calculation from the curves of the rotating moment, is in the better consent with the experimental data, than the results of the calculations, based on the calculation from MCE constants and turn angles of the magnetization vectors.

This work was supported by RFBR Grants No. 09-02-01274, No. 10-02-00721, and No. 10-02-90016, as well as by the Federal Target Program "Research and scientific pedagogical staff of innovative Russia."

- [1] N. S. Akulov, und L. W. Kirensky. Journal of Physics **3**, No. 1, 31-34. (1940).  
 [2] Belov, K.P., Talalaeva, E.V., Chernikova, L.A., Ivanova, T.I., Ivanovskii, V.I. and Kazakov, G.V. Sov Phys JETP **45**, 307-310 (1977)  
 [3] A. S. Ermolenko. IEEE Transactions on Magnetics, Vol. MAG-12, No. 6, 992-996. (1976)  
 [4] S. A. Nikitin, K. P. Skokov, Yu. S. Koshkid'ko, Yu.G. Pastushenkov, T. I. Ivanova, PRL **105**, 137205 (2010)  
 [5] Y.S. Koshkid'ko, K.P. Skokov, Yu.G. Pastushenkov, S.A. Nikitin, T.I. Ivanova, Solid State Phenomena, **168 -169** (2011) 134  
 [6] K. P. Skokov, Bull. Russ. Acad. Sci., Phys. 71, 1518 (2007).

24PO-I1-27

## AB INITIO AND MONTE CARLO INVESTIGATIONS OF THE MAGNETIC EXCHANGE AND CURIE TEMPERATURE OF $\text{Ni}_{50}\text{Mn}_{25+x}\text{Sn}_{25-x}$ ALLOYS

*Sokolovskiy V.<sup>1</sup>, Buchelnikov V.<sup>1</sup>, Zagrebin M.<sup>1</sup>, Entel P.<sup>2</sup>*

<sup>1</sup> Chelyabinsk State University, Br. Kashirinykh str. 129, Chelyabinsk, Russia

<sup>2</sup> University of Duisburg-Essen, Lothar str. 1, Duisburg, Germany

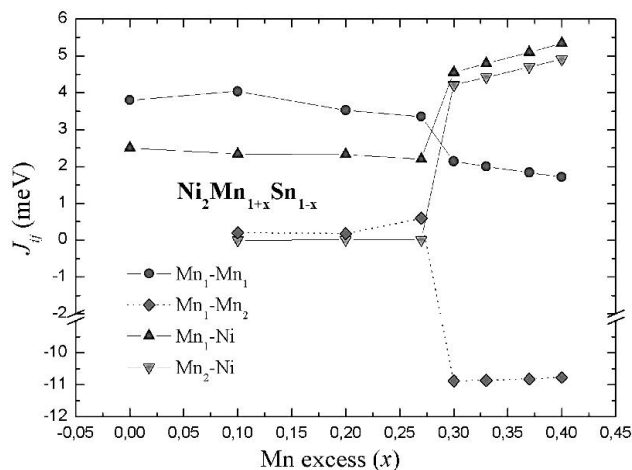
The ferromagnetic (FM) shape memory alloys Ni-Mn-X (X =In, Sn, Sb) alloys have drawn more attention recently. Some interesting properties, such as a magnetoresistance, exchange bias effect, direct and inverse magnetocaloric effect, are applicable in developing actuator materials, in spintronics, magnetic recording and materials for magnetic refrigeration [1].

In the case of Ni-Mn-Sn alloys, the stoichiometric  $\text{Ni}_{50}\text{Mn}_{25}\text{Sn}_{25}$  alloy has the  $L2_1$  structure, in which the Sn atoms occupy the site (0, 0, 0), the Mn atoms occupy the (1/2, 1/2, 1/2) and the Ni atoms locate at the sites (1/4, 1/4, 1/4) and (3/4, 3/4, 3/4). For the case of non-stoichiometric  $\text{Ni}_2\text{Mn}_{1+x}\text{Sn}_{1-x}$  alloys, the excess of Mn atoms are occupied the Sn sites and these atoms interact antiferromagnetically (AF) with the surrounding Mn atoms on the regular Mn sites [1].

In this work, we present *ab initio* and Monte Carlo calculations of exchange magnetic constants and the Curie temperatures of stoichiometric and non-stoichiometric Heusler  $\text{Ni}_{50}\text{Mn}_{25+x}\text{Sn}_{25-x}$  alloys. Calculations have been carried out for the high temperature austenitic  $L2_1$  structure (the space group is  $Fm\bar{3}m$ ). The ferromagnetic behavior and  $L2_1$  structure observe in the range  $0 \leq x \leq 0.4$ . The alloys with  $0.4 \leq x \leq 0.6$  undergo a martensitic transition from the high temperature  $L2_1$  structure to the orthorhombic  $4O$  one. The magnetic exchange constants have been calculated for several alloys by the Munich SPR-KKR (Spin Polarized Relativistic Korringa-Kohn-Rostoker code) package [2]. The Curie temperatures have been calculated by Monte Carlo method using Heisenberg model.

In our simulations, we have found that the excess of Mn atoms leads to decrease the  $\text{Mn}_1\text{-Mn}_1$  interaction and to increase  $\text{Mn}_1\text{-Ni}$ , and  $\text{Mn}_2\text{-Ni}$  interactions (here,  $\text{Mn}_1$  and  $\text{Mn}_2$  denote atoms at regular Mn and Sn sites, respectively). Moreover the  $\text{Mn}_1\text{-Mn}_2$  interaction for alloys with  $x > 0.28$  is the AF one and it is the largest of all exchange parameters. It should note that alloys with  $x > 0.28$  are closed to alloys with the martensitic transformation. The AF interactions are also responsible for the drop in the thermomagnetization curves of Ni-Mn-Sn alloys at the structural phase transition.

Our *ab initio* calculations have shown that the Curie temperatures and dependencies of magnetic exchange constants from the distance between the atoms for Ni-Mn-Sn alloys are in good agreement with experimental dependencies of exchange constants for these compounds [3].



Support by RFBR (grants 10-02-96020-r-ural, 11-02-00601, and 10-02-92110), RF President RF Grant MK-1891.2010.2 and FSYS-03/11 of ChelSU is acknowledged.

- [1] A. Planes, L. Manosa, and M. Acet, *J. Phys.: Condens. Matter*, **21** (2009) 233201.  
 [2] H. Ebert. *Electronic Structure and Physical Properties of Solids*, ed. H. Dreysse (Springer, Lecture Notes in Physics, Berlin, 1999) Vol. 535 p. 191.  
 [3] T. Kanomata et al., *Mater. Science Forum*, 583 (2008) 119.

24PO-I1-28

## MAGNETOCALORIC EFFECT IN $\text{R}_2\text{Fe}_{17-x}\text{Mn}_x$ , $\text{R} = \text{Ce}, \text{Lu}$

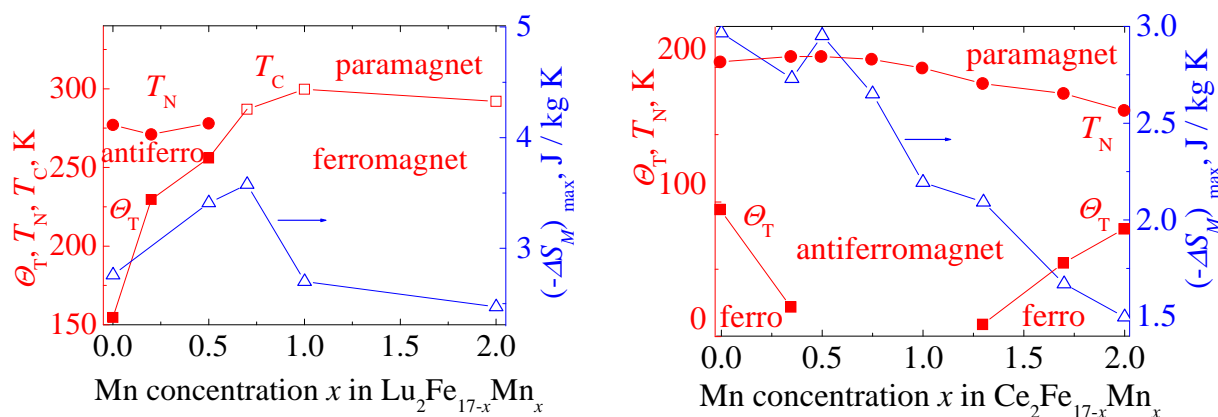
*Kuchin A.G.*<sup>1</sup>, *Iwasieczko W.*<sup>2</sup>

<sup>1</sup> Institute for Metal Physics, 18 S. Kovalevskaya Str., 620041 Ekaterinburg, Russia

<sup>2</sup> Institute of Low Temperature and Structure Research, P.O. Box 1410, 59-950 Wroclaw, Poland

In spite of the fact that both  $\text{Lu}_2\text{Fe}_{17}$  and  $\text{Ce}_2\text{Fe}_{17}$  binary compounds exhibit almost the same magnetic properties, their solid solutions with Mn in the range of  $x = 0 - 2$  behave differently (see Figs.). The  $\text{Lu}_2\text{Fe}_{17-x}\text{Mn}_x$  compounds with  $x = 0 - 0.5$  are ferromagnets at low temperatures and antiferromagnets at high temperatures with a nearly constant Néel temperature  $T_N \sim 278$  K. The temperature of the “ferromagnet-antiferromagnet” phase transition rapidly increases from 135 K with growing content of Mn, and the compounds from the range  $x = 0.7 - 2$  are ferromagnets only

with the practically unchanged Curie temperature,  $T_C(0.7) = 287$  K. The peak entropy change  $-\Delta S_M$  is 3.6 J/kg K at  $T = 300$  K in the  $\text{Lu}_2\text{Fe}_{16.3}\text{Mn}_{0.7}$  compound, as estimated from the isothermal magnetization data taken in the field 5 T. The increase of the MCE in the  $\text{Lu}_2\text{Fe}_{17-x}\text{Mn}_x$  system may be conditioned by the fact that the low- and high-temperature magnetic phase transitions are moving closer. These first- and second-order magnetic transitions merge for the composition  $\text{Lu}_2\text{Fe}_{16.3}\text{Mn}_{0.7}$ , where the associated entropy change is maximal. The  $\text{Ce}_2\text{Fe}_{17-x}\text{Mn}_x$  compounds with small Mn concentrations ( $x < 0.5$ ) are ferromagnets at low temperatures and helical antiferromagnets at high temperatures. The compounds with  $x = 0.5 - 1$  are helical antiferromagnets and those with  $x = 1.3 - 2$  are helical ferromagnets or helical antiferromagnets at low and high  $T$ , respectively. The Néel temperature  $T_N$  of the  $\text{Ce}_2\text{Fe}_{17-x}\text{Mn}_x$  compounds decreases almost monotonously with increasing Mn content, whereas the change of the temperature of ferromagnetic ordering  $\Theta_T(x)$  is non-monotonous.  $\Theta_T$  and  $T_N$  also approach each other in the  $\text{Ce}_2\text{Fe}_{17-x}\text{Mn}_x$  compounds,  $x = 1.3 - 2$  with increasing content of Mn, but  $-\Delta S_M$  does not increase, unlike the case of the  $\text{Lu}_2\text{Fe}_{17-x}\text{Mn}_x$  system. This discrepancy may be determined by different types of the ground magnetic state (collinear ferromagnetic in  $\text{Lu}_2\text{Fe}_{17-x}\text{Mn}_x$  and helical ferromagnetic in  $\text{Ce}_2\text{Fe}_{17-x}\text{Mn}_x$  with  $x = 1.3 - 2$ ). The peak entropy change decreases drastically by half in the  $\text{Ce}_2\text{Fe}_{17-x}\text{Mn}_x$  ( $x = 0 - 2$ ) system, which is traceable to a monotonic decrease of magnetization with increasing Mn content and the helical type of magnetic states in the compounds.



Support by UD RAS (No. 09-P-2-1008) is acknowledged.

24PO-I1-29

## MAGNETIC AND STRUCTURE PROPERTIES OF THIN FILM Ni-Mn-In HEUSLER ALLOY GROWN BY PULSED LASER DEPOSITION

Grunin A.<sup>1</sup>, Goikhman A.<sup>1</sup>, Rodionova V.<sup>1,2</sup>

<sup>1</sup> Immanuel Kant Baltic Federal University, 236041 Kaliningrad, Russia

<sup>2</sup> Moscow State University, Moscow, 119991, Russia

In recent years the problem of environment and energy saving attracts a lot of attention affecting materials research scientific activity. For example, the concept of room-temperature magnetic refrigeration was developed. It is a refrigeration technology using magnetocaloric effect instead of gas compressing-expanding cycles, more efficient and potentially capable of replacing the conventional refrigerators.

Ni-Mn-Ga and Ni-Mn-In Heusler alloys are promising candidates for basic materials of next generation magnetic refrigeration technologies due to absence of toxic hazards and relatively lowcost of initial materials from the economical-social point of view. Large values of magnetocaloric effect (MCE) near the room temperature was observed in some of these alloys owing to proximity of structural (martensitic,  $T_m$ ) and magnetic (Curie,  $T_c$ ) phase transitions.

The main idea of this work is formation of non-stoichiometric Ni-Mn-In Heusler alloy thin films under optimized growth conditions and investigation of their structural and magnetic properties.

Thin film structures were prepared by pulsed laser deposition (PLD) technique, using Nd:YAG laser with 532 and 1064nm wavelengths. Samples were grown in an ultra-high vacuum ( $\sim 10^{-9}$ – $10^{-10}$  Torr) chamber. The crystal structure, phase composition and magnetic properties were investigated by Rutherford backscattering spectroscopy (RBS), Auger electron spectroscopy (AES) with ion profiling system, Raman scattering spectroscopy and vibrating sample magnetometry techniques, respectively.

We have shown, that different stoichiometric  $\text{Ni}_{50}\text{Mn}_{(33.9+34.3)}\text{In}_{(15.7+16.1)}$  target ablation with wide number of different laser parameters (wavelength, energy, frequency etc.) does not lead to formation stoichiometric Ni-Mn-In layer: thin films strongly differ from targets in chemical composition. As grown In concentration on Ni-Mn-In thin films was much less than in the initial target:  $\sim 7\%$  of In were observed by RBS in thin film samples, while target In concentration is approximately 15%. Thin film indium concentration is decreasing, by increasing growth temperature (substrate T) and at  $T_s=580^\circ\text{C}$  it was observed less than 1% of In in sample.

The optimal temperatures of thin films annealing, which was performing immediately after the growth in a vacuum chamber, were also found. Ni-Mn-In layer was capped with Pt protective layer to prevent In evaporation during the vacuum annealing and to prevent oxidation of thin film on atmosphere. For Ni-Mn-In/Pt structures it was shown that at  $T=400^\circ\text{C}$  of vacuum annealing the maximum of indium concentration “starting movement” from volume to surface. At vacuum annealing temperature  $T=600^\circ\text{C}$  total intermixing of Ni-Mn-In and Pt layers was observed by AES ion profiling. The optimal vacuum annealing temperature was selected as  $T=350^\circ\text{C}$ , because at this temperature In concentration maxima lies within the sample thickness. It also was confirmed by annealing sample without Pt layer.

And at the next stage we have made series of experiments with co-deposition of two independent targets  $\text{Ni}_{50}\text{Mn}_{34.3}\text{In}_{15.7}:\text{In}$ . As a result we have achieved increasing of In concentration in the thin film samples. These changes of stoichiometry should lead to changes of the critical temperatures  $T_c$  and  $T_m$ . To confirm this, we checked the structural and magnetic properties of samples.

24PO-I1-30

## SPECIFIC HEAT OF $\text{MnCoGe}$ TYPE COMPOUNDS AT MARTENSITIC PHASE TRANSITIONS

*Markin P.E.<sup>1,2</sup>, Mushnikov N.V.<sup>1</sup>, Proshkin A.V.<sup>1</sup>, Belyaev S.V.<sup>2</sup>*

<sup>1</sup> Institute of Metal Physics, Ural Branch of RAS, S. Kovalevskaya 18, 620990 Ekaterinburg, Russia

<sup>2</sup> Ural State University, Lenin av. 51, 620083 Ekaterinburg, Russia

The structural, magnetic and thermal properties of  $\text{Mn}_{1-\delta}\text{Co}_{1-\delta}\text{Ge}$ ,  $\delta = 0.01, 0.02, 0.03, 0.035$  compounds were investigated by means of X-ray diffraction, magnetization and specific heat measurements in the temperature interval 4.2 – 340 K. According to X-ray diffraction studies, the compounds with  $\delta = 0.01$  and 0.035 have the  $\text{TiNiSi}$ -type orthorhombic and  $\text{Ni}_2\text{In}$ -type hexagonal crystal structure, respectively, in the temperature interval mentioned above. Both crystallographic

phases are ferromagnets, however, the magnetization and Curie temperature of the orthorhombic phase is higher. Near room temperature the compound with  $\delta = 0.02$  exhibits a first order spontaneous structural martensitic transformation from the ferromagnetic orthorhombic TiNiSi-type phase to the paramagnetic hexagonal Ni<sub>2</sub>In-type phase, while in the compound with  $\delta = 0.03$  the same transformation occurs at lower temperature between ferromagnetic orthorhombic phase and ferromagnetic hexagonal phase. These transitions are accompanied by the entropy changes  $\Delta S = 33.8 \text{ J/(kg}\cdot\text{K)}$  for  $\delta = 0.02$  and  $28 \text{ J/(kg}\cdot\text{K)}$  for  $\delta = 0.03$ .

The chemical compositions of the samples are very close to each other. Therefore, in the temperature intervals where the compounds have the same orthorhombic or hexagonal structures their behavior of the specific heat is very similar. Independently on the composition, the data form two universal temperature dependences - one for the hexagonal state and another for the orthorhombic state. The entropy changes associated with the spontaneous structural transitions for the compounds with  $\delta = 0.02, 0.03$  are equal to the differences between the entropies of the stable hexagonal ( $\delta = 0.035$ ) and stable orthorhombic ( $\delta = 0.01$ ) compounds taken at the transition temperatures. We obtained the changes of the magnetic, lattice and electronic entropies at the spontaneous structural transition by examining the differences of respective entropy contributions of hexagonal and orthorhombic modifications.

The electronic specific heat coefficients  $\gamma$  for the orthorhombic and hexagonal phases were determined from the low-temperature parts of the specific heat data to be  $10 \text{ mJ/(mol}\cdot\text{K}^2)$  and  $28 \text{ mJ/(mol}\cdot\text{K}^2)$ , respectively. The lattice contribution was analyzed in the Debye model. The Debye temperature of the hexagonal modification was determined from the high-temperature part of the specific heat data ( $T > 300 \text{ K}$ ), where the hexagonal phase is paramagnetic. The Debye temperature of the orthorhombic modification was determined from the high-temperature part of the specific heat data for the isostructural compound NiMn<sub>0.2</sub>Ti<sub>0.8</sub>Ge, which Curie temperature is much smaller than that for the MnCoGe orthorhombic compound.

It was found that when the sample undergoes the structural transition, the magnetic entropy exhibits maximal variation. However the changes of the lattice and electronic entropies are also important and must be taken into account. The lattice entropy change has the opposite sign and partly compensate the variation of the magnetic and electronic entropies at the phase transition.

The study is partially supported by RFBR (projects 10-02-96019 and 09-02-00272).

24PO-I1-31

## MAGNETIC PROPERTIES AND MAGNETOCALORIC EFFECT OF Gd<sub>3</sub>Ni IN CRYSTALLINE AND AMORPHOUS STATES

*Shishkin D.A.<sup>1</sup>, Baranov N.V.<sup>1,2</sup>, Proshkin A.V.<sup>1,2</sup>, Andreev S.V.<sup>2</sup>, Volegov A.S.<sup>2</sup>*

<sup>1</sup> Institute of Metal Physics, Russian Academy of Science, 620990, Ekaterinburg, Russia;

<sup>2</sup> Institute of Physics and Applied Mathematics, Ural State University, 620083, Ekaterinburg, Russia

\*e-mail: shishkin@imp.uran.ru

Pure Gd metal and Gd based alloys and compounds are considered as promising candidates for magnetic refrigeration in different temperature ranges. The aim of the present work is to study the influence of rapid quenching of the melt on the magnetic properties and magnetocaloric effect (MCE) in Gd<sub>75</sub>Ni<sub>25</sub> alloy. The crystalline counterpart of this alloy is the intermetallic compound

Gd<sub>3</sub>Ni which exhibits the maximal rare earth content within Gd-Ni binary system and shows an antiferromagnetic (AF) order below the Neel temperature  $T_N \approx 100$  K [1]. The amorphous Gd<sub>75</sub>Ni<sub>25</sub> sample was prepared by a melt-spinning technique in argon atmosphere. The magnetization measurements were performed by using a Quantum Design SQUID magnetometer. From the magnetization data, the isothermal magnetic entropy change ( $\Delta S_M$ ) was calculated by using the Maxwell relation [2].

The measurements performed for the liquid quenched (LQ) Gd<sub>75</sub>Ni<sub>25</sub> alloy have revealed that this alloy exhibits a ferromagnetic behavior in a low-field region (see *Fig. 1*). Under application of a magnetic field, the magnetization of the LQ alloy increases sharply reaching a high value at low fields unlike the crystalline Gd<sub>3</sub>Ni compound which shows the phase transition from AF to the field-induced ferromagnetic state with increasing field above the critical field  $H_c \sim 40$  kOe. The Curie temperature of the LQ alloy is found to be 117 K which exceeds the  $T_N$  value for the crystalline Gd<sub>3</sub>Ni compound. For the LQ alloy, the calculation of the isothermal magnetic entropy change has given a higher maximal value of  $\Delta S_M = -7.44$  J kg<sup>-1</sup> K<sup>-1</sup> at a field change of 50 kOe in comparison with  $\Delta S_M \approx -5.20$  J kg<sup>-1</sup> K<sup>-1</sup> for the crystalline Gd<sub>3</sub>Ni compound [1] (see inset in *Fig. 1*). Furthermore, for the LQ alloy, the refrigerant capacity (RC) characterizing the refrigerant efficiency of a material is found to be also much higher than that for the crystalline compound (676 J kg<sup>-1</sup> and 107 J kg<sup>-1</sup> [1], respectively). Our results have shown that the rapid quenching of the melt modifies substantially the magnetic state of Gd<sub>3</sub>Ni and improves the MCE.

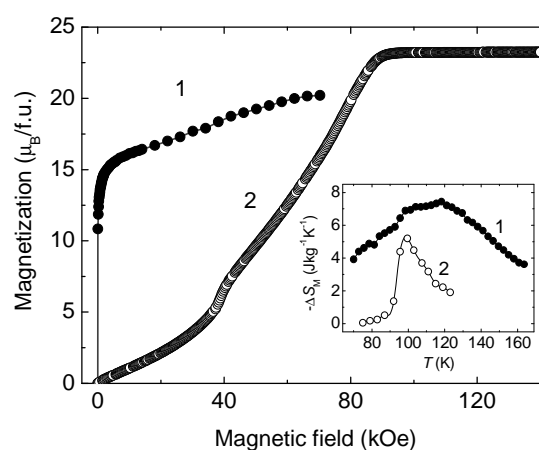


Fig.1. Magnetization of Gd<sub>3</sub>Ni alloy at  $T = 5$  K in amorphous (1) and crystalline (2) states. The inset shows temperature dependences of the magnetic entropy change at a field change of 50 kOe.

The present work was supported by the program of the Presidium RAS (Project No 09-P-2-1035) and RFBR (Grant 10-02-96028).

[1] N.V. Tristan, S.A. Nikitin, T. Palewski, K. Skokov, J. Warchulska, *J. Magn. Magn. Mater.*, **334** (2002) 40–44

[2] S.K. Tripathy, K.G. Suresh and A.K. Nigam, *J. Magn. Magn. Mater.*, **306** (2006) 24–29

## THERMOMECHANICAL PROPERTIES OF NiMnIn FERROMAGNETIC SHAPE MEMORY ALLOY

Hernando B.<sup>1</sup>, Koledov V.<sup>2</sup>, Kuchin D.<sup>2</sup>, Khovailo V.<sup>2</sup>, Garcia J.<sup>3</sup>, Shavrov V.<sup>2</sup>, Mashirov A.<sup>2</sup>, Kalimullina E.<sup>2</sup>, Chatterjee S.<sup>3</sup>, Majumdar S.<sup>3</sup>

<sup>1</sup> Depto. de Física, Universidad de Oviedo, Oviedo – Asturias, 33007, Spain

<sup>2</sup> Kotelnikov Institute of Radioengineering and Electronics of RAS, Moscow, 125009, Russia

<sup>3</sup> Department of SSP, Indian Association for the Cultivation of Science, Kolkata, 700 032, India  
rexby@list.ru

Recently much interest has been paid to the investigation of new Heusler alloys NiMnX:Me (X = Sn, In, Sb, Me = 3d transition metal) with shape memory effect (SME), because they demonstrate unusual sequence of magnetic and structural transitions strongly sensitive to magnetic field and composition [1]. The purpose of the present work is to study the magnetic properties and SME in off-stoichiometric Ni-Mn-In Heusler alloys by measurements of magnetization (M) and bending strain ( $\epsilon$ ) versus temperature (T) for different loads. The samples were prepared by argon arc-melting technique and subsequent annealing in vacuum [1]. Typically M(T) curves show the signature of Curie point and 1<sup>st</sup> order metamagnetostructural transition (MMT) marked by thermal hysteresis. MMT is accompanied by pure SME, which is proved by  $\epsilon(T)$  measurements. Unexpectedly, the sample with composition Ni<sub>50</sub>Mn<sub>34</sub>In<sub>16</sub> has demonstrated the evidence of a two-step martensitic transition (figs. 1 and 2), which is evident both in M(T) and  $\epsilon(T)$  data.

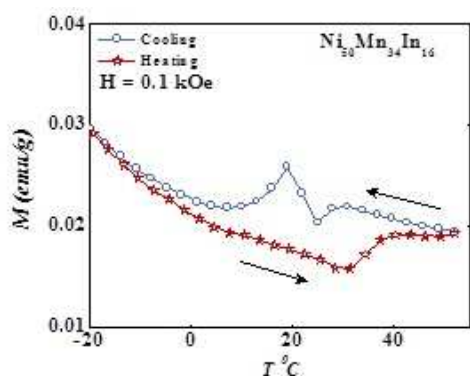


Fig. 1. Magnetization versus temperature for Ni<sub>50</sub>Mn<sub>34</sub>In<sub>16</sub> alloy.

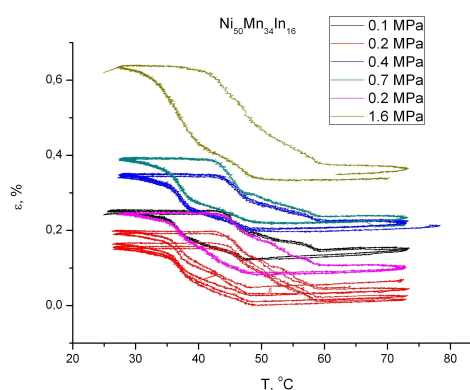


Fig. 2. Bending strain versus temperature curves for different loads for Ni<sub>50</sub>Mn<sub>34</sub>In<sub>16</sub> alloy.

Further investigations should clarify the nature of the two-stage structural transformation in off-stoichiometric Ni-Mn-In alloys and the possibility of magnetic field control of SME.

The work was supported by RFBR 10-02-92662, 10-02-96020, 11-02-90502, MAT2009-13108-C02-01 and DST (India).

[1] S. Chatterjee *et al.*, Phys. Rev. B **81**, 214441 (2010).



## MAGNETOCALORIC EFFECT IN Ho-Er-Gd-Co MULTICOMPONENT COMPOUNDS

Ćwik J.<sup>1</sup>, Palewski T.<sup>2</sup>, Nenkov K.<sup>1,2</sup>, Lyubina J.<sup>3</sup>, Gutfleisch O.<sup>2</sup>

<sup>1</sup> International Laboratory of High Magnetic Fields and Low Temperatures, Gajowicka 95, 53-421 Wrocław, Poland.

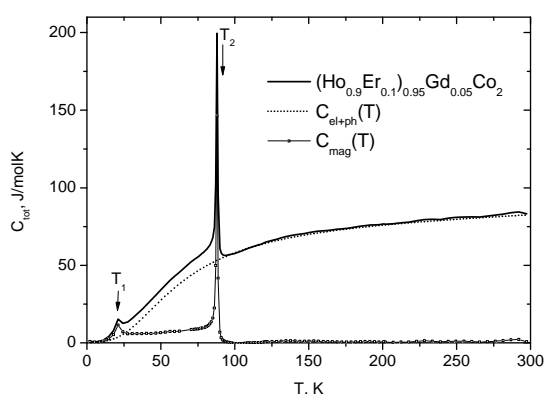
<sup>2</sup> IFW Dresden, Institute of Metallic Materials, Postfach 270016, 01171 Dresden, Germany

<sup>3</sup> Department of Materials, Imperial College London, Exhibition Road, London, SW7 2AZ, United Kingdom

We report magnetic and magnetocaloric properties of the polycrystalline series of  $(\text{Ho}_{0.9}\text{Er}_{0.1})_{1-x}\text{Gd}_x\text{Co}_2$  ( $x = 0.05, 0.1$  and  $0.15$ ) solid solutions. These samples were synthesized using high purity rare earth metals and cobalt. The X-ray diffraction patterns taken at room temperature revealed that all compounds have the C15 cubic Laves phase  $\text{MgCu}_2$  type structure. Magnetization measurements were carried out using a vibration sample magnetometer with a step motor in applied fields up to 14 T using a Bitter-type magnet. The heat capacity was measured using Quantum Design PPMS 14 Heat Capacity System in a temperature range of 2 - 295 K without the magnetic field and in a magnetic field of 1 and 2 T.

The solid solutions  $(\text{Ho}_{0.9}\text{Er}_{0.1})_{1-x}\text{Gd}_x\text{Co}_2$  with  $x = 0.05, 0.1$  and  $0.15$  have two magnetic phase transitions. The first one is observed in the low temperature region ( $T_1$ ), below 22 K and the second one is observed in the higher temperature region ( $T_2$ ), below 125 K. The substitution of Gd for  $\text{Ho}_{0.9}\text{Er}_{0.1}\text{Co}_2$  in the  $(\text{Ho}_{0.9}\text{Er}_{0.1})_{1-x}\text{Gd}_x\text{Co}_2$  solid solutions leads to an decrease of the magnetic ordering temperature  $T_1$  from 21.2 K ( $x = 0.05$ ) to 20.6 K ( $x = 0.15$ ) and increase of the magnetic ordering temperature  $T_2$  from 88.2 K ( $x = 0.05$ ) to 124.7 K ( $x = 0.15$ ). The first magnetic transition is associated with a magnetic Er sublattice, while the second transition is associated with the Ho and Gd sublattice. Both magnetic and heat capacity measurements showed that all the samples have two magnetic phase transitions.

The magnetocaloric effect has been estimated in terms of isothermal magnetic entropy change for all solid solutions in magnetic fields up to 3 T. The raising amount of the Gd in  $(\text{Ho}_{0.9}\text{Er}_{0.1})_{1-x}\text{Gd}_x\text{Co}_2$  samples on magnetic and magnetocaloric properties will be discussed.



Total heat capacity  $C_{\text{tot}}(T)$  of  $(\text{Ho}_{0.9}\text{Er}_{0.1})_{0.95}\text{Gd}_{0.05}\text{Co}_2$  measured in zero magnetic field

24PO-I1-34

## SHAPE MEMORY EFFECT IN MICROSIZED SAMPLES OF FERROMAGNETIC HEUSLER ALLOYS

*Akatyeva K.<sup>1</sup>, Afonina V.<sup>1</sup>, Irzhak A.<sup>2</sup>, Khovailo V.<sup>2</sup>, Koledov V.<sup>1</sup>, Shavrov V.<sup>1</sup>, von Gratoski S.<sup>1</sup>, Albertini F.<sup>3</sup>, Fabbrici S.<sup>3</sup>*

<sup>1</sup> Kotelnikov Institute of Radioengineering and Electronics of RAS, Moscow, 125009 Russia

<sup>2</sup> Moscow Institute of Steel and Alloys, Moscow, 119049, Russia

<sup>3</sup> Istituto dei Materiali per l'Electronica ed il Magnetismo IMEM-CNR, Parma, 43010, Italy  
Listina\_13@mail.ru

Since the discovery of giant magnetic-field-induced strains in Ni-Mn-Ga ferromagnetic alloy with the shape memory effect (SME) much of works have been done with purpose to apply this phenomenon to micromechanics. Unfortunately, the SME is intrinsically irreversible. Usually, external force biasing or special procedure of 'training' of the alloy for 'two-way' SME should be applied. This is not convenient for microsized samples of the alloy. Recently, the new two-layer composite scheme is proposed, which allow obtaining of the reversible deformation using only one-way SME [1]. In the present work we describe the preparation and study of microsized composites with SME on the base of 50  $\mu\text{m}$  thick Ni-Mn-Ga Heusler alloy melt spun ribbons (see figure).

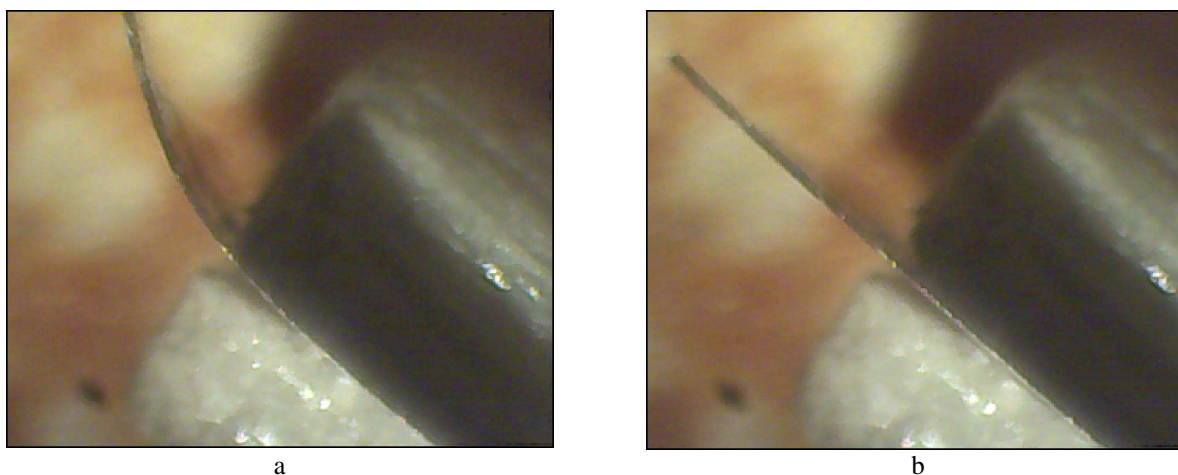


Fig. Pure SME in melt spun ribbon of Ni-Mn-Ga alloy. Sample is in martensite (a) and in austenite (b).

The microsized samples preparation and experiments on thermally actuated SME are achieved in vacuum chamber of FEI Strata 201 FIB device. The sample size is approximately  $10 \times 3 \times 1 \mu\text{m}^3$ . The thicknesses of the layer with SME of the composite are down to  $0.5 \mu\text{m}$  and less. The experiments on thermal actuation and prospects of magnetic field control of the new type of actuators are discussed.

The work was supported by RFBR grants No 10-02-92662, 10-02-96020, 11-02-90502 and RAS-CNR joint research Program.

[1]. A. V. Irzhak, V. S. Kalashnikov, V. V. Koledov, et al. Technical Physics Letters. V. 36, p. 329–332 (2010).

24PO-I1-35

## INDEPENDENCE OF MAGNETIC PART OF HEAT CAPACITY IN THE VICINITY OF $T_C$

*Zverev V.I.<sup>1,2</sup>, Gimaev R.R.<sup>1,2</sup>, Tishin A.M.<sup>1,2</sup>, Mudryk Ya.<sup>3</sup>, Gschneidner K.A.Jr.<sup>3,4</sup>,  
Pecharsky V.K.<sup>3,4</sup>*

<sup>1</sup> Faculty of Physics, M.V. Lomonosov Moscow State University, 119991, Moscow, Russia

<sup>2</sup> Advanced Magnetic Technologies and Consulting LLC, 142190, Troitsk, Russia

<sup>3</sup> The Ames Laboratory, U.S. Department of Energy, Iowa State University, Ames, IA 50011-3020, USA

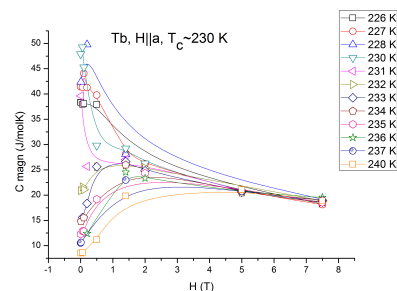
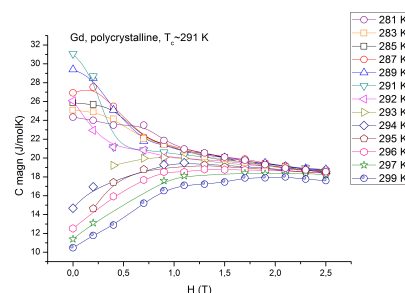
<sup>4</sup> Department of Materials Science and Engineering, Iowa State University, Ames, IA 50011-2300, USA

It is well known that the largest values of the magnetocaloric effect at temperatures near ambient, are observed in the proximity of spontaneous magnetic phase transitions. Advancing the fundamental and applied science of magnetocaloric materials, therefore, requires better understanding of the behavior of these materials in the vicinity of critical points.

Although in temperature and magnetic field coordinates, the regions where the phase transitions are observed are of great interest for magnetism, there is no reliable theory that can describe the whole spectrum of phenomena occurring at these points. Even the well known Landau theory of second order phase transitions [1] considers the phase transition itself without the applied magnetic field, but it remains silent with respect to what happens in the presence of magnetic field.

Here, we show how the applied magnetic field affects the magnetic part of the heat capacity near the temperature of magnetic phase transformations by using one of the most promising magnetocaloric materials – Gd, and two other rare-earth metals, i.e. Tb and Ho as examples.

Detailed measurements of the temperature dependence of heat capacity in varying magnetic field were carried out using high purity samples of polycrystalline Gd and single crystals of Tb and Ho. The magnetic contributions to the heat capacity of the samples were determined by subtracting off the lattice and electronic contributions. Results for Gd and Tb are presented in the figures. We argue that the regions where the magnetic heat capacity remains nearly constant (and magnetic field independent) correspond to phase transformations in non-zero magnetic field. The theoretical foundation for this argument is based on the fundamental thermodynamic principles. The physical meaning of the observed independence of the magnetic heat capacity on the applied magnetic field will be discussed in detail. The magnetic sublattice at these conditions may be considered insensitive to the application of magnetic field.



Work at the Ames Laboratory (heat capacity measurements) is supported by the Office of Basic Energy Sciences, Materials Sciences Division of the Office of Science of the U.S. Department of Energy, under contract No. DE-AC02-07CH11358 with Iowa State University (YaM, VKP and KAG). AMT, VIZ and RRG acknowledge support by the AMT&C Group Ltd., UK.

[1] L.D. Landau and E.M. Lifshitz, Statistical Physics, (Butterworth-Heinemann, Oxford, 1980).

## PRESSURE INDUCED AF-F-AF MAGNETIC PHASE TRANSFORMATIONS IN Pd SUBSTITUTED FeRh COMPOUND

Chirkova A.M.<sup>1</sup>, Baranov N.V.<sup>1,2</sup>, Volegov A.S.<sup>1</sup>, Stepanova E.A.<sup>1</sup>

<sup>1</sup> Ural State University, 620083 Ekaterinburg, Russia

<sup>2</sup> Institute of Metal Physics of the RAS, 620990 Ekaterinburg, Russia

In the nearly equiatomic Fe-Rh alloys a first-order magnetic phase transformation from the low-temperature antiferromagnetic (AF) state to the high-temperature ferromagnetic (F) state occurs upon heating at a critical temperature  $T_t \approx 320$ -400 K. The AF-F transition is accompanied by significant changes in different physical properties [1, 2]. The change of the Fe:Rh ratio around the 1:1 composition, the substitution of Fe or Rh by other d-elements as well as the application of the hydrostatic pressure [1-3] is observed to affect the magnetic state and critical temperature. In particular, the applied pressure expands the AF region and may induce the AF state in ferromagnetically ordered alloys [2-3]. As shown in [1], the partial substitution of Pd for Rh leads to substantial nonmonotonic change of the AF-F transition temperature with minimal value  $T_t \approx 125$  K at  $x = 0.08$ , whereas the lattice parameter of the  $\text{Fe}_{0.49}(\text{Rh}_{1-x}\text{Pd}_x)_{0.51}$  alloys increases linearly with the Pd concentration [4]. The  $\text{Fe}_{0.49}(\text{Rh}_{1-x}\text{Pd}_x)_{0.51}$  alloys are AF-ordered below  $T_t$  at  $0 < x < 0.12$ , and F-ordered at  $x > 0.13$  in the whole temperature range up to the Curie temperature  $T_C \approx 650$  K, where the ferromagnetic order disappears.

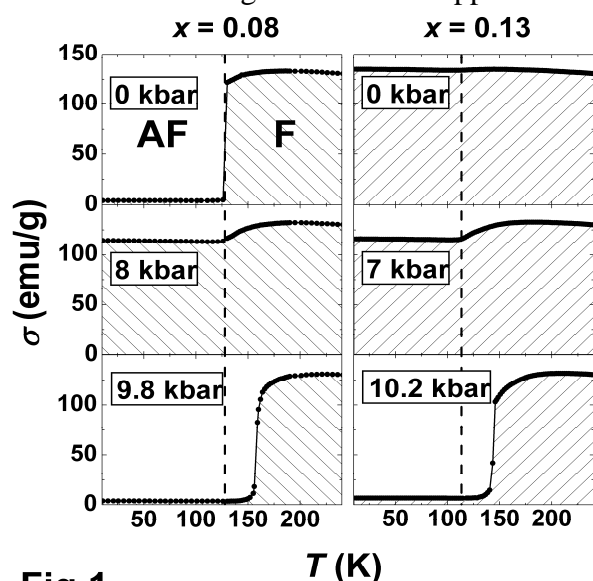


Fig.1

The aim of the present work is to study the effect of hydrostatic pressure on the magnetic state of  $\text{Fe}_{0.49}(\text{Rh}_{1-x}\text{Pd}_x)_{0.51}$  alloys. Two compositions with  $x = 0.08$  and  $x = 0.13$  were selected. Unlike the ferromagnetically ordered alloy with  $x = 0.13$ , the sample with the Pd content  $x = 0.08$  exhibits the AF-order below  $T_t \approx 125$  K [1]. The temperature dependence of the magnetization was measured in an applied magnetic field of 10 kOe under hydrostatic pressures up to 10 kbar (Fig.1). It has been found that in the F-ordered alloy ( $x = 0.13$ ), the pressure  $P > 7$  kbar induces the AF state below  $T_t \approx 125$  K and shifts the transition temperature toward  $T_t \approx 145$  K with increasing pressure up to 10.2 kbar. Surprisingly, the 8 kbar pressure applied to the sample with  $x = 0.08$  is observed to induce a metastable F state instead of broadening the AF region (shown in Fig 1), while further growth of the pressure up to 9.8 kbar reinstates the AF state. Unusual behavior of the magnetic state of the Pd substituted ( $x = 0.08$ ) sample under applied pressure is attributed to the peculiarities of the electronic density of states (DOS) in this alloy near the Fermi level. Both the substitution of Pd for Rh and the change of interatomic distances under applied pressure are suggested to affect the DOS value and the ground magnetic state in  $\text{Fe}_{0.49}(\text{Rh}_{1-x}\text{Pd}_x)_{0.51}$ .

[1] N.V. Baranov, E.A. Barabanova, *J. Alloys Compd.*, **219** (1995) 139.

[2] L.I. Vinokurova, A.V. Vlasov, N.I. Kulikov, M. Pardavi-Horvath, *J. Magn. Magn. Mater.*, **25** (1981) 201.

[3] K. Kamenev, Z. Arnold, J. Kamarad, N.V. Baranov, *J. Alloys Compd.*, **252** (1997) 1.

[4] K. Nishimura, Y. Nakazawa, L. Li, K. Mori, *Mater. Trans., JIM*, **49** (2008) 1753.

## STUDY OF MAGNETIC AND STRUCTURAL PROPERTIES OF Ni-Mn-Ga HEUSLER ALLOYS WITH THE HELP OF HUBBARD MODEL AND AB INITIO CALCULATIONS

*Zagrebin M.A., Buchelnikov V.D., Sokolovskiy V.V., Motylev I.A.*

Chelyabinsk State University, Br. Kashirinykh Str. 129, 454001 Chelyabinsk, Russia

Heusler Ni-Mn-Ga alloys are interesting for practical applications because of the numerous unusual effects such as a shape memory effect in ferromagnetic state, a giant magnetocaloric effect and etc. The strong magnetoelastic interaction between the magnetic and structural subsystems is the reason of these effects [1]. Experimental data shows that properties (such as elastic moduli, exchange parameters, magnetic moment etc.) of these alloys depends on stoichiometry [2,3]. In our study we investigate structural and magnetic properties with the help of Hubbard model and first principles calculations [4-6]. These investigations allow us to explain experimentally observed concentration dependences of structural and magnetic properties of Ni-Mn-Ga.

Macroscopic free energy is obtained from the microscopic Hubbard Hamiltonian and it is [4]

$$F = F_0 + \frac{1}{2}a_2e^2 + \frac{1}{3}a_3e^3 + \frac{1}{4}a_4e^4 + \frac{1}{2}b_2m^2 + \frac{1}{4}b_4m^4 + \frac{1}{2}Ce^2m^2, \quad (1)$$

where  $e$  is the tetragonal distortion,  $m$  is the normalized magnetization,  $a_i$  are the elastic modulus,  $b_i$  are the exchange constants and  $C$  is the magnetoelastic constant. Coefficients  $a_i$ ,  $b_i$ , and  $C$  depend on the DOS and the DOS derivatives at  $E_F$  and temperature  $T$  [4]. We can obtain their concentration dependencies using DOS calculations. Equilibrium value of lattice constant of Ni-Mn-Ga is calculated with the help of QUANTUM ESPRESSO simulation package [5]. Received value is 5.82 Å and it is the same as experimentally observed [7]. This value we used for further calculations of DOS and other properties for different concentrations of  $\text{Ni}_{2+x}\text{Mn}_{1-x}\text{Ga}$  in austenite and martensite states. These calculations carried out with the help of Spin-Polarized Relativistic Korringa-Kohn-Rostoker (SPR-KKR) simulation package [6]. Using SPR-KKR package we have calculated DOS, exchange parameters and magnetic moment of  $\text{Ni}_{2+x}\text{Mn}_{1-x}\text{Ga}$  for concentration range  $0 \leq x \leq 0.39$ . Calculated results shown that magnetic moment of stoichiometric  $\text{Ni}_2\text{MnGa}$  is 4.07  $\mu\text{B}$  and it is decreased with increasing of Ni excess  $x$  until 2.58  $\mu\text{B}$  for  $\text{Ni}_{2.39}\text{Mn}_{0.61}\text{Ga}$ . This behavior allows us to describe experimentally observed concentration dependence of magnetic moment in  $\text{Ni}_{2+x}\text{Mn}_{1-x}\text{Ga}$  system [2]. Using calculated DOS we can construct theoretical  $T$ - $x$  phase diagram of  $\text{Ni}_{2+x}\text{Mn}_{1-x}\text{Ga}$  alloys by the help of minimizing free energy (1).

Work was supported by grants National Council of Enlightener Organizations and RFBR grants 10-02-96020\_ural and 11-02-00601.

- [1] P. Entel et al, *Materials Science Forum*, **635** (2010) 3.
- [2] V.V. Khovaylo et al, *Phys. Rev. B.*, **72**, (2005) 224408.
- [3] P. Lazpita et al, *New J. of Phys.*, **13**, (2011) 033039.
- [4] M.A. Zagrebin et al, *MRS Proceedings*, **1310** (2010) ff03-08
- [5] P. Giannozzi et al, *J. Phys.: Condens. Matter*, **21** (2009) 395502.
- [6] H. Ebert, *Lecture Notes in Physics*, **535** (1999) 191.
- [7] P.J. Webster et al, *Phil. Magazine B*, **49** (1984) 295.

24PO-I1-38

## RELAXATION OF THE MAGNETIZATION NEAR THE MAGNETIC PHASE TRANSITION IN GADOLINIUM

*Kamantsev A.<sup>1</sup>, Koledov V.<sup>1</sup>, Shavrov V.<sup>1</sup>, Afanasyev A.<sup>2</sup>, Buchelnikov V.<sup>2</sup>, Taskaev S.<sup>2</sup>*

<sup>1</sup> Kotelnikov Institute of Radio Engineering and Electronics of RAS, 11/7 Mokhovaya str., 125009 Moscow,

<sup>2</sup> Chelyabinsk State University, 129 Br. Kashyrinyh str., 454001 Chelyabinsk, Russia  
kama@cplire.ru

The research in the field of the new technology of refrigeration at room temperature based on magnetic materials with phase transitions (PT) attracts much attention last years. In spite of the fact that magnetic PT were investigated theoretically and experimentally for a long time, at the moment there is no deep understanding of the question of the kinetic phenomena going on with magnetic PT, which is crucial in development of this technology. Practically it is very important to know the fundamental physical restrictions on speed of relaxation processes of order parameter (magnetization) near critical point of PT. Theoretically [1], relaxation processes near the 2<sup>d</sup> order PT point are described by Landau-Khalatnikov equation:  $\frac{d\eta}{dt} = -\gamma \frac{\partial \Omega}{\partial \eta}$ , where  $\eta$  – order parameter,  $t$  – time,  $\Omega$  – thermodynamic potential,  $\gamma$  – kinetic coefficient.

The aims of present work are the following:

- 1) To develop the theoretical basement of the experimental method for the measurement of the time of establishment of the equilibrium value of order parameter after fast heating and cooling of the sample in the form of thin plate near PT critical temperature.
- 2) Theoretical study of heat exchange processes between the water coolant and the plate made of magnetocaloric material in order to estimate the time response of heating and cooling.
- 3) To estimate achievable magnitude of power-to-weight ratio of magnetocaloric refrigerator or thermal pump with working body made of gadolinium.

In present work the computer modeling was carried out in COMSOL system. The geometrical model of method was constructed by means of the graphic interface. Numerical simulation was done using 2D and 3D grids in the geometry corresponding to experimental method. The system of the equations consisting of Navier–Stokes, heat conductivity and continuity was solved by finite element method. The coolant motion along sample with different velocities was calculated, the heat diffusion and convection were taken into account.

The relaxation times of Gd plate temperature in cases of heating and cooling was determined. It is shown, that the process of cooling (heating) of the sample is irregular and depends on the type of coolant flow: laminar or turbulent. The flow type influences considerably the magnetic behavior of the sample.

Support by RFBR grants 10-02-96020-r-ural, 11-02-00601, 10-02-92110 and RF President grant MK-1891.2010.2 is acknowledged.

[1] L.D Landau, I.M. Khalatnikov, *Doklady Akademii Nauk USSR*, **96** (1954) 469.

24PO-I1-39

## ANNEALING AND MAGNETIC FIELD INFLUENCE ON THE MARTENSITIC TRANSITION IN $\text{Ni}_{45.8}\text{Mn}_{42.6}\text{In}_{11.6}$ SHAPE MEMORY ALLOY RIBBONS

González L.<sup>1\*</sup>, García J.<sup>1</sup>, Nazmunnahar M.<sup>2</sup>, Rosa W.O.<sup>1</sup>, Escoda Ll.<sup>3</sup>, Suñol J.J.<sup>3</sup>, Prida V.M.<sup>1</sup>, Koledov V.V.<sup>4</sup>, Shavrov V.G.<sup>4</sup>, Hernando B.<sup>1</sup>

<sup>1</sup> Departamento de Física, Universidad de Oviedo, Calvo Sotelo s/n, 33007-Oviedo, Spain.

<sup>2</sup> Dpto. Física de Materiales, Univ. País Vasco UPV/EHU, Apdo. 1072, 20080 San Sebastián, Spain.

<sup>3</sup> Girona University, Campus Montilivi, ed. PII, Lluís Santaló s/n, 17003 Girona, Spain

<sup>4</sup> Kotelnikov Institute of Radio Engineering and Electronics, RAS, Moscow 125009, Russia.

\* [gonzalezlorena.uo@uniovi.es](mailto:gonzalezlorena.uo@uniovi.es)

A Heusler  $\text{Ni}_{45.8}\text{Mn}_{42.6}\text{In}_{11.6}$  alloy has been prepared by arc-melting and produced in a ribbon shape by rapid solidification using melt-spinning technique. The as-quenched sample presents an austenite-martensite structural transformation in the temperature range from 50 K up to 400 K, with start and finish temperatures of the martensitic phase transformation were  $M_s = 236$  K and  $M_f = 166$  K, while the ones found for the austenite were  $A_s = 237$  K and  $A_f = 268$  K respectively. We report the influence either of short-time vacuum annealing, during 10 minutes at 923 K, 973 K, 1023 K and 1073 K, and or magnetic field on the martensitic transition of that non-stoichiometric Heusler alloy ribbon. Thermomagnetic Measurements were performed on as-quenched and annealed ribbons by a VersaLab VSM in the 50 – 400 K temperature range applying different magnetic fields up to 3 T. Hysteresis loops were also recorded at different temperatures. Structural transformation is highly sensitive to both, applied field and annealing temperature. The annealing treatment shifts characteristic martensitic transition temperatures and a disclose of the austenite-martensite structural transformation can be appreciated at low applied field around 50 Oe that disappears when the field is increased in ribbons annealed at above 973 K. The observed magnetic and structural transitions could be explained by the existence of a strong dependence of exchange interactions on interatomic distances [1-3].

[1] T. Kanomata, et al., J. Magn. Magnet. Mater. **321** (2009) 773.

[2] V.V. Khovaylo et al., Phys. Rev. B **80** (2009) 144409

[3] K.R. Priolkar et al, European Phys. Lett. (2011)

24PO-I1-40

## MAGNETIC TRANSITIONS AND THE MAGNETIC CHARACTERISTICS OF THE MARTENSITIC TRANSFORMATIONS IN A Fe-Mn-Co ALLOY

Yüksel M.<sup>1</sup>, Ağan S.<sup>2</sup>

<sup>1</sup> Vocational school of health sciences Fatih University, 06370 Ostim /Ankara, TURKEY.

<sup>2</sup> Department of Physics, Kırıkkale University, 71450, Kırıkkale, TURKEY.

In this study, the magnetic transitions and the magnetic characteristics of the thermally induced martensitic transformations in Fe-13.2%Mn-5.3%Co alloy have been investigated. The microstructure analysis of diffusionless phase transformations forming in the alloy were performed by scanning electron microscopy (SEM), and the magnetic properties were revealed by Mössbauer

spectroscopy and AC susceptibility. SEM observations reveal that two types of thermal-induced martensites,  $\epsilon$  (h.c.p.) and  $\alpha'$  (b.c.c.) martensites, form in the austenite grains of the alloy. Mössbauer spectra at room temperature reveal a paramagnetic character with a singlet for the  $\gamma$  (f.c.c.) austenite and  $\epsilon$  martensite phases and a ferromagnetic character with a broad sextet for  $\alpha'$  martensite phase. In addition, measurement of the AC susceptibility of the alloy shows that the magnetic transition from the paramagnetic order to magnetic disordered occurs below room temperature at 258 K.

24PO-I1-41

## RELATION BETWEEN MAGNETOCALORIC EFFECT AND THERMAL HYSTERESIS OF MARTENSITIC TRANSITION IN Ni-Mn-X ALLOYS

*Titov I.S.<sup>1</sup>, Gonzalez-Alonso D.<sup>2</sup>, Acet M.<sup>1</sup>, Krenke T.<sup>3</sup>, Manosa L.<sup>2</sup>, Planes A.<sup>2</sup>*

<sup>1</sup> University Duisburg-Essen, Department of Physics, AG Farle, Duisburg, Germany

<sup>2</sup> Departament d'Estructura i Constituents de la Matèria, Facultat de Física, Universitat de Barcelona, Barcelona, Catalonia, Spain

<sup>3</sup> Thyssen Krupp Electrical Steel GmbH, D-45881 Gelsenkirchen, Germany

The presence of a large positive entropy change around the martensitic transformation in both  $\text{Ni}_{48.56}\text{Mn}_{34.94}\text{Sn}_{16.50}$  and in  $\text{Ni}_{50}\text{Mn}_{35.34}\text{In}_{14.66}$  is expected to lead to substantial cooling on applying a magnetic field. However, unlike in Ni-Mn-In, because of the relatively low shift of the transition temperature in Ni-Mn-Sn cooling would be somewhat limited. In both cases we measure direct temperature change under applying and removing a 5 T magnetic field around the reverse and forward martensitic transition. In case of Ni-Mn-Sn we detect cooling on applying a magnetic field (inverse MCE) and again further cooling on removing the field (conventional MCE). When the field is applied again once more we detect only conventional MCE on both removing and applying field due to the irreversibility of the thermodynamical state of the alloy after first application of field. In Ni-Mn-In, the irreversibility is reduced due to the strong shift in the martensitic transformation temperature with applied field (about 10K/T), and thus the initial state can be partially recovered. The results are discussed in relation to the width of the hysteresis and its thermal shift with applied magnetic field.

Support by SPP1239 is acknowledged.



## THE EFFECT OF STRUCTURAL STATE ON MAGNETIC AND MAGNETOCALORIC PROPERTIES OF MICRO- AND NANOCRYSTALLINE Gd

*Nikitin S.A.<sup>1</sup>, Smarzhenskaya A.I.<sup>1</sup>, Semisalova A.S.<sup>1</sup>, Kaminskaya T.P.<sup>1</sup>, Tereshina I.S.<sup>2</sup>,  
Burkhanov G.S.<sup>2</sup>, Chistyakov O.D.<sup>2</sup>, Dobatkin S.V.<sup>2</sup>*

<sup>1</sup> Lomonosov Moscow State University, Faculty of Physics, 119991 Moscow, Russia

<sup>2</sup> Baikov Institute of Metallurgy and Materials Science RAS, 119991 Moscow, Russia

In recent years the magnetic properties of alloys with micro- and nanocrystalline structure were extensively studied. The magnetization process, magnetic hysteresis and forced magnetization in these materials are not sufficiently studied, though their prospects are of no doubt. The study of magnetization processes in modeling objects like Gd acquires a special significance.

The purpose of this work was the investigation of magnetic and magnetocaloric properties of Gd with micro- and nanocrystalline state.

We used Gd as starting material which was purified by double vacuum distillation. An original furnace has been designed and purification regimes have been developed [1]. The purified Gd (of 99.96 wt % purity) is characterized by low contents of metallic and interstitial elements, in particular, oxygen, whose concentration was decreased by two orders of magnitude as a result of the purification. A method widely employed to produce nanocrystalline state in materials involves severe plastic deformation (SPD) [2]. This method is specific because it allows to avoid the starting material contamination with impurities and to perform the fabrication of pore-free samples suitable for structural and magnetic measurements.

SPD was performed in a Bridgman anvil by means of torsion under high hydrostatic pressure of 4 GPa at room temperature with achieved true strain of 5 revolutions on samples with initial sizes of 10 mm in diameter and 0.6 mm in height. Magnetic properties have been investigated using vibrating sample magnetometer in magnetic fields up to 12 kOe at the temperature range 200–350 K.

The structural state of the samples was investigated by “SMENA” Scanning Probe Microscope, operating in a semi-contact mode, and also using a phase contrast method. The scanning was performed with a silicon cantilevers. The AFM investigations have revealed the presence of structural elements with the sizes of 30–250 nm.

The comparative investigation of magnetic properties of the bulk Gd and the same material after SPD processing has been performed. The isothermal magnetic entropy change was calculated from magnetization measurements near the ferromagnetic-paramagnetic phase transition at  $T_C=293$  K using Maxwell relations. Our experiments have shown that in conventional Gd at  $T=T_C$   $\Delta S_M \approx 2.6$  J/kg·K, while in nanocrystalline Gd  $\Delta S_M \approx 1.6$  J/kg·K, with a wide “diffuse” phase transition.

The explanation for obtained results is that in nanocrystalline Gd the size of nanograins is comparable with the domain wall width and the forced magnetization near  $T_C$  is defined by exchange correlation interactions between adjacent grains. In this case the forced magnetization is accompanied with the magnetic spin ordering, opposed to both thermal fluctuations and discontinuity of local exchange energy.

The work is supported by RFBR, pr. N 10-03-00848 and N 10-02-00721.

[1] O.D. Chistyakov, G.S. Burkhanov, N.B. Kol’chugina, N.N. Panov, *Vysokochistye veshchestva*, **3** (1994) 57 (in Russian).

[2] R.Z. Valiev, *Russ. Nanotekhnologii*, **1-2** (2006) 208 (in Russian).



**24 August**

Wednesday

17:30-19:00

poster session  
24PO-I2

**“Spintronics and  
Magnetotransport”**

24PO-I2-1

## MAGNONIC CRYSTAL FOR SENSITIVE MAGNETIC FIELD SENSORS

Takagi T.<sup>1</sup>, Noda J.<sup>1</sup>, Ueno T.<sup>1</sup>, Baryshev A.V.<sup>1,2</sup>, Inoue M.<sup>1</sup>

<sup>1</sup> Toyohashi University of Technology, Toyohashi 441-8580, Japan

<sup>2</sup> Ioffe Physico-Technical Institute, Saint-Petersburg 194021, Russia

We have experimentally demonstrated that a *magnonic crystal* - an artificial magnetic structure for controlling propagation of magnetostatic waves - can be used as an extremely sensitive sensor for detecting magnetic fields. Functional characteristics of the sensor were studied at room temperature and in a normal noisy space without considering any magnetic shielding.

Highly sensitive detection of a magnetic field at room temperature is one of the key techniques of the brain-computer interfaces [1]. To realize this technique without inserting undesirable electrodes into the brain, we require a very sensitive magnetic field sensor that can enable the detection of a localized three-dimensional magnetic field originating from the brain at room temperature. In this work we discuss a *magnonic crystal* [2] which is an artificial magnetic material for the propagation of magnetic waves. We show that a magnonic crystal can be used as an extremely sensitive magnetic field sensor that is functional at room temperature.

The *magnonic crystal*—an analogy of photonic crystal [3] – is a ferromagnetic periodical structure exhibiting band gaps corresponding to attenuation of magnetic waves, which is supported either by the magnetostatic coupling or exchange coupling of spins, depending on the frequency (wavelength) of the waves. Periodicity can be easily introduced for magnetostatic surface waves (MSSW) propagation. This is because the wave propagates by confining its energy to the surface of the medium, and the MSSW magnonic band gap is obtained merely by periodically modulating the surface of medium. For such a periodic surface modulation, use of a set of periodic metal stripes directly formed on the surface is a simple way for obtaining a one-dimensional MSSW magnonic crystal.

Under the bias field of  $H_0 = 200$  Oe, the magnonic crystal exhibited a clear and deep band gap of -59.4 dB at approximately 3.00 GHz; the resonant strength  $Q$  of this band gap was considerably high. The frequency of the band gap was found to be very sensitive to the magnetic field applied to the crystal. Our experiments showed that the magnonic crystal exhibited its high potential for magnetic field measurement without considering any magnetic shielding. This sensitivity was more than 10 times that of the giant magneto-impedance (GMI) element. If the sensitivity of this magnetic field sensor by magnonic crystal reaches the level of that of the superconducting quantum interference device (SQUID), numerous applications including the brain-computer interface can be explored for the advancement of human life.

[1] D. J. Krusienski and J. R. Wolpaw, *Int. Rev. Neurobiol.* **86**, 147 (2009).

[2] M. E. Dokukin, K. Togo, M. Inoue, *J. Magn. Soc. Jpn.* **32**, 103 (2008).

[3] J. D. Joannopoulos, R. Meade, *J. Winn*, *Photonic Crystals*, Princeton University Press, Princeton NJ (1995).

## MAGNETIC-FIELD-DRIVEN MICROWAVE DETECTION EFFECT IN A MANGANITE-BASED MAGNETIC TUNNEL STRUCTURE

*Rautskiy M.V.<sup>1</sup>, Volkov N.V.<sup>1,2</sup>, Eremin E.V.<sup>1,2</sup>, Patrin G.S.<sup>1,3</sup>*

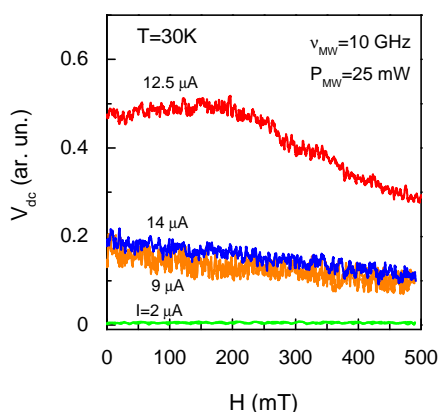
<sup>1</sup> L.V. Kirensky Institute of Physics SB RAS, Krasnoyarsk, 660036, Russia

<sup>2</sup> Siberian State Aerospace University, Krasnoyarsk, 660014, Russia

<sup>3</sup> Siberian Federal University, Krasnoyarsk, 660041, Russia

The methods of studying the spin-dependent effects in materials under the combined external factors allow obtaining more information on the observed phenomena as compared to the traditional investigation methods and make it possible to find effective ways of controlling the spin-polarized current in nanostructures.

Here we present the data on the microwave detection properties of a magnetic tunnel structure LSMO/LSM<sub>1-δ</sub>O/MnSi, where LSMO (La<sub>0.7</sub>Sr<sub>0.3</sub>MnO<sub>3</sub>) and MnSi are ferromagnetic conducting layers separated by a potential barrier formed by an LSM<sub>1-δ</sub>O manganite layer depleted in manganese. The results of investigation of the transport properties in current-in-plane (CIP) geometry were reported previously in [1]. In the experiments on the microwave radiation detection, we also used the planar geometry. The structure under study exhibits the microwave detection effect; the value of rectified voltage  $V_{dc}$  depends on magnetic field  $H$  (see the figure). The value of



$V_{dc}$  and the behavior of the  $V_{dc}(H)$  dependence are affected by bias current  $I_{dc}$  through the structure. The maximum value of the effect and the most pronounced variations in a magnetic field are observed at the bias current value corresponding to the highest nonlinearity of the current-voltage characteristic (CVC). When  $I_{dc}$  is tuned out in the smoother portions of the CVC, the detection effect value decreases; at zero bias, the effect vanishes. The nonlinearity of the CVC is apparently responsible for the detection properties of the structure under investigation, whereas the dependence on  $H$  originates from the CVC variation in magnetic field: with increasing field, the dependence tends to become smoother and, in the limit, linear. As a consequence,  $V_{dc}$  decreases with increasing  $H$ .

It is not improbable that in the investigated structure in CIP geometry under certain conditions the mechanism based on the interrelation between the spin-polarized current and the spin dynamics may be implemented [2]. It is confirmed, in particular, by the observed magnetic-field-dependent detection effect at low temperatures and large bias currents. The signal is observed in the fields far above 100 mT, where the CVC is already linear and invariable with increasing  $H$ .

This study was supported by the Russian Foundation for Basic Research, project no. 11-02-00367-a); Presidium of the Russian Academy of Sciences, program 21.1; the Division for Physical Sciences of the Russian Academy of Sciences, program 2.4.4.1; the Siberian Branch of Russian Academy of Sciences, projects nos. 5 and 134; and the Federal target program, State contract NK-556P\_15.

[1] N.V. Volkov, C.G. Lee, P.D. Kim, et al., J. Phys. D: Appl. Phys., 42 (2009) 205009.

[2] A.A. Tulapurkar, Y. Suzuki, A. Fukushima, et al., Nature (London), 438 (2005) 339.

24PO-I2-3

## PLANAR HALL EFFECT IN STRAINED MANGANITE THIN FILMS

*Borisenko I.V., Ovsyannikov G.A., Shakhunov V.A.*

Kotel'nikov Institute of Radio Engineering and Electronics, Russian Academy of Sciences,  
Moscow, Russia.

In recent years nanoscale magnetic materials and devices are in the field of interest due to their possible applications in future spintronics. Magnetoresistive methods like anisotropic magnetoresistance or planar Hall effect (PHE) was successfully implemented for evaluating the magnetic state of semiconductor ferromagnetic structures [1]. Manganites are the most studied magnetic oxide compounds and considered to be possible candidate for spintronic and magnetoelectric device applications. Magnetic and electronic properties of manganites strongly depend on both mechanical strain imposed by substrate and doping. In this work we studied the effect of planar Hall effect in thin optimally doped manganite films epitaxially grown on substrates with different symmetries of crystalline structure.

Thin films of  $\text{La}_{2/3}\text{Sr}_{1/3}\text{MnO}_3$  ( $T_{\text{Curie}} \approx 370\text{K}$ ) with thickness of 40nm were epitaxially grown by pulsed laser deposition technique on (110) $\text{NdGaO}_3$  and (001) $\text{SrTiO}_3$ . Manganite films were patterned into hall bars with thickness of 50  $\mu\text{m}$  by Ar ion beam milling through photoresist mask. (110) $\text{NdGaO}_3$  has orthorhombic symmetry and provoke in LSMO film strains of different polarity while (001) $\text{SrTiO}_3$  is of cubic symmetry and causes biaxial tensile strain. PHE describes the situation when the biasing current and the magnetization both lies in the film plane and the lateral resistance  $R_{xy}$  depends on the angle between them ( $\alpha$ ) only:  $R_{xy} = R_0 \cdot \sin(2\alpha)$ . Analyzing  $R_{xy}(H)$  dependencies for several direction of magnetic films we conclude that films grown on  $\text{NdGaO}_3$  substrate have strong uniaxial magnetic anisotropy while films on  $\text{SrTiO}_3$  either have no anisotropy or weak biaxial anisotropy which enhances while temperature goes down. These results were compared to ones reported earlier [2]. The magnitude of the PHE was about 0,5  $\Omega$  at 300K which is by several orders of magnitude larger than in metallic ferromagnetics but significantly decreases at lower temperatures.

Supported by "School" 5423.2010.2, SEC 02.740.11.0795, RFBR 11-02-01234-a and Programs of RAS.

[1] H.X. Tang et al., *Phys.Rev.Lett.* **90**, 107201 (2003).

[2] G.A. Ovsyannikov, A.M. Petrzhhik, I.V. Borisenko, A.A. Klimov, Yu.A. Ignatov, V.V. Demidov, and S.A. Nikitov, *JETP* **108**, p. 48 (2009).

## DYNAMIC TRANSFORMATION OF MAGNETIC VORTICES IN SPIN-VALVE NANO-COLUMNAR ELECTRICAL MICROWAVE SIGNAL GENERATOR

*Ekomasov A.<sup>1</sup>, Azamatov Sh.<sup>1</sup>, Khvalkovskiy A.<sup>2</sup>, Zvezdin K.<sup>2</sup>, Ekomasov E.<sup>1</sup>*

<sup>1</sup> Bashkir State University, 450074, Ufa, Validy Str., 32, Russia

<sup>2</sup> Prokhorov General Physics Institute RAS, 119991, Moscow, Vavilov Str., 38, Russia

In 2007 the discovery of giant magnetoresistance effect (GMR), initiated an active research in the field of spintronics, received the Nobel Prize in Physics (A. Fert, P. Grunberg). Currently, the magnetoresistance effects are already used in the hard drive industry. The recently observed phenomenon of switching and excitation of oscillation of the magnetization using the spin-polarized current is of great interest. These phenomena are due to the effect of spin transfer predicted by J. Slonczewski and L. Berger in 1996 [1-2]. One of the promising applications of these phenomena is the so-called Spin-Transfer nanogenerators (STNO) of microwaves, based on the spin transfer effect. Most of these structures have two magnetic layers separated by nonmagnetic spacer. When the current of fairly high density flows through them, the magnetization oscillations at a frequency of about 0.3-3 GHz arise in this system. Due to the GMR effect or tunneling magnetoresistance the resistance of the system changes at the same frequency, which can be used to create nanoscale microwave generators of electricity.

In this paper we consider STNO, in which both magnetic layers are in the vortex state. The magnetic dynamics of such system has been numerically studied using micromagnetic package SpinPM. In particular, we studied the dynamic processes of transformation of magnetic vortices (vortex core switching), for different currents, the external magnetic field and the magnetic layers shape (two round layers, oval and round, two oval). It has been found that with increasing current, the switching core field reduced similar to the dependences observed in the experimental work [3]. Also there is a substantial change in the value of the switching field depending on the shape of the magnetic layers.

This work has been supported by RFBR grant 10-02-01162.

[1] J. Slonczewski, *J. Magn. Magn. Mater.* **L1** (1996) 159.

[2] L. Berger, *Phys. Rev.* **B 54** (1996) 9353.

[3] N. Locatelli, V.V. Naletov, J. Grollier, G. de Loubens, V. Cros, C. Deranlot, C. Ulysse, G. Faini, O. Klein, A. Fert arXiv:1005.0290v2.

24PO-I2-5

## EXCHANGE BIAS IN Co/IrMn AND NiFe/IrMn STRUCTURES INDUCED BY DEPOSITION IN PRESENCE OF MAGNETIC FIELD

*Dzhun I.O.<sup>1</sup>, Chechenin N.G.<sup>1</sup>, Dushenko S.A.<sup>1,2</sup>, Konstantinova E.A.<sup>2</sup>*

<sup>1</sup> Skobeltsyn Institute of Nuclear Physics

<sup>2</sup> Faculty of Physics Lomonosov Moscow State University, Leninskie Gory, Moscow 119991, Russian Federation

One of the methods to saturate an antiferromagnetic layer in a ferromagnetic/antiferromagnetic (F/AF) structure is the deposition in presence of a constant magnetic field applied in plane of substrate. In this work we have investigated bilayer structures with IrMn antiferromagnetic layer. In comparison with Fe<sub>50</sub>Mn<sub>50</sub>-alloy we have investigated before, Ir<sub>30</sub>Mn<sub>70</sub> represents higher Neel temperature (hence the exchange bias blocking temperature) and thermal stability. Due to development of magnetic sensory it is important to obtain exchange bias of a desirable magnitude. That is why the dependencies of the exchange bias field magnitude on different parameters such as layer materials and thicknesses are of great importance. On the other hand, many effects concerning the exchange bias represent also fundamental interest. Here we report on our investigation of exchange bias, uniaxial anisotropy and intrinsic resonance field in F/AF structures for different AF layer thicknesses and F layer materials. The multilayer structures Si/Ta/Co(7nm)/IrMn(15nm)/Ta and Si/Ta/NiFe(7nm)/IrMn(15nm)/Ta were deposited by DC magnetron sputtering in argon at the pressure of  $3 \cdot 10^{-3}$  Torr with the magnetic field of 420 Oe applied in the plane of the substrate during the deposition. The Si/Ta/Co(7nm)/Ta and Si/Ta/NiFe(7nm)/Ta structures with free, i.e. not pinned by exchange interaction F layers, were also deposited for a comparison. A set of Si/Ta/NiFe(10nm)/IrMn( $t_{AF}$ )/Ta samples was also made in order to investigate the dependence of magnetic properties on the IrMn antiferromagnetic layer thickness  $t_{AF}$ . The magnetic properties of the samples were studied using the angular dependence of the ferromagnetic resonance field. It was shown that non-zero exchange bias of 14 Oe appears at room temperature in contrast to the structures with FeMn layer. These structures are also characterized with higher uniaxial anisotropy of 134 Oe and lower intrinsic resonance field (higher Co-layer saturation magnetization). The surface of samples with IrMn-layer was smoother than that for structures with FeMn. The exchange bias field increased up to 85 Oe when NiFe was deposited instead of Co layer. It can be explained by lower coercivity of NiFe. The intrinsic resonance field of the free NiFe layer is larger than that of free Co layer (750 and 596 Oe respectively), while the uniaxial anisotropy changes slightly (from 92 to 82 Oe). In the case of Co/IrMn bilayer structure the uniaxial anisotropy was significantly higher than that of free Co layer, while the intrinsic resonance field was lower than that of the free layer. Conversely, in the case of NiFe-layer the uniaxial anisotropy of the F/AF structure is lower than that of the free layer, while the intrinsic resonance fields were the same. The exchange bias thickness dependence had non-monotonic shape with two maxima at 15 and 60 nm antiferromagnetic layer thickness.

This work is supported by Federal Agency of Science and Innovations (contract 02.740.11.0242, contract 02.740.11.0389). The FMR study was performed at User Facilities Center of M.V. Lomonosov Moscow State University.



24PO-I2-6

## GIANT MAGNETORESISTANCE IN NiFe/IrMn/Cu/NiFe – BASED SPIN-VALVE STRUCTURES

*Dushenko S.A.<sup>1,2</sup>, Chechenin N.G.<sup>1,2</sup>, Chernykh P.N.<sup>1</sup>, Dzhan I.O.<sup>1</sup>*

<sup>1</sup> Skobeltsyn Institute of Nuclear Physics

<sup>2</sup> Faculty of Physics Lomonosov Moscow State University, Leninskie Gory, Moscow 119991, Russian Federation

The GMR effect in the ferromagnetic/antiferromagnetic based spin-valves was studied. Experimental samples were deposited by magnetron sputtering on Si (100) substrate using the magnetron ATC ORION-5 produced by AJA INTERNATIONAL in the argon atmosphere at the pressure of  $3 \cdot 10^{-3}$  Torr. The exchange bias was induced in the spin-valve structures by applying constant magnetic field of 400 Oe along the sample surface during the deposition. The deposition rates for each layer were evaluated by measuring the thickness of dummy layers using the Rutherford backscattering. Samples with the structure Si/Ta(15nm)/NiFe(t1)/IrMn(15nm)/Cu(t2)/NiFe(10nm)/Ta(15nm) were made. The dependence of their resistance from the external magnetic field was measured at the room temperature. In the set of the samples with different t1 (thickness of the pinned ferromagnetic layer) fast reduction of the GMR effect with the increase of t1 was observed. In the other set of samples with different thickness of the spacer layer t2 of Cu it was found that the absolute value of the effect (maximal difference in the resistance) didn't change significantly from sample to sample (absolute value of the effect is about the 0.04 Ohm), but the magnetic field of the resistance peak position and its width strongly depended on the Cu thickness. Though the nature of this effect isn't completely clear we assume that it arises from the changes in the uniformity of the Cu spacer layer when its thickness is small on the one hand, and the increasing role of the conductivity of this layer with the increasing thickness in comparison with the conductivity of the whole structure on the other hand.

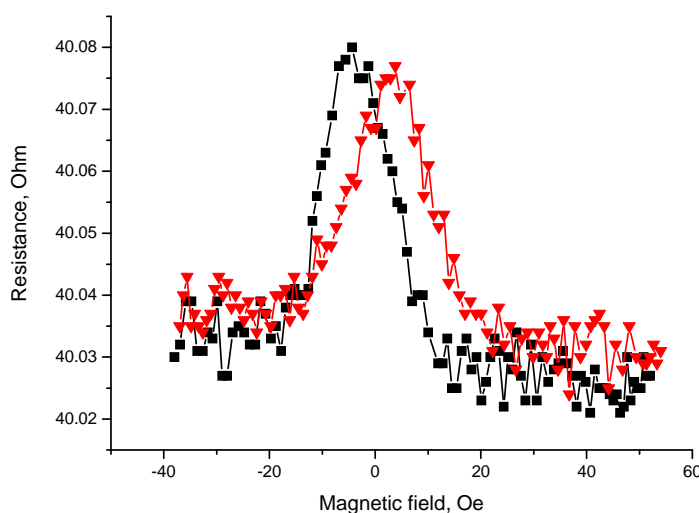


Figure 1. Magnetoresistance for the structure Si/Ta(15nm)/NiFe(7nm)/IrMn(15nm)/Cu(1nm)/NiFe(10nm)/Ta(15nm) for the increasing (squares) and decreasing (triangles) external magnetic field.

This work is supported by Federal Agency of Science and Innovations (contract 02.740.11.0242, contract 02.740.11.0389).

## ELECTROLUMINESCENCE OF InGaAs/GaAs QUANTUM SIZE HETEROSTRUCTURES WITH GaAs BARRIER MODIFIED BY DELTA-Mn DOPING

*Dorokhin M.V.<sup>1</sup>, Danilov Yu.A.<sup>1</sup>, Demina P.B.<sup>1</sup>, Kulakovski V.D.<sup>2</sup>, Prokof'eva M.M.<sup>1</sup>,  
Vikhrova O.V.<sup>1</sup>, Zaitsev S.V.<sup>2</sup>, Zvonkov B.N.<sup>1</sup>*

<sup>1</sup> Physico-Technical Research Institute of Nizhny Novgorod State University, 603950 Nizhny  
Novgorod, Gagarine Av., 23/3, Russia

<sup>2</sup> Institute of Solid State Physics, RAS, 142432 Chernogolovka, Institutsky pr. 2, Russia

The important feature of currently developing newest light-emitting devices (LEDs) is the capability of emitting a circularly polarized light. The latter feature makes such LED's attractive as a key element of the spintronics [1]. Prospective devices of this kind are the light-emitting Au/n-GaAs Schottky diodes with a  $\delta$ <Mn>-doped layer inserted near an InGaAs/GaAs quantum well (QW). Our previous investigations have shown the possibility of obtaining both high electroluminescence (EL) intensity and circular polarization [2]. In the present work we investigate the properties of InGaAs/GaAs heterostructures with  $\delta$ <Mn>-doped GaAs barrier.

The structures were grown by two-stage epitaxial growth method. An  $\text{In}_x\text{Ga}_{1-x}\text{As}/\text{GaAs}$  QW ( $x = 0.1-0.2$ ) and the thin (3 nm) spacer GaAs layer were grown on  $n^+$ -GaAs (or  $i$ -GaAs) substrates by MOCVD at 600°C. At the next stage the  $\delta$ <Mn>-doping and a GaAs cap layer growth were carried out at 400°C in the same reactor by the laser sputtering of a Mn and GaAs targets, respectively. The details are described elsewhere [2]. The nominal thickness of  $\delta$ <Mn> layer ( $Q_{\text{Mn}}$ ) was varied from 0.1 to 1.8 monolayers (ML). The reference sample contained no  $\delta$ -layer.

The type of conductivity and 2D concentration of carriers in the QW/ $\delta$ <Mn> structure were determined by the Hall effect measurements of the samples grown on  $i$ -GaAs substrates. All samples have a  $p$ -type conductivity with concentrations of holes up to  $1 \times 10^{12} \text{ cm}^{-2}$  at 77 K and  $1.5 \times 10^{13}$  at 300 K. The hole mobility was up to  $685 \text{ cm}^2/\text{V}\cdot\text{s}$  at 77 K and  $70 \text{ cm}^2/\text{V}\cdot\text{s}$  at 300 K

It was found that a conduction channel in the QW remains even at low temperatures.

The forward bias EL at 77 K demonstrated strong enhancement of the EL intensity in comparison with that of the similar samples without  $\delta$ -doping. The EL intensity non-monotonously depends on the Mn content as well as on a spacer layer thickness. The maximum of the EL was obtained for the sample with  $Q_{\text{Mn}} = 0.1$  ML. The best thickness of a spacer between  $\delta$ <Mn> and a QW was found to be 10 nm. The enhancement of the EL is believed to be due to increased hole injection into the QW with a help of the inserted acceptor  $\delta$ <Mn>-layer. This supposition is approved by  $I$ - $V$  characteristics measurements that show the peculiarities on the  $I$ - $V$  curves related with additional hole current flowing.

The EL at the magnetic field was measured at 1.5 K in a liquid He cryostat with the superconducting magnet. The magnetic field  $B$  was normal to the QW plane. In the magnetic field the EL radiation becomes circularly polarized. The degree of polarization varies for different samples from 12% to 48 % and strongly depends on the  $\delta$ <Mn> parameters. However the polarization degree for samples with  $\delta$ <Mn>-doping always exceeds that of reference samples evidencing about the affect of  $\delta$ <Mn> on hole spin polarization in the QW.

This work was supported by RFBR (projects 08-02-00548 and 08-02-97038), Ministry of Education of Russian Federation (project 2.2.2.2.4737).

[1] A.M. Nazmul, S. Sugahara, M. Tanaka // Phys. Rev. B. **67**, 241308, (2003).

[2] Yu.A. Danilov, P.B. Demina, M.V. Dorokhin, et.al. // Euro-Asian Symp. "Magnetism on a nanoscale". Abstract Book. Kazan, 23-26 August 2007, P.121.

24PO-I2-8

## PRESSURE TRANSDUCER BASED ON MAGNETIC PHASE TRANSITION

Mollaev A.Yu.<sup>1</sup>, Kamilov I.K.<sup>1</sup>, Arslanov R.K.<sup>1</sup>, Marenkin S.F.<sup>2</sup>, Arslanov T.R.<sup>1</sup>, Zalibekov U.Z.<sup>1</sup>

<sup>1</sup> Institute of Physics, Daghestan Scientific Center of the Russian Academy of Science, 367003, Makhachkala, Russia

<sup>2</sup> Institute of common and inorganic chemistry of the Russian Academy of Science, 119991, Moscow, Russia

The high mobility of charge carriers, small effective mass of electrons and great relations of electron mobility to hole mobility are the characteristic features of new ferromagnetic semiconductors CdGeP<sub>2</sub>:Mn with T<sub>c</sub>=320 K on the basis of A<sup>II</sup>B<sup>IV</sup>C<sup>V</sup><sub>2</sub> group. The semiconductor structures based on them are the promising materials for creation of pressure transducers used both as the pressure calibrator in high pressure devices and as the command element reference. In present work is offered a new physical approach based on the metamagnetic phase transition.

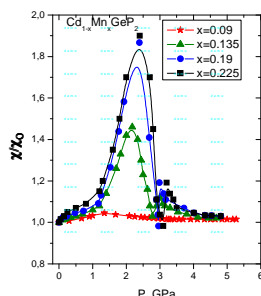


Fig.1. The baric dependence of magnetic susceptibility  $\chi/\chi_0(P)$  for Cd<sub>1-x</sub>Mn<sub>x</sub>GeP<sub>2</sub> with different level of Mn.

The baric dependences of relative magnetic susceptibility ( $\chi/\chi_0(P)$ ) are measured at high hydrostatic pressures up to 6 GPa in polycrystalline samples of Cd<sub>1-x</sub>Mn<sub>x</sub>GeP<sub>2</sub> with ( $x=0.09 \leq x \leq 0.225$ ) at increase in pressure and a region of room temperatures. The measurements are carried out in high pressure device of “Toroid” type [1] and the magnetic susceptibility is estimated by a frequency method [2].

The magnetic phase transitions are revealed in all studied samples of p-Cd<sub>1-x</sub>Mn<sub>x</sub>GeP<sub>2</sub> with ( $x=0.09 \leq x \leq 0.19$ ) except the base (CdGeP<sub>2</sub>), when pressure increases. (Fig. 1). A maximum of ( $\chi/\chi_0(P)$ ) shifts towards the high pressures with increasing of Mn percentage. A maximum value rises with increasing of Mn percentage. According to analysis of ( $\chi/\chi_0(P)$ ) dependence in these samples occurs the metamagnetic phase transition – a

transition from low magnetization state to the high magnetization.

The offered transducers based on metamagnetic phase transition are small-size and technological in production. The magnetic susceptibility is used as indicator of properties. Since the phase transition of the magnetic susceptibility has a sharp peak of sufficiently high intensity, which is measured easily, offered transducers can be recommended as a command element in technological processes for production of super solids and precious-stone materials. They do not require the ohmic contacts, changing a percentage of Mn from 0.09 to 0.225 one can change a pressure value from P=1.34 GPa to P=2.4 GPa.

This work was supported by Program of Presidium of RAS “Thermophysics and mechanics of external energetic influences and physics of high compressed material” and Section of High Compressed Material.

[1] L. G. Khvostantsev, et al., Phys Status. Solidi. **A64** (1981) 379.

[2] A. Yu. Mollaev, et al., Inorganic materials. **37** (2001) 4327.

## ELECTRO-ASSISTED MAGNETIZATION SWITCHING IN ASYMMETRIC SPIN-VALVES

*Sohatsky V.*

T. Shevchenko Kiev University, Dep. of Radiophysics, 01033 Kiev, Ukraine

Spin transistor (ST), that could be used as a logic element or nonvolatile memory cell have continuous interest for spintronics since it could have attractive characteristics of switching, amplification and non-volatility. Such a ST must satisfy some contrary conditions as high sensitivity to electric and magnetic fields, high operating frequency and amplification capability (voltage, current, power gains), low power consumption, not complicated structure, low-cost technology, etc. The also problem of the ST is needs of high spin polarization and a distance of polarized spin transport enough for effective polarization detecting. The essential component of many STs is a spin-valve (SV), that must have high magnetoresistance (MR), not small own resistivity and spatial dimensions, low remagnetizing field, high speed switching, etc.

In order to improve characteristics of the SV incorporated in a ST it is possible to: 1) choose the orientation of bias magnetic field and magnetic anisotropy axes (Fig1a,b); 2) choose the thickness of the ferromagnetic layers that determine the interlayer interaction (Fig1c-e); 3) use polarized current passed through the SV to assist it remagnetization.

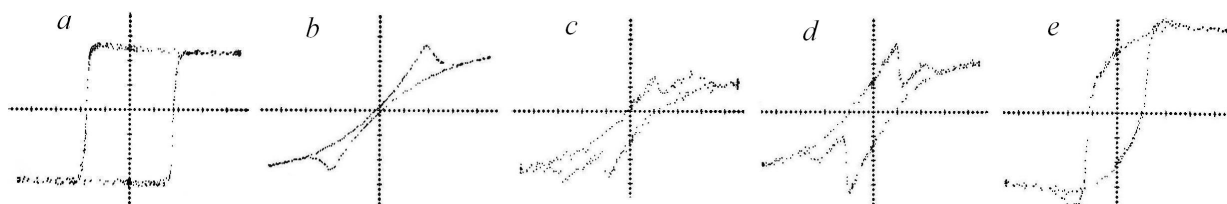


Fig1. View of MOKE hysteresis loops shape for choosing the SV remagnetizaion mode.

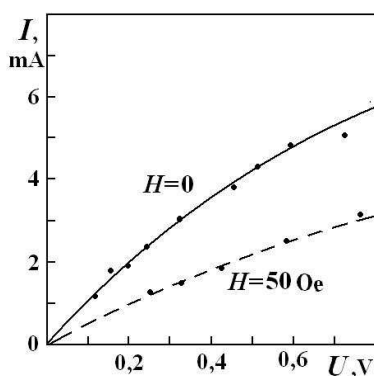


Fig.2. Output currents vs input voltage & bias field

The stack film structure was deposited on Si substrate with conducting channel and contacting electrodes for modeling the field-effect pseudo-ST with incorporated SVs of 2 types: with conductive (Fe/Cu/FeNi) or dielectric (Fe/MgO/NiFe) sublayer. The  $I$ - $V$  characteristics of such a ST were measured in a bias magnetic field mode; the remagnetization hysteresis curves were obtained with MOKE-magnetometer. Although such a ST could operate in a binary regime it's fit for modeling of all the ST functions. The output current depended on input voltage and applied magnetic field as shown on the graph (Fig.2). The power consumption of the ST with external magnetic field source is higher than it's need when the source is a component of the ST. Lack of amplification in a presented geometry was confirmed by evaluation of the energy balance, that moreover assumed

decreasing of the SV cell size (with corresponding increasing of demagnetizing). The possible way to overcome the above problems is to use in one ST two SVs with various remagnetizing fields and MR. The second SV (with higher MR) should be used for control the ST current and the first SV (with lower switching field) for control remagnetization current of the second SV. Another way that was also tried out in our experiments was a remagnetization assisted by polarized current. This complicate the ST construction, however the possibilities for amplification enhancement were attempted experimentally and confirmed by evaluations in both cases.

## OBSERVATION OF THE GRIFFITHS PHASE ANALOG IN THE Nd<sub>0.5</sub>Sr<sub>0.5</sub>MnO<sub>3-δ</sub> FILMS WITH A DEFICIT OF OXYGEN

Solin N.I.<sup>1</sup>, Medvedev Yu.V.<sup>2</sup>, Khokhlov V.A.<sup>2</sup>, Korolev A.V.<sup>1</sup>, Prokhorov A.Yu.<sup>2</sup>

<sup>1</sup>Institute of Metal Physics, S.Kovalevskaya str., 18, Yekaterinburg, 620041, Russia,

<sup>2</sup>Donetsk Institute for Physics & Engineering, 83114, Donetsk, R.Luxemburg str., 2, Ukraine

email: solin@imp.uran.ru

Even in the best crystals of manganites there are intrinsic inhomogeneities (the quenched disorder) which determine the colossal magnetoresistance effect. The existence of nanoclusters in doped manganites up to a temperature  $T \approx T_C$  ( $T^*$  is analog of the Griffiths temperature) which is of

the order of the Curie temperature ( $T_C$ ) of conducting manganites is predicted [1]. With  $x=0,5-\delta$  the quenched disorder arises from an inconsistency between the sizes of Nd and Sr ions, from the existence of the charge order, the anion vacancies and from the proximity to the ferromagnet - antiferromagnet transition boundary.

The work is devoted to the observation of nanoclusters in the paramagnetic region from the magnetotransport properties of Nd<sub>0.5</sub>Sr<sub>0.5</sub>MnO<sub>3-δ</sub> films. The 120 nm thick films were prepared by

the rf-magnetron sputtering. Magnetism ( $T_C$  from 145 K up to 235 K) and magnetoresistance occur on these films annealing in oxygen. Resistance at  $T > T_C = 145$  K is described by the Efros-Shklovskii law:  $\log \rho(H=0) \sim (T_0/T)^{1/2}$ , where  $T_0 \sim 1/Rls$  and the magneto-resistance  $MR \equiv \rho(H=0)/\rho(H)$  is related with the change of  $Rls$  ( $Rls$  is size of localized states) [2]. The relative change of the size of localized states  $\Delta Rls/Rls^0$  in the magnetic field  $H$  has the form [3]:

$$\Delta Rls/Rls^0 \equiv [Rls(T,H) - Rls(T,H=0)]/Rls(T,H=0) = 1 - 1/[1 - (T/T_0)^{1/2} * LnMR]^2 \quad (1).$$

The relative change  $\Delta Rcl/Rcl^0$  of the size of clusters  $Rcl$  in the magnetic field at the carriers  $\theta$  self-localization in the paramagnetic matrix has the form [3, 4]:

$$\Delta Rcl/Rcl^0 \equiv [Rcl(T,H) - Rcl(T,H=0)]/Rcl(T,H=0) = b H^2 / [5 T (T-\theta)], \quad (2)$$

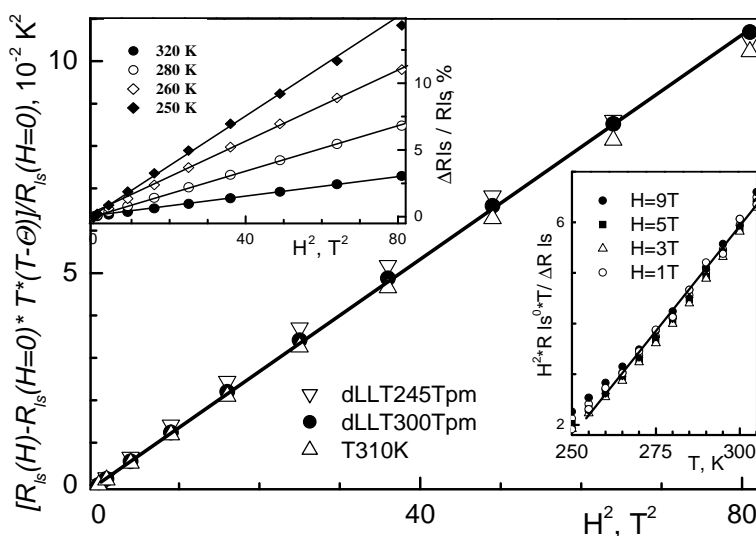
with  $T > \theta$ ,  $\theta$  is the Weiss temperature,  $b$ -the known value. The regularities of  $Rls$  upon magnetic field intensity  $H$  (fig. and the upper inset) and temperature  $T$  (the lower inset) determined from (1) are well described by the expression (2) in the model [4] of phase separation into metallic droplets with small radius  $Rcl$  within the paramagnetic matrix.

The results confirm the conclusion [1] about the existence of Griffiths phase analog. In Nd<sub>0.5</sub>Sr<sub>0.5</sub>MnO<sub>3-δ</sub> films the value  $T^* \approx 280-310$ K is close to the value  $T_C = 285$ K of Nd<sub>2/3</sub>Sr<sub>1/3</sub>MnO<sub>3</sub>.

This work was supported by Scientific Program of Far Eastern Division and Ural Division RAS and "Novel Materials and Structures" of the Department of Physics of RAS.

[1] J. Burgy et al., Phys. Rev. Letters, **87**, 277202(2001).

[2] C.M.Varma. Phys. Rev. B **54**, 7328(1996).



the rf-magnetron sputtering. Magnetism ( $T_C$  from 145 K up to 235 K) and magnetoresistance occur on these films annealing in oxygen. Resistance at  $T > T_C = 145$  K is described by the Efros-Shklovskii law:  $\log \rho(H=0) \sim (T_0/T)^{1/2}$ , where  $T_0 \sim 1/Rls$  and the magneto-resistance  $MR \equiv \rho(H=0)/\rho(H)$  is related with the change of  $Rls$  ( $Rls$  is size of localized states) [2]. The relative change of the size of localized states  $\Delta Rls/Rls^0$  in the magnetic field  $H$  has the form [3]:

$$\Delta Rls/Rls^0 \equiv [Rls(T,H) - Rls(T,H=0)]/Rls(T,H=0) = 1 - 1/[1 - (T/T_0)^{1/2} * LnMR]^2 \quad (1).$$

The relative change  $\Delta Rcl/Rcl^0$  of the size of clusters  $Rcl$  in the magnetic field at the carriers  $\theta$  self-localization in the paramagnetic matrix has the form [3, 4]:

$$\Delta Rcl/Rcl^0 \equiv [Rcl(T,H) - Rcl(T,H=0)]/Rcl(T,H=0) = b H^2 / [5 T (T-\theta)], \quad (2)$$

with  $T > \theta$ ,  $\theta$  is the Weiss temperature,  $b$ -the known value. The regularities of  $Rls$  upon magnetic field intensity  $H$  (fig. and the upper inset) and temperature  $T$  (the lower inset) determined from (1) are well described by the expression (2) in the model [4] of phase separation into metallic droplets with small radius  $Rcl$  within the paramagnetic matrix.

The results confirm the conclusion [1] about the existence of Griffiths phase analog. In Nd<sub>0.5</sub>Sr<sub>0.5</sub>MnO<sub>3-δ</sub> films the value  $T^* \approx 280-310$ K is close to the value  $T_C = 285$ K of Nd<sub>2/3</sub>Sr<sub>1/3</sub>MnO<sub>3</sub>.

This work was supported by Scientific Program of Far Eastern Division and Ural Division RAS and "Novel Materials and Structures" of the Department of Physics of RAS.

[1] J. Burgy et al., Phys. Rev. Letters, **87**, 277202(2001).

[2] C.M.Varma. Phys. Rev. B **54**, 7328(1996).

[3] N.I.Solin, JETPLetters, **91**,675 (2010)

[4] M. Yu. Kagan and K. I. Kugel', Phys. Usp. **44**, 553 (2001)

24PO-I2-11

## NEW MAGNETORESISTANCE RESULTS FOR GdB<sub>6</sub>

Anisimov M.A.<sup>1</sup>, Bogach A.V.<sup>1</sup>, Glushkov V.V.<sup>1</sup>, Demishev S.V.<sup>1</sup>, Samarin N.A.<sup>1</sup>, Filipov V.B.<sup>2</sup>,  
Shitsevalova N.Yu.<sup>2</sup>, Kuznetsov A.V.<sup>3</sup>, Sluchanko N.E.<sup>2</sup>

<sup>1</sup> Low Temperatures and Cryogenic Engineering Department, A.M. Prokhorov General Physics Institute of Russian Academy of Science, 38 Vavilov str., Moscow 119991, Russia

<sup>2</sup> Institute for Problems of Material Science of NAS, 3 Krzhyzhanovskii str., Kiev 03680, Ukraine

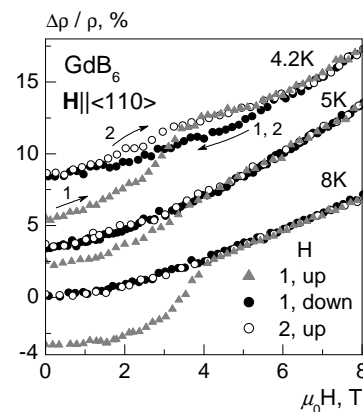
<sup>3</sup> Moscow Engineering Physics Institute, 31 Kashirskoe sh., Moscow 115409, Russia

E-mail: anisimov.m.a@gmail.com, nes@lt.gpi.ru

Among strongly correlated electronic systems the rare-earth (RE) hexaborides have attracted considerable interest due to variety of magnetic ground states. Most of RB<sub>6</sub> (R-Ce, Pr, Nd, Gd, Tb, Dy, Ho) are antiferromagnetic (AF) metals except of ferromagnetic EuB<sub>6</sub>, diamagnetic LaB<sub>6</sub> and narrow band semiconductors SmB<sub>6</sub> and YbB<sub>6</sub>. In present work the transport properties of gadolinium hexaboride (GdB<sub>6</sub>) have been investigated. Although Gd<sup>3+</sup> ion does not have the orbital degrees of freedom ( $L=0$ ,  $S=7/2$ ) the compound GdB<sub>6</sub> demonstrates the complex magnetic phase diagram. At zero magnetic field two successive phase transitions in (i) AF commensurate (C) with the wave vector  $\mathbf{k}=[\frac{1}{4}, \frac{1}{4}, \frac{1}{2}]$  and (ii) L states are observed in GdB<sub>6</sub> at  $T_N \sim 15\text{K}$  and  $T^* \sim 10\text{K}$ , respectively [1, 2]. However the nature of (ii) phase of GdB<sub>6</sub> is still the subject of discussion.

To shed more light on the features of ground state formation the comprehensive study of transverse magnetoresistance (MR) has been carried out on the high quality single crystals of GdB<sub>6</sub> ( $T_N \sim 15.5\text{K}$ ,  $T^* \sim 4.7\text{K}$ ) in the wide range of temperatures 2-40K and magnetic fields up to 8T. The data obtained allow to establish the crossover of magnetoresistance from negative (-MR,  $T > T_N$ ) to positive (+MR,  $T^* < T < T_N$ ) regime at  $T_N$ . The transition to L phase below  $T^*$  is accompanied by the complex behavior of MR with field hysteresis on the curves  $\Delta\rho(H)/\rho$  (see symbols  $\circ$  and  $\bullet$  on Figure) in the temperature range 2-4.7K. Along with the aforementioned field hysteresis which is detected in the slow rate heating from low to high temperatures an additional field hysteresis (see symbol  $\blacktriangle$  on Figure) was found for the first time in L and C phases of GdB<sub>6</sub>. The hysteresis feature was observed in the fast rate heating from low temperatures (2-3K) and only in the first scan of magnetic field (see the numbers of scan on Figure). This influence of the temperature prehistory on the MR behavior in GdB<sub>6</sub> is related to the remagnetization process.

The analysis of  $\Delta\rho(H)/\rho$  allows to separate three contributions to MR of GdB<sub>6</sub>. In addition to the (1) negative contribution ( $-\Delta\rho/\rho \sim H^2$ ) interpreted in the framework of Yosida model [3], (2) a linear ( $\Delta\rho/\rho \sim H$ ) and (3) nonlinear ferromagnetic components were also observed. The obtained results of MR analysis in GdB<sub>6</sub> are close to conclusions of [4]. According to the procedure of [4] where these contributions were naturally interpreted for AF metals PrB<sub>6</sub> and NdB<sub>6</sub> in terms of spin-polaron model, the (3) component should be ascribed to the ferromagnetic nanodomains (spin-polarized  $5d$ -states) embedded in the metallic matrix of GdB<sub>6</sub>.



- [1] S.Kunii, K.Takeuchi, et al., J. Magn. Magn. Mat., **52** (1985) 275.  
 [2] S.E.Luca, M.Amara et al., Physica B, **350** (2004) E39.  
 [3] K. Yosida, Phys. Rev. **107** (1957) 396.  
 [4] M.A.Anisimov, A.V.Bogach, V.V.Glushkov et al., JETP, **109** (2009) 815.

24PO-I2-12

## LOW DOPED $\text{La}_{0.54}\text{Ho}_{0.11}\text{Sr}_{0.35}\text{Mn}_{1-x}\text{V}_x\text{O}_3$ MANGANITES: CATION DISORDER INFLUENCE ON TRANSPORT PHENOMENA AND MAGNETIC PROPERTIES

*Craus M.-L.O.<sup>1,2</sup>, Cornei N.<sup>3</sup>, Oprea A.<sup>1,4</sup>, To T.L.<sup>2</sup>*

<sup>1</sup> National Institute of Research and Development for Technical Physics, Mangeron 47, Iasi, Romania

<sup>2</sup> Joint Institute for Nuclear Research, Joliot-Curie 6, Dubna, Russia

<sup>3</sup> "Al. I. Cuza" University, Chemistry Department, Blvd. Carol I 11, Iasi, Romania

<sup>4</sup> Universitatea Bucuresti, Physics Department, Bucharest- Magurele, Romania.

Simple perovskites with  $\text{ABO}_3$  structure are known as potential magnetoresistive materials ( $B = \text{Mn}$  or transition elements). Electronic phase diagrams of these oxides are complex, various states are stabilized by changing the carrier concentration, temperature or magnetic field intensity. Substitution of trivalent elements A with bivalent alkali-earth (Ca, Sr, Ba) leads to a change of the concentration of the carriers, while a substitution with isovalent rare earth elements produces a

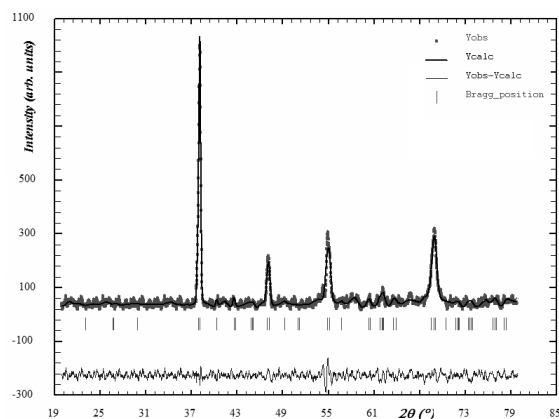


Figure 1 Diffractogram of LHMVO ( $x=0.03$ ) manganite (difference between observed and calculated data-bottom: FullProf program)

variation of carrier bandwidth. Ferromagnetism and metallic behavior appear due Zener mechanism, The  $\text{La}_{0.54}\text{Ho}_{0.11}\text{Sr}_{0.35}\text{Mn}_{1-x}\text{V}_x\text{O}_3$  samples were prepared by sol gel method to improve the purity and homogeneity of the samples. Stoichiometric amounts of  $\text{La}_2\text{O}_3$ ,  $\text{Ho}_2\text{O}_3$ ,  $\text{SrCO}_3$ ,  $\text{MnO}_2$  and  $\text{V}_2\text{O}_5$  (99.9%) were dissolved in nitric acid. Citric acid and ethylene glycol were added to the previous solution. The mixture was heated giving a black-brown powder, which was pressed, heated at  $800^\circ\text{C}$  for 17 hours, grinded, cold pressed and finally sintered in air at  $1200^\circ\text{C}$  during 8 hours. The sintered samples were investigated by XRD, to determine phase composition, atoms positions,

lattice parameters, microstrains and average size of coherent crystalline blocks. XRD data were handled by means of CellRef and FullProf programs. The samples contain only orthorhombic perovskite phase (s. Fig. 1). It was established that the samples contain only simple perovskite phases, except the samples with  $x \geq 0.1$ . The substitution of Mn with V leads to nonmonotonous variations of the lattice constants and unit cell volume of the manganite phase. We supposed that this behavior is due to the variation of the oxygen concentration and to the presence of a small amount of a foreign monoclinic phase, as  $\text{P2}_1$  or  $\text{La}(\text{V})\text{O}_3$  (V can be partially substituted by Mn). Measurements of specific magnetization ( $\sigma$ ) with temperature was performed by VSM method, between 77 and 400 K, at  $H = 14$  kOe. We observed that at low temperature the molar magnetization is practically independent on the V concentration. The observed variation of the

molar magnetization was attributed to the variation of the additional oxygen concentration ( $\delta$ ), which have a maximum with the V concentration (s. Tab.3). The resistance of the samples vs temperature was determined by four probes method. A decrease of the Curie temperature with V concentration was observed. The variation of samples resistance with temperature was determined by four probes method, between 7 and 300 K, by using a magnetic field with  $H_{\max}=1.15$  T. The presence of a electronic insulator/semiconductor phase is indicated indirectly in the curve of variation of the resistance with temperature for the sample corresponding to  $x=0.1$

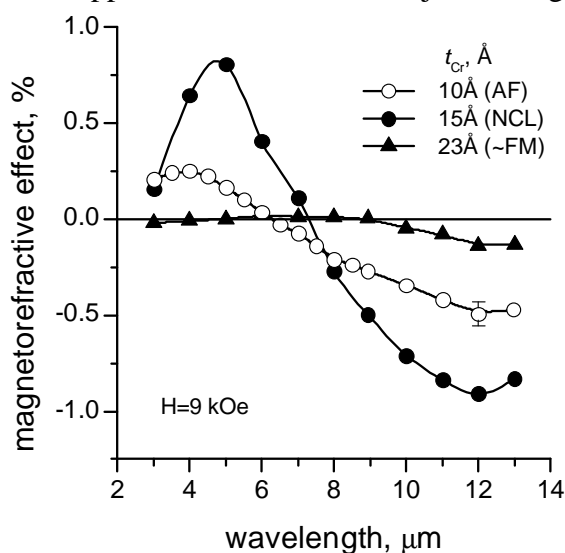
24PO-I2-13

## DEPENDENCE OF SCATTERING PARAMETERS OF CONDUCTION ELECTRONS ON MAGNETIC ORDERING IN SUPERLATTICES WITH GMR EFFECT

*Lobov I.D., Kirillova M.M., Romashev L.N., Milyaev M.A., Ustinov V.V.*

Institute of Metal Physics, Ural Division, Russian Academy of Sciences, Ekaterinburg, Russia

Giant magnetoresistance in multilayer and granular structures is related to the asymmetry of spin-dependent scattering of conduction electrons at interfaces and in ferromagnetic layers. Thus, the information about the parameters of the interfacial scattering of conduction electrons in multilayer nanostructures plays the key role in understanding the peculiarities of magnetotransport properties of these materials. Previously, we developed an approach [1] for determination of the parameters of interfacial spin-dependent scattering of conduction electrons in layered metallic nanostructures. This approach is based on the joint using of magnetorefractive effect (high-frequency analog of



giant magnetoresistive effect), transverse Kerr effect, and optical ellipsometry. In this study, we applied the approach mentioned to Fe/Cr superlattices with various type of magnetic ordering in the absence of applied magnetic field: antiferromagnetic (AF), noncollinear (NCL), and approximately ferromagnetic one ( $\sim$  FM). The magnetorefractive effect is studied in the infrared spectral region of 2–13  $\mu\text{m}$  (see in figure) in molecular-beam epitaxy-grown  $[\text{Fe}(t_{\text{Fe}}, \text{\AA})/\text{Cr}(t_{\text{Cr}}, \text{\AA})]_n$  superlattices with different thicknesses of chromium and iron layers ( $t_{\text{Cr}}=10\text{--}23$   $\text{\AA}$ ,  $t_{\text{Fe}}=10\text{--}27$   $\text{\AA}$ ). The magnetic and magnetoresistive measurements are fulfilled on the same samples. We analyze the magnetorefractive spectra in the framework of Jacquet-Valet model [2]. Relaxation times  $\tau_i^{\uparrow(\downarrow)}$  and scattering probabilities  $P_i^{\uparrow(\downarrow)}$  of

conduction electrons at interfaces, as well as spin asymmetry coefficient  $\gamma_{\text{Fe/Cr}(100)}$  we obtained from simulation of the magnetorefractive spectra in the intraband absorption region ( $\lambda > 8$   $\mu\text{m}$ ) where contribution of the interband transitions of electrons to optical absorption of iron becomes minimal. The experimental estimations of the spin-dependent scattering parameters of conduction electrons we compare with the available theoretical results.



Support by the Russian Foundation for Basic Research under Grant No. 10-02-00590-a, and the Program of the Russian Academy of Science Presidium “The principles of fundamental researches of nanotechnologies and nanomaterials” under Grant No 09-P-2-1037 is gratefully acknowledged.

[1] I.D. Lobov, M.M. Kirillova, A.A. Makhnev, L.N. Romashev and V.V. Ustinov, *Phys. Rev. B* **81** (2010) 134436.

[2] J. C. Jacquet and T. Valet, in *Magnetic Ultrathin Films, Multilayers and Surfaces*, edited by E. Marinero, MRS Symposia Proceedings **384** (Materials Research Society, Pittsburgh, 1995), p. 477.

24PO-I-14

## THE SPIN-DEPENDANT RESONANT TUNNELING THROUGH THE METALLIC SPHERE INSIDE THE BARRIER

*Titova M.*

Faculty of Physics M.V.Lomonosov Moscow State University Leninskie Gory, Moscow 119991  
Russia

The investigation of electrons scattering by a point impurity located in an insulating barrier between two ferromagnetic layers has shown that the change of a localization of the impurity in the barrier strongly affected magnetude and spin-polarisation of the tunnel current. Until recent years, the problem of the influence of a ffnite size impurity on current-voltage characteristic (I-V) has not been solved. However, impurity's size and its shape strongly affect I-V characteristic.

The goal of our investigation was to consider a case of a spherical impurity placed into an insulating barrier layer in structure F1/O/F2, F1;2 being the ferromagnetic layers, O the insulator, magnetizations directed at angle  $\theta$  relatively to each other. Current voltage characteristics for “up” and “down” spin-polarized currents were obtained, resonant tunneling depending on parameter  $kOR$ ;  $k_0$  being wave vector of impurity's material, R the radius of the sphere, was established.

24PO-I2-15

## MAGNETIC STRUCTURE OF CUBIC MnGe STUDIED BY POWDER NEUTRON DIFFRACTION

*Makarova O.L.<sup>1,2</sup>, Tsvyashchenko A.V.<sup>3,4</sup>, Mirebeau I.<sup>2</sup>, Andre G.<sup>2</sup>, Fomicheva L.N.<sup>3</sup>, Ray N.<sup>2</sup>*

<sup>1</sup>National Research Center «Kurchatov Institute», 123182, Moscow, Russia

<sup>2</sup>Laboratoire Leon Brillouin, CEA/SACLAY, 91191, Gif-sur-Yvette, France

<sup>3</sup>Vereshchagin Institute for High Pressure Physics, Russian Academy of Sciences, 142190, Troitsk, Russia

<sup>4</sup>Skobeltsyn Institute of Nuclear Physics, MSU, Vorob'evy Gory 1/2, 119991 Moscow, Russia

The magnetically ordered B20-compounds (space group  $P2_13$ ) are chiral cubic helimagnets. The formation of the long period magnetic modulations is closely connected to the lack of inversion symmetry in the B20 structure and described as a destabilization of a ferromagnetic configuration due to small antisymmetric Dzyaloshinskii-Moriya (DM) contribution into expansion of the free

energy [1]. Among B20 compounds, MnSi and FeGe have attracted renewed interests. Both compounds present unusual physical properties associated with the change in the spiral direction, such as topological spin texture, partially ordered magnetic state akin of partial order in liquid crystals [2].

It is expected that the manganese germanides with the B20 structure have transport and magnetic properties similar to those of the silicides, but no systematic investigations have been carried out yet because of the complexity of the sample synthesis. Recently, it became possible to obtain cubic polycrystalline samples of MnGe under high pressure synthesis. Magnetic structure of cubic MnGe has been determined by powder neutron diffraction. Below 160K, MnGe has a helical spin structure with the propagation vector  $k = (0, 0, \xi)$ , where  $\xi = 0.1$ . The period of modulation decreases as temperature decreases in a continuous way. At  $T = 40\text{K}$ , the propagation vector locks in to the commensurate value  $k = (0, 0, 1/6)$ .

This work was supported by the Russian Foundation for Basic Research (Grant 11-02-00029).

[1] P.Bak, M.H.Jensen Theory of helical magnetic structures and phase transitions in MnSi and FeGe. *J. Phys. C: Solid St. Phys.*, 13, L881, (1980)

[2] Uchida, M., Onose, Y., Matsui, Y. & Tokura, Y. Real-space observation of helical spin order. *Science* 311, 359\_361 (2006)., C. Pfleiderer, D. Reznik, L. Pintschovius, H. v. Löhneysen, M. Garst & A. Rosch Partial order in the non-Fermi-liquid phase of MnSi *Nature* 427, 227-231 (2003)

24PO-I2-16

## ASYMMETRIC VOLTAGE DEPENDENCIES OF THE TUNNEL MAGNETORESISTANCE IN MAGNETIC TUNNEL JUNCTIONS

*Useinov A.<sup>1</sup>, Gooneratne C.<sup>1</sup>, Useinov N.<sup>2</sup>, Kosel J.<sup>1</sup>*

<sup>1</sup> 4700 KAUST, Thuwal 23955-6900, Kingdom of Saudi Arabia

<sup>2</sup> Kazan Federal University, Kremlevskaya str.18, Kazan 420008, Russian Federation

In this work, we theoretically study the values of the tunnel magnetoresistance (*TMR*) as a function of the applied voltage ( $V_a$ ) in single and in double barrier magnetic tunnel junctions (SMTJs, DMTJs) and estimate the possible difference of the *TMR*- $V_a$  curves for negative and positive voltages in the homojunctions.

In the case of perfectly fabricated homogeneous junctions, the *TMR*- $V_a$  branches as well as its spin-polarization values (and its spin-asymmetry *SA*) must be identical for negative and positive values of  $V_a$ . However, as a matter of fact, in many cases there are differences between the two branches due to different electronic states (*E*-states) [1-3] for both sides. Asymmetric *E*-states arise due to non-equal sputtering conditions, lattice mismatch of the deposited layers, layers thicknesses, impurities, annealing regimes etc.

Two essentially different *TMR*- $V_a$  behaviors were observed for the DMTJs as reported in literature [3, 4]. Both types and their asymmetries can be calculated in range of our theoretical model. The first one is *TMR*, which is monotonously decreasing as the voltage is increasing. In this case, the double barrier system can be represented as two junctions connected in series (JCIS). Asymmetric voltage dependence of JCIS based on CoFeB/MgO interfaces was experimentally investigated within a wide range of annealing regimes [3].

The second type of *TMR* behavior was observed by Liang [4] and represents the junctions as entire tunnel system. When the middle magnetic layer thickness of the DMTJ is less than 1.3 nm, electrons tunnel the entire double structure at once and *TMR-V<sub>a</sub>* curves have peak-like behavior where the heights of the peaks for the positive and negative voltage branches can be different due to the *E*-states' asymmetry too. In this regime the electron's energy relaxation in the middle magnetic layer is much less than in the case of JCIS and, in particular, hot electrons change the *TMR-V<sub>a</sub>* behavior.

Based on the two-current model, we present a quasi-classical approach together with quantum tunneling conditions and explain different types of *TMR* behaviors versus *V<sub>a</sub>*. Numerical results are in agreement with the DMTJs as well as SMTJs experimental data.

[1] A. Useinov, R. Deminov, N. Useinov, and L. Tagirov, *Phys. Stat. Solidi B*, **247** (2010) 1797.

[2] A. Useinov, J. Kosel, *IEEE Trans in Magn.* (submitted as INTERMAG- 2011 proceedings).

[3] G. Feng, S. van Dijken, J. F. Feng, J. M. D. Coey, et.al, *J. Appl. Phys.*, **105** (2009) 033916.

[4] L. Jiang, H. Naganuma, M. Oogane, and Y. Ando, *Appl. Phys. Express*, **2**, (2009) 083002.

24PO-I2-17

## SPIN TRANSFER TORQUE EFFECT IN MULTILAYER STRUCTURES ON THE BASIS OF MAGNETIC TUNNEL JUNCTION

*Popkov A.F., Dyomin G.D., Mazurkin N.S., Korneev V.I.*

Moscow Institute of Electronic Technology, 124489 Moscow, Russia

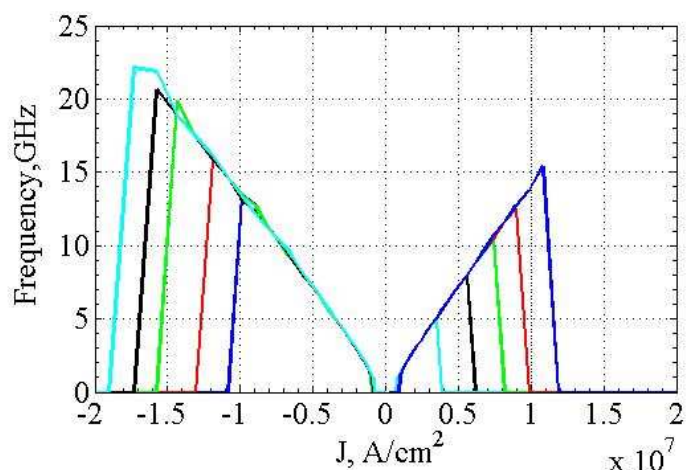
The spin-transfer effect is calculated for the tunnel junction consisting of multilayered magnetic hetero-structure including normal (NM), ferromagnetic (FM) and isolation (I) layers (NM/FM/I/FM/NM) in which one of the ferromagnetic layers is acting as a full polarizer. In the frame of ballistic approach we derive the current-induced torque in the magnetic film taking into account of autoelectronic emission mechanism in this multilayer. We generalize previously obtained results [1] of the calculation of field emission currents for the collinear magnetizations to the case of a tilted free layer magnetization. All calculations are based on the solving Schrodinger equation for corresponding spinor components and the subsequent thermodynamic average of spin flow. Within the Slonczewski's approach [2], the current-induced torque may be calculated as spin-angular momentum acting on a ferromagnet per total current  $I_e$ . It can be presented by as following

$$\frac{\partial \hat{\mathbf{m}}_R}{\partial t} = G(\theta) I_e \hat{\mathbf{m}}_R \times \hat{\mathbf{m}}_L \times \hat{\mathbf{m}}_R$$

where  $\hat{\mathbf{m}}_{L,R}$  are unit vectors of magnetizations in the left and right electrodes, and polarization parameter

$$G(\theta) = \frac{\hbar \gamma}{2dMI_e} \frac{\langle Q_{S\perp} \rangle}{\sin \theta} \quad \text{may be}$$

determined after the calculation of the transverse component of a spin flow density  $Q_{S\perp}$  where  $d$  is the width of unpinned magnetic layer and  $M$  is its



magnetization.

The obtained results are used then for the calculation of current thresholds of induced switching of nanosized magnetic heterostructures. Fig 1 shows results of our calculations of the dependence of precession frequency on tunneling current flowing parallel to the varied magnetic field ( $\vec{J} \parallel \vec{H}$ ) for the CPP geometry (current perpendicular to the plane). For the considered geometry it turned out that threshold currents equal approximately  $10^6 \text{ A/cm}^2$ . Obtained results shows that spin polarized field emission may be used for spin torque writing in the nano-sized nonvolatile memory cells.

The work is supported by the Education Ministry of RF, contr. # 2.1.1/5169.

[1] A.A.Shokri, A.Saffarzadeh, *J. Phys.: Condens. Matter.* **16** (2004) 445.

[2] J.Slonczewski, *J. Magn. Magn. Mater.* **159** (1996) L1.

24PO-I2-18

## MAGNETIC PROPERTIES OF $\text{Fe}_{1-x}\text{Co}_x\text{Si}$ SINGLE CRYSTALS

*Yurkin G.Yu.<sup>1</sup>, Patrin G.S.<sup>1,2</sup>, Isaeva T.N.<sup>1</sup>*

<sup>1</sup> L.V. Kirensky Institute of Physics SB RAS, Krasnoyarsk, 660036, Russia

<sup>2</sup> Siberian Federal University, prospect Svobodny, 79, Krasnoyarsk, 660041, Russia

In the present paper the results of experimental investigation of magnetic properties of  $\text{Fe}_{1-x}\text{Co}_x\text{Si}$  monocrystalline samples are shown in the temperature range from 4.2 to 800 K. Measurements were carried out with MPMS. Samples were synthesized by the close-spaced vapor transport technique [1]. Technique was chosen as simplest and it is similar to equilibrium state of the crystal growth. Average size of synthesized crystals is up to 2 mm. Concentration of cobalt is equal to  $x = 0.005 \div 0.025$ . According to X-ray analysis the structure of all synthesized samples corresponds to FeSi structure. The low-temperature magnetic properties of FeSi both single crystal and polycrystalline solid have been explained by the theory of impurity centers originated from crystal nonstoichiometric. Polycrystalline  $\text{Fe}_{1-x}\text{Co}_x\text{Si}$  samples in the impurity limit ( $x \leq 0.01$ ) have been studied recently [3]. It was found out that the qualitative dependence of susceptibility of

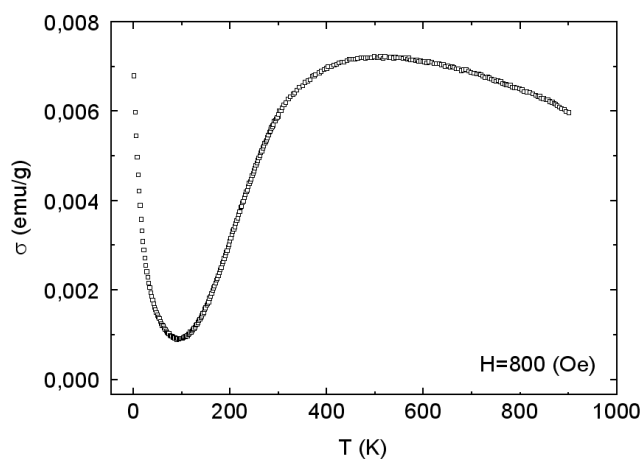


Fig.1. Temperature dependence of magnetization of nominally pure FeSi crystal.

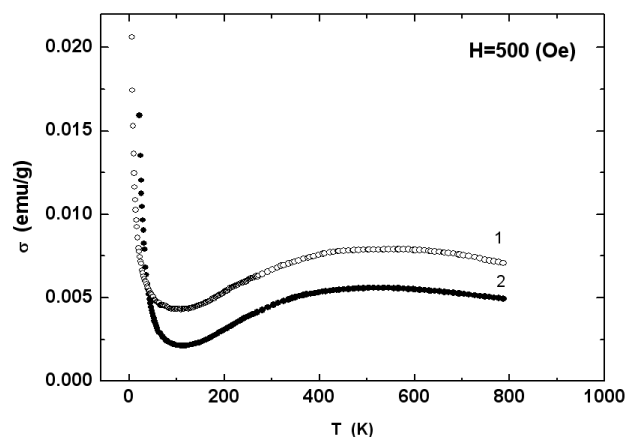


Fig.2. Temperature dependence of magnetization of  $\text{Fe}_{1-x}\text{Co}_x\text{Si}$  monocrystalline. (1- $x=0.025$ , 2- $x=0.005$ ).

polycrystalline  $\text{Fe}_{1-x}\text{Co}_x\text{Si}$  samples is similar to it for pure FeSi (Pic. 1), but the absolute value of susceptibility increases. In order to study low-temperature magnetic properties of  $\text{Fe}_{1-x}\text{Co}_x\text{Si}$ , monocrystalline samples having perfect structure have been grown. In these case concentration of cobalt is also within impurity limits and up spin subband is shifted in such a way that valence and carrier band are not overlapped. Picture 2 shows the temperature dependence of magnetization of  $\text{Fe}_{1-x}\text{Co}_x\text{Si}$  monocrystals. It is clear that low-temperature tail of magnetization is also common with  $\text{Fe}_{1-x}\text{Co}_x\text{Si}$  monocrystals when  $x \leq 0.01$ . These data indicates that reason of low-temperature tail of magnetization appearance is magnetic clusters originated from crystal nonstoichiometric.

[1] J. Ouvrard, R. Wandji, B. Roques, *J. Cryst. Growth*, **13** (1972) 406.

[2] G.S. Patrin, V.V. Beletsky, D.A. Velikanov, G.Yu. Yurkin, *PSS*, **48** (2006) 658.

[3] G.S. Patrin, V.V. Beletsky, D.A. Velikanov, G.Yu. Yurkin, *JETP*, **139** (2011) 351

24PO-I2-19

## MAGNETIC, TRANSPORT AND OPTICAL PROPERTIES OF $\text{Ca}_{1-x}\text{Eu}_x\text{MnO}_3$ SINGLE CRYSTALS

*Loshkareva N.N., Naumov S.V., Solin N.I., Mostovshchikova E.V., Korolyov A.V., Arbutova T.I., Telegin S.V.*

Institute of Metal Physics UD of RAS, 620990 Ekaterinburg, Russia

In electron-doped manganites  $\text{Ca}_{1-x}\text{Ln}_x\text{MnO}_3$ , where Ln is rare earth ion, the crystal and magnetic structure strong change at doping in rather narrow range of concentrations  $0 < x < 0.2$ , charge and orbital ordering occur, and the phase separation of different scale takes place. The study of these features of  $\text{CaMnO}_3$ -based manganites is of interest of the physics of strongly correlated systems. In one of the first papers on electron-doped manganites, the magnetic and transport properties of  $\text{Ca}_{1-x}\text{Eu}_x\text{MnO}_3$  polycrystals have been studied [1]. As shown recently [2,3], the study of single crystals gives a more clear information about the interaction of magnetic and electronic subsystems in electron-doped manganites. In particular, it was found that the magnetoresistance of  $\text{Ca}_{1-x}\text{Ce}_x\text{MnO}_3$  single crystals have features near three phase transitions [3].

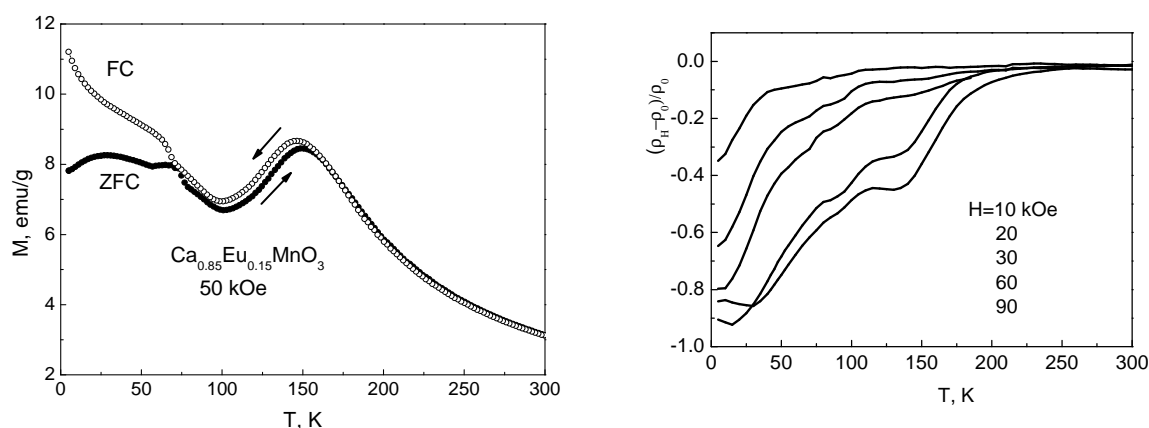


Fig.1 Temperature dependence of magnetization (left panel) and magnetoresistance (right panel) of  $\text{Ca}_{0.85}\text{Eu}_{0.15}\text{MnO}_3$  single crystal.

In the present work we investigate  $\text{Ca}_{1-x}\text{Eu}_x\text{MnO}_3$  single crystals, where  $x = 0.10, 0.125, 0.15$ , grown by floating zone method, and discuss the relationship of magnetic, transport and optical properties, and effects of nonstoichiometry. Figure 1 shows the temperature dependence of magnetization and magnetoresistance for  $\text{Ca}_{0.85}\text{Eu}_{0.15}\text{MnO}_3$  single crystal. Maximum of the  $M(T)$  at 150 K is associated with the temperature of the orbital/charge ordering in the monoclinic structure and phase transition from paramagnetic state to antiferromagnetic one of  $C$ -type. Growth of the magnetization below 100 K is due to phase transition to antiferromagnetic state of  $G$ -type with a ferromagnetic contribution, which occurs in a small volume of the crystal. Features of magnetoresistance occur near the phase transitions and have a different nature.

The work was supported by the project of Presidium of RAS (grant No.09-P-2-1004), Integration project of the Ural Division – Siberian Division of RAS (grant No.09-C-2-1016), and RFBR (grant No.10-02-00068).

- [1] I.O. Troyanchuk, N.V. Kasper, N.V. Samsonenko., et al. *J.Phys.:Condens.Matter.* **8** (1996) 10627.  
 [2] N.N.Loshkareva, A.V. Korolyov, N.I. Solin, et al. *JETP* **102** (2006) 248.  
 [3] N.N. Loshkareva, A.V. Korolyov, N.I. Solin, et al. *JETP* **108** (2009) 88.

24PO-I2-20

## ELECTRON AND MAGNETIC PROPERTIES IN $\text{A}^{\text{II}}\text{B}^{\text{IV}}\text{C}^{\text{V}}_2\text{:Mn}$ AT HIGH PRESSURE UP TO 7 GPa

Mollaev A.Yu.<sup>1</sup>, Kamilov I.K.<sup>1</sup>, Arslanov R.K.<sup>1</sup>, Marenkin S.F.<sup>2</sup>, Arslanov T.R.<sup>1</sup>, Zalibekov U.Z.<sup>1</sup>

<sup>1</sup> Institute of Physics, Daghestan Scientific Center of the Russian Academy of Science, 367003, Makhachkala, Russia

<sup>2</sup> Institute of common and inorganic chemistry of the Russian Academy of Science, 119991, Moscow, Russia

In high-temperature ferromagnetic semiconductors  $\text{Cd}_{1-x}\text{Mn}_x\text{GeAs}$  ( $x=0\div 0.36$ ) and  $\text{Cd}_{1-x}\text{Mn}_x\text{GeP}_2$  ( $x=0\div 0.225$ ) there is carried out a complex investigation of electric and magnetic properties. The baric dependences of the specific resistance  $\rho$ , Hall coefficient  $R_H$ , and relative magnetic susceptibility  $\chi/\chi_0$  are measured. The  $\rho(P)$  and  $R(P)$  are measured in high-pressure device of “Toroid” type [1, 2] when pressure rises and falls up to 7 GPa. The magnetic susceptibility is estimated by a method described in the work [3]. Structural phase transitions are found in baric dependences of  $\rho(P)$  and  $R_H(P)$  in both compounds at increase and decrease in pressure. A position of phase transitions sifts towards the high pressures when a percentage of Mn increases. All phase transitions are reversible in  $\text{Cd}_{1-x}\text{Mn}_x\text{GeAs}_2$ , in  $\text{Cd}_{1-x}\text{Mn}_x\text{GeP}_2$  samples with  $x \leq 0.135$  the phase transition is accompanied by partial decomposition of a substance, what confirms the X-ray diffraction study before and after pressure applying on dependences  $(\chi/\chi_0)P$ . In all samples of both compounds there are observed the magnetic phase transitions which shift towards high pressures with increase in percentage of Mn. When pressure decreases the hysteresis emerges. A magnetic phase transition is not revealed in base samples of  $\text{CdGeAs}$  and  $\text{CdGeP}$ . We interpret the observed phase transitions as non-magnetic phase transition [4]. The temperature dependences of normal and abnormal Hall coefficients are calculated from magnetic-field dependences of Hall resistance for  $\text{Cd}_{1-x}\text{Mn}_x\text{GeAs}_2$  ( $x=0\div 0.36$ ) by the method of interactive graphical plotting.

This work was supported by Program of Presidium of RAS “Thermophysics and mechanics of external energetic influences and physics of high compressed material” and Section of High Compressed Material.

- [1] L.G. Khvostantsev, L.P. Vereshagin, A.P. Novikov. High Temp.-High Pressure. 9 (1977) 6 32.  
 [2] A.Yu. Mollaev, R.K. Arslanov, L.A. Saypulaeva, S.F. Marenkin. Inorganic materials. 37 (2001) 4 405.  
 [3] A.Yu. Mollaev, I.K. Kamilov, S.F. Marenkin, R.K. Arslanov, U.Z. Zalibekov, T.R. Arslanov, A.A. Abdullaev, I.V. Fedorchenko. Inorganic materials. 46 (2010) 9 1029.  
 [4] A.Yu. Mollaev, I.K. Kamilov, R.K. Arslanov, T.R. Arslanov, U.Z. Zalibekov, V.M. Novototzev, S.F. Marenkin. Jetf Letters. 91 (2010) 9 524.

24PO-I2-21

## SPIN-POLARIZED CURRENT IN THE MAGNETIC NANO WIRE

*Kanjouri F.<sup>1</sup>, Babazadeh H.L.<sup>2</sup>, Esmailian A.H.<sup>3</sup>*

<sup>1</sup> Physics Department, Tarbiat Moallem University, Tehran, Iran

<sup>2</sup> Plasma Physics Center, Science and Reaserch Branch, Islamic Azad University (IAU), Tehran, Iran

<sup>3</sup>Department of Physics, Qom Branch, Islamic Azad University, Qom, Iran

One of the most important magneto resistance effects is the tunneling magneto resistance (TMR), which is caused by spin dependent tunneling processes.

In this paper we calculated the tunneling magneto resistance (TMR) of a nano wire which consists of a non-magnetic insulator nano wire with circle cross section between two ferromagnetic leads which are made of the same material. The calculation performed in the framework of free –electron model at zero temperature. We consider not only the contributions of the conductive electrons at the Fermi level but also those bellow the Fermi level to the tunneling.

We consider spin dependent transport in the ballistic regime, and we suppose that the linear size of the one-dimensional nano wire is much smaller than the spin coherence length. In this length scale, the effect of scattering is lower intensely. So in this way, the topological shape of system has important role to calculate the TMR. In presence of insulator in the middle level, the applied potential will be gathered on two ends of it and so as we will see the thickness of this level has an important role in the results. Considering two separate conducting channels with different spins we can define two different energy levels named as “higher-spin-Fermi-level”, and “lower-spin-Fermi-level” which are the reasons of spin current.

Our calculations show that the TMR ratio decreases with increasing the applied voltage and increases with decreasing thickness of nano wire.

- [1] M.Ye.Zhuravlev, H.O.Lutz, A.V.Vedyayev, Preprint cond-mat/0002325v1  
 [2] B.J.Spisak, M.Woloszyn and A.paja, acta Physica polonica a 115(2009)226

24PO-I2-22

## ROOM-TEMPERATURE FERROMAGNETISM IN (III,Mn)Sb SEMICONDUCTORS

Danilov Yu.A.<sup>1</sup>, Zvonkov B.N.<sup>1</sup>, Kudrin A.V.<sup>1</sup>, Vikhrova O.V.<sup>1</sup>, Plankina S.M.<sup>2</sup>, Dunaev V.S.<sup>2</sup>,  
Nezhdanov A.V.<sup>2</sup>, Drozdov Yu.N.<sup>3</sup>

<sup>1</sup> Physico-Technical Research Institute of the Nizhny Novgorod State University, Nizhny Novgorod, Russia

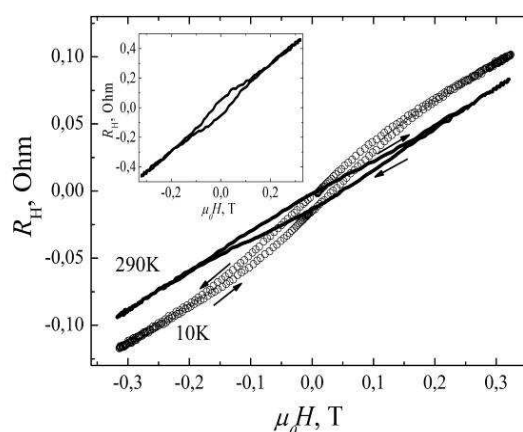
<sup>2</sup> N.I. Lobachevsky State University of Nizhny Novgorod, Nizhny Novgorod, Russia

<sup>3</sup> Institute for Physics of Microstructures, RAS, Nizhny Novgorod, Russia

The results of investigation the properties of (III,Mn)Sb layers fabricated by laser deposition are presented. The GaMnSb and InMnSb layers were grown on semi-insulating GaAs (100) substrates by alternating laser ablation of semiconductor GaSb (or InSb) and metal Mn target. Process performed in MOCVD reactor in hydrogen flow. The quantity of manganese was controlled by time of target sputtering and characterized by a technological parameter  $Y_{Mn} = t_{Mn}/(t_{Mn}+t_s)$ , where  $t_{Mn}$  and  $t_s$  is a time of Mn and semiconductor sputtering. The  $Y_{Mn}$  parameter was varied in range of 0.06 – 0.33 and in range 0.06 – 0.25 for GaMnSb and InMnSb, respectively. The growth process was performed at substrate temperature 300°C or 400°C for GaMnSb and 200°C for InMnSb.

Investigations of x-ray diffraction and Raman scattering showed reasonably good crystal quality of GaMnSb and InMnSb layers. Study of transversal Kerr effect at 300 K revealed a hysteresis loop in the dependences of the relative change of reflected light intensity on magnetic field that indicate the presence of ferromagnetic properties. The magnetic field dependences of Hall resistance ( $R_H(H)$ ) confirmed the ferromagnetic properties GaMnSb layers. For all GaMnSb samples the  $R_H(H)$  dependences were nonlinear with clear hysteresis. It should be note that the sign of anomalous Hall effect coefficient depended on temperature and growth conditions.

In contrast to GaMnSb layers, InMnSb samples were not ferromagnetic at room temperature. The investigations of transversal Kerr effect did not reveal ferromagnetism at 300 K, and anomalous Hall effect was observed only at low temperatures (< 70 K).



$R_H(H)$  dependences at 290 and 10 K for GaMnSb layer ( $Y_{Mn} = 0.33$ ). The inset shows  $R_H(H)$  dependence at 10 K for InMnSb layer ( $Y_{Mn} = 0.17$ ).

Support by Federal target program «Scientific and scientific-pedagogical personnel of the innovative Russia» in 2009-2013 and by the RFBR (grant no. 11-02-00645-a)



24PO-I2-23

## HIGH SENSITIVE AND THERMAL STABLE CoFe/Cu MULTILAYERS

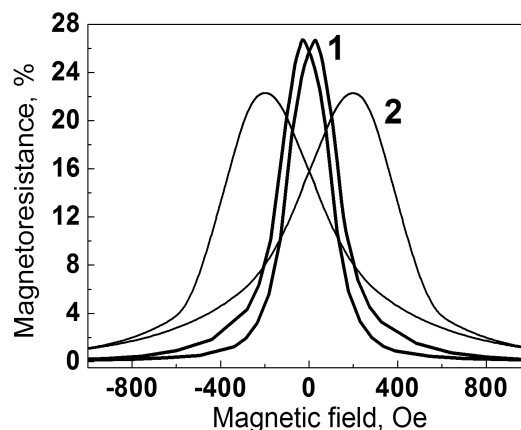
Milyaev M.A., Naumova L.I., Proglyado V.V., Krinitsina T.P., Bannikova N.S., Ustinov V.V.  
Institute of Metal Physics, Ural Branch of RAS, Ekaterinburg, Russia

Multilayers CoFe/Cu display a high and reproducible GMR ratio ( $\Delta R/R > 20\%$ ) at room temperature, high magnetoresistive sensitivity comparable with that in permalloy films and high thermal stability [1, 2]. It was found that the material as well thickness of the buffer layer affect significantly both GMR ratio and magnetic hysteresis [3, 4]. In the present work we have investigated dependence of the coercive force and GMR ratio on parameters of  $[\text{CoFe/Cu}]_n$  multilayers: material and thickness buffer layer, number ( $n$ ) of CoFe-Cu bilayers. The optimal annealing procedure (temperature and duration) was determined for multilayers with different buffer layers.

$[\text{Co}_{90}\text{Fe}_{10}(15\text{A})/\text{Cu}(23\text{A})]_n / \text{Cr}(10\text{A})$  multilayers with Cr, Fe, Cu and  $\text{Co}_{90}\text{Fe}_{10}$  buffer layer were grown at room temperature on  $\text{Al}_2\text{O}_3(10\bar{1}2)$ , glass and naturally oxidated (100)Si substrates by DC magnetron sputtering under argon pressure of 0.1 Pa. The base pressure of residual gases in the deposition chamber was  $10^{-7}$  Pa. The annealing was performed in a separate chamber under pressure of  $10^{-5}$  Pa. Magnetoresistance was measured by the four-point probe method in current-in-plane geometry at room temperature. Crystallographic and microstructural information was obtained by transmission electron microscopy and X-ray diffraction.

We found that the  $\text{Co}_{90}\text{Fe}_{10}$  alloy is the most preferable material to improve magnetoresistive characteristics. The maximal GMR ratio  $\Delta R/R = 23.7\%$  was found for buffer layer thickness  $t_{\text{CoFe}} = 15\text{A}$  and for number of bilayers  $n = 8$ . Annealing during 1 hour at temperature  $T = 300^\circ\text{C}$  increased the GMR ratio up to  $\Delta R/R = 26.7\%$  (curve 1). The magnetoresistive sensitivity determined as the maximum of resistivity derivation was about  $0.17\%/\text{Oe}$ . Annealing at  $T > 320^\circ\text{C}$  decreases GMR ratio.

The highest thermal stability was found in superlattices with Cr buffer layer with thickness  $t_{\text{Cr}} > 20\text{A}$ , where GMR ratio was nearly changeless after 1 hour annealing at different temperatures in the range  $(20 \div 420)^\circ\text{C}$ . The main distinction of the  $[\text{CoFe/Cu}]_n$  multilayers with Cr buffer layer is a wide magnetic hysteresis (curve 2) caused probably by a formation of antiferromagnetic ordering in thin Cr layers.



The research was supported by RFBR, project No. 10-02-00590, and Program of Presidium of the Russian Academy of Sciences, project No. 09-P-2-1037.

- [1] Saito Y., Hashimoto S., Inomata K., IEEE Trans. on magn., **28**, №23 (1992) 2751.
- [2] D. Wang, J. Anderson, J.M. Daughton., IEEE Trans. on magn. **33**, №5 (1997) 3520.
- [3] Gangopadhyay S., Shen J.X., et al., IEEE Trans. on magn., **31**, № 6 (1995) 3933.
- [4] M.A. Milyaev, L.I. Naumova, V.V. Proglyado, T.P. Krinitsina, N.S. Bannikova and V.V. Ustinov, Solid State Phenomena, **168-169** (2011) 303.

## MAGNETOTRANSPORT PROPERTIES OF $R_3M$ COMPOUNDS

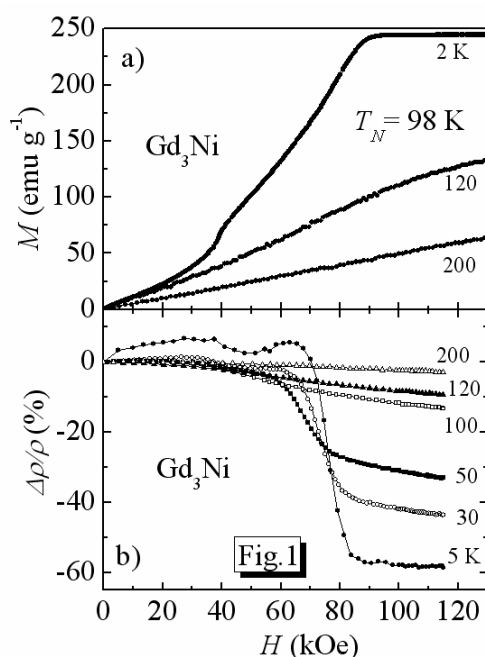
Proshkin A.V.<sup>1,2</sup>, Gubkin A.F.<sup>1</sup>, Baranov N.V.<sup>1,2</sup>

<sup>1</sup> Institute of Metal Physics RAS, 620219 Ekaterinburg, Russia

<sup>2</sup> Ural State University, 620083 Ekaterinburg, Russia

The rare earth (R) - 3d transition metal (M)  $R_3M$  compounds are known to exhibit the complicated non-collinear magnetic structures and a rich variety of field-induced magnetic phase transitions. Some unusual features in the behavior of the specific heat and transport properties were observed in  $R_3M$  not only below magnetic ordering temperatures but also in the paramagnetic state [1]. In particular, the electrical resistivity  $\rho(T)$  of the compounds  $R_3M$  ( $M = \text{Co}, \text{Ni}, \text{Rh}$ ) in a wide temperature range above magnetic critical temperatures was suggested to include an additional contribution associated with the presence of short-range magnetic correlations and spin-fluctuations [1]. The heat capacity and magnetocaloric effect are influenced by these short-range magnetic correlations as well [1, 2]. The aim of the present work is to study the magnetic state and magnetotransport properties of  $R_3M$  ( $R = \text{Gd}, \text{Tb}, \text{Y}; M = \text{Ni}, \text{Co}$ ) compounds.

In  $\text{Gd}_3\text{Ni}$ , application of a magnetic field below the Neel temperature  $T_N = 98$  K is observed to lead to the phase transition from the antiferromagnetic (AF) state to the field-induced ferromagnetic (F) state (Fig.1a), which is in agreement with previous data [3]. As shown in Fig.1b, the AF-F transformation under application of a magnetic field above 90 kOe is accompanied by a giant reduction of the electrical resistivity ( $\Delta\rho/\rho \sim -57\%$  at  $T = 5$  K). The  $\Delta\rho/\rho$  value decreases with increasing temperature. The giant magnetoresistance effect in  $\text{Gd}_3\text{Ni}$  below  $T_N$  may be attributed to the reconstruction of the Fermi surface through the AF-F transition. The magnetization curves of  $\text{Gd}_3\text{Ni}$  are found to exhibit a non-Brillouin shape at temperatures up to  $\sim 150$  K (see Fig. 1a), i.e. well above  $T_N$ . An analogous behavior of the magnetization in the isostructural antiferromagnetic compound  $\text{Tb}_3\text{Ni}$ . These data together with specific heat results [4] allowed us to suggest that short-range antiferromagnetic correlations persist in  $R_3M$  compounds well above magnetic ordering temperatures. The existence of a short-range magnetic order above the magnetic ordering temperature up to  $T \sim 5T_N$  is confirmed by neutron diffraction measurements performed for  $\text{Tb}_3\text{Ni}$  and  $\text{Tb}_3\text{Co}$  compounds. The additional magnetic contribution to the electrical resistivity which determines the low values of the temperature coefficient of resistivity observed in  $R_3M$  compounds in the paramagnetic state



may be associated with conduction electron scattering by these short-range magnetic regions (magnetic clusters) and spin-fluctuations induced by the f-d-exchange in the d band.

This work was supported by the program of the Presidium of RAS (Project No 09-II-2-1035).

[1] N.V. Baranov et al., *J. Alloys and Comp.*, **329** (2001) 22.

[2] S.K. Tripathy, K.G. Suresh, A.K. Nigam, *J. Magn. Magn. Mat.*, **306** (2006) 24.

[3] G.J. Primavesi and K.N.R. Taylor, *J. Phys. F: Metal Phys.*, **2** (1972) 761.

[4] N.V. Tristan et al., *Physica B*, **344** (2004) 462.

## SPIN POLARIZED CONDUCTANCE IN DOUBLE-BARRIER MAGNETIC TUNNEL JUNCTION

Useinov N.Kh., Tagirov L.R.

Kazan Federal University, 420008, Kazan, Russian Federation

We present a theoretical study of the spin-polarized conductance in double-barrier magnetic tunnel junctions (DMTJ):  $FM^L/I_1/FM^W/I_2/FM^R$ , where the magnetization of the middle ferromagnetic layer  $FM^W$  can be aligned parallel (P) or antiparallel (AP) with respect to the fixed magnetizations of the left  $FM^L$  and right  $FM^R$  ferromagnetic electrodes. The two dielectric layers  $I_{1(2)}$  of the lateral size comparable with the mean-free paths of conduction electrons serve as tunnel barriers. In Fig. 1, the large parabolic curves present dispersion low for the spin-up electrons ( $\uparrow$ -arrows) and correspond to the spin-up majority conductance sub-bands. The small parabolic curves belong to the spin-down minority sub-bands with spin-down electrons ( $\downarrow$ -arrows). The arrows inside the brackets of the middle layer show the electron spin-direction for the AP case. The spin-dependent conduction channels passing through the minority or majority sub-bands are determined by the tunneling trajectory of an electron conserving the spin projection. They are shown at the bottoms of the sub-bands as dash-dot-dot lines and dashed lines for the P-case and as dash-dot and solid lines for the AP-case, respectively.

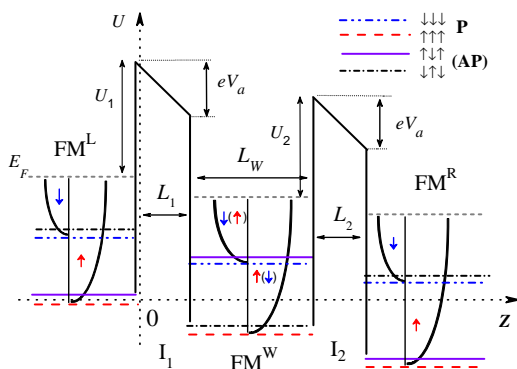


Fig. 1. The schematic potential profile of the DMTJ with applied bias  $V_a$ .  $U_{1(2)}$  are the heights of the barriers above Fermi energy  $E_F$ ,  $L_{1(2)}$  are the thickness of the respective barriers, and  $L_W$  is the thickness of the middle layer  $FM^W$ .

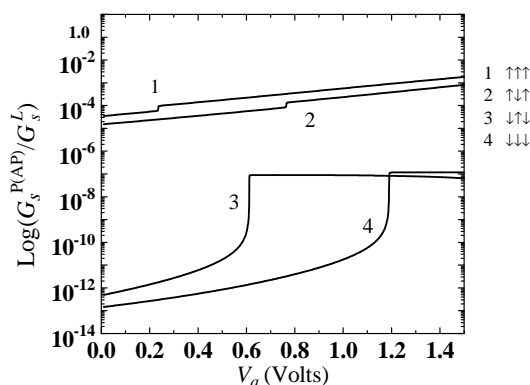


Fig. 2 Tunnel conductance as a function of the dc bias for four configurations of the spin-conduction channels at each of the P and AP magnetic moments alignment. The arrows correspond to the arrows in Fig. 1.

Figure 2 shows conductance as a function of the bias voltage for some values of the conduction bands spin-polarization (correspond to experiments) on the left  $FM^L$ , right  $FM^R$  ferromagnetic electrodes and of the middle ferromagnetic layer  $FM^W$ . The other parameters of the DMTJ as follows:  $L_{1(2)} = 12 \text{ \AA}$ ,  $L_W = 13.6 \text{ \AA}$  and  $U_{1(2)} = 1.8 \text{ eV}$ . In the free-electron model [1], the spin-polarized conductance is proportional to the product of the transmission coefficient (TC) and cosine of the incidence angle of an electron trajectory in the  $FM^L$  layer. The calculations with exact solution for TC show that the tunnel conductance has staircase character for each of the conduction channels. The number of steps depends on the middle layer thickness and the magnetization configuration of DMTJ, thus producing giant magnetoresistance.

The work was supported by RFBR, project No. 10-02-91225-CT\_a.

[1] A.N. Useinov, R.G. Deminov, *et al*, *Phys. Status Solidi B*, **247** (2010) 1797.

## ELECTRICAL PROPERTIES OF $\text{Bi}_{24}(\text{CoBi})\text{O}_{40}$ SOLID SOLUTIONS WITH CHARGE ORDERING

*Aplesnin S.S.<sup>1</sup>, Udod L.V.<sup>1</sup>, Sitnikov M.N.<sup>1</sup>, Galyas A.I.<sup>2</sup>*

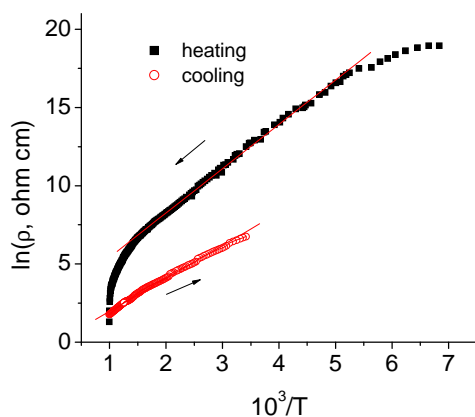
<sup>1</sup>M. F. Reshetneva Aircosmic Siberian State University, Krasnoyarsk, 660014, Russia

<sup>2</sup>State Scientific Production Association "Material Science Center of the National Academy of Sciences of Belarus", 220072 Minsk, Belarus

e-mail: [luba@iph.krasn.ru](mailto:luba@iph.krasn.ru)

Compounds with mixed valencies shows a wide variety of electrical properties. For example, the conductivity of  $\text{Co}_3\text{O}_4$  and  $\text{Mn}_3\text{O}_4$  which contain bi- and trivalent cations is low in comparison with  $\text{Fe}_3\text{O}_4$ . The high conductivity is due to the combined effect of mixed valence of the iron ions on the same octahedral sublattice and the small distance between neighboring octahedral sites in  $\text{Fe}_3\text{O}_4$ . The electron transition may occur either between cations on tetrahedral and octahedral sites located at a relative large distance, or between cations on octahedral sites in the substances  $\text{Co}_3\text{O}_4$  and  $\text{Mn}_3\text{O}_4$ . Charge ordering in these compounds interrelates with spin and orbital degree of freedom. The effect of charging ordering on transport properties without these interactions is investigated on  $\text{Bi}_{24}(\text{CoBi})\text{O}_{40}$  consisting of the ions with filled  $6s^2$  and empty  $6s$  shells.

The aim of this study is to investigate the influence of charge ordering on the resistivity and thermoelectromotive force in the temperature range  $80 \text{ K} < T < 1000 \text{ K}$ . According to the data of X-ray diffraction analysis, the synthesized substance has the chemical formula  $\text{Bi}_{24}(\text{CoBi})\text{O}_{40}$  and the crystal structure is cubic symmetry with the I23 space group and the lattice parameter is  $a = 10.1917(1) \text{ \AA}$  [1]. The presence of an impurity phase  $\text{Co}_3\text{O}_4$  in number of 23% was detected in the synthesized samples.



The temperature dependence of resistivity for  $\text{Bi}_{24}(\text{CoBi})\text{O}_{40}$  is shown in figure. The temperature hysteresis of resistivity at heating and at cooling is observed. The resistance of sample after cooling increase according to the logarithmic law versus the measurement time at the fixed temperature. Crystal structure is retained and X-ray diffraction peaks is shifted towards small angles in results of that the constant lattice is rised by 0.4%. The decrease of resistance is associated with increase of a constant lattice that shows on interrelation of electric and structural properties. The temperature dependence of thermoelectromotive force is well described by typical semi-conductor dependence  $\alpha$

$(T) \sim \Delta E/kT$  with the activation energy is  $\Delta E = 0.23 \text{ eV}$  at  $150 \text{ K} < T < 250 \text{ K}$ . A mixed state consisting of semi-conductor and metal is possible exists in the temperature range  $250 \text{ K} < T < 950 \text{ K}$  where  $\alpha(T)$  is described by fitting function  $\alpha(T) = A/T + B T$ , where  $A = 162$ ,  $B = 0.0003$ .

So, semiconductor  $\text{Bi}_{24}(\text{CoBi})\text{O}_{40}$  has charge ordering up to  $T = 250 \text{ K}$ , above this temperature probably there is coexistence of regions with uniform distribution of a charge on bismuth ions, and domains with three and five valence of bismuth ions. Heating of sample  $\text{Bi}_{24}(\text{CoBi})\text{O}_{40}$  causes the uniform charge distribution and the phase transition to a metal state at  $T = 950 \text{ K}$ .

[1] C.C. Aplesnin, L.V. Udod, M.C. Molokeev, Abstract "Magnetic Materials, New Technologies", 149 (2010).

24PO-I2-27

## THE EFFECT OF ANIONIC DOPING ON STRUCTURAL AND ELECTRICAL PROPERTIES OF $\text{MnSe}_{1-x}\text{Te}_x$ CHALCOGENIDES

*Aplesnin S.<sup>1,2</sup>, Romanova O.<sup>1,2</sup>, Eremin E.<sup>1,2</sup>, Ryabinkina L.<sup>1</sup>, Demidenko O.<sup>3</sup>, Makovetskii G.<sup>3</sup>, Yanushkevich K.<sup>3</sup>*

<sup>1</sup> L.V. Kirensky Institute of Physics SB RAS, Krasnoyarsk, 660036, Russia

<sup>2</sup> M. F. Reshetneva Aircosmic Siberian State University, Krasnoyarsk, 660014, Russia

<sup>3</sup> State Scientific Production Association "Material Science Center of the National Academy of Sciences of Belarus", Minsk, 220072, Belarus

Magnetic semiconductors showing the metal – insulator phase transitions and the phenomenon of colossal magnetoresistance are perspective materials for spintronics. It is possible the  $\text{MnSe}_{1-x}\text{Te}_x$  solid solutions possess such properties. MnSe and MnTe are antiferromagnetics with different types of structure and with semiconductor type of conductivity at temperatures below room [1]. These compositions are characterised by the polaron mechanism of conductivity which is sensitive to the slightest changes in elementary cells of magnetic and crystal subsystems.

Synthesis of  $\text{MnSe}_{1-x}\text{Te}_x$  ( $0 \leq X \leq 0.4$ ) samples with step on concentration  $X=0.1$  is carried out by the of method solid - state reaction with use of a temperature step mode. X-ray researches show that the anion replacement in  $\text{MnSe}_{1-x}\text{Te}_x$  system with increase in the tellurium concentration leads to reduction of diffraction reflexes intensity. Smooth shift of reflexes (422), (420), (331), (400) angular positions on the wide  $2\theta$  angles towards smaller values is observed that testifies to increase in the elementary cell sizes. The reduction of the diffraction reflexes intensity on X-ray patterns, most likely, is attributed to crystal distortions formation at anion substitution and disorder increasing in the cubic structure of  $Fm\bar{3}m(225)$  space group. Despite of this, linear increase of parameter  $a$  and an elementary crystal cell of samples with increase in the tellurium concentration allows to draw a conclusion that in the  $0 \leq X \leq 0.4$  concentration range in  $\text{MnSe}_{1-x}\text{Te}_x$  system exist solid solutions with space group  $Fm\bar{3}m(225)$  structure. The unit cell parameter  $a$  changes linearly.

Resistivity measurements were performed using a standard four-probe compensation method at the direct current in the temperature range 77 – 300 K in magnetic field up to 10 kOe. The effect of the magnetic field on the transport properties was studied using two methods. Firstly, the change of resistivity was measured as a function of temperature for the  $\text{MnSe}_{1-x}\text{Te}_x$  solid solutions with the magnetic field and without. Secondly current-voltage characteristics were studied at a fixed temperature in zero magnetic field and in the field  $H = 10$  kOe. The current-voltage characteristics of the manganese chalcogenides  $\text{MnSe}_{1-x}\text{Te}_x$  at  $T < 100$  K are linear and independent on magnetic field. It has been established that resistivity of the samples in magnetic field decreases. The maximum change ( $\delta_H$ ) has been found in the range of the Neel temperature for the composition  $X = 0.1$  ( $T_N=135$  K) and for  $X = 0.2$  ( $T_N=130$  K) the change is smaller by an order of magnitude. For higher concentrations  $X=0.3$  and  $0.4$  magnetoresistance has not been found.

This work was supported by the Russian Foundation for Basic Research project № 09-02-00554\_a; № 09-02-92001-NNS\_a; № 11-02-98018 p\_sibir\_a; ADTP "Development of scientific potential of the higher school" № 2.1.1/401

[1] S.S. Aplesnin, L.I. Ryabinkina, O.B. Romanova, D.A.BalaeV, K.I. Yanushkevich, O.F. Demidenko, N.S. Miroshnitchenko, *PSS*, **49** (2007) 1984

24PO-I2-28

## LINewidth REDUCTION OF SPIN TRANSFER DRIVEN EXCITATIONS DUE TO MODE COUPLING

Gusakova D.<sup>1</sup>, Quinsat M.<sup>1,2</sup>, Sierra J.F.<sup>1</sup>, Tiberkevich V.<sup>3</sup>, Slavin A.<sup>3</sup>, Ebels U.<sup>1</sup>, Dieny B.<sup>1</sup>, Buda-Prejbeanu L.D.<sup>1</sup>, Cyrille M.C.<sup>2</sup>

<sup>1</sup> SPINTEC, UMR-8191, CEA-INAC/CNRS/UJF/G-INP, 17 rue des Martyrs, 38054 Grenoble, France

<sup>2</sup> CEA-LETI, MINATEC, DRT/LETI/DIHS, 38054 Grenoble, France

<sup>3</sup> Dep. of Physics, Oakland Univ. Rochester, MI 48309, USA

One fundamental question on the spin transfer nano-oscillators (STNO) properties concerns the origin of linewidth broadening and the way to reduce it. Here we show that the dynamic interaction between a current induced auto-oscillation mode with the eigen ferromagnetic (FMR) modes of any magnetic layer composing the STNO structure may lead to an important linewidth reduction of emitted signal. We study numerically an STNO composed of a free layer (FL) and a synthetic antiferromagnet (SAF), see Figure 1(a). The dynamical interactions are the exchange between two layers of the SAF and the mutual spin torque interaction between the FL and SAF layer. Taking these interactions as well as a white Gaussian thermal noise field into account the Landau-Lifshitz-Gilbert equation has been solved simultaneously for all three layers in a macrospin approach. Due to the mutual spin torque interaction the FL auto-oscillation frequency vs field experiences a distortion and flattening when its frequency is close to the SAF eigen mode, see Figure 1(b). This leads to a reduction of FL precession amplitude while the amplitude of the SAF increases. By analysing the phase and amplitude noise extracted from simulated signal we interpret the change of slope in frequency dependence as the reduction of the nonlinearity of the FL oscillations. The reduction of nonlinearity leads to a drastic decrease of the linewidth (Fig. 1(c)) which is of interest for applications.

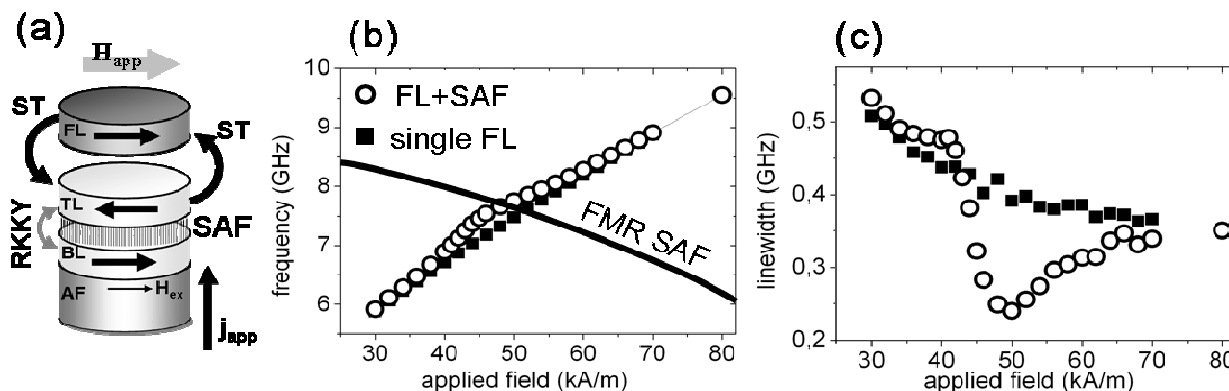


Figure 1. (a) studied STNO structures. (b), (c) FL in-plane precession frequencies and linewidths vs applied field. Open circles correspond to the frequency dependence of dynamically coupled structure and squares correspond to that calculated for the single FL. Solid black line corresponds to the SAF eigen mode frequencies.

## ELECTRICAL RESISTANCE OF $\text{Sm}_{0.25}\text{Mn}_{0.75}\text{S}$ SPIN GLASS

*Aplesnin S.S.<sup>1,2</sup>, Kharkov A.M.<sup>1</sup>, Eremin E.V.<sup>2</sup>, Sokolov V.V.<sup>3</sup>*

<sup>1</sup> M. F. Reshetneva Aircosmic Siberian State University, Krasnoyarsk, 660014, Russia

<sup>2</sup> L.V. Kirensky Institute of Physics, Siberian Branch of Russian Academy of Sciences, Krasnoyarsk, 660036, Russia

<sup>3</sup> Institute of Inorganic Chemistry, Siberian Branch of Russian Academy of Sciences, Novosibirsk, Russia

The at present, much attention is focused on the materials with the strong correlation between magnetic and electrical properties [1]. In view of practical applications, these compounds are promising for the creation of microelectronic elements; as far as the fundamental studies are concerned, the most intriguing are the materials containing variable-valence elements undergoing metal-insulator transitions and magnetic phase transformations including variations in magnetic properties at preservation of magnetic symmetry.

One might expect that upon cation substitution of a manganese ions by samarium ions the pressure imposed by the nearest neighborhood may induce an electrons in d-band, that causes ferromagnetic exchange between manganese ions located near boundary of samarium cluster. A competition between ferro- and antiferromagnetic interactions can give rise to a new magnetic structure.

The metallic type of conductivity establish for  $\text{Sm}_{0.25}\text{Mn}_{0.75}\text{S}$  and mechanism of electrical resistivity is attributed to scattering electrons on the acoustic phonons and magnetic scattering on uncompensated antiferromagnetic manganese clusters at  $T < 180$  K (Fig.1a). Spin-glass state is found in  $\text{Sm}_{0.25}\text{Mn}_{0.75}\text{S}$  on the basis of frequency and field magnetization dependencies. Temperature associated with relaxation maximum increases logarithmically with frequency. Using ideas and methods of Anderson localization theory authors [2] obtain simple formula for, which connect the mobility edge with short-range order characteristics of the magnetic subsystem - static spin correlators.

$$\rho^{th} = \rho_0 \exp\left[\frac{(1 - \langle S_0 \cdot S_1 \rangle / S^2) / (1 + \langle S^z \rangle / S)}{W / 4kT}\right] \quad (1)$$

Where  $W$  is the conductivity band width,  $\langle S_0 \cdot S_1 \rangle$  is spin-spin correlation between nearest neighbors,  $\langle S^z \rangle$  - average

magnetization. We used the Monte Carlo (MC) method for calculation the magnetic characteristics for  $18 \times 18 \times 18$ ,  $22 \times 22 \times 22$  lattice with 50000–100000 Monte Carlo steps per site with periodical boundary conditions. Spin-spin correlation and magnetization were simulated for ferromagnetic and for AFM with random ferromagnetic and antiferromagnetic exchange. Using MC results for  $\langle S_0 \cdot S_1 \rangle$  and  $\langle S^z \rangle$  we fit formula (1) to experimental data, that were determined as difference  $\Delta\rho = \rho_1^{ex} - \rho_2^{fit}$  (Fig.1a). The best agreement is achieved for the band width with  $W=3$  eV and spontaneous magnetization tends to zero (Fig.1b). A random-bond model with off-diagonal disorder depending on an instant spin configuration gives a quantitative description of the experimental dependence  $\rho(T)$ .

This study was supported by the Russian Foundation for Basic Research project № 09-02-00554\_a; № 09-02-92001-NNS\_a.

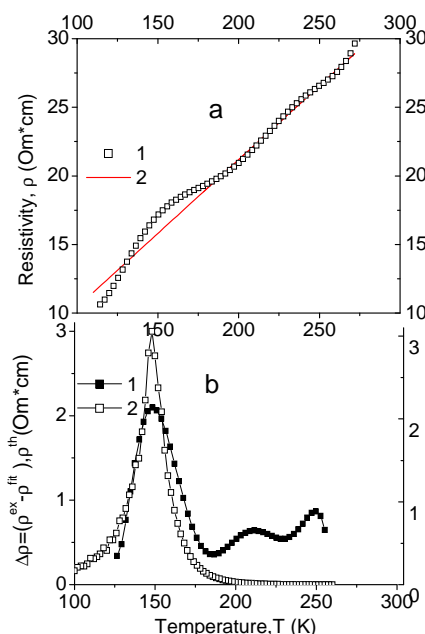


Fig.1 Experimental (1) and fitting (2) dependence of the electrical resistivity versus temperature for  $\text{Sm}_{0.25}\text{Mn}_{0.75}\text{S}$

- [1] Ehrenstein W., Mazur N., Scott J. *Nature*, **442** (2006) 759.  
 [2] Auslender M.I., Kogan E.M., Tretyakov S.V. *Phys. stat. sol.*, **148** (1988) 295.

24PO-I2-30

## EFFECT OF THE SYMMETRY OF SPIN PINNING AT RESONANT FIELD OF SPIN-WAVE RESONANCE SPECTRA IN THREE-LAYER MAGNETIC FILMS

*Bazhanov A.G., Zyuzin A.M.*

Mordovia State University, 430005, Saransk, Russia

The aim of this work was experimental investigation and theoretical calculation of the values of resonance fields  $H_n$  of spin-wave resonance (SWR) with gradual change in the symmetry boundary conditions (spin pinning symmetry). Smooth change in the symmetry of spin pinning, a gradual decrease in the thickness  $h_{pin}$  of the upper layer with high damping (pinning layer) in a three-layer film by layer-etching. The study found that as the thickness  $h_{pin}$  where the boundary conditions are gradually moving from symmetric to asymmetric,

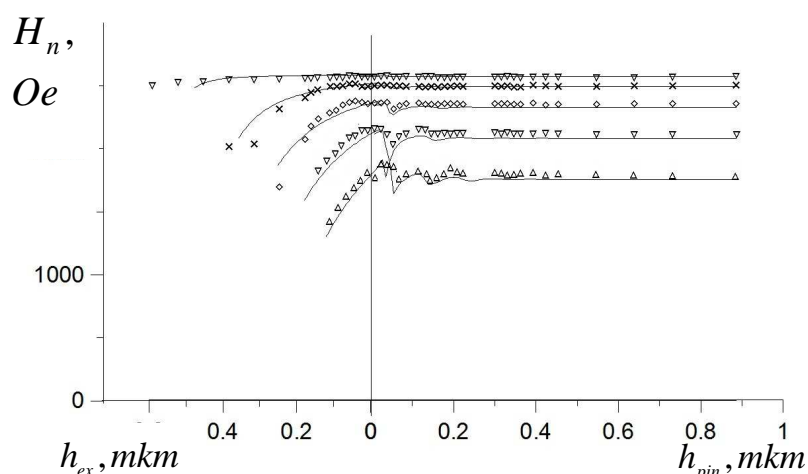


Fig.1. Dependence of the resonant mode fields of the spin-wave resonance on the thickness of the pinning layer  $h_{pin}$  for parallel orientation of the external field relative to the film. Badges - experiment, solid line - calculation.

the resonant field of zero spin-wave (SW) mode  $H_0$  remains almost unchanged (fig.1). For the first and subsequent modes for  $h_{pin} \leq 0.4$  mkm a change in the value  $H_n$  close to periodic. In this case, the amplitude changes of the resonant fields increases with increasing mode number  $n$ . At full etching thickness  $h_{pin}$  of the top of the pinning layer, where the boundary conditions are asymmetric, the resonance field starts to decrease monotonically. A further decrease in the thickness of the excitation layer  $h_{ex}$  values  $H_n$  also decrease monotonically.

To explain these results was calculated, which recorded the equations of motion of the magnetization for each of the layers, as well as the exchange boundary conditions at the interface between layers [1, 2]. Conducted in this paper, the calculation showed that the observed change in the value  $H_n$  due to the fact that at thicknesses  $h_{pin}$  greater length damped spin waves in the pinning layer  $h_{pin} > l$  no effect on the value of the wave phase at the interlayer boundary is not happening. When  $h_{pin} \leq 0.4$  mkm length damped spin waves in the pinning layer  $l$  becomes comparable to the value  $h_{pin}$  and the value of the wave phase at the interlayer boundary begins to



state the spin fluctuations on the free boundary. Phase value, in turn, greatly affects the wave numbers  $k_{1n}, k_{2n}', k_{2n}''$ , which determine, in turn, the resonance fields  $H_n$  of SW modes.

- [1] A.G. Gurevich, G.A. Melkov. *Magnetic oscillations and waves* (Nauka, Moscow, 1994).  
 [2] A.G. Bazhanov. The Physics Metals and Metallography. **101**(2006) 354.

24PO-I2-31

## SPIN HALL EFFECT INDUCED BY SOUND

*Lyapilin I.I.*

Institute for Metal Physics, RAS, 620041, Yekaterinburg, Russia

Among the effects, in which the spin-orbit interaction plays a dominant role and which recently have intensively been studied in low dimensional system it is worth noting the spin Hall effect (SHE) [1-3].

The effect is manifested in the form of a spin current directed perpendicular to the normal current, which takes place in an electric field. The SHE has been observed experimentally [4, 5]. Note that upon the SHE external electric field which directly affects the kinetic degrees of freedom of electrons is transmitted to the spin subsystem through the spin-orbit interaction.

There are, however, mechanisms of interaction with external fields under which the energy of the external field is transmitted simultaneously to both electronic subsystems (kinetic and spin). One of these interactions is the interaction of ultrasonic waves with free conduction electrons.

We analysed cases when the interactions with sound, depends both on the translational and spin operators. We have considered the system of conduction electrons in a constant magnetic field, which interact with the field of lattice displacements and impurities.

We have examined the effects associated with the absorption and redistribution of energy between the subsystems of the kinetic and spin degrees of freedom in the vicinity of the resonance frequencies in the quadratic approximation in the amplitude of displacements. The macroscopic equations for momentum balance, spin components and energy balance of subsystems are obtained by the nonequilibrium statistical operator which is determined under the linear approximation in drift velocity and intensity of sound waves.

The analysis of the macroscopical equations of balance is carried out which evidences the possibility of realization of spin Hall effect induced by sound waves (acoustic spin Hall effect). Besides, the resonant change of conductivity caused by various width of channels transferring the sound wave energy between electronic subsystems is studied.

- [1] M.I. Djakonov, V.I. Perel, Physics Letters. **35A** (1971) 459  
 [2] J.E.Hirsh, Phys.Rev.Lett., **83** (1999) 834.  
 [3] S.Zhang. Phys.Rev.Lett., **85** (2000) 393.  
 [4] Y.K. Kato, R.C. Myers, A.C. Gossard,\etal, Science. **306**, (2004) 1910.  
 [5] J. Wunderlich, B. Kaestner, J. Sinova, \etal, Phys.Rev. Lett., **94** (2005 ) 047204.

## QUANTUM HALL FERROMAGNETIC-PARAMAGNETIC TRANSITION IN P-Si/SiGe/Si QUANTUM WELLS IN A TILTED MAGNETIC FIELD

*Drichko I.L.<sup>1</sup>, Smirnov I.Yu.<sup>1</sup>, Suslov A.V.<sup>2</sup>, Mironov O.A.<sup>3</sup>, Leadley D.R.<sup>4</sup>*

<sup>1</sup>A.F. Ioffe Physico-Technical Institute, St. Petersburg, 194021, Russia

<sup>2</sup>National High Magnetic Field Laboratory, Tallahassee, 32310, USA

<sup>3</sup>Warwick SEMINANO R&D Centre, Coventry CV4 7EZ, UK

<sup>4</sup>Department of Physics, University of Warwick, Coventry CV4 7AL, UK

Magnetoresistance components  $\rho_{xx}$  and  $\rho_{xy}$  of two heterostructures *p*-Si/SiGe/Si with  $p=2 \times 10^{11} \text{ cm}^{-2}$  and  $7.2 \times 10^{10} \text{ cm}^{-2}$  and with anisotropic *g*-factor were measured in a tilted magnetic field of up to 18 T in the temperature range of 0.2 – 2.2 K. We analyzed dependences of the conductivity  $\sigma_{xx}$ , its activation energy  $\Delta E$  and the filling factor  $\nu$  on the tilt angle  $\theta$ .

As seen from Fig. 1 in the sample with  $p=2 \times 10^{11} \text{ cm}^{-2}$  for  $\theta > 50^\circ$  minima at  $\nu=2$  shifts toward lower fields. At  $\theta \approx 59.5^\circ$ , two oscillations appear. With further increase of  $\theta$  the new oscillation shifts left and grows in amplitude while the former oscillation disappears. There is a range of  $\theta = (59.5-61)^\circ$  in which both types of oscillations coexist. Fig. 2 shows that in the vicinity of  $\nu=2$  at  $\theta \approx 60^\circ$  activation energy  $\Delta E(\theta)$  undergoes a minima,  $\sigma_{xx}(\theta)$  in turn shows a maxima. Moreover,  $\nu(\theta)$  shows a sharp jump. These facts allowed us to conclude that at  $\theta \approx 60^\circ$  at  $\nu \approx 2$  the crossing of the Landau levels  $0\uparrow$  and  $1\downarrow$  occurs. This leads to the first order quantum Hall ferromagnetic-paramagnetic (F-P) phase transition.

F-P transition is expected to be accompanied by the formation of ferromagnetic domains, which in accordance with [1] should be manifested by an anisotropy of the magnetoresistance. We tilted the sample in two orientations:  $B_{\parallel} \parallel I$  and  $B_{\parallel} \perp I$  (Fig. 1), but however did not observe any anisotropy.

In the sample with  $7.2 \times 10^{10} \text{ cm}^{-2}$  no transition was observed. For both samples we have obtained the dependences of the effective *g*-factor on the tilt angle, which led us to conclusion that the F-P transition in the *p*-Si/SiGe/Si structure in the tilted field is a result of a violation of the *g*-factor axial symmetry due to disorder.

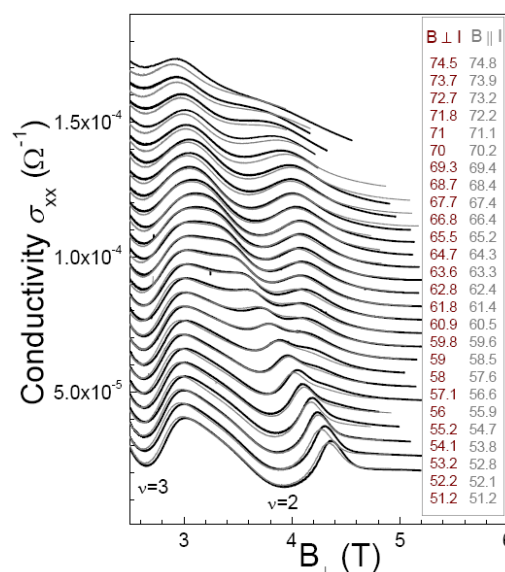


Fig. 1.  $\sigma_{xx}$  vs  $B_{\perp}$  at  $\theta=(51-75)^\circ$  and two orientations:  $B_{\parallel} \parallel I$  and  $B_{\parallel} \perp I$ . The curves are shifted on  $5 \times 10^{-6} \Omega^{-1}$  for clarity.  $T=0.3$  K.

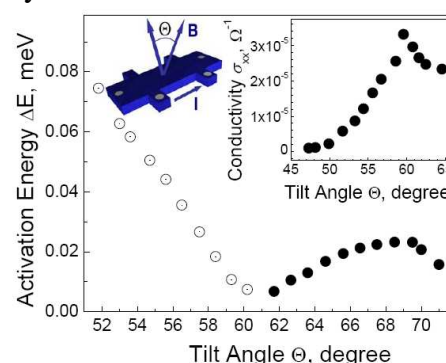


Fig. 2. Activation energy on  $\theta$ . Inset: Conductivity  $\sigma_{xx}$  vs  $\theta$  at  $\nu=2$ ;  $T=0.3$  K.

Support by RFBR 11-02-00223, NSF DMR-0654118, Program of RAS “Spintronika” is acknowledged.

[1] J.T. Chalker, et al, *Phys. Rev. B*, **66** (2002) 161317.

## MAGNETORESISTIVE PROPERTIES OF Gd/Ti MULTILAYERS

Svalov A.V.<sup>1,2</sup>, Vas'kovskiy V.O.<sup>1</sup>, Barandiaran J.M.<sup>2</sup>, Orue I.<sup>3</sup>, Sorokin A.N.<sup>1</sup>,  
Kurlyandskaya G.V.<sup>1,2</sup>

<sup>1</sup> Ural State University named after A.M.Gorky, 620083, Ekaterinburg, Russia

<sup>2</sup> Universidad del País Vasco (UPV-EHU), Dpto. Electricidad y Electrónica,  
P. Box 644, 48080 Bilbao, Spain

<sup>3</sup> SGiker, Universidad del País Vasco (UPV/EHU), 48080 Bilbao, Spain

The magnetoresistance (MR) of Gd thin films and Gd containing granular structures has not been systematically studied [1,2]. However, magnetic and resistive properties of such systems show strong dependence on the size of rare earth entities and can demonstrate interesting behaviour [3,4].

In this work  $[\text{Gd}/\text{Ti}]_n$  multilayered structures were prepared by rf-sputtering and comparatively studied by different methods. The thickness of the Gd layers ( $L_{\text{Gd}}$ ) was varied from 0.9 to 12 nm. The thickness of non-magnetic spacers of Ti was varied from 0.5 to 2 nm. The magneto-resistance was measured in a Cryogenics Ltd. system using a conventional four-point probe technique both in the transverse (current flow perpendicular to the applied field) and longitudinal configurations in a magnetic field up to 100 kOe in the temperature range of 2 to 270 K. A magnetic field was applied and an electric current was flowing in the plane of the sample.

For all  $[\text{Gd}/\text{Ti}]_n$  samples the basic tendency was a decrease of the resistance with an increase of the applied magnetic field and an absence of saturation, even for the magnetic field of 100 kOe. The negative MR was observed in both (longitudinal and transverse) configurations, i.e. it did not depend on the relative orientation of magnetization with respect to the current flow. Therefore, one can designate this effect as a GMR-like magnetoresistance.

At low fields the MR curves presented two local maxima in the longitudinal configuration and two minima in the transverse configuration. The field values of these extrema coincided with a coercive field of the multilayers.

Thus, both anisotropic and isotropic magnetoresistance contributions were observed in  $[\text{Gd}/\text{Ti}]_n$  multilayers. A decrease of the  $L_{\text{Gd}}$  leads to a decrease in the AMR contribution to the total magnetoresistance. A change of the temperature leads to a variation in the relative AMR and GMR-like contributions to the total MR value. For all temperatures, the shape of the resulting MR curves is typical for GMR-like magnetoresistance. The analysis of the shape of the negative isotropic MR curves in  $[\text{Gd}/\text{Ti}]_n$  multilayers shows that they can be attributed to both GMR and the high field isotropic magnetoresistance. But one can give the preference to the high field isotropic magnetoresistance on the basis of the comparative evaluation of the complex of the temperature and thickness dependencies of MR.

This work was supported by RFBR (grant 11-02-00288-a), Spanish MEC (project MAT2008-06542-C04\_02), and SAIOTEK MAGNOSEN grant.

[1] M. Vaezzadeh, B. George, G. Marchal, *Phys. Rev B*, **50** (1994) 6113.

[2] Q. Xiao, J.S. Jiang, C.L. Chien, *Phys. Rev. Lett.*, **68** (1992) 3749.

[3] D. Diercks, A.V. Svalov, M. Kaufman, V.O. Vas'kovskiy, G.V. Kurlyandskaya, *IEEE Trans. Magn.*, **46** (2010) 1515.

[4] A.V. Svalov, G.V. Kurlyandskaya, V.O. Vas'kovskiy, A.N. Sorokin, D. Diercks, *J. Appl. Phys.*, **109** (2011) 023914-6.

24PO-I2-34

## THE KINETIC EQUATION FOR NON-EQUILIBRIUM ORBITAL ANGULAR MOMENTUM

*Kurkin M.I.<sup>1</sup>, Orlova N.B.<sup>2</sup>*

<sup>1</sup> Institute of Metal Physics UrB RAS, S. Kovalevskaya st. 18, 620041, Ekaterinburg, Russia,

<sup>2</sup> Department of Applied and Theoretical Physics, Novosibirsk State Technical University, Karl Marx av. 20, 630092 Novosibirsk, Russia

The phenomenon of quenching of the orbital magnetism in crystals can be formulated as a condition:

$$\langle L^\alpha \rangle = 0; \quad \alpha = x, y, z. \quad (1)$$

The condition (1) is caused by the equivalence of any two opposite directions for the orbital angular momentum  $L$  in an electric field of ions in the crystal lattice. The condition for this equivalence is the equality:

$$\langle m|H|m \rangle = E_m; \quad E_m = E_{-m}, \quad (2)$$

$H$  is the Hamiltonian of an electron in a crystal field,  $m$  is the magnetic quantum number. From (2) it follows that the transitions between states with  $m$  and  $(-m)$  are permitted by the energy conservation rule. However they are prohibited by the angular momentum conservation ( $\Delta L - \hbar\Delta m = 2\hbar m$ ). The role of the crystal lattice in this transition ensures the  $\Delta L + \Delta L_{latt} = 0$  equality. However, the lattice deformation associated with  $\Delta L_{latt}$  requires the energy  $\Delta E_{latt}$ , so the transitions under consideration are forbidden by the energy conservation law. The requirements of the both conservation laws can be reached if we consider also the relaxation of lattice deformations. Such relaxation can turn the local deformation at the  $m \rightarrow -m$  transition point to a uniform rotation of the entire sample following by its transfer to the support holding the sample.

We used the dynamic equations for the components of the orbital angular momentum operator  $\hat{L}^z$  and  $\hat{L}^\pm = \hat{L}^x \pm i\hat{L}^y$ :

$$i\hbar \frac{d}{dt} \hat{L}^\alpha = [\hat{L}^\alpha, \hat{H}] = \hat{L}^\alpha \hat{H} - \hat{H} \hat{L}^\alpha$$

with the Hamiltonian:

$$\hat{H} = \varepsilon_u b^+ b - \varepsilon_L \hat{L}^z - V \hat{L}^+ b - V^* \hat{L}^- b^+, \quad (3)$$

Here  $b$  and  $b^+$  is the creation and annihilation operators of lattice deformation,  $\varepsilon_u$  is the energy of the deformation,  $\varepsilon_L$  is the effective field lattice orienting  $L$  respectively to the selected crystal axis  $z$ ,  $V$  is the parameter of interaction  $L^\pm$  with the  $b$  and  $b^+$ . The relaxation of strain  $b$  and  $b^+$  was taken into account in the approximation of  $\tau_{ph}$  relaxation time. The interaction was considered in a  $V$  square approximation. For the values  $\langle \hat{L}^z \rangle = L^z$  we obtained the Bloch type equation

$$\frac{d}{dt} L^z = -L^z / T_1, \quad \frac{1}{T_1} = \frac{2|V|^2}{(\varepsilon_u + \varepsilon_L)^2} \cdot \frac{1}{\tau_{ph}}. \quad (4)$$

In the report we would like to discuss the effect of the  $\tau_{ph}$  dependence on the rate of deformation change.

This work was partly supported by Russian Foundation for Basic Research (project 11-02-00093).

## MAGNETIC AND ANISOTROPIC PROPERTIES STUDY OF Fe<sub>3</sub>Si/MgO STRUCTURES BY FERROMAGNETIC RESONANCE

Astashenok A.V., Zyubin A.Yu., Orlova A.N., Goikhman A.Yu., Kupriyanova G.S., Nevolin V.N.  
Immanuel Kant Baltic Federal University, 236041, A. Nevskogo, 14, Kaliningrad, Russia

One of the important problems today is a development of new materials and combinations for applications in field of spintronics. The perspective material for such tasks is ferromagnetic Fe<sub>3</sub>Si. It has a high Curie temperature of 850K and has ferromagnetic half-metal properties with 43% spin polarization. The most interesting structures are fully *epitaxial* ferromagnetic – isolator – ferromagnetic type structures based on MgO [1]. Information about magnetic and anisotropy properties depending on grow conditions is very important for understanding.

In the present work, we correspond on the utilizing ferromagnetic resonance (FMR) method for the control of the ferromagnetic and absence of paramagnetic phases and impurities, and the orientation properties of the formed polycrystalline and epitaxial structures. The structures were analysed on the modernised EPR Radiopan equipment with the operation frequency of 9,4 GHz. The resonator of a rectangle type E102 was used. The modulation frequency was 100 kHz.

We have analyzed the structures formed by the pulsed laser deposition (PLD) technique on the equipment of the thin-layer materials laboratory of the National nuclear research university “MEPHI” [2,3]. Experiments on ferromagnetic silicide Fe<sub>3</sub>Si formation in crystal phase were held by co-deposition of Fe and Si on the MgO substrate in the relevant stechiometric ratio regarding to the epitaxial conditions of growth, i.e. the preparation of the substrate with vacuum annealing before the formation up to T=600 °C and the deposition at the high T= 250-450 C. It was made a series of samples with different coefficient of co-deposition to find optimal conditions of Fe<sub>3</sub>Si epitaxial growth. The thickness of Fe<sub>3</sub>Si was 240Å. The chemical structure was controlled by Auger spectroscopy method with ion profiling.

The sample 1, synthesized by the co-deposition Fe:Si with the ratio 10:9 did not demonstrate the angle dependence of the signal in the plain geometry. We detected the change of the signal intensity at the film rotation around its normal position ( $\theta=90^\circ$ ,  $\varphi$  is the changing angle) and the change of the resonance signal position at the film rotation in plain against the magnetic field direction. In the samples of MgO/Fe<sub>3</sub>Si, synthesized at the ratio Fe:Si as 11:3, which was chosen at the calculation of the dispersion coefficient of these materials, in contrast to the sample 1, we detected the dependence of the resonance signal in both geometries, which is the evidence of the crystal state and oriented structure formation.

The analysis showed that parameters of FMR spectra of multilayer structures are very sensitively to magnetic and anisotropic properties of Fe<sub>3</sub>Si/MgO thin film structures and depend on growing conditions and Si content. Results of experiment data simulation gave us possibility to extract magnetic anisotropy constants, proved by known results for same structures. The extracted magnetic parameters such as anisotropy constants, linewidths and resonance field position were studied.

The work was performed within the frames of the State contract No. 02.740.11.0550 and No. P148 dated from April 15<sup>th</sup>, 2010.

[1] S.S.P. Parkin, C. Kaiser, A. Panchula, P.M. Rice, B. Hughes, M. Samat, S. Yang, *Nature Mat.*, **3** (2004) 862.

[2] R. Mantovan, M. Georgieva, M. Fanciulli, A. Goikhman, N. Barantsev, Yu. Lebedinskii and A. Zenkevich, *Phys. Stat. Sol. (a)*, **205** (2008) 1753.

[3] R. Mantovan, C. Wiemer, A. Lampereti, M. Georgieva, M. Fanciulli, A. Goikhman, N. Barantsev, Yu. Lebedinskii and A. Zenkevich, *Hyperfine Interactions*, **191** (2009) 41.

24PO-I2-36

## CO-TUNNELING CURRENT THROUGH THE TWO-LEVEL QUANTUM DOT COUPLED TO MAGNETIC LEADS: A ROLE OF EXCHANGE INTERACTION

*Sharafutdinov A.U.<sup>1</sup>, Burmistrov I.S.<sup>2</sup>*

<sup>1</sup> Moscow Institute of Physics and Technology, 141700 Moscow, Russia

<sup>2</sup> L.D. Landau Institute for Theoretical Physics, Kosygina street 2, 117940 Moscow, Russia

As is well-known, in the Coulomb blockade regime transport through the quantum dot is determined by co-tunneling processes. We present analytical results for the current through the two-level quantum dot with exchange interaction in the presence of fully-polarized (parallel or antiparallel) ferromagnetic leads. We demonstrate that the current-voltage characteristics has staircase structure which is sensitive to the spin of the quantum dot. In addition, we find that in the antiparallel case, contribution of inelastic co-tunneling to the current depends on the phases of tunneling amplitudes due to the presence of exchange interaction on the quantum dot. The details can be found in A.U. Sharafutdinov and I.S. Burmistrov, arXiv:1103.2425

24PO-I2-37

## THE VOLUME MAGNETOSTRICTION IN DILUTED MAGNETIC SEMICONDUCTORS CdGeAs<sub>2</sub> AND CdGeP<sub>2</sub> DOPED BY MANGANESE AT ROOM TEMPERATURES INDUCED BY HIGH PRESSURES

*Mollaev A.Yu.<sup>1</sup>, Kamilov I.K.<sup>1</sup>, Arslanov R.K.<sup>1</sup>, Marenkin S.F.<sup>2</sup>, Arslanov T.R.<sup>1</sup>, Zalibekov U.Z.<sup>1</sup>*

<sup>1</sup> Institute of Physics, Daghestan Scientific Center of the Russian Academy of Science, 367003, Makhachkala, Russia

<sup>2</sup> Institute of common and inorganic chemistry of the Russian Academy of Science, 119991, Moscow, Russia

The given work presents the experimental results on relative volume compressibility  $\Delta V(P)/V_0$  from the pressure  $P \leq 7$  GPa at room temperatures in diluted magnetic semiconductors Cd<sub>1-x</sub>Mn<sub>x</sub>GeAs<sub>2</sub> ( $x=0 \div 0.36$ ) and p-Cd<sub>1-x</sub>Mn<sub>x</sub>GeP<sub>2</sub> ( $x=0.09 \leq x \leq 0.225$ ). The measurements are carried out in a high pressure device of toroid type at the hydrostatic pressure up to  $P \leq 7$  GPa in region room temperatures. A detailed description of a method of the experiment is given in work [1]. The synthesis of the samples and technological modes of their growth are described in work [2].

Compressibility is measured by the tensometric technique as in [3]. The measured samples have a cylinder shape of 1mm in a height and 3 mm in a diameter.

An extinction of ferromagnetic state under the pressure in Cd<sub>1-x</sub>Mn<sub>x</sub>GeAs<sub>2</sub> ( $x=0 \div 0.36$ ) reveals as a sharp decrease in lattice compressibility and increase in bulk modulus beginning from  $P > 4.5$  GPa. The bulk modulus rises in wide pressure ranges above 4.5 GPa and gradually increases close to 7 GPa, what indicates that the magnetic transition “ferromagnetic-paramagnetic” occurred at this pressure.

The anomalies of magnetic properties are found on the  $\Delta V(P)/V_0$  dependences in Cd<sub>1-x</sub>Mn<sub>x</sub>GeP<sub>2</sub> ( $x=0.09 \leq x \leq 0.225$ ) at  $P > 3.5$ . In our opinion the obtained results show that magnetic phase transitions take place in all studied samples. A transition from the magnetic-ordered phase into the magnetic-disordered phase occurs near a critical pressure  $P_c > 3.5$  GPa. High pressures significantly decrease

the Curie temperature ( $T_c$ ) in all researched polycrystals. The values for volume magnetostriction (coefficient of spontaneous magnetization) are determined from the  $\Delta V(P)/V_0$  dependences. The calculations of bulk modulus  $B$  carried out by means of scaling expression allow to estimate the values of bulk modulus in magnetic-ordered and magnetic-disordered phases.

This work was supported by Program of Presidium of RAS “Thermophysics and mechanics of external energetic influences and physics of high compressed material” and Section of High Compressed Material.

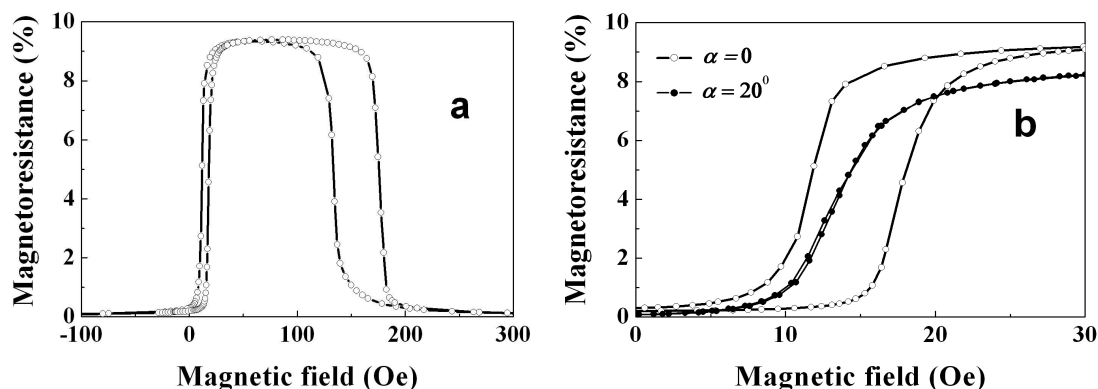
- [1] L. G. Khvostantsev, L. P. Vereshagin, A. P. Novikov. High Temp.-High Pressure. **9** (1977) 6 32.  
 [2] S. F. Marenkin, V. M. Novotortzev, K. K. Palkina et al., Inorganic materials. **40** (2004) 2 135.  
 [3] O. B. Tsiok, V. V. Bredikhin, V. A. Sidorov and L. G. Khvostantsev, High Pressure Res. **15** (2008) 32.

24PO-I2-38

## LOW HYSTERESIS TOP SPIN-VALVES WITH FeMn AND IrMn ANTIFERROMAGNETIC LAYERS

*Milyaev M., Naumova L., Proglyado V., Krinitsina T., Ustinov V.*  
 Institute of Metal Physics, Ural Branch of RAS, Ekaterinburg, Russia

Objects of our investigations are “spin-valve” nanostructures consisting of two ferromagnetic (FM) layers separated by a nonmagnetic spacer layer, one of FM layers being pinned by an antiferromagnetic (AFM) layer. At the top spin-valve structure, the AFM layer and the adjacent pinned FM layer are located in the upper part of the multilayer, whereas the free FM layer is on a buffer layer in the bottom part. Important spin-valve characteristics for various applications are: giant magnetoresistance (GMR) ratio, exchange bias field, magnetoresistive sensitivity, thermal stability, and low hysteresis caused by free layer magnetization reversal [1,2]. A way to decrease considerably the free layer hysteresis is demonstrated in the present work.



Samples Ta(50A)/Fe<sub>20</sub>Ni<sub>80</sub>(20A)/Co<sub>90</sub>Fe<sub>10</sub>(55A)/Cu(24 A)/Co<sub>90</sub>Fe<sub>10</sub>(55A)/Fe<sub>50</sub>Mn<sub>50</sub>(150A)/Ta(20A) (sample 1) and Ta(20A)/Fe<sub>20</sub>Ni<sub>80</sub>(25A)/Co<sub>90</sub>Fe<sub>10</sub>(20A)/Cu(24A)/Co<sub>90</sub>Fe<sub>10</sub>(25A)/Mn<sub>83</sub>Ir<sub>17</sub>(50A)/Ta(20A) (sample 2) were prepared by DC magnetron at room temperature on glass and naturally oxidated (100)Si substrates sputtering in high purity argon under the pressure of 0.1 Pa. The base pressure of residual gases in the chamber was  $10^{-7}$  Pa. Magnetic field of  $H = 110$  Oe was applied in the film plane during multilayer deposition. Magnetoresistance was measured at room temperature with four-point probe method in current-in-plane geometry using with varying

angle ( $\alpha$ ) between the magnetic field vector and the in-plane anisotropy axis induced in AFM metal during deposition in magnetic field.

In Fig.(a) is shown a typical for spin-valve structures magnetoresistance curve measured for sample 1. Fig.(b) demonstrates the reduction of low field hysteresis for this sample by the factor of 30 when magnetic field is applied under the angle  $\alpha = 20^\circ$  to the anisotropy axis in the film plane. Similar properties were detected for the sample 2 with  $\text{Mn}_{83}\text{Ir}_{17}$  antiferromagnetic layer in which the GMR ratio was found to be 11%.

The work is supported by RFBR, project No. 10-02-00590, and by the Program of Presidium of the Russian Academy of Sciences, project No. 09-P-2-1037.

[1] H. Kanai, K. Yamada et al, IEEE Transactions On Magnetics, **32** (1996), 3368.

[2] S. Tumanski: Thin Film Magnetoresistive Sensors, IOP Publishing Ltd (2001), p. 229.

24PO-I2-39

## ELECTRICAL AND OPTICAL PROPERTIES OF FERROMAGNETIC Co-BASED HEUSLER ALLOYS

*Fomina K.A.<sup>1</sup>, Marchenkov V.V.<sup>1</sup>, Shreder E.I.<sup>1</sup>, Eisterer M.<sup>2</sup>, Weber H.W.<sup>2</sup>*

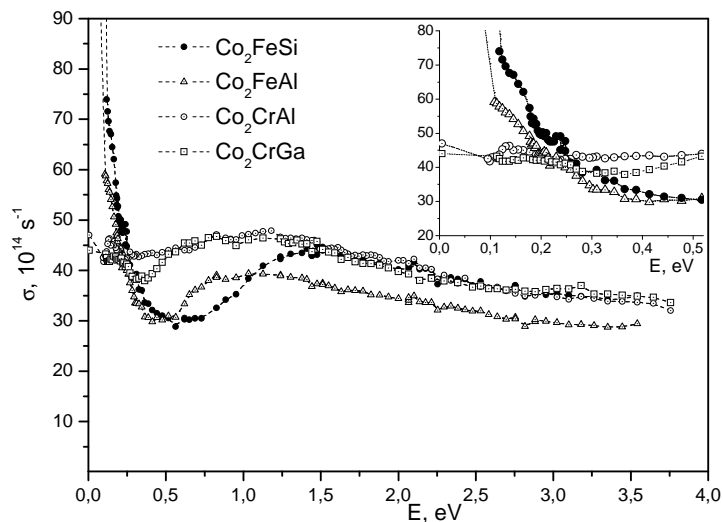
<sup>1</sup> Institute of Metal Physics, Kovalevskaya Str. 18, Ekaterinburg 620041, Russia

<sup>2</sup> Atominstytut, Vienna University of Technology, Stadionallee 2, Vienna 1020, Austria

Heusler alloys are of great interest due to their unique functional properties. Some of them have been predicted to be in a half-metallic state [1-3]. The main feature of the electronic structure of half-metallic ferromagnets is the presence of an energy gap at the Fermi level in one spin subband and a metallic character of the density of states in the other one. This can lead to 100% spin polarization of the current carriers. Such alloys can be used as promising materials for spintronic devices.

The electrical and optical properties of  $\text{Co}_2\text{CrGa}$ ,  $\text{Co}_2\text{CrAl}$ ,  $\text{Co}_2\text{FeAl}$  and  $\text{Co}_2\text{FeSi}$  Heusler alloys have been studied. The electroresistivity has been measured in the temperature interval from 4.2 to 370 K and the optical conductivity has been studied in the spectrum range  $\lambda = (0.3 - 13) \mu\text{m}$  at room temperature. The electroresistivity and the optical conductivity of  $\text{Co}_2\text{FeAl}$  and  $\text{Co}_2\text{FeSi}$  are typical for metals. An abnormal behavior of the electroresistivity has been observed and the optical properties in the IR range have been studied also for  $\text{Co}_2\text{CrGa}$  and  $\text{Co}_2\text{CrAl}$  alloys, i.e., the electrical resistivity demonstrates a semiconductor-like behavior, and the optical conductivity has no contribution (very weak or negative Drude-type growth) from the intraband absorption of the conduction electrons.

The data analysis, based on existing band calculations, allows us to conclude





that the anomalous behavior of these properties is determined by the electronic states near and at the Fermi level. The electronic states in the subband with spin up give the main contribution to the interband transitions in the IR range, but they practically do not contribute to the static conductivity (resistivity). There are almost no charge carries in the other electronic subband with spin down. Hence, the interband transitions occur only at energies above the semiconductor gap value.

This work was partly supported by the Austrian Academy of Sciences.

[1] R.Y. Umetsu, K. Kobayashi et al, *Appl. Phys. Lett.* **85** (2004) 2011

[2] J. Kübler G. H. Fecher and C. Felser, *Phys. Rev. B* **76** (2007) 024414

[3] B. Balke, S. Wurmehl et al, *Sci. Technol. Adv. Mater.* **9** (2008) 014102

24PO-I2-40

## MAGNETOSTATIC MECHANISM OF PHASE-LOCKING OF SPIN-TRANSFER NANO-OSCILLATORS

Zvezdin K.<sup>1</sup>, Safin A.<sup>1,2</sup>, Krasheninnikov A.<sup>1</sup>, Belanovsky A.<sup>1</sup>, Khvalkovsky A.<sup>1</sup>, Dussaux A.<sup>3</sup>,  
Locatelli N.<sup>3</sup>, Bortolotti P.<sup>3</sup>, Grollier J.<sup>3</sup>, Cros V.<sup>3</sup>, Fert A.<sup>3</sup>

<sup>1</sup> Prokhorov General Physics Institute, Russian Academy of science, 119991, Moscow, Vavilov Str.,  
38, Russia

<sup>2</sup> Moscow Power Engineering Institute (Technical University), Moscow, 111250,  
Krasnokazarmennaya Str., 14, Russia

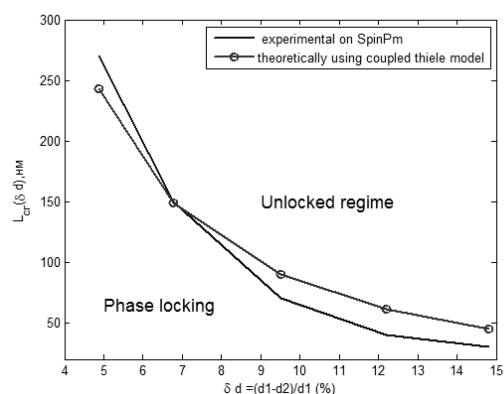
<sup>3</sup> Unité Mixte de Physique CNRS/Thales and Université Paris Sud 11, 1 ave Augustin Fresnel,  
91767 Palaiseau, France

Modern spin-transfer nano-oscillators (STNO) [1,2] are characterized by a very narrow line width, they are well tunable and its production is compatible with CMOS semiconductor technical cycle, causing great applied interest. However, the use of STNO in telecommunication is limited by very low output power generated frequencies. This problem is intended to be solved through the increase in power of a single vortex STNO and phase synchronization of ensemble of such devices.

In this work, the synchronization of two vortex STNOs by magnetostatic mechanism with the help of micromagnetic simulations has been explored. To explain and interpret the results, the analytic model of synchronization in linear relationship between vortices has been built using coupled Thiele equations [1,2].

With the help of the SpinPM solver, a full-scale micromagnetic research of spectral characteristics of coupled vortex dynamics has been performed. The dependence of critical locking interdot distance as a function of difference between diameters of the disks has been obtained (shown on figure). On this figure the analytical dependence using theoretical approach (coupled Thiele equations) is compared to the modeling data.

A dynamical equation for phase difference  $\Psi$  between two cores has been found. This is Adler like equation which can be represented as  $d\Psi/dt = \Delta\Omega - \rho \cdot \sin(\Psi + \alpha)$ , where  $\Delta\Omega$  – frequency difference between two partial oscillators,  $\rho$  – maximum mismatch correction and  $\alpha$  is the angle. In general all these parameters  $\Delta\Omega$ ,  $\rho$ ,  $\alpha$  depend



on the current time in a nonlinear manner. This complex dynamic of synchronized objects defines nontrivial character of synchronization zone (Arnold tongue) has been observed experimentally using SpinPM.

[1] Y. Gaididei et al, *Int. J. of Quant.* **110** (2010) 83.

[2] B. Dussaux et al, *Nat. Comm*, **10** (2010) 1038.

24PO-I2-41

## NON-NEWTONIAN DYNAMICS OF THE FAST MAGNETIC VORTEX MOTION

*Avanesyan G.G.<sup>1</sup>, Khvalkovskiy A.V.<sup>1</sup>, Kulagin N.E.<sup>2</sup>, Zaspel C.E.<sup>3</sup>, Zvezdin K.A.<sup>1</sup>, Ivanov B.A.<sup>4</sup>*

<sup>1</sup>A.M. Prokhorov General Physics Institute, Russian Academy of Sciences, 119991, Moscow, Russia

<sup>2</sup>State University of Management, 109542, Moscow, Russia

<sup>3</sup>Department of Environmental Sciences, University of Montana-Western, Dillon MT 59725, USA

<sup>4</sup>Institute of Magnetism, National Academy of Sciences of Ukraine, Kiev 03142, Ukraine

A magnetic vortex is a curling magnetization distribution in at magnetic submicron dots, with the magnetization pointing perpendicularly to the dot plane within the ten nanometer size vortex core. This unique magnetic object has attracted much attention recently because of the fundamental interest to specific properties of such a nanoscale spin structure. The direction of the core polarization (“up” or “down”) can store a bit of information, and this is of considerable practical interest for new applications in magnetic memory technology. The switching process of such elements includes ultra fast motion (at the tens of picoseconds time scale) of the vortex core [1]. Due to this reason the fast dynamics of the magnetic vortices attracts much attention last years.

In our numerical and analytical work, we study a sub-ns dynamics of the magnetic vortex in a submicron size disc made of a soft magnetic material. In the numerical micromagnetic simulations we consider a circular disc made of permalloy with the diameter 300 nm and with the thickness 10 nm. We excite the vortex dynamics by the action of the sub-ns pulses of magnetic field or spin – polarized current of different amplitudes and durations. This dynamics consists of beside the gyrotopic motion (circular motion within sub – GHz diapason), high frequency modes in GHz diapason. All this range of dynamics could be explained by third order non-Newtonian equation for the vortex core coordinate  $\mathbf{X}$  [2]:

$$G_3(\mathbf{e}_z \times \frac{d^3\mathbf{X}}{dt^3}) + M \frac{d^2\mathbf{X}}{dt^2} + G(\mathbf{e}_z \times \frac{d\mathbf{X}}{dt}) = \mathbf{F} \quad (1)$$

Eq. (1) is the generalization of the familiar first order Thiele equation with standard gyroconstant  $G = 2\pi L M_s / \gamma$ , describing slow gyroscopic motion only. The values of effective mass  $M$  and higher gyroconstant  $G_3$  for different magnets are obtained by comparison of the analytical theory and numerical data [2]. For vortex state magnetic dots  $G_3 = \eta_G R / 4\pi\gamma^3 M_s$  and  $M = \eta_M L / \gamma^2$ , where the coefficients  $\eta \sim 1$ [2].

We present some new results obtained recently for this system. First, we describe the non – linear regime of the vortex excitation. Second, we present the numerical results obtained for the excitation by spin – polarized current.

[1] R. Hertel, S. Gliga, M. Fahnle et al., *Phys. Rev. Lett.* **98**, 117201 (2007).

[2] B.A. Ivanov, G.G. Avanesyan, A.V. Khvalkovskiy, N.E. Kulagin, C.E. Zaspel, K.A. Zvezdin, JETP Let. **91**, 190-195 (2010).

24PO-I2-42

## **ELECTROMAGNETIC WAVES ABSORPTION IN THE SYSTEMS WITH NON-COLLINEAR MAGNETIC STRUCTURES**

*Udalov O.G., Karashtin E.A.*

Institute for physics of microstructures RAS, (603950) GSP-105, Nizhny Novgorod, Russia

The systems with inhomogeneous magnetization show a variety of interesting properties, such as giant magnetoresistance, spin transfer torque, “topological” Hall effect et. al. These properties are actively studied at the time. Recently one more interesting phenomenon is theoretically predicted in the system with non-collinear magnetic structure [1], namely transition of electrons between the states with different spin orientation under the impact of alternative linearly polarized electric field. These transitions cause the additional absorption peak in the region of the frequencies  $\omega_j = J/\hbar$ , where  $J$  is spin splitting of conduction electron band. The diluted magnetic semiconductor is considered in the work [1]. In the present work this effect is theoretically investigated in two another systems, namely in the medium with magnetic spiral and in the magnetic superlattice containing two magnetic layers with non-collinear magnetization per period.

In the work it is demonstrated that the transitions of electrons between different spin states also arise magnetic spiral and magnetic superlattices (with non-collinear magnetization spatial distribution). This leads to additional absorption peak appearing.

In the case of magnetic spiral the electric field should be polarized along the spiral axis. High frequency conductivity of the medium with magnetic spiral has a peak near exchange splitting of conduction band. Due to high symmetry of magnetic spiral there are not any other peaks in the high frequency region. In the work [2] the absorption of electromagnetic waves is investigated experimentally for holmium (that shows helical magnetic order under temperature below  $T_n = 133$  K). In the region of exchange splitting of conduction band a peak appears when the temperature is below 133 K. This peak disappears when the strong external magnetic field (making the magnetization to be uniform) is applied to the crystal. The peak has maximum magnitude for the electromagnetic field polarized along the helical axis. The results of our calculation can qualitatively explain the behavior of the peak.

In the case of magnetic superlattice the electric field should be polarized along the direction of magnetization variation. Due to low symmetry (comparing to helix) of the system two type of absorption peaks arise in the high frequency region. First one appears due to transition of electron between minibands formed because of periodicity of the superlattice. These peaks exist both for the cases of collinear and non-collinear magnetization distribution. Another one appears due to transition of electrons with changing of its spin orientation. This type of absorption appears near the frequency  $\omega_{sl} = (m_{av}J)/(\hbar m_{sat})$  ( $m_{sat}$  is saturation magnetization of single layer,  $m_{av}$  is the average magnetization of the superlattice) only in non-collinear case. Inserting the spin-independent periodic potential in the system the peaks of the first type can be shifted in the region of frequency higher than  $\omega_{sl}$ . Therefore the electron transitions between different “spin subbands” can be observed in principle in such a system.

This research was supported by the FTP “Scientific and scientific-pedagogical personnel of innovative Russia” (contracts No P2618, P348), RFBR (project 11-02-00294-a), and the “Dynasty” foundation.

- [1] L.S. Khazan, Yu.G. Rubo, V.I. Sheka // *Phys. Rev. B*, **47**, 20, 13180 (1993).  
 [2] P. Weber and M. Dressel, *J. Magn. Magn. Mater.* **272-276**, E1109 (2004).

24PO-I2-43

## AB-INITIO STUDY OF ELECTRONIC AND MAGNETO-OPTICAL PROPERTIES OF InSb:Mn AND InAs:Mn

*Kulatov E.<sup>1</sup>, Titov A.<sup>1</sup>, Uspenskii Yu.<sup>2</sup>*

<sup>1</sup> A.M. Prokhorov General Physics Institute of RAS, 38 Vavilov str. Moscow 119991, Russia

<sup>2</sup> P.N. Lebedev Physical Institute of RAS, 53 Leninskii prosp. Moscow 117924, Russia

Diluted ferromagnetic semiconductors attract considerable attention for semiconductor-based spintronics, as in these devices the spin degree of freedom of carriers can be magnetically and electrically manipulated. The magneto-optical (MO) Kerr spectra and electronic properties of  $\text{In}_{1-x}\text{Mn}_x\text{Sb}$  and  $\text{In}_{1-x}\text{Mn}_x\text{As}$  ( $x=1.56, 3.125$  and  $6.25\%$ ) are calculated using the relativistic, full-potential linear augmented plane-wave method as implemented in WIEN2k [1]. Density-functional calculations presented here are performed within a supercell ( $2 \times 2 \times 2$  and  $4 \times 4 \times 4$ ) schemes. All atomic positions in cell are optimized by minimization of the forces acting on atoms. The energy difference between ferromagnetic and antiferromagnetic collinear orderings has been calculated for the uniform and dimer Mn-pair geometries in order to find the ground state distribution of the Mn atoms in InSb(As) hosts. We find the preference of the dimer ferromagnetic configuration of Mn dopants.

Our calculated optical spectra show marked features in the infrared region. The amplitude and energy position of our calculated MO resonance in  $\text{In}_{1-x}\text{Mn}_x\text{Sb}$  ( $x=1.56\%$ ) are found to be in good agreement with corresponding experimental MO spectra at 2500 nm[2]. Although the MO property is a rather complicated function of the on-diagonal and off-diagonal components of the optical conductivity tensor, present calculation provides a clear insight about its origin in this material. The large ( $\sim 3^\circ$ ) Kerr effect observed in InSb:Mn can be understood as a combined effect of the on- and off-diagonal components, nearly maximal exchange splitting of Mn 3d states and the large spin-orbit coupling of Sb. The frequency-dependent optical properties, namely reflectivity, absorption coefficient, refractive index, extinction coefficient and unscreened plasma frequencies are also given.

Support by Russian Foundation for Basic Research (RFBR No 10-02-00698-a, 10-02-00118-a, 09-02-91078-CNRS-a) and Program of Russian Academy of Sciences “Strongly correlated electrons in solids and structures” and “Basic investigations of nanotechnologies and nanomaterials” is acknowledged.

- [1] P.Blaho, K.Schwarz, G.K.H.Madsen, D.Kvasnicka, and J.Luitz, *Wien2k, An Augmented Plane Wave+Local Orbitals Program for Calculating Crystal Properties* (Karlheinz Schwarz, Techn. Universitat Wien, Austria, 2001).  
 [2] C. Thurn, V.M. Axt, A. Winter, H. Pascher, H. Krenn, X. Liu, J.K. Furdyna, T. Wojtowicz, *Phys. Rev. B*, **80**, (2009) 195210.

## SUPPRESSION OF FERROMAGNETISM IN $\text{Eu}_x\text{Ca}_{1-x}\text{B}_6$

Glushkov V.<sup>1</sup>, Kuznetsov A.<sup>2</sup>, Sannikov I.<sup>2</sup>, Bogach A.<sup>1</sup>, Anisimov M.<sup>1</sup>, Demishev S.<sup>1</sup>, Ivanov V.<sup>1</sup>,  
Dukhnenko A.<sup>3</sup>, Levchenko A.<sup>3</sup>, Shitsevalova N.<sup>3</sup>, Sluchanko N.<sup>1</sup>

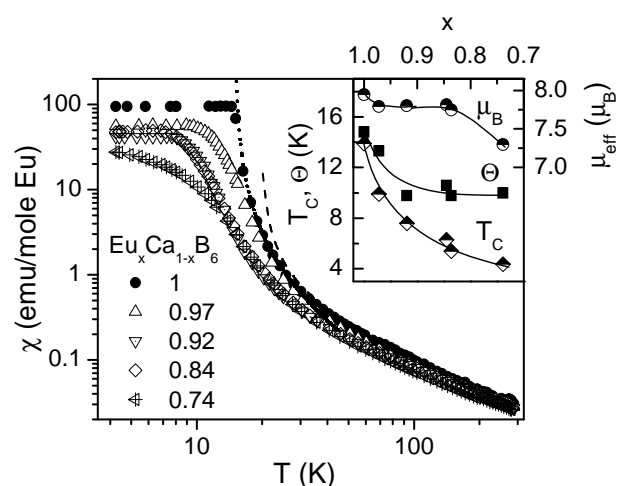
<sup>1</sup> A.M.Prokhorov General Physics Institute of RAS, 38, Vavilov str., Moscow 119991, Russia

<sup>2</sup> National Research Nuclear University MEPhI, 31, Kashirskoe Shosse, Moscow, 115409 Russia

<sup>3</sup> Institute for Problems of Materials Science NAS, 3, Krzhyzhanovsky str., 03680, Kiev, Ukraine

Moving in the  $\text{Eu}_x\text{Ca}_{1-x}\text{B}_6$  series from nonmagnetic insulator  $\text{CaB}_6$  to ferromagnetic semimetal  $\text{EuB}_6$  (Curie temperature  $T_C=13.9$  K) induces long range magnetic ordering in the  $\text{Eu}^{2+}$  magnetic sublattice at  $x>x_M\sim 0.3$  [1], which is followed by the metal-insulator transition (MIT) with the onset of metallic state at the Eu content  $x>x_C\sim 0.8$  [2]. This observation agrees qualitatively with the quantum MIT scenario predicted recently for this system with colossal magnetoresistive effect ( $\rho(0)/\rho(H)\sim 7\cdot 10^5$  for  $x=0.74$  [2]) within double exchange approach [3]. However, a lack of detailed information about the evolution of the magnetic properties in the Eu-rich  $\text{Eu}_x\text{Ca}_{1-x}\text{B}_6$  compounds doesn't allow to shed light on the intricate interplay between charge transport and magnetism in vicinity of the concentration driven MIT [2,4].

Here we report the magnetic properties of the  $\text{Eu}_x\text{Ca}_{1-x}\text{B}_6$  single crystals ( $0.74\leq x\leq 1$ ) studied in the wide range of temperatures (1.8-300 K) and magnetic fields (up to 5 T). At high temperatures the temperature dependences of low field magnetic susceptibility follow the Curie-Weiss behaviour  $\chi\sim(T-\Theta_p)^{-1}$  (shown by dashed line for the  $\text{EuB}_6$   $\chi(T)$  curve in Figure). The effective magnetic moment of the  $\text{Eu}^{2+}$  ion estimated from the data (see inset in Figure) is found to fall down from the free ion value  $\mu_{\text{eff}}\approx 7.93\mu_B$  for  $x=1$  to  $\mu_{\text{eff}}\approx 7.3\mu_B$  for  $x=0.74$  ( $\mu_B$  - Bohr magneton) when Eu content decreases entering into the dielectric phase ( $x<x_C$ ). At the same time, a universal behavior of magnetic susceptibility  $\chi\sim(T-\Theta)^{-\alpha}$  ( $\alpha=1.5$ ) (see, e.g., dotted line for the  $\text{EuB}_6$   $\chi(T)$  curve in Figure) is observed close to the Curie temperature in the paramagnetic states at both metallic ( $x>x_C$ ) and dielectric ( $x<x_C$ ) sides of the MIT. Note also that the gradual decrease of  $T_C$  with the increase of Ca content is accompanied by the concentration independent behaviour of  $\Theta(x)$  and  $\Theta_p(x)$  parameters detected at  $x<0.9$  (inset in Figure). The established anomalous evolution of the effective exchange constants and the parameters of  $\text{Eu}^{2+}$  magnetic state in these Eu-rich compounds is discussed in terms of magnetic and electronic phase separation realized in vicinity of the concentration driven quantum MIT.



Support by RFBR 11-02-00623 project and Federal Programme “Scientific and Educational Human Resources of Innovative Russia” is acknowledged.

[1] G.A. Wigger et al., *Phys. Rev. Lett.*, **93** (2004) 147203.

[2] V. Glushkov et al., *JETP*, **111** (2010) 246.

[3] V.M. Pereira et al., *Phys. Rev. Lett.*, **93** (2004) 147202.

[4] G.Caimi et al., *Phys. Rev. Lett.*, **96** (2006) 016403.

24PO-I2-45

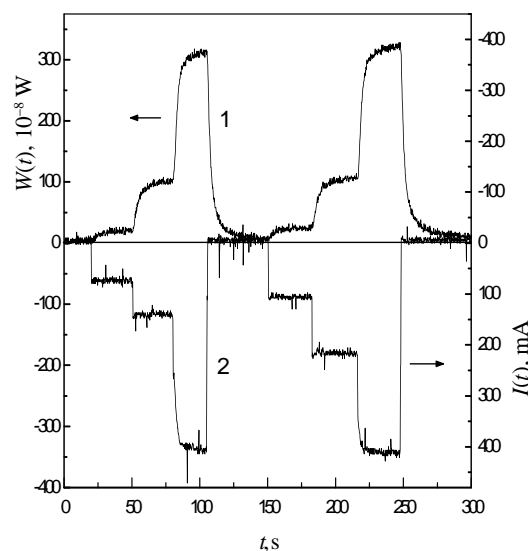
## SPIN-INJECTION TERAHERTZ RADIATION IN MAGNETIC JUNCTION

Chigarev S.G.<sup>1</sup>, Epshtein E.M.<sup>1</sup>, Gulyaev Yu.V.<sup>1</sup>, Malikov I.V.<sup>2</sup>, Mikhailov G.M.<sup>2</sup>, Panas A.I.<sup>1</sup>,  
Zilberman P.E.<sup>1</sup>

<sup>1</sup> Kotel'nikov FIRE RAS, 141190, Fryazino, Moscow District, RF.

<sup>2</sup> IPTM & HPM RAS, 142432, Chernogolovka, Moscow District RF.

Electromagnetic radiation of 1 – 10 THz range is observed at room temperature in a structure with a point contact between a ferromagnetic rod and a thin ferromagnetic film under electric current of high enough density. The radiation is due to nonequilibrium spin injection between the components of the structure. By estimates, the injection can lead to inverted population of the spin subbands. The radiation power exceeds by orders of magnitude the thermal background (with the Joule heating taking into account) and follows the current without inertia, as it may be seen from the picture. It is seen that the radiation tracks all the variations of the current, where  $W(t)$  is a power of THz radiation and  $I(t)$  is an electrical current through the point contact,  $t$  is a current time. The only smooth character of the radiation pulse fronts under abrupt jumps of the current and a small smooth "tail" near zero may be related with thermal effects. Such a suppression of the thermal radiation is due to very good thermal conductivity of our specimen. The spin-polarized current injects spin and disturbs spin equilibrium near the contact (see review [1]). According the estimates in Ref. [2], this can lead to inversion of the spin subband population. We show here that such an inversion really takes place in our structure under high currents because of opposite directions of the magnetic fluxes inside and outside the ferromagnetic rod.



Supported by grant RFBR #10-02-00030-a

[1] Yu.V.Gulyaev, P.E. Zilberman, A.I. Panas, E.M. Epshtein. *Physics-Uspekhi*, **52**, 335 (2009).

[2] Yu.V.Gulyaev, P.E. Zilberman, S.G. Chigarev, E.M. Epshtein. *JCTE*, **55**, 1132 (2010).

## THERMODYNAMIC EFFECTS OF THE SPIN ORDERING OF ELECTRONS IN HYBRIDIZED STATES ON THE IMPURITIES OF TRANSITION ELEMENTS

*Okulov V.I.<sup>1</sup>, Pamyatnykh E.A.<sup>2</sup>, Zabaznov Yu.V.<sup>2</sup>*

<sup>1</sup> Institute for Metal Physics UD RAS, Ekaterinburg, Russia

<sup>2</sup> Ural State University, Ekaterinburg, Russia

The present report shows the results of the theoretical study of the effects of manifesting the spontaneous spin polarization of electron hybridized donor d-states system in conduction band of a crystal. On the basis of the theory, developed in [1,2], we present the justification of the spin polarization phenomenon of the given type and give the description of temperature and concentration dependences of both spin splitting of electron energies and corresponding electron contributions to thermodynamic quantities (electron specific heat, elastic modulus, magnetic susceptibility), using the model of exchange Fermi-liquid interaction constants. In the framework of this model the spin splitting of the peaks of density of states, characterizing the localized component of hybridized states, is described by the constant  $\beta$ , which in the case of full polarization (one peak was filled only) proved to be equal

$$\beta = \psi n^i \quad (1)$$

Here  $\psi$  is the interaction constant and  $n^i$  is the concentration of localized component. Thereby the polarization of component  $\beta_c$ , characterizing homogeneous density (conduction electrons), takes also place and equal to:

$$\beta_c = (\psi_{ci}/\psi)\beta \quad (2)$$

Here  $\psi_{ci}$  is the interaction constant, characterizing the interaction of the components of free motion and localization of different states. Formulas (1) and (2) are valid, when the value of  $\beta$  exceeds the interval of hybridization. In the case of partial filling of spin splitting peaks the polarization is considered in [3]. Therefore we have shown that spontaneous spin polarization of electrons in hybridized states is accompanied by the polarization of conduction electrons in energy interval of hybridization. This result is of important significance as far as it gives a justified conclusion concerning the polarization of conducting electrons under the effect of direct interaction rather than indirect less effective interaction. We have considered specific low-temperature anomalies of thermodynamic properties due to hybridization of the states of polarized electrons. It was also shown that the fact of spin polarization can be established, in particular, from the temperature dependences, the form of which is essentially dependent on the interaction parameters.

This work was supported by the Russian Foundation for Basic Research (Grant no. 09-02-01389) and by the Program of the Physical Sciences Branch of RAS (Grant no. 09-2-T2-1037) and Russian-American Program BRHE.

[1] V.I. Okulov, *Phys.Met.Metallogr.*, **100** (2005) 23.

[2] V.I. Okulov, E.A. Pamyatnykh, V.P. Silin, *Fiz.Nizk.Temp.*, **35** (2009) 891.

[3] V.I. Okulov, E.A. Pamyatnykh, Yu.V. Zabaznov, *Solid St.Phenom.*, **168-169** (2011) 489.





Wednesday

**24 August**

17:30-19:00

poster session  
24PO-J1

**“Diluted Magnetic  
Semiconductors”**

24PO-J1-1

## THE PROPERTIES OF $\text{Si}_{1-x}\text{Mn}_x$ FILMS PRODUCED BY THE PULSED LASER DEPOSITION METHOD WITH DROPLET VELOCITY SEPARATION TECHNIQUE

*Rocheva V.V.<sup>1</sup>, Rylkov V.V.<sup>2,3</sup>, Nikolaev S.N.<sup>2</sup>, Khaydukov E.V.<sup>1</sup>, Khramova O.D.<sup>1</sup>, Perov N.S.<sup>4</sup>, Semisalova A.S.<sup>4</sup>, Aronzon B.A.<sup>2,3</sup>, Novodvorsky O.A.<sup>1</sup>, Panchenko V.Ya.<sup>1</sup>*

<sup>1</sup> Institute on Laser and Information Technologies of RAS, 140700 Shatura, Moscow Region, Russia

<sup>2</sup> National Research Centre, Kurchatov Institute, 123182 Moscow, Russia

<sup>3</sup> Institute for Theoretical and Applied Electromagnetics, 125412 Moscow, Russia

<sup>4</sup> Faculty of physics, M.V. Lomonosov MSU, 119991 Moscow, Russia

The results of structural and transport properties studies of 60 nm  $\text{Si}_{1-x}\text{Mn}_x$  films with various Mn ( $x = 0.33-0.5$ ) content are presented. The films are produced by the pulsed laser deposition method (PLD) with using of the deposited particles velocity separation [1]. The method [1] allows to avoid the hitting of the droplets on the growing film which presence is a primary factor of film quality loss in PLD. The deposition was carried out on  $\text{Al}_2\text{O}_3$  (0001) substrates at the 340 °C with the rate of 1.5 nm/min.

The atomic-force microscopy analysis of the films has shown their high quality – the surface roughness is about 1 nm.

It was revealed that the films demonstrate ferromagnetic properties in the anomalous Hall effect (AHE) at sufficiently high temperatures ( $T \geq 200$  K) and possess essentially nonmonotonic dependence of resistance on Mn content (Fig. 1). The  $R_{xx}$  film resistance initially falls and then grows at the Mn concentration increase, and the temperature behavior of  $R_{xx}$  changes its character from metal type to dielectric one. Under these conditions the AHE dramatically falls – more than 100 times for  $x = 0.5$  in comparison with  $x = 0.36$  and changes the sign (Fig. 1). The possible reasons of unusual behavior of the transport properties are discussed.

The work is partially supported by RFBR (grants 10-07-00492 and 11-07-00359).

[1] O.A. Novodvorsky, A.A. Lotin, E.V. Khaydukov, *Utility model RF patent 89906*, Published 20.12.2009, bulletin 35.

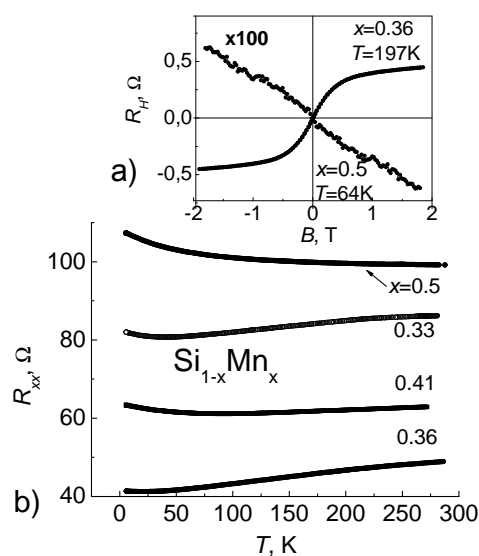


Fig. 1. a) Dependences of the Hall resistance on magnetic field for the samples with  $x = 0.36$  at  $T = 197$  K and  $x = 0.5$  at  $T = 64$  K ( $R_H$  is magnified 100 times). b) Temperature dependences of the resistance in  $\text{Si}_{1-x}\text{Mn}_x$  films.

24PO-J1-2

**MAGNETISM IN DILUTED MAGNETIC SEMICONDUCTING OXIDES***Lisboa-Filho P.<sup>1</sup>, Arruda L.B.<sup>1</sup>, Pereira A.L.J.<sup>1</sup>, Leite D.M.G.<sup>1</sup>, da Silva J.H.D.<sup>1</sup>, Ortiz W.A.<sup>2</sup>*<sup>1</sup> UNESP Univ Estadual Paulista, Faculdade de Ciências, Departamento de Física, Bauru, Brazil<sup>2</sup> UFSCar Universidade Federal de São Carlos, Departamento de Física, São Carlos, Brazil

The understanding and control of ferromagnetism in diluted magnetic semiconducting oxides (DMO) is a special challenge in solid state physics and materials science due to its impact on magneto-optical devices and spintronics. Several studies and mechanisms have been proposed to explain ferromagnetism in DMO compounds since the theoretical prediction of room-temperature ferromagnetism by Dietl and co-workers [1]. However, genuine and intrinsic ferromagnetism in 3d-transition metal-doped n-type ZnO and TiO<sub>2</sub> semiconductors is still a controversial issue [2, 3]. Today, major works correlate the observation of a ferromagnetic response to oxygen interstitials ( $I_O$ ), oxygen vacancies ( $V_O$ ) and/or zinc vacancies ( $V_{Zn}$ ) [4].

In this contribution, structural and magnetic properties of cobalt-ZnO and cobalt-TiO<sub>2</sub> nanostructures and manganese-TiO<sub>2</sub> thin films were investigated.

The ZnO:Co and TiO<sub>2</sub>:Co samples were prepared by varying cobalt molar concentration, ultrasonic exposure time and post-annealing heat-treatments parameters. The obtained results show that single phase powder samples can be obtained by the sonochemical method; however, cobalt nanoclusters can be detected depending on synthesis conditions. A careful study on the structural and morphological features of the prepared nanostructures was carried out revealing a surface amorphization and a possible induction of a zincblend phase due to the ultrasonic treatment. For sonochemically treated samples, although a paramagnetic response is always present, ferromagnetism could be detected even for non-doped samples.

Pure and Mn doped TiO<sub>2</sub> films were also grown by sputtering technique onto a-SiO<sub>2</sub> substrates. The prepared samples have predominant anatase crystal phase, however the increase of O<sub>2</sub> flow during film growth and the Mn incorporation favor the mix between anatase and rutile. Several magnetic measurements were carried out and even for the Mn doped-films a conclusive ferromagnetic signature was not observed.

Support by FAPESP and CNPq is acknowledged.

[1] T. Dietl, et al.; *Science* **287**, 1019 (2000)

[2] M. J. D. Coey et al.; *Nature Materials* **4**, 173 (2005)

[3] M. A. Garcia et al.; *JAP* **105**, 013925 (2009)

[4] Xu Zuo et al. ; *JAP* **105**, 07C508 (2009)

24PO-J1-3

## MAGNETIC LOCAL STRUCTURE OF $^{57}\text{Fe}$ PROBE ATOMS AND MAGNETIC PHASE TRANSITIONS IN $\text{RNiO}_3$

*Rusakov V.S.<sup>1</sup>, Presniakov I.A.<sup>1</sup>, Sobolev A.V.<sup>1</sup>, Demazeau G.<sup>2</sup>, Gapochka A.M.<sup>1</sup>,  
Gubaydulina T.V.<sup>1</sup>, Matsnev M.E.<sup>1</sup>, Lukyanova E.N.<sup>1</sup>*

<sup>1</sup> M.V. Lomonosov Moscow State University, Moscow, Russia

<sup>2</sup> Institut de la Chimie de la Matiere Condensee de Bordeaux, Bordeaux, France

$\text{RNiO}_3$  ( $R$  = rare-earth, Y) perovskites are being investigated with renewed interest in recent years due to their unusual electronic/magnetic properties. This family undergoes two transitions, an insulator-metal transition at  $T_{\text{IM}}$  and an antiferromagnetic ordering at  $T_{\text{N}}$  ( $T_{\text{N}} = T_{\text{IM}}$  for  $R = \text{Pr}$  and  $\text{Nd}$ , whereas  $T_{\text{N}} < T_{\text{IM}}$  for  $R = \text{Sm} \rightarrow \text{Lu}$ ).  $T_{\text{IM}}$  and  $T_{\text{N}}$  are systematically related with a variation of the Ni-O-Ni bond angle driven by the size of rare earth. Below  $T_{\text{N}}$ , for the large rare-earth nickelates the magnetic ordering was characterized by the propagation vector  $k = (1/2, 0, 1/2)$ . In this magnetic structure, each  $\text{Ni}^{3+}$  ion is coupled ferromagnetically to three nearest neighboring  $\text{Ni}^{3+}$  ions and antiferromagnetically to three remaining neighbors through the oxygen ions of the ( $\text{NiO}_6$ ) octahedra.

For the first time the nickelates  $\text{RNiO}_3$  ( $R$  = rare-earth) have been investigated by  $^{57}\text{Fe}$  probe Mössbauer spectroscopy. The results concerning the investigation of hyperfine interactions for  $^{57}\text{Fe}$  probe atoms above and below the magnetic ordering temperature ( $T_{\text{N}}$ ) are presented. The magnetic susceptibility measurements show that doped iron cations, stabilized in the lattice, lead to decreasing the magnetic ordering temperature ( $T_{\text{N}}$ ). Comparison of the ordering temperature found by magnetization measurements with a temperature dependence of magnetic hyperfine fields at  $^{57}\text{Fe}$  in  $\text{RNi}_{0.98}\text{Fe}_{0.02}\text{O}_3$  showed for  $R = \text{Pr}, \text{Nd}$  compounds a first-order magnetic phase transitions, while a second-order transition for  $R = \text{Sm} \rightarrow \text{Lu}$  compounds. At  $T \ll T_{\text{N}}$ , the  $^{57}\text{Fe}$  spectra are resolved into two magnetic sextets with considerably different magnetic hyperfine fields but with the same value of isomer shift. Such a particular magnetic environment of  $\text{Fe}^{3+}$  cations located in the same crystallographic sites has been attributed to the unusual magnetic ordering in  $\text{RNiO}_3$  caused by the presence of magnetic “frustrated bonds”. In the light of orbital ordering model suggested by the neutron diffraction studies, the partial substitution of  $\text{Ni}^{3+}(t_{2g}^6 e_g^1)$  by  $\text{Fe}^{3+}(t_{2g}^3 e_g^2)$  may induce significant topological frustration of  $\text{Fe}^{3+}$  spins in surroundings of  $\text{Ni}^{3+}$  orbitals, leading to two different magnetic environments around  $\text{Fe}^{3+}$  ions below  $T_{\text{N}}$ . The present results may be an evidence of the important role of the orbital ordering in determining the electronic properties of the Ni(III) perovskites.

24PO-J1-4

## EFFECTS OF IRON IMPLANTATION AND POST ANNEALING ON THE STRUCTURAL AND MAGNETIC PROPERTIES OF RUTILE ( $\text{TiO}_2$ )

*Vakhitov I.R.<sup>1</sup>, Dulov E.N.<sup>1</sup>, Lyadov N.M.<sup>2</sup>, Nuzhdin V.I.<sup>2</sup>, Khaibullin R.I.<sup>1,2</sup>, Tagirov L.R.<sup>1,2</sup>*

<sup>1</sup> Kazan (Volga region) Federal University, 420008, Kazan, Russian Federation

<sup>2</sup> Kazan Physical-Technical Institute, 420029, Kazan, Russian Federation

The work refers to the ion-beam synthesis and study of a new class of magnetic materials - diluted magnetic oxide semiconductors, which are promising for practical applications in spintronics and

magnetic optoelectronics. In the report we present the influence of iron implantation and subsequent thermal annealing on the modification of structural and physical properties of the wide-gap semiconductor rutile (TiO<sub>2</sub>).

Single crystalline (100)- and (001)- plates of TiO<sub>2</sub> were implanted with 40 keV Fe<sup>+</sup> ions to high dose of  $1.5 \times 10^{17}$  ion/cm<sup>2</sup>. Subsequent thermal annealing of the implanted samples was carried out either in vacuum ( $\sim 10^{-6}$  Torr) or in air at temperature in the range of 300-1200 K for 30 min. The elemental-phase composition and magnetic properties of the implanted rutile were investigated by scanning electron microscopy (SEM), depth-resolved conversion electron Mossbauer spectroscopy (CEMS), coil magnetometry and differential thermomagnetic analysis.

SEM and CEMS studies show that, the Fe concentration in the irradiated regions is about 30 at.%. Such high concentration of iron obviously should lead to the precipitation of impurities in the form of iron nanoparticles. Elemental microanalysis shows that there is only the implanted impurity of iron and host elements: titanium and oxygen with a reduced content of the latter. As a result of implantation, optical transparency of TiO<sub>2</sub> plates is significantly reduced due radiation damages. Subsequent thermal treatment leads to recovery of the crystalline structure of TiO<sub>2</sub>, as well to the coloring of the studied samples of rutile in various color tones depending on the environment and the temperature of annealing. The surface morphology of the samples is smooth, in general, without any new formations, both after implantation and after annealing. CEMS shows the presence of three iron-based phases in the implanted region: ferromagnetic  $\alpha$ - Fe phase, related to iron nanoparticles, and two paramagnetic phases of solid solutions - Fe<sup>2+</sup><sub>x</sub>Ti<sub>1-x</sub>O<sub>2- $\delta$</sub>  and Fe<sup>3+</sup><sub>x</sub>Ti<sub>1-x</sub>O<sub>2- $\delta$</sub> . There are significant changes in the magnetic phase composition with depth. Fe-implanted samples of TiO<sub>2</sub> reveal the ferromagnetism at room temperature with the shape anisotropy of “easy plane”, which is characteristic for thin magnetic films, as well as magneto-crystalline 2- and 4-fold anisotropy in the plane of (100)- and (001)-samples, respectively. The latter implies that ion-synthesized nanoparticles of Fe coherently embedded in the tetragonal structure of rutile. The magnetic anisotropy also decreases with increasing the temperature of annealing, and ferromagnetism disappears when the samples are annealed in air (T<sub>ann</sub> = 750° K) and vacuum (T<sub>ann</sub> = 900° K), due to oxidation of the iron nanoparticles.

Support by RFBI, grant No 10-02-01130, and Ministry of Education and Science of the Russian Federation, contract No P902, is acknowledged.

24PO-J1-5

## **STRUCTURAL AND MAGNETIC STUDIES OF ZINK OXIDE (ZnO) IMPLANTED WITH 3D TRANSITION IONS: Mn, Co, Fe and Ni.**

*Gumarov A.I.<sup>1</sup>, Lyadov N.M.<sup>2</sup>, Valeev V.F.<sup>2</sup>, Güler S.<sup>3</sup>, Rameev B.Z.<sup>2,3</sup>, Faizrakhmanov I.A.<sup>2</sup>,  
Khaibullin R.I.<sup>1,2</sup>, Tagirov L.R.<sup>1,2</sup>*

<sup>1</sup> Kazan (Volga Region) Federal University, 420008 Kazan, Russia

<sup>2</sup> Zavoisky Physical-Technical Institute, 420029 Kazan, Russia

<sup>3</sup> Gebze Institute of Technology, 41400 Gebze-Kocaeli, Turkey

Single-crystal (1120)- and (0001)-face oriented plates of ZnO were implanted with 40 keV Mn<sup>+</sup>, Co<sup>+</sup>, Fe<sup>+</sup> or Ni<sup>+</sup> ions to the dose of  $1.5 \times 10^{17}$  ions/cm<sup>2</sup> to create magnetic semiconductor nanomaterials. The influence of the chemical type of the 3d-dopant on the structural and magnetic properties of ZnO have been studied by using scanning electron microscopy (SEM), optical

spectroscopy in UV-visible light ranges, ferromagnetic resonance (FMR) and vibrating sample magnetometry.

In the case of  $Mn^{+}$  ion implantation of ZnO, the implanted samples showed paramagnetic behavior at room temperature. In contrast to the Mn-implanted samples, Co-implanted ZnO plates reveal room temperature ferromagnetism. Moreover we found strong influence of crystallographic orientation of ZnO plates on their magnetic anisotropy induced the  $Co^{+}$  ion implantation. We observed strong two-fold in-plane magnetic anisotropy in the Co-implanted (1120) ZnO (see fig.). Anisotropic ferromagnetism is

typical for ZnO only for the reason that we did not observe the evidences for magnetic anisotropy in corundum ( $Al_2O_3$ ) implanted with Co ions for the same crystallographic orientation of the surface and to same dose. Formation of anisotropic nanoparticles of cobalt in the irradiated region of ZnO may be responsible for this particular ferromagnetism. Alternatively, the Co-implanted (0001)-plates show isotropic in-plane ferromagnetism. In this case the ferromagnetism can be induced by magnetic  $Co^{2+}$  ions substituting zinc cations in structural position according to the optical data. Magnetic resonance studies of Co-implanted (0001) ZnO show both wide signals of FMR and narrow line of ESR related to  $Co^{2+}$  ions in the wurtzite structure of ZnO. Also room temperature ferromagnetism has been observed in both Fe- and Ni- implanted single-crystal ZnO plates. Our studies show that the main source of ferromagnetism in these samples is formation of the ferromagnetic Fe or Ni nanoparticles during the high dose implantation.

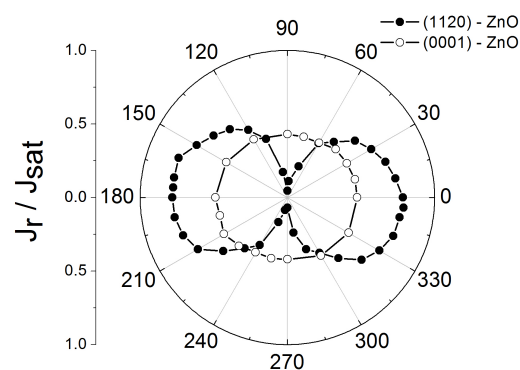


**Fig.** In-plane magnetic anisotropy in Co-implanted ZnO. Here  $J_r$  is remanence,  $J_s$  is saturation magnetization

Support by joint RFFI-TUBITAK Programme, grant №10-02-91225-CT\_a, and Ministry of Education and Science of the Russian Federation, contract No.P902, is acknowledged.

24PO-J1-6

## EPR STUDY OF OXYGEN VACANCIES ELECTROMIGRATION IN Ar-IMPLANTED RUTILE ( $TiO_2$ )

Zhiteytshev E.R.<sup>1</sup>, Bazarov V.V.<sup>1</sup>, Khaibullin R.I.<sup>1,2</sup>, Ulanov V.A.<sup>3</sup>, Azevedo A.M.<sup>4</sup>, Sobolev N.A.<sup>4</sup>

<sup>1</sup> E.K. Zavoisky Physical-Technical Institute of RAS, 420029 Kazan, Russia

<sup>2</sup> Solid State Physics Department, Kazan Federal University, 420008 Kazan, Russia

<sup>3</sup> Kazan State Power Engineering University, 420066 Kazan, Russia

<sup>4</sup> Departamento de Física and I3N, Universidade de Aveiro, 3810-193 Aveiro, Portugal

Titanium dioxide ( $TiO_2$ ) had attracted considerable attention due to potential applications in a variety of areas, viz., solar cells, photocatalysis, spintronics, etc. Recently it was shown that the reduced  $TiO_2$  samples reveal ferromagnetic properties at low temperatures. The observed ferromagnetism of the reduced  $TiO_2$  has been associated with spin polarization of electrons trapped by oxygen vacancies,  $O_v$  (so-called bounded magnetic polarons, an analogue of F-centers). However, the features of this phenomenon remain unclear up to now.

In this work we report electron paramagnetic resonance (EPR) studies of oxygen vacancies created in  $TiO_2$  by 40 keV  $Ar^{+}$  ion implantation to a high fluence of  $1.5 \times 10^{17}$  ion/cm<sup>2</sup>. First, it was established that high-energy argon implantation in the colorless plates of (001)-oriented single

crystalline rutile ( $\text{TiO}_2$ ) results in a blue color induced by high concentration of oxygen vacancies in the implanted region of the sample. Secondly, we developed original methods of oxygen vacancies migration under an applied DC electric field with the aim of changing the concentration of these point defects in the samples under study. Fast radiation-enhanced electromigration of oxygen vacancies became visually observable. Around the negative electrode, the initial blue color of the sample changed into the dark blue-grey one due to an increased density of oxygen vacancies, while the region around the positive electrode lost the coloration. Then the sample was divided in a dark and a light half for subsequent EPR studies. Angular dependences of the EPR spectra were taken in the X- and Q- microwave bands (9.5 GHz and 36.8 GHz, respectively) at different temperatures in the range from 4–300 K. Several types of EPR centers related to oxygen vacancies, trivalent titanium ions and  $\text{O}_V\text{-Ti}^{3+}$  defect complexes have been identified. Also we observed a strong redistribution of the EPR line intensities between the dark and light half of the sample. Thus, EPR showed that the concentrations of the oxygen vacancies or their complexes have different values in these sample parts in accordance with our visual observations. The EPR lines of oxygen vacancies vanish when the sample temperature rises above 30 K. We conclude that the EPR lines disappearance is a result of the oxygen vacancy recharging at  $T > 30$  K due to the transition of an electron trapped by the vacancy to the conduction band of rutile.

The work has been supported by RFBR through grant 10-02-01130-a, and by the Ministry of Education and Science of the Russian Federation through contract no. P902. A.M.A. acknowledges financial support by the University of Aveiro.

24PO-J1-7

### PECULIARITIES IN OPTICAL AND MAGNETO-OPTICAL SPECTRA OF THE GaMnSb LAYERS GROWN BY LASER ABLATION

*Gan'shina E.A.<sup>1</sup>, Golik L.L.<sup>2</sup>, Kovalev V.I.<sup>2</sup>, Kun'kova Z.E.<sup>2</sup>, Temiryazeva M.P.<sup>2</sup>, Danilov Yu.A.<sup>3</sup>, Vikhrova O.V.<sup>3</sup>, Zvonkov B.N.<sup>3</sup>, Novikov A.I.<sup>1</sup>, Vinogradov A.N.<sup>1</sup>*

<sup>1</sup> Department of Physics, Moscow State University, 119991 Moscow, Russia

<sup>2</sup> Institute of Radioengineering and Electronics, RAS, 141190 Fryazino, Russia

<sup>3</sup> Nizhny Novgorod State University, 603950 Nizhny Novgorod, Russia

In this work we present the results of researches of optical and magneto-optical properties of GaMnSb layers, deposited by pulse laser ablation on GaAs(001) substrates. Mn content in the layers was controlled by the sputtering time ratio of Mn and GaSb targets,  $Y_{Mn} = t_{Mn}/t_{Mn} + t_{GaSb}$ . For the layers under study  $Y_{Mn} = 0.06 - 0.5$ , temperature of the substrate during the growth  $T_g = 300$  or  $400^\circ\text{C}$  and thickness of the layers  $D \approx 100\text{-}200$  nm. Electrical properties of such GaMnSb layers were studied in [1]. These layers demonstrated the semiconducting character of the conductivity temperature dependence and the ferromagnetic behaviour at room temperature. Anomalous Hall effect was observed for a series of these layers.

Spectral ellipsometry ( $E = 1.25\text{-}3.5$  eV) and the transversal Kerr effect (TKE) ( $E = 0.5\text{-}4$  eV) were used to study the GaMnSb layers. We studied also surface topography and microscopic magnetic structure of the layers using atomic- and magnetic force microscopy (MFM). Spectra of the optical constants ( $n$ ,  $k$  and  $\varepsilon_1$ ,  $\varepsilon_2$ ) obtained from the ellipsometry spectra confirm a high crystal quality of several studied samples, but at the same time they testify to the presence of a metallic phase, which can arise during the growth of the layers. Observed transformation of the ellipsometry spectra

indicates an increase in a fraction of the metallic phase in the layers with increasing the  $Y_{\text{Mn}}$  value. All samples exhibit magnetic contrast, which is not correlated with the surface topography. At room temperature a strong resonant band is observed in the TKE spectra of the GaMnSb layers with low Mn content ( $Y_{\text{Mn}} = 0.06$  and  $0.09$ ) in the energy range  $E \approx 0.5-1.5$  eV. A number of weaker features is observed at the higher energies,  $E \geq 1.5$  eV. The peculiarities in the TKE spectra of the GaMnSb layers become sharper and more intensive under cooling, and their spectral shape is conserved. The ratio of intensities of the TKE bands in the low energy and high energy regions changes as the  $Y_{\text{Mn}}$  value increases. Earlier the analogous resonant band was observed at the similar energies in the TKE spectra of the GaAs:MnAs granular films [2] and InMnAs layers grown by the laser ablation [3]. In [3] it was shown that the resonant TKE band could be caused by excitation of surface plasmons in the MnAs nanoclusters embedded in the  $\text{In}_{1-x}\text{Mn}_x\text{As}$  host. In our opinion, the resonant band in the TKE spectra of the GaMnSb layers is due to excitation of the surface plasmons in MnSb nanoclusters, which arose during the growth of the layers. Nature of the features observed in the TKE spectra of the GaMnSb layers in the high energy range is also discussed. Possible causes of the transformation of the ellipsometry and TKE spectra of the studied GaMnSb layers with increasing  $Y_{\text{Mn}}$  are analyzed.

Support by the Program of the Presidium of RAS No. 27 is acknowledged.

- [1] Yu.A. Danilov, B.N. Zvonkov, A.V. Kudrin, et al., *Proceedings of the XV Intern. Symp. "Nanophysics and Nanoelectronics"*, **1** (2011) 129.  
 [2] H. Akinaga, M. Mizuguchi, T. Manago, et al., *J. Magn. Magn. Mat.*, **242-245** (2002) 470.  
 [3] E.A. Gan'shina, L.L. Golik, V.I. Kovalev, et al., *J. Phys.: Cond. Matter*, **22** (2010) 396002.

24PO-J1-8

## **MAGNETIZATION STEPS AND EXCHANGE COUPLING IN DILUTED MAGNETIC SEMICONDUCTORS**

*Isber S.*

Department of Physics, American University of Beirut, Bliss Street, P. O. Box 11-0236, Beirut, Lebanon.

Magnetization step (MS) spectroscopy of magnetic clusters is a powerful tool in understanding the basic phenomenon of exchange coupling between various magnetic moments in Diluted Magnetic Semiconductors (DMS). From MS positions of the external magnetic field, interesting information, like the strength of the exchange interaction between two paramagnetic ions, and the energy-level splittings of the paramagnetic ion due to crystal field, as well as the absolute signs of the spin-Hamiltonian parameters can be obtained. Magnetization measurements shows that the exchange coupling between  $\text{Eu}^{2+}$  ions in Tin (Sn) and lead (Pb) Chalcogenides IV-VI semiconductors is antiferromagnetic. The crystal field effect on the MS of magnetic clusters will be also discussed for these compounds.



24PO-J1-9

## SYNTHESIS OF FERROMAGNETIC $Mn_xGe_{1-x}$ PHASES BY INTERLAYER SOLID-STATE REACTIONS

Zhigalov V.S.<sup>1,2</sup>, Myagkov V.G.<sup>1</sup>, Bykova L.E.<sup>1</sup>, Matsynin A.A.<sup>1,2</sup>

<sup>1</sup> Kirensky Institute of Physics, Russian Academy of Sciences, Siberian Branch, Krasnoyarsk, 660036 Russia

<sup>2</sup> Reshetnev Siberian State Aerospace University, Krasnoyarsk, 660014 Russia

Nanomaterials with the structure 3d metal/semiconductor of  $Mn_xGe_{1-x}$  type have been widely discussed in the literature as promising candidates for spintronics applications. Spintronic materials should be proof against external factors, possess required magnetic properties, and be manufacturable.

In this study, conditions of the formation of  $Mn_xGe_{1-x}$  phases in Mn/Ge film bilayers upon thermal treatment are studied and the magnetic properties of the obtained materials are considered.

Figure 1 presents the dependence of saturation magnetization on annealing temperature. One can see that during synthesis, as a result of the interlayer solid-state reaction, two ferromagnetic phases are formed at temperatures of about 200 and 500°C. The features of the magnetization behavior with varying annealing temperature are related to the formation of certain  $Mn_xGe_{1-x}$  phases that arise at 200, 350, and 500 °C. To identify these phases, we used X-ray diffraction. Curie temperature of the first ferromagnetic phase is ~300°C. We suppose this phase is  $Mn_5Ge_3$  [1].

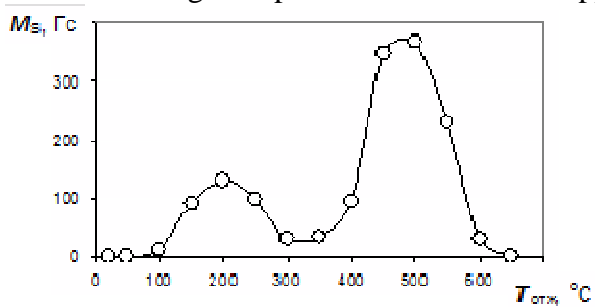


Fig. 1. Saturation magnetization of the Mn/Ge bilayer versus annealing temperature. MS values were taken at room temperature

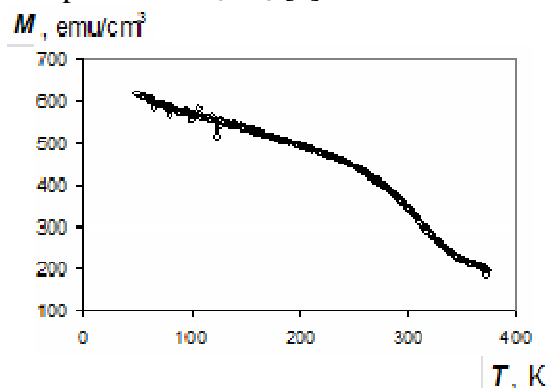


Fig. 2. Temperature dependence of saturation magnetization for the film annealed at 500°C

Figure 2 shows the temperature dependence of saturation magnetization of the second phase. It follows from this dependence that the sample is magnetically ordered at temperatures above room temperature. The estimated Curie temperature is  $T_C \sim 360$  K and the saturation magnetization at room temperature is  $\sim 360$  emu/cm<sup>3</sup>. The minimum Curie temperature of the sample exceeds the data on the Curie temperatures of the  $Mn_xGe_{1-x}$  samples reported in the literature [1].

This study was supported by the Departmental Target Program “Development of Scientific Potential of the Higher School” (2009--2011), project no.1.1/9193.

- [1] R.B. Morgunov and A.I. Dmitriev, *Russ. Khim. Zh.*, 2009, vol. LIII, no. 2, p. 36-45.  
 [2] V.S. Zhigalov, V.G. Myagkov, O.A. Bayukov et al., *Pis'ma Zh. Eksp. Teor. Fiz.*, 2009, vol. 89, no. 12, p. 725-729.  
 [3] V.G. Myagkov, V.S. Zhigalov, L.E. Bykova et al., *Pis'ma Zh. Eksp. Teor. Fiz.*, 2010, vol. 92, no. 10, p. 757-761.

24PO-J1-10

## INSULATOR-METAL TRANSITION IN DILUTED MAGNETIC SEMICONDUCTOR $\text{Pb}_{1-x-y}\text{Sn}_x\text{V}_y\text{Te}$ UNDER PRESSURE

*Skipetrov E.P.<sup>1</sup>, Golovanov A.N.<sup>1</sup>, Kovalev B.B.<sup>1</sup>, Skipetrova L.A.<sup>1</sup>, Mousalitin A.M.<sup>2</sup>, Slynko E.I.<sup>3</sup>, Slynko V.E.<sup>3</sup>*

<sup>1</sup> Faculty of Physics, Moscow State University, 119991 Moscow, Russia

<sup>2</sup> Moscow Institute of Steel and Alloys, 119049 Moscow, Russia

<sup>3</sup> Institute of Materials Science Problems, 58001 Chernovtsy, Ukraine

Doping of  $\text{A}^4\text{B}^6$  narrow-gap semiconductors with transition elements (Ti, V, Cr) induces appearance of deep impurity levels in the electronic structure and turns them into the diluted magnetic semiconductors (DMS) [1]. Substituting ions in the metal sublattice, impurities may exist in the crystal in the electrically neutral 2+ or electrically active 3+ states. In sufficiently doped samples the pinning of Fermi level by impurity level takes place. Impurity level (impurity band) is partially filled with electrons, density of states, occupied with electrons, corresponds to the concentration of 2+ impurity ions, while density of empty states – to the concentration of 3+ impurity ions. Thus magnetic properties of these DMS are determined not only by the total amount of magnetic impurities introduced, but also by concentrations and magnetic moments of impurity ions in the different charge states (by the energy position of the level relative to the band edges and occupancy of the level with electrons) [1,2]. There are two principal routes to govern these parameters of electronic structure: variation of the nonmagnetic matrix composition in the alloys ( $\text{Pb}_{1-x}\text{Sn}_x\text{Te}$ ,  $\text{Pb}_{1-x}\text{Ge}_x\text{Te}$  etc.) and application of external pressure.

In order to investigate the electronic structure rearrangement in  $\text{Pb}_{1-x}\text{Sn}_x\text{Te}$  alloys, doped with vanadium, under pressure in the present work the galvanomagnetic properties in weak magnetic fields ( $4.2 \leq T \leq 300$  K,  $B \leq 0.07$  T) as well as Shubnikov-de Haas effect ( $T=4.2$  K,  $B \leq 7$  T) in  $\text{Pb}_{1-x-y}\text{Sn}_x\text{V}_y\text{Te}$  ( $x=0.05-0.20$ ,  $y \leq 0.01$ ) under hydrostatic pressure  $P \leq 15$  kbar have been studied.

It is shown that increase of vanadium impurity content leads to the p-n-conversion and transition to the insulating phase due to the pinning of Fermi level by the donor-type deep vanadium impurity level, situated under the bottom of conduction band. Under pressure the decrease of activation energy of vanadium level, n-p-inversion of the conductivity type at low temperatures and insulator-metal transition are revealed. In the metallic phase sharp increase of the Hall mobility and appearance of Shubnikov-de Haas oscillations at helium temperature, indicating an increase of the free hole concentration under pressure, are observed.

Experimental results are explained assuming the linear shift of vanadium deep level down to the valence band, sequential intersection of the level with the middle of the gap and with the valence band top under pressure and opposite movement of the level with the increase of temperature at the fixed pressure. It is shown that under pressure deep vanadium level moves almost parallel to the conduction band bottom. Intersection of the level with the valence band top leads to the flowing of electrons from the valence band to the level, inducing insulator-metal transition, changing in the impurity band occupancy and in the magnetic properties of the investigated alloy. The pressure and temperature coefficients of vanadium deep level energy are determined and the diagram of the electronic structure rearrangement for  $\text{Pb}_{1-x-y}\text{Sn}_x\text{V}_y\text{Te}$  alloys under pressure is proposed.

This work was supported by RFBR (Grant No 11-02-01298).

[1] T. Story, E. Grodzicka, B. Witkowska et al., *Acta Phys. Polon. A*, **82** (1992) 879.

[2] E.P. Skipetrov, M.G. Mikheev, F.A. Pakpur et al., *Semiconductors*, **43** (2009) 297.

24PO-J1-11

## INFLUENCE OF MAGNETIC IMPURITIES ON FIGURE OF MERIT OF $\text{Bi}_2\text{Te}_3$ , $\text{Sb}_2\text{Te}_3$ AND $\text{Bi}_2\text{Se}_3$

*Kulbachinskii V., Kytin V., Kudryashov A., Tarasov P.*

Low Temperature Physics Department, Physics Faculty, M.V. Lomonosov Moscow State University, 119991 GSP-1, Moscow, Russia

Temperature dependence of Seebeck coefficient  $S$ , electrical conductivity, thermal conductivity and figure of merit of  $p\text{-Bi}_2\text{Te}_3$ ,  $\text{Sb}_2\text{Te}_3$  and  $n\text{-Bi}_2\text{Se}_3$  doped by Fe or Cr were carried out in the temperature interval  $7 < T < 300$  K. At  $T = 4.2$  K Shubnikov-de Haas and Hall effect have been measured. By increasing the Fe content, the hole concentration decreases in  $p\text{-Bi}_{2-x}\text{Fe}_x\text{Te}_3$ , while the electron concentration increases in  $n\text{-Bi}_{2-x}\text{Fe}_x\text{Se}_3$ . The same was observed in  $\text{Sb}_{2-x}\text{Cr}_x\text{Te}_3$ . This demonstrates that Fe or Cr act as donors.  $S$  increases in  $p\text{-Bi}_{2-x}\text{Fe}_x\text{Te}_3$  and  $\text{Sb}_{2-x}\text{Cr}_x\text{Te}_3$  with increasing Fe or Cr content, while it decreases in  $n\text{-Bi}_{2-x}\text{Fe}_x\text{Se}_3$ .

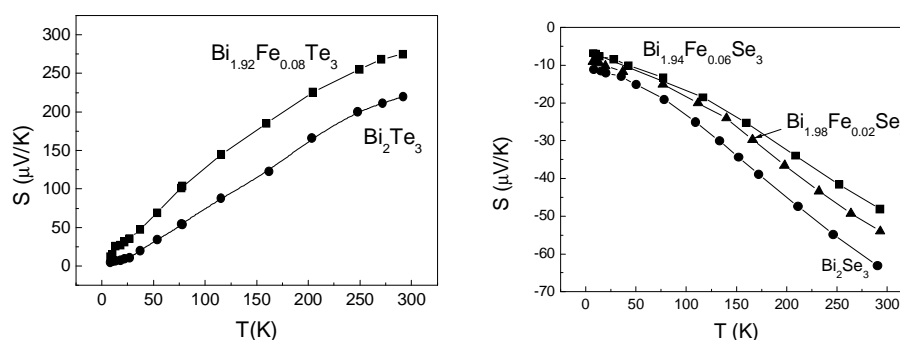


Fig.1 Temperature dependence of the thermopower  $S$  of  $p\text{-Bi}_{2-x}\text{Fe}_x\text{Te}_3$  and  $n\text{-Bi}_{2-x}\text{Fe}_x\text{Se}_3$ .

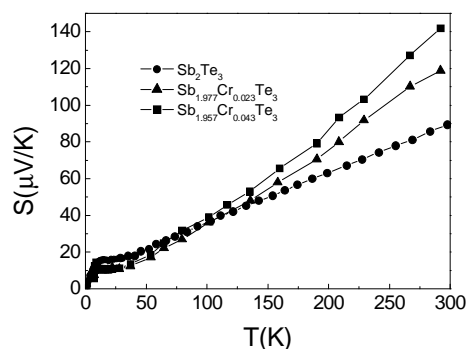


Fig.2 Temperature dependence of the thermopower  $S$  of  $\text{Sb}_{2-x}\text{Cr}_x\text{Te}_3$

In diluted magnetic semiconductors  $p\text{-Bi}_2\text{Te}_3$  and  $n\text{-Bi}_2\text{Se}_3$  concentrations of Fe with  $x \leq 0,08$  in the formula  $\text{Bi}_{2-x}\text{Fe}_x\text{Te}_3$  and  $x \leq 0,06$  in the formula  $\text{Bi}_{2-x}\text{Fe}_x\text{Se}_3$  have been achieved. In  $\text{Bi}_{2-x}\text{Fe}_x\text{Te}_3$  ferromagnetism was found with the Curie temperature,  $T_c$ , increasing as a function of  $x$  up to  $T_c = 12$  K for  $x = 0.08$  [1,2]. In  $n\text{-Bi}_{2-x}\text{Fe}_x\text{Se}_3$  samples ferromagnetism was not detected.

We have measured the thermoelectric power  $S$ , in the temperature range  $7\text{K} < T < 300\text{K}$ .  $S$  increases in  $\text{Bi}_{2-x}\text{Fe}_x\text{Te}_3$  due to Fe doping while  $S$  decreases in  $\text{Bi}_{2-x}\text{Fe}_x\text{Se}_3$  (fig. 1).

Figure of merit  $ZT$  decreases in  $\text{Bi}_{2-x}\text{Fe}_x\text{Te}_3$  due to Fe doping at  $7\text{K} < T < 300\text{K}$  while  $ZT$  decreases in  $\text{Bi}_{2-x}\text{Fe}_x\text{Se}_3$  at  $77\text{K} < T < 300\text{K}$  and increases at  $7\text{K} < T < 77\text{K}$ .

In  $\text{Sb}_{2-x}\text{Cr}_x\text{Te}_3$  a ferromagnetic phase has been revealed [3]. In fig. 2 we plot temperature dependence of  $S$  of  $\text{Sb}_{2-x}\text{Cr}_x\text{Te}_3$ . Thermal conductivity decreases in  $\text{Sb}_{2-x}\text{Cr}_x\text{Te}_3$  as compared with  $\text{Sb}_2\text{Te}_3$ . Figure of merit  $ZT$  decreases in  $\text{Sb}_{2-x}\text{Cr}_x\text{Te}_3$  due to Cr doping at  $7\text{K} < T < 140\text{K}$  while  $ZT$  increases in  $\text{Sb}_{2-x}\text{Cr}_x\text{Te}_3$  at  $140\text{K} < T < 300\text{K}$ .

[1] V.A. Kulbachinskii, A.Yu. Kaminskii, K. Kindo et al., JETP Lett., v.**73**, (2001) 352.

[2] V.A. Kulbachinskii, A.Yu. Kaminskii, K. Kindo et al., Phys. Lett. A, v.**285**, (2001) 173.

24PO-J1-12

## STRUCTURAL, ELECTRICAL AND MAGNETIC PROPERTIES OF InSb-MnSb EUTECTICS

*Kochura A.V.<sup>1,2</sup>, Lashkul A.<sup>2</sup>, Alam M.<sup>1</sup>, Shakhov M.S.<sup>2</sup>, Marenkin S.F.<sup>3</sup>, Fedorchenko I.V.<sup>3</sup>,  
Lahderanta E.<sup>2</sup>*

<sup>1</sup> South - West State University, Kursk, Russia

<sup>2</sup> Laboratory of Physics, Lappeenranta University of Technology, PO Box 20, FIN-53851,  
Lappeenranta, Finland

<sup>3</sup> Institute of General and Inorganic Chemistry of Russian Academy of Sciences, Moscow, Russia

A number of possibilities for spin manipulation are opened by the embedding of ferromagnetic materials with high Curie temperature ( $T_c$ ) to non-magnetic semiconductors. As high-temperature ferromagnetic compounds are using Mn-V compounds: MnAs ( $T_c=318$  K), MnSb ( $T_c=585$ K), MnP ( $T_c=290$  K). MnSb embedded to InMnSb matrix can improve applicable properties these material. For example, by occurring the magneto-optical effect, enhancing the coercivity and  $T_c$ , as it observed in a similar GaMnAs-MnAs system.

Magnetic wires are promising material for spintronics and its incorporating to diluted semiconductor matrix is perspective way for fabrication new two-phase magnetic systems. The example of such system is the directly solidified InSb-MnSb eutectic alloys, which shows anisotropic behavior if the inclusions consist of thin needles in parallel alignment. Among possibility growing of monocrystals with high carrier mobility advantage its systems is exhibition degrees of freedom associated with MnSb wires inherent shape anisotropy.

The directly solidified InSb-MnSb eutectic alloys were growth by the Bridgman-Stockbarger method. The composition of the crystals was studied with atomic absorption analysis, scanning electron (SEM) and atomic force (AFM) microscopy. For detection of possible minority phases x-ray powder diffraction (XRD) analysis was carried out. The XRD patterns of probes from center part of boule had only InSb and MnSb (NiAs-type) peaks and additionally a little traces of InMn<sub>3</sub> and Mn<sub>2</sub>Sb when probes was taken from edge of boule. By Laue pattern examination was determined the preferred crystallographic directions of InSb matrix [110] and MnSb rods [001] to growth direction. SEM and AFM investigations showed that needle inclusions were distributed uniformly with the longest side oriented along a growth axis. The mean diameter and the length of inclusions were  $2r = 12 \mu\text{m}$  and  $l > 1 \text{ mm}$ , respectively.

The temperature dependences of longitudinal resistivity  $\rho(T)$  for the InSb-MnSb eutectic were examined in the range 1.6 – 320 K. Metallic-like behavior is predominant for all direction of current to needles. Only at  $T < 20$  K for sample with transverse arrangement MnSb rods and current  $\rho(T)$  become semiconductor-like. With help of theory of two-phase systems consisting of cylindrical aligned in one direction rods, needles, or fibres embedded in continuous matrix, we divide conductivities in axial and transverse directions, which are in good agreement with conductivities of Mn-Sb alloys and InSb crystals.

The field dependences of magnetoresistance were investigated in pulsed magnetic field up to 25 T in the range 1.6 – 320 K. Maximal negative magnetoresistance was observed at  $T = 1.6$  K (-6%). At  $T < 10$  K magnetoresistance consist of a negative component prevailing up to 2 - 5 T, and an upturn with increasing magnetic field due to a classical positive contribution.

Temperature  $M(T)$  and field dependences of magnetization measured at magnetic field up to 50 kG in the range 3 – 600 K showed that samples were ferromagnetic with  $T_c \approx 600$  K and small coercivity. Strong influence of anisotropy on magnetic properties was observed at low ( $\sim 1$  kG) magnetic fields.

Support by RFBR (projects no. 11-02-00363, 10-03-00666) is acknowledged.

24PO-J1-13

## FMR STUDY OF MAGNETIC ANISOTROPY OF HIGH- $T_c$ MnSi FILMS

Kapelnitsky S.V.<sup>1,4</sup>, Drovosekov A.B.<sup>2</sup>, Semisalova A.S.<sup>3</sup>, Chuev M.A.<sup>4</sup>, Lomov A.A.<sup>4</sup>, Perov N.S.<sup>3</sup>,  
Lesnikov V.P.<sup>5</sup>, Podolskii V.V.<sup>5</sup>

<sup>1</sup> NRC "Kurchatov Institute", 123182 Moscow, Russia

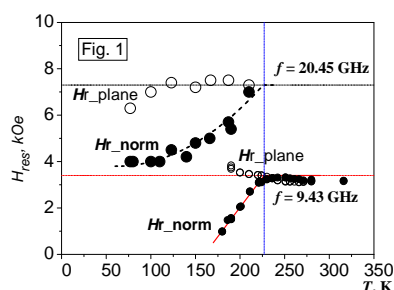
<sup>2</sup> Kapitza Institute for Physical Problems RAS, 119334 Moscow, Russia

<sup>3</sup> Faculty of physics, M.V. Lomonosov MSU, 119992 Moscow, Russia

<sup>4</sup> Institute of Physics and Technology RAS, 117218 Moscow, Russia

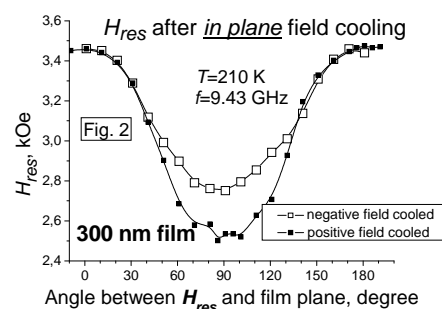
<sup>5</sup> Institute of Applied and Theoretical Electrodynamics RAS, 127412 Moscow, Russia

Ferromagnetic resonance (FMR) at 9.43 GHz and 20.45 GHz is used to study  $\text{Si}_{1-x}\text{Mn}_x$  ( $x \sim 0.35$ ) thin films prepared by laser plasma epitaxy on single crystal GaAs substrate at grow temperature 300 K. The thicknesses of layers under study were 300 nm and 80 nm. In the measurements at 9.43 GHz the first derivative of microwave absorption with respect to magnetic field was recorded, at 20.45 GHz an absorption signal was detected.



The Curie temperature,  $T_c$  determined from the FMR data is about  $T_c \approx 230$  K for the 300 nm film and  $T_c > 300$  K for 80 nm sample, which exceeds by an order of magnitude  $T_c$  for bulk disilicides. These results are in agreement with the results obtained by magneto-optical Kerr effect and the magnetization measurements. High  $T_c$  in thin films of similar composition were recently found in the investigation of the anomalous Hall effect [1].

In the 300 nm sample, the resonance field for the external field lying in the film plane ( $H_{r\_plane}$ ) was higher than that for the external field normal to film plane ( $H_{r\_norm}$ ) (Fig.1). Resonance field in the sample plane is isotropic. This evidences for the presence of a strong uniaxial magnetic anisotropy field with easy axis being normal to the 300 nm film plane, in contrast to the 80 nm film. The corresponding uniaxial anisotropy field for 300 nm film at 77 K comprises 1.7 kOe, that is much higher than demagnetizing field  $H_{dem} = 4\pi M_s \approx 400$  Oe. The angular dependence of resonance field for the 80 nm film indicates negligible net magnetic anisotropy field besides demagnetizing field of the layer. It was found for the 300 nm film that in-plane field cooling in the field 8 kOe leads to change in resonant field  $H_{r\_norm}$  i.e. in direction orthogonal to that of field in cooling, whereas in-plane resonance field  $H_{r\_plane}$  stay unchanged (Fig. 2). This can be related to the existence of antiferromagnetic or non-collinear magnetic clusters with exchange coupling to the ferromagnetic matrix.



The work is partially supported by RFBR (grants 10-07-00492, 10-07-00624, 10-02-01110).

[1] B.A. Aronzon, V.V. Rylkov, S.N. Nikolaev, V.V. Tugushev, *et al*, *Preprint Cond-Mat*. No1012.0715 (2010).

24PO-J1-14

## DISTRIBUTION OF Mn AND GALVANOMAGNETIC PROPERTIES FOR DELTA<Mn>-DOPED GaAs STRUCTURES

Danilov Yu.A.<sup>1</sup>, Drozdov M.N.<sup>2</sup>, Drozdov Yu.N.<sup>2</sup>, Dunaev V.S.<sup>3</sup>, Kudrin A.V.<sup>1</sup>, Vikhrova O.V.<sup>1</sup>, Zvonkov B.N.<sup>1</sup>

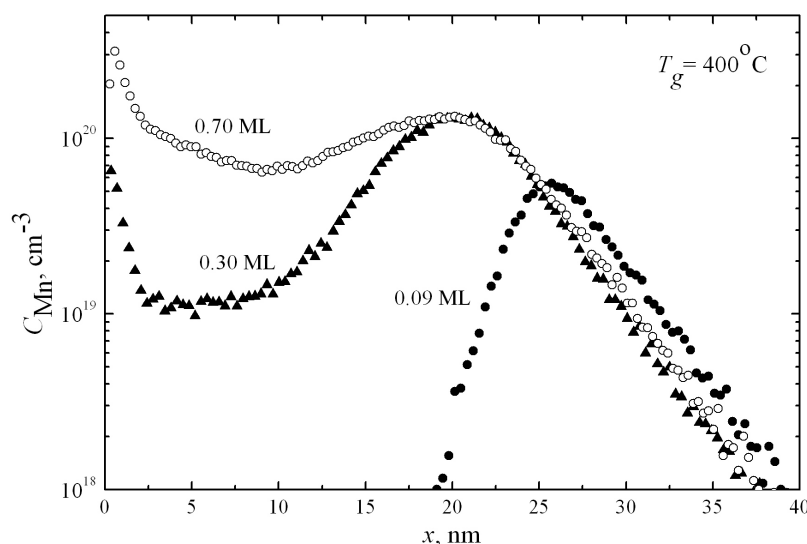
<sup>1</sup> Physico-Technical Research Institute of the Nizhny Novgorod State University, Nizhny Novgorod, Russia

<sup>2</sup> Institute for Physics of Microstructures, RAS, Nizhny Novgorod, Russia

<sup>3</sup> N.I. Lobachevsky State University of Nizhny Novgorod, Nizhny Novgorod, Russia

Delta-doped layers of Mn in GaAs are the subject of intensive studying of a number of research groups involved in the development of semiconductor spintronic devices. In this study, structures were grown by the combined method MOCVD and laser sputtering. A buffer layer of undoped GaAs was formed on a substrate SI-GaAs (001) at 600 - 650°C, then the substrate temperature was lowered to 350 - 450°C, and a delta-layer was formed by laser sputtering of metallic Mn in the flow of arsine. Content of Mn in the delta-layer ( $Q_{Mn}$ ) was controlled by the deposition time and determined in monolayer (ML) units. Then at the same low temperature a top layer with thickness of  $\approx 25$  nm was formed by laser sputtering of a GaAs wafer. The structures were investigated by elemental composition profiling with secondary ion mass spectrometry (TOF.SIMS-5). Galvanomagnetic properties (Hall effect and magnetoresistance) were studied in the temperature range of 10 - 300 K.

X-ray diffraction on similar structures containing InGaAs QW as below the delta-layer shown that the top layer is a monocrystalline GaAs. Figure shows the spatial distribution of Mn. Clearly, at the low  $Q_{Mn}$  values the depth distribution is almost symmetric with respect to position of the delta-layer ( $x_{Mn}$ ) in GaAs.



However, since the  $Q_{Mn} = 0.18$  ML, there is a significant redistribution of Mn atoms to the surface. After reaching a maximum at the  $Q_{Mn} = 0.30$  ML the concentration of Mn atoms at  $x_{Mn}$  almost unchanged, and an excess impurity segregates with growth front of the top layer GaAs. These results are in agreement with the data of Hall effect measurements. The all structures had  $p$ -type of conductivity. Galvanomagnetic measurements at low

temperatures shown anomalous Hall effect and negative magnetoresistance that it is an evidence of ferromagnetism in the structures with GaAs delta <Mn>-doped layer. At temperatures  $< 35$ K the Hall resistance dependences on magnetic field ( $R_H(H)$ ) were nonlinear without a hysteresis loop. The absence of the hysteresis on the  $R_H(H)$  dependences can be related to in-plane orientation of easy magnetization axis. Also, it was shown, that the segregated Mn atoms are in an electrically inactive state.

24PO-J1-15

## ANOMALOUS AND PLANAR HALL EFFECTS IN FERROMAGNETIC FILMS $\text{Si}_{1-x}\text{Mn}_x$ ( $x \approx 0.35$ )

*Semisalova A.S.<sup>1</sup>, Rylkov V.V.<sup>2,3</sup>, Aronzon B.A.<sup>2,3</sup>, Vasiliev A.L.<sup>2</sup>, Nikolaev S.N.<sup>2</sup>, Roddatis V.V.<sup>2</sup>,  
Granovsky A.B.<sup>1</sup>, Gan'shina E.A.<sup>1</sup>, Perov N.S.<sup>1</sup>, Lesnikov V.P.<sup>4</sup>, Podolskii V.V.<sup>4</sup>*

<sup>1</sup> Faculty of physics, M.V. Lomonosov MSU, 119991 Moscow, Russia

<sup>2</sup> NRC "Kurchatov Institute", 123182 Moscow, Russia

<sup>3</sup> Institute of Theoretical and Applied Electromagnetics RAS, 125412 Moscow, Russia

<sup>4</sup> Physicotechnical Research Institute of Lobachevsky SUNN, 603950 Nizhnii Novgorod, Russia

Based on Si or Ge diluted magnetic semiconductors are of primary interest for spintronics. Most efforts have been focused on the case when the volume fraction of embedded in Si magnetic or paramagnetic ions is quite small (<5-8%). In this case it is difficult to obtain strong ferromagnetism at room temperature and high level of spin polarization of current carriers. Recently, it has been shown that the anomalous Hall effect (AHE) resistivity for the case of thin films  $\text{Si}_{1-x}\text{Mn}_x$  with a high content of embedded Mn ions ( $x \approx 0.35$ ) is predominant up to room temperature and exhibits the considerable hysteresis up to  $\sim 230$  K [1,2]. It can be considered as the first evidence of possibility to obtain high spin polarization in Si:Mn in the vicinity of room temperature. The Hall effect measurements in [1,2] were carried out for thin films  $\text{Si}_{1-x}\text{Mn}_x$  ( $x \approx 0.35$ ) of small thickness (40-80 nm), therefore the influence of substrate due to interface and strain was noticeable. In this report, we present last results on structural, magnetic, magneto-optical and magnetotransport properties of more thick films, focusing on Hall effect behavior.

The films  $\text{Si}_{1-x}\text{Mn}_x$  ( $x \approx 0.35$ ) of thickness  $\approx 300$  nm were deposited from laser plasma on GaAs substrates at the growth temperature  $T_g = 300^\circ\text{C}$  (see for details [1,2]). Both magnetic and magneto-optical measurements confirm the long-range ferromagnetic order at relatively high temperatures  $T < T_C \approx 220$  K, exceeding the Curie temperature of  $\text{Mn}_4\text{Si}_7$  type silicides ( $\approx 50$  K). We observed also AHE in these samples. Surprisingly, the AHE resistivity was found to be opposite in sign and about 50 times smaller than that for the samples of thickness 80 nm, obtained at the same conditions on GaAs substrates. At the temperatures  $T \leq 10$  K being considerably smaller than Curie temperature of  $\text{Si}_{1-x}\text{Mn}_x$  alloy ( $T_C \approx 220$  K) we found the planar Hall effect with magnitude at least ten times greater than AHE.

These peculiarities of Hall effect can be caused by the presence in the samples various stable phases of  $\text{MnSi}_{2-y}$  disilicides with close to each other component content ( $y = 0.25-0.28$ ). The change of disilicide type during the film growth and the appearance of the antiferromagnetic inclusions of  $\text{Mn}_5\text{Si}_3$  type in the ferromagnetic matrix  $\text{MnSi}_{2-y}$  can result in the change of AHE sign and its self-compensation. At the same time, since the planar Hall effect is due to spontaneous anisotropy of magnetoresistance this phenomenon is not so much sensitive to the presence of various phases. The high-resolution electron microscopy data confirm the presence of  $\text{Mn}_5\text{Si}_3$  phase and small gradient of Mn concentration along the axis of films growth.

The work is partially supported by RFBR (grants 09-02-00309, 10-07-00492, and 10-07-00624) and RNP 2.1.1/2833.

[1] S.N. Nikolaev, B.A. Aronzon, V.V. Rylkov *et al.*, *JETP Letters*, **89**, (2009) 603.

[2] B.A. Aronzon, V.V. Rylkov, S.N. Nikolaev *et al.*, [arXiv:1012.1175v1](https://arxiv.org/abs/1012.1175v1) (2010).

24PO-J1-16

## EFFECT OF $\delta$ -<Mn>-LAYER'S MAGNETIZATION ON THE PHOTOLUMINESCENCE OF QUANTUM WELL IN InGaAs/GaAs HETEROSTRUCTURES

Talantsev A.<sup>1</sup>, Dmitriev A.<sup>1</sup>, Zaitsev S.<sup>2</sup>, Koplak O.<sup>3</sup>, Morgunov R.<sup>1</sup>

<sup>1</sup> IPCP RAS, Acad. Semenov av. 1, Chernogolovka, Russia

<sup>2</sup> ISSP RAS, Acad. Ossipyan st. 2, Chernogolovka, Russia

<sup>3</sup> Kyiv National University, Kiev, Ukraine

The influence of orientation of surfaces GaAs on magnetic properties, spin dynamics and photoluminescence of heterostructures with quantum well InGaAs/GaAs and  $\delta$ -<Mn>-layer was observed [1]. The temperature dependencies of magnetic momentum, ESR-spectra, and temperature dependencies of photo-luminescence polarization of quantum well for singular and vicinal heterostructures InGaAs/GaAs/ $\delta$ -<Mn> are qualitatively different (Fig.1).

In singular InGaAs/GaAs/ $\delta$ -<Mn> heterostructures temperature dependence of magnetization follows the Bloch's "3/2" law, as in ordered bulk ferromagnets.

In vicinal InGaAs/GaAs/ $\delta$ -<Mn> heterostructures temperature dependence of magnetization follows the predictions of percolation theory in disordered ferromagnets. Despite the fact that in the investigated heterostructures, carriers in the quantum well and paramagnetic manganese ions in the delta-manganese layer are separated from each other, temperature dependence of circular polarization  $P_C$  of photoluminescence for the singular and vicinal samples qualitatively follows the dependence of magnetic moment on the temperature. This means that magnetic field of  $\delta$ -<Mn>-layer induces spin polarization of charge carriers in quantum well.

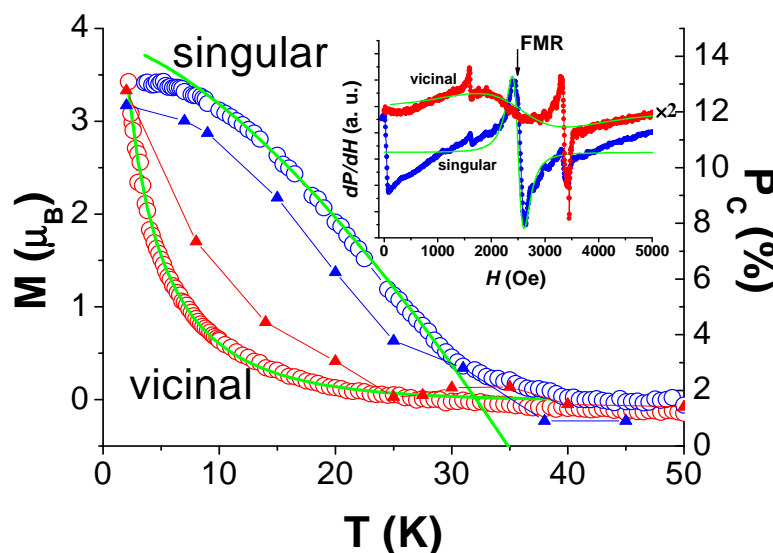


Fig. 1. Temperature dependencies of magnetization  $M$  of  $\delta$ -Mn-layer ( $\mu_B$  – Bohr's magneton) and circular polarization  $P_C$  of photoluminescence of quantum well in singular and vicinal samples. Open symbols mark temperature dependencies of magnetization  $M$  of singular and vicinal samples in magnetic field of 1 kOe (solid lines depict the approximation by Bloch law and percolation formula). Solid (triangular) symbols mark dependencies of the degree of circular polarization  $P_C$  in singular and vicinal samples on temperature in magnetic field of 2 kOe and 5 kOe, respectively (lines are guides for eyes). The inset depicts the electron spin resonance spectra of singular and vicinal samples at the temperature  $T = 4$  K. Line FMR corresponds to magnetic resonance in  $\delta$ -Mn-layer [2].

The work is supported by the Grant of the President of Russia MK-1764.2011.3.

[1] A.I. Dmitriev, A.D. Talantsev et al., *JETP*, **112** (2011) article in press.

[2] A.I. Dmitriev, R.B. Morgunov et al., *JETP*, **112** (2011) 317.



24PO-J1-17

## PERCOLATIVE METAL-INSULATOR TRANSITION IN MAGNETIC SEMICONDUCTORS

*Meilikhov E.Z., Farzetdinova R.M.*

Kurchatov Institute, 123182 Moscow, Russia

The role of large-scale fluctuations of the electric potential in traditional (non-magnetic) doped semiconductors is well known. Such a fluctuating potential appears usually in highly-compensated semiconductors where concentrations of charged impurities (donors and acceptors) are high and the concentration of screening mobile charge carriers is low, that results in a large screening length, defining the spatial scale of electric potential fluctuations. In that case, the average amplitude of the fluctuation potential is also high that leads to the localization of charge carriers and results in the activation character of the system conductivity: it is controlled by the thermal activation of charge carriers from the Fermi level to the percolation level and falls down exponentially with lowering temperature. In the absence of the impurity compensation, the charge carrier concentration is so high that any perturbations of the electro-static nature are effectively screened, and the spatial scale of the potential coincides with the extent of impurity density fluctuations. The depth of such a short-scale potential relief is relatively shallow and does not lead to the charge carrier localization - the conductivity keeps to be metal one.

In diluted (but nevertheless, highly-doped) magnetic semiconductors (of  $\text{Ga}_{1-x}\text{Mn}_x\text{As}$  type), in addition to above mentioned fluctuations of the electric potential, the new perturbation source appears - specifically, fluctuations of the “magnetic potential” concerned with fluctuations of the local magnetization in such a semiconductor. That potential is, in fact, the potential of the exchange interaction of mobile charge carriers with magnetic impurities (for instance, via the RKKY mechanism) which fluctuates in accordance with fluctuations of the concentration and the local magnetization of those impurities.

Within the “wells” of the magnetic potential, mobile charge carriers with a certain spin direction are accumulated while the carriers of the opposite spin direction are pushed out. The spatial scale of magnetic fluctuations is now determined not by the electrostatic screening but by the characteristic length of the magnetic interaction of impurities and the correlation length of their arrangement in the semiconductor bulk. However, in diluted magnetic semiconductors, there is usually  $l \sim l_s$  and, thus, spatial scales of the magnetic (exchange) and Coulomb potentials agree closely.

That means the constructive superposition of both reliefs, and so the average total amplitude of the potential relief becomes to be higher. The medium arises where the concentration and the spin polarization of charge carriers are strongly non-uniform, and the degree of that non-uniformity is substantially defined by the local magnetization of the system. Increasing magnetization with lowering temperature promotes strengthening the spatial localization of charge carriers and in a number of cases could stimulate the metal-insulator transition. Percolative metal conductivity, characteristic for non-uniform systems, changes into the conductivity of the activation type. That occurs when under some external factors (such as temperature, magnetic field, etc.) the Fermi level falls below the percolation level. One of possible mechanisms is as follows. The fluctuating potential leads to appearing the density of states tail into which both the percolation and Fermi levels are pulled. Rates of those levels' movement are different, and if they change the relative position the metal-insulator transition occurs.

It is just the model that is investigated in the present work.



Wednesday

**24 August**

17:30-19:00

poster session  
24PO-J2

**“Low Dimensional  
Magnetism”**

24PO-J2-1

**MAGNETOTHERMAL TRANSPORT IN SPIN-LADDER SYSTEMS***Shlagman O., Shimshoni E.*

Bar-Ilan University, Ramat-Gan 52900, Israel

We develop a theoretical model aimed to explain the results of a recent experiment on the spin-1/2 ladder compound (**BPCB**) [1] which measured a dramatic dependence of the thermal conductivity on a magnetic field  $B$  (Magnetothermal conductivity). The results show a double-minimum feature in the thermal conductivity isotherms, symmetric with respect to the field

$B_{middle} = \frac{B_{c1} + B_{c2}}{2}$  which corresponds to the center of the spinon-band in these systems [2]. Our

theory for the thermal transport accounts for the  $B$ -dependent coupling of spinons to lattice phonon modes. We employ a mapping of the ladder Hamiltonian in a strong magnetic field onto an XXZ spin-chain in a weak effective field ( $B_{eff} = B - B_{middle}$ ) and consequently to a Luttinger liquid of Jordan-Wigner Fermions at a chemical potential  $B_{eff}$ . The resulting Bosonized representation provides a low-energy theory for the spinon excitations and their coupling to the phonons. The latter gives rise to hybridization of spinons and phonons and the formation of new eigenmodes. Similarly to an earlier work on spin-chains [3], we show that the interplay of umklapp and disorder scattering dominates the relaxation of heat current, yielding magnetothermal effects consistent with the experimental observation.

[1] A. V. Sologubenko et. al., Phys Rev B. **80**, 220411@ (2009).

[2] R. Chitra and T. Giamarchi, Phys. rev. B **55**, 5816 (1997).

[3] E. Shimshoni, D. Rasch, P. Jung, A. V. Sologubenko and A. Rosch, Phys.rev. B **79**, 064406 (2009).

24PO-J2-2

**STUDY OF THE MAGNETIC STRUCTURE OF A TRIMER WITH A COULOMB INTERACTION AND A VARIABLE NUMBER OF ELECTRONS***Piskunova N.I.<sup>1,2,3,4</sup>, Aplesnin S.S.<sup>3,4</sup>*<sup>1</sup> Omsk State Agrarian University, Omsk, 644008<sup>2</sup> F.M. Dostoevsky State University, Omsk, 644077, Russia<sup>3</sup> M.F. Reshetnev Siberian Aerospace State University, Krasnoyarsk, 660014, Russia<sup>4</sup> L.V. Kirensky Institute of Physics, SB RAS, Krasnoyarsk, 660036, Russia*e-mail: apl@iph.krasn.ru, light\_mylife@mail.ru*

Intensive development of nanotechnologies allows clusters of arbitrary shapes and various sizes to be produced [1]. The development of modern nanotechnologies has stimulated interest in the noncollinear magnetism. Simultaneous consideration of collinear and multiparticle correlations is a complex and still not completely solved problem.

In this paper, we consider an isolated trimer (an triangular cluster [2]) that is located, for example, in a polymer matrix or in a colloidal solution and that is in equilibrium with its environment. Our goal is to investigate the electronic structure of a trimer and to establish the dependence of the chemical potential on the intersite Coulomb interaction and changes in hopping integrals for a variable number of particles [3].

We solve the above problems for three limiting cases in the Hubbard model [3]: the on-site Coulomb repulsion is less than ( $U < W$ ), approximately equal to ( $U \approx W$ ), and much greater than ( $U \gg W$ ) the conduction band width.

The eigenvalue spectrum and the corresponding state vectors by exact diagonalization, based on which we determined the trimer magnetization  $M = \sum_i^N (n_{i,\sigma} - n_{i,-\sigma})$  has been calculated [3]. At constant volume, the chemical potential is defined via the change in the system's energy,  $\mu = -\Delta E/\Delta n$ , when the number of particles changes from three to two.

During research for the trimer with the variable number of electrons the range of the intersite Coulomb interaction and an interval of the magnetic fields, changing energy level splitting near the chemical potential, by more than an order have been found. The removal of the magnetic degeneracy in the trimer under the influence of the intersite Coulomb interaction and the formation of a singlet pairs of electrons under trimer deformation have been established.

This work was supported by the Ministry of Education and Science of the Russian Federation as part of the "Development of the Scientific Potential of Higher School" Program (project nos. 2.1.1./401, 2.1.1/930) and the Russian Foundation for Basic Research (project nos. 09-02-00554-a, 09-02-92001-NNS-a, 10-02-00507, 10-02-00787, 11-02-90709-mob\_tr).

[1] C.P. Poole, Jr. and F. J. Owens, *Introduction to Nanotechnology* (Wiley, New York, 2003).

[2] *Frustrated Spin Systems*, Ed. by H. T. Diep (World Scientific, London, 2004).

[3] S.S. Aplesnin, N.I. Piskunova, *JETP*, **112** (2011) 127.

24PO-J2-3

## THERMODYNAMIC AND SPECTROSCOPIC STUDY OF QUASI-ONE-DIMENSIONAL MIXED-SPIN SYSTEM $(Y_{1-x}Nd_x)_2BaNiO_5$

*Popova E.A.<sup>1</sup>, Klimin S.A.<sup>2</sup>, Popova M.N.<sup>2</sup>, Tristan N.<sup>3</sup>, Klingeler R.<sup>3</sup>, Büchner B.<sup>3</sup>, Vasiliev A.N.<sup>4</sup>*

<sup>1</sup> Moscow State Institute of Electronics and Mathematics (Technical University),

109028 Moscow, Russia

<sup>2</sup> Institute of Spectroscopy, RAS, 142190 Troitsk, Moscow region, Russia

<sup>3</sup> Leibniz-Institute for Solid State and Materials Research IFW Dresden, 01171 Dresden, Germany

<sup>4</sup> Low Temperature Physics Department, Moscow State University, 119991 Moscow, Russia

The crystal structure (*Immm*) of the  $R_2BaNiO_5$  (R=rare earth or Y) compounds contains spin-S=1 chains composed by flattened  $NiO_6$  octahedra sharing their corners. The chains are interconnected through the  $R^{3+}$  and  $Ba^{2+}$  ions. While  $Y_2BaNiO_5$  is a typical Haldane gap system [1], members of the family  $R_2BaNiO_5$  containing magnetic  $R^{3+}$  ions order antiferromagnetically. The Neel temperature range from 12 K (R=Tm) to 61 K (R=Dy). In the series of compounds  $(Y_{1-x}Nd_x)_2BaNiO_5$   $T_N$  depends on  $x$ .

The magnetic properties of  $(Y_{1-x}Nd_x)_2BaNiO_5$  ( $x = 1, 0.25, 0.15, 0.05$ ) were studied by means of spectroscopic, magnetic susceptibility, and specific heat measurements in the temperature range

0.3–350 K. We have found three peculiarities in magnetic behavior of the compounds studied. First, the magnetic ordering is manifested by the  $\lambda$ -type anomaly in the temperature dependence of the specific heat  $C(T)$  and by the splitting of  $\text{Nd}^{3+}$  Kramers doublets,  $\Delta(T)$ , in the optical spectra. The Neel temperature decreases with decreasing concentration of neodymium and, for  $x=1$  and  $x=0.25$ , is in good agreement with the available neutron scattering data [2]. The observed  $\Delta(T)$  also decreases with decreasing  $x$ , which results in a reduced magnetic moment of the neodymium subsystem..

Second, the Schottky anomaly is present below  $T_N$  in the temperature dependence of both specific heat and magnetic susceptibility  $\chi(T)$ . It is caused by a temperature-driven population of the upper component of the split ground Kramers doublet of  $\text{Nd}^{3+}$ . The value of the splitting  $\Delta(T)$  found from the spectra was used to calculate contributions of the Nd subsystem into magnetic susceptibility and specific heat. To fit the experimental data, the Nd - Ni and Nd - Nd interactions had to be taken into account.

Third, an extra anomaly was observed in the  $\chi(T)$  and  $C(T)$  dependences at about 3 K in every compound. We tentatively assign this peculiarity to the presence of nickel-chain breaks. We give an estimate for the contribution from the triplet state originating from an extra spin of a chain segment split by internal and external magnetic fields.

We argue that the behavior of nickel subsystem differs from that of ordinary antiferromagnets. At high temperatures, while the contribution of the Nd subsystem into magnetic susceptibility follows the Curie-Weiss law, the Ni subsystem behaves like the Haldane-gap system, the contribution of which is independent of the concentration  $x$  (in contrast to the rare-earth subsystem).

Support of the RAS under the Programs for Basic Research is acknowledged.

[1] J. Darriet and L.P. Regnault, Solid State Commun. **86** (1993) 409.

[2] T. Yokoo, Z. Zheludev, M. Nakamura, and J. Akimitsu, Phys.Rev. B **55** (1997) 11516.

24PO-J2-4

## MAGNETIC INTERACTIONS IN DELAFOSSITES

*Korshunov A.S., Kudasov Yu.B., Maslov D.A., Pavlov V.N.*

Russian Federal Nuclear Center – VNIIEF, Mira str. 37, Sarov, 607188, Russia

SarFTI, National Research Nuclear University “MEPhI”, Dukhov str. 6, Sarov, 607188, Russia

The delafossite structure compounds provide good examples of antiferromagnets on a triangular lattice giving an evidence of the influence of geometrical frustration on these magnetic systems. These compounds are quasi two-dimensional and are highly frustrated between neighbouring triangular layers as well as within a layer. Delafossites demonstrate complex step-like magnetization curves at low temperatures in applied external magnetic field.

Among delafossites  $\text{CuFeO}_2$ , which is a naturally occurring mineral, was historically the first known compound of this type [1]. Its natural structure is characterized by the space group  $R3m$  formed by two-dimensional triangular lattice layers stacked rhombohedrally along the  $c$  axis [2]. Another compound discussed  $\text{AgFeO}_2$  has two polytypes of crystal structures, that is,  $R3m$  and  $P6_3/mmc$  [3].

In present work we have done *ab initio* magnetic structure calculation of the hexagonal polytype  $P6_3/mmc$  of  $\text{AgFeO}_2$  and a similar hypothetical structure for  $\text{CuFeO}_2$  to obtain magnetic interaction parameters. This trick makes it possible to simplify drastically the calculation of the magnetic

structure of  $\text{CuFeO}_2$ . The calculation reveals a significant interlayer antiferromagnetic interaction. We have shown that it can cause a collinear magnetic structure instead of the  $120^\circ$ -ordering anticipating for Heisenberg  $\text{Fe}^{3+}$  ions. The model including the strong interlayer interactions allows to describe the steps in the magnetization curves observed experimentally.

The work was supported by Russian Foundation for Basic Research (#10-02-00530-a) and Russian Federal Education Agency (AVCP # 2.1.1/7216).

[1] A. Pabst, *Amer. Mineral.*, **31** (1946) 539.

[2] O. A. Petrenko, G. Balakrishnan, M. R. Lees et. al., *Phys. Rev. B*, **62** (2000) 8983.

[3] A. Vasiliev, O. Volkova, I. Presniakov et. al., *J. Phys.: Condens. Matter*, **22** (2010) 016007.

24PO-J2-5

## CRYSTAL-FIELD LEVELS AND MAGNETIC ORDERING OF $\text{R}_2\text{BaNiO}_5$ (R=Ho, Dy, Sm)

*Galkin A.S.<sup>1</sup>, Klimin S.A.<sup>1</sup>, Popova M.N.<sup>1</sup>, Mill B.V.<sup>2</sup>*

<sup>1</sup> Institute of Spectroscopy RAS, Fizicheskaya 5, Troitsk 142190, Moscow region, Russia

<sup>2</sup> Moscow State University, Physics Department, 119899 Moscow, Russia

The family of the chain nickelates  $\text{R}_2\text{BaNiO}_5$  (with R = rare earth or Y) have attracted a considerable attention recently after observation of the Haldane gap in  $\text{Y}_2\text{BaNiO}_5$ . Nickelates with  $\text{R}^{3+}$  carrying non-zero magnetic moment are known to exhibit a 3D magnetic ordering. Nevertheless, the Haldane gap, being an intrinsic property of one-dimensional system composed of magnetic ions with integer-value spins, survives in nickelates even in the three-dimensional magnetically ordered state [1]. Besides, in  $\text{Ho}_2\text{BaNiO}_5$  the magnetoelectric effect has recently been found [2]. To get a deeper insight into this interesting model system, we have undertaken a detailed optical study of the crystal-field (CF) levels and magnetic ordering in  $\text{R}_2\text{BaNiO}_5$  (R=Ho, Dy, Sm).

In this work, we have measured transmittance spectra of the polycrystalline samples  $\text{R}_2\text{BaNiO}_5$  (R=Ho, Dy, Sm) in a broad range of frequencies ( $2000\text{-}20000\text{ cm}^{-1}$ ) and temperatures ( $4.2\text{-}300\text{K}$ ) using Fourier-transform spectrometers BOMEM DA3.002 and BRUKER IFS 125HR. Positions of  $\text{Dy}^{3+}$ ,  $\text{Ho}^{3+}$ ,  $\text{Sm}^{3+}$  CF levels have been determined. It is shown that the ground CF levels are responsible for the peculiarities in the temperature dependences of magnetic susceptibility and heat capacity. Magnetic ordering is investigated on the basis of the temperature dependence of the positions of  $\text{Dy}^{3+}$ ,  $\text{Ho}^{3+}$ ,  $\text{Sm}^{3+}$  CF levels. Unusually large shifts of spectral lines observed at the magnetic ordering are, probably, associated with magnetoelastic and magnetoelectric interactions leading to changes of the crystal field.

This work was supported by the Russian Academy of Sciences under the Programs for Basic Research.

[1] A. Zheludev, J.M. Tranquada, T. Vogt, and D.J. Buttrey, *Phys. Rev. B* **54** (1996) 7210.

[2] G. Néner and T. T. Palstra, *Phys. Rev. B* **76** (2007) 024415.

24PO-J2-6

## MAGNETIC PROPERTIES OF THE ANTIFERROMAGNETIC SPIN-1/2 CHAIN SYSTEM $\beta$ -TeVO<sub>4</sub>

*Savina Yu.<sup>1</sup>, Bludov O.<sup>1</sup>, Pashchenko V.<sup>1</sup>, Gnatchenko S.<sup>1</sup>, Lemmens P.<sup>2</sup>, Berger H.<sup>3</sup>*

<sup>1</sup> B.I. Verkin Institute for Low Temperature Physics and Engineering, NASU,  
61103 Kharkov, Ukraine

<sup>2</sup> Institute for Condensed Matter Physics, TU Braunschweig, D-38106 Braunschweig, Germany

<sup>3</sup> Inst. Phys. Mat. Complexe, EPFL, CH-1015 Lausanne, Switzerland

Vanadium oxides with the V<sup>4+</sup> ions ( $S = 1/2$ ) are excellent model systems for one-dimensional spin-1/2 quantum magnets. In this work the magnetic properties of the new one-dimensional compound  $\beta$ -TeVO<sub>4</sub> were investigated in the temperature range 1.9 – 400 K and magnetic fields up to 5 T using a Quantum Design SQUID magnetometer MPMS-XL5. The crystal structure of  $\beta$ -TeVO<sub>4</sub> consists of zigzag chains parallel to the  $c$ -axis formed by slightly distorted square pyramids VO<sub>5</sub> sharing corners. In compounds built up of the corner-sharing topology, the nearest-neighbor exchange coupling may be more than an order of magnitude smaller than for edge-sharing case and an important role of the next-nearest neighbor interactions take place.

Magnetic data shows an axial anisotropy of magnetic properties respect to the  $b$ -axis, which is due to a small anisotropy of the  $g$ -tensor for the V<sup>4+</sup> ions. Magnetic susceptibility shows the presence of a broad crossover at  $T^* = 130$  K, which indicates a changing of effective exchange interactions character: above 130 K – weak ferromagnetic (FM) and below 130 K – the predominant antiferromagnetic (AF) correlations. In low-temperature range ( $T < 5$  K) the observed three features at  $T = 2.28, 3.28, 4.65$  K can be interpreted as a phase transitions for the studied system: a long-range-ordered AF state at  $T_N = 4.65$  K and the further modifications of AF ordered phase (2.28; 3.28 K). Similar series of few phase transitions were observed for quasi-one-dimensional helicoidal magnetic compounds [1].

A fit of the magnetic susceptibility in the frame of few low-dimensional spin-1/2 models was performed. The best qualitative agreement with the experiment in the wide temperature range ( $5 < T < 400$  K) was obtained for an AF uniform exchange coupling model with the intrachain AF coupling constant  $J/k_B = 21.4 \pm 0.2$  K. The estimated values of other exchange integrals (AF or FM nature) don't exceed a few Kelvin.

[1] L. Capogna, M. Mayr, P. Horsch, M. Raichle, R.K. Kremer, M. Sofin, A. Maljuk, M. Jansen and B. Keimer, Phys. Rev. B **71**, 140402R (2005).



**CHARGE CARRIERS LOCALIZATION AT  $T \approx 210$  K  
AND FIRST ORDER PHASE TRANSITION AT  $T \approx 30$  K  
IN  $\alpha'$ -(BEDT-TTF)<sub>2</sub>IBr<sub>2</sub> MONOCRYSTALS DETECTED BY ESR**

*Chernenkaya A.<sup>1</sup>, Morgunov R.<sup>1</sup>, Dmitriev A.<sup>1</sup>, Kirman M.<sup>1</sup>, Tanimoto Y.<sup>2</sup>*

<sup>1</sup> IPCP RAS, Acad. Semenov av. 1, Chernogolovka, Russia

<sup>2</sup> Faculty of Pharmacy, Osaka- Ohtani University, Tondabayashi 584-8540, Japan

BEDT-TTF (bis(ethylenedithio) tetrathiafulvalene) based organic metals undergo promising physical properties such as Wigner-crystallization, superconductivity, photo-induced phase transition, and non-linear optical harmonics. The layered structure of these compounds provides a strong anisotropy of electrical conductivity of  $\alpha'$ -(BEDT-TTF)<sub>2</sub>IBr<sub>2</sub> crystals. Several transition temperatures were detected in  $\alpha'$ -(BEDT-TTF)<sub>2</sub>IBr<sub>2</sub> crystals. Localization of charge carriers (holes) was observed at  $T < 210$  K. This process is not accompanied by changes in crystal lattice parameters [1,2]. One more jump-like transition was observed in these crystals at  $T \approx 30$  K [3,4].

In  $\alpha'$ -(BEDT-TTF)<sub>2</sub>IBr<sub>2</sub> single crystals, charge ordering was observed near 208 K. It was accompanied sharp changes of the temperature dependencies of ESR parameters: integral intensity (magnetic susceptibility), g-factor and linewidth  $\Delta H$ . In  $\alpha'$ -(BEDT-TTF)<sub>2</sub>IBr<sub>2</sub> single crystals, localization of charge carriers occurs in regular positions of the unit cell. In  $\alpha'$ -(BEDT-TTF)<sub>2</sub>IBr<sub>2</sub> single crystals, exchange narrowing of the ESR lines and sharp decrease of static and dynamic magnetic susceptibilities were observed at low temperatures ( $T < 50$  K). The difference between static and dynamic magnetic susceptibilities appears in  $\alpha'$ -(BEDT-TTF)<sub>2</sub>IBr<sub>2</sub> single crystals at high temperatures ( $T > 50$  K). This difference is due to the frequency of thermally activated hopping of charge carriers is higher than the frequency of microwave field in the ESR spectrometer.

For studying  $\alpha'$ -(BEDT-TTF)<sub>2</sub>IBr<sub>2</sub> single crystals at low temperatures <sup>12</sup>C, <sup>13</sup>C and D isotopes enriched samples were used. It was found that all types of samples show temperature hysteresis of ESR line-widths, g-factors and integral magnetic susceptibility at temperature  $T \approx 30$  K. Low-temperature and low-temperature phases were found to be disappeared and appeared at different temperatures depending on cooling or heating conditions. The calculation of number of spins per cell shows: a high-temperature phase (at  $T = 290$  K) 1 spin is for  $0.7 \pm 0.4$  unit cells and in low-temperature phase (at  $T = 12$  K) 1 spin is for  $1.42 \pm 0.5 \cdot 10^8$  cells.

First order phase transition occurs in  $\alpha'$ -(BEDT-TTF)<sub>2</sub>IBr<sub>2</sub> of all types of samples. High-temperature phase and low-temperature phase give different ESR signals. The thermal prehistory and the defect formation during thermal cycling effect the temperature hysteresis in  $\alpha'$ -(BEDT-TTF)<sub>2</sub>IBr<sub>2</sub>. These factors are stronger than the isotopic substitution.

[1] R. Morgunov, A. Dmitriev, A. Chernenkaya, K. Yamamoto, K. Yakushi, Y. Tanimoto. *Physica B* 405, 138 (2010).

[2] Morgunov R., Dmitriev A., Chernenkaya A., Yamamoto K., Yakushi K., Tanimoto Y. *JETP*, 111, 5, 857 (2010).

[3] Y. Yue, K. Yamamoto, C. Nakano, M. Uruichi, K. Yakushi, M. Inokuchi, T. Hiejima and A. Kawamoto. *Physica B* 405, 11, 232 (2010).

[4] M. Kirman, A. Dmitriev, A. Chernenkaya, R. Morgunov. *Fiz. Tverd. Tela* 53, 6, 1203 (2011) [Solid State Physics].

## EFFECT OF THE BOND DISORDER ON THE MAGNETIC EXCITATIONS OF THE SPIN-GAP MAGNET PHCC.

Skoblin G.M.<sup>1,2</sup>, Glazkov V.N.<sup>2</sup>, Hiiivonen D.<sup>3</sup>, Yankova T.S.<sup>4</sup>, Zheludev A.<sup>3</sup>

<sup>1</sup> Moscow Institute of Physics and Technology, 141700 Dolgoprudny, Russia

<sup>2</sup> Kapitza Institute for Physical Problems RAS, 119334 Moscow, Russia

<sup>3</sup> Department of Solid State Physics, ETH Zurich, Switzerland

<sup>4</sup> M.V.Lomonosov Moscow State University, Moscow, Russia

Quantum magnets with site or bond disorder are considered as possible candidates for the formation of new Bose-glass phase [1]. Recently studied spin gap magnet PHCC ((C<sub>4</sub>H<sub>12</sub>N<sub>2</sub>)(Cu<sub>2</sub>Cl<sub>6</sub>)) [2] is a prominent candidate for the test of this hypothesis, since it allows to grow bromine-substituted single crystals with Br concentration up to 10%.

Electron spin resonance technique was used to study magnetic excitations of the pure and Br-doped PHCC (Br concentration  $x=5\%$  and  $10\%$ ). Orientation and frequency dependences of the resonance absorption were studied for these samples at different temperatures. Doping leads to the broadening of the resonance lines, since the bond-disorder shortens excitations lifetime. However, the intensity of absorption decreases with decreasing temperature for all samples, indicating that the spin gap state survives even at highest doping level. At high temperatures (10 K) we observe single resonance absorption line, which can be described by certain effective g-factor. We have found, that the g-factor value decreases with doping (Figures 1,2). Observed g-factor renormalization provides possible clue to the increase of critical field with doping, as observed in magnetization measurements. At low temperatures (1.8-3 K) the resonance absorption is split into several components due to the effects of anisotropic interactions. (Figure 2). This splitting is also concentration dependent: the doping level affects both amplitude of the splitting and its angular dependence. Our findings show the complicated interplay of disorder and anisotropic interactions in the spin-gap systems.

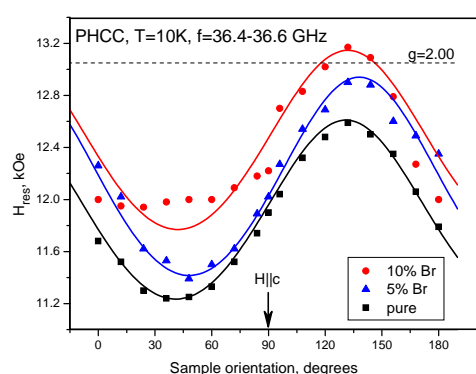


**Figure 1.** Angular dependences of resonance fields for different samples. Symbols – experiment, curves –guide to the eye.

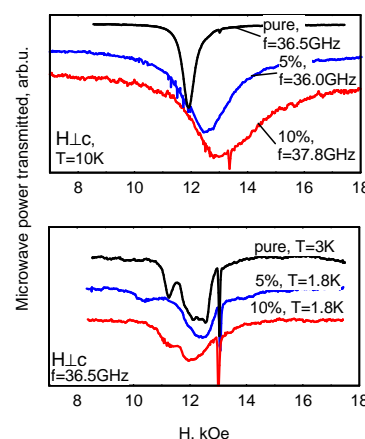


**Figure 2.** Comparison of the ESR absorption spectra at 10K (top) and at 1.8...3K (bottom). Narrow sharp line is a DPPH marker ( $g=2.00$ ).

Authors acknowledge support from Russian Foundation for Basic Research.

[1] O. Nohadani, S. Wessel and S. Haas, Phys.Rev.Letters **95**, 227201 (2005).

[2] M.B. Stone, C. Broholm, D.H. Reich et al., New Journal of Physics **9**, 31 (2007).

## DETERMINISTIC AND NON-DETERMINISTIC SWITCHING IN CHAINS OF MAGNETIC HYSTERONS

Tanasa R., Stancu A.

Faculty of Physics, Alexandru Ioan Cuza University, 700506, Iasi, Romania

The recent years were characterized by an important scientific and technological effort to design and manipulate nanostructures [1] in several fields of physics and materials science. Many factors have contributed to these evolutions, but maybe the most important one is represented by the advance in production and preparation techniques. Now, one could easily produce magnetic structures with controlled geometry [2,3], with nearly zero dispersion in their magnetic properties, i.e. almost identical particles. The question of paramount importance is related to the magnetic response of such a system that follows the linear response theory, or new features appear due to long range effect of magnetic interaction field.

In this paper we are addressing this problem starting from a very simple structure that is a one dimensional chain of magnetic elements, evenly distributed at distance " $d$ " along the network, while their intrinsic anisotropy axis is perpendicular to the chain. The equilibrium configuration is obtained with a standard Monte Carlo algorithm at zero Kelvin. Also, the magnetic field created by all elements in the system, i.e. interaction field, was calculated with a Fast Fourier Transform (FFT) technique. We have evaluated Major Hysteresis Loops (MHL) while lattice constant " $d$ ", was systematically modified. From Fig.1, it is clear that under the influence of the interaction fields several magnetic entities within the chain switch at positive external magnetic field. Another feature is the stability plateaus that spans over positive and negative magnetic fields. Such a behaviour is a clear fingerprint of a novel mechanism that could not be integrated in the nucleation and growth processes family.

In our simulations, we considered distance variation in steps of 0.1 % of unity length and external field resolution of 0.03%. A statistical analysis was necessary to extract the relevant data from more than one thousand individual runs. In Fig. 2, we are showing the switching field and plateaus length for distances varied from  $d=0.8$  up to  $d=2$ . We are observing that when " $d$ " increases, the plateaus length decreases while the switching field collapses to the coercitivity field ( $H_c=-1$ ).

In the full paper, we shall provide a explanation of these MHLs starting from an analytical evaluation of the interaction field function of neighborhood number, and we shall present, using a phase diagram chart, the periodical behavior these systems prefers.

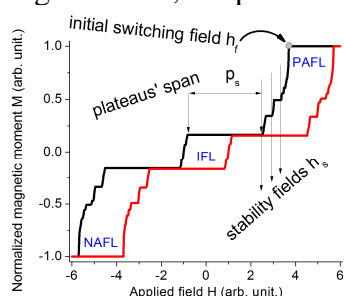


Fig. 1

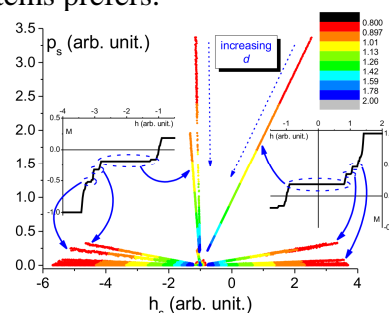


Fig. 2

Support by Romanian CNCSIS-CORELSYS 294 is acknowledged.

[1] J.J. Rehr, *Nature* **440** (2006) 618.

[2] S. Jain, A.O. Adeyeye, N. Singh, *Nanotechnology* **21** (2010) 285702.

[3] R.F. Wang, C. Nisoli, R.S. Freitas, J. Li, W. McConville, B.J. Cooley, M.S. Lund, N. Samarth, C. Leighton, V. H. Crespi, P. Schiffer, *Nature* **439** (2006) 303.

## ESR IN NEW SPIN DIMER SYSTEM $\text{Ba}_3\text{Cr}_2\text{O}_8$

Gavrilova T.P.<sup>1</sup>, Eremina R.M.<sup>1</sup>, Deisenhofer J.<sup>2</sup>, Loidl A.<sup>2</sup>

<sup>1</sup> Zavoisky Physical -Technical Institute, 420029, Sibirsky tract, 10/7, Kazan Russia

<sup>2</sup> Institute for Physics, Augsburg University, D-86135 Augsburg, Germany

The dimerization of a magnetic  $S=1/2$  system, namely the formation of a spin-singlet ground state at low temperature with opening of a gap ( $\Delta$ ) in the excitation spectrum, has been observed to date in a variety of inorganic crystals. In the limit of weak interdimer interactions, the problem maps exactly into the physics of Bose-Einstein Condensates (BEC), as explained in a recent review [1] and references therein. Upon application of an external magnetic field above a critical value ( $H_c$ ), one can excite triplons into the network of  $S=0$  dimers, a direct analogy to increasing the density of Bosons in a condensate, here tunable by the strength of the magnetic field.

Very recently, a new family of dimerized antiferromagnet, namely  $\text{A}_3\text{M}_2\text{O}_8$  ( $A = \text{Ba}, \text{Sr}$ ,  $M = \text{Mn}, \text{Cr}$ ), has shown Bose-Einstein condensation of magnons ( $H_c = 12.5$  Tesla for  $\text{Ba}_3\text{Cr}_2\text{O}_8$  [2]). The systems also uniquely show the presence of dimerized  $\text{MO}_4^{3-}$  tetrahedra with an M ion in the unusual  $5+$  oxidation state and the presence of competing exchange interactions, since the dimers are arranged in a triangular lattice presenting a high degree of geometrical frustration. The fitting of the temperature dependence of the magnetic susceptibility in  $\text{Ba}_3\text{Cr}_2\text{O}_8$  by modified Bleaney-Bowers equation with interdimer interactions confirmed the formation of a spin-singlet ground state at low temperature and allowed to determine the intradimer isotropic exchange interaction  $J^{\text{is}} = 27.3$  K [3].

All these interesting facts stimulated our study of  $\text{Ba}_3\text{Cr}_2\text{O}_8$  single crystals by the ESR method. ESR measurements were performed at X-band (9.47 GHz) frequency in the temperature range

$4.2 < T < 300$  K. The ESR spectrum consists of one Lorentzian-shaped line with  $g \sim 2$ . The experimental angular dependencies of ESR linewidths in two different planes are presented in Fig.1. Black curves correspond to the theoretical calculations. It was necessary to take into consideration the intradimer symmetric and antisymmetric anisotropic exchange interaction to fit the experimental data. The presence of DM interaction was confirmed also by high-frequency ESR measurement [4].

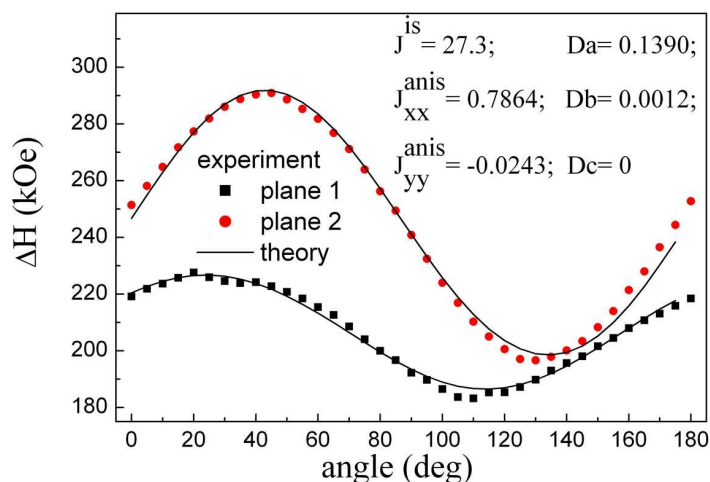


Fig. 1. Angular dependencies of ESR linewidth in  $\text{Ba}_3\text{Cr}_2\text{O}_8$  in X-band at  $T=12$  K

We acknowledge partial support by the program UMNİK 8765r/11225.

- [1] T. Giamarchi, C. Rueegg, and O. Tchernyshyov, *Nature Physics* **4**, 198 (2008).
- [2] A. Aczel, H. Dabkowska, G. Luke, et al. *Comm. APS, March-Meet. Abst.*: **32**, 00013 (2008).
- [3] T. Nakajima, H. Mitamura, and Yu. Ueda, *JPSJ* **75**, 054706 (2006).
- [4] M. Kofu, H. Ueda, H. Nojiri, et al. *PRL* **102**, 177204 (2009).

24PO-J2-11

## INVESTIGATION OF FRUSTRATED HEISENBERG CHAIN IN THE PRESENCE OF DZVALOSHINSKII-MORIYA INTERACTION

Vahedi J.<sup>1</sup>, Mahdavifar S.<sup>2</sup>

<sup>1</sup> Department of Physics, Islamic Azad University of Sari, 48164-194, Sari, Iran

<sup>2</sup> Department of Physics, University of Guilan, 41335-1914, Rasht, Iran

We consider the one-dimensional (1D) isotropic frustrated ferromagnetic spin-1/2 model with added Dzyaloshinskii-Moriya (DM) interaction. We study the effect of a uniform DM interaction on the ground state phase diagram of the model using the analytical cluster method and numerical Lanczos technique. Cluster method results, show that the classical ground state phase diagram of the model consists of only a single phase: "spiral". The quantum corrections of the DM interaction effect on the ground state phase diagram is determined by a very accurate numerical experiment. A very rich phase diagram including the gapless Luttinger liquid, the gapped spiral and Dimer orders is observed in different sectors of the quantum phase diagram. We also calculate the concurrence in the three ground state phases, and find that only next nearest neighbors are entangled.

24PO-J2-12

## THERMODYNAMIC PROPERTIES AND ELECTRONIC STRUCTURE OF HoB<sub>2</sub>

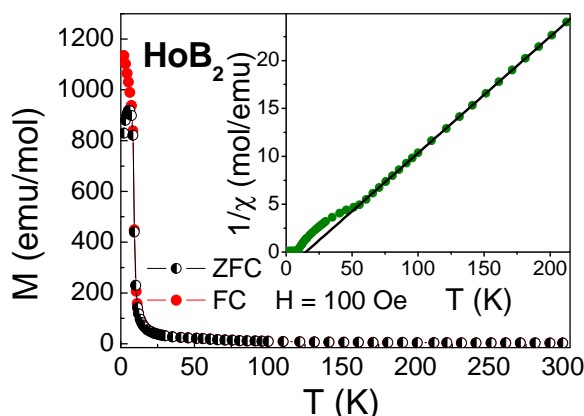
Volkov D.V.<sup>1</sup>, Volkova O.S.<sup>1</sup>, Matovnikov A.V.<sup>2</sup>, Novikov V.V.<sup>2</sup>, Dorgiev V.V.<sup>1</sup>, Vasiliev A.N.<sup>1</sup>

<sup>1</sup> M.V. Lomonosov Moscow State University, 119992 Moscow, Russia

<sup>2</sup> Bryansk State University, 241036 Bryansk, Russia

Various phenomena of f-electron magnetism are exhibited in the rare-earth diborides RB<sub>2</sub>. These metallic compounds with different rare-earths from Tb to Yb show [1] complicated character of magnetic transitions, relatively strong magnetocrystalline anisotropy and specific features of low-temperature heat capacity.

The RB<sub>2</sub> compounds crystallize in the hexagonal AlB<sub>2</sub>-type structure, space group P6/mmm. The single-phase polycrystalline HoB<sub>2</sub> and LuB<sub>2</sub> samples were successfully synthesized through intermediate hydride phase (HoB<sub>2</sub>) and at high pressure (LuB<sub>2</sub>). Temperature and field dependences of magnetization were measured for HoB<sub>2</sub> from 2 to 300 K in the fields up to 7 T. Temperature dependences of heat capacity were measured for HoB<sub>2</sub> and LuB<sub>2</sub> from 5 to 300 K. The temperature dependence of heat capacity C<sub>p</sub>(T) of HoB<sub>2</sub> shows two peaks indicating two phase transitions at T<sub>1</sub>=53 K and T<sub>2</sub>=8.2 K. In the temperature dependence of the magnetic susceptibility (see figure), the peak of C<sub>p</sub>(T) at T<sub>2</sub> corresponds to a steep rise of the magnetization below 10 K. The anomaly of C<sub>p</sub>(T) around T<sub>1</sub> can be compared with a clear deviation of the inverse magnetic susceptibility



$1/\chi(T)$  from the high-temperature Curie-Weiss behavior detected below  $\sim 60$  K (see inset in the figure). A Curie-Weiss fit of the inverse magnetic susceptibility for  $50 \text{ K} \leq T \leq 300 \text{ K}$  yields an effective magnetic moment  $\mu_{\text{eff}} = 8.1 \mu_B$  and a positive Weiss temperature  $\theta_{\text{CW}} = 15 \text{ K}$ . The temperature dependence of magnetization at the field of 1 T and magnetization curves in the fields up to 7 T suggest that the magnetic ordering phenomena in  $\text{HoB}_2$  are more complicated than simple ferromagnetic ordering in, contrast to the case of  $\text{TmB}_2$  [2]. The magnetic specific heat  $C_{\text{mag}}(T)$  and magnetic entropy  $S_{\text{mag}}(T)$  of  $\text{HoB}_2$  were determined with the help of our data for the specific heat of  $\text{LuB}_2$ , which is a good nonmagnetic lattice reference compound in this case, and were used to investigate possible crystal-field effects.

For the electronic structure calculations the full-potential local-orbital scheme FPLO (version: fplo 7.00 – 28) within the local (spin) density approximation LSDA+U [3,4] for a correct description of the correlated 4f states was used. The total energies calculated for the supercell with  $a = a_{\text{HoB}_2}$  and  $c = 2c_{\text{HoB}_2}$  show that the total energy of the ferromagnetic model is lower than that for the antiferromagnetic model by 0.051 mHartree, which is equivalent to a temperature of 7.9 K. This value is in good agreement with  $\theta_{\text{CW}} = 15 \text{ K}$  and  $T_C = 8.2 \text{ K}$ . The calculated electronic density of states shows the localized 4f states of Ho well below the Fermi level in the region between -5 eV and -7 eV. They do not mix noticeably with the valence-band states and thus can only interact via an RKKY type of interaction.

Support by RFBR and FPP is acknowledged.

[1] K.H.J. Buschow, Boron and Refractory Borides (Berlin, Heidelberg, 1977) p.494.

[2] T. Mori, T. Takimoto, A. Leithe-Jasper et al., Phys. Rev. B 79 (2009) 104418.

[3] K. Koepf and H. Eschrig, Phys. Rev. B 59 (1999) 1743.

[4] J.P. Perdew and Y. Wang, Phys. Rev. B 45 (1992) 13244.

24PO-J2-13

## TRANSPORT PROPERTIES OF INTERMETALLIC COMPOUNDS $\text{RCoGe}_2$ (R = Ce and La)

Kuo Y.K.<sup>1</sup>, Lue C.S.<sup>2</sup>

<sup>1</sup> Department of Physics, National Dong Hwa University, Hualien 97401, Taiwan

<sup>2</sup> Department of Physics, National Cheng Kung University, Tainan 70101, Taiwan

The electronic and magnetic properties of the cerium-based ternary intermetallic compound compounds with the general formula  $\text{RMX}_2$  ( $M =$  transition metals,  $X = \text{Si}$  or  $\text{Ge}$ ) has been of considerable interest recently. The physical properties of this class of materials show a wide range of variation depending on the degree of localization of the 4f electrons of cerium. As a result, a variety of different novel magnetic/nonmagnetic ground states, such as heavy-fermion (HF), antiferromagnetic (AF), mixed-valence (MV) and intermediate-valence (IV) etc, are observed due to the competition between Kondo and RKKY interactions [1]. Among those compounds,  $\text{CeCoGe}_2$  is of particular interest due to its peculiar physical properties, such as it has a rather high Kondo temperature  $T_K \sim 250 \text{ K}$ , the Ce ion is in the normal trivalent state, and it is the first Kondo system clearly interpreted by the Coqblin-Schrieffer model with  $j = 5/2$  [2-4].

In this study, measurements of the electrical resistivity ( $\rho$ ), Seebeck coefficient ( $S$ ), and thermal conductivity ( $\kappa$ ) on  $\text{CeCoGe}_2$  have been performed in the temperature range 10 - 300 K to

investigate the electronic structure. For comparison, the nonmagnetic counterpart LaCoGe<sub>2</sub> has also been studied. It is found that the temperature dependence of resistivity  $\rho(T)$  of CeCoGe<sub>2</sub> shows a weak variation in  $T$  at high temperatures, while  $\rho(T)$  decreases more rapidly below 80 K. This behavior of  $\rho(T)$  is similar to that of the earlier reported results [2], and the drop in  $\rho(T)$  is associated with the onset of Kondo coherence with which the conduction electrons interact with local magnetic moments. On the other hand,  $\rho(T)$  exhibits a metallic-like behavior for the nonmagnetic LaCoGe<sub>2</sub>. The temperature dependence of Seebeck coefficient  $S(T)$  is found to be positive in CeCoGe<sub>2</sub> over the measured temperature range, indicating that predominant charge carriers are electrons for the thermoelectric transport. On the contrary,  $S(T)$  is found to be negative in LaCoGe<sub>2</sub> with a noticeable contribution of phonon-drag effect at low temperatures. It is noted that the magnitude of  $S$  for CeCoGe<sub>2</sub> is one or two orders of magnitude larger than that of LaCoGe<sub>2</sub>, and the enhancement of  $S$  in CeCoGe<sub>2</sub> could be attributed to the strong correlations between the conduction electrons and the magnetic moments of the localized  $f$ -electrons. Instead of a linear temperature dependence in  $S(T)$  as observed in LaCoGe<sub>2</sub>, CeCoGe<sub>2</sub> exhibits a broad maximum in  $S(T)$  at about 75 K, at which the sudden drop in  $\rho(T)$  occurs. This is a typically behavior for Ce-based Kondo lattice compounds. A low- $T$  peak in thermal conductivity is seen for both compounds due to the reduction of thermal scattering at low temperatures. A detailed analysis of the thermal conductivity by separating lattice and electronic contribution and the comparison with the electrical resistivity indicates a more ordered state for LaCoGe<sub>2</sub> than CeCoGe<sub>2</sub>.

This work is supported by the National Science Council of Taiwan under Contract Nos NSC-97-2628-M-259-001-MY3 (YKK) and NSC-98-2112-M-006-011 (CSL).

- [1] G.R. Stewart, Rev. Mod. Phys. **56**, 755 (1984).
- [2] B.K. Lee *et al.*, Phys. Rev. B **69**, 085113 (2004).
- [3] B.K. Lee *et al.*, Phys. Rev. B **71**, 214433 (2005).
- [4] C.R. Rotundu and B. Andraka, Phys. Rev. B **74**, 224423 (2006).

24PO-J2-14

## MAGNETIC AND RESONANT PROPERTIES OF NEW LITHIUM NICKEL ANTIMONATE Li<sub>3</sub>Ni<sub>2</sub>SbO<sub>6</sub>

*Zvereva E.A.<sup>1</sup>, Savelieva O.A.<sup>1</sup>, Volkova O.S.<sup>1</sup>, Vasiliev A.N.<sup>1</sup>, Nalbandyan V.B.<sup>2</sup>,  
Evstigneeva M.A.<sup>2</sup>, Medvedeva L.I.<sup>2</sup>, Wolter A.<sup>3</sup>, Büchner B.<sup>3</sup>*

<sup>1</sup> Faculty of Physics, Moscow State University, 119991 Moscow, Russia

<sup>2</sup> Chemistry Faculty, Rostov State University, Rostov-on-Don 344090, Russia

<sup>3</sup> Leibniz Institute for Solid State and Materials Research IFW Dresden, D-01171 Germany

Two structurally identical Li<sub>3</sub>Ni<sub>2</sub>SbO<sub>6</sub> samples were obtained by ion exchange from Na<sub>3</sub>Ni<sub>2</sub>SbO<sub>6</sub> at 570 K and by solid-state synthesis at 1420 K. In contrast to earlier known orthorhombic 3D framework polymorph, Li<sub>3</sub>Ni<sub>2</sub>SbO<sub>6</sub> studied in this work is a monoclinic (C2/m) 2D layered superstructure of the rock-salt type. Rietveld refinement of the powder XRD data revealed cation-ordered “honeycomb” Ni<sub>2</sub>SbO<sub>6</sub> layers alternating with Li<sub>3</sub> layers and no signs of Li/Ni substitution. The magnetic measurements were performed in a MPMS Quantum design SQUID magnetometer. The susceptibility was measured under 0.1 T magnetic field in the temperature range 2-300 K. An isothermal magnetization curve was obtained for magnetic fields  $B \leq 5$  T at T=2 K. Electron spin

resonance (ESR) studies were carried out using X-band spectrometer Adani ( $f \approx 9.4$  GHz,  $B \leq 0.7$  T,  $T = 6-470$  K).

It was found that the magnetic susceptibility passes through maximum upon a decrease of the temperature then falls on the third. Such a behavior indicates an onset of antiferromagnetic ordering at low temperature. Neel temperature  $T_N$  determined from the maximum was found to be  $\sim 16$  K. Above  $T_N$ , the magnetic susceptibility follows the Curie-Weiss law  $\chi = \chi_0 + C/(T - \Theta)$ . The Curie-Weiss temperature is about zero indicating rather delicate balance between ferro- and antiferromagnetic interactions in this compound. Effective magnetic moment estimated from the Curie constant is  $4.3 \mu_B$  that is in a satisfactory agreement with theoretical estimations for nickel ion  $Ni^{2+}$  ( $S=1$ ). The 2 K  $M(H)$  isotherm has a slight upward curvature suggesting the possible presence of spin flop transition in an applied field.

ESR data are in line with magnetization measurements. ESR spectra in the paramagnetic phase ( $T > T_N$ ) show a single Lorentzian shape line ascribable to  $Ni^{2+}$  ion in octahedral coordination. Absorption at  $T > T_N$  is characterized by isotropic temperature-independent effective g-factor  $g = 2.150 \pm 0.001$  and the linewidth which decreases when the recording temperature is lowered, passes through a minimum at  $T = 120$  K and eventually changes the trend. Upon further decrease in temperature, the linewidth rapidly grows up to maximum around  $T_N$ . Temperature dependence of g-value also demonstrates sharp anomaly in the vicinity of  $T_N$ ; however, the visible shift of the resonant field to higher magnetic fields begins only in the immediate proximity to Neel temperature. It indicates that the linewidth shows a larger pre-ordering magnetic effect, possibly from short-range magnetic fluctuations upon approaching AFM ordering transition from above. An analysis of the anomalous line broadening at low temperature has been performed in the framework of Huber's theory developed for canonical antiferromagnetic and spin-glass systems and satisfactory agreement has been achieved.

Superexchange magnetic interaction has been rationalized in accordance with the Goodenough-Kanamori rules. Superexchange interaction via the half-occupied Ni  $e_g$  ( $d_z^2$ ,  $d_{x^2-y^2}$ ) orbitals was assumed to be ferromagnetic since Ni-O-Ni bond angles are closer to  $90^\circ$  within mixed-cation layers of Ni and Sb. At the same time, interaction between layers is obviously antiferromagnetic providing antiferromagnetic behavior of this compound in general.

The work was supported by the Russian Foundation for Basic Research (grant 11-03-01101) and International Centre for Diffraction Data (grant-in-aid 00-15).



**24 August**

Wednesday

17:30-19:00

poster session  
24PO-K1

**“Micromagnetics”**

24PO-K1-1

## THE FORMATION OF MAGNETIC DOMAIN STRUCTURES ON A MECHANICAL STRESSED SURFACE OF $\text{DyFe}_{11}\text{Ti}$ SINGLE CRYSTALS

*Semenova E.M., Lyakhova M.B., Murzanov M.S., Kutcher D.S., Pastushenkov Yu.G.*

Tver State University, 170002, Sadoviy lane 35, Tver, Russia

Investigation of magnetic domain structure (DS) of mono- and polycrystalline tetragonal  $\text{Dy}(\text{Fe,Ti})_{12}$  compound were carried out by the methods of optical and magnetic force microscopy. This compound is characterized by a “easy axis” (EA) type of magnetocrystalline anisotropy (MCA) at room temperature [1,2]. It was found that nonequilibrium DS formed on surface of  $\text{DyFe}_{11}\text{Ti}$  after mechanical polishing of the samples.

The stripe domain structure reveals on a prismatic plane (100) of single crystal  $\text{DyFe}_{11}\text{Ti}$  in the equilibrium state by flat iron garnet film (Fig. 1a). The boundaries of the stripe domains are oriented along the crystallographic axis [001]. DS on prismatic plane (100) is not detected by the method of polar Kerr effect. However, a stripe domain structure reveals on the surface of the crystal by the polar Kerr effect after mechanical polishing, but the orientation of domain walls in this case is perpendicular to the [001] (Fig. 1b). At the same time, the stripe domains in volume of single crystal is still oriented along the crystallographic c axis. Fig.1c shows that after mechanical impact on the surface of the sample the indicator film garnet reveals simultaneous presence of stripe domains oriented in two perpendicular directions: the stripe DS perpendicular to the [001] direction on the surface and stripe DS parallel the same direction in the volume. The surface domain structure is stable for several hours at room temperature, then it disappears and is not detected by any method. Thus, the surface domain structure, which is formed after mechanical action on the surface

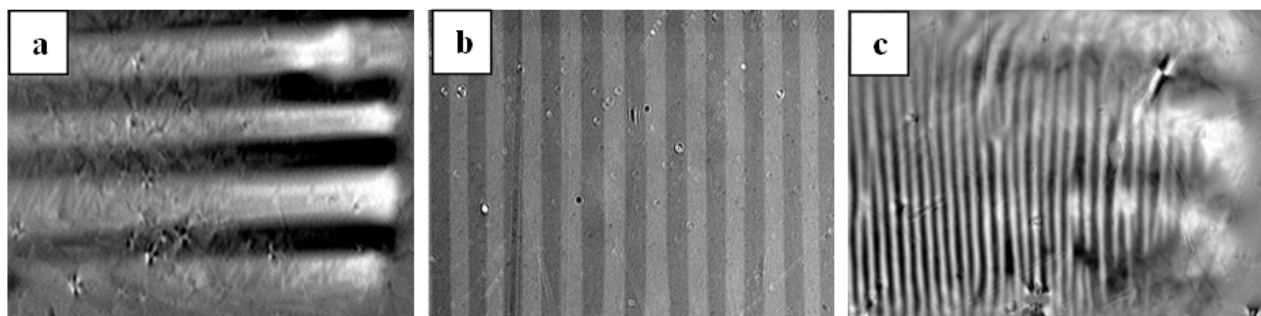


Fig.1. Magnetic DS on prismatic plane of single  $\text{Dy}(\text{Fe,Ti})_{12}$  crystal.

of the crystal, is nonequilibrium. Heating of the sample accelerates the relaxation process. The tight layer that occurs on the crystal surface after mechanical polishing is the reason of the observed phenomenon. A peculiarity of this layer is induced anisotropy with axis is perpendicular to the [001]. The evidence of this assumption is the behavior of the DS on the basal plane under similar conditions.

In this work the causes and behavior of nonequilibrium domain structure on the surface of mono- and polycrystalline  $\text{DyFe}_{11}\text{Ti}$  compound were investigated. A physical model describing the observed phenomenon was proposed.

Support by RFBR №09-02-01274 and the Federal program Scientific and pedagogical staff of innovative Russia.

- [1] L.M. Garcia, J. Bartolome, P.A. Algarabel, M.R. Ibarra and M.D. Kuz'min, *J. Appl. Phys.*, 73 (1993) 5908.  
 [2] X.C. Kou, T.S. Zhao, R. Grössinger, H.R. Kirchmayr, X.Li and E.R. de Boer, *Phys. Rev. B*, 47 (1993) 3231.

24PO-K1-2

## **SPIN-REORIENTATION TRANSITIONS AND MAGNETIC DOMAIN STRUCTURE IN RE-3d INTERMETALLIC COMPOUNDS**

*Pastushenkov Yu.G., Skokov K.P., Lyakhova M.B., Semenova E.M., Petrenko A.V., Simonov V.V., Zeziulina P.A.*

Tver State University, 170100, Tver, Zheliabova Str. 33, Russia

The domain structure (DS) in the single crystals of RE-3d intermetallic compounds of 1:5 and 2:17 stoichiometry in a wide temperature range (10-350 K) in the absence of the magnetic field and in the magnetic fields up to 0.2 T was investigated by magneto-optical Kerr effect.  $\text{RCo}_5$  (R=Nd, Dy, Ho) and  $\text{R}_2\text{Fe}_{17}$  (R=Nd, Gd, Tb, Dy, Ho, Er) intermetallics were chosen as the objects of the investigation.

By the example of  $\text{HoCo}_5$  compound the transformation of the domain structure of the hexagonal crystal in the whole temperature interval of magnetic phase transitions “easy axis”-“easy cone” and “easy cone”-“easy plane” was investigated in the details for the first time. Significant temperature changes of the DS were observed only in the compounds with spin-reorientation phase transitions ( $\text{NdCo}_5$ ,  $\text{DyCo}_5$ ,  $\text{HoCo}_5$ ) in the absence of the magnetic field. Significant temperature DS changes were not observed in  $\text{R}_2\text{Fe}_{17}$  compounds with “easy plane” type of anisotropy in the whole region of the magnetic ordering. Quantitative parameters of the DS were determined for all compounds. The DS models for the materials with “easy plane” and “easy cone” types of anisotropy were proposed.

In both groups of the compounds investigations of the temperature behavior of the DS in the magnetic field were carried out. For  $\text{RCo}_5$  compounds the field was placed at the right angle to the  $c$  axis of the sample. For  $\text{R}_2\text{Fe}_{17}$  compounds the magnetic field was placed in the basal plane along one of the three axes of easy magnetization. In  $\text{R}_2\text{Fe}_{17}$  compounds the widening of the temperature range of the DS, typical for the anisotropy type “easy cone”, in the magnetic field was observed. This behavior corresponds to the data of the magnetic measurements [1]. In  $\text{Ho}_2\text{Fe}_{17}$  compound a specific behavior of the DS in the temperature interval of 10-100 K was found. In this temperature region at the placement of the magnetic field an active rebuilding of the DS was observed. As the result of the rebuilding, the DS, containing 2 magnetic phases, magnetized along one of the easy directions in the basic plane, the third magnetic phase with the magnetization along the direction of the magnetic field appeared. The field, in which the third magnetic phase appeared, was increasing at the approach of the temperature to 100 K. In other compounds of 2:17 stoichiometry an active rebuilding of the DS was not found.

The received data about the character and the parameters of the DS were used at the analysis of the magnetocaloric effect in the magnetic phase transition regions in the given compounds [2,3].

This work was supported by RFBR Grants No. 09-02-01274, No. 10-02-00721, and No. 10-02-90016, as well as by the Federal Target Program “Research and scientific pedagogical staff of innovative Russia.”

- [1] A.S. Ermolenko, *IEEE Trans. on Magnetics*, Vol. MAG-12 (1976) 992.

- [2] S.A. Nikitin, K.P. Skokov, Yu.S. Koshkid'ko, Yu.G. Pastushenkov, T.I. Ivanova, *PRL* **105** (2010) 137205.
- [3] K.P. Skokov, Yu.G. Pastushenkov, Yu.S. Koshkid'ko, G. Shuetz, D. Goll, T.I. Ivanova, S.A. Nikitin, E.M. Semenova, A.V. Petrenko. *J. Magn. Magn. Mater.* 323 (2011) 447–450.

24PO-K1-3

## **SIMULATION OF THE NONLINEAR DYNAMICS OF THE DOMAIN WALLS IN MAGNETICS WITH AN OPTIONAL TWO-DIMENSIONAL MODULATION OF THE MAGNETIC PARAMETERS**

*Ekomasov E.G., Murtazin R.R., Gumerov A.M., Ekomasov A.E.*  
Bashkir State University, 450074, Ufa, Russia

It is known that in real magnetics the appearance of magnetic parameters local changes happens due to structural and chemical non-homogeneities and local influence (mechanical, thermal or solar) [1]. As it is usually difficult to make a precise (microscopic) calculation, one is to model the functions, which describe the parameters of a non-homogeneous material [2,3]. The case is especially interesting, when the size of a magnetic non-homogeneity and the size, describing a non-homogeneity of parameters of a stuff, are of the same order. It results in considerable complication of Landau-Lifshitz equation for the magnetization. Although the task of excitation and distribution of the magnetization waves, under certain conditions, is reduced to the studies of the modified sine-Gordon equation with floating factor [2-4]. The investigation of the big perturbations influence on the solution of the modified sine-Gordon equation in general case can be investigated only with the help of numerical methods. In dynamic, when a temporally or spatial non-homogeneous perturbation acts in the area of such non-homogeneities (or defects), under certain conditions, a strongly non-linear waves of magnetic character can be aroused. Such waves are weakly investigated.

We have investigated for the case of 2D nonhomogeneity of the constant of the magnetic anisotropy (NCMA) of the origin and evolution of the magnetic nonhomogeneities of pulson and 2D soliton types, localized in defect region. The description of the program on which the calculations were made is presented in [5]. The dependence of the shape of the localization of the excited magnetic nonhomogeneities from the shape of the defect region was found. The analytical expressions of the multisoliton type describing the magnetic nonhomogeneities of both types are proposed. The dependences of maximum deflection magnetization in magnetic nonhomogeneities of pulson and 2D-soliton types on time, nonhomogeneities region characteristics and DW speed were received. The dependence of the frequency of the pulson pulsation mode and 2D-soliton from the NCMA parameters was obtained. We made a comparison with the one-dimensional case [3] and showed the analogy. The dependence of the amplitude and width of the stable 2D-soliton from the wall velocity and the NCMA parameters was found. The dependences of the maximum amplitude solitary bending waves on the DW speed and on the nonhomogeneities region characteristics in the case of DW inertial motion and DW motion in the external magnetic fields were found. The analytical form of the amplitude solitary bending waves, that gives qualitative description of our results, was found.

- [1] S.V. Vonsovskii, *Magnetism*, Nauka, Moscow (1971).
- [2] D.I. Paul, *J.Phys.C: Solid State Phys*, **12**, (1979) 585.

- [3] M.A. Shamsutdinov, I.U. Lomakina, V.N. Nazarov, A.T. Harisov, D.M. Shamsutdinov, Ferro- and antiferromagnetodynamic. Nonlinear oscillations, waves and solitons, Nauka, Moscow (2009).  
 [4] E.G. Ekomasov, Sh.A. Azamatov, R.R. Murtazin, FMM **105**, (2008) 341.  
 [5] E.G. Ekomasov, Sh.A. Azamatov, R.R. Murtazin, FMM, **108**, (2009) 566.  
 [6] E.G. Ekomasov, R.R. Murtazin, A.M. Gumerov, Chronicles of the Consolidated Fund of Electronic Resource <Science and education >, № **5** (2010).  
 URL: <http://ofernio.ru/portal/newspaper/ofernio/2010/5.doc>

24PO-K1-4

## ANALYTIC REPRESENTATION OF BLOCH WALLS IN THIN FERROMAGNETIC FILMS

*Semenov V.S.*

Trapeznikov Institute of Control Sciences, Russian Academy of Sciences,  
 ul. Profsoyuznaya 65, Moscow, 117997 Russia

In thin ferromagnetic films, the domains of opposite magnetization are separated by  $180^\circ$  domain walls (DW). We consider the film thickness  $2D$  and the easy axis parallel to  $Z$ -axis.  $180^\circ$  DW separates two domains magnetized along  $\pm z$ -axis. The DW magnetization distribution is determined by changing magnetization  $\vec{M} = M_S \vec{m} = M_S (m_x \vec{i} + m_y \vec{j} + m_z \vec{k})$  ( $|\vec{M}| = M_S$  is saturated magnetization of the film);  $\vec{i}, \vec{j}, \vec{k}$  are ors along  $x, y, z$ - axe, respectively. The direction cosine  $m_x, m_y, m_z$  are coincided along with  $x, y$  and  $z$ -axe of rectangular coordinate system. This paper deals with two-dimensional models, that is direction cosine  $m_x(x, y), m_y(x, y), m_z(x, y)$  are dependant of  $x$  and  $y$ , and they are not dependant of  $z$ .

To calculate direction cosine  $(m_x, m_y, m_z)$  of magnetization vector  $\vec{M}$  we use the potential function  $A(t, s) = p(t) g(s)$ , where  $p(t)$  gives changing magnetization along the DW width, and  $g(s)$  - along film thickness. The direction cosine

$$m_x(t, s) = -\frac{\partial A(t, s)}{\partial s} = -p(t) \frac{dg(s)}{ds} = p g_s, \quad m_y(t, s) = \frac{\partial A(t, s)}{\partial t} = \frac{dp(t)}{dt} g(s) = p_t g,$$

$$m_z(t, s) = \sqrt{1 - m_x^2 - m_y^2}.$$

To provide the existence of such DW it is necessary to complement as follows:

1.  $m_x(t \rightarrow |\infty|, s) \rightarrow 0, m_y(t \rightarrow |\infty|, s) \rightarrow 0, m_z(t \rightarrow |\infty|, s) \rightarrow \pm(\mp)1$ ;
2.  $m_x^2(t, s) + m_y^2(t, s) + m_z^2(t, s) \leq 1$ ;
3. in the DW region, there must be bending line  $t_0(s)$ , along which the magnetization direction of film thickness changes to opposite one:

$$m_x^2(t_0(s), s) + m_y^2(t_0(s), s) = p^2 g_s^2 + p_t^2 g^2 = 1, \quad p g_s^2 + p_{tt} g^2 = 0, \quad \text{where } p_{tt} = d^2 p / dt^2.$$

To obtain two-dimensional magnetization distribution related to two-dimensional Bloch DW the function  $p(t)$  in the bending line region ( $t_1 \leq t \leq t_0$ ) has to change monotonously from maximal value  $p_{\max} = p(t = t_0)$  to some value  $p_1 = p(t = t_1)$  and its derivative has to change from  $p_{t0} = p_t(t = t_0) = 0$  to maximal value  $p_{t\max} = p_t(t = t_1)$ . Unknown function  $g$  and its derivative  $g_s$

are finding from bending line existence condition:  $g^2 = 1/(p_t^2 - p p_{tt})$ ,  $g_s^2 = -(p_{tt}/p)g^2$ . To calculate these numerical values the region  $t_1 \leq t \leq t_0$  is divided into  $n$  intervals:  $\Delta t = (t_0 - t_1)/n$ . Each value of  $t_i = (i-1)\Delta t$  ( $1 \leq i \leq n+1$ ) corresponds to two meanings  $g(s_i)$  and  $g_s(s_i)$ . From the derivative value we find the meanings of  $\Delta s_i = (g(s_{i+1}) - g(s_i))/g_s(s_i)$  and further we find the meanings of  $s_{i+1} = \sum_{i=1}^i \Delta s_i$ . So we determine changing functions  $g(s)$  and  $g_s(s)$  along the film thickness, that is we obtain the necessary condition of domain wall energy calculation.

24PO-K1-5

## INFLUENCE OF ONE-DIMENSIONAL DEFECTS ON THE DYNAMICS OF NEW PHASE NUCLEI CLOSE TO THE POINT OF THE FIRST ORDER PHASE TRANSITION IN MAGNETS

*Shafeev R.<sup>1</sup>, Nazarov V.<sup>2</sup>, Shamsutdinov M.<sup>1</sup>, Lomakina I.<sup>1</sup>*

<sup>1</sup> Bashkir State University, 32, Zaki Validi st., 450074, Ufa, Russia

<sup>2</sup> Institute of Molecular and Crystal Physics, 151, Pr. Oktyabrya, 450075, Ufa, Russia

Studying the dynamics of magnetic heterogeneities near the point of spin-reorientation first order phase transition in magnets containing various defects is a topical problem in condensed-matter physics [1, 2]. This is due to broad application of magnetization reversal processes in contemporary instruments of information storage and transmission.

The present paper is related to studying the nucleus of the domain of totally stable phase near the point of spin-reorientation first order phase transition in magnets with non-uniform distribution of magnetic anisotropy constant and exchange interaction parameter using the solitonic model. The investigations were carried out by the means of approximative integration [3] based on the application of the law of energy variation and the number of spin deviations and taking into account of damping.

Analysis of the numerical experiment shows the following results. Depending on the width of the magnetic anisotropy defect  $d = D/\delta_0$  ( $\delta_0$  is a characteristic size of the phase boundary) the new phase nucleus having the amplitude higher than critical can disappear (A), consolidate on the defect (B), or outgrow the boundaries of the defect area (C) leading to the formation of new phase domain (see Fig. 1). Parameter  $k$  on the figure is the relative value of local variation of the magnetic anisotropy constant. If the initial amplitude of the nucleus is less than critical it weakly depends on the defect size and disappears turning into an attenuating breather. The non-uniform distribution of the exchange interaction parameter against the coordinate insignificantly influences the dynamics of new phase nucleus comparing to the contribution of

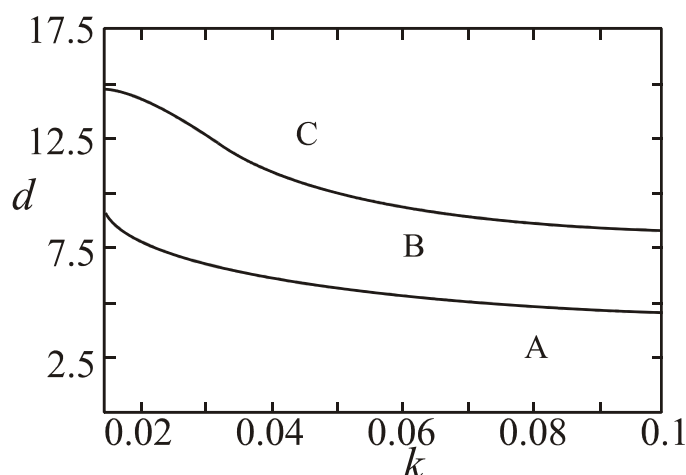


Fig. Areas of disappearance (A), consolidation on the defect (B) and outgrowth of the defect (C) of the initial magnetic heterogeneity as the interacting 90-degree phase walls.

magnet anisotropy defect. Presence of the areas with non-uniform parameter  $A$  in the sample leads to the shift of the lines separating the areas shown on figure in the way to increase the width of the defect  $d$ . In this way presence of areas with lower anisotropy can lead to the formation of new phase nuclei before the point of first order phase transition, that is in the depth of the old (stable) phase before reaching the temperature of equilibrium phase transition.

[1] Tereshina E.A. et al, *FTT*, **50**, (2008) 54–60.

[2] Chetkin M.V. et al, *FTT*, **40**, (1998) 1656.

[3] Shamsutdinov M.A. et al., *Ferro- i antiferromagnetodinamika.*, M.: Nauka, (2009) 456.

24PO-K1-6

## NUCLEATION PROCESSES IN SPIN-REORIENTATION PHASE TRANSITION OF TYPE II IN REAL MAGNETS

*Vakhitov R., Magadeev E., Gareeva E., Yumaguzin A.*

Bashkir State University, Z. Validi st. 32, Ufa, Russia

Investigations show that phenomenological method applied to spin-reorientation phase transition (SRPT) of type I allows to study two mechanisms of nucleation in similar ways [1,2]. The first one is the “wall” mechanism, being described as a generation of stretches in domain wall (DW) structure in a vicinity of SRPT, being new phase nuclei. The second one is the fluctuation one, i.e. appearance of magnetization fluctuations in the transition region (deviation of the magnetization vector  $\mathbf{M}$  from the equilibrium state to the direction of  $\mathbf{M}_0$  orientation, corresponding to the metastable phase), disappearing quickly, however condensing on crystal defects, thus becoming new phase nuclei. In phenomenological theory they are matched by 0-degree DW ( $0^0$ -DW), appearing as solutions of Euler-Lagrange equations for the considered magnet. These inhomogeneities [2] are the model representation of large-scale magnetization fluctuations and allow exploring SRPT of type I in real magnets. Nevertheless there is no such a mechanism of nucleation if SRPT of type II analysis, because of the absence of reasons for described solutions to appear in the vicinity of transition.

In this paper the magnetization distribution around a  $\delta$ -shaped defect is considered, also magnetic inhomogeneities generating on it are shown to have a  $0^0$ -DW-like structure. That made it possible to explore nucleation processes in SRPT of type II in a bounded magnet with defects, using a  $0^0$ -DW as a model representation of new phase nuclei. It is shown that obtained conformities for the fluctuation mechanism of nucleation in SRPT of type II are similar to those found earlier for SRPT of type I. That allows using the considered model for the analysis of other scripts of remagnetization of magnets, where defects play a remarkable role.

[1] K.P. Belov et al., *Orientational transitions in rare-earth magnets*, M.:Nauka, (1979) 320.

[2] R.M.Vakhitov, A.R Yumaguzin, *Fizika tverdogo tela*, **43** (2001) 65.

24PO-K1-7

## INVESTIGATION OF NONLINEAR MAGNETOELASTIC OSCILLATIONS IN THREE-LAYER STRUCTURE

*Dianov M.Y.<sup>1</sup>, Vlasov V.S.<sup>1</sup>, Kotov L.N.<sup>1</sup>, Shcheglov V.I.<sup>2</sup>, Shavrov V.G.<sup>2</sup>*

<sup>1</sup> Syktyvkar State University, 167001 Syktyvkar, Oktybrsky 55, Russia

<sup>2</sup> Institute of Radioengineering and Electronics of RAS, 125009 Moscow, Mokhovaya 11-7, Russia

Investigation of nonlinear dynamic systems is the topical area of modern science. One of the trends in this area is the study of nonlinear magnetic and magnetoelastic effects in magnetically ordered media. The fundamental significance of this problem is related to the general problem of interaction of magnetic fields with matter, the scope of applications of these results lies in the creation of various RF and microwave devices. Particularly one of the practical implementations can be the creation of powerful sources of ultrasound [1, 2].

This work deals with the problem of hypersound excitation in three-layer structure consisting of two ferrite layers with magnetoelastic properties located on the nonmagnetic substrate. Nonmagnetic layer located between ferrite layers. In this paper the equations of motion of the elastic medium and Landau-Lifshitz equation with allowance for the direction and polarization of the external magnetic fields and the same elastic properties of all layers, boundary conditions was obtained effective system of ordinary nonlinear differential equations to model magnetoelastic oscillations. It was assumed that the ferrite layers and the nonmagnetic layer is monocrystalline with a cubic crystal lattice. The computational model taken into account the demagnetizing and magnetoelastic fields as the internal magnetic fields for ferrite layers. In this case, we considered only the homogeneous mode of the magnetization oscillations and the coupled with magnetization transverse elastic oscillations. The averaging of elastic strain on the thickness of magnetic layers was used into the expression for the magnetoelastic field in Landau-Lifshitz equation. The system of equations was solved numerically by Runge-Kutta method. The efficiency of autooscillation excitation and hypersound oscillations amplitude at different parameters of the material and external fields was investigated based on numerical solutions of the equations system. Influence of elastic and magnetic eigenfrequencies detuning to the excited hypersound amplitude was determined. The possibility of increasing the effective hypersound excitation frequency area comparing with magnetoelastic devices with linear hypersound excitation regime was showed due to ferrite resonators nonlinearity. The excitation of hypersound oscillation different modes including the autooscillating mode also was showed. Properties of magnetoelastic autooscillations were investigated. In particularly the range of ferrite layers and the nonmagnetic layer material parameters, the amplitudes of the external fields for the magnetoelastic autooscillations existing were determined. The properties of the magnetoelastic autooscillations with the same in a single layer ferrite film were compared. The magnetoelastic oscillations modulation depth increasing comparing with the single ferrite layer case was identified.

This work was supported by RFBR (grant 10-02-01327).

[1] V.S. Vlasov, L.N. Kotov, V.G. Shavrov, V.I. Shcheglov, *Journal of Communications Technology and Electronics*, **54** (2009) 821.

[2] S.N. Karpachev, V.S. Vlasov, L.N. Kotov, *Vestnik Moskovskogo Universiteta. Fizika*, **6** (2006) 60.



## MICROMAGNETIC MODEL OF MAGNETIC AFTEREFFECT IN $\text{Sm}(\text{Co,Cu})_5$ SINGLE CRYSTALS

*Salev P., Kuznetsova Yu., Suponev N., Dygteva O.*  
Tver State University, 33, Zhelyabova st., Tver, Russia

The model of magnetic aftereffect based on microstructure and domain structure investigation in  $\text{Sm}(\text{Co,Cu})_5$  single crystals is presented. X-ray diffraction study points to single phase state with hexagonal 1:5 structure of all samples. Consequently we suppose that these precipitates are caused by variation of Cu concentration. The supposition is confirmed by the high-resolution TEM images of samples [1]. Our images of liquation precipitates with different Cu concentration were obtained using SOLVER P47 scanning probe microscope by means of the lateral force method (Fig.).

We conclude such precipitates cause the exchange parameter and anisotropy constants local variations, so they may serve as domain wall pinning sites. Thermal fluctuations may help the domain wall to overcome these pinning sites in magnetic field. The total time required for overcome one pinning site follows from Arrhenius equation:

$$t = \tau \exp\left(\frac{\Delta E_{AK}}{k_B T}\right), \quad (1)$$

where  $\tau$  is average thermal fluctuations field period and  $\Delta E_{AK}$  is total magnetic energy difference due to local variations of the exchange parameter and anisotropy constants.

Estimation of  $\tau$  value follows from the equation for thermal fluctuation field [2]:

$$H_{th} = \sqrt{\frac{2\alpha k_B T}{\mu_0 \tau \gamma M_s \Delta_{xyz}^3}}, \quad (2)$$

The energy of thermal fluctuation field should be equivalent to  $\Delta E_{AK}$  to overcome domain walls pinning sites:

$$E_{th} = \mu_0 M_s H_{th} = \Delta E_{AK}, \quad (3)$$

Combining equation (1)-(3) we obtain the final equation for estimation the  $\tau$  value:

$$\tau = \frac{2\mu_0 \alpha M_s k_B T}{\gamma (\Delta E_{AK})^2 d^3}, \quad (3)$$

where  $d$  is the average size of precipitations.

Computer simulations of magnetic aftereffect based on this model were carried out. It was obtained a good correlation whit experimental data.

Support by RFBR №09-02-01274 and the Federal program Scientific and pedagogical staff of innovative Russia.

[1] Y. Zhang, A. Gabay, Y. Wang, G. C. Hadjipanayis, J. Magn. Mat. **272–276** (2004) e1899–e1900

[2] W. F. Brown, Jr., Phys. Rev. **130** (1963) 1677

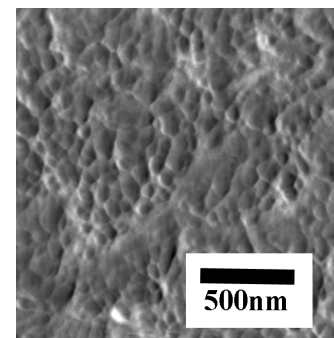


Fig. AFM topography of base plane  $\text{SmCo}_3\text{Cu}_2$

## NON-COLLINEAR STATES IN A CHAIN OF SINGLE-DOMAIN MAGNETIC PARTICLES

*Fraerman A.A.<sup>1</sup>, Muhamatchin K.R.<sup>1,2</sup>*

<sup>1</sup> Institute for Physics of Microstructures, Russian Academy of Sciences  
Nizhniy Novgorod 603950 GSP 105, Russia

<sup>2</sup> Department of Physics, Nizhniy Novgorod State University,  
Gagarin Avenue 23, Nizhniy Novgorod 603950, Russia

Non-collinear magnetization structures, such as helimagnets, can exist in the systems with exchange interactions; however the exchange energy is the same for both sign of spiral wave vector. Degeneracy can be removed in the presence of the spin-orbit interaction, whose contribution to the energy of the ferromagnet can be described phenomenologically by the Lifshitz-type invariants. We find it interesting to explore the possibility of modeling of the exchange and relativistic interactions (appearing in magnets) in the systems of single-domain magnetic particles interacting magnetostatically. Interaction proportional to the scalar product of the magnetization  $\vec{m}_1 \vec{m}_2$  simulates exchange and terms  $m_i m_k$  simulate the Lifshitz-type invariants.

We study the ground state of the chain of magnetic dipoles and conclude that a state with non-collinear magnetization distribution can exist. In order to prove it, we consider one-dimensional lattice with two different dipoles in the cell and the difficult axis of magnetization parallel to the translation vector. In this case the competition of long-range "exchange forces" leads to the formation of the helical structure, whose period is determined by a ratio of the dipole moments  $V_1/V_0$ :  $q \approx \pi \pm \exp[1 - (\ln 2)(1+V)/(1-V)]$ , where  $V=2(V_1/V_0)/(1+(V_1/V_0)^2)$ . The "left" and the "right" helices have the equal energy. Also, we consider a medium with heterogeneous permeability, which is a half the ideal diamagnetic (superconductor) or paramagnetic (e.g. Permalloy). In particular, we explore the ground state of the chain of magnetic dipoles with two

identical particles in the elementary cell ( $a$  is the distance between the dipoles in the cell), located along the Z-axis at a distance  $l/2$  ( $l$  is the distance between the dipole and its reflection) from the surface of the superconductor (XZ -plane), assuming that the London penetration depth is to zero and the superconductor is a perfect diamagnetic. For such a system an additional term  $[q \text{rad} \mu \times \vec{d}] [\vec{m}_1 \times \vec{m}_2]$  in the interaction energy of two dipoles appears,  $\vec{d}$  is the translation vector. The term removes leads to appearing of non-collinear state in the system. This state consists of two homogeneously magnetized sub lattices. The angle between magnetizations of these sub lattices is determined by the system geometry (Figure 1).

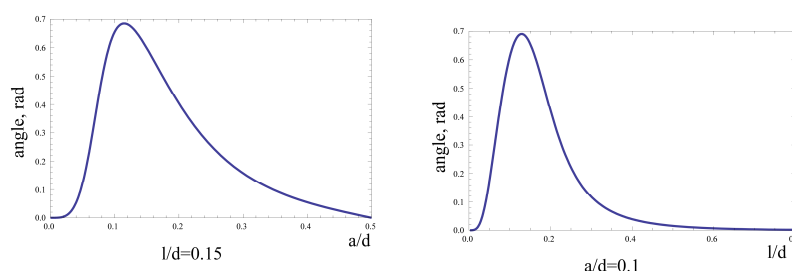
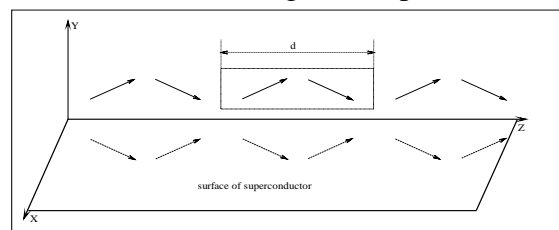


Fig.1. Angle between magnetizations of sub lattices as function  
a)  $l/d$   
b)  $a/d$

24PO-K1-10

## THE TYPES OF STABLE SPIRAL DOMAINS IN FERRITE-GARNET FILM

Mamalui Ju.A., Siryuk Ju.A., Smirnov V.V.

Donetsk National University, 24, Universitetskaya str., 83001 Donetsk, Ukraine.

Stable spiral domain structure ferrite-garnet film ( $(TmBi)_3(FeGa)_5O_{12}$  with easy axis  $\langle 111 \rangle$ , Neel temperature  $T_N = 437K$ , compensation point  $T_C = 120K$ , quality factor  $Q > 5$ ) has been investigated. Stable spiral domain structure (SDS) has been formed under influence of pulse magnetic field perpendicular the plain of film and bias filed  $H = 0$  or  $H \neq 0$ . They are conserved after switch off the pulse field. Two type of equilibrium SDS () has been studied. The first type is spiral domain (SD) surrounded of CMD lattice and the second type is hexagonal lattice of spiral domain. Dependence of the type of SDS from forming condition has been experimentally proved.

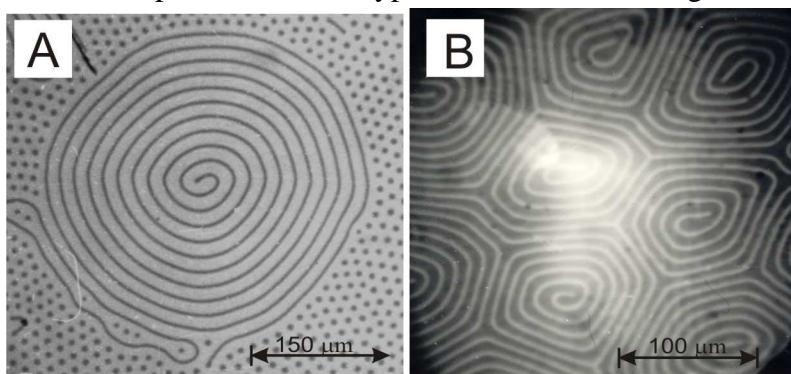


Fig.1. Spiral domain structure.

1. *Spiral domain in surrounding of CMD lattice.* Two strip domain separated by  $180^\circ$  domain boundary twisted into Archimedean spiral (fig.1.A). Influence of bias field on parameters of SD (radius, number of turns, length and period of stripe domain generating spiral) has been investigated. For analyzing experimental results conception of magnetostatic pressure has been

used. Proved that condition of equal of magnetostatic pressures both phase produce to coexistence of two domain phase “SD-lattice of CMD” [1]. Magnetostatic pressure of CMD lattice not only stabilized spiral domain but also determine:

- 1) the possibility of forming a spiral domain, its form, size;
- 2) the behavior of the SD as the temperature ( $T$ ) or magnetic field  $H$  change;
- 3) the temperature region of the spiral domain formation.

The effect of  $T$  or  $H$  on the SD, surrounded by CMD lattice, was investigated. It is shown that a change of  $T$  or  $H$  phase transitions in CMD lattice cause phase transitions in the SD [2].

2. *Lattice of spiral domains.* Each cell of SD lattice is a hexagon, inside which there is a spiral domain, consisting of 5-8 convolutions (fig.1.B). The direction of twisting spiral is any. Outer ends of the spiral are fixed either on the nodal three- radial points, or at another remote spiral, creating its coils. SD lattice is energetically favorable and stable at field formation. When you change or an increase of  $T$  or  $H$  phase transitions in SD lattice did not occur. It disappears by reducing the length of the spirals. In the SD lattice such stabilization is absent, which is in the spiral domain, surrounded by CMD lattice.

[1] Ju.A. Mamalui, Ju.A. Siryuk, j.Fiz. tverd. Tela, **43**, №8 (2001) 1458.

[2] Ju.A. Mamalui, Ju.A. Siryuk, j.Functional materials, **15**, №3 (2008) 376.

## THE CELLULAR DOMAIN STRUCTURE IN FERRITE-GARNET FILM

*Mamalui Ju.A., Siryuk Ju.A., Smirnov V.V.*

Donetsk National University, 24, Universitetskaya str., 83001 Donetsk, Ukraine.

Experimentally studied the characteristics of "hard" honeycomb domain structure (HDS) as the magnetic field ( $H$ ) or temperature ( $T$ ) in epitaxial ferrite-garnet film change. Domain wall structure effect on the features of the HDS was shown.

The film of  $(TmBi)_3(FeGa)_5O_{12}$  compound (the easy axis  $\langle 111 \rangle$ , the Neel temperature  $T_N = 437K$ , the point of magnetic compensation of  $T_C = 120K$ , the quality factor  $Q > 5$ ) have been studied. The studies were performed on a magneto-optical device, which provides for the action of two magnetic fields perpendicular to the plane of the film: a pulsed field and bias field  $H$  of two directions. If  $H$  coincides with the direction of magnetization inside the bubble, then  $H < 0$ , if  $H$  is the opposite –  $H > 0$ . Direction  $H < 0$  applies to create a honeycomb DS.

1. *Effect of magnetic field on domain structure.* At  $H = 0$  a hexagonal lattice of bubbles by a pulsed field is formed. This lattice is the equilibrium at the temperature of formation. It corresponds to the minimum energy. Equilibrium lattice parameter  $y = d/a = 0.74$ , where  $d$  – diameter of the bubble,  $a$  – lattice constant. This is "hard" lattice, i.e. pulsed field creates a vertical Bloch lines (VBL), which are uniformly distributed in the domain walls of the bubble. When  $H < 0$  lattice is transformed into HDS (fig.1.A). Bubbles obtain the shape of a hexagon, and VBL are moved to those parts of the domain walls that form the vertex angles of honeycomb domain. Thus, the hexagonal honeycomb domain structure separated by stripes having a  $180^\circ$  domain wall. With increasing  $H < 0$  the number of VBL in the domain boundaries is decreases. Domain increases, and there is an "explosion" of the honeycomb domain structure, i.e. phase transition of the HDS in the cellular structure (fig.1.B). Under pulsed field this structure is transformed again into a

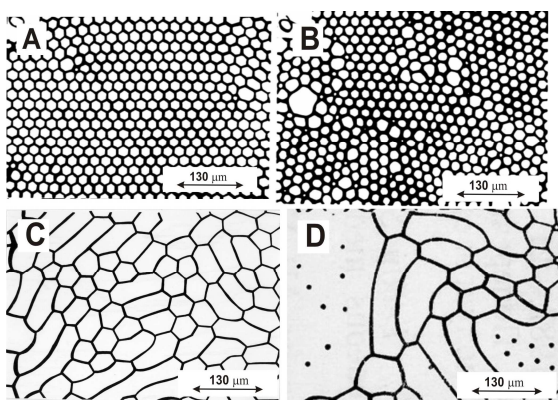


Fig.1. The types of domain structure.

larger honeycomb domain structure. This DS resembles a "net" (fig.1.C). With increasing  $H < 0$  under a pulsed field those stripe areas which share the vertex angles of honeycomb domains with the assembled VBL, turn into bubbles. The remaining sections of stripe collapse (fig.1.D). A lattice with a small bubble packing density  $y = d/a = 0.3$  is creating. And the bubbles in them have the polarity of the stripes that had previously surrounded the honeycomb structure.

2. *Effect of temperature on the honeycomb domain structure.* When the temperature of equilibrium SDS, which created at 300K, is stored in a temperature range at both ends of which a phase transition one of the first kind distinguished by its character. When the compensation point approaches there occur a phase transition of HDS to the cluster structure. At a distance from the compensation point is a phase transition into a new HDS with more options and a decrease in the number of domains. The conception of magnetostatic pressure was used for analyzing the experimental results.

Equilibrium SDS previously created at 300K exists in some range of temperature. At both ends of this range a phase transition one of the first kind distinguished by its character is appear. A phase transition of HDS in the cluster structure has been occurred move on to compensation point. A phase transition into a new HDS with greater parameters and with decrease numbers of domains has been appeared under moving in opposite direction. For analyzing experimental results conception of magnetostatic pressure has been used.

## TWO TYPES OF SPIN-REORIENTATION PHASE TRANSITIONS IN FERRITE-GARNET FILM

*Mamalui Ju.A., Siryuk Ju.A., Bezus A.V.*

Donetsk National University, 24, Universitetskaya str., 83001 Donetsk, Ukraine.

Features of domain structure (DS) of ferrite-garnet film of composition  $(YBi)_3(FeGa)_5O_{12}$  (the easy magnetization axis  $\langle 111 \rangle$ , the Neel temperature  $T_N = 421K$ , point of magnetic compensation  $T_k = 223K$ ) have been studied. The film possesses mixed anisotropy: the crystallographic cubic ( $K_1$ ) and the axial induced the growth ( $K_u$ ). The ratio of anisotropy constants depends on temperature  $K_u/K_1 = f(T)$  and this influences DS features. The DS is examined by the Faraday effect. The spin-reorientation phase transition (SRPT) is fixed by the method of color registering. Study of DS features is based on theoretical simulation of visual experimental data.

It has been determined that the domain boundary (DB) is most sensitive to changes in the ratio of anisotropy constants. In DB there is a collection of spins of different orientation [1]. For a definite value of the ratio of anisotropy constants the corresponding orientation of spins in DB becomes of advantage, in view of the energy, and in this region of DB there is a phase transition.

There were two spin-reorientation phase transitions in the film to the both sides of compensation

point. For  $T \geq 360K$ , the cylindrical magnetic domains (CMD) are observed, i.e. there exists the axial phase. The domain boundary is a  $180^\circ$  Bloch one. For  $T = 360K$ , at some sites of CMD round boundaries, there occurs a phase transition from the  $180^\circ$  Bloch DB to a broader  $180^\circ$  DB in which the plane of spin turn is at an angle to axis  $\langle 111 \rangle$ . In DB, the phase transition is induced by the first-order spin-reorientation phase transition from axial phase to angular one. The transition develops through nucleation and it is the hysteresis-free one. New phase nucleus is domain boundary of the initial phase. A 15K temperature range in which axial and angular phases coexist has been determined experimentally. The interval is defined by successive phase transitions over the whole of CMD domain boundary length. The boundary between axial and angular phases is not visual. This can be explained by considering a new phase nucleus as a static soliton whose dimensions are growing with changes in anisotropy constants ratio

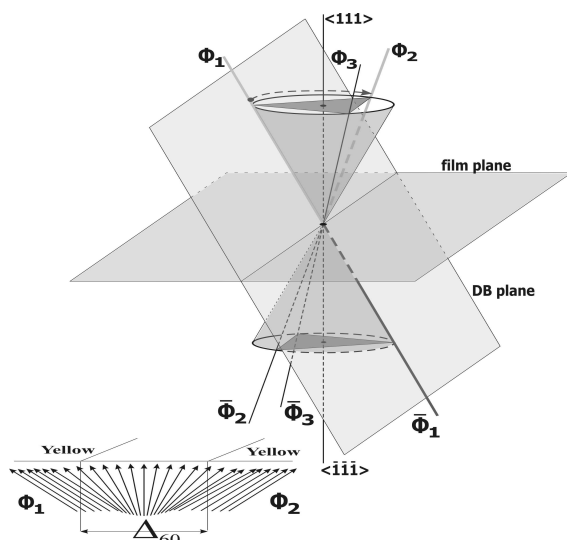


Fig.1. The model of 60-deg domain boundary.

whose dimensions are growing with changes in anisotropy constants ratio  $K_u/K_1 = f(T)$  [2].

In the low-temperature region (173-178K) there is a gradual phase transition in DB from  $180^\circ$  twisted to  $60^\circ$  and than to  $120^\circ$  boundary (Fig.1). The phase transition in DB induces the hysteresis-free second-order spin-reorientation phase transition from one angular phase to another angular phase in the whole volume of the sample. The angular phases are sequentially changed in conformity with the character of phase transition in DB under spin reorientation.

[1] A.A.Bezlepkin, S.P.Kuntsevich, Ju.A.Popkov, Fiz. Nizk. Temperatur, **15** (1989) 875.

[2] R.M.Vakhitov, A.R. Jumaguzin, Fiz. Tverd. Tela, **43** (2001) 65.

## DYNAMICS OF VORTEX SPIN-TORQUE NANOOSCILLATOR WITH BROKEN AXIAL SYMMETRY

*Skirdkov P.N.<sup>1</sup>, Zvezdin K.A.<sup>1</sup>, Cros V.<sup>2</sup>, Grollier J.<sup>2</sup>, Zvezdin A.K.<sup>1</sup>*

<sup>1</sup> A. M. Prokhorov General Physics Institute of RAS, Vavilova 38, 119991 Moscow, Russia

<sup>2</sup> Unite Mixte de Physique CNRS/Thales and Universite Paris Sud 11, 1 ave A. Fresnel, 91767  
Palaiseau, France

High-frequency dynamics of magnetic vortices induced by the spin transfer effect observed recently in nanopillars and nanocontacts have raised a strong interest [1,2]. The associated microwave emissions in such vortex spin-torque nanooscillators (STNOs) can occur without any external magnetic field and at low current densities, together with large powers (up to one microwatt and narrow line width less than 1 MHz) comparatively to single-domain spin transfer nanooscillators.

But the properties of these devices are usually analyzed in axial geometry [3,4]. We have studied the dynamics of magnetization in a vortex spin torque nanooscillator with broken axial symmetry caused by a planar polarizer by analytical calculations and micromagnetic modelling using the finite-difference SpinPM solver. The change of various parameters of the STNO such as critical current and frequency of the vortex rotation due to spin-torque has been investigated. The occurrence of a planar polarizer breaks the axial symmetry and changes the dynamics of vortex in this case in comparison with a pure axial polarizer. Analytical expression for the spin-torque induced by the planar polarizer has been obtained using Landau–Lifshitz–Gilbert equation. We have considered the following two approaches: the travelling wave ansatz (TWA) and the image vortex ansatz (IVA) (see e.g. [5]). We have studied the impact of choosing one of these approaches on the result and discussed the differences between them. The dynamics of this system has been studied analytically using Thiele-like equation. The results have been compared with micromagnetic simulations.

Other possibilities of the axial symmetry breaking such as occurrence of the defects of the structure have also been considered. We have studied the following kinds of defects: the elliptic-like structure, the small cutoff and the displacement of the nanodisks centers. An attempt of their analytical description using the analogy with planar polarizer has been done. The obtained results have been compared with micromagnetic simulations. Applicability of this approach has been discussed. The impact of different types of defects on the magnetization dynamics has been studied by micromagnetic stimulation.

[1] A. Dussaux et al., *Nature Communications*, **1** (2010) 8.

[2] A. Chanthbouala et al., *Nature Physics Letters*, published online: 10 April 2011.

[3] A.V. Khvalkovskiy et al., *Applied Physics Letters*, **96** (2010) 212507.

[4] N. Locatelli et al., *Applied Physics Letters*, **98** (2011) 062501.

[5] Y. Gaididei et al., *International Journal of Quantum Chemistry*, **110** (2010) 83–97.

## SPIN-TRANSFER MEMRISTIVE EFFECT IN MAGNETIC NANOSTRUCTURES

*Zvezdin K.A.<sup>1</sup>, Belanovsky A.D.<sup>1</sup>, Chanthbouala A.<sup>2</sup>, Grollier J.<sup>2</sup>, Cros V.<sup>2</sup>*

<sup>1</sup> Prokhorov General Physics Institute, Russian Academy of science,  
119991, Moscow, Vavilov Str., 38, Russia

<sup>2</sup> Unité Mixte de Physique CNRS/Thales and Université Paris Sud 11, 1 ave Augustin Fresnel,  
91767 Palaiseau, France

The existence of memristor was first postulated in 1971 by Leon Chua of UC Berkeley [1].

Memristor is a two-terminal device which resistance depends on the magnitude and polarity of the applied current and the duration of the current pulse. If the power supply is off, memristor remembers the last state, and stores this information until the next current switching on. Until recently Memristors remain exclusively the subject of theoretical research, but in 2008 at HP Labs, by a group led by R.S. Williams it was shown a working prototype of nanoscale memristor based on ion transport in semiconductor nanostructures[2].

Great attention to the memristor is caused both by its fundamental importance as the fourth basic passive element in circuit design, and by the wide possibilities of their practical application in electronics. Development of the nanoscale memristor production technology will radically improve the performance of such devices as multibit nonvolatile memory and logic, neurochips, power electronics devices, shock-resistive circuits, information security systems, etc.

Recently, several schemes of spintronic memristor have been proposed, based on the excitation of magnetization dynamics by spin-polarized current. In this case, one of the most interesting and promising spintronic circuits memristor is based on the spin-polarized current controlled domain wall motion [3,4]. Here we report on the micromagnetic simulation of the memresistive properties of memristive properties of multilayered structures with domain wall controlled by spin-polarized current flowing perpendicular to the sample plane.

[1] L.O. Chua, Memristor—the missing circuit element, *IEEE Trans. Circuit Theory*, vol. 18, no. 5, pp. 507–519, 1971.

[2] D.B. Strukov, G.S. Snider, D.R. Stewart, and R.S. Williams, —The missing memristor found. *Nature*, vol. 453, pp. 80–83 (2008).

[3] A.V. Khvalkovskiy, K.A. Zvezdin, Ya.V. Gorbunov, V. Cros, J. Grollier, A. Fert and A.K. Zvezdin. High domain wall velocities due to spin currents perpendicular to the plane. *Phys. Rev. Lett.* 102, 067206 (2009).

[4] A. Chanthbouala, R. Matsumoto, J. Grollier, V. Cros, A. Anane, A. Fert, A.V. Khvalkovskiy, K.A. Zvezdin, K. Nishimura, Y. Nagamine, H. Maehara, K. Tsunekawa, A. Fukushima, and S. Yuasa, *Nature Physics*, (2011), doi:10.1038/nphys1968.

## EXCITATION OF SPIN SELF-OSCILLATIONS IN A MAGNETIC FILM BY CURRENTS OF SINGLE AND DOUBLED STRIP-LIKE CONTACTS

*Mazurkin N.S., Korneev V.I., Popkov A.F.*

Moscow institute of electronic technology, 124489 Zelenograd, Moscow, Russia  
e-mail: edenlab@mail.ru

Development of nano-sized microwave generators based on spin torque transfer is nowadays one of the actual tasks in spintronics. Basic problems here lie in the low power generation, necessary condition for to decrease critical currents and increase quality factor of oscillations. To solve these problems it is learned possibility to come from metal to tunnel contacts, to use excitation of macroscopic coherent spin oscillations by domain walls and vortices in mesoscopic structures and the usage of mutual and external synchronization in the system of nanocontacts. The tunnel dielectric interlayer can be by the order of value and more to enlarge the power of generation, but very strong decreases the factor of quality. The usage of coherent modes as such as vortex oscillations significantly increases this factor, but decreases the frequency division of resonant oscillations. One of the promising ways to enlarge the power and the quality factor of spin self-oscillations at high frequencies is the usage of phase synchronization for multiple generators created on the common magnetic platform. In this view it is interesting to consider autooscillations in a magnetic film induced by the system of contacts having strip-like form and nano-sized width.

In this paper on the basis of numerical solutions of magnetodynamics equations [1] taking into account of spin transfer effects we analyze strongly nonlinear eigen modes of spin self-oscillations excited in a magnetic film by spin polarized currents created by strip-like single and double contacts. We consider in detail the case of axial symmetry of vertical magnetization and spin polarization, including into the consideration of nonuniform exchange interaction, magnetostatic and external magnetic field effects. In the considered case of axial symmetry it is possible to describe spin precession with a fixed frequency by transformed magnetodynamic equations reduced to the system of ordinary equations. It allows us to find all possible nonlinear modes of localized self-oscillations excited not only by a single, but also by double strip-like contacts. An example of such a solution is shown on Fig. 1. These modes are used then for the full micromagnetic simulation and analysis of their time evolution and modes living. It was shown that in the distributed system for the support of spin precession with the fixed frequency it is necessary to supply higher currents than in the macrospin model. In the case of double contacts effects of phase synchronization and assisting effects arise at higher frequencies than for those predicted by a low amplitude perturbation theory. Elaborated approach allows one to find spin oscillation modes and frequency division of phase synchronization for arbitrary number of current nanocontacts in the dependence of parameters of the distributed system.

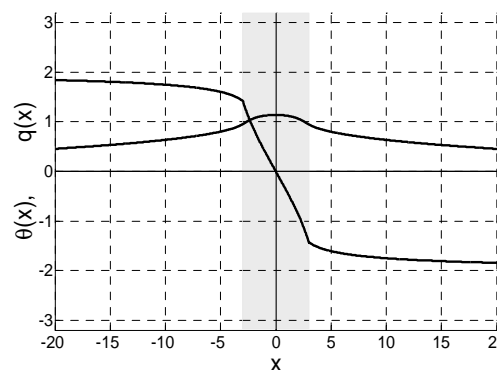


Fig. 1. Precession angle and wave number of the first mode of spin oscillations

The work is supported by the Education Ministry of RF, contr.# 2.1.1/5169.

[1] *Slonczewski J.C.* Current-driven excitation of magnetic multilayers // *J. Magn. Magn. Mater.* 159, L1 (1996).



## DYNAMICS OF DOMAIN WALL IN FERROMAGNET WITH INHOMOGENEOUS MAGNETOELECTRIC INTERACTION

*Nikolaev Yu.Ye., Kharisov A.T., Shamsutdinov M.A.*

Bashkir State University, Validi st., 32, Ufa, Russian Federation

The media with interconnected magnetic and electric properties generate much interest nowadays. Due to magnetoelectric interaction, an electric field may substantially influence various properties of magnets [1]. Of special topicality are the studies dedicated to the influence of inhomogeneous magneto-electric interaction (IMEI) on the characteristics of magnetic domain walls. I. Dzyaloshinskii predicted the movement of Neel domain walls under the influence of a gradient electric field [2], whereas the paper [3] disclosed a shift of domain walls in iron garnets exposed to an electric field.

This paper investigates the influence of an electric field on the structure and dynamics of the domain wall in iron garnets in a single-sublattice model. The energy density describing IMEI is written as [2]:

$$F_{me} = -b\mathbf{E}(\mathbf{m}\text{div}\mathbf{m} + [\mathbf{m}\times\text{rot}\mathbf{m}]),$$

where  $\mathbf{E}$  is electric field intensity,  $b$  is the IMEI parameter,  $\mathbf{m} = \mathbf{M}/M_0$ ,  $M_0 = |\mathbf{M}|$  is saturation magnetization.

It has been shown that in a weak electric field which is parallel to the easy magnetization axis ( $\mathbf{E} \parallel z$ ), a wall is formed having a structure that is intermediate between the Bloch wall and the Neel one. As some critical field is exceeded, the intermediate wall turns into the Neel one. Domain wall dynamics in a gradient electric field has been investigated both analytically and numerically. It has been established that due to IMEI the domain wall is set in motion by an electric field. The dependencies of motion characteristics on the value of the gradient electric field have been obtained, as well as the value of the damping parameter.

Fig. 1 shows the angle  $\psi$  of magnetization deflection from its equilibrium value as the domain wall moves depending on the value of the electric field gradient  $e$ . The dotted line represents the result of the numerical solution, whereas the solid line has been obtained analytically. A good agreement has been observed of the results of the numerical studies and those of the approximation analysis.

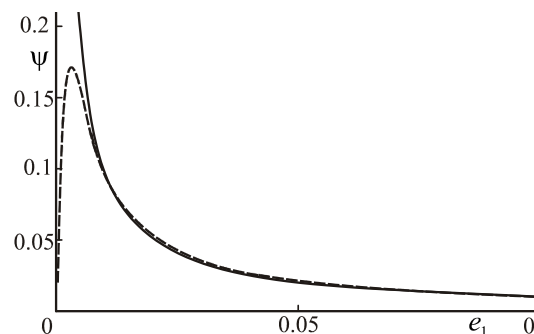


Fig. 1. Dependence of angle  $\psi$  on  $e$

[1] M. Fiebig, Revival of the magnetoelectric effect, *J. Physics D: Appl. Phys.*, **38**, (2005), 123–152.

[2] I.E. Dzyaloshinskii, Magnetoelectricity in ferromagnets, *EPL*, **83**, (2008). 67001.

[3] A.S. Logginov, G.A. Meshkov, A.V. Nikolaev, E.P. Nikolaeva, A.P. Pyatakov, A.K. Zvezdin, Room temperature magnetoelectric control of micromagnetic structure in iron garnet films, *Appl. Physics. Lett.*, **93**, (2008), 182510.

24PO-K1-17

## DOMAIN WALL DYNAMICS IN MOLECULAR FERRIMAGNET

### $[\text{Mn}^{\text{II}}(\text{HL-pn})(\text{H}_2\text{O})][\text{Mn}^{\text{III}}(\text{CN})_6]\cdot 2\text{H}_2\text{O}$

*Morgunov R.B.<sup>1</sup>, Mushenok F.B.<sup>1</sup>, Koplak O.V.<sup>2</sup>*

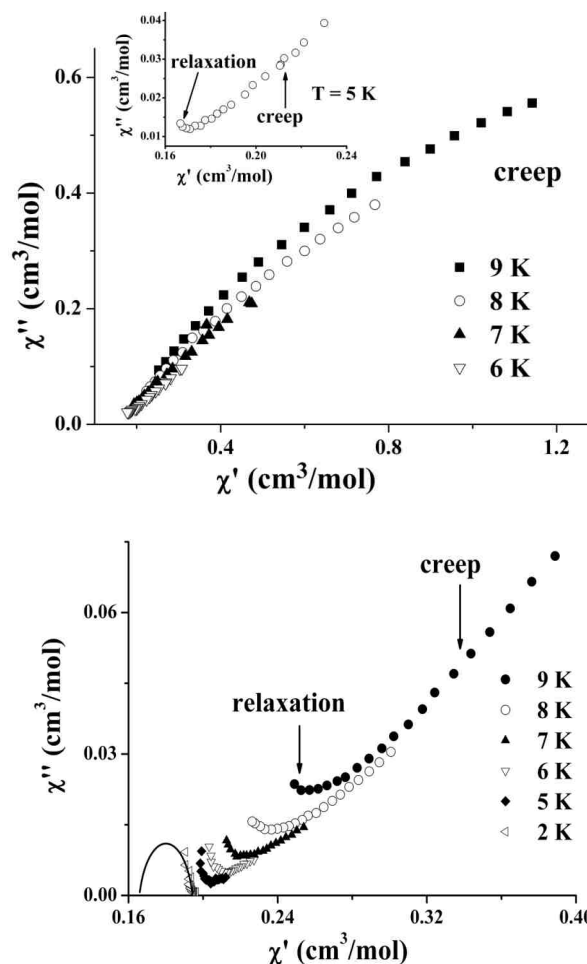
<sup>1</sup> Institute of Problems of Chemical Physics, 142432, Chernogolovka, Russia

<sup>2</sup> University of Kyiv and NAS of Ukraine 01033, Kyiv, Ukraine

Synthesis of molecular magnets provides broad opportunities for tailoring of magnetic properties in solid-state materials by using a controllable design of atomic and spins structures. On this route, the influence of chirality of crystal and spin structures on ESR spectra and coercivity was observed in chiral (R) and racemic (rac) molecular ferrimagnets  $[\text{Mn}^{\text{II}}(\text{HL-pn})(\text{H}_2\text{O})][\text{Mn}^{\text{III}}(\text{CN})_6]\cdot 2\text{H}_2\text{O}$  (BN). Magnetic properties of BN crystals obtained both in static and high-frequency regimes do not elucidate the low-frequency spin dynamics which is primarily caused by motion of domain walls in a random potential field of defects and Peierls relief. In this work we analyzed various regimes of domain wall motion in chiral BN-R and racemic BN-rac crystals using AC magnetic susceptibility.

The contributions of switching, slide, creep and Debye relaxation modes of the domain wall motion in chiral BN-R and racemic BN-rac samples were distinguished. In chiral BN-R crystals, transitions to the creep and Debye relaxation modes were observed at  $T=7$  and  $5$  K, whereas in racemic BN-rac crystals the same transitions occurred at higher temperatures  $T=13$  and  $9$  K, respectively.

Thus, we observed influence of chirality on the transition temperatures in slide to creep to relaxation modes. At the same time, chirality does not affect the switching and slide modes of the domain wall motion.



Cole-Cole diagram ( $\chi''$  vs  $\chi'$ ) in chiral BN-R (up) and racemic BN-rac (down) samples at  $T = 2 - 9$  K. The inset shows  $\chi''(\chi')$  dependence in BN-R crystals at  $T = 5$  K.

**24 August**

Wednesday

17:30-19:00

poster session  
24PO-K2

**“Magnetism in Biology  
and Medicine”**

24PO-K2-1

**RUNNING PULSE MAGNETIC FIELD INFLUENCE ON LYMPHOCYTES***Vyshenskaya T.<sup>1</sup>, Safronova E.<sup>1</sup>, Rodionova V.<sup>1,2</sup>, Ivanov A.<sup>3</sup>*<sup>1</sup> Lomonosov Moscow State University, Faculty of Physics, Magnetism division,  
119991 Moscow, Russia<sup>2</sup> Immanuel Kant Baltic Federal University, 236041 Kaliningrad, Russia<sup>3</sup> OAO "EPZ", 391351 Ryazanskaya obl, Elatma, Russia

Magnetic fields now are widely used for therapy. It was shown that effect on human body and cell cultures strongly depends on magnetic field parameters [1]. The mostly effective for medical purposes is the device ALMAG (product of OAO "EPZ") working in a running pulse mode in a range of biologically active frequencies 4-16 Hz.

For registration cell reaction on magnetic field we used coherent phase microscope (CPM) Airyscan developed in the Institute for Radioengineering, Electronics and Automation (Moscow, Russia) [2]. One of important advantages of this method is a high sensitivity of CPM method to changes in physical-chemical properties of biological samples. The optical path length difference (OPLD) or phase thickness measured with CPM instruments in different domains of the object, serves as the informative optical parameter used for visualization of individual cells or intracellular organelles. Metabolically-dependent variations of CPM images reflect changes in the functional state of biological objects.

We studied influence of ALMAG-01 field on a functional state of immune system cells – lymphocytes. The tube with a cell's suspension was radiated with a pulse magnet field (frequency 6.25 Hz, 20 mT) for a 10 min (time of a single standard medical procedure) under 37 °C. Control tube was incubated under the same conditions.

After the procedure functional state of cells was studied by a CPM method [2]. The main measured value was phase thickness of individual cells. As was previously shown [3] for individual cells their phase thickness and, correspondingly, mean refractive index, correlate with a functional state.

The results show that the device ALMAG-01 doesn't change functional state of lymphocytes, but reversibly rearrange chromatin distribution inside cell nucleus. After 1.5 h after the procedure the distribution on phase thickness of cells in suspension becomes as it was before the magnetic field procedure.

[1] Binhi V.N. Magnetobiology, Academic Press 2002 San Diego - San Francisco - New York - Boston - London - Sydney – Tokyo.

[2] Tychinsky V.P., Tikhonov A.N. "Interference Microscopy in Cell Biophysics. Principles and methodological aspects of Coherent Phase Microscopy", Cell Biochemistry and Biophysics, 58(3): 107-1016 (2010).

[3] Tychinsky V.P., Kretushev A.V., Vyshenskaya T. V., Tikhonov A.N. Coherent phase microscopy in cell biology: visualization of metabolic states, Biochim. Biophys. Acta. 1708: 362-366 (2005).

## MAGNETIC TWEEZERS BASED ON AMORPHOUS FERROMAGNETIC MICROWIRES FOR BIOLOGIC APPLICATION

Safronova E.<sup>1</sup>, Rodionova V.<sup>1,2</sup>, Vyshenskaya T.<sup>1</sup>, Attaullakhanov F.<sup>3</sup>, Perov N.<sup>1</sup>

<sup>1</sup> Lomonosov Moscow State University, Faculty of Physics, Magnetism division, 119991 Moscow, Russia

<sup>2</sup> Immanuel Kant Baltic Federal University, 236041 Kaliningrad, Russia

<sup>3</sup> Lomonosov Moscow State University, Faculty of Physics, Biophysics division, 119991 Moscow, Russia

In comparison with optical tweezers [1], widely used for the manipulation of nano- and micro-objects in medicine and biology, magnetic tweezers (technique using inhomogeneous magnetic field to move magnetic objects) has an important advantage: the controlled object is not affected directly by the electro-magnetic field of high intensity and therefore it is not overheated. There are numerous successful implementation of this technique. For example, in [2] magnetic tweezers were used to stretch the DNA molecule by means of manipulation of attached magnetic nanoparticles. Permanent magnets with a specially designed ends were used as sources of magnetic field. The magnetic glass-covered microwires have several advantages [3, 4] and could be more effectively used as magnetic micromanipulators. This work is aimed to demonstrate the properties of the magnetic tweezers built using two glass-covered magnetic microwires.

Magnetic properties of the microwires were investigated by vibrating sample magnetometer – “LakeShore” VSM (7400 series), in the field range  $\pm 10$  kOe, and by the hand-made vibrating sample magnetometer with high magnetic field resolution – 0.02 Oe in the low magnetic fields. It was found that microwires made of  $\text{Fe}_{77,5}\text{B}_{15}\text{Si}_{7,5}$  ( $d = 100 \mu\text{m}$ ,  $d$ -diameter of microwires) and  $\text{Co}_{83}\text{Fe}_7\text{C}_1\text{Si}_7\text{B}_2$  ( $d = 30 \mu\text{m}$ ) alloys, can be used for making magnetic tweezers, due to their low coercivity ( $H_C = 0.9$  Oe and  $H_C = 0,024$  Oe, correspondingly) and rather high permeability. Owing to these properties the magnitude of their magnetic induction can be simply controlled by changing the external magnetic field. Theoretical estimations show that the force  $F$ , which a microwire exerts on the object with characteristic size of  $r = 1 \mu\text{m}$  at the distance of  $50 \mu\text{m}$  is sufficient to move the object:  $F \sim 0,7$  nN. Value of force  $F = -\text{grad}(MB)$  varies, depending on the magnetic moment of the manipulated object,  $M$ , and induction out of microwires,  $B$ .

For the pilot study the microparticles Carboxyl Ferro-Magnetic ( $r = 1 \text{ mkm}$ ,  $r$  – radius of the particle) were used as a manipulated object. The displacement of microparticles caused by the magnetic field of the microwires was observed with help of the metallographic microscope MIM 8. The magnetization of the microwires (the manipulators) was realized by the electromagnets. The magnetic field in the location of the particles was calibrated against the data of  $\text{Co}_{83}\text{Fe}_7\text{C}_1\text{Si}_7\text{B}_2$  microwire bend in the magnetic field of the  $\text{Fe}_{77,5}\text{B}_{15}\text{Si}_{7,5}$  microwire (the task of the mechanics about the beam bend was used). The possibility of the magnetic particles movement in different directions via the microwires magnetic field was shown. The critical magnetic field for uncontrollable behavior of magnetic particles was determined.

[1] Ashkin A., Phys. Rev. Lett. **24**, 156 (1970). DOI:10.1103/PhysRevLett.24.156

[2] Seidel R., Klaun D., [http://www.biotec.tu-dresden.de/cms/fileadmin/research/biophysics/practical\\_handouts/magnetictweezers.pdf](http://www.biotec.tu-dresden.de/cms/fileadmin/research/biophysics/practical_handouts/magnetictweezers.pdf)

[3] Zhukova V., Zhukov A., Gonzalez J., Blanco J.M., J. Magn. Magn. Mater. 254-255 (2003) 182-184.

[4] Larin V.S., Torcunov A.V., Zhukov A., Gonzalez J., Vazquez M., Panina L., J. Magn. Magn. Mater. 249 (2002) 39-45.

## APPLICATION OF FERRIMAGNETIC NANO-PARTICLES IN CHEMOTHERAPY, HYPERTHERMIA AND MRI CONTRASTING

*Brusentsov N.A.<sup>1</sup>, Pirogov Yu.A.<sup>2</sup>, Polyanski V.A.<sup>3</sup>, Golubeva I.S.<sup>1</sup>, Anisimov N.V.<sup>2</sup>, Gulyaev M.V.<sup>2</sup>,  
Nikitin M.P.<sup>4</sup>, Yuriev M.V.<sup>4</sup>, Brusentsova T.N.<sup>4</sup>, Nikitin P.I.<sup>4</sup>*

<sup>1</sup> N.N. Blokhin Russian Cancer Research Center, RAMS, Moscow, 115478, Russia

<sup>2</sup> Research Center for Magnetic Tomography and Spectroscopy,

M.V. Lomonosov Moscow State University, Moscow, 119991, Russia

<sup>3</sup> Institute of Mechanics, Moscow State University, Moscow, 117192, Russia

<sup>4</sup> A.M. Prokhorov General Physics Institute, RAS, Moscow, 119991, Russia

Last time, developments of chemotherapy drugs on the base of ferrimagnetic substances became high interest subject in medicine and medical physics. Tissues absorbing the preparation change sharply magnetic characteristics - magnetic susceptibility and times of spin relaxation. Therefore selective accumulation of drug just in a lesion zone creates good conditions for monitoring and forcing of treatment process for account of magnetic hyperthermia application with following extraction of breakup substances. For visualization of lesion, it is suitable to use magnetic resonance imaging (MRI) method. In the case, ferrimagnetic preparation may be considered as a contrast agent which stimulates strong lowering of MRI-signal in the drug accumulation zone.

We synthesized citrate-ferrite (CF) particles containing  $\text{Fe}_3\text{O}_4$  with size 25-50 nm, applied them for early diagnostics of tumor in metastasis stage and tested the preparation in experiments on the female mice C57Bl/6j with inoculated adenocarcinoma of mammary gland in nodule form (the size about 10 mm). Besides electric sensor control with application of BioMag equipment [1], it was used 7 Tesla MRI scanner BioSpec 70/30 (Bruker Co.) to inspect the process. The mice were anesthetized by intra-abdominal injection of Zoletil 100 preparation. Hyperthermia (heating up to +46 °C during 30 min) fulfilled with help of NdFeB bandage creating alternate (0.88 MHz) magnetic field 0.2 Tesla from 150 W power current source [2,3].

Citrate-ferrite accumulation in tumor affected hypodermic region was revealed on MRI images in some (2-24) hours as MRI signal lowering. It was particularly visible on T2\* images resulted by gradient echo method that is equivalent to negative contrast agent influence [3]. Additional tool promoting to higher CF concentration in tumor tissue appeared using of the foregoing alternate magnetic field. Variable gradient magnetic fields of MRI scanner also promoted to the same process.

CF preparation was injected to 8 mice in 1.0 ml quantity. Combination of chemotherapy and magnetic hyperthermia for Ca755 tumors with dimensions about 10 mm diameter supplies 60% lowering of metastasis volume and raises survival rate of female mice up to 300%. In the case of 15-mm tumors, application of the procedure described above with systematic repetition of the therapy after relapse enlarges survival potential up to 220%.

Citrate-ferrite nano-particle drugs for chemotherapy in combination with magnetic hyperthermia are the good tool of tumor treatment. Simultaneously, these particles act as powerful contrast agent during MRI observation of the process because they are accumulated inside tumor and give strong magnetic resonance signal from paramagnetic  $\text{Fe}_3\text{O}_4$  clusters.

[1] M. Nikitin, P. Vetoshko, N. Brusentsov, P. Nikitin, *J. Magn. Magn. Mat.*, **321** (2009) 1658.

[2] U. Hafeli, K. Gilmore, A. Zhou, S. Lee, M. Hayden, *J. Magn. Magn. Mat.*, **311** (2007) 323.

[3] N. Brusentsov, Yu. Pirogov, N. Anisimov, et al., *Am. Inst. Phys.*, **1311** (2010) 447-451.

24PO-K2-4

## MAGNETIC PROPERTIES AND APPLICATION OF BIOMINERAL PARTICLES

*Stolyar S.V.*<sup>1,2</sup>, *Bayukov O.A.*<sup>1,2</sup>, *Ladygina V.P.*<sup>3</sup>, *Iskhakov R.S.*<sup>1,2</sup>, *Balaev D.A.*<sup>1,2</sup>, *Ishenko L.A.*<sup>1</sup>,  
*Inzhevatin E.V.*<sup>1,3</sup>, *Dobretsov K.G.*<sup>4</sup>

<sup>1</sup> Siberian Federal University, Krasnoyarsk, Russia

<sup>2</sup> Kirensky Institute of Physics, Siberian Branch of RAS, Krasnoyarsk, Russia

<sup>3</sup> ISCOESR of Krasnoyarsk Science Centre, Siberian branch of RAS, Krasnoyarsk, Russia

<sup>4</sup> Clinical hospital of Krasnoyarsk railway station

Advantages of microorganisms as potential sources of nanoparticles consist in ability in controllable growing of their biomass and the production of nanocrystals with assigned characteristics. In this work the method of ferrihydrite nanoparticles synthesis by biomineralization of iron with iron-reducing bacteria is proposed. The *Klebsiella oxytoca* bacterial culture isolated from sapropel of the Borovoe Lake (Krasnoyarsk Territory) was used. Ferrihydrite is antiferromagnetic with temperature of magnetic ordering higher than room temperature ( $T_N=340$  K). In consequence of small sizes of particles ( $d<100$  Å) magnetic moments of  $\text{Fe}^{3+}$  ions on the surface of particles are non-compensated and form parasitic integral magnetic moment. The method of Mössbauer spectroscopy showed four nonequivalent positions for ferric iron in investigated bacterial ferrihydrite. Quadrupole splitting of these positions have well defined disjoint range of values:  $\text{QS}\{\text{Fe}^{3+}(1)\}=0.43-0.67$  mm/s,  $\text{QS}\{\text{Fe}^{3+}(2)\}=0.83-1.07$  mm/s,  $\text{QS}\{\text{Fe}^{3+}(3)\}=1.22-1.52$  mm/s and  $\text{QS}\{\text{Fe}^{3+}(4)\}=1.59-1.93$  mm/s.

The changes of structures and magnetic properties of nanoparticles in the process of microorganism cultivation depending on culture aging, illumination etc were disclosed. Some aspects of biological application of nanoparticles were investigated, in particular ability of sorption some antibiotics on their surfaces was shown, survival of animals after intraperitoneal injection of nanoparticles was studied, and possibility of control of their movement in cartilaginous and bone tissues with the help of magnetic field were shown.

24PO-K2-5

## A BASIC THEORY OF IMMUNOMAGNETIC SEPARATION

*Kashevsky S.B.*

A.V. Luikov Heat and Mass Transfer Institute, National Academy of Sciences of Belarus  
15, P. Brovki Str., 220072, Minsk, Belarus

Presently, immunomagnetic cell separation became an important addition to optical and other traditional means of studying cells. Remarkably, the introduction of this method into industry was so swift that many of its scientific and engineering aspects still remain unexamined. A widespread scheme of immunomagnetic separation is precipitation of labeled cells on the lateral surface of a vertical test tube in the nonuniform magnetic field created by a transversally magnetized rod-like permanent magnet positioned right up against the tube. Here we consider the basic model that embodies the key properties of such mode of separation, namely the set of diametrically magnetized cylindrical rod and the adjacent cylindrical container. We assume the magnet to be of infinite length (with diameter  $R_m$ , and magnetization  $I_m$ ), magnetic beads contain a superparamagnetic filler with

the volume concentration  $c$ , magnetization curve of beads can be approximated by simple function (supporting experiments are presented)

$$I = I_s(1 + I_s/\chi H)^{-1}, \quad I_s = cI_{sb}, \quad I_{sb} \text{ is the saturation magnetization of magnetic particles,}$$

and consider the inertialess motion of labeled cell ignoring complications arising from magnetic and hydrodynamic interactions within a real multicomponent suspension. The choice of cylindrical magnet is interesting because the spatial distribution of its magnetic field magnitude is axially symmetric,

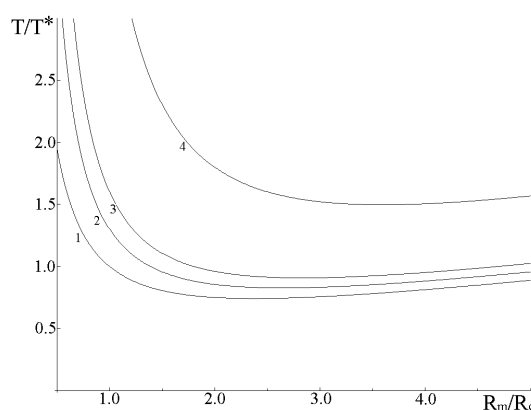
$$H = 2\pi I_m R_m^2 / R^2, \quad R \text{ is the distance to the magnet axis,}$$

so that magnetic extraction of labeled cells proceeds in the same manner at any azimuthal position of the cylindrical container around the magnet. Under the above simplifying conditions, explicit relations are derived between main performance characteristics of the system and its geometrical and physical parameters. They are the time  $T$  of full separation, the optimal magnet to container radii ratio,  $\rho$ , which minimizes the separation time  $T$ , and dynamic separation function  $\varphi(t_s)$  that characterizes a fraction of cells,  $\varphi$ , deposited on the surface of the container in time interval  $t_s$ . The separation time is obtained in the form

$$T = \frac{T^*}{10} [3 + 5k + (1+k)\rho + (4 + 40k/3)\rho^{-1} + (2 + 20k)\rho^{-2} + 16k\rho^{-3} + 16k\rho^{-4}/3]$$

( $R_c$  is the container radius,  $M_s$  is the effective magnetic moment of a labeled cell at saturation,  $\eta$  is the liquid viscosity,  $d$  is the cell diameter). The time  $T^* = 15\eta d R_c^2 / (M_s I_m)$  determines the full separation time for the case  $R_c = R_m$ , and  $k=0$ .

Figure illustrates the function  $T(R_m/R_c)$  for different  $k$ :  $k=0$  (1), 0.05 (2), 0.1 (3), 0.5 (4). Parameter  $k$  is zero if the beads are magnetically saturated, increasing  $k$  indicate departure from the saturation.



Apart from being of utility for designing cylindrical systems, the constructed theory can serve as the basic one for comparative characteristic of systems with different shapes, as well as for studying the effects of such factors as magnetic interaction of beads and hydrodynamic entrainment of unlabeled cells by the labeled.

24PO-K2-6

## SYNTHESIS AND INVESTIGATION OF $\text{La}_{1-x}\text{Ag}_y\text{MnO}_3$ FINE PARTICLES

*Kushnir A.E.<sup>1</sup>, Markelova M.N.<sup>1</sup>, Kaul A.R.<sup>2</sup>*

<sup>1</sup> Lomonosov Moscow State University, department of Materials Sciences, Moscow, Russia

<sup>2</sup> Lomonosov Moscow State University, Chemistry department, Moscow, Russia

Local hyperthermia is one of the most effective methods of cancer treatment that is based on cancer cells hypersensitivity to heating in comparison with the healthy ones. Injecting ferromagnetic particles with Curie temperature ( $T_c$ ) in the range of 43-50 °C in the place of the tumour localization we provide local overheat. In our work it was suggested to use solid solutions on the basis of  $\text{La}_{1-x}\text{Ag}_y\text{MnO}_{3+d}$  with perovskite structure. These solid solutions allow preparation of the materials with necessary  $T_c$ . The purpose of the work lies in the research of the dependence of magnetic properties of  $\text{La}_{1-x}\text{Ag}_y\text{MnO}_{3+d}$  powders on a method and synthesis conditions. The



major methods of such solid solutions preparation are the so-called "paper" method and the method of aerosol pyrolysis.  $\text{La}_{0.8}\text{Ag}_{0.17}\text{MnO}_{3+d}$  powder was synthesized by both methods. These two techniques are quite different: in case of the "paper" method of synthesis, the powder is obtained by burning ashless paper filters impregnated with special solution and further annealing at 800 °C,  $p(\text{O}_2)=1$  bar, for 30 hours. In case of synthesis by aerosol pyrolysis the powder is obtained by running the aerosol, generated by ultrasound, through the hot reactor. However, for the final materials preparation by aerosol pyrolysis we need additional oxidation of the product at 800 °C,  $p(\text{O}_2)=1$  bar. In our work we studied the influence of annealing oxidising time (5, 30 and 100 hours) on magnetic properties of powders. Thus, thorough study of the powders properties synthesized by "paper" method and method of pyrolysis with various time of oxidation is carried out. All samples were investigated by X-ray diffraction (XRD) that showed that samples were single-phase with the structure of rhombohedrally deformed perovskite. The cation structure control was carried out by energy-dispersive X-ray (EDX) and mass spectrometry with the inductive-connected plasma. Duration of pyrolysis powders oxidation does not influence the structural nature of a material (we see no shifts or lines broadening on X-ray pattern). However, magnetic properties of samples vary essentially:  $T_c$  grows with the increase of oxidation time that can be connected with samples sintering. Using method of iodometric titration it was additionally demonstrated that average degree of oxidation of manganese does not depend on the oxidation time thus confirming the dependence of magnetic properties from samples sintering. Temperature of stabilisation ( $T_s$ ) study in variable magnetic field showed other dependences:  $T_s$  and capacity of a warming up reach the maximum at 30 hours that we connect with the peculiarities of samples preparation for the given measurements in which course splitting of fritted units takes place leading to the fall of  $T_s$  and capacity of a warming up.

24PO-K2-7

## MÖSSBAUER AND MAGNETIC STUDY OF SOLID PHASES FORMED BY DISSIMILATORY IRON-REDUCING BACTERIA

*Chistyakova N.I.*<sup>1</sup>, *Rusakov V.S.*<sup>1</sup>, *Shapkin A.A.*<sup>1</sup>, *Pigalev P.A.*<sup>1</sup>, *Kazakov A.P.*<sup>1</sup>, *Zhilina T.N.*<sup>2</sup>,  
*Zavarzina D.G.*<sup>2</sup>, *Lančok A.*<sup>3</sup>, *Kohout J.*<sup>4</sup>, *Greneche J.-M.*<sup>5</sup>

<sup>1</sup> Faculty of Physics, M.V. Lomonosov Moscow State University,  
Leninskie gory, 119991 Moscow, Russia

<sup>2</sup> Winogradsky Institute of Microbiology, Russian Academy of Sciences,  
Prospect 60-letiya Oktyabrya 7/2, 117312 Moscow, Russia

<sup>3</sup> Institute of Inorganic Chemistry, v.v.i., 25608 Husinec – Řež, Czech Republic

<sup>4</sup> Faculty of Mathematics and Physics, Charles University, Ovocný trh 5 116 36 Praha 1,  
Czech Republic

<sup>5</sup> Laboratoire de Physique de l'Etat Condensé, UMR CNRS 6087  
Université du Maine F72085 Le Mans Cedex 9, France

One of the possible ways of iron mineral formation is an extracellular reduction of amorphous Fe (III) oxides and hydroxides by dissimilatory iron-reducing bacteria. Thermophilic anaerobic iron-reducing bacterium *Thermincola ferriacetica* (strain Z-0001) was isolated from the ferric sediments of hot springs Stolbovskie of Kunashir Island ( $T=60-65$  °C and pH 6.8–7.0). Anaerobic alkaliphilic bacterium *Geoalkalibacter ferrihydriticus* (strain Z-0531) was isolated from bottom sediments from the weakly mineralized soda Lake Khadyn, optimal conditions of strain growth were pH 8.6,

T = 35°C. Both bacteria used amorphous synthesized ferrihydrite (SF) as an electron acceptor, and acetate (CH<sub>3</sub>COO<sup>-</sup>) as an electron donor for the anaerobic growth.

The kinetics of iron mineral formation by *T. ferriacetica* have been investigated earlier by Mossbauer spectroscopy methods [1-2]. For more detailed analysis of solid phases which were formed during the bacterium growth we prepared the new series of samples obtained by *T. ferriacetica*. The concentration of Fe(III) that was contained in SF was 90 mM. The incubation time varied from 1 to 10 days. For the cultivation of *G. ferrihydriticus* the sodium acetate (2 g/l) and varied concentration of the SF 5 mM – 150 mM were added to the anaerobic prepared alkaline mineral medium. The anthraquinone-2,6-disulfonate (AQDS) with concentrations 0 g/l – 1 g/l was also added to the cultivation medium as the additional electron acceptor.

Mössbauer investigations of solid phases that were formed during the reduction of SF by *T. ferriacetica* and *G. ferrihydriticus* were carried out at room, liquid nitrogen and liquid helium temperatures in the presence or the absence of an external magnetic field (6 T). The magnetization M(T,H) was measured using VSM (Lake Shore 7400 System) in the temperature interval 80-300 K and magnetic field up to 10 kOe. It was performed ZFC and FC measurements of M(T) and measurements of hysteresis loops at some temperatures.

It was shown that the samples obtained during the growth of *T. ferriacetica* and the magnetically ordered phases formed by *G. ferrihydriticus* were nonstoichiometric magnetite, or a mixture of magnetite and maghemite. The samples obtained during exponential phase of growth of *T. ferriacetica* were consistent with the presence of superparamagnetic nanoparticles. AQDS concentration affects the size of particles of magnetically ordered phases formed by *G. ferrihydriticus*.

[1] N.I. Chystyakova, V.S. Rusakov, D.G. Zavarzina, et al., Czechoslovak Journal of Physics 50, (2005) 781.

[2] Chistyakova N.I., Rusakov V.S., Koksharov Yu.A., Zavarzina D.G., Greneche J.-M., *Solid State Phenomena* **152-153** (2009) 431.

24PO-K2-8

## STRUCTURAL AND MAGNETIC CHARACTERISTICS OF NEW NANOBIOMAGNETICS ON THE BASIS OF POLYMERIC MATRIX

*Aleksandrova G.<sup>1</sup>, Pokatilov V.<sup>2</sup>, Konovalova A.<sup>2</sup>*

<sup>1</sup> A.E. Favorsky Irkutsk Institute of Chemistry SB RAS, 1 Favorsky st. 664033 Irkutsk, RF

<sup>2</sup> Moscow State Institute of Radioengineering, Electronics and Automation.

78 Vernadsky av. 119454, Moscow, RF

Magnetic properties of nanoparticles, quite different from those of usual magnets, are determined by numerous factors. The most important ones are particles' chemical composition, size and shape. As for magnetic particles dispersed in polymeric matrices, matrix nature, type of dispersion, as well as particle-particle and matrix-particle relationships are also relevant. The given work is aimed to establish the dependence between composition and magnetic state of magnetite particles dispersed in biocompatible polysaccharide matrix.

Nanodispersed magnetite has been obtained by a modified hydrolytic sol gel method. An important technological feature of the technique used is the participation of polysaccharide arabinogalactan as stabilizing matrix in the reaction. Structures and morphologies of the ferroarabinogalactan samples has been characterized by a wide complex of spectral methods,

including atomic absorption and X-ray phase analyses, UV and IR spectroscopy, transmission and scanning electron microscopy.

Magnetic states of iron ions in the nanobiocomposites of magnetite contents of 2.9-17.3 % have been determined by the Mössbauer spectroscopy at room temperature. Size effect has been shown as a change of magnetic properties of the samples at varying ratio between magnetic component and dielectric arabinogalactan matrix. Contributions of paramagnetic, superparamagnetic and ferromagnetic components into magnetic state of the nanoparticles depending on the content of magnetite in the samples has been estimated. Dependence between magnetic state of iron ions and size distribution of magnetically active nanoparticles has been established.

The dependence found between magnetic and structural characteristics of the nanobiocomposite create the prerequisites for expedient synthesis of new magnetically active materials. Controlled space-isolation of particles, biocompatibility and moderate magnetization make these materials promising as magnetically controlled diagnostic and therapeutic agents.

Support by SB RAS integrate project № 47 is acknowledged.

24PO-K2-9

## **COMPARISON OF METHODS IN COMPLEXITY ANALYSIS OF FOETAL HEART RATE VARIABILITY FROM MAGNETOCARDIOGRAM**

*Amoroso M.<sup>1,2</sup>, Rassi D.<sup>2</sup>*

<sup>1</sup> University of the West Indies, St. Augustine, Trinidad & Tobago

<sup>2</sup> Swansea University, Wales, UK

Continuous foetal monitoring methods that can improve the classification of foetal signals into reassuring, non-reassuring and ominous category are a very useful aid to clinicians in making decisions for intervention in the final trimester. Previous results from other research in this area have indicated that analysis of complexity in the foetal signal may be of utility in distinguishing foetal states when used along with more frequently used linear parameters.

This study investigates the complexity of the foetal HRV signal during periods of high correlation between HF and LF determined by the method of time domain analysis described in Rassi et al, 2002. Recording from normal foetuses are first analysed to determine whether baseline complexity remains within a range such that changes may precede or be associated with a non-reassuring foetal state. Using foetal R-R heart rate variability traces from 20-minute magnetocardiographic recordings, each recording is processed by filtering the HF, LF, VLF frequency ranges recommended by the Task Force of the European Society of Cardiology and the North American Society of Pacing and Electrophysiology, 1996, and extracting dominant spontaneous oscillations using ensemble elementary mode decomposition. The signals are subjected to complexity analysis determining Lempel Ziv complexity and sample entropy, where parameter values are compared at intervals for the duration of the recording.

## LAWS OF ELASTICITY IN THE PHYSICAL PROCESSES INFLUENCE OF PARAMETERS (TPH) ON THE PROPERTIES AND STRUCTURAL PHASE TRANSITIONS

*Polyakov P.I.<sup>1</sup>, Mazur A.S.<sup>2</sup>*

<sup>1</sup> Inst. For Phys. of Mining Processes, R. Luxemburg sr., 72, Donetsk, 83114, Ukraine

<sup>2</sup> Inst. for Phys. and Eng. n.a. O.O. Galkin, R. Luxemburg sr., 72, Donetsk, 83114, Ukraine

The present paper deals with the analysis of experimental results taking into account mechanisms brought by the bulk elastic energy transformed by the thermodynamic parameters, temperature, magnetic fields, high hydrostatic pressure (T-H-P). An effect of the external parameters is considered through the separation of critical lines and points of the “cooling-heating” effect in the course of analysis of linear elastic evolution of properties in sign alternating and crossing effects of elastic stress energy as well as their value for structural reorganizations at reversible volume changes (structural phase transformations of types I and II). [1,2]

An explanation of the direct and reverse hysteresis effect in the range of the structural phase transitions I and II is suggested and the secondary signs of changes of phase state properties in the wide range of structures are formulated. The regularities of formation of a structural phase transition at 0 K are stated with separating the position of the triple point and the change of the properties and phase states with the elements of superconducting and conducting properties. [3]

We have marked out regularities of changes of  $\text{Eu}_{0.55}\text{Sr}_{0.45}\text{MnO}_3$ ,  $\text{Sm}_{1-x}\text{Sr}_x\text{MnO}_3$  properties and its isotopic analogue with oxygen substitution in the course of formation of the structural phase transition of type I at 0 K and evolution of the boundaries of phase states. We suggest new approaches for defining of critical lines and points in physical processes of the separation of the boundaries of phase states. [4,5]

We have carried out the analysis of elastic linear changes of resistivity and the jump of properties under the effect of three parameters in polycrystal  $\text{La}_{0.56}\text{Ca}_{0.24}\text{MnO}_3$ . Using the examples of linear changes of resistivity, structure parameters, magnetization and magnetostriction of the structural phase transitions of types I and II in metals, semiconductors, dielectrics under T-P-H influence, the governing role of the laws of bulk elasticity is defined [2]. The analysis described below underlines the dominating role of elastic internal stresses (EI stresses) with the energy that formed the dynamics of interactions determining the structure state, properties and critical phase transformations in magnet-containing media.

[1] P.I. Polyakov, S.S. Kucherenko, JMMM. 278 (2004) 138-155

[2] P.I. Polyakov, T.A. Ryumshyna. Magnetism and Laws of Bulk Elasticity. TransWorld Research Network. Kerala. India. (2009).

[3] A.D. Bruce, R.A. Cowley. Structural Phase Transitions. Taylor, Fransis Ltd., London, 1981.

[4] A.I. Abramovich, O.Yu. Gorbenko, A.R. Kaul, L.I. Koroleva and A.A. Michurin, Phys. Tverd. Tela. 46(9) (2004) 1657.

[5] A.M. Kadomtseva, Yu.V. Popov, G.P. Vorob'ev, K.I. Kamilov, V.Yu. Ivanov, A.A. Muhin and A.M. Balbashov, Phys. Tverd. Tela. 42(6) (2000) 1077.

24PO-K2-11

## OPTICAL ACTIVITY OF OIL SOLUTIONS

Edelman I.<sup>1</sup>, Sokolov A.<sup>1</sup>, Zablude V.<sup>1</sup>, Petrakovskaya E.<sup>1</sup>, Martyanov O.<sup>2</sup>, Shubin A.<sup>3</sup>, Idrisov A.<sup>3</sup>

<sup>1</sup> Kirensky Institute of Physics SB RAS, Krasnoyarsk, Russia

<sup>2</sup> Borekov Institute of Catalysis SB RAS, Novosibirsk, Russia

<sup>3</sup> Siberian Federal University, Krasnoyarsk, Russia

Magnetic circular dichroism (MCD), optical absorption and electron paramagnetic resonance (EPR) in mineral oil and its component solutions have been investigated. Crude oil from several fields was dissolved in gasoline in various concentrations. Asphaltite (№2) and asphaltenes (№1,3) solutions were investigated too. Elemental composition of samples was determined by X-ray fluorescent analysis (RFA) with EDXRF Quant X-ARL. Optical absorption spectral dependences were measured in range of 250-2250 nm. MCD was measured using the light polarization modulation technique in the wavelength region of 300-600 nm with an accuracy  $10^{-5}$  and spectral resolution  $\sim 20 \text{ cm}^{-1}$ . EPR spectra were recorded with the ST/X-2544 spectrometer. All measurements were made at room temperature.

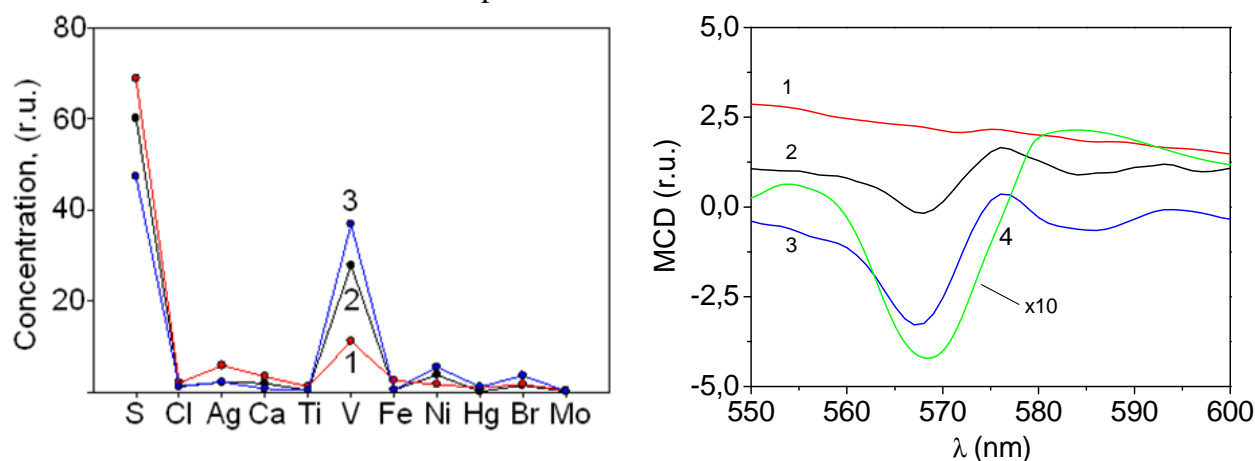


Fig. 1. Left: elemental composition of 3 samples mentioned above; right: MCD spectra of the same samples (curves 1-3, correspondingly) and of the oil solution (curve 4).

All asphaltite and asphaltene samples and some oil solution contain different vanadil (vanadic etio-porphyrins with the general chemical formula  $C_{32}H_{36}N_4OV$ ) concentration. Besides, other paramagnetic element Ni presents in samples.

According to EPR data all investigated samples contain vanadil. The vanadil line is centered at  $H=321.88 \text{ mT}$ , line width is  $1.6 \text{ mT}$ . The radical line at  $H=325.3 \text{ mT}$  of  $0.8 \text{ mT}$  width is observed near to vanadil line. The vanadil line intensity is approximately proportional to this element concentration in a sample. Weak features are observed near 400 and 570 nm in the optical absorption spectra. MCD has been revealed in the region of 570 nm only for samples containing vanadil, i.e. MCD is due to  $V^{4+}$ . The  $V^{4+}$  optical spectra were investigated in several works and the line near 400 nm was shown to be associated with charge transfer transition  $O^{2-}-V^{4+}$  [1]. The line 570 nm is too weak in the absorption spectra, and possible because of this reason it is not referred in literature, but it is very well resolved in the MCD spectrum. The nature of this line and perspective of its using for the oil analysis are discussed.

The work is supported by Siberian Branch of RAS Integration Project №.118.

[1] Sviridov D.T., Sviridova R.K., Smirnov U.F. Optical spectra of transition metal ions in crystals, M., "Nauka", 1976.

## RELATION OF SOIL MAGNETIC PROPERTIES WITH INDUSTRIAL POLLUTION

*Samsonova V.<sup>1</sup>, Rodionova V.<sup>1,2</sup>, Koptsik S.<sup>1</sup>, Perov N.<sup>1</sup>*

<sup>1</sup> Lomonosov Moscow State University, Faculty of Physics, 119991 Moscow, Russia

<sup>2</sup> Immanuel Kant Baltic Federal University, 236041 Kaliningrad, Russia

For study of the polluted soils (for the detection and characterisation of pollution level) the magnetic measurements and methods are used in addition to the soil chemical and the geological analysis. Measurements of soils magnetic susceptibility proved to be suitable for the quick analysis of large territory and for spatial delineation of polluted regions [1, 2]. Moreover magnetic control methods are cheaper and can give information about the composition, shape and size of particles of ferrimagnetic minerals. For the correct magnetic detection of pollution composition and level the correlations between magnetic and soil properties are important.

In present work the results of the investigations of soil magnetic properties in the surroundings of the “Pechenganikel” smelter (Russia) are presented. The soils probes were taken from the surface organogenic and underlying mineral horizons of podzols at intensively studied [3] heavy polluted (1, 8 km) and background (41 km from the smelter) sites. The probes were sieved and homogenised with the help of the mills with agate balls. The influence of the pollution level, the soil depth, and the type of the pretreatment on magnetic properties was studied and the correlation between magnetic and soil-science results was analyzed.

For magnetic properties investigations we used the vibrating sample magnetometer by “LakeShore” (7400 System). All samples show ferromagnetic behavior. The hysteresis loops and the temperature dependence of the magnetic properties were measured for few samples of each soil probe in temperature range 80-400 K and at the magnetic field up to 16 kOe. The ZFC-FC curve at magnetic field of 500 Oe for the soil probe taken at 8 km from organogenic horizon is presented in the figure. The observed blocking temperature is 330 K. At the temperature  $T=120$  K the abrupt decreasing of the magnetic moment appears and at the temperature  $T=230$  K there are few appreciable peculiarities. We suppose that these transitions are evidences of Verwey and Moren transitions, correspondingly, and conclude that in these soils two types of iron-oxides –  $\alpha\text{Fe}_2\text{O}_3$  and  $\alpha\text{Fe}_3\text{O}_4$  can be identified. The particle size can be determined through common method [4] using detected blocking temperature.

The results suggest the relationship between the magnetic properties of the soil samples, prehtreatment and the distance from the smelter. The results can be used for development of magnetic methods of environmental monitoring. We conclude that the magnetic measurements provide detailed information about the composition, state, and the grain size of iron-oxides, the most common ferromagnetic minerals in soils.

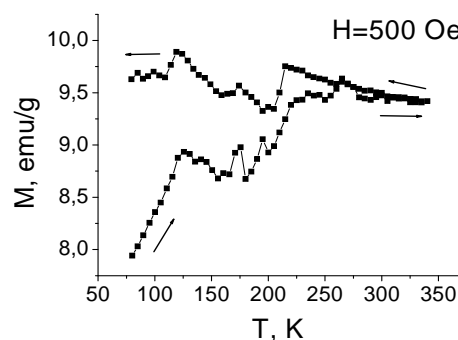
Support by Russian Foundation for Basic Research (project 11-04-01794) is acknowledged.

[1] H. Fialova et al., *J. Appl. Geophys.* **59** (2006) 273– 283.

[2] A. Schmidt et al., *J. Geochem. Explor.* **85** (2005) 109–117.

[3] S. Koptsik et al., *J. Environ. Monit.* **5** (2003) 441–450.

[4] A.V. Prunova et al., *J. Magn. Magn. Mater.* **321** (2009) 3502-3506.



The temperature dependence (ZFC-FC) of the soil magnetic properties in the magnetic field of 500 Oe.

24PO-K2-13

## ROTATING-SAMPLE MAGNETOMETER FOR THE CRYSTAL FIELD PARAMETERS MEASURING.

*Gimaev R.R.<sup>1,2</sup>, Spichkin Y.I.<sup>2</sup>, Tishin A.M.<sup>1,2</sup>*

<sup>1</sup> Faculty of Physics, M.V. Lomonosov Moscow State University, 119991, Moscow, Russia

<sup>2</sup> Advanced Magnetic Technologies and Consulting LLC, 142190, Troitsk, Russia

The method for measuring of the crystal field parameters by means of rotating-sample magnetometer is presented. The measurement is performed by registering the 2<sup>nd</sup>, 4<sup>th</sup> and 6<sup>th</sup> harmonics of the measuring signal, which is proportional to the change of the sample magnetization due to rotation of the sample in magnetic field exceeding the saturation field. Experimentally measured temperature dependence of the amplitudes of these harmonics is used to calculate the crystal field parameters within the frames of the theoretical model proposed in [1].

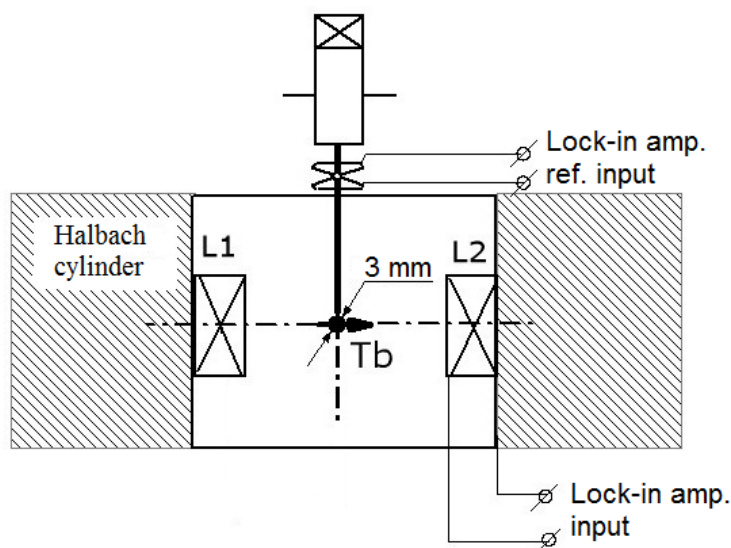
The signal is measured by a digital lock-in amplifier, and the temperature change and stabilization is conducted by a PID controller. The sample and coils (L1, L2) location in the Halbach magnet working bore is presented in the figure. Measurements are made in the automatic mode. The experiment is run by the program, which is written using the LabView 8.2 package.

The program algorithm consists of the blocks stated below:

- 1) Initialization block,
- 2) Block of setting and stabilization of the sample temperature,
- 3) Block of measurement and presentation of raw data in the graph,
- 4) Block of mathematical processing of experimental data,
- 5) Block of saving experimental data to file.

Magnitude of the expected signal was estimated. Test measurements of magnetization of the Tb single crystal along a axis in the permanent magnetic field 2.7 T at room temperature was performed. The results show that

sensitivity of the instruments and the proposed design of the equipment allow to determine crystal field parameters of heavy rare-earth metals. Testing of the control software showed that computer-device communications and execution of the software blocks were correct.



[1] Kuz'min M.D., *Appl. Phys. Lett.*, **84** (2004) 2605

24PO-K2-14

## DNA(Gd<sup>3+</sup>): MAGNETIC PROPERTIES OF NEUTRON ABSORPTION AGENT

*Nikiforov V.N., Koksharov Yu.A.*

M.V. Lomonosov Moscow State University, Faculty of Physics,  
119991, Moscow, Leninskie gory, Russia

<sup>157</sup>Gd is a potential perspective agent for neutron capture cancer therapy. Gd bound to DNA is actual task for use in EPR and NMR investigations because gadolinium ions could be detected as molecular magnetic marker in diagnostics. In the presented work the calculation of concentration of gadolinium in DNA was provided on the base on the SQUID magnetic susceptibility experiments and EPR experiments. The SQUID and EPR data support the fact that Gd – DNA binding for plasmid and cholesteric-phase DNA's takes place. The magnetic investigations give us opportunity to calculate the concentration of Gd<sup>3+</sup> ions binding with DNA. The magnetic results presented are in good accordance with neutron capture data.

The first type of DNA samples was water solution of 2 mg plasmid pEGFP-N1 (A-type) and pDsRed2-C1 (B-type) in 2 ml of water. Molar weight was 2915 kDa. The samples A, B were not treated by gadolinium salts. Ax1, Ax2, Ax3, Ax4 were treated by GdCl<sub>3</sub>, in ratio 1:1, 1:2 and 1:3, Bx1, Bx2, Bx3, Bx4 were treated by Gd(NO<sub>3</sub>)<sub>3</sub>, in the same ratios.

The second type of the samples presented, were molecules of DNA in cholesteric phase. At first, DNA molecules by means of ultrasonic treatment were cutted on 600000 Da parts. The length of molecules was controlled by electrophoresis. Then, were obtained liquid crystal dispersion of DNA molecules (sample 1, with mass 6 mg) The presence of cholesteric phase of molecules of DNA in the sample was detected by means of a circular dichroism spectrum. X-ray analysis confirms presence in the sample of the ordered phase and gives DNA concentration value corresponds to cholesteric phase. The samples of DNA, DNA with La, DNA with Gd were investigated. Constructions DNA with Gd (samples 2,3,4, mass of each sample equals 3 mg ) were synthesized from pure DNA by GdCl<sub>3</sub> water solution treatment. The various ratios between Na and Gd are used.

The maximum local concentration of gadolinium in sample achieve 200 mg/ml (from magnetic data, see below) at ratio Gd/Na higher than 10 times (sample 2). In samples 3 and 4 this ratio equals 3 and 1 consequently. Particles of liquid crystal dispersion keep magnetic properties during more than 1 month. Existence of liquid crystal particles with 4500-5000 Å dimensions are being confirmed with AFM microscopy data.

The calculation of concentration of gadolinium in DNA based on the magnetic susceptibility experiments and EPR experiments. SQUID (superconducting quantum interferometer device) magnetometer is rather sensitive for detecting magnetic response from DNA. EPR experiment is used for determining of g- factor. Measured magnetic susceptibility  $\chi = \text{Pm/H}$  was fitted by the Curie-Weiss equation with constant value of  $\chi_0$ . Namely  $\chi = \chi_0 + C/(T - \Theta)$ , where C is Curie constant,  $\Theta$  – paramagnetic Curie temperature. The calculated value of  $\chi_0$ , C and  $\Theta$  for samples are presented.

	X <sub>0</sub> , emu/gOe	C, emu K/g Oe	Θ, K	Dia- or paramagnetism
DNA	3.5 10 <sup>-6</sup>	8 10 <sup>-5</sup>	-0.4	para
DNA La	1.3 10 <sup>-6</sup>	1.54 10 <sup>-4</sup>	-2.0	para
DNA Gd N2	8.8 10 <sup>-6</sup>	0.02360	4.2	para



24PO-K2-15

## QUADRUPOLE MAGNETIC FIELD PROTECTION FOR MARS SPACECRAFT

Ahmadi T.

Student at Smart High School, Sanandaj, Kurdistan, Iran

In order to travel to the mars, we have to travel outside the Earth for a long time but there are two sources of radiation threaten the health of astronauts and the interior part of spaceship, solar particle events (SPEs) and galactic cosmic radiation (GCR). There isn't any doubt that magnetic field shielding is better than passive shields[1]. This strength of estimated magnetic fields could pass SPEs easily but it passes GCRs partially. GCR consists of protons, alpha particles, and nuclei of heavier elements. We have to provide a method to protect spacecraft from ALL fundamental sources of radiation in deep space.

In a dipolar field, intensity of magnetic field is not homogenous while protection magnetic field has to be homogenous to deflect particles. So the best shape for field is semi-quadrupole field is consisting of two dipolar. These two dipolar fields are generating by two torus-solenoid rings far from spaceship. The strength of magnetic field is high near rings and less near spaceship.

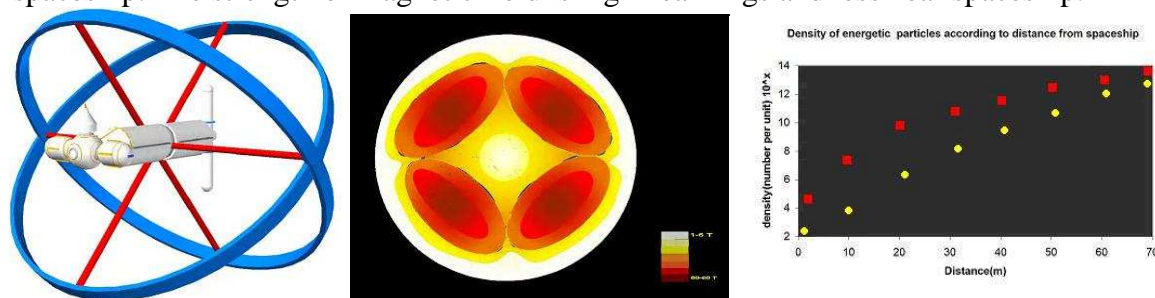


FIG.1) rings with MOK, the intensity of semi-quadrupole field ( $B = \mu I / 4\pi \int d\ell \times \mathbf{r} / r^2$ ) density of two simulated storms basic on the distance from MOK (Red=2.2 MeV, Yellow=400KeV)

Properties of torus-solenoid rings: Thickness of each torus: 1 cm, height of each one: 13 m, number of loops of the solenoid hid in each ring torus: 6500, Radius X= 30 m, Radius Y =18 m, angle between two rings = 90° weight of protection structure= 200-340 tones

Properties of semi-quadrupole field: field intensity near structure: 60 Tesla, field intensity interior the spaceship: 1.5-2.5 Tesla, magnetic field intensity in the boundaries of fields (fields of two rings) =45 Tesla, direction of magnetic field: anti-aligned with solar magnetic field.

The pressure of this solar storm on magnetic field is around  $4 \times 10^5$  gr/cm<sup>3</sup> while magnetic field deviation of protection magnetic field due to a plasma pressure for 2.2 MeV energy is 0.5 and for a storm with 360-410 KeV is 0.3. Radius of magnetopause in this field given by:

$$R_{mp} = (0.8 \times 10^{-8} B^2 / n m i V^2)^{1/6}$$

Radius of magnetopause is 38 meters ( for 2.2 MeV) and 43 meters (for 410 KeV).

It is important that a storm with these properties is not existed. A solar storm consists of particles with various energy and a storm which all of its particles were 2.2 MeV is simulated only for magnetic field examination.

Dyson-Harrop Satellite has the sufficient capacity to produce around electrical current [2]. This system produces at least  $1.7 \times 10^6$  V. Produced energy by DHS is primarily determined by the capacitance of Receiver and RB max (the minimal distance from the main-wire). RB, max is the distance of main wire from cylinder. Basic on the real data simulation, magnetic field of DHS attracts 13 m<sup>3</sup> of a solar storm's electrons and deflect this volume of protons during 50 seconds.

This torus is so thin but it can shield whole the spacecraft will a high strength magnetic field but its mass is less than other designs while it can shield a great part of spaceship.

[1] Shiga D, too much radiation for astronauts to make it to Mars, *New Scientist* 2726, 2009

[2] Harrop B *et al*, (2010), the detection of a Dyson-Harrop Satellite, *Astrobiology Science Conference 2010*

24PO-K2-16

## INVESTIGATION OF RADIATION AND MAGNETIC EFFECTS AT BUBBLE CAVITATION IN LIQUID JET

Kornilova A.<sup>1</sup>, Vysotskii V.<sup>2</sup>, Sysoev N.<sup>1</sup>, Hait E.<sup>1</sup>, Korneeva Y.<sup>1</sup>, Tomak V.<sup>3</sup>

<sup>1</sup> Moscow State University, Russia

<sup>2</sup> Kiev National Shevchenko University, Kiev, Ukraine

<sup>3</sup> Moscow State Bauman Technical University, Russia

In the work the results of investigation of intensive X-Ray radiation in supersonic water jet in free space and near the end of water output channel at super-high pressures of water (200...3000 atm) [1,2] are presented. Results of experiments and theoretical calculation show that the intensive acoustic shock waves connected with the cavitation processes are a source of intensive X-Ray radiation. Frequency of this X-Ray radiation depends on substance in which shock waves extends and is transformed. Comparison of spectra of X-radiation from different surfaces at cavitation of water jet is presented on Fig.1. The soft part of X-Ray radiation with energy  $E_x \approx 1$  keV was generated by the surface of supersonic free water jet in the area of cavitation. The energy of radiation from the surface of water output channel (made of stainless steel) was  $E_x \approx 2$  keV. In the case of additional lead cover of this surface the energy was  $E_x \approx 4.5-5$  keV.

The total activity of cavitation-induced X-Ray generation was about  $Q \approx 0.1$  Ci.

The different radiation phenomena were also detected by X-Ray photo-plates (see Fig.2).

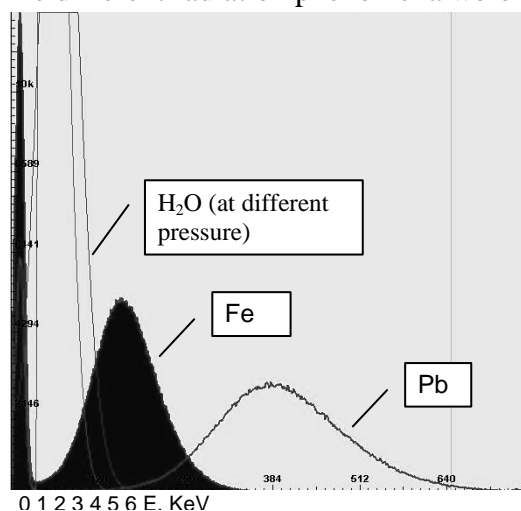


Fig. 1. X-radiation from different surfaces at cavitation of water jet.

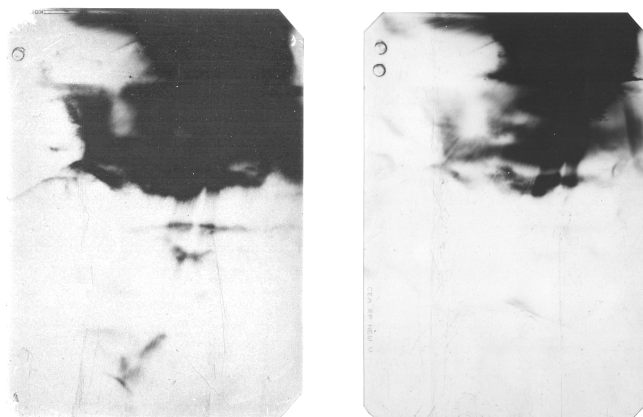


Fig. 2. The image on two X-ray films situated in coaxial geometry around cylindrical rod with cavitating water jet. The left film was situated more close to a rod.

The problems of action of cavitation induced shock waves on the magnetic properties of walls of cavitation chamber (including demagnetization and magnetic phase transitions) are also discussed.

[1] A.A. Kornilova, V.I. Vysotskii, N.N. Sysoev, A.V. Desyatov. *Jour. of Surface Investigation. X-ray, Synchrotron and Neutron Techniques*, 2009, V. 3, #2, 275.

[2] A.A. Kornilova, V.I. Vysotskii, N.N. Sysoev, N.K. Litvin, V.I. Tomak, A.A. Barzov. *Jour. of Surface Investigation. X-ray, Synchrotron and Neutron Techniques*, 2010, V.4, #6, 1008.

Wednesday

**24 August**

17:30-19:00

poster session

24PO-M

**“High Frequency  
Properties and  
Metamaterials”**

24PO-M-1

## WAVEGUIDE PROPERTIES OF PLANAR STRUCTURES BASED ON THE LEFT-HANDED MEDIA

*Sannikov D.G.*

Department of Radiophysics and Electronics, Ulyanovsk State University, L.Tolstoy str., 42,  
Ulyanovsk, 432970, Russian Federation

The very rapidly developing physics of metamaterials with negative refractive index (left media), which unique properties offer significant opportunities for developing radically new instruments and devices. One of the promising applications of left-handed media in the field of optoelectronics can be planar guiding structures [1-3].

The report focuses on the analysis of the dispersion relations in planar structures with different combinations of left and right layers. Based on the ray approach we investigate conditions for the existence of bulk and surface TE and TM modes, as well as a criterion for the degeneracy of the waveguide modes. The analysis shows that the dispersion characteristics of bulk and surface TE and TM modes in a three-layer waveguides depend strongly on the relationship of permittivity and permeability, as well as the degree of asymmetry of the structure. The propagation of bulk ( $m = 0$ ) and surface ( $m_s = 0, 1$ ) modes in these structures are limited to three values of the normalized propagation constant. We propose new types of optical microcavities, whose operation is associated with the capture of photons inside the active guiding layer 2 surrounded by a semi-infinite dielectric (3) and metamaterial (1) or two left-handed media (1 and 3) (Fig. 1).

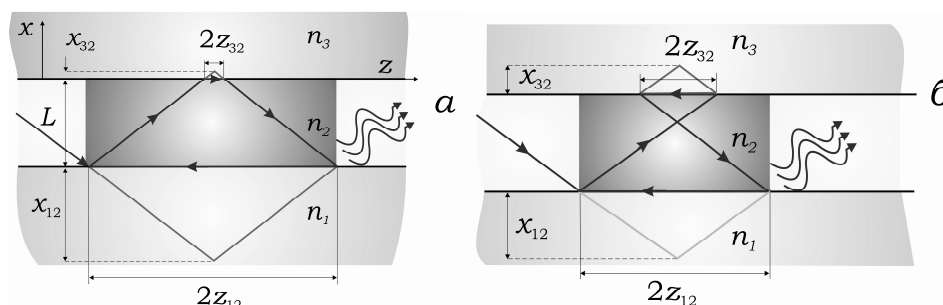


Fig. 1. The microcavity cavities based on amplifying guiding layer with dielectric and metamaterial (a) and both left handed metamaterial clads.

Supported by the Ministry of Education and Science (state contract № 02.740.11.0224 from 7.7.2009; P119 from 12.04.2010).

- [1] Shadrivov I.V., Sukhorukov A.A., Kivshar Y.S. *Phys.Rev.E.* **67** (2003) 057602.
- [2] Vukovic S.M., Aleksic N.B., Timotijevic D.V. *Opt. Comm.* **281** (2008) 1500
- [3] Wang Z. H., Xiao Z. Y., Li S. P. *Opt. Comm.* **281** (2008) 607.

24PO-M-2

## **IS MnSi AN ITINERANT-ELECTRON MAGNET? RESULTS OF ESR EXPERIMENTS**

*Demishev S.V., Semeno A.V., Bogach A.V., Glushkov V.V., Sluchanko N.E., Samarin N.A.,  
Chernobrovkin A.L.*

Prokhorov General Physics Institute, Russian Academy of Sciences, ul. Vavilova 38,  
Moscow, 119991 Russia

High-frequency (60 GHz) electron spin resonance (ESR) has been studied in manganese monosilicide, MnSi, single crystals [1]. The measurements performed within the 4.2-300 K temperatures range at the applied magnetic field up to 70 kOe have demonstrated that the magnetic resonance in MnSi is due to localized magnetic moments of the Heisenberg type with the  $g$ -factor depending only slightly on temperature,  $g \sim 1.9-2.0$ . At the same time, it has been found that the ESR linewidth is determined by spin fluctuations and can be quantitatively described in the wide temperature range ( $4.2 \text{ K} < T < 60 \text{ K}$ ) in the framework of the Moriya theory using the  $SL(T)$  function. The revealed deviations from the model of weak itinerant-electron magnetism commonly used for the description of the magnetic properties of MnSi indicate a possible spin\_polaron nature of the unusual magnetic properties of this strongly correlated metal [1].

Support by by the Ministry of Education and Science of the Russian Federation (state program “Scientific and Pedagogical Personnel of Innovative Russia”), by the Russian Academy of Sciences (program “Strongly Correlated Electrons in Metals, Semiconductors, and Magnetic Materials”), and by the Russian Foundation for Basic Research (project no.11\_02\_00123\_a).

[1] S.V.Demishev et. al., *JEPT Letters*, **93**, (2011) 213.

24PO-M-3

## **ELECTROMAGNETIC WAVE PROPAGATION THROUGH MULTI-LAYER STRUCTURES CONSIST OF THIN MAGNETIC FILMS WITH IMPEDANCE BOUNDARY CONDITIONS**

*Antonets I.V.<sup>1</sup>, Kotov L.N.<sup>1</sup>, Shavrov V.G.<sup>2</sup>, Shcheglov V.I.<sup>2</sup>*

<sup>1</sup> Syktivkar State University, 167001, Syktivkar, Russia

<sup>2</sup> Institute of Radioengineering and Electronics of RAS, 125009, Moscow, Russia

The multi-layer magnetic structures are of great interest for different types of microwave analog signal processing devices using electromagnetic wave propagation [1]. In this region is very important to find the simple methods of calculation wave amplitudes in separate layers and coefficients of wave reflection and penetration in whole structure. As a preliminary task we investigated the propagation of single-dimension wave through three media with arbitrary permittivity and permeability and found the propagation waves amplitudes. This task was solved by straight method consisting of stitching individual solutions on media boundaries and averaging method consisting of using average impedance boundary conditions. By comparison of these methods we have shown that the straight method calculations are ideologically more simple but

averaging method yields more simple formulas. We have shown that general ideological loading in averaging method is in the conclusion of outside average impedance boundary conditions. This task is very difficult in magnetic media because of tensor character magnetic permeability near the condition of ferromagnetic resonance. We have shown that for isotropic medium with scalar permeability for every layer there is two average impedance conditions and for isotropic medium with tensor permeability there is four boundary conditions. The reason of this circumstance is that the in tensor media propagate two kinds of electromagnetic waves: gyro-magnetic and gyro-electric. This waves are connected each other and may be divided only when dc bias magnetic field is parallel or perpendicular to wave propagation direction. For our task we found the complete universal inside and outside average impedance boundary conditions. By averaging method with universal boundary conditions and also by straight method we solved the electro-dynamical tasks about normal and inclined incidence of electromagnetic waves vertical and horizontal polarization to the media dividing surfaces. There was shown the unity of all above mentioned tasks with single-dimension task and possibility obtaining the electro-dynamical tasks solutions from single-dimension task solution by substitution of coefficients and variables. This developed mathematical methods were applied to solve tasks for multi-layer magnetic structures consist of two and three layers placed between two external media with different parameters. It was shown the possibility reduction of the electro-dynamical tasks to single-dimension task for scalar permeability in the cases of normal and inclined incidence and for tensor permeability only for normal incidence. Also we have found the complete inside reflection conditions from different layers of multi-layer structures. For the wave having vertical polarization we found the conditions elimination of reflection which are generalization of Brewster law on the multi-layer structures. We have shown that in magnetic media by Brewster condition the angle between wave vectors of reflected and penetrated waves is not equal to  $90^\circ$ . In the case of normal wave incident there is the quantitative correlation between permeability and permittivity when wave reflection is absent.

This work is supported by RFFR, Grant: № 10-02-01327-a.

[1] J.Adam, L.Davis, G.Dionne, E.Schloemann, S.Stitzer // IEEE Tr. MTT. 2002.V.50.№3. P.721.

24PO-M-4

## **SECOND ORDER MAGNETIZATION PRECESSION BY REORIENTATION TRANSITION**

*Vlasov V.S.<sup>1</sup>, Kotov L.N.<sup>1</sup>, Shavrov V.G.<sup>2</sup>, Shcheglov V.I.<sup>2</sup>*

<sup>1</sup> Syktivkar State University, Syktivkar, Russia

<sup>2</sup> Institute of Radioengineering and Electronics of RAS, 125009, Moscow, Russia

The development of works by nonlinear physics stimulates the investigation of wave processes in nonlinear media. The striking example of this phenomenon is electromagnetic waves propagation in ferrite films where nonlinearity arise by very small wave amplitude. Usually the magnetization precession is accompanied by parametrical excitation of exchange spin waves [1,2]. The electromagnetic energy pumping into spin-wave reservoir keeps the angular precession amplitude on the level of one-two degrees. For the prevention of spin waves excitation the bias dc magnetic field is directed along to normal to the film surface. In this case the precession frequency is equal to the spin wave spectrum bottom and precession angles may be so large as several tens degrees [3].

Usually the dc bias magnetic field  $H_0$  is more than film demagnetizing field  $4\pi M_0$ , that is to say:  $H_0 \geq 4\pi M_0$ . In this case the magnetization vector in equilibrium position is oriented along the biasing dc magnetic field. In interval  $0 < H_0 < 4\pi M_0$  take place the reorientation phase transition in which the magnetization vector orientation is between the film plane and bias field direction. We have investigate large amplitude magnetization precession by orientation phase transition.

So by  $H_0 < 4\pi M_0$  the magnetization vector equilibrium position is deflected from dc field direction. The variable magnetic field  $h$  having right circular polarization oriented in perpendicular to dc bias field induces the forced magnetization vector precession. In this case the magnetization vector performs the circular precession around the equilibrium position and itself position moves onto the cone surface. The precession portrait on co-ordinate plane of magnetization vector components  $m_x, m_y$  is the circumference on which is put the spiral in the form of epicycle. The magnetization vector end moves uniform on the epicycle and epicycle centre moves on the other circumference with centre in the point corresponding to projection of bias field vector onto the film plane. This motion is the second order precession. Cause of this motion is in inequality of gyroscopic forces operate on the magnetization vector in positions corresponding to maximum and minimum distance from dc field direction. We have shown that second order precession have five regimes: (1) simple circular small-amplitude precession, (2) equilibrium position precession without center encircle, (3) nonsubsiding equilibrium position precession with center encircle, (4) subsiding equilibrium position precession with center encircle, (5) simple circular large-amplitude precession. The transition from one regime to another is determined by variable magnetic field amplitude. These phenomena may be used for different types of microwave analog signal processing devices.

This work is supported by RFBR, Grant: № 10-02-01327-a.

[1] H. Suhl. // J.Phys.Chem.Sol. 1957. V.1. №4, P.209.

[2] A.G. Gurevich, G.A. Melkov // Magnetic oscillations and waves. M.: Nauka. 1994.

[3] A.G. Temiryazev, M.P. Tikhomirova, P.E. Zilberman. // J. Appl. Phys. 1994. V.76. №12. P.5586.

24PO-M-5

## **MAGNETIC SUSCEPTIBILITY OF COMPOSITE MEDIUM CONSISTED OF UNIAXIAL FERRITE PARTICLES**

*Shcheglov V.I., Zubkov V.I.*

Institute of Radioengineering and Electronics of RAS, Moscow, Russia

The composite media consisted of discrete elements are in great attention [1,2]. Here we have investigated such medium consisted of uniaxial spherical ferrite particles embedded in nonmagnetic insulating matrix. We calculated the dynamic magnetic susceptibility of this medium biased by uniform dc magnetic field. All ferrite particles have the same uniaxial magnetic anisotropy but the anisotropy axis orientations of each individual particle are different in correspond with a priori given probability law. The interaction between particles is absent. The first stage of task is calculation of magnetic susceptibility tensor for one separate particle. Then it is performed the addition above all particles in unit of volume. We have shown that all tensor components are

complex with nonzero real and imaginary parts. Some of calculated tensor components have the form [3]:

$$\chi_{xx} = \frac{(\Omega_1 + i\Omega\alpha)\cos^2\varphi_a \cos^2\theta_m + (\Omega_2 + i\Omega\alpha)\sin^2\varphi_a}{4\pi[\Omega_1\Omega_2 - (1+\alpha^2)\Omega^2 + i\alpha\Omega(\Omega_1 + \Omega_2)]};$$

$$\chi_{xz} = \frac{-(\Omega_1 + i\Omega\alpha)\cos\varphi_a \sin\theta_m \cos\theta_m - i\Omega \sin\varphi_a \sin\theta_m}{4\pi[\Omega_1\Omega_2 - (1+\alpha^2)\Omega^2 + i\alpha\Omega(\Omega_1 + \Omega_2)]}; \quad \text{where } \Omega = \frac{1}{4\pi M_0} \cdot \frac{\omega}{\gamma},$$

$$\Omega_1 = \frac{1}{4\pi M_0} [H_a \sin^2(\theta_a - \theta_m) + H_0 \cos\theta_m]; \quad \Omega_2 = \frac{1}{4\pi M_0} \{H_a \cos[2(\theta_a - \theta_m)] + H_0 \cos\theta_m\};$$

$M_0$  – saturation magnetization;  $H_a$  – anisotropy field;  $H_0$  – external bias field;  $\alpha$  – dissipation parameter;  $\gamma$  – gyromagnetic ratio;  $\theta_a$  and  $\varphi_a$  – angular co-ordinates of anisotropy axis;  $\theta_m$  – polar angle of equilibrium orientation magnetization vector. The whole tensor components have the form:

$$\chi_{ik} = \frac{2}{3} \cdot \left(\frac{r}{d}\right)^3 \cdot \sum_{n=0}^{n_{max}} \left( \sum_{m=0}^{m_{max}} \chi_{ik}^{(n,m)} \right) \cdot \left[ \sum_{n=0}^{n_{max}} \frac{\sin(n \cdot \theta_0)}{\theta_0} \right]^{-1}, \quad \text{where: } r - \text{ferrite sphere radius, } d -$$

distance between neighbouring particles,  $n$  and  $m$  – angular numbers of anisotropy axis positions,  $n_{max} = \pi/\theta_0$ ,  $m_{max} = 2\pi \sin(n \cdot \theta_0)/\theta_0$ ,  $\theta_0$  – angular step. When the distribution of anisotropy axis orientations individual particles is equivalent-probable above the whole space from nine tensor components are nonzero only five the same as in anti-symmetrical tensor of isotropic medium:  $\chi_{xx}$ ,  $\chi_{xy}$ ,  $\chi_{yx}$ ,  $\chi_{yy}$ ,  $\chi_{zz}$ . In this case are there the equalities:  $\chi_{xx} = \chi_{yy}$ ,  $\chi_{xy} = -\chi_{yx}$ . The most distinction from isotropic medium is considerable more frequency range (in five-ten times or more). When the distribution of anisotropy axis orientations individual particle is not equivalent-probable and subordinates to other law the all nine tensor components are nonzero. So the composite medium susceptibility tensor has certain symmetrical and anti-symmetrical properties.

[1] А. Виноградов // Электродинамика композитных материалов. М.: УРСС. 2001.

[2] J. Pendry, A. Holden, W. Stewart, I. Youngs // Phys. Rev. Lett. 1996. V.76. №25. P.4773.

[3] V.I.Zubkov, V.I.Shcheglov // J. Comm. Tech. El. 2010. V.55. №4. P.457.

24PO-M-6

## MAGNETOSTATIC WAVE DISPERSION IN MAGNETIC FILM BY ORIENTATION TRANSITION

*Shcheglov V.I., Zubkov V.I.*

Institute of Radioengineering and Electronics of RAS, Moscow, Russia

The magnetostatic volume and surface waves (MSVW and MSSW) in ferrite films and structures are of great interest for different types of microwave analog signal processing devices using wave propagation [1]. The dispersion properties of such waves have many variety of forms. Owing to gyrotropy of medium the directions of phase and group velocity vectors in these waves may be very different. According to magnetization conditions there may be as forward so backward waves. In majority of papers there investigate waves in films magnetized for saturation along the direction of external bias field. In this work we describe the magnetostatic waves (MSW) investigations in conditions when magnetization vector is not parallel to bias field direction [2].



We have investigated the MSW propagation in longitudinal magnetized ferrite film having normal uniaxial anisotropy in conditions of orientation phase transition in the whole field interval from zero to transition field. We have found the dispersion relation for quasi-surface (QS) and quasi-volume (QV) MSW, potentials, fields and dynamic magnetizations for waves of both types by wave propagation along the film plane. The frequency boundaries between QV and QS waves regions have the form:

$$\Omega_{1,2} = \sqrt{(\Omega_A^2 - \Omega_H^2) \pm \frac{\Omega_A^2 \mp \sqrt{\Omega_A^4 - 4\Omega_H^2(\Omega_A^2 - \Omega_H^2)} \cdot \cos^2 \varphi}{2\Omega_A}}, \quad \text{where the normalized}$$

frequencies are:  $\Omega = \frac{\omega}{4\pi\gamma M_0}$ ;  $\Omega_H = \frac{H_0}{4\pi M_0}$ ;  $\Omega_A = \frac{K/M_0 - 2\pi M_0}{2\pi M_0}$ , and:  $M_0$  – saturation magnetization,  $K$  – anisotropy constant,  $H_0$  – dc bias field,  $\omega$  – frequency,  $\varphi$  – angle between wave vector and normal vector to the dc field direction,  $\gamma$  – gyro-magnetic constant.

Also we have found the frequency boundaries between existence regions of QV and QS waves and limit frequencies when wave number goes to zero or infinity. It was shown that limit frequencies of both wave types decrease when field increase and lower frequency limit in phase transition field goes to zero (safe mode) and upper frequency limit goes to square root from anisotropy field. The frequency region of QV MSW is limited from top and upper by two frequency regions of QS MSW. When anisotropy field is varied the general structure of frequency limits for both wave types is maintained but extent along both frequency and bias field axis varies proportional to anisotropy field. When wave vector orientation vary from perpendicular to parallel from bias field the frequency region of QV MSW increase and frequency region of QS MSW decrease. The wave vector orientation interval for QS MSW in film surface is limited by cut-off angle but for QV MSW the cut-off angle is absent.

- [1] J.Adam, L.Davis, G.Dionne, E.Schloemann, S.Stitzer // IEEE Tr.MTT. 2002.V.50.№3. P.721.  
 [2] V.I.Zubkov, V.I.Shcheglov, J. // J.Comm.Tech. El. (Russia). 2000. V.45. №4. P.471.

24PO-M-7

## **ON THE MANIFESTATION OF RELATIONSHIP BETWEEN DISPERSION AND POWER CHARACTERISTICS OF MAGNETOSTATIC WAVES IN FERRITE STRUCTURES**

*Lock E.H., Vashkovsky A.V.*

Kotel'nikov Institute of Radio Engineering and Electronics of Russian Academy of Sciences  
 (Fryazino branch), 141190, Vvedensky sq.1, Fryazino, Moscow region, Russia

Ferrite-dielectric-metal (FDM) structure is characterized by one rare property: dispersion characteristic of a dipole spin wave (magnetostatic wave (MSW)) in this structure may have one or two extremum points. Thus, in some intervals of wave number the wave is forward, and in the other intervals – backward. As a distinct from other structures, where the wave is always forward or always backward, it is of interest to consider, how fundamental relationships between the propagation number, phase and group velocities, Poynting vector and power flow manifest themselves when the wave number changes near extremum points.

Basing on the Maxwell's equations the dispersion characteristics of MSW with extremum points were calculated for FDM structure (Fig. 1, curves 2, 3). Then the corresponding partial and total

power fluxes were calculated for the FDM structure geometries with extremum points on dispersion characteristics (Fig. 2). As it is seen from comparison of Fig.1 and Fig.2, when the wave number  $k_y$  changes near extremum points, then the total power flow  $\Pi$  changes its value from positive to negative or from negative to positive (for more details see [1]).

Similar calculations were carried out in magnetostatic approximation also. A comparison of magnetostatic approximation results with calculations based on Maxwell's equations shows that magnetostatic approximation formulas (currently used for calculation of the MSW Poynting vector and MSW power flow) are wrong. A correct formulas is proposed in [1].

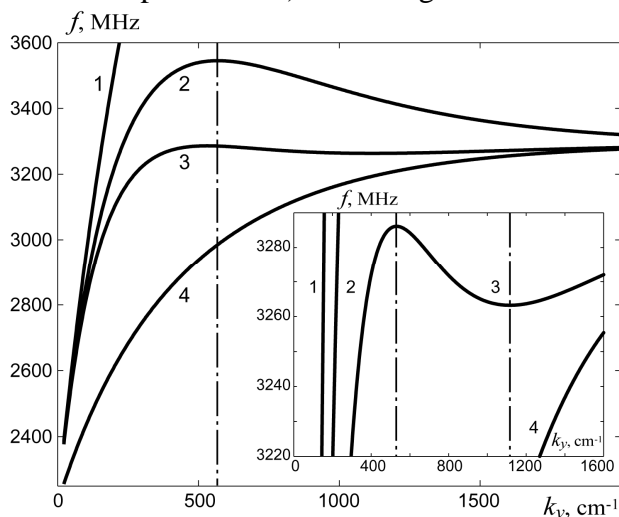


Fig. 1. Dispersion of FDM structure for various vacuum gap thickness  $w$ : 1 –  $w = 0$ , 2 –  $w = 10 \mu\text{m}$ , 3 –  $w = 15.5 \mu\text{m}$ , 4 –  $w \rightarrow \infty$ .

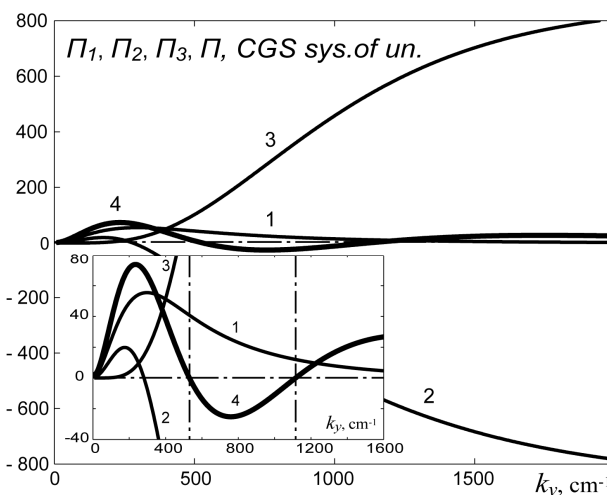


Fig. 2. Power fluxes of FDM structure for  $w = 15.5 \mu\text{m}$  for in vacuum half-space (1), in ferrite (2), in vacuum gap (3) and total flux (4 bold line).

Support of Program “Development of the Scientific Potential of High School” (project No. 2.1.1/1081) is acknowledged.

[1] A.V. Vashkovsky, E.H. Lock, *Physics-Uspeski*, **54**(3), (2011) in press.

24PO-M-8

## ON THE ANGULAR WIDTH OF DIFFRACTIVE BEAM IN ANISOTROPIC 2-D GEOMETRIES

Lock E.H.

Kotel'nikov Institute of Radio Engineering and Electronics of Russian Academy of Sciences  
(Fryazino branch), 141190, Vvedensky sq.1, Fryazino, Moscow region, Russia

The laws of geometrical optics and the formula, describing angular width of diffractive beam as a ratio of incident wavelength  $\lambda_0$  and slit length  $D$ , are examples of well-known physical laws for isotropic media. Evidently the question is appear: is it possible to deduce similar universal formula for 2-D geometries of anisotropic media? So an attempt is taken to obtain such formula through the study of spin wave diffraction in ferrite slab (for more details see [1]).

To describe dipole spin waves, named usually magnetostatic waves (MSWs), let's use magnetostatics equations  $\text{rot } \mathbf{h} = 0$  and  $\text{div } \mathbf{b} = 0$  and introduce magnetostatic potential  $\Psi$  in agree

with formula  $\mathbf{h} = \text{grad}\Psi$  (see [2]). Due to potential  $\Psi$  is scalar function, the study of MSW diffraction become simpler – and we can follow in general by the widely known analytical way, applied for isotropic media, with taking into account noncollinear character of MSW. In particular, for diffraction of the plane surface MSW (MSSW) on the wide slit (MSSW with noncollinear wavevector  $\mathbf{k}$  and group velocity vector  $\mathbf{V}$  is incident on the slit in opaque thin screen with arbitrary orientation) it was shown, that angular distribution of magnetic potential  $\Psi$  in the far-field region is described by the expression of type  $\sim \sin\Phi/\Phi$ , where the phase function  $\Phi$  is more complex, than for isotropic media. It is possible to obtain analytical formula, describing angular width  $\Delta\psi$  of main diffractive MSSW beam in the far-field region:

$$\Delta\psi = \frac{\lambda_0}{D} \left| \frac{d\psi}{d\varphi}(\varphi_0) \right| F \quad (1)$$

Here  $D$  is the length of slit,  $\lambda_0$  – the wavelength of incident MSSW,  $\varphi_0$  – the orientation of the wave vector  $\mathbf{k}_0$  of incident MSSW,  $d\psi/d\varphi$  and  $\psi(\varphi)$  – respectively, derivative and dependence of MSSW group velocity vector orientation angle  $\psi$  on MSSW wavevector orientation angle  $\varphi$ ,  $F$  – function, depending on  $\varphi_0$ , slit orientation  $\theta$  and angular derivative of isofrequency dependence (ID) at  $\varphi = \varphi_0$ . All angles are counted respect to collinear propagation axis, along which vectors  $\mathbf{k}$  and  $\mathbf{V}$  are collinear. Thus, the angular width  $\Delta\psi$  is defined substantially by mathematic properties of ID for the certain wave. If vector  $\mathbf{k}_0$  is normal to the slit line, then  $F \equiv 1$ . In this case for isotropic media (whose ID is circumference, dependence  $\psi(\varphi)$  has the form  $\psi = \varphi$  and  $d\psi/d\varphi \equiv 1$ ) we find from (1) well-known expression  $\Delta\psi = \lambda_0/D$ .

There is a hope, that formula (1), deduced for MSW, will be valid for any anisotropic media and structures for 2-D geometries, including metamaterial structures, that characterized by ID too. As it is seen from the formula (1) an unusual phenomenon may be appear in anisotropic 2-D geometries: if incident wave is characterized by such value  $\varphi_0$  that  $d\psi/d\varphi = 0$  at  $\varphi = \varphi_0$  then  $\Delta\psi = 0$ ! It means, the diffractive beam conserve its wide during propagation! Mention must be made, that ID for not any medium contains the point(s), where  $d\psi/d\varphi = 0$ , but such points present on ID for MSSWs with frequencies near the beginning of the spectrum.

This work is partially supported by the Program “Development of the Scientific Potential of High School” (project No. 2.1.1/1081).

[1]. Lock E. H. *Electronic Journal «Investigated in Russia»* **084** (2010) 975

[2] Damon R. W., Eshbach J. R. *J. Phys. Chem. Solids* **19** (1961) 308

24PO-M-9

## DEPENDENCE OF THE FERROMAGNETIC RESONANCE MODES ON THE EXTERNAL MAGNETIC FIELD IN DOUBLE LAYERED FERROMAGNETIC FILMS

*Shulga N.V., Doroshenko R.A.*

Institute of molecule and crystal physics, 450075, Ufa, Prospekt Oktyabrya 151, Russia

The ferromagnetic resonance in the exchange coupled ferromagnetic bilayer film in an inclined external magnetic field has been investigated. Film layers have finite thickness and possess with the anisotropies of the easy plane and easy axis types.

Double-layer structures have been investigated earlier in the approximation of thin layers in a case when the thickness of the interlayer magnetic inhomogeneity is much greater than the thickness of the layers. Two resonant modes, divided by a forbidden region, have been described for example in [1]. The model removes the restriction on the thickness of the layers has been constructed in [2]. This model is based on the assumption that the external field is large and the layers of the film are uniformly magnetized in the field.

In general, the problem can be solved only numerically. The ground state of the system has been obtained by discretizing and numerically minimizing the energy functional. The calculations of the ferromagnetic resonance has been performed in accordance with the method proposed in [3,4]. Dynamic response of the magnetic system to small homogeneous exciting external magnetic field is determined by the solution of the discretized on a one-dimensional grid of the Landau-Lifshitz equation.

Dependencies of the resonant frequency, the width of the resonance absorption lines, as well as profiles on the resonance modes on the magnitude and direction of the external magnetic field were investigated. The calculations are performed for a wide range of parameters, according to their characteristics, the structure closest to the bilayer films of iron garnets [2]. The obtained results are in accordance with the results for systems consisting of thin layers and systems placed in a saturating magnetic field, however, taking into account the heterogeneity of the magnetization reveals some features of the FMR modes of behavior depending on thickness of the layers.

The influence of interlayer exchange on the behavior of the resonant modes decreases with increasing thickness of the layers and approaches to the behavior of the FMR frequency of mono layers. The influence of interlayer exchange on both branches of the ferromagnetic resonance is found when the thickness of the layers decrees. In particular it has been observed a decrease of the value of the field at which the reversal of magnetization of the film occurs, which leads to a corresponding modification of the field dependence of the ferromagnetic resonance frequency.

The dependences of the FMR frequencies on the exchange coupling constant for the case when the two film layers are magnetized in the external field direction was obtained. For thin films revealed that the upper branch increases monotonically, while the lower branch reaches saturation with increasing the interlayer exchange constant. The canting angle of the upper branch decreases with increasing thicknesses of the layers.

[1] A. V. Kobelev, Ya. G. Smorodinsky, *Fiz. Tverd. Tela*, **31** 10 (1989) 6.

[2] A. L. Sukstansky, G. I. Yampolskaya, *Fiz. Tverd. Tela*, **42** (2000) 866.

[3] S.Labbe, P.-Y. Bertin, *J. Magn. Magn. Mater.*, **206** (1999) 93.

[4] N. Vukadinovic, M. Labrune, J. Ben Youssef, A. Marty, J. C. Toussaint, H. Le Gall, *Phys.Rev.B*, **65** (2001) 054403-1.

## AMPLIFICATION OF EVEN HARMONICS IN NONLINEAR MAGNETOIMPEDANCE RESPONSE OF AMORPHOUS WIRES IN PRESENCE OF LONGITUDINAL ALTERNATING MAGNETIC FIELD

*Buznikov N.A.<sup>1</sup>, Antonov A.S.<sup>2</sup>, Rakhmanov A.A.<sup>2</sup>*

<sup>1</sup> Scientific-Research Institute of Natural Gases and Gas Technologies – GAZPROM VNIIGAZ,  
142717 Razvilka, Leninsky District, Moscow Region, Russia

<sup>2</sup> Institute for Theoretical and Applied Electrodynamics, Russian Academy of Sciences,  
125412 Moscow, Russia

An interest in soft magnetic amorphous wires is related to their unusual physical properties and possible use in different applications. One of the striking phenomena observed in such wires is the giant magnetoimpedance (GMI) effect. The GMI implies a strong dependence of the sample impedance on an external magnetic field. The GMI effect is usually studied at low amplitudes of the driving current, when the voltage response is proportional to the wire impedance. At higher current amplitudes, the relation between changes in the sample magnetization and the driving current becomes nonlinear, and the voltage signal consists of a variety of harmonics [1]. This mode is often referred to as the nonlinear magnetoimpedance.

In recent years, the appearance of higher harmonics in the magnetoimpedance response has been detected and analyzed in Co-based amorphous wires [2–5]. The nonlinear mode occurs when the magnetic field induced by the alternating current is of the order of the anisotropy field, and the origin of the nonlinear voltage response is related to the magnetization reversal of a part of a wire [2]. It has been demonstrated that although the first harmonic dominates in the voltage, even harmonics have higher sensitivity to external magnetic field [3]. Even harmonics appear in the presence of helical anisotropy in a wire, when there is an asymmetry in the circular magnetization process. The asymmetry may be reinforced by application of torsional stress [4] or by superimposition of bias current on the driving alternating current [5].

In this work, we propose a new method to generate even harmonics in the nonlinear magnetoimpedance, which consists of simultaneous excitation of the wire by a driving current and a longitudinal alternating magnetic field. The rotational model to calculate the voltage across the wire with a circular anisotropy is developed. The frequency spectrum of the voltage is studied in the low-frequency approximation, when the skin effect can be neglected. It is shown that the appearance of even harmonics in the voltage response arises from the asymmetry in the magnetization reversal process due to the presence of the longitudinal alternating magnetic field. The dependences of even harmonic amplitudes on the external magnetic field, the current amplitude and the alternating magnetic field amplitude are analyzed. The ranges of alternating field amplitude and current amplitude to achieve a maximal field sensitivity of the second harmonic are found. The nonlinear effect studied may be promising for the development of sensors of a weak magnetic field.

- [1] R.S. Beach, N. Smith, C.L. Platt, F. Jeffers, A.E. Berkowitz, *Appl. Phys. Lett.*, **68** (1996) 2753.
- [2] C. Gómez-Polo, M. Vázquez, M. Knobel, *J. Magn. Magn. Mater.*, **226–230** (2001) 712.
- [3] J.G.S. Duque, A.E.P. de Araújo, M. Knobel, A. Yelon, P. Ciureanu, *Appl. Phys. Lett.*, **83** (2003) 99.
- [4] J.G.S. Duque, C. Gómez-Polo, A. Yelon, P. Ciureanu, A.E.P. de Araújo, M. Knobel, *J. Magn. Magn. Mater.*, **271** (2004) 390.
- [5] S.K. Pal, A.K. Panda, A. Mitra, *J. Magn. Magn. Mater.*, **320** (2008) 496.

## PLASMON INDUCED MODIFICATION OF THE TMOKE IN NI OPAL SLABS

Grunin A.A., Sapoletova N.A., Napolskii K.S., Eliseev A.A., Fedyanin A.A.  
Lomonosov Moscow State University 119991 Moscow, Russia

The optical and magneto-optical properties of two-dimensional slabs of Ni inverse opals with the 560 nm – period were studied. The form and geometrical parameters of such structures are usually characterized by normalized thickness, which is the ratio of the nickel layer thickness to the diameter of microspheres in the opal slab. Optical properties of metal inverse opal slabs dependent strongly on the normalized thickness, because not only delocalized surface plasmons but also localized plasmons can be excited in such structures [1]. In this paper, Ni inverse opal slabs with normalized thickness in the range from 0.2 to 1.1 are studied. Due to hexagonal packing, opal slab has six reciprocal vectors and, consequently, only two configurations with the azimuthal angles between reciprocal vector and plane of incidence of  $\psi=0^{\circ}$  and  $\psi=30^{\circ}$  are important. As well as in 1D structures, surface plasmons (SPP) can be excited in 2D structures in a narrow spectral range where phase-matching conditions are fulfilled. This was observed as dips in reflection spectra for the *p*-polarized light. The Transversal Kerr Effect (TKE) spectra of Ni inverse opal slabs measured at the angle of incidence  $\theta=60^{\circ}$  for two azimuthal angles of  $\psi=0^{\circ}$  and  $\psi=30^{\circ}$  are shown in Fig. 1. The peak positions in the TKE spectra are in the vicinity of dips in reflection spectra and correspond to phase-matching conditions of SPP excitation for the azimuthal configurations. The TKE enhancement of about 2-4 times is observed. The TKE enhancement yielded by surface plasmon excitation are agreed with TKE results obtained for 1D Ni subwavelength gratings [2]. The excitation of localized plasmons in contrast to delocalized plasmons does not lead to TKE modification.

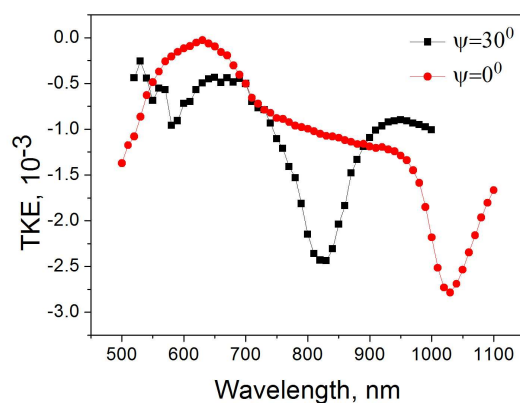


Fig. 1: The spectral dependences of transversal Kerr effect in 2D nickel inverse opal slabs for two azimuthal angles, angle of incidence  $\theta=60^{\circ}$ .

- [1] T. A. Kelf, Y. Sugawara, R. M. Cole, and J. J. Baumberg, Localized and delocalized plasmons in metallic nanovoids, *Phys. Rev. B.*, vol 74, p. 245415, 2006.  
[2] A.A.Grunin, A. G. Zhdanov, A. A. Ezhov, E. A. Ganshina, and A. A. Fedyanin, Surface-plasmon-induced enhancement of magneto-optical Kerr effect in all-nickel subwavelength nanogratings, *Appl. Phys. Lett.*, vol.97, p. 261908, 2010.

## FEATURES OF MAGNETIC PROPERTIES AND FMR OF CoFeZr/Si LAYERED NANOSYSTEMS DUE TO THEIR INNER STRUCTURE

Chekrygina Ju.<sup>1</sup>, Devizenko A.<sup>1</sup>, Kalinin Yu.<sup>2</sup>, Lebedeva E.<sup>3</sup>, Syr'ev N.<sup>3</sup>, Shipkova I.<sup>1</sup>, Sitnikov A.<sup>2</sup>, Vyzulin S.<sup>4</sup>

<sup>1</sup> National Technical University "Kharkov Polytechnic Institute", 61002, Kharkov, Ukraine

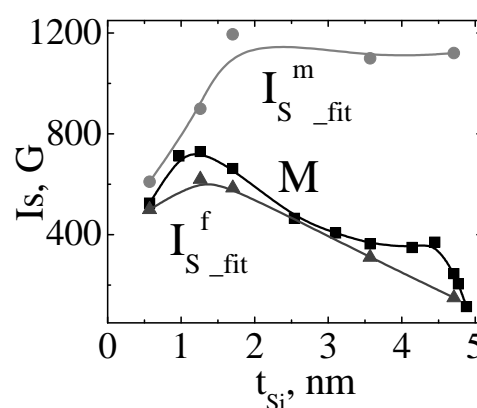
<sup>2</sup> Voronezh State Technical University, Voronezh, 394026, Russia

<sup>3</sup> Lomonosov Moscow State University, 119991 Moscow, Russia

<sup>4</sup> Kuban State University, 350040 Krasnodar, Russia

The results of studying static magnetic properties, ferromagnetic resonance (FMR) as well as glancing angle X-ray diffraction spectra (GAXRD) of [CoFeZr( $t_m$ )/Si( $t_{Si}$ )]<sub>40</sub> multilayer nanosystems are presented. Two groups of the samples were investigated. The first group samples had the layer thicknesses in the ranges of  $t_m = 2 - 3$  nm,  $t_{Si} = 0.5 - 5$  nm and the second ones were in the intervals  $t_m = 7 - 12$  nm,  $t_{Si} = 1 - 13$  nm. The samples were fabricated by ion-beam sputtering in argon atmosphere onto silicon substrates at Voronezh State Technical University. In-plane hysteresis loops were measured using a high sensitivity vibrating sample magnetometer with fields up to 1000 Oe. FMR spectra measurements were performed with EPR-spectrometer at a frequency of 9.27 GHz. XRD spectra were obtained on general purposes X-Ray diffractometer using Cu $\kappa\alpha$ -1 radiation applying  $\theta$ - $2\theta$  scans in 0- 5° glancing angle interval.

Analysis of the changes of hysteresis loop parameters, mean static saturation magnetization  $I_S$  and dynamic magnetization  $M$  (determined from FMR data) when  $t_{Si}$  increasing shows that inner structure of nanosystems under study differs from programmed in experiment size-composition sequence. Taking into account the possibility of silicides formation at metal-Si interfaces we have performed a computer simulation of GAXRD spectra for a multilayer interference structure. The following parameters were varied: composition of bi- or three-layers (such as Me/Si, Me/silicide, Me/silicide/Si), thickness of the layers, density and roughness of the each component. The best coincidence of experimental and theoretical GAXRD spectra has been achieved if a system consisted of metal alloy phase, MeSi<sub>2</sub> silicide and Si multilayers. It was shown that the estimated total magnetic layer thickness decreased from ~60 nm to ~7 nm when silicon content in the system increased ( $t_{Si}$  changed from 0.5 nm to 5 nm). We have calculated the mean film magnetization  $I_{S_{fit}}^f$  values and the magnetic layer magnetization  $I_{S_{fit}}^m$  using the measured values of magnetic momenta but fitted thickness of the whole nanostructure and that of all magnetic layers, respectively. These data for the first group samples are shown in the Figure along with dynamic magnetization  $M$  values. The second group samples revealed the weak dependence of  $M$  values on  $t_{Si}$ . These  $M$  values were near the bulk material magnetization (1100-1300 G). Matters of discussion are critical layer and interlayer thickness below which a resonance response corresponds to the effective medium rather than to individual magnetic layer.



## INHOMOGENEOUS BROADENING OF FERROMAGNETIC RESONANCE LINE DURING RECRYSTALLIZATION PROCESS IN AMORPHOUS RIBBONS

*Iskhakov R.S.<sup>1,3</sup>, Komogortsev S.V.<sup>1,3</sup>, Chekanova L.A.<sup>1</sup>, Kuznetsov P.A.<sup>2</sup>, Gavriluk A.A.<sup>4</sup>,  
Semenov A.L.<sup>4</sup>, Morozov I.L.<sup>4</sup>*

<sup>1</sup> Institute of Physics SB RAS, Krasnoyarsk 660036, Russia

<sup>2</sup> Central Research Institute of Structural Materials, "Prometey", 191015, St-Petersburg, Russia

<sup>3</sup> Siberian University of Technology, Krasnoyarsk, 660049, Russia

<sup>4</sup> Irkutsk State University, Irkutsk, 664003, Russia

Nanocrystalline and amorphous ferromagnetic alloys possess excellent soft magnetic properties due to exchange softening [1]. In these materials, the magneto-crystalline anisotropy is randomly fluctuating on a scale much smaller than the domain wall width and is therefore averaged out within exchange correlation length. In the present paper, we will present experimental results on ferromagnetic resonance (FMR) linewidth as a function of annealing conditions, as well as the annealing-temperature dependence of the crystallite size, coercive field, and the magnetic anisotropy field in the  $\text{Fe}_{73.5}\text{CuNb}_3\text{Si}_{13.5}\text{B}_9$  and  $\text{Fe}_{64}\text{Co}_{21}\text{B}_{15}$  alloy ribbons. We shall show the interrelationship of these quantities, demonstrate that these parameters are all related to nanoparticle crystallization, and indicate how they can be examined by extending random anisotropy theory.

Melt-spun ribbons  $\text{Fe}_{73.5}\text{CuNb}_3\text{Si}_{13.5}\text{B}_9$  produced at FSUE CRISM "PROMETHEY" have been investigated as a function of annealing time at different temperatures. When annealed at moderate temperatures,  $\text{Fe}_{73.5}\text{CuNb}_3\text{Si}_{13.5}\text{B}_9$  is characterized by an extremely low coercive field, and high magnetic permeability. At a high critical temperature ( $\sim 590^\circ\text{C}$ ), the grain size rapidly increases with annealing temperature. This onset of crystallization is accompanied by a relatively abrupt increase in the FMR linewidth (Fig.1), the magnetic anisotropy field, and the coercive field. We extend the scaling arguments of Herzer to explain these obviously related phenomena.

Samples of  $\text{Fe}_{64}\text{Co}_{21}\text{B}_{15}$  alloy ribbons prepared as stripes cut along the length of the original ribbon with trapezium shape (width varies from 0.5 cm to 0.2 cm) and its geometrical parameters are 30  $\mu\text{m}$  thick, 10 cm long. Along the length of the ribbons run the current with density in the range of  $1.2 \cdot 10^7$ — $3.4 \cdot 10^7$   $\text{A/m}^2$  during 2 minutes. The heat, released during the current flow with such density is the reason of structural transitions in the investigated ribbons. FMR spectra of investigated samples characterized by single peak with different width of peak those changes with annealing. It was determined that dependence of the FMR line width  $\Delta H$  from current density is nonmonotonic and it is characterized by two areas with negative gradient ( $1.2 \cdot 10^7$   $\text{A/m}^2 \div 1.5 \cdot 10^7$   $\text{A/m}^2$  and  $2.2 \cdot 10^7$   $\text{A/m}^2 \div 3.4 \cdot 10^7$   $\text{A/m}^2$ ) and by the range with positive gradient ( $1.5 \cdot 10^7$   $\text{A/m}^2 \div 2.2 \cdot 10^7$   $\text{A/m}^2$ ). Decreasing of  $\Delta H$  value may be explained by relaxation internal stress in the amorphous phase and accompanying this process of decreasing effective magnetic anisotropy energy induced by magnetoelastic coupling. Specific resistance of ribbons treated current with densities up to  $1.8 \cdot 10^7$   $\text{A/m}^2$  is invariable after that increasing on the 50%.

Support by Federal Program "Development of the Scientific Potential of Higher Education" (project no. RNP 2.1.1/11470), Federal Target Program "Research and Research-Pedagogical Personnel of Innovation Russia for 2009-2013", Russian Foundation for Basic Research (project 11-03-00471-a) are acknowledged.

[1] M. Rubinstein, V. G. Harris, and P. Lubitz, *J. Magn. Magn. Mater.* **234** (2001) 306



## ELECTROMAGNETIC CRYSTAL AS A LOW-REFLECTIVITY MATERIAL

*Bychkov I.V., Zotov I.S., Fediy A.A.*

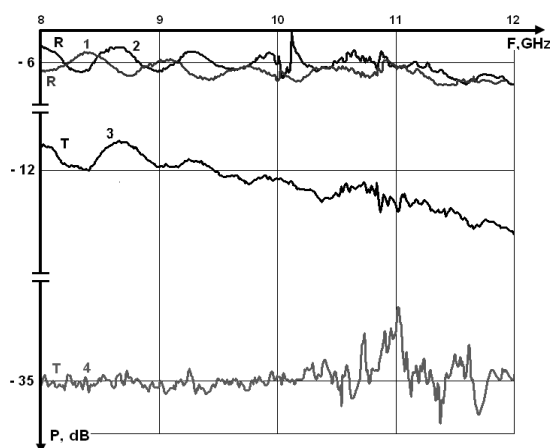
Chelyabinsk State University, Chelyabinsk, Russia.

The work contains the results of experiments on the study of reflection (R) and transmission coefficients (T) of electromagnetic waves that are characteristic for composite materials consisting of a dielectric matrix ( $\text{CaSO}_4 \cdot 2\text{H}_2\text{O}$ ) with graphite additives and a dielectric matrix which have a regular conducting structure in the form of graphite stems representing an electromagnetic crystal [1] and their compositions. The research was carried out for the SHF range 8-12 GHz by the means of wave guiding with the use of a voltage standing-wave-ratio meter.

Three types of samples were studied. The first one represented a dielectric matrix ( $\text{CaSO}_4 \cdot 2\text{H}_2\text{O}$ ) with the additives of flake graphite, the size of samples was  $10 \text{ mm} \times 10 \text{ mm} \times 23 \text{ mm}$ . By changing concentration of conducting switching it is possible to vary electro-dynamics characteristics of a composite material within the broad limits. For example, when mass concentration of graphite is 5%, a sample has low reflection coefficient (curve 2) though the transmission coefficient remains quite high (curve 3) which makes it virtually inapplicable for the purpose of screen age and premises protection.

The second type of samples represented a dielectric matrix ( $\text{CaSO}_4 \cdot 2\text{H}_2\text{O}$ ) with an electromagnetic crystal.

The crystal is formed by graphite conducting stems (with the diameter 0.7 mm) which in their turn form a square lattice with different spacing, the size of the samples –  $10 \text{ mm} \times 10 \text{ mm} \times 23 \text{ mm}$ . The results of measurement of reflection and transmission coefficients proved that the material behaved like a metal wall providing that there is a normal dip of the wave, the transmission coefficient is -35 dB, but at the same time quite a high reflection coefficient is close to 1 (according to the norm of reflection for a brass plate) [2]. The third sample represented a double-layer composite material composed of the layer from the first sample and the layer from the second sample with the crystal of a regular lattice (5 mm). Electromagnetic radiation struck normally to the surface of the first layer. This sample showed good screening characteristics (curve 4) but its reflection coefficient was rather low (curve 1) and can be compared with the first type of samples. The results of the research showed the possibility of getting low-reflection covers with good screening characteristics providing that there is a combination of absorbent and composite material based on the electromagnetic crystal.



[1] P.A. Belov, S.A. Tretyakov, A.J. Viitanen. Dispersion and reflection properties of artificial media formed by regular lattices of ideally conducting wires. *J. of Electromagn. Waves and Appl.*, Vol.16, No.8, 1153-1170, 2002.

[2] I.V.Bychkov, I.S.Zotov, A.A.Fediy. Reflection properties of electromagnetic crystal based composite material. Fourth International Congress on Advanced Electromagnetic Materials in Microwaves and Op-tics. 13th-18th September 2010 in Karlsruhe, Germany. ©

24PO-M-15

## MAGNETIC PROPERTIES OF THE LAYERED PERMALLOY AND FINEMET FILMS FOR GMI ELEMENTS

*Buchkevich A.A., Savin P.A., Lepalovskij V.N., Volchkov S.O., Vas'kovskiy V.O.*  
Ural State University, Russia, Ekaterinburg

The highly sensitive sensors based of giant magnetoimpedance (GMI) are advanced for production of magnetic field sensors in engineering, biophysics etc.

The properties of sensors is most dependent from the material (medium sensory) which using for construction of final industrial product. It was known that to achieve high values of GMI effect is required original magnetically soft material.

In this work we compared the magnetic properties of permalloy ( $\text{Fe}_{19}\text{Ni}_{81}$ ) and finemet ( $\text{Fe}_{72,5}\text{Cu}_{1,1}\text{Nb}_{1,9}\text{Mo}_{1,5}\text{Si}_{14,2}\text{B}_{8,7}$  (FM) films. The films were deposited by r. f. sputtering on the glass substrates. The thickness of magnetic layers were varied (Fig. 1). In order to reduce coercive force of the film with thickness of 500 nm were introduced Cu interlayers of 3 nm (Fig. 2). It was include varying the number of interlayers of copper, the thickness 30 Å. The deposition was spent in a planar magnetic field. The hysteresis loops was observed using the Kerr effect and a the VSM.

The magnetoimpedance measurements executed on element with size 1 mm×10 mm show considerable distinction in value in sample with layering into magnetic layers (up to 220%).

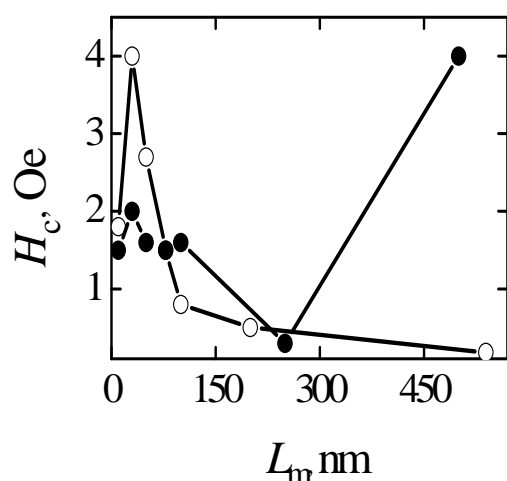


Figure 1 shows the dependence of  $H_c$  ( $L$ ) which has a tendency to decrease with increasing thickness, associated apparently with the decrease of influence of the surface. In this case, the thickness of the 30 nm has a maximum, possibly associated with the change of type of domain walls. With increasing the thickness appeared transcritical state, which is observed only in permalloy, with thickness of 500 nm.

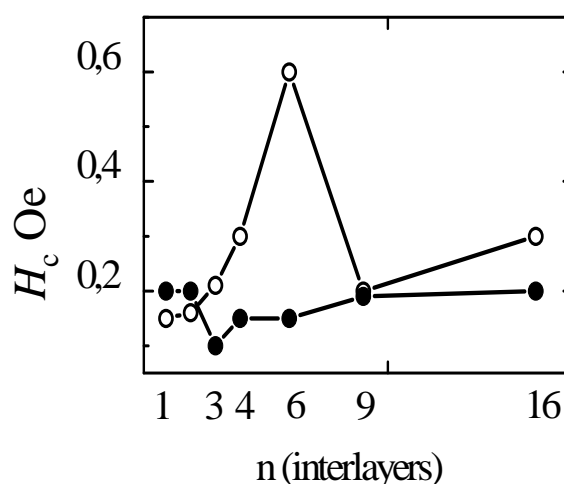


Figure 2 shows the dependence of  $H_c(n)$ , where  $n$  – the number of copper interlayers (the thickness 3nm) made in the magnetic layers of total thickness of 5000 Å. Layering is blocking the appearing of the transcritical state in permalloy, and a minimum of  $H_c$  is observed in the three layering film (0.1 Oe). The same layering of the finemet multilayer structure only increase a coercive force (maximum with 6 layers of copper (0.6 Oe)), while finemet monolayer 5400 Å had a coercive force of 0.18 Oe.

## HYBRID SURFACE–BULK MAGNETOSTATIC WAVES IN THE WAVEGUIDE PRODUCED BY A NONUNIFORM MAGNETIC FIELD

*Annenkov A.Yu., Gerus S.V.*

Kotel'nikov Institute of Radio Engineering and Electronics of Russian Academy of Sciences  
(Fryazino branch), 141190, Fryazino, Russia

The results of computer simulation of magnetic modes in a waveguide created in a ferrite film by the nonuniform magnetic field of the complicated shape are presented. As a model of a field distribution the stepped configuration consisting of two rectangular channels A and B is chosen. The field distribution is shown on fig. 1. It is possible to obtain in the certain frequency range simultaneous existence of a surface MSW in one channel and volume MSW in other one by selecting parameters of steps of a magnetic field. The Walker's generalized equation for a magnetostatic scalar potential was solved by the grid method [1,2]. The discovered solution has shown, that complicated distribution pattern of a wave function is formed as a result of interacting modes of initial channels. The hybrid wave functions consisting of areas with surface and volume mode distributions of MSW are obtained.

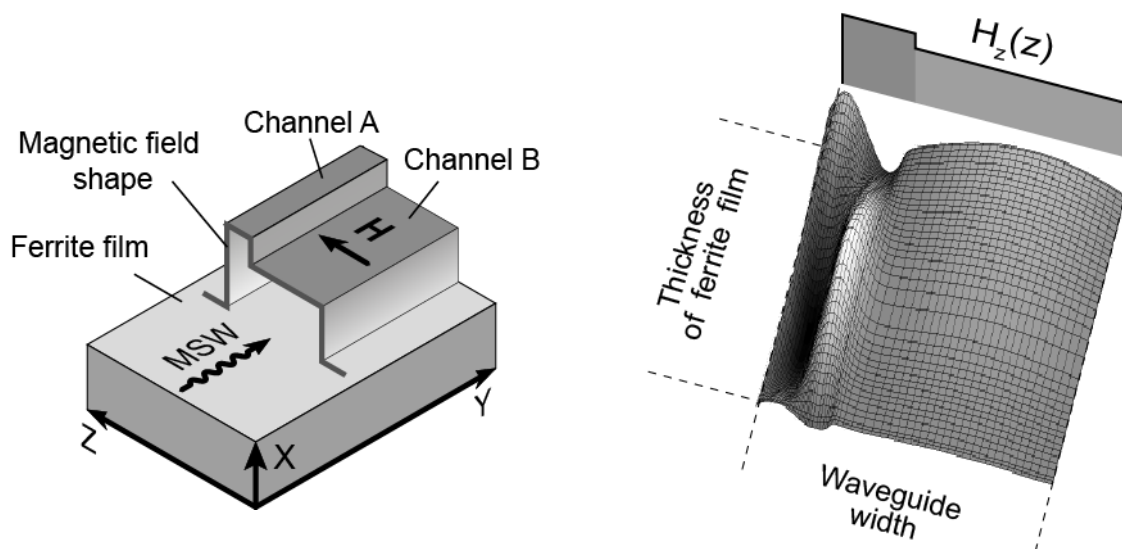


Fig. 1. Configuration of a waveguide magnetic field

Fig. 2. Distribution of a scalar magnetic potential of a hybrid wave

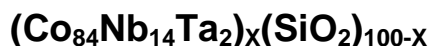
On fig. 2 the 3D distribution of a hybrid magnetic wave is shown. In a right-hand of a waveguide this distribution looks like a surface MSW, and in left-hand - like volume MSW.

[1] A.Yu.Annenkov, S.V.Gerus, S. I. Kovalev, *Technical Physics*, Vol. 47, No. 6, 2002, pp. 737–741.

[2] A.Yu.Annenkov, S.V.Gerus, S. I. Kovalev, *Technical Physics*, Vol. 49, No. 2, 2004, pp. 238–244.

24PO-M-17

## MAGNETIC AND ELECTRICAL PROPERTIES OF NEW MULTILAYER HETEROGENEOUS STRUCTURES BASED ON COMPOSITES



*Aleshnikov A.A., Kalinin Yu.E., Sitnikov A.V., Fedosov A.G.*

Dept. Solid State Physics, Voronezh State Technical University, Russia

Research of the structure of composites  $(\text{Co}_{84}\text{Nb}_{14}\text{Ta}_2)_x(\text{SiO}_2)_{100-x}$  revealed the presence of columnar structure of clusters of metal grains in the perpendicular direction to the plane of films which are formed during heterogeneous material synthesis (picture 1). The study looks at the possibility of restriction of film columnar structure growth with the help of creation of interlayers from composite produced in the active gas medium.

The films of heterogeneous systems based on ferromagnetic alloy  $\text{Co}_{84}\text{Nb}_{14}\text{Ta}_2$  and silicon oxide were produced with the help of ion-beam sputtering.

Solid composites  $(\text{Co}_{84}\text{Nb}_{14}\text{Ta}_2)_x(\text{SiO}_2)_{100-x}$  were synthesized. Their growth was carried out in the Ar medium on stationary and rotating substrate (base), in the Ar medium with incorporation of 3,5 partial % of  $\text{O}_2$ . Multilayer heterogeneous systems  $\{[(\text{Co}_{84}\text{Nb}_{14}\text{Ta}_2)_{65}(\text{SiO}_2)_{35}]/[(\text{Co}_{84}\text{Nb}_{14}\text{Ta}_2)_{65}(\text{SiO}_2)_{35}+\text{O}_2]\}_n$  and  $\{[(\text{Co}_{84}\text{Nb}_{14}\text{Ta}_2)_x(\text{SiO}_2)_{100-x}]/[(\text{SiO}_2)]\}_{128}$  were also synthesized.

Concentration dependences of electrical resistivity ( $\rho$ ) of composites and multilayer heterogeneous structures are typical for percolation systems with phases which differ considerably in the rate of their conductivity.

The analysis of given results shows that incorporation of oxygen leads to the increase of  $\rho$  value in the studied composites. It is revealed that dependences of  $\rho(x)$  in the multilayer heterogeneous structures  $\{[(\text{Co}_{84}\text{Nb}_{14}\text{Ta}_2)_x(\text{SiO}_2)_{100-x}]/[(\text{Co}_{84}\text{Nb}_{14}\text{Ta}_2)_x(\text{SiO}_2)_{100-x}+\text{O}_2]\}_n$  differ insignificantly from this composite  $(\text{Co}_{84}\text{Nb}_{14}\text{Ta}_2)_x(\text{SiO}_2)_{100-x}$  characteristics.

The research of transfer curves showed the presence of significant component of perpendicular magnetic anisotropy ( $H_a$ ) in both composite and multilayer  $\{[(\text{Co}_{84}\text{Nb}_{14}\text{Ta}_2)_{65}(\text{SiO}_2)_{35}]/[(\text{Co}_{84}\text{Nb}_{14}\text{Ta}_2)_{65}(\text{SiO}_2)_{35}+\text{O}_2]\}_n$  films. The exception is multilayer heterogeneous structures  $\{[(\text{Co}_{84}\text{Nb}_{14}\text{Ta}_2)_x(\text{SiO}_2)_{100-x}]/[(\text{SiO}_2)]\}_{128}$ , as well as  $\{[(\text{Co}_{84}\text{Nb}_{14}\text{Ta}_2)_x(\text{SiO}_2)_{100-x}]/[(\text{Co}_{84}\text{Nb}_{14}\text{Ta}_2)_x(\text{SiO}_2)_{100-x}+\text{O}_2]\}_n$  produced with the help of cyclic evaporation in Ar atmosphere with pressure  $9,6 \cdot 10^{-4}$  torr during 58 seconds and in the mixed atmosphere (Ar with pressure  $9,6 \cdot 10^{-4}$  torr and  $\text{O}_2$  with pressure  $3,4 \cdot 10^{-4}$  torr) during 34 seconds in which  $H_a$  perpendicular component was reduced considerably.

Characteristics of concentration dependences of real ( $\mu'$ ) and imaginary ( $\mu''$ ) parts of complex magnetic permeability correlate with dependences of transfer curves of studied systems. Research showed that  $\mu'(x)$  at frequency 50 MHz in compositions over percolation threshold was increase from 15-20 in composites  $(\text{Co}_{84}\text{Nb}_{14}\text{Ta}_2)_x(\text{SiO}_2)_{100-x}$  till 50-60 in multilayer structures  $\{[(\text{Co}_{84}\text{Nb}_{14}\text{Ta}_2)_x(\text{SiO}_2)_{100-x}]/[(\text{SiO}_2)]\}_{128}$ .

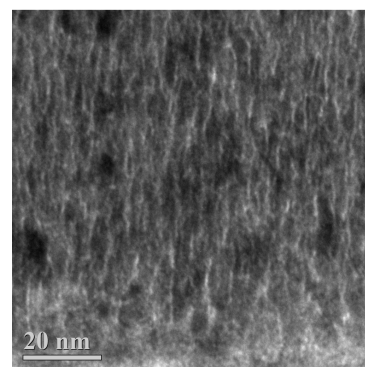


Fig. 1. Microphotograph of the cross-section of film of composite  $(\text{Co}_{84}\text{Nb}_{14}\text{Ta}_2)_{65}(\text{SiO}_2)_{35}$

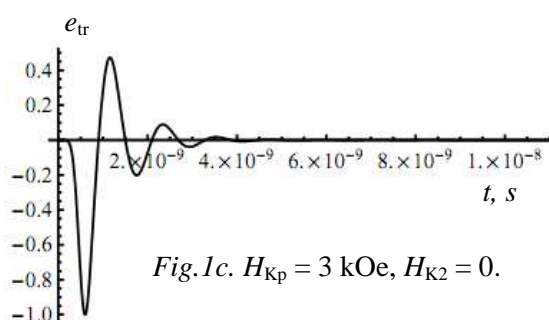
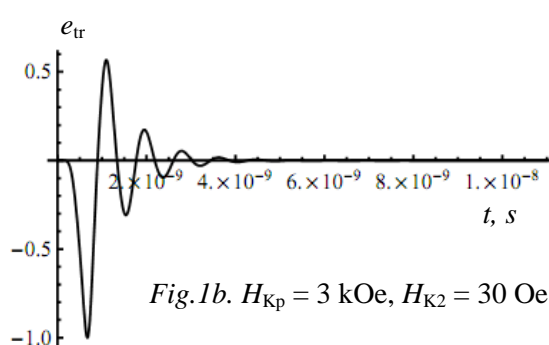
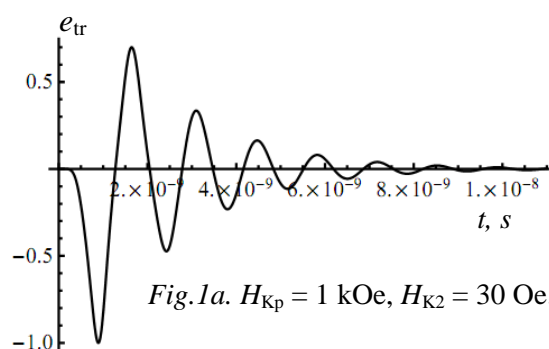
This work was supported by RFBR (grants № 09-02-97506 p\_центр\_a)

## ANALYSIS OF IN-PLANE ANISOTROPY INFLUENCE ON NONLINEAR MAGNETIZATION OSCILLATIONS ACCOMPANYING 90° PULSED REVERSAL PROCESSES IN REAL FERRITE-GARNET FILMS

*Kolotov O.S., Matyunin A.V., Nikoladze G.M., Polyakov P.A.*  
M.V. Lomonosov Moscow State University, Faculty of Physics,  
Leninskie Gory, Moscow 119991, Russia

An effect of planar anisotropy on the damping of magnetization oscillations arising during pulsed reversal processes in magnetic films and plates was discerned in works [1, 2]. The effect was confirmed experimentally in the case of free magnetization oscillations in ferrite-garnet films [2]. Theoretical calculations [3] show that the similar effect should be observed in the case of nonlinear magnetization oscillations. At value of in-plane anisotropy  $H_{Kp}$  close to 9–10 kOe oscillations should almost disappear. However, the calculations were carried out without taking into account real ferrite-garnet film properties. In particular, the presence of biaxial anisotropy in a film plane has not been considered. In this work it is shown that biaxial anisotropy results in a slight changing of oscillations intensity and their decay time. The transverse 90° magnetization signals calculated for three different films are shown in the presented figures. Here  $e_{tr}$  is the instantaneous voltage related to the absolute value of the voltage at the first extreme point. In the calculations it was supposed that saturation magnetization  $M_S = 16$  Gs, magnetizing field amplitude  $H_m = 30$  Oe, bias field  $H_0 = 4$  Oe and Landau-Lifshitz damping constant  $\lambda = 14 \cdot 10^6$  Hz. The duration of a pulse front is equal to 0.3 ns.

The signal presented in Fig. 1a corresponds to the film with  $H_{Kp} = 1$  kOe and biaxial anisotropy field  $H_{K2} = 30$  Oe. The next signal (Fig. 1b) was obtained for the film with  $H_{Kp} = 3$  kOe and  $H_{K2} = 30$  Oe. And Fig. 1c corresponds to the last one with  $H_{Kp} = 3$  kOe and  $H_{K2} = 0$  Oe.



- [1] E.N. Il'icheva et al., *Phys. of Solid State*, **45**, №6, (2003) 1087.  
 [2] Yu. A. Durasova et al., *Tech. Physics*, **54**, №2, (2009) 309.  
 [3] O.S. Kolotov et al., *Tech. Physics*, **56**, №1, (2011) 78.

## STRESS-IMPEDANCE EFFECT IN NANOCRYSTALLINE FeSiBNbCu ALLOY IN TEMPERATURE RANGE (297÷433) K

Semirov A.V.<sup>1</sup>, Bukreev D.A.<sup>1</sup>, Moiseev A.A.<sup>1</sup>, Derevyanko M.S.<sup>1</sup>, Lukshina V.A.<sup>2</sup>, Volkova E.G.<sup>2</sup>,  
Kurlyandskaya G.V.<sup>3</sup>

<sup>1</sup> East Siberian State Academy of Education, Irkutsk, Russia

<sup>2</sup> Institute of Metal Physics, Ural Division, RAS, Ekaterinburg, 620041 Russia

<sup>3</sup> Ural State University, Ekaterinburg, 620083 Russia

The temperature dependence of the impedance of nanocrystalline Fe<sub>73.5</sub>Si<sub>16.5</sub>B<sub>6</sub>Nb<sub>3</sub>Cu<sub>1</sub> ribbons on mechanical stresses was studied in the temperature range (297÷433) K. For nanocrystallization rapidly quenched amorphous ribbons were subjected to the field annealing for 1 hour at 793 K with a transverse magnetic field of 3 kOe applied in plane of the ribbon. According to X-ray and transmission electron microscopy studies the fine nanocrystalline structure ( $\alpha$ -Fe + Fe<sub>3</sub>Si) was formed during the heat treatment with the average grain size about 10 nm. The analysis of the shape of the inductive hysteresis loops had shown that the samples can be described as rather soft ferromagnets with saturation induction of 1.2 T and coercive force of about 0.04 Oe. An in-plane transverse magnetic anisotropy with the value of the anisotropy constant about 10 J/m<sup>3</sup> was induced during the annealing. Measurements of the impedance were carried out with using the Agilent 4294A impedance analyzer in frequency range of alternating current (0.1÷50) MHz at its effective value of 10 mA. External tensile mechanical stresses ( $\sigma$ ) were varied in the interval of 0 to 190 MPa. For numerical evaluation of the changes of stress impedance effect (SI) value of the SI ratio  $((\Delta Z/Z)_\sigma)$  was calculated as follow:  $((\Delta Z/Z)_\sigma) = 100 \times (Z(\sigma) - Z(\sigma=0))/Z(\sigma=0)$ .

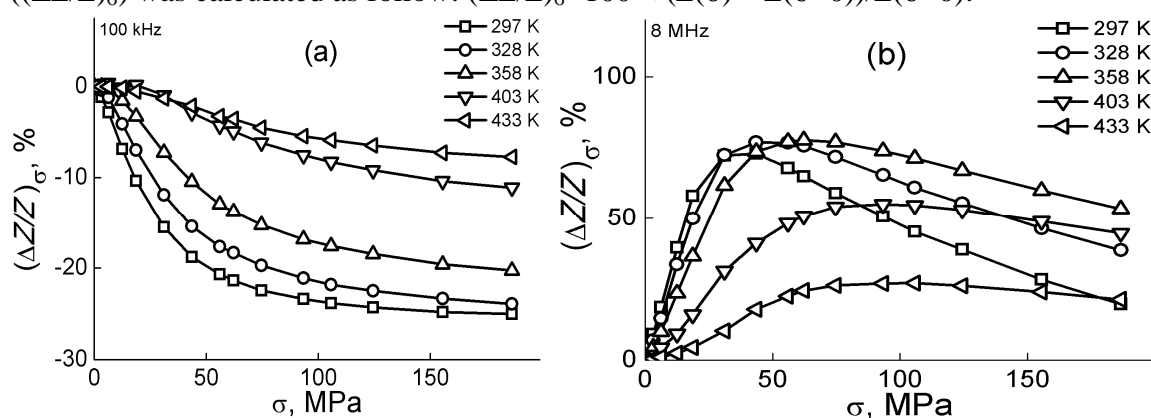


Fig.1.

For all temperatures under consideration a decrease of the impedance was observed with an increase of the tensile stresses for all frequencies of the alternating current below 0.5 MHz (Fig. 1, a). The sensitivity of  $((\Delta Z/Z)_\sigma)$  with respect to the value of the mechanical stresses decreases with the increase of the temperature. The value of the impedance increases to certain maximum with an increase of the mechanical stresses for the frequencies between 0.5 MHz and certain frequency followed by the impedance decrease (Fig. 1, b). The SI reaches the value about 100% at sensitivity above 2 %/MPa at frequencies of about 40 MHz. The maximum value of the  $((\Delta Z/Z)_\sigma)$  moves to range of higher  $\sigma$  values with the temperature increase. The maximum value of the SI shows small changes up to the temperature about 360 K and then decreases rather quickly.

The investigations were supported by Russian Foundation for Basic Research (09-08-00406-a).

## DC-BIAS CURRENT INFLUENCE ON TEMPERATURE DEPENDENCE OF THE CO-BASED AMORPHOUS WIRES IMPEDANCE

*Semirov A.V., Moiseev A.A., Bukreev D.A., Derevyanko M.S.*  
East Siberian State Academy of Education, Irkutsk, Russia

The dc-bias current influence on temperature dependence of the amorphous  $\text{Co}_{66}\text{Fe}_4\text{Nb}_{2.5}\text{Si}_{12.5}\text{B}_{15}$  wire impedance was investigated. The samples were subjected to soft heat treatment during 100 hours under the temperature of 150 °C. The amorphous state of the samples was confirmed by the X-ray structure investigations. The impedance properties were investigated using automated system of magnetoimpedance spectroscopy based on impedance analyzer Agilent 4294A [1]. The investigations were done in the frequency range of alternating current from 100 kHz to 100 MHz at effective value of the current 1mA. The value of the dc-bias current was changed in the interval of  $\pm 60$  mA. The temperature of the sample was varied in the range from 20 °C to 130 °C.

It is ascertained that the changing of the bias current value leads to changing of the temperature dependence of the impedance  $Z(t)$  in the whole ac frequency range. The behavior and variation of  $Z(t)$  depends on ac frequency at which it was measured.

The impedance of the samples monotone falls with the temperature increasing at the ac frequencies below 8 MHz and the dc-bias current intensity up to 30 mA. In this case  $Z(t)$  dependence is near to linear dependence (Fig. 1, a). But its dependence becomes nonlinear when the bias current intensity above 30 mA.

When the ac frequencies above 8 MHz  $Z(t)$  dependence is similar to linear in the range of bias current values up to 10 mA (Fig. 1, b). The impedance increases in the whole temperatures interval for bias current interval from 10 mA to 30 mA. The  $Z(t)$  dependence is nonlinear decreasing. The temperature dependence of the impedance ( $Z(t)$ ) curve have weak maximum when the bias current above 30 mA. When the bias current goes on increases the maximum becomes more expressive and shifts to range of greater values of the temperatures.

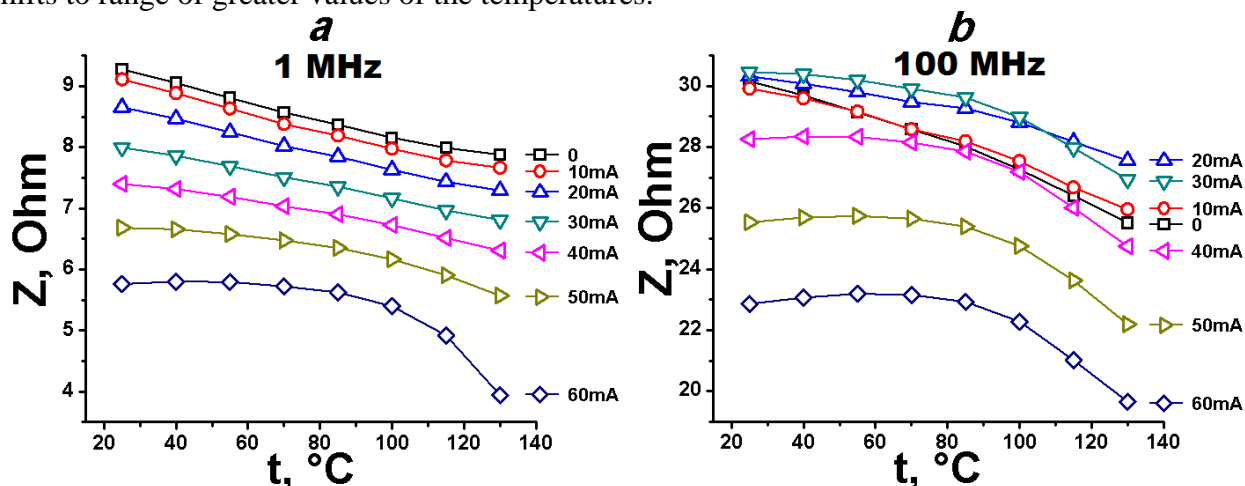


Fig. 1.

The investigations were supported by Russian Foundation for Basic Research (09-08-00406-a).

[1] Semirov A. V., Moiseev A. A., Bukreev D. A. et al., *Nauch. Priborostroen.* (in Russian), **20** (2010) 42–45.

## SPECTRAL PROPERTIES OF SUPERLATTICES WITH ANISOTROPIC INHOMOGENEITIES. THE TRANSITION FROM 3D TO 2D DISORDER

Ignatchenko V.A.<sup>1</sup>, Pozdnyakov A.V.<sup>2</sup>

<sup>1</sup> L.V. Kirensky Institute of Physics, SB RAS, 660036, Krasnoyarsk, Russia

<sup>2</sup> Siberian Federal University, (branch), 662971, Zheleznogorsk, Russia

In the papers [1,2] effects of inhomogeneities with anisotropic correlation properties on the dispersion laws and damping of waves in an initially sinusoidal superlattice were studied. The correlation function had different correlation radii  $k_{\parallel}$  and  $k_{\perp}$ , along the superlattice axis  $z$  and in the  $xy$  plane, respectively. The anisotropy of the correlations was characterised by the parameter  $\kappa = k_{\perp} / k_{\parallel}$  that changed from 1 to 0 when the correlation wave number  $k_{\perp}$  changed from  $k_{\perp} = k_{\parallel}$  (isotropic 3D inhomogeneities) to  $k_{\perp} = 0$  (1D inhomogeneities). The changes of the Green's

function and the density of states during that transition between the 3D and 1D disorders were investigated.

In the present paper we study Green's function for the situation of the smooth transition between the 3D and 2D inhomogeneities. This transition corresponds to the change of the reciprocal parameter  $\kappa_1 = k_{\parallel} / k_{\perp}$  from 1 to 0 when correlation number  $k_{\parallel}$  changes from  $k_{\parallel} = k_{\perp}$  to  $k_{\parallel} = 0$  (Fig. 1). Here  $\nu = (\omega - \omega_0) / \alpha g M$  is the normalized frequency,  $\Lambda_p$  is the width of the gap (forbidden zone) in the spectrum of the superlattice at the boundary of the Brillouin zone, and  $\nu_r$  is the frequency of the center of this gap.

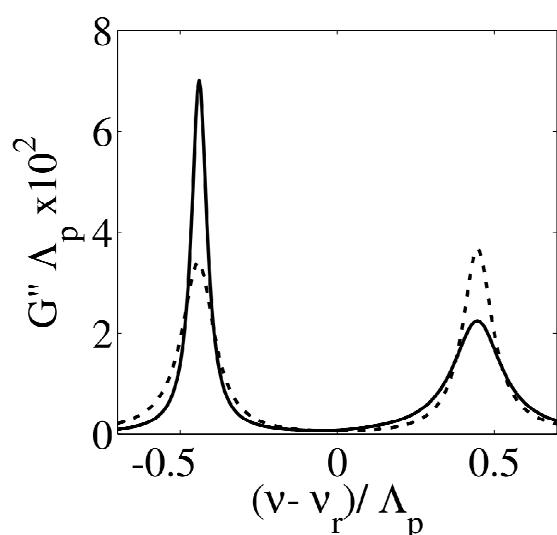


Fig. 1. The imaginary part of the Green's function  $G''(\nu)$  for the case  $\kappa_1 = 1$  (dashed curve) and  $\kappa_1 = 0$  (solid curve).

Fig 1 shows how the imaginary part of the Green's function  $G''(\nu)$  changes during the transition between the 3D and 2D inhomogeneities. For the 3D case ( $\kappa_1 = 1$ , dashed curve)  $G''(\nu)$  has two

symmetric peaks in the points  $(\nu - \nu_r) / \Lambda \approx \pm 0.5$ . With the decrease of  $k_{\parallel}$  the effects asymmetry appears in the behavior of the dynamic susceptibility peaks: the peak corresponding to the lower-frequency edge of the forbidden band shifts to the band center and its height increases, while the peak corresponding to the higher-frequency band edge broadens and decreases sharply in height before vanishing (solid curve).

Support by the Program No. 27.1 of the RAS Presidium, the State Contract No. 02.740.11.0220 on the FTP, and the Program RNP 2.1.1/3498 is acknowledged.

[1] V.A. Ignatchenko, A.A. Maradudin, and A.V. Pozdnyakov, *Zh. Eksp. Teor. Fiz.*, **78** (2003) 9.

[2] V.A. Ignatchenko and A.V. Pozdnyakov, *Solid State Phenomena*, **168–169** (2011) 85.



## INFLUENCE OF INTERFACES ON SPIN WAVE SPECTRA OF PLANAR MAGNONIC CRYSTALS

*Sokolovskyy M.L., Krawczyk M.*

Faculty of Physics, Adam Mickiewicz University, Umultowska 85, 61-614 Poznań, Poland

In recent years, attention among the scientists devoted to the theory of metamaterials has increased significantly because of the possibility to achieve new properties that otherwise do not exist in nature. Metamaterials with periodic modulation of one or more structural parameters are promising for applications. The fundamental feature of periodic structures is the presence of forbidden-frequency gaps ('band gaps') in their spectrum, in which no propagation is allowed. Electromagnetic bandgap metamaterials control the propagation of light. This is accomplished with either a class of metamaterial known as photonic crystals, or another class known as left-handed materials. Both are novel classes of artificially engineered structures, and both control and manipulate the propagation of electromagnetic waves. Periodically modulated magnetic materials can be regarded as the magnetic counterpart of photonic crystals, with spin waves acting as information carriers. As opposed to magnonics, photonics is a more developed field of research and technology. However, magnonic crystals are better candidates for miniaturization, since the wavelength of spin waves is several orders of magnitude shorter than that of electromagnetic waves of the same frequency.

In this work we consider 1D and 2D planar magnonic crystals with nanoscale sizes. Imperfections are always present in the real materials. In the case of fabrication of periodic structures using the nanolithography [1] we have to consider imperfections at the interfaces. Due to the lack of precision there could appear either alloy of different materials or empty spaces between them. In this work we investigate the influence of air spacers at the interfaces between the magnetic materials on the spin wave spectra of the considered structures. The spin wave spectra are calculated using the plane-wave method [2]. The calculations are performed for the case of nonuniform static dipolar field. At the same time the finite thickness of the studied structures is taken into account. We find that the presence of air spacers with a thickness of a few nanometers enables the opening of band gaps in magnonic crystals.

The research leading to these results has received funding from the European Community's Seventh Framework Programme (FP7/2007-2013) under Grant Agreement nr233552 for the MAGNONICS project.

[1] Z.K. Wang, et al., *Appl. Phys. Lett.*, **94** (2009) 083112.

[2] M. L. Sokolovskyy, M. Krawczyk, *J. Nanopart. Res.*, available online, doi: 10.1007/s11051-011-0303-5.

## AUTORESONANT GENERATION OF BOSE-EINSTEIN CONDENSATE OF MAGNONS IN PERPENDICULARLY MAGNETIZED FERROMAGNETIC FILM

*Kharisov A.T.<sup>1</sup>, Kalyakin L.A.<sup>2</sup>, Shamsutdinov M.A.<sup>1</sup>*

<sup>1</sup> Bashkir State University, Validi st., 32, Ufa, Russian Federation

<sup>2</sup> Institute of Mathematics with Computer Center of the Ufa Science Center of Russian Academy of Sciences, Chernishevskogo st., 112, Ufa, Russian Federation

The properties of the Bose-Einstein condensate (BEC) of magnons in ferromagnetic films are currently actively investigated both theoretically [1–3] and experimentally [4, 5]. The case primarily considered is that of the ferromagnetic film magnetized in a magnetic field which is parallel to the film's plane. There is a paper [2] where a prediction is made that the BEC of magnons may exist in perpendicularly magnetized films. It has been shown in [6] that such films may feature autoresonant excitation of a non-linear precessional motion of magnetization. The present paper outlines the theory of autoresonant generation of the BEC of high-density magnons by radio-frequency and low-amplitude fields in perpendicularly-magnetized fine easy-plane ferromagnetic films. Autoresonance is understood as a phenomenon of automatic adjustment of the frequency of a non-linear oscillating system to match the frequency of a weak external input as well as a considerable resonant growth of the oscillation amplitude. Such an adjustment of the frequency and the resonant growth of the oscillation amplitude of a nonlinear system take place under autophasing. The essence of the autophasing effect is that the difference between the phase of the weak exciting field and that of the nonlinear system's oscillations (while continuing to be a limited value) changes but slightly over a long period of time [7].

In perpendicularly magnetized easy-plane ferromagnetic films, with the resonant field slowly decreasing, a capture of magnetization is possible by low-amplitude RF fields. There takes place an adjustment of the phase and the frequency of the magnons to match the RF field frequency and an autoresonant generation of a Bose-Einstein condensate of the magnons which correspond to the homogeneous precession of magnetization. The studies show that in the model based on the combined Gross-Pitaevskii and Ginzburg-Landau equation, with autophasing present, a BEC can be generated, this BEC possessing considerable density.

The paper is supported by the grants of the Russian Foundation for Basic Research # 09-01-92436 and # 10-01-00186, as well as of the Scientific School-2215.2008.01.

- [1] A. I. Bugrij, V. M. Loktev, *Low Temperature Physics*, **33** (2007) 37.
- [2] I.S. Tupitsyn, P.C.E. Stamp, A.L. Burin, *Phys. Rev. Lett.*, **100** (2008) 257202.
- [3] Sergio M. Rezende, *Phys. Rev. B.*, **79** (2009) 174411.
- [4] S.O. Demokritov, V.E. Demidov, O. Dzyapko, G.A. Melkov, A.A. Serga, B. Hillebrands, A.N. Slavin, *Nature*, **443** (2006) 430.
- [5] B.A. Malomed, O. Dzyapko, V.E. Demidov, S.O. Demokritov, *Phys. Rev. B*, **81** (2010) 024418.
- [6] M.A. Shamsutdinov, L.A. Kalyakin, A. T. Kharisov, *Technical Physics*, **55** (2010) 860.
- [7] L.A. Kalyakin, M.A. Shamsutdinov, *Theoretical and Mathematical Physics*, **160** (2009), 960.

## MAGNETOELECTRIC INTERACTION IN NICKEL ALLOYS LAYERED STRUCTURES

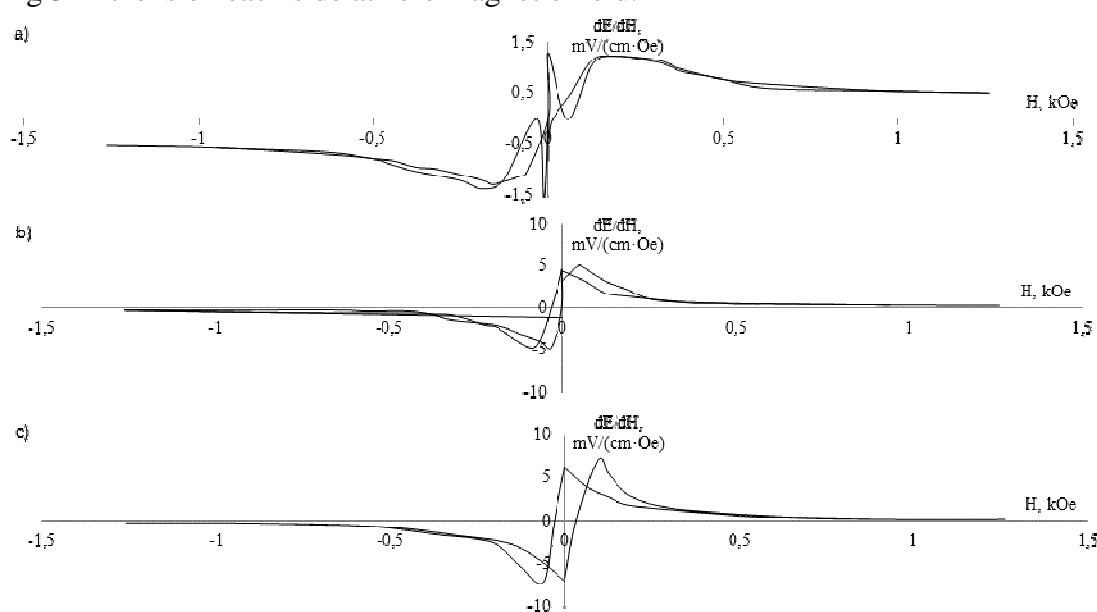
*Poddubnaya N.N.<sup>1</sup>, Stognij A.I.<sup>2</sup>, Novitskii N.N.<sup>2</sup>*

<sup>1</sup> SEE Institute of eTechnical Acoustic, 13 Ludnikov Ave, 210017, Vitebsk, Belarus

<sup>2</sup> SSPA Scientific and Practical Materials Research Center, 17 Brovki St., 220072 Minsk, Belarus

Magnetolectric properties of laminated structures piezoelectric/metal has been studied. Piezoelectric ceramics components are selected, lead zirconate titanate thick 0.4 mm. Metallic layers formed by chemical and electrolytic deposition of nickel and cobalt alloys, layer by layer deposition of nickel and its alloy with cobalt, layer by layer deposition of layers of nickel and cobalt. The thickness of the magnetic metal coating was 20-40 microns. Ion-beam deposition obtained by the structure of Co/PZT/Co with a coating of cobalt 1, 2 and 3 microns.

Linear magnetolectric coefficient of voltage has been studied in Co/PZT structures at low frequencies showed that the shape of hysteresis loops of the magnetolectric determined dependence of the magnetostrictive cobalt with a thickness of metal coating to 2 microns. With increasing thickness of the magnetostrictive metal is greatly affected by the piezoelectric properties. Maximum magnetolectric properties up to 10 mV/(cm·Oe) observed in structures with a thick coating 3 microns on each side at zero magnetic field.



Magnetolectric coefficient of voltage in Co/PZT/Co structures with thick coating  
a) - 1 microns, b) - 2 microns, c) - 3 microns.

Studies of magnetolectric properties of structures Ni/PZT [1] show a significant magnetolectric effect (up to 90 mV/(cm·Oe) in the bilayer). Structures obtained by coprecipitation of cobalt and nickel, and interleaving layers of nickel and cobalt have obviously expressed the magnetic properties, but do not exhibit the magnetolectric properties. Presumably, this behavior is due to a lack of magnetostrictive properties in the foam of cobalt and a nickel - cobalt obtained by electrolytic deposition.

[1] N.N. Paddubnaya, V.M. Laletin, A.I. Stognij, N.N. Novitskii / Dependence of magnetolectric effect in layered lead zirconate-titanate / nickel heterostructures on the interface type // Functional materials 17, No 3, 2010

## MAGNETOIMPEDANCE OF FeNi THIN FILM MEANDERS

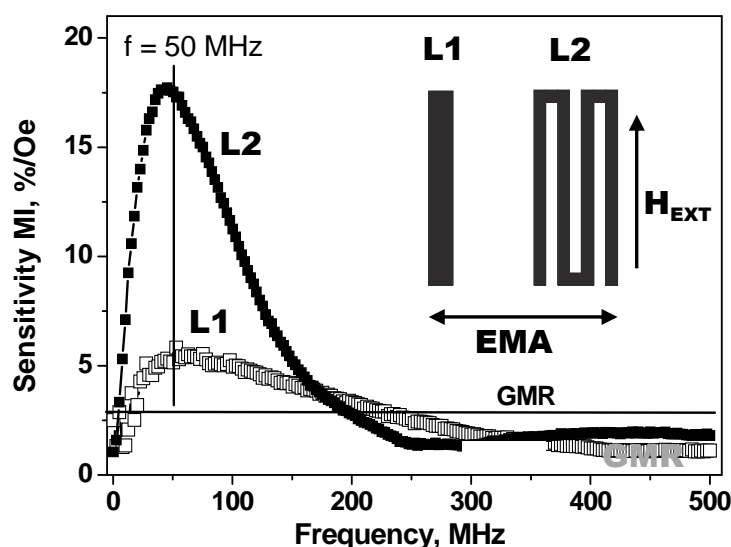
Volchkov S.O.<sup>1</sup>, Uvchenko A.A.<sup>1</sup>, Lepalovskij V.N.<sup>1</sup>, Fernandez E.<sup>2</sup>, Kurlyandskaya G.V.<sup>1,2</sup>

<sup>1</sup> Department of Magnetism and Magnetics Nanomaterials, Ural State University, Ekaterinburg, Russian Federation

<sup>2</sup> Depto Electricidad y Electrónica, Universidad del País Vasco UPV-EHU, Leioa, Spain

Magnetoimpedance effect (MI) was extensively studied in recent years as a basis of many technological applications [1-2]. Many works were devoted to the influence of topology on MI of thin film based elements [1-3]. The new class of MI elements (meander shaped) was discussed and studied recently [4]. It is characterized by the increase of the total length of the MI element, preserving the minimum area occupied in the technological device. In the present work a comparative study of magnetoimpedance of  $\text{Fe}_{19}\text{Ni}_{81}/[\text{Cu}/\text{Fe}_{19}\text{Ni}_{81}]_4/\text{Cu}/\text{Fe}_{19}\text{Ni}_{81}/[\text{Cu}/\text{Fe}_{19}\text{Ni}_{81}]_4$  multilayers was done in two cases: stripe shape (L1) with width 1 mm and a meander (L2) of an approximately four times higher total length (L2) with width 0.5 mm.

Both types of structures were fabricated using lithography techniques and multilayered films were deposited at the same time by rf-sputtering in the field of 100 Oe. The structures were fabricated in such way that the easy magnetization axis (EMA) was kept along the short side of the sample (see Figure). The  $\text{Fe}_{19}\text{Ni}_{81}$  layers were separated by a 3.2 nm thick non-magnetic Cu layers in order to avoid the transition into “transcritical” state [5]. The thickness of the FeNi and central copper layer were 100 nm and 500 nm respectively. The longitudinal MI was measured in a microstrip line [6] in a frequency range of 1 MHz to 500 MHz. MI ratio ( $\Delta Z/Z$ ) was defined with respect to the maximum applied magnetic field of 150 Oe. The MI sensitivity was calculated as  $s(\%/Oe) = (\Delta Z/Z)/\Delta H$ , where  $\Delta H = 0.1$  Oe. The maximum MI sensitivity value for L1 sample was 5.4 %/Oe (exceeding the value of the maximum sensitivity of 3 %/Oe for giant magnetoresistance (GMR) sensors). The maximum MI sensitivity of the meander structure was 17 %/Oe. In both cases the maximum values of  $\Delta Z/Z = 22\%$  for L1 sample and  $\Delta Z/Z = 75\%$  for L2 sample were reached at a low frequency of about 50 MHz, convenient for applications. The increase of MI in the meander structure can be explained by the contribution of the additional inductance. The obtained results can be useful for the optimization of the miniaturized MI detectors design.



The authors thank Prof. V.O. Vaskovskiy for helpful discussion. This work was supported by MAGNOSEN Grant.

- [1] A.S. Antonov, S. N. Gadetskii, et al, Fiz. Met. Metalloved. 83 (6), 61 (1997).
- [2] L.V. Panina, K. Mohri, Sens. Actuators A, 2000, 81, 71.
- [3] S.O. Volchkov, A.V. Svalov, G.V. Kurlyandskaya, Russian Phys. Journal, 52(8), 2009, 769.
- [4] L. Chena, Y. Zhou, C. Leia, Z.M. Zhoua and W. Dinga JMMM, V 322, I. 19, P. 2834-2839.
- [5] A.V. Svalov, I.R. Aseguinolaza, A. Garcia-Arribas et al. IEEE Trans. Magn. 2010. 46, 333.
- [6] D. de Cos, A. García-Arribas, J. M. Barandiarán, Sens. Actuators A, 2004, 115, 368.

## USING OF MODEL CONNECTED OSCILLATORS FOR THE DESCRIPTION OF MAGNETIC SPECTRA

*Ivanov A.P.<sup>1</sup>, Kotov L.N.<sup>1</sup>, Vlasov V.S.<sup>1</sup>, Poleshikov S.M.<sup>2</sup>, Asadullin F.F.<sup>2</sup>, Shcheglov V.I.<sup>3</sup>,  
Shavrov V.G.<sup>3</sup>*

<sup>1</sup> Syktyvkar State University, 167001 Syktyvkar, Oktybrsky 55, Russia

<sup>2</sup> Syktyvkar Forest Institute, 167000 Syktyvkar, Lenina 39, Russia

<sup>3</sup> Institute of Radioengineering and Electronics of RAS, 125009 Moscow, Mokhovaya 11-7, Russia

For modeling of magnetic domain walls movement in volume samples under the alternating fields action coupled oscillators mechanical models representing the dot weights connected by elastic interaction can be used as shown in works [1-2]. Describing the processes due to the nonlinear dynamics of the domain structure is very important, since the revealed behavior can be applied in the development of new generations of information storage devices in which information readout is based on translational motion of the domain structure without disc rotation [3]. Let us consider model of domains as system mechanical oscillators located on a ring with nonlinear coupling between oscillators. On such ring it is possible to observe translational and oscillation motion. Parametrical excitation of such system in the absence of nonlinearity of elastic forces leads to occurrence damping modulation oscillations without dependence on depth modulation parameter. Presence of nonlinearity of elastic forces compels translational motion of the system as whole. It has been established that such motion is provided with obligatory presence at interaction potential of even orders nonlinearities [4].

The given work is continuation of the work [4]. The model offered in the work [4] is used here for the description of magnetic spectra of the magnetic samples in the low-frequency area caused by the domains motion. The domain dynamics is described on the basis of the numerical solution of differential equations for a system of connected oscillators. The numerical solution of the system of differential equations as in the work [4] was found using Runge–Kutta integration. The expression for the magnetic susceptibility of magnetic samples of the limited sizes on the basis of mechanical oscillators' model was defined. Features of low-frequency area of frequency spectra where the magnetic susceptibility doesn't depend on frequency of the field have been revealed. The area specifies independence oscillator velocity on the frequency. Spectra of the ferromagnetic materials limited samples on frequency and amplitude of the alternating field including for nanosized samples was calculated. For example, spectra magnetic nanowires which can be used in memory devices and spintronics devices were calculated [3].

This work was supported by RFBR (grant 10-02-01327).

[1] W G Zengt, J X Zhangt and G G Siuf, *J. Phys.: Condens. Matter*, **3** (1991) 4783.

[2] M.M. Solov'ev, B.N. Filippov, *Fiz. Met. Metaloved.*, **98** (2004) 12.

[3] S.S.P. Parkin, M. Hayashi, L. Thomas, *Science*, **320** (2008) 190.

[4] A.P. Ivanov, L.N. Kotov, V.S. Vlasov, F.F. Asadullin, S.M. Poleshchikov, V.V. Koledov, V.I. Shcheglov, V.G. Shavrov, *Bulletin of the Russian Academy of Sciences: Physics*, **75** (2011) 187.

## COMPLEX CONDUCTIVITY SPECTRUM OF THIN COMPOSITE FILMS: EXPERIMENT AND MODELING

Vlasov V.S.<sup>1</sup>, Kotov L.N.<sup>1</sup>, Lasek M.P.<sup>1</sup>, Kalinin Yu.E.<sup>2</sup>, Sitnikov A.V.<sup>2</sup>

<sup>1</sup> Syktyvkar State University, 167001 Syktyvkar, Oktybrsky 55, Russia

<sup>2</sup> Voronezh State Technical University, 394026 Voronezh, Moskovsky Pr. 14, Russia

This paper proposes a new way of measuring the frequency dependence of the module RF and microwave complex conductivity of composite metal-dielectric films. We studied the film of the following compositions:  $(\text{Co}_{45}\text{-Fe}_{45}\text{-Zr}_{10})_x(\text{Al}_2\text{O}_3)_y$ ,  $(\text{Cu}_{100})_x(\text{Al}_2\text{O}_3)_y$  with magnetic and nonmagnetic metal phase and the same dielectric phase. The metal phase concentration varied in the limits,  $3 < y < 12$ ,  $y = 21-30$   $x$ . The most pronounced dependences of the complex conductivity on frequency were obtained for films with the concentration of metal phase  $x$  below the percolation threshold ( $x \leq 0.42$ ). The different behavior of the complex conductivity on the frequency for films of magnetic and nonmagnetic nanocomposites was revealed. The complex conductivity of the magnetic nanocomposites films decreases rapidly with increasing frequency in comparison with films from non-magnetic nanocomposites. After reaching the minimum complex conductivity for films with magnetic nanocomposites the conductivity increases linearly with increasing frequency. The minimum in the dependence of the complex conductivity for films with non-magnetic nanocomposites shifted to the frequency of  $\sim 4$  times compared with the films with magnetic composites. The dependence of the modulus of the complex conductivity on frequency for non-magnetic nanocomposites has the form close to parabolic. The model of equivalent electrical circuit of magnetic and nonmagnetic nanogranular composite films which describes the experimental results of the frequency dependence of complex conductivity of the films was proposed. Calculations of spectrums of complex conductivity of thin composite films at a various concentration of metal and dielectric phases were made on the base of the model. The model of equivalent electrical circuit is the improvement of the model proposed in the work [1]. The model takes into account the magnetic properties of composite films comparing with the model in the work [1]. Thus the magnetic properties of the films have the significant contribution to the complex conductivity, reflecting and absorbing properties of the films. These facts have shown in the work. The technique of measuring the modulus of the complex conductivity was proposed. From the complex conductivity data we can easily obtain the dependence of the nanogranular composite films magnetic permeability on the frequency.

This work was supported by RFBR (grant 10-02-01327).

[1] Kalinin Yu.E., Kotov L.N., Petrunev S.N., Sitnikov A.V., *Izvestiya RAN. Seriya fizicheskaya*, **69** (2005) 1191.

## EFFECT OF MAGNETIC IMPEDANCE AMORPHOUS RIBBONS

### $\text{Fe}_{74}\text{P}_{18}\text{Mn}_5\text{V}_3$

*Kondusov V.<sup>1</sup>, Kondusov V.<sup>1</sup>, Kalinin Yu.<sup>1</sup>, Vavilova V.<sup>2</sup>, Paliy N.<sup>2</sup>*

<sup>1</sup> Voronezh State Technical University, Voronezh, 394026, Russia

<sup>2</sup> Institute of Metallurgy and Materials Science, Moscow, 119991, Russia

Effect of magnetic impedance was investigated in magnetic fields up to 80 kA/m and frequency of the alternating current flowing through the sample from 0.05 MHz to 100 MHz on samples of length 17 mm, 1 mm wide, made of amorphous ribbon of  $\text{Fe}_{74}\text{P}_{18}\text{Mn}_5\text{V}_3$  thickness 30 microns. The long side of the specimen was parallel to the long side of the original tape. Measuring the relative variation of the magnetic impedance (ie,  $\Delta Z/Z_0$  (%)) on the external magnetic field (H) implemented an automated installation of PC-based, developed by the authors, based on well-known scheme used, consisting of series-connected high resistance resistor and the sample [1]. Installation can take the field dependence of samples in the frequency range of 50 kHz - 100 MHz and in fields up to 80 kA/m. Removing the model dependence of 50 points was carried out in 5 minutes, the numerical results of measurements are automatically recorded in a text file that is used to construct the plot of a specialized program.

Figure 1 shows typical experimental magnetic field dependence of the impedance of the investigated amorphous ribbons for a few of the exciting current frequency  $f$ . It is clearly seen that with increasing  $f$  the transformation curve of the type "single peak in the curve of the "double peak".

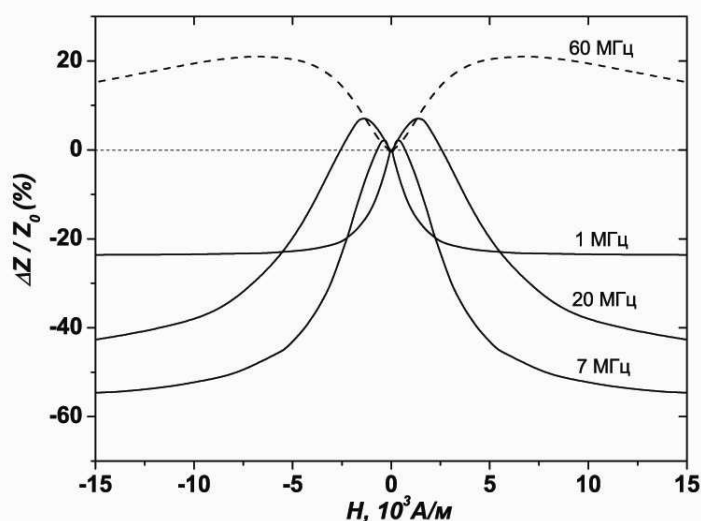


Figure 1. Relative changes in the magnetic impedance (i.e.,  $\Delta Z/Z_0$  (%)) rapidly quenched amorphous ribbons  $\text{Fe}_{74}\text{P}_{18}\text{Mn}_5\text{V}_3$  on the external magnetic field (H) for the currents of different frequencies.

Analysis of the results of studies of the magnetic impedance effect suggests that such a change in  $\Delta Z/Z_0$  (%) depending on the external magnetic field (H) due to the influence of the magnetic impedance of the different mechanisms of magnetization of the sample.

[1] O.L. Sokol-Kutilovskiy // FMM. 1997. T.84. release 3. P.51-54.





**25 August** Thursday

9:30-11:00

plenary lectures  
25PL-A

25PL-A-1

## ODD TRIPLET SUPERCONDUCTIVITY IN SUPERCONDUCTOR-FERROMAGNET STRUCTURES

*Efetov K.B.*

Ruhr University Bochum, Germany

Novel unusual effects in superconductor-ferromagnet (S/F) heterostructures are discussed. The main attention is paid to the triplet component of the superconducting condensate generated in these systems due to the presence of the ferromagnet. This component is odd in frequency and even in the momentum, which makes it insensitive to non-magnetic impurities. The triplet component is not destroyed even by a strong exchange field and can penetrate the ferromagnet over long distances. It is generated as soon as the magnetic moment of the ferromagnet is not homogeneous in space, which can be made experimentally in a controllable way. What is important, the odd triplet component is generated in the *conventional s-wave* and *d-wave* superconductors put into a contact with the ferromagnets. In the latter case, the ferromagnet can even enhance the superconductivity. The generation of superconductivity in the strong ferromagnet is not the only unusual effect. In its turn, the ferromagnet moment can be induced in the superconductor on distances of the order of the superconducting coherence length, which may be classified as the inverse proximity effect. We review recent experiments where the long range penetration of the superconductivity through a strong ferromagnet and the inverse proximity effects have been observed.

25PL-A-2

## SYMMETRY AND MAGNETOELECTRIC INTERACTION IN MULTIFERROICS

*Zvezdin A.K.<sup>1</sup>, Pyatakov A.P.<sup>1,2</sup>*

<sup>1</sup> A.M. Prokhorov General Physics Institute, Russian Academy of Science, Vavilova 38, Moscow 119991, Russia

<sup>2</sup> Faculty of Physics, M.V. Lomonosov Moscow State University, Leninskie gory, Moscow, 119991, Russia

In the last decade there was a remarkable progress in physics of multiferroics (materials with several order parameters), particularly in the understanding of magnetoelectric coupling mechanisms [1-4]. In the review [5] that summarizes the achievement of the initial period of multiferroic era the emphasis was put on the biquadratic coupling between magnetic and ferroelectric order parameters  $F^{ME} = -\frac{1}{2} \sum_{ss'} \beta_{ss'}^{ijkl} P^i P^j M_s^k M_{s'}^l$ , where  $\mathbf{P}$  is polarization and  $\mathbf{M}_s$  is

magnetization of sublattices ( $s$  is the number of magnetic sublattice). Nowadays other types of magnetoelectric interactions linear in electric polarization are brought to the forefront as they are responsible for magnetically induced ferroelectricity. They can be divided into two general classes:

The first one is the homogeneous magnetoelectric interaction that are described by terms  $F_{\text{hom}}^{ME} = -\alpha_{klm} P_k M_l L_m$  or  $F_{\text{hom}}^{ME} = -\alpha_{klm} P_k L_l L_m$  where  $\mathbf{P}$ ,  $\mathbf{M}$  and  $\mathbf{L}$  are ferroelectric, magnetic and antiferromagnetic order parameters, respectively. They are responsible for ferroelectrically induced

weak ferromagnetism in proper ferroelectrics and toroidal ordering [6] as well as ferroelectric polarization induced by antiferromagnetic ordering [7].

The second one is inhomogeneous magnetoelectric interaction (or spin flexoelectricity) that is described by Lifshitz-like invariant  $F_{inhom}^{ME} = -\gamma_{ijkl} P_i n_j \nabla_k n_l$ , where  $\mathbf{P}$  is the electric polarization, and  $\mathbf{n}$  is the magnetic order parameter vector. The interrelation between spatial modulation of order parameter and electric polarization, known as flexoelectric effect in liquid crystals, in the case of magnetic media causes various effects:

- Improper ferroelectric polarization induced by magnetic ordering in multiferroics [4], and electric polarization associated with magnetic domain walls [8]
- Spatially modulated spin structures stabilized by electric polarization in proper ferroelectrics [6] and chiral domain structure in magnetic films with broken central symmetry [8]
- The pinning of antiferromagnetic domain structure at ferroelectric domain walls as well as spin modulation induced by ferroelectric domains [9].

Support by RFBR grant 10-02-13302-RT-omi is acknowledged.

- [1] N.A. Hill, J. Phys. Chem. B **104** (2000) 6694.
- [2] M. Fiebig, J. Phys. D: Appl. Phys. **38** (2005) R123.
- [3] D. Khomskii, Physics, **2** (2009) 20.
- [4] S.-W. Cheong, M. Mostovoy, Nature Materials, **6** (2007) 13.
- [5] G. A. Smolenskii, I. Chupis, Sov. Phys. Usp. **25** (1982) 475.
- [6] A. Kadomtseva et al, JETP Lett. **79** (2004) 571.
- [7] A. K. Zvezdin et al, JETP Letters, **81** (2005) 272.
- [8] A.P. Pyatakov et al, EPL, **93** (2011) 17001.
- [9] Z. V. Gareeva, A. K. Zvezdin, EPL, **91** (2010) 47006.



**25 August**

Thursday

11:30-13:00

14:30-17:00

oral session

25TL-A

25RP-A

25OR-A

**“Diluted Magnetic  
Semiconductors”**

25TL-A-1

## SPIN PHOTOCURRENTS IN DILUTED MAGNETIC NANOSTRUCTURES

*Bel'kov V.*

Ioffe Physical-Technical Institute, Russian Academy of Sciences, 194021 St. Petersburg, Russia

The generation of spin currents in low-dimensional semiconductor structures has recently attracted a lot of interest. A pure spin current is formed by oppositely directed and equal flows of spin-up and spin-down electrons. While the net electrical current is zero, the spin current is finite and leads to a spatial spin separation. Spin-dependent effects can be greatly enhanced due to exchange interaction between electrons and magnetic ions in diluted magnetic semiconductors (DMS). The strength of these effects can be widely tuned by temperature, magnetic field, concentration of the magnetic ions and nanostructure design.

Here we report on the observation of zero-bias spin separation in (Cd,Mn)Te/(Cd,Mg)Te and "hybrid" AlSb/InAs/(Zn,Mn)Te DMS heterostructures. In the latter samples manganese ions are separated from InAs quantum well (QW) by monolayer-scale spacer of pure ZnTe. By that, we obtain *n*-type III-V magnetic QWs. We show that the free carrier absorption of microwave or terahertz radiation causes a pure spin current flow. The effect is probed in an external magnetic field which converts the spin current into a net electric current. This conversion is greatly enhanced in DMS compared to non-magnetic structures. The application of an external magnetic field results not only in a giant Zeeman spin splitting of the conduction band but evokes also spin-dependent exchange scattering of free electrons by magnetic impurities. Both effects destroy the cancellation of spin-up and spin-down electron flows yielding a net electric current. We demonstrate that spin-dependent exchange scattering of electrons by magnetic impurities plays an important role in electric photocurrent generation, providing yet another handle to manipulate spin-polarized currents.

To generate spin photocurrents we heat the electron gas by low power continuous-wave linearly polarized terahertz (2.54 THz) or microwave (95 GHz) radiation. Free carrier absorption only is induced at these frequencies. To align the  $\text{Mn}^{2+}$  spins and to convert the spin flows into a charge current an in-plane magnetic field  $B$  was applied. In this experimental geometry both the cyclotron motion and Landau quantization of the two-dimensional electrons are excluded.

At low magnetic fields the photosignals  $U$  are linear in  $B$  and the signal polarity reverses with the change of the magnetic field direction. A central observation is that cooling of the DMS samples changes the signal polarity and substantially increases absolute value of the photoresponse. This behaviour is not found in reference non-magnetic QWs. While at moderate temperatures the signal depends linearly on magnetic field, at the lowest temperature of 1.8 K the photocurrent saturates at high  $B$ . The increase of the radiation power  $P$  results in the decrease of the normalized signal  $U/P$ , indicating a reduction of the exchange enhanced spin splitting due to increased temperature of Mn-ion-system. Temperature, magnetic field and excitation intensity dependences are typical for the magnetization of DMS and are controlled by the exchange interaction of two-dimensional electrons with manganese ions.

We show experimentally and theoretically that two mechanisms are responsible for the amplification of a spin photocurrent in DMS: Giant Zeeman splitting of the conduction band states and spin-dependent carrier scattering by localized  $\text{Mn}^{2+}$  spins polarized by an external magnetic field. In a degenerated electron gas at weak magnetic fields the scattering mechanism dominates the spin current conversion.

25TL-A-2

## UNUSUAL HIGH FIELD MAGNETOTRANSPORT IN Ge:Mn MAGNETIC SEMICONDUCTORS

*Gerber A.*

School of Physics and Astronomy, Tel Aviv University, Ramat Aviv 69978 Tel Aviv, Israel

An interest in Mn doped Ge was initiated by the search of magnetic semiconductors for spintronics applications. Although no room temperature macroscopic ferromagnetism has been found, the material reveals a number of unusual and puzzling magnetotransport properties. These include the field driven metal-insulator transition, probably associated with a strong magnetic disorder, a huge magnetoresistance of thousands of percent and suppression of the extraordinary Hall effect in magnetically ordered state by high magnetic field. In the insulating state we find a peculiar magnetoresistance following the  $3/2$  power law from zero up to 60 T field with no sign of saturation. We argue that the non-saturating power-law magnetoresistance is a distinctive property of a wide variety of conducting materials that has no explanation in the framework of the existing theories.

25RP-A-3

## HIGH-TEMPERATURE FERROMAGNETISM IN Si:Mn ALLOYS WITH PHASE SEGREGATION

*Tugushev V.V.<sup>1,2</sup>, Men'shov V.N.<sup>1,2</sup>, Caprara S.<sup>2,3</sup>, Chulkov E.V.<sup>2,4</sup>*

<sup>1</sup> NRC Kurchatov Institute, Kurchatov Square 1, 123182 Moscow, Russia

<sup>2</sup> Donostia International Physics Center, P. de Manuel Lardizabal 4, 20018 San Sebastian, Spain

<sup>3</sup> Dipartimento di Fisica, Università di Roma "La Sapienza", P. Aldo Moro 2, 00185 Rome, Italy

<sup>4</sup> UPV/EHU and Centro Mixto CSIC-UPV/EHU, Apartado 1072, 20080 San Sebastian, Spain

A possible mechanism for high-temperature ferromagnetic (FM) order in Si:Mn alloys is proposed. Our theoretical findings provide a general picture for understanding numerous intriguing magnetic properties observed in these alloys, which are semiconducting or metallic, depending on the Mn content, are suggested to undergo phase separation. In the phase-separated state, again depending on the Mn content, Mn atoms can be gathered within nanometer-sized particles or micrometer-sized islands composed of the  $\text{MnSi}_{2-z}$  precipitate with  $z \approx (0.25-0.30)$ , which are embedded in the Mn-poor silicon matrix. We consider the  $\text{MnSi}_{2-z}$  precipitate to be the  $\text{MnSi}_{1.7}$  silicide host containing a certain amount of magnetic defects associated with unbound Mn 3d orbitals. The  $\text{MnSi}_{1.7}$  silicide is considered to be a weak itinerant ferromagnet, where sizable spin fluctuations ("paramagnons") exist far above its intrinsic Curie temperature, leading to a strong enhancement of the exchange coupling between the local moments of the defects [1]. As a result, a significant enhancement of the temperature of onset of long-range order among the local moments may be achieved. We associate this temperature with the global Curie temperature of the precipitate.

A phenomenological model is developed to determine the spatial structures and characteristics of ferromagnetic order for the cases of a bulk precipitate and of precipitate particles of various shapes. Furthermore, local magnetic moments can be present not only inside the precipitate particle but also at the boundary between this particle and the silicon matrix. We showed that, for a precipitate

particle, FM ordering may be augmented thanks to the enhanced concentration of local moments at the boundary [2]. Allowing for the presence of strong quenched disorder in the precipitate, we describe short-range FM order in the system. Under the assumption that quenched disorder in the defects positions exists within the precipitate, the origin of specific features of high-temperature magnetism can be attributed to the short-range order in the form of FM droplets. Finally, experimental data on Si:Mn alloys are interpreted on the basis of obtained theoretical results.

Support by RFBR and Ikerbasque Foundation is acknowledged.

[1] V.N.Men'shov, V.V.Tugushev, and S.Caprara, *Eur.Phys.Journ. B* **77** (2010)337.

[2] V.N.Men'shov, V.V.Tugushev, S.Caprara, and E.V.Chulkov, *Phys.Rev.B* **83** (2011) 035201.

25OR-A-4

## SPIN DYNAMICS IN MAGNETIC SEMICONDUCTOR NANOSTRUCTURES

*Dmitriev A.<sup>1</sup>, Zaitsev S.<sup>2</sup>, Koplak O.<sup>3</sup>, Morgunov R.<sup>1</sup>*

<sup>1</sup> IPCP RAS, Acad. Semenov av. 1, Chernogolovka, Russia

<sup>2</sup> ISSP RAS, Acad. Ossipyan st. 2, Chernogolovka, Russia

<sup>3</sup> T. Shevchenko University of Kiev, Volodymyrska st. 64, Kiev, Ukraine

The requirements imposed on the geometrical size, energy consumption, and operation rate of modern electronic semiconductor devices increase rapidly. This poses the problem of the search and introduction of alternative materials and structures based on nonclassical principles into engineering. One of the solutions to this problem is the design of spintronic devices in which their properties are controlled both the electron charge and the electron spin. Spintronics based on diluted magnetic semiconductors nanostructures appears to be more attractive and realistic as it opens new opportunities for the fine adjustment of relationship among magnetic, electrical transport and optical properties. The fundamental principles of physics of macroscopic diluted magnetic semiconductors were developed previously.

This work is devoted to study of spin dynamics, magnetic and magnetotransport properties of diluted magnetic semiconductors nanostructures [1-3]:

- ordered  $\text{Ge}_{1-x}\text{Me}_x$  nanowires (Me = Mn, Co, Cr, Fe;  $x \approx 1 - 3$  at. %) grown in nanopores of anodized aluminum oxide by supercritical fluids method,
- $\text{Ge}_{1-x}\text{Mn}_x$  nanofilms ( $x \approx 2 - 8$  at. %) grown by manganese ion implantation in germanium single crystals,
- heterostructures with InGaAs quantum well and Mn  $\delta$ -doped GaAs nanolayer grown by metal-organic epitaxy and laser scattering).

The aim of the work is following:

- a comparative analysis of the role of diluted magnetic semiconductors geometrical sizes and dimensions in magnetic and electrical transport properties,
- study of the relationship between magnetic, electrical and optical properties of functional diluted magnetic semiconductors nanostructures with limited or intermediate fractal dimension and percolational magnetic order,
- control of spin polarization of charge carriers in diluted magnetic semiconductors nanostructures.

A comparison of the microwave magnetoresistance, electron spin resonance spectra and static magnetization of  $\text{Ge}_{1-x}\text{Mn}_x$  thin films and nanowires has indicated that the sample size affects the



spin-dependent scattering of charge carriers, Curie temperature, the magnetization, and the spin dynamics in  $\text{Ge}_{1-x}\text{Mn}_x$  nanostructures [1-2]. Effect of Mn  $\delta$ -doped GaAs layer magnetization on photoluminescence polarization of quantum well in GaAs-based heterostructures was found [3]. Fundamental basis for properties optimization (different methods of doping, annealing, size and dimension limitations) of ordered diluted magnetic semiconductors nanostructures III-V and IV groups was discussed.

These results are the experimental basis for development of the theory of percolation phase transition in diluted magnetic semiconductors nanostructures.

Support by the Grant of the President of Russia MK-1764.2011.3.

[1] R.B. Morgunov, A.I. Dmitriev et al., *Phys. Rev. B* **80**, (2009) 085205.

[2] R.B. Morgunov, A.I. Dmitriev et al., *J. Appl. Phys.* **105**, (2009) 093922.

[3] A.I. Dmitriev, R.B. Morgunov et al., *JETP* **112**, (2011) 317.

25TL-A-5

## MAKING NITRIDE SEMICONDUCTORS MAGNETIC

*Bonanni A.*

Institut für Halbleiter- und Festkörperphysik, Johannes Kepler University, Linz, Austria

We summarise our recent work on controlling and elucidating the magnetism and exchange interactions in GaN and related systems grown by MOVPE and doped with either Fe [1-6] or Mn [7-9] and co-doped with donors (Si) [3,4,8] or acceptors (Mg) [3]. In particular, we show that a significant contribution of the  $d$  orbitals to the bonding leads to the self-organized aggregation of Fe cations at the growth surface driving the material systems to the state of condensed magnetic semiconductor (CMS), *i.e.* to a semiconducting matrix with Fe-rich nanoscale chemical or crystallographic phase separations [10,11]. The correlation between the presence of different Fe-rich phases with peculiar and welldefined magnetic behaviour is highlighted together with the ways proposed for the realisation of a single-phase CMS. Furthermore, we demonstrate – by employing a range of nano characterization tools – that Mn in GaN occupies random cation positions at least up to  $x = 3\%$ . Moreover, we present experimental results on the determination of the coupling strength between Mn ions in GaN and show how by co-doping with Si the dominant interaction can be tuned from ferromagnetic to antiferromagnetic [8].

[1] A. Bonanni, M. Kiecana, C. Simbrunner, Tian Li, M. Sawicki, M. Wegscheider, M. Quast, H. Przybylinska, A. Navarro-Quezada, R. Jakieła, A. Wolos, W. Jantsch, and T. Dietl, *Paramagnetic GaN:Fe and ferromagnetic (Ga,Fe)N: The relationship between structural, electronic, and magnetic properties*, *Phys. Rev. B* **75**, 125210 (2007).

[2] W. Pacuski, P. Kossacki, D. Ferrand, A. Golnik, J. Cibert, M. Wegscheider, A. Navarro-Quezada, A. Bonanni, M. Kiecana, M. Sawicki, T. Dietl, *Observation of strong-coupling effects in a diluted magnetic semiconductor (Ga,Fe)N*, *Phys. Rev. Lett.* **100**, 037204 (2008).

[3] A. Bonanni, A. Navarro-Quezada, Tian Li, M. Wegscheider, R.T. Lechner, G. Bauer, Z. Matej, V. Holy, M. Rovezzi, D'Acapito, M. Kiecana, M. Sawicki, and T. Dietl, *Controlled aggregation of magnetic ions in a semiconductor. Experimental demonstration*, *Phys. Rev. Lett.* **101**, 135502 (2008).

- [4] M. Rovezzi, F. D'Acapito, A. Navarro-Quezada, B. Faina, T. Li, A. Bonanni, F. Filippone, A. Amore Bonapasta, T. Dietl, *Local structure of (Ga,Fe)N and (Ga,Fe)N:Si investigated by x-ray absorption fine structure spectroscopy*, *Phys. Rev. B* **79**, 195209 (2009).
- [5] A. Navarro-Quezada, W. Stefanowicz, Tian Li, B. Faina, M. Rovezzi, R. T. Lechner, T. Devillers, F. d'Acapito, G. Bauer, M. Sawicki, T. Dietl, and A. Bonanni, *Embedded magnetic phases in (Ga,Fe)N: the key role of growth temperature*, *Phys. Rev. B* **81**, 205206 (2010).
- [6] I. A. Kowalik, A. Persson, M.A. Nino, A. Navarro-Quezada, B. Faina, A. Bonanni, T. Dietl, D. Arvanitis, *Element specific characterization of heterogeneous magnetism in (Ga,Fe)N films*, arXiv:1011.0847.
- [7] W. Stefanowicz, D. Sztenkiel, B. Faina, A. Grois, M. Rovezzi, T. Devillers, A. Navarro-Quezada, T. Li, R. Jakiela, M. Sawicki, T. Dietl, and A. Bonanni, *Magnetism of dilute (Ga,Mn)N*, *Phys. Rev. B* **81**, 235210 (2010).
- [8] A. Bonanni, M. Sawicki, T. Devillers, W. Stefanowicz, B. Faina, Tian Li, T. E. Winkler, D. Sztenkiel, A. Navarro-Quezada, M. Rovezzi, R. Jakiela, A. Meingast, G. Kothleitner, and T. Dietl, *Ga1-xMnxN – Experimental Probing of Exchange Interactions between Localized Spins in a Dilute Magnetic Insulator*, arXiv:1008.2083.
- [9] J. Suffczynski, A. Grois, W. Pacuski, A. Golnik, J. A. Gaj, A. Navarro-Quezada, B. Faina, T. Devillers, A. Bonanni, *Effects of s, p -- d and s -- p exchange interactions probed by exciton magnetospectroscopy in (Ga,Mn)N*, *Phys Rev. B.* **83**, 094421 (2011).
- [10] A. Bonanni, Topical Review, *Ferromagnetic nitride-based semiconductors doped with transition metals and rare earths*, *Semicond. Sci. and Technol.* **22**, 41 (2007).
- [11] A. Bonanni and T. Dietl, *A story of high-temperature ferromagnetism in semiconductors*, *Chem. Soc. Rev.* **39**, 528 (2010).

25OR-A-6

## FERROMAGNETISM AND MULTIFERROIC BEHAVIOR IN Cu-DOPED ZnO

*Ding J*

Department of Materials Science & Engineering, National University of Singapore,  
Singapore 119260, Singapore

Room temperature ferromagnetism has been observed in Cu-doped ZnO. Our experimental results have shown that ferromagnetism is strongly dependent on the sample preparation condition. The ordinary substitution of  $\text{Zn}^{2+}$  by  $\text{Cu}^{2+}$  doesn't result in ferromagnetism. Our soft x-ray magnetic circular dichroism and x-ray absorption studies have shown that the ferromagnetism is attributed to the presence of oxygen vacancies and  $\text{Cu}^{1+}$  ions. Based on first-principles calculations, we propose a microscopic "indirect double-exchange" model, in which alignments of localized large moments of Cu in the vicinity of the oxygen vacancy  $\text{V}_\text{O}$  are mediated by the large-sized vacancy orbitals [1]. More recently, we have obtained multiferroic behaviour in Cu-doped ZnO with a higher doping concentration. The presence of Cu ions can enhance electric resistivity significantly. Ferroelectricity has been observed in ZnO doped with 8% of Cu accompanied with room temperature ferromagnetism. Magnetic domain structure has been observed and it can be manipulated with electric field, probably due to migration of oxygen vacancies. In addition, change of magnetization has been obtained after poling with electric field [2].

- [1] T. S. Heng, D.-C. Qi, T. Berlijn, J. B. Yi, K. S. Yang, Y. Dai, Y. P. Feng, I. Santoso, C. S'anchez-Hanke, X. Y. Gao, Andrew T. S. Wee, W. Ku, J. Ding and A. Rusydi, "Room-

temperature ferromagnetism of Cu-doped ZnO films probed by soft X-ray magnetic circular dichroism”, *Physical Review Letters* 104 (2010) 197601.

[2] T.S. Heng, M.F. Wong, D.C. Qi, J.B. Yi, A. Kumar, A. Huang, F.C. Kartawidjaja, S. Smadici, P. Abbamonte, C. Sánchez-Hanke, S. Shannigrahi, J.M. Xue, J. Wang, Y.P. Feng, A. Rusydi, K.Y. Zeng and J. Ding, “Mutual Ferromagnetic – Ferroelectric Coupling in Multiferroic Copper Doped ZnO”, *Advanced Materials* (accepted)

25TL-A-7

## CORRELATION BETWEEN STRUCTURE AND MAGNETISM OF Co:ZnO EPITAXIAL FILMS

Ney A.

Universität Duisburg-Essen, Experimentalphysik, Lotharstr. 1, 47057 Duisburg, Germany

Dilute magnetic semiconductors (DMS) are envisioned as sources of spin-polarized carriers for future semiconductor devices which simultaneously utilize spin and charge of the carriers. The hope of discovering a DMS with ferromagnetic order up to room temperature (RT) still motivates research on suitable DMS materials such as Co:ZnO.

We have used hard x-ray absorption spectroscopy (XAS) and in particular x-ray linear dichroism (XLD) and x-ray magnetic circular dichroism (XMCD) to study Co:ZnO with element specificity. For Co:ZnO films grown by pulsed laser deposition we could demonstrate by means of XLD that more than 95% of the Co dopant atoms occupy substitutional Zn lattice sites [1]. This could be generalized to other preparation techniques such as reactive magnetron sputtering lateron and meaningful quality indicators based on XAS could be established [2]. For all phase-pure Co:ZnO films the M(H) curves recorded by SQUID as well as XMCD at the Co K-edge consistently reveal paramagnetic behaviour [1,2] with a significant single ion anisotropy [3]. Furthermore it could be established that Co-O-Co pairs in Co:ZnO couple antiferromagnetically [1]. No significant changes to the magnetic properties were found upon Al-codoping leading to highly n-type Co:ZnO films as long as structural integrity is assured by the XAS-based quality indicators [4].

Here it will be shown that the antiferromagnetic interactions of Co-O-Co can be directly evidenced by high field XMCD measurements up to 17 T which bare the potential to quantify the strength of the magnetic coupling. In addition, the structural and magnetic properties of phase-separated, superparamagnetic Co:ZnO films will be researched using a combination of XAS-based techniques and transmission electron microscopy (TEM). The TEM results are consistent with both SQUID and XAS-based findings highlighting the fact that phase pure Co:ZnO is a model system for an anisotropic dilute paramagnet where the Co dopant concentration can be varied over a large concentration range from the impurity limit up to the coalescence limit (~20%) of the wurtzite lattice.

Support by the Germany Research Foundation (DFG) through the Heisenberg-Programme is gratefully acknowledged.

[1] A. Ney et al., *Phys. Rev. Lett.* **100** (2008) 157201

[2] A. Ney et al., *New. J. Phys.* **12** (2010) 013020

[3] A. Ney et al. *Phys. Rev. B* **81** (2010) 054420

[4] A. Ney et al. *Phys. Rev. B* **82** (2010) 041202(R)

25OR-A-8

## MAGNETIC AND MAGNETO-OPTICAL PROPERTIES OF $\text{Ti}_{1-x}\text{V}_x\text{O}_{2-\delta}$ SEMICONDUCTOR OXIDE FILMS WITH A VARIOUS RESISTIVITY

Orlov A.F.<sup>1</sup>, Balagurov L.A.<sup>1</sup>, Kulemanov I.V.<sup>1</sup>, Perov N.S.<sup>2</sup>, Gan'shina E.A.<sup>2</sup>, Fetisov L.Yu.<sup>2</sup>, Semisalova A.S.<sup>2</sup>, Rubacheva A.D.<sup>2</sup>, Yashina L.V.<sup>2</sup>, Rogalev A.<sup>3</sup>, Smekhova A.<sup>3</sup>

<sup>1</sup>Institute for Rare Metals, Moscow, 119017, Russia

<sup>2</sup>Moscow State University, Moscow, 119992, Russia

<sup>3</sup>European Synchrotron Radiation Facility, Grenoble Cedex, France

Dilute magnetic semiconductors have attracted a huge attention because of their potential application in semiconductor spin electronics and new generation magnetic memory systems. Room temperature ferromagnetic ordering in a titanium oxide doped with vanadium was early investigated mainly in the papers of N.H. Hong et al. [1]. In this report, we present the results of the study of ferromagnetic semiconductor oxides  $\text{Ti}_x\text{V}_{1-x}\text{O}_{2-\delta}$  structure, magnetic and magneto-optical parameters at various V contents and the wide range of resistivity values changing from a deep dielectric down to a degenerate semiconductor.

Films of  $\text{Ti}_{1-x}\text{V}_x\text{O}_{2-\delta}$  on substrates of either  $\text{LaAlO}_3$  or rutile  $\text{TiO}_2$  having (001) orientation were grown by RF magnetron sputtering of metallic alloy targets in the argon-oxygen atmosphere. The concentration of V impurity (x) in the films was 3, 10 or 18% at. The grown films revealed the structure either anatase or rutile with the (001) crystallography orientation and the resistivity changed in the range of  $10^{-3} - 10^6 \Omega\cdot\text{cm}$ . Study of the V impurity chemical state by technique of X-ray photoelectron spectroscopy have shown that in the films with a small concentration of V (3% at.) the whole impurity is in the oxidized state. The character of bulk sensitive XANES spectrum at the V K edge in the film with 3% V also confirms the ionic state of V atoms. Aiming to transfer more impurity into a solid solution, the samples with a high impurity content were heated in vacuum up to temperature of 950 °C which corresponds to the solid solution area at the phase diagram, and then the samples were fast quenched in vacuum.

The room temperature magnetization of the films was found in the whole resistivity range from a deep dielectric down to a degenerate semiconductor. Ferromagnetism in the films of  $\text{TiO}_2:\text{V}$  system has always an intrinsic origin because the possible clusters of V impurity are paramagnetic. The maximum magnetization of  $42 \text{ emu}\cdot\text{cm}^{-3}$  that corresponds to 4.8 Bohr magneton per V atom was observed at the films with 3% V. When the temperature decreases from 400 to 80 K the saturation magnetic moment increases from  $1.5\cdot 10^{-4}$  up to  $3.3\cdot 10^{-4}$  emu.

The magneto-optical transversal Kerr effect spectra were measured at room temperature by dynamic method in the 1.4–3.2 eV energy range in the applied magnetic field up to 3 kOe. The magneto-optical response in the  $\text{TiO}_2:\text{V}$  was observed only in certain samples with high magnetic moment and was significantly lower than in the  $\text{TiO}_2:\text{Co}$  that stipulated by the lack of any magnetic inclusions in the films of  $\text{TiO}_2:\text{V}$ .

Support by RFBR, Grant # 10-02-00804a, is acknowledged.

[1] N.H. Hong, A.G. Ruyter, F. Prellier, J. Sakai. *J. Appl. Phys.*, **97**, 10D323 (2005).

25OR-A-9

**AMORPHOUS GRAIN BOUNDARIES IN FERROMAGNETIC ZnO**

*Mazilkin A.A.<sup>1,2,3</sup>, Protasova S.G.<sup>1,2,3</sup>, Straumal B.B.<sup>1,2,3</sup>, Schütz G.<sup>2</sup>, Tietze Th.<sup>2</sup>, Goering E.<sup>2</sup>, Baretzky B.<sup>3</sup>, Myatiev A.A.<sup>4</sup>, Straumal P.B.<sup>4,5</sup>*

<sup>1</sup> Institute of Solid State Physics, Russian Academy of Sciences, Chernogolovka,  
Moscow district, 142432 Russia

<sup>2</sup> Max-Planck-Institut für Intelligent Systeme (former MPI Metallforschung), Heisenbergstrasse 3,  
70569 Stuttgart, Germany

<sup>3</sup> Karlsruher Institut für Technologie, Institut für Nanotechnologie, Hermann-von-Helmholtz-Platz  
1, 76344 Eggenstein-Leopoldshafen, Germany

<sup>4</sup> National University of Science and Technology “Moscow Institute of Steel and Alloys – MISiS”,  
Leninsky prospect 4, 119991 Moscow, Russia

<sup>5</sup> Institut für Materialphysik, Universität Münster, Wilhelm-Klemm-Str. 10,  
D-48149 Münster, Germany

The nanograined thin films of undoped ZnO were synthesized by the wet chemistry (“liquid ceramics”) method from butanoate precursors. Films consist of the dense equiaxial nanograins, and possess ferromagnetic properties with saturation magnetization up to  $20 \cdot 10^{-6}$  emu (about  $2 \cdot 10^{-3}$   $\mu$ Bohr/f.u.) and coercivity of 10 mT. Structural investigations by the x-rays diffraction and high-resolution transmission electron microscopy reveal that the crystalline wurtzite grains do not contact each other and are completely surrounded by a layer of amorphous phase. The amorphous layers form a kind of continuous foam-like network, where the amorphous intergranular phase amount could be increased by the synthesis parameters. Simultaneously, the saturation magnetization increases as well. We suppose that the defects in the intergranular amorphous “foam” are responsible for the ferromagnetic behavior of undoped ZnO.

25OR-A-10

**FERROMAGNETISM IN HOMOGENOUS Fe,Sn CODOPED  $\text{In}_2\text{O}_3$  FILMS**

*Jiang F.-X., Xu X.-H.*

School of Chemistry and Materials Science, Shanxi Normal University, Linfen 041004,  
People’s Republic of China

In recent years, transition metals (TMs) doped  $\text{In}_2\text{O}_3$  magnetic semiconductors were extensively studied due to potential applications in spintronic devices. Fe as a dopant has been paid more attention due to its high solubility in the  $\text{In}_2\text{O}_3$  host lattice [1,2]. Very recently, codoping Fe together with other dopants was found to be able to significantly influence the magnetic and transport property [3].

In this paper, we choose Sn to codoped Fe- $\text{In}_2\text{O}_3$  films mainly because Sn could provide one extra electron into naturally *n*-type  $\text{In}_2\text{O}_3$  films.  $(\text{In}_{0.92}\text{Fe}_{0.05}\text{Sn}_{0.03})_2\text{O}_3$  films were deposited on sapphire substrates at 600 °C by pulsed laser deposition.

The x-ray diffraction patterns showed the main (222) and (400) orientation peaks of  $\text{In}_2\text{O}_3$ , and no peak of any secondary phase was observed in the spectra. Figure 1 shows the magnetic-field dependence of magnetization at 5 K and 300 K for  $(\text{In}_{0.92}\text{Fe}_{0.05}\text{Sn}_{0.03})_2\text{O}_3$  film. The saturated magnetization of the film is about 0.2  $\mu_B/\text{Fe}$  and the coercive fields is approximately 540 Oe at 300 K. The zero-field-cooled (ZFC) and field-cooled (FC) measurements of the magnetization

dependence on temperature for  $(\text{In}_{0.92}\text{Fe}_{0.05}\text{Sn}_{0.03})_2\text{O}_3$  film are shown in Fig. 2. It can be seen that there is no blocking temperature ( $T_B$ ) in the  $(\text{In}_{0.92}\text{Fe}_{0.05}\text{Sn}_{0.03})_2\text{O}_3$  film in the whole temperature range of 2-380 K, suggesting that there is no tiny ferromagnetic nonoclusters. The X-ray absorption spectra analysis further revealed that the  $\text{Fe}^{3+}$  ions were dominating in the film and a small amount of  $\text{Fe}^{2+}$  ions were also presented, but no metallic Fe was observed, which was consistent with the results of ZFC/FC. The above results indicated that the observed ferromagnetism in  $(\text{In}_{0.92}\text{Fe}_{0.05}\text{Sn}_{0.03})_2\text{O}_3$  film was due to substitution of Fe and Sn for In and was intrinsic. Codoping Sn in Fe-doped  $\text{In}_2\text{O}_3$  films can increase the carrier density of the film, suggesting a carrier-mediated ferromagnetism.

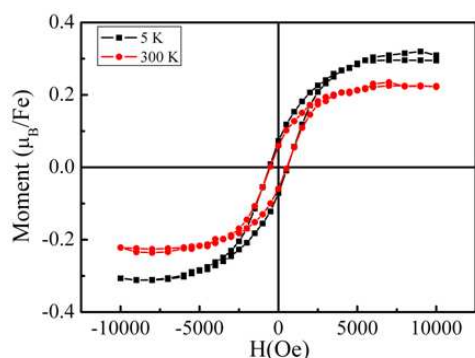


Fig. 1. The M-H dependence of magnetization at 5 K and 300 K for  $(\text{In}_{0.92}\text{Fe}_{0.05}\text{Sn}_{0.03})_2\text{O}_3$  film.

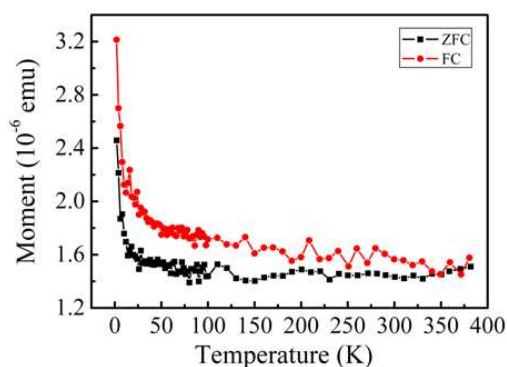


Fig. 2. The ZFC/FC magnetization curves of the  $(\text{In}_{0.92}\text{Fe}_{0.05}\text{Sn}_{0.03})_2\text{O}_3$  film.

[1] Y. K. Yoo, et al, *Appl. Phys. Lett.*, **86** (2005) 042506.

[2] X. H. Xu, et al, *Appl. Phys. Lett.*, **94** (2009) 212510.

[3] H. W. Ho, et al, *J. Phys.: Condens. Matter.*, **20** (2008) 475204.

25OR-A-11

## LOCAL ATOMIC AND ELECTRONIC STRUCTURE OF DILUTED MAGNETIC SEMICONDUCTORS

Finkelstein L.D.<sup>1</sup>, Kurmaev E.Z.<sup>1</sup>, Chang G.S.<sup>2</sup>, Green R.<sup>2</sup>, Moewes A.<sup>2</sup>, Dinia A.<sup>3</sup>

<sup>1</sup> Institute of Metal Physics, Russian Academy of Sciences-Ural Division,  
620990 Yekaterinburg, Russia

<sup>2</sup> Department of Physics and Engineering Physics, University of Saskatchewan, 116 Science Place,  
Saskatoon, SK, S7N 5E2, Canada

<sup>3</sup> Institut de Physique et Chimie des Matériaux de Strasbourg (IPCMS), UMR 7504 ULP-CNRS  
(ULP-ECPM), 23 rue du Loess, BP 43, F-67034, Strasbourg Cedex 2, France

The results of resonant inelastic X-ray scattering (RIXS) measurements of diluted magnetic semiconductors (DMS) are presented. We have measured RIXS spectra of  $3d$ -impurity atoms of  $\text{Ti}_{1-x}\text{Co}_x\text{O}_2$  [1],  $\text{Zn}_{1-x}\text{Co}_x\text{O}$  [2],  $\text{Zn}_{1-x}\text{Mn}_x\text{O}$  [3],  $\text{Cu}_{2-x}\text{MnO}$  [4],  $\text{Zn}_{1-x-y}\text{Co}_x\text{Al}_y\text{O}$  [5],  $\text{Zn}_{1-x-y}\text{Co}_x\text{Ag}_y\text{O}$  [6],  $\text{Ce}_{1-x}\text{Co}_x\text{O}_2$  [7] and found that  $3d$ -impurity atoms occupy not only cation sites but also interstitials. The resonantly excited  $3d$ -metal x-ray emission spectra of ferromagnetic samples show that the ratio of integral intensities for Co  $L_2$  and  $L_3$  emission lines significantly decreases with respect to nonmagnetic samples. This is due to  $L_2L_3M_{4,5}$  Coster-Kronig transitions and suggests that ferromagnetic samples have  $n$ -type charge carriers and Me-Me bonds between substitutional and

interstitial  $3d$ -impurity atoms are present while Me–O bonds are dominant in nonmagnetic samples where  $3d$ -impurity atoms substitute cation sites. The oxygen  $K$ -emission and absorption spectra of diluted magnetic oxides are found to be insensitive to  $3d$ -metal doping which suggests that the oxygen vacancies are not responsible for change of conductivity of the samples. It is shown that X-ray nonresonant and resonantly excited  $3d$ -impurity atoms in DMS can be used for microscopic estimation of change of number of carriers in relation with the preparation conditions.

We gratefully acknowledge the Russian Science Foundation for Basic Research (Projects 11-02-00022), Canada Research Chair program and the Region Alsace for financial support.

- [1] G. S. Chang, E. Z. Kurmaev, D.W. Boukhvalov, L. D. Finkelstein, D. H. Kim, T.-W. Noh, A. Moewes and T. A. Callcott, *J. Phys.: Condens. Matter* 18 (2006) 4243.
- [2] G. S. Chang, E. Z. Kurmaev, D. W. Boukhvalov, L. D. Finkelstein, S. Colis, T. M. Pedersen, A. Moewes, and A. Dinia, *Phys. Rev. B* 75 (2007) 195215.
- [3] G. S. Chang, E. Z. Kurmaev, S. W. Jung, H.-J. Kim, G.-C. Yi, S.-I. Lee, M. V. Yablonskikh, T. M. Pedersen, A. Moewes and L. D. Finkelstein, *J. Phys.: Condens. Matter* 19 (2007) 276210.
- [4] G. S. Chang, E. Z. Kurmaev, DW Boukhvalov, A. Moewes, L. D. Finkelstein, M. Wei and J. L. MacManus-Driscoll, *J. Phys.: Condens. Matter* 20 (2008) 215216.
- [5] G. S. Chang, E. Z. Kurmaev, D. W. Boukhvalov, L. D. Finkelstein, A. Moewes, H. Bieber, S. Colis and A. Dinia, *J. Phys.: Condens. Matter* 21 (2009) 056002.
- [6] G. S. Chang, E. Z. Kurmaev, L. D. Finkelstein, A. Moewes, H. Bieber, S. Colis and A. Dinia (to be published).
- [7] A. Bouaine, R. J. Green, S. Colis, P. Bazylewski, G. S. Chang, A. Moewes, E. Z. Kurmaev, and A. Dinia, *J. Phys. Chem. C* 115 (2011)1556.





**25 August**

Thursday

11:30-13:00

14:30-17:00

oral session

25TL-B

25RP-B

25OR-B

**“Soft and Hard  
Magnetic Materials”**

25TL-B-1

## MICROMAGNETIC MODELS OF GLASS-COATED MICROWIRES WITH CIRCUMFERENTIAL ANISOTROPY

Torrejon J.<sup>1,2</sup>, Thiaville A.<sup>1</sup>, Adenot-Engelvin A.L.<sup>3</sup>, Vazquez M.<sup>2</sup>

<sup>1</sup> Lab. Physique des Solides, CNRS-Univ. Paris-Sud, 91405 Orsay, France

<sup>2</sup> Instituto de Ciencia des Materiales, CSIC, 28049 Madrid, Spain

<sup>3</sup> CEA, DAM, Le Ripault, 37260 Monts, France

Glass-coated microwires with effective circumferential anisotropy have been investigated by micromagnetics. The soft ferromagnetic nucleus of such wires, as a consequence of the amorphous structure together with a negative magnetostriction, shows a continuous and non-uniform magnetic structure like a vortex, with coupled axial core and circular outer shell regions. The theoretical approach is based on a one-dimensional micromagnetic model where exchange, anisotropy (of magnetoelastic origin) and magnetostatic energies are considered. This model is valid as long as the circular symmetry of the sample is not broken. We assume here that the circumferential anisotropy does not depend on the radial coordinate, corresponding to dominant glass cover induced stresses.

The model predicts first the static structures, at equilibrium as well as under an axial field [1]. One can therefore evaluate the size of the core region as a function of exchange energy coefficient, circular anisotropy constant, nucleus radius and axial field strength. In particular, the critical nucleus radius  $R_c$  below which the magnetization is fully axial was analytically obtained, as  $R_c = q_1 \Delta / \sqrt{1 - H/H_K}$ , where  $\Delta = \sqrt{A/K}$  is the Bloch wall width parameter linked to the exchange ( $A$ ) and anisotropy ( $K$ ) energy terms,  $H$  the applied axial field,  $H_K = 2K/(\mu_0 M_s)$  the anisotropy field, and  $q_1 \approx 1.8412$  the first zero of the derivative of the Bessel function of order one.

More recently, the model was extended to study the magnetization dynamics under an axial a.c. field, neglecting the skin effects. Similarly to previous work about soft films with a non-uniform magnetization structure across the sample thickness (due to a variation of anisotropy across the thickness) [2], it was found here that the permeability can be obtained as the sum of the macrospin-like permeabilities over a series of eigenmodes. These modes are obtained as the solutions of a Schrödinger equation where the potential derives from the rest solution, with exchange and anisotropy terms.

Comparison with experimental measurements (applying the a.c. field in a coaxial APC7 setup, with a sample realized by winding a microwire, using the parameters determined from VSM loops) will be presented.

Support by the EC-Marie Curie Programme is acknowledged.

[1] J. Torrejon, A. Thiaville, A.L.-L. Adenot-Engelvin, M. Vazquez, O. Acher, *J. Magn. Magn. Mater.*, **323** (2011) 283.

[2] V. Dubuget, A. Thiaville, F. Duverger, S. Dubourg, O. Acher, A.-L. Adenot-Engelvin, *Phys. Rev. B* **80** (2009) 134412.

25TL-B-2

## MICROWAVE RESPONSE OF FERROMAGNETIC NANOWIRE ARRAYS

*Carignan L.P.<sup>1</sup>, Boucher V.<sup>1</sup>, Caloz C.<sup>2</sup>, Yelon A.<sup>1</sup>, Ménard AD.<sup>1</sup>*

<sup>1</sup> Département de génie physique and Regroupement Québécois sur des Matériaux de Pointe,  
École Polytechnique Montréal, Canada

<sup>2</sup> Electrical Engineering Department, École Polytechnique de Montréal, Canada

Electroplated arrays of ferromagnetic nanowires (FMNWs) provide new possibilities for the engineering of microwave materials, due to their relatively inexpensive fabrication process and their compatibility with microwave integrated circuit technologies. However, these increased design flexibility and integrability are provided at the cost of higher microwave losses as compared to state-of-the-art ferrites and garnets currently used in microwave devices. While we have developed quantitative models of the magnetic permeability, correctly predicting the electromagnetic dispersion of a variety of samples [1], the understanding and reduction of the microwave losses remain the biggest challenge for these promising materials.

We present our recent advances in modeling and measuring the microwave response of FMNW arrays. The systems studied consist of Ni, CoFeB and NiFe alloys, electroplated into nanoporous alumina membranes. Overall, magnetometry (including FORC measurements), ferromagnetic resonance, and microwave transmission line experiments are well accounted for by considering the systems as two sub-arrays of interacting macrospins, leading to relatively simple quantitative expressions for the microwave responses as a function of material and geometrical parameters of the arrays. These are used to quantify the interwire interactions, clarify the magnetization processes, and demonstrate the reconfigurable double resonance properties of self-biased arrays [2-3]. Surprisingly, the ferromagnetic resonance linewidth exhibits a rather weak frequency dependence, indicating a small phenomenological Gilbert damping parameter and suggesting that the losses are dominated by extrinsic mechanisms. Above a certain frequency, usually between 30 and 40 GHz, the FMNW arrays start to exhibit losses which are competitive compared to those of more conventional materials. The relative contributions of different loss mechanisms are reviewed and material challenges currently limiting their use are highlighted.

Support by NSERC is acknowledged.

[1] V. Boucher, *et al.*, Phys. Rev. B, **80**, (2009) 224402.

[2] L.P. Carignan, *et al.*, Appl. Phys. Lett, **95** (2009) 062505.

[3] V. Boucher, *et al.*, Appl. Phys. Lett, **98** (2011) 112502.

25RP-B-3

## COOPERATION BETWEEN K.P. BIELOV GROUP AND WROCLAW SCIENTIFIC CENTER

*Suski W.*<sup>1,2</sup>

<sup>1</sup> International Laboratory of High Magnetic Fields and Low Temperatures, P.O. Box 4714,  
50-985 Wrocław 47, Poland

<sup>2</sup> Polish Academy of Sciences, W. Trzebiatowski Institute of Low Temperature and Structure  
Research, P.O.Box 1410, 50-950 Wrocław 2, Poland  
w.suski@int.pan.wroc.pl

Discovery of ferromagnetism in the uranium trihydride by Trzebiatowski and his coworkers [1] in early fifties came as the total surprise to the scientific community. In spite of the fact that this phenomenon found confirmation in other scientific laboratories (for review see [2]) and magnetic ordering has been detected in other binary compounds of uranium with nonmetallic components, Trzebiatowski, being a chemist by education was looking for physicists having some experience in research on the *f*-electron materials to undertake the common investigation of the uranium compounds. For obvious reasons such cooperation with Western laboratories was excluded, but due to the initiative of Trzebiatowski, Wrocław's scientists had an opportunity to meet K.P.Bielov and his coworkers on the subsequent conferences in Wrocław (LT-Physics), in Dresden (Magnetismus) and in Erevan (School on *f*-electron materials) in the late sixties. At that time we already knew that uranium monochalcogenides were ferromagnetic, oxychalcogenides were antiferromagnetic as well as the uranium monopnictides and dipnictides whereas the  $U_3X_4$  pnictides appeared to be ferromagnetic. Also very soon, the single crystals of some of these binary compounds obtained by transport method with reasonable dimensions became available. Unfortunately, our experimental facilities were seriously limited. Up to the beginning of the seventies we had no liquid helium and magnetic fields used in our experiments were 0.5 T at maximum. Moreover, the single crystals which we had at our disposal could not be used to determine their magnetocrystalline anisotropy or magnetostriction.. Therefore we took opportunity of measurements in Belov Laboratory, however, due to administrative regulation, being employees of Polish Academy of Sciences we used to come to Moscow due to cooperation with Kapitza Institute. We paid several visits to MGU and as a result 6 common papers were published, mostly in prestigious physical journals, Next International Laboratory of High Magnetic Fields and Low Temperature was organized in Wrocław which appeared to be a convenient area of cooperation of the scientists from Socialist Countries, unfortunately, in early period only coworkers of respective Academies of Sciences had an access. This situation changed when our countries became „normal” and now former students of K.B. Belov are frequent visitors both in Laboratory and at Institute, particularly the group of S.A. Nikitin from MGU, coworkers of Yu.G. Pastushenkov from Physics Department of Tver University and of G.S. Burkhanov from Baykov Institute RAS in Moscow. Obviously, the cooperation is at present extended to new multicomponent materials including hydrides and new phenomena as new superconductivity, strongly correlated electrons and magnetocaloric effect.

[1] W.Trzebiatowski,AŚliwa and B.Staliński, *Roczniki Chemii* **26**(1952)110, *ibid.* **28**(1954)12.

[2] R.Troć and W.Suski, *J.Alloys Comp.* **219**(1995) 1.

25RP-B-4

## PROPERTIES AND APPLICATIONS OF TiO<sub>2</sub> COATED NANOSTRUCTURED MATERIALS

Gómez-Polo C.<sup>1</sup>, Larumbe S.<sup>1</sup>, Soto-Armañanzas J.<sup>1</sup>, Olivera J.<sup>1</sup>, Pérez-Landazabal J.I.<sup>1</sup>,  
Mendizabal I.<sup>2</sup>, Korili S.A.<sup>2</sup>, Gil A.<sup>2</sup>

<sup>1</sup> Department of Physics, Public University of Navarra, Campus of Arrosadia,  
31006 Pamplona, Spain

<sup>2</sup> Department of Applied Chemistry, Public University of Navarra, Campus of Arrosadia,  
31006 Pamplona, Spain

The study of the so-called nanostructured materials represents a topic of growing interest in the last decades. Among them, those systems with components with differentiated characteristics (i.e. ferromagnetic and sensing/photocatalytic properties) stand out. The combination of various technological properties in the same unit enables the design of optimized new materials with multifunctional capabilities.

The aim of this work is to present some recent results in the field of multifunctional nanostructured materials, characterized by the coexistence of ferromagnetic and metal oxide semiconductor (TiO<sub>2</sub>) components. Two systems will be analyzed: nanocrystalline soft magnetic alloys (wires) and metal oxide ferromagnetic nanoparticles. In both cases, a TiO<sub>2</sub> coating is introduced to provide the multifunctional characteristic to the samples. In the first case, nanocrystalline wires with nominal composition Fe<sub>73.5-x</sub>Cr<sub>x</sub>Si<sub>13.5</sub>Cu<sub>1</sub>B<sub>9</sub>Nb<sub>3</sub> ( $x = 3$  and  $7$ ) were used, initially obtained in amorphous state by the in-rotating-water quenching technique (diameter about 130  $\mu\text{m}$ ). The control of the Curie temperature of the residual amorphous phase through the crystalline volume fraction [1] enables the design of temperature detectors for environmental applications [2]. The TiO<sub>2</sub> coating is employed as gas sensing element for the detection of humidity or gases as CO and CO<sub>2</sub>. In the second system, metal oxide ferromagnetic nanoparticles (Fe<sub>3</sub>O<sub>4</sub>, NiFe<sub>2</sub>O<sub>4</sub>) are obtained by sol-gel procedure and a TiO<sub>2</sub> coating is subsequently introduced. The main interest of these systems is in the field of depuration of water employing the photocatalytic properties of the TiO<sub>2</sub> coating. The ferromagnetic core enables the magnetic separation of the photocatalyst from the treated water under the application of an external magnetic field. However, in these nanoparticle systems the introduction of the surface coating could lead to deterioration of the magnetic response (i.e. spin surface disordered effects). Accordingly, surface effects, occurrence of spin-glass behaviour and exchange-bias effects, should be analyzed in order to achieve the optimum magnetic response for the magnetic separation application.

[1] C. Gómez-Polo, J.I. Pérez-Landazábal, V. Recarte, M. Vázquez, A. Hernando, *Phys. Rev. B* **70** (2004) 094412.

[2] C. Gómez-Polo, L.M. Socolovsky, M. Knobel, M. Vázquez, *Sensors Letters* **5** (2007) 196.

25TL-B-5

## FAST DOMAIN WALL DYNAMICS IN AMORPHOUS AND NANOCRYSTALLINE MAGNETIC MICROWIRES

Varga R.<sup>1</sup>, Richter K.<sup>1</sup>, Klein P.<sup>1</sup>, Zhukov A.<sup>2</sup>, Vázquez M.<sup>3</sup>

<sup>1</sup> Inst. Phys., Fac. Sci., UPJS, Park Angelinum 9, 04154 Kosice, Slovakia

<sup>2</sup> Dept. Física de Materiales, Fac. Química, UPV/EHU, San Sebastian, Spain

<sup>3</sup> ICMN CSIC, Cantoblanco, Madrid, Spain

Domain wall dynamics is used in many spintronic devices to transfer or store information [1,2]. The speed of such devices depends on the domain wall propagation velocity.

Extremely fast domain wall propagation has been found in amorphous glass-coated microwires [3,4]. However, because of their amorphous nature these microwires are in metastable state. Hence, the domain wall dynamics is very unstable with time and temperature [5,6].

In the given contribution, we show the three possible reasons for fast domain wall propagation. Firstly, it is the low anisotropy that results in low domain wall damping. Secondly, it is the presence of two perpendicular anisotropies that can be averaged out each other. Finally it is the existence of radial domain structure just below the surface of microwires that shields the domain wall from pinning on the surface of the wire.

Moreover, we show how the domain wall dynamics in glass-coated microwires can be stabilized, keeping the domain wall velocity high. It is possible either by thermal treatment of amorphous microwires, or by using nanocrystalline structure of metallic core. Nanocrystalline materials consist of nanocrystalline grains embedded randomly in amorphous matrix. They combine excellent soft magnetic properties of amorphous materials with the high time and thermal stability of crystalline structure. Velocities up to 3000 m/s can be observed in the FeCoMoB-based nanocrystalline microwire.

Support by the project NanoCEXmat Nr. ITMS 26220120019, Slovak grant APVV-0266-10 and VEGA grant No.1/0076/09 is acknowledged.

[1] S. S. P. Parkin, M. Hayashi, and L. Thomas, *Science* **320** (2008), 190.

[2] D.A. Allwood, G. Xiong, C.C. Faulkner, D. Atkinson, D. Petit, R.P. Cowburn, *Science* **309** (2005), 1688.

[3] J. D. Santos, Á. Ruiz, R. F. Cobos, I. Ribot, V. Vega, P. Álvarez, M. L. Sánchez, J. L. Sánchez Ll., V. M. de la Prida and B. Hernando, *Phys. Status Solidi A*, **206** (2009), 618.

[4] R. Varga, A. Zhukov, J. M. Blanco, M. Ipatov, V. Zhukova, J. Gonzalez, P. Vojtaník, *Phys. Rev. B* **76**, (2007), 132406.

[5] G. Infante, R. Varga, G. A. Badini-Confaloneri, and M. Vázquez, *Appl. Phys. Lett.* **95**, 012503 (2009).

[6] R. Varga, K. L. Garcia, M. Vázquez, and P. Vojtanik, *Phys. Rev. Lett.* **94** (2005), 017201.

25RP-B-6

## ON MAGNETOSTATIC INTERACTION IN REMAGNETIZATION PROCESS OF FE-RICH MICROWIRES

Gawroński P.<sup>1</sup>, Tomkowicz J.<sup>1</sup>, Zhukov A.<sup>2,3</sup>, Zhukova V.<sup>2</sup>, Blanco J.M.<sup>4</sup>, Gonzalez J.<sup>2</sup>

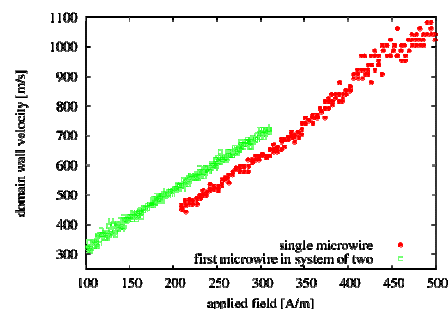
<sup>1</sup> Faculty of Physics and Applied Computer Science, AGH UST, 30-059, Cracow, Poland

<sup>2</sup> Dept. Física de Materiales, UPV/EHU, 20018, San Sebastian, Spain

<sup>3</sup> IKERBASQUE, Basque Foundation for Science, 48011 Bilbao, Spain

<sup>4</sup> Dept. Fis. Apl. I, EUPDS, UPV/EHU, Plaza de Europa, 1, 20018, San Sebastian, Spain

We studied the remagnetization process in systems consisting of two glass coated microwires of the nominal composition of  $\text{Fe}_{75}\text{B}_{15}\text{Si}_{10}$  produced by Taylor Ulitovsky method [1]. The diameter of the metallic core varied from 8 to 18  $\mu\text{m}$  and the glass coating thickness from 8 to 15  $\mu\text{m}$ . The magnetostatic interaction between the microwires manifests itself in appearance of a characteristic plateau in the hysteresis loop, at the magnetic field when two microwires are magnetized in the opposite directions [2]. We studied experimentally the effect of magnetic field frequency and the amplitude peculiarities of such magnetostatic interaction, particularly conditions when this plateau disappears for microwires with the various ratio of the metallic core to the glass coating and on domain wall (DW) propagation in system of interacting microwires. We measured the influence of the stray field produced by one microwire on the velocity of DW in the neighbouring microwire. In Figure 1 we present the dependence of the velocity of DW on the amplitude of the applied field. One of the plots (circles) refers to a single microwire, and another (squares) – to one of two microwires, which presents remagnetization at lower applied field. The velocity of DW in the latter microwire is larger than in the single microwire. We assume, that the stray field of the neighbouring microwire increases the effective field acting on the microwire that is first to remagnetise. The experimental dependencies of the switching field on the frequency and of the velocity of DW on the applied field, when combined with the local remagnetization profile, allow to reconstruct numerically the shape of the hysteresis loop for one and two wires systems, as well as to obtain the dependence of the critical frequency where the plateau vanishes.



This work was partially supported by the “Krakow Interdisciplinary Ph.D.-Project in Nanoscience and Advances Nanostructures” operated within Foundation for Polish Science MPD Programme cofinanced by European Regional Development Fund, by EU ERA-NET under project “SoMaMicSens” (MANUNET-2010-Basque-3), by EU under FP7 “EM-safety” project, by Spanish Ministry of Science and Innovation, under Project MAT2010-18914 and by the Basque Government under Saiotek 09 MICMAGN project (S-PE09UN38).

[1] A. Zhukov, J. Gonzalez, J.M. Blanco, M. Vazquez, V. Larin, J. Mater. Res. 15 (2000) 2107.

[2] A.Chizhik, A.Zhukov, J.M.Blanco, R.Szymczak, J.Gonzalez, JMMM 249/1-2 (2002) 99-103.

25OR-B-7

## THE INFLUENCE OF POWDER PARTICLE SIZE ON BEHAVIOR OF HOT PLASTIC DEFORMATION, STRUCTURE AND MAGNETIC PROPERTIES OF NdFeB DIE-UPSET MAGNETS

Wojciech L.

Electrotechnical Institute, street: Sklodowskiej – Curie 55/61, 50–369 Wrocław, Poland

lipiec@iel.wroc.pl

The influence of powder particle size on behaviour of hot plastic deformation, structure and magnetic properties of NdFeB die-upset magnets have been examined.

It was found, that powder particle size strongly affected on plastic properties of material during hot deformation process. Precursors made of powder with the smallest particles (0 – 32  $\mu\text{m}$ ) shown bigger plastic resistance than those made of powder with the larger ones (32 – 88 or 88 – 350  $\mu\text{m}$ ). For the same pressing force and temperature, applied within hot plastic deformation process, precursors made of the smallest particle powder allowed to obtain only 56 % deformation, while the another: 65% deformation. X-ray diffraction analysis shown that, precursors made of the smallest particles powder allowed to produce anisotropic magnets with much worse texture than those ones made of larger particles. This result was confirmed by SEM examinations. Imagines, made for die-upset magnets, for whom small particles was applied, indicated that only small part of grains undergo alignment, while very good texture appears in microstructure of magnets produced of larger particles. Such behaviour of material is connected with the contents of large grains in depend on the size of powder particle applied in production process of isotropic precursors, what was detailed described elsewhere [1 ÷ 2].

The above results lead to conclusion, that small powder particles, introducing more large grains into material than big powder particles, cause the increase of plastic resistance of material during hot plastic deformation process what makes alignment less efficiency. Magnetic properties of die-upset magnets are strongly influenced by the phenomenon. The best sample made of (0 – 32  $\mu\text{m}$ ) powder fraction allowed to obtain following magnetic properties:  $J_r = 1,15 \text{ T}$ ;  $jH_c = 110 \text{ kA/m}$ ;  $(BH)_{max} = 80 \text{ kJ/m}^3$ . While the best sample made of (32 – 88  $\mu\text{m}$ ) powder fraction received:  $J_r = 1,35 \text{ T}$ ;  $jH_c = 900 \text{ kA/m}$ ;  $(BH)_{max} = 350 \text{ kJ/m}^3$ .

[1] W. Lipiec, H.A. Davies, *The influence of the powder densification temperature on the microstructure and magnetic properties of anisotropic NdFeB magnets aligned by hot deformation*, Journal of Alloys and Compounds, Vol 491, 18 (2010), pp 694 ÷ 697,

[2] W. Lipiec, *The correlation between the size of powder particles and the microstructure of anisotropic Nd-Fe-B magnets aligned by hot plastic deformation*, Proceedings of the 21<sup>st</sup> Workshop on Rare-Earth Permanent Magnets and their Applications, Bled, Slovenia, 29 Aug. – 2 Sept. (2010), pp. 73 ÷ 76.



25OR-B-8

**THE  $\gamma \rightarrow \alpha$  PHASE TRANSITION IN CERIUM IS NOT ISOSTRUCTURAL:  
THEORY AND EXPERIMENT**

*Nikolaev A.V.<sup>1,3</sup>, Tsvyashchenko A.V.<sup>2,3</sup>, Velichkov A.I.<sup>4</sup>, Salamatin A.V.<sup>4</sup>, Fomicheva L.N.<sup>2</sup>,  
Ryasny G.K.<sup>3</sup>, Sorokin A.A.<sup>3</sup>, Kochetov O.I.<sup>4</sup>, Budzynski M.<sup>5</sup>, Michel K.H.<sup>6</sup>*

<sup>1</sup> Institute of Physical Chemistry and Electrochemistry, RAS, 117915, Moscow, Russia

<sup>2</sup> Vereshchagin Institute for High Pressure Physics, RAS, 142190, Troitsk, Russia

<sup>3</sup> Skobeltsyn Institute of Nuclear Physics, MSU, 119899, Moscow, Russia

<sup>4</sup> Joint Institute for Nuclear Research, PO Box 79, Moscow, Russia

<sup>5</sup> Institute of Physics, M. Curie-Sklodowska University, 20-031 Lublin, Poland

<sup>6</sup> Department of Physics, University of Antwerp, Groenenborgerlaan 171,  
2020, Antwerpen, Belgium

Usually different crystallographic forms of a same element are distinguished by their crystal space symmetry. In some cases, for example in metallic cerium, there are two well defined thermodynamic phases:  $\gamma$  and  $\alpha$ , which apparently have the same face centred cubic lattice. The existence of such twin phases in cerium has become a challenge to the theory and prompted the search of a main factor responsible for the difference. Here we show both theoretically and experimentally that the well known  $\gamma$ - $\alpha$  phase transition in cerium is not really isostructural. Recent experimental results (time-differential perturbed angular correlation spectroscopy, TDPAC) are interpreted as evidence for quadrupolar electronic charge density ordering and symmetry lowering at the  $\gamma \rightarrow \alpha$  transition while the lattice remains face-centered cubic.



**25 August**

Thursday

11:30-13:00

oral session

25TL-C

25OR-C

**“Magnetic Oxides”**

25TL-C-1

## MAGNETO-OPTIC STUDIES OF MAGNETIC OXIDES

*Gehring G.A., Alshammari M., Fox A.M.*

Department of Physics and Astronomy, University of Sheffield, Sheffield S3 7RH UK

This talk will present some previously published and new work on magneto-optic studies of oxides made in Faraday geometry. This is the only technique available to study the magnetic properties of gap states in magnetic semiconductors and is also very suitable for the study of thin films of manganites and ferrites.

In this geometry the magnetic circular dichroism is related to the difference in absorption for left and right circularly polarised light and for light of angular frequency  $\omega$  is related to the off-diagonal component of the dielectric constant by  $MCD = \frac{\omega L}{2nc} \text{Im} \epsilon_{xy}(\omega)$  where  $n = \sqrt{\epsilon_{xx}(\omega)}$  and  $L$  is the film thickness for media that are sufficiently transparent that  $n$  is approximately real. Thus the MCD, measured at a given frequency gives information about the initial and final states involved in the electronic transition that occurs at that frequency.

Early work of the Sheffield group [1,2,3] showed that the MCD spectrum in doped oxides, ZnO and TiO<sub>2</sub>, appears as a peak below the band edge arising from spin polarised conduction electrons in the host oxide. A signal characteristic of Co<sup>2+</sup> is also seen in some samples. The magnetic hysteresis loop can also be measured using MCD as well as using standard magnetometry.

More recently we have shown that it is possible to use optical methods to decompose the signal from samples of ZnO that contain metallic cobalt into a part that arises from the metallic nanoparticles and a part that is due to the polarised electrons in the host [4,5]. We have also observed similar spectra in doped In<sub>2</sub>O<sub>3</sub> [6] and were able to show that the MCD signal scaled with the magnetisation both as a function of Co doping and temperature [7].

The method has also been used to study the Verwey transition in Fe<sub>3</sub>O<sub>4</sub> [8] and to observe the temperature dependence of the conduction electron polarisation in manganites [9]. Recent work on samples of GdMnO<sub>4</sub> has shown that the optical response from the transition arising from the transfer of an electron between Mn sites has a different field and temperature dependence from that arising from a transition from the oxygen  $p$  states to a Mn site [10]. This, very unusual behaviour will be discussed in the talk.

We should like to thank K.A.C.S.T. (Saudi Arabia) and the Royal Saudi Embassy for financial support for M.A.

- [1] Neal *et al Phys. Rev Lett* **96**, (2006) 197208.
- [2] Branford, W. R *et al Phys. of Semicond., Pts A and B AIP Conf. Proc.* **893** (2007) 1199.
- [3] Behan *et al Phys. Rev Lett* **100** (2008) 047206.
- [4] Score D.S. *et al Proc ICM J. Phys.: Conf. Ser.* **200**, (2010) 062024.
- [5] Score D.S *et al submitted for publication.*
- [6] Jiang, FX; *et al. J. Appl. Phys.* **109** (2011) 053907.
- [7] Hakimi, A.M.H.R. *et al submitted for publication*
- [8] Neal, J.R. *et al J. Mag. Mag. Mater.* **310** (2007) E246.
- [9] Nath T.K. *et al J. Appl. Phys.* **105 Issue: 7 (2009)** 07D709.
- [10] Alshammari M. *et al to be published.*

25TL-C-2

**FERROMAGNETIC LANTHANUM MANGANITES***Bebenin N.G.*

Institute of Metal Physics, UD RAS, 18 Kovalevskaya St., Ekaterinburg 620990, Russia

The strong interaction between charge carriers, localized magnetic moments and crystal lattice in ferromagnetic manganites  $\text{La}_{1-x}\text{D}_x\text{MnO}_3$  where D is a divalent ion gives rise to many interesting effects observed preferably in a vicinity of the Curie temperature  $T_C$ . Colossal magnetoresistance (CMR) is, perhaps, most popular but such phenomena as giant magnetocaloric effect, giant magnetotransmission, magnetostriction, magnetothermopower, etc., are also intensively studied. The aim of this work is to overview results on the physical properties of CMR manganites published mainly during last 5-10 years. We first describe the crystal lattice and structural transitions with special emphasis on coexistence of different crystal phases. Then the magnetic phase diagrams for D = Ca, Sr, Ba reported for polycrystalline and single-crystalline samples are considered. The electronic structure of the CMR manganites is discussed on the basis of the results of band structure calculations and some optical experiments. The main part of the review is devoted to the transport properties. We report and analyze the experimental data on resistivity, magnetoresistance, Hall effect and thermopower. Special attention is paid to the critical behavior of resistivity near  $T_C$  in the manganites with the second order magnetic transition. The CMR effect in the materials with the first order transition is considered in close connection with the magnetic inhomogeneity. Optical properties are discussed from the viewpoint of the change of electronic band structure due to change in temperature. Finally we briefly review magnetocaloric effect and magnetostriction.

The work was supported by RFBR grant No. 09-02-00081 and the Program №18 of Presidium of RAS.

25OR-C-3

**MAGNETIC POLARONS IN  $\text{CaMnO}_3$ :  $^{17}\text{O}$  NMR data**

*Mikhalev K.<sup>1</sup>, Verkhovskii S.<sup>1</sup>, Volkova Z.<sup>1</sup>, Gerashenko A.<sup>1</sup>, Buzlukov A.<sup>1</sup>, Yakubovskii A.<sup>2</sup>, Kaul A.<sup>3</sup>, Trokiner A.<sup>4</sup>, Kumagai K.<sup>5</sup>*

<sup>1</sup> Institute of Metal Physics, UB of RAS, Ekaterinburg 620990, Russia

<sup>2</sup> Russian Research Centre "Kurchatov Institute", Moscow 123182, Russia

<sup>3</sup> Moscow State University, Moscow 119991, Russia

<sup>4</sup> Laboratoire de Physique du Solide, LPEM, CNRS, E.S.P.C.I., Paris 75231, France

<sup>5</sup> Graduate School of Sciences, Hokkaido University, Sapporo 060-0811, Japan

The intriguing inhomogeneities in doped manganese oxides are widely discussed. Ferromagnetic (FM) nanosize domains frozen in the antiferromagnetic (AF) lattice are considered as an intrinsic property of the magnetic ground state of the parent AF insulators lightly doped with holes or with electrons [1]. In some cases these domains can be considered as small size FM-dressed polarons with spin and charge fluctuations [2].

We report  $^{17}\text{O}$  NMR results evidencing the existence of magnetic polarons (MP) in the AF state as well as in the paramagnetic state of a  $\text{CaMnO}_{3-x}$  ( $T_N = 123$  K). The sample is lightly electron doped due to a small amount of oxygen vacancies ( $x < 0.01$ ).

The  $^{17}\text{O}$  NMR spectra show two lines with very different local magnetic environments [3]. The more intense line is due to the AF matrix. The thermal dependence of the magnetic moment of the AF sublattice deduced from the  $^{17}\text{O}$  linewidth is typical for insulating three-dimensional Heisenberg antiferromagnets. The less intense, strongly shifted line directly evidences the existence of FM domains embedded in the AF spin lattice. The extremely narrow line in zero magnetic field indicates a nearly perfect alignment of the manganese spins in the FM domains which also display an unusually weak temperature dependence of their magnetic moment. We show that these FM entities start to move above 40 K in a slow-diffusion regime with the activation energy about 15 meV. These static and dynamic properties bear a strong similarity with those of a small size MP.

In the paramagnetic state far above  $T_N$  the spin density of the mobile electrons is equally shared between manganese and the local spin density probed by  $^{17}\text{O}$  spin in the regular lattice of the  $\text{Mn}^{4+}$  ions follow a Curie-Weiss law. But when approaching  $T_N$  the spin density of the doped electrons becomes inhomogeneously distributed. Below 160 K an increasing fraction of the mobile carriers become FM-dressed. These electrons form the MP.

According to the  $^{17}\text{O}$  echo decay-rate data, MP become unstable with increasing temperature. Their rate of hopping changes and approaches the metallic-like. The energy barrier required to excite these electrons into the  $\text{O}(2s2p)\text{-Mn}(e_g)$  conducting band is estimated as  $E_a = 1100(200)$  K. Nevertheless, on the basis of  $^{17}\text{O}$  NMR data sensitive to low-frequency spin dynamics of the mobile carriers, we cannot define in what degree their mobility at elevated temperature approaches the one existing in conducting band of metal.

This work was supported by RFBR (Grant No. 09-02-00310).

[1] C. Chiorescu, J.L. Cohn, J.J. Neumeier, *Phys. Rev. B*, **76** (2007) 020404(R).

[2] M.B. Salamon, M. Jaime, *Rev. Mod. Phys.*, **73** (2001) 583.

[3] A. Trokiner, S. Verkhovskii, A. Yakubovskii et al, *Phys. Rev. B*, **79** (2009) 214414.

25OR-C-4

## **EFFECT OF ELECTRON-LATTICE INTERACTION ON PHASE SEPARATION IN MAGNETIC OXIDES WITH TWO TYPES OF CHARGE CARRIERS**

*Kugel K.I., Rakhmanov A.L., Sboychakov A.O.*

Institute for Theoretical and Applied Electrodynamics, Russian Academy of Sciences,  
Izhorskaya Str. 13, Moscow, 125412 Russia

A typical feature of the strongly correlated electron systems is the formation of inhomogeneous states. The nature of such inhomogeneities is usually related to electron correlations, but their specific manifestations can include the effects of different degrees of freedom existing in the solids: spin, charge, orbital, and lattice. Here we study the effect of electron-lattice interaction for strongly correlated electron systems described by the two-band Hubbard model. The electron-lattice interaction is chosen in the following form

$$H_{e-ph} = \sum_{\langle ij \rangle \sigma} \lambda a_{i\sigma}^+ a_{j\sigma} + \sum_{i\sigma} \lambda_b n_{ib},$$

where  $a_{i\sigma}^+$  and  $a_{i\sigma}$ , are the creation and annihilation operators in the wider ( $a$ ) band and  $n_{ib}$  is the operator of the particle number in the narrower ( $b$ ) band,  $\langle \dots \rangle$  means the summation over nearest neighbors. So, a two-fold effect of electron-lattice interaction is taken into account: in non-diagonal terms, it changes the effective bandwidth, whereas in diagonal terms, it shifts the positions of the bands and the chemical potential. Following the approach of Refs. [1,2], we analyze the model in the framework of the mean-field approach, considering phonons as a classical static elastic field.

We demonstrate that if the electron-lattice interaction is strong enough, there appears a competition between states with different values of strains and the transition between these states can occur in a jump-like manner. We also show that the electron-lattice interaction produces a pronounced effect on the conditions of the electronic phase separation since it influences the value of the bandwidth ratio and the relative positions of the bands [3].

The obtained results should be important for the systems with strong electron-lattice interaction, especially for those containing Jahn-Teller ions, such as manganites and cuprates. In these compounds, electron-lattice coupling could be the main driving force of the phase separation determining the structure of the phase-separated state and characteristic scales of inhomogeneities.

The work was supported by the Russian Foundation for Basic Research (projects 10-02-92600-KO and 11-02-00708).

[1] A.O. Sboychakov, A.L. Rakhmanov, K.I. Kugel, *Phys. Rev. B*, **76** (2007) 195113.

[2] K.I. Kugel, A.L. Rakhmanov, A.O. Sboychakov, N. Poccia, A. Bianconi, *Phys. Rev. B*, **78** (2008) 165124.

[3] A.O. Sboychakov, A.L. Rakhmanov, K.I. Kugel, *J. Phys.: Condens. Matter*, **22** (2010) 415601.





**25 August** Thursday

14:30-17:00

memorial session  
25OR-C

25OR-C-5

**MAGNETISM DIVISION OF MSU: 80 YEARS OF MAGNETIC RESEARCH***Perov N.*

Faculty of Physics, MSU, Leninskie Gory, GSP-1, Moscow, Russia

Magnetic Laboratory was created in Moscow State University by professor Vladimir Arkad'ev. Vladimir Arkad'ev entered MSU in 1904. On the first year he began to work in professor Umov's group. He studied the propagation of magnetic waves along iron rod. In 1906 Vladimir Arkad'ev received invitation from professor Lebedev to work in his group.

During First World War Arkad'ev took part in the chemical defense field. In 1918 Arkad'ev returned in MSU where he founded Moscow Magnetic Laboratory, which exists for a long time on the enthusiasm of their members. After 1923 it began to be funded from All-Russian Electro-technical Institute at All-Russian Soviet of People's Economy, and since 1926 glavnauka began to fund Magnetic Laboratory. The main fields of research were developing the theory of electromagnetic field, general and magnetic spectroscopy, magnitostatics, magnetic relaxation, magnistraction and electric oscillations.

In the July of 1930 there had been reorganization in the MSU and as a result in the December of 1931 appeared the first in the USSR Magnetism Department. As the head of new department professor Nikolay Akulov was assigned. And when the faculty structure restored in MSU Magnetism Department was member of Faculty of Physics. Only during first year of work Akulov and his pupils laid down the foundations of general theory of mono- and polycrystall magnetizing, foundations of theory of galvanomagnetic and galvanoelastic effects, and foundations of theory of magnitostriktion.

At Second World War Magnetism Department as a part of MSU was evacuated in Sverdlovsk. After 1943 University returned to Moscow. The number of students achieved the before-war level only at 1947. But after death of Stalin in 1953 following with arrest and shooting of Beria, Akulov's opponents tried to catch the opportunity and remove Akulov from his position. And as a result Akulov was dismissed from MSU in 1954.

During the period since 1954 till 1987 the head of magnetism division was Eugeny Kondorsky. He was a creator of the theory of micromagnetism, initiated the work on magnetism division in the field of biomagnetism. Professor Kondorsky participated in defense research. During the years when he was a head of magnetism division the great school of magnioptics was created by professor Georgy Krinchik.

Since 1987 till nowadays the head of magnetism division is Anatoly Vedyayev. Professor Vedyayev is a founder of scientific school in transport properties of magnetic and composites materials. At the moment magnetism division is a consolidated collective which moves towards the glorious future in the magnetism science.

25OR-C-6

## TO THE CENTENARY OF K.P. BELOV

*Khohlov D., Nikitin S.*

Faculty of Physics, MSU, Leninskie Gory, GSP-1, Moscow, Russia

November 4, 2011 marks 100 years of well-known physicist magnetologist, honored scientist of the RSFSR, winner of the State and the Lomonosov Prize, Professor, Dr.Sci. Konstantin Petrovich Belov. K.P. Belov is a graduate of Moscow University. After graduating from MSU in 1934, he continued his work within its walls as a postgraduate student, then an assistant, associate professor, professor. From 1954 to 1988 years Belov was a head of one of the largest departments of Moscow State University - Department of General Physics for Science Faculties, where students of geological, geographical, biological faculties receive physical education. Under the leadership of K.P. Belov the physics textbooks were created. The talented scientist and organizer created a scientific laboratory at the Department of Magnetism and Research Laboratory of Magnetism at Physics Faculty of MSU. A school of physicists magnetologists associated with K.P. Belov is widely known in Russia and abroad. 8 theses of doctor of science and 50 Ph.D theses have been prepared under prof. K.P. Belov supervision. Pupils of prof. K.P. Belov work fruitfully in many universities and scientific laboratories in Russia and in several foreign countries.

The beginning of scientific activity of K.P. Belov associated with the study of magnetoelastic and electrical phenomena in ferromagnetic metals and its alloys. Dependencies of the exchange energies on interatomic distances are important for understanding of the properties of invar materials used in technical devices.

Extensive researches under the leadership of K.P. Belov were carried out in the field of magnetism of ferrites. Due to high electrical resistance of ferrites they are used in the technique applications in an alternating electromagnetic field (radio frequency and microwave technology). Researches of K.P. Belov and his collaborators related to the study of magnetic phase transitions, magnetostriction, magnetocaloric and galvanomagnetic phenomena and revealed the essential features of magnetic ordering and conductivity processes in ferrites. Investigations of K.P. Belov always reflect the latest trends in science. Thus, in 80's years of last century, a study of magnetic semiconductors were carried out at MSU, as a result a new class of magnetic semiconductors with high Curie temperatures (above room temperature) and the presence of special magnetic states – ferrons were found.

Professor K.P. Belov is one of the founders of research in the field of magnetic phase transitions. The spin reorientation transitions were studied intensively. These papers have fundamental contribution for the theory of magnetism. In the Russia, a systematic studies of rare-earth magnets began under the leadership of K.P. Belov at Moscow University, and later this area was developed in a large number of research centers in Russia. The rapid development of studies on magnetic and other physical and chemical properties of rare earth compounds was due to the need to expand the arsenal of materials for technical applications.

The research laboratory provided significantly results in physics of magnetism of rare earth metals, their alloys and compounds. A new phenomenon - giant magnetostriction (the diploma of invention), a huge magnetic anisotropy and large magnetocaloric effect were discovered in rare earth metals and compounds. Spin reorientation in orthoferrites and garnets and a number of other phenomena were investigated.

Many of these physical phenomena are of great practical importance. The giant magnetostriction in the rare-earth and uranium alloys was found There are a great strains under magnetic field, which 1000 times more than in classical magnetic materials. This effect is promising for use in sonar, for the generation of ultrasound, to control the laser beams, the engines micromovings, etc.

Researches on the study of rare-earth magnets are highly appreciated: prof. K.P. Belov, a group of department staff and academic institutions have been awarded the USSR State Prize for the study of magnetism of rare earth and uranium compounds.

The results of the fruitful and intense creative activity of prof. K.P. Belov and his team of physicists are summarized in nine monographs. These books give a great contribution to the physics of magnetic phenomena. Excellent organizational skills, great scientific advances and high human qualities of Konstantin Petrovich Belov are widely known in the scientific world.

25OR-C-8

## **BOROVIK-ROMANOV ANDREI STANISLAVOVICH**

*Kreines N.M.*

P.L. Kapitza Institute for Physical Problems, Kosygin str.,2, Moscow, 119973, Russia

Andrei Stanislavovich Borovik-Romanov, a prominent Russian physicist, was born on March 18<sup>th</sup>, 1920 in Leningrad (died on July 31<sup>st</sup>, 1997). His education at Moscow State University (MSU) was interrupted by World War II when he had joined the Soviet Army as a volunteer. After the war he finished his education in MSU. In 1956 he was invited by P.L. Kapitza to the Institute for Physical Problems (now Kapitza Institute for Physical Problems) where he spent the most fruitful part of his professional life (till July 1997).

The first fundamental results obtained by A.S. Borovik-Romanov were in field of magnetism. He has discovered the weak ferromagnetism in antiferromagnets and suggested that this phenomenon can be explained by a non-collinear spin ordering, the idea stimulating a lot of succeeding experiments and intense theoretical studies. Another result related to these studies was the discovery of piezomagnetism of antiferromagnets.

From the magnetostatic properties of weak ferromagnets A.S. Borovik-Romanov switched to studying their dynamic behavior. Here he was both a theoretician and experimentalist. He obtained a number of fundamental results. He found an antiferromagnetic resonance in easy-plane antiferromagnets and described its spectrum, discovered the parametric excitation of spin waves, and observed the inelastic light scattering by thermal and parametrically excited magnons and phonons. The experimental results were in good agreement with principal theoretical predictions.

In the late seventies A.S. Borovik-Romanov has essentially changed his field of research initiating the construction of the first (and till present unique) soviet nuclear demagnetization cryostat for studies of quantum liquids at ultralow temperatures. In 1982 his research group started NMR experiments in superfluid <sup>3</sup>He and in a short time got a number of new exciting results concerning the spin dynamics of superfluid <sup>3</sup>He. A macroscopic spin transport due to spin supercurrents, a spin analog of a Josephson phenomenon and phase slips were observed. A new dynamical homogeneously precessing domain maintained by spin supercurrent was discovered. A.S. Borovik-Romanov has shown that all these effects, while occurring in spin system, have many similarities to superconductivity and superfluidity.

In recent years A.S. Borovik-Romanov returned to studies of magnetic resonance (NMR) of quasi-one-dimensional antiferromagnets.

All the scientific research of A.S. Borovik-Romanov is marked with his special style. He considered it very important to change his topics from time to time or at least the experimental methods.

A.S. Borovik-Romanov was an outstanding physicist as well as a great organizer of science and teacher. From 1963 to 1984 he was a vice-director and from 1984 to 1991 took up a director post at Kapitza Institute. He was a Professor and had a chair at Moscow Institute of Physics and

Technology and was an editor-in-chief of a Journal of Experimental and Theoretical Physics and JETP Letters.

In 1966 A.S. Borovik-Romanov was elected as a corresponding member of the USSR Academy of Sciences, and became full member in 1972.

25OR-C-9

## SCHOOL OF S.V. VONSOVSKY AND MODERN MAGNETISM

*Irkhin V.Yu.*

Institute of Metal Physics, 620990, Ekaterinburg, S. Kovalevskoy str. 18, Russia

The Ural school in magnetism and solid state theory was founded by Academician S.V. Vonsovsky (1910-1998). The theoretical work started from the fundamental papers by S.P. Shubin and S.V. Vonsovsky on the polar [1] and  $s$ - $d(f)$  exchange [2] models. Being formulated already in the first half of XX century, these models still work successfully in the physics of electron correlations and magnetism. They provide also a basis for original theoretical concepts treating new physical phenomena.

The polar model (most frequently, in the simplest form proposed by J. Hubbard) is extremely useful for the problems of localized and itinerant magnetism of  $d$ -electrons (many-electron vs. one-electron pictures, formation of local magnetic moments, metal-insulator transition etc.).

The  $s$ - $d(f)$  exchange Hamiltonian describing the interaction between two systems of localized and itinerant electrons was written down in the second quantization form by S.V. Vonsovsky and E.A. Turov [3]. This initiated numerous investigations of magnetic and transport properties.

Professor Yu.P. Irkhin (1930-2008) with collaborators investigated a number of transport phenomena in ferro- and antiferromagnets, especially magnetic resistivity and the anomalous Hall effect. An important contribution was made to rare-earth magnetism, including the theory of exchange interactions for complicated atomic configurations and the explanation of giant magnetic anisotropy [4].

Yu.P. Irkhin elaborated also the second quantization procedure for many-electron systems within the framework of the atomic representation of Hubbard's  $X$ -operators. These ideas turned out to be very fruitful: modern treatments of the Hubbard model include various slave-boson and slave-fermion representations, formation of exotic quasiparticles with non-standard statistics, etc.

Another famous pupil of Vonsovsky is Academician Yu.A. Izyumov (1933-2010) who is known by his works in magnetic neutronography, symmetry theory in magnetism, the problem of coexistence of magnetism and superconductivity. As for model investigations, he worked on non-standard diagram techniques in the Heisenberg and Hubbard model. During 1990-s, after discovery of high- $T_c$  superconductors, Yu.A. Izyumov made many efforts to popularize the Hubbard model.

At present, the many-electron models discussed are widely used for description of transition-metal, rare-earth and actinide compounds (manganites with colossal magnetic resistivity, Kondo lattices, systems with heavy fermions and non-Fermi-liquid behavior, etc.).

[1] S. Schubin and S. Wonsowsky, Proc. Roy. Soc. A**145**, 159 (1934); Zs. Sow. Phys. **7**, 292 (1935); **10**, 348 (1936).

[2] S. V. Vonsowskii, Zh. Eksp. Theor. Fiz. **16**, 981 (1946); Magnetism. New York, Wiley, 1974.

[3] S. V. Vonsovsky, E.A. Turov, Zh. Eksp. Theor. Fiz. **24**, 419 (1953).

[4] Yu. P. Irkhin, Usp.Fiz.Nauk **154**, 321 (1988).

25OR-C-10

## SERGEJ VLADIMIRIVICH TYABLIKOV (1921 – 1968) AS ONE OF THE FOUNDERS OF THE MODERN QUANTUM THEORY OF MAGNETISM

*Kotelnikova O.A.<sup>1</sup>, Rudoy Yu.G.<sup>2</sup>, Tyablikov V.S.<sup>1</sup>*

<sup>1</sup> Lomonosov State University, 119991, Vorobievsky Gory, Moscow, Russia,  
Dept of Magnetism; E-mail: olgakot@magn.ru, vlad@magn.ru

<sup>2</sup> People's Friendship University of Russia, 117198, Mikluho-Maclaya, 6, Moscow,  
Dept of Theoretical Physics; E-mail: rudikar@mail.ru

At September 7<sup>th</sup> of this year there occurs the 90<sup>th</sup> anniversary of Professor Sergej Vladimirovich Tyablikov – one of the most prominent researchers in the modern quantum theory of magnetism; in fact, he was one of the founders of this field. Prof. S.V. Tyablikov was born at September 7<sup>th</sup>, 1921 at the City of Klin in Moscow Region. At the year 1947 he got PhD degree at Moscow State University under Prof. A.A. Vlasov guidance.

Later on Prof. S.V. Tyablikov became one of the first and most outstanding representatives of the scientific school created by N.N. Bogoliubov. Starting from 1947 and up to the end of his life at March 17<sup>th</sup>, 1968 S.V. Tyablikov worked at the famous Steklov Mathematical Institute of the former Soviet Academy of Science. From 1962 he became the permanent Head of the Statistical Physics Department and from 1966 he was also the scientific leader of the Condensed Physics Department at that time created at the Theoretical Physics Laboratory in the Joint Institute of Nuclear Research at the Dubna City near Moscow.

The main S.V. Tyablikov's scientific achievements include the following issues: 1) operator perturbation theory for the degenerate energy level of metal (so called polar model of metal, 1949); 2) the method of approximate secondary quantization method for spin operators and the procedure for constructing of effective spin Hamiltonians (1956); 3) formulation (with N.N. Bogoliubov) of the method of advanced and retarded temperature Green functions (1959) – one of the most fruitful in the modern statistical physics and condensed matter physics; 4) the well known, simple and effective, "Tyablikov approximation" (1959) in the quantum theory of magnetism. All these results are published in systematical way in two monographies [1,2], which are well known among theoretical physicists throughout the world.

[1] V.L. Bonch-Bruевич, S.V. Tyablikov (1962): *The Green Function Method in Statistical Mechanics*. North Holland Publishing Co., Amsterdam.

[2] S.V. Tyablikov (1967): *Methods of Quantum Theory of Magnetism*. Plenum Publishing Co., New York.

25OR-C-11

## THE SCIENTIFIC LEGACY OF E.A. TUROV

*Mens`chenin V.V., Kurkin M.I.*

Institute of Metal Physics, Ural Division of RAS; menschenin@imp.uran.ru

The activity of E.A. Turov covers all fundamental trends in the theory of magnetism. He and his disciples obtained basic results which influenced and continue to affect significantly the development of modern concept in this field of physics:

- a symmetrized approach to the investigation of the magnetoordered material properties was devised;
- the quantum-mechanical theory of the magnetic resonance in magnetics and the methodology of its using for the investigation of the magnetic material properties were developed;
- the kinetic phenomena in magnetic media was theoretically studied in detail;
- the dynamic of domain boundaries and other soliton-like objects was examined.

As a completion of certain steps E.A. Turov published fundamental surveys and original monographs on all this trends in Russian and foreign editions. Of special note are the monographs "Physical properties of magnetoordered crystals" and "Nuclear magnetic resonance in ferro- and antiferromagnetics". Both of these books are the handbooks for several generations of physicists-magnetologists. These monographs have the stimulating effect on the development of corresponding trends of investigation in magnetic science. E.A. Turov is also a co-author of a number of collective monographs on the actual problems of physics, for example, "Ferromagnetic resonance" (reprinted abroad in 1966), "Spin waves and magnetic excitation" (published by "North-Holland" in 1988) and others. In the last 15 years of life E.A. Turov published several more monographs which are of much interest for specialists, teachers and students in the field of physics of magnetic phenomena. These are "Kinetic, optic and acoustic properties of antiferromagnets" (1990), "Nuclear magnetic resonance in magnetoordered materials and its application" (1990), "The foundations of material medium electrodynamics in variable and non-uniform fields" (2000), "Symmetry and magnetic properties of antiferromagnets" (2001) (the last three monographs are written in co-authorship).

In the last years Eugeny Akimovich was interested in the studying of magnetic ordering influence on high-frequency properties of magnetics. Static magnetoelectrical properties are being studied for a long time; magnetism in dynamics has a considerable history as well. But these investigations were carried out in variable magnetic fields. Magnetodynamics in variable electrical fields is that gap which E.A. Turov and his collaborators undertook to fill.

As a competent physicist-magnetologist of our country E.A. Turov was a member of magnetic committee of International Union of pure and applied physics, a member of bureau of "Magnetism" and "Solid-state theory" sections of Scientific council of Russian Academy of Sciences on condensed medium physics, a scientific consultant of "Physical encyclopedia" edition over a number of years.





**25 August**

Thursday

11:30-13:00

14:30-17:00

oral session

25TL-D

25RP-D

25OR-D

**“Low Dimensional  
Magnetism”**

25RP-D-1

## INFLUENCE OF FIELD ON FRUSTRATIONS IN LOW-DIMENSIONAL MAGNETS

Kassan-Ogly F.A.<sup>1</sup>, Filippov B.N.<sup>1</sup>, Murtazaev A.K.<sup>2</sup>, Ramazanov M.K.<sup>2</sup>, Badiev M.K.<sup>2</sup>

<sup>1</sup> Institute of Metal Physics, Ural Division RAS, ul. S.Kovalevskoi 18, Ekaterinburg, 620990 Russia

<sup>2</sup> Institute of Physics, DSC, RAS, Makhachkala 367003, Daghestan, Russia

The phenomena of frustrations appearance and suppression of phase transition or, on the contrary, the phase transition appearance and suppression of frustrations are studied on the base of exact analytical solutions for 1D Ising model, 3-state, and 4-state standard Potts models with allowance for the interactions between nearest  $J$  and next-nearest neighbors  $J'$ , for 6-state, 8-state, and 12-state modified Potts models with allowance for the interaction between only nearest neighbors  $J$ . In all the models investigated we obtained exact numbers and values of frustrating fields depending, in particular, on mutual orientation of the field and spin directions.

In 2D case on the example of Ising model we studied these phenomena by the numerical “replica Monte Carlo method”, taking into account the interactions only between nearest neighbors  $J$  and an external magnetic field of arbitrary value.

We formulated the notion of thermodynamic order parameter and obtained the expressions for the entropy and heat capacity in terms of this order parameter. We also introduced the notion of frustration measure ( $f$ ) in tight connection with the order parameter.

It is shown that when passing across any frustration point (either in presence or absence of magnetic field) cardinal changes of magnetic structure take place.

Figure 1 shows  $f(T,H)$  in 1D Ising model with competing interactions  $J < 0$  and  $J' < 0$  and Fig.2 shows heat capacity in 2D Ising model in frustrating field ( $H=4.0$ ) and above and below it.

The frustrations phenomena in low-dimensional (1D and 2D) magnetic systems without allowance for an external magnetic field are thoroughly discussed in our previous works [1,2].

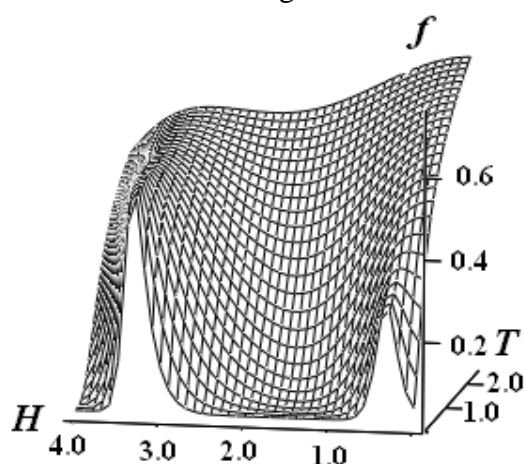


Fig.1. Frustration measure.

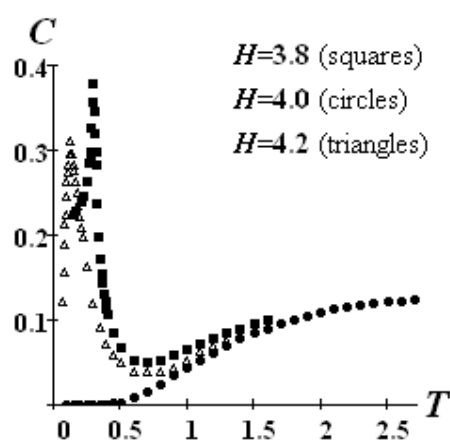


Fig.2. Heat capacity.

Support by RFBR project 11-02-00932a and project 10-02-00130 is acknowledged.

[1] F.A. Kassan-Ogly and B.N. Filippov, *Solid State Phenomena* **168-169** (2011) 427.

[2] F.A. Kassan-Ogly, B.N. Filippov, V.V. Men'shenin, A.K. Murtazaev, M.K. Ramazanov, and M.K. Badiev, *Solid State Phenomena* **168-169** (2011) 435.

25OR-D-2

## THERMODYNAMIC PROPERTIES OF LANGASITE FAMILY COMPOUNDS

### $\text{Pb}_3\text{TeCo}_3\text{V}_2\text{O}_{14}$ AND $\text{Pb}_3\text{TeMn}_3\text{As}_2\text{O}_{14}$

Markina M.<sup>1</sup>, Mill B.<sup>1</sup>, Vasiliev A.<sup>1</sup>, Klingeler R.<sup>2,3</sup>, Büchner B.<sup>3</sup>

<sup>1</sup> Physical Faculty, Moscow State University, 119992 Moscow, Russia

<sup>2</sup> Kirchhoff Institute for Physics, University of Heidelberg, D-69120 Heidelberg, Germany

<sup>3</sup> Leibniz Institute for Solid State and Materials Research, D-01069 Dresden, Germany

Recently, new compounds with  $\text{Ca}_3\text{Ga}_2\text{Ge}_4\text{O}_{14}$  crystal structure (sp. gr.  $P321$ ) containing  $\text{Co}^{2+}$  and  $\text{Mn}^{2+}$  ions in  $3f$  position were discovered [1]. In the crystal structure the magnetic ions are placed in  $ab$ -plane in the oxygen tetrahedra forming a trianglular network [1,2]. Their initial magnetic study revealed an antiferromagnetic ordering at 7–13 K [2]. In the present work we investigate the magnetic susceptibility and specific heat of  $\text{Pb}_3\text{TeCo}_3\text{V}_2\text{O}_{14}$  and  $\text{Pb}_3\text{TeMn}_3\text{As}_2\text{O}_{14}$  in the range 1.8–350 K using Quantum Design MPMS and PPMS devices.

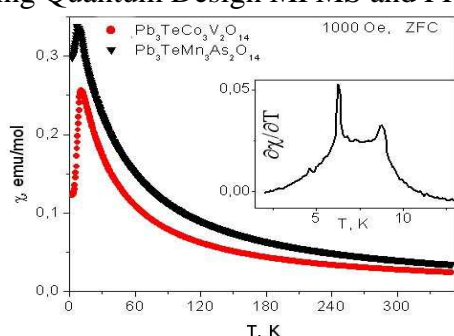


Fig.1. Magnetic susceptibility of  $\text{Pb}_3\text{TeCo}_3\text{V}_2\text{O}_{14}$  and  $\text{Pb}_3\text{TeMn}_3\text{As}_2\text{O}_{14}$ . Inset:  $\partial\chi/\partial T$  curve of  $\text{Pb}_3\text{TeCo}_3\text{V}_2\text{O}_{14}$

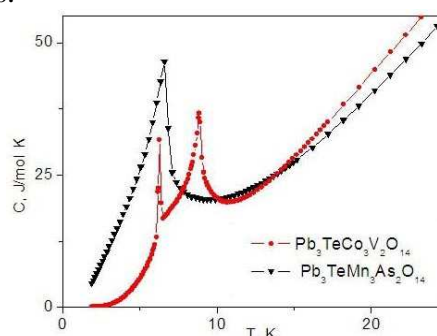


Fig.2. Specific heat of  $\text{Pb}_3\text{TeCo}_3\text{V}_2\text{O}_{14}$  and  $\text{Pb}_3\text{TeMn}_3\text{As}_2\text{O}_{14}$ .

Temperature dependences of the magnetic susceptibility  $\chi(T)$  of  $\text{Pb}_3\text{TeCo}_3\text{V}_2\text{O}_{14}$  and  $\text{Pb}_3\text{TeMn}_3\text{As}_2\text{O}_{14}$  are shown in Fig.1. The  $\chi(T)$  curves follow the Curie-Weiss law in the range 20–350 K. The values of the effective magnetic moment are  $4.3 \mu_B$  for  $\text{Co}^{2+}$  in  $\text{Pb}_3\text{TeCo}_3\text{V}_2\text{O}_{14}$  and  $5.1 \mu_B$  for  $\text{Mn}^{2+}$  in  $\text{Pb}_3\text{TeMn}_3\text{As}_2\text{O}_{14}$ . The Neel temperatures  $T_N$  determined as a maxima of  $\chi(T)$  are 10.8 K for  $\text{Pb}_3\text{TeCo}_3\text{V}_2\text{O}_{14}$  and 7.1 K for  $\text{Pb}_3\text{TeMn}_3\text{As}_2\text{O}_{14}$ . For  $\text{Pb}_3\text{TeCo}_3\text{V}_2\text{O}_{14}$  we found the double peak structure on the  $\partial\chi/\partial T$  curve (see Inset to Fig.1). This double anomaly was also found in the specific heat temperature dependence  $C(T)$  for  $\text{Pb}_3\text{TeCo}_3\text{V}_2\text{O}_{14}$  (Fig 2). The anomalies are seen at  $T_1 = 8.9$  K and  $T_2 = 6.3$  K. Below  $T_N$  the  $C(T)$  curve shows exponential decrease. The Debye temperature for  $\text{Pb}_3\text{TeCo}_3\text{V}_2\text{O}_{14}$  is  $\Theta_D = 350$  K. For  $\text{Pb}_3\text{TeMn}_3\text{As}_2\text{O}_{14}$  the  $C(T)$  curve shows almost linear behavior down to 1.8 K. The scaling procedure using the  $C(T)$  data of nonmagnetic analogue  $\text{Pb}_3\text{TeZn}_3\text{As}_2\text{O}_{14}$  in a range 1.8–80 K gave the magnetic entropy 34 J/mol·K for  $\text{Pb}_3\text{TeCo}_3\text{V}_2\text{O}_{14}$  and 46 J/mol·K for  $\text{Pb}_3\text{TeMn}_3\text{As}_2\text{O}_{14}$  that agrees well with theoretical estimations 34.6 and 44.7 J/mol·K. Unusual properties of  $\text{Pb}_3\text{TeCo}_3\text{V}_2\text{O}_{14}$  and  $\text{Pb}_3\text{TeMn}_3\text{As}_2\text{O}_{14}$  allow predicting the multiferroic features of them. Lately the multiferroic properties of  $\text{Fe}^{3+}$ -based langasite family compound were discovered. The magnetic ordering in  $\text{Ba}_3\text{NbFe}_3\text{Si}_2\text{O}_{14}$  is accompanied by anomalies of crystal lattice parameter, dielectric permittivity and polarization [3,4].

This work was supported by RFBR Grants 09-02-00444 and 10-02-00641.

[1] B.V. Mill, *Russ. J. Inorg. Chem.*, **54**, (2009) 1205.

[2] V.Yu. Ivanov, et al., *Solid State Phenomena*, **152-153**, (2009).

[3] K. Marty et al., *Phys. Rev. B* **81**, (2010) 054416.

[4] H.D. Zhou et al., *Chem. Mater.*, **21**, (2009) 156.

25OR-D-3

## STRUCTURE AND MAGNETISM OF $(\text{Cu}_x)\text{LaNb}_2\text{O}_7$ with $X = \text{Cl}, \text{Br}$

*Tsirlin A.A., Rosner H.*

Max Planck Institute for Chemical Physics of Solids, Nöthnitzer Str. 40, 01187 Dresden, Germany

Crystal structure plays decisive role for magnetic properties and microscopic physics of quantum magnets. Fine details of the atomic arrangement dramatically influence individual exchange couplings, thereby accurate structure determination based on high-quality diffraction data is essential for understanding the physics. In this contribution, we will present the subtle interplay between structure and magnetism in the family of layered Dion-Jacobson-type compounds represented by  $(\text{CuX})\text{LaNb}_2\text{O}_7$  oxyhalides with  $X = \text{Cl}$  and  $\text{Br}$ . In these compounds, magnetic  $(\text{CuX})$  layers are separated by non-magnetic  $\text{LaNb}_2\text{O}_7$  blocks having perovskite structure. While early studies put  $(\text{CuX})\text{LaNb}_2\text{O}_7$  forward as novel examples of spin-1/2 frustrated-square-lattice magnetism, experimental data are by far inconsistent with any expectations for the square-lattice model. In particular,  $(\text{CuCl})\text{LaNb}_2\text{O}_7$  is a dimer-like gapped magnet, whereas  $(\text{CuBr})\text{LaNb}_2\text{O}_7$  behaves as a three-dimensional antiferromagnetic system with the Néel order below  $T_N = 33$  K. This temperature is comparable to the energy scale of exchange couplings and contrasts with the expected two-dimensionality of the system.

A crucial and so far overlooked feature of  $(\text{CuX})\text{LaNb}_2\text{O}_7$  oxyhalides is the presence of weak atomic displacements that break the initially proposed tetragonal crystallographic symmetry, and lead to the superstructure formation. Microscopically, these displacements tend to lift the orbital degeneracy of  $\text{Cu}^{+2}$ , although unlike in conventional Jahn-Teller systems both Cu atoms, Cl ligands, and even oxygen atoms of the perovskite block change their positions to form orthorhombic superstructures. We use high-resolution synchrotron x-ray and neutron diffraction data to establish the correct low-temperature structures of  $(\text{CuX})\text{LaNb}_2\text{O}_7$ . In both Cl and Br compounds, atomic displacements can be separated into two groups inducing distinct sets of superstructure reflections. In  $(\text{CuCl})\text{LaNb}_2\text{O}_7$ , ordered displacements of Cu and Cl atoms below 640 K are followed by cooperative tilts of  $\text{NbO}_6$  octahedra below 500 K. The Br compound shows an opposite sequence of structural transformations, with cooperative octahedral tilts preceding the displacements of Cu and Br atoms. Proposed models of the low-temperature crystal structures fully conform to spectroscopic data obtained from nuclear magnetic resonance and Raman scattering.

To unravel magnetic properties of  $(\text{CuX})\text{LaNb}_2\text{O}_7$ , we perform extensive microscopic modeling based on density functional theory band structure calculations supplied with quantum Monte-Carlo simulations for resulting spin models. Consistent description of thermodynamic and neutron-scattering data leads to the following conclusions: i) neither  $(\text{CuCl})\text{LaNb}_2\text{O}_7$  nor  $(\text{CuBr})\text{LaNb}_2\text{O}_7$  are frustrated-square-lattice magnets; ii) despite the apparent crystallographic two-dimensionality, spin lattices of these compounds are three-dimensional; iii) strong hybridization between Cu  $3d$  and Cl/Br  $p$  states induces non-trivial long-range couplings that form spin dimers and cause gapped ground state in the Cl compound, or stabilize antiferromagnetic long-range order in the Br compound.

Our results evidence the crucial role of the precise structure determination and efficient microscopic modeling in understanding peculiar low-temperature behavior of quantum magnets. Basic trends of structural changes and their interplay with magnetism are relevant for a broad family of  $\text{Cu}^{+2}$  oxyhalides, and will be applied to an ongoing work on the 1/3-magnetization plateau in  $(\text{CuBr})\text{Sr}_2\text{Nb}_3\text{O}_{10}$  and related compounds.

25OR-D-4

## FINITE SIZE EFFECTS AND STAGGERED MAGNETIZATION IN THE SPIN-1/2 HONEYCOMB LATTICE COMPOUND $\text{InCu}_{2/3}\text{V}_{1/3}\text{O}_3$

Vavilova E.<sup>1,2</sup>, Yehia M.<sup>2</sup>, Moeller A.<sup>3,4</sup>, Taetz T.<sup>4</sup>, Loev U.<sup>5</sup>, Klingeler R.<sup>6</sup>, Kataev V.<sup>2</sup>, Buechner B.<sup>2</sup>

<sup>1</sup> Zavoisky Physical Technical Institute of the RAS, 420029, Kazan, Russia

<sup>2</sup> IFW Dresden, D-01171 Dresden, PO BOX 270116, Germany

<sup>3</sup> University of Houston, Department of Chemistry and Texas Center for Superconductivity, Houston, TX 77204, USA

<sup>4</sup> Institut für Anorganische Chemie, Universität zu Köln, 50939 Köln, Germany

<sup>5</sup> Technische Universität Dortmund, Theoretische Physik I, 44221 Dortmund, Germany

<sup>6</sup> Heidelberg University, Heidelberg, Germany

We present the results of investigations of the ground state of the quasi two-dimensional spin-1/2 honeycomb lattice compound  $\text{InCu}_{2/3}\text{V}_{1/3}\text{O}_3$ . In this system uncorrelated finite size structural domains occurring in the honeycomb planes are expected to inhibit long range magnetic order. In the same time high field electron spin resonance data show the development of two collinear antiferromagnetic sublattices below 20 K, nuclear magnetic resonance show the presence of the staggered internal field on V and In nuclei positions. A reorientation of spin sublattices in a field of 5.7 T has been clearly identified in the magnetization and magnetic resonance data. Our experimental results are corroborated by the Quantum Monte-Carlo study of the finite size honeycomb spin layers coupled in the third dimension. It reveals a sharp development of the staggered magnetization at a finite temperature that in the thermodynamic limit would correspond to a phase transition to the AFM long-range ordered state [1].

[1] A. Yehia, et al., Phys. Rev. B **81**, 060414 (2010).

25OR-D-5

## MAGNETIC AND TRANSPORT PROPERTIES OF Co ADATOM ON Pt(111) SURFACE

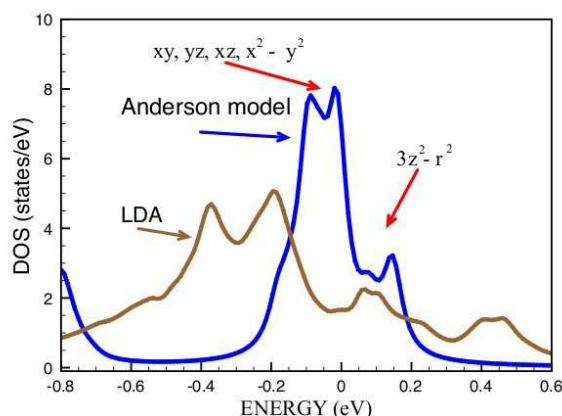
Mazurenko V.<sup>1</sup>, Iskakov S.<sup>1</sup>, Valentyuk M.<sup>1</sup>, Rudenko A.<sup>1</sup>, Lichtenstein A.<sup>2</sup>

<sup>1</sup> Ural Federal University, St. Mira 19, Ekaterinburg, Russia

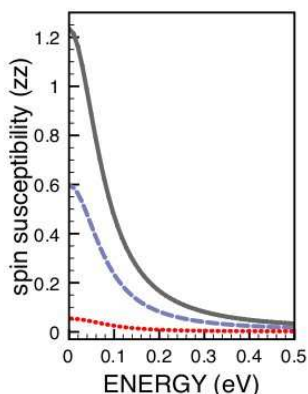
<sup>2</sup> University of Hamburg, 20355 Hamburg, Germany

The strong Coulomb correlations effects on the electronic and magnetic structure of an individual Co atom deposited on the Pt(111) surface in the paramagnetic phase have been investigated. The first-principles LDA calculations demonstrated a peak below the Fermi level that originated from the 3d states of the cobalt adatom. The width of the peak is considerably larger than that observed in the STM experiment [1].

Using a realistic five d-orbital impurity Anderson model at low temperatures with parameters



determined from the first-principles calculations we found a striking change of the electronic structure in comparison with the LDA results. The spectral function calculated with full rotationally invariant Coulomb interaction is in good agreement with the quasiparticle region of the STM conductance spectrum [1].



In the framework of the Kubo's linear response theory the spin-spin correlation function was calculated. It gives us information about localization of the magnetic moments of the 3d orbitals. We found that the 3d orbitals of the yz and xz symmetry strongly hybridized with Pt states demonstrate an itinerant type of magnetism. On the other hand the correlation function of the 3z<sup>2</sup>-r<sup>2</sup> orbital displays a peak at the zero energy, which corresponds to the localized Heisenberg-type model.

Based on the obtained results we conclude that the dI/dV spectrum near the zero voltage is of the itinerant nature and, as a consequence, demonstrates a weak response to the applied magnetic field.

Support by the grant program of President of Russian Federation MK-406.2011.2, the scientific program "Development of scientific potential of universities" N 2.1.1/779 and by the scientific program of the Russian Federal Agency of Science and Innovation N 02.740.11.0217 is acknowledged.

[1] F. Meier, L. Zhou, J. Wiebe and R. Wiesendanger, *Science* **320**, 82 (2008).

25OR-D-6

## MAGNETIC ORDERING IN QUASI-1D HEISENBERG MAGNETS: THE ROLE OF FRUSTRATION

*Janson O.*

Max-Planck Institute for Chemical Physics of Solids, Noethnitzer Str. 40, D-01187 Dresden,  
Germany

Strong quantum fluctuations impede long-range magnetic ordering in one-dimensional Heisenberg systems even at zero temperature. At first sight, this rigorous theoretical result contrasts to the experimental evidence for an antiferromagnetic order in most of real-material Heisenberg chain compounds. However, for real materials, a three-dimensional magnetic coupling regime is inherent. This way, the magnetic ground state results from a subtle interplay of strong quantum fluctuations and the interchain coupling regime, in particular, its topology as well as the strength of individual couplings.

Since the interchain couplings are typically one or more orders of magnitude smaller than the dominant intrachain coupling, their accurate experimental evaluation is very difficult. Using density functional theory band-structure calculations, we were able to evaluate the numerical values for the leading interchain couplings. Subsequent simulations of the resulting magnetic models yield excellent agreement with the available experimental data, such as the long-range magnetic ordering temperature and the propagation vector of the magnetically ordered state.

In this study, we address the microscopic magnetic models of several spin-1/2 compounds that were recently proposed to imply the physics of Heisenberg chain: CuSe<sub>2</sub>O<sub>5</sub>, (NO)Cu(NO<sub>3</sub>)<sub>3</sub>, and CaCu<sub>2</sub>(SeO<sub>3</sub>)<sub>2</sub>Cl<sub>2</sub>. Extensive comparison between several systems gives evidence that the magnetic

ordering temperature, besides the size of the intra- and interchain couplings, crucially depends on the presence of the magnetic frustration.

25OR-D-7

## LARGE THERMO-MAGNETIC EFFECTS IN QUASI ONE-DIMENSIONAL SPIN SYSTEMS

*Shimshoni E.*

Department of Physics, Bar-Ilan University, Ramat Gan 52900, Israel

Recent measurements of thermal transport in quantum spin chains and ladders compounds exhibit remarkable magneto-thermal effects upon tuning of an external magnetic field. I will discuss a theoretical approach to the study of thermal conductivity, which accounts for the dominant role of approximate conservation laws in such systems and possibly explain the data. In particular, the interplay of weak impurity and umklapp scattering is shown to yield "dip" features in the magneto-thermal conductivity, consistent with the experimental observation. Moreover, the theory predicts that in sufficiently clean spin-1/2 systems, a dramatic variation of the thermal conductivity manipulated by a magnetic field is possible, even in compounds with very high exchange coupling. Finally, it is suggested that such magneto-thermal effects can generally serve as a useful probe of the Fermi surface of spinons in a spin-liquid state in arbitrary dimension.

25OR-D-8

## ION-ION INTERACTIONS IN FRUSTRATED $Tb_2Ti_2O_7$ : SPECTROSCOPIC STUDY

*Klimin S.A.<sup>1</sup>, Narozhnyy M.V.<sup>1</sup>, Popova M.N.<sup>1</sup>, van Loosdrecht P.H.M.<sup>2</sup>*

<sup>1</sup> Institute for spectroscopy RAS, 142190 Troitsk, Moscow region, Russia

<sup>2</sup> Material Science Center, University of Groningen, 9747 AG Groningen, the Netherlands

Frustrated magnetism in rare-earth (RE) titanates  $R_2Ti_2O_7$  ( $R$  stands for a RE element) with pyrochlore structure leads to an unusual magnetic state known as spin ice (SI) [1]. In the SI state, the  $R^{3+}$  ions situated in the corners of the  $R_4$  tetrahedra are magnetically arranged in each polyhedron. The magnetic moments are directed along the three-fold axes of tetrahedron at the angle  $109^\circ$  between each other. However, the arrangement of magnetic moments in each pair of nearest tetrahedra that have common vertex is frustrated. Frustration leads to the absence of a long-range magnetic order. SI state was established only for a few titanates ( $R = Dy$  and  $Ho$ ). It can be realized under the condition of the Ising-type anisotropy of the  $R^{3+}$  ion, driven by the crystal field (CF) [2]. The  $Tb^{3+}$  ion in the terbium titanate is also known to possess the Ising-type anisotropy [2], nevertheless, the SI state does not realize in  $Tb_2Ti_2O_7$ . The reason for this could be the low-lying CF-levels of  $Tb^{3+}$ . The CF splitting of the ground  $Tb^{3+}$  multiplet in  $Tb_2Ti_2O_7$  was studied by neutron scattering [3] and Raman spectroscopy [4] and the data are somewhat contradictory. This study was undertaken to obtain the information on low-lying CF levels of  $Tb^{3+}$  in  $Tb_2Ti_2O_7$  by means of transmission spectroscopy.

The absorption spectra for  $Tb_2Ti_2O_7$  were measured in broad spectral ( $1800-8000\text{ cm}^{-1}$ ) and temperature ( $1.7 - 300\text{ K}$ ) ranges. From the spectra, the CF energies for the ground multiplet were derived. First excited state of  $Tb^{3+}$  ion is located with energy  $\sim 1.5\text{ meV}$ . Other levels are situated at

10, 14 and 17 meV, in coincidence with [3]. Very unusual behavior of spectral lines at low temperatures ( $T < 15$  K) was registered. We interpret this behavior in terms of the strong interionic interaction that leads to transformation of terbium energetic spectrum. Our suggestion is confirmed by the unusual behavior of CF energies which demonstrate a dispersion according to the recent neutron data [5]. The strong interionic interaction leads to the mixing of ground and first excited (1.5 meV) states, thus Ising type anisotropy is not realized for  $Tb_2Ti_2O_7$ .

Support by RAS (under the Programs for Fundamental Research) is acknowledged.

[1] A.P. Ramirez, et al., Nature **399**, 333 (1999).

[2] B. Z. Malkin, A. R. Zakirov, M. N. Popova, S. A. Klimin, E. P. Chukalina, E. Antic-Fidancev, Ph. Goldner, P. Aschehoug, G. Dhalenne, Phys. Rev. B **70**, 075112 (2004).

[3] J.S. Gardner, B.D. Gaulin, A.J. Berlinsky, P. Waldron, S.R. Dunsiger, N.P. Raju, J.E. Greedan. Phys. Rev. B **64**, 224416 (2001).

[4] T.T.A. Lummen, et al., Phys. Rev. B **77**, 214310 (2008).

[5] I. Mirebeau, P. Bonville, and M. Hennion, Phys. Rev. B **76**, 184436 (2007).

25OR-D-9

## MAGNETIC ANISOTROPY OF 2D ANTIFERROMAGNET WITH TRIANGULAR LATTICE $CuCrO_2$

*Prozorova L.A.<sup>1</sup>, Svistov L.E.<sup>1</sup>, Tsurkan V.<sup>2</sup>, Vasiliev A.M.<sup>1</sup>*

<sup>1</sup> P.L. Kapitza Institute for Physical Problems RAS, Moscow, Russia

<sup>2</sup> Center for Electronic Correlations and Magnetism EKM, Experimentalphysik V,  
Universität Augsburg, Germany

For more than a decade, the study of frustrated antiferromagnets has been a fascinating subject of condensed-matter physics. Unconventional types of magnetic ordering and phases in frustrated quantum spin chains are attractive issues, because they appear under a fine balance of the exchange interactions and are sometimes caused by much weaker interactions or fluctuations.

$CuCrO_2$  compound is an example of the quasi-two dimensional antiferromagnet ( $S=3/2$ ) on a triangular lattice with easy axis anisotropy. At temperatures lower than transition temperatures ( $T_{N1}=23.6$  K and  $T_{N2}=24.2$  K) the magnetic system of  $CuCrO_2$  is long range ordered in the triangular planes and has short range correlations between planes. The planar spiral spin structure with the incommensurate vector  $(0, 328; 0, 328; 0)$  was recently detected in  $CuCrO_2$  compound [1]. The small deviation from 120-degree magnetic structure is probably caused by small distortion of triangular lattice, so that the exchange parameter along one side of the triangle differs from two others (Fig. 1). In our work we study the magnetic structure of  $CuCrO_2$  single crystals using the ESR technique. The frequency and angle dependencies of ESR spectra can be well described in the model of a planar spiral spin structure with biaxial anisotropy [2]. One anisotropy axis is directed along  $C_3$   $(0,0,1)$  and the second is arranged along  $(1,-1,0)$ . The weak in-plane anisotropy is connected with the distortion of triangular planes mentioned above. The in-plane anisotropy does not change at the spin-reorientation transition, which means that this distortion is not connected with magnetostriction.



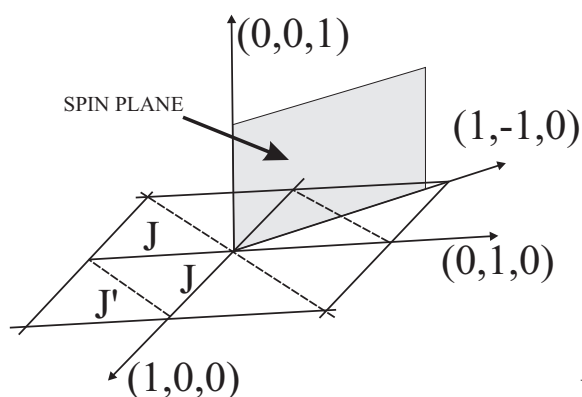


Fig. 1

The value of anisotropy of the exchange susceptibility of the spin structure, the constants of anisotropy and the fields of spin reorientation transitions were obtained.

The work has been supported by RFBR Grant № 10-02-01105-a.

[1] M. Poienar, F. Dumay, C. Martin, V. Hardy, A. Maignan, and G. Andre, Phys. Rev. B **79**, 0144412 (2009).

[2] K. Kimura, H. Nakamura, S. Kimura, M. Hagiwara, and T. Kimura, Phys. Rev. Lett. **103**, 107201 (2009).

25OR-D-10

### SPIN-RESONANT MODE IN IRON-PNICTIDE SUPERCONDUCTORS

*Inosov D.S.<sup>1</sup>, Park J.T.<sup>1</sup>, Yaresko A.<sup>1</sup>, Graser S.<sup>2</sup>, Sun D.L.<sup>1</sup>, Bourges Ph.<sup>3</sup>, Sidis Y.<sup>3</sup>, Li Y.<sup>1</sup>, Kim J.-H.<sup>1</sup>, Haug D.<sup>1</sup>, Ivanov A.<sup>4</sup>, Hradil K.<sup>5,6</sup>, Schneidewind A.<sup>5,7</sup>, Link P.<sup>5</sup>, Faulhaber E.<sup>7,5</sup>, Glavatsky I.<sup>8</sup>, Lin C.T.<sup>1</sup>, Keimer B.<sup>1</sup>, Hinkov V.<sup>1</sup>*

<sup>1</sup> Max-Planck-Institut für Festkörperforschung, Heisenbergstraße 1,  
70569 Stuttgart, Germany

<sup>2</sup> Center for Electronic Correlations and Magnetism, Institute of Physics, University of Augsburg,  
D-86135 Augsburg, Germany

<sup>3</sup> Laboratoire Léon Brillouin, CEA-CNRS, CEA Saclay, 91191 Gif-sur-Yvette Cedex, France

<sup>4</sup> Institut Laue-Langevin, 156X, 38042 Grenoble cedex 9, France

<sup>5</sup> Forschungsneutronenquelle Heinz Maier-Leibnitz (FRM II), Technische Universität München,  
D-85747 Garching, Germany

<sup>6</sup> Institut für Physikalische Chemie, Universität Göttingen, 37077 Göttingen, Germany

<sup>7</sup> Gemeinsame Forschergruppe HZB – TU Dresden, Helmholtz-Zentrum Berlin  
für Materialien und Energie, D-14109 Berlin, Germany

<sup>8</sup> Helmholtz-Zentrum Berlin für Materialien und Energie GmbH, Glienicke Str. 100,  
D-14109 Berlin, Germany

The proximity of superconductivity and antiferromagnetism in the phase diagram of iron arsenides, the apparently weak electron-phonon coupling and the “resonance peak” in the superconducting spin excitation spectrum have fostered the hypothesis of magnetically mediated Cooper pairing. However, since most theories of superconductivity are based on a pairing boson of sufficient spectral weight in the normal state, detailed knowledge of the spin excitation spectrum above the superconducting transition temperature,  $T_c$ , is required to assess the viability of this

hypothesis. Using inelastic neutron scattering we have studied the spin excitations in optimally doped  $\text{BaFe}_{1.85}\text{Co}_{0.15}\text{As}_2$  ( $T_c = 25$  K) and  $\text{BaFe}_{1.91}\text{Ni}_{0.09}\text{As}_2$  ( $T_c = 18$  K) over a wide range of temperatures and energies [1]. We present the results in absolute units and find that the normal state spectrum carries a weight comparable to underdoped cuprates. In contrast to cuprates, however, the spectrum agrees well with predictions of the theory of nearly antiferromagnetic metals [2], without complications arising from a pseudogap or competing incommensurate spin-modulated phases. We also show that the temperature evolution of the resonance energy follows the superconducting energy gap, as expected from conventional Fermi-liquid approaches. Our observations point to a surprisingly simple theoretical description of the spin dynamics in the iron arsenides and provide a solid foundation for models of magnetically mediated superconductivity

[1] Inosov D S, Park J T, Bourges P, Sun D L, Sidis Y, Schneidewind A, Hradil K, Haug D, Lin C T, Keimer B and Hinkov V, *Nature Phys.* **6**, 178 (2010).

[2] Moriya T, *Spin Fluctuations in Itinerant Electron Magnetism* (Springer-Verlag, Berlin Heidelberg, 1985).

25OR-D-11

## HIGH PRESSURE PHASE DIAGRAM OF Ce-BASED HEAVY FERMIONS

*Larrea J.<sup>1</sup>, Paschen S.B.<sup>1</sup>, Lorenzer A.<sup>1</sup>, Sidorenko A.<sup>1</sup>, Teyssier J.<sup>2</sup>, Ronnow H.M.<sup>3</sup>*

<sup>1</sup> Institute of Solid State Physics, Vienna University of Technology, Austria

<sup>2</sup> Department of Physics of Condensed Matter, University of Geneva, Switzerland

<sup>3</sup> Laboratory for Quantum Magnetism, Ecole Polytechnique Federale de Lausanne, Lausanne, Switzerland

We report our electrical transport, specific heat and magnetic susceptibility investigation under high pressure on the two heavy fermion compounds:  $\text{Ce}_3\text{Pd}_{20}\text{Si}_6$  and  $\text{CeCoGe}_{2.3}\text{Si}_{0.7}$ , which are believed to be close to a quantum critical point (QCP).

At ambient pressure,  $\text{Ce}_3\text{Pd}_{20}\text{Si}_6$  shows two successive phase transitions:  $T_L = 0.3$  K and  $T_U = 0.5$  K which have been tentatively attributed to antiferromagnetic and quadrupolar order. On the other hand,  $\text{CeCoGe}_{2.3}\text{Si}_{0.7}$  undergoes an antiferromagnetic transition at  $T_N = 6$  K [2]. It is expected that for the latter system disorder plays an important role when approaching the QCP. We will present temperature-pressure phase diagrams and suggest mechanisms that account for the quantum criticality in both compounds.

"Financial support by the European Research Council (ERC Advanced Grant No 227378) is acknowledged."

[1] S. Paschen et al., *J. Magn. Magn. Mater.*, 316, 90 (2007)

[2] D. Eom et al., *J. Phys. Soc. Jpn.* 67, 2495 (1998)

25OR-D-12

## NON-ZHANG-RICE STATES AND UNCONVENTIONAL ORBITAL MAGNETISM IN CUPRATES

*Moskvin A.S.<sup>1</sup>*

Ural State University, 620083 Ekaterinburg, Russia

Both theoretical considerations and experimental data point towards a more complicated nature of the valence hole states in doped cuprates than it is predicted by simple Zhang-Rice (ZR) model. Actually, we deal with a competition of conventional hybrid Cu 3d-O 2p  $b_{1g} \propto d_{x^2-y^2}$  state and purely oxygen nonbonding state with  $a_{2g}$  and  $e_{u,x,y} \propto p_{x,y}$  symmetry [1]. Accordingly, the ground state of such a non-ZR hole center  $[\text{CuO}_4]^{5-}$  as a cluster analog of  $\text{Cu}^{3+}$  ion should be described by a complex  ${}^1A_{1g}-{}^{1,3}B_{2g}-{}^{1,3}E_u$  multiplet with several competing charge, orbital, and spin order parameters [2], both of conventional ones (e.g., spin moment or Ising-like orbital magnetic moment) and unconventional, or hidden ones (e.g., intra-plaquette's staggered order of Ising-like oxygen orbital magnetic moment, orbital toroidal moment or combined spin-quadrupole ordering). The non-ZR hole  $[\text{CuO}_4]^{5-}$  centers should be considered as singlet-triplet pseudo-Jahn-Teller (ST-PJT) centers prone to strong vibronic coupling. Both hole- and electron-doped cuprates are believed to form an electron-hole Bose liquid [3], or a system of electron  $[\text{CuO}_4]^{7-}$  centers moving in a lattice formed by hole  $[\text{CuO}_4]^{5-}$  centers, in other words, these ST-PJT hole centers are an essential element of both hole and electron doped cuprates. In particular, these specify many features of the pseudogap regime which manifests clearly seen competing orders. However, the non-ZR structure of hole centers seems to be a detrimental factor for high- $T_c$  superconductivity. We believe that a large body of puzzling effects governed by the non-ZR structure of the hole centers are secondary ones and are not of primary importance for high- $T_c$  superconductivity. Recent discovery of many unconventional phenomena within a pseudogap phase, in particular, that of broken time reversal and rotational (tetragonal) symmetries associated primarily with electronic inequivalence at the two O sites within the  $\text{CuO}_2$  unit cell do provide a strong support of the non-ZR nature of the hole centers with obvious incorporation of nonbonding oxygen orbital. We address recent experimental findings of the hidden order by circular magnetooptics, magnetic elastic neutron scattering, and  $\mu\text{SR}$  measurements in different cuprates. All these merely provide a novel information about the peculiarities of the non-ZR structure of the hole centers rather than about the microscopic origin of high- $T_c$  superconductivity. However, we need to understand these phenomena to understand high- $T_c$  puzzle itself.

The RFBR Grant No. 10-02-96032 is acknowledged for financial support.

[1] A.S. Moskvin, Yu.D. Panov, *Fiz. Nizk. Temp. (Low Temp. Phys.)*, **37** (2011) 334.

[2] A.S. Moskvin, *JETP Lett.*, **80** (2004) 697.

[3] A.S. Moskvin, *Low Temp. Phys.*, **33** (2007) 234.



**25 August**

Thursday

11:30-13:00

14:30-17:00

oral session

25TL-E

25RP-E

25OR-E

superconductivity

**“Magnetic Soft Matter”**

25TL-E-1

## MEAN-FIELD DESCRIPTION OF THE ORDER – DISORDER PHASE TRANSITION IN FERRONEMATICS

Raikher Yu.L.<sup>1</sup>, Zakhlevnykh A.N.<sup>2</sup>, Stepanov V.I.<sup>1</sup>

<sup>1</sup> Institute of Continuous Media Mechanics, Ural Branch, Russian Academy of Sciences,  
Perm, 614013, Russia

<sup>2</sup> Physical Department, Perm State University, Perm, 614990, Perm, Russia

The Maier-Saupe theory, despite its mature age, remains the main theoretical tool in describing complicated liquid-crystalline systems, each time confirming anew the power of physically solid phenomenology. However, in the physics of ferronematics (or, wider, ferroliquid crystals) it was untouched for a long time. The cause is that the overwhelming majority of interesting and applicationally prospective ideas and problems concerning ferronematics (FN) are justly related to their behavior in the liquid-crystalline (*ordered*) state, while above the transition point (in the *disordered* state) these composites are believed to be very much alike usual magnetic fluids.

Nowadays, when synthesis of stable thermotropic FN ceased to be a rare and exotic event (see, [1,2], for example), the time came for more detailed investigation of their properties and, in particular, the origin of the ordered phase. From the very idea of FN, i.e., the suspensions of ferromagnetic particles in mesomorphic matrices, one should expect that application of an external magnetic field should modify the parameters of the transition. In fact, in FN, as a composite system, these modifications are two-fold. The first effect stems just from the presence of a solid admixture that (*i*) excludes some volume from the mesophase and (*ii*) needs some energy for its orientation together with the host substance [3]. The second class of effects is of the “opposing” sense: it accounts for the orientational action exerted on the host on the part of the suspended particles in result of the orientation of the latter by the field. Both types of the effects might augment as well as decrease the transition point (Curie temperature) of FN.

The issue that is essential for all these effects, is the coupling between the particle subsystem and the host matrix. In the simplest case this orientational interaction is described by a single material parameter depending simultaneously on the anisotropy of the surface tension at the particle-matrix interface, on the geometry of the particles [4] and on the particle concentration.

The mean-field theory allows us to build up a consistent and fairly simple model describing the isotropic – nematic transition in dilute FNs. Extending the work carried out in [5], we predict possible situations, which might be encountered in FN, and estimate the magnitudes of the transition temperature shifts expected for really existing FN suspensions.

Partial financial support from RFBR projects 10-02-96022 and 09-02-91070 is acknowledged. We are grateful to P. Kopčanský for drawing this interesting subject to our attention.

[1] N. Tomašovičová, P. Kopčanský, M. Koneracká, L. Tomčo, V. Závišová, M. Timko, N. Éber, K. Fodor-Csorba, T. Tóth-Katona, A. Vajda, J. Jadzyn, *J. Phys.: Condens. Matter* **20** (2008) 204123.

[2] O. Buluy, S. Nepijko, V. Reshetnyak, E. Ouskova, V. Zadorozhnii, A. Leonhardt, M. Ritschel, G. Schönhense, Yu. Reznikov, *Soft Matter* **7** (2011) 644.

[3] M.V. Gorkunov, M.A. Osipov, *Soft Matter* **7** (2011) Advanced article: DOI: 10.1039/c0sm01398f.

[4] S.V. Burylov, Yu.L. Raikher, *Phys. Rev. E* **50** (1994) 358.

[5] R. Akhmetzyanov, A.N. Zakhlevnykh, Yu.L. Raikher, In: *Magnetic Properties of Ferrocolloids*, Sverdlovsk: Ural Branch of Acad. Sci. USSR, pp.63–74 (1988), in Russian.

25RP-E-2

## MAGNETIC-FIELD INDUCED ISOTROPIC TO NEMATIC PHASE TRANSITION IN FERRONEMATICS

Kopčanský P.<sup>1</sup>, Tomašovičová N.<sup>1</sup>, Koneracká M.<sup>1</sup>, Závěšová V.<sup>1</sup>, Timko M.<sup>1</sup>, Hnatič M.<sup>1</sup>, Éber N.<sup>2</sup>, Tóth-Katona T.<sup>2</sup>, Jadzyn J.<sup>3</sup>, Honkonen J.<sup>4</sup>

<sup>1</sup> Institute of Experimental Physics, Slovak Academy of Sciences, Watsonova 47, Košice, Slovakia

<sup>2</sup> Research Institute for Solid State Physics and Optics, HAS, H-1525 Budapest, P.O.Box 49, Hungary

<sup>3</sup> Institute of Molecular Physics, PAS, 16 Smoluchowskiego str., 60179 Poznan, Poland

<sup>4</sup> Department of Physical Sciences, University of Helsinki, Gustav Hällstromin katu 2, Helsinki, Finland

It has long been known that the possibility exists in liquid crystals for an external magnetic field to substantially alter the nematic-isotropic transition temperature [1]. However, the effect has not been produced experimentally as the critical fields were estimated well over 100 T for traditional liquid crystal materials. The first experimental observation of the predicted magnetic-field dependence of the nematic-isotropic phase transition temperature has been recently carried out [2] on a powerful electromagnet ( $H$  up to 30 T). To demonstrate the effect, a „non-traditional” (bent-core) nematic liquid crystal material was used. The effect of the phase transition temperature shift was  $\sim 0.8$  °C at magnetic field 30 T.

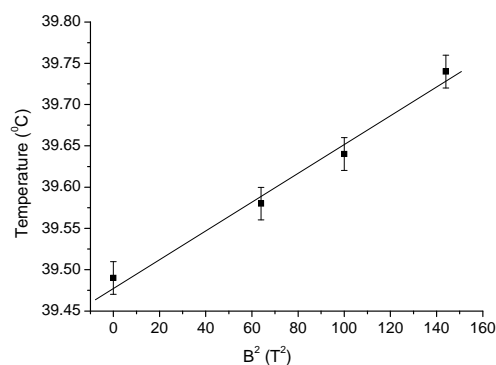


**Fig. 2.** Isotropic-nematic transition temperature vs. applied magnetic field (line represents the best linear fit).

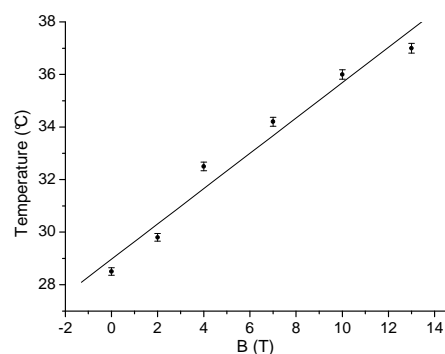


**Fig. 3.** Isotropic-droplet state transition temperature vs. applied magnetic field (line represents the best linear fit).

In this work this effect was demonstrated in a „traditional” calamitic nematic 6CHBT and in 6CHBT dissolved in phenyl isothiocyanate doped with magnetic nanoparticles. In the first case the shift in temperature was about 0.2 °C (12 T) and dependence of phase transition temperature on the external magnetic fields was quadratic (see Fig.1) while in the second case the shift was about 9 °C (13 T) and the dependence was linear (see Fig.2).

The work was supported by the Slovak Academy of Sciences grant VEGA No. 0077 and Centre of Excellence Nanofluid, APVV-0171-10, Education Agency for Structural Funds of EU in frame of project 26220120033 and the Grenoble High Magnetic Field Laboratory with support of EC from the 7th FP-Contract No 228043-EuroMagNET II.

[1] W. Helfrich, *Phys. Rev. Lett.*, **24** (1970) 201.

[2] T. Ostapenko, et al., *Phys. Rev. Lett.*, **101** (2008) 247801.

## MAGNETIC PROPERTIES OF FERROFLUID EMULSIONS

Ivanov A.O.<sup>1</sup>, Kuznetsova O.B.<sup>1</sup>, Subbotin I.M.<sup>1</sup>, Dikanskii Yu.I.<sup>2</sup>

<sup>1</sup> Urals State University, Lenin Av., 51, 620000 Ekaterinburg, Russia

<sup>2</sup> Stavropol State University, 355009 Stavropol, Russia

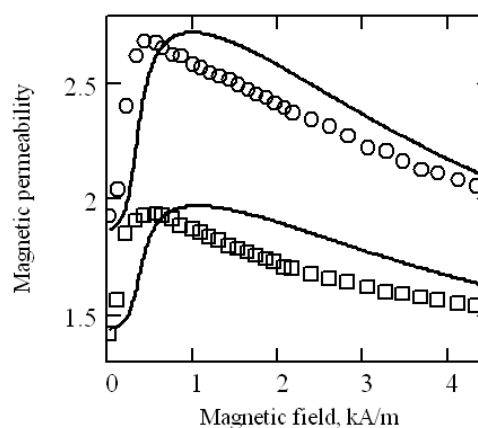
Ferrofluid emulsions are the colloidal suspensions of droplets, filled with a ferrofluid and suspended in neutral nonmiscible liquids. Typical droplet diameter is of the order 1 – 10  $\mu\text{m}$ ; and they are spherical in a field absence. An externally applied magnetic field induces the droplet magnetic moments and tends to elongation of droplets along a field direction. The suspension may be inverted to get the “inversed” ferrofluid emulsion, representing the suspension of liquid droplets in a carrier ferrofluid.

Recently the nonmonotonic magnetic response was experimentally reported [1] for the emulsions of kerosene-based ferrofluid in nonmiscible aviation oil. Under the action of a uniform external magnetic field the magnetic permeability of such ferrofluid emulsion demonstrates the rapid weak field growth and further long-tail decay in stronger magnetic fields (see Fig., experimental dots). The effect could be observed only for emulsions with a rather weak interfacial tension ( $\sim 10^{-5}$  N/m and less), and it is more pronounced for emulsions with higher values of the droplet volume fraction. In Fig. the boxes are related to the emulsion with the droplet volume fraction of 20%, and the circles correspond to the volume fraction of 35% [1].

The effect could be theoretically explained on the basis of the following physical idea. In weak fields the magnetization of ferrofluid inside the droplets might be considered as being linearly dependent on a magnetic field strength with a constant value of the ferrofluid magnetic susceptibility. Simultaneously, the droplet elongation results in the decrease of demagnetizing field inside the droplets. So, in weak magnetic field one could expect more rapid growth of the induced droplet magnetic moment than the linear dependence on external field strength; and, thus, the emulsion magnetic permeability is an increasing function of field strength.

In stronger magnetic field the droplets are already highly elongated. So, the field strengthening is not accompanied by further significant decrease of the demagnetizing field; and the further droplet elongation terminates. On the other hand the magnetic susceptibility of the ferrofluid reduces with a field. Thus, the effective magnetic permeability of the ferrofluid suspension becomes decreasing.

The theoretical model, combining the known magnetization behaviour of the ferrofluid, the solution of magnetostatic problem for the magnetic field geometry inside and outside the elongated droplet, and the droplet energy minimization approach for obtaining the droplet elongation at moderate value of an externally applied uniform magnetic field, fully substantiate the described physical conception (see Fig., curves).



Support by MES RF is acknowledged.

[1] Yu.I. Dikanskii, A.R. Zakinyan, N.Yu. Konstantinov, *Technical Physics*, **53** (2008) 19.



## DYNAMIC MAGNETIZATION OF A NANODISPERSE SYSTEM INDUCED BY AN ACOUSTIC WAVE

*Polunin V.M., Storozhenko A.M., Ryapolov P.A.*

South-West State University, 50 Lyet Oktyabrya st., 94, Kursk, Russian Federation

Acoustic oscillations of a magnetized magnetic fluid (MF) are accompanied by the emission of electromagnetic waves (acoustomagnetic effect) [1]. The radiated waves can be registered with the aid of an inductor coil, where these waves induce the electro-motive force proportional to the amplitude of the MF magnetization oscillations.

Assuming that the MF behaves superparamagnetically, the amplitude of the induced e.m.f in relative units can be presented as a function of the Langevin parameter  $\xi$  [2]. Besides the oscillations of the magnetic nanoparticle concentration, this amplitude includes the contributions from:

- temperature variations in the adiabatic sound wave;
- the dynamic demagnetizing field induced in a magnetized fluid by the sound wave.

Theoretical curves describing these mechanisms are shown in Fig. 1.

The expression for thermal contribution reads:

$$\Omega(\xi) \equiv k'D(\xi),$$

where  $k'=qc^2/C_p$ ,  $q$  is the thermal expansion coefficient;  $c$  is the speed of acoustic wave propagation;  $C_p$  is the specific heat capacity at constant pressure;  $D(\xi)=\xi^{-1}-\xi\text{sh}^{-2}\xi$ .

The dynamic demagnetizing field contribution is described by the formula

$$Y_1(\xi) \equiv L(\xi) - \frac{L(\xi)}{1+k''D(\xi)/\xi},$$

where  $L(\xi)=c\text{th}\xi-\xi^{-1}$  is the Langevin function;  $k''=N_d\mu_0M_S m^*/(k_0T)$ ;  $N_d$  is the dynamic demagnetizing factor;  $M_S$  denotes MF saturation magnetization;  $m^*$  is the ferroparticle magnetic moment,  $T$  denotes absolute temperature,  $k_0=1.38 \cdot 10^{-23} \text{ J} \cdot \text{K}^{-1}$ ,  $\mu_0=4\pi \cdot 10^{-7} \text{ H/m}$ .

The summary effect of these two mechanisms can be presented by the dependence:

$$Y_+(\xi) = \frac{L(\xi) \cdot k''D(\xi)/\xi + \Omega(\xi)}{1+k''D(\xi)/\xi}.$$

As seen from Fig. 1, in a general case each of the two mechanisms to about the same extent contributes to the acoustomagnetic effect. However, choosing an appropriate sample, one can reduce significantly any of the two factors or both of them. For example, the thermal component might be eliminated if to use a carrier liquid with a low thermal expansion coefficient, while the dynamic demagnetizing field becomes negligible in highly diluted MF samples.

In Fig. 2 are shown in relative units the magnetization curve  $\beta_M$ , the acoustomagnetic effect curve  $\beta$  and the difference between the latter. As expected, the "difference" curve has a maximum, whose

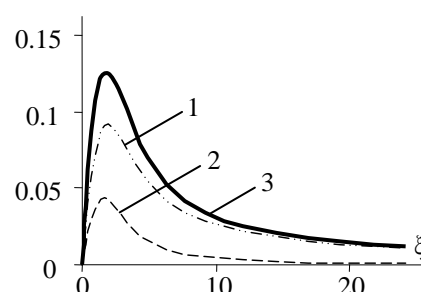


Fig. 1. 1 –  $\Omega$ , 2 –  $Y_1$ , 3 –  $Y_+$ .

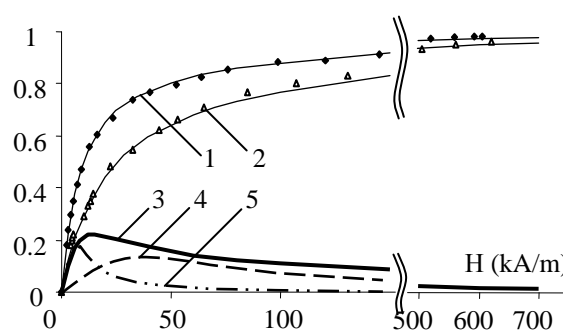


Fig. 2. 1 – the relative magnetization  $\beta_M(H)$ , 2 – the relative acoustomagnetic effect curve  $\beta(H)$ , 3 – the "difference" curve  $\beta_M(H)-\beta(H)$ , 4 –  $Y_+$  ( $d=d_{\min}=9 \text{ nm}$ ), 5 –  $Y_+$  ( $d=d_{\max}=16 \text{ nm}$ ).

magnitude and position are determined by the joint contribution of the thermal vibrations and the dynamic demagnetizing field to the magnetization perturbation. We show that the “difference” curve obtained in our experiments is in satisfactory agreement with the theoretical dependence  $Y_+(H)$  corresponding to the case of a monodisperse MF consists of nanoparticles with diameter  $d$ .

- [1] V. M. Polunin, Acoustic effects in magnetic fluids, Moscow: Fizmatlit, 2008. P. 34  
 [2] V. M. Polunin, N. S. Kobelev et al. *Magneto hydrodynamics*. **46** (2010) 31.

25TL-E-5

## DIPOLAR COLLOIDS IN AC MAGNETIC FIELD

*Cebers A., Belovs M.*

University of Latvia, Riga, Zellu 8, LV-1002, Latvia

Dipolar systems in AC fields are active systems with a rich emergent behaviour. As an example a system of micron size ferromagnetic particles floating on the surface of liquid should be mentioned [1]. In this system the formation of dynamic self-organized states are found which generate a liquid flow and a self-propulsion of the chains of particles [2]. In [3] it is found that ferromagnetic particles due to the dipolar interaction exhibit different synchronization phenomena under the action of an AC magnetic field. This class of phenomena includes the synchronous oscillations in a weak field, synchronous rotation at large fields and dynamic staggered states.

The arising states in a system of  $N$  particles are characterized by a vectorial order parameter defined by

$$\vec{V} = \frac{1}{N} \sum_{i=1}^N \vec{n}_i .$$

Here  $\vec{n}_i$  is the unit vector along the magnetic moment of the particle. The system is described by parameters  $\varepsilon = mH_0 / \zeta\omega$  and  $\lambda\varepsilon = H_{dip} / H_0$ , which characterize the ratio of the period of an AC field  $2\pi / \omega$  to the characteristic time of dipole relaxation and the ratio of dipolar field of neighbour particle  $H_{dip}$  to the strength of AC field  $H_0 = (0, 0, H_0 \sin(\omega t))$ . The radius vectors of dipoles are on the line in the plane with a normal  $(\cos(\alpha), 0, -\sin(\alpha))$ .

In Fig.1 the order parameter absolute value in dynamic ordered state of the system of 7 dipoles is shown ( $\varepsilon = 2; \lambda = 0.01 / \varepsilon; \alpha = \pi / 20$ ). Initial configuration is random. We see that dipoles a long periods of time are in dynamic ordered state where they synchronously oscillate in AC field. The perfect ferromagnetic ordered state is broken at definite short intervals of time when the mean value of magnetic dipolar moments switches to the opposite direction along x axis.

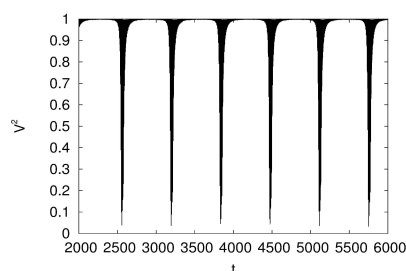


Fig.1

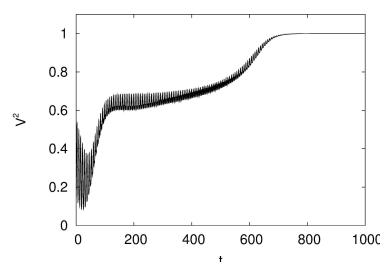


Fig.2

In larger ensembles in dependence on initial conditions pure ferromagnetic states or ferromagnetic states with domain structure may be formed. This is illustrated by Fig.2 for ensemble of 24 dipoles at  $\varepsilon = 0.4$  (other parameters are the same, initial configuration is random).

- [1] A.Snezhko, I.S.Aranson, and W.-K.Kwok, *Phys.Rev.Lett.*,96 (2006) 078701  
 [2] A.Snezhko, I.S.Aranson, and W.-K.Kwok, *Phys.Rev.Lett.*,99 (2007) 158301  
 [3] M.Belovs, and A.Cebers. *Euromech Colloquium 526* (2011) 13

25RP-E-6

## LONGITUDINAL AND TRANSVERSAL POLYMERIZATION MAGNETIC FIELD EFFECTS ON THE MICROSTRUCTURE OF A MAGNETIC ELASTOMER

Balasoiu M.<sup>1,2</sup>, Bica I.<sup>3</sup>, Dokukin E.B.<sup>2</sup>, Kuklin A.I.<sup>2</sup>, Rogachev A.V.<sup>2</sup>, Soloviov D.V.<sup>2</sup>, Jigounov A.<sup>4</sup>, Lebedev V.T.<sup>5</sup>, Raikher Yu.L.<sup>6</sup>

<sup>1</sup> National Institute of Physics and Nuclear Engineering, Bucharest, Romania

<sup>2</sup> Joint Institute of Nuclear Research, Dubna, Russia

<sup>3</sup> West University of Timisoara, Department of Electricity and Magnetism, Timisoara, Romania

<sup>4</sup> Institute of Macromolecular Chemistry, ASCzR Prague

<sup>5</sup> Petersburg Nuclear Physics Institute, Gatchina, Russia

<sup>6</sup> Institute of Continuum Media Mechanics, Ural Branch of RAS, Perm, Russia

New generation of magnetic elastomers represents a new type of composites consisting of small magnetic particles, usually in the nano- or micrometer range, dispersed in a highly elastic polymeric matrix. Combination of magnetic and elastic properties leads to a number of striking phenomena that are exhibited in response to magnetic fields. Since the magnetic fields are convenient stimuli from the point of signal control, therefore it is of great importance to develop and study such flexible polymeric systems [1].

For example, functionalized nanocomposites consisting of magnetic nanoparticles embedded in dielectric matrices have a significant potential for the electronics industry [2].

In the simplest form a polymer nanocomposite is a blend of small particles (the diameter is less than 100 nm), incorporated in a polymer matrix. Polymer nanocomposites are characterized by the convergence of three different length scales: the average radius gyration of the polymer molecules ( $R_G$ ), the average diameter of the nanoparticles ( $2r$ ), and the average nearest-neighbor distance between the particles ( $d$ ), as shown in Fig. 1.

Application of a magnetic field during the polymerization process of the magnetic elastomer induces changes at the level of these length scales and/or the formation of anisotropic structures which significantly can change the electromagnetic properties of the composite.

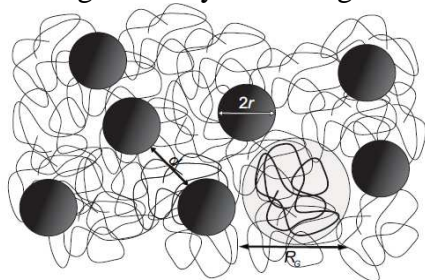


Fig. 1. A schematic illustration of a polymer nanocomposite. The average radius of the nanoparticles ( $2r$ ) (filled dark circles), the average radius of gyration of the polymer molecules ( $R_G$ ) (the thick black line inside the filled light-gray circle) and the average nearest-neighbor distance ( $d$ ) between the nanoparticles are of the same magnitude.

Magnetic elastomers samples with induced longitudinal or transversal anisotropy are prepared and investigated by means of small angle X-ray and neutron scattering [3]. The case of moderate particle concentration is detailed analyzed.

- [1] S. Abramchuk, E. Kramarenko, G. Stepanov, et.al, *Polym. Adv. Technol.* **18** (2007) 883  
 [2] J.V.T. Timonen, R.H.A. Raas, O. Ikkeda et al., in A. Aldea, V. Barsan, *Trends in nanophysics*, Springer, 2010, p.257  
 [3] M. Balasoiu, V.T. Lebedev, D.N. Orlova, I. Bica, *Crystallography Reports* (2011) (submitted).

25RP-E-7

## **SIMULATION OF DIPOLAR MAGNETOSTRICTION IN SOFT MAGNETIC ELASTOMERS**

*Stolbov O.V., Raikher Yu.L.*

Institute of Continuous Media Mechanics, Ural Branch of Russian Academy of Sciences,  
614013, Perm, Russia

The origin of dipolar magnetostriction in soft magnetic elastomers (SMEs) is discussed, i.e., their ability to shrink/ elongate having been subjected to a uniform magnetic field in the absence of mechanical loading. Qualitative analysis shows that the effect of the field on a SME is twofold: one of the mechanisms is universal and manifests itself on the macroscopic scale, while the other is strongly dependent on the mesoscopic details of spatial distribution of the magnetic filler particles in the elastic matrix.

In the present work we report the results of numerical modeling of the deformational response of a SME sphere to a uniform magnetic field. The sample is treated as an elastic matrix, over the bulk of which a number of spherical magnetically soft ferromagnetic particles are distributed at random. In the absence of field the particles do not interact; under the field they magnetize and get coupled by the standard pairwise magnetodipole interaction. Assuming that the magnetization law of the ferromagnet is linear, one gets an easily solvable set of linear equations, which enables to find the local fields and the induced magnetic moments for all the particles. With these data, the magnetostatic energy of the sample is evaluated, and the dipolar force experienced by each particle is found by numerical differentiation of this functional.

To find the field-induced deformations, a continuum approach is employed. Both the particles and the matrix are treated as elastic media albeit with substantially different values of the moduli. This allows us to define the elastic modulus of the SME sphere as a piecewise-constant function that is finite in any point of the sample. Under assumption that the ferromagnet is much more rigid than the elastomer, the dependence of the results on the mechanical properties of the particles is virtually eliminated. The elastic problem is solved by finite-element method with the aid of Escript/Finley library [1]. To obtain the shrinking/elongation characteristics of the sample independent of surface rippling that inevitably occurs under magnetizing, the deformed sample is first transformed (with a least-square procedure) in an equivalent ellipsoid, and the major axes of the latter are evaluated. Then from these numbers the strain parameter is constructed.

Calculations are performed on a sphere containing 480 particles, whose positions are distributed at random, the only restriction is that the particle overlap is forbidden; the volume fraction of the magnetic phase is maintained equal to 30%. After averaging over about hundred realizations of the system, we find that the strain parameter is essentially positive. These new results we compare to the solution of a true continuum (single-phase) problem [2]. It turns out that the present modeling yields the strain parameter that is several times smaller than that obtained in continuum modeling.

This discrepancy could be corrected by introducing additional “cross” terms responsible for the magnetostriction in the free energy function of the continuum approximation.

We note that in our new model can allow for negative magnetostriction as well. The latter emerges if, when generating the initial distribution, close neighboring of the particles is forbidden, i.e., short-range spatial correlations are suppressed.

The work was done under auspices of projects 09-P-1-1010 from RAS, 02.740.11.0442 and AATP 2.1.1/4463 from RMES, 11-02-9600 from RFBR.

[1] L. Gross, L. Bourgouin, A. Hale., H. Muhlhaus, *Phys. Earth Planet. Interiors* **163** (2007) 23.

[2] O.V. Stolbov, Yu.L. Raikher, *J. Magn. Magn. Mater.* 289 (2005) 62.

25RP-E-8

## INVESTIGATION OF THE PROPERTIES OF MAGNETIC NANOPARTICLES IN SOFT SUBSTANCES

*Kantorovich S.<sup>1,2</sup>, Weeber R.<sup>2</sup>, Klinkigt M.<sup>2</sup>, Prokopyeva T.<sup>1</sup>, Holm C.<sup>2</sup>*

<sup>1</sup> Ural State University, Lenin av. 51, Ekaterinburg, 620000, Russia

<sup>2</sup> Institute for Computational Physics, University of Stuttgart, Pfaffenwaldring 27, 70569, Stuttgart, Germany

The behaviour of magnetic nanoparticles in the soft nonmagnetic media can be tuned in two different ways: one can change the properties of the carrier matrix and its coupling with magnetic particles, or the prepare magnetic nanoparticles which effective interactions differ from the regular magnetic dipole-dipole one. Our theoretical and computer simulation studies are devoted both to the study of magneto-elastic coupling in, so-called, ferrogels, and to the study of magnetically capped particles, and magnetic particles of various shapes.

Growing interest to magnetic gels or ferrogels, namely, hydrogels with embedded magnetic particles, can be easily justified by the possibility of using these systems in actuators, artificial muscles, and drug delivery. The properties of ferrogels are dictated by the coupling of magnetic response, dipole- dipole interaction, and the elastic properties of the polymer-gel matrix. A manifestation of this coupling can be observed in the deformation of a macroscopic ferrogel body in a uniform or gradient magnetic field. However, the lack of understanding of this coupling hinders industrial application of a magnetic gel. We have put forward two different models of the particle coupling to the matrix, and have shown, that depending on the density and distribution of magnetic particles, the gel can shrink perpendicularly to the field direction or shrink in a uniform manner.

Referring to specifically designed magnetic particles, one can introduce the particles, only a small part of the surface of which is magnetic, in other words particles with magnetic caps. It turned out that already the simple model of a particle with the magnetic dipole moment, shifted radially from the centre of mass, could show very particular properties. For example, these particles, depending on the shift of the magnetic dipole moment, exhibit a transition of the ground state configuration from the typical head-to-tail one (in case of the dipole moment being slightly shifted from the centre of mass) to an antiparallel pair of magnetic moments at higher shifts. Recent advances in the synthesis of particles opened a wide perspective in studying more complex systems, such as magnetic Janus particles or magnetic nanorods.

In the present contribution we would summarise the results obtained analytically and via various simulation techniques, in order to compare the state of art in the field to the known experimental

results.

This research has been carried out within the financial support by RFBR Grant No.08-02-00647-a, AVCP Grant No. 2.1.1/1535, FASI No. 02.740.11.0202, and the Grant of President RF MK-6415.2010.2 and Alexander von Humboldt Foundation.

25RP-E-9

## THERMO-REVERSIBLE HYDROFERROGELS BASED ON MAGNETIC NANOPARTICLES TEMPLATED IN TRIBLOCK COPOLYMER MESOPHASES

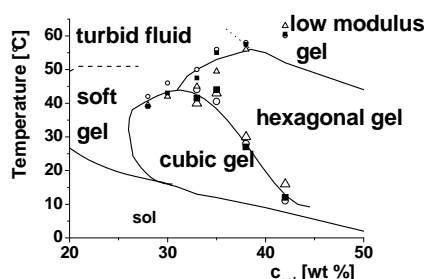
*Krekhova M.<sup>1</sup>, Lang T.<sup>2</sup>, Richter R.<sup>2</sup>, Schmalz H.<sup>1</sup>*

<sup>1</sup> Makromolekulare Chemie II, Universität Bayreuth, D-95440 Bayreuth

<sup>2</sup> Experimentalphysik V, Universität Bayreuth, D-95440 Bayreuth

Hybrid systems composed of magnetic nanoparticles embedded in a covalently cross-linked polymer matrix (ferrogels, FGs) have been investigated by various research groups [1]. In contrast to these permanent ferrogels, the viscoelastic properties of physically cross-linked FGs are characterized by a reversible gelation, e.g. induced by temperature or pH changes, making such gels an exciting type of magnetic soft matter [2].

In our current work thermo-reversible hydroferrogels have been prepared via gelation of water based ferrofluids (FFs) using an ABA-type triblock copolymer (Pluronic<sup>TM</sup> P123) as gelator. P123 consists of a thermo-responsive poly(propylene oxide) (PPO) middle block and two poly(ethylene oxide) (PEO) end blocks (PEO<sub>20</sub>PPO<sub>70</sub>PEO<sub>20</sub>). P123 based hydrogels are “inverse”-gels, i.e. liquid at low temperatures and gelation occurs upon heating due to micellisation above the lower critical solution temperature of the PPO middle block. P123 exhibits a temperature induced transition between a cubic and a hexagonal micellar gel phase. These mesophases were utilized as templates to achieve a defined arrangement of the magnetic nanoparticles (maghemite and cobalt ferrite) in the corresponding hydroferrogels [3].



Phase diagram for neat gels (○) and maghemite based FGs (●  $c_{FF} = 11$  wt %, ▲  $c_{FF} = 14$  wt %).

Long-term stable homogeneous FGs can be prepared from FFs with a maximum maghemite content of 14 wt% and cobalt ferrite content of 8 wt%. A combination of rheology and  $\mu$ -DSC was applied as an alternative method to construct the phase diagram of P123 based hydroferrogels (see Fig.). Magnetization experiments on FGs show that the incorporation of the maghemite nanoparticles ( $d = 8 \pm 2$  nm) into the gel matrix has no significant influence on the superparamagnetism and the magnetic moment distribution. In the case of cobalt ferrite ( $d = 6 \pm 2$  nm), the FFs exhibit the familiar superparamagnetic curve. In contrast, the corresponding FGs exhibit a hysteretic magnetization curve. The observed hysteresis indicates a strong coupling between the gel matrix and the magnetic moment of the blocked cobalt ferrite nanoparticles, which show a predominantly Brownian-type relaxation. Magneto-rheometric measurements have been carried out in order to investigate the impact of magnetic fields on the mechanical properties of the hydroferrogels.

Support by the German Science Foundation (Research Group FOR 608) is acknowledged.

- [1] M. Zrínyi et al., *Polym. Gels Netw.*, **5** (1997) 415; M. Zrínyi, *Colloid Polym. Sci.*, **278** (2000) 98; S. Abramchuk et al., *Polym. Adv. Technol.*, **18** (2007) 513.  
 [2] M. Krekhova, G. Lattermann, *Mater. Chem.*, **18**, (2008) 2842; G. Lattermann, M. Krekhova, *Macromol. Rapid Commun.*, **27** (2006) 137; **27** (2006) 1968; C. Gollwitzer et al., *Soft Matter* **5** (2009) 2093.  
 [3] M. Krekhova et al., *Langmuir*, **26** (2010) 19181.

25RP-E-10

## MICROSTRUCTURE OF MAGNETORHEOLOGICAL ELASTOMERS

*Günther D., Borin D., Odenbach S.*

TU Dresden, Institute of Fluid Mechanics, George-Bähr-Str. 3, 01062, Dresden, Germany

Magnetorheological elastomers (MREs) are a kind of multiphase multifunctional composites consisting of an elastic matrix filled with micron-sized magnetic particles.

Many previous studies have already dealt with the mechanical properties of this class of materials [1-3]. However, the characterization of the structural composition of the MREs has been considered very poor up to now, although it represents a fundamental basis of the observed mechanical behavior. Earlier, sporadic attempts have been made to analyze the inner structure of MREs using electron microscopy methods, scanning electron microscopy (SEM) and X-ray diffraction measurements (XRD) [4-6]. These techniques have the inherent disadvantage of sample destruction, which do not allow the subsequent evaluation of the mechanical properties of manufactured MREs. The analysis of three dimensional structures is also not possible using these methods.

The primary goal of the present work was the structural characterization of anisotropic, i.e. structured during the curling process in an applied magnetic field, MREs with different mass concentrations by using computed tomography (CT) methods.

The characterization by CT not only preserves the structure of the sample but also yields a three-dimensional map of the sample geometry. Anisotropic MRE samples with a concentrations  $\varphi=5, 15$  and 35 weight % of soft magnetic particles have been produced and investigated regarding to the morphological characteristics of their structures by CT. It has been shown that even small changes in the mass content of the magnetic filler led to the formation of completely different morphologies, which were reproducible for all samples. There were the familiar column formations in patterns with a mass content of  $\varphi=5\%$  iron powder. Increasing the matter content of 15% resulted to the formation of tubular structures. Samples with  $\varphi=35\%$  had a densely-packed structure, where the particle formations broke up. Meanders emerged, which contained no iron particles and penetrated the sample over the entire height like canyons.

This experimentally obtained information is in contrast to the models usually used for the theoretical modelling and calculations of MREs properties.

This project is funded by the European Union and the Free State of Saxony.

- [1] M.R. Jolly, J.D. Carlson, B.C. Munoz, *J.Intell. Mater. Sys. Struct.*, **7** (1996) 613.  
 [2] G. V. Stepanov, S. S. Abramchuk, D. A. Grishin, L. V. Nikitin, E. Yu. Kramarenko, A. R. Khokhlov, *Polymer*, **48** (2007) 488.  
 [3] G. Y. Zhou, *Smart Mater. Struct.*, **12** (2003) 139.

- [4] Wei Zhang, Xing-long Gong, Tao-lin Sun, Yan-ceng Fan, Wan-quan Jiang, *Chin. J. Chem. Phys.*, **23** (2010) 226.
- [5] W. H. Li, Y. Zhou, T. F. Tian, *Rheol. Acta*, **49** (2010) 733.
- [6] M. Balasoiu, M. L. Craus, E. M. Anitas, I. Bica, J. Plestil, A. I. Kuklin, *Phys. Solid State* **52** (2010) 917.

25RP-E-11

## MAGNETORHEOLOGICAL AND DEFORMATION PROPERTIES OF MAGNETICALLY CONTROLLED ELASTOMER WITH HARD MAGNETIC FILLER

*Stepanov G.V.<sup>1</sup>, Kramarenko E.Yu.<sup>2</sup>, Chertovich A.V.<sup>2</sup>*

<sup>1</sup> Institute of Chemistry and Technology of Organoelement Compounds,  
Sh. Entuziastov 128, Moscow, 111123, Russia

<sup>2</sup> Faculty of Physics, Moscow State University, Moscow, 119991, Russia.

A study on the change in elasticity of MCEs containing HM-filler in the magnetic field and after magnetization in various fields was carried out. Samples were prepared on the base of silicone polymer matrix with hard magnetic filler (FeNdB). Filler dispersity varied in the range of 1-100 microns. Filler properties in the annealing process in hydrogen and in the air, as well as under the mechanical stress during grinding were studied. During such influence, the hardness of the magnetic filler decreases slightly, and it becomes magnetically nonuniform. Deformation and magnetorheological properties of materials in magnetic fields up to 300 mT were studied. A distinctive feature of the samples with hard magnetic filler if compared with previously synthesized is their residual magnetization after placing them in the magnetic field, meanwhile samples acquire properties characteristic for the materials based on soft magnetic filler placed in the magnetic field [1].

Parameters - the elasticity and viscosity of such materials we measured by shift method on a rotational rheometer. It was observed that during stepwise measurement of the magnetic field strength viscosity increases much faster than the elasticity. This effect can be used in the construction of controlled dampers [2].

The magnetic properties study of the MCE has shown that with decreasing concentration of the magnetic filler in the composite elastic modulus of the material decreases and the coercivity of the material decreases, as shown it is in the table.

This result contradicts the well-known fact in which the coercive force of the composite increases with decreasing concentration of the magnetic filler, as a result of the reduction the demagnetizing factor influence. In our case, the composite anomalous behavior can be attributed to the rotation and movement of magnetized particles inside an elastic polymer matrix. Magnetization of the composite is mainly connected with possible filler particle rotation rather than particle magnetization under the action of magnetic field.

FeNdB Concentration	Ms, emu/g	Hc, Oe
100%	-	1855
80%	104	1740
75%	109	1271



This work was supported by the federal target program Research and Scientific–Pedagogical Personnel of Innovative Russia (State contract P2290).

[1] Chertovich A V, Stepanov G V, Kramarenko EY and Khokhlov A R, *Macromolecular Materials and Engineering* 2010. V.295. № 4. P. 336 – 341.

[2] Patent 2411404 RF, F16F 9/53, F16F15/03. Controlled device damping / Stepanov G V, Kramarenko EY, Khokhlov A R Vikulenkov A.V.

25RP-E-12

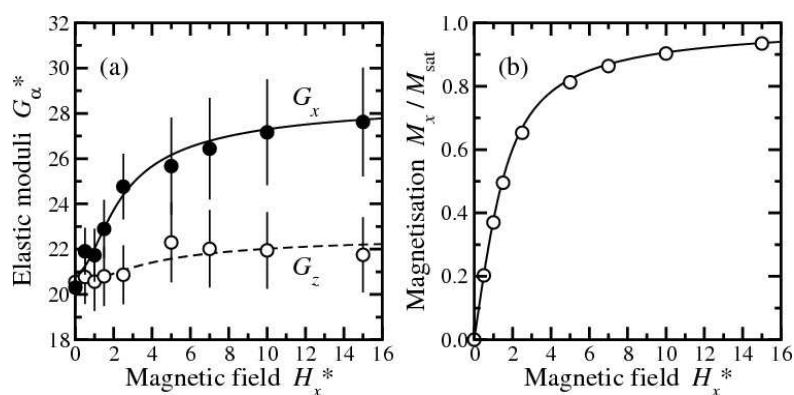
## COMPUTER SIMULATIONS OF FERROGELS

*Camp P.J., Wood D.S.*

School of Chemistry, The University of Edinburgh, West Mains Road, Edinburgh EH9 3JJ, UK

The effects of uniform magnetic fields on the mechanical and magnetic properties of ferrogels are examined using computer simulations. This contribution is focused on *chemical* ferrogels, which are prepared by initiating cross-linking reactions between polymers introduced to a colloidal suspension of magnetic nanoparticles [1]. These materials exhibit interesting properties: applying a uniform magnetic field during preparation leads to a mechanically anisotropic ferrogel; and the elastic moduli of the ferrogel can be altered reversibly by applying a uniform magnetic field, either parallel or perpendicular to the field applied during preparation.

Figure 1. (a) Elastic moduli of an isotropic ferrogel (with 9.5% v/v magnetic loading) as functions of the magnetic field strength: (points) simulation data; (lines) fits. (b) Magnetisation curve: (points) simulation data; (line) second-order modified mean-field theory [3]. All data are plotted in dimensionless units.



In this work, the colloidal suspension is modelled as a fluid of dipolar hard spheres, and particle configurations are generated using Monte Carlo simulations; the ferrogel is then formed by trapping the spheres in an elastic matrix (mimicking the effects of the cross-linked polymers). Monte Carlo simulations are used to determine the interparticle correlations, elastic moduli, and magnetisation curve of the ferrogel [2]. Figure 1(a) shows an example of the dependence of the elastic moduli  $G_x$  of an isotropic ferrogel on a uniform magnetic field applied in the  $x$  direction; figure 1(b) shows the corresponding magnetisation curve  $M_x(H_x)$ . It is found that the elastic moduli in the  $x$  and  $z$  directions are proportional to  $M_x^2$  and  $M_x^4$ , respectively. Using the magnetisation curve from Ivanov and Kuznetsova's second-order modified mean-field theory [3] – which has been tested rigorously against simulation data [4] – the theoretical relationships between the elastic moduli and the magnetic field can be obtained; these are shown as the lines in figure 1(a). In this presentation, results for different ferrogels will be described, and the experimentally observed trends will be explained by reference to the microscopic organisation of the magnetic nanoparticles in the gel matrix.

- [1] Z. Varga, G. Filipcsei, M. Zrínyi, *Polymer*, **47** (2006), 227.  
 [2] D.S. Wood, P.J. Camp, *Phys. Rev. E*, **83** (2011), 011402.  
 [3] A.O. Ivanov, O.B. Kuznetsova, *Phys. Rev. E*, **64** (2001), 041405.  
 [4] A.O. Ivanov, S.S. Kantorovich, E.N. Reznikov, C. Holm, A.F. Pshenichnikov, A.V. Lebedev, A. Chremos, P.J. Camp, *Phys. Rev. E*, **75** (2007), 061405.

25OR-E-13

## **MAGNETIC NANOSTRUCTURES BASED ON MAGNETIC NANOPARTICLES AND POLYMERS: SYNTHESIS AND CHARACTERIZATION**

*Turcu R.P.<sup>1</sup>, Craciunescu I.<sup>1</sup>, Nan A.<sup>1</sup>, Rednic L.<sup>1</sup>, Leostean C.<sup>1</sup>, Vekas L.<sup>2</sup>*

<sup>1</sup> National R&D Institute for Isotopic and Molecular Technologies,  
400293 Cluj-Napoca, Romania

<sup>2</sup> Romanian Academy – Timisoara Branch, CFATR, Lab. Magnetic Fluids,  
300223 Timisoara, Romania

In a hybrid magnetic nanoparticle – polymer system the specific composition of the polymeric material allows for the functionalization, different morphology design and control of the magnetic nanoparticle properties.

We report the synthesis and characterization of magnetic nanostructures designed either as core-shell nanoparticles or microgels by using water-based magnetic nanofluids and different polymers as starting materials. Correlation between the synthesis parameters and particle size distribution, magnetostatic properties, chemical surface composition, coating efficiency and embedding/encapsulation mechanisms of magnetic nanoparticles and particle clusters in polymers were investigated by TEM/HRTEM, DLS, VSM, XPS, FTIR.

The water based magnetic nanofluid (MF/W) samples used were provided by Lab MF-CFATR Timisoara and consist of magnetite nanoparticles coated by double layers of lauric acid (LA+LA) or oleic acid (OA+OA), dispersed in water according to the procedure described in [1].

Functionalized core-shell type magnetic nanostructures were obtained by coating the magnetite nanoparticles of the magnetic nanofluid MF/W/(LA+LA) with pyrrole copolymer shells with attached biomolecules like glucose, biotin and cholesterol. These core-shell magnetic nanostructures have superparamagnetic behavior and relatively good magnetization values (saturation magnetization in the range 15-60 emu/g), making them suitable for further applications in biotechnology and biomedicine.

Thermoresponsive magnetic microgels were obtained by using water based magnetic nanofluid and free radical polymerization of N-isopropylacrylamide. Moreover, the copolymerisation of monomers N-isopropylacrylamide and acrylic acid or methacrylic acid allow tuning the sensitivity of microgels to temperature and pH by adjusting the polymer content. Magnetic microgels contain clusters of magnetite nanoparticles coated with double layer of surfactants (oleic acid or lauric acid) encapsulated into polymeric spheres having hydrodynamic diameters in the range 50-200 nm. The magnetization curve of magnetic microgels dried sample, at room temperature shows superparamagnetic behavior, as expected for magnetite nanoparticles of small sizes (less than 10 nm), stabilized by double layer of surfactant. High magnetization values ( $M_S = 30-40$  emu/g) means that our synthesis procedure favours close packing of surfactated magnetite nanoparticles and allows the encapsulation of a relatively high concentration of magnetite nanoparticles into the polymer spheres.

Support by the European project FP7 No. 229335 MAGPRO<sup>2</sup>LIFE and the Romanian project 83EU/2010 is acknowledged. PhD Fellow A. Taculescu and Dr. C.Coca-Podaru from Lab MF-CFATR Timisoara are thanked for MF/W samples.

[1] D. Bica, L. Vékás, M.V. Avdeev, O. Marinica, V. Socoliuc, M. Balasoiu, V.M. Garamus, *Journal of Magnetism and Magnetic Materials* **311** (2007) 17.



**25 August**

Thursday

11:30-13:00

oral session

25TL-F

25RP-F

25OR-F

**“Magnetophotonics”**

25RP-F-1

## OPTICAL AND MAGNETO-OPTICAL PROPERTIES OF GARNET COMPOSITE FILMS WITH SQUARELY ARRANGED AU PARTICLES

*Uchida H.<sup>1</sup>, Mizutani Y.<sup>2</sup>, Nakai Y.<sup>1</sup>, Fedyanin A.A.<sup>3</sup>, Inoue M.<sup>2</sup>*

<sup>1</sup> Tohoku Institute of Technology, Taihaku, Sendai 982-8577, Japan

<sup>2</sup> Toyohashi University of Technology, Tempaku, Toyohashi 441-8580, Japan

<sup>3</sup> Moscow State University, Moscow 119992, Russia

A bismuth-substituted yttrium iron garnet (Bi:YIG) is a magneto-optical (MO) material for visible and infrared light regions. Original MO effect of the Bi:YIG is not that large, but it is able to be enhanced by localized surface plasmon resonance (LSPR) in a composite film with Au particles. We demonstrated this phenomenon in composite films using randomly arranged Au particles [1]. In this article, we describe optical and magneto-optical properties of composite films with periodically arranged Au particles. Structural effects to Faraday rotation are discussed.

Fig. 1(a) shows squarely arranged Au particles on a quartz substrate: a periodicity of 250 nm and a diameter of 121 nm. On these particles a Bi:YIG film with a thickness of 60 nm was deposited by the RF magnetron sputtering method. Fig. 1(b) shows transmittance spectra of the composite films with periodicities of 250 and 500 nm, respectively. There exist several absorption bands induced by LSPR. The large absorption bands appeared at a wavelength of 730 nm (periodicity: 250 nm) and at 920 nm (periodicity: 500 nm), which are induced by coupled plasmon excited in groups of several Au particles. The largest enhancements of Faraday rotation for the respective composites were obtained at these LSPR wavelengths (fig.1(c)). In addition, small absorption bands in shorter wavelength side are seen; enhanced Faraday rotations are also small, which are induced by single plasmon in individual Au particles. Relationship of the structure and the optical property is discussed.

[1] H. Uchida, Y. Mizutani, Y. Nakai, A. A. Fedyanin and M. Inoue, *J. Phys. D: Appl. Phys.* 44 (2011) 064014.

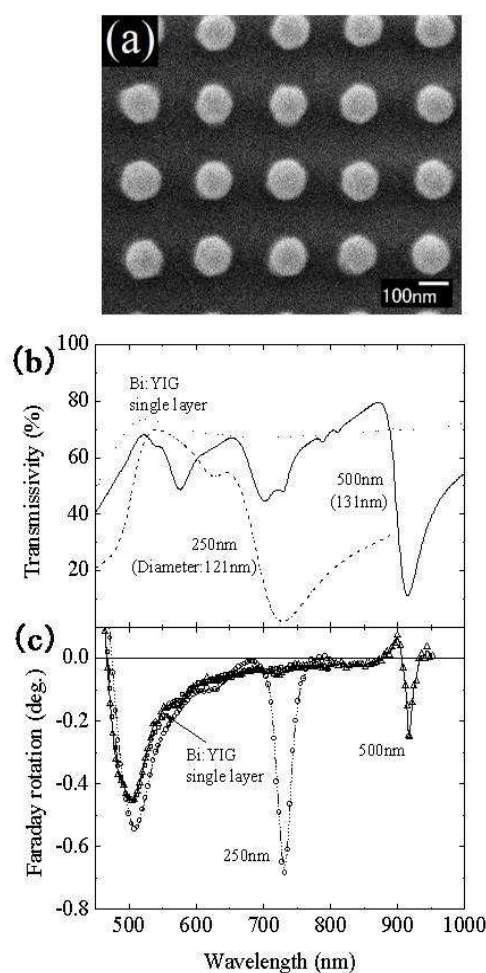


Fig. 1 (a) A SEM image of squarely arranged Au particles with a periodicity of 250 nm. (b) Transmittivity and (c) Faraday rotation spectra of the Bi:YIG composite films. Periodicities and diameters are indicated.

## PLASMONIC EFFECTS IN MAGNETOPHOTONIC CRYSTALS

Grunin A.A.<sup>1</sup>, Chetvertukhin A.V.<sup>1</sup>, Baryshev A.V.<sup>2</sup>, Dolgova T.V.<sup>1</sup>, Uchida H.<sup>3</sup>, Inoue M.<sup>2</sup>,  
Fedyanin A.A.<sup>1</sup>

<sup>1</sup> Faculty of Physics, Lomonosov Moscow State University, Moscow 119991, Russia

<sup>2</sup> Toyohashi University of Technology, Tempaku, Toyohashi 441-8580, Japan

<sup>3</sup> Tohoku Institute of Technology, Taihaku, Sendai 982-8577, Japan

Recent achievements in magnetophotonic crystals (MPCs) [1], which are photonic crystals fabricated from transparent magnetic materials open prospective for their use as magnetophotonic microdevices intended for controlling the magneto-optical response at the micro- and submicroscale. Practical realization of magnetophotonic devices based on MPCs requires magnetic materials with low absorption that ensures considerable photonic band gap effect. In metals, the only possibility to realize the effects analogous to photonic band gap is the excitation of surface plasmon-polaritons (SPPs) in planar periodically nanostructured metal films which are called as plasmonic crystals. Dispersion law of SPPs becomes modified as a function of metal profile and many effects in propagation of SPPs analogous to electromagnetic waves in photonic crystals, such as guiding, spatial localization and anomalous slowing can be observed. SPP-crystals are generally fabricated from noble metals because of large SPP propagation length. In this paper, both approaches of plasmonic and magnetophotonic crystals are combined for realization of a scheme of magneto-optical Kerr effect enhancement utilizing resonant excitation of SPPs in 1D and 2D plasmonic subwavelength nanogratings fabricated entirely from magnetic metal [2]. The use of subwavelength nanostructuring of the nickel film allows the fulfilment of phase-matching conditions for the SPPs excitation and enhancement of longitudinal (LKE) and transversal (TKE) magneto-optical Kerr effects.

Samples of 1D and 2D plasmon-assisted magnetophotonic crystals consist of magnetic nickel film spatially corrugated in one or two directions with the period of 320 nm and 400 nm for 1D and 2D case, respectively. The phase-matching condition between the electromagnetic wave incident on the subwavelength nanograting and the SPP propagating along the sample surface involves the reciprocal vector of 1D or 2D spatial MPC lattice by using the (-1)-st diffraction order. Sharp and angle-dependent resonant drop in specular reflection corresponding to the Wood's anomaly is observed. The drop in reflectivity indicates additional channel for the light energy redistribution associated with the excitation of the SPP mode as the (-1)th diffraction order starts propagating along the sample surface. Angular dependence of this feature is defined by the SPP dispersion relation. Spectral dependences of reflected light polarization rotation and intensity modulation measured in LKE and TKE configurations, respectively, show significant enhancement in the spectral vicinity of the Wood's anomaly. The TKE value is approximately one order of magnitude larger in comparison with the plain nickel film. The TKE spectrum in the vicinity of the SPP resonance has an asymmetrical shape and even changes the sign.

[1] M. Inoue, R. Fujikawa, A. Baryshev, A. Khanikaev, P.B. Lim, H. Uchida, O. Aktsipetrov, A. Fedyanin, T. Murzina, and A. Granovsky, *J. Phys. D*, **39**, (2006) R151.

[2] A.A. Grunin, A.G. Zhdanov, A.A. Ezhov, E.A. Ganshina, A.A. Fedyanin, *Appl. Phys. Lett.*, **97**, (2010) 261908.

25RP-F-3

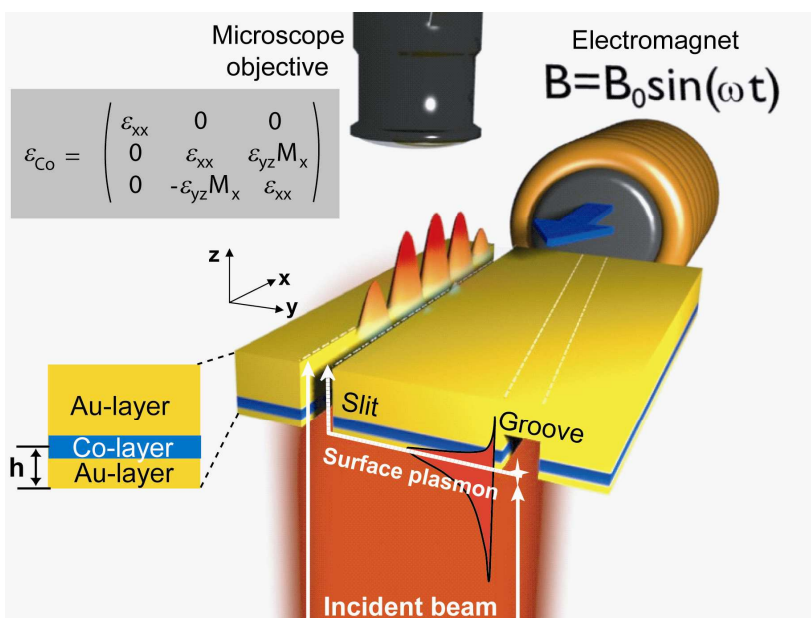
## ACTIVE MAGNETO-PLASMONICS IN HYBRID MULTILAYER STRUCTURES

Temnov V.V.

MIT, 77 Massachusetts Avenue, Cambridge, MA 02139, USA

Nanostructured metal surfaces are presently used to effectively couple light to surface plasmons. This technology is also key to on-chip miniaturization of plasmonic sensors. We present a new plasmonic sensor, based on a tilted slit-groove interferometer, milled into a single noble metal film [1] or into a hybrid metal-ferromagnet-metal structure [2]. Surface plasmons are excited at the groove and propagate towards the slit, where they interfere with incident light (Fig. 1). Due to the tilt angle the optical transmission through the slit shows a pronounced periodic interference pattern. A modulation of the complex surface plasmon wave vector results in a measurable change of the contrast and phase shift of the plasmonic interference pattern [1].

The wave vector of surface plasmons in our hybrid magneto-plasmonic metal-ferromagnet-metal (Au/Co/Au) multilayer structure may be changed by switching in-plane magnetization in cobalt using a weak periodic external magnetic field of the order of a few mT (Fig. 1). The magneto-optical shift of plasmonic interference fringes results into the local transmission changes through the slit. The magneto-plasmonic intensity modulation depth reaches values up to 2% in this geometry. It can be further increased by covering the microinterferometer with high-index dielectric material [3], suggesting an application as a magneto-plasmonic switch. The experiments with different multilayer structures, where the depth  $h$  of a 6nm thin cobalt layer is varied in the range of 8...48 nm allow us to measure the electromagnetic field distribution of surface plasmon and directly measure the skin depth of light [2]. When combined with time-resolved optical pump-probe spectroscopy, our technique allows to monitor ultrafast processes at laser-excited surfaces with femtosecond time resolution [1].



The experiments with different multilayer structures, where the depth  $h$  of a 6nm thin cobalt layer is varied in the range of 8...48 nm allow us to measure the electromagnetic field distribution of surface plasmon and directly measure the skin depth of light [2]. When combined with time-resolved optical pump-probe spectroscopy, our technique allows to monitor ultrafast processes at laser-excited surfaces with femtosecond time resolution [1].

Support by Deutsche Forschungsgemeinschaft and EU Network of Excellence PhOREMOST is acknowledged.

[1] V.V. Temnov et al, *Optics Express* **17**, (2009) 8423.

[2] V.V. Temnov et al., *Nature Photonics* **4**, (2010) 107.

[3] D. Martin-Becerra et al., *Appl. Phys. Lett.* **97**, (2010) 183114.



25OR-F-4

## ENHANCED MAGNETO-OPTICAL EFFECTS IN MAGNETOPLASMONIC CRYSTALS

Belotelov V.I.<sup>1,2</sup>, Akimov I.A.<sup>3</sup>, Pohl M.<sup>3</sup>, Kotov V.A.<sup>1,4</sup>, Vengurlekar A.S.<sup>5</sup>, Gopal A.V.<sup>5</sup>,  
Yakovlev D.<sup>3</sup>, Zvezdin A.K.<sup>1</sup>, Bayer M.<sup>4</sup>

<sup>1</sup> A.M. Prokhorov General Physics Institute RAS, Moscow, 119991, Russia

<sup>2</sup> M.V. Lomonosov Moscow State University, Moscow, 119992, Russia

<sup>3</sup> Dortmund University, Dortmund, 44221, Germany

<sup>4</sup> V.A. Kotelnikov Institute of Radio Engineering and Electronics RAS, Moscow, 125009, Russia

<sup>5</sup> Tata Institute of Fundamental Research, Mumbai, 400005, India

Magneto-optical (MO) materials are of great interest for their use in integrated optical circuits. However, as the MO effects are rather weak, current focus is on enhancement of these effects for device realization.

We have fabricated a new magneto-optical material that consists of a smooth film of iron garnet that is covered by a nanostructured layer of gold, and have shown how the excitation of SPPs in this magnetoplasmonic crystal affects its magneto-optical properties [1]. Numerical

calculations showed that TMOKE parameter  $\delta$  for a bare iron garnet film is very small ( $\delta \sim 10^{-5}$ ). When the film is covered by a smooth gold layer, the TMOKE can be resonantly enhanced up to  $\delta \sim 5 \cdot 10^{-3}$  if the SPP is excited in the Kretschmann configuration, but it can be observed

only in reflection because the transmission almost vanishes. However, when the gold layer is nanostructured, extraordinary optical transmission occurs and value of  $\delta$  can reach  $1.5 \cdot 10^{-2}$ . A unique property of the TMOKE in the transmission geometry is that the effect occurs mainly due to the metal/magnetic dielectric interface and does not depend on the bulk component. We also demonstrate that the TMOKE is highly selective because enhancement only occurs for the resonances related to the excitation of SPPs at the metal/magnetic dielectric interface.

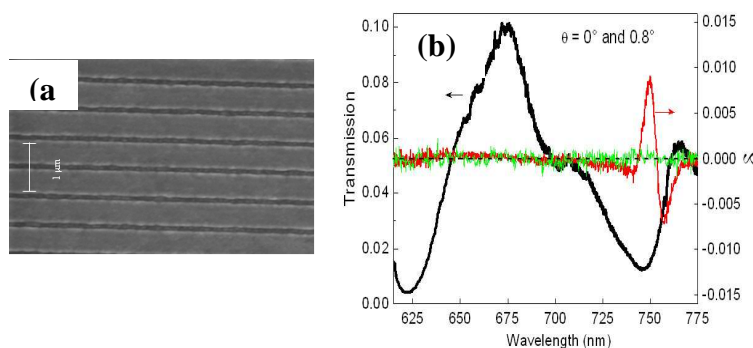


Fig. 1 (a) SEM image of the grating structure. Grating period is 595 nm, gold line width is 484 nm and gold thickness is 120 nm. (b) Transmission MOKE enhancement at non-normal incidence of  $0.8^\circ$  (Red line) along with the transmission spectrum (Black line) and absence of MOKE at normal incidence (Green line).

Support by RFBR and grant of Russia President for young scientists (MK-3123.2011.2) is acknowledged.

[1] V.I. Belotelov, I.A. Akimov, M. Pohl, V.A. Kotov, S. Kasture, A.S. Vengurlekar, A.V. Gopal, D. Yakovlev, A.K. Zvezdin, M. Bayer, *Nature Nanotechnology* **6**, (2011).

25OR-F-5

## FEATURE OF THE OPTICAL TAMM STATE FORMED IN DEGENERATE BAND GAPS

*Merzlikin A.M.<sup>1</sup>, Vinogradov A.P.<sup>1</sup>, Girich A.A.<sup>2</sup>, Tarapov S.I.<sup>2</sup>*

<sup>1</sup> Institute for Theoretical and Applied Electromagnetics of RAS, Moscow 125412, Russia

<sup>2</sup> Institute of Radiophysics and Electronics of NASU, Kharkov, 61085, Ukraine

Almost all applications of photonic crystals are connected with light propagation control. Particularly a lot of attention has been focused on the possibility of managing its transparency or reflection by external means, as for example, by means of a magnetic field.

This communication devoted to investigation of electromagnetic wave propagation and localization into periodic structure made of anisotropic and gyrotropic layers. It is shown that hybrid wave, which is an eigensolution in anisotropic/gyrotropic periodical system, may be described in term of admittance, but contrary to the isotropic case it is tensor quantity.

The possibility to control unpolarized light by use of an external magnetic field is shown. The key feature of this control is the formation of a special type of band gap, namely, the formation of gyrotropic degenerate band gaps [1-4]. These band gaps are formed by the coupling of ordinary and extraordinary Bloch waves upon application of an external magnetic field, which causes the transformation of linearly polarized eigenmodes into circularly polarized ones. These additional BG are formed inside the Brillouin zone, which makes it different from the common ones existing at the boundaries of the Brillouin zones. The main feature of such band gaps is polarization degeneracy of the Bragg reflection, i.e. these BG are simultaneously formed for both polarizations.

It is shown that if the frequency of the Tamm state lies in the degenerated band gap then its structure qualitatively differs from the structure of a well-known Tamm state localized at the interface between two 1D PC made of isotropic materials [5]. As a consequence of anisotropy of hybrid wave admittance to construct such a Tamm state at least three evanescent Bloch waves are demanded. The new condition for Tamm states is deduced.

Support by RFBR (project 10-02-90466) is acknowledged.

[1] A.M. Merzlikin, A.P. Vinogradov, A.V. Dorofeenko, M. Inoue, M. Levy, A.B. Granovsky, *Physica B: Condensed Matter*, **394** (2007) 277.

[2] A.A. Jalali, M. Levy, *Journal of the Optical Society of America B*, **25** (2008) 119.

[3] A.M. Merzlikin, M. Levy, A.A. Jalali, A.P. Vinogradov, *Phys. Rev. B*, **79** (2009) 195103.

[4] F. Wang, A. Lakhtakia, *Applied Phys. Lett.*, **92** (2008) 011115.

[5] Phys. Rev. Lett T. Goto, A.V. Dorofeenko, A.M. Merzlikin, A.V. Baryshev, A.P. Vinogradov, M. Inoue, A.A. Lisyansky, A.B. Granovsky, *Phys. Rev. Lett.*, **101** (2008) 113902.

**25 August**

Thursday

14:30-17:00

oral session

25TL-F

25RP-F

25OR-F

**“Magnetic Oxides”**

25TL-F-6

## SPIN-STATE DEGREE OF FREEDOM AND PHASE INHOMOGENEITY IN CORRELATED ELECTRON SYSTEMS

*Ishihara S.*

Department of Physics, Tohoku University, Sendai 980-8578 Japan

Core Research for Evolutional Science and Technology (CREST), Sendai 980-8578, Japan

Novel electric and magnetic phenomena observed in correlated electron systems are responsible for competition and cooperation between multi-electronic phases with delicate energy balances. In some transition-metal ions, there is the spin-state degree of freedom, i.e. multiple spin states due to the different electronic configurations in a single ion. A prototypical example is the perovskite cobaltites  $R_{1-x}A_x\text{CoO}_3$  (R: rare-earth ion, A: alkaline earth ion) where transitions between the multiple spin states occur by changes of the carrier concentration, temperature and other parameters. In  $\text{Co}^{3+}$  with a  $d^6$  configuration, there are three possible spin states, the high-spin (HS) state with  $S=2$ , the intermediate-spin (IS) state with  $S=1$ , and the low-spin (LS) state with  $S=0$ . The several magnetic, electric and transport measurements have been done in insulating and metallic cobaltites, and report inhomogeneous features. It is widely believed that the observed giant magneto-resistance effect in the lightly doped region results from electronic and magnetic inhomogeneity.

We address the issues of the spin-state transition and the phase separation associated with the spin state degree of freedom by analysing the multi-orbital correlated electron model. I will introduce the following two issues:

(1) The electronic structure in chemical carrier doped system with spin-state degree of freedom is examined [1]. The multi-orbital Hubbard model is analysed by the exact diagonalization method and the variational Monte-Carlo method in finite size clusters. In this model, we introduce two orbitals termed A and B in each site in a crystal. When the electron number per site is two, the lowest two electronic structures are  $|B^2\rangle$  and  $|A^1B^1\rangle$  which correspond to LS and HS, respectively. We find that the electronic phase separation is realized between the non-magnetic band insulator and the HS ferromagnetic metal. The different band widths play an essential role in the present electronic phase separation. Implications for perovskite cobaltites are discussed.

(2) We study the photo-induced spin state change in itinerant correlated electron system, motivated from the pump-probe experiments in perovskite cobaltites [2]. The effective models before and after photon-pumping are derived from the two-orbital Hubbard model and are analysed by the exact diagonalization method. When a photon is introduced in the low-spin band insulator, we found a spin-polarized bound state of photo-excited hole and the high-spin state. This bound state directly reflects the optical pump-probe spectra. These results well explain the recent femto-second spectroscopy experiments in perovskite cobaltites [3].

This work is in collaboration with Y. Kanamori, R. Suzuki, and T. Watanabe in Tohoku University.

[1] R. Suzuki, T. Watanabe and S. Ishihara, *Phys. Rev. B* 80, 054410-1-5 (2009)

[2] Y. Kanamori, H. Matsueda, and S. Ishihara, arXiv:1103.0608.

[3] Y. Okimoto, *et al.* arXiv:1103.1204.

25RP-F-7

## MAGNETIC PROPERTIES OF COBALTITE NANOPARTICLES

*Wisniewski A.<sup>1</sup>, Fita I.<sup>1,2</sup>, Markovich V.<sup>3</sup>, Puzniak R.<sup>1</sup>, Iwanowski P.<sup>1</sup>*

<sup>1</sup> Institute of Physics, Polish Academy of Sciences,  
Aleja Lotnikow 32/46, 02-668 Warsaw, Poland

<sup>2</sup> Donetsk Institute for Physics & Technology, National Academy of Sciences,  
83114 Donetsk, Ukraine

<sup>3</sup> Department of Physics, Ben-Gurion University of the Negev, 84105 Beer-Sheva, Israel

Recently, properties and functionality of cobaltite nanoparticles have attracted a lot of attention. It is primarily due to their particular feature to change the  $\text{Co}^{3+}$  spin state. The spin state of bulk  $\text{LaCoO}_3$  evolves with increasing temperature from the nonmagnetic low-spin (LS) state ( $S = 0$ ) to an intermediate-spin (IS) state ( $S = 1$ ) at  $\approx 100$  K and then to a mixture of IS state and high-spin (HS) state ( $S = 2$ ) above 300 K.

Magnetic properties of  $\text{LaCoO}_3$  and  $\text{La}_{0.8}\text{Ca}_{0.2}\text{CoO}_3$  nanoparticles with particle size ranging from 8 to 50 nm, prepared by the glycine-nitrate method, were investigated in temperature range 5 - 320 K, magnetic field up to 50 kOe and under hydrostatic pressure up to 10 kbar. The x-ray and magnetization measurements for  $\text{LaCoO}_3$  nanoparticles with different size, showed that with increasing the surface-to-volume ratio the lattice parameters expand distinctly due to a surface effect and the ferromagnetic moment increases simultaneously. The observed correlation between FM moment and lattice parameters agrees well with the appearance of FM state in expanded lattice of tensile films, giving support that ferromagnetism of  $\text{LaCoO}_3$  nanoparticles results from the IS state induced by an expansion of the unit-cell and/or an increase of Co-O bond length. On the other hand, an applied hydrostatic pressure suppresses strongly the ferromagnetic phase, leading to its full disappearance at 10 kbar. It was shown that ferromagnetism in  $\text{LaCoO}_3$  is attributed to ferromagnetically coupled IS  $\text{Co}^{3+}$  ions which appear/disappear with expanding/compressing the lattice and/or Co-O bonds. For  $\text{La}_{0.8}\text{Ca}_{0.2}\text{CoO}_3$  nanoparticles, with particle downsizing, a noticeable expansion of unit cell, with concomitant changes in the rhombohedral structure towards the cubic one, was observed. It was found that the increased surface-disorder effect strongly suppresses the ferromagnetic state in  $\text{La}_{0.8}\text{Ca}_{0.2}\text{CoO}_3$  nanoparticles leading to a decrease, by factor of about 2, both in spontaneous magnetization  $M_S$  and Curie temperature  $T_C$ , when particle's size decreases from 23 to 8 nm. The effective magnetic moment was found also to decrease distinctly due to the strong interdependence between Co-O-Co interactions and Co spin state. The size-induced magnetic disorder drives the  $\text{La}_{0.8}\text{Ca}_{0.2}\text{CoO}_3$  nanoparticles to a dominant glassy behavior for 8 nm particles. The applied pressure suppresses  $T_C$ ,  $M_S$ , and coercive field  $H_C$ , like it is observed for bulk  $\text{La}_{0.8}\text{Ca}_{0.2}\text{CoO}_3$ . However, in nanoparticles the pressure effect on  $T_C$  is stronger, while  $H_C$  diminishes with pressure much slower than in bulk material.

## COMPARATIVE STUDY OF HETEROGENEOUS MAGNETIC STATE ABOVE $T_C$ IN $\text{La}_{0.82}\text{Sr}_{0.18}\text{CoO}_3$ COBALTE AND $\text{La}_{0.9}\text{Sr}_{0.1}\text{MnO}_3$ MANGANITE

*Ryzhov V.A.<sup>1</sup>, Lazuta A.V.<sup>1</sup>, Molkanov P.L.<sup>1</sup>, Khavronin V.P.<sup>1</sup>, Kurbakov A.I.<sup>1</sup>, Runov V.V.<sup>1</sup>,  
Mukovskii Ya.M.<sup>2</sup>, Pestun A.E.<sup>2</sup>, Privezentsev R.V.<sup>2</sup>*

<sup>1</sup> Petersburg Nuclear Physics Institute, Orlova Coppice, Gatchina,  
Leningrad obl. 188300, Russia

<sup>2</sup> Moscow State Steel and Alloys Institute, Leninskii prospekt 4, Moscow 119049, Russia

The formation of an inhomogeneous magnetic state at some  $T^*$  above the Curie temperature,  $T_C$ , caused by origination of the ferromagnetic (F) metallic clusters in the paramagnetic matrix of hole doped manganites has been well established [1]. However, a reason for this and properties of the forming state remain the subject of much discussion. We previously revealed such the feature in the doped by different ways  $\text{Nd}_{1-x}\text{Ba}_x\text{MnO}_3$ ,  $\text{La}_{0.88}\text{MnO}_x$  manganites with insulating (I) as well as metallic (M) ground states [2]. The close resemblance of this state properties was found in these compounds that suggests a possible universality of this feature in manganites, exhibiting the F ordering. Study of this state in the doped cobaltites is the topic of the current research activity. We present here the results of studying the clustered state origination in the  $\text{La}_{0.9}\text{Sr}_{0.1}\text{MnO}_3$  (LaSrMn) and  $\text{La}_{0.82}\text{Sr}_{0.18}\text{CoO}_3$  (LaSrCo) single crystals with close values of  $T_C \sim 140$  K to compare the peculiarities of this state in doped cobaltites and manganites. The studies include the data on the transport and magnetic properties (the linear and nonlinear (second and third order) susceptibilities) for both samples as well as an analysis of the crystal structure (neutron diffraction) and small angle polarized neutron scattering (SAPNS) for the powdered cobaltite. The LaSrCo (rhombohedral  $R\bar{3}c$  space group) as well as LaSrMn (orthorhombic  $Pbnm$  space group) reveal the F ground state. The clusters exhibit strong nonlinear properties in a weak field due to their F moment. At measurements of the second harmonic of magnetization  $M_2$  in the parallel steady  $H$  and small  $ac$  magnetic fields this provides a characteristic signal with extremum in  $H \sim 30$  Oe and  $H$ -hysteresis that allows one to control  $T$ -evolution of clustered state. The  $H$ -hysteresis observation in  $M_2(H)$ , due to its symmetry

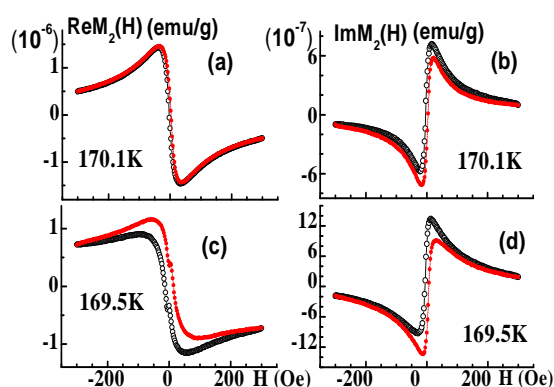


Fig.1.  $\text{Re}M_2$  (panels a, c) and  $\text{Im}M_2$  (panels b, d) for LaSrMn (panels a, b) and LaSrCo (panels c, d) crystals at  $T = 170.1$  K and  $169.5$  K respectively. Solid/open symbols present the  $M_2(H)$  curves at direct/reverse  $H$ -scan.

properties, evidences the F spontaneous moment presence.  $M_2$  and SAPNS data indicate  $T^* \approx 265$  K ( $252$  K)  $> T_C \approx 140$  K in LaSrMn (LaSrCo). Obtained at close  $T > T_C$   $M_2$ -signals (Fig.1) show clearly a presence of the F clusters that arise by the first order manner in both samples. The amplitudes and  $H$ -positions of the  $M_2$  extremes are near that evidences similarity of the F cluster parameters. Their  $T$ -behaviour is also consistent. Some distinctions (they are larger in  $\text{Re}M_2$ ) of signals are due to a difference of cluster dynamic characteristics in these samples and noticeable contribution of a paramagnetic matrix (in critical regime) to  $M_2$  response in LaSrMn. The last is well seen at approaching to  $T_C$ .

Support by the Program of Presidium RAS No 21 (project 4.4.1.8) and RFBR (Grant No 09-02-01509-a) is acknowledged.

[1] E. Dagotto, *New J. of Phys.*, **7** (2005) 67.

[2] В.А. Рыжов и др., *ЖЭТФ*, **94** (2002) 803; V.A. Ryzhov et al., *JMMM*, **300** (2006) e159.

## COLLECTIVE VOLUME PLASMONS IN MATERIALS WITH NANOSCALE PHASE SEPARATION

Sarychev A.K.<sup>1</sup>, Boyarintsev S.O.<sup>1</sup>, Rakhmanov A.L.<sup>1</sup>, Kugel K.I.<sup>1</sup>, Sukhorukov Yu.P.<sup>2</sup>

<sup>1</sup> Institute for Theoretical and Applied Electrodynamics, Russian Academy of Sciences,  
Izhorskaya Str. 13, Moscow, 125412 Russia

<sup>2</sup> Institute of Metal Physics, Ural Branch, Russian Academy of Sciences, S. Kovalevskaya Str. 18,  
Ekaterinburg, 620990 Russia

Nanoscale phase separation, that is, a spontaneous formation of random or ordered inhomogeneities in a chemically homogeneous medium, is a common property of the materials with strongly correlated electrons. Among a vast number of these materials, there are such important systems as high- $T_c$  superconductors and magnetic oxides with colossal magnetoresistance. The phase-separated materials can be considered as natural metamaterials since the spatial scale of inhomogeneities is less than the wavelength  $\lambda$  of the incident electromagnetic wave. Among important phenomena found here, we could mention a wide peak in reflection  $R$ , transmission  $T$ , and absorption  $A$  in the infrared range [1,2,3] and the enhancement of Raman scattering in the same wavelength range [4]. These phenomena observed in single crystals and high-quality films are temperature dependent and can be attributed to inhomogeneous structure of the studied samples.

We show that the phase separation can provoke such exciting optical phenomena as anomalous absorption, giant field fluctuations, and orders of magnitude enhanced Raman scattering. We study here a 3D metal-insulator nanocomposite. Such a system is usually described in terms of the effective media theory (EMT). However, the EMT is (i) an uncontrollable approach and (ii) it cannot be used for the analysis of a local field distribution in inhomogeneous media. In this paper, we use computer simulations of the nanocomposite. We compute the local electric field distribution,  $E(\mathbf{r})$ , and find specific excitations, giant fluctuations of  $E(\mathbf{r})$  in a characteristic volume including a number of metallic droplets, as it is seen from Fig. 1. The giant fluctuations are of special importance for the description of optical effects sensitive to the local field, like the Raman scattering, optical nonlinearities, etc. We name these excitations collective volume plasmons (CVP). We also compute the dependence of the averaged system permittivity  $\epsilon$  on frequency  $\omega$  and content of the metallic phase  $p$ , and calculate reflection and absorption coefficients of the system. We predict peaks in  $R(\omega)$  and  $A(\omega)$  within a wide range of metal content  $p$  in agreement with experimental results obtained for  $\text{La}_{0.7}\text{Ca}_{0.3}\text{MnO}_3$  manganite single crystals and high-quality thin films in the infrared spectral range [5].

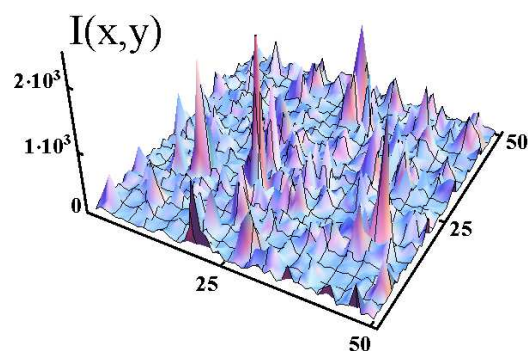


Fig. 3 Intensity of the local electric field  $I=|E(x,y,z)/E_0|^2$  at a fixed value of  $z$ ;  $\lambda = 5\mu\text{m}$

- [1] Ch. Hartinger *et al.*, *Phys. Rev. B* **73** (2006) 024408.
- [2] A. Rusydi *et al.*, *Phys. Rev. B*, **78** (2008) 125110.
- [3] P. Gao *et al.*, *Phys. Rev. B*, **78** (2008) 220404.
- [4] M. Seikh *et al.*, *Pramana – J. Phys.*, **64** (2005) 119.
- [5] A.B. Granovsky, Yu.P. Sukhorukov, *et al.*, *Zh. Eksp. Teor. Fiz.* **139** (2011) 90 [*JETP* **112** (2011) 77].





**25 August**

Thursday

11:30-13:00

14:30-17:00

oral session

25TL-G

25RP-G

25OR-G

**“Magnetism and  
Superconductivity”**

25TL-G-1

## NANOSCALE STRUCTURES AND GIANT NERNST EFFECT BELOW THE PSEUDOGAP IN HIGH- $T_c$ SUPERCONDUCTORS

Saarela M.<sup>1</sup>, Kusmartsev F.V.<sup>2</sup>

<sup>1</sup> Department of Physics, University of Oulu, P.O.Box 3000, FIN-90014 Oulu, Finland

<sup>2</sup> Department of Physics, Loughborough University, Loughborough LE11 3TU, UK

Observations of a large Nernst signal in an extended region above the critical temperature  $T_c$  in hole-doped cuprates provides an accurate tool to study fluctuations in the pseudogap region. We show that the nanoscale structures in these layered superconductors may be caused by localized negative charges, which can collect a cluster of charge carriers around them. Our results support the scenario that superfluidity vanishes because long-range phase coherence is destroyed by a charge density wave instability induced by localized charges and the over-screening of the long-ranged part of the Coulomb interaction, which is enhanced due to decreasing charge carrier density [1]. When the carrier density is low enough localized charges begin to trap particles and form bound states of clusters of charge carriers, which we call Coulomb bubbles. These bubbles are embedded inside the superconductor and form nuclei of the new insulating state. The growth of a bubble is terminated by the Coulomb force and each of them has a quantized charge and a fluctuating phase. When clusters first appear they are covered by superfluid liquid due to the proximity effect and invisible. However, when the charge carrier density decreases the size of bubbles increases and the superconducting proximity inside them vanishes. The insulating state arises via a percolation of these insulating islands, which form a giant percolating cluster that prevents the flow of the electrical supercurrent through the system. We present an effective Hamiltonian, which takes into account the Jahn–Teller distortion of the apical oxygen and provides two bands, the band of charge carriers and the localized impurity band causing the clustering. Our results are consistent with the two-component picture for cuprates deduced earlier by Gorkov and Teitelbaum [2] from the analysis of the Hall effect data and ARPES spectra. The Coulomb clusters are also observed in Scanning Tunneling Microscope (STM) experiments [3] and are responsible for the pseudogap [4].

[1] F. Kusmartsev, M. Saarela, *Supercond. Sci. Technol.* **22** (2009) 014008.

[2] L.P. Gorkov, G.B. Teitelbaum, *Phys. Rev. Lett.* **97** (2009) 247003 (2009).

[3] Y. Kohsaka et al., *Nature* **454**, 1072 (2008).

[4] T. Kondo et al., *Nature* **457** (2009) 376.

25TL-G-2

## RENORMALIZED MEAN FIELD APPROACH TO HIGH-TEMPERATURE SUPERCONDUCTIVITY: COMPARISON TO EXPERIMENT

*Spalek J.<sup>1,2</sup>, Jedrak J.<sup>1</sup>*

<sup>1</sup> Institute of Physics, Jagiellonian University, Reymonta 4, 30-059 Krakow, Poland

<sup>2</sup> Faculty of Physics and Applied Computer Science, AGH, 30-59 Krakow, Poland

High-temperature superconductivity in the cuprate oxides is analyzed using the method developed recently in our group, the so-called statistically consistent Gutzwiller-Fukushima method for the extended  $t$ - $J$  model [1]. The following results are compared directly with experiment:

- (i) the upper critical concentration for the disappearance of superconductivity;
- (ii) the doping dependence of the superconducting quasi-particle energy in the antinodal direction; and
- (iii) the Fermi velocity as a function of doping.

The results agree (semi)quantitatively with the data at the optimal doping and in the overdoped regime. The conclusion we draw is that the  $t$ - $J$  model in the newly devised mean-field version reflects the overall features of the high-temperature superconductors, at least in the unconventional-Fermi-liquid regime. Full analysis requires inclusion of antiferromagnetism, as well as the treatment of the pseudogap appearance. We discuss briefly those issues and in particular, the magnetism induced localization within the model. It should be stressed that the results compare favourably with the best variational quantum Monte Carlo results, whenever the detailed comparison of the two methods is applicable. We discuss also briefly at the beginning the application of  $t$ - $J$  model to the superconductivity in strongly correlated systems in a historical prospective, as it involves directly the spin-singlet pairing induced by the kinetic exchange interactions, a purely magnetic, real-space mechanism.

Support Ministry of Science and Higher Education and of The Foundation for Polish Science (FNP) through the project TEAM is gratefully acknowledged.

[1] J. Jedrak and J. Spalek, *Phys. Rev. B* **83** (2011) 104512; *ibid.* **81** (2010) 073108.

25RP-G-3

## METALLIC CONTAMINANT DETECTION SYSTEM USING MULTI-CHANNEL HIGHT $T_c$ SQUIDS

*Tanaka S.<sup>1</sup>, Kitamura Y.<sup>1</sup>, Hatsukade Y.<sup>1</sup>, Ohtani T.<sup>2</sup>, Suzuk S.<sup>2</sup>*

<sup>1</sup> Toyohashi University of Technology, 1-1 Hibarigaoka Tempaku-cho Toyohashi, Aichi 441-8580 Japan

<sup>2</sup> Advance Food Technology Co., Ltd., 333-9 Hamaike Nishimiyuki-cho Toyohashi, Aichi 441-8113, Japan

We have developed the magnetic metallic contaminant detectors using multiple high  $T_c$  SQUID gradiometers for industrial products. Finding ultra-small metallic contaminants is a big issue for manufacturers producing commercial products. The quality of industrial products such as lithium

ion batteries can be deteriorated by the inclusion of tiny metallic contaminants. When the contamination does occur, the manufacturer of the product suffers a great loss to recall the tainted products. Outer dimension of metallic particles less than 50 micron can not be detected by a conventional X-ray imaging. Therefore a high sensitive detection system for small foreign matters is required. However most of the case, the matrix of an active material coated sheet electrode is magnetized and the magnetic signal from the matrix is large enough to mask the signal from contaminants. Thus we have developed a detection system based on a SQUID gradiometer and a horizontal magnetization to date. For practical use, we should increase the detection width of the system by employing multiple sensors. In this paper, we present the eight channel high-T<sub>c</sub> SQUID gradiometer system for inspection of sheet electrodes of a lithium ion battery with width of at least 60 mm to 70 mm. Eight SQUID gradiometers were mounted with separation of 9.0 mm. As a result, small iron particles of about 50 micron in a sheet were successfully measured. This result suggests the system is the promising tool for the detection of contaminants in a lithium ion battery.

This work was supported in part by Knowledge Cluster Initiative from Ministry of Education, Culture, Sports, Science and Technology.

- [1] S. Tanaka, H. Fujita, Y. Hatsukade, T. Nagaishi, K. Nishi, H. Ota, T. Otani, and S. Suzuki, "A food contaminant detection system based on high-T<sub>c</sub> SQUIDs," *Supercond. Sci. Technol.*, vol. 19, pp. S280-S283, March, 2006.
- [2] H. J. Krause, G. I. Panaitov, N. Wolter, D. Lomparski, W. Zander, Y. Zhang, E. Oberdoerffer, D. Wollersheim, and W. Wilke, "Detection of Magnetic Contaminations in Industrial Products Using HTS SQUIDs," *IEEE Trans. on Appl. Supercond.*, vol. 15, pp. 729-732, June, 2005.
- [3] M. Bick, P. Sullivan, D. L. Tilbrook, J. Du, B. Thorn, R. Binks, C. Sharman, K. E. Leslie, A. Hinsch, K. Macrae, and C. P. Foley, "A SQUID-based metal detector: comparison to coil and X-ray systems," *Supercond. Sci. Technol.*, vol. 18, pp. 346-351, March, 2005.
- [4] S. Tanaka, H. Fujita, Y. Hatsukade, T. Otani, S. Suzuki, and T. Nagaishi, "A High T<sub>c</sub> SQUID Micro-detector with a high performance magnetic shield for industrial products," *Supercond. Sci. Technol.*, vol. 20, pp. S385-S388, March, 2007.
- [5] S. Tanaka, T. Akai, Y. Hatsukade, T. Ohtani, Y. Ikeda, S. Suzuki, and H. A. K. Tanabe, "High T<sub>c</sub> SQUID Detection System for Metallic Contaminant in Lithium Ion Battery," *IEEE Trans. Magn.*, vol. 45, pp. 4510-4513, October, 2009.

25OR-G-4

**SPIN DEPENDENT SUPERCONDUCTING TRANSPORT  
IN HYBRID OXIDE HETEROSTRUCTURE  
WITH SUPERCONDUCTING/MAGNETIC INTERFACE**

*Ovsyannikov G.A.<sup>1,2</sup>, Constantinian K.Y.<sup>1</sup>, Shadrin A.V.<sup>1,2</sup>, Kislinski Y.V.<sup>1</sup>, Zaitsev A.V.<sup>1</sup>*

<sup>1</sup> Kotel'nikov Institute of Radio Engineering and Electronics,  
Russian Academy of Sciences, 125009, Moscow, Russia

<sup>2</sup> Department of Microtechnology and Nanoscience, Chalmers University of Technology,  
S41296, Gothenburg, Sweden

Here we report on the experimental studies of the dc and rf current transport in across the oxide superconductor/magnetic interfaces in hybrid thin film S-N-M-D Mesa HeteroStructures (MHS) of Nb/Au/M/YBa<sub>2</sub>Cu<sub>3</sub>O<sub>7-δ</sub> with areas from 10×10 up to 50×50 μm<sup>2</sup>. Here Nb is a conventional *s*-wave superconductor (S), YBa<sub>2</sub>Cu<sub>3</sub>O<sub>7-δ</sub> (YBCO) is an oxide superconductor (S<sub>d</sub>) with dominant *d*-wave order parameter, Au is the normal metal (N), and M is magneto-active interlayer or Ca<sub>1-x</sub>Sr<sub>x</sub>CuO<sub>2</sub> (CSCO) that is a quasi-two dimensional Heisenberg antiferromagnetic cuprate[1,2] or La<sub>1-y</sub>Ca<sub>y</sub>MnO<sub>3</sub> that is a the mixed-valence manganite exhibiting both antiferromagnetism or ferromagnetism depending on Ca doping (y value). Since epitaxial growth of oxide films the sharp interface between superconducting and magneto-active thin film is realized. The critical current density of MHS exponentially decrease with the thickness d<sub>s</sub> of CSCO interlayer while characteristic resistance increase. Finally the critical current is observed in MHS with CSCO interlayer up to d<sub>s</sub>=50 nm. Experimental data well correspond to the theoretical model of two superconductor separate by several (upto 20) magnitoractive layers with antiferromagnetic ordering. The MHS are found to have higher sensitivity to an applied magnetic field then conventional Josepson junction due to controlling of critical current by the canting of layer magnetization. We have no observed critical current in MHS with LSMO interlay for d<sub>s</sub>=5 nm.

Support by the Russian Academy of Sciences, Russian Foundation of Basic Research (11-02-01234-a), Scientific school grant 5423.2010.2, Ministry of Education and Science of Russian Federation, contract 02.740.11.0795.

[1] P. Komissinskiy, G.A. Ovsyannikov, I.V. Borisenko et al., Phys. Rev. Lett.. **99** (2007) 017004.

[2] G.A. Ovsyannikov, K.Y. Constantinian, Yu.V. Kislinski, et al. Superconductor Science and Technology **24** (2011) 055012.

25TL-G-5

## THE ORDER PARAMETER OF IRON PNICTIDES REVEALED BY THE SPECIFIC HEAT

Hsieh Y.S.<sup>1</sup>, Lin J.-Y.<sup>1</sup>, Yang H.D.<sup>2</sup>, Chareev D.<sup>3</sup>, Vasiliev A.N.<sup>4</sup>

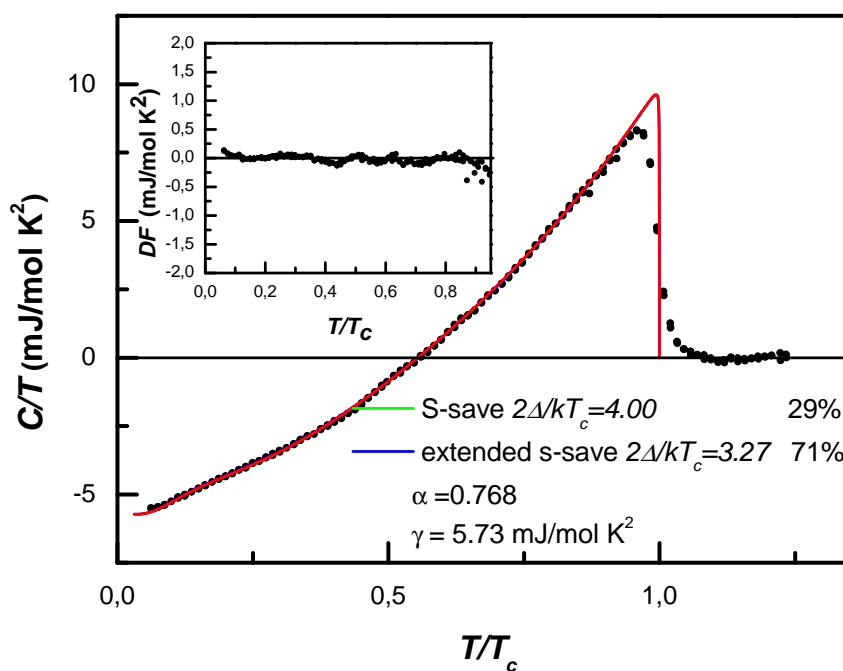
<sup>1</sup> Institute of Physics, National Chiao Tung University, Hsinchu 30010, Taiwan

<sup>2</sup> Department of Physics, National Sun Yat-Sen University, Kaohsiung 804, Taiwan

<sup>3</sup> Institute of Experimental Mineralogy, Chernogolovka, Moscow Region 142432, Russia

<sup>4</sup> Department of Low-Temperature physics, Moscow State University, Moscow 119991 Russia

We have measured the low-temperature specific heat of FeSe single crystals with in-plane or out-of-plane magnetic fields. The symmetry of the order parameter and the mixed state will be discussed for both compounds. The zero field specific heat can be well fit in to a two-gap model with an isotropic *s*-wave and an extended *s*-wave, consistent with the very recent theoretical calculations. The mixed state data further confirm the existence of an isotropic and a very anisotropic order parameter.



25TL-G-6

**MAGNETIC PROPERTIES OF NOVEL FeSe(Te) SUPERCONDUCTORS**

*Grechnev G.E.<sup>1</sup>, Panfilov A.S.<sup>1</sup>, Fedorchenko A.V.<sup>1</sup>, Desnenko V.A.<sup>1</sup>, Gnatchenko S.L.<sup>1</sup>,  
Tsurkan V.<sup>2,3</sup>, Deisenhofer J.<sup>2</sup>, Loidl A.<sup>2</sup>, Chareev D.<sup>4</sup>, Volkova O.S.<sup>5</sup>, Vasiliev A.N.<sup>5</sup>*

<sup>1</sup> B.Verkin Institute for Low Temperature Physics and Engineering,

National Academy of Sciences of Ukraine, 47 Lenin Ave., Kharkov 61013, Ukraine

<sup>2</sup> Experimental Physics 5, Center for Electronic Correlations and Magnetism,

Institute of Physics University of Augsburg, Augsburg 86159, Germany

<sup>3</sup> Institute of Applied Physics, Academy of Sciences of Moldova, Chisinau MD 2028, Moldova

<sup>4</sup> Institute of Experimental Mineralogy, Russian Academy of Sciences, Chernogolovka,  
Moscow District 142432, Russia

<sup>5</sup> Moscow State University, Physics Department, Moscow 119991, Russia

Magnetization studies for FeSe<sub>1-x</sub>Te<sub>x</sub> systems (0<x<1) were carried out in magnetic fields up to 50 kOe and in the temperature range 2-300 K. In these systems the superconducting transitions were observed in the range from 8 K to 14.2 K at ambient pressure. For the most samples, a nonlinear behavior of the magnetization curves in the normal state gives evidence of a commonly observed presence of ferromagnetic impurities in the studied compounds. By taking these impurity effects into account, the intrinsic magnetic susceptibility  $\chi$  was estimated to increase gradually with Te content. At ambient pressure, a drastic drop in  $\chi(T)$  with decreasing temperature was observed in FeTe at  $T_N=70$  K, which appears to be closely related to the antiferromagnetic ordering.

Also, magnetic susceptibility  $\chi$  of FeSe<sub>1-x</sub>Te<sub>x</sub> systems was studied under pressures at fixed temperatures of 55, 78 and 300 K. These measurements were performed both for polycrystalline and single crystalline samples. The obtained results have revealed a puzzling growth of susceptibility under pressure for tellurium-rich compositions, and this effect is enhanced with lowering of temperature. This strong positive pressure effect on  $\chi$  does not depend qualitatively on the magnetic state of the sample. The estimated spontaneous change in volume of FeTe at the antiferromagnetic ordering is shown to be large enough and presumably hidden from direct detection because of the close interplay of the antiferromagnetic and structural phase transitions.

To shed light on the observed magnetic properties of FeSe<sub>1-x</sub>Te<sub>x</sub> and the pressure effects in  $\chi$ , the *ab initio* calculations of the volume dependent band structure and the exchange enhanced paramagnetic susceptibility were performed for these systems within the local spin density approximation. It is found that FeSe<sub>1-x</sub>Te<sub>x</sub> systems are close to magnetic instability with dominating enhanced spin paramagnetism. The calculated values of the density of states at the Fermi level and paramagnetic susceptibility exhibit the strong dependence on the structural parameters, such as unit cell volume  $V$  and especially the height  $Z$  of chalcogen species from the Fe plane. With appropriate values of these parameters the reasonable agreement between calculated and experimental values of  $\chi$  at ambient pressure could be obtained. In the course of the calculations, the puzzling experimental pressure effect on  $\chi$  can be explained in terms of the pressure dependence of  $V$  and  $Z$ , the latter determining the dominant positive contribution.

This work has been supported by the Russian-Ukrainian RFBR-NASU project 43-02-10 and 10-02-90409.

25TL-G-7

## INTERPLAY BETWEEN MAGNETIC AND SUPERCONDUCTOR ORDER IN NON-STOICHIOMETRIC Pnictide

*Kikoin K.*

Tel-Aviv University, Lebanon str., 69978, Tel-Aviv, Tel-Aviv

It is shown that As vacancies in LaFeAsO superconductor pnictide induce strong enhancement of paramagnetic response both in normal and superconducting state. Although As vacancies themselves are non-magnetic defects, they are able to form localized magnetic moments due to strong covalent bonding with neighboring Fe ions. The microscopic theory of magnetic moment formation in semi-metallic state of non-stoichiometric LaFeAsO is constructed in a framework of appropriately modified Anderson-Wolf's model. Experimental manifestations of enhanced paramagnetism and the influence of magnetic fluctuations on superconductor pairing are also discussed.

25RP-G-8

## RADIATIVE DARK-BRIGHT INSTABILITY AND THE CRITICAL CASIMIR EFFECT IN DQW EXCITON CONDENSATES

*Hakioffglu T.<sup>1,2</sup>*

<sup>1</sup> Department of Physics, Bilkent University, 06800 Ankara, Turkey

<sup>2</sup> Institute of Theoretical and Applied Physics, 48740 Turunffc, Muffgla, Turkey

It is already well known that the radiative interband interaction in the excitonic normal liquid in semiconducting double quantum wells is responsible for a negligible splitting between the energies of the dark and bright excitons enabling to consider a four fold spin degeneracy. This also lead many workers to naively consider the same degeneracy in studying the condensate. On the other hand, the non-perturbative aspects of this interaction in the condensed phase, e.g. its consequences on the order parameter and the dark-bright mixture in the ground state have not been explored. In this work, we demonstrate that the ground state concentrations of the dark and the bright exciton condensates are dramatically different beyond a sharp interband coupling threshold where the contribution of the bright component in the ground state vanishes [1,2]. This shows that the effect of the radiative interband interaction on the condensate is nonperturbative. We also observe in the free energy, a discontinuous derivative with respect to the layer separation at the entrance to the condensed phase, indicating a strong critical Casimir force [3]. An estimate of its strength shows that it is measurable. Measuring the Casimir force is challenging, but at the same time it has a conclusive power about the presence of the long-sought condensed phase.

[1] T. Hakioffglu and Mehmet Sffahin, Phys. Rev. Lett. 98, 166405 (2007).

[2] M.A. Can and T. Hakioffglu, Phys. Rev. Lett. 103, 086404 (2009).

[3] T. Hakioffglu and Ege Özgün, Sol. State Comm. to appear.



25RP-G-9

## THEORY OF MAGNETISM IN IRON PnictIDES AND SELENIDES

Antropov V.P.<sup>1</sup>, Belashchenko K.D.<sup>2</sup>, van Schilfgaard M.<sup>3</sup>, Ke L.<sup>1</sup>

<sup>1</sup> Ames Laboratory, Ames, IA, USA

<sup>2</sup> Nebraska State University, Lincoln, NE, USA

<sup>3</sup> Arizona State University, Tempe, AZ, USA

A formation of magnetic phases and magnetic interactions in iron pnictides and selenides are studied using electronic structure calculations and model analysis. The construction of the generic spin Hamiltonian in  $\text{CaFe}_2\text{As}_2$  is discussed. We show that introduction of strong biquadratic exchange provides an alternative and more natural explanation of the neutron scattering experiments and produce symmetry-respecting spin Hamiltonian [1]. A nature of biquadratic term is discussed in details. The analysis of thermal properties with the proposed Hamiltonian produces a reasonable value of the Neel temperature and shows the appearance of first order transition of pure magnetic origin. We claim that such 3D model of spin interactions with biquadratic term included should be considered as most appropriate model of magnetic interactions in iron pnictides.

Using linear-response density-functional theory, magnetic excitations in the striped phase of  $\text{CaFe}_2\text{As}_2$  are studied as a function of local moment amplitude [2]. We find a new kind of excitation: sharp resonances of Stoner-like (itinerant) excitations at energies comparable to the Néel temperature, originating largely from a narrow band of Fe d states near the Fermi level, and coexist with more conventional (localized) spin waves. Both kinds of excitations can show multiple branches, highlighting the inadequacy of a description based on a localized spin model. Consequences for the spin fluctuations related superconductivity are discussed.

[1] A. L. Wysocki, K. D. Belashchenko, V. P. Antropov. *Nature Physics* (6 March 2011) doi:10.1038/nphys1933.

[2] L. Ke, M. van Schilfgaard, J. Pulikkotil, T. Kotani, and V. P. Antropov. *Phys. Rev. B* **83**, (2011) 060404

25OR-G-10

## STUDIES OF $\text{EuRh}_3\text{B}_2$ AND $\text{EuRh}_4\text{B}_4$ COMPOUNDS SYNTHESIZED UNDER HIGH PRESSURE AND TEMPERATURE

Smekhova A.<sup>1,3</sup>, Fomicheva L.<sup>2</sup>, Tsvyashchenko A.<sup>2</sup>, Sidorov V.<sup>2</sup>, Wilhelm F.<sup>3</sup>, Rogalev A.<sup>3</sup>

<sup>1</sup> M.V.Lomonosov Moscow State University, Moscow, Russia

<sup>2</sup> Vereshchagin Institute for High Pressure Physics RAS, Troitsk, Russia

<sup>3</sup> European Synchrotron Radiation Facility, Grenoble, France

In this report we present the results of a thorough study of  $\text{EuRh}_3\text{B}_2$  and  $\text{EuRh}_4\text{B}_4$  compounds that have been synthesized by a non-common method under high pressure – temperature conditions for the first time.  $\text{EuRh}_3\text{B}_2$  system attracts a lot of attention since the origin of its magnetic response remains unclear [1];  $\text{EuRh}_4\text{B}_4$  compound is interesting because of possible coexistence of magnetic and superconducting states at low temperatures [2].

Synthesized samples have been characterized structurally and magnetically by X-ray diffraction, macroscopic electrical resistivity, ac-susceptibility and SQUID measurements as well as element-

and shell-selective X-ray absorption spectroscopy (XANES) and X-ray magnetic circular dichroism (XMCD) techniques.

Macroscopic measurements have shown the presence of the ferromagnetic phase in both systems below 83 K. The superconducting phase in the  $\text{EuRh}_4\text{B}_4$  system was found by the electrical-resistivity method below 5.8 K.

Element-selective XANES and XMCD measurements at the Eu  $L_{2,3}$  absorption edges have shown the presence of the two valence states of Eu ions in both compounds: the magnetic  $\text{Eu}^{2+}$  ions with a paramagnetic behavior and the “non-magnetic”  $\text{Eu}^{3+}$  one (see Fig.1). A double structure of the XANES white line has been found at the Rh  $L_{2,3}$  absorption edges for both samples, but with a different energy splitting. XMCD signal at the rhodium  $L_{2,3}$  edges has demonstrated a sizable induced magnetic polarization of Rh 4d states.

Aforementioned studies allow to conclude that ferromagnetism of the  $\text{EuRh}_3\text{B}_2$  sample has not pure itinerant nature and originates from localized magnetic moments of  $\text{Eu}^{2+}$  ions and Rh atoms; and that magnetic  $\text{Eu}^{2+}$  ions in  $\text{EuRh}_4\text{B}_4$  compound do not suppress superconductivity.

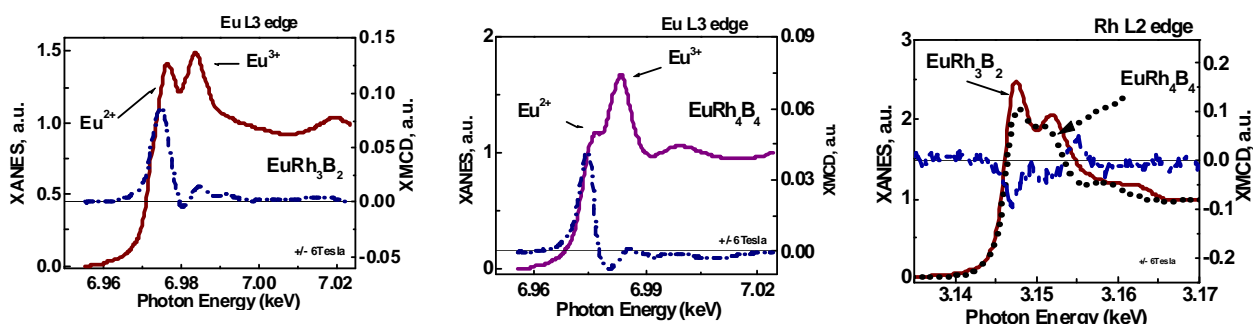


Fig. 1. XANES (left scale) and XMCD (right scale) spectra of  $\text{EuRh}_3\text{B}_2$  (left panel) and  $\text{EuRh}_4\text{B}_4$  (central panel) recorded at the Eu  $L_3$  absorption edge and at the Rh  $L_2$  absorption edge (right panel). At the right panel the XMCD spectra have shown only for the  $\text{EuRh}_3\text{B}_2$  sample. All spectra have been measured at low temperature and with an external magnetic field up to  $\pm 6$  Tesla.

- [1] S.K. Malik, R.Vijayaraghavan, W.E. Wallace, et al., *J. Magn. Magn. Mater.*, **37** (1983) 303.  
 [2] I. Felner, I. Nowik, *Phys. Rev. Lett.*, **45** (1980) 2128.

25OR-G-11

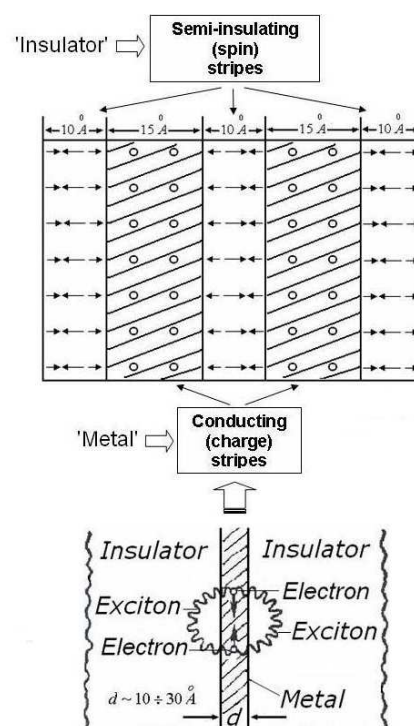
## HTSC DUE TO GINZBURG SANDWICH FORMED NATURALLY BY MAGNETISM IN LAYERS OF COPPER OXIDES AND IRON PNICTIDES

*Mazov L.S.*

Institute for Physics of Microstructures, Russian Academy of Science, Nizhny Novgorod, Russia

As known, below the Neel temperature  $T_N$ , in the insulating (semi-metallic), basal planes of undoped copper oxides (iron pnictides), the uniform (striped), antiferromagnetic (AF) ordering arises, because of commensurate in character magnetic (AF SDW) phase transition, with total (copper oxides) or partial (iron pnictides) dielectrization of electron energy spectra. The feature of these AF-ordered basal planes is a presence of low-energy ( $< 3$  eV) charge-transfer (CT) excitons, corresponding to interband CT-transition in  $\text{CuO}_2$  (or FeAs) plane with excitonic peak in near-IR range of in-plane optical absorption spectrum (OAS). Since in result two atomic sites involved appear to be spinless then CT-excitons move through the lattice in this plane coherently, without

disturbance of its AF spin background [1]. In doped copper oxides (iron pnictides), as it was demonstrated by us before [1], superconducting transition is preceded by magnetic (AF SDW) phase transition in the pseudogap regime ( $T_{\bar{n}} < T < T_{SDW}^{onset} \approx T^* < T_N$ ), due to partial dielectrization of electron energy spectrum [1,2]. Because of incommensurability of the SDW state with the lattice period, it generates the CDW with one-half wavelength  $\lambda_{CDW} = \lambda_{SDW} / 2$ , and hence the wave of lattice distortions. So-formed SDW/CDW state in basal planes results in a sequence of alternating, semi-insulating, AF-ordered spin (S) and conducting, charge (C) stripes (upper panel in Figure). The S-stripes provide above CT-excitonic peak in OAS up to metallic level of doping [1,3]. The picture obtained is reminiscent that for Ginzburg sandwich (GS): insulator-metal-insulator (I/M/I) (lower panel in Figure) [2]: excitons with characteristic energy essentially higher than Debye one, propagating in GS outer plates, provide high-temperature Cooper pairing of conduction electrons in the GS metallic spacer. The parameters of C- and S-stripes in copper oxides (iron pnictides) are exactly within the optimal range of parameters for GS (see Table). Such a picture is a first, clear evidence for a Little-Ginzburg exciton mechanism of HTSC in these compounds, with in-plane GS-scenario [1-3], when I/M/I-structure is naturally formed by magnetism. Moreover, similar compounds with higher energy of CT-excitons in AF-ordered layers are promising for room- $T_c$  superconductivity.



Parameter	Theory	Experiment (cuprates)
$d$ (nm)	1-3	1.5
$n$ ( $\text{cm}^{-3}$ )	$10^{18} - 10^{23}$	$10^{21} - 5 \cdot 10^{22}$
Exciton energy (eV)	0.3 - 3	1.5
Exciton band width (eV)	0.1 - 0.3	< 0.5

- [1] L.S.Mazov, *J.Supercond.Nov.Magn.*, **20** (2007) 579; [arXiv.org/abs: 0805.4097](https://arxiv.org/abs/0805.4097); [0911.4089](https://arxiv.org/abs/0911.4089).  
 [2] *Problem of HTSC* (Edited by V.L.Ginzburg and D.A.Kirzhnits, Moscow, Nauka Pr., 1977).  
 [3] L.S.Mazov, in: *Proc. of 2<sup>nd</sup> Int. Conf. "Applied Superconductivity -2011"* (to centenary of discovery of superconductivity), 4 March 2011, Moscow, Russia; CD-ROM: BPSC-3.4, 3 pp.



**25 August** Thursday

11:30-13:00

oral session  
25OR-H

**“Multiferroics”**

25OR-H-1

### **ELECTRIC-FIELD EFFECTS IN MULTIFERROIC BiFeO<sub>3</sub>: BASIC PROPERTIES AND NOVEL ELECTRONIC DEVICES**

*Kiryukhin V.<sup>1</sup>, Lee S.<sup>1</sup>, Choi T.<sup>1</sup>, Choi Y.J.<sup>1</sup>, Ramazanoglu M.<sup>1</sup>, Ratcliff W.<sup>2</sup>, Cheong S.-W.<sup>1</sup>*

<sup>1</sup> Physics Department, Rutgers University, Piscataway, NJ 08854, USA

<sup>2</sup> NCNR, National Institute of Standards and Technology, Gaithersburg, MD 20899, USA

BiFeO<sub>3</sub> (BFO) is a room-temperature multiferroic combining large electric polarization (P) and long-wavelength spiral magnetic order. Significant efforts have been devoted to studies of thin-film BFO model multiferroic devices, and local control of magnetization by an electric field has been demonstrated recently. However, the extant thin films typically consist of a poorly controlled patchwork of ferroelastic domains severely impeding experimental work. We report growth of mm-sized single crystals consisting of a single ferroelectric (FE) domain. Switching between two (out of 8) unique directions of P by an electric field is demonstrated. Magnetic moments are strongly coupled to the lattice, and rotate together with P when the field is applied. Electric field can be used to control the populations of the 3 equivalent magnetic domains with different directions of the spiral wave vector in FE single-domain samples. In particular, a FE monodomain sample with a single-wave-vector magnetic spiral can be prepared. The spiral has the same helicity in the entire sample. All these effects are reversible. Thus, electric field can be used to control the ferroelectric and magnetic states, and even the magnetic helicity of the sample.[1,2] This level of control makes possible realization of model electronic devices based on single crystals of BFO. We report demonstration of a novel diode device whose forward direction can be switched reversibly by an electric pulse. We also demonstrate significant photovoltaic effect in BFO.[3] Finally, we discuss recent results on the effects of varying temperature and applied uniaxial pressure on the magnetic structure of BFO.

[1] S. Lee, W. Ratcliff II, S.-W. Cheong, and V. Kiryukhin, *Appl. Phys. Lett.* **92**, 192906 (2008).

[2] S. Lee, T. Choi, W. Ratcliff II, R. Erwin, S.-W. Cheong, and V. Kiryukhin, *Phys. Rev. B* **78**, 100101(R) (2008).

[3] T. Choi, S. Lee, Y.J. Choi, V. Kiryukhin, S.-W. Cheong, *Science* **324**, 63 (2009).

25OR-H-2

### **QUANTUM THEORY OF MAGNETOELECTRICITY IN RARE-EARTH FERROBORATES**

*Plokhov D.I.<sup>1</sup>, Popov A.I.<sup>1,2</sup>, Plis V.I.<sup>2</sup>, Zvezdin A.K.<sup>1</sup>*

<sup>1</sup> A.M. Prokhorov General Physics Institute of Russian Academy of Sciences  
38 Vavilov Str., 119991, Moscow, Russia

<sup>2</sup> Moscow Institute of Electronic Technology, 5 Pas. 4806, 124498, Zelenograd, Moscow, Russia

In recent years magnetoelectric and related multiferroic materials are paid considerable attention focused onto both fundamental understanding and novel applications. In these aspects, rare-earth

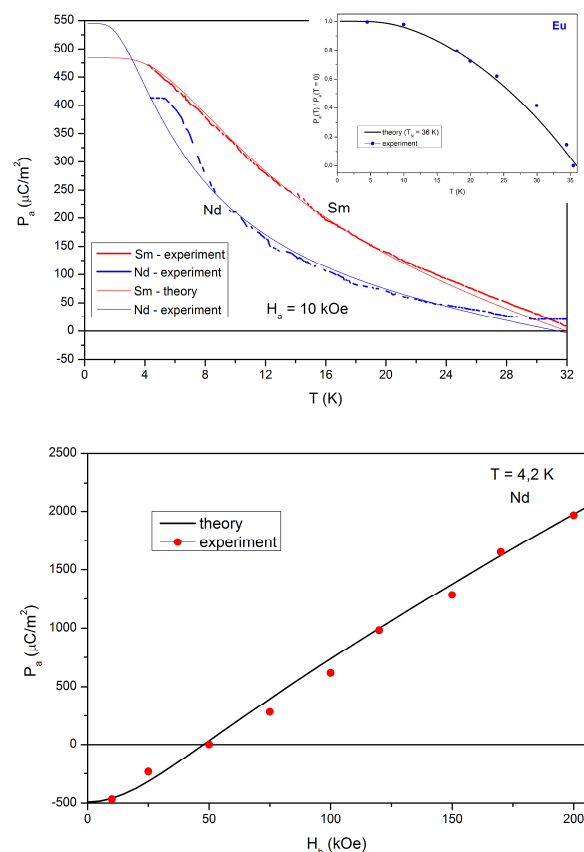
(RE) ferroborates  $RFe_3(BO_3)_4$ , a new class of multiferroics, is especially interesting due to a possible effect of an electric polarization control with an external magnetic field.

The RE ferroborates have a rhombohedral crystal structure with the  $R32$  space group. The magnetoelectricity of the ferroborates is determined by the RE ions. The Hamiltonian of the RE ion  $R^{3+}$  ( $R = Nd, Sm, Eu$ ) in ferroborates reads  $H = H_{CF} + H_{MF}$ , where  $H_{CF}$  is the crystal field (CF) Hamiltonian and  $H_{MF}$  is the ion Hamiltonian in the effective exchange and external magnetic fields. At the  $R^{3+}$  sites in the RE ferroborates with  $D_3$  symmetry the crystal field can be described by six independent real CF parameters.

The iron subsystem is described by means of two magnetic sublattices antiferromagnetically coupled by an exchange field. In the external magnetic field above  $H_{flop} \sim 10$  kOe antiferromagnetic vector  $\mathbf{L}$  becomes uniform over the sample and perpendicular to the field. The magnetization process is then determined by the rare-earth subsystem and the spin-flip of the Fe sublattices ( $H_{flip} \sim 1000$  kOe). The temperature dependences of the exchange and spin-flip fields are calculated in the frame of the molecular field theory. The subsystem of RE ions can be considered as a paramagnetic due to the smallness of RE-RE exchange interactions.

It is considered two mechanisms of magnetoelectricity in RE ferroborates: electronic, due to the electric dipole moments of RE ions, and ionic, due to displacement of the ions from the equilibrium in a magnetic field.

The temperature (for the Nd, Sm, and Eu ferroborates) and the field (for the Nd ferroborate) dependencies for the electric polarization are obtained. The comparison of the theoretical calculations with the experimental data [1] shows their good agreement.



The work is supported by the RFBR (grants 10-02-01162, 10-02-90475, and 11-02-91067).

[1] A.M. Kadomtseva et al., *J. Low Temp. Phys.*, **36** (2010) 640.

## THE INFLUENCE OF MAGNETOELECTRIC INTERACTIONS ON THE DOMAIN WALLS IN MULTIFERROIC

Gareeva Z.V.<sup>1</sup>, Zvezdin A.K.<sup>2</sup>

<sup>1</sup> Institute of Molecular and Crystal Physics, Russian Academy of Sciences, 450075 Ufa, Russia

<sup>2</sup> A.M. Prokhorov General Physics Institute, Russian Academy of Sciences, 119991 Moscow, Russia

A range of new phenomena are revealed in thin multiferroics films with domain structures. The physical properties of a material in a vicinity of domain walls appear to be different from the properties of a bulk. The novel functionalities of the domain walls connected with control of magnetic properties by electric parameters and vice versa are the subject of active scientific discussions [1-3]. One of the bright examples is the discovery of the conductivity of BiFeO<sub>3</sub> domain walls [2]. The latest experimental findings [3] focus also on the enhancement of magnetization in a vicinity of ferroelectric domain walls.

However the comprehension and origin of intrinsic electric properties and domain walls magnetism in multiferroics are under discussion, they can be attributed to change of a crystallographic structure, action of strains of a substrate and magnetoelectric pinning [4, 5].

The present research reports the novel mechanism of domain origin giving rise to electric polarization and magnetization in thin multiferroic film. The electric polarization induced by non – uniform distribution of magnetic moments and magnetization have been investigated. To understand the peculiarities of these properties the distribution of antiferromagnetic vector over multiferroic film has been considered. The following regularities have been found out

1) The character of micromagnetic distribution is closely connected with the patterning of ferroelectric domains.

2) Magnetic spins stick out from the rotational plane in a vicinity of ferroelectric boundaries interlocking on the ferroelectric walls.

3) The magnetic walls energy becomes a periodical function on the parameter  $\xi_0 = x_0 / \Delta$ ,  $\Delta = \sqrt{A / |K_2|}$  characterizing the displacement of magnetic wall relative to ferroelectric domain structure (Fig) (here  $A=2 \cdot 10^{-7}$  erg/cm,  $|K_2|=1 \cdot 10^6$  erg/cm<sup>3</sup>).

The properties of the magnetically induced polarization and the physical nature of magnetization occurring in multiferroic with stripe-like ferroelectric domain structure have been discussed.

Magnetism and polarization in thin multiferroic film are the contentious subjects to this date. Traditional treatment links emerging magnetic moments with homogeneous Dzyaloshinskii – Moria magnetoelectric interaction. It has been shown that the non – homogeneous mechanism i.e. flexomagnetoelectric interaction should be taken into account as well.

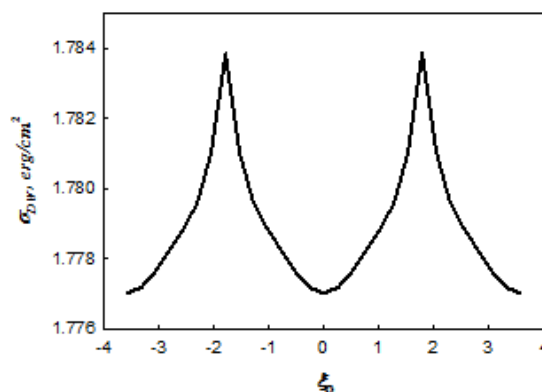


Fig. Dependence of the magnetic domain wall energy  $\sigma_{DW}$  on the parameter  $\xi_0$  characterizing the displacement of the magnetic domain wall relative to the ferroelectric domain structure.

[1] H. Béa and P. Paruch, *Nature Materials*, **8** (2009) 168.

[2] J. Seidel et al. *Nature Materials*, **8** (2009) 229.

[3] Q. He et al. American Physical Society, APS March Meeting 2010, abstract S1.084.

[4] Z.V. Gareeva, A.K. Zvezdin, *Phys. Sol. Stat.*, **52** (2010) 1714.

[5] Z.V. Gareeva, A.K. Zvezdin, *Europhys.Lett.* **91**(2010) 47006.



25OR-H-4

## THE WAVES OF CHARGE DENSITY AND DENSITY IN THE REGION OF PHASE TRANSITION TO THE INCOMMENSURATE MAGNETIC STRUCTURE IN OXIDES $RMn_2O_5$

*Menshenin V.V.<sup>1</sup>, Nikolaev V.V.<sup>1</sup>, Dmitriev A.V.<sup>2</sup>*

<sup>1</sup> Institute of Metal Physics of Ural Division of RAS

<sup>2</sup> Ural Federal University

menshenin@imp.uran.ru

The physical properties of oxides  $RMn_2O_5$  (R- rare-earth ion) were intensively studied in the last fifteen years. In recent times the interest to such systems has increased in connection with the detection of strong bond in them between the long-range magnetic order and electric polarization.

Basing on the sequential group-theoretical approach, the possibility of description of magnetic phase transitions to incommensurate magnetic structures within the Landau theory in oxides  $RMn_2O_5$  and also in the case, when Lifshitz invariants have the exchange nature, but don't contain coordinate derivatives along the coordinate axis normal to plane, in which the wave structure vector holds the general position is shown analytically in the paper.

It is stated, that in manganates the transition from antiferromagnetic phase to long-period structure can be described as a phase transition of second order at spatial symmetry of system  $Pbam$ . Experimental data which show, that it can be the second order transition, were found in paper [1]. This paper shows the heat capacity jumps in manganates in the region of investigated transition. We are not aware of the literature evidences describing the reveal of hidden transition heat and giving the ground to treat the investigated transition as the first genus transition. Nonlinear equations, describing the extremum conditions of thermodynamic potential, can be solved exactly by the way of separation of coordinate dependencies by x and z components of four-component order parameter. Coordinate dependence of solution along z axis has a view of solitary wave of kink type. The found x axis solution has the oscillating character what points to the formation of long-period structure in oxides  $RMn_2O_5$  below 24 K.

It was stated, that owing to this transition, the electric polarization decreases and has inhomogeneous distribution in the sample in the form of solitary nonlinear wave of charge density. It became clear, that electric polarization is a superposition of two components, one of which was generated at temperatures higher than 24K, and the second occurred due to the appearance of long-period structure.

It is shown, that the close to transition deformations, allowed by the system symmetry, don't change the system symmetry, but lead to the change of density, forming as well a nonlinear solitary density wave.

Basing on the group-theoretical analysis it was stated, that due to the low local symmetry of ions  $Mn^{3+}$  positions, the wave functions hybridization of d-electrons of ions  $Mn^{3+}$  and p-electrons of oxygen atoms can occur. The possibility of this hybridization leads to the presence of electron polarization of manganese ions along b – axis of the crystal. Since the hybridization of wave functions stipulates, as well, for the origin of indirect exchange interaction between manganese ions, the electric polarization in the whole sample will appear only together with the establishment of the long-range magnetic order related with the indirect exchange of manganese ions. At the same time the exact magnetic symmetry does not contain inversion. admitting the appearance of polarization.

[1] Phys.Rev.Lett., 2004,v.93, p.107207-2.

25OR-H-5

## MAGNETIC-FIELD-TUNED ELECTRIC POLARIZATION OF MICROMAGNETIC STRUCTURES

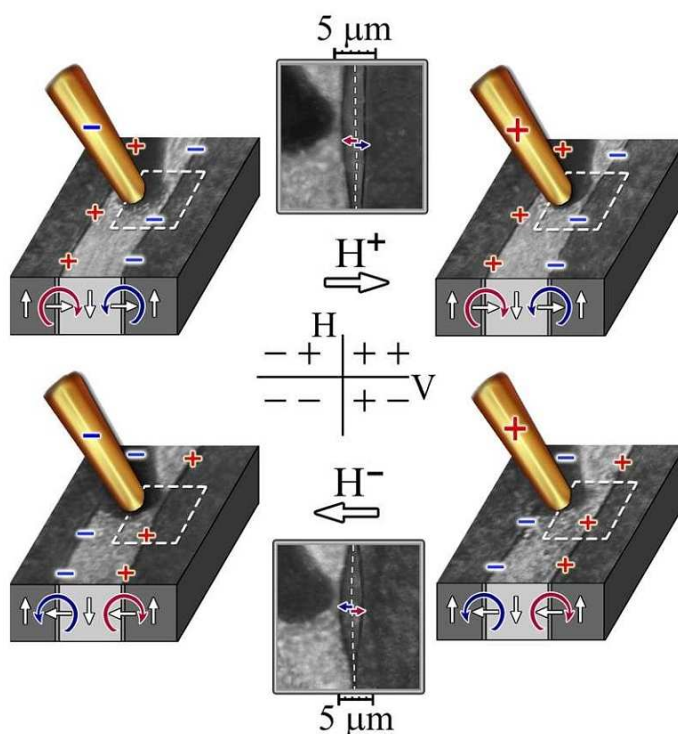
*Sergeev A.S., Sechin D.A., Pavlenko O.V., Pyatakov A.P., Nikolaeva E.P., Nikolaev A.V.*  
Faculty of Physics, M.V. Lomonosov Moscow State University, Moscow, Russia

Multiferroics are materials with coexisting and often coupled ferromagnetic and ferroelectric orders. In so-called spiral multiferroics such magnetoelectric coupling is caused by existence of spin spiral, i.e. cycloidal spiral ordering, which gives rise to the ferroelectricity. Multiferroicity is not however strongly required property of the material to exhibit magnetoelectric coupling. Every magnetic insulator can conceivably show it due to the inhomogeneous magnetoelectric interaction [1]. Because of this interaction spatial regions with certain magnetic inhomogeneities are electrically charged.

Particularly, Neel-type domain walls should carry electric charge and thus undergo an effect of external electric field. This phenomenon was observed in [2]. We used iron garnet films and non-magnetic copper wire. When electrical voltage of 1 kV was applied to the wire, domain walls attracted or repelled from the wire tip depending on the sign of the voltage. This effect was detected as a slight wall shift from its equilibrium state. It is also noteworthy that all the domain walls in the film had the same sign of surface electric charge in that case.

The fact that micromagnetic structure of the domain wall plays essential role in discussed phenomenon we proved in our recent experiments in which in-plane magnetic field  $H$  of 60 Oe was applied [3]. External magnetic field is of magnitude, which is insufficient for domain structure destroying, but at the same time it is large enough to change micromagnetic structure of the wall, as is schematically shown on the figure.

Let us consider up left subfigure. There are two domain walls depicted there. The magnetization direction in the middle of both walls is defined by the direction of the external in-plane magnetic field  $H$ . The sense of the magnetization vector rotation is different, and namely it is clockwise in the left wall and counterclockwise in the right one. According to the theory of inhomogeneous magnetoelectric effect, the sense of the magnetization vector rotation defines the electric polarization direction and thus the sign of the domain wall surface charge. Hence, under the influence of the electric field at given voltage polarity of the wire one of neighbouring domain walls should attract to the tip and another one should repel from it. Corresponding behaviour of domain walls was observed experimentally. Top and bottom square insets in the figure are superimposed photos of domain wall shifts from the equilibrium state depicted as a dashed line.



Support of RFBR grant №10-02-13302-RT-omi and Dynasty foundation is gratefully acknowledged.

- [1] V.G. Bar'yakhtar, V.A. L'vov and D.A. Yablonskii, JETP Lett., **37** (1983), 673  
 [2] A.S. Logginov *et al.*, Appl. Phys. Lett., **93** (2008), 182510  
 [3] A.P. Pyatakov *et al.*, EPL, **93** (2011), 17001

25OR-H-6

## MAGNETIC PROPERTIES AND STRUCTURE OF $Gd_{1-x}Nd_xCr(BO_3)_4$ : OPTICAL SPECTROSCOPY STUDIES

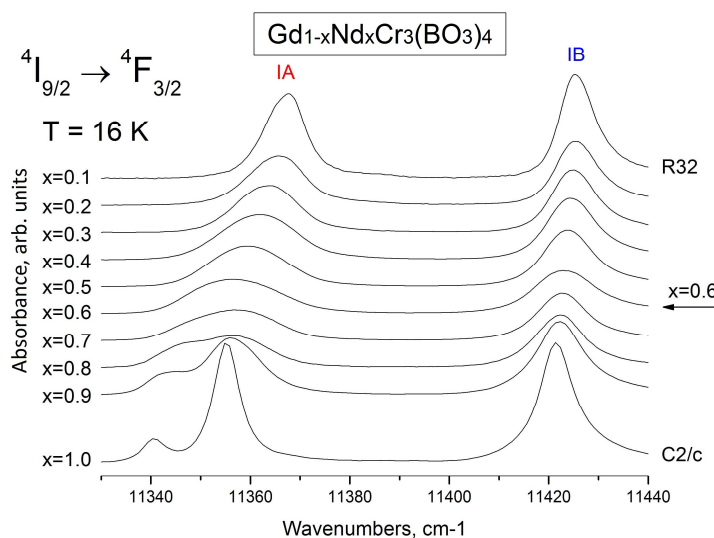
Boldyrev K.N.<sup>1</sup>, Popova M.N.<sup>1</sup>, Borovikova E.Yu.<sup>2</sup>, Dobrecova E.A.<sup>2</sup>, Maltsev V.V.<sup>2</sup>, Leonyuk N.I.<sup>2</sup>

<sup>1</sup> Institute of Spectroscopy RAS, 142190 Troitsk, Moscow region, Russia

<sup>2</sup> Department of Crystallography and crystal chemistry, Moscow State University,  
119991 Moscow, Russia

Borates with the general formula  $RM_3(BO_3)_4$  ( $R = Y, La - Lu$ ;  $M = Al, Ga, Sc, Fe, Cr$ ) have a trigonal structure of the natural mineral huntite. Recent studies of the rare-earth iron borates  $RFe_3(BO_3)_4$  have shown that these compounds exhibit a variety of phase transitions. Their magnetic properties are governed by the presence of two interacting magnetic subsystems, i.e. the  $Fe^{3+}$  and the  $R^{3+}$  ones. It turns out that the magnetic structure of  $RFe_3(BO_3)_4$  changes as a function of temperature, external magnetic field and substitutions in the rare-earth subsystem. Some compounds belonging to the family of rare-earth iron borates (with  $R=Gd, Nd, Pr, Tb, Ho, Sm$ ) display a considerable magnetoelectric coupling and their electric (magnetic) properties can be controlled by the magnetic (electric) field. This is a promising finding in view of possible device applications. Up to now, only little was known about the properties of the rare-earth borates  $RCr_3(BO_3)_4$  with another magnetic ion, i.e. chromium. The first results on thermodynamic and optical properties  $NdCr_3(BO_3)_4$  have been presented in the paper [1].

In this work, we have undertaken the first investigation of the optical properties of combined rare-earth chromium borates  $Gd_{1-x}Nd_xCr_3(BO_3)_4$ .  $NdCr_3(BO_3)_4$  demonstrates splitting of the  $Nd^{3+}$  Kramers doublets in the internal magnetic field that appears due to the antiferromagnetic phase transition at temperature  $T_N=8.2$  K [1]. Also similar effect in  $Gd_{0.99}Nd_{0.01}Cr_3(BO_3)_4$  was observed at the temperature  $T = 7.0$  K, and we assume that this phase transition corresponds to the antiferromagnetic ordering. The series of  $Gd_{1-x}Nd_xCr_3(BO_3)_4$  single crystals were grown. Analysis of the phonon spectra indicates that  $NdCr_3(BO_3)_4$  crystals possess monoclinic  $C2/c$  structure, but  $GdCr_3(BO_3)_4$  possess trigonal  $R32$  structure. From optical spectroscopy we have found, that at  $x<0.6$  that crystals has  $R32$  phase, but at  $x>0.6$  structure phase is  $C2/c$ . Also magnetic ordering of these crystals were analysed by optical spectroscopy.



This work was supported by the Russian Foundation for Basic Research (grant N10-02-01071), Federal Target-purpose Program “Scientific and Educational Personnel of Innovative Russia”, by the Russian Academy of Sciences under the Programs for Basic Research and by the Grant of the President of Russia (Grant No MK-143.2010.5).

[1] E.A.Popova, N.I.Leonyuk, M.N.Popova, E.P.Chukalina, K.N.Boldyrev, Tristan N., Klingeler R., and Büchner B., Thermodynamic and optical properties of  $\text{NdCr}_3(\text{BO}_3)_4$ , Phys. Rev. B, 76 (2007).

**25 August**

Thursday

14:30-17:00

oral session

25TL-H

25RP-H

25OR-H

**“Spintronics and  
Magnetotransport”**

25TL-H-7

## HIGHLY SPIN POLARIZED CURRENT WITH HALF METALLIC FERROMAGNETS

*Tezuka N., Saito T., Yoshida M., Jiang L., Zhou G., Sugimoto S.*  
Tohoku University, Aobayam 6-6-02, Aoba-ku, Sendai, Japan

Highly spin polarized current is an important subject for developing spintronics devices, because such current bring in large tunnel magnetoresistance (TMR) ratio or high spin injection efficiency into semiconductor. Several methods have been predicted or reported to obtain high spin polarization current. High TMR ratios have been obtained for magnetic tunnel junctions with FeCo or FeCoB electrodes and MgO barrier, which is a result of coherent spin polarized tunneling of electrons with half-metallic  $\Delta_1$  symmetry in the MgO(001) barrier. The others are using half-metallic ferromagnets (HMFs) electrodes, which are metallic in one spin direction and semiconducting in the other at the Fermi level, exhibit 100% spin polarization, or using an insulating ferromagnetic barrier, whose barrier height depends on the spin direction. Full Heusler alloys, in particular, are promising as a half metal, because a number of which have been predicted to be HMFs, and have a high Curie temperature. After our first observation of the TMR effect using a  $\text{Co}_2(\text{Fe,Cr})\text{Al}[1]$ , the magnetic tunnel junctions (MTJs) using full-Heusler alloy electrodes have been extensively studied. We will report the TMR observation for the MTJ using Heusler electrodes, and spin injection into semiconductor, especially for  $\text{Co}_2\text{Fe}(\text{Al,Si})$ .

We investigated the structure and magnetic properties of the  $\text{Co}_2\text{Fe}(\text{Al,Si})$  (CFAS) films on MgO (001), MgO(110) and GaAs(001) substrates. Next we fabricated the MTJs with CFAS full-Heusler alloys as electrodes and a MgO or Al-oxide barriers, and fabricated the CFAS/GaAs junctions to detect the spin injection efficiency into semiconductor. The junctions are microfabricated using the electron beam lithography and Ar ion milling.

The structure was changed by the substrate and post annealing temperatures, in which the fully epitaxial and polycrystalline CFAS films were obtained with the different disorder structure. By optimizing the fabrication condition, we have successfully grown the highly ordered CFAS full-Heusler films for MTJs on a Cr-buffered MgO(001) substrates. As a result the maximum TMR ratios of 386% and 832% were obtained measured at room temperature and 9 K, respectively, for a junction consisting of Cr/CFAS/MgO/CFAS/CoFe/Ta. The tunneling spin polarization estimated by Julliere's equation was 0.81 at room temperature and 0.90 at 9 K[2].

The *n*-GaAs layer and CFAS thin films were deposited by MBE on GaAs(001) substrates. The clear rectifying characteristics were observed in the CFAS/*n*-GaAs junctions with various doped densities, indicating the formation of Schottky barrier between CFAS/*n*-GaAs interface. From the comparison of the bias dependences of conductance for junctions with higher ordered CFAS and with lower one, it was indicated that the  $L2_1$  phase contributes to electrical transport properties. Finally, the spin injection signal was observed at 5 K by 3-terminal Hanle measurement, and spin relaxation time was estimated to be 380 ps [3], which value was longer than past report's one.

We will present the result of structural, magnetic and electrical transport properties of CFAS and other Co based full-Heusler films deposited on MgO(001), MgO(110) and GaAs(001) in more detail, and also report the spin filtering effect using  $\text{CoFe}_2\text{O}_4$  insulating barrier briefly.

This work was partly supported by Grant-in-Aid for Scientific Research (B) (22360002), Asahi glass foundation, and Strategic Japanese-German Joint Research Program "ASPIMATT".

- [1] K. Inomata, S. Okamura, R. Goto and N. Tezuka, *Jpn. J. Appl. Phys.*, **42**, (2003) L419.  
 [2] N. Tezuka, N. Ikeda, F. Mitsunashi, and S. Sugimoto, *Appl. Phys. Lett.*, **94**, (2009) 162504.  
 [3] T. Saito, N. Tezuka, and S. Sugimoto, *IEEE Transactions on Magnetics*, in press.

25RP-H-8

## MAGNETIC TUNNEL STRUCTURES: TRANSPORT PROPERTIES CONTROLLED BY BIAS, MAGNETIC FIELD, MICROWAVE AND OPTICAL RADIATION

*Volkov N.V.*<sup>1,2</sup>, *Eremin E.V.*<sup>1,2</sup>, *Tarasov A.S.*<sup>1,2</sup>, *Varnakov S.N.*<sup>1,2</sup>, *Ovchinnikov S.G.*<sup>1,2</sup>, *Patrin G.S.*<sup>1,3</sup>

<sup>1</sup> L.V. Kirensky Institute of Physics SB RAS, Krasnoyarsk, 660036, Russia

<sup>2</sup> Siberian State Aerospace University, Krasnoyarsk, 660014, Russia

<sup>3</sup> Siberian Federal University, Krasnoyarsk, 660041, Russia

The spin-polarized electron transport in magnetic tunnel structures has been a subject of intense studies. Various spin-dependent effects observed in these structures are interesting for both fundamental research and application. We report the features of the spin-dependent transport in several magnetic systems with tunnel junctions.

The first system is the manganite-based magnetic tunnel structure *La<sub>0.7</sub>Sr<sub>0.3</sub>MnO<sub>3</sub>/manganite depleted layer/MnSi*, where the depleted layer forms a potential barrier between the ferromagnetic electrodes *La<sub>0.7</sub>Sr<sub>0.3</sub>MnO<sub>3</sub>* ( $T_C = 250$  K) and *MnSi* ( $T_C = 30$  K). The structure was studied in unconventional CIP geometry, where current channel switching driven by a bias current and a magnetic field was discovered [1]. Switching between the conducting layers is responsible for a novel mechanism of magnetoresistance whose value can be controlled by a bias current. Switching and, consequently, magnetoresistance can be controlled also by optical radiation. In addition, in this tunnel structure the magneto-dependent effect of microwave detection was found. The origin of this effect is the interplay of the spin-polarized current and the spin dynamics in the ferromagnetic layers induced by a microwave radiation.

The second system is a Fe/SiO<sub>2</sub>/p-Si hybrid structure, in which the features of the transport properties in CIP geometry are also related to the effect of current-channel switching between the top ferromagnetic layer and the semiconductor substrate. In this structure, however, a principal role is played by a Schottky barrier formed near the SiO<sub>2</sub>/p-Si interface, as opposed to the first case where a tunnel barrier is formed only by an insulating layer. Resistivity of the Schottky barrier and, hence, current channel switching depends on temperature and sign and value of the bias current. This makes it possible to control the current-channel switching effect and, consequently, the transport properties of the structure within some limits. The transport properties of the structure can also be controlled by a magnetic field and optical radiation.

The third system under study is a granular manganite material that represents a cooperative assembly of the magnetic tunnel junctions. This system exhibits a great value of magnetoresistance and the magnetic-field-driven microwave detection effect. The magnetoresistance and rectification effects in the granular manganite sample are caused by a ramified network of the magnetic tunnel junctions, which are formed by ferromagnetic conducting grains with insulator boundaries. Magnetoresistance originates from the spin-dependent tunnel current between the grains, while the rectification effect is based on the interplay between the spin-polarized current through the tunnel junctions and magnetic resonance induced inside the grains forming the junctions.

This study was supported by the RFBR, project no. 11-02-00367-a; Presidium of the Russian Academy of Sciences, program 21.1; the Division for Physical Sciences of the Russian Academy of Sciences, program 2.4.4.1; the Siberian Branch of the Russian Academy of Sciences, projects nos. 5 and 134; and the Federal target program, State contract NK-556P\_15.

[1] N.V. Volkov, C.G. Lee, P.D. Kim et al., *J. Phys. D: Appl. Phys.*, **42** (2009) 205009.

[3] N.V. Volkov, E.V. Eremin, M.V. Rautskii et al., *JMMM*, **323** (2011) 1001.

25OR-H-9

## THE EFFECT OF HEAT TREATMENTS ON THE STRUCTURAL AND MAGNETIC PROPERTIES OF $\text{Fe}_3\text{O}_4/\text{Fe}$ BILAYERS

Goikhman A.<sup>1</sup>, Kupryanova G.<sup>1</sup>, Zenkevich A.<sup>2</sup>, Mantovan R.<sup>3</sup>, Fanciulli M.<sup>3,4</sup>, Rodionova V.<sup>1,5</sup>, Perov N.<sup>5</sup>

<sup>1</sup> Immanuel Kant Baltic Federal University, Kaliningrad, Russia

<sup>2</sup> National Research Nuclear University MEPhI, Moscow, Russia

<sup>3</sup> Laboratorio MDM IMM-CNR, Agrate Brianza (MB), Italy

<sup>4</sup> Dipartimento di Scienza dei Materiali, Università di Milano Bicocca, Milano, Italy

<sup>5</sup> Faculty of Physics, Moscow State University, Moscow, Russia

The effect of heat treatments on the structural and magnetic properties of bi-layered  $\text{Fe}/\text{Fe}_3\text{O}_4$  thin films grown by pulsed laser deposition on the pre-oxidized amorphous  $\text{SiO}_2/\text{Si}$  substrates has been investigated. The initially amorphous  $\text{FeO}_x$  films with  $\text{Fe}:\text{O}=3:4$  stoichiometry deposited at room temperature on top of the polycrystalline Fe underlayer were further subjected to the vacuum thermal annealing and the evolution of structural vs. magnetic properties was investigated by the combination of Raman scattering spectroscopy, conversion electron Mössbauer spectroscopy, ferromagnetic resonance spectroscopy, and vibrating sample magnetometry. The magnetic properties of as grown  $\text{Fe}/\text{FeO}_x$  bilayer exhibit similar parameters as for a single Fe layer with no

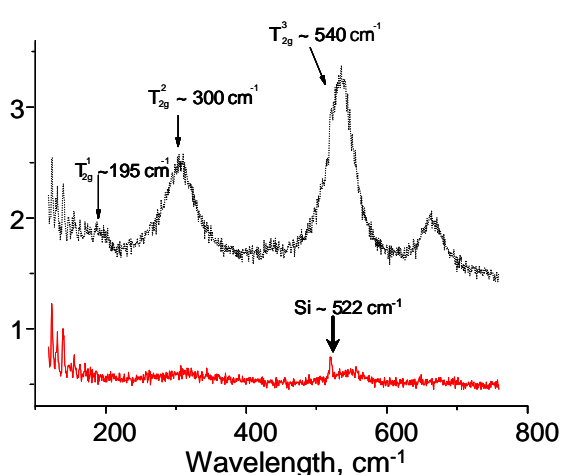


Fig. 1 Raman spectra taken for  $\text{Fe}_3\text{O}_4/\text{Fe}$  bilayer in XY geometry upon room temperature deposition (solid, bottom) and upon annealing at  $T=450^\circ\text{C}$  (dashed, top).

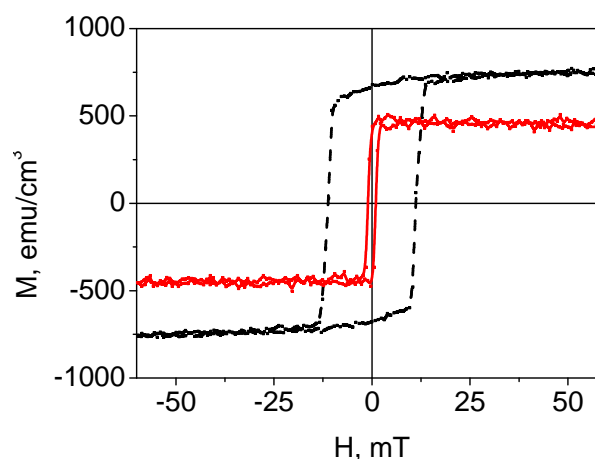


Fig. 2 Hysteresis loop obtained on  $\text{Fe}_3\text{O}_4/\text{Fe}$  bilayer upon room temperature deposition before (solid) and upon (dashed) annealing the structure at  $T=450^\circ\text{C}$  (dashed).

visible contribution from amorphous iron oxide. Following the annealing at  $T=450^\circ\text{C}$  the formation of the coupled ferromagnetic phase in  $\text{Fe}_3\text{O}_4/\text{Fe}$  bilayers exhibiting the coercive force  $H_c \sim 10\text{ mT}$



and the saturation magnetization  $M_s \sim 700 \text{ emu/cm}^3$  is revealed. The evolution of magnetic structure directly correlates with the crystallization of the magnetite phase in the iron oxide layer.

The support by the grants from Russian Ministry of Education and Science is acknowledged.

25OR-H-10

## CURRENT-INDUCED MAGNETO-TORSIONAL OSCILLATIONS IN NANOROD WITH ANTIFERROMAGNETIC LAYER

*Gomonay O.V.<sup>1,2</sup>, Loktev V.M.<sup>2</sup>*

<sup>1</sup> National Technical University of Ukraine "KPI",

ave Peremogy, 37, 03056 Kyiv, Ukraine; *malyshen@ukrpak.net*

<sup>2</sup> Bogolyubov Institute for Theoretical Physics NAS of Ukraine, Metrologichna str. 14-b, 03143,  
Kyiv, Ukraine; *vloktev@bitp.kiev.ua*

Nanoelectromagnetomechanical systems (NEMMS) operate at the boundary between the classical and the quantum world and thus are of great interest from both fundamental and technological applications. In particular, they could be used for the detection and control of the quantum states of coupled systems [1] or for designing devices for high-precision measurements [2]. Most of the NEMMS constructions use ferromagnetic materials for the magnetic-to-mechanical energy conversion (see, e.g. [3]). However, antiferromagnetic (AFM) materials usually show much stronger magnetoelastic coupling and much higher susceptibility to external magnetic field and thus can be used as the effective magneto-mechanical converters.

In the present paper we consider the possibility to induce the magneto-torsional oscillations in a small particle of AFM. Like in FM, the spin-polarized current that flows through the surface of AFM induces the spin-torques and results in oscillations and/or rotation of AFM vector. We study the linear dynamics of the AFM and shift vectors in the presence of the spin-polarized current in a finite-size sample. The model accounts for magnetoelastic coupling between AFM and shift vector and boundary conditions for free surface.

We show that depending on the geometry of a sample the ac spin-polarized current may induce an acoustic vibration with the wavelength of the order of the sample size or parametric downconversion with the emission of the acoustic waves.

The results obtained make a groundwork for the development the NEMMS device on the basis of AFM materials.

[1] P. Mohanty, G. Zolfagharkhani, S. Kettemann, *et al*, Phys. Rev. B, **70**, 195301 (2004), G. Sonne, R. Shekhter, L. Gorelik, *et al*, Phys. Rev. B, **78**, 144501 (2008).

[2] J. P. Davis, D. Vick, D. C. Fortin *et al*, Appl. Phys. Lett. **96**, 072513 (2010).

[3] A. A. Kovalev, G. E. W. Bauer, A. Brataas, Jpn. J. Appl. Phys., **45**, 3878 (2006).





permanent magnet based  
**MAGNETIC FIELD GENERATORS**  
 for fundamental and applied researches

- **modeling, design and fabrication** of magnetic field sources and other magnetic systems
- **high-intensity field** sources, **3 T and more** permanent magnet systems
- **high-uniform** magnetic field sources (homogeneity up to  $10^{-4}$ )
- magnetic systems with **complicated configuration** of the field
- **adjustable field sources**, field changing rate upto **10 T/sec**
- assembling of magnetic **systems according to customer specification**
- the **best quality magnetic materials**



<http://www.amtc.ru>  
<http://www.amtc.org>  
 e-mail: [sale@amtc.org](mailto:sale@amtc.org)  
[kopel@amtc.org](mailto:kopel@amtc.org)  
 tel/fax: +7 (495) 777 72 26



AMT&C, LLC offers automated measuring setups allowing to measure magnetic and thermal properties depending on the magnetic field.

## SCIENTIFIC MEASURING EQUIPMENT



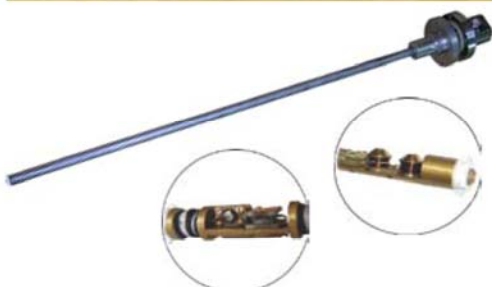
**Magnetocaloric Measuring Setup (MMS)** includes adjustable permanent magnet based magnetic field generator, liquid nitrogen cryostat, measuring insert, computer controlled measuring system and has the following working parameters:

- variable **magnetic field** strength - from **-1.9 to +1.9 T**
- variable magnetic **field change rate** - from **0.05 to 6 T/s**
- operating **temperature region** – **150 + 365 K**
- sample dimensions (min-max) - (1-2)×(2-5)×(8-10) mm
- **automatic and manual** measuring modes



**Setup for magnetocaloric materials express testing**

- operating **temperature range** – from **-10 C to 80 C**
- maximum magnetic **field strength** – **1 T**
- magnetic **field changing rate** – **2.5 T/sec**
- sample dimensions – **2×4×8 mm**
- magnetocaloric effect measuring range - from **0.1 K**



### **Variable temperature measuring inserts**

suitable for using together with adjustable magnetic field sources with application for:

- magnetometry (ac susceptibility, dc susceptibility and magnetization measurements, torque magnetometry, low field measurements)
- heat capacity measurements
- electro-transport measurements
- thermal transport measurements.

<http://www.amtc.ru>  
<http://www.amtc.org>  
 e-mail: [sale@amtc.org](mailto:sale@amtc.org)  
[kopel@amtc.org](mailto:kopel@amtc.org)  
 tel/fax: +7 (495) 777 72 26

## Author Index

### A

Aaltio I. ....	556	Almuchametova A.R. ....	462
Aarts J. ....	514	Alshammari M. ....	836
Abakumov P.V. ....	102	Alves S. ....	568
Abbasi N. ....	444	Amato A. ....	89
Abdel-Hafiez M. ....	564	Amelichev V.A. ....	375
Abe M. ....	325	Ammar S. ....	622
Abramov N. ....	515	Amoroso M. ....	771
Abramova G. ....	152	Anandakumar S. ....	324
Abrikosov I.A. ....	553	Ando K. ....	13, 586
Abylkalykova R.B. ....	382	Andre G. ....	681
Acet M. ....	26, 292, 298, 638, 639, 664	Andreev A.S. ....	111
Ackerbauer S. ....	555	Andreev A.V. ....	86, 88, 90, 418
Adenot-Engelvin A.L. ....	826	Andreev N.V. ....	481
Afanasiev D. ....	309	Andreev S.V. ....	135, 136, 654
Afanasyyev A. ....	662	Andreeva M. ....	132
Afonina V. ....	658	Anghel L. ....	226
Agalidy Yu. ....	201	Anisimov A.V. ....	279
Ağan S. ....	663	Anisimov M. ....	709
Ageev N.V. ....	130	Anisimov M.A. ....	427, 678
Ağıl H. ....	597	Anisimov N.V. ....	766
Agostinelli E. ....	276	Anisimov V.I. ....	598
Ahmadi T. ....	777	Anitas E. ....	430
Airriyan E.L. ....	641	Annenkov A.Yu. ....	795
Akatyeva K. ....	658	Anokhin D. ....	238
Akimov I.A. ....	881	Antipov E. ....	169
Akmaldinov K. ....	401	Antipov S.D. ....	117, 118
Aksenov V.L. ....	242, 347, 513, 571	Antonets I.V. ....	781
Aksoy S. ....	292, 298, 639	Antonov A.N. ....	123
Aktsipetrov O.A. ....	213	Antonov A.S. ....	789
Aktürk S. ....	638, 639	Antropov V.P. ....	301, 897
Aladyshkin A.Yu. ....	345	Aplesnin S. ....	693
Alam M. ....	724	Aplesnin S.S. ....	270, 692, 695, 732
Albertini F. ....	292, 658	Aprili M. ....	354
Aldashev I.A. ....	270	Aquino R. ....	317, 318, 570
Aleksandrova G. ....	770	Arai K.I. ....	320
Alekseyev S. ....	450	Arango Y. ....	562
Aleshnikov A.A. ....	139, 796	Arbuzov V. ....	182
Algarabel P. ....	292	Arbuzova T. ....	182
Ali N. ....	550, 626, 631, 636	Arbuzova T.I. ....	685
Aliev A.M. ....	554, 642	Arefev A.I. ....	641
Aliev F.G. ....	620	Argyriou D. ....	605
Alling B. ....	553	Ariake J. ....	20
Almasy L. ....	226	Ari-Gur P. ....	295, 556
		Arima T. ....	604
		Arnold Z. ....	292
		Aronzon B.A. ....	533, 714, 727
		Arroyo F. ....	55
		Arruda L.B. ....	715

Arslanov R.K.	675, 686, 702
Arslanov T.R.	675, 686, 702
Artyukhin S.	605
Arzhnikov A.K.	30, 456, 465
Arzumanian G.M.	226
Arzuza L.C.C.	546
Asadullin F.F.	805
Astakhov G.V.	62
Astashenok A.V.	701
Astashonok A.	131
Atalay F.E.	415
Atalay S.	415, 416
Atkinson D.	23
Atkinson R.	614
Atoneche F.	200
Attanasio C.	514, 594
Attaullakhanov F.	765
Atxitia O.U.	338
Auffret S.	254, 266, 267, 285
Avakumov R.	443
Avanesyan G.G.	706
Avdeev M.	503
Avdeev M.V.	242, 571, 575
Averkiev N.S.	532
Averkin S.V.	609
Awad A.A.	620
Azamatov Sh.	671
Azarevich A.N.	504, 505
Azevedo A.M.	718
Aznaurova G.Y.	193

---

## **B**

Babaev A.B.	193
Babaoğlu M.G.	597
Babazadeh H.L.	687
Babos M.	58
Babushkina N.A.	174, 181, 194
Bader S.D.	321
Badgley K.E.	25
Badiev M.K.	516, 850
Bagrets A.	16
Baker S.	276
Bakhvalova T.N.	220
Bakulina A.S.	400
Bakursky S.	351
Balaev A.	128
Balaev A.D.	184, 399
Balaev D.A.	106, 767
Balagurov L.A.	820

Balakhonov S.V.	154
Balasoiu M.	226, 239, 243, 867
Balbashov A.M.	63, 67, 479, 492, 495
Baltz V.	285
Balymov K.G.	122, 134, 426
Bandiera S.	254, 266, 267
Bannikov V.V.	192
Bannikova N.S.	689
Bañobre-López M.	22
Bányai I.	58
Barandiaran J.M.	699
Barandiarán J.M.	291, 297
Baranov N.V.	153, 157, 640, 654, 660, 690
Baretzky B.	821
Barilo S.	474
Barker J.	206, 337
Barmin Yu.V.	469
Barnaš J.	12
Barnes S.E.	354
Barsukov I.	21
Barthelemy M.	330
Barvinschi P.	314
Baryshev A.V.	202, 587, 668, 879
Batalov S.V.	453
Bataronov I.L.	469
Batdalov A.B.	642
Battiato M.	331
Bayer M.	61, 881
Bayri N.	415, 416
Bayukov O.A.	161, 176, 767
Bazarov V.V.	718
Bazhanov A.G.	696
Bazhanov D.I.	145
Beaurepaire E.	16
Bebenin N.G.	195, 619, 837
Beckmann D.	348
Bedarev V.A.	474
Behr G.	89
Belanovsky A.	705
Belanovsky A.D.	364, 759
Belashchenko K.D.	25, 259, 897
Belenli I.	597
Bel'kov V.	814
Belobrov P.I.	307, 442
Belogorokhov I.A.	424
Belotelov V.I.	210, 881
Belousov V.A.	159
Belova L.M.	391
Belovs M.	866
Belozorov E.V.	412
Belozorov D.	621
Belyaev I.V.	385

Belyaev S.V. ....	653	Borovikova E.Yu. ....	907
Belzig W. ....	75	Bortolotti P. ....	13, 705
Belzik M. ....	227	Bosak A. ....	607
Berezovets V.A. ....	534	Bottyán L. ....	347
Berger A. ....	557	Bou Matar O. ....	617
Berger H. ....	484, 736	Boucher V. ....	827
Bergeret F.S. ....	77	Bourges Ph. ....	857
Berkov D. ....	359	Bovenspiensen U. ....	338
Berkov D.V. ....	357	Bowen M. ....	16
Béron F. ....	546	Boyarintsev S.O. ....	887
Bersuker I.B. ....	177	Bringer A. ....	332
Berzhansky V. ....	201	Brisson A. ....	571
Berzhansky V.N. ....	212	Brûlet A. ....	571
Besedin S.P. ....	242	Brunne D. ....	61
Bessonov V. ....	219	Brunner K. ....	62
Bezdushnyi R.V. ....	393	Bruno P. ....	12
Bezmaternikh L.N. ....	494	Brusentsov N.A. ....	232, 766
Bezmaternykh L.N. ....	64, 158, 474, 606, 607	Brusentsova T.N. ....	766
Beznosikov D.S. ....	632	Buchelnikov V. ....	295, 639, 647, 650, 662
Beznosov A. ....	186, 187	Buchelnikov V.D. ....	293, 488, 551, 628, 646, 661
Bezus A.V. ....	757	Buchkevich A.A. ....	794
Bezus E.A. ....	210	Büchner B. ...	89, 429, 561, 562, 564, 596, 733, 743, 851
Bhatt V. ....	83	Buda-Prejbeanu L. ....	254
Bianchi A.D. ....	510	Buda-Prejbeanu L.D. ....	694
Bica I. ....	239, 867	Budzynski M. ....	833
Bichurin M.I. ....	493, 609	Buechner B. ....	853
Bienkowski K. ....	93	Buettgen N. ....	565
Bigot J.-Y. ....	330	Bugayev Ye.A. ....	130
Bilych I. ....	496	Bukharaev A.A. ....	269
Binns C. ....	276	Bukreev D.A. ....	391, 798, 799
Birge N.O. ....	344	Bulatov T.A. ....	406
Blackburn S. ....	510	Buling A. ....	37
Blanco J.M. ....	545, 831	Buřka B.R. ....	15
Blon T. ....	263	Bulvina Yu.S. ....	159
Bludov O. ....	736	Bunda S. ....	189
Bludov O.M. ....	484	Bunda V. ....	189
Bluegel S. ....	332	Buravtsova V. ....	209
Blugel S. ....	582	Burdick G.W. ....	203
Bodunova A.S. ....	486	Bürgler D.E. ....	146
Boehm M. ....	152	Burkhanov G. ....	629
Bogach A. ....	709	Burkhanov G.S. ....	393, 665
Bogach A.V. ....	427, 504, 505, 624, 678, 781	Burmistrov I.S. ....	702
Bogomazova O.B. ....	365, 460	Burton J.D. ....	258
Boldyrev K.N. ....	907	Bush A.A. ....	489, 565
Bonanni A. ....	817	Butenko A. ....	268
Bondarenko G.N. ....	161, 399	Buzlukov A. ....	837
Bondarev A.V. ....	469	Buznikov N.A. ....	789
Bontempi E. ....	151	Bychkov I.V. ....	488, 793
Borich M.A. ....	476	Bykova L.E. ....	161, 721
Borin D. ....	871	Byzov I.V. ....	282
Borisenko I.V. ....	501, 670		
Bork A. ....	16		

---

**C**

Caicedo J.....	38
Caloz C.....	827
Camp P.J.....	873
Capan C.....	510
Caprara S.....	534, 815
Carbone C.....	21
Cardoso S.....	55
Carignan L.P.....	827
Carrey J.....	51, 263
Carva K.....	331
Casoli F.....	292
Cebers A.....	866
Cerda J.....	229
Chakhalian J.....	599
Chang C.-R.....	357
Chang G.S.....	822
Chang J.-H.....	357
Chanthbouala A.....	759
Chantrell R.W.....	206, 337
Chappert C.....	356
Chareev D.....	894, 895
Charikova T.B.....	506
Chatterjee S.....	656
Chaudret B.....	51, 263
Chebotkevich L.A.....	107, 112, 141
Chechenin N.G.....	143, 672, 673
Chekanova L.....	128
Chekanova L.A.....	127, 142, 792
Chekrygina Ju.....	791
Chen H.-H.....	357
Chen P.J.....	278
Cheong S.-W.....	902
Cherepanov V.M.....	100, 322, 327, 432
Chérif S.M.....	614
Chernavsky P.....	166
Chernenkaya A.....	737
Chernenko V.A.....	297, 648
Chernenkov Yu.P.....	409, 417
Chernichenko A.....	148
Chernikov R.V.....	389, 390, 391, 437
Chernikov S.....	114
Chernobrovkin A.L.....	154, 781
Cherny A.S.....	388
Chernykh P.N.....	673
Chernyshov A.....	535
Chertovich A.V.....	872
Chervinskii D.....	89
Chetkin M.....	66
Chetvertukhin A.V.....	202, 332, 879
Chiba D.....	529
Chichkov V.....	515
Chichkov V.I.....	481
Chien C.L.....	156
Chigarev S.G.....	710
Chiriac H.....	539
Chirikov D.N.....	228
Chirkova A.M.....	660
Chistyayev V.A.....	373
Chistyakov O.....	436, 629
Chistyakov O.D.....	393, 665
Chistyakova N.I.....	769
Chizhik A.....	545
Chizhik M.V.....	125, 127
Chizhik N.A.....	405
Choi T.....	902
Choi Y.J.....	902
Choi Y.-S.....	84
Chshiev M.....	260, 445
Chubykalo-Fesenko O.....	338
Chudnovsky E.M.....	517
Chuev M.A.....	100, 322, 327, 432, 725
Chugunov A.A.....	115
Chukalina E.P.....	610
Chulkov E.V.....	303, 534, 815
Chumak A.V.....	589
Churagulov B.R.....	154
Chushkin Y.....	569
Chuvildiev V.N.....	120
Chzhan A.V.....	150
Chzhan V.....	629
Çiçek Ö.....	597
Cirillo C.....	514, 594
Coke A.....	556
Constantinian K.Y.....	511, 893
Coppola P.....	318
Cornei N.....	430, 679
Coşkun A.....	638, 639
Côté M.....	510
Couper C.....	314
Cox D.....	137
Craciunescu I.....	874
Craus M.-L.....	430
Craus M.-L.O.....	679
Cristescu C.P.....	243
Cros V.....	13, 705, 758, 759
Curély J.....	281
Cwik J.....	629
Ćwik J.....	657



Cyrille M.C. ....694

**D**

da Silva J.H.D. ....715  
 Daemen L.L. ....28  
 Damay F. ....607  
 Damianova R. ....393  
 Danilov S. ....182  
 Danilov V. ....229  
 Danilov Yu.A. ....674, 688, 719, 726  
 Darton N.J. ....54  
 Davydenko A.V. ....107, 155  
 Davydov A.B. ....533  
 de Jong J.A. ....63, 67  
 De Oliveira H. ....571  
 de Teresa J.M. ....55  
 Deen P.P. ....292  
 Deisenhofer J. ....740, 895  
 Déjardin P.-M. ....164, 366  
 del Val J.J. ....542  
 Dellmann T. ....89, 140  
 Delong L.D. ....83  
 Demazeau G. ....171, 178, 716  
 Demidenko O. ....693  
 Demidov A.A. ....477  
 Demidov E.S. ....286  
 Demidov V.E. ....14  
 Demidov V.V. ....501  
 Demina P.B. ....674  
 Deminov R.G. ....77, 507  
 Demirci Ç.E. ....639  
 Demishev S. ....709  
 Demishev S.V. ..154, 427, 504, 505, 624, 678,  
 781  
 Demokritov S.O. ....14  
 Denisov I.A. ....307, 442  
 Denisova E. ....128, 402  
 Denisova E.A. ....142  
 Dennis C.L. ....278  
 Depeyrot J. ....317, 318, 570, 576  
 Derevyanko M.S. ....391, 798, 799  
 Desnenko V. ....186, 187  
 Desnenko V.A. ....895  
 Devizenko A. ....791  
 Devolder T. ....356  
 Deyev S.M. ....327  
 Dhesi S.S. ....557  
 Dhochak K. ....533  
 Dianov M.Y. ....752

Dieleman D. ....620  
 Diény B. ....254, 260, 266, 267, 285, 694  
 Dietl T. ....528  
 Dikanskii Yu.I. ....864  
 Dikansky Yu.I. ....244, 251  
 Ding J. ....818  
 Ding Y. ....478, 480  
 Dinia A. ....822  
 Djemia P. ....614  
 Djuraev D.R. ....216  
 Dmitriev A. ....728, 737, 816  
 Dmitriev A.V. ....905  
 Dmitrieva N.V. ....407  
 Dmitrieva T. ....425  
 Dmytriiev O. ....360, 590  
 Dobatkin S.V. ....665  
 Dobbrow C. ....227  
 Dobrecova E.A. ....907  
 Dobretsov K.G. ....767  
 Dobromyslov M.B. ....102  
 Dobroserdova A. ....229  
 Dobysheva L.V. ....465  
 Doerr M. ....436, 645  
 Dokukin E.B. ....867  
 Dolgiy A. ....129  
 Dolgova T.V. ....202, 332, 879  
 Dolya S. ....186  
 Domingo N. ....276  
 Dorgiev V.V. ....741  
 Dorofeenko A.V. ....208, 223  
 Dorokhin M.V. ....674  
 Doroshenko R.A. ....787  
 Dragoshanskii Yu.N. ....422  
 Drechsler S.-L. ....561, 562  
 Drowniak J.L. ....377  
 Drichko I.L. ....698  
 Drobosyuk M. ....647  
 Drobosyuk M.O. ....646  
 Drokina T.V. ....176  
 Drovosekov A.B. ....133, 146, 725  
 Drozdov M.N. ....726  
 Drozdov Yu.N. ....688, 726  
 Drulis H. ....436, 629  
 Dubenko I. ....293, 550, 636  
 Dubenko I.S. ....626, 631  
 Dubois E. ....569  
 Dubovik M.N. ....362  
 Dubrovina N.V. ....213  
 Ducati C. ....557  
 Ducruet C. ....254, 266, 267  
 Dugaev V.K. ....12  
 Dianov J. ....263

Duginov V.N.	243
Dukhnenko A.	709
Dulov E.N.	716
Dunaev V.S.	688, 726
Dunaevsky S.M.	467
Dunets O.V.	121
Durr H.A.	590
Dürr H.A.	206, 337
Dushenko S.A.	143, 672, 673
Dussaux A.	13, 705
Dvornik M.	590
Dyadkin V.A.	29
Dyakonov V.P.	548
D'yakonov V.P.	490
Dygteva O.	753
Dyomin G.D.	683
Dzhumaliev A.S.	408
Dzhun I.O.	143, 672, 673
Dzyapko O.	14

---

## *E*

Ebels U.	267, 694
Éber N.	863
Eckerlebe H.	29
Economou E.N.	95
Edel'man I.S.	204
Edelman I.	215, 281, 773
Efetov K.B.	810
Efimets Yu.Yu.	110
Efimkin D.K.	42
Efimova V.	230
Efremova M.A.	154
Efros A.L.	304
Eggert S.	310
Egorov S.B.	115
Eisterer M.	704
Ekholm M.	553
Ekomasov A.	671
Ekomasov A.E.	748
Ekomasov E.	671
Ekomasov E.G.	365, 462, 748
Ekomasov E.G.	460
El Moussaoui S.	584
Elfimova E.	230, 245, 246, 577
Eliseev A.A.	790
Eliseeva S.V.	149
Elokhina L.	175
Elsukova A.	26
Emura S.	552

Enachescu C.	481
Endo Y.	370
Enikeev R.	295
Entel P.	290, 551, 628, 650
Epshtein E.M.	710
Eremin E.	693
Eremin E.V.	109, 142, 158, 423, 477, 669, 695, 911
Eremin I.M.	600
Eremin M.V.	501, 600
Eremina R.M.	491, 740
Eriksson O.	309, 457
Ermakov K.E.	107
Erokhin S.	359
Ershov N.V.	409, 417
Ertekin E.	597
Eschrig M.	74
Escoda Ll.	296, 663
Eshchenko R.	424
Esmailian A.H.	444, 687
Espinosa D.	568
Evans P.R.	614
Evans R.F.L.	206, 337
Evers F.	16
Evstigneeva M.A.	429, 743

---

## *F*

Fabbrici S.	292, 658
Fähler S.	290
Faizrakhmanov I.A.	717
Fan J.	56
Fanciulli M.	912
Fang D.	14
Fannin P.C.	314
Farle M.	21, 26, 137, 283, 298
Farzetdinova R.M.	530, 729
Faulhaber E.	857
Fayziev Sh.Sh.	216
Fayzullin R.R.	646
Fazzini P.F.	263
Fediy A.A.	793
Fedorchenko A.V.	895
Fedorchenko I.V.	724
Fedorov V.I.	409, 417
Fedosov A.G.	139, 796
Fedyanin A.A.	202, 332, 790, 878, 879
Feher A.	186, 187, 189
Feofanov A.K.	592
Feofanov V.S.	232

Ferguson A.J. ....	14	Gafarov A.Y. ....	377
Fernandez E.....	804	Gaidukova I.Yu.....	645
Fernando G.W.....	42	Gajc M. ....	93
Fert A. ....	13, 705	Galakhov V.R. ....	37, 282
Fertman E.....	186, 187	Galkin A.S. ....	735
Fetisov L. ....	243, 635	Galyas A.I. ....	270, 692
Fetisov L.Y. ....	489	Gamza M. ....	555
Fetisov L.Yu. ....	820	Gamzatov A.G.....	642
Fidan A.....	416	Gan`shina E. ....	38
Fiebig M.....	482	Gan`shina E. ....	209, 219
Figueiredo Neto A.M.....	568	Gan`shina E.A... 130, 583, 607, 648, 719, 727, 820	
Filatov E.Yu.....	405	Ganeev V.R.....	101
Filimonov D.S.....	160	Gapihan E. ....	254
Filimonov Y. ....	397	Gapochka A.M.....	171, 178, 716
Filimonov Y.A. ....	408	Gapontsev A.V. ....	147
Filimonov Yu. ....	615	Garamus V.....	430
Filipov V.B. ....	427, 504, 505, 624, 678	Garcia C.....	542
Filippov B.N.....	362, 407, 850	Garcia J. ....	295, 633, 656
Filomeno C.L.....	576	García J. ....	276, 663
Finkelstein L.D. ....	598, 822	García-Muñoz J.L. ....	495
Fiorani D. ....	276	García-Santiago A. ....	517
Firsin A.A. ....	35	Gareev R. ....	271
Firsova N.....	482	Gareeva E.....	751
Fisher L.M.....	174	Gareeva Z.V.....	904
Fisk Z. ....	510	Garlea V.O.....	556
Fita I. ....	885	Gatiyatov R.G. ....	269
Fitzsimmons M.R.....	25	Gaudin G.....	285
Flachbart K.....	504, 505	Gaviko V.S. ....	87, 394, 407, 413
Flores A.G.....	103, 398	Gavrilenko V.I. ....	531
Fomicheva L. ....	897	Gavrilkin S.....	520
Fomicheva L.N. 428, 434, 435, 512, 636, 681, 833		Gavrilkin S.Yu.....	504
Fomina K.A.....	704	Gavrilov A.I.....	240
Fominov Ya.V.....	77, 507	Gavrilova T.P.....	491, 740
Fox A.M. ....	836	Gavriluk A.A. ....	792
Fraerman A.A.....	30, 754	Gavrilyuk A.A. ....	403, 404
Freitas P.P. ....	55	Gawroński P.....	831
Friedland K.-J.....	268	Ge Y.....	556
Fritzsche J. ....	345	Gehring G.A. ....	836
Fu X.L. ....	151	Geiler A.L. ....	373
Fukunaga H.....	543, 544	Gencer A. ....	597
Fukushima A. ....	13	Gendler T.S.....	123, 126
Furdyna J.....	535	Gerashenko A. ....	474, 837
Furukawa N.....	604	Gerasimov E.G. ....	87, 394, 413
Fuse K. ....	325	Gerasimov M. ....	585
<hr/>			
<b>G</b>		Gerber A. ....	815
Gabani S.....	504, 505	Gerlach S. ....	334
Gabbasov R.R. ....	327	Gerus S.V.....	795
		Gervits N.E. ....	160, 472, 521
		Geshev J.....	277
		Ghazale J.J. ....	446
		Ghidini M.....	557

Gil A.....	829	Gornostyrev Yu.N.....	417
Gimaev R.R.....	659, 775	Gorunov G.E.....	117, 118
Gippius A.A. ....	160, 472, 521, 565	Goto T.....	587
Girich A.A.....	207, 882	Gottlieb M.....	52, 227
Gizhevskii B.A.....	37	Goujeon M.....	51
Gladkikh D.V.....	251	Goulon J.....	607
Gladkov A.A.....	233, 237	Govor G.A. ....	644
Glatz A. ....	347	Granovsky A.....	542
Glavatskyy I.....	857	Granovsky A.....	38, 635
Glazkov V.N.....	565, 738	Granovsky A.B. 208, 220, 223, 550, 626, 630, 631, 648, 727	
Glazkova Ya.S. ....	171	Granovsky S.....	140
Glebov A.V.....	400	Granovsky S.A.....	645
Glebov V.A. ....	400	Graser S. ....	857
Glushkov V.....	709	Grazú V.....	55
Glushkov V.V. ...	427, 504, 505, 624, 678, 781	Greben'kova Yu.....	148
Gnatchenko S. ....	218, 736	Grebennikov A.A.....	138
Gnatchenko S.L.....	474, 484, 895	Grebennikov V.I.....	458, 461
Goering E. ....	821	Grebenshchikov Yu.B.....	280
Gofryk K. ....	428	Grechnev G.E. ....	895
Goikhman A.....	635, 652, 912	Green R.....	822
Goikhman A.Yu.....	701	Gregg J.F.....	589
Goiran M.....	531, 533	Grein R.....	74
Goldobin E. ....	79, 346	Greneche J.-M.....	769
Golik L.L.....	719	Grenier S.....	151
Golosov D. ....	268	Gribkov B.A. ....	286
Golovanov A.N.....	722	Gribov I.....	376
Golubeva I.S.....	766	Grigoriev S.V.....	29
Golubiatnikov A.N.....	252	Grigorieva N.Yu. ....	475
Golubov A.....	78	Grin Yu. ....	555
Golubov A.A.....	77, 350, 507	Grishina O.V.....	389, 390, 391, 437
Gomes J.A.....	570	Grollier J.....	13, 705, 758, 759
Gómez-Polo C.....	829	Groshev A.G.....	30
Gomonay O.V.....	913	Gruber J.B.....	203
Gonchar L.E.....	35, 183	Gruner M.E.....	290
Goncharova O.A. ....	142	Grunin A.....	652
Gonzalez J.....	545, 618, 635, 831	Grunin A.A. ....	790, 879
Gonzalez L. ....	295, 633	Gschneider K.A.Jr. ....	659
González L. ....	276, 663	Gu G.....	562
Gonzalez-Alonso D.....	664	Gubaydulina T.V. ....	171, 178, 716
Goodilin E.A. ....	388	Gubernatorov V.V. ....	422
Gooneratne C. ....	682	Gubkin A.F. ....	433, 640, 690
Gopal A.V.....	881	Gudim I.....	496
Gopin A.V.....	237	Gudim I.A.....	477, 606
Gorbatov O.....	417	Gudin S.A. ....	147
Gorbenko O.Yu.....	174	Gudkov V.V.....	177
Gorbunov D.I.....	418	Gudoshnikov S.A.....	280
Goren Y.....	52	Guénon S. ....	345
Gorin A. ....	396	Guimarães A.P.....	23
Gorkovenko A.N.....	116	Güler S.....	717
Gorn N.....	359	Gulyaev M.V. ....	766
Gorn N.L.....	357	Gulyaev Yu.V.....	710
Gornakov V.S.....	278		

Gumarov A.I. ....	717
Gumerov A.M. ....	365, 460, 748
Günther D. ....	871
Gupta A. ....	132
Gürlich C. ....	346
Gusakova D. ....	694
Gusev A. ....	89
Gusev M. Yu. ....	367
Gusev S.N. ....	286
Gusliencko K.Y. ....	620
Gutfleisch O. ....	643, 657
Gutiérrez J. ....	291, 297

---

## H

Hait E. ....	778
Hajdu A. ....	242
Hajdú A. ....	58
Hakioffglu T. ....	896
HannulaS.-P. ....	556
Harin E.V. ....	386, 423
Harres A. ....	277
Harus G.I. ....	506
Hasanov S. ....	630, 635
Hasegawa R. ....	540
Hatsukade Y. ....	891
Haug D. ....	857
Heimes A. ....	74
Heinonen O. ....	83
Hekking F.W.J. ....	77
Hellsvik J. ....	309
Hendren W.R. ....	614
Hendry E. ....	222
Hérault J. ....	254
Herbst F. ....	622
Hernandez J.M. ....	517
Hernando B. ....	276, 295, 296, 554, 633, 656, 663
Herranz G. ....	38
Hess C. ....	89
Heyderman L. ....	584
Heyer O. ....	174
Hillebrands B. ....	589
Hinkov V. ....	857
Hinzke D. ....	334
Hnatič M. ....	863
Holdsworth P. ....	560
Holm C. ....	229, 869
Honda A. ....	163
Honda N. ....	20, 163

Honkonen J. ....	863
Horimai H. ....	340, 341
Hosseini M.G. ....	141
Hovorka O. ....	557
Hradil K. ....	857
Hrkac G. ....	356
Hsieh Y.S. ....	894
Hsu J.C. ....	480
Hu Q.M. ....	637
Hübler F. ....	348
Hudl M. ....	276
Hueso L.E. ....	557
Hung D.S. ....	480
Hurt D. ....	510
Hüvonen D. ....	738

---

## I

Iakubov I.T. ....	372, 373
Ibaev J. ....	508
Ibarboure E. ....	571
Ibarra M.R. ....	55
Ichkitidze L.P. ....	509
Idrisov A. ....	773
Ignatchenko V.A. ....	302, 459, 463, 800
Ignatchik O. ....	510
Ignatenko A.N. ....	500
Ignatov A.I. ....	92
Igoshev P.A. ....	44
Iguchi S. ....	604
Ihle D. ....	46
Il'inykh I.A. ....	126
Il'ichev E. ....	592
Iliev L. ....	393
Iljin A.I. ....	155
Ilyn M. ....	542, 635
Ilyushin. A. ....	395
Iñiguez J. ....	103, 398
Inkina N.A. ....	188
Inosov D.S. ....	857
Inoue A. ....	438
Inoue M. ....	202, 340, 341, 587, 668, 878, 879
Inyushkin A.V. ....	181
Inzhevatin E.V. ....	767
Ionescu A. ....	54
Ipatov M. ....	618
Irkhin V. Yu. ....	44, 845
Irmak A.E. ....	638, 639
Irzhak A. ....	658
Isaev E.I. ....	28

Isaeva T.N. ....	684
Isber S. ....	720
Ishchenko L.A. ....	226
Ishchenko T.V. ....	624
Ishenko L.A. ....	767
Ishihara S. ....	884
Iskakov S. ....	853
Iskhakov R. ....	128, 402
Iskhakov R.S. ....	125, 127, 142, 226, 399, 423, 767, 792
Iskhakova L.D. ....	492
Islamov A. ....	430
Isobe M. ....	608
Istomin S. ....	169
Istomin Yu. ....	572
Itoh A. ....	206, 275, 333, 337, 584
Iunin Y.L. ....	156
Iusan D. ....	457
Ivankov A.I. ....	226
Ivanov A. ....	94, 230, 246, 764, 857
Ivanov A.A. ....	506
Ivanov A.O. ....	864
Ivanov A.P. ....	805
Ivanov B.A. ....	309, 706
Ivanov M. ....	482
Ivanov S.I. ....	385
Ivanov V. ....	709
Ivanov V.E. ....	223
Ivanov V.Yu. ....	428, 492, 494, 495, 606
Ivanov Yu.P. ....	107, 155
Ivanova G.V. ....	414
Ivanova N.B. ....	158
Ivanova O. ....	281
Ivanova O.S. ....	626
Ivanova T.I. ....	634, 649
Ivanovskii A.L. ....	192
Ivantsov R. ....	281
Ivantsov R.D. ....	204
Iwanowski P. ....	885
Iwasieczko W. ....	651

---

## J

Jadzyn J. ....	863
Janson O. ....	854
Jantaratana P. ....	619
Jedrak J. ....	891
Jensen N. ....	605
Jernenkov K.N. ....	513
Jiang F.-X. ....	821

Jiang L. ....	910
Jigounov A. ....	226, 867
Jodlauk S. ....	174
Johansson B. ....	28
Joshi L. ....	264

---

## K

Kabanov Yu.P. ....	278
Kabychenkov A. ....	464
Kachel T. ....	206, 337
Kachur I. ....	218
Kachur I.S. ....	474
Kaczorowski D. ....	534
Kadomtseva A.M. ....	492, 495, 606
Kafesaki M. ....	95
Kajňaková M. ....	186, 187
Kakazei G. ....	621
Kalashnikov I. ....	449
Kalashnikova A.M. ....	63, 64, 67
Kalenkov M.S. ....	349
Kalimullina E. ....	656
Kalinikos B.A. ....	475
Kalinin Yu. ....	128, 209, 791, 807
Kalinin Yu.E. ....	108, 110, 111, 121, 139, 165, 796, 806
Kalinov A.V. ....	174, 194
Kalish A.N. ....	210
Kalitka V.S. ....	181, 554, 642
Kalmykov S. ....	234
Kalmykov Yu.P. ....	366
Kalyakin L.A. ....	802
Kamali S. ....	132
Kamantsev A. ....	662
Kamarad J. ....	292
Kamenev A. ....	174
Kamenev A.A. ....	194
Kameneva M.Yu. ....	197
Kamentsev K.E. ....	489
Kamikawatoko T. ....	543
Kamilov I.K. ....	675, 686, 702
Kamilov K.I. ....	642
Kaminskaya T.P. ....	117, 665
Kaminski B. ....	61
Kamzin A.S. ....	101, 323
Kandaurova G.S. ....	361
Kanjouri F. ....	444, 687
Kantarci N. ....	439
Kantorovich S. ....	229, 869
Kapelnitsky S.V. ....	725

Karashtin E.A.	707	Khasanov R.	89
Karavainikov A.V.	212	Khasawneh M.A.	344
Karenowska A.D.	589	Khatsko E.N.	388
Karminskaya T.	78, 351	Khavronin V.P.	173, 886
Karminskaya T.Yu.	77, 507	Khaydukov E.V.	714
Karpenkov A.	643	Khaydukov Yu.N.	347, 513
Karpenkov A.Yu.	641	Khenkin L.V.	235
Karpenkov D.Yu.	641	Khivintsev Y.	397
Karpova T.	376	Khizriev K.Sh.	124
Kartashev A.V.	176	Khohlov D.	843
Karzanov V.V.	286	Khokhlov D.R.	424
Kaschenko M.	174	Khokhlov N.E.	210
Kashevsky B.	572	Khokhlov V.A.	677
Kashevsky S.	572	Kholin D.I.	133, 146
Kashevsky S.B.	767	Kholopov V.L.	235, 248
Kashirin M.A.	118, 121, 138, 159	Khomskii D.I.	34, 36, 174
Kashkin D.	585	Khovailo V.	295, 633, 656, 658
Kashurkin O.Yu.	372, 375	Khovaylo V.	647
Kassan-Ogly F.A.	850	Khovaylo V.V.	293, 646
Kataev V.	562, 853	Khramova O.D.	714
Katanin A.A.	44	Khusainov M.	351, 353, 503
Kato K.	320	Khvalkovskiy A.	671
Katsnelson M.I.	309	Khvalkovskiy A.V.	13, 706
Katsumata K.	325	Khvalkovsky A.	705
Kaul A.	38, 837	Kida N.	65
Kaul A.R.	174, 181, 194, 768	Kiessling A.	541
Kawabata S.	74, 77	Kikoin K.	896
Kawasaki K.	587	Kim C.G.	324
Kay K.Mc.	254	Kim D.-H.	321
Kazak N.V.	158, 607	Kim I.	608
Kazakov A.	550	Kim J.-H.	857
Kazakov A.P.	626, 630, 631, 769	Kim J.-V.	356
Kazakova O.	137	Kim K.H.	608
Kazei Z.A.	197	Kim S.-K.	84
Kazhan V.A.	236	Kimel A.	200
Kazin P.E.	240	Kimel A.K.	337
Kazuhiro N.	411	Kimel A.V.	62, 63, 67, 206, 309, 584
Ke L.	897	Kimmel G.	556
Keimer B.	857	Kimura A.	294
Keshri S.	264	Kiparisov S.Ya.	106, 150
Ketov S.V.	406	Kirillova M.M.	680
Ketsko V.A.	172	Kirilyuk A.	62, 63, 67, 200, 206, 274, 309, 337, 584
Ketterson J.B.	83	Kirilyuk A. I.	309
Keune W.	262	Kirman M.	737
Khaibullin R.I.	204, 716, 717, 718	Kirschner J.	151
Khaire T.S.	344	Kiryukhin V.	902
Kharchenko A.	621	Kiseleva T.Yu.	126
Kharisov A.T.	761, 802	Kisielewski J.	582
Kharkov A.M.	695	Kisielewski M.	582
Kharlamova A.	419	Kislinski Y.V.	893
Kharrasov M.Kh.	454	Kislinskii Y.V.	511
Khasanov N.A.	113		

Kitamura Y.....	891	Koplak O.V.....	762
Klauss H.-H.....	140	Koptsik S. ....	774
Klauss H.–H.....	89	Koralewski M. ....	57
Klein P. ....	830	Korenev S.V. ....	405
Kleiner R.....	79, 345, 346	Korenev V.L. ....	62
Kleinerman N.M. ....	162, 412, 417	Korili S.A.....	829
Klenov N.....	351	Korneev V.I. ....	683, 760
Klimenko E.M.....	235	Korneeva Y.....	778
Klimin S. ....	174	Kornilov A.A. ....	117
Klimin S.A. ....	733, 735, 855	Kornilov V.M. ....	261
Klimov S. ....	451	Kornilova A. ....	778
Klingeler R...89, 561, 562, 564, 733, 851, 853		Korolev A.V. ....	640, 677
Klinkigt M.....	869	Korolev D. ....	245, 574
Klos A. ....	93	Korolev V. ....	245, 574
Kłos J.W.....	379	Koroleva L.I.....	168, 627
Klose C.....	344	Korolyov A. ....	140
Knyazev Yu.V.....	211	Korolyov A.V. ....	685
Kobayashi K.....	529	Korotin M.A. ....	45
Kobayashi N.....	320	Korovin V.M.....	236
Kobyakov A.V. ....	104	Korovushkin A.E. ....	237
Kocharian A.N. ....	42	Korshunov A.S. ....	734
Kochetov O.I.....	833	Korznikova G.F. ....	410
Kochura A.V. ....	724	Korzun A.Yu.....	404
Koelle D. ....	79, 345, 346	Koschny Th.....	95
Kohlstedt H. ....	346	Kosel J. ....	682
Kohn K. ....	610	Koshkid'ko Yu.S. ....	293, 649
Kohout J. ....	769	Koshkodaev D.S. ....	240
Kojima K.....	320	Kostromitin K.I.....	293, 628
Koksharov Yu.A. ....	776	Kostromitina N. ....	175, 182
Kolano-Burian A.....	548	Kostromitina N.V. ....	37
Koledintseva M.Y. ....	377	Kostyrko T.....	15
Koledov V.....295, 296, 633, 656, 658, 662		Kostyuchenko V.V. ....	284
Koledov V.V.....	554, 632, 663	Kotelnikova O.A.....	47, 846
Kolesnikov E.A.....	123	Kotov L.N. 108, 110, 111, 632, 752, 781, 782, 805, 806	
Kolmychek I.A.....	583	Kotov V.A.....	212, 881
Kolokoltsev O.....	217	Kovac J. ....	57
Kolotov O.S. ....	797	Kovač J. ....	189
Komissarova L.Kh. ....	232	Kovalenko V.....	520
Komogortsev S.....	128	Kovalev B.B. ....	722
Komogortsev S.V.....142, 399, 405, 423, 792		Kovalev V.I.....	719
Kondratenko V.V.....	130	Kovnir K.A. ....	390
Kondusov V. ....	807	Kozeeva L.P.....	197
Kondyan S.....	152, 623	Kraetchmer W.....	565
Koneracká M.....	863	Kramarenko E.Yu. ....	872
Konoto M. ....	13	Kramer R.B.G.....	345
Konovalov P.N.....	626	Krapf A. ....	520
Konovalova A. ....	483, 770	Krasheninnikov A.....	705
Konovalova A.O. ....	472	Krasheninnikov A.V. ....	13
Konstantinova E.A.....	143, 672	Krasnorusski V.N. ....	435
Kopcansky P. ....	57	Krasnorussky V.N.....	428
Kopčanský P. ....	863	Kravchenko S.V.....	268
Koplak O.....	26, 728, 816		



Krawczyk M.....	801	Kurbatova Yu.....	66
Kreines N.M.....	133, 146, 844	Kurebayashi H.....	14
Krehova M.....	870	Kurkin M.I.....	147, 339, 700, 847
Krenke T.....	664	Kurkin T.S.....	226
Krikunov A.I.....	386, 423	Kurlyanskaya G.V.....	619, 699, 798, 804
Krinitsina T.....	703	Kurmaev E.Z.....	282, 598, 822
Krinitsina T.P.....	689	Kurtanov N.I.....	383
Krishtopenko S.S.....	531	Kushnir A.E.....	768
Krokhotin A.I.....	644	Kushnir S.E.....	240
Krug von Nidda.....	491	Kushnir V.N.....	514, 594
Kruglyak V.V.....	222, 590	Kusmartsev F.V.....	890
Krumme B.....	262	Kutcher D.S.....	746
Krutikova E.....	238	Kuz'min M.....	88
Krutyanskiy V.L.....	583	Kuz'mova A.V.....	194
Krylov V.I.....	512, 636	Kuzemsky A.L.....	466
Krynetskii I.....	520	Kuzian R.....	561
Ku C.S.....	478	Kuzmenko A.....	60
Kubota H.....	13	Kuzmenko A.M.....	494, 606
Kubota T.....	438	Kuzmenko A.P.....	102
Kuchin A.G.....	211, 437, 651	Kuzmin D.A.....	488
Kuchin D.....	656	Kuzmin L.....	595
Kudakov A.D.....	367	Kuzmin Yu.I.....	211
Kudasov Yu.B.....	444, 734	Kuzmova T.....	174
Kudrevatykh N.V.....	120, 135, 136	Kuznetsov A.....	166, 577, 709
Kudriavtsev Yu.....	534	Kuznetsov A.A.....	232
Kudrin A.M.....	118	Kuznetsov A.R.....	417
Kudrin A.V.....	688, 726	Kuznetsov A.V.....	427, 678
Kudryashov A.....	723	Kuznetsov P.A.....	399, 792
Kudryavtcev V.O.....	391	Kuznetsova O.B.....	864
Kugel K.I.....	36, 174, 533, 838, 887	Kuznetsova Yu.....	753
Kuklin A.I.....	226, 239, 867	Kuzovnikov A.....	402
Kulagin D.V.....	487	Kuzovnikova L.....	402
Kulagin N.E.....	473, 706	Kveglis L.I.....	382
Kulakovski V.D.....	674	Kytin V.....	723
Kulatov E.....	708	Kyzyrgulov I.R.....	454
Kulatov E.T.....	43, 305, 424		
Kulbachinskii V.....	723		
Kulemanov I.V.....	820		
Kulesh N.A.....	122, 134, 426	<b>L</b>	
Kulikov D.....	448		
Kulkova S.....	637	Lachaize S.....	51, 263
Kumagai K.....	474, 837	Lachinov A.N.....	261
Kumar P.....	213	Lacroix C.....	350
Kun'kova Z.E.....	719	Lacroix L.-M.....	51, 263
Kunikin S.A.....	251	Ladygina V.P.....	767
Kuo Y.K.....	515, 742	Lafrentz M.....	61
Kupriyanov M.....	78, 351	Lagae L.....	356
Kupriyanov M.Yu.....	77, 79, 350, 507, 514, 594	Lagarkov A.N.....	372, 373
Kupriyanova G.....	131	Lahderanta E.....	724
Kupriyanova G.S.....	701	Lähderanta E.....	196
Kupryanova G.....	912	Lamonova K.....	89
Kurbakov A.I.....	173, 886	Lančok A.....	769

Lang T.....	870	Lin C.T.....	857
Lapa P.N.....	624	Lin J.-Y.....	894
Lara A. ....	620	Lindner J.....	21, 137
Lardé R.....	285	Link P.....	857
Larin V.S.....	630	Lisboa-Filho P. ....	715
Larrea J.....	858	Lisin V.N. ....	269
Larumbe S.....	829	Lisovskii F.V. ....	486
Lasek M.P. ....	806	Liu H.-L. ....	68
Lashkul A.....	196, 724	Liu X.....	535
Laureti S.....	276	Liubimov B.Ya. ....	280
Laval J.Y.....	185	Llandro J.....	54
Lázpita P. ....	291, 297	Lobo D.N.....	552
Lazuta A.V.....	173, 886	Lobov I.D.....	680
Le Guyader L. ....	584	Locatelli N. ....	13, 705
Leadley D.R. ....	698	Lock E.H.....	785, 786
Lebedev A.V.....	579	Loev U. ....	853
Lebedev V.T.....	867	Loewenhaupt M.....	561, 645
Lebedeva E.....	791	Lofland S.E.....	515
Lechevallier L. ....	285	Logginov A.S.....	486
Lecommandoux S. ....	571	Loginov N.....	585
Lee B.W. ....	214	Lograsso T.M.....	28
Lee H.Y.....	478	Logunov M. ....	396, 585
Lee J.H. ....	260	Loidl A.....	740, 895
Lee K.S.....	84	Loktev V.M.....	913
Lee S. ....	902	Lomakina I.....	750
Lee Z.H. ....	56	Lomayeva S.F.....	374
Leite D.M.G. ....	715	Lomov A.A. ....	725
Leithe-Jasper A. ....	555	Lopatin Yu.G. ....	120
Lemmens P.....	484, 736	Lopatina E.A.....	406
Leonyuk N.I. ....	907	Lopez J.M. ....	258
Leostean C.....	874	López-Quintela M.A.....	22
Lepalovskij V.N.....	116, 223, 794, 804	Lorenz T.....	174
Lepeshev A. ....	402	Lorenz W.E.A.....	561
Leskova J.V.....	183	Lorenzer A. ....	858
Lesniak M.S. ....	321	Loshkareva N.....	175
Lesnikov V.P.....	286, 534, 725, 727	Loshkareva N.N.....	37, 685
Letellier F.....	285	Lozovik Yu.E.....	42
Levchenko A. ....	709	Łuczak J.....	15
Levchenko G.....	578	Lue C.S. ....	515, 742
Levchenko G.G. ....	191, 487	Luetkens H.....	89
Levchuk S.A.....	286	Lukoyanov A.V. ....	211
Levina V.V.....	123, 126	Lukshina V.A.....	407, 409, 417, 798
Levshin N.L. ....	367	Lukyanova E.N.....	716
Levy M.....	213	Lupu N. ....	438
Levy S. ....	201	Lyadov N.M.....	716, 717
Li C.M.....	637	Lyakhova M.B.....	383, 746, 747
Li L.....	148	Lyanda-Geller Y. ....	535
Li L.A.....	104	Lyapilin I.I. ....	697
Li X.P.....	56	Lysenko S.N. ....	579
Li Y. ....	857	Lyubina J. ....	657
Lichtenstein A.....	853	Lyubutin I.S.....	548
Lim P.B. ....	340		

---

**M**

Maccherozzi F.....	557
Maekawa S.....	10, 354
Maeter H.....	89
Magadeev E.....	751
Magnitskaya M.V.....	305
Mahdavifar S.....	741
Mahloojian M.R.....	444
Mahmoodi R.....	141
Maignan A.....	607
Majumdar S.....	656
Makagonov V.A.....	118
Makagonov V.A.....	121
Makarov S.I.....	262
Makarova O.L.....	681
Makhnev A.A.....	479
Makino A.....	438
Makinose Y.....	325
Maklakov S.A.....	372, 375
Maklakov S.S.....	375
Makovetskii G.....	693
Makovetskii G.I.....	485
Maksimov E.G.....	305
Malakhovskii A.....	215, 218
Malakhovskii A.V.....	474
Malek J.....	561
Maleyev S.V.....	29, 300
Malikov I.V.....	710
Malinina R.....	400
Maltsev V.V.....	907
Mamalui Ju.A.....	755, 756, 757
Mamedov T.N.....	243
Mamonova M.....	451
Manchon A.....	260
Manfrini M.....	356
Manosa L.....	664
Mañosa L.....	292
Mansurova M.....	217
Mantovan R.....	912
Maratkanova A.N.....	374
Marchenkov V.V.....	637, 704
Marenkin S.F.....	675, 686, 702, 724
Marin C.N.....	314
Marinho E.P.....	576
Marinica O.....	575
Marins de Castro M.....	266
Marinz de Castro M.....	254, 267
Markelova M.N.....	768
Markin P.E.....	653
Markina M.....	169, 851
Markovich V.....	885
Marquina C.....	55
Marten T.....	553
Martin C.....	607
Martinez E.....	82
Martins F.H.....	570
Martovitsky V.....	520
Martyanov O.....	773
Marzo J.....	55
Mashirov A.....	196, 295, 656
Mashirov A.....	633
Maslov D.A.....	444, 734
Maslova I.S.....	564
Mateos P.....	103
Mathieu R.....	276
Mathur N.D.....	557
Matovnikov A.V.....	741
Matsnev M.E.....	171, 178, 716
Matsukura F.....	529
Matsushita N.....	325
Matsynin A.A.....	721
Matyunin A.V.....	797
Maydykovskiy A.I.....	213
Maykin V.Yu.....	177
Maziewski A.....	200, 582
Mazilkin A.A.....	821
Mazov L.S.....	898
Mazur A.S.....	772
Mazurenko V.....	853
Mazurkin N.S.....	683, 760
McLeod J.A.....	598
Meckenstock R.....	21, 137, 298
Medvedev Yu.V.....	677
Medvedeva I.V.....	637
Medvedeva L.I.....	743
Medvedeva M.....	447
Meffre A.....	51, 263
Mehdaoui B.....	51
Meilikhov E.Z.....	530, 729
Meiszterics A.....	226
Melenev P.V.....	314
Melnikov N.B.....	458, 461
Melnikov S.A.....	385
Melnikova L.....	57
Men`shov V.N.....	303, 815
Ménard D.....	827
Mendelev V.....	577
Mendizabal I.....	829
Mengotti E.....	584

Mens`chenin V.V.....	847	Molenkamp L.W.....	62
Menshenin V.V.....	905	Molkanov P.L.....	173, 886
Mentink J.H.....	309, 457	Mollaev A.Yu.....	675, 686, 702
Menushenkov A.P.....	389, 390, 391, 437	Molokeev M.S.....	176, 184
Menushenkov V.P.....	384, 389, 391, 406, 421	Monod Ph.....	185
Menzel D.....	29	Moreira A.F.L.....	318
Merazzo K.J.....	103	Morgunov R.....	728, 737, 816
Merzlikin A.M.....	92, 207, 882	Morgunov R.B.....	762
Meshkov G.A.....	364	Moritz J.....	285
Mestnik Filho J.....	570	Morosov A.I.....	306
Metlushko V.....	620	Morozov A.S.....	168, 627
Meyerheim H.L.....	151	Morozov I.L.....	404, 792
Michel K.H.....	833	Morozova N.A.....	165
Michelini F.....	43	Morozova N.V.....	403, 404
Michels A.....	359	Moshchalkov V.V.....	345, 505
Migunov V.....	283	Moshnyaga V.....	482
Mikhailov G.M.....	710	Moskvin A.....	520
Mikhailov V.....	201	Moskvin A.S.....	521, 562, 859
Mikhailova M.P.....	534	Moskvin E.V.....	29
Mikhailovsky Yu.O.....	630	Moskvina N.....	376
Mikhalev K.....	837	Mostovoy M.....	605
Mikhaylovskiy R.V.....	222, 590	Mostovshchikova E.V.....	37, 685
Miki H.....	293	Motylev I.A.....	661
Mill B.....	851	Mousalitin A.M.....	722
Mill B.V.....	735	Moya X.....	557
Milyaev I.M.....	410	Mozul K.A.....	114
Milyaev M.....	424, 703	Mrabti H.El.....	366
Milyaev M.A.....	680, 689	Mudryk Ya.....	659
Minina E.....	229	Muhamatchin K.R.....	754
Mints R.G.....	346	Mukhamedganov E.....	148
Miroux S.....	571	Mukhamedzhanov E.Kh.....	513
Mirebeau I.....	681	Mukhin A.A.....	492, 494, 495, 606
Mironov O.A.....	698	Mukovskii Y.M.....	515
Mironyuk A.N.....	509	Mukovskii Ya.M.....	173, 195, 481, 491, 886
Mischenko I.N.....	322	Mulyukov Kh.....	633
Mishina E.....	482	Münzenberg M.....	338
Mitroova Z.....	57	Murphy A.P.....	614
Mitrukovskiy S.I.....	583	Murtazaev A.....	508
Mitsiuk V.I.....	644	Murtazaev A.K.....	124, 516, 850
Mitsuteru I.....	411	Murtazaev A.K.....	193
Mitzin K.V.....	504	Murtazin R.R.....	365, 460, 462, 748
Mizokawa T.....	34	Murzanov M.S.....	746
Mizumoto T.....	588	Murzina T.V.....	583
Mizusawa K.....	275	Musabirov I.....	633
Mizutani Y.....	878	Mushenok F.B.....	762
Moeller A.....	853	Mushnikov N.V.....	87, 394, 412, 413, 414, 433, 653
Moewes A.....	598, 822	Myagkov V.G.....	161, 721
Mohammadi N.....	444	Myatiev A.A.....	821
Moiseev A.A.....	391, 798, 799	Mysik A.A.....	282
Moiseev K.D.....	534		
Moiseyev A.....	455		
Mokhovikov A.Yu.....	403, 404		

---

**N**

Nagaosa N.....	73, 605
Nagy B. ....	347
Nahas Y.....	16
Nakagawa T. ....	325
Nakai T.....	320
Nakai Y. ....	878
Nakano M.....	543, 544
Nakayama H.....	543
Nalbandyan V.B.....	429, 743
Naletova V. ....	234
Nan A. ....	874
Nane O. ....	439
Napolskii K.S.....	790
Narozhnyy M.V. ....	855
Nasirpouri F. ....	141
Naumov S.....	175, 182
Naumov S.V.....	37, 685
Naumova L.....	703
Naumova L.I. ....	689
Nazarov V. ....	750
Nazarov V.N. ....	462
Nazmunnahar M.....	663
Nechepurenko I.A. ....	223
Nedopekin O.V. ....	77, 507
Nedukh S.....	621
Nefedov I.M. ....	345
Nénert G.....	608
Nenkov K. ....	657
Neustroev N.S.....	367
Neverov V.N.....	506
Nevolin V.N.....	701
Ney A. ....	819
Nezhdanov A.V.....	688
Neznakhin D.S. ....	120, 135, 136
Ng W.C. ....	56
Nikiforov A.E.....	35, 183
Nikiforov V.N.....	776
Nikitenko V.I. ....	156, 278
Nikitenko Yu.V.....	347, 513
Nikitin A.L. ....	233, 237
Nikitin L.V. ....	233, 237, 439
Nikitin M.P. ....	322, 326, 327, 766
Nikitin P.I.....	326, 766
Nikitin S. ....	843
Nikitin S.A. ....	393, 549, 634, 644, 649, 665
Nikitov S. ....	397, 585, 615
Nikoladze G.M.....	797
Nikolaev A.L. ....	237
Nikolaev A.V.....	833, 906
Nikolaev S.N.....	714, 727
Nikolaev V.V.....	905
Nikolaev Yu.Ye. ....	761
Nikolaeva E.P. ....	906
Nikulin A.A. ....	583
Nikulin Y.V. ....	408
Nipan G.D.....	172
Nishimoto S. ....	561
Nizhankovskii V. ....	534
Nobuhiro M. ....	411
Noda J. ....	668
Nolting F.....	584
Nomerovannaya L.V.....	479
Nomura K. ....	605
Nordblad P.....	276
Nosov A.....	376
Noudem J.....	185
Novakova A.A. ....	123, 126, 235
Novikov A. ....	209
Novikov A.I. ....	130, 648, 719
Novikov I.M. ....	117
Novikov V.V.....	741
Novitskii N.....	200
Novitskii N.N.....	490, 803
Novitskij N.N.....	172
Novodvorsky O.A.....	714
Novokshonov S.G.....	470
Novosad V. ....	321
Novoselov K.S.....	10
Nowak U.....	334
Nozieres J.P. ....	254
Nurgaliev T.....	170
Nuzhdin V.I. ....	716

---

**O**

Odenbach S.....	871
Ogloblichev V.....	474
Ognev A.V.....	112, 141
Ohno H.....	529
Ohtani T.....	891
Okada K.....	132, 325
Okame S.....	275
Okulov V.I. ....	180, 711
Oliveira W. ....	276
Olivera J.....	829
Olkhovik L.P.....	323
Olkov S.A. ....	422

Ono T. ....	529	Park J.T. ....	857
Oppeneer P.M. ....	331	Park S.Y. ....	214
Oprea A. ....	430, 679	Parshin A.P. ....	385
Orlov A.F. ....	820	Paschen S.B. ....	858
Orlov A.V. ....	326	Pascua G. ....	89
Orlov Yu. ....	14	Pashchenko M.I. ....	474
Orlova A. ....	131	Pashchenko V. ....	736
Orlova A.N. ....	701	Pashchenko V.A. ....	484
Orlova N.B. ....	339, 700	Pashkevich M. ....	200
Orlova T.S. ....	185	Pashkevich Yu. ....	89
Ortiz W.A. ....	715	Pastushenkov Yu. ....	643
Orue I. ....	297, 699	Pastushenkov Yu.G. ....	641, 649, 746, 747
Osewski P. ....	93	Pathak A.K. ....	550, 626, 631
Osipov A.V. ....	372, 375	Patrin G. ....	148
Osipov M.A. ....	517	Patrin G.S.. 104, 105, 106, 144, 150, 669, 684, 911	
Ospennikova O.G. ....	385	Patrin K.G. ....	104, 105
Ossau W. ....	62	Patselov A. ....	424
Ostatochnikov V.A. ....	149	Paula F.L.O. ....	570
Ostler T.A. ....	206, 337	Pavlenko O.V. ....	906
Ostrovskaya N.V. ....	464	Pavlov E. ....	615
Ouchi K. ....	20	Pavlov V.N. ....	734
Ovchenkova I.A. ....	634	Pavlov V.V. ....	61
Ovchinnikov S. ....	14	Pavlukhina O. ....	639
Ovchinnikov S.G. ....	109, 158, 548, 607, 911	Pavlyk L.P. ....	420
Ovechkina N.A. ....	37	Pawar S.H. ....	518
Overby M. ....	535	Pawar S.S. ....	518
Ovsyannikov G.A. ....	501, 511, 670, 893	Pawlak D.A. ....	93
Ozawa T. ....	320	Pecharsky V.K. ....	659
Özçelik B. ....	439	Peddis D. ....	276
Ozherelyev V.V. ....	469	Peighambari S.M. ....	141
<hr/>			
<b>P</b>		Pelmeneva A.V. ....	403
Pal'chik M.G. ....	106	Penciu R. ....	95
Palandage K. ....	42	Pereira A.L.J. ....	715
Palewski T. ....	629, 649, 657	Pérez-Landazabal J.I. ....	829
Paliy N. ....	807	Pernechele C. ....	292
Pamyatnykh E.A. ....	180, 711	Pernod P. ....	617
Pamyatnykh L.A. ....	361	Perov N. ....	166, 243, 401, 635, 765, 774, 842, 912
Pamyatnykh S.Y. ....	361	Perov N.S.. 118, 130, 235, 489, 513, 630, 714, 725, 727, 820	
Panas A.I. ....	710	Perzynski R. ....	314, 317, 569, 570
Panchenko V.Y. ....	322, 327	Pestun A.E. ....	173, 886
Panchenko V.Ya. ....	714	Peters L. ....	309
Panfilov A.S. ....	895	Petkovic I. ....	354
Pankov F. ....	201	Petrakovskaya E.A. ....	104
Pankratov N.Yu. ....	644	Petrakovskii G. ....	623
Pankrats A. ....	152, 623	Petrakovskii G.A. ....	176
Paoluzi A. ....	292	Petrakovskya E. ....	773
Papusoi C. ....	254, 267	Petrashov V.T. ....	349
Parfeniev R.V. ....	534	Petrenko A.V. ....	747
		Petrov D.A. ....	204, 374

Petrov S.V. ....	563	Polyakov V.V. ....	144
Petrov V.M. ....	493, 609	Polyakova K.P. ....	144
Petrova A.E. ....	28	Polyanski V.A. ....	766
Petrzhik A.M. ....	501, 511	Pomerantseva E.A. ....	388
Petukhov D.S. ....	506	Ponosov Yu.S. ....	37, 282
Phillips L. ....	557	Pontius N. ....	206, 337
Pichugin A.Yu. ....	270	Poperechny I.S. ....	315
Pigalev P.A. ....	769	Popkov A.F. ....	473, 683, 760
Pilyuk E. ....	196	Popkov S.I. ....	184
Pirogov A.N. ....	433	Popov A.I. ....	902
Pirogov Yu.A. ....	766	Popov A.P. ....	279
Pirota K.R. ....	546	Popov S.E. ....	35
Piryatinskaya V. ....	218	Popov Yu.F. ....	492, 495, 606
Piryatinskaya V.G. ....	474	Popova D. ....	332
Pisarev R.V. ....	61, 63, 64, 67, 610	Popova E.A. ....	733
Piskorskiy V.P. ....	385	Popova M.N. ....	610, 733, 735, 855, 907
Piskunov Yu. ....	474	Porcari G. ....	292
Piskunova N.I. ....	732	Portemont C. ....	254, 266, 267
Pismenova N.E. ....	191	Posth O. ....	137, 298
Pivkina M.N. ....	117, 118	Postivey N. ....	215
Plakida N.M. ....	46	Potapov A.P. ....	407, 409
Planes A. ....	292, 664	Povarov K.Yu. ....	563
Plankina S.M. ....	688	Pozdnyakov A.V. ....	800
Platunov M.S. ....	158	Pratt Jr.W.P. ....	344
Pleschov V.G. ....	153	Prebeanu L. ....	254
Plis V.I. ....	902	Prejbeanu I.L. ....	266, 267
Plokhov D.I. ....	902	Preobrazhensky V. ....	617
Plotkin Z. ....	52	Presniakov I.A. ....	171, 178, 521, 716
Plyashkevich M.L. ....	231	Prevost B. ....	510
Pochylski M. ....	57	Prida V.M. ....	276, 296, 663
Poddubnaya N.N. ....	490, 803	Priolkar K.R. ....	552
Podlivaev A.I. ....	517	Prischepa S. ....	78
Podolski V.V. ....	534	Prischepa S.L. ....	514, 594
Podolskii V.V. ....	286, 725, 727	Privezentsev R.V. ....	173, 886
Podyalovskii D.I. ....	557	Proglyado V. ....	703
Pohl M. ....	881	Proglyado V.V. ....	689
Pokatilov V. ....	425, 483, 770	Prokhorov A.Yu. ....	677
Pokatilov V.S. ....	382, 434, 472	Prokhorov I. ....	572
Pokholok K.V. ....	160	Prokof'eva M.M. ....	674
Pokhrel M. ....	203	Prokopieva T. ....	229
Pokrovskiy S.V. ....	517	Prokopov A.R. ....	212
Poleshikov S.M. ....	805	Prokopyeva T. ....	869
Polevoy S.Yu. ....	207	Proshin ....	351
Polikarpov M.A. ....	100, 322, 327, 432	Proshin Yu. ....	353, 503, 519
Politova G. ....	629	Proshkin A.V. ....	653, 654, 690
Pollard R.J. ....	614	Protasova S.G. ....	821
Polukhin D.S. ....	459	Prozorova L.A. ....	565, 856
Polunin V.M. ....	865	Prudnikov P. ....	447, 448, 449, 450, 452
Polushkin N.I. ....	616	Prudnikov V. ....	450
Polyakov A. ....	510	Prudnikov V.N. ....	550, 626, 630, 631
Polyakov P.A. ....	797	Prudnikova M.V. ....	626, 631
Polyakov P.I. ....	772	Prudnikov V. ....	451

Przybylski M.....	151
Puertas S.....	55
Pugach N.....	595
Pugach N.G.....	79
Pukhov A.A.....	208, 223
Puzik I.I.....	123
Puzniak R.....	885
Pyanzina E.....	229
Pyatakov A.P.....	364, 486, 810, 906
Pyatygin A.I.....	422
Pytalev D.....	174

---

## Q

Quinsat M.....	694
----------------	-----

---

## R

Radkovskaya A.....	98
Radu I.....	206, 337
Radyush Yu.V.....	485
Raikher Yu.L.....	226, 314, 315, 317, 573, 862, 867, 868
Raj K.....	314
Rajh T.....	321
Rajput S.S.....	264
Rakhimov S.A.....	203
Rakhmanov A.A.....	789
Rakhmanov A.L.....	36, 838, 887
Rakhmatullin I.I.....	460
Ramazanoglu M.....	902
Ramazanov M.K.....	516, 850
Ramazanova A.....	574
Rameev B.Z.....	717
Ramos A.....	151
Raposo V.....	103, 398
Raquet B.....	533
Rasing T.....	524
Rasing Th.....	62, 63, 67, 200, 206, 309, 337, 457, 584
Rassi D.....	771
Ratcliff W.....	902
Rautskii M.V.....	104
Rautskiy M.V.....	669
Ray N.....	681
Raymond L.....	43
Razdolski I.....	67
Razmadze A.G.....	377
Rednic L.....	874
Reid A.H.M.....	62
Reininger T.....	541
Ren Y.....	295
Reser B.I.....	458, 461
Respaud M.....	51, 263
Ressouche E.....	495
Richter J.....	561
Richter K.....	830
Richter R.....	870
Righi L.....	292
Rinkevich A.....	376
Ritter C.....	608, 645
Rivas B.....	22
Rivas J.....	22
Rivkin K.....	83
Robert A.....	569
Roche S.....	445
Rocheva V.V.....	714
Rod I.....	137
Roddatis V.V.....	727
Rodionova V.....	166, 401, 635, 652, 764, 765, 774, 912
Rodionova V.V.....	630
Rodmacq B.....	254, 267, 285
Rodriguez Fernández J.....	297
Rogachev A.V.....	226, 867
Rogalev A.....	607, 820, 897
Rohrkamp J.....	174
Rojas D.P.....	297
Rokhinson L.....	535
Romanova O.....	693
Romashev L.N.....	680
Ronkin M.....	376
Ronning F.....	428
Ronnow H.M.....	858
Rosa W.....	295
Rosa W.O.....	296, 663
Rosenfeld E.V.....	87
Roshchin I.V.....	25
Rosner H.....	555, 852
Rossen S.....	457
Rosta L.....	226
Roussigné Y.....	614
Rozanov K.N.....	372, 374, 375, 378
Rozhansky I.V.....	532
Rozhkova E.A.....	321
Rozhnovskaya A.....	287, 419
Rozova M.G.....	160
Rubacheva A.D.....	820
Ruban A.V.....	417, 553
Rudenko A.....	853



Rudnev I.A.	517
Rudoy Yu.G.	47, 846
Rumyantseva V.V.	113
Runov V.V.	886
Rusakov V.S.	171, 178, 521, 716, 769
Rusakov V.V.	314
Ryabinkina L.	693
Ryapolov P.A.	865
Ryasny G.K.	833
Rybakov Yu.P.	308
Ryjikov I.	419
Rykova A.I.	388
Rylkov V.V.	533, 714, 727
Ryoma M.	411
Ryzhikov I.A.	372, 375
Ryzhkovskii V.M.	644
Ryzhov V.A.	173, 886

---

## S

Saarela M.	890
Saber F.S.	446
Sabiryanova E.A.	120
Sablina K.A.	184
Sadecka K.	93
Sadovskii M.V.	72
Sadykov A.	474
Sadykov R.A.	428, 435, 636
Safin A.	705
Safran S.	597
Safronova E.	166, 764, 765
Sagdatkireeva M.B.	113
Sahara M.	544
Said-Galiyev E.E.	118
Saito H.	586
Saito T.	910
Sakai H.	604
Sakharov V.	397
Sakurai H.	340
Salamatin A.V.	833
Sales B.C.	565
Saletsky A.M.	145, 626
Salev P.	753
Samancioğlu Y.	638, 639
Samanta T.	636
Samardak A.S.	112, 141
Samarin N.A.	427, 624, 678, 781
Samohvalov E.A.	429
Samsonova V.	166, 774
Sánchez M.L.	296
Sánchez T.	296
Sandhu A.	214
Sandratskii L.	151
Sandre O.	571
Sannikov D.G.	780
Sannikov I.	709
Sanson C.	571
Santos J.D.	296
Sapoletova N.A.	790
Sapozhnikov M.V.	286
Sapronova N.V.	184
Sardar D.K.	203
Sarıkürkcü C.	639
Sarychev A.	94
Sarychev A.K.	887
Sarychev M.N.	177
Sato M.	73
Sato T.	333
Savchenko A.G.	384, 421
Savchenko A.S.	487
Savelieva O.A.	429, 743
Savin P.A.	794
Savina Yu.	736
Savina Yu.O.	484
Sazanova L.A.	188
Sboychakov A.O.	36, 838
Scharinger S.	346
Schavrov V.	633
Schegoleva N.N.	282
Schlickeiser F.	334
Schmalz H.	870
Schmaus S.	16
Schmidt A.	227
Schneider C.M.	335
Schneidewind A.	857
Schnelle W.	555
Schöps O.	64
Schrefl T.	356
Schreiber R.	146
Schultz L.	290
Schütz G.	821
Sechin D.A.	906
Sedin Yu.Yu.	517
Selezneva N.V.	153, 157
Seleznyova K.	215
Semchenko V.V.	382
Semenenko V.N.	373
Semeno A.V.	154, 624, 781
Semenov A.L.	403, 404, 792
Semenov V.S.	749
Semenova E.M.	383, 641, 746, 747
Semenova O.R.	241

Sementsov D.I.....	149	Shikov A.A. ....	28
Semirov A.V. ....	391, 798, 799	Shimizu R. ....	333
Semisalova A.S. 118, 130, 665, 714, 725, 727, 820		Shimshoni E.....	732, 855
Senina V.A. ....	117	Shin K.H. ....	260
Seredkin V.A.....	144, 150, 204	Shinde K.P. ....	518
Serga A.A.....	589	Shinkevich S. ....	310
Sergeev A.S.....	906	Shipkova I. ....	791
Serikov V.V. ....	162, 412, 417	Shishkin D.A.....	654
Serrate D. ....	55, 292	Shishkov S.Yu. ....	100
Shabanova N. ....	520	Shitsevalova N.....	709
Shadrin A.V. ....	511, 893	Shitsevalova N.Yu. ....	427, 504, 505, 624, 678
Shadrin V.V. ....	488	Shkuratov V.Y. ....	489
Shadrina A.L. ....	176	Shlagman O. ....	732
Shafeev R. ....	750	Shlimak I.....	268
Shagalov A.G.....	453	Shmatov G.A. ....	361
Shah W.H.....	179	Shoji Y.....	588
Shakhov M.S.....	724	Shreder E.I. ....	704
Shakhunov V.A.....	670	Shubin A. ....	773
Shalygin A. ....	94, 287	Shubin Yu.V. ....	405
Shalyguina E. ....	287, 419	Shulenina A.V.....	242
Shamonina E. ....	97	Shulga N.V. ....	787
Shamsutdinov M.A. ....	761, 802	Shull R.D. ....	156, 278
Shamsutdinov M. ....	750	Shurina E.V.....	114
Shapaeva T.....	66	Shusharina N.....	635
Shapaeva T.B. ....	365	Sichelschmidt J. ....	565
Shapiro A.Ya.....	563	Sidis Y. ....	857
Shapkin A.A.....	769	Sidorenko A. ....	858
Shaposhnikov A.N. ....	212	Sidorenko A.S.....	593
Sharafullin I.F. ....	454	Sidorov V.....	897
Sharafutdinov A.U. ....	702	Sidorov V.A.....	428, 435
Sharipova M.I.....	332	Sidorov V.V.....	389, 391
Sharko S.A. ....	490	Sidorov V.A.....	434
Sharma G.....	132	Sierra J.F.....	694
Shatruk M.M. ....	390	Silva F.G. ....	317
Shavrov V. ....	295, 656, 658, 662	Simon Ch. ....	607
Shavrov V.G.....	205, 487, 632, 663, 752, 781, 782, 805	Simonov V.V. ....	747
Shcheglov V.I.....	752, 781, 782, 783, 784, 805	Simonovsky A.Ya.....	235, 248
Shchegoleva N.N. ....	116	Simovski C.R.....	92
Shchetinin I.V. ....	400	Singh K. ....	607
Sheftel E.N. ....	386, 423	Siryuk Ju.A. ....	755, 756, 757
Shein I.R. ....	192	Sitnikov A. ....	128, 209, 791
Shelehev E.V. ....	384, 391	Sitnikov A.V. ....	108, 110, 111, 121, 139, 159, 165, 796, 806
Shelushinina N.G. ....	506	Sitnikov M.N. ....	692
Shen N.H.....	95	Sizanov A.....	468
Shenkman O. ....	52	Skipetrov E.P. ....	722
Sherman E.Ya. ....	12	Skipetrova L.A.....	722
Sherokalova E.M.....	153, 157	Skirdkov P.N.....	758
Sherstobitova E.A. ....	433, 640	Sklenar J.....	83
Shevchenko A.D. ....	388	Skoblin G.M. ....	738
Shigapov I.M.....	600	Skokov K. ....	643
		Skokov K.P. ....	293, 641, 649, 747

Skorikov N.A. ....	598	Spichkin Y.I. ....	231, 775
Skourski Y. ....	86, 88, 436, 561, 645	Spirin A. ....	585
Skryabina O.V. ....	156	Srinivasan G. ....	493
Skumryev V. ....	495	Stadler S. ....	550
Slavin A. ....	694	Stamm C. ....	206, 337
Slavin A.N. ....	589	Stan C. ....	243
Sluchanko N. ....	709	Stancu A. ....	363, 481, 739
Sluchanko N.E. ....	427, 504, 505, 624, 678, 781	Starostenko S.N. ....	372, 378
Slyngo E.I. ....	722	Starykh O.A. ....	563
Slyngo V.E. ....	722	Stashkevich A.A. ....	614
Smagin V.V. ....	476	Stashkova L.A. ....	394
Smarzhevskaya A.I. ....	644, 665	Staub U. ....	65
Smekhova A. ....	607, 820, 897	Stebliy M.E. ....	112
Smelova E.M. ....	145	Stefanski A. ....	93
Smirnitskaya G.V. ....	117	Steneteg P. ....	553
Smirnov A.I. ....	563, 565	Stepanov A.L. ....	204
Smirnov I.Yu. ....	698	Stepanov G.V. ....	233, 872
Smirnov R.F. ....	641	Stepanov V.I. ....	315, 317, 573, 862
Smirnov V.V. ....	755, 756	Stepanova E.A. ....	426, 660
Smolnikov A. ....	474	Stepantsov E. ....	219
Snegirev V.V. ....	197	Stetsenko P.N. ....	117, 118
Sobolev A.V. ....	171, 178, 521, 716	Stishov S.M. ....	28
Sobolev N.A. ....	718	Stognei O.V. ....	138, 159
Socoliuc V. ....	575	Stognij A. ....	200
Söderberg O. ....	556	Stognij A.I. ....	172, 490, 803
Soga D. ....	568	Stolbov O.V. ....	868
Sohatsky V. ....	676	Stoleriu L. ....	481
Sokolik A.A. ....	42	Stolyar S.V. ....	125, 127, 226, 767
Sokolov A. ....	215, 773	Stone M.B. ....	562
Sokolov B.Yu. ....	216	Storozhenko A.M. ....	865
Sokolov V.V. ....	695	Straumal B.B. ....	821
Sokolovskiy V. ....	639, 650	Straumal P.B. ....	821
Sokolovskiy V.V. ....	293, 551, 628, 661	Stromberg F. ....	262
Sokolovskyy M.L. ....	801	Strugatsky M. ....	215
Solin N. ....	175	Stupakiewicz A. ....	200, 582
Solin N.I. ....	677, 685	Subbotin I.M. ....	864
Solodov E. ....	387	Sugimoto S. ....	910
Solontsov A. ....	301	Sukhachev A. ....	215, 218
Soloviov D.V. ....	226, 867	Sukhachev A.L. ....	474
Soloviov S.V. ....	473	Sukhorukov Yu. ....	38, 219
Solzi M. ....	292	Sukhorukov Yu.P. ....	220, 887
Sorokin A.A. ....	833	Sukhorukova O.S. ....	205
Sorokin A.N. ....	122, 699	Sukovatitsina E.V. ....	141
Sorokin A.O. ....	468	Sultan M. ....	338
Sotnikov A. ....	562	Sun D.L. ....	857
Soto-Armañanzas J. ....	829	Suñol J.J. ....	296, 663
Sotskiy V.V. ....	235	Sunyaev D.A. ....	501
Soukoulis C.M. ....	95	Suponev N. ....	753
Sousa R. ....	254	Suponev N.P. ....	383
Sousa R.C. ....	266, 267	Susan-Resiga D. ....	575
Spalek J. ....	891	Suski W. ....	828
Spasova M. ....	26, 283	Suslov A.V. ....	698

Suvorov A.A.	177
Suzuk S.	891
Svalov A.V.	134, 699
Sviridova T.A.	384, 389, 391, 481
Svistov L.E.	565, 856
Swietlik R.	17
Sycheva T.S.	422
Syljuåsen O.F.	310
Syms R.R.A.	95
Syr'ev N.	791
Syromyatnikov A.	468
Syromyatnikov A.V.	304, 468
Sysoev N.	778
Syvorotka I.I.	420
Szewczyk A.	484
Szymczak H.	490, 548
Szymczak R.	548, 627

---

## T

Tabachkova N.Yu.	481
Tabakaev A.I.	144
Taetz T.	853
Tagirov L.R.	77, 507, 593, 691, 716, 717
Taguchi Y.	604
Takagi T.	668
Takahashi M.	538
Takei R.	588
Takemura Y.	50
Talantsev A.	728
Taldenkov A.N.	174, 181, 194
Tan R.P.	263
Tan S.	571
Tanaka S.	891
Tanaka Y.	73
Tanasa R.	739
Taniguch T.	325
Tanimoto Y.	737
Tankeyev A.P.	476
Tarakanov O.	419
Tarapov S.	621
Tarapov S.I.	207, 882
Tarassenko A.S.	487
Tarassenko S.V.	205, 487
Tarassenko T.N.	485
Tarasov A.S.	109, 911
Tarasov P.	723
Taşarkuyu E.	638, 639
Taskaev S.	295, 647, 662
Taskaev S.V.	551, 646

Tejada J.	517
Tekielak M.	582
Telegin A.	38, 219
Telegin A.V.	220
Telegin S.	175
Telegin S.V.	685
Telegina I.	436
Temerov V.	218, 496, 623
Temerov V.L.	474
Temiryazeva M.P.	486, 719
Temnov V.V.	880
Teplykh A.E.	640
Terent'ev P.B.	394
Terent'ev P.E.	640
Terentyev P.B.	87, 414
Tereshina E.	436
Tereshina E.A.	90, 393
Tereshina I.	436, 629
Tereshina I.S.	393, 665
Testa A.M.	276
Teysser J.	858
Tezuka N.	910
Thévenot J.	571
Thiaudière E.	571
Thiaville A.	826
Thompson J.D.	428, 434
Thorat N.D.	518
Tiberkevich V.	694
Tiberkevich V.S.	589
Tietze Th.	821
Tikhomirov O.A.	170
Tikhonov E.V.	43, 424
Timirgazin M.A.	456
Timko M.	57, 863
Tishin A.M.	231, 659, 775
Titov A.	708
Titov A.A.	43, 305
Titov I.	292
Titov I.S.	664
Titov S.V.	366
Titova E.	245
Titova M.	681
Tkachenko N.V.	323
Tkachev A.V.	160, 472, 521
Tkacheva E.S.	244
To T.L.	679
Tobash P.H.	434
Tokunaga Y.	604
Tokura Y.	604
Tolentino H.C.N.	151
Tomak V.	778
Tomašovičová N.	863

Tombacz E. ....	242
Tombác E. ....	58
Tomkowicz J. ....	831
Tong S.Y. ....	371
Tonnerre J.-M. ....	151
Toriumi S. ....	333
Torrejon J. ....	826
ToSoong T.H. ....	56
Tóth-Katona T. ....	863
Tourinho F.A. ....	317, 318, 570, 576
Tovstolytkin A.I. ....	557
Tranquada J.M. ....	562
Tretyakov S.A. ....	92
Tretyakov Yu.D. ....	240, 388
Tripathi V. ....	533
Tristan N. ....	733
Trohidou K.N. ....	276
Trokiner A. ....	837
Tronov A.A. ....	286
Trubina A. Yu. ....	188
Trukhanov A.V. ....	172
Trukhanov S.V. ....	172, 190
Trunova A. ....	26
Tsai C.C. ....	83
Tsaregorodsev R.O. ....	513
Tsarevskii S. ....	503
Tsikalov D.S. ....	463
Tsirlin A.A. ....	852
Tskhadadze G.A. ....	634
Tsukamoto A. ....	206, 275, 333, 337, 584
Tsurkan V. ....	856, 895
Tselik A.M. ....	562
Tsvetkov D. ....	175
Tsvyashchenko A. ....	897
Tsvyashchenko A.V. ....	428, 434, 435, 512, 636, 681, 833
Tsymbal E.Y. ....	255, 258, 265
Tsysar K.M. ....	145
Tu C.S. ....	478
Tugarinov V. ....	152, 623
Tugushev V.V. ....	303, 534, 815
Tumanov V. ....	519
Tung M.J. ....	371
Turcu R.P. ....	874
Turkov V. ....	234
Turkov V.K. ....	108, 110, 111
Turpanov I. ....	148
Turpanov I.A. ....	104
Turysheva E. ....	246
Tyablikov O.A. ....	160
Tyablikov V.S. ....	846
Tyatyushkin A.N. ....	247

Tzurin V.A. ....	282
------------------	-----

---

## U

Ubizskii S.B. ....	420
Uchida H. ....	202, 878, 879
Udalov O.G. ....	707
Udod L.V. ....	692
Ueda Y. ....	608
Ueno S. ....	525
Ueno T. ....	668
Uimin M.A. ....	282
Ulanov V.A. ....	718
Ulaschik S. ....	572
Ulasov I. ....	321
Ulyanov A.N. ....	191
Ulyashev A.M. ....	108, 632
Umkhaeva Z. ....	395
Ünlü G. ....	26, 638, 639
Urcelay-Olabarria I. ....	495
Useinov A. ....	682
Useinov N. ....	682
Useinov N.Kh. ....	691
Ushakova O. ....	400
Usov N.A. ....	280
Uspenskaya L.S. ....	115, 170
Uspenski Yu.A. ....	424
Uspenskii Yu. ....	708
Uspenskii Yu.A. ....	43, 305
Ustinov V. ....	703
Ustinov V.V. ....	195, 680, 689
Uvarov V.N. ....	388
Uvchenko A.A. ....	804

---

## V

Vahaplar K. ....	206, 337
Vahedi J. ....	741
Vakhitov I.R. ....	716
Vakhitov R. ....	751
Valeev R.A. ....	385
Valeev V.F. ....	717
Valentyuk M. ....	853
Valenzuela L. ....	546
Valenzuela R. ....	622
Valiev U.V. ....	203
van den Brink J. ....	561
van Loosdrecht P.H.M. ....	855

van Schilfgaarde M. ....	897	Volchkov S.O. ....	794, 804
Vanacken J. ....	505	Volegov A.S. ....	120, 135, 136, 157, 654, 660
Varga R. ....	542, 830	Volkov D.V. ....	741
Varlamov A.A. ....	347	Volkov N. ....	496
Varnakov S.N. ....	109, 911	Volkov N.V. ....	109, 184, 669, 911
Varvaro G. ....	276	Volkov V.V. ....	242
Vas'kovskiy V.O. ....	619	Volkova E.G. ....	407, 798
Vas'kovskiy V.O. ....	116, 122, 134, 699, 794	Volkova O. ....	562
Vas'kovsky V.O. ....	426	Volkova O.S. ....	171, 178, 429, 564, 741, 743, 895
Vasenko A.S. ....	77, 350	Volkova Z. ....	837
Vashkovsky A.V. ....	785	Volochnaev M.N. ....	382
Vasil'ev A.D. ....	158	Volodin A.P. ....	481
Vasil'ev A.N. ....	171, 178	Vomir M. ....	330
Vasiliev A. ....	169, 562, 851	Vompe A. ....	166
Vasiliev A.L. ....	727	Vompe A.A. ....	235
Vasiliev A.M. ....	856	von Gratowski S. ....	658
Vasiliev A.N. ....	429, 564, 608, 733, 741, 743, 894, 895	von Löhneysen H. ....	348
Vasiliev V. ....	376	Vonesch H. ....	330
Vavilova E. ....	562, 853	Vorob'ev G.P. ....	492, 495, 606
Vavilova V. ....	807	Vorob'eva N.V. ....	261
Vazquez M. ....	826, 830	Voronina E. ....	140
Vedyayev A.V. ....	265, 456	Vorotynova O. ....	152
Vekas L. ....	571, 874	Vyas K.N. ....	54
Vékás L. ....	575	Vyshenskaya T. ....	764, 765
Velev J.P. ....	258	Vysotskii V. ....	778
Vélez S. ....	517	Vysotsky S. ....	615
Velichko E.S. ....	383	Vyzulin S. ....	791
Velichkov A.I. ....	833		
Veligzhanin A. ....	281	<hr/>	
Velikanov D. ....	148, 281, 623	<b>W</b>	
Velikanov D.A. ....	176, 184, 405		
Vengurlekar A.S. ....	881	Waintal X. ....	445
Verkhovskii S. ....	474, 837	Walowski J. ....	338
Verklov M.M. ....	385	Wang R.L. ....	637
Vershinin A.V. ....	162, 412	Wang T.H. ....	478
Vetoshko P.M. ....	326	Watanabe K. ....	90, 436
Vickers M.E. ....	557	Weber H.W. ....	704
Vikhrova O.V. ....	674, 688, 719, 726	Weeber R. ....	869
Vila L. ....	254, 266, 267	Wei D.H. ....	480
Vilkov E. ....	455	Wei F.L. ....	101
Vinai G. ....	285	Weides M. ....	346
Vinnikov L.Ya. ....	599	Weis C. ....	262
Vinogradov A.N. ....	719	Weiß S. ....	290
Vinogradov A.P. ....	92, 208, 223, 882	Wende H. ....	21, 262
Vinokur V.M. ....	347	Werner R. ....	345
Vishnevskii V. ....	201	Wienholdt S. ....	334
Vladimirov A.A. ....	46	Wilhelm F. ....	607, 897
Vladimirova E. ....	376	Wirtz C. ....	137
Vlasov A. ....	443	Wisniewski A. ....	885
Vlasov V.S. ....	108, 110, 111, 632, 752, 782, 805, 806	Wizent N. ....	561

Wojciech L.....	832
Wolf M.J. ....	348
Wolter A.....	429, 743
Wolter A.U.B. ....	564
Wood D.S.....	873
Wosnitza J.....	86, 88, 510
Wu K.T.....	478, 480
Wulfhekel W.....	16

---

## X

Xu L.S. ....	637
Xu X.-H.....	821
Xu Z. ....	562

---

## Y

Yabukami S.....	320
Yada K. ....	73
Yagmur V.....	415, 416
Yagodkin Yu.D.....	400, 406, 421
Yagupov S.....	215
Yakinci M.E.....	439
Yakovchuk V.Yu. ....	105, 125
Yakovlev D.....	881
Yakovlev D.R.....	61
Yakubovskii A. ....	837
Yakubovsky A.....	474
Yakushiji K. ....	13
Yamada T.K.....	16
Yamaguchi M.....	370
Yamakawa K.....	20
Yamashita F. ....	543, 544
Yanai T.....	543
Yanai Y. ....	544
Yang C.P. ....	637
Yang D.S.....	191
Yang H. ....	445
Yang H.D. ....	894
Yang H.X. ....	260
Yang M.-D. ....	371
Yang R. ....	637
Yankova T.....	565
Yankova T.S.....	738
Yanmaz E.....	597
Yanovskiy A.A. ....	248
Yanushkevich K.....	693
Yanushkevich K.I.....	270, 485

Yao Y.D.....	478, 480
Yaresko A.....	857
Yarikov S.A. ....	105
Yaroslavtsev A.A.....	390, 437
Yashina L.V.....	820
Yasin S.....	86, 177
Yatsyk I.V.....	491
Yehia M. ....	853
Yelkhova T.M.....	231
Yelon A.....	827
Yelsukov E.P. ....	374
Yelsukov Eu.....	140
Yeremenko A.V.....	388
Yerin C.V.....	249
Yermakov A.Ye.....	282
Yevstafyev O. ....	617
Yildiz F. ....	151
Yoda Y.....	132
Yokoyama T. ....	73
Yoo M.W. ....	84
Yoshida M. ....	910
Young B.-L.....	515
Yshkova V. ....	574
Yu. ....	351
Yuasa S. ....	13, 586
Yücel A.....	639
Yüksel M. ....	663
Yumaguzin A.....	751
Yurasov A.N.....	220
Yurasov N.....	220
Yurchenko V.M.....	205
Yuriev M.V.....	326, 766
Yurkin G.Yu. ....	405, 684
Yushkevich Y. ....	614
Yushkov V.I.....	104
Yusifovich A.A.....	270

---

## Z

Zabaznov Yu.V.....	180, 711
Zabluda V. ....	215, 773
Zagrebin M. ....	639, 650
Zagrebin M.A. ....	293, 661
Zaichenko S. ....	166
Zaikin A.D. ....	349
Zainullina R.I.....	195
Zaitsev A.V.....	511, 893
Zaitsev R.O.....	601
Zaitsev S. ....	728, 816
Zaitsev S.V. ....	674

Zakharenko M. ....	166	Zhigalov V.S. ....	721
Zakharov K. ....	169	Zhilina T.N. ....	769
Zakharov Yu. ....	443	Zhiteytsev E.R. ....	718
Zakhlevnykh A.N. ....	241, 862	Zhou G. ....	910
Zakhvalinskii V. ....	196	Zhukov A. ....	542, 545, 618, 630, 635, 648, 830, 831
Zakinyan A.R. ....	244	Zhukov A.P. ....	626, 631
Zaleski A. ....	629	Zhukov A.V. ....	250
Zalibekov U.Z. ....	675, 686, 702	Zhukova D.A. ....	634
Zaliznyak I.A. ....	562	Zhukova V. ....	542, 618, 635, 831
Zarefy A. ....	285	Zhuravlev M.Ye. ....	265
Zaripova L.D. ....	101	Zilberman P.E. ....	710
Zarubin A.V. ....	44	Zimmermann K. ....	234
Zarzuela R. ....	517	Zolotaryov A.Yu. ....	130
Zashchirinskii D.M. ....	168, 627	Zotov A.V. ....	155
Zaspel C.E. ....	706	Zotov I.S. ....	793
Zasukhin S.V. ....	133	Zotova O.V. ....	439
Zavarzina D.G. ....	769	Zubarev A.Yu. ....	228
Závišová V. ....	863	Zubavichus Y. ....	281
Zayats A. ....	583	Zubin A. ....	131
Zayats A.V. ....	614	Zubkov V.I. ....	783, 784
Zayets V. ....	586	Zubov V.E. ....	367
Zeer G. ....	152	Zubritsky S.M. ....	403
Zeidis I. ....	234	Zuev D.M. ....	240
Zenkevich A. ....	912	Zverev V.I. ....	659
Zenkov A.V. ....	188	Zvereva E.A. ....	429, 743
Zenkov E.V. ....	188	Zvezdin A.K. ....	13, 210, 473, 758, 810, 881, 902, 904
Zeziulina P.A. ....	747	Zvezdin K. ....	671, 705
Zhang Y. ....	438	Zvezdin K.A. ....	13, 364, 706, 758, 759
Zhang Z.Q. ....	438	Zvonkov B.N. ....	674, 688, 719, 726
Zharkov S. ....	152	Zvyagin A. ....	496
Zhekov K. ....	496	Zvyagina G. ....	496
Zheludev A. ....	565, 738	Zyablovsky A.A. ....	208
Zherlitsyn S. ....	86, 177	Zyubin A.Yu. ....	701
Zhernenkov K.N. ....	347	Zyuzin A.M. ....	696
Zhernenkov M. ....	25		
Zhevstovskikh I.V. ....	177		